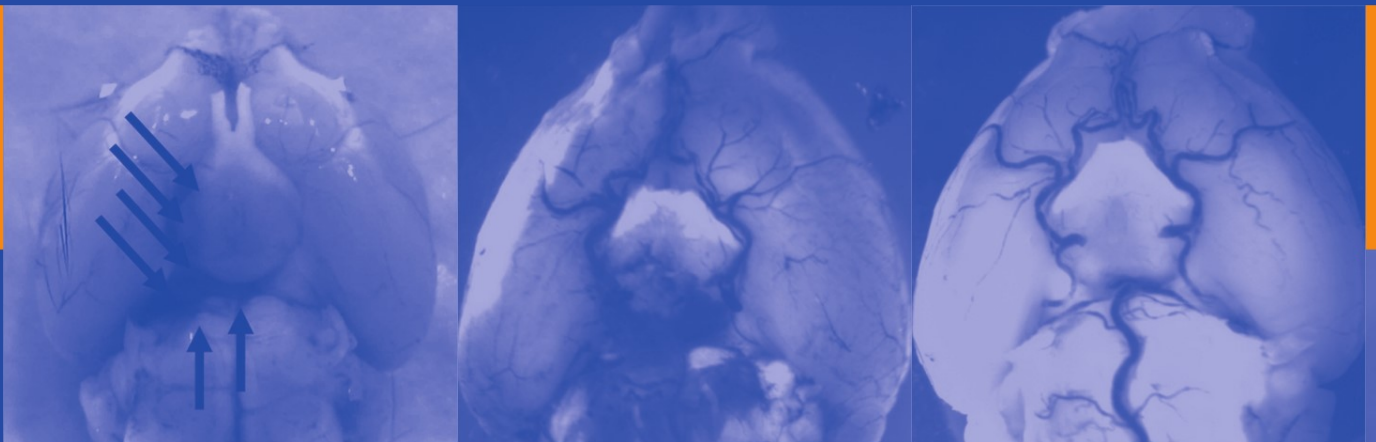


J. H. Zhang · A. Colohan
Editors

Intracerebral Hemorrhage Research

From Bench to Bedside



Acta Neurochirurgica
Supplements

Editor: H.-J. Steiger

Intracerebral Hemorrhage Research
From Bench to Bedside

Edited by
John H. Zhang, Austin Colohan

Acta Neurochirurgica
Supplement 111

SpringerWienNewYork

John H. Zhang
Department of Physiology and Pharmacology, School of Medicine,
Loma Linda University, Loma Linda, CA 92354, USA
e-mail: jhzhang@llu.edu

Austin Colohan
Department of Neurosurgery, Loma Linda University Medical Center,
Loma Linda, CA 92354, USA
e-mail: acolohan@llu.edu

This work is subject to copyright.

All rights are reserved, whether the whole or part of the material is concerned, specifically those of translation, reprinting, re-use of illustrations, broadcasting, reproduction by photocopying machines or similar means, and storage in data banks.

Product Liability: The publisher can give no guarantee for all the information contained in this book. This does also refer to information about drug dosage and application thereof. In every individual case the respective user must check its accuracy by consulting other pharmaceutical literature. The use of registered names, trademarks, etc. in this publication does not imply, even in the absence of a specific statement, that such names are exempt from the relevant protective laws and regulations and therefore free for general use.

©2011 Springer-Verlag/Wien
Printed in Germany
SpringerWienNewYork is part of Springer Science+Business Media
springer.at

Typesetting: SPI, Pondichery, India

Printed on acid-free and chlorine-free bleached paper
SPIN: 12752751

Library of Congress Control Number: 2011928407

With 143 (partly coloured) Figures

ISSN 0065-1419
ISBN 978-3-7091-0692-1 e-ISBN 978-3-7091-0693-8
DOI: 10.1007/978-3-7091-0693-8
SpringerWienNewYork

Preface

On March 9–11, 2010, the Third International Conference on Intracerebral Hemorrhage was held at the exquisite Rancho Las Palmas Resort in Rancho Mirage, California. No one could have asked for a better venue – beautiful weather, lush gardens, and a location city that attracts millions of people from all over the world each year, i.e., the world-renowned city of Palm Springs.

Surrounded by the snow-capped mountains and the peaceful sounds of circulating swimming pools, this year's conference was home to the largest gathering of intracerebral hemorrhage researchers from all over the world. For two full and productive days, a total of 66 invited oral presentations accompanied by 56 posters presented themes ranging from Predisposed Factors, Experimental Models, Inflammation and Immune Systems, Hematoma Clearance, Oxidative Stress, Neuroprotection, Vascular Responses, AVM Hemorrhage, Hemorrhage Transformation, Subarachnoid Hemorrhage, Neonatal Brain Injury, Surgical Brain Injury, Clinical Trials, Clinical Treatment, Surgical Management, and Neuro-ICU, just to name a few.

Looking back, the Third International Conference on Intracerebral Hemorrhage was historic for several reasons. First and foremost, this was the first independent conference on intracerebral hemorrhage, distinct from the first two international conferences on intracerebral hemorrhage that were satellite symposiums, part of an established neuroscience conference. Second, this conference was by far the largest meeting dedicated to intracerebral hemorrhage research, with more than 100 researchers and clinicians in attendance to exchange ideas and to discuss recent advances in basic science research and clinical practice. Third, the largest volume of presentations by far were submitted to this year's conference, including well over 122 oral and poster papers, compared with 21 at the First International Conference on Intracerebral Hemorrhage held in Ann Arbor, MI, on June 4, 2005, and 45 papers at the Second International Conference on Intracerebral Hemorrhage, which was held in Shanghai on November 10–11, 2007. Fourth, a total of 22 clinical and basic science experts served as session chairs as well as on the International Advisory Board this year, compared with 10 members who served on the International Advisory Board at the First International Conference and 17 members at the Second International Conference. And finally, one of the greatest successes of this conference was the broad coverage of topics presented – with a total of 17 themes focusing on secondary brain injuries, animal modeling, and clinical manifestations, just to name a few, compared with two themes of human and animal studies at the First International Conference and five themes at the Second International Conference, respectively. What all these points tell us is that there is growing interest in cerebral hemorrhage research and strong support for researchers in this field of academic activities.

One of the highlights of the Third International Conference on Intracerebral Hemorrhage was the award ceremony held on March 10th where this year's recipients of the coveted Julian T. Hoff Fellowship were announced. The three young researchers who received the honorable Hoff Fellowship in Intracerebral Hemorrhage Research were: Dr. Zheng Chen, a neurosurgeon from Fudan University in China, Dr. Anatol Manaenko, a neurobiologist from Loma Linda

University in California, and Dr. Paul R. Gigante, a neurosurgeon from Columbia University in New York. Toward the latter half of the ceremony, Dr. David Mendelow presented the audience with some exciting news about next year's conference. He announced next year's plan to host the Fourth International Intracerebral Hemorrhage Conference jointly with both the Vascular and Neurotrauma EANS annual meeting on May 2–5, 2011 in the beautiful city of Newcastle upon Tyne in England. This was definitely some exciting news.

Many of the attendees of the Third International Conference on Intracerebral Hemorrhage submitted papers of their presentations to be published in the special issue of *Acta Neurochirurgica*, which has been named "Intracerebral Hemorrhage Research: From Bench to Bedside." A total of 75 papers were divided into Animal Models, Pathophysiology of Cerebral Hemorrhage, Experimental Treatment for Cerebral Hemorrhage, Cerebral Hemorrhage, Clinical Manifestations, Prognosis of Cerebral Hemorrhage, and Clinical Management. These articles represent the recent advances in hemorrhagic brain injury research presented by highly respected laboratories around the world.

Lastly, we would like to thank our administrative personnel: Annette Brock, Kimberly Zaugg, and Stacia Christiansen, who did a remarkable job taking care of all the meeting affairs. Finally, we would like to thank Professor Hans-Jakob Steiger, the associate editor for special issues of *Acta Neurochirurgica*, for supporting the publication of this volume of recent advances in intracerebral hemorrhage research.

CA, USA

John H. Zhang, M.D., Ph.D
Austin Colohan, M.D

Acknowledgement

International Organization Committee

J. Aronowski

A. Colohan

S. Fagan

D. Greenberg

D.F. Hanley

D. Heistad

Y. Hua

R.F. Keep

E.H. Lo

R.L. Macdonald

A.D. Mendelow

G. Rosenberg

X. Qin

F.R. Sharp

N. Shimamura

L. Shutter

J. Tang

S.E. Tsirka

H. Suzuki

W.L. Young

G. Xi

J.H. Zhang

Contents

Cerebral Hemorrhage Animal Models

History of Preclinical Models of Intracerebral Hemorrhage	3
Q. Ma, N.H. Khatibi, H. Chen, J. Tang, and J.H. Zhang	
Comparison of Different Preclinical Models of Intracerebral Hemorrhage	9
A. Manaenko, H. Chen, J.H. Zhang, and J. Tang	
Cerebral Amyloid Angiopathy-Related Microhemorrhages in Alzheimer’s Disease: A Review of Investigative Animal Models	15
H. Chen and J.H. Zhang	
Multiparametric Characterisation of the Perihemorrhagic Zone in a Porcine Model of Lobar ICH	19
B. Orakcioglu, M. Kentar, Y. Uozumi, E. Santos, P. Schiebel, A. Unterberg, and O.W. Sakowitz	
Developing a Model of Chronic Subdural Hematoma	25
J. Tang, J. Ai, and R.L. Macdonald	
A Mouse Model of Intracranial Aneurysm: Technical Considerations	31
Y. Tada, Y. Kanematsu, M. Kanematsu, Y. Nuki, E.I. Liang, K. Wada, H. Makino, and T. Hashimoto	
The Postpartum Period of Pregnancy Worsens Brain Injury and Functional Outcome After Cerebellar Hemorrhage in Rats	37
T. Lekic, R.P. Ostrowski, H. Suzuki, A. Manaenko, W. Rolland, N. Fathali, J. Tang, and J.H. Zhang	
Hyperglycemia and Hemorrhagic Transformation of Cerebral Infarction: A Macroscopic Hemorrhagic Transformation Rat Model	43
T. Tsubokawa, H. Joshita, Y. Shiokawa, and H. Miyazaki	
Hemorrhagic Transformation Induced by Acute Hyperglycemia in a Rat Model of Transient Focal Ischemia	49
Y. Xing, X. Jiang, Y. Yang, and G. Xi	

A Novel Preclinical Model of Germinal Matrix Hemorrhage Using Neonatal Rats	55
T. Lekic, A. Manaenko, W. Rolland, J. Tang, and J.H. Zhang	
Pathophysiology of Cerebral Hemorrhage	
Intracranial Hemorrhage: Mechanisms of Secondary Brain Injury	63
J. Lok, W. Leung, S. Murphy, W. Butler, N. Noviski, and E.H. Lo	
Clot Formation, Vascular Repair and Hematoma Resolution After ICH, a Coordinating Role for Thrombin?	71
R.F. Keep, G. Xi, Y. Hua, and J. Xiang	
The Dual Role of Src Kinases in Intracerebral Hemorrhage	77
D.-Z. Liu and F.R. Sharp	
Brain Arteriovenous Malformation Pathogenesis: A Response-to-Injury Paradigm	83
H. Kim, H. Su, S. Weinsheimer, L. Pawlikowska, and W.L. Young	
The Evolving Landscape of Neuroinflammation After Neonatal Hypoxia-Ischemia	93
N. Fathali, N.H. Khatibi, R.P. Ostrowski, and J.H. Zhang	
Red Blood Cell Lysis and Brain Tissue-Type Transglutaminase Upregulation in a Hippocampal Model of Intracerebral Hemorrhage	101
F. Zhao, S. Song, W. Liu, R.F. Keep, G. Xi, and Y. Hua	
Cytoprotective Role of Haptoglobin in Brain After Experimental Intracerebral Hemorrhage	107
X. Zhao, S. Song, G. Sun, J. Zhang, R. Strong, L. Zhang, J.C. Grotta, and J. Aronowski	
Effects of Aging on Autophagy After Experimental Intracerebral Hemorrhage	113
Y. Gong, Y. He, Y. Gu, R.F. Keep, G. Xi, and Y. Hua	
Effects of Gender on Heart Injury After Intracerebral Hemorrhage in Rats	119
Z. Ye, Q. Xie, G. Xi, R.F. Keep, and Y. Hua	
Iron Accumulation and DNA Damage in a Pig Model of Intracerebral Hemorrhage	123
Y. Gu, Y. Hua, Y. He, L. Wang, H. Hu, R.F. Keep, and G. Xi	
Subarachnoid Hemorrhage Causes Pulmonary Endothelial Cell Apoptosis and Neurogenic Pulmonary Edema in Mice	129
H. Suzuki, T. Sozen, Y. Hasegawa, W. Chen, K. Kanamaru, W. Taki, and J.H. Zhang	

Hemoglobin Expression in Neurons and Glia After Intracerebral Hemorrhage	133
Y. He, Y. Hua, R.F. Keep, W. Liu, M.M. Wang, and G. Xi	
Experimental Treatment for Cerebral Hemorrhage	
Isoflurane Preconditioning Affords Functional Neuroprotection in a Murine Model of Intracerebral Hemorrhage	141
P.R. Gigante, G. Appelboom, B.Y. Hwang, R.M. Haque, M.L. Yeh, A.F. Ducruet, C.P. Kellner, J. Gorski, S.E. Keesecker, and E.S. Connolly Jr.	
The Neuroprotective Effects of Cyclooxygenase-2 Inhibition in a Mouse Model of Aneurysmal Subarachnoid Hemorrhage	145
R. Ayer, V. Jadhav, T. Sugawara, and J.H. Zhang	
Sonic Hedgehog Agonist Fails to Induce Neural Stem Cell Precursors in a Porcine Model of Experimental Intracranial Hemorrhage	151
J. Tong, J.M. Latzman, J. Rauch, D.S. Zagzag, J.H. Huang, and U. Samadani	
NC1900, an Arginine Vasopressin Analogue, Fails to Reduce Brain Edema and Improve Neurobehavioral Deficits in an Intracerebral Hemorrhagic Stroke Mice Model	155
A. Manaenko, T. Lekic, J.H. Zhang, and J. Tang	
Geldanamycin Reduced Brain Injury in Mouse Model of Intracerebral Hemorrhage	161
A. Manaenko, N. Fathali, S. Williams, T. Lekic, J.H. Zhang, and J. Tang	
Combined Systemic Thrombolysis with Alteplase and Early Hyperbaric Oxygen Therapy in Experimental Embolic Stroke in Rats: Relationship to Functional Outcome and Reduction of Structural Damage	167
L. Küppers-Tiedt, A. Manaenko, D. Michalski, A. Guenther, C. Hobohm, A. Wagner, J.H. Zhang, and D. Schneider	
Neutrophil Depletion Diminishes Monocyte Infiltration and Improves Functional Outcome After Experimental Intracerebral Hemorrhage	173
L.H. Sansing, T.H. Harris, S.E. Kasner, C.A. Hunter, and K. Kariko	
Hydrogen Inhalation is Neuroprotective and Improves Functional Outcomes in Mice After Intracerebral Hemorrhage	179
A. Manaenko, T. Lekic, Q. Ma, R.P. Ostrowski, J.H. Zhang, and J. Tang	
Deferoxamine Reduces Cavity Size in the Brain After Intracerebral Hemorrhage in Aged Rats	185
T. Hatakeyama, M. Okauchi, Y. Hua, R.F. Keep, and G. Xi	
Post-treatment with SR49059 Improves Outcomes Following an Intracerebral Hemorrhagic Stroke in Mice	191
A. Manaenko, N. Fathali, N.H. Khatibi, T. Lekic, K.J. Shum, R. Martin, J.H. Zhang, and J. Tang	

Deferoxamine Affects Heat Shock Protein Expression in Heart after Intracerebral Hemorrhage in Aged Rats	197
H. Hu, L. Wang, M. Okauchi, R.F. Keep, G. Xi, and Y. Hua	
Neuroprotection by Melatonin after Germinal Matrix Hemorrhage in Neonatal Rats	201
T. Lekic, A. Manaenko, W. Rolland, K. Virbel, R. Hartman, J. Tang, and J.H. Zhang	
Endothelin Receptor-A (ET_a) Inhibition Fails to Improve Neonatal Hypoxic-Ischemic Brain Injury in Rats	207
N.H. Khatibi, L.K. Lee, Y. Zhou, W. Chen, W. Rolland, N. Fathali, R. Martin, R. Applegate, G. Stier, and J.H. Zhang	
FTY720 is Neuroprotective and Improves Functional Outcomes After Intracerebral Hemorrhage in Mice	213
W.B. Rolland II, A. Manaenko, T. Lekic, Y. Hasegawa, R. Ostrowski, J. Tang, and J.H. Zhang	
Thrombin Preconditioning Reduces Iron-Induced Brain Swelling and Brain Atrophy	219
S. Song, H. Hu, Y. Hua, J. Wang, and G. Xi	
Capsaicin Pre-treatment Provides Neurovascular Protection Against Neonatal Hypoxic-Ischemic Brain Injury in Rats	225
N.H. Khatibi, V. Jadhav, S. Charles, J. Chiu, J. Buchholz, J. Tang, and J.H. Zhang	
Effects of Recombinant Osteopontin on Blood-Brain Barrier Disruption After Subarachnoid Hemorrhage in Rats	231
H. Suzuki, Y. Hasegawa, R. Ayer, T. Sugawara, W. Chen, T. Sozen, K. Kanamaru, W. Taki, and J.H. Zhang	
Protective Effect of Hydrogen Gas Therapy After Germinal Matrix Hemorrhage in Neonatal Rats	237
T. Lekic, A. Manaenko, W. Rolland, N. Fathali, M. Peterson, J. Tang, and J.H. Zhang	
Pretreatment with Normobaric and Hyperbaric Oxygenation Worsens Cerebral Edema and Neurologic Outcomes in a Murine Model of Surgically Induced Brain Injury	243
D. Westra, W. Chen, R. Tsuchiyama, A. Colohan, and J.H. Zhang	
Beneficial Effect of Hyperbaric Oxygenation After Neonatal Germinal Matrix Hemorrhage	253
T. Lekic, A. Manaenko, W. Rolland, R.P. Ostrowski, K. Virbel, J. Tang, and J.H. Zhang	
Thrombin Preconditioning Attenuates Iron-Induced Neuronal Death	259
H. Hu, S. Yamashita, S. Song, Y. Hua, R.F. Keep, and G. Xi	

Granulocyte Colony-Stimulating Factor Treatment Provides Neuroprotection in Surgically Induced Brain Injured Mice	265
N.H. Khatibi, V. Jadhav, M. Saidi, W. Chen, R. Martin, G. Stier, J. Tang, and J.H. Zhang	
Tamoxifen Treatment for Intracerebral Hemorrhage	271
Q. Xie, J. Guan, G. Wu, G. Xi, R.F. Keep, and Y. Hua	
Prostaglandin E₂ EP₁ Receptor Inhibition Fails to Provide Neuroprotection in Surgically Induced Brain-Injured Mice	277
N.H. Khatibi, V. Jadhav, B. Matus, N. Fathali, R. Martin, R. Applegate, J. Tang, and J.H. Zhang	
Mucosal Tolerance to Brain Antigens Preserves Endogenous TGFβ-1 and Improves Neurological Outcomes Following Experimental Craniotomy	283
N. Jafarian, R. Ayer, J. Eckermann, W. Tong, N. Jafarian, R.L. Applegate II, G. Stier, R. Martin, J. Tang, and J.H. Zhang	
Effects of Progesterone and Testosterone on ICH-Induced Brain Injury in Rats	289
Z. Chen, G. Xi, Y. Mao, R.F. Keep, and Y. Hua	
Drug Repurposing for Vascular Protection After Acute Ischemic Stroke	295
W. Guan, A. Kozak, and S.C. Fagan	
Erythropoietin Attenuates Inflammatory Factors and Cell Death in Neonatal Rats with Intracerebral Hemorrhage	299
M. Chau, D. Chen, and L. Wei	
Protective Effects of Hydrogen on Fetal Brain Injury During Maternal Hypoxia	307
W. Liu, O. Chen, C. Chen, B. Wu, J. Tang, and J.H. Zhang	
Cerebral Hemorrhage Clinical Manifestations	
Neuroglobin Expression in Human Arteriovenous Malformation and Intracerebral Hemorrhage	315
K. Jin, X. Mao, L. Xie, and D.A. Greenberg	
Intracerebral Hemorrhage and Meteorological Factors in Chongqing, in the Southwest of China	321
X. Li, J.H. Zhang, and X. Qin	
Timing Pattern of Onset in Hypertensive Intracerebral Hemorrhage Patients	327
J. Feng, J.H. Zhang, and X. Qin	
“Weekend Effects” in Patients with Intracerebral Hemorrhage	333
F. Jiang, J.H. Zhang, and X. Qin	

Disparities in Medical Expenditure and Outcomes Among Patients with Intracranial Hemorrhage Associated with Different Insurance Statuses in Southwestern China	337
Y. Kong, Y. Wang, J.H. Zhang, X. Wang, and X. Qin	
Clinical Analysis of Electrolyte Imbalance in Thalamic Hemorrhage Patients Within 24 H After Admission	343
Z. Guo, T. Wang, J.H. Zhang, and X. Qin	
Characteristics of Pulse Pressure Parameters in Acute Intracerebral Hemorrhage Patients	349
T. Tao, T. Wang, J.H. Zhang, and X. Qin	
Electrocardiographic Abnormalities in Patients with Intracerebral Hemorrhage	353
Q. Liu, Y. Ding, P. Yan, J.H. Zhang, and H. Lei	
ECG Change of Acute Subarachnoid Hemorrhagic Patients	357
Q. Liu, Y.-H. Ding, J.H. Zhang, and H. Lei	
Diagnosis and Treatment of Hemorrhagic Pituitary Adenomas	361
G. Huo, Q.-L. Feng, M.-Y. Tang, and D. Li	
Characteristics of Acute Cerebral Hemorrhage with Regard to Lipid Metabolism and Glycometabolism Among Different Age Groups	367
X. Wang, Y. Kong, H. Chen, J.H. Zhang, and Y. Wang	
Prognosis of Cerebral Hemorrhage	
The Role of a High Augmentation Index in Spontaneous Intracerebral Hemorrhage to Prognosticate Mortality	375
L.H. Keong, Ab R.I. Ghani, M.S. Awang, S. Sayuthi, B. Idris, and J.M. Abdullah	
Effect of Minimally Invasive Aspiration in Treatment of Massive Intracerebral Hemorrhage	381
G. Li, X. Qin, G. Pen, W. Wu, J. Yang, and Q. Yang	
Retrospective Analysis of the Predictive Effect of Coagulogram on the Prognosis of Intracerebral Hemorrhage	383
Y. Wang, X. Wang, Y. Kong, F. Li, and H. Chen	
Risk Factors of Early Death in Patients with Hypertensive Intracerebral Hemorrhage During Hospitalization	387
X. Hu, J.H. Zhang, and X. Qin	
Effects of Early Serum Glucose Levels on Prognosis of Patients with Acute Intracerebral Hemorrhage	393
Y. Wang, T. Wang, J.H. Zhang, and X. Qin	

Prognosis Study of 324 Cases with Spontaneous Intracerebral Hemorrhage in Chongqing, China	399
Q. Li, X.-Y. Qin, J.H. Zhang, and J. Yang	
Retrospective Analysis of the Predictive Effect of Routine Biochemical Results on the Prognosis of Intracerebral Hemorrhage.	403
H. Chen, F. Li, X. Wang, Y. Kong, and Y. Wang	
Clinical Management	
Alteplase (rtPA) Treatment of Intraventricular Hematoma (IVH): Safety of an Efficient Methodological Approach for Rapid Clot Removal.	409
J. Bartek Jr., J. Hansen-Schwartz, O. Bergdal, J. Degn, B. Romner, K.L. Welling, and W. Fischer	
Decompressive Hemi-craniectomy Is Not Necessary to Rescue Supratentorial Hypertensive Intracerebral Hemorrhage Patients: Consecutive Single-Center Experience	415
N. Shimamura, A. Munakata, M. Naraoka, T. Nakano, and H. Ohkuma	
Intravascular Hypothermia for Acute Hemorrhagic Stroke: A Pilot Study	421
J.M. Abdullah and A. Husin	
Use of Intralesional tPA in Spontaneous Intracerebral Hemorrhage: Retrospective Analysis.	425
W.D. Johnson and P.A. Bouz	
Endoscopic Surgical Treatment for Pituitary Apoplexy in Three Elderly Patients over the Age of 80	429
Y. Hasegawa, S. Yano, T. Sakurama, Y. Ohmori, T. Kawano, M. Morioka, H. Chen, J.H. Zhang, and J.-I. Kuratsu	
Proton Pump Inhibitor Prophylaxis Increases the Risk of Nosocomial Pneumonia in Patients with an Intracerebral Hemorrhagic Stroke	435
L. Ran, N.H. Khatibi, X. Qin, and J.H. Zhang	
Author Index	441
Subject Index	445

Cerebral Hemorrhage Animal Models

History of Preclinical Models of Intracerebral Hemorrhage

Qingyi Ma, Nikan H. Khatibi, Hank Chen, Jiping Tang, and John H. Zhang

Abstract In order to understand a disease process, effective modeling is required that can assist scientists in understanding the pathophysiological processes that take place. Intracerebral hemorrhage (ICH), a devastating disease representing 15% of all stroke cases, is just one example of how scientists have developed models that can effectively mimic human clinical scenarios. Currently there are three models of hematoma injections that are being used to induce an ICH in subjects. They include the microballoon model introduced in 1987 by Dr. David Mendelow, the bacterial collagenase injection model introduced in 1990 by Dr. Gary Rosenberg, and the autologous blood injection model introduced by Dr. Guo-Yuan Yang in 1994. These models have been applied on various animal models beginning in 1963 with canines, followed by rats and rabbits in 1982, pigs in 1996, and mice just recently in 2003. In this review, we will explore in detail the various injection models and animal subjects that have been used to study the ICH process while comparing and analyzing the benefits and disadvantages of each.

Keywords ICH · Animals · Microballoon · Collagenase

Q. Ma, H. Chen, and J. Tang (✉)
Department of Physiology and Pharmacology,
Loma Linda University, School of Medicine,
Risley Hall, Room 219, Loma Linda, CA 92354, USA
e-mail: jtang@llu.edu

N.H. Khatibi
Department of Anesthesiology, Loma Linda University,
School of Medicine, Loma Linda, CA, USA

J.H. Zhang
Department of Physiology and Pharmacology,
Loma Linda University, School of Medicine,
Risley Hall, Room 219, Loma Linda, CA 92354, USA and
Department of Anesthesiology, Loma Linda University,
School of Medicine, Loma Linda, CA, USA and
Department of Neurosurgery, Loma Linda University,
School of Medicine, Loma Linda, CA, USA

Introduction

Intracerebral hemorrhage (ICH) is a devastating disease accounting for roughly 15% of all stroke types. As many as 50,000 individuals are affected annually in the United States, with a large number of those individuals facing chronic morbidities and early mortalities.

Over the years, basic science research has focused on reducing and/or blocking the cascade of harmful events in ICH with the goal of improving clinical outcomes. But in order to effectively study the mechanisms behind these events, proper modeling is needed that can mimic pathophysiologic processes in humans. Studies on various animal models began in 1963 with canines, followed by rats and rabbits in 1982, pigs in 1996, and mice just recently in 2003. These animal subjects have been thoroughly studied individually and compared to human models looking for a parallel between the two groups.

As important as it is to find an animal subject that will mimic processes in the human brain, creating the actual hematoma is another challenge. Currently there are three models of injections that are being used to induce an ICH in subjects. They include the microballoon model introduced in 1987 by Dr. David Mendelow, the bacterial collagenase injection model introduced in 1990 by Dr. Gary Rosenberg, and the autologous blood injection model introduced by Dr. Guo-Yuan Yang in 1994 [1–3].

In this retrospective review, the history behind the development of the ICH model will be presented and discussed. Furthermore, the advantages and disadvantages of each model type and animal subject will be evaluated.

ICH Models

Microballoon Model

In 1987, Sinar et al. [2] made a microballoon insertion model in rats as a way to study the mass effects of ICH.

A microballoon mounted on a no. 25 blunted needle was inserted into the right caudate nucleus after a burr hole had been created on the skull. The microballoon was inflated to 0.05 mL over a period of 20 s and was kept inflated for 10 min before being deflated. At the end of the study, the authors looked at brain histology, intracranial pressure, and cerebral blood flow. They found the microballoon model to be successful in producing an effective brain lesion with an extensive area of ischemic damage noted on the right caudate nucleus. Additionally, there was a reduction in cerebral blood flow and an increase in intracranial pressure at the site of damage.

The advantage of the microballoon model, according to Rojas et al. [4], is that it mimics the space-occupying aspect of the hematoma. The disadvantage is it fails to address the potential effects of blood and subsequent substances released by the clot formation. This could potentially be the reason why there is a smaller degree of ischemia in this model versus what would be expected with an equivalent volume of blood [5, 6].

Collagenase Injection Model

Collagenases are proteolytic enzymes that degrade the basement membrane and interstitial collagen [7]. Additionally, they have been shown through immunocytochemical studies to surround blood vessels [8]. As a result, in 1990, Rosenberg et al. made a new model for spontaneous ICH using bacterial collagenase injections directly in the brains of Sprague-Dawley rats [1]. In this model, male rats were placed in a stereotactic apparatus, and 2 μ l of saline containing 0.01–0.1U bacterial collagenase (type XI or VII) was infused into the left caudate nucleus over 9 min. Bleeding occurred as early as 10 min after collagenase injection, with edema also seen at the site of hemorrhage [1]. Other modifications to this model were made, including: injection site changes, adjustments to collagenase concentration, injection rates/volumes, and heparinization. This model conceptually integrates small vessel breakdown to produce hemorrhage and allows a controllable amount of variability in hemorrhage size [9]. The advantage of this model is its ability to mimic spontaneous intraparenchymal bleeding in humans while avoiding the technical difficulties with handling blood [10]. It also mimics the hematoma expansion of continuous bleeding that occurs naturally in ICH patients [11, 12]. The disadvantages of this model are related to bacterial collagenase's ability to introduce a significant inflammatory reaction [10].

Blood Injection Model

The blood injection ICH model has become the standard for experimental ICH. The first recorded publication using arterial blood as a single injectable agent was conducted by Ropper et al. in 1982 [13]. Using a 27-gauge cannula, fresh

blood from the ventricle of a donor rat was infused over 1 s into the right caudate nucleus of the subject ICH rat. This method did not account for key sources of variability. Hence, in 1984, a variation of Ropper's model was performed by Bullock et al. [14] to study the changes in intracranial pressure and cerebral blood flow. Instead of using donor blood, Bullock used a 22-gauge needle that bridged the right caudate nucleus to the femoral artery. For the first time, the study was able to look at ICH under arterial pressure – thus effectively evaluating the pathophysiology of ICH. One of the main disadvantages of this method was the lack of reproducibility because of the potential variations in blood pressure.

This is why in 1994 a study at the University of Michigan by Yang et al. [3], discovered that the use of a microinfusion pump could address the concerning issues that had confronted previous authors. Using a microinfusion pump, a constant rate of autologous blood (extracted from the femoral artery) was infused into the right caudate nucleus, creating a controllable and reproducible hematoma. This single blood injection model has been applied to most of the recent ICH studies. Unfortunately, one of the major issues with Yang's technique was the reflux of blood up the needle tract and into the ventricular system or extension into the subdural space with a more rapid injection rate. Additionally, the inability of this technique to reproduce the systemic arterial pressure that can influence the hematoma size is also seen as a slight disadvantage. Finally, the use of the femoral artery created problems down the road when it came time to assess neurobehavioral deficits.

To address the concern of blood reflux up the needle tract, a double injection model was created just 2 years later. In 1996, a study led by Deinsberger et al. [15] at the Justus Liebig University in Germany modified the single arterial blood injection model originally designed by Yang and instead used a double arterial blood injection model. What Deinsberger and his team proposed was injecting 5 μ l of fresh autologous blood into the caudate nucleus and waiting 10 min to allow for clot formation. This way, when it was time to inject the rest of the autologous blood to mimic the hematoma, the chances of reflux would be minimized significantly. This was the main advantage of the double blood injection model over the single injection model – it minimized blood reflux through the needle tract. The disadvantages, however, were the obvious difficulties with infusion and increased potential of clot formation because of the time lag between injections.

Large Animal Models

Monkeys

Chimpanzees and rhesus monkeys share over 90% of their DNA with humans in addition to physiologic, structural

and size similarities, making them ideal candidates for pre-clinical study. In 1982, Segal et al. [16] used macaque monkeys to demonstrate the effects of local therapy on hematoma formation using the thrombolytic urokinase. Their treatment was given after injection of 6 mL autologous blood into the right internal capsule. Additionally, in 1988, Bullock et al. [17] used adult Vervet monkeys to demonstrate and quantify a 90–120 min decrease in the regional cerebral blood flow (rCBF) following an ICH. A key refinement to the primate model made by Bullock was the use of a catheter that infused blood directly from the femoral artery into the right caudate, thereby keeping the infusion pressure closer to arterial pressure and reducing complications from blood handling and delay.

The experiments using monkeys were costly, and the various levels of restrictions and regulations were concerning [4]. Hence, their use in ICH modeling was quickly discontinued.

Canines

Like monkeys, canines have long been the subject of medical research across the same range of fields, most notably having contributed to cardiovascular physiology [18]. But like monkeys, use of canines in research involves similarly stringent criteria and cost. In 1963, Whisnant et al. [19] developed a model for experimental ICH by performing single injections of 0.5–1.5 mL of fresh autologous venous blood into the basal nuclei or deep white matter region in canines – producing varying sizes of ICH. In 1975, Sugi et al. [20] used canines to develop a single autologous arterial blood injection model, noting lactate elevations in CSF after injection. In 1999, Qureshi et al. [21] made single autologous blood injections (7.5 mL) over 20–30 min under arterial pressure into the deep white matter adjacent to the basal ganglia of canines. The needle was pointed 20° lateral to the vertical axis. The complications encountered in this study were the increased frequency of transtentorial herniation. Hence, they then used smaller injection volumes ranging from 2.8 to 5.5 mL, which successfully induced formation of ICH with fewer complications [22]. In 1999, Lee et al. [23] made use of an infusion pump for injection of 3–5 mL of non-heparinized autologous arterial blood into the temporo-parietal cortex. This method took 8 min in canine subjects and allowed for the formation of consistently sized clots.

In 1985, the microballoon method was used by Takasugi et al. [24] who modified this method by injecting venous blood directly into the balloon as an attempt to minimize reflux. This model mimicked both the increased pressure and blood volume following ICH. Using this model, Takasugi was able to classify the chronological stages after ICH and concluded that the increased repair time after ICH was correlated to the degree of histologic injury to the surrounding tissue rather than to the size of the hematoma itself.

Pigs

Known for their large, gyrated brain and well-developed white matter, the large hematoma volume in pigs post-ICH enables a closer examination of the area compared to other animal species [25]. In 1996, Wagner et al. [25] developed a lobar hemorrhage model in pigs where 1.7 mL of autologous arterial blood was slowly injected using an infusion pump into the frontal white matter. The slow injection reduced the likelihood of ventricular rupture or leakage of blood along the needle track. Compared with rapid infusions at high pressures, this method more closely modeled ICH in humans where bleeding generally originates from small intraparenchymal arteries. In 2000, Kuker et al. [26] injected 0.5–2.0 mL of venous blood with a blood reservoir into the anterior frontal lobe to study the characteristics of hematomas using magnetic resonance imaging. This study used Takasugi's method of prior microballoon catheter insertion to reduce needle pathway reflux. A different study in 2002 led by Rohde et al. [32] modified this model into a double-injection procedure (with a main injection of 2–3 mL of autologous venous blood with blood reservoir in their study) to better prevent post-injection reflux.

Pigs were also used in collagenase injection models. Collagenase infusions of 10 µL by micro-infusion pump over 20–30 min were made into the right somatosensory cortex by Mun-Bryce et al. [27] in 2001. This study examined tissue excitability following ICH and evaluated the outcomes using magnetic resonance imaging in addition to electro- and magneto-encephalography. Use of collagenase, which is released from injured cells [5], does address the clinically relevant phenomenon of vasogenic edema following ICH. The levels of collagenase, however, are far above those encountered in clinical ICH and therefore correlations must take this into account.

Small Animal Models

Rabbits

Rabbits were first used by Kaufman et al. in 1985 [28] in a single autologous blood injection model. The study failed to yield conclusive results, and in fact, the rabbit died shortly after injection. A decade later, arterial blood was injected using an infusion pump by Koeppen et al. [29]. Arterial blood extracted from the ear was injected into the right thalamus and, to minimize reflux, needle withdrawal was delayed. The study found that subjects exhibited a reduction in neurobehavioral deficits.

Compared to larger animal models, use of rabbits is less costly, meets a higher success rate, and allows for an extended period of study with less mortality. Qureshi et al. in 2001 [30] modified this model in order to look at patterns of cellular

injury. In this model, a 30-gauge needle penetrated the brain, while autologous arterial blood was infused into the white matter of the left frontal lobe. Instead of using arterial blood, Gustafsson et al. in 1999 [31] used autologous venous blood that was injected manually in the brain. Although a hematoma did form, the use of venous blood differs from what is seen in humans.

Rats

The earliest rat model using a single arterial blood injection method was conducted in 1982 by Ropper et al. [13]. The study reported that blood, not the mass effect as was previously postulated, was responsible for the changes in regional cerebral blood flow. Unfortunately, because of the nature of the design, certain outcomes could not be evaluated – the disadvantage of using donor blood introduces various immune reactions, while the lack of arterial pressure fails to mimic a true human ICH experience. Additionally, variability in outcomes was an issue because of the potential for reflux up the needle tract and the potential for blood volume discrepancies. Several of these issues were addressed later by Bullock et al. in 1984 [14]. For instance, blood infusion was conducted more rapidly under arterial pressure and in a smaller time window (10 s); however, it was difficult to reproduce reliably. The blood pressure variations from animal to animal resulted in different injury volumes, and the small time window required significant technical mastery. This was followed by development of a method that instead held the rate of infusion constant using microinfusion pumps [6]. The use of microinfusion pumps allowed production of a controllable and reproducible lesion with a slower injection rate and a lower pressure than in an arterial pressure model (100 mmHg). A remaining shortcoming was that a more rapid injection rate resulted in a variable reflux of blood along the needle track and poorly reproducible lesions.

To address the issue of needle tract reflux, the double injection method was developed by Deinsberger et al. in 1996 [15]. In this model, a smaller volume of blood was first infused, allowing for clot formation and a reduction in blood reflux. While technically challenging, this technique met with great success in reproducibility and minimization of pathway reflux. The use of venous blood in the single blood injection model was addressed by Masuda et al. in 1988 [33]. While they described a significant success rate in the production of intraparenchymal hematomas, the use of venous blood did not faithfully replicate the conditions in the major form of clinical ICH, which involves rupture of an arterial vessel.

In 1990, Rosenberg et al. established a new model for spontaneous ICH using bacterial collagenase infused directly

into the brain in Sprague-Dawley rats [1]. This model was especially popular because it was the closest mimicker of spontaneous ICH in human beings [10].

Mice

The ICH model in mice was derived from experiments in rats. A single arterial blood injection into the right basal ganglia in mice was described by Nakamura et al. in 2004 [34]. This study compared the effects of autologous arterial blood, donor whole blood, and saline injections on brain edema development. The study found that donor blood injection was associated with a significantly greater increase in edema in the ipsilateral cortex compared to an autologous blood injection model.

In 2003, Belayev et al. [35] placed a cannula into the left striatum and injected 5 μ l of heparinized cardiac blood from a donor mouse. Following the injection, 7 min were given for clotting to occur, and a final injection of blood was given (10 μ l). Double injection methods, such as this one in mice, were met with great success because of their consistency. Soon after, in 2006, a triple injection method in mice was developed by Ma et al. using venous blood [36]. Two infusions of 5 μ l of blood were separated by a 7-min pause for clot formation. After the second infusion, a 1-min pause was given for additional formation, followed by a 20- μ l infusion of blood. This method also produced consistent outcomes.

In 2008, Rynkowski et al. [37] published a protocol for a modified double blood injection model in mice. In this model, 30 μ l of autologous blood from the central tail artery was injected directly into the right striatum in two steps as previously described [35]. In both the double and triple injection mouse models, potential immunoreactive blood from other mice was used, and although heparinized to minimize clot formation, it prevented proper study of pathologic processes associated with the hematoma formation.

In 1997, Choudri et al. [38] first utilized the previously established rat model for collagenase injection in mice by infusing 1 μ l of bacterial collagenase into the right basal ganglia over 4 min. This was followed by Clark et al. in 1998 [39] who performed a 2-min injection of 0.5- μ l-volume collagenase into the right caudate and globus pallidus, followed by a 3-min delay to reduce tract reflux. Additionally, Clark's group performed a 28-point neurobehavioral evaluation at 24 and 48 h. Neurobehavioral scoring has since been adopted by other groups as a way to follow functional differences with administration of various substances meant to worsen or improve the injury in ICH [6, 39, 40].

Both rats and mice have been widely used in research because of their feasibility and ease with which to anesthetize them compared to larger animals. Transgenic systems

exist primarily in mice, making this the optimal model for studying genomic effects on ICH and secondary mechanisms of injury. However, the relatively small size makes them difficult to implement techniques that are used in larger animals.

Conclusion

In this review, we looked at the three main models that have been developed to understand the physiology behind ICH – microballoon infusion, collagenase injection, and the autologous blood injection model. Additionally, we compared the various animals species that have been used to conduct these experiments, including monkeys, canines, pigs, rabbits, mice, and rats. Although there are no ideal subjects or models that can mimic the natural process in humans, each model can be used to study certain aspects of the pathophysiological process behind an ICH. In the future, the ideal ICH model should have characteristics that can model spontaneous intracerebral hemorrhage in humans and allow for effective studies on physiology, procedural interventions, and mechanisms of secondary brain injury.

Acknowledgement This study is partially supported by NIH NS053407 to J.H. Zhang and NS060936 to J. Tang.

Conflict of interest statement We declare that we have no conflict of interest.

References

- Rosenberg GA, Mun-Bryce S, Wesley M, Kornfeld M (1990) Collagenase-induced intracerebral hemorrhage in rats. *Stroke* 21:801–807
- Sinar EJ, Mendelow AD, Graham DI, Teasdale GM (1987) Experimental intracerebral hemorrhage: effects of a temporary mass lesion. *J Neurosurg* 66:568–576. doi:10.3171/jns.1987.66.4.0568
- Yang GY, Betz AL, Chenevert TL, Brunberg JA, Hoff JT (1994) Experimental intracerebral hemorrhage: relationship between brain edema, blood flow, and blood-brain barrier permeability in rats. *J Neurosurg* 81:93–102. doi:10.3171/jns.1994.81.1.0093
- Rojas H, Zhang JH (2008) Animal models of spontaneous intracerebral hemorrhage. In: Zhang JH (ed) *Advancements in neurological research*. Research SignPost, pp 39–89, ISBN:978-81-308-0225-1
- Nath FP, Jenkins A, Mendelow AD, Graham DI, Teasdale GM (1986) Early hemodynamic changes in experimental intracerebral hemorrhage. *J Neurosurg* 65:697–703. doi:10.3171/jns.1986.65.5.0697
- Wu B, Ma Q, Khatibi N, Chen W, Sozen T, Cheng O, Tang J (2010) Ac-YVAD-CMK decreases blood-brain barrier degradation by inhibiting caspase-1 activation of interleukin-1 β in intracerebral hemorrhage mouse model. *Transl Stroke Res* 1(1):57–64
- Harris ED Jr, Krane SM (1974) Collagenases (third of three parts). *N Engl J Med* 291:652–661
- Montfort I, Perez-Tamayo R (1975) The distribution of collagenase in normal rat tissues. *J Histochem Cytochem* 23:910–920
- James ML, Warner DS, Laskowitz DT (2008) Preclinical models of intracerebral hemorrhage: a translational perspective. *Neurocrit Care* 9:139–152. doi:10.1007/s12028-007-9030-2
- Andaluz N, Zuccarello M, Wagner KR (2002) Experimental animal models of intracerebral hemorrhage. *Neurosurg Clin N Am* 13:385–393
- Fujii Y (1972) Studies on induced hypothermia for open heart surgery. II. Adequate flow of hypothermic perfusion in the dog. *Nippon Geka Hokan* 41:149–159
- Kazui S, Naritomi H, Yamamoto H, Sawada T, Yamaguchi T (1996) Enlargement of spontaneous intracerebral hemorrhage. Incidence time course. *Stroke* 27:1783–1787
- Ropper AH, Zervas NT (1982) Cerebral blood flow after experimental basal ganglia hemorrhage. *Ann Neurol* 11:266–271. doi:10.1002/ana.410110306
- Bullock R, Mendelow AD, Teasdale GM, Graham DI (1984) Intracranial haemorrhage induced at arterial pressure in the rat. Part 1: description of technique, ICP changes and neuropathological findings. *Neurol Res* 6:184–188
- Deinsberger W, Vogel J, Kuschinsky W, Auer LM, Boker DK (1996) Experimental intracerebral hemorrhage: description of a double injection model in rats. *Neurol Res* 18:475–477
- Segal R, Dujovny M, Nelson D et al. (1982) Local urokinase treatment for spontaneous intracerebral hematoma. *Clin Res* 30:412A
- Bullock R, Brock-Utne J, van Dellen J, Blake G (1988) Intracerebral hemorrhage in a primate model: effect on regional cerebral blood flow. *Surg Neurol* 29:101–107
- Fujii Y, Tanaka R, Takeuchi S, Koike T, Minakawa T, Sasaki O (1994) Hematoma enlargement in spontaneous intracerebral hemorrhage. *J Neurosurg* 80:51–57. doi:10.3171/jns.1994.80.1.0051
- Whisnant JP, Sayre GP, Millikan CH (1963) Experimental intracerebral hematoma. *Arch Neurol* 9(6):586–592
- Sugi T, Fujishima M, Omae T (1975) Lactate and pyruvate concentrations, and acid-base balance of cerebrospinal fluid in experimentally induced intracerebral and subarachnoid hemorrhage in dogs. *Stroke* 6:715–719
- Qureshi AI, Wilson DA, Hanley DF, Traystman RJ (1999) No evidence for an ischemic penumbra in massive experimental intracerebral hemorrhage. *Neurology* 52:266–272
- Qureshi AI, Wilson DA, Traystman RJ (1999) Treatment of elevated intracranial pressure in experimental intracerebral hemorrhage: comparison between mannitol and hypertonic saline. *Neurosurgery* 44:1055–1063, discussion 1063–1054
- Lee EJ, Hung YC, Lee MY (1999) Anemic hypoxia in moderate intracerebral hemorrhage: the alterations of cerebral hemodynamics and brain metabolism. *J Neurol Sci* 164:117–123. doi:S0022-510X(99)00068-4 [pii]
- Takasugi S, Ueda S, Matsumoto K (1985) Chronological changes in spontaneous intracerebral hematoma – an experimental and clinical study. *Stroke* 16:651–658
- Wagner KR, Xi G, Hua Y, Kleinholz M, de Courten-Myers GM, Myers RE, Broderick JP, Brott TG (1996) Lobar intracerebral hemorrhage model in pigs: rapid edema development in perihematomal white matter. *Stroke* 27:490–497
- Kuker W, Thiex R, Rohde I, Rohde V, Thron A (2000) Experimental acute intracerebral hemorrhage. Value of MR sequences for a safe diagnosis at 1.5 and 0.5 T. *Acta Radiol* 41:544–552
- Mun-Bryce S, Wilkerson AC, Papuashvili N, Okada YC (2001) Recurring episodes of spreading depression are spontaneously elicited by an intracerebral hemorrhage in the swine. *Brain Res* 888:248–255. doi:S0006-8993(00)03068-7 [pii]
- Kaufman HH, Pruessner JL, Bernstein DP, Borit A, Ostrow PT, Cahall DL (1985) A rabbit model of intracerebral hematoma. *Acta Neuropathol* 65:318–321

29. Koeppen AH, Dickson AC, McEvoy JA (1995) The cellular reactions to experimental intracerebral hemorrhage. *J Neurol Sci* 134(Suppl):102–112. doi:0022510X9500215N [pii]
30. Qureshi AI, Ling GS, Khan J, Suri MF, Miskolczi L, Guterman LR, Hopkins LN (2001) Quantitative analysis of injured, necrotic, and apoptotic cells in a new experimental model of intracerebral hemorrhage. *Crit Care Med* 29:152–157
31. Gustafsson O, Rossitti S, Ericsson A, Raininko R (1999) MR imaging of experimentally induced intracranial hemorrhage in rabbits during the first 6 hours. *Acta Radiol* 40:360–368
32. Rohde V, Rohde I, Thix R, Ince A, Jung A, Duckers G, Groschel K, Rottger C, Kuker W, Muller HD, Gilsbach JM (2002) Fibrinolysis therapy achieved with tissue plasminogen activator and aspiration of the liquefied clot after experimental intracerebral hemorrhage: rapid reduction in hematoma volume but intensification of delayed edema formation. *J Neurosurg* 97:954–962. doi:10.3171/jns.2002.97.4.0954
33. Masuda T, Dohrmann GJ, Kwaan HC, Erickson RK, Wollman RL (1988) Fibrinolytic activity in experimental intracerebral hematoma. *J Neurosurg* 68:274–278. doi:10.3171/jns.1988.68.2.0274
34. Nakamura T, Xi G, Hua Y, Schallert T, Hoff JT, Keep RF (2004) Intracerebral hemorrhage in mice: model characterization and application for genetically modified mice. *J Cereb Blood Flow Metab* 24:487–494. doi:00004647-200405000-00002 [pii]
35. Belayev L, Saul I, Curbelo K, Busto R, Belayev A, Zhang Y, Riyamongkol P, Zhao W, Ginsberg MD (2003) Experimental intracerebral hemorrhage in the mouse: histological, behavioral, and hemodynamic characterization of a double-injection model. *Stroke* 34:2221–2227. doi:10.1161/01.STR.0000088061.06656.1E
36. Ma B, Zhang J (2006) Nimodipine treatment to assess a modified mouse model of intracerebral hemorrhage. *Brain Res* 1078:182–188. doi:S0006-8993(06)00158-2 [pii]
37. Rynkowski MA, Kim GH, Komotar RJ, Otten ML, Ducruet AF, Zacharia BE, Kellner CP, Hahn DK, Merkow MB, Garrett MC, Starke RM, Cho BM, Sosunov SA, Connolly ES (2008) A mouse model of intracerebral hemorrhage using autologous blood infusion. *Nat Protoc* 3:122–128. doi:nprot.2007.513 [pii]
38. Choudhri TF, Hoh BL, Solomon RA, Connolly ES Jr, Pinsky DJ (1997) Use of a spectrophotometric hemoglobin assay to objectively quantify intracerebral hemorrhage in mice. *Stroke* 28:2296–2302
39. Clark W, Gunion-Rinker L, Lessov N, Hazel K (1998) Citicoline treatment for experimental intracerebral hemorrhage in mice. *Stroke* 29:2136–2140
40. Thix R, Mayfrank L, Rohde V, Gilsbach JM, Tsirka SA (2004) The role of endogenous versus exogenous tPA on edema formation in murine ICH. *Exp Neurol* 189:25–32. doi:10.1016/j.expneurol.2004.05.021

Comparison of Different Preclinical Models of Intracerebral Hemorrhage

Anatol Manaenko, Hank Chen, John H. Zhang, and Jiping Tang

Abstract Intracerebral hemorrhage (ICH) is the most devastating type of stroke. It is characterized by spontaneous bleeding in brain parenchyma and is associated with a high rate of morbidity and mortality. Presently, there is neither an effective therapy to increase survival after intracerebral hemorrhage nor a treatment to improve the quality of life for survivors. A reproducible animal model of spontaneous ICH mimicking the development of acute and delayed brain injury after ICH is an invaluable tool for improving our understanding of the underlying mechanisms of ICH-induced brain injury and evaluating potential therapeutic interventions. A number of models have been developed. While different species have been studied, rodents have become the most popular and widely utilized animals used in ICH research. The most often used methods for experimental induction of ICH are injection of bacterial collagenase and direct injection of blood into the brain parenchyma. The “balloon” method has also been used to mimic ICH for study. In this summary, we intend to provide a comparative overview of the technical methods, aspects, and pathologic findings of these types of ICH models. We will also focus on the similarities and differences among these rodent models, achievements in technical aspects of the ICH model, and discuss important aspects in selecting relevant models for study.

Keywords Animal model · ICH · Intracerebral hemorrhage · Stroke · Rat · Mouse · Rodent

A. Manaenko, H. Chen, J.H. Zhang, and J. Tang (✉)
Department of Physiology and Pharmacology,
Loma Linda University, School of Medicine, Risley Hall,
Room 219, Loma Linda, CA 92350, USA
e-mail: jtang@llu.edu

Introduction

Intracerebral hemorrhage (ICH) is a devastating disease accounting for approximately 5–15% of all types of stroke. In the United States, as many as 50,000 individuals are affected annually with a large number of those individuals facing chronic morbidities and early mortalities. ICH is more than twice as common as subarachnoid hemorrhage (SAH); it results in more disability and death than SAH or ischemic stroke [1]. Currently, there is neither an effective therapy to increase survival after intracerebral hemorrhage nor a treatment to improve the quality of life for survivors [2]. For improvement of existing therapies and development of new ones, an animal model that mimics the clinical situation and effects of intracerebral hemorrhage as closely as possible is absolutely essential.

The effects of intracerebral hemorrhage upon brain tissue are biphasic. Initial injury occurs in response to the expanding hematoma imposing shear force and mass effect upon the cerebral tissues [3]. Intracerebral bleeding leads to increased intracranial pressure, which could lead to transtentorial herniation secondary to the resulting mass effect [4]. A later phase involves multiple “toxic” factors present in activated blood components [5], infiltration of the brain by systemic immunocells [6], activation of microglia [7], and hematoma-induced apoptotic death of neuronal and glial cells in the surrounding parenchymal rim [8] followed by progressive rupture of the blood-brain barrier and rising brain edema [9].

In creating a model, it should be kept in mind that although in most patients’ bleeding stops soon after ictus, secondary bleeding is often observed. Fuji et al. reported that hematoma extension happens in 14% of patients in the first 24 h after ICH [10]. Similarly, Kazui et al. observed hematoma enlargement in 17% of patients during the first 6 h and in 22% of patients during first 24 h after ICH onset [11]. In this review, we will describe the most common models of ICH. Because rodents are the most used experimental animals in ICH models, we will concentrate on technique details of ICH induction in those species and compare the technical and pathological advantages and short-term outcomes of the existing models.

Single Blood Injection

The most straightforward method for the introduction of blood and hematoma formation in the brain is singular injection. In rodents, blood injection was first used by Ropper et al. in 1982 [12]. The authors used Sprague-Dawley rats as experimental subjects. They permanently implanted a 27-gauge needle in the right basal ganglia, allowed the animals to awake, and infused 0.24–0.28 ml of whole or centrifuged blood from another rat, without anesthesia, over 1 s. In the control animals, they inserted plastic polymer. Two out of their eight subjects died. The authors reported early and delayed hyperperfusion of one or both cortical regions of brain. Comparison between ICH and control animals demonstrated that the subsequent effects were caused by blood and not by mass effect. One clear advantage of this model is that it does not require use of anesthetized animals. There are several shortcomings in this model. By using donor blood, there is always a risk of inflammatory reaction not typically seen in the clinical setting. Also, blood infusion was done not under arterial blood pressure. It does not mimic the clinical situation seen in humans.

To overcome this disadvantage, Bullock et al. presented another model of ICH 2 years later. They stereotactically inserted a needle filled with non-heparinized blood and connected it via a catheter to the femoral artery. As soon as the needle was inserted, the catheter was opened, and blood flowed until arrested spontaneously. A disadvantage of this model is that it is not well reproducible. Blood pressure variations from animal to animal were considered to have resulted in the observed variation in injury volumes. The authors reported a variation in hemorrhage sizes ranging between 6% and 43%.

Nath and coauthors tried to improve the model to make it more reproducible by producing hemorrhage via the pumping of a predetermined amount of whole blood [13]. They withdrew arterial blood and placed this blood into a 25- μ L tube, which they connected to a no. 25 needle. The infusion system was filled prior to needle placement. They used a constant pressure reservoir set to 100 mmHg. Blood was injected over approximately 10 s. To avoid blood clotting, the injection was performed within 2.5 min after withdrawal. The authors injected 25, 50, or 100 μ L of blood, and did not observe any relationship between the volume of hemorrhage and the degree of resultant hematoma.

A similar technique was presented by Yang et al. in 1994 [14]. However, this group instead used a constant pressure reservoir and micropump. They withdrew autologous blood from the femoral artery into a syringe of 1 mL, mounted it immediately to an infusion pump, and then infused 100 μ L of blood. They then placed the glue around the hole and quickly removed the needle. The needle was introduced vertically. (One modification of this technique is the introduction of the

needle at an angle of 20° to help avoid disruption of blood in the vertical space [15]). Although Yang and coauthors injected a predetermined amount of blood, this model failed to reproduce the dynamic interplay between systemic arterial pressure and brain tissue resistance [14].

In general, all models produced one solid hematoma noted to occur in up to 50% of patients in a clinical setting, as well as mimic the mass effect of a hematoma and reproduce the toxic effects of blood elements, but these characteristics are not well reproducible. The success rate in lesion production is low, and ruptures in the ventricular and subdural spaces have been noted. Bullock discussed 70.8% success after they operated on 24 animals and observed rupture into the ventricular space in 4 and into the subdural space in 3 [16]. Nath et al. indicated that the hematomas produced varied in size and shape, and often in addition to the intracerebral clot there was some surface collection [13]. Yang did not mention success rates in his publication [14]. Masuda failed to produce hematomas in 7% and mentioned that in most cases some extension into the ventricular system was observed [17].

To overcome these disadvantages, two other models were developed: the microballoon and multiple blood injection models. To improve upon the blood injection model, Deinsberger presented the double injection model in 1996 [18]. They figured out that the most adequate total hematoma volume is 50 μ L and separated the blood into two parts. First they injected 15 μ L of blood and waited 7 min for the building of the blood clot along the needle. Then they injected the major volume of blood: 35 μ L. The model was successful. This technique led to hematomas consisting of a clot in the caudate nucleus linked to a thin elongated clot in the white matter by a small clot along the needle track. Only one animal out of 13 had an extension of hematoma into the subdural space.

This technique is widely used and was adapted to mice, too. Belayev et al. in 2003 used mice, which is more challenging because of the smaller sizes [3]. The authors used a 30-gauge stainless steel cannula. Each mouse received a 5- μ L injection of either whole blood or CSF over 3 min, followed 7 min later by 10 μ L injected over 5 min with a microinfusion pump. Sham animals received just needle trauma. Blood was taken from the heart of a donor mouse, which was flushed with heparin before blood withdrawal. The injection cannula was slowly withdrawn 10 min after the second injection, and the wound was sutured. The authors evaluated the neurological deficit 60 min after blood injection and determined that the animals after blood, but not after CSF and only needle trauma developed significant neurological deficits. Histological examination of the brain after 48-h survival revealed the presence of a localized hematoma in all animals with blood infusion. The measured hematoma volume in the blood injection group was highly reproducible. In contrast, the CSF and cannula groups showed only a small

non-hemorrhagic lesion. Residual swelling of the ipsilateral hemisphere at 48 h was 5.7% in hematoma mice and 1.5% in the CSF group.

Further improvement of the model was done by Ma et al. in 2006 [20]. They developed a triple injection model. The blood was rapidly taken from the orbital veins (not from the heart as Belayev did [19]) of a donor mouse using a glass capillary. During the ICH process, the injection was paused for 7 min after the first 5 μ l (to generate a clotting along the needle track), then paused for 1 min after the second 5 μ l (important to reinforce the clotting), and the remaining 20 μ l was injected in the following 4 min. Sham animals were subjected to the same manipulations as the ICH mice, but no blood was injected.

Microballoon-Induced Formation of ICH

Microballoon insertion was developed by Sinar and coauthors in 1987 as a way to study the mass effects of ICH [21]. A microballoon was mounted on a no. 25 blunted needle and inserted stereotaxically into the right caudate nucleus. The burr hole was then sealed with dental cement. After a 30-min stabilization period, the balloon was inflated to 50 μ l over a period of 20 s with radiopaque contrast medium. In the sham-treated control group, the balloon was inserted but not inflated. Brain edema formation was successfully produced, much as occurs in the presence of any intracerebral mass, but the potentially significant effects of the presence of blood and clot in ICH cannot be addressed by this method.

Microballoon insertion alone can only demonstrate the mass effects of an introduced volume. This model does not reproduce such factors as the toxicity of blood elements and blood brain barrier disruption. While one can use this model for evaluation of the potential benefits of surgical hematoma evacuation, even in this kind of experiment there is a limitation. This model does not mimic the surgical brain injury caused by hematoma evacuation.

Collagenase Injection

Hematoma expansion and vasogenic edema following ICH has been considered to result from elevated local concentrations of collagenase released from injured cells [1] following tissue injury [10, 11]. From this concept, models for study of spontaneous ICH were developed using collagenase. Rosenberg et al. used microinfusion pumps to deliver 2- μ l volumes of 0.01–0.1 units of bacterial collagenase into the left caudate nucleus over a 9-min period [22]. Initial bleeding could be seen as early as 10 min after collagenase injection.

Different authors observed the expansion of hematoma at 1 and 4 h [22, 23]. However, in 1995 Brown et al. noted the presence of fresh blood much later as well [24].

Choudri performed collagenase injection in mice via 4-min infusion of bacterial collagenase into the right basal ganglia [25]. Clark performed a 2-min, 0.5- μ l injection into the right caudate and globus pallidus of mouse subjects, with a 3-min pause after the injection to minimize pathway reflux [26]. Later studies have shown similar adjustments in injection parameters [7], often raising the needle-withdrawal delay and the infusion course. Such adjustments to procedural parameters may improve the accuracy and precision of this model. In addition to the achievement of greater injury from the generation of a spontaneous ICH in this model, a key point is that the histological changes observed in the brain after collagenase injection have been consistent with the changes noted in human brain tissue after ICH [27]. The model does not involve the handling of blood products and the associated technical complications. This model allowed for successful evaluation of intracerebral hemorrhage, edema formation, and histological changes resulting from the spontaneous hemorrhages that followed infusion [22]. This model mimics spontaneous ICH.

However, studies have used collagenase levels significantly greater than the levels of endogenous collagenase in clinical ICH, which may not allow this model to faithfully emulate the pathologic alterations involved in ICH in the clinical setting. The disadvantages of this model are related to bacterial collagenase's ability to introduce a significant inflammatory reaction. Moreover, in opposition to the ICH in patients where the solid hematoma is a result of bleeding from the arterial source in brain tissue, bleeding in the collagenase model is diffuse and results from rupture of small blood vessels around the site of collagenase injection.

Comparison of the Collagenase and Blood Models

Hematoma Size

Direct comparison of the collagenase and blood injection models was performed by MacLellan and coauthors [23]. The authors used the previously described model of blood injection used in rats [16]. They took 100 μ l of blood from the tail (it was not clearly established whether the blood was venous or arterial). They then injected the withdrawn blood over 10 min into the striatum through a small burr hole made 3.5 mm to the right of and at the anteroposterior level of the bregma to a depth of 6.0 mm. The authors then used the same coordinates to administer an injection of 0.2 U of

bacterial collagenase in 1.0 μl sterile saline (as described [28]). They performed a hemoglobin assay to compare the hematomas produced by injection of collagenase with that produced following direct injection of 100 μl of blood directly into the striatum. One hour after the operation, the hematomas of both models were comparable (approximately 65 μl in the blood infusion model versus 50 μl in the collagenase model). The hematoma in the blood injection model remained stable during the first 4 h. Well in agreement with a previous publication [24], MacLellan observed a significant increase in hematoma size within this time period in the collagenase model.

Hematoma size and lesion volume were evaluated at later time points using magnetic resonance imaging (MRI). From the imaging the authors [23] concluded that, despite similar initial hematoma volumes measured by using hemoglobin assay at 4 h, the injury observed between 4 and 6 weeks was greater in the collagenase model. The authors explained that as opposed to the blood model (in which the blood remains pooled), blood in the collagenase model diffuses from the hemorrhage site into the parenchyma. They also conclude that the hematoma observed in the blood model resolved more quickly in comparison with that seen in the collagenase model.

Functional Outcome

Functional outcomes were evaluated using a neurological deficit scale as described previously [29]. They established a baseline by testing the animals prior to ICH and continued evaluation through 28 days after induction of ICH. While on day 1 the hematoma volumes in both models were comparable, neurological evaluation revealed significant aggravation of the neurological deficits in the collagenase versus blood injection subjects. Complete recovery was observed in the blood infusion model at day 21. From this time point onward, no recovery was noted to occur in the collagenase model.

Takamatsu et al. noted the lack of spontaneous recovery in the collagenase model of ICH [30]. Takamatsu evaluated neurological motor deficits using four tests from days 1 after ICH induction. In contrast to MacLellan's group who tested for 28 days, Takamatsu performed neurological testing up to a maximum of 15 days, and did not observe improvement of neurological deficits between days 10 and 15, which leads to the conclusion that there is no spontaneous recovery in that model [30]. Kim et al. performed testing for 35 days after collagenase injection and reported about the lack of spontaneous recovery even up to day 35 [31]. Beray-Berthat et al. extended the time of observation after collagenase-induced ICH up to 56 days. They used five different neurological

tests and reported that they revealed long-term deficits at up to 2 months following ICH [32].

In contrast, Karki et al. induced ICH by infusion of 100 μl of nonheparinized autologous whole blood into the right striatum adjacent to the SVZ (exact coordinates undisclosed). Karki assessed the functional outcome using the neurological severity score between day 1 and day 28, and found partial recovery [33]. Similar results were observed using the "corner test" (common for evaluation of neurological deficits, by measuring the number of times an animal turns to the right or left after placement in a corner). Grasso et al. injected 100 μl of autologous whole blood under stereotactic guidance into the right basal ganglia, and evaluated for neurological deficits using a neurologic symptom score and the "corner test" at days 1, 7 and 14. The authors did not observe spontaneous recovery in neurological scoring and noted only slight recovery in the corner test [34]. Yang et al. injected 100 μl of nonheparinized autologous blood stereotactically and evaluated for neurological deficits at days 1, 4, 7, and 14 using the neurological severity score and corner test. They demonstrated a time-dependent resolution of the neurological deficit. Even if on the last day of observation deficits were still present, this time-dependent resolution suggests that complete spontaneous recovery is possible [14]. Similar results were presented by Seyfried et al., who injected 100 μl of blood stereotactically and evaluated for neurological deficits through severity scoring and corner test at days 1, 7, and 14. The authors observed a clear time-dependent resolution of neurological deficits in both tests [35].

It appears that the injection of collagenase causes severe injury with persistent neurological deficits without spontaneous recovery, similar to that observed in the clinical setting. Because spontaneous recovery in this model is possible, the value of the blood injection model for long-term study may be limited. MacLellan et al. [20] pointed out that because of the described differences between the models, it is valuable to utilize both models in testing for the potential beneficial effects of therapeutics.

Blood-Brain Barrier

MacLellan et al. also evaluated time-dependent development of blood-brain-barrier disruption by using MRI in both induction models. They reported that at all tested time points (12 h, 2 and 4 days), disruption of the blood-brain barrier caused by collagenase injection was significantly higher in comparison with the blood model. The authors observed a time-dependent increase in blood-brain barrier permeability in the collagenase model, but not in the in blood model of induction [23].

Knight et al. observed only small increases in blood-brain barrier permeability in the surrounding rim of the hematoma 1 day after injection of 100 μ l autologous blood. This parameter remained slightly elevated through day 14, where the authors observed decreases in permeability at the rim area [36]. In the collagenase model, Rosenberg et al. investigated the blood-brain barrier disruption via another method, measurement of [14C]-sucrose uptake in the brain from the blood. The blood-brain barrier in the collagenase model was noted to be open 30 min after ICH induction. [14C]-Sucrose uptake in the brain tissue was noted to stay significantly elevated for 7 days [37]. Taken together, it seems that the damage caused by ICH induction via blood injection is moderate when compared with the outcomes from collagenase injection.

Cell Death

Because infiltration of brain parenchyma with immunologic cells such as neutrophils is considered to be a significant mechanism leading to cell death [7], there was a study directly comparing brain injury in the collagenase and blood models of ICH [38]. The authors compared the inflammatory reactions and cell death following collagenase versus blood injection in the brains of rats. The authors first collected mixed (arterial and venous) blood by cutting the tip of the tail, then injected that blood or 0.4 U of collagenase following coordinates similar to those used by MacLellan [33] (3 mm lateral to the midline, 0.02 mm anterior to the coronal suture, 5.5 mm below the surface of the skull). The authors reported that neutrophil infiltration of the striatal or cortical tissue around the hematoma was observed at 1 day in both models. However, only in the collagenase model was there a significant difference at this time point compared with the other observed time point. The neutrophils were almost completely diminished in number at day 3 in the blood model and still present in the collagenase model.

Similar temporal patterns of neutrophil infiltration have been observed by other authors. Pelling et al. observed significant neutrophil infiltration at day 2 after collagenase-induced ICH [9]. Wang observed neutrophil infiltration at day 1 and 3 in the same model [39]. MacLellan et al. reported significant neutrophil infiltration at day 4 after collagenase injection [40]. In the blood model Gong et al. also observed peak neutrophil infiltration on day 1. While neutrophils were still present at day 3, at later time points (at day 7 and 10), the authors observed a marked decrease in the number of neutrophils present [41].

Xue et al. [38]. investigated the number of dying neurons (identified by cytoplasmic pyknosis or eosinophilia) in both models. They reported that the number of dying neurons in

the penumbra peaked at day 2 in both models. But the measured differences between day 2 and the other evaluated time points (1 and 4 h; 1, 2, 3, 7, and 21 days) were significant only in the collagenase model. Dying neurons were observed through day 7 in the blood model and through day 21 in the collagenase model.

Conclusion

In conclusion we can say that the blood injection and collagenase models are technically similar. They are easy to perform and are reproducible; the size of hematoma in these two models is well controllable. The location of hematoma formation is easier to control in the collagenase model. Since in the blood model the amount of liquid injected into the brain is significantly higher, there is always a risk of blood disruption in the subarachnoid and ventricular spaces. The collagenase model mimics the time-dependent extension of the hematoma, which has been observed in a relatively small portion of patients. Damage caused by comparable initial hematoma was significantly higher in the collagenase model subjects. Damage resulted in extension of the hematoma over time, with greater tissue and neuron loss, greater BBB disruption, and lack of spontaneous neurological recovery in animals after collagenase compared to blood injection.

Acknowledgement This study was partially supported by NIH NS053407 to J.H. Zhang and NS060936 to J. Tang.

Conflict of interest statement We declare that we have no conflict of interest.

References

1. Woo D, Broderick J (2002) Spontaneous intracerebral hemorrhage: epidemiology and clinical presentation. *Neurosurg Clin N Am* 13: 265–279
2. D'Ambrosio A, Sughrue ME, Yorgason J, Mocco J, Kreiter K, Mayer S, McKhann G, Connolly E (2005) Decompressive hemicraniectomy for poor-grade aneurysmal subarachnoid hemorrhage patients with associated intracerebral hemorrhage: clinical outcome and quality of life assessment. *Neurosurgery* 56:12–19
3. Aronowski J, Hall C (2005) New horizons for primary intracerebral hemorrhage treatment: experience from preclinical studies. *Neurol Res* 27:268–279
4. Badjatia N, Rosand J (2005) Intracerebral hemorrhage. *Neurologist* 11:311–324
5. Xi G, Keep RF, Hoff JT (1998) Erythrocytes and delayed brain edema formation following intracerebral hemorrhage in rats. *J Neurosurg* 89:991–996
6. Xue M, Del Bigio M (2003) Comparison of brain cell death and inflammatory reaction in three models of intracerebral hemorrhage in adult rats. *J Stroke Cerebrovasc Dis* 12(3):152–159

7. Wang J, Tsirka SE (2005) Tuftsin fragment 1–3 is beneficial when delivered after the induction of intracerebral hemorrhage. *Stroke* 36(3):613–618
8. Felberg R, Grotta C, Shirzadi A, Strong R, Narayana P, Hill-Felberg S, Aronowski J (2002) Cell death in experimental intracerebral hemorrhage: the “black hole” model of hemorrhagic damage. *Ann Neurol* 51:517–524
9. Qureshi A, Ling G, Khan J, Suri M, Misholczi L, Guterman L, Hopkins L (2001) Quantitative analysis of injured, necrotic, and apoptotic cells in a new experimental model of intracerebral hemorrhage. *Crit Care Med* 29:152–157
10. Fujii Y, Takeuchi S, Sasaki O, Minakawa T, Tanaka R (1998) Multivariate analysis of predictors of hematoma enlargement in spontaneous intracerebral hemorrhage. *Stroke* 29:1160–1166
11. Kazui S, Naritomi H, Yamamoto H, Sawada T, Yamaguchi T (1996) Enlargement of spontaneous intracerebral hemorrhage. Incidence time course. *Stroke* 27:1783–1787
12. Rosenberg GA, Mun-Bryce S, Wesley M, Kornfeld M (1990) Collagenase-induced intracerebral hemorrhage in rats. *Stroke* 21:801–807
13. Peeling J, Yan H-J, Corbett D, Xue M, Del Bigio MR (2001) Effect of FK-506 on inflammation and behavioral outcome following intracerebral hemorrhage in rat. *Exp Neurol* 167:341–347
14. Yang D, Knight RA, Han Y, Karki K, Zhang J, Ding C, Chopp M, Seyfried DM (2011). Vascular recovery promoted by atorvastatin and simvastatin after experimental intracerebral hemorrhage: magnetic resonance imaging and histological study. *J Neurosurg* 114:1135–1142
15. Kim J-M, Lee S-T, Ch K, Jung K-H, Song E-C, Kim S-J, Sinn D-I, Kim S-E, Park D-K, Kang K-M, Hong NH, Park H-K, Won C-H, Kim K-H, Kim M, Lee SK, Roh J-K (2007) Systemic transplantation of human adipose stem cells attenuated cerebral inflammation and degeneration in a hemorrhagic stroke model. *Brain Res* 1183:43–50
16. Bullock R, Mendelow AD, Teasdale GM, Graham DI (1984) Intracranial haemorrhage induced at arterial pressure in the rat. Part 1: description of technique, ICP changes and neuropathological findings. *Neurol Res* 6:184–188
17. Nath FP, Jenkins A, Mendelow AD, Graham DI, Teasdale GM (1986) Early hemodynamic changes in experimental intracerebral hemorrhage. *J Neurosurg* 65:697–703
18. Deinsberger W, Vogel J, Kuschinsky W, Auer LM, Boker DK (1996) Experimental intracerebral hemorrhage: description of a double injection model in rats. *Neurol Res* 18:475–477
19. Belayev L, Saul I, Curbelo K, Busto R, Belayev A, Zhang Y, Riyamongkol P, Zhao W, Ginsberg MD (2003) Experimental intracerebral hemorrhage in the mouse: histological, behavioral, and hemodynamic characterization of a double-injection model. *Stroke* 34:2221–2227
20. MacLellan C, Silasi G, Poon G, Edmundson C, Buist R, Peeling J, Colbourne F (2008) Intracerebral hemorrhage models in rat: comparing collagenase to blood infusion. *J Cereb Blood Flow Metab* 28:516–522
21. Takamatsu Y, Ishida A, Hamakawa M, Tamakoshi K, Jung G, Ishida K (2010) Treadmill running improves motor function and alters dendritic morphology in the striatum after collagenase-induced intracerebral hemorrhage in rats. *Brain Res* 1355:165–173
22. Rosenberg GA, Estrada E, Kelley RO, Kornfeld M (1993) Bacterial collagenase disrupts extracellular matrix and opens blood-brain barrier in rat. *Neurosci Lett* 160(1):117–119
23. MacLellan CL, Davies LM, Fingas MS, Colbourne F (2006) Influence of hypothermia on outcome after intracerebral hemorrhage in rats. *Stroke* 37:1266–1270
24. Brown M, Kornfeld M, Mun-Bryce S, Sibbitt R, Rosenberg G (1995) Comparison of magnetic resonance imaging and histology in collagenase-induced hemorrhage in the rat. *J Neuroimaging* 5(1):34
25. Choudhri TF, Hoh BL, Solomon RA, Connolly ES Jr, Pinsky DJ (1997) Use of a spectrophotometric hemoglobin assay to objectively quantify intracerebral hemorrhage in mice. *Stroke* 28:2296–2302
26. Clark W, Gunion-Rinker L, Lessov N, Hazel K (1998) Citicoline treatment for experimental intracerebral hemorrhage in mice. *Stroke* 29:2136–2140
27. Del Bigio MR, Yan HJ, Buist R, Peeling J (1996) Experimental intracerebral hemorrhage in rats. Magnetic resonance imaging and histopathological correlates. *Stroke* 27:2312–2319, discussion 2319–2320
28. Ropper AH, Zervas NT (1982) Cerebral blood flow after experimental basal ganglia hemorrhage. *Ann Neurol* 11:266–271
29. Masuda T, Dohrmann GJ, Kwaan HC, Erickson RK, Wollman RL (1988) Fibrinolytic activity in experimental intracerebral hematoma. *J Neurosurg* 68:274–278. doi:10.3171/jns.1988.68.2.0274
30. Wang J, Fields J, Zhao C, Langer J, Thimmulappa RK, Kensler TW, Yamamoto M, Biswal S, Dore S (2007) Role of Nrf2 in protection against intracerebral hemorrhage injury in mice. *Free Radic Biol Med* 43:408–414
31. Knight RA, Han Y, Nagaraja TN, Whitton P, Ding J, Chopp M, Seyfried DM (2008) Temporal MRI assessment of intracerebral hemorrhage in rats. *Stroke* 39:2596–2602
32. Beray-Berthet V, Delifer C, Besson VC, Girgis H, Coqueran B, Plotkine M, Marchand-Leroux C, Margail I (2010) Long-term histological and behavioural characterisation of a collagenase-induced model of intracerebral haemorrhage in rats. *J Neurosci Meth* 191:180–190
33. Karki K, Knight RA, Han Y, Yang D, Zhang J, Ledbetter KA, Chopp M, Seyfried DM (2009) Simvastatin and atorvastatin improve neurological outcome after experimental intracerebral hemorrhage stroke. *Stroke* 40:3384–3389
34. Grasso G, Graziano F, Sfacteria A, Carletti F, Meli F, Maugeri R, Passalacqua M, Certo F, Fazio M, Buemi M, Iacopino DG (2009) Neuroprotective effect erythropoietin darbepoetin alfa after experimental intracerebral hemorrhage. *Neurosurg* 65(4):763–769
35. Sinar EJ, Mendelow AD, Graham DI, Teasdale GM (1987) Experimental intracerebral hemorrhage: effects of a temporary mass lesion. *J Neurosurg* 66:568–576
36. Ma B, Zhang J (2006) Nimodipine treatment to assess a modified mouse model of intracerebral hemorrhage. *Brain Res* 1078:182–188
37. Seyfried DM, Han Y, Yang D, Ding J, Shen LH, Savant-Bhonsale S, Chopp M (2010) Localization of bone marrow stromal cells to the injury site after intracerebral hemorrhage rats. *J Neurosurg* 112:329–335
38. Xue M, Del Bigio MR (2000) Intracerebral injection of autologous whole blood in rats: time course of inflammation and cell death. *Neurosci Lett* 283:230–232
39. Weiss SJ (1989) Tissue destruction by neutrophils. *N Engl J Med* 320:365–376
40. MacLellan CL, Auriat A, McGie SC, Yan RH, Huynh HD, De Butte MF, Colbourne F (2006) Gauging recovery after hemorrhagic stroke in rats: implications for cytoprotection studies. *J Cereb Blood Flow Metab* 26:1031–1042
41. Gong C, Hoff JT, Keep RF (2000) Acute inflammatory reaction following experimental intracerebral hemorrhage rat. *Brain Res* 871:57–65

Cerebral Amyloid Angiopathy-Related Microhemorrhages in Alzheimer's Disease: A Review of Investigative Animal Models

Hank Chen and John H. Zhang

Abstract There is a growing understanding of cerebral amyloid angiopathy (CAA), which accounts for the majority of primary lobal intracerebral hemorrhages (ICH) among the elderly [1] and is cited as the cause of 20% of spontaneous ICHs in patients over 70 years of age [2]. The basis for this disease process is the deposition and formation of eventually destructive amyloid plaques in the walls of brain vessels, predominantly arterial but not excluding venules and capillaries [3]. Investigation of the pathophysiology and therapies for CAA-associated hemorrhages have been made possible through animal models utilizing species that develop CAA in a similar fashion to humans, such as the squirrel monkey, rhesus monkey, dog and mutant and transgenic mouse strains, which exhibit the age-related development of amyloid plaques, progressive neurodegeneration and CAA-associated hemorrhages. The disease course in these animal models resembles that seen in the clinical setting for patients with CAA. Rodent studies have been able to demonstrate the strong role of CAA and CAA-associated microhemorrhages in the pathogenesis and progression of CAA with and without AD [4]. This review will present the existing understanding of CAA-associated microhemorrhages frequently observed in AD, different animal models, involved imaging and the role of animal models in the development of therapeutics including immunotherapies such as anti-A β antibodies for the treatment of CAA and its associated microhemorrhages.

Keywords Alzheimer's disease · Amyloid · Angiopathy · Intracerebral · Microhemorrhage · Stroke · Animal model · Mouse · Rat

H. Chen and J.H. Zhang (✉)
Department of Physiology and Pharmacology,
Loma Linda University, School of Medicine,
Risley Hall, Room 219, Loma Linda, CA 92350, USA
e-mail: jhzhang@llu.edu

CAA-Associated Microhemorrhages

Cerebral amyloid angiopathy (CAA) is regarded as a clinical high-risk factor for spontaneous intracerebral hemorrhage and lobar hemorrhage [5], predominantly in the temporal and occipital lobes [6]. The principle form of cerebral amyloid found in the aging human brain and Alzheimer's disease (AD) is β -amyloid (A β), a cleavage product of the acute phase reactant amyloid- β precursor protein (A β PP). Deposition of neuron-derived A β onto vascular smooth muscle cells in blood vessel walls leads to thinning and degradation of the tunica media [7], with development of vasculitis, aneurysm-like vasodilatation, fibrinoid necrosis and eventual vessel disruption [7]. A β PP/A β aggregates have been cited to function as a potentially important anticoagulant and vascular sealant in vessel injury [8], which becomes important when addressing potential therapies to remove the A β deposits leading to microhemorrhage and central to the progressive neurodegeneration in AD [9].

Non-Human Primate Model

CAA has been found to occur in non-human primates ranging from lemurs to chimpanzees. The most studied of these are the rhesus macaque and squirrel monkey, showing similarities between CAA in humans and non-human primates: age-related increases in frequency and severity of CAA, preferential deposition in the neocortex and independence of CAA from amyloid plaque formation. While the strongest genetic relationship is shared by humans and other primates, extensive specific study of CAA-related microhemorrhages has not been pursued in this animal group, possibly because of the great cost and significant complexity of the management, handling and procedural requirements involved in primate research [4].

Murine Model

Cerebral deposition of amyloid in plaques and vessels has been consistently observed in mutated and transgenic mouse strains. Such strains have been a popular choice for the study of CAA-related hemorrhages. In the APPDutch mutant, PDAPP, TG2576 (APP^{sw}) and APP23-transgenic mouse strains, CAA has been demonstrated to consistently lead to multiple and recurrent spontaneous cerebral hemorrhages [10]. As in humans, an age-related increase in the frequency and severity of CAA exists, there is predominant involvement of the neocortex, and the development of CAA appears to be independent from formation of amyloid plaques [11, 12]. Findings have suggested the involvement of molecular processes such as MMP-9 induction and degradation of the extracellular matrix (ECM) [13], and processes such as the perivascular microglial activation noted in APP Dutch mice can be further studied together with functional outcomes after CAA-related hemorrhage by utilizing these mouse strains exhibiting spontaneous intracerebral microhemorrhages [14]. The presence of apoE was found to be critical to the development of CAA-associated microhemorrhages in transgenic mouse strains, noting a statistically significant reduction in CAA and microhemorrhage events in the strains lacking apoE [15].

Canine Model

CAA occurs naturally in canines, with canine A β being structurally identical to that found in humans. Spontaneous CAA-related hemorrhage has been consistently reported to occur in older dogs, usually over 13 years of age. Canine amyloid deposition has been shown to concentrate in the intercellular spaces of the tunica media in blood vessels in a similar fashion to humans [16]. The positive correlation between CAA and intracerebral hemorrhage that exists in humans has also been established in canines [17].

Discussion

Diagnostic tools for detecting physical and metabolic changes in the AD brain include MRI, fMRI, PET, CT and SPECT, which are all imaging methods that can continue to be refined using animal models to enhance detection of AD and CAA-related microhemorrhages [18]. Existing treatments for AD, such as cholinesterase inhibitors, *N*-methyl *D*-aspartate (NMDA) antagonists and non-steroidal anti-inflammatory drugs (NSAIDs), do not directly address the production and deposition of senile plaque A β . Removal of

these deposits has been regarded as a potential means of halting the progression of AD [9]. Racke et al. used a transgenic mouse model to demonstrate attenuation of CAA-associated microhemorrhage by immunotherapy against deposited A β [11]. Strategies have since revolved around the same concept: reduction of A β production, blocking A β deposition in vessel walls, halting molecular events involved in A β -induced vessel degeneration, suppression of A β -induced inflammation and neurotoxicity, and removal of A β from the brain. Earlier trials of immunotherapy directed at removing A β were met with complications of encephalitis and meningitis, possibly because of the removal of protective A β deposits and A β PP/A β aggregates together with the target A β senile plaque deposits [11]. While animal models, such as the TG2576 mouse strain, have allowed for enhanced and accelerated development of more specifically A β mimotope-targeted vaccines and immunotherapies [19], the limitations of animal models must not be overlooked. For instance, use of transgenic or knockout rodents may not replicate clinical conditions to screen for possible complications. One immunotherapy medication did not successfully pass phase II trials because of clinical signs of encephalitis and meningitis that may have resulted from the removal of the non-senile plaque A β [8], which may not have had the same protective role in rodents and therefore did not present itself as a complication prior to clinical trials. Another issue is that of route of administration; for example, developed therapies given by intracerebroventricular injection (ICV), often used in mouse models, will require additional testing via alternate routes to translate successfully into the clinical setting.

Acknowledgement This study is partially supported by NIH NS053407 to J.H. Zhang

Conflict of interest statement We declare that we have no conflict of interest.

References

1. O'Donnell HC, Rosand J, Knudsen KA, Furie KL, Segal AZ, Chiu RI, Ikeda D, Greenberg SM (2000) Apolipoprotein E genotype and the risk of recurrent lobar intracerebral hemorrhage. *New Engl J Med* 342:240–245
2. Jellinger KA (2002) Alzheimer disease and cerebrovascular pathology: an update. *J Neural Transm* 109:813–836
3. Mandybur TI (1975) The incidence of cerebral amyloid angiopathy in Alzheimer's disease. *Neurology* 25:120–126
4. Walker LC (1997) Animal models of cerebral β -amyloid angiopathy. *Brain Res* 25:70–84
5. Greenberg SM, O'Donnell HC, Schaefer PW, Kraft E (1999) MRI detection of new hemorrhages: potential marker of progression in cerebral amyloid angiopathy. *Neurology* 53:1135–1138
6. Rosand J, Muzikansky A, Kumar A, Wisco JJ, Smith EE, Betensky RA, Greenberg SM (2005) Spatial clustering of hemorrhages in probably cerebral amyloid angiopathy. *Ann Neurol* 58:459–462

7. Okazaki H, Reagan TJ, Campbell RJ (1979) Clinicopathologic studies of primary cerebral amyloid angiopathy. *Mayo Clin Proc* 54:22–31
8. Atwood CS, Bishop GM, Perry G, Smith MA (2002) Amyloid- β : a vascular sealant that protects against hemorrhage? *J Neurosci Res* 70:356
9. Hardy J, Selkoe DJ (2002) The amyloid hypothesis of Alzheimer's disease: progress and problems on the road to therapeutics. *Science* 297:353–356
10. Herzig MC, Winkler DT, Burgermeister P, Pfeifer M, Kohler E, Schmidt SD, Danner S, Abramowski D, Stürchler-Pierrat C, Bürki K, van Duinen SG, Maat-Schieman MLC, Staufenbiel M, Mathews PM, Jucker M (2004) A β is targeted to the vasculature in a mouse model of hereditary cerebral hemorrhage with amyloidosis. *Nat Neurosci* 7:954–960
11. Racke MM, Boone LI, Hepburn DL, Parsadainian M, Bryan MT, Ness DK, Pirooz KS, Jordan WH, Brown DD, Hoffman WP, Holtzman DM, Bales KR, Gitter BD, May PC, Paul SM, DeMattos RB (2005) Exacerbation of cerebral amyloid angiopathy-associated microhemorrhage in amyloid precursor protein transgenic mice by immunotherapy is dependent on antibody recognition of deposited forms of amyloid β . *J Neurosci* 25:629–636
12. Thakker DR, Weatherspoon MR, Harrison J, Keene TE, Lane DS, Kaemmerer WF, Stewart GR, Shafer LL (2009) Intracerebroventricular amyloid- β antibodies reduce cerebral amyloid angiopathy and associated micro-hemorrhages in aged Tg2576 mice. *Proc Natl Acad Sci USA* 106(11):4501–4506, Epub 2009 Feb 25
13. Lee JM, Yin K, Hsin I, Chen S, Fryer JD, Holtzman DM, Hsu CY, Xu J (2005) Matrix metalloproteinase-9 in cerebral-amyloid angiopathy-related hemorrhage. *J Neuro Sci* 229–230:249–254
14. Winkler DT, Bondolfi L, Herzig MC, Jann L, Calhoun ME, Wiederhold KH, Tolnay M, Staufenbiel M, Jucker M (2001) Spontaneous hemorrhagic stroke in a mouse model of cerebral amyloid angiopathy. *J Neurosci* 21:1619–1627
15. Fryer JD, Taylor JW, DeMattos RB, Bales KR, Paul SM, Parsadainian M, Holtzman DM (2003) Apolipoprotein E markedly facilitates age-dependent cerebral amyloid angiopathy and spontaneous hemorrhage in amyloid precursor protein transgenic mice. *J Neurosci* 23:7889–7896
16. Prior R, D'Urso D, Frank R, Prikulis I, Wihl G, Pavlakovic G (1996) Canine leptomenigeal organ culture: a new experimental model for cerebrovascular β -amyloidosis. *J Neurosci Methods* 68:143–148
17. Uchida K, Nakayama H, Goto N (1991) Pathological studies on cerebral amyloid angiopathy, senile plaques and amyloid deposition in visceral organs in aged dogs. *J Vet Med Sci* 53:1037–1042
18. Jeong S-W, Jung K-H, Chu K, Bae H-J, Lee S-H, Roh J-K (2004) Clinical and radiologic differences between primary intracerebral hemorrhage with and without microbleeds on gradient-echo magnetic resonance images. *Arch Neurol* 61:905–909
19. Wilcock DM, Colton CA (2009) Immunotherapy, vascular pathology, and microhemorrhages in transgenic mice. *CNS Neurol Disord Drug Targets* 8:50–64

Multiparametric Characterisation of the Perihemorrhagic Zone in a Porcine Model of Lobar ICH

Berk Orakcioglu, M. Kentar, Y. Uozumi, E. Santos, P. Schiebel, A. Unterberg, and O.W. Sakowitz

Abstract Objectives: To describe early perihemorrhagic changes after lobar intracerebral hemorrhage (ICH) using multiparametric neuromonitoring [intracranial pressure (ICP), cerebral blood flow (CBF), tissue oxygenation ($P_{br}O_2$), microdialysis (MD)].

Methods: Seven anaesthetized male swine were examined over 12 h. Four cerebral probes were inserted around the ICH (ICP, MD, CBF and $P_{br}O_2$). A right frontal autologous arterial ICH (1.5 mL) was induced in all animals.

Results: Initial ICH creation was hampered by using a soft 22-G cannula. A modified injection technique with a 90° bent steel cannula (20 G) allowed for an 87.5% success rate in ICH formation. After induction of ICH, ICP significantly increased from 2 mmHg to 9 mmHg. No significant $P_{br}O_2$ or CBF reduction occurred during the monitoring period. Consequently, microdialysis did not indicate overall mean deterioration in the hematoma group over time. The indicator of ischemia (extracellular lactate) did not increase significantly during the monitoring period. Individual monitoring episodes demonstrated hypoxic episodes with consecutive metabolic derangement. These effects were reversible by optimizing CPP and FiO_2 .

Conclusion: We established a reproducible cortical ICH model using multiparametric neuromonitoring. Subtle changes in ICP were observed. No evidence for the existence of a perihemorrhagic ischemic area was found, hypothetically because of the small hematoma size. Individual animals underwent critical $P_{br}O_2$ and CBF decreases with consecutive metabolic derangement. The effect of larger

hematoma volumes should be evaluated with this setup in future studies to study volume-dependent deterioration.

Keywords ICH · Multiparametric monitoring · $P_{br}O_2$ · CBF · ICP · Microdialysis

Introduction

The acute changes in the perihemorrhagic zone (PHZ) of spontaneous ICH remain unclear. In theory, depression of perfusion may lead to metabolic changes because of lack of tissue oxygenation. Some previous studies using $P_{br}O_2$ measurement and microdialysis have shown evidence of perihemorrhagic tissue hypooxygenation or of an increase in extracellular concentrations of glutamate after ICH [1, 2]. Currently no experimental model exists that simultaneously measures intracranial pressure, oxygenation, perfusion and metabolism in the PHZ of ICH. Therefore, we utilized human cerebral multimodal monitoring probes (ICP, $P_{br}O_2$, CBF and microdialysis) to study the PHZ in a porcine model of lobar ICH.

Methods

Animal Preparation

Animal protocols for the experiments were approved by the institutional animal care and use committee (protocol no.: 35-9185.81/G-60/06). A standardized operative setup was followed as described elsewhere [3]. Seven male swine with an average mean weight of 30.1 ± 1.62 (SD) kg were anesthetized with ketamine (10 mg/kg), midazolam (5 mg/kg) and azaperone (40 mg/kg) administered by intramuscular injection. Animals were orally intubated and mechanically ventilated ($F_iO_2=0.3$). Anesthesia was maintained using 1.5% isoflurane inhalation. Rectal and brain temperatures (T_r , T_{br})

B. Orakcioglu (✉)
Department of Neurosurgery, University Hospital Heidelberg,
Im Neuenheimer Feld 400, 69120 Heidelberg, Germany
e-mail: berk.orakcioglu@med.uni-heidelberg.de

M. Kentar, Y. Uozumi, E. Santos, P. Schiebel, A. Unterberg,
and O.W. Sakowitz
Department of Neurosurgery, Ruprecht-Karl-University,
Heidelberg, Germany

were continuously monitored. Rectal temperature was maintained between 35.5°C and 37°C. After surgical exposure of the right femoral artery, a 4-F catheter was placed for permanent monitoring of mean arterial blood pressure (MAP). A venous line was placed in the right ear vein, and capillary oxygen saturation (SO₂) was monitored from the left ear.

Operative Procedure

Five burr holes (diameter: 5 mm) were placed over the right hemisphere. One burr hole was placed parietally through which the ICP probe (Neurovent-P®, Raumedic AG, Helmbrechts, Germany) was placed. Immediately along the coronal suture three burr holes were placed 0.8, 1.2 and 1.6 cm off midline, respectively. Through these burr holes the monitoring probes were inserted next to each other. Medially the thermodiffusion regional CBF probe (Hemedex td-rCBF, Codman®, USA) was followed by the P_{br}O₂ probe (Neurovent®-TO, Raumedic AG, Helmbrechts, Germany) and microdialysis probe (CMA 70, Solna, Sweden) most laterally (Fig. 1). All intraparenchymal devices were introduced and secured transcutaneously prior to insertion into the brain. An equilibration period of 2 h was allowed for the probes to run in and the animals to stabilize. Further frontally, a soft 22-G cannula for induction of the ICH was introduced via the fifth burr hole, which was located 1.5 cm in front of the coronal suture and 0.8 cm lateral to the sagittal suture. In seven subjects (data not shown completely), an autologous arterial hematoma was created following the description of Quereshi et al. and Hemphil et al. [1, 4]. Polyvinyl chloride tubing was attached to a stopcock at the distal end of the spinal needle and to the femoral artery. At the initiation of hematoma formation, autologous blood was introduced into the brain under arterial pressure via this tubing. However, we aimed to target the cortico-subcortical area in order to avoid deep-seated ICH location. The injected hematoma volume was 1.5 mL. Neither the catheters nor the syringes were flushed with heparin. Following first experiences with the described injection method, we adapted the technique and used a 90° bent steel 20-G cannula. After catheter placements and ICH injection, the burr holes were sealed with bone wax and monitoring was conducted for 10 h to complete the monitoring period of 12 h. Postmortem cranial vaults were opened completely, brains were removed, and intraparenchymal catheter locations and ICH size and position were macroscopically inspected (Fig. 2).

Monitoring

All relevant physiological parameters, such as mean arterial pressure (MAP), intracranial pressure (ICP), cerebral

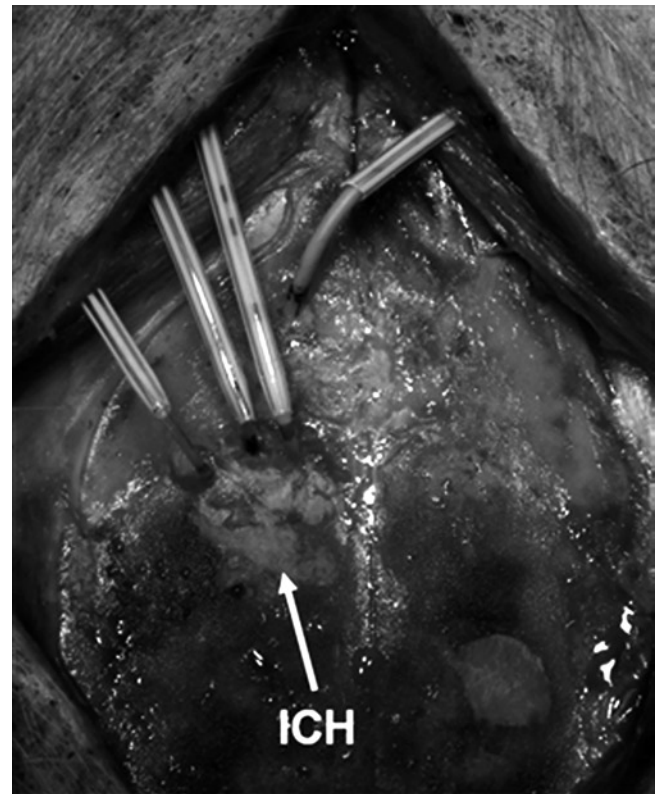


Fig. 1 Photograph illustrating the catheter positioning in relation to the injection site of the hematoma. Most parietally the ICP probe is introduced. Just in front of the coronal suture three monitoring probes are placed next to each other. Most medial is the CBF probe followed by the P_{br}O₂ probe and microdialysis probe. Frontally, the burr hole site for the hematoma is marked (*white arrow*)

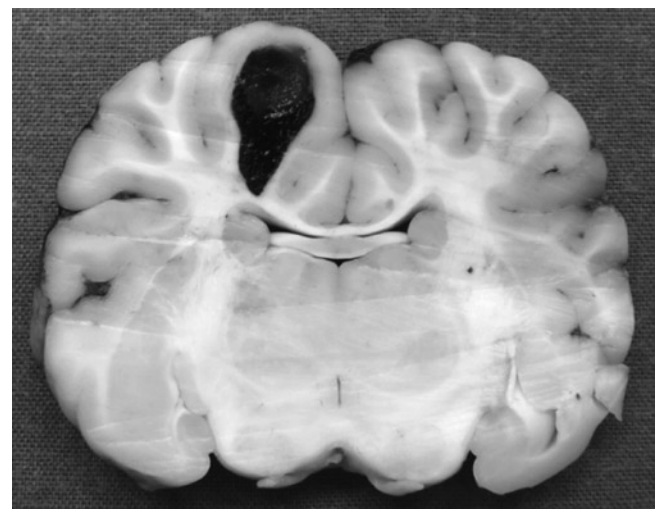


Fig. 2 Typical cortico-subcortical ICH in the right frontal lobe with extension to the fronto-parietal region. Total ICH volume was confirmed after sectioning of the brain postmortem

perfusion pressure (CPP), brain and rectal temperature (T_b, T_r), heart rate (HR), oxygen saturation (SO₂), P_{br}O₂ and rCBF, were continuously recorded. Microdialysates were

perfused with a rate of 0.3 $\mu\text{L}/\text{min}$, and samples were taken every 30 min. The microdialysis vials were collected and analyzed after the experiment was finished. All other parameters were recorded online. Blood-gas analyses were achieved every 2 h. The experiments did not test any therapeutic measure in all but one animal in which an increase of FiO_2 and regulation of CPP were allowed.

Statistical Analysis

For statistical analysis we used a standard software package (SPSS 14.0). All data were normally distributed. A paired Student's *t*-test was used. The 95% confidence interval was calculated for the mean difference of all parameters. The $p < 0.05$ level was used to assess significance.

Results

Using the ICH injection technique with the soft cannula, an ICH of intended volume was formed in 7/11 (64%) of animals. The improved technique resulted in an 87.5% success rate. The monitoring results were as follows: ICP increased shortly after hematoma formation and rose until it reached a plateau at 8 mmHg after 6 h of monitoring. This increase was statistically significant ($p < 0.001$). The early ICP increase was adjoined by an increase in CBF from 27 mL/100 mg/min to 34 mL/100 mg/min after 3 h. After 10 h CBF decreased to baseline values. $\text{P}_{\text{br}}\text{O}_2$ stayed unchanged for 6 h after the hematoma placement. However, towards the end of the experiment $\text{P}_{\text{br}}\text{O}_2$ reached 30 mmHg. Metabolic mean values did not show any evidence of parenchymal ischemia as neither extracellular glutamate (not displayed) nor lactate increased significantly compared to baseline measurements. These results are displayed in Table 1. Individual monitoring episodes demonstrated immediate dramatic oxygen decrease and subsequent increase of metabolic indicators of cerebral ischemia. These effects were reversible by increasing the fraction of inhaled oxygen (FiO_2) from 30% to 80% and modulation of CPP (Fig. 3).

Discussion

The theory that cerebral ischemia contributes to secondary neuronal injury after ICH has been discussed in several publications, but the results of different groups are inconsistent, and there is an ongoing debate about the existence of a “perihemorrhagic penumbra” [1, 2, 5–7]. Experimental projects are often subject to the criticism that results cannot be transferred into human pathologies. For example, assessing CBF with laser Doppler flowmetry in rats is not comparable to online CBF recording using a td-CBF probe in patients. However, multimodal monitoring tools are progressing as useful tools in the setting of various types of stroke [8–11]. Therefore, this study was performed on the basis of a multimodal monitoring approach with cerebral probes used in the clinical setting (ICP, CBF, $\text{P}_{\text{br}}\text{O}_2$ and microdialysis).

As superficial lobar hematomas are more amenable to effective therapy such as surgical evacuation, we at first investigated experimental ICH in pigs as described. The injection method that we used has been previously described by Qureshi et al. and Hemphil et al. [1, 4]. We adapted this method to the porcine anatomy. The injection technique was modified using a 90° angled 20-G steel cannula, which reliably led to the formation of consistent ICH of intended volume. Using this model, hypoxic episodes were found, but metabolic or histological correlates were not assessed. Others found that glutamate, as an indicator of pending ischemia, significantly increased in the early phase after ICH formation [2]. The authors concluded that the exact role of these amino acids in the pathogenesis of neuronal injury observed in ICH needs to be defined.

From previous publications it was reported that cerebral perfusion may be reduced in tissues surrounding the hematoma. In this context, Belayev et al. performed a combined study of perfusion monitoring by laser Doppler flow and neurobehavioral tests in mice after ICH. A significantly reduced perfusion (35–50%) was sustained over 90 min and went along with substantial neurological deficits in these animals [12]. An MRI study at 7 T in rats additionally showed that cerebral perfusion may be diminished around the hematoma, which correlated to histological cell loss [13]. Similarly, relevant perfusion reductions measured by MRI were seen in

Table 1 Table showing mean values \pm SD of ICP, CBF and $\text{P}_{\text{br}}\text{O}_2$ and extracellular lactate measured by microdialysis during four time points (TP1: 30 min prior to ICH; TP2: 3 h post ICH; TP3: 6 h post ICH; TP 4: 10 h post ICH). ICP increased because of the injected volume, CBF and $\text{P}_{\text{br}}\text{O}_2$ moderately decreased. Lactate values do not show any relative increase compared to the baseline measurement

Parameter	TP1	TP2	TP2	TP3
Time				
ICP [mmHg]	1.03 \pm 3.53	6.44 \pm 5.05	8.67 \pm 5.75	7.21 \pm 3.77
$\text{P}_{\text{br}}\text{O}_2$ [mmHg]	23.27 \pm 16.97	20.12 \pm 15.78	21.25 \pm 15.25	29.74 \pm 15.88
CBF (mL/100 mg/min)	30.04 \pm 9.41	33.20 \pm 15.07	30.6 \pm 13.73	26.84 \pm 12.48
Lactate (mmol/L)	3.18 \pm 1.30	2.55 \pm 1.51	4.19 \pm 1.85	4.19 \pm 2.44

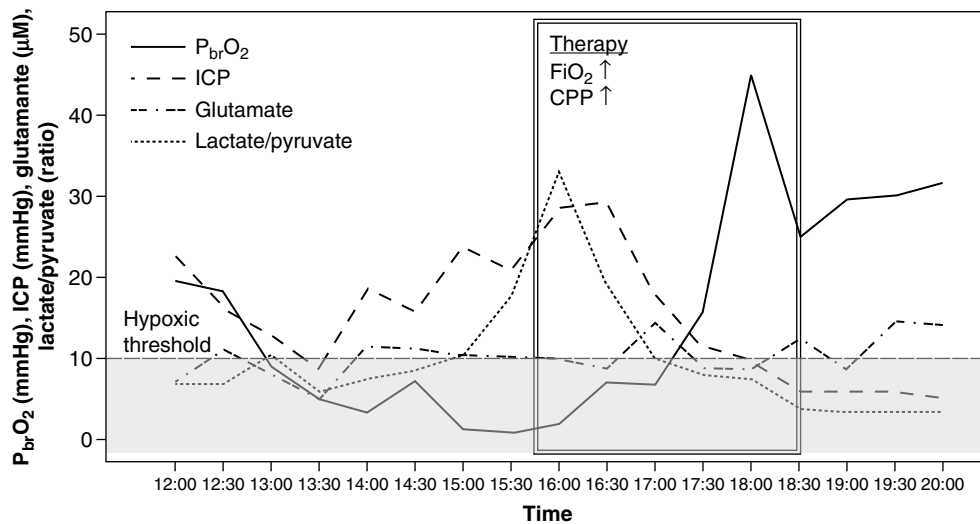


Fig. 3 Original recording episode of an individual animal illustrating the $P_{br}O_2$, lactate/pyruvate ratio, glutamate and ICP. At 12.00 h the ICH was created. One can appreciate that ICP increased from 8 mmHg to 11 mmHg, and tissue oxygenation dramatically decreased subsequently under the hypoxic threshold (below grey dashed line) of 10 mmHg. As an early indicator of pending ischemia lactate/pyruvate ratio and

extracellular glutamate increased up to clearly pathological values. Regulation of CPP from 55 mmHg to 60 mmHg and increase of FiO_2 from 30% to 80% (initiation 15.45 h, double lined box) led to reversal of the $P_{br}O_2$ decrease and the metabolic deterioration. The usefulness of additional monitoring is evident as ICP did not indicate any critical circumstance in this subject

18 patients [14]. However, it remains difficult to establish perihemorrhagic perfusion and structural patterns using artifact-prone tools like MRI. In our previous results we found that there is no relevant ischemic tissue in the immediate surrounding of the hematoma as measured by DWI, although we were able to show that perfusion is reduced on the affected side (5–27%) in comparison to the healthy side [6].

There are limitations to our study. We do not present histological correlates to our findings. However, once more significant perihemorrhagic changes are evident, histopathological studies seem mandatory. Effects on functional recovery cannot be proved as neurological assessments were not performed as the animals were sacrificed at the end of the study.

In conclusion, we examined continuous multiparametric characteristics of small volume ICH in swine in the acute phase. We improved the injection technique of ICH that resulted in an acceptable success rate of hematoma creation of approximately 90%. In the current study only subtle changes in ICP but no changes in CBF, $P_{br}O_2$ and microdialysis were observed. With the use of larger hematoma volumes, one might be able to elicit perfusion and tissue oxygen changes with subsequent impact on metabolic indices. Future studies should therefore focus on increasing hematoma size and elucidate the effects of contralateral hematomas (to differentiate purely volume-/ICP-dependent effects from ischemic/neurotoxic effects). Our model could also allow studying en vogue but yet unclear phenomena like cortical spreading depolarizations in their role in the pathophysiology of the PHZ in ICH.

Conflict of interest statement We declare that we have no conflict of interest.

References

- Hemphill JC 3rd, Morabito D, Farrant M, Manley GT (2005) Brain tissue oxygen monitoring in intracerebral hemorrhage. *Neurocrit Care* 3:260–270
- Qureshi AI, Ali Z, Suri MF, Shuaib A, Baker G, Todd K, Guterman LR, Hopkins LN (2003) Extracellular glutamate and other amino acids in experimental intracerebral hemorrhage: an in vivo microdialysis study. *Crit Care Med* 31:1482–1489
- Orakcioglu B, Sakowitz OW, Neumann J-O, Kentar MM, Unterberg AW, Kiening KL (2010) Evaluation of a novel brain tissue oxygenation probe in an experimental swine model. *Neurosurgery* 67(6):1716–1722
- Qureshi AI, Hanel RA, Kirmani JF, Yahia AM, Hopkins LN (2002) Cerebral blood flow changes associated with intracerebral hemorrhage. *Neurosurg Clin N Am* 13:355–370
- Carhuapoma JR, Wang PY, Beauchamp NJ, Keyl PM, Hanley DF, Barker PB (2000) Diffusion-weighted MRI and proton MR spectroscopic imaging in the study of secondary neuronal injury after intracerebral hemorrhage. *Stroke* 31:726–732
- Orakcioglu B, Becker K, Sakowitz OW, Herweh C, Kohrmann M, Huttner HB, Steiner T, Unterberg A, Schellinger PD (2008) MRI of the perihemorrhagic zone in a rat ICH model: effect of hematoma evacuation. *Neurocrit Care* 8(3):448–455
- Schellinger PD, Fiebich JB, Hoffmann K, Becker K, Orakcioglu B, Kollmar R, Juttler E, Schramm P, Schwab S, Sartor K, Hacke W (2003) Stroke MRI in intracerebral hemorrhage: is there a perihemorrhagic penumbra? *Stroke* 34:1674–1679
- Meixensberger J, Jaeger M, Vath A, Dings J, Kunze E, Roosen K (2003) Brain tissue oxygen guided treatment supplementing ICP/ CPP therapy after traumatic brain injury. *J Neurol Neurosurg Psychiatry* 74:760–764

9. Sakowitz OW, Sarrafzadeh AS, Benndorf G, Lanksch WR, Unterberg AW (2001) On-line microdialysis following aneurysmal subarachnoid hemorrhage. *Acta Neurochir Suppl* 77:141–144
10. Unterberg AW, Sakowitz OW, Sarrafzadeh AS, Benndorf G, Lanksch WR (2001) Role of bedside microdialysis in the diagnosis of cerebral vasospasm following aneurysmal subarachnoid hemorrhage. *J Neurosurg* 94:740–749
11. Vajkoczy P, Roth H, Horn P, Lucke T, Thome C, Hubner U, Martin GT, Zapletal C, Klar E, Schilling L, Schmiedek P (2000) Continuous monitoring of regional cerebral blood flow: experimental and clinical validation of a novel thermal diffusion microprobe. *J Neurosurg* 93:265–274
12. Belayev L, Saul I, Curbelo K, Busto R, Belayev A, Zhang Y, Riyamongkol P, Zhao W, Ginsberg MD (2003) Experimental intracerebral hemorrhage in the mouse: histological, behavioral, and hemodynamic characterization of a double-injection model. *Stroke* 34:2221–2227
13. Knight RA, Han Y, Nagaraja TN, Whitton P, Ding J, Chopp M, Seyfried DM (2008) Temporal MRI assessment of intracerebral hemorrhage in rats. *Stroke* 39:2596–2602
14. Pascual AM, Lopez-Mut JV, Benlloch V, Chamarro R, Soler J, Lainez MJ (2007) Perfusion-weighted magnetic resonance imaging in acute intracerebral hemorrhage at baseline and during the 1st and 2nd week: a longitudinal study. *Cerebrovasc Dis* 23:6–13

Developing a Model of Chronic Subdural Hematoma

Jingyang Tang, Jinglu Ai, and R. Loch Macdonald

Abstract Chronic subdural hematoma (CSDH) is a common neurosurgical condition that has a high incidence in the increasing elderly population of many countries. Pathologically, it is defined as a persistent liquefied hematoma in the subdural space more than 3 weeks old that is generally encased by a membranous capsule. CSDHs likely originate after minor head trauma, with a key factor in its development being the potential for a subdural cavity to permit its expansion within, which is usually due to craniocerebral disproportion. The pathogenesis of CSDH has been attributed to osmotic or oncotic pressure differences, although measurements of these factors in the CSDH fluid do not support this theory. Current belief is that CSDH arises from recurrent bleeding in the subdural space, caused by a cycle of local angiogenesis, inflammation, coagulation and ongoing fibrinolysis. However, because of a lack of detailed knowledge about the precise mechanisms, treatment is often limited to surgical interventions that are invasive and often prone to recurrence. Thus, it is possible that an easily reproducible and representative animal model of CSDH would facilitate research in the pathogenesis of CSDH and aid with development of treatment options.

Keywords Chronic subdural hematoma · Acute subdural hematoma · Subdural hygroma · Animal models · Mild traumatic brain injury

J. Tang and J. Ai
Division of Neurosurgery, Keenan Research Centre in the Li Ka Shing Knowledge Institute of St. Michael's Hospital, 30 Bond Street, Toronto, ON M5B 1W8, Canada

R.L. Macdonald (✉)
Division of Neurosurgery, Keenan Research Centre in the Li Ka Shing Knowledge Institute of St. Michael's Hospital, 30 Bond Street, Toronto, ON M5B 1W8, Canada
Department of Surgery, University of Toronto, Toronto, ON, Canada
e-mail: macdonaldlo@smh.ca

Introduction

Chronic subdural hematoma (CSDH) is a common neurosurgical problem that is more common with increasing age, coagulopathy, alcohol abuse and neurodegenerative disorders such as Alzheimer's disease [1]. CSDH also is common in infants, so there is a somewhat U-shaped age distribution. Most cases, however, affect patients over 65 years old [2]. The incidence of CSDH is not well documented, and in possibly the only epidemiologic study in the computed tomography era, the overall incidence was 13 per 100,000 per year, ranging from 3.4 in people under 65–58 in those over 65 [3]. The incidence would be predicted to increase as the mean age of the world population increases and the use of predisposing drugs, such as antiplatelet and anticoagulant drugs, increases.

Characterization and Origin of CSDH

Chronic subdural hematomas have been pathologically defined as liquefied hematomas within a membranous capsule that persist in the subdural space. Up to 50% of patients give a history of minor head trauma in the 3 months preceding onset of symptoms [4]. The time from occurrence to liquefaction is variable, probably at least a week, and usually more than 3 weeks after minor trauma [2]. The hematoma is encased in a membranous capsule, with the outer membrane on the dural side comprised of vascularised granulation tissue up to 1 cm thick [5]. This layer has been identified to be of a type of reparative or inflammatory tissue that includes fibroblasts, collagen fibrils and a network of capillaries with endothelial cell fenestrations and open gaps between the individual endothelial cells [6]. In contrast, the inner membrane is much thinner, usually 30–300 µm thick, relatively acellular and avascular, mainly fibrocollagenous and similar

to the semi-permeable arachnoid membrane [7]. The hematoma itself contains liquid with fresh erythrocytes, low concentrations of coagulation factors, no fibrinogen and increased fibrinolytic activity [1]. Its age can be determined by the degree of eosinophilia within the subdural hematoma membrane [5] and roughly by the appearance on computed tomography [8].

CSDH may evolve from acute subdural hematoma (ASDH) or subdural hygroma [2]. ASDH is characterized by a solid subdural clot without a membrane and develops into a CSDH in less than 1% of cases. Subdural hygroma is accumulation of cerebrospinal fluid in the subdural space, also without a membrane, but can eventually contain mixed fluids, develop a membrane and evolve into a CSDH. Subdural hygromas are more common in the infant or senior populations, are usually caused by mild trauma to the head and are often bilateral.

Development of CSDH has been correlated with the availability of potential subdural space for its growth and expansion [2]. In the elderly, cerebral atrophy creates craniocerebral dysproportion. Similarly, recurrence of CSDH after treatment is also correlated with failure of the brain to expand after surgery [9].

Pathogenesis

Virchow described CSDH as “pachymeningitis hemorrhagica chronica interna” and considered it to be an inflammatory or infectious condition with secondary bleeding [10]. Trotter was among the first to suggest that trauma was the key factor in the origin [11]. In 1925, Putnam and Cushing proposed that recurrent bleeding from the thin-walled neovasculature within the outer neomembrane caused expansion of CSDH [12]. Subsequently, Gardner and others theorized that expansion of the CSDH was due to increased osmolarity or oncotic pressure in the hematoma, which caused the hematoma to imbibe water [13]. Some experiments and measurements of CSDH fluid osmolarity and oncotic pressure do not support this theory [14].

Current literature now supports the hypothesis that CSDHs arise from repeated bleeding into the subdural cavity, although this is based on observation without any scientific confirmation [15]. Minor trauma causes tearing of veins that traverse the potential subdural space where the veins have their thinnest walls [7]. Recurrent hemorrhage activates clotting wound-healing reactions [16]. The accumulated blood induces inflammation and fibrinolysis, further weakening local blood vessels and facilitating repeated bleeding into the cavity. Hong et al. measured higher interleukin-6, vascular

endothelial growth factor and basic fibroblast growth factor concentrations in CSDH with recurrence, suggesting a role of inflammation in the propagation of CSDH [1]. Within the hematoma fluid itself, there is a high concentration of fibrinolytic proteins such as tissue-type plasminogen activators, plasmin- α 2-plasmin inhibitor complex, and fibrin and fibrinogen degradation products [17] that prevent clotting and allow the blood to remain in a liquefied form. As the outer membrane forms around the hematoma and becomes vascularized, capillaries that are prone to bleeding develop within the membrane [9]. Their proliferative potential and fragile nature, in combination with the increased fibrinolytic activity in the CSDH fluid, theoretically create a cycle of bleeding, coagulation, inflammation, angiogenesis and fibrinolysis that causes CSDH.

Treatment and Complications

The diagnosis of CSDH can be made by cranial computed tomography or magnetic resonance imaging. Symptomatic patients generally undergo some form of treatment. A survey of Canadian Neurosurgical Society members found CSDH was most often treated using two burr holes [18]. Other methods, such as using one burr hole, twist drill craniostomy, craniotomy, and each method with or without irrigation and insertion of a drainage tube, are also employed with varying consequences in regard to recurrence, morbidity, and mortality rates [9]. One randomized trial supported use of burr holes with a drain compared to burr holes without a drain [19], and metaanalysis of the literature also supported use of burr holes or a twist drill craniostomy [20].

Animal Models

Attempts have been made to develop an animal model of CSDH in order to facilitate understanding of its pathogenesis and to explore treatment options, such as medical methods. However, most of the experiments have been met with limited success. Watanabe, et al. used dogs and monkeys to study the effects of subdural and subcutaneous hematomas [21]. While a liquefied mass could be produced by subdural injections, these hematomas spontaneously resolved after 15 days, and no persistent CSDH developed. We hypothesize that this is because there is no craniocerebral dysproportion in young, healthy animals. Apfelbaum and colleagues used similar methods in cats and found a similar time course with an outer membrane developing after 8 days, but with

disappearance of the hematomas by 21 days [22]. Finally, it was reported that the neurotoxin 6-aminonicotinamine probably caused ex vacuo hydrocephalus 9 days after injection into neonatal mice [23]. The mice also developed neurological and physiological side effects because of the neurological damage. By 20 days after injection, hematomas spontaneously developed in the parieto-occipital regions. These lasted for 10 days until the animals tended to die. Histology of the hematomas showed similarities to human CSDH.

The most successful attempt at an animal model was by Labadie and Glover [24]. They used various combinations of human platelet-free plasma, autologous hemolyzed blood or autologous whole blood, and injected or implanted these into the subcutaneous space over the thoracic spine of rats. Approximately 50% of the 154 clots implanted developed into enlarging liquefied hematomas and displayed compa-

rable organization and development to human CSDH [24]. The authors reported that treatment of rats with dexamethasone prevented expanding hematoma formation in this model [25].

As chronic expanding hematomas are also known to form in other parts of the body such as major muscles, the liver and serous cavities, it is possible that a subcutaneous model of CSDH is an acceptable substitute. We have had difficulty replicating prior experiments in rats. Implantation of clotted pig blood into the subcutaneous space over the thoracic spine of mice is currently being performed (Figs. 1 and 2). Skin necrosis over large clots sometimes occurs. Clots persist for up to 21 days and histologically show similar histology to clots isolated from human CSDH cases, but more study is still needed to quantify the direct interactions between the clot and the local tissue.

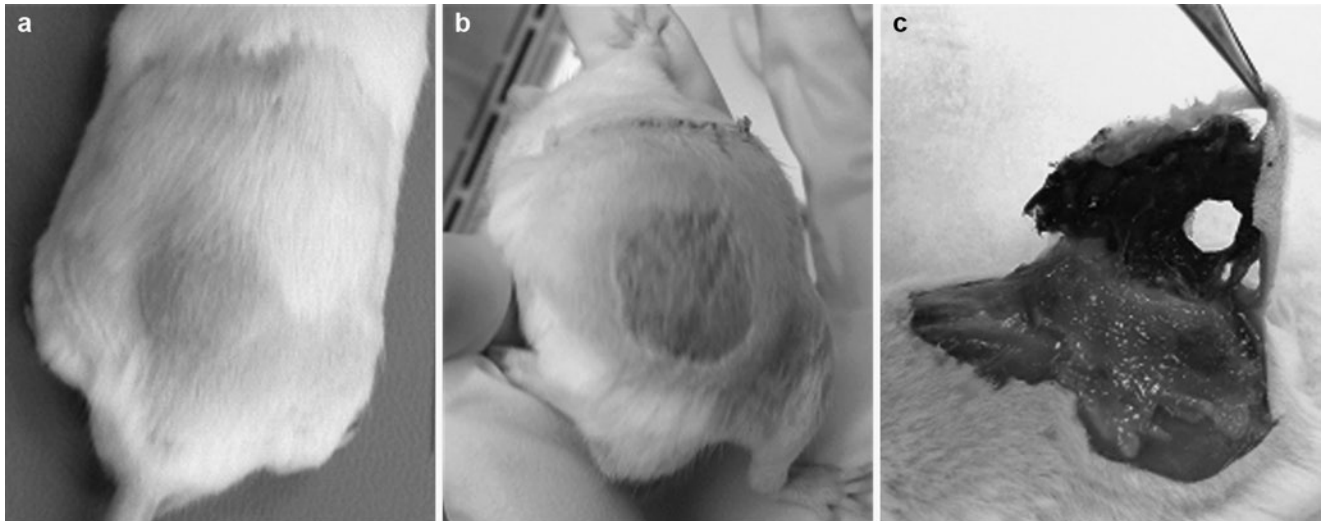
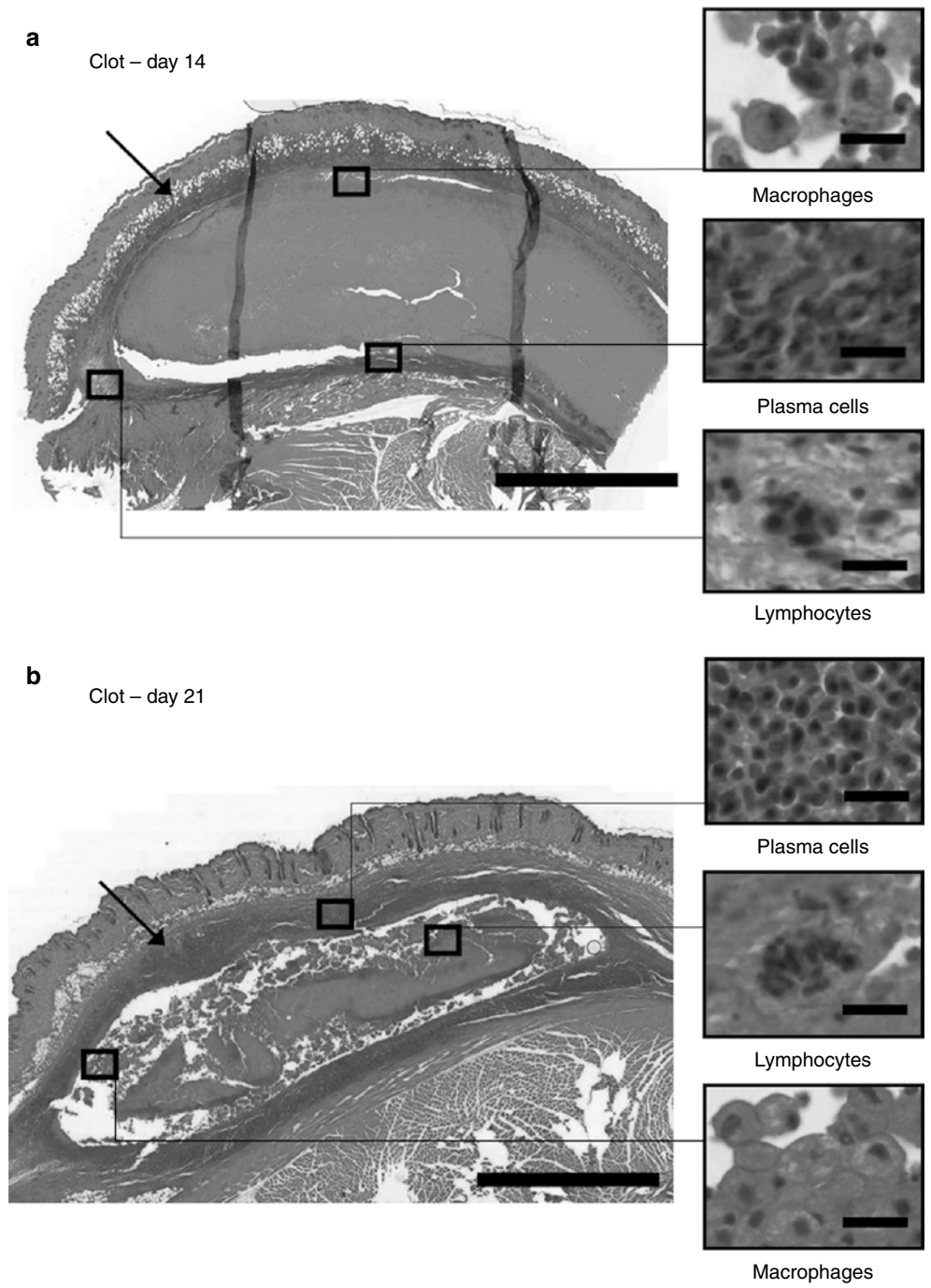


Fig. 1 Implantation of a 6-mL clot on the dorsal side of the mouse (a). Beginning stage of development of necrotic skin over the clot (b). Ulceration of the necrotic skin with complete detachment between the necrotic tissue and the surrounding healthy dermis (c)

Fig. 2 Histology of mouse subcutaneous clots. Hematoma removed 14 days after implantation shows a thick inflammatory cell layer surrounding the tissue, with eosinophilia in the clot-tissue interface (a). Hematoma removed 21 days after surgery shows a layer of inflammatory cells around the clot with white blood cell infiltration (b). (Hematoxylin and eosin, whole block on left scale bar=5,000 μm, cells on right scale bar=20 μm)



Conflict of interest statement We declare that we have no conflict of interest.

References

- Hong HJ, Kim YJ, Yi HJ, Ko Y, Oh SJ, Kim JM (2009) Role of angiogenic growth factors and inflammatory cytokine on recurrence of chronic subdural hematoma. *Surg Neurol* 71:161–165
- Lee KS, Bae WK, Doh JW, Bae HG, Yun IG (1998) Origin of chronic subdural haematoma and relation to traumatic subdural lesions. *Brain Inj* 12:901–910
- Kudo H, Kuwamura K, Izawa I, Sawa H, Tamaki N (1992) Chronic subdural hematoma in elderly people: present status on Awaji Island and epidemiological prospect. *Neurol Med Chir (Tokyo)* 32:207–209
- Mori K, Maeda M (2001) Surgical treatment of chronic subdural hematoma in 500 consecutive cases: clinical characteristics, surgical outcome, complications, and recurrence rate. *Neurol Med Chir (Tokyo)* 41:371–381
- Golden J, Frim DM, Chapman PH, Vonsattel JP (1994) Marked tissue eosinophilia within organizing chronic subdural hematoma membranes. *Clin Neuropathol* 13:12–16
- Killeffer JA, Killeffer FA, Schochet SS (2000) The outer neomembrane of chronic subdural hematoma. *Neurosurg Clin N Am* 11:407–412
- Yamashita T (2000) The inner membrane of chronic subdural hematomas: pathology and pathophysiology. *Neurosurg Clin N Am* 11:413–424
- Lee KS, Bae WK, Bae HG, Doh JW, Yun IG (1997) The computed tomographic attenuation and the age of subdural hematomas. *J Korean Med Sci* 12:353–359
- Ramachandran R, Hegde T (2007) Chronic subdural hematomas – causes of morbidity and mortality. *Surg Neurol* 67:367–372
- Virchow R (1857) Das haematom der dura mater. *Verch Phys Med Ges (Wurzburg)* 7:134–142
- Trotter W (1914) Chronic subdural haemorrhage of traumatic origin, and its relation to pachymeningitis haemorrhagica interna. *Br J Surg* 2:271–291
- Putnam T, Cushing H (1925) Chronic subdural hematoma: its pathology, its relation to pachymeningitis hemorrhagica, and its surgical treatment. *Arch Surg* 11:329–393
- Gardner WJ (1932) Traumatic subdural hematoma with particular reference to the latent interval. *Arch Neurol Psychiatry* 27:847–858
- Stoodley M, Macdonald RL, Wehl CC, Zhang ZD, Lin G, Johns L, Kowalczyk A, Ghadge G, Roos RP (2000) Effect of adenoviral-mediated nitric oxide synthase gene transfer on vasospasm after experimental subarachnoid hemorrhage. *Neurosurgery* 46:1193–2003
- Labadie EL, Glover D (1974) Chronic subdural hematoma: concepts of physiopathogenesis. A review. *Can J Neurol Sci* 1:222–225
- Fujisawa H, Ito H, Saito K, Ikeda K, Nitta H, Yamashita J (1991) Immunohistochemical localization of tissue-type plasminogen activator in the lining wall of chronic subdural hematoma. *Surg Neurol* 35:441–445
- Fujisawa H, Nomura S, Kajiwara K, Kato S, Fujii M, Suzuki M (2006) Various magnetic resonance imaging patterns of chronic subdural hematomas: indicators of the pathogenesis? *Neurol Med Chir (Tokyo)* 46:333–338
- Cenic A, Bhandari M, Reddy K (2005) Management of chronic subdural hematoma: a national survey and literature review. *Can J Neurol Sci* 32:501–506
- Santarius T, Kirkpatrick PJ, Ganesan D, Chia HL, Jalloh I, Smielewski P, Richards HK, Marcus H, Parker RA, Price SJ, Kirillos RW, Pickard JD, Hutchinson PJ (2009) Use of drains versus no drains after burr-hole evacuation of chronic subdural haematoma: a randomised controlled trial. *Lancet* 374:1067–1073
- Weigel R, Schmiedek P, Krauss JK (2003) Outcome of contemporary surgery for chronic subdural haematoma: evidence based review. *J Neurol Neurosurg Psychiatry* 74:937–943
- Watanabe S, Shimada H, Ishii S (1972) Production of clinical form of chronic subdural hematoma in experimental animals. *J Neurosurg* 37:552–561
- Apfelbaum RI, Guthkelch AN, Shulman K (1974) Experimental production of subdural hematomas. *J Neurosurg* 40:336–346
- Aikawa H, Suzuki K (1987) Experimental chronic subdural hematoma in mice. Gross morphology and light microscopic observations. *J Neurosurg* 67:710–716
- Labadie EL, Glover D (1976) Physiopathogenesis of subdural hematomas. Part 1: histological and biochemical comparisons of subcutaneous hematoma in rats with subdural hematoma in man. *J Neurosurg* 45:382–392
- Glover D, Labadie EL (1976) Physiopathogenesis of subdural hematomas. Part 2: inhibition of growth of experimental hematomas with dexamethasone. *J Neurosurg* 45:393–397

A Mouse Model of Intracranial Aneurysm: Technical Considerations

Yoshiteru Tada*, Yasuhisa Kanematsu*, Miyuki Kanematsu, Yoshitsugu Nuki, Elena I. Liang, Kosuke Wada, Hiroshi Makino, and Tomoki Hashimoto

Abstract Intracranial aneurysms can be induced by a single stereotaxic injection of elastase into the cerebrospinal fluid at the right basal cistern in hypertensive mice. This mouse model produces large aneurysm formations with an incidence of 60–80% within 3–4 weeks. Intracranial aneurysms in this model recapitulate key pathological features of human intracranial aneurysms. Several technical factors are critical for the successful induction of intracranial aneurysms in this model. Precise stereotaxic placement of the needle tip into the cerebrospinal fluid space is especially important. Aneurysm formations in this model can serve as a simple and easily interpretable outcome for future studies that utilize various inhibitors, knockout mice, or transgenic mice to test roles of specific molecules and pathways in the pathophysiology of intracranial aneurysms.

Y. Tada, Y. Nuki, E.I. Liang, K. Wada,
and H. Makino
Department of Anesthesia and Perioperative Care, University
of California, 1001, Potrero Avenue, No. 3C-38, San Francisco,
CA, USA and
Center for Cerebrovascular Research,
University of California, San Francisco, CA, USA

Y. Kanematsu
Department of Neurosurgery, Institute of Health Biosciences,
The University of Tokushima, Tokushima, Japan

M. Kanematsu
Department of Thoracic, Endocrine Surgery and Oncology,
Institute of Health Biosciences, The University of Tokushima,
Tokushima, Japan

T. Hashimoto (✉)
Department of Anesthesia and Perioperative Care, University
of California, 1001, Potrero Avenue, No. 3C-38, San Francisco,
CA, USA and
Center for Cerebrovascular Research, University
of California, San Francisco, CA, USA and
Department of Anesthesia and Perioperative Care, University
of California, 1001 Potrero Avenue, No. 3C-38, San Francisco,
CA 94110, USA
e-mail: hashimot@anesthesia.ucsf.edu

Keywords Intracranial aneurysm · Animal model · Macrophage · Matrix metalloproteinase · Hypertension · Inflammation · Mouse

Introduction

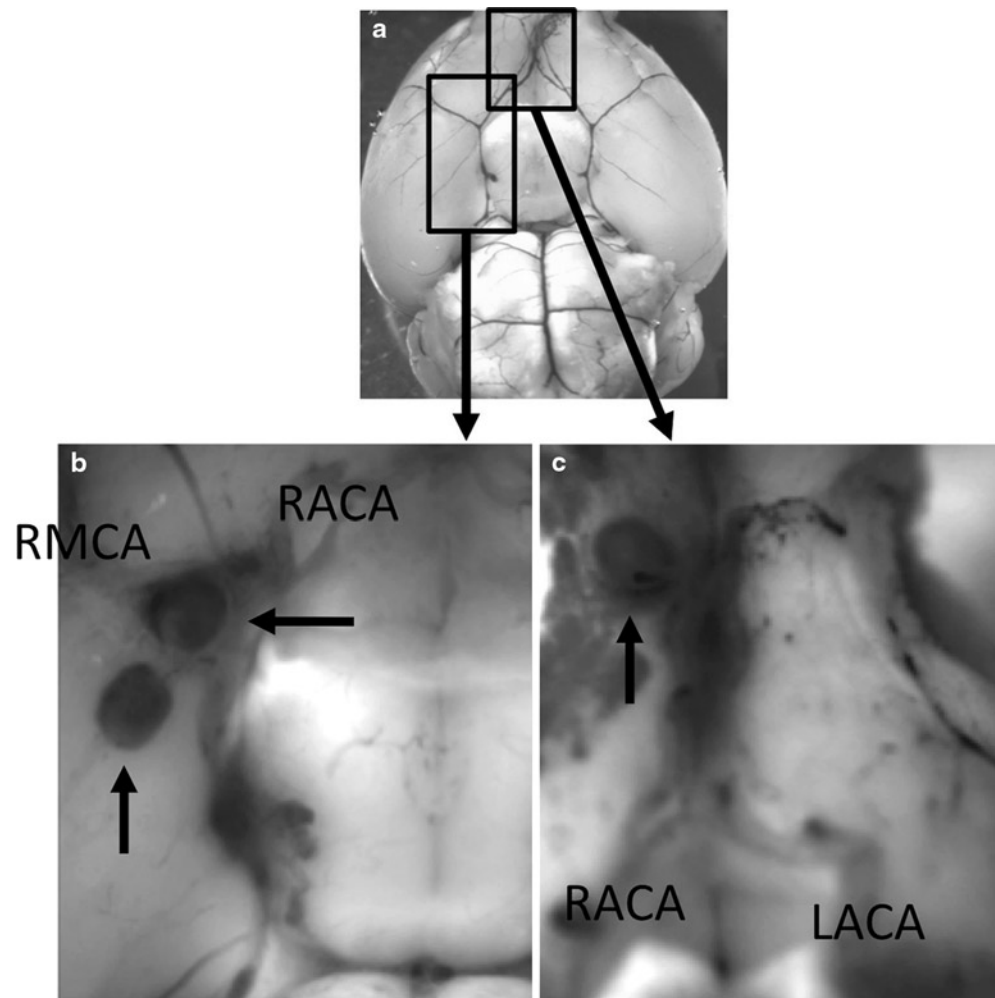
Despite recent advances in diagnosis and treatment, the mechanisms for formation, growth, and subsequent rupture of intracranial aneurysms are not well understood [1]. In order to understand the pathophysiology of intracranial aneurysms and identify therapeutic targets for the prevention of aneurysmal rupture, an animal model of intracranial aneurysm would be useful. Recently, we have developed a new mouse model of intracranial aneurysm that recapitulates key pathological features of human intracranial aneurysms [2]. This model produces large intracranial aneurysms within a short incubation time of 2–3 weeks. In this article, we will discuss technical considerations that are critical for the successful application of this model for future studies.

Overview of Elastase-Induced Intracranial Aneurysm in Hypertensive Mice

In this model, two well-known clinical factors associated with human intracranial aneurysms – hypertension and the degeneration of elastic lamina – are combined to induce intracranial aneurysm formation in mice [2]. Hypertension is associated with the formation and rupture of intracranial aneurysms. Degeneration of the elastic lamina is a key pathological change of intracranial aneurysms. Fragmentation of the elastic lamina alone is considered a pre-aneurysmal

*Authors Yoshiteru Tada and Yasuhisa Kanematsu contributed equally to this study

Fig. 1 Representative aneurysms. (a) Control brain. (b) Aneurysms were found at the bifurcation at the right middle cerebral artery and the internal carotid artery and at the proximal part of right middle cerebral artery. (c) Aneurysm at the right anterior cerebral artery. (RACA right anterior cerebral artery, LACA left anterior cerebral artery, RMCA right middle cerebral artery). Arrows in Figure 1b and 1c indicate aneurysms



change that can eventually mature into an aneurysm. In this model, hypertension is induced by continuous infusion of angiotensin II; degradation of the elastic lamina is induced by a single injection of elastase into the cerebrospinal fluid using a stereotaxic method. This model produces large intracranial aneurysms at an incidence of 60–80% within 3–4 weeks. Aneurysms are formed in the circle of Willis and its major branches. Figure 1 shows a control brain (a) and representative aneurysms (b, c) from this model.

There are dose-dependent effects of angiotensin II and elastase on the incidence of aneurysms in this model. Neither angiotensin II nor elastase alone could induce aneurysms, indicating that synergistic effects of elastase and hypertension are needed for the aneurysm formation in our model. When hypertension-induced vascular remodeling is coupled with elastase-induced inflammation, abnormal vascular remodeling may occur. Intracranial aneurysm formation may represent maladaptive vascular remodeling that is mediated by hemodynamic changes and inflammation [3].

Histologically, intracranial aneurysms formed in this model closely resemble human intracranial aneurysms. Part of the aneurysmal wall in this model is often thickened. Although endothelial

and smooth muscle cell layers are sometimes fragmented, they are generally present throughout the aneurysmal wall, showing that the intracranial aneurysms formed in this model are true aneurysms, not pseudo-aneurysms.

Aneurysms formed in this model are generally large and easily distinguishable from the normal arteries without using histological assessment. Aneurysm formations in this model can serve as a simple and easily interpretable outcome for future studies that utilize various inhibitors, knockout mice, or transgenic mice to test roles of specific molecules and pathways in the pathophysiology of intracranial aneurysms. For example, using this model, we have shown critical roles of matrix metalloproteinases (MMPs) in the formation of intracranial aneurysms [2].

Angiotensin II-Induced Hypertension

Angiotensin II infusion through an implanted osmotic pump is a well-established, well-characterized model of hypertension in mice [4–6]. A horizontal skin incision approximately

1 cm long should be made on one side of the back at 1 cm cephalad from the base of the tail. The small pocket between the skin and muscle layers that will contain the osmotic pump can be made using a pair of forceps. The osmotic pump can be implanted into this pocket, and the skin should be closed with sutures. This procedure takes only 5–10 min with a minimum amount of training. Proper suturing of the incision is very important since the wound dehiscence can result in unexpected explantation of the osmotic pump. Frequent monitoring of the wound site is needed, and the additional sutures can be added as needed.

Using angiotensin II infusion, a rise in systolic blood pressure can be detected as early as 1 week, and hypertension can be maintained for up to 6 weeks. Norepinephrine infusion or deoxycorticosterone acetate (DOCA)-salt treatment can also be used to induce hypertension in mice [5, 6]. DOCA-salt hypertension may be useful when non-hemodynamic effects of angiotensin II need to be avoided. Angiotensin II can exert various effects on the vasculature in addition to its hypertensive effect, including induction of reactive oxygen species and promotion of inflammation [5]. It should be noted that in our experience, the rise in blood pressure in these two methods was milder than that in angiotensin II-induced hypertension; hypertension became less significant after 3 weeks using norepinephrine infusion or deoxycorticosterone acetate (DOCA)-salt treatment. Angiotensin II-induced hypertension may be more consistent and sustained.

Blood Pressure Measurement

To monitor successful induction and maintenance of systemic hypertension, blood pressure measurement is critical. Since repeated measurements of blood pressure are needed, the tail cuff method is used in our laboratory (ML125M, ADInstruments). In our experience, this method provides accurate estimates for systolic blood pressure. Our preliminary data showed a highly significant correlation between the systolic blood pressure values using the tail cuff method and the mean blood pressure values obtained from the direct measurement using a femoral artery catheter.

Blood pressure measurement of conscious mice requires a series of training of mice. Some strains of mice, such as C57BL/6 J mice, appear to have high locomotor activity and resistance to restraint, even after training for blood pressure measurements [4]. Alternatively, blood pressure measurement can be performed on anesthetized mice. Systolic blood pressure can be reliably measured when mice are under a steady state of isoflurane anesthesia [2, 5]. This would require a continuous monitoring of isoflurane concentration in the anesthesia chamber or mask. We have conducted an experiment comparing systolic blood pressure values between conscious state and anesthetized state.

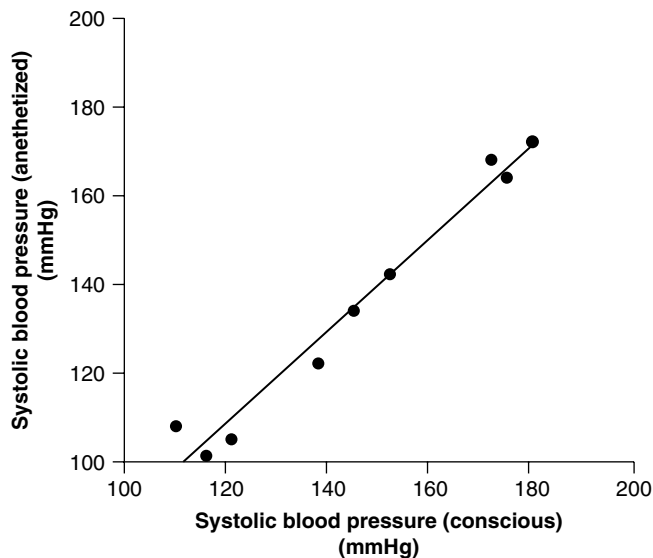


Fig. 2 Correlation of systolic blood pressure between conscious and anesthetized state. There was a close correlation between systolic blood pressure measured in a conscious state and systolic blood pressure measured in an anesthetized state ($y = 1.05x - 17$, $R^2 = 0.96$, $P < 0.05$)

In three groups of mice, blood pressure was measured in both conscious and anesthetized states. Mice received either phosphate-buffered saline, angiotensin II at 500 ng/kg/min, or angiotensin II at 1,000 ng/kg/min through osmotic pumps ($n = 3$ in each group). After two consecutive days of acclimation training, mice underwent “conscious” blood pressure measurement. Immediately after the blood pressure measurements were taken in the conscious state, mice were anesthetized with isoflurane, and blood pressure was measured at the steady state of isoflurane anesthesia (after 15 min of equilibration with isoflurane concentration at 1.5%). As shown in Fig. 2, there was a close correlation between systolic blood pressure measured under conscious state and that under anesthetized state ($R^2 = 0.96$, $P < 0.05$). As we have expected, systolic blood pressure measured under anesthetized state was slightly lower than that under conscious state ($y = 1.05x - 17$), reflecting the blood pressure lowering effect of isoflurane. We have previously shown that isoflurane anesthesia does not mask effects of antihypertensive agents [5]. These data showed that systolic blood pressure measurement under a steady isoflurane anesthesia can be reliably used to monitor changes in blood pressure in mice.

Stereotaxic Injection of Elastase

The detailed method for the single stereotaxic injection of elastase into the cerebrospinal fluid at the right basal cistern has been described previously [2]. Briefly, the tip of a 26-gauge needle (10 μ l syringe, Model 701, with 26 g 2 inches,

Hamilton Replacement needle Point style 3, Fisher Scientific) was stereotaxically placed in the right basal cistern using the coordinates obtained from Mouse Brain Atlas (2.4–2.8 mm posterior to the bregma, 0.9–1.1 mm lateral to the midline, and 4.9–5.1 mm ventral to the skull surface). Elastase (E7885, porcine pancreatic elastase, lyophilized powder, 20 mg, Sigma Aldrich) was dissolved in PBS, and 2.5 μl of the elastase solution (0–35 milli-units) was injected at 0.2 $\mu\text{l}/\text{min}$. This part of the procedure will take approximately 30–40 min. Significant variations may exist in the potency of elastase activity in different lots or different preparations of commercially available elastase [7, 8]. It may be prudent to use elastase from the same lot in each set of experiments.

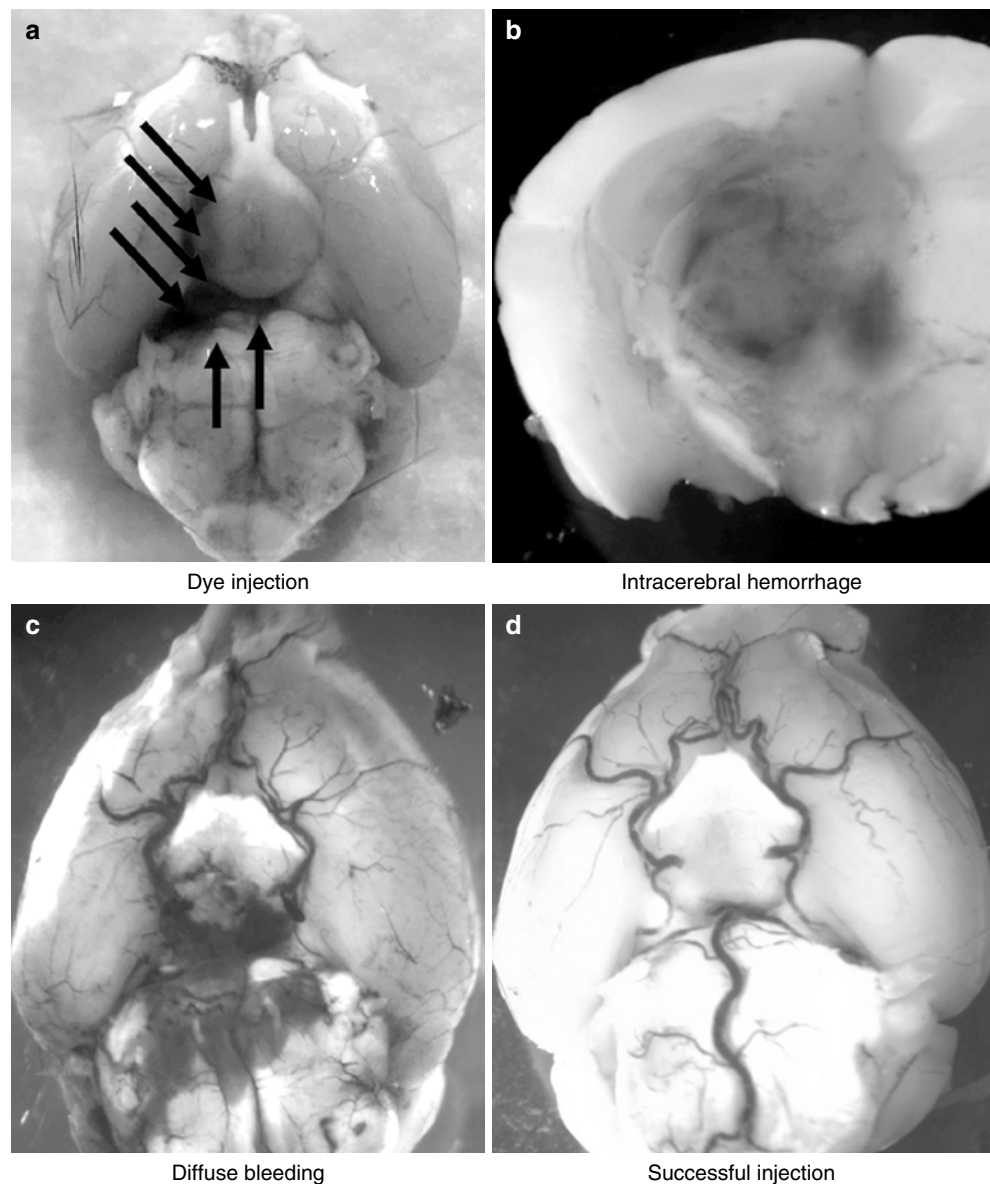
In our experience, we found that the stereotaxic coordinates need to be adjusted depending on the operator and the age of mice. Therefore, a series of test injections using dye

(bromophenol blue) was extremely important to ensure the correct placement of the needle tip at the right basal cistern. The coordinates we described in the original paper [2] should be regarded as a guideline. Each researcher should perform a series of test injections to adjust for the appropriated coordinates before starting the actual experiments. Figure 3a shows a result of typical successful test injections. The mouse was sacrificed immediately after injection; bromophenol blue dye was observed along the right half of the circle of Willis. It appears that at least ten test injections are needed before each operator establishes the appropriate coordinates that yield stable aneurysm induction. We routinely perform a test injection once every ten mice to ensure the correct needle placement.

The depth of the needle is another critical factor for the successful induction of aneurysm in this model. If the needle depth is too shallow, the injection of elastase into the brain

Fig. 3 Inspection of brain tissues 1 day after injection of dye or elastase. **(a)** Test injection of dye. Immediately after a stereotaxic injection of bromophenol blue (2.5 μl) into the cerebrospinal fluid at the right basal cistern, the mouse brain was extracted. The dye was observed along the right half of the circle of Willis. Arrows indicate the dye.

(b) Intracerebral hemorrhage due to elastase injection into the brain parenchyma. If the needle depth is too shallow, an injection of elastase results in intracerebral hemorrhage. **(c)** Diffuse bleeding from the brain surface. If the needle tip is too close to the surface of the brain, the injection of elastase into the cerebrospinal fluid can result in diffuse hemorrhage from the surface of the brain, even when the needle tip is inside the subarachnoid space. **(d)** Successful injection of elastase. When the brain was inspected 1 day after elastase injection, there was no diffuse bleeding from the surface of the brain or intracerebral hemorrhage, indicating a successful placement of the needle



parenchyma results in intracerebral hemorrhage similar to the collagenase-induced intracerebral hemorrhage (Fig. 3b) [9–11]. If the needle tip is too close to the surface of the brain, the injection of elastase into the cerebrospinal fluid can result in diffuse hemorrhage from the surface of the brain, even when the needle tip is inside the subarachnoid space (Fig. 3c). This might be due to compartmentalization of the subarachnoid space.

We recommend that the operator should find the depth at which the needle tip touches the surface of the dura matter or skull base. Then, the operator can use the depth that is approximately 0.3–0.4 mm shallower than the dura or skull base for subsequent test injections using dye. The spread of dye along the right half of the circle of Willis should be confirmed (Fig. 3a). If the dura matter is intensely stained with the dye, subdural injection should be suspected. After establishing the needle depth for successful injections, the operator should perform test injections of elastase and sacrifice the animals 1 day after injection. Lack of diffuse bleeding from the surface of the brain or intracerebral hemorrhage would indicate the successful placement of the needle (Fig. 3d).

The surgical procedures for the aneurysm induction seem to cause significant perioperative stress to mice. Water intake of some of the postoperative mice seemed to have decreased during the first 2 postoperative days. Therefore, we inject 500 μ l of saline subcutaneously once a day for the first 2 postoperative days in all mice.

Conclusion

Elastase-induced intracranial aneurysms in hypertensive mice represents an easily reproducible animal model that yields a high incidence of large intracranial aneurysms within a practical incubation time. There are several technical issues that are critical for the successful use of this model. This model can be used to study molecular pathways that are potentially involved in the pathophysiology of intracranial aneurysms.

Sources of Funding This study was funded by NIH R01NS055876 (TH) and NIH P01NS044155 (TH).

Conflict of interest statement We declare that we have no conflict of interest.

References

1. Shi C, Awad IA, Jafari N, Lin S, Du P, Hage ZA, Shenkar R, Getch CC, Bredel M, Batjer HH, Bendok BR (2009) Genomics of human intracranial aneurysm wall. *Stroke* 40:1252–1261
2. Nuki Y, Tsou TL, Kurihara C, Kanematsu M, Kanematsu Y, Hashimoto T (2009) Elastase-induced intracranial aneurysms in hypertensive mice. *Hypertension* 54:1337–1344
3. Hashimoto T, Meng H, Young WL (2006) Intracranial aneurysms: links between inflammation, hemodynamics and vascular remodeling. *Neurol Res* 28:372–380
4. Daugherty A, Manning MW, Cassis LA (2000) Angiotensin II promotes atherosclerotic lesions and aneurysms in apolipoprotein E-deficient mice. *J Clin Invest* 105:1605–1612
5. Kanematsu Y, Kanematsu M, Kurihara C, Tsou TL, Nuki Y, Liang EI, Makino H, Hashimoto T (2010) Pharmacologically induced thoracic and abdominal aortic aneurysms in mice. *Hypertension* 55:1267–1274
6. Weiss D, Kools JJ, Taylor WR (2001) Angiotensin II-induced hypertension accelerates the development of atherosclerosis in apoE-deficient mice. *Circulation* 103:448–454
7. Carsten CG III, Calton WC, Johanning JM, Armstrong PJ, Franklin DP, Carey DJ, Elmore JR (2001) Elastase is not sufficient to induce experimental abdominal aortic aneurysms. *J Vasc Surg* 33:1255–1262
8. Ding YH, Danielson MA, Kadirvel R, Dai D, Lewis DA, Cloft HJ, Kallmes DF (2006) Modified technique to create morphologically reproducible elastase-induced aneurysms in rabbits. *Neuroradiology* 48:528–532
9. Kitaoka T, Hua Y, Xi G, Hoff JT, Keep RF (2002) Delayed argatroban treatment reduces edema in a rat model of intracerebral hemorrhage. *Stroke* 33:3012–3018
10. Rosenberg GA, Mun-Bryce S, Wesley M, Kornfeld M (1990) Collagenase-induced intracerebral hemorrhage in rats. *Stroke* 21:801–807
11. Tang J, Liu J, Zhou C, Alexander JS, Nanda A, Granger DN, Zhang JH (2004) Mmp-9 deficiency enhances collagenase-induced intracerebral hemorrhage and brain injury in mutant mice. *J Cereb Blood Flow Metab* 24:1133–1145

The Postpartum Period of Pregnancy Worsens Brain Injury and Functional Outcome After Cerebellar Hemorrhage in Rats

Tim Lekic, Robert P. Ostrowski, Hidenori Suzuki, Anatol Manaenko, William Rolland, Nancy Fathali, Jiping Tang, and John H. Zhang

Abstract *Background:* Intracerebral hemorrhage (ICH) is one of the most common causes of maternal deaths related to the postpartum period. This is a devastating form of stroke for which there is no available treatment. Although premenopausal females tend to have better outcomes after most forms of brain injury, the effects of pregnancy and child birth lead to wide maternal physiological changes that may predispose the mother to an increased risk for stroke and greater initial injury.

Methods: Three different doses of collagenase were used to generate models of mild, moderate and severe cerebellar hemorrhage in postpartum female and male control rats. Brain water, blood-brain barrier rupture, hematoma size and neurological evaluations were performed 24 h later.

Results: Postpartum female rats had worsened brain water, blood-brain barrier rupture, hematoma size and neurological evaluations compared to their male counterparts.

Conclusion: The postpartum state reverses the cytoprotective effects commonly associated with the hormonal neuroprotection of (premenopausal) female gender, and leads to greater initial injury and worsened neurological function after cerebellar hemorrhage. This experimental model can be used

for the study of future treatment strategies after postpartum brain hemorrhage, to gain a better understanding of the mechanistic basis for stroke in this important patient subpopulation.

Keywords Postpartum · Neurological deficits · Intracerebral hemorrhage · Stroke

Introduction

Intracerebral hemorrhage (ICH) is a devastating complication of pregnancy that accounts for 1 out of 14 deaths within this subpopulation in the United States [1]. ICH is the least treatable form of stroke [2] and has an approximate 20% mortality rate when related to pregnancy [1]. Survivors retain significant brain injury and life-long neurological deficits [3, 4], with most rehabilitating patients remaining unable to be “independent” 6 months later [5]. Matched for age and gender, the relative risk for ICH is increased 30-fold during the postpartum period [6].

Almost half of the cases of postpartum ICH occur in patients with eclampsia [7], and this is associated with hemostatic elevations of aquaporin-4 (AQP4) expression, brain edema and blood-brain barrier (BBB) disruption [8]. The cerebellum contains some of the highest levels of AQP4 [9] and is one of the brain locations with the greatest AQP4 increases during the postpartum period [10]. Therefore, this brain region could be a good model to study maternal mechanisms of ICH occurring during the postpartum period.

Clostridial collagenase is a stereotaxically infused enzyme that mimics spontaneous (ICH) vascular rupture, permitting investigations targeting hemostasis and neurobehavioral outcome [11–17]. We therefore hypothesized that unilateral cerebellar collagenase infusion in postpartum rats could model important clinical features [18–24]. This experimental approach may increase the pathophysiological understanding of this disease to direct future applications of therapeutic interventions [25].

T. Lekic, R.P. Ostrowski, H. Suzuki, A. Manaenko, W. Rolland, and J. Tang
Departments of Physiology, Loma Linda University,
School of Medicine, Loma Linda, CA 92354, USA

N. Fathali
Department of Human Pathology and Anatomy, Loma Linda
University, School of Medicine, Loma Linda CA 92354, USA

J.H. Zhang (✉)
Departments of Physiology, Loma Linda University,
School of Medicine, Loma Linda, CA 92354, USA and
Department of Human Pathology and Anatomy, Loma Linda
University, School of Medicine, Loma Linda CA 92354, USA and
Department of Neurosurgery, Loma Linda University,
School of Medicine, Loma Linda, CA 92354, USA and
Department of Physiology, Loma Linda University,
School of Medicine, Riskey Hall, Room 223, Loma Linda,
CA, 92354, USA
e-mail: johnzhang3910@yahoo.com

Materials and Methods

The Animals and General Procedures

One hundred and nine adult Sprague-Dawley rats (290–345 g; Harlan, Indianapolis, IN) were used. All procedures were in compliance with the *Guide for the Care and Use of Laboratory Animals* and approved by the Animal Care and Use Committee at Loma Linda University. Surgeries were carried out using isoflurane anesthesia with aseptic techniques, and animals were given food and water during recovery [13, 14].

Model of Cerebellar Hemorrhage

Anesthetized animals were secured prone onto a stereotaxic frame (Kopf Instruments, Tujunga, CA) before an incision was made over the scalp. The following stereotaxic coordinates were measured from the bregma: 11.6 mm (caudal), 2.4 mm (lateral) and 3.5 mm (deep). A (1-mm) borehole was drilled, and then a 27-gauge needle was inserted. Collagenase VII-S (0.2 U/ μ l, Sigma, St Louis, MO) was infused by microinfusion pump (rate=0.2 μ l/min, Harvard Apparatus, Holliston, MA). The syringe remained in place for 10 min to prevent back-leakage before being withdrawn. Then the borehole was sealed with bone wax, the incision sutured closed and animals allowed to recover. Control surgeries consisted of needle insertion alone. A thermostat-controlled heating blanket maintained the core temperature (37.0°C \pm 0.5°C) throughout the operation.

Cerebellar Water

Water content was measured using the wet-weight/dry-weight method [26]. Quickly after sacrifice the brains were removed, and tissue weights were determined before and after drying for 24 h in a 100°C oven, using an analytical microbalance (model AE 100; Mettler Instrument Co., Columbus, OH) capable of measuring with 1.0- μ g precision. The data were calculated as the percentage of water content: (wet weight – dry weight)/wet weight \times 100.

Neurological Score

This was assessed using a modified Luciani scale [24], which is a summation of scores (maximum=9) given for (1) decreased body tone, (2) ipsilateral limb extensions and (3) dyscoordination (0=severe, 1=moderate, 2=mild, 3=none). Scores are represented as percent of sham.

Animal Perfusion and Tissue Extraction

Animals were fatally anesthetized with isoflurane (\geq 5%) followed by cardiovascular perfusion with ice-cold PBS for the hemoglobin and Evans blue assays, and immunoblot analyses. The cerebella were then dissected and snap-frozen with liquid nitrogen and stored in –80°C freezer, before spectrophotometric quantifications or protein extraction.

Hematoma Volume

The spectrophotometric hemoglobin assay was performed as previously described [26], where extracted cerebellar tissue was placed in glass test tubes with 3 mL of distilled water, then homogenized for 60 s (Tissue Miser Homogenizer; Fisher Scientific, Pittsburgh, PA). Ultrasonication for 1 min lysed erythrocyte membranes (then centrifuged for 30 min), and Drabkin's reagent was added (Sigma-Aldrich) into aliquots of supernatant that reacted for 15 min. Absorbance, using a spectrophotometer (540 nm; Genesis 10uv; Thermo Fisher Scientific, Waltham, MA), was calculated into hemorrhagic volume on the basis of a standard curve [27].

Vascular Permeability

Under general anesthesia, the left femoral vein was catheterized for 2% intravenous Evans blue injection (5 ml/kg; 1 h circulation). Extracted cerebellar tissue was weighed, homogenized in 1 ml PBS, then centrifuged for 30 min, after which 0.6 ml of the supernatant was added with equal volumes of trichloroacetic acid, followed by overnight incubation and re-centrifugation. The final supernatant underwent spectrophotometric quantification (615 nm; Genesis 10uv; Thermo Fisher Scientific, Waltham, MA) of extravasated dye, as described [28].

Western Blotting

As routinely done [26], the concentration of protein was determined using DC protein assay (Bio-Rad, Hercules, CA). Samples were subjected to SDS-PAGE, then transferred to a nitrocellulose membrane for 80 min at 70 V (Bio-Rad). Blotting membranes were incubated for 2 h with 5% nonfat milk in Tris-buffered saline containing 0.1% Tween 20 and then incubated overnight with the following primary antibodies: anti-AQP4 (1:200; Santa Cruz Biotechnology, Santa Cruz, CA), anti-collagen IV (1:500; Chemicon,

Temecula, CA) and anti-zonula occludens (ZO)-1 (1:500; Invitrogen Corp., Carlsbad, CA). This was followed by incubation with secondary antibodies (1:2,000; Santa Cruz Biotechnology) and processed with ECL plus kit (Amersham Bioscience, Arlington Heights, Ill). Images were analyzed semiquantitatively using Image J (4.0, Media Cybernetics, Silver Spring, MD).

Statistical Analysis

Statistical significance was considered at $P < 0.05$. Data were analyzed using analysis of variance (ANOVA). Significant interactions were explored with T -test (unpaired) and Mann-Whitney rank sum test when appropriate.

Results

Collagenase infusion led to dose-dependent elevations of cerebellar water and neurodeficit (Figs. 1a, b). Compared to male controls, cerebellar water was significantly elevated in postpartum females at 0.2 and 0.4 units collagenase and neurodeficit across all doses ($P < 0.05$). Kaplan-Meier survival analysis demonstrated a significantly increased mortality rate (Fig. 1c, $P < 0.05$) in postpartum females (approximately 30%) compared to male controls (0%). Collagenase infusion (0.6 U) led to a greater hematoma size (Fig. 2a) and vascular permeability (Fig. 2b) in postpartum females compared to male controls ($P < 0.05$). Immunoblots of shams (Fig. 3a) showed greater AQP4, and diminished COL-4 (collagen-IV) and ZO-1 expressions in postpartum females compared to male controls ($P < 0.05$), while collagenase infusion (0.6 U) injury was equivalent and did not cause any additional changes compared to respective shams (Fig. 3b, $P < 0.05$).

Discussion

Intracerebral hemorrhage (ICH) is the least treatable form of stroke clinically and is a devastating complication after pregnancy accompanied by life-long neurodeficits [1–6]. This study infused collagenase into the unilateral (right) side of the cerebellar hemisphere of postpartum rats as an approach to model these features, since available animal models to study the pathophysiological basis of these outcomes are lacking.

Our results are in support of the clinical evidence for cerebral vascular vulnerability in the postpartum period. Around half of the cases of ICH in this patient population will have eclampsia [7], and this is related to hemostatically relevant increases of aquaporin-4 (AQP4) expression, blood-brain

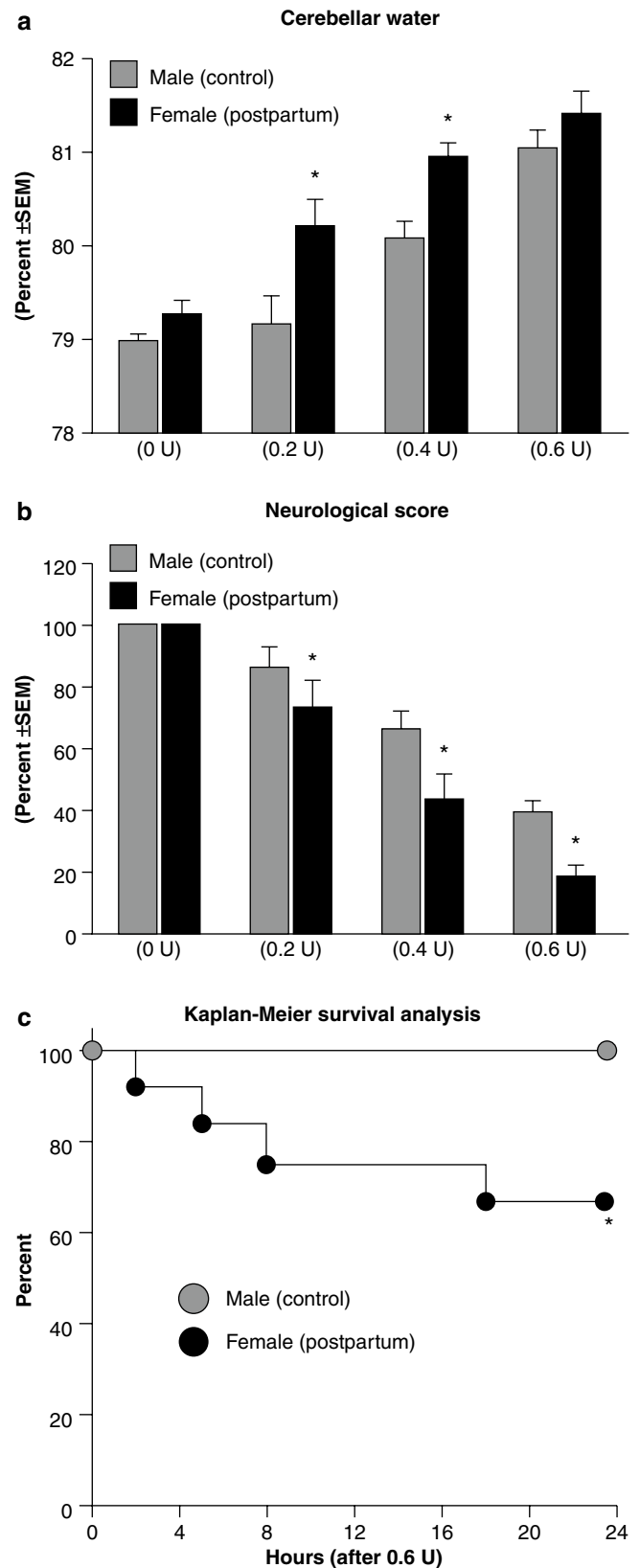


Fig. 1 Postpartum worsens outcomes at 24 h after collagenase infusion. (a) Cerebellar water, (b) neurological score and (c) survival analysis; groups consisted of males (control) and females (postpartum), receiving doses of 0, 0.2, 0.4 and 0.6 units collagenase. The values are expressed as mean \pm SEM, $n = 5$ (per group), * $P < 0.05$ compared with male (control)

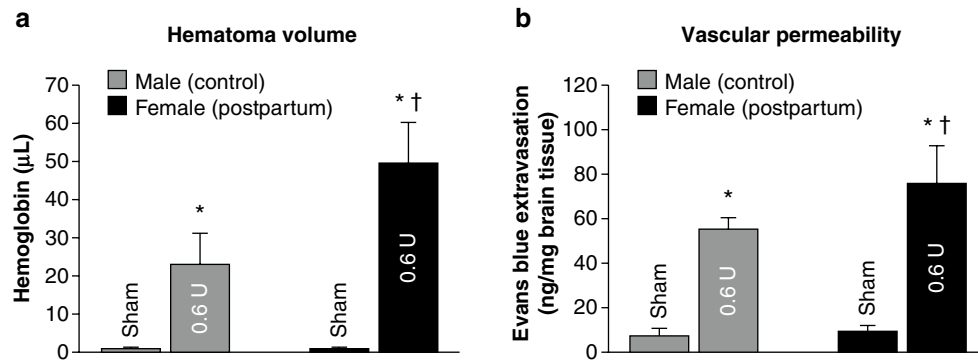


Fig. 2 Postpartum increases vascular rupture at 24 h after collagenase infusion. (a) Hematoma volume and (b) vascular permeability; the values are expressed as mean \pm SD. Groups consisted of males (control)

and female (postpartum), receiving doses of 0 and 0.6 units collagenase, $n=5$ (per group), * $P<0.05$ compared with respective shams and † $P<0.05$ compared with male (0.6 units, control)

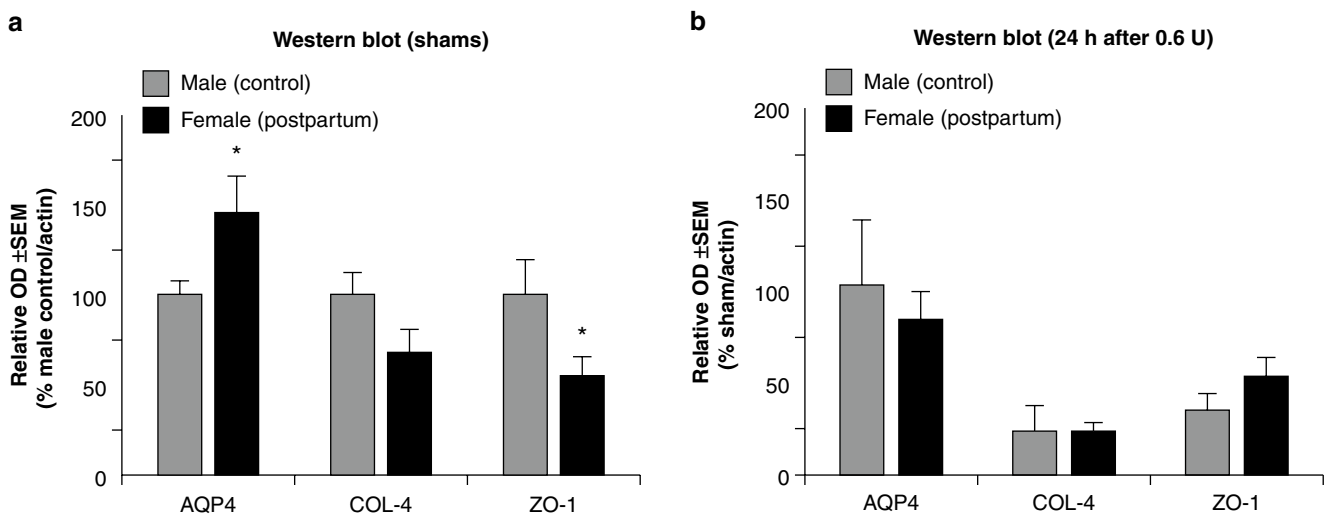


Fig. 3 Postpartum rats have increased vascular vulnerability. (a and b) Semi-quantification of immunoblots for AQP4, collagen-IV (COL-4) and ZO-1 groups consisted of males (control) and females (postpartum),

receiving doses of 0 and 0.6 units of collagenase. The values are expressed as mean \pm SEM, $n=5$ (per group), * $P<0.05$ compared with males (control)

barrier (BBB) disruption and brain edema [8]. In agreement, we found greater AQP4, and diminished COL-4 (collagen-IV) and ZO-1 expressions in the cerebella of postpartum female shams compared to the male controls. The collagenase model is an ideal method for study since it did not alter these levels any further; however, the increased vascular vulnerability in postpartum animals led to greater brain edema, neurodeficit, BBB rupture and hematoma size across most doses studied. The lack of significant difference in cerebellar water at the highest collagenase dose (0.6 U) is likely either a reflection of mortality (i.e., severely injured animals died) or due to the high baseline AQP4 expressions leading to an edematous outflow.

In summary, we have characterized a highly reliable and easily reproducible experimental model of intracerebral hemorrhage using postpartum rats. Since the cerebellum contains some of the highest levels of AQP4 [9] with the greatest AQP4 increase during the postpartum period [10], this ICH model provides a basis for studying the clinical and

pathophysiological features of this disease while establishing a foundation for performing further preclinical therapeutic investigations.

Acknowledgement This study is partially supported by NIH NS053407 to J.H. Zhang and NS060936 to J. Tang.

Conflict of interest statement We declare that we have no conflict of interest.

References

- Bateman BT, Schumacher HC, Bushnell CD, Pile-Spellman J, Simpson LL, Sacco RL, Berman MF (2006) Intracerebral hemorrhage in pregnancy: frequency, risk factors, and outcome. *Neurology* 67:424–429. doi:67/3/424 [pii] 10.1212/01.wnl.0000228277.84760.a2
- Ciccone A, Pozzi M, Motto C, Tiraboschi P, Sterzi R (2008) Epidemiological, clinical, and therapeutic aspects of primary

- intracerebral hemorrhage. *Neurol Sci* 29(Suppl 2):S256–257. doi:10.1007/s10072-008-0955-9
3. Skriver EB, Olsen TS (1986) Tissue damage at computed tomography following resolution of intracerebral hematomas. *Acta Radiol Diagn (Stockh)* 27:495–500
 4. Broderick JP, Adams HP Jr, Barsan W, Feinberg W, Feldmann E, Grotta J, Kase C, Krieger D, Mayberg M, Tilley B, Zabramski JM, Zuccarello M (1999) Guidelines for the management of spontaneous intracerebral hemorrhage: a statement for healthcare professionals from a special writing group of the Stroke Council, American Heart Association. *Stroke* 30:905–915
 5. Gebel JM, Broderick JP (2000) Intracerebral hemorrhage. *Neurol Clin* 18:419–438
 6. Kittner SJ, Stern BJ, Feeser BR, Hebel R, Nagey DA, Buchholz DW, Earley CJ, Johnson CJ, Macko RF, Sloan MA, Wityk RJ, Wozniak MA (1996) Pregnancy and the risk of stroke. *N Engl J Med* 335:768–774
 7. Sharshar T, Lamy C, Mas JL (1995) Incidence and causes of strokes associated with pregnancy and puerperium. A study in public hospitals in Ile France. Stroke Pregnancy Study Group. *Stroke* 26:930–936
 8. Quick AM, Cipolla MJ (2005) Pregnancy-induced up-regulation of aquaporin-4 protein in brain and its role in eclampsia. *FASEB J* 19:170–175. doi:10.1096/fj.04-1901hyp
 9. Verkman AS (2002) Physiological importance of aquaporin water channels. *Ann Med* 34:192–200
 10. Wiegman MJ, Bullinger LV, Kohlmeyer MM, Hunter TC, Cipolla MJ (2008) Regional expression of aquaporin 1, 4, and 9 in the brain during pregnancy. *Reprod Sci* 15:506–516. doi:10.1177/1933719107311783
 11. Foerch C, Arai K, Jin G, Park KP, Pallast S, van Leyen K, Lo EH (2008) Experimental model of warfarin-associated intracerebral hemorrhage. *Stroke* 39:3397–3404. doi:10.1161/STROKEAHA.108.517482
 12. MacLellan CL, Silasi G, Poon CC, Edmundson CL, Buist R, Peeling J, Colbourne F (2008) Intracerebral hemorrhage models in rat: comparing collagenase to blood infusion. *J Cereb Blood Flow Metab* 28:516–525. doi:10.1038/sj.jcbfm.9600548
 13. Lekic T, Hartman R, Rojas H, Manaenko A, Chen W, Ayer R, Tang J, Zhang JH (2010) Protective effect of melatonin upon neuropathology, striatal function, and memory ability after intracerebral hemorrhage in rats. *J Neurotrauma* 27:627–637. doi:10.1089/neu.2009.1163
 14. Hartman R, Lekic T, Rojas H, Tang J, Zhang JH (2009) Assessing functional outcomes following intracerebral hemorrhage in rats. *Brain Res* 1280:148–157. doi:10.1016/j.brainres.2009.05.038
 15. Andaluz N, Zuccarello M, Wagner KR (2002) Experimental animal models of intracerebral hemorrhage. *Neurosurg Clin N Am* 13:385–393
 16. Thiex R, Mayfrank L, Rohde V, Gilsbach JM, Tsirka SA (2004) The role of endogenous versus exogenous tPA on edema formation in murine ICH. *Exp Neurol* 189:25–32. doi:10.1016/j.expneurol.2004.05.021S0014488604001840 [pii]
 17. Rosenberg GA, Mun-Bryce S, Wesley M, Kornfeld M (1990) Collagenase-induced intracerebral hemorrhage in rats. *Stroke* 21:801–807
 18. Rosenberg GA, Kaufman DM (1976) Cerebellar hemorrhage: reliability of clinical evaluation. *Stroke* 7:332–336
 19. St Louis EK, Wijdicks EF, Li H (1998) Predicting neurologic deterioration in patients with cerebellar hematomas. *Neurology* 51:1364–1369
 20. Kelly PJ, Stein J, Shafiqat S, Eskey C, Doherty D, Chang Y, Kurina A, Furie KL (2001) Functional recovery after rehabilitation for cerebellar stroke. *Stroke* 32:530–534
 21. Dolderer S, Kallenberg K, Aschoff A, Schwab S, Schwarz S (2004) Long-term outcome after spontaneous cerebellar haemorrhage. *Eur Neurol* 52:112–119. doi:10.1159/000080268 ENE2004052002112 [pii]
 22. Thach WT (1996) On the specific role of the cerebellum in motor learning and cognition: clues from PET activation and lesion studies in man. *Behav Brain Sci* 19:411–431
 23. Strick PL, Dum RP, Fiez JA (2009) Cerebellum and nonmotor function. *Annu Rev Neurosci* 32:413–434. doi:10.1146/annurev.neuro.31.060407.125606
 24. Baillieux H, De Smet HJ, Paquier PF, De Deyn PP, Marien P (2008) Cerebellar neurocognition: insights into the bottom of the brain. *Clin Neurol Neurosurg* 110:763–773. doi:10.1016/j.clineuro.2008.05.013 [pii]
 25. NINDS ICH Workshop Participants (2005) Priorities for clinical research in intracerebral hemorrhage: report from a National Institute of Neurological Disorders and Stroke workshop. *Stroke* 36:e23–41. doi:10.1161/01.STR.0000155685.77775.4c [pii]
 26. Tang J, Liu J, Zhou C, Alexander JS, Nanda A, Granger DN, Zhang JH (2004) Mmp-9 deficiency enhances collagenase-induced intracerebral hemorrhage and brain injury in mutant mice. *J Cereb Blood Flow Metab* 24:1133–1145. doi:10.1006/j.cbfm.2004.10000-00007 [pii]
 27. Choudhri TF, Hoh BL, Solomon RA, Connolly ES Jr, Pinsky DJ (1997) Use of a spectrophotometric hemoglobin assay to objectively quantify intracerebral hemorrhage in mice. *Stroke* 28:2296–2302
 28. Saria A, Lundberg JM (1983) Evans blue fluorescence: quantitative and morphological evaluation of vascular permeability in animal tissues. *J Neurosci Methods* 8:41–49

Hyperglycemia and Hemorrhagic Transformation of Cerebral Infarction: A Macroscopic Hemorrhagic Transformation Rat Model

Tamiji Tsubokawa, Hiroo Joshita, Yoshiaki Shiokawa, and Hiroshi Miyazaki

Abstract The recombinant tissue plasminogen activator (t-PA) is a useful therapy for acute ischemic stroke patients, but there is a major risk factor of hemorrhagic transformation. Hyperglycemic patients are not able to admit t-PA because hyperglycemia exaggerates ischemic brain and vascular damage following transient focal cerebral ischemia and frequently induces hemorrhagic transformation of the infarct during reperfusion. However, the mechanisms underlying hemorrhagic transformation induced by hyperglycemia are still unknown. Furthermore, previous reports focused upon microscopic hemorrhage rather than macroscopic hemorrhagic transformation. In order to make these problems clear, it is necessary to establish an experimental model that induces constant macroscopic hemorrhagic transformation in the infarct area caused by middle cerebral artery occlusion and the reperfusion model on the hyperglycemic rat. This experimental study can establish the model in which macroscopic hemorrhagic transformation occurs following 1.5 h occlusion and 24 h reperfusion by using the intraluminal thread method on hyperglycemic rats. It might be useful to determine the mechanisms and understand why hyperglycemia exaggerates the causes inducing macroscopic hemorrhagic transformation in the infarct area, and this reproducible model provides a platform for evaluating treatment strategies.

Keywords Hemorrhagic transformation · Hyperglycemia · Ischemia · Reperfusion

Introduction

Hyperglycemia is risk factor for aggravated brain injury during human cerebral ischemia [1, 2]. Although thrombolytic therapy with tissue plasminogen activator (tPA) in ischemic stroke can improve clinical outcome when delivered soon after stroke onset [3], tPA also increases the risk of hemorrhagic transformation [4, 5]. It is also reported that hyperglycemia aggravates ischemic injury after reperfusion, causing hemorrhagic transformation for hyperglycemia in treatment with t-PA usage [6, 7].

In experimental transient ischemia models using hyperglycemic rats, blood brain barrier (BBB) disruption is caused mainly by severe oxidative stress with increased activity of matrix metalloproteinase-9 (MMP-9) in the ischemic area during reperfusion [8–13]. Recently studies have suggested that hyperglycemia exacerbates hemorrhagic transformation [7, 12, 13].

However, the mechanisms underlying hemorrhagic transformation induced by hyperglycemia are still unknown. Furthermore, previous reports focused upon microscopic hemorrhage rather than macroscopic hemorrhagic transformation. In this study, we established a macroscopic hemorrhagic infarct model in the hyperglycemic rat to study mechanisms underlying the human observation that hyperglycemia worsens stroke outcome.

Materials and Methods

The experimental protocol was approved by the Local Animal Care Committee of Saitama Cardiovascular and Respiratory Center. Twenty-four adult male Sprague-Dawley

T. Tsubokawa (✉)

Department of Neurosurgery, Saitama Cardiovascular and Respiratory Center, Kumagaya, Saitama, Japan and
Department of Neurosurgery, Kyorin University, Tokyo, Japan and
Department of Neurosurgery, Saitama Cardiovascular and Respiratory Center, 1696 Itai, Kumagaya, Saitama, 360-0105, Japan
e-mail: tsubokawa-nsu@umin.ac.jp

H. Joshita

Department of Neurosurgery, Saitama Cardiovascular and Respiratory Center, Kumagaya, Saitama, Japan

Y. Shiokawa

Department of Neurosurgery, Kyorin University, Tokyo, Japan

H. Miyazaki

Department of Neurosurgery, Kugayama Hospital, Tokyo, Japan

rats weighing between 270 and 350 g were divided randomly into two groups: the normoglycemia and hyperglycemia groups.

A preliminary study was performed to determine the adequate occlusion time for inducing BBB dysfunction, infarct with brain edema and mortality. In accordance with the results of the preliminary experiment [14], in this experiment, 1.5 h ischemia and 24 h reperfusion are applied as a transient reperfusion model.

Middle Cerebral Artery Occlusion (MCAO) and Reperfusion Model

Rats were weighed prior to surgery. Anesthesia was induced with ketamine (80 mg/kg i.p.) and xylazine hydrochloride (8 mg/kg i.p.) followed by atropine (0.1 mg/kg i.s). A heating pad and a heating lamp were used to maintain the rectal temperature between $36.5 \pm 0.5^\circ\text{C}$. Rats were intubated, and respiration was maintained with a small animal respirator. Rats were subjected to MCAO as described by Yin et al. [15], with some modifications. Briefly, with the use of an operating microscope, the left common carotid artery, internal carotid artery (ICA) and external carotid artery (ECA) were surgically exposed. The ECA was then isolated and coagulated. A 4–0 silicon-coated nylon suture (Doccol Co., Albuquerque, NM) was inserted into the ICA through the ECA stump and gently advanced to occlude the MCA. The mean arterial blood pressure, heart rate, arterial blood gases and blood glucose levels before, during, and after ischemia were analyzed. After 90 min of MCA occlusion, the suture was removed to restore blood flow, the neck incision was closed, and the rats were allowed to recover. After the experiment, the animals were housed individually until sacrifice. All animals had free access to food and water.

Hyperglycemia Model

Hyperglycemia was induced by intraperitoneal injection of 50% glucose (5 mL/kg) after anesthesia, and the blood sugar level was 507 ± 51.4 mg/dL at 15 min after injection. On the other hand, the blood sugar level was 183 ± 32.8 mg/dL in the normoglycemia group.

Macroscopic Observation and TTC Staining

Two groups were used for evaluation of infarction volume. At 24 h after MCAO, rats were deeply anesthetized

with ketamine and perfused transcardially with ice-cold phosphate-buffered saline. Then rats were decapitated, and the brains were rapidly removed. All brains were carefully evaluated for macroscopic hemorrhagic changes before 2% 2,3,5-triphenyltetrazolium chloride (TTC; Sigma, Germany) staining. The tissue was sliced into 2-mm-thick coronal sections, and the slices were stained in TTC for 30 min at 37°C in the dark [15]. Four coronal sections per animal were then photographed. TTC stains both neuronal and glial cells with a deep red pigment. In areas where neuronal loss occurs, TTC does not stain and tissue remains white.

Morphological Assessment

At 24 h after the MCAO, the rats were anesthetized, and transcardially perfused with PBS and 4% paraformaldehyde as described previously [15]. For hematoxylin and eosin staining, slices were stained with hematoxylin for 3 min and eosin for 30 s.

Statistics

Data are presented as means \pm SEM. Statistical differences between the various groups were assessed by a Mann-Whitney rank sum test. A value of $p < 0.05$ was considered statistically significant.

Results

Physiological Data

No statistical differences were observed between the normoglycemia and the hyperglycemia groups with regard to mean arterial blood pressure, heart rate, arterial blood gases and body weight. There was a significant difference in blood glucose levels between the normoglycemia group and the hyperglycemia group, as expected.

Brain Infarction and Hemorrhagic Transformation

Hemorrhagic transformation was not observed in the normoglycemia group. Hemorrhagic transformation was

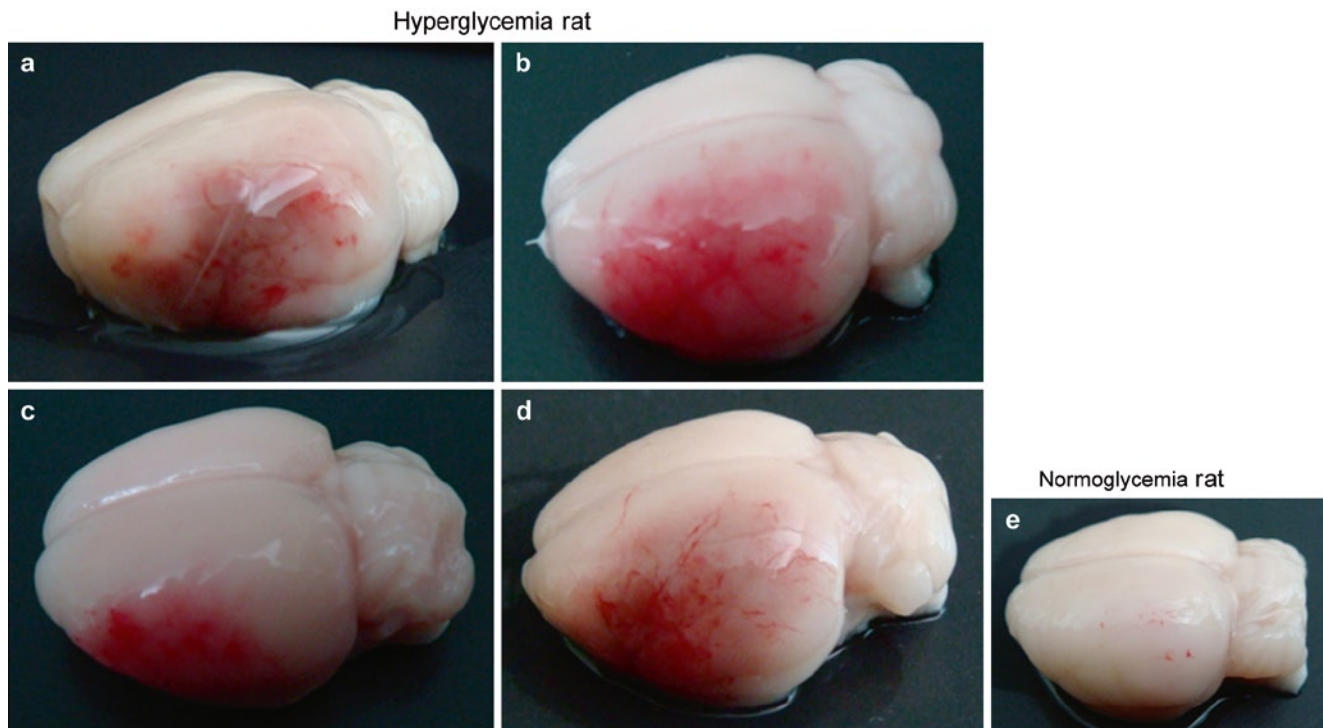


Fig. 1 Hemorrhagic transformation is seen macroscopically in the ipsilateral MCA territory on the hyperglycemia group (a–d). Hemorrhagic transformation is not observed in the normoglycemia group (e)

seen macroscopically in the ipsilateral MCA territory in the hyperglycemia group. All hyperglycemic rats had hemorrhagic transformation in the infarct area, but hemorrhage did not extend outside of the infarct area (Fig. 1). It was significantly increased in the hyperglycemia group to induce hemorrhagic transformation ($p < 0.05$). Representative samples of TTC-stained brain sections in the normoglycemia and hyperglycemia groups are shown in Fig. 2. The H&E staining revealed extravasation of blood from the microvessels into the surrounding brain parenchyma (Fig. 3).

Discussion

Hyperglycemia is linked to a worse outcome after transient ischemia in rats by aggravation of the ischemic change and hemorrhagic transformation in the infarct area [6–13]. The aggravating factors may be related to the severity of ischemic brain damage and capillary endothelium damage caused by oxidative stress and enhanced MMP-9, which induces small pericapillary hemorrhage [8–13]. It has not yet been clearly demonstrated why hyperglycemia

aggravates ischemic reperfusion injuries. Also, it is not yet clear why small pericapillary hemorrhage at the early stage of reperfusion escalates to macroscopic hemorrhage by 24 h after reperfusion in all hyperglycemia rats. There have been no previous reports of macroscopic hemorrhagic transformation, except small blood leakages near broken capillaries in a rat hyperglycemic reperfusion model [7, 11–13].

Therefore, to investigate treatments to prevent aggravation of ischemic-reperfusion brain damage caused by hyperglycemia, it is necessary to establish an ideal ischemic-reperfusion model in order to reproducibly induce hemorrhagic lesions with a consistent size in the infarct area. As shown for the model reported here, consistent macroscopic hemorrhagic transformation in the infarcted area was produced after 50% glucose solution administered as an intraperitoneal injection, followed by 1.5 h of MCA occlusion and 24 h of reperfusion.

This model should prove to be useful for probing mechanisms that connect hyperglycemia to aggravation of reperfusion brain damage, as well as identifying better treatments to inhibit the aggravating effects of hyperglycemia on the reperfusion hemorrhagic transformation.

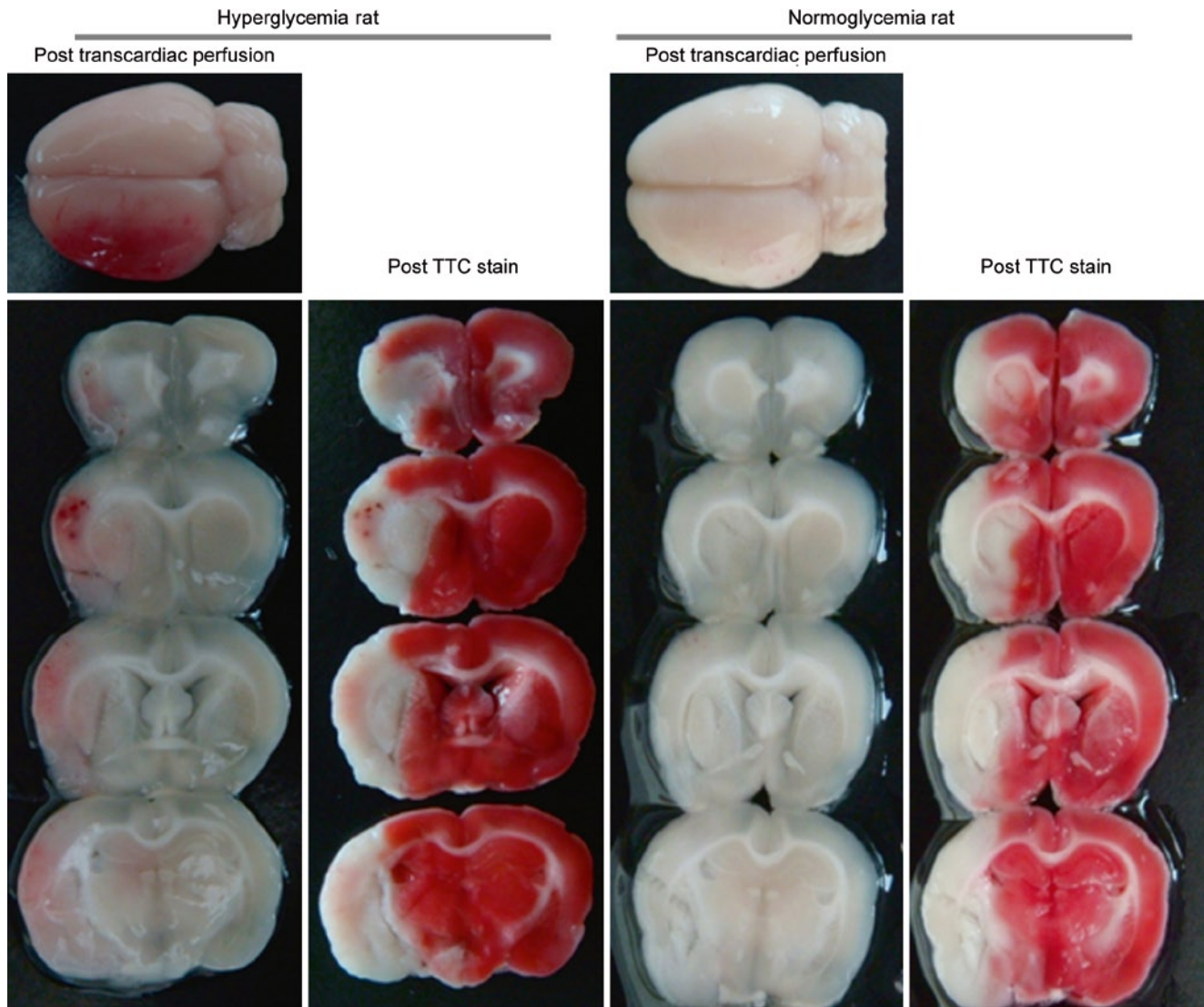


Fig. 2 The area of infarction is demonstrated by TTC staining 1.5 h ischemia/24 h reperfusion at the MCA. Normoglycemia rat is shown on the *left side*, which has an infarct located in the left MCA perfusion area

with slight brain edema, but not any hemorrhage at the infarcted area. On the *right side*, the hyperglycemia rat has hemorrhage in the infarcted area with severe brain edema

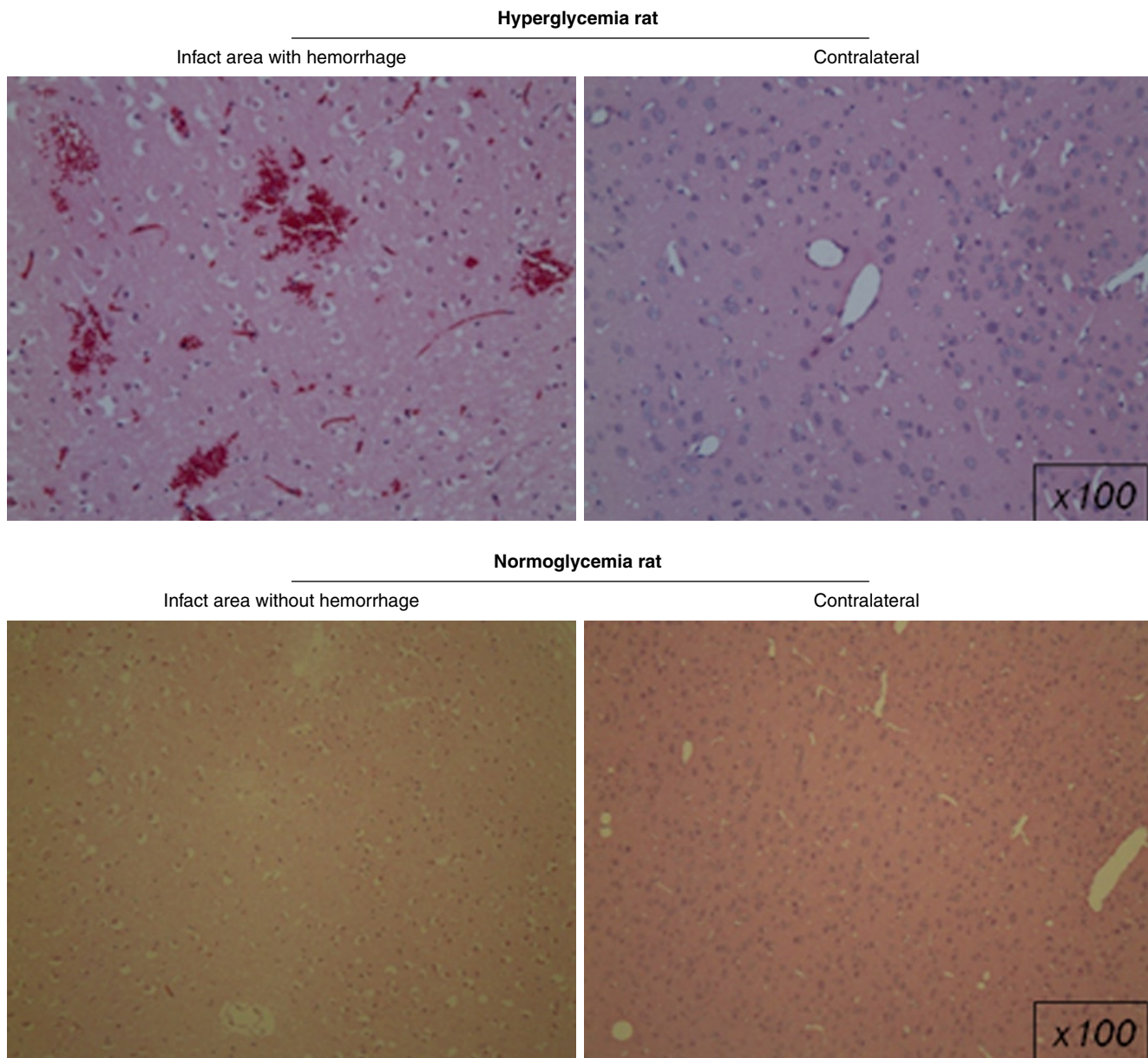


Fig. 3 At 24 h after reperfusion, there is macroscopic hemorrhagic transformation as the erythrocytes leak from the microvessels into the surrounding brain parenchyma on hematoxylin and eosin staining.

But no leakage erythrocytes were observed on the ischemic area in the normoglycemia group

Conflict of interest statement We declare that we have no conflict of interest.

References

1. Kushner M, Nencini P, Reivich M, Rango M, Jamieson D, Fazekas F, Zimmerman R, Chawluk J, Alavi A, Alves W (1990) Relation of hyperglycemia early in ischemic brain infarction to cerebral anatomy, metabolism, and clinical outcome. *Ann Neurol* 28:129–135
2. McCormick MT, Muir KW, Gray CS, Walters MR (2008) Management of hyperglycemia in acute stroke: how, when, and for whom? *Stroke* 39:2177–2185
3. NINDS RT-PA Stroke Study Group (1995) Tissue plasminogen activator for acute ischemic stroke. *N Engl J Med* 333:1581–1587
4. Hacke W, Kaste M, Fieschi C, Toni D, Lesaffre E, Boysen G, Bluhmki E, Hoxter G, Mahagne MH (1995) Intravenous thrombolysis with recombinant tissue plasminogen activator for acute hemispheric stroke. The European Cooperative Acute Stroke Study (ECASS). *JAMA* 274:1017–1025
5. NINDS RT-PA Stroke Study Group (1997) Intracerebral hemorrhage after intravenous t-PA therapy for ischemic stroke. *Stroke* 28:2109–2118

6. Bruno A, Levine SR, Frankel MR, Brott TG, Lin Y, Tilley BC, Lyden PD, Broderick JP, Kwiatkowski TG, Fineberg SE (2002) Admission glucose level and clinical outcomes in the NINDS rt-PA stroke trial. *Neurology* 59:669–674
7. de Courten-Myers GM, Kleinholz M, Holm P, DeVoe G, Schmitt G, Wagner KR, Myers RE (1992) Hemorrhagic infarct conversion in experimental stroke. *Ann Emerg Med* 21:120–126
8. Bemeur C, Ste-Marie L, Montgomery J (2007) Increased oxidative stress during hyperglycemic cerebral ischemia. *Neurochem Int* 50:890–904
9. Dietrich WD, Alonso O, Busto R (1993) Moderate hyperglycemia worsens acute blood-brain barrier injury after forebrain ischemia in rats. *Stroke* 24:111–116
10. Ennis SR, Keep RF (2007) Effect of sustained-mild and transient-severe hyperglycemia on ischemia-induced blood-brain barrier opening. *J Cereb Blood Flow Metab* 27:1573–1582
11. Kamada H, Yu F, Nito C, Chan PH (2007) Influence of hyperglycemia on oxidative stress and matrix metalloproteinase-9 activation after focal cerebral ischemia/reperfusion in rats: relation to blood-brain barrier dysfunction. *Stroke* 38:1044–1049
12. Kawai N, Stummer W, Ennis SR, Betz AL, Keep RF (1999) Blood-brain barrier glutamine transport during normoglycemic and hyperglycemic focal cerebral ischemia. *J Cereb Blood Flow Metab* 19:79–86
13. Qin Z, Karabiyikoglu M, Hua Y, Silbergleit R, He Y, Keep RF, Xi G (2007) Hyperbaric oxygen-induced attenuation of hemorrhagic transformation after experimental focal transient cerebral ischemia. *Stroke* 38:1362–1367
14. Tsubokawa T, Jadhav V, Solaroglu I, Shiokawa Y, Konishi Y, Zhang JH (2007) Lecithinized superoxide dismutase improves outcomes and attenuates focal cerebral ischemic injury via antiapoptotic mechanisms in rats. *Stroke* 38:1057–1062
15. Yin D, Zhou C, Kusaka I, Calvert JW, Parent AD, Nanda A, Zhang JH (2003) Inhibition of apoptosis by hyperbaric oxygen in a rat focal cerebral ischemic model. *J Cereb Blood Flow Metab* 23:855–864

Hemorrhagic Transformation Induced by Acute Hyperglycemia in a Rat Model of Transient Focal Ischemia

Yingqi Xing, Xinmei Jiang, Yi Yang, and Guohua Xi

Abstract Hemorrhagic transformation (HT) is a major factor limiting the use of tissue plasminogen activator for stroke. HT has been found in animals undergoing transient focal cerebral ischemia with hyperglycemia. This study examined the incidence rate, location and content of HT.

Rats were divided into two groups: the hyperglycemic group and normoglycemic group. Rats received an injection of 50% glucose (6 ml/kg, i.p.) or an equivalent volume of saline 15 min before 2-h transient middle cerebral artery occlusion (tMCAO) with reperfusion. Rats were killed 4, 8 or 24 h later and used for blood–brain barrier permeability, hemoglobin content, brain edema, and infarct volume measurements. Mortality and HT incidence rates were also evaluated. We found that all hyperglycemic rats had HT, and two out of six normoglycemic rats had HT 24 h after tMCAO. Hyperglycemic rats had more severe Evans blue leakage ($p < 0.05$) and brain edema ($p < 0.05$) in the ipsilateral hemisphere. However, infarct volumes were the same in hyperglycemic and normoglycemic rats. In conclusion, acute hyperglycemia reliably and

consistently resulted in hemorrhagic transformation in a rat model of transient focal cerebral ischemia. The model is useful for experimental assessment of new therapies for HT.

Keywords Hemorrhagic transformation · Hyperglycemia · Middle cerebral artery occlusion

Introduction

Hemorrhagic transformation (HT) in ischemic stroke is common and represents an almost natural event in the process of cerebral infarction [1–4]. There is currently no effective treatment to limit the occurrence of HT after stroke. A major factor limiting the use of tissue plasminogen activator (tPA) to reduce ischemic brain damage in patients is HT [5, 6].

Hyperglycemia has a major role in post-ischemic HT. In experimental transient middle cerebral artery occlusion (tMCAO) models, acute hyperglycemia increases HT [7]. The present study investigated mortality rate, location and content of HT formation, brain infarct volume, brain edema formation, blood-brain barrier (BBB) permeability, and neurologic deficits after transient focal cerebral ischemia with reperfusion in a hyperglycemic rat model.

Materials and Methods

Animal Preparation and Middle Cerebral Artery Occlusion

Animal study protocols were approved by the University of Michigan Committee on the Use and Care of Animals. A total of 58 male Sprague-Dawley rats (Charles River Laboratories; Portage, MI) weighing 275–300 g were used in this study. Rats were fasted for 12 h before surgery, but had free access to water. Anesthesia was induced by inhalation of

Y. Xing

Department of Neurology, The First Hospital, Jilin University, Changchun, People's Republic of China and
Department of Neurosurgery, University of Michigan, Ann Arbor, MI, USA

X. Jiang

Department of Neurology, The First Hospital, Jilin University, Changchun, People's Republic of China

Y. Yang (✉)

Department of Neurology, The First Hospital, Jilin University, Changchun, People's Republic of China and
Department of Neurology, The First Hospital, Jilin University, 71 Xinmin Street, Changchun 130021, People's Republic of China
e-mail: doctor_yangyi@hotmail.com

G. Xi (✉)

Department of Neurosurgery, University of Michigan, 5018 BSRB, Ann Arbor, MI 48109–2200, USA
e-mail: guohuaxi@umich.edu

5% isoflurane in a nitrous oxide/oxygen mixture (70/30). Rectal temperature was maintained at 37.5°C with use of a feedback-controlled heating pad.

Middle cerebral artery occlusion was induced using the filament model as previously described, with some modifications [8, 9]. The suture was removed after 2 h of occlusion. The animal was allowed to awaken and recover with free access to food and water.

The left femoral artery was catheterized for continuous blood pressure monitoring. Blood was obtained from the catheter for analysis of pH, PaO₂, PaCO₂, hematocrit, and glucose.

Experimental Groups

Rats were divided into two groups, the hyperglycemic and normoglycemic groups. All rats had tMCAO. Fifteen minutes prior to MCAO, hyperglycemic rats had an intraperitoneal injection of 50% glucose (6 mL/kg). Normoglycemic rats received an equivalent volume of saline. There were four parts of this study. First, rats ($n=5-6$) were killed 2 h after reperfusion for Evans blue content measurement. Second, brain water content ($n=5-9$) was determined 8 h after MCAO. Third, rat brains were sampled ($n=5-14$) for hemoglobin content determination 24 h after MCAO. Fourth, rats ($n=6-8$) were used for histology examination, including measurements of infarct volume and brain swelling, 24 h after MCAO. Mortality and HT were also examined at 24 h after MCAO.

BBB Integrity

Evans blue dye (2% in saline, 4 m/kg) was given intravenously 2 h after MCAO, immediately after the intraluminal filament removal. Two hours after Evans blue injection, the chest wall was opened under lethal anesthesia, and the brains were perfused with 0.1 mol/l phosphate-buffered saline through the left ventricle to remove the intravascular localized dye until colorless perfusion fluid was obtained from the right atrium. After decapitation, the brain was removed and dissected into left and right hemispheres, and each hemisphere was weighed. Brain samples were then placed in 3 ml 50% trichloroacetic acid solution, and then homogenized and centrifuged (10,000 rpm for 20 min). The supernatant was measured at 610 nm for absorbance by a spectrophotometer (Ultrospec 3; Pharmacia LKB). The concentration of Evans blue was quantified from a linear standard curve and was expressed as micrograms per gram of brain tissue.

Hemoglobin Measurement

HT formation was also quantified by spectrophotometric assay of brain hemoglobin content [10]. At 24 h after MCAO,

the animals were perfused transcordially with 0.1 mol/l phosphate-buffered saline under deep anesthesia until the outflow fluid from the right atrium was colorless. The brain was rapidly removed and dissected into two parts, the left and the right hemispheres. The hemispheric brain tissue was then homogenized in 0.1 mol/l phosphate-buffered saline followed by 30-min centrifugation (13,000 g). Then 200 μ l reagent (QuantiChrom Hemoglobin Assay Kit; BioAssay Systems) was mixed with 50 μ l supernatant. After 15 min, optical density was determined by a spectrophotometer (Ultrospec 3; Pharmacia LKB) at 400 nm wavelength. The total hemispheric hemoglobin content was calculated as milligrams per hemisphere by hemoglobin standard.

Brain Water Content Measurement

Eight hours after MCAO, animals were anesthetized and decapitated as described in our previous study [11]. The brains were removed and dissected into three parts: the cerebellum and left and right hemispheres. Brain samples were immediately weighed on an electronic balance (model AE 100; Mettler Instrument) to obtain the wet weight. Brain samples were then dried in a gravity oven at 100°C for 48 h to obtain the dry weight. Brain water content was then calculated as (wet weight-dry weight)*100/wet weight.

Histology

Twenty-four hours after MCAO, the animals were reanesthetized and perfused intracardially with 4% paraformaldehyde in 0.1 mol/l phosphate-buffered saline (pH 7.4). Brains were removed and kept in 4% paraformaldehyde for 6 h, and then immersed in 25% sucrose for 3–4 days at 4°C. The brains were embedded in the mixture of 25% sucrose and optimal cutting temperature compound (Sakura Finetek), and 20 μ m-thick coronal frozen sections were made on a cryostat. After disposing the 2-mm anterior part of the forebrain, slices for every 2 mm-thick interval distance were stained with crystal violet or hematoxylin-eosin (H&E). The crystal violet staining was used for measurements of infarct volume, and the H&E staining was used to measure the brain swelling. In total, five slices of each brain were stained and analyzed.

1. To quantify infarct volume, the areas of infarction at five coronal levels throughout the brain were identified, and the infarct and hemispheric volumes were measured with National Institutes of Health Image by an investigator blind to the treatments. To avoid artifacts in volume measurement from brain edema within the infarct, infarct volume was calculated by measuring and subtracting the volume of the noninfarcted ipsilateral hemisphere from the volume of the contralateral hemisphere [12].

2. The extent of brain swelling was determined by the ratio of the ipsilateral hemispheric volume to the contralateral for edema formation. Swelling was measured and analyzed by whole hemisphere and by region (basal ganglia).

Statistical Analysis

Results are expressed as mean \pm SD. Statistical significance was analyzed by two-tailed Student's *t* test and Mann-Whitney *U* test for continuous variable, and by χ^2 test for mortality and HT formation rate. Statistical significance was considered at $p < 0.05$.

Results

Physiological variables were measured immediately before the introduction of MCAO. The levels of pH, PO₂, and PCO₂ were in the normal range. Blood glucose levels were significantly higher in the hyperglycemic rats compared with the normoglycemic rats (385.6 ± 73.7 to 123.7 ± 39.2 mg/dL, $p < 0.05$). Hyperglycemia increased the mortality rate in this tMCAO model (18.9% vs. 0 in normoglycemic group, $p < 0.05$, χ^2 test).

Evans blue content was increased in the ipsilateral hemisphere as compared with the contralateral hemisphere in both groups at 4 h after MCAO ($p < 0.01$, Fig. 1). Evans blue content 4 h after MCAO was higher in hyperglycemic

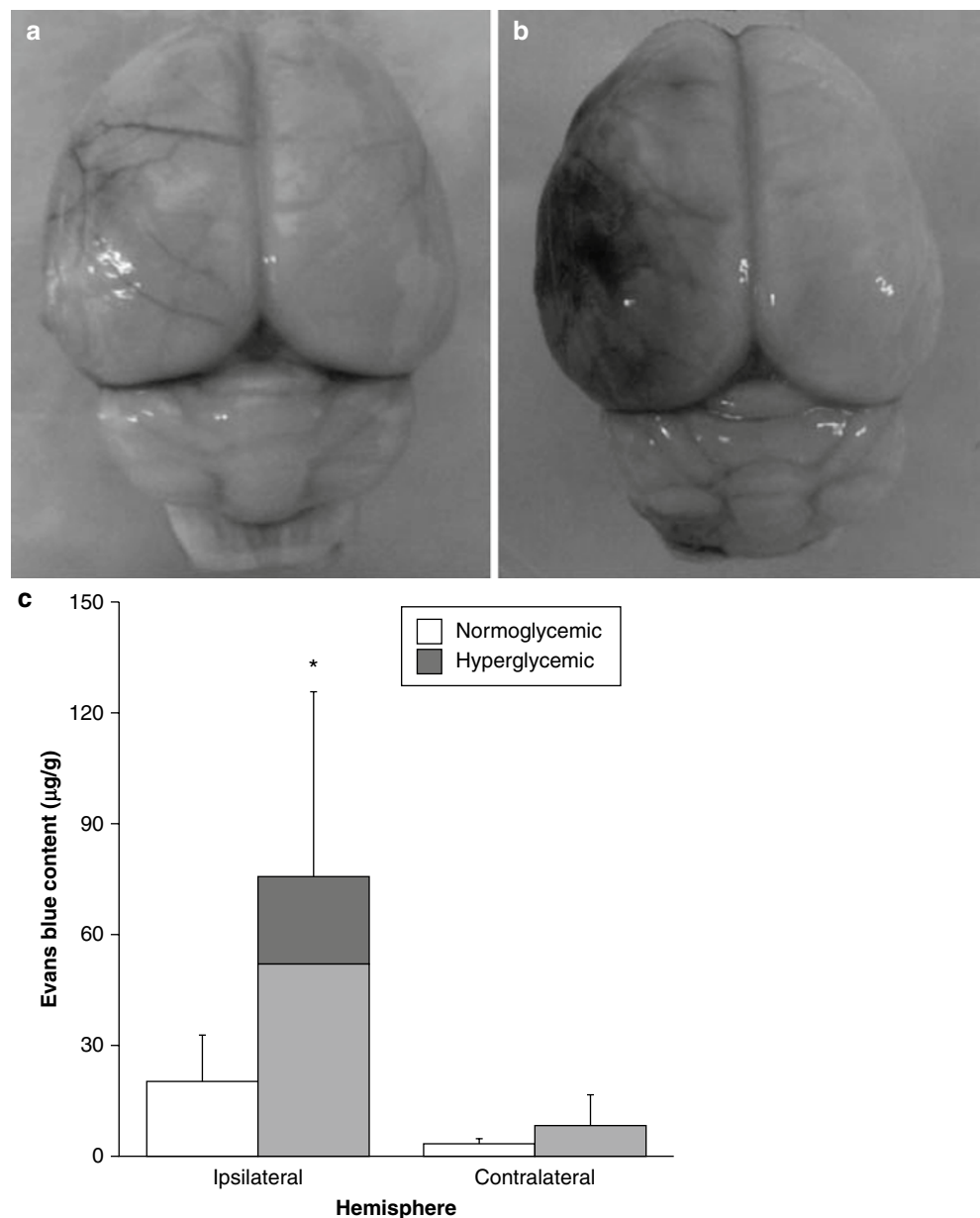


Fig. 1 Evans blue leakage in the rat brain 4 h after tMCAO with normoglycemia (a) or hyperglycemia (b). (c) Quantification of brain Evans blue contents after tMCAO. Values are mean \pm SD, $n = 5-6$, * $p < 0.05$ vs. normoglycemia

animals than that in normoglycemic animals ($76.1 \pm 49.6 \mu\text{g/g}$ vs. 20.5 ± 12.6 , $p < 0.05$, Fig. 1).

All six hyperglycemic rats had HT, but only two out of six normoglycemic rats had HT 24 h after MCAO. Hemorrhage was either petechial or confluent petechial hemorrhage, occurring mostly in the basal ganglia (91%, Fig. 2a–f). Hemoglobin contents 24 h after MCAO were significantly higher in hyperglycemic animals than in normoglycemic animals (601 ± 309 vs. $383 \pm 140 \mu\text{g}$, $p < 0.05$, Fig. 2g).

Brain swelling occurred in the ipsilateral hemisphere after MCAO. Hyperglycemia increased the brain swelling ratio in the basal ganglia (1.8 ± 0.5 vs. 1.3 ± 0.3 in the normoglycemia, $p < 0.05$). Also, brain water content of the ipsilateral hemisphere was higher in hyperglycemic animals than in normoglycemic animals (82.1 ± 1.3 vs. 80.7 ± 0.5 , $p < 0.05$; Fig. 3).

There was a tendency for hyperglycemia to increase the total infarct volume in the ipsilateral hemispheres, but statistical

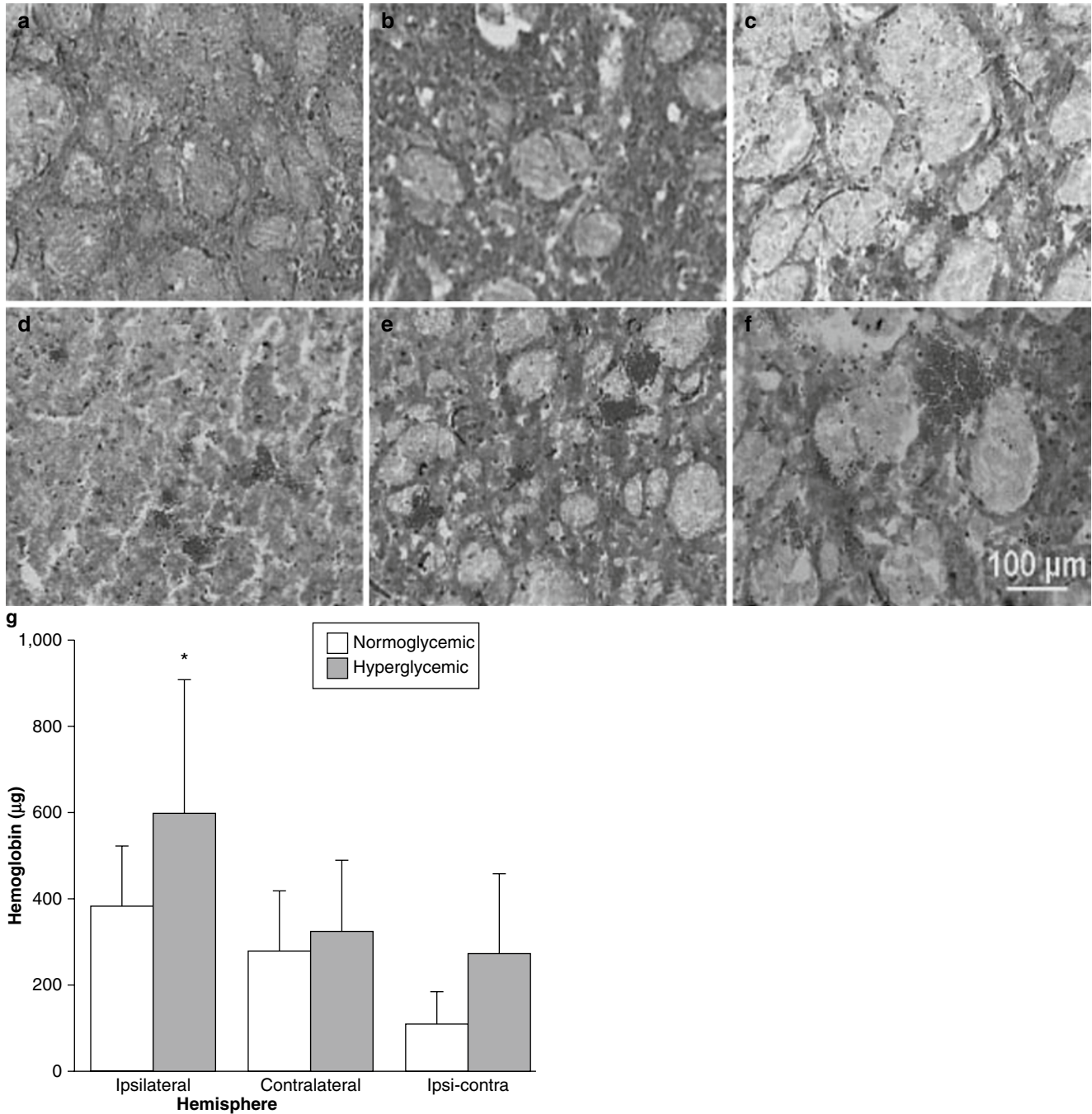


Fig. 2 Hemorrhagic transformation 24 h after tMCAO with normoglycemia (a–c) or hyperglycemia (d–f). (g) Hemoglobin contents in brain 24 h after tMCAO. Values are mean \pm SD, $n = 5$ –14. * $p < 0.05$ vs. normoglycemia

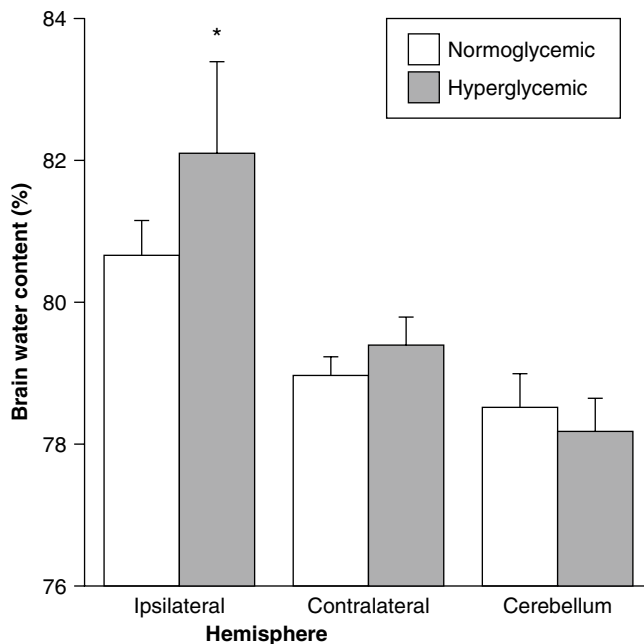


Fig. 3 Brain water content 24 h after tMCAO. Values are mean \pm SD, $n=5-9$, * $p<0.05$ vs. normoglycemia

significance was not reached (164.3 ± 93.4 vs. 117.1 ± 49.8 mm³, in normoglycemic rats, $p>0.05$).

Discussion

The findings of our current study are: (1) HT occurs in all hyperglycemic rats after tMCAO; (2) most HTs are located in the basal ganglia; (3) hyperglycemia increases BBB leakage at 4 h and brain water content at 24 h following tMCAO. These results suggest the animal models of HT will be useful for experimental assessment of new therapies for HT.

In experimental animal models of MCAO with reperfusion, hyperglycemia induces HT [7, 13]. Although the precise mechanisms that enhance HT are unknown, acidosis may be involved in hyperglycemia-induced HT [13]. The resultant cellular acidosis includes enzymatic dysfunction, enhanced free radical production through increased iron-catalyzed hydroxyl radical production [14], depressed mitochondrial function by inhibited ADP-stimulated respiratory activity [15], induction of endonucleases that may initiate programmed cell death [16], increased intracellular Ca²⁺ accumulation [17], and cellular swelling [18]. Recent studies indicate that hyperglycemia can increase the production of matrix metalloproteinases, reactive oxygen species, and proinflammatory cytokines that might result in vascular damage and lead to hemorrhage [19].

Hyperglycemia has a major impact on post-ischemic HT. In experimental tMCAO models, acute hyperglycemia induced by glucose administration augments ischemic injury and

increases HT [7, 20, 21]. Human data also show that hyperglycemia is a very strong predictor of HT in patients undergoing tPA therapy [19].

In conclusion, acute hyperglycemia can induce HT in rats with transient focal cerebral ischemia.

Conflict of interest statement We declare that we have no conflict of interest.

References

- Bozzao L, Angeloni U, Bastianello S, Fantozzi LM, Pierallini A, Fieschi C (1991) Early angiographic and CT findings in patients with hemorrhagic infarction in the distribution of the middle cerebral artery. *Am J Neuroradiol* 12:1115–1121
- Hornig CR, Dorndorf W, Agnoli AL (1986) Hemorrhagic cerebral infarction—a prospective study. *Stroke* 17:179–185
- Moulin T, Crepin-Leblond T, Chopard JL, Bogousslavsky J (1994) Hemorrhagic infarcts. *Eur Neurol* 34:64–77
- Paciaroni M, Agnelli G, Corea F, Ageno W, Alberti A, Lanari A, Caso V, Micheli S, Bertolani L, Venti M, Palmerini F, Biagini S, Comi G, Previdi P, Silvestrelli G (2008) Early hemorrhagic transformation of brain infarction: rate, predictive factors, and influence on clinical outcome: results of a prospective multicenter study. *Stroke* 39:2249–2256
- Lyden PD, Zivin JA (1993) Hemorrhagic transformation after cerebral ischemia: mechanisms and incidence. *Cerebrovasc Brain Metab Rev* 5:1–16
- Wang X, Lo EH (2003) Triggers and mediators of hemorrhagic transformation in cerebral ischemia. *Mol Neurobiol* 28:229–244
- de Courten-Myers GM, Kleinholz M, Wagner KR, Myers RE (1989) Fatal strokes in hyperglycemic cats. *Stroke* 20:1707–1715
- Karabiyikoglu M, Hua Y, Keep RF, Ennis SR, Xi G (2004) Intracerebral hirudin injection attenuates ischemic damage and neurologic deficits without altering local cerebral blood flow. *J Cereb Blood Flow Metab* 24:159–166
- Longa EZ, Weinstein PR, Carlson S, Cummins R (1989) Reversible middle cerebral artery occlusion without craniectomy in rats. *Stroke* 20:84–91
- Choudhri TF, Hoh BL, Solomon RA, Connolly ES Jr, Pinsky DJ (1997) Use of a spectrophotometric hemoglobin assay to objectively quantify intracerebral hemorrhage in mice. *Stroke* 28:2296–2302
- Xi G, Keep RF, Hoff JT (1998) Erythrocytes and delayed brain edema formation following intracerebral hemorrhage in rats. *J Neurosurg* 89:991–996
- Lin TN, He YY, Wu G, Khan M, Hsu CY (1993) Effect of brain edema on infarct volume in a focal cerebral ischemia model in rats. *Stroke* 24:117–121
- de Courten-Myers GM, Kleinholz M, Holm P, DeVoe G, Schmitt G, Wagner KR, Myers RE (1992) Hemorrhagic infarct conversion in experimental stroke. *Ann Emerg Med* 21:120–126
- Siesjo BK, Bendek G, Koide T, Westerberg E, Wieloch T (1985) Influence of acidosis on lipid peroxidation in brain tissues in vitro. *J Cereb Blood Flow Metab* 5:253–258
- Hillered L, Ernster L, Siesjo BK (1984) Influence of in vitro lactic acidosis and hypercapnia on respiratory activity of isolated rat brain mitochondria. *J Cereb Blood Flow Metab* 4:430–437
- Kalimo H, Rehnörona S, Soderfeldt B, Olsson Y, Siesjo BK (1981) Brain lactic acidosis and ischemic cell damage: 2. Histopathology. *J Cereb Blood Flow Metab* 1:313–327
- OuYang YB, Mellergard P, Kristian T, Kristianova V, Siesjo BK (1994) Influence of acid-base changes on the intracellular calcium concentration of neurons in primary culture. *Exp Brain Res* 101:265–271

18. Kraig RP, Petito CK, Plum F, Pulsinelli WA (1987) Hydrogen ions kill brain at concentrations reached in ischemia. *J Cereb Blood Flow Metab* 7:379–386
19. Garg R, Chaudhuri A, Munschauer F, Dandona P (2006) Hyperglycemia, insulin, and acute ischemic stroke: a mechanistic justification for a trial of insulin infusion therapy. *Stroke* 37:267–273
20. Kawai N, Keep RF, Betz AL (1997) Hyperglycemia and the vascular effects of cerebral ischemia. *Acta Neurochir Suppl* 70:27–29
21. Venables GS, Miller SA, Gibson G, Hardy JA, Strong AJ (1985) The effects of hyperglycaemia on changes during reperfusion following focal cerebral ischaemia in the cat. *J Neurol Neurosurg Psychiatry* 48:663–669

A Novel Preclinical Model of Germinal Matrix Hemorrhage Using Neonatal Rats

Tim Lekic, Anatol Manaenko, William Rolland, Jiping Tang, and John H. Zhang

Abstract *Background:* Germinal matrix hemorrhage (GMH) is a neurological disorder associated with very low birth weight premature infants. This event can lead to post-hemorrhagic hydrocephalus, cerebral palsy, and mental retardation. This study developed a novel animal model for pre-clinical investigations.

Methods: Neonatal rats underwent infusion of clostridial collagenase into the right germinal matrix (anterior caudate) region using stereotaxic techniques. Developmental milestones were evaluated over 10 days, cognitive function at 3 weeks, and sensorimotor function at 4 weeks after collagenase infusion. This was accomplished by anthropometric quantifications of cranial, cerebral, cardiac, and splenic growths.

Results: Collagenase infusion led to delays in neonatal developmental milestones, followed by cognitive and sensorimotor dysfunctions in the juvenile animals. Cranial growth was accelerated during the first week after injury, and this was followed by significant brain atrophy, splenomegaly, and cardiac hypertrophy 3 weeks later.

Conclusion: This study characterized the developmental delays, mental retardation, and cerebral palsy features resembling the long-term clinical course after germinal matrix hemorrhage in premature infants. Pre-clinical testing of therapeutics in this experimental model could lead to improved patient outcomes while expanding upon the pathophysiological understanding of this disease.

Keywords Animal models · Neurological deficits · Stroke, experimental

T. Lekic, A. Manaenko, W. Rolland, and J. Tang
Department of Physiology, Loma Linda University,
School of Medicine, Loma Linda, CA 92354, USA

J.H. Zhang (✉)
Department of Physiology, Loma Linda University,
School of Medicine, Loma Linda, CA 92354, USA and
Department of Neurosurgery, Loma Linda University,
School of Medicine, Loma Linda, CA 92354, USA and
Department of Physiology, Loma Linda University, School of
Medicine, Risley Hall, Room 223, Loma Linda, CA, 92354, USA
e-mail: johnzhang3910@yahoo.com

Introduction

Germinal matrix hemorrhage (GMH) is the rupture of immature blood vessels within the subventricular (anterior caudate) progenitor cell region of neonatal brains [1] during the first 7 days of life [2]. GMH occurs in 20–25% of very low birth weight (VLBW $\leq 1,500$ g) premature infants [3–5] and affects 3.5/1,000 births in the United States each year [6]. This is an important clinical problem, since the consequences are hydrocephalus (post-hemorrhagic ventricular dilation), cognitive and motor developmental delay, cerebral palsy, and mental retardation [4, 7]. However, available animal models to study the pathophysiological basis of these outcomes are lacking [8].

An important research priority is the development and validation of experimental models of brain hemorrhage for translational studies of human conditions [9]. Elevated MMP-2 and MMP-9 are associated with GMH induction in humans [10, 11]. Stereotaxic collagenase infusion is one of the most commonly used methods in adult experimental intracerebral hemorrhage (ICH) studies [12, 13] and functions as an MMP to lyse the extracellular-matrix around blood vessels to cause vascular rupture [13, 14]. This approach enables investigations of neurological and brain injury outcomes [12–19].

In this study, we hypothesized that unilateral germinal-matrix collagenase infusion in neonatal rats would model features similar to clinical GMH [4, 7]. With this approach, applications of therapeutic strategies can be tested to improve outcomes and to gain a better pathophysiological understanding of this disease [9].

Methods and Materials

Animal Groups and General Procedures

This study was in accordance with the National Institutes of Health guidelines for the treatment of animals and was approved by the Institutional Animal Care and Use Committee

at Loma Linda University. Timed pregnant Sprague-Dawley rats were housed with food and water available *ad libitum*. Postnatal day 7 (P7) pups were blindly assigned to the following ($n=8$ /group): sham (naive), needle (control), and collagenase infusion. All groups were evenly divided within each litter.

Experimental Model of GMH

Using an aseptic technique, rat pups were gently anesthetized with 3% isoflurane (in mixed air and oxygen) while placed prone on a stereotaxic frame. Betadine sterilized the surgical scalp area, which was incised in the longitudinal plane to expose the skull and reveal the bregma. The following stereotaxic coordinates were determined: 1 mm (anterior), 1.5 mm (lateral) and 3.5 mm (ventral) from bregma. A bore hole (1 mm) was drilled, into which a 27-gauge needle was inserted at a rate of 1 mm/min. A microinfusion pump (Harvard Apparatus, Holliston, MA) infused 0.3 units of clostridial collagenase VII-S (Sigma, St Louis, MO) through a Hamilton syringe. The needle remained in place for an additional 10 min after injection to prevent “back-leakage.” After needle removal, the burr hole was sealed with bone wax, the incision sutured closed, and the animals were allowed to recover. The entire surgery took an average of 20 min. Upon recovering from anesthesia, the animals were returned to their dams. Needle controls consisted of needle insertion alone without collagenase infusion, while naive animals did not receive any surgery.

Developmental Milestones

Animals were assessed over 10 days after collagenase infusion. For the righting reflex, time needed for the rat pups to completely roll over onto all four limbs after being placed on their backs was measured [20]. For negative geotaxis, the time needed for complete rotation (180°) after being placed head down on a slope (20° angle), was recorded [20]. The maximum allotted time was 60 s/trial (two trials/day).

Cognitive Measures

Higher order brain function was assessed during the third week after collagenase infusion. The T-Maze assessed short-term (working) memory [21]. Rats were placed into the stem (40 cm × 10 cm) of a maze and allowed to explore until one arm (46 cm × 10 cm) was chosen. From the sequence of ten

trials, of left and right arm choices, the rate of spontaneous alternation (0% = none and 100% = complete, alternations/trial) was calculated, as routinely performed [22, 23]. The Morris water maze assessed spatial learning and memory on four daily blocks, as described previously in detail [16, 17]. The apparatus consisted of a metal pool (110 cm diameter), filled to within 15 cm of the upper edge, with a platform (11 cm diameter) for the animal to escape onto, that changed location for each block (maximum = 60 s/trial), and was digitally analyzed by Noldus Ethovision tracking software. Cued trials measured place learning with the escape platform visible above water. Spatial trials measured spatial learning with the platform submerged, and probe trials measured spatial memory once the platform had been removed. For the locomotor activity, in an open field, the path length in open-topped plastic boxes (49 cm-long, 35.5 cm-wide, 44.5 cm-tall) was digitally recorded for 30 min and analyzed by Noldus Ethovision tracking software [17].

Sensorimotor Outcome

At 4 weeks after collagenase infusion, animals were tested for functional ability. Neurodeficit was quantified using a summation of scores (maximum = 12), given for (1) postural reflex, (2) proprioceptive limb placing, (3) back pressure towards the edge, (4) lateral pressure towards the edge, (5) forelimb placement, and (6) lateral limb placement (2 = severe, 1 = moderate, 0 = none), as routinely performed [22]. For the rotarod, striatal ability was assessed using an apparatus consisting of a horizontal, accelerated (2 rpm/5 s), rotating cylinder (7 cm diameter × 9.5 cm wide), requiring continuous walking to avoid falling recorded by photobeam circuit (Columbus Instruments) [16, 17]. For foot fault, the number of complete limb missteps through the openings, was counted over 2 min while exploring over an elevated wire (3 mm) grid (20 cm × 40 cm) floor [23].

Assessment of Growth

Over 28 days after collagenase infusion, the head (width and height) and rump-to-crown (length) measurements were performed using a Boley Gauge (Franklin Dental Supply, Bellmore, NY), as previously described [24]. Head width was measured anterior to the side of the ears, head height from posterior to the adjacent mandible, and rump-to-crown was the greatest cranial (caudal) to tail (rostral) extension. At the completion of experiments, the brains were removed, and hemispheres separated by a midline incision (loss of brain weight has been used as the primary variable to estimate

brain damage in juvenile animals after neonatal brain injury [25]). For organ weights, the spleen and heart were separated from surrounding tissue and vessels. The quantification was performed using an analytical microbalance (model AE 100; Mettler Instrument Co., Columbus, OH) capable of 1.0 μg precision.

Statistical Analysis

Significance was considered at $P < 0.05$. Data were analyzed using analysis of variance (ANOVA), with repeated measures (RM-ANOVA) for long-term neurobehavior. Significant interactions were explored with conservative Scheffe *post hoc* and Mann-Whitney rank sum tests when appropriate.

Results

Collagenase infusion delayed the developmental acquisition of eye opening, negative geotropism and righting reflex by 2–3 days (Fig. 1a–c, $P < 0.05$). Three weeks after GMH, significant deficits were discovered in spatial learning and memory (Fig. 2a, b, $P < 0.05$), T-maze (working) memory (Fig. 2c, $P < 0.05$), and hyperactivity, in the open field (decreased corner time and increased center crossings, Fig. 2d, e, $P < 0.05$). Juvenile animals had significant sensorimotor dysfunction, as revealed by the neurodeficit score, accelerating rotarod and foot fault (Fig. 3a–c, $P < 0.05$). These dysfunctions were associated with increased cranial size at 7 days (Fig. 4a, $P < 0.05$), and dysfunctional growth of the body, brain, heart, and spleen (Fig. 4b–e, $P < 0.05$) 3 weeks later.

Discussion

Germinal matrix hemorrhage (GMH) is an important problem affecting approximately 12,000 births in the United States each year [6]. The clinical consequences of GMH are developmental delay, cerebral palsy, and mental retardation [4, 7]. In this study collagenase was infused into the germinal matrix of neonatal rats as an approach to model these features, since animal models to study the basis of these outcomes are lacking [8].

This neonatal rat model of GMH resembles the neurological consequences seen in the pediatric population after hemorrhagic brain injury. Collagenase infusion led to developmental delays in the neonates that were followed by cognitive and sensorimotor dysfunction in the juvenile

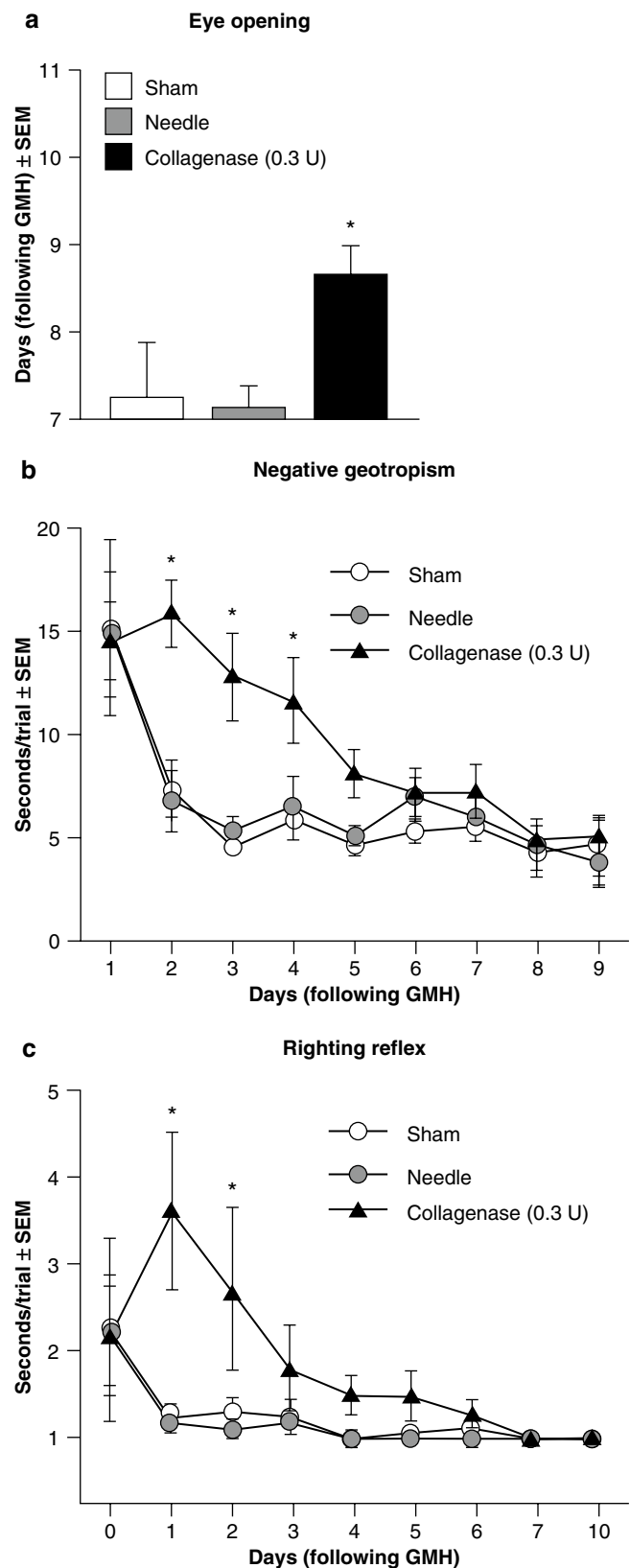


Fig. 1 Developmental delays: Neonates were assessed for (a) eye opening latency, (b) negative geotropism, and (c) righting reflex, over 10 days after collagenase infusion. Values expressed as mean \pm SEM, $n = 8$ (per group), * $P < 0.05$ compared with controls (sham and needle trauma)

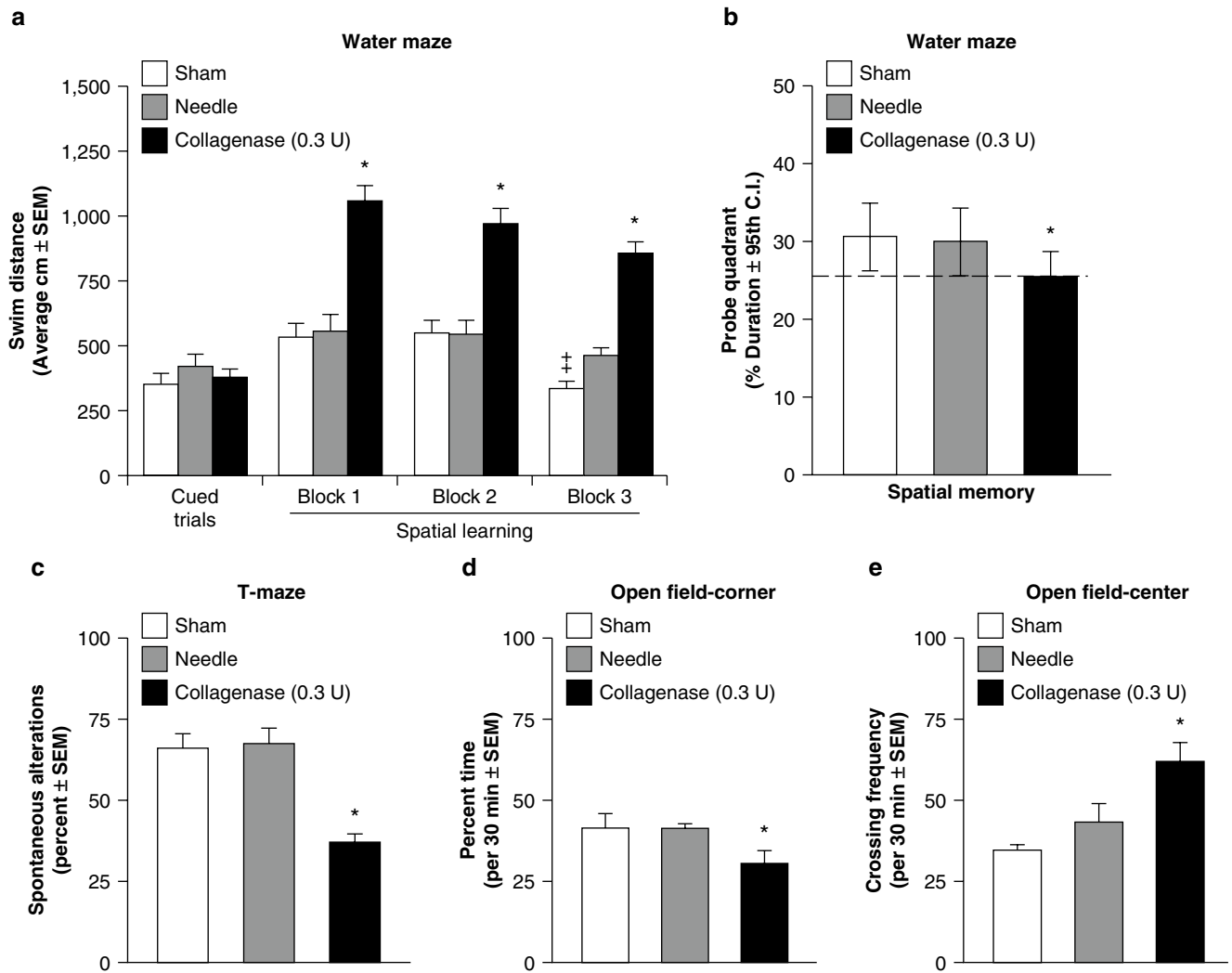


Fig. 2 Cognitive dysfunction: Higher order function was measured at the 3rd week after collagenase infusion. (a) Cued and spatial learning water maze, (b) probe (spatial memory) water maze, (c) T-maze, (d) open field (percent time in corner), and (e) open field (center crossing frequency). Values expressed as mean \pm 95th C.I. (probe quadrant) or mean \pm SEM (all others), $n=8$ (per group), $*P<0.05$ compared with controls (sham and needle trauma) and $^{\dagger}P<0.05$ compared with block 1 (spatial learning water maze)

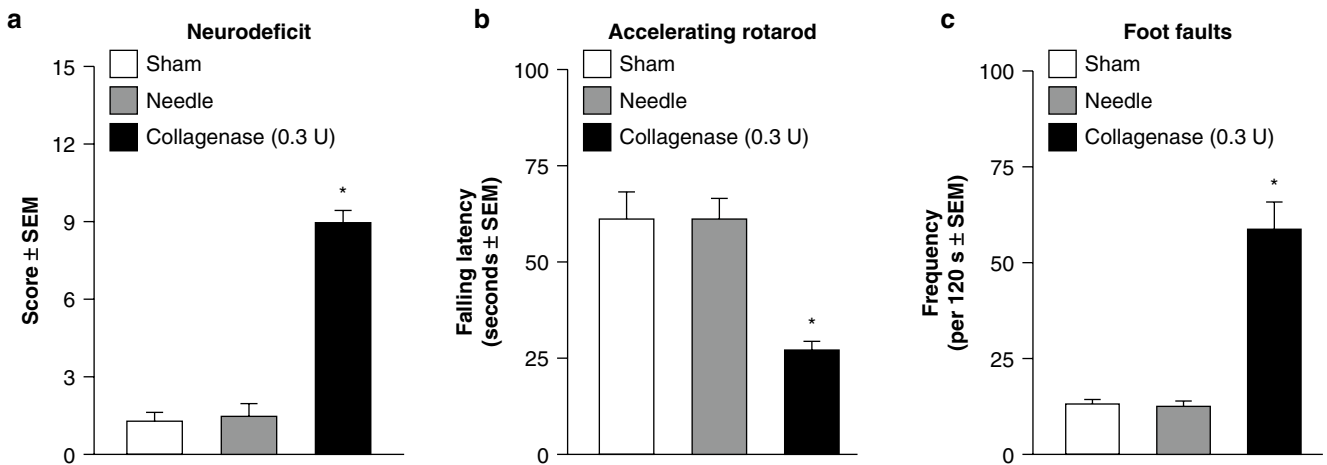


Fig. 3 Sensorimotor dysfunction: Cerebral palsy measurements were performed in the juveniles at 1 month after collagenase infusion. (a) Neurodeficit score, (b) rotarod, and (c) foot fault. Values expressed as mean \pm SEM, $n=8$ (per group), $*P<0.05$ compared with controls (sham and needle trauma)

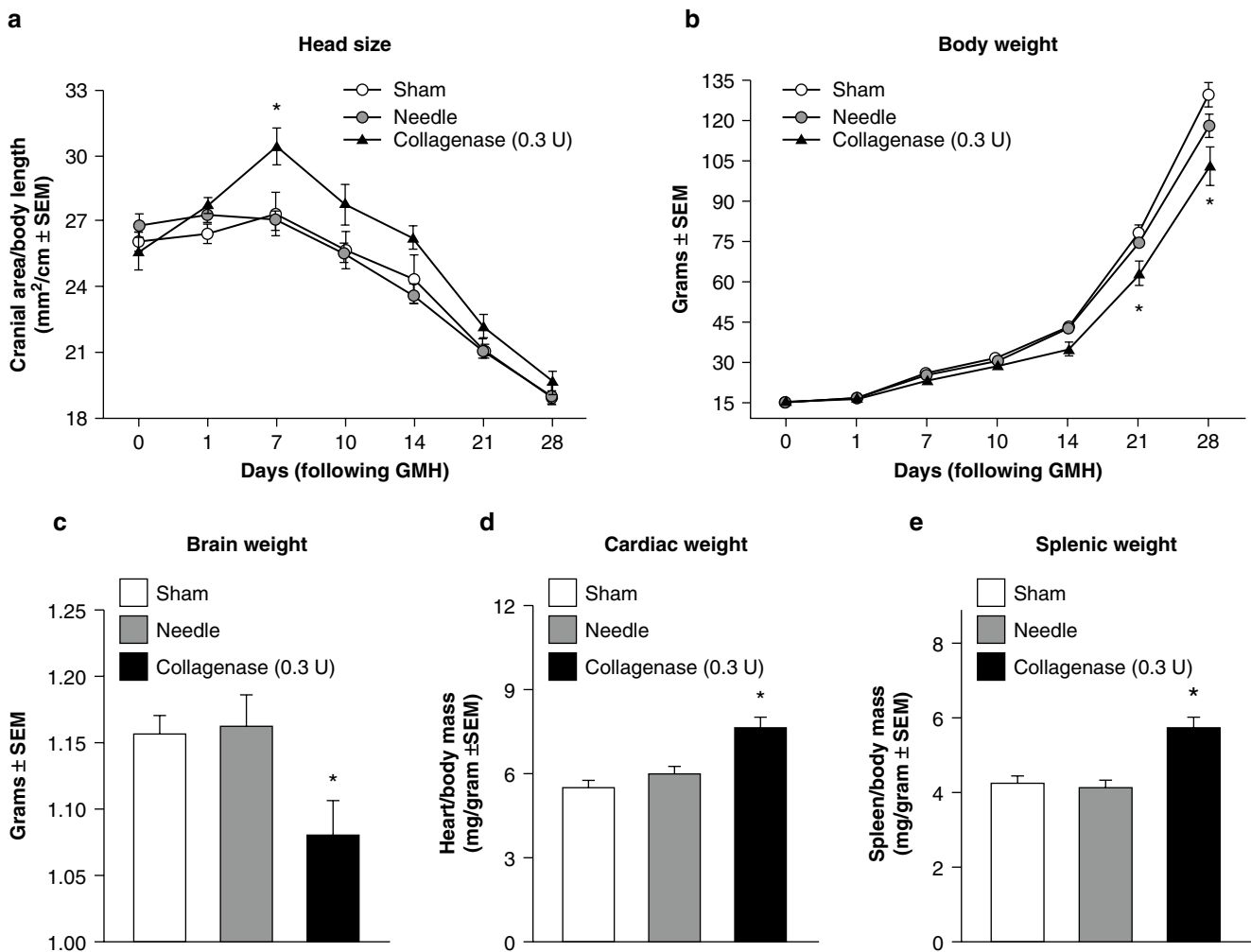


Fig. 4 Cranial and somatic pediatric growth: 1 month assessment of (a) head size (cranial area/body length), (b) body weight, (c) brain weight, (d) cardiac weight and (e) splenic weight. Values expressed as

mean ± SEM, $n=8$ (per group), * $P<0.05$ compared with controls (sham and needle trauma)

developmental stage. The cranium was enlarged compared to somatic growth during the first week, with significant brain atrophy 3 weeks later. This presentation is likely a reflection of hydrocephalic cerebrospinal fluid build-up, leading to cranial expansion and compression of the brain tissue into an atrophic developmental growth pattern. Splenomegaly and cardiac hypertrophy presented at 1 month after injury, and this could either be a reflection of the disproportionate somatic growth or of prolonged peripheral hemostatic or inflammatory consequences of the brain bleed.

In summary, we have characterized a highly reliable and easily reproducible experimental model of germinal matrix hemorrhage using neonatal rats. This provides the basis for studying the clinical and pathophysiological features of this disease, and establishes a foundation for performing further preclinical therapeutic investigations.

Acknowledgement This study is partially supported by NIH NS053407 to J.H. Zhang and NS060936 to J. Tang.

Conflict of interest statement We declare that we have no conflict of interest.

References

- Ballabh P (2010) Intraventricular hemorrhage in premature infants: mechanism of disease. *Pediatr Res* 67:1–8. doi:10.1203/PDR.0b013e3181c1b176
- Kadri H, Mawla AA, Kazah J (2006) The incidence, timing, and predisposing factors of germinal matrix and intraventricular hemorrhage (GMH/IVH) in preterm neonates. *Childs Nerv Syst* 22:1086–1090. doi:10.1007/s00381-006-0050-6
- Vohr BR, Wright LL, Dusick AM, Mele L, Verter J, Steichen JJ, Simon NP, Wilson DC, Broyles S, Bauer CR, Delaney-Black V, Yolton KA, Fleisher BE, Papile LA, Kaplan MD (2000) Neurodevelopmental and functional outcomes of extremely low birth weight infants in the National Institute of Child Health and Human Development Neonatal Research Network, 1993–1994. *Pediatrics* 105:1216–1226
- Murphy BP, Inder TE, Rooks V, Taylor GA, Anderson NJ, Mogridge N, Horwood LJ, Volpe JJ (2002) Posthaemorrhagic ventricular

- dilatation in the premature infant: natural history and predictors of outcome. *Arch Dis Child Fetal Neonatal Ed* 87:F37–F41
5. Vermont-Oxford (1990) The Vermont-Oxford Trials Network: very low birth weight outcomes for 1990. Investigators of the Vermont-Oxford Trials Network Database Project. *Pediatrics* 91:540–545
 6. Heron M, Sutton PD, Xu J, Ventura SJ, Strobino DM, Guyer B (2010) Annual summary of vital statistics: 2007. *Pediatrics* 125: 4–15. doi:10.1542/peds.2009-2416 [pii]
 7. Ballabh P, Braun A, Nedergaard M (2004) The blood-brain barrier: an overview: structure, regulation, and clinical implications. *Neurobiol Dis* 16:1–13. doi:10.1016/j.nbd.2003.12.016S0969996103002833 [pii]
 8. Balasubramaniam J, Del Bigio MR (2006) Animal models of germinal matrix hemorrhage. *J Child Neurol* 21:365–371
 9. NINDS ICH Workshop Participants (2005) Priorities for clinical research in intracerebral hemorrhage: report from a National Institute of Neurological Disorders and Stroke workshop. *Stroke* 36:e23–e41. doi:01.STR.0000155685.77775.4c [pii] 10.1161/01.STR.0000155685.77775.4c
 10. Cockle JV, Gopichandran N, Walker JJ, Levene MI, Orsi NM (2007) Matrix metalloproteinases and their tissue inhibitors in preterm perinatal complications. *Reprod Sci* 14:629–645. doi:14/7/629 [pii]10.1177/1933719107304563
 11. Schulz CG, Sawicki G, Lemke RP, Roeten BM, Schulz R, Cheung PY (2004) MMP-2 and MMP-9 and their tissue inhibitors in the plasma of preterm and term neonates. *Pediatr Res* 55:794–801. doi:10.1203/01.PDR.0000120683.68630.FB01.PDR.0000120683.68630.FB [pii]
 12. MacLellan CL, Silasi G, Poon CC, Edmundson CL, Buist R, Peeling J, Colbourne F (2008) Intracerebral hemorrhage models in rat: comparing collagenase to blood infusion. *J Cereb Blood Flow Metab* 28:516–525. doi:9600548 [pii]10.1038/sj.jcbfm.9600548
 13. Rosenberg GA, Mun-Bryce S, Wesley M, Kornfeld M (1990) Collagenase-induced intracerebral hemorrhage in rats. *Stroke* 21: 801–807
 14. Yang GY, Betz AL, Chenevert TL, Brunberg JA, Hoff JT (1994) Experimental intracerebral hemorrhage: relationship between brain edema, blood flow, and blood-brain barrier permeability in rats. *J Neurosurg* 81:93–102
 15. Foerch C, Arai K, Jin G, Park KP, Pallast S, van Leyen K, Lo EH (2008) Experimental model of warfarin-associated intracerebral hemorrhage. *Stroke* 39:3397–3404. doi:STROKEAHA.108.517482 [pii]10.1161/STROKEAHA.108.517482
 16. Lekic T, Hartman R, Rojas H, Manaenko A, Chen W, Ayer R, Tang J, Zhang JH (2010) Protective effect of melatonin upon neuropathology, striatal function, and memory ability after intracerebral hemorrhage in rats. *J Neurotrauma* 27:627–637. doi:10.1089/neu.2009.1163
 17. Hartman R, Lekic T, Rojas H, Tang J, Zhang JH (2009) Assessing functional outcomes following intracerebral hemorrhage in rats. *Brain Res* 1280:148–157. doi:S0006-8993(09)00957-3 [pii]10.1016/j.brainres.2009.05.038
 18. Andaluz N, Zuccarello M, Wagner KR (2002) Experimental animal models of intracerebral hemorrhage. *Neurosurg Clin N Am* 13:385–393
 19. Thiex R, Mayfrank L, Rohde V, Gilsbach JM, Tsirka SA (2004) The role of endogenous versus exogenous tPA on edema formation in murine ICH. *Exp Neurol* 189:25–32. doi:10.1016/j.expneurol.2004.05.021S0014488604001840 [pii]
 20. Thullier F, Lalonde R, Cousin X, Lestienne F (1997) Neurobehavioral evaluation of lurcher mutant mice during ontogeny. *Brain Res Dev Brain Res* 100:22–28. doi:S0165380697000102 [pii]
 21. Hughes RN (2004) The value of spontaneous alternation behavior (SAB) as a test of retention in pharmacological investigations of memory. *Neurosci Biobehav Rev* 28:497–505. doi:S0149-7634(04)00073-9 [pii]10.1016/j.neubiorev.2004.06.006
 22. Fathali N, Ostrowski RP, Lekic T, Jadhav V, Tong W, Tang J, Zhang JH (2010) Cyclooxygenase-2 inhibition provides lasting protection against neonatal hypoxic-ischemic brain injury. *Crit Care Med* 38:572–578. doi:10.1097/CCM.0b013e3181cb1158
 23. Zhou Y, Fathali N, Lekic T, Tang J, Zhang JH (2009) Glibenclamide improves neurological function in neonatal hypoxia-ischemia in rats. *Brain Res* 1270:131–139. doi:S0006-8993(09)00520-4 [pii]10.1016/j.brainres.2009.03.010
 24. Saad AY (1990) Postnatal effects of nicotine on incisor development of albino mouse. *J Oral Pathol Med* 19:426–429
 25. Andine P, Thordstein M, Kjellmer I, Nordborg C, Thiringer K, Wennberg E, Hagberg H (1990) Evaluation of brain damage in a rat model of neonatal hypoxic-ischemia. *J Neurosci Methods* 35:253–260

Pathophysiology of Cerebral Hemorrhage

Intracranial Hemorrhage: Mechanisms of Secondary Brain Injury

Josephine Lok, Wendy Leung, Sarah Murphy, William Butler, Natan Noviski, and Eng H. Lo

Abstract ICH is a disease with high rates of mortality and morbidity, with a substantial public health impact. Spontaneous ICH (sICH) has been extensively studied, and a large body of data has been accumulated on its pathophysiology. However, the literature on traumatic ICH (tICH) is limited, and further investigations of this important topic are needed. This review will highlight some of the cellular pathways in ICH with an emphasis on the mechanisms of secondary injury due to heme toxicity and to events in the coagulation process that are common to both sICH and tICH.

Keywords Intracranial hemorrhage · Heme toxicity · Iron toxicity · Coagulation · Inflammation · Vascular response

Introduction

ICH is a disease with high rates of mortality and morbidity, with a substantial public health impact. ICH can be classified as spontaneous or traumatic. Spontaneous ICH (sICH)

has been extensively studied, and a large body of data has been accumulated on its pathophysiology. However, the literature on traumatic ICH (tICH) is limited. The need to investigate the specific mechanisms of tICH is underscored by the fact that ICH is a well-known feature of severe TBI, and carries a high risk of morbidity and mortality. Progression of the hemorrhage is associated with poor clinical outcomes [1, 2]. This is true not only of large hemorrhages, but also of microbleeds detected only on susceptibility-weighted imaging (SWI) and not on routine CT or MRI [3]. Moreover, these detrimental sequelae often extend beyond the area of the hemorrhage. Metabolic changes have been found in regions remote from focal hemorrhagic lesions, suggesting diffuse injury after human traumatic brain injury [4]. In a rat TBI model, the severity of intracerebral hemorrhage was correlated with the degree of final cortical atrophy [5]. In addition, TBI itself may induce coagulopathy, which further increases the extent of intracerebral hemorrhage and the incidence of poor outcome associated with such injuries [6].

The management of traumatic intracerebral hemorrhage (tICH) presents a paradox. On one hand, current management of severe TBI is directed towards preservation of adequate cerebral perfusion pressure (CPP). This approach frequently requires therapies that raise the arterial blood pressure when increased intracranial pressure (ICP) does not respond to efforts to return it to normal levels. On the other hand, increasing the blood pressure in traumatic injuries will likely increase blood loss. Since the progression of the hemorrhage is greatest in the first 24 h, while the edema formation begins immediately after trauma and commonly peaks within 48–72 h, the current CPP-driven management may be detrimental in terms of ICH progression. Ideally, the management to optimize CPP and to control ICH should be coordinated in the temporal progression of TBI. In addition to increasing the blood pressure pharmacologically to maintain adequate cerebral perfusion pressure, strategies to reduce hemorrhage progression and to address the harmful effects of the hemorrhage are needed. To achieve this goal, an understanding of the

J. Lok (✉) and W. Leung
Neuroprotection Research Laboratory, Massachusetts General Hospital, Boston, MA, USA and
Department of Pediatrics, Pediatric Critical Care Medicine, Massachusetts General Hospital, Boston, MA, USA
e-mail: jlok1@partners.org

S. Murphy and N. Noviski
Department of Pediatrics, Pediatric Critical Care Medicine, Massachusetts General Hospital, Boston, MA, USA

W. Butler
Department of Neurosurgery, Massachusetts General Hospital, Boston, MA, USA

E.H. Lo
Neuroprotection Research Laboratory, Massachusetts General Hospital, Boston, MA, USA, and
Department of Neurology, Massachusetts General Hospital, Boston, MA, USA and
Department of Radiology, Massachusetts General Hospital, Boston, MA, USA

pathophysiology of tICH is essential. Although there are significant differences between tICH and sICH, they share common processes, and a review of the literature on sICH could shed light on the mechanisms of injury in tICH.

This review will highlight some of the cellular pathways in ICH with an emphasis on the mechanisms of secondary injury due to heme toxicity and to events in the coagulation process that are common to the different types of sICH and tICH.

Release of Free Heme

Heme is a major component of hemoproteins, including hemoglobin, myoglobin, cytochromes, guanylate cyclase, and nitric oxide synthase. Free heme is deposited in tissue only in pathological conditions. Hemorrhage, ischemia, edema, and mechanical injury damage are all processes that may result in the release of heme from hemoproteins [7]. Intracellular heme originates from cytoplasmic hemoproteins and from mitochondrial cytochromes located in neurons and glia [8]. Extracellular heme is released from dying cells and from extravasated hemoglobin from red blood cells [9]. The release of oxyhemoglobin (oxyHb) leads to superoxide anion (O_2^{\bullet}) and hydrogen peroxide (H_2O_2) release as oxyhemoglobin undergoes auto-oxidation to methemoglobin. Free heme is degraded by heme oxygenase-1 (HO-1) and heme oxygenase-2 (HO-2) into Fe^{2+} , CO, and one isomer of biliverdin, which rapidly reduces to free bilirubin. Free heme is lipophilic and enhances lipid peroxidation [10]. Free iron is extremely toxic to cells it reacts with H_2O_2 to form hydroxyl radicals, and degrades membrane lipid peroxides to yield alkoxy- and peroxy- radicals, which cause further chain reactions of free radical-induced damage [10, 11]. The result is oxidative damage to lipids, DNA, and proteins, leading to caspase activation and neuronal death [12]. Additionally, damage to endothelial cells causes BBB breakdown, resulting in vasogenic edema, increased ICP, and ischemia [13–15]. The effect of bilirubin formation after TBI is unclear. At low physiologic nanomolar concentrations in the healthy brain, bilirubin has potent antioxidative properties, but at high concentrations, it can act as a neurotoxin [7]. The level at which it is neuroprotective vs. neurotoxic is not clear, especially in the complex environment after TBI. The role of CO generation is also controversial, and may have both beneficial and detrimental effects on the vascular smooth muscle [7].

Because of the potential harmful effects of Hb breakdown, HO-1 and HO-2 activity may be detrimental after TBI. HO inhibitors have been shown to reduce edema in models of ischemia, hemorrhage, and trauma [16–18]. However, there is also evidence that HO-1 is neuroprotective [16]. These discrepancies may result from the model used, and the brain region or even the cell type studied. In cell culture, for

example, HO-1, induced in reactive astrocytes and microglia/macrophages, protects cortical astrocytes but not neurons from oxidative stress after exposure to Hb and H_2O_2 [17, 18]. Other investigations show that the anti-oxidant activity of bilirubin/biliverdin redox cycling [19], and the administration of deferoxamine, a scavenger for ferric iron that improved spatial memory in a rodent model of ICH [20].

Haptoglobin (Hp), a glycoprotein that binds free Hb almost irreversibly, is a potential endogenous neuroprotectant after ICH [13, 21, 22]. In the Hb-Hp complex, the iron moiety is situated within the hydrophobic pocket of Hb, preventing its oxidative and cytotoxic activities [23]. Hp binding also facilitates the clearance of free Hb by monocytes and macrophages, and promotes iron recycling [24]. In addition to preventing Hb-induced oxidative cellular damage to cells, Hp-Hb binding protects Hb itself from oxidative damage. This is especially important since oxidative changes to Hb results in its inability to bind to Hp or to the Hb scavenger receptor CD163 on macrophages [25], which mediate Hb endocytosis and clearance. Interestingly, the presence of free Hb alone could induce a state of hypohaptoglobinemia [11], making the induction of Hp expression even more crucial. The Hp level in the brain is low at baseline [11], but its expression can be induced in the brain and in peripheral blood by intracerebral injection of blood [11]. Overexpression of Hp, induced pharmacologically with sulforaphane [an activator of nuclear factor-erythroid 2-related factor (Nrf2)], reduces brain injury after experimental ICH [11].

Oligodendrocytes appear to be the major producer of Hp in the CNS [11]. Since oligodendrocytes are closely associated with axons, they are uniquely situated to decrease the effects of heme toxicity on white matter tracts, which are positioned along the path of blood extravasation during aSAH. In fact, Hp-overexpressing mice show better axonal integrity than Hp-null mice [11]. This function of oligodendrocytes adds to their known activities in protecting axons from excitotoxic and oxidative stress. In addition to protecting neurons, Hp also protects oligodendrocytes themselves from heme toxicity [11], ensuring continued intracranial production of Hp. Thus, Hp is a promising endogenous agent that can be utilized to limit Hb-mediated toxicity in ICH.

Activation of Coagulation

Coagulation disorders are common after TBI, including both hypercoagulability and coagulopathy. In the presence of coagulopathy, there is a significant increase in the risk of morbidity and mortality from TBI. Tissue factor (TF), a protein present in endothelial cells and leukocytes and a key physiological initiator of the coagulation cascade, is released into the general circulation following injury to brain vessels [26].

Cerebral vessels have a rich store of TF and play a central role in inducing CNS and systemic coagulopathy [26, 27]. The large amount of TF released can overwhelm normal control mechanisms that prevent excessive coagulation. With significant hemorrhage, anti-thrombin, clotting factors, and platelets are consumed. At the same time, the expression of plasminogen activator-inhibitor (PAI-1) expression is increased, inhibiting the fibrinolytic system [28]. Tissue hypoperfusion and activation of the protein C pathway have also been implicated in the early coagulopathy seen in TBI [29]. These factors contribute to DIC, which is seen in up to 25% of patients with severe TBI. DIC-induced coagulopathy may develop within hours of injury [30]. On the other hand, TF-dependent activation of coagulation can cause both microvascular and macrovascular fibrin thrombi formation. Excessive microthrombi formation may obstruct flow in small vessels and is proposed to be a cause of delayed ischemia in investigations of aSAH [31]. To illustrate the complexity of the coagulation system, several thrombin-mediated processes will be highlighted here as examples of the many interactions within the coagulation pathways.

Thrombin has been shown to be a potent inducer of microparticle release from platelets and endothelial cells [32]. MPs are small vesicles consisting of a small amount of cytosol and a bilayer plasma membrane with surface antigens from the cell of origin. MP release occurs during many types of apoptogenic, procoagulant, or proinflammatory stimulation [33]. These stimuli trigger the migration of procoagulant phospholipids, such as phosphatidylserine, to the outer leaflet of the plasma membrane, with subsequent membrane budding resulting in MP release. Phosphatidylserine on MP surfaces creates an additional procoagulant surface for the assembly of clotting enzyme complexes [28]. MPs also provide a reservoir of circulating TF and enhance the catalytic efficiency of the TF/factor VIIa complex [28].

In addition to promoting fibrin clot formation, thrombin also mediates vasoconstriction through the thrombin receptor, PAR1, found on endothelial cells [34]. When cleaved by thrombin, activated PAR1 mediates vasoconstriction and upregulates its own expression, increasing the vessel responsiveness to thrombin [34]. These processes potentiate vasoconstriction, which limits bleeding but can worsen ischemia after TBI. PAR1 activation also directly triggers inflammation [35] and increases BBB permeability, edema, and cell death [32], illustrating the complex dynamics within the coagulation system.

Activation of Platelets

Beyond their crucial role in hemostasis, activated platelets have important secondary effects on the vasculature. The interaction of platelets with the exposed collagen of the blood

vessel and with activated leukocytes contributes to platelet degranulation and to the formation of adhesion molecules in the endothelium [36]. These events trigger the release of eicosanoids and free radicals from granulocytes, increasing oxidative stress in the microenvironment of the hemorrhage. Platelets also directly contribute to vasoconstriction after ICH. Platelets and mast cells release 5-HT when activated. 5-HT has many actions, including increasing vascular permeability [36], and vasoconstriction in large cerebral arteries but vasodilation in small cerebral arteries [37, 38]. It also stimulates the sensory fibers of the trigeminovascular system, which release substance P (SP) antidromically [39], contributing to the effects of neurogenic inflammation. In experimental SAH, platelets also interact with perivascular nerves as follows: release of SP from these nerves stimulates the arachidonic acid cascade within platelets [40], contributing to inflammation through products of AA metabolism such as prostaglandins and leukotrienes.

Activation of Leukocytes

Leukocyte-endothelial cell interactions, mediated by intercellular adhesion molecule-1 (ICAM-1), lymphocyte function-associated antigen-1 (LFA-1), macrophage antigen-1 (Mac-1), and endothelial (E)-selectin, constitute another important element in the inflammatory response [41]. These interactions are believed to contribute to the development of vasospasm in aSAH. Infiltrating neutrophils may secrete TNF α and pro-inflammatory proteases, and generate ROS [42]. Dying leukocytes may stimulate macrophages to release proinflammatory mediators [43]. Mast cells migrate to vessel walls after SAH and release histamine when stimulated by bradykinin [44]. In studies of cerebral ischemia, leukocyte-endothelial cell adhesion helps to initiate and propagate reperfusion injury. Mice that have received neutralizing antibodies against leukocyte adhesion receptors and mutant mice that are genetically deficient in these adhesion receptors [45] experience less microvascular dysfunction and tissue injury following ischemia/reperfusion. If the same holds true for post-traumatic hemorrhage, then anti-leukocyte strategies should be explored as a therapeutic option.

Actions of Microglia, Astrocytes, and Oligodendrocytes

In studies of SAH, activated microglia have phagocytic activities that help to clear the hematoma. Thus, microglial activation and macrophage infiltration can be beneficial after hemorrhage. However, activated microglia also release

cytokines [46–48], ROS [49, 50], and nitric oxide [51, 52], all of which also contribute to hemorrhage-induced brain injury. In animal models of ICH, use of anti-microglial strategies, such as tetracycline derivatives, has resulted in reduced injury size, edema, and improved neurologic function [53], but has not yet been substantiated in clinical studies. Importantly, these therapies must maintain the beneficial actions of microglia while decreasing their proinflammatory activities.

Astrocytes modulate the neuronal response to brain injury through the production of angiogenic and neurotrophic factors. For instance, they influence neuronal sensitivity to glutamate toxicity by regulating the expression of the NMDA receptor subunit and the glutamate transporter excitatory amino acid carrier [54]. Interestingly, astrocytes could also modulate microglial ROS production [49] and thus play a role in limiting the harmful effects of microglial ROS release, without compromising the other positive effects of microglial activation. Oligodendrocytes also play an important role. As discussed earlier, one of their responses to hemorrhage is the increased expression of haptoglobin [11], which binds free heme and limits heme-induced toxicity.

The Vascular Response

The different cells within the blood vessels respond differently to the presence of extravascular blood [55]. Cerebral arteries contain three structural layers: the external layer (the adventitia) contains axons of the perivascular nerves in a collagen sheath; the media contains smooth muscle; the internal layer (the intima) contains endothelial cells and the basement membrane. Oxyhemoglobin, released by lysed red blood cells, is pathogenic for all three layers [55]. In the adventitia, the loss of nerve fibers has been reported after sICH [56, 57]. This type of denervation could be expected to result in loss of neurogenic control of cerebral arteries [55] and impairment of autoregulation. In the media, myonecrosis occurs with loss of contractile protein in the smooth muscle [58, 59]; additionally, the amount of interstitial collagen increases [58]. Together, these processes contribute to arterial narrowing, which is not vasospasm-mediated [60]. In the intima layer, matrix metalloproteinases (MMPs) are released after hemorrhage. MMPs degrade the basement membrane and tight junction proteins, resulting in disruption of the BBB. Local substances released by multiple cell types also affect the permeability of the BBB [61]. Perivascular nerve fibers release CGRP, 5-HT, and SP, which contribute to mast cell release of histamine [55], increasing inflammation.

Endothelial cells themselves release substances that can be detrimental in the setting of TBI. An example is

endothelin, a potent vasoconstrictor, which helps to limit hemorrhage but may aggravate ischemic secondary injury after TBI. After ICH, endothelial cells also upregulate the expression of receptors to SUR1 and to angiotensin I (AT1) [62, 63]. These responses also contribute to vasoconstriction. SUR1 [63] and ET-1 [55] have the additional effect of increasing BBB permeability. Specific antagonists to SUR1, AT1 receptors, and ET-1 [55, 62, 63] have been shown to reduce cerebral edema and improve outcome in animal models of ICH and trauma. These are only a few examples of the diverse responses triggered in cerebral endothelial cells after ICH, which have been studied most extensively in the context of vasospasm after aSAH. It has been pointed out that vasospasm also plays a role in the different types of hemorrhage after TBI [64, 65], but it is unclear whether the treatment of post-traumatic vasospasm improves outcome.

Recent studies show that endothelial microparticles (MP) are released into the circulation at high proportions in TBI. In TBI, the proportion of endothelial MPs (compared to platelet MPs) was found to be higher than in many other disease entities, including spontaneous SAH, which is known to cause extensive cerebral endothelial damage [28]. This finding suggests that severe TBI and tICH result in more extensive endothelial activation than sICH, exacerbating the prothrombotic and proinflammatory signaling pathways in TBI.

Conclusion

Intracerebral hemorrhage initiates many cellular responses beyond those that restore hemostasis, and these responses may contribute to secondary brain injury (see Fig. 1). ICH is often accompanied by increased ICP, ischemia, oxidative damage, vasogenic edema, and cytotoxic edema. These processes disrupt mitochondrial energetics and lead to neuronal cell death. Heme toxicity, iron toxicity, and activation of coagulation are obviously key elements in both sICH and tICH. Thus, the data on cellular mechanisms in sICH may be applicable to the understanding of tICH. However, there are also significant differences among the different types of traumatic and spontaneous ICHs. These differences include: the distribution of the various hemorrhage subtypes (subdural, subarachnoid, intraparenchymal, or intraventricular) in spontaneous vs. traumatic bleeds, the extent and rate of hemorrhage progression, the degree and duration of increased intracranial pressure, and the presence of blood beneath the subarachnoid layer vs. the dura. Additionally, the presence of concomitant injuries in TBI may influence the response to ICH. Thus, specific research on the pathophysiology of tICH and the recovery process is needed in order to identify specific therapeutic targets for these processes.

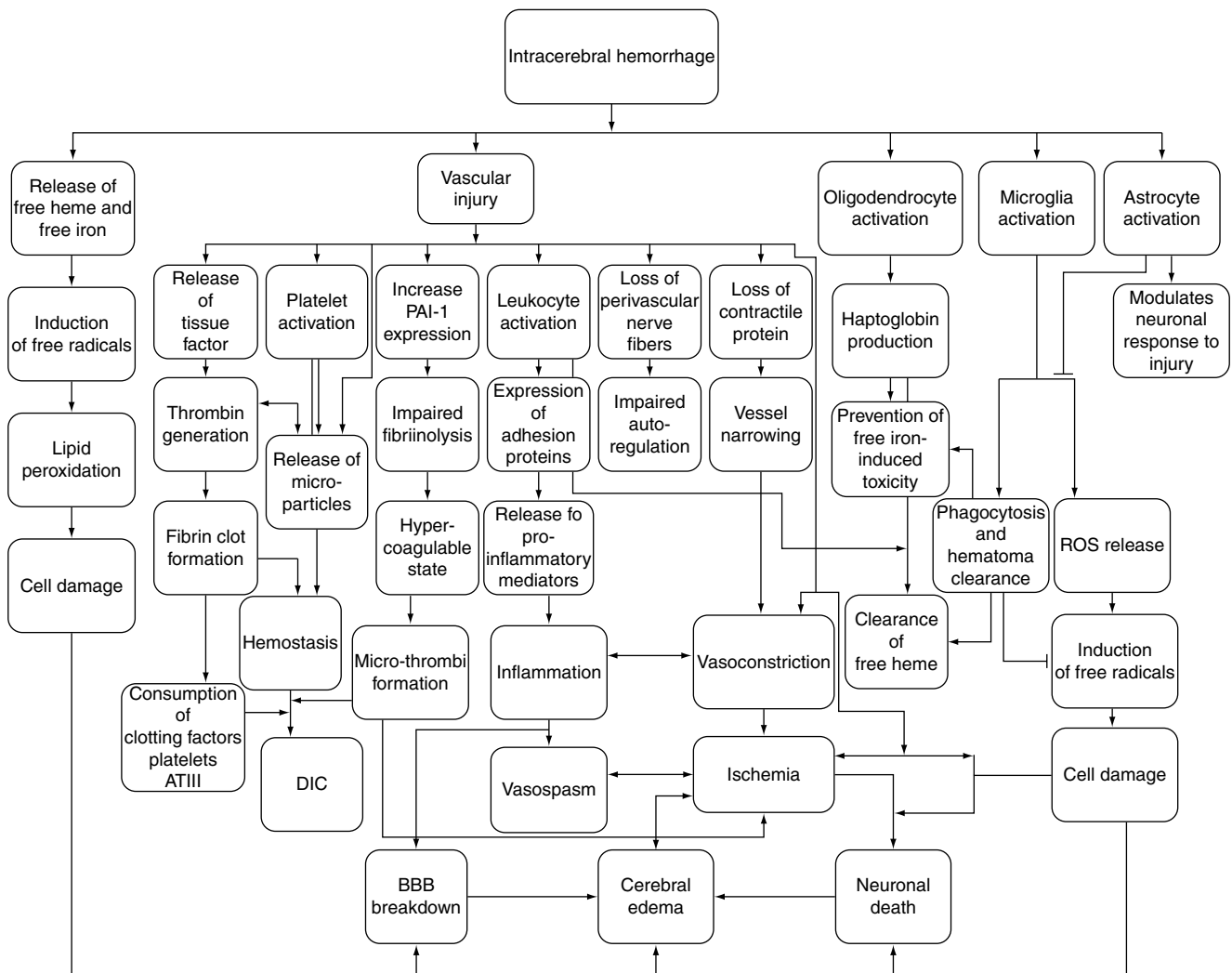


Fig. 1 Representative pathways of secondary brain injury after ICH

Acknowledgement This manuscript is supported by NIH grant K08NS057339 to JL.

Conflict of interest statement The authors declare no conflict of interest.

References

- Narayan RK, Maas AI, Servadei F, Skolnick BE, Tillinger MN, Marshall LF (2008) Progression of traumatic intracerebral hemorrhage: a prospective observational study. *J Neurotrauma* 25: 629–639
- White CL, Griffith S, Caron JL (2009) Early progression of traumatic cerebral contusions: characterization and risk factors. *J Trauma* 67:508–514, discussion 514–505
- Park JH, Park SW, Kang SH, Nam TK, Min BK, Hwang SN (2009) Detection of traumatic cerebral microbleeds by susceptibility-weighted image of MRI. *J Korean Neurosurg Soc* 46:365–369
- Wu HM, Huang SC, Hattori N, Glenn TC, Vespa PM, Hovda DA, Bergsneider M (2004) Subcortical white matter metabolic changes remote from focal hemorrhagic lesions suggest diffuse injury after human traumatic brain injury. *Neurosurgery* 55:1306–1315, discussion 1316–1307
- Immonen RJ, Kharatishvili I, Grohn H, Pitkanen A, Grohn OH (2009) Quantitative MRI predicts long-term structural and functional outcome after experimental traumatic brain injury. *Neuroimage* 45:1–9
- Narayan RK, Maas AI, Marshall LF, Servadei F, Skolnick BE, Tillinger MN (2008) Recombinant factor VIIA in traumatic intracerebral hemorrhage: results of a dose-escalation clinical trial. *Neurosurgery* 62:776–786, discussion 786–778
- Chang EF, Claus CP, Vreman HJ, Wong RJ, Noble-Haesslein LJ (2005) Heme regulation in traumatic brain injury: relevance to the adult and developing brain. *J Cereb Blood Flow Metab* 25:1401–1417
- Wagner KR, Sharp FR, Ardizzone TD, Lu A, Clark JF (2003) Heme and iron metabolism: role in cerebral hemorrhage. *J Cereb Blood Flow Metab* 23:629–652
- Sharp FR, Massa SM, Swanson RA (1999) Heat-shock protein protection. *Trends Neurosci* 22:97–99

10. O'Brien PJ, Little C (1969) Intracellular mechanisms for the decomposition of a lipid peroxide. II. Decomposition of a lipid peroxide by subcellular fractions. *Can J Biochem* 47:493–499
11. Zhao X, Song S, Sun G, Strong R, Zhang J, Grotta JC, Aronowski J (2009) Neuroprotective role of haptoglobin after intracerebral hemorrhage. *J Neurosci* 29:15819–15827
12. Wang X, Mori T, Sumii T, Lo EH (2002) Hemoglobin-induced cytotoxicity in rat cerebral cortical neurons: caspase activation and oxidative stress. *Stroke* 33:1882–1888
13. Keep RF, Xiang J, Ennis SR, Andjelkovic A, Hua Y, Xi G, Hoff JT (2008) Blood-brain barrier function in intracerebral hemorrhage. *Acta Neurochir Suppl* 105:73–77
14. Thiex R, Tsirka SE (2007) Brain edema after intracerebral hemorrhage: mechanisms, treatment options, management strategies, and operative indications. *Neurosurg Focus* 22:E6
15. Bhasin RR, Xi G, Hua Y, Keep RF, Hoff JT (2002) Experimental intracerebral hemorrhage: effect of lysed erythrocytes on brain edema and blood-brain barrier permeability. *Acta Neurochir Suppl* 81:249–251
16. Ferris CD, Jaffrey SR, Sawa A, Takahashi M, Brady SD, Barrow RK, Tysoe SA, Wolosker H, Baranano DE, Dore S, Poss KD, Snyder SH (1999) Haem oxygenase-1 prevents cell death by regulating cellular iron. *Nat Cell Biol* 1:152–157
17. Regan RF, Chen J, Benvenisti-Zarom L (2004) Heme oxygenase-2 gene deletion attenuates oxidative stress in neurons exposed to extracellular hemin. *BMC Neurosci* 5:34. doi:10.1186/1471-2202-5-34
18. Rogers B, Yakopson V, Teng ZP, Guo Y, Regan RF (2003) Heme oxygenase-2 knockout neurons are less vulnerable to hemoglobin toxicity. *Free Radic Biol Med* 35:872–881
19. Baranano DE, Rao M, Ferris CD, Snyder SH (2002) Biliverdin reductase: a major physiologic cytoprotectant. *Proc Natl Acad Sci USA* 99:16093–16098
20. Nakamura T, Keep RF, Hua Y, Schallert T, Hoff JT, Xi G (2004) Deferoxamine-induced attenuation of brain edema and neurological deficits in a rat model of intracerebral hemorrhage. *J Neurosurg* 100:672–678
21. Xi G, Keep RF, Hoff JT (1998) Erythrocytes and delayed brain edema formation following intracerebral hemorrhage in rats. *J Neurosurg* 89:991–996
22. Wada T, Oara H, Watanabe K, Kinoshita H, Yachi A (1970) Autoradiographic study on the site of uptake of the haptoglobin-hemoglobin complex. *J Reticuloendothel Soc* 8:185–193
23. Allison AC, Rees WA (1957) The binding of haemoglobin by plasma proteins (haptoglobins); its bearing on the renal threshold for haemoglobin and the aetiology of haemoglobinuria. *Br Med J* 2:1137–1143
24. Wang Y, Kinzie E, Berger FG, Lim SK, Baumann H (2001) Haptoglobin, an inflammation-inducible plasma protein. *Redox Rep* 6:379–385
25. Buehler PW, Abraham B, Vallelian F, Linnemayr C, Pereira CP, Cipollo JF, Jia Y, Mikolajczyk M, Boretti FS, Schoedon G, Alayash AI, Schaer DJ (2009) Haptoglobin preserves the CD163 hemoglobin scavenger pathway by shielding hemoglobin from peroxidative modification. *Blood* 113:2578–2586
26. Stein SC, Smith DH (2004) Coagulopathy in traumatic brain injury. *Neurocrit Care* 1:479–488
27. Keimowitz RM, Annis BL (1973) Disseminated intravascular coagulation associated with massive brain injury. *J Neurosurg* 39:178–180
28. Morel N, Morel O, Petit L, Hugel B, Cochard JF, Freyssinet JM, Sztark F, Dabadie P (2008) Generation of procoagulant microparticles in cerebrospinal fluid and peripheral blood after traumatic brain injury. *J Trauma* 64:698–704
29. Cohen MJ, Brohi K, Ganter MT, Manley GT, Mackersie RC, Pittet JF (2007) Early coagulopathy after traumatic brain injury: the role of hypoperfusion and the protein C pathway. *J Trauma* 63:1254–1261, discussion 1261–1252
30. Halpern CH, Reilly PM, Turtz AR, Stein SC (2008) Traumatic coagulopathy: the effect of brain injury. *J Neurotrauma* 25:997–1001
31. Vergouwen MD, Vermeulen M, Coert BA, Stroes ES, Roos YB (2008) Microthrombosis after aneurysmal subarachnoid hemorrhage: an additional explanation for delayed cerebral ischemia. *J Cereb Blood Flow Metab* 28:1761–1770
32. Sugawara T, Jadhav V, Ayer R, Chen W, Suzuki H, Zhang JH (2009) Thrombin inhibition by argatroban ameliorates early brain injury and improves neurological outcomes after experimental subarachnoid hemorrhage in rats. *Stroke* 40:1530–1532
33. Morel O, Morel N, Freyssinet JM, Toti F (2008) Platelet microparticles and vascular cells interactions: a checkpoint between the haemostatic and thrombotic responses. *Platelets* 19:9–23
34. Kai Y, Maeda Y, Sasaki T, Kanaide H, Hirano K (2008) Basic and translational research on proteinase-activated receptors: the role of thrombin receptor in cerebral vasospasm in subarachnoid hemorrhage. *J Pharmacol Sci* 108:426–432
35. Xi G, Reiser G, Keep RF (2003) The role of thrombin and thrombin receptors in ischemic, hemorrhagic and traumatic brain injury: deleterious or protective? *J Neurochem* 84:3–9. doi:10.1046/j.1471-4159.2003.01268.x [pii]
36. Akopov S, Sercombe R, Seylaz J (1996) Cerebrovascular reactivity: role of endothelium/platelet/leukocyte interactions. *Cerebrovasc Brain Metab Rev* 8:11–94
37. Auer LM, Leber K, Sayama I (1985) Effect of serotonin and its antagonist ketanserin on pial vessels. *J Cereb Blood Flow Metab* 5:517–522
38. Muhonen MG, Robertson SC, Gerdes JS, Loftus CM (1997) Effects of serotonin on cerebral circulation after middle cerebral artery occlusion. *J Neurosurg* 87:301–306
39. Khalil Z, Helme RD (1990) Serotonin modulates substance P-induced plasma extravasation and vasodilatation in rat skin by an action through capsaicin-sensitive primary afferent nerves. *Brain Res* 527:292–298. doi:0006-8993(90)91149-B [pii]
40. Gece A, Kis B, Mezei Z, Telegdy G (1999) Effects of inflammatory neuropeptides on the arachidonate cascade of platelets. *Int Arch Allergy Immunol* 118:166–170
41. Wang J, Dore S (2007) Inflammation after intracerebral hemorrhage. *J Cereb Blood Flow Metab* 27:894–908
42. Weiss SJ (1989) Tissue destruction by neutrophils. *N Engl J Med* 320:365–376
43. Stern M, Savill J, Haslett C (1996) Human monocyte-derived macrophage phagocytosis of senescent eosinophils undergoing apoptosis. Mediation by alpha v beta 3/CD36/thrombospondin recognition mechanism and lack of phlogistic response. *Am J Pathol* 149:911–921
44. Lee PY, Pearce FL (1990) Histamine secretion from mast cells stimulated with bradykinin. *Agents Actions* 30:67–69
45. Ishikawa M, Zhang JH, Nanda A, Granger DN (2004) Inflammatory responses to ischemia and reperfusion in the cerebral microcirculation. *Front Biosci* 9:1339–1347
46. Gregersen R, Lambertsen K, Finsen B (2000) Microglia and macrophages are the major source of tumor necrosis factor in permanent middle cerebral artery occlusion in mice. *J Cereb Blood Flow Metab* 20:53–65
47. Hanisch UK (2002) Microglia as a source and target of cytokines. *Glia* 40:140–155. doi:10.1002/glia.10161
48. Stoll G, Schroeter M, Jander S, Siebert H, Wollrath A, Kleinschnitz C, Bruck W (2004) Lesion-associated expression of transforming growth factor-beta-2 in the rat nervous system: evidence for down-regulating the phagocytic activity of microglia and macrophages. *Brain Pathol* 14:51–58

49. Min KJ, Yang MS, Kim SU, Jou I, Joe EH (2006) Astrocytes induce hemeoxygenase-1 expression in microglia: a feasible mechanism for preventing excessive brain inflammation. *J Neurosci* 26:1880–1887
50. Wang J, Tsirka SE (2005) Tuftsin fragment 1–3 is beneficial when delivered after the induction of intracerebral hemorrhage. *Stroke* 36:613–618
51. Mander P, Borutaite V, Moncada S, Brown GC (2005) Nitric oxide from inflammatory-activated glia synergizes with hypoxia to induce neuronal death. *J Neurosci Res* 79:208–215
52. Khan M, Sekhon B, Giri S, Jatana M, Gilg AG, Ayasolla K, Elango C, Singh AK, Singh I (2005) S-Nitrosoglutathione reduces inflammation and protects brain against focal cerebral ischemia in a rat model of experimental stroke. *J Cereb Blood Flow Metab* 25:177–192
53. Van Den Bosch L, Tilkin P, Lemmens G, Robberecht W (2002) Minocycline delays disease onset and mortality in a transgenic model of ALS. *NeuroReport* 13:1067–1070
54. Canolle B, Masmejean F, Melon C, Nieoullon A, Pisano P, Lortet S (2004) Glial soluble factors regulate the activity and expression of the neuronal glutamate transporter EAAC1: implication of cholesterol. *J Neurochem* 88:1521–1532. doi:10.1046/j.1471-4159.2003.02301.x [pii]
55. Sercombe R, Dinh YR, Gomis P (2002) Cerebrovascular inflammation following subarachnoid hemorrhage. *Jpn J Pharmacol* 88:227–249
56. Uemura Y, Sugimoto T, Okamoto S, Handa H, Mizuno N (1987) Changes of neuropeptide immunoreactivity in cerebrovascular nerve fibers after experimentally produced SAH. Immunohistochemical study in the dog. *J Neurosurg* 66:741–747
57. Fein JM, Flor WJ, Cohan SL, Parkhurst J (1974) Sequential changes of vascular ultrastructure in experimental cerebral vasospasm. Myonecrosis of subarachnoid arteries. *J Neurosurg* 41:49–58
58. Mayberg MR, Okada T, Bark DH (1990) The significance of morphological changes in cerebral arteries after subarachnoid hemorrhage. *J Neurosurg* 72:626–633
59. Gomis P, Kacem K, Sercombe C, Seylaz J, Sercombe R (2000) Confocal microscopic evidence of decreased alpha-actin expression within rabbit cerebral artery smooth muscle cells after subarachnoid haemorrhage. *Histochem J* 32:673–678
60. Yamamoto Y, Bernanke DH, Smith RR (1990) Accelerated non-muscle contraction after subarachnoid hemorrhage: cerebrospinal fluid testing in a culture model. *Neurosurgery* 27:921–928
61. Grossetete M, Phelps J, Arko L, Yonas H, Rosenberg GA (2009) Elevation of matrix metalloproteinases 3 and 9 in cerebrospinal fluid and blood in patients with severe traumatic brain injury. *Neurosurgery* 65:702–708
62. Jung KH, Chu K, Lee ST, Kim SJ, Song EC, Kim EH, Park DK, Sinn DI, Kim JM, Kim M, Roh JK (2007) Blockade of AT1 receptor reduces apoptosis, inflammation, and oxidative stress in normotensive rats with intracerebral hemorrhage. *J Pharmacol Exp Ther* 322:1051–1058
63. Simard JM, Kilbourne M, Tsybalyuk O, Tosun C, Caridi J, Ivanova S, Keledjian K, Bochicchio E, Gerzanich V (2009) Key role of sulfonylurea receptor 1 in progressive secondary hemorrhage after brain confusion. *J Neurotrauma* 26(12): 2257–2267
64. Armin SS, Colohan AR, Zhang JH (2006) Traumatic subarachnoid hemorrhage: our current understanding and its evolution over the past half century. *Neurol Res* 28:445–452
65. Armin SS, Colohan AR, Zhang JH (2008) Vasospasm in traumatic brain injury. *Acta Neurochir Suppl* 104:421–425

Clot Formation, Vascular Repair and Hematoma Resolution After ICH, a Coordinating Role for Thrombin?

Richard F. Keep, G. Xi, Y. Hua, and J. Xiang

Abstract Following intracerebral hemorrhage (ICH) there is a sequential response involving activation of the coagulation cascade/platelet plug formation, vascular repair, upregulation of endogenous defense mechanisms and clot resolution. How these responses are coordinated and modified by different hematoma sizes has received little attention. This paper reviews evidence that thrombin can modulate and may coordinate the components of the endogenous response. This has potential consequences for treatment of ICH with a number of modalities.

Keywords Thrombin · Coagulation · Vascular repair · Hematoma resolution · Iron-handling proteins

Introduction

The endogenous response to an intracerebral hemorrhage (ICH) involves: (1) clot/platelet plug formation to stop the bleed, (2) vascular repair and (3) clot resolution. As clot resolution can release potentially neurotoxic chemicals (e.g., iron), there is also (4) upregulation of endogenous defense mechanisms that may counteract the effects of those chemicals (e.g., iron chelators;[1]). To avoid re-bleeding, which might

occur if the clot resolved prior to completion of vascular repair or potential neurotoxicity if clot resolution occurs prior to induction of defense mechanisms, these responses must be coordinated (Fig. 1). Therapeutically, a number of approaches have been used to enhance the endogenous response. For example, Factor VIIa has been given to promote clotting [2], surgery with and without tissue plasminogen activator (tPA) has been used to accelerate clot removal [3], thiazolidinediones have been given to modulate clot phagocytosis by microglia [4], and deferoxamine has been administered to enhance iron defense [5].

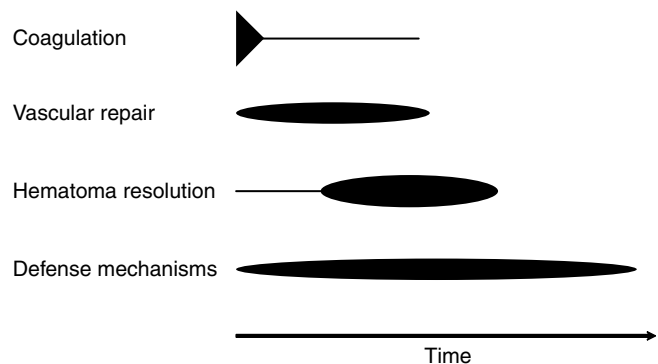


Fig. 1 The sequential endogenous response to ICH. While the coagulation cascade is activated immediately upon hemorrhage, there will be continued production of thrombin and fibrin until sufficient vascular plugging and repair have occurred to prevent further entry of fibrinogen and prothrombin. The time course of vascular repair after ICH has not been well studied. It is probably initiated immediately after ictus and is sufficient to prevent further hemorrhage by the time that hematoma resolution is complete. Fibrinolysis begins almost immediately after the hemorrhage. However, in the early stages after ICH, fibrin deposition exceeds lysis. Resolution occurs when lysis exceeds fibrin deposition (decreased thrombin cleavage of fibrinogen) and when there is clearance of cellular elements of the hematoma. The time course of resolution varies with hematoma size (*see text*). The induction of endogenous defense mechanisms involves (at least in part) the production of new protein. This involves a time delay after ictus (e.g., iron handling proteins peak 24–72 h after ICH in the rat)

R.F. Keep (✉)
Department of Neurosurgery, University of Michigan,
Ann Arbor, MI, USA and
Department of Molecular & Integrative Physiology,
University of Michigan, Ann Arbor, MI, USA and
R5018 Biomedical Science Research Building,
University of Michigan, 109 Zina Pitcher Place,
Ann Arbor, MI 48109-2200, USA
e-mail: rkeep@umich.edu

G. Xi, Y. Hua, and J. Xiang
Department of Neurosurgery, University of Michigan,
Ann Arbor, MI, USA

While information is available about parts of the endogenous response (e.g., the coagulation cascade and the role of microglia, leukocytes, complement and plasminogen activators in clot resolution), less is known about coordination of the endogenous responses and how they might be modulated by ICH severity. One potential coordinator of the endogenous responses is thrombin. This paper examines this potential role and highlights some therapeutic consequences.

Normal Natural History of Clot Formation and Resolution After ICH

After cerebrovascular rupture, there is almost instantaneous activation of the coagulation cascade and the start of clot formation. In about two-thirds of patients, bleeding stops soon after ictus, but in the remaining patients there is continued hematoma expansion for part of the first day [6], an expansion phase that is increased in patients on oral anticoagulant therapy [7]. In humans, the hematoma has been reported to then resolve over weeks, although this depends upon clot size [8]. It should be noted that even after the physical hematoma resolves, hematoma degradation products can still remain in the brain. Thus, high levels of iron are still found in the rat brain 28 days after ICH even though the hematoma has resolved [1].

Thrombin Generation and Coagulation After ICH

Thrombin, by converting fibrinogen to fibrin (and by stabilization of the fibrin clot via activation of Factor XIII), is central to the coagulation cascade. However, it also has other effects on the coagulation cascade, activating Factor XI, as well as cofactors VIII and V, and stimulating platelets. These effects serve to amplify the coagulation cascade. The actions of thrombin are carried out by either enzyme activity (e.g., conversion of fibrinogen to fibrin) or cell thrombin receptors (e.g., platelet activation). Three protease-activated receptors (PAR-1, -3 and -4) are thrombin receptors [9].

While thrombin is produced almost instantaneously from prothrombin at the ictus, there may be continued production until the injury site is completely plugged, preventing further entry of prothrombin into the brain. As noted above, in some patients, this may take several hours.

Thrombin and Vascular Repair

Vascular repair after ICH has received little attention. Repair entails reestablishment of the endothelial barrier, but also

involves changes in other elements of the neurovascular unit (e.g., astrocytes, pericytes and vascular smooth muscle cells). Circulating endothelial progenitor cells may also be involved in re-endothelialization [10, 11]. Thrombin has profound effects on cerebral endothelial cell proliferation and shape [12, 13]. It also has marked effects on other elements of the neurovascular unit. Thus, for example, it changes astrocyte shape [14], indirectly causes pericyte contraction [15] and induces smooth muscle cell proliferation [16]. Thrombin can also cause migration of progenitor cells from the subventricular zone to sites of injury [17].

Thrombin and Clot Resolution

There is a surprising lack of definitive evidence about the relative importance of different mechanisms in clearing intracerebral hematomas. Perihematomal levels of plasminogen activators are increased after ICH [18], but the relative importance of tPA and urokinase (uPA) in fibrinolysis after ICH is uncertain. Both tPA and uPA have been used clinically to aid in clot removal, although there is, to date, no evidence that this reduces ICH-induced injury in patients [19]. Removal of the cellular constituents of the hematoma involves several processes. Erythrocyte energy failure can cause cell lysis, complement activation inserts a membrane attack complex in the cell membrane leading to lysis, and there can be phagocytosis of the erythrocytes and cell elements [4, 20, 21]. Phagocytosis can be carried out by microglia or invading macrophages from the bloodstream [4, 21].

Thrombin has the potential to impact both fibrinolysis and the clearance of cellular components of the hematoma. Thrombin indirectly impacts fibrinolysis as fibrin (and particularly partially degraded fibrin) enhances plasminogen activator activity leading to greater plasmin production [22]. Thrombin also directly induces cerebral endothelial cells to produce uPA [13]. ICH-induced inflammation is also regulated by thrombin. It upregulates inflammatory mediators, activates microglia and promotes leukocyte influx into brain [6]. Thrombin can also cause activation of the complement cascade in the brain, including membrane attack complex formation [23]. These results indicate that thrombin modulates clot resolution as well as clot formation.

Thrombin and Endogenous Defense Mechanisms

A number of mechanisms that may limit brain injury are upregulated after ICH. For example, there is a marked increase in the expression of iron-handling proteins such as ferritin, transferrin and transferrin receptor [1]. These changes

may reduce the iron toxicity that can follow hematoma resolution [6]. While expression of iron handling proteins is regulated by a number of systems, intracerebral thrombin triggers a marked increase in transferrin and the transferrin receptor expression in brain [24]. As thrombin is produced immediately upon hemorrhage, the upregulation in iron handling proteins occurs early after ICH [1], allowing the proteins to be present before the onset of erythrocyte lysis within the hematoma. Iron itself can also upregulate the expression of iron handling proteins [25], but if iron release during hematoma resolution were to be the sole signal for upregulation, there would be potential iron-induced neurotoxicity in the hours necessary for protein upregulation.

Thrombin Inhibition After ICH

Understanding the temporal effects of thrombin in ICH not only requires knowledge of its production and targets, it also requires information about what factors inhibit thrombin's action and how these change after ICH. Protease nexin-1 (PN-1) is the main thrombin inhibitor present in brain. It is highly expressed in astrocytes, but there is also evidence for neuronal expression [9]. PN-1 (mRNA and protein) is upregulated in the brain after rat ICH [26]. Plasminogen activator inhibitor (PAI)-1 can also inhibit thrombin, and it too is upregulated after ICH [27]. However, although these inhibitors may inhibit free thrombin, a substantial amount of

thrombin remains bound within the hematoma where it is protected from inactivation [28]. Thus, as the hematoma resolves there is continual release of thrombin from the hematoma. The action of that thrombin will depend on access to targets (for example, fibrinogen and platelets).

Thrombin as a Coordinator of the Endogenous Responses and Therapeutic Consequences

A temporally coordinated endogenous response to ICH involving coagulation/platelet plug formation, vascular repair, hematoma resolution and upregulation of defense mechanisms necessitates some crosstalk between these different events. The pleiotropic effects of thrombin suggest that it may be involved in such coordination (Fig. 2). As described above, it is central to the coagulation cascade and platelet plug formation, it affects vascular repair and hematoma resolution, and it can induce some of the endogenous defense mechanisms. Thrombin is initially formed at the onset of hemorrhage, and this is important for coagulation and platelet plug formation. This early production of thrombin may also be important for initiating vascular repair and providing the signal for upregulation of defense mechanisms, such as iron handling proteins.

The release of clot-bound thrombin may also provide a way of coordinating hematoma resolution with vascular

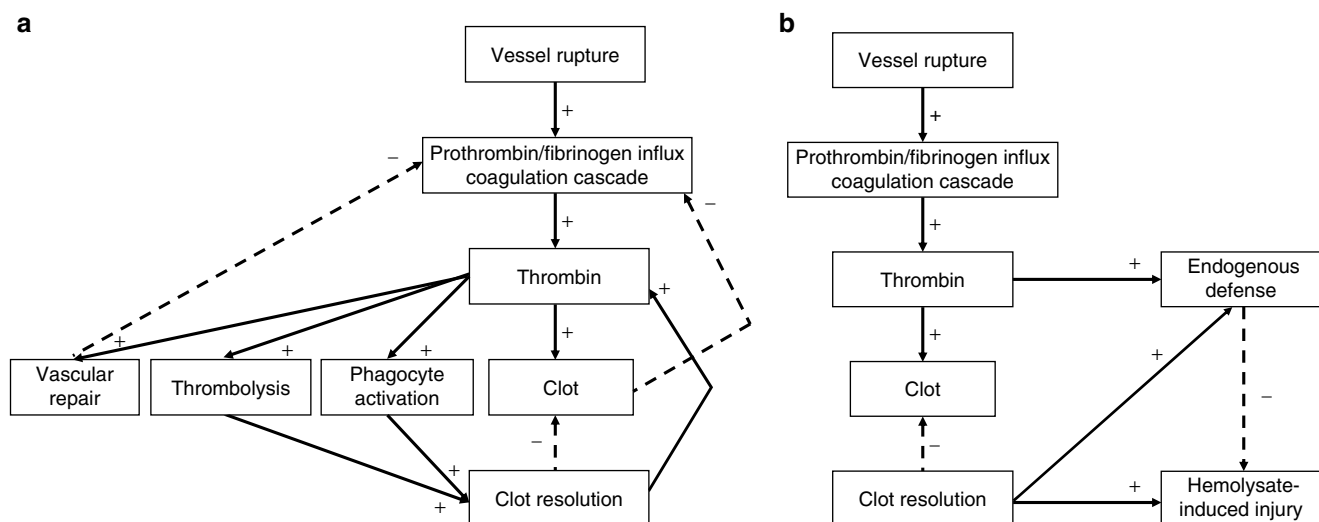


Fig. 2 Thrombin impacts many elements of the endogenous response to ICH. **(a)** The production of thrombin serves to seal the site of initial rupture via production of a clot/platelet plug, and it is also involved in regulating vascular repair. Thrombin is also involved in clot resolution. By sealing the rupture, clotting and vascular repair can stop further entry of prothrombin and fibrinogen into the brain, preventing further fibrin deposition. In addition, thrombin activates microglia, promotes macrophage entry into the brain (both cell types are involved in hema-

toma phagocytosis) and can accelerate fibrinolysis, aiding hematoma resolution. Because thrombin is present within the clot, hematoma resolution may cause its release, which may serve to produce more fibrin if the vasculature has not been fully repaired. **(b)** Thrombin is also involved in upregulating defense mechanisms in the brain (e.g., iron-handling proteins), which may reduce clot-derived neurotoxicity. While clot-derived factors may also upregulate defense mechanisms, thrombin upregulation may occur, earlier providing greater protection

repair. If hematoma degradation occurs before vascular repair is fully achieved, leakage of fibrinogen from the damaged vessel may be cleaved by thrombin from the degrading hematoma to form a new fibrin clot. This might provide a quicker response than activation of the coagulation cascade and creation of thrombin from prothrombin leaking from the bloodstream. In addition, the continual release of clot-bound thrombin from the resolving hematoma may provide a signal to maintain upregulation of phagocytosis and defense mechanisms until the clot has finally resolved. If this is the case, thrombin may also participate in ending the endogenous response to ICH. As the vessel is repaired and the hematoma resolves, there will be a decline in extravascular thrombin, and this may be a signal for the cessation of the inflammatory response and the return of defense mechanisms to normal levels. This potential role of thrombin requires further examination.

ICH severity varies from microbleeds to hematomas of over 100 mL. Presumably, the extent of the endogenous response needs to vary with the size of the hematoma. As the amount of prothrombin entering the brain with the hemorrhage varies with the size of the hematoma, thrombin production would reflect the severity of the hemorrhage and may regulate the endogenous response to match ICH size.

A role for thrombin in coordinating the endogenous response would have several therapeutic consequences. Thrombin has been the target in clinical and preclinical ICH trials. Increasing thrombin production to prevent hematoma expansion was the basis of the Factor VIIa trial [2]. While that trial showed that Factor VIIa could reduce hematoma growth, it did not improve outcome. In contrast, there is preclinical evidence that thrombin can participate in ICH-induced injury [29], and delayed thrombin inhibition with argatroban improved outcome in a rat ICH model [30]. These results reflect the differential time-dependent roles of thrombin in ICH.

Clot removal has been examined extensively as a method of reducing ICH-induced injury without, as yet, significant clinical benefit [19]. The poor outcome in patients that had ultra-early clot removal because of rebleeds [31] reflects the importance of ensuring that vascular repair has occurred prior to clot removal/resolution. Whether more delayed clot removal may have unanticipated effects on ICH-induced injury by affecting the endogenous response to ICH by removing clot-bound thrombin has not been examined (e.g., will it affect the upregulation of endogenous defense mechanisms?).

Summary

Thrombin has pleiotropic effects on the response of the brain to ICH, including roles in coagulation/platelet plug formation, vascular repair, clot resolution and upregulation

of endogenous defense mechanisms, and may act as a coordinator of the endogenous response. Understanding the integration of the response of the brain to ICH may give insight into how better to modulate that response to reduce ICH-induced injury.

Acknowledgments This work was supported by the National Institutes of Health grants NS34709 (RFK), NS017760 (GX) and NS039866 (GX). The content is solely the responsibility of the authors and does not necessarily represent the official views of the NIH.

Conflict of interest statement We declare that we have no conflict of interest.

References

1. Wu J, Hua Y, Keep RF, Nakamura T, Hoff JT, Xi G (2003) Iron and iron-handling proteins in the brain after intracerebral hemorrhage. *Stroke* 34:2964–2969
2. Mayer SA, Brun NC, Begtrup K, Broderick J, Davis S, Diringer MN, Skolnick BE, Steiner T (2008) Efficacy and safety of recombinant activated factor VII for acute intracerebral hemorrhage. *N Engl J Med* 358:2127–2137
3. Mendelow AD, Unterberg A (2007) Surgical treatment of intracerebral haemorrhage. *Curr Opin Crit Care* 13:169–174
4. Zhao X, Sun G, Zhang J, Strong R, Song W, Gonzales N, Grotta JC, Aronowski J (2007) Hematoma resolution as a target for intracerebral hemorrhage treatment: role for peroxisome proliferator-activated receptor gamma in microglia/macrophages. *Ann Neurol* 61:352–362
5. Hua Y, Nakamura T, Keep RF, Wu J, Schallert T, Hoff JT, Xi G (2006) Long-term effects of experimental intracerebral hemorrhage: the role of iron. *J Neurosurg* 104:305–312
6. Xi G, Keep RF, Hoff JT (2006) Mechanisms of brain injury after intracerebral haemorrhage. *Lancet Neurol* 5:53–63
7. Huttner HB, Steiner T (2010) Coagulopathy-related intracerebral hemorrhage. In: Carhuapoma JR, Mayer SA, Hanley DF (eds) *Intracerebral hemorrhage*. Cambridge University Press, Cambridge, pp 58–70
8. Dolinskas CA, Bilaniuk LT, Zimmerman RA, Kuhl DE (1977) Computed tomography of intracerebral hematomas. I. Transmission CT observations on hematoma resolution. *Am J Roentgenol* 129:681–688
9. Xi G, Reiser G, Keep RF (2003) The role of thrombin and thrombin receptors in ischemic, hemorrhagic and traumatic brain injury: deleterious or protective? *J Neurochem* 84:3–9
10. Hristov M, Weber C, Hristov M, Weber C (2008) Endothelial progenitor cells in vascular repair and remodeling. *Pharm Res* 58:148–151
11. Urbich C, Dimmeler S, Urbich C, Dimmeler S (2004) Endothelial progenitor cells: characterization and role in vascular biology. *Circ Res* 95:343–353
12. Nagy Z, Kolev K, Csonka E, Pek M, Machovich R (1995) Contraction of human brain endothelial cells induced by thrombogenic and fibrinolytic factors. An in vitro cell culture model. *Stroke* 26:265–270
13. Shatos MA, Orfeo T, Doherty JM, Penar PL, Collen D, Mann KG (1995) Alpha-thrombin stimulates urokinase production and DNA synthesis in cultured human cerebral microvascular endothelial cells. *Arterioscler Thromb Vasc Biol* 15:903–911
14. Cavanaugh KP, Gurwitz D, Cunningham DD, Bradshaw RA (1990) Reciprocal modulation of astrocyte stellation by thrombin and protease nexin-1. *J Neurochem* 54:1735–1743

15. Dodge AB, Hechtman HB, Shepro D (1991) Microvascular endothelial-derived autacoids regulate pericyte contractility. *Cell Motil Cytoskeleton* 18:180–188
16. Stouffer GA, Runge MS (1998) The role of secondary growth factor production in thrombin-induced proliferation of vascular smooth muscle cells. *Sem Thromb Hemost* 24:145–150
17. Yang S, Song S, Hua Y, Nakamura T, Keep RF, Xi G (2008) Effects of thrombin on neurogenesis after intracerebral hemorrhage. *Stroke* 39:2079–2084
18. Masuda T, Dohrmann GJ, Kwaan HC, Erickson RK, Wollman RL (1988) Fibrinolytic activity in experimental intracerebral hematoma. *J Neurosurg* 68:274–278
19. Mendelow AD, Gregson BA, Fernandes HM, Murray GD, Teasdale GM, Hope DT, Karimi A, Shaw MD, Barer DH (2005) Early surgery versus initial conservative treatment in patients with spontaneous supratentorial intracerebral haematomas in the International Surgical Trial in Intracerebral Haemorrhage (STICH): a randomised trial. *Lancet* 365:387–397
20. Hua Y, Xi G, Keep RF, Hoff JT (2000) Complement activation in the brain after experimental intracerebral hemorrhage. *J Neurosurg* 92:1016–1022
21. Zhao X, Grotta J, Gonzales N, Aronowski J, Zhao X, Grotta J, Gonzales N, Aronowski J (2009) Hematoma resolution as a therapeutic target: the role of microglia/macrophages. *Stroke* 40:S92–S94
22. Eastman D, Wurm FM, van Reis R, Higgins DL (1992) A region of tissue plasminogen activator that affects plasminogen activation differentially with various fibrin(ogen)-related stimulators. *Biochemistry* 31:419–422
23. Gong Y, Xi GH, Keep RF, Hoff JT, Hua Y (2005) Complement inhibition attenuates brain edema and neurological deficits induced by thrombin. *Acta Neurochir Suppl* 95:389–392
24. Hua Y, Keep RF, Hoff JT, Xi G (2003) Thrombin preconditioning attenuates brain edema induced by erythrocytes and iron. *J Cereb Blood Flow Metab* 23:1448–1454
25. Wagner KR, Sharp FR, Ardizzone TD, Lu A, Clark JF, Wagner KR, Sharp FR, Ardizzone TD, Lu A, Clark JF (2003) Heme and iron metabolism: role in cerebral hemorrhage. *J Cereb Blood Flow Metab* 23:629–652
26. Wu H, Zhao R, Qi J, Cong Y, Wang D, Liu T, Gu Y, Ban X, Huang Q, Wu H, Zhao R, Qi J, Cong Y, Wang D, Liu T, Gu Y, Ban X, Huang Q (2008) The expression and the role of protease nexin-1 on brain edema after intracerebral hemorrhage. *J Neurol Sci* 270:172–183
27. Hua Y, Xi G, Keep RF, Wu J, Jiang Y, Hoff JT (2002) Plasminogen activator inhibitor-1 induction after experimental intracerebral hemorrhage. *J Cereb Blood Flow Metab* 22:55–61
28. Liu CY, Nossel HL, Kaplan KL (1979) The binding of thrombin by fibrin. *J Biol Chem* 254:10421–10425
29. Lee KR, Colon GP, Betz AL, Keep RF, Kim S, Hoff JT (1996) Edema from intracerebral hemorrhage: the role of thrombin. *J Neurosurg* 84:91–96
30. Kitaoka T, Hua Y, Xi G, Hoff JT, Keep RF (2002) Delayed argatroban treatment reduces edema in a rat model of intracerebral hemorrhage. *Stroke* 33:3012–3018
31. Morgenstern LB, Demchuk AM, Kim DH, Frankowski RF, Grotta JC (2001) Rebleeding leads to poor outcome in ultra-early craniotomy for intracerebral hemorrhage. *Neurology* 56:1294–1299

The Dual Role of Src Kinases in Intracerebral Hemorrhage

Da-Zhi Liu and Frank R. Sharp

Abstract Src kinase signaling has been implicated in multiple mechanisms of intracerebral hemorrhage (ICH). These include (1) thrombin-mediated mitogenic stress, (2) excitatory amino acid (AA)-mediated excitatory toxicity, (3) vascular endothelial growth factor (VEGF) and matrix metalloproteinases (MMPs)-mediated changes of vascular permeability, (4) cytokines-mediated inflammatory responses, and (5) others. These work together after ICH, causing brain injuries in the acute stage and self-repair in the recovery stage. We found that acute administration of the Src inhibitor, PP2, blocks the blood-brain barrier (BBB) breakdown and brain edema that occurs after ICH. However, delayed and chronic administration of PP2 prevents the BBB repair and edema resolution after ICH. These results led us to suggest that the two contradictory findings share the same principles at least in part via activation of Src kinases in acute or recovery stages after ICH. Acute Src kinase activation after ICH leads to BBB damage, and chronic Src kinase activation after ICH leads to BBB repair.

Keywords Src kinases · Blood-brain barrier · Vasogenic edema · Neurogenesis · Neuronal apoptosis · Intracerebral hemorrhage

Introduction

A series of studies show that inhibition of Src, a family of non-receptor tyrosine kinases, attenuates blood-brain barrier (BBB) breakdown, vasogenic edema, mitogen-activation protein kinase (MAPK) activation, neuronal cell cycle reactivation, and subsequent neuronal death in the acute stage (0–24 h) after subarachnoid hemorrhage (SAH) or intracerebral hemorrhage (ICH) [1–5].

In contrast, inhibition of Src kinases blocks BBB repair and brain edema resolution in the recovery stage (7–14 days) after ICH, in part because Src kinase proto-oncogene members stimulate proliferation of newborn brain endothelial cells and perivascular astrocytes in the “neurovascular niche” that repair the damaged BBB [4]. Although there are no direct reports on Src kinase-mediated neurogenesis after ICH, Src kinases increase the numbers of newborn neuronal cells in the dentate gyrus (DG) via activation of the mitogenic signaling cascade in the recovery stage (7days) after cerebral ischemia [6].

Mitogenic signaling encourages cells to re-enter the cell cycle. The cell cycle is regarded as the central process leading to cellular proliferation (e.g., neural progenitor cells). However, increasing evidence over the last decade supports the notion that neuronal cell cycle re-entry results in post-mitotic death [7]. This suggests inhibition of the cell cycle could block not only neural progenitor cell proliferation, but also neuronal apoptosis.

Therefore, any therapeutics that prevent neuronal death by blocking mitogenic signaling may have limited benefit because they may also prevent neurogenesis. This may provide at least a partial explanation for the contradictory phenomena of acute or chronic administration of Src kinase inhibitor in the preclinical treatment of ICH and ischemia, since inhibition of Src kinase activation has been shown to reduce progenitor cell proliferation. This might subsequently block BBB repair, edema resolution and decrease neurogenesis after brain injuries [4, 6].

Activation of Src Kinases Mediates Acute Brain Injuries After ICH

We previously reported that the expression of Lyn, one of the Src family kinases, was upregulated 21-fold following ICH [8, 9], and activity of Src kinases increased 3–5-fold at 4 h after experimental ICH [2, 3]. In the follow-up function

D.-Z. Liu (✉) and F.R. Sharp
Department of Neurology and the MIND Institute,
University of California at Davis Medical Center,
Sacramento, CA 95817, USA
e-mail: dzliu@ucdavis.edu

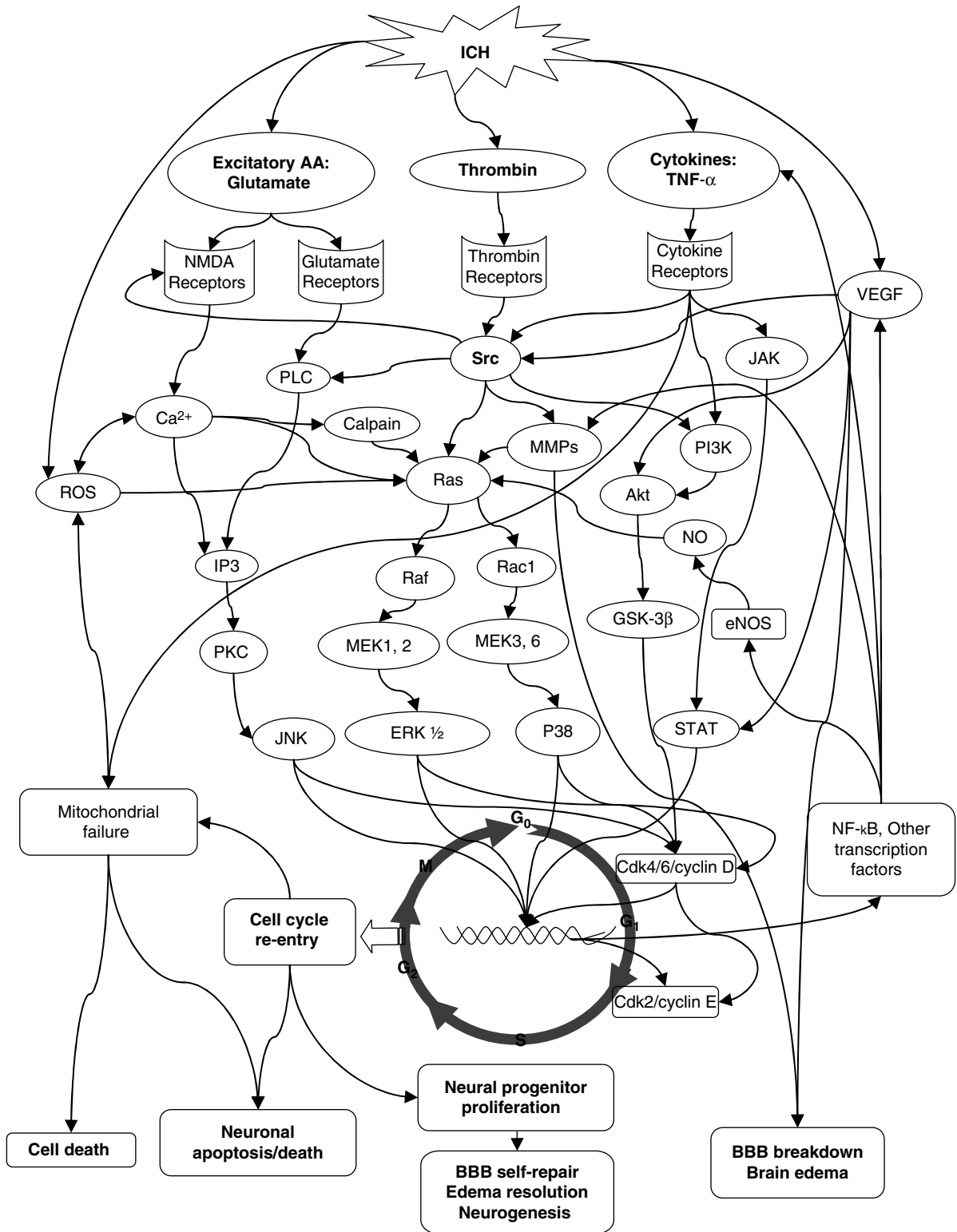


Fig. 1 The mitogenic signal pathways, initiated by mitogenic molecules, lead to blood-brain barrier (BBB) breakdown, vasogenic edema, mitogen-activation protein kinase (MAPK) activation, neuronal cell cycle reactivation and subsequent death, and as well as BBB repair,

brain edema resolution and neurogenesis. The arrows do not necessarily indicate direct binding and/or activation of the downstream molecules; intermediate proteins or kinases may exist

study, we showed acute administration of Src kinase inhibitor, PP2, decreased local cerebral glucose utilization (LCGU) and activity of Src kinases, attenuated BBB breakdown, brain edema and cell death around ICH, and improved behavioral function following ICH [2–4, 10]. These findings suggest that activation of Src kinases mediates brain injuries in the acute stage after ICH. The possible Src kinase related-mechanisms that lead to acute brain injuries after ICH include: (1) ICH/VEGF//Src/MMPs/BBB breakdown and brain edema; (2) ICH/glutamate/NMDA receptors (regulated by Src/Ca²⁺/ROS/mitochondrial failure/cell death (Fig. 1).

Molecules and Signaling That Lead to Cell Cycle Re-entry via Activation of Src Kinases After ICH

Intracerebral hemorrhage results in the release of a wide variety of molecules, including thrombin, heme and iron [11], ROS [12, 13], NO [14], vascular endothelial growth factor (VEGF) [15], excitatory amino acids such as glutamate [16], various inflammatory cytokines such as interleukin-1 (IL-1), IL-6 and IL-10, tumor necrosis factor- α (TNF- α) [17–20], and others (Fig. 1).

Most of these molecules are able to trigger mitogenic signaling. The signaling of one molecule is often modified or augmented by another (Fig. 1). For example, mitochondrial failure results in the release of ROS, which enhances TNF- α production [21]. Intracellular TNF- α accumulation in turn causes mitochondrial failure [22] and promotes ROS generation, producing a vicious cycle. The signaling can also be accelerated by one molecule on its own, such as the auto-crine cycling of NO, mediated by the inducible enzymes NO/Ras/Raf/MEK-1/ERK 1, 2/NF- κ B/NO [23]. These kinds of positive feedback make it possible to elevate molecules abruptly, either as a normal physiological response to ICH or as the cause of ICH-induced damage itself.

Src kinases are important upstream regulators in the process of mitogenic signaling transduction. As shown in Fig. 1, examples of some Src kinase-mediated signaling pathways that lead to brain injuries by forcing neuronal cell cycle re-entry include: (1) ICH/VEGF//Src/Ras/ERK or P38/cell cycle re-entry, (2) ICH/thrombin/thrombin receptors/Src/Ras/ERK or P38/cell cycle re-entry, (3) ICH/glutamate/NMDA receptors (regulated by Src)/Ca²⁺/calpain/Ras/ERK or P38/cell cycle re-entry, (4) ICH/glutamate/PLC (enhanced by Src)/JNK/cell cycle re-entry, and (5) ICH/TNF- α /TNF- α receptor/PI3K (enhanced by Src)/Akt/GSK-3 β /cell cycle re-entry.

Cell Cycle Re-entry Induces Apoptosis of Neurons

Under physiological conditions, neurons are subjected to a variety of stimuli and signals. These include mitogenic signals that promote re-entry into the cell cycle and also a series of anti-mitogenic factors that strive to maintain the neuron at rest [23]. However, once brain injuries occur, this balance is lost. For example, some cell cycle proteins (e.g., cyclin D, PCNA and GADD34) are produced in mature neurons very soon after experimental rat brain ischemia [24–27]. In an in vitro ICH model, we and others observed that neurons did not proceed to S phase, but rather died via apoptosis after the G0/G1 transition [3, 28]. However, A β challenged neurons could proceed through S phase before dying [29], but these neurons became trapped in S phase.

Tumor cells that enter the cell cycle neither finish dividing nor revert to their G0 quiescent state [27, 30–32]. On the other hand, a neuron that re-enters the cell cycle cannot revert to an earlier G0 either, because the transitions through the mitotic cell cycle are irreversible processes [33]. Presumably, the failure to complete the cell cycle in these stressed neurons triggers specific apoptotic or other cell death mechanisms to rid the tissue of these cells. Since Src kinase inhibition can block mitogenic signaling that is activated after ICH, Src kinase inhibition appears to be a candidate strategy for the treatment of ICH.

Cell Cycle Re-entry Induces Proliferation of Neural Progenitor Cells

Neurogenesis arises from brain progenitor cells rather than from differentiated adult neurons. It is now clear that neurogenesis occurs in the brain of adult mammals [34–37]. This neurogenesis may be associated with maintenance or restoration of neurological function after brain ischemia and ICH, suggesting that neurogenesis is functionally important to recovery [4, 37]. In addition, elevated mitogenic signaling after ICH would produce proliferation of endothelial cells and glial cells to fix the disrupted BBB. This could be an explanation for the finding that inhibition of Src kinase activation blocked BBB repair and brain edema resolution, and reduced progenitor cell proliferation, leading to decreased neurogenesis after brain ischemia and ICH [4, 6].

Future Directions

Future studies will need to address which specific Src family members (e.g., c-Src, c-Yes, Fyn, Lck, Lyn, Hck, Blk, c-Fgr) may mediate ICH-induced brain injuries or neurogenesis separately. It is even possible that different Src family members might mediate BBB breakdown and BBB repair. Moreover, it is necessary to search for small molecular compounds that are more specific for certain Src family members that might mediate different aspects of the injury caused by ICH.

Acknowledgements This study was supported by NIH grant NS054652 (FRS)

Conflict of interest statement We declare that we have no conflict of interest.

References

- Kusaka G, Ishikawa M, Nanda A, Granger DN, Zhang JH (2004) Signaling pathways for early brain injury after subarachnoid hemorrhage. *J Cereb Blood Flow Metab* 24(8):916–925
- Ardizzone TD, Zhan X, Ander BP, Sharp FR (2007) SRC kinase inhibition improves acute outcomes after experimental intracerebral hemorrhage. *Stroke* 38(5):1621–1625
- Liu DZ, Cheng XY, Ander BP, Xu H, Davis RR, Gregg JP, Sharp FR (2008) Src kinase inhibition decreases thrombin-induced injury and cell cycle re-entry in striatal neurons. *Neurobiol Dis* 30(2):201–211
- Liu DZ, Ander BP, Xu H, Shen Y, Kaur P, Deng W, Sharp FR (2010) Blood brain barrier breakdown and repair after thrombin-induced injury. *Ann Neurol* 67(4):526–533
- Sharp F, Liu DZ, Zhan X, Ander BP (2008) Intracerebral hemorrhage injury mechanisms: glutamate neurotoxicity, thrombin, and Src. *Acta Neurochir Suppl* 105:43–46
- Tian HP, Huang BS, Zhao J, Hu XH, Guo J, Li LX (2009) Non-receptor tyrosine kinase Src is required for ischemia-stimulated neuronal cell proliferation via Raf/ERK/CREB activation in the dentate gyrus. *BMC Neurosci* 10:139
- Liu DZ, Ander BP, Sharp FR (2010) Cell cycle inhibition without disruption of neurogenesis is a strategy for treatment of central nervous system diseases. *Neurobiol Dis* 37:549–557
- Tang Y, Lu A, Aronow BJ, Wagner KR, Sharp FR (2002) Genomic responses of the brain to ischemic stroke, intracerebral haemorrhage, kainate seizures, hypoglycemia, and hypoxia. *Eur J Neurosci* 15(12):1937–1952
- Lu A, Tang Y, Ran R, Ardizzone TL, Wagner KR, Sharp FR (2006) Brain genomics of intracerebral hemorrhage. *J Cereb Blood Flow Metab* 26(2):230–252
- Ardizzone TD, Lu A, Wagner KR, Tang Y, Ran R, Sharp FR (2004) Glutamate receptor blockade attenuates glucose hypermetabolism in perihematomal brain after experimental intracerebral hemorrhage in rat. *Stroke* 35(11):2587–2591
- Hua Y, Keep RF, Hoff JT, Xi G (2007) Brain injury after intracerebral hemorrhage: the role of thrombin and iron. *Stroke* 38(2 Suppl):759–762
- Matz PG, Fujimura M, Lewen A, Morita-Fujimura Y, Chan PH (2001) Increased cytochrome c-mediated DNA fragmentation and cell death in manganese-superoxide dismutase-deficient mice after exposure to subarachnoid hemolysate. *Stroke* 32(2):506–515
- Wu J, Hua Y, Keep RF, Schallert T, Hoff JT, Xi G (2002) Oxidative brain injury from extravasated erythrocytes after intracerebral hemorrhage. *Brain Res* 953(1–2):45–52
- Jung KH, Chu K, Jeong SW, Han SY, Lee ST, Kim JY, Kim M, Roh JK (2004) HMG-CoA reductase inhibitor, atorvastatin, promotes sensorimotor recovery, suppressing acute inflammatory reaction after experimental intracerebral hemorrhage. *Stroke* 35(7):1744–1749
- Lee CZ, Xue Z, Zhu Y, Yang GY, Young WL (2007) Matrix metalloproteinase-9 inhibition attenuates vascular endothelial growth factor-induced intracerebral hemorrhage. *Stroke* 38(9):2563–2568
- Qureshi AI, Ali Z, Suri MF, Shuaib A, Baker G, Todd K, Guterman LR, Hopkins LN (2003) Extracellular glutamate and other amino acids in experimental intracerebral hemorrhage: an in vivo microdialysis study. *Crit Care Med* 31(5):1482–1489
- Dziedzic T, Bartos S, Klimkowicz A, Motyl M, Slowik A, Szczudlik A (2002) Intracerebral hemorrhage triggers interleukin-6 and interleukin-10 release in blood. *Stroke* 33(9):2334–2335
- Rincon F, Mayer SA (2004) Novel therapies for intracerebral hemorrhage. *Curr Opin Crit Care* 10(2):94–100
- Castillo J, Davalos A, Alvarez-Sabin J, Pumar JM, Leira R, Silva Y, Montaner J, Kase CS (2002) Molecular signatures of brain injury after intracerebral hemorrhage. *Neurology* 58(4):624–629
- Mayne M, Ni W, Yan HJ, Xue M, Johnston JB, Del Bigio MR, Peeling J, Power C (2001) Antisense oligodeoxynucleotide inhibition of tumor necrosis factor-alpha expression is neuroprotective after intracerebral hemorrhage. *Stroke* 32(1):240–248
- Brown DM, Donaldson K, Borm PJ, Schins RP, Dehnhardt M, Gilmour P, Jimenez LA, Stone V (2004) Calcium and ROS-mediated activation of transcription factors and TNF-alpha cytokine gene expression in macrophages exposed to ultrafine particles. *Am J Physiol Lung Cell Mol Physiol* 286(2):L344–L353
- Qureshi AI, Mendelow AD, Hanley DF (2009) Intracerebral haemorrhage. *Lancet* 373(9675):1632–1644
- Copani A, Nicoletti F (2005) Cell-cycle mechanisms and neuronal cell death. *Kluwer Academic/Plenum*, New York
- Imai H, Harland J, McCulloch J, Graham DI, Brown SM, Macrae IM (2002) Specific expression of the cell cycle regulation proteins, GADD34 and PCNA, in the peri-infarct zone after focal cerebral ischaemia in the rat. *Eur J Neurosci* 15(12):1929–1936
- Li Y, Chopp M, Powers C, Jiang N (1997) Immunoreactivity of cyclin D1/cdk4 in neurons and oligodendrocytes after focal cerebral ischemia in rat. *J Cereb Blood Flow Metab* 17(8):846–856
- Guegan C, Levy V, David JP, Ajchenbaum-Cymbalista F, Sola B (1997) c-Jun and cyclin D1 proteins as mediators of neuronal death after a focal ischaemic insult. *NeuroReport* 8(4):1003–1007
- Katchanov J, Harms C, Gertz K, Hauck L, Waeber C, Hirt L, Priller J, von Harsdorf R, Bruck W, Hortnagl H et al (2001) Mild cerebral ischemia induces loss of cyclin-dependent kinase inhibitors and activation of cell cycle machinery before delayed neuronal cell death. *J Neurosci* 21(14):5045–5053
- Rao HV, Thirumangalakudi L, Desmond P, Grammas P (2007) Cyclin D1, cdk4, and Bim are involved in thrombin-induced apoptosis in cultured cortical neurons. *J Neurochem* 101(2):498–505
- Copani A, Condorelli F, Caruso A, Vancheri C, Sala A, Giuffrida Stella AM, Canonico PL, Nicoletti F, Sortino MA (1999) Mitotic signaling by beta-amyloid causes neuronal death. *FASEB J* 13(15):2225–2234

30. Kuan CY, Schloemer AJ, Lu A, Burns KA, Weng WL, Williams MT, Strauss KI, Vorhees CV, Flavell RA, Davis RJ et al (2004) Hypoxia-ischemia induces DNA synthesis without cell proliferation in dying neurons in adult rodent brain. *J Neurosci* 24(47):10763–10772
31. Pallas M, Camins A (2006) Molecular and biochemical features in Alzheimer's disease. *Curr Pharm Des* 12(33):4389–4408
32. Yang Y, Mufson EJ, Herrup K (2003) Neuronal cell death is preceded by cell cycle events at all stages of Alzheimer's disease. *J Neurosci* 23(7):2557–2563
33. Novak B, Tyson JJ, Gyorffy B, Csikasz-Nagy A (2007) Irreversible cell-cycle transitions are due to systems-level feedback. *Nat Cell Biol* 9(7):724–728
34. Brandt MD, Storch A (2008) Neurogenesis in the adult brain: from bench to bedside? *Fortschr Neurol Psychiatr* 76(9): 517–529
35. Shen J, Xie L, Mao X, Zhou Y, Zhan R, Greenberg DA, Jin K (2008) Neurogenesis after primary intracerebral hemorrhage in adult human brain. *J Cereb Blood Flow Metab* 28(8): 1460–1468
36. Neundorfer B (2008) Does the neurogenesis in the adult brain show the way into the future? *Fortschr Neurol Psychiatr* 76(9):511
37. Liu J, Solway K, Messing RO, Sharp FR (1998) Increased neurogenesis in the dentate gyrus after transient global ischemia in gerbils. *J Neurosci* 18(19):7768–7778

Brain Arteriovenous Malformation Pathogenesis: A Response-to-Injury Paradigm

Helen Kim, Hua Su, Shantel Weinsheimer, Ludmila Pawlikowska, and William L. Young

Abstract Brain arteriovenous malformations (AVMs) are a rare but important cause of intracranial hemorrhage (ICH) in young adults. In this paper, we review both human and animal studies of brain AVM, focusing on the: (1) natural history of AVM hemorrhage, (2) genetic and expression studies of AVM susceptibility and hemorrhage, and (3) strategies for development of a brain AVM model in adult mice. These data target various mechanisms that must act in concert to regulate normal angiogenic response to injury. Based on the various lines of evidence reviewed in this paper, we propose a “response-to-injury” model of brain AVM pathogenesis.

H. Kim

Center for Cerebrovascular Research, Department of Anesthesia and Perioperative Care, University of California, San Francisco, CA, USA and

Department of Epidemiology and Biostatistics
University of California, San Francisco, CA, USA and
Institute for Human Genetics, University of California, San Francisco, CA, USA

H. Su and S. Weinsheimer

Center for Cerebrovascular Research, Department of Anesthesia and Perioperative Care, University of California, San Francisco, CA, USA

L. Pawlikowska

Center for Cerebrovascular Research, Department of Anesthesia and Perioperative Care, University of California, San Francisco, CA, USA and
Institute for Human Genetics, University of California, San Francisco, CA, USA

W.L. Young (✉)

Center for Cerebrovascular Research, Department of Anesthesia and Perioperative Care, University of California, San Francisco, CA, USA and
Department of Neurological Surgery, University of California, San Francisco, CA, USA
Department of Neurology, University of California, San Francisco, CA, USA and
Department of Anesthesia and Perioperative Care, University of California, 1001 Potrero Avenue, Rm. 3C-38, San Francisco, 94110, CA, USA
e-mail: ccr@anesthesia.ucsf.edu

Keywords Brain arteriovenous malformations · Intracranial hemorrhage · Gene expression · Genetics · Angiogenesis · Inflammation · Animal models

Brain arteriovenous malformations (AVM) represent a relatively infrequent but important source of neurological morbidity in relatively young adults [1]. Brain AVMs have a population prevalence of 10–18 per 100,000 adults [2, 3], and a new detection rate (incidence) of approximately 1.3 per 100,000 person-years [4, 5]. The basic morphology is of a vascular mass, called the nidus, that directly shunts blood between the arterial and venous circulations without a true capillary bed. There is usually high flow through the feeding arteries, nidus, and draining veins. The nidus is a complex tangle of abnormal, dilated channels, not clearly artery or vein, with intervening gliosis.

Seizures, mass effect, and headache are causes of associated morbidity, but prevention of new or recurrent intracranial hemorrhage (ICH) is the primary rationale to treat AVMs, usually with some combination of surgical resection, embolization, and stereotactic radiotherapy. The risk of spontaneous ICH has been estimated in retrospective and prospective observational studies to range from 2% to 4% per year [6], but approximately 50% of patients present initially with a bleed. Other than non-specific control of symptoms, e.g., headache and seizures, primary medical therapy is lacking.

Treatment of unruptured AVMs is controversial and has led to an ongoing randomized clinical trial to test whether the best medical therapy has better outcomes than procedural intervention (<http://clinicaltrials.gov/ct/show/NCT00389181>). Because of the complexity of AVM treatment and a wide range of expert opinions, it is unlikely that a single clinical trial can settle all of the questions related to management strategies. Thus, understanding the pathogenesis of AVM formation and progression to ICH will be important for informing patient management decisions.

In this review, we propose a novel “response-to-injury” paradigm to explain sporadic brain AVM pathogenesis, based on findings from clinical research studies of AVM patients

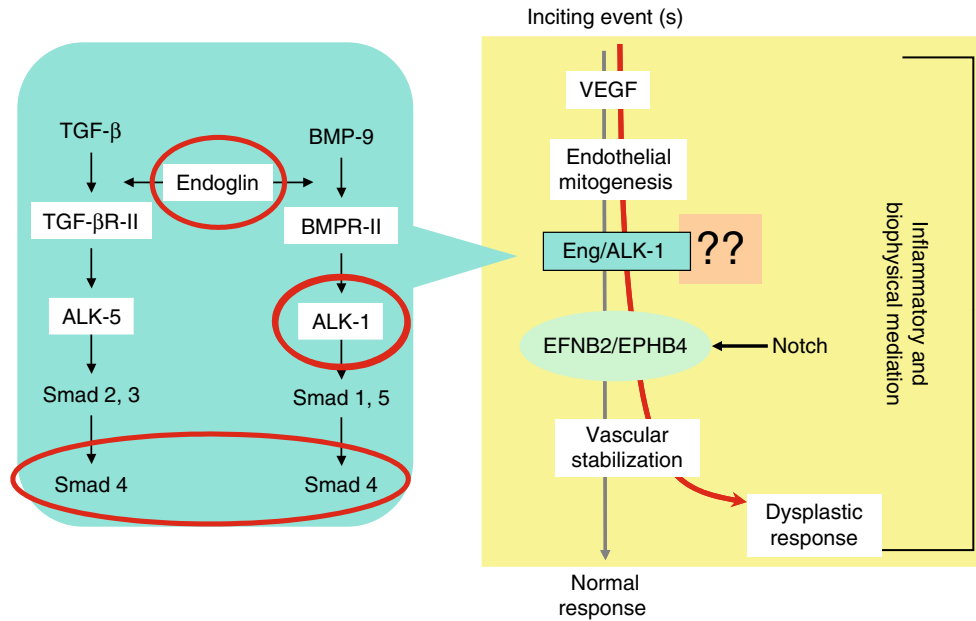


Fig. 1 “Response-to-injury” paradigm for formation of brain AVMs. In the normal circulation, an injury upregulates the expression of angiogenic factors, such as VEGF, which induces EC mitogenesis; newly formed vessels will develop into a stable neovasculature under normal conditions (*gray arrow*). In addition to EC mitogenesis, formation of stable vessels also involves recruitment of mural cells including pericytes and, in the case of arterial or venous structures, smooth muscle. All of these processes involve TGF- β signaling. The blue box on the left details the canonical TGF- β signaling pathway. The genes that are mutated in HHT are circled in red; BMP-9 may also be a physiological

ligand for ALK-1 signaling. In the presence of certain genetic backgrounds, this otherwise normal injury repair process can lead to a vascular dysplastic response (*red arrow*) when signaling through aberrant ALK-1 and/or ENG, or in a closely related pathway (*question marks*). Other contributory pathways may include EFNB2 and EPHB4 imbalance, possibly through involvement of Notch signaling. Additional modifier influences are indicated, and may include increased endothelial shear stress from the high flow rates through a fistulous A-V connection. Inflammation and involvement of circulating precursor cells may also be relevant

and animal models investigating AVM formation to date. Figure 1 shows a speculative synthesis of pathways involved in AVM pathogenesis. Inciting event(s), while not known, might include sequelae of even modest injury from an otherwise unremarkable episode of trauma, infection, inflammation, irradiation, or a mechanical stimulus such as compression. The normal response to these inciting events would involve angiogenesis, endothelial mitogenesis, and vascular stabilization. However, when superimposed on an underlying structural defect, such as a microscopic developmental venous anomaly or some sort of venous outflow restriction in a microcirculatory bed, or an underlying genetic background, such as mutations in key angiogenic genes, the normal injury response is shifted towards an abnormal dysplastic response. In the next few sections, we will review the available data on factors involved in the abnormal “response-to-injury” in AVMs.

Evidence for Abnormal Angiogenesis and Inflammation in AVM

Studies of surgically resected AVM tissue suggest an active angiogenic and inflammatory lesion rather than a static congenital anomaly. Several groups [7, 8] have shown that a

prominent feature of the AVM phenotype is relative overexpression of vascular endothelial growth factor (VEGF-A) at both the mRNA and protein level. Extrapolating from animal models, VEGF may contribute to the hemorrhagic tendency of AVMs [9]. The vascular phenotype of AVM tissue may be explained, in part, by an inadequate recruitment of periendothelial support structures, which is mediated by angiopoietins and TIE-2 signaling. For example, angiopoietin-2 (ANG-2), which allows loosening of cell-to-cell contacts, is overexpressed in the perivascular region in AVM vascular channels [10].

A key downstream consequence of VEGF and ANG-2 signaling, contributing to the angiogenic phenotype, is matrix metalloproteinase (MMP) expression. MMP-9 expression, in particular, appears to be at least an order of magnitude higher in AVM than in control tissue [11, 12], with levels of naturally occurring MMP inhibitors, TIMP-1 and TIMP-3, also increased, but to a lesser degree. Additional inflammatory markers that are overexpressed include myeloperoxidase (MPO) and interleukin 6 (IL-6), both of which are highly correlated with MMP-9 [11, 13]. MMP-9 expression is correlated with the lipocalin-MMP-9 complex, suggesting neutrophils as a major source. In a subset of unruptured, non-embolized AVMs, neutrophils (MPO) and macrophages/microglia (CD68) were all prominent in the vascular wall and

intervening stroma of AVM tissue, whereas T and B lymphocytes were present but rarely observed [14]. Higher immunoglobulin levels have been reported in AVM tissue than in control brain [15].

Exactly how the dysplastic response propagates is not known, but recruitment of progenitor cell populations may be one source influencing AVM growth and development, and is an area in need of further exploration. For example, endothelial progenitor cells (EPCs) are present in the nidus of brain and spinal cord AVMs, and may mediate pathological vascular remodeling and impact the clinical course of AVMs. Gao et al. demonstrated that both brain and spinal AVM tissues displayed more CD133-, SDF-1-, and CD68-positive signals than epilepsy and basilar artery control tissues [16]. EPCs, identified as CD133 and KDR double stained-positive cells, were increased in the brain and spinal cord AVM nidus, mainly at the edge of the vessel wall. The expression of SDF-1 was co-localized with CD31-positive and α -smooth muscle cell expression, and was predominantly found within the vessel wall. More generally, circulating bone-marrow derived cells have a major role in both microcirculatory angiogenesis [17, 18] and conductance vessel remodeling [19, 20]. If AVM pathogenesis involves these two processes, it is reasonable to infer that bone-marrow derived cells may have an underappreciated role in lesion formation and growth. An unresolved issue with all stem cell interactions is the extent to which progenitor cells actually integrate into existing tissue compartments, or whether they provide a nursing function by supplying critical components of the repair response such as cytokines, growth factors, and enzymes to the tissue, i.e., do progenitor cells supply “troops” or merely “ordinance.”

Evidence for Genetic Influences in AVMs

Candidate genes and pathways for brain AVM pathogenesis have been suggested by Mendelian disorders, which exhibit AVMs as part of their clinical phenotype, and gene expression studies. AVMs in various organs, including the brain, are highly prevalent in patients with hereditary hemorrhagic telangiectasia (HHT, OMIM#187300), an autosomal dominant disorder of mucocutaneous fragility. Compared to sporadic lesions, brain AVMs in HHT tend to be smaller and are more likely to have single draining veins, be located superficially, and be multiple. However, they are generally similar to the sporadic lesions and cannot be distinguished individually on the basis of their angioarchitecture.

The two main subtypes of HHT (HHT1 and 2) are caused by loss-of-function mutations in two genes [21] originally implicated in TGF- β signaling pathways (Fig. 1). The first is endoglin (*ENG*), which encodes an accessory protein of TGF- β receptor complexes. The second is activin-like kinase

1 (*ALK1*, or *ACVLR1*), which codes for a transmembrane kinase also thought to participate in TGF- β signaling. There are hundreds of reported mutations in *ALK1* and *ENG* [22], but the functional effect appears to be haplo-insufficiency rather than a mutation-specific set of dysfunctions. A third candidate gene for AVM pathogenesis is *SMAD4*, encoding a downstream participant in TGF- β and bone morphogenic protein (BMP) signaling. *SMAD4* is mutated in a combined syndrome of juvenile polyposis and HHT [23]. These HHT mutations can be viewed as risk factors for brain AVM since the prevalence in HHT1 (*ENG*) is 1,000-fold higher and HHT2 (*ALK1*) is 100-fold higher compared to the prevalence of brain AVMs in the general population (10/100,000) [24].

At the earliest stages of vascular development, mice lacking *Alk-1* (*Acvrl1*) form systemic A-V fistulae from fusion of major arteries and veins [25]. Endothelial cell-specific ablation of the murine *Alk-1* gene causes vascular malformations to form during development, whereas mice harboring an EC-specific knockout of *Alk-5* (the type I TGF- β receptor) or *Tgfb2* show neither vascular malformation formation nor any other perturbation in vascular morphogenesis [26]. The exact signaling pathways for ALK-1 and ENG are complex and interrelated, and their relative importance and cellular specificity are controversial [27]. ENG interacts with multiple TGF- β -related signaling pathways and interacts with TGFBR2 (the type II TGF- β receptor) as well as with type I TGF- β receptors, ALK-1 and ALK-5 [28]. ENG can also bind ligands besides TGF- β , including activins and BMP family members [29, 30]. Regardless of the exact signaling mechanism leading to vascular malformation, it is clear that mutations and likely genetic variation in TGF-beta signaling genes are important players in the “response-to-injury” paradigm of AVM pathogenesis.

Candidate Gene Studies in Non-HHT AVM Patients

The mechanism of AVM initiation is as yet unknown. Even if it involves a structural aberration or mechanical insult – per se not a heritable trait – the subsequent growth and behavior of the lesion may still be influenced by genetic variation. For example, multiple genetic loci influence VEGF-induced angiogenesis [31, 32]. Therefore, a pathogenesis that involves a “response-to-injury” at any level may be at least partially influenced by heritable aspects of such a response.

Candidate gene studies of sporadic AVM cases have identified single nucleotide polymorphisms (SNPs) in several genes associated with risk of AVM susceptibility and/or progression to ICH. Previously, SNPs in *ALK1* (IVS3-35A>G) and *ENG* (207G>A) were found to be associated with an increased risk of AVM [33]. The *ALK1* finding was later replicated in an independent cohort of AVM patients from

Germany [34, 35]. Additionally, common SNPs in interleukin (IL) genes have been associated with increased risk of AVM among certain race-ethnic groups. Among Hispanics, a promoter SNP in *IL-6* (−174G>C) was associated with a two-fold increased risk of AVM after adjusting for age, sex, and genetic ancestry. Among self-reported Caucasians, common SNPs in *IL-1β*, two promoter (−31T>C and −511C>T) and one exonic (+3953C>T), were also associated with an increased risk of AVM susceptibility [36]. The *IL-1β* promoter polymorphisms have also been reported to have functional effects on *IL-1β* transcription. Thus, genetic variation in these cytokines may contribute to AVM pathogenesis by enhancing or maintaining a proinflammatory state necessary for lesion formation.

Evidence for genetic influences on the clinical course of AVM rupture resulting in intracranial hemorrhage (ICH) has also been reported in three different settings: presentation with ICH [36–38], new ICH after diagnosis [39, 40], and ICH after treatment [41]. The same *IL-6* promoter polymorphism (−174G>C) was associated with clinical presentation of ICH [37], and the high-risk G allele correlated with increasing *IL-6* mRNA and protein levels in AVM tissue [13]. More recently, SNPs in the *EPHB4* gene, encoding a tyrosine kinase receptor involved in embryogenic arterial-venous determination, were also reported to be associated with increased risk of ICH presentation [38]. Loss of function mutations in *EphB4* (receptor) and *Efnb2* (ligand) cause vascular defects and AVM formation in mice similar to that observed in *Notch1* gain-of-function mutants, but these results suggest that different mechanisms can lead to the same phenotype [42].

Not surprisingly, SNPs in inflammatory genes also appear to influence the risk of ICH in the natural course of AVMs, including promoter SNPs in *TNF-α* (−238G>A) [39] and *IL1B* (−31T>C and −511C>T) [36]. In addition to their association with spontaneous ICH in the natural, untreated course, both *APOE* ε2 [40] and *TNF-α*-238 A [39] alleles appear to confer greater risk for post-radiosurgical and post-surgical hemorrhage [41].

Genome-Wide SNP and Expression Studies in AVM Patients

A drawback of candidate gene studies is that, while they are hypothesis driven, they represent at best an educated guess as to which genes are involved. An alternative approach is to conduct a genome-wide association (GWAS) or expression-profiling study. The GWAS approach relies upon scanning all common variations in the genome utilizing microarrays that feature hundreds of thousands to millions of SNPs or probes covering known genes. GWAS can identify associated genes if the causal variants are common in the general

population and have shown moderate success for several common complex diseases. An advantage of the GWAS approach is the ability to uncover completely novel biological mechanisms. For example, inflammation was not previously known to be causally involved in age-related macular degeneration (AMD), but a series of studies published in 2005, including the first successful example of GWAS [43], implicated the Y204H polymorphism in the complement factor H gene with risk of AMD [44]. These genetic findings were subsequently replicated in several independent cohorts and have paved the way for development of new therapeutic interventions [44]. Preliminary results from the first GWAS study in Caucasian brain AVM patients have recently been reported [45].

Genome-wide expression profiling can also be used to identify genes that are likely to have a functional role in the disease process. The basic premise is that different patient groups (diseases) can be distinguished by their gene expression “signature,” defined as the unique and consistent pattern of up- and down-regulation of genes. Two small genome-wide expression studies of brain AVM tissue have identified overexpression of inflammatory and angiogenesis-related genes, including *VEGFA*, *ENG*, *ANGPT2*, *ITGAV*, *VEGFR1* (*FLT1*), and *MMP9* [7, 46]. Decreased expression was observed for *TIE1*, *TEK* (*TIE2*), and *ANGPT1* [7, 46].

Increasingly, there is interest in performing genome-wide expression profiling of peripheral blood to identify vascular disease-specific gene expression signatures that may serve as clinically useful molecular biomarkers [47–50]. Identifying blood biomarkers for ICH may have clinical utility in identifying high-risk AVM patients, especially those who come to clinical attention without ICH. The first such study in brain AVM patients has recently been published in abstract form [51], demonstrating differential blood expression profiles in ruptured compared to unruptured brain AVM patients. Pathway analysis of differentially expressed genes implicated inflammatory pathways and VEGF, MAPK, and Wnt signaling, which has relevance for AVM model development as discussed below. Integration of data from multiple genome-wide approaches, including both SNP genotype and gene expression data, may offer additional insight into disease mechanisms.

Experimental AVM Models

Model systems for studying AVM are needed to test mechanistic hypotheses and develop novel therapies. We have previously discussed the development of cerebral microvascular dysplasia, a surrogate model for brain AVM [52]. There has been considerable progress in AVM model development during the past year.

A logical approach to animal models is to focus on genes that are clearly related to the human disease phenotype, which for AVM are those genes described above leading to HHT. It is known that both *Eng*^{+/-} [53] and *Alk1*^{+/-} [54] adult mice develop vascular lesions in various organs, but spontaneous lesions in the brain are quite modest, and only seen in older *Eng*^{+/-} mice using scanning electron microscopy [55]. Our group showed that more pronounced forms of cerebral microvascular dysplasia can be induced using VEGF stimulation in *Eng*^{+/-} or *Alk1*^{+/-} mice [56–58], which can be enhanced by local increases in tissue perfusion rates in the *Alk1*^{+/-} background [56]. Recently, we found that, for a given degree of virally mediated VEGF overexpression, *Eng*^{+/-} mice have more severe cerebrovascular dysplasia than *Alk1*^{+/-} mice, which simulates the relative penetrance of brain AVM in HHT patients (HHT1 > HHT2) (Fig. 2c) [57]. These experiments result in enlarged, dysmorphic vascular structures at the capillary level, not the large vessels seen in the human disease.

Oh and colleagues have developed several innovative inducible knockout systems using a novel endothelial Cre transgenic line [26, 59]. Antenatal conditional deletion of *Alk1* causes severe cerebrovascular dysplasia and apparent fistula formation (Fig. 2a). Interestingly, conditional *Alk1* deletion in adult mice induced AV fistulas and hemorrhage in the lung and GI tracks, but not in skin or brain. Importantly, upon induction of skin wounding, *Alk1* deleted mice developed vascular dysplasia and direct A-V connections, suggesting an abnormal response to injury (Fig. 2b). Direct A-V connections have also been detected in the retina of *Eng*-deficient neonatal mice [60]. The combination of local angiogenic stimulation (Matrigel+VEGF/FGF) and *Eng* loss led to gross venous enlargement [60]. These results suggest that physiological or environmental factors, in addition to genetic variation, are required for *Alk1* and *Eng*-deficient vessels to develop vascular malformations in adult mice. In support of this notion, Walker et al. recently described cerebrovascular dysplasia and apparent A-V shunting after focal VEGF stimulation in mice subjected to regional conditional *Alk1* deletion [61].

An additional mechanism of potential interest – especially to the phenomenon of AVM rupture – was suggested by a recent study by Lebrin et al. [62]. Thalidomide reduced epistaxis and enhanced blood vessel stabilization in nasal mucosa of HHT patients. In *Eng*^{+/-} mice, thalidomide treatment stimulated mural cell coverage and thus rescued vessel wall defects partially through upregulation of platelet-derived growth factor-B (PDGF-B) expression in endothelial cells and stimulated mural cell activation.

Notch signaling appears important for the determination of arterial and venous fate, a process that seems to depend on local levels of VEGF [63]. There is empirical evidence that proteins involved in Notch signaling – including the receptor,

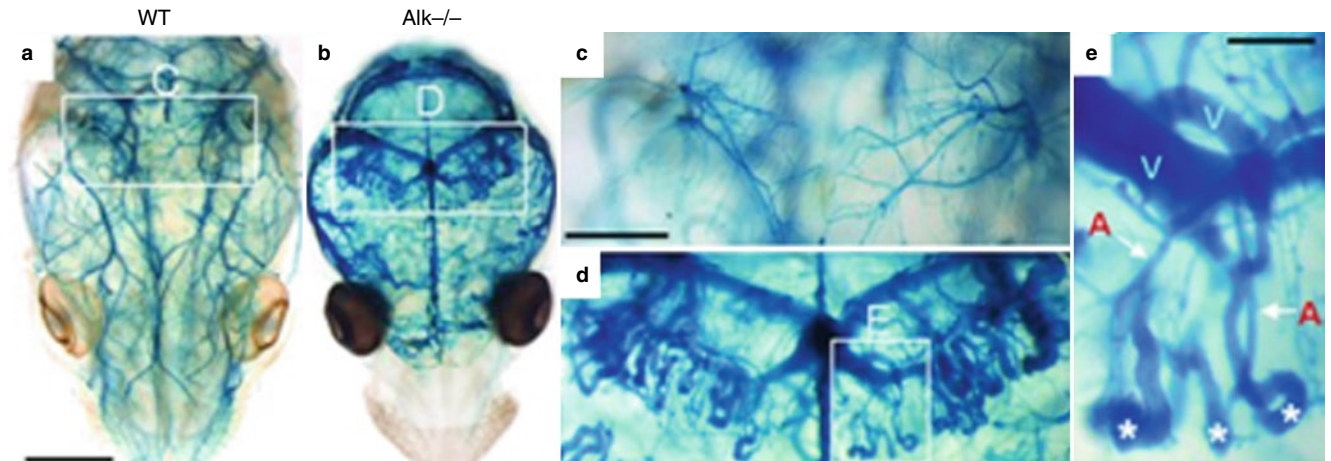
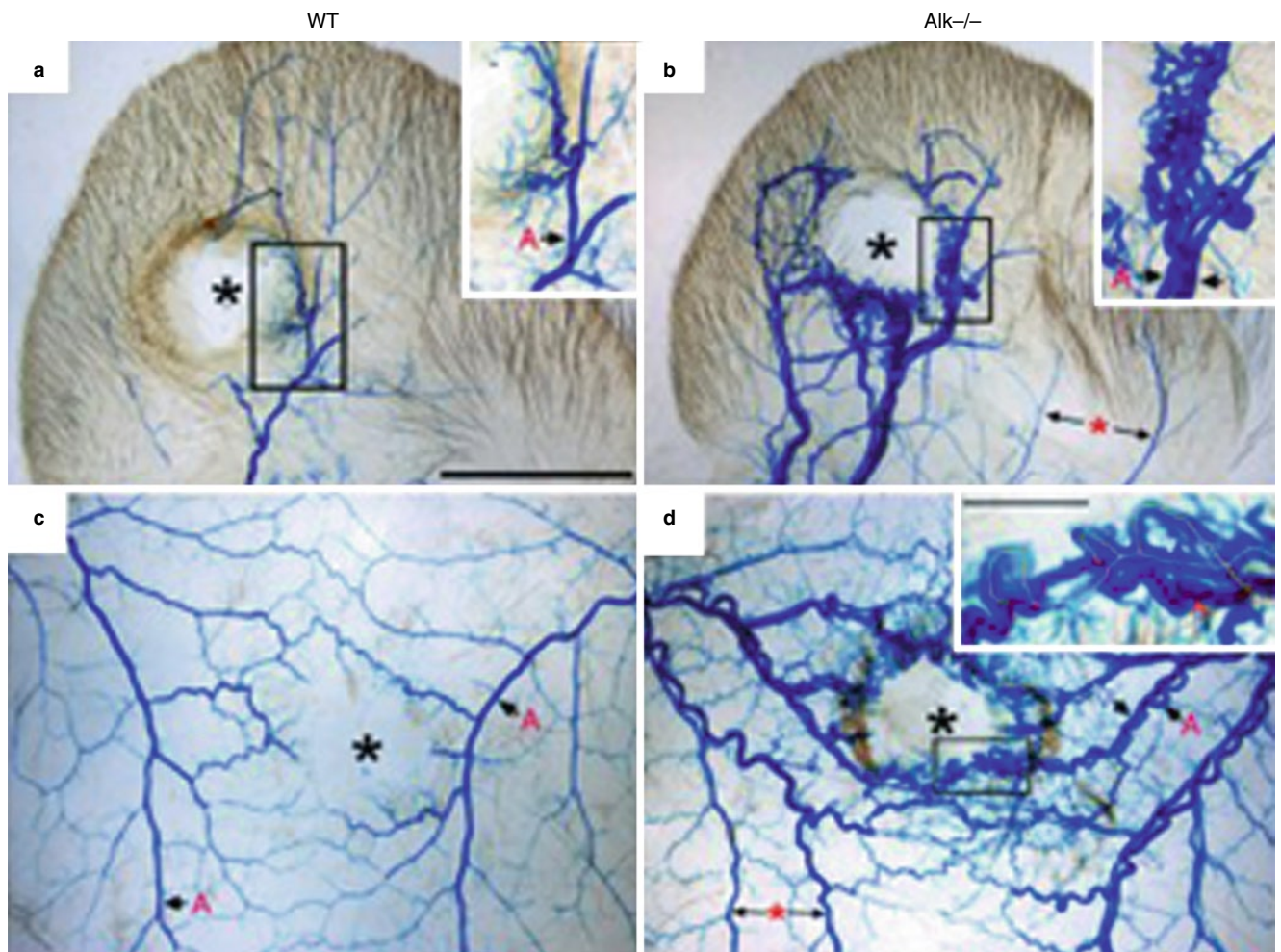
its ligands, and downstream signals – are expressed in excised surgical specimens [64, 65]. Animal experiments support a potential link with the human disease. Using conditional endothelial expression, Murphy and colleagues used a tetracycline-responsive promoter to suppress overexpression during development and then, by withdrawal of doxycycline, overexpressed the intracellular signaling portion of Notch-4 (*int3*) in early post-natal mice. They observed a rapidly lethal phenotype, which mimicked aspects of human AVMs, including dysplastic posterior fossa vasculature with apparent A-V shunting.

Taken together, both genetic manipulation and angiogenic stimulation appear to be important aspects of AVM model development. The angiogenic stimulus can be varied, for example via injury, exogenous growth factor delivery, or the use of young, perinatal animals that have high inherent angiogenic activity in the brain. An ideal AVM model should strive to contain the following components: (1) *anatomic*: nidus of abnormal vessels of varying sizes at micro- and macro-circulatory levels; (2) *physiologic*: A-V shunting, hemodynamically significant, i.e., sufficient to decrease feeding artery or increase draining venous pressures; (3) *biological*: alterations in angiogenic and inflammatory protein expression, involvement of or intersection with known genetic pathways; (4) *clinical*: relative quiescence, spontaneous hemorrhage into the parenchyma or CSF spaces. Currently, such an ideal animal model that would more closely mimic the human phenotype has not been developed in adults. However, insights from the current AVM models suggest that regional conditional gene deletion plus angiogenic stimulation may promote the ideal AVM development in adult mouse brain.

Since submission of this article, Walker et al. [66] have reported on focal VEGF stimulation coupled with regional homozygous deletion of *Alk1* in the adult mouse brain. This report describes post-natal vascular malformations with phenotypic aspects of human bAVM, including arteriovenous shunting, which provides additional proof-of-principle for the scenario shown in Fig. 1.

Summary and Synthesis of Data Regarding the Etiology and Pathogenesis of AVM

Elucidating the mechanisms and factors influencing AVM lesion formation and progression to ICH offers promise for developing innovative treatments and better risk stratification for clinical management or clinical trial design. Further, study of brain AVM could be a powerful platform from which to gain insights into general vascular biologic mechanisms relevant to a wide variety of diseases affecting the vascular system.

A**B**

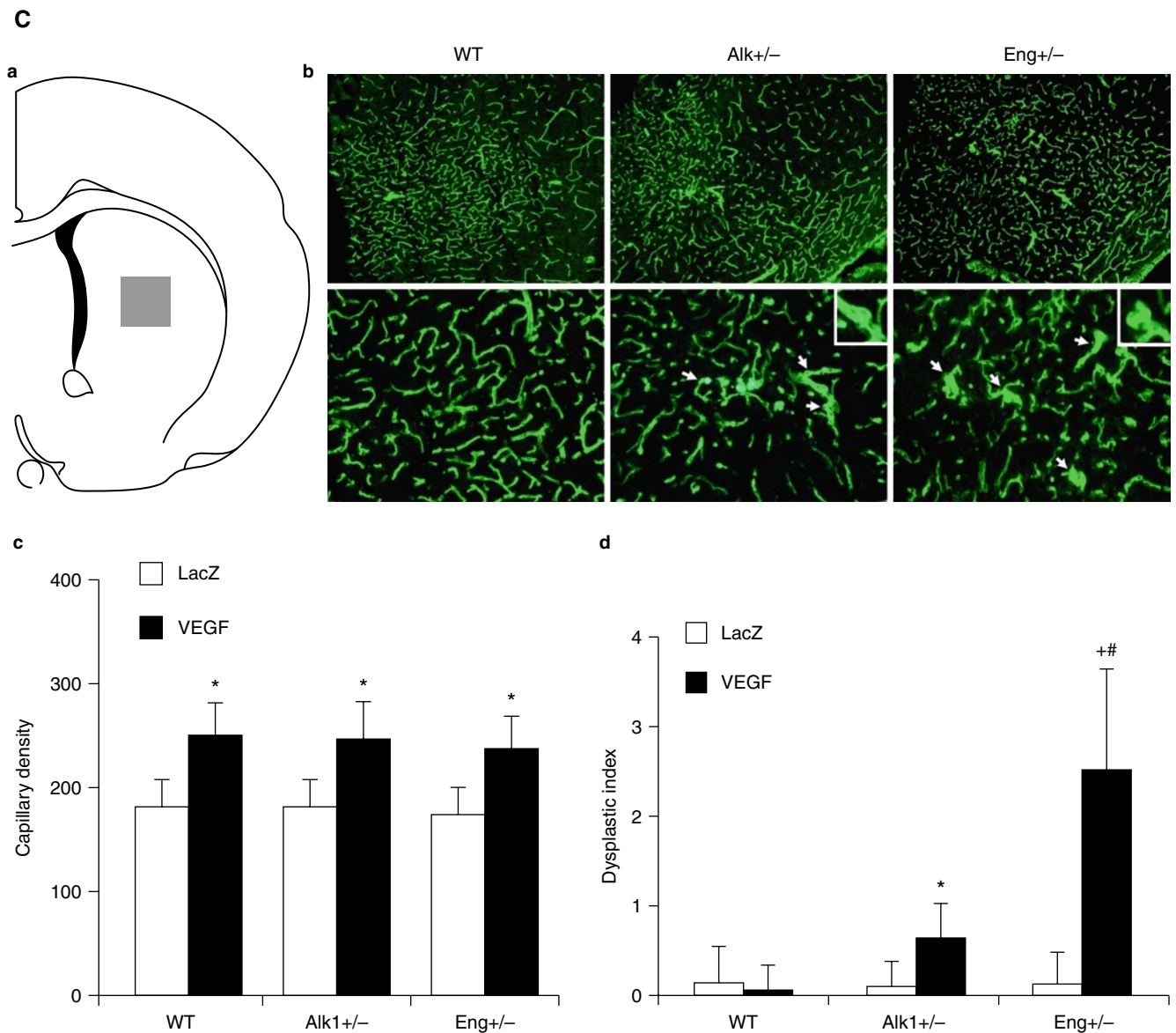


Fig. 2 (continued)

Fig. 2 Brain AVM in *Alk1* or *Eng* deficient mice. (A) Endothelial *Alk1* deletion results in AVMs in the brain [59]. (a–e) Dissection microscopic views of vascular images of control (WT, a, c) and mutant (*Alk1*^{-/-}; b, d, e) in postnatal day 3 mouse brains by latex dye injected into the left ventricle of the heart. Magnified views of blood vessels in the hippocampal area (d, e). Asterisks indicate peculiar looping of vessels at the distal tips of arteries shunting to veins (e). A artery, V vein. (B) Wounding can induce *de novo* AVM formation in *Alk1*-deleted adult mice [59]. Vascular patterns shown by latex dye injected into the left heart of control (WT, a, c) and mutant (*Alk1*^{-/-}, b, d) mice bearing wounds in the ear (a, b) or dorsal skin (c, d), 8 days after induction of *Alk1* gene deletion. The images were taken after clearing in organic solvents. Center of the wound is indicated by asterisks. Note that only mutant mice

developed AV shunts shown by the presence of latex dye in both arteries and veins. AV shunting and abnormal vascular morphologies were apparent only in the wound areas. Blood vessels away from the wound indicated by arrows with asterisks (b and d) showed normal appearance. Inset in d shows a magnified view of AV fistulas formed in the rim area of the mutant wound. (C) Overexpression of VEGF in the striatum of *Alk1* and *Eng* haplo-insufficient mice resulted in vascular dysplasia [57]. (a) Injection site (grey square). (b) Angiogenic foci and dysplastic capillaries (arrows). Inserts are enlarged images of dysplastic capillaries. Scale bars: 100 μ m (top panel) and 50 μ m (bottom panel). (c, d) Capillary density and dysplasia index. * p <0.05, vs. AAV-LacZ group. # p <0.05, vs. AAV-VEGF-transduced WT or *Alk1*^{+/-} mice. VEGF AAV-VEGF-injected mice, LacZ AAV-LacZ-injected mice

Acknowledgments The authors gratefully acknowledge the UCSF Brain AVM study project members <http://avm.ucsf.edu>; the other Principal Investigators (Nancy Boudreau, Tomoki Hashimoto, Charles E. McCulloch, Stephen Nishimura) of P01 NS044155 (Young), “Integrative Study of Brain Vascular Malformations”; and Voltaire Gungab for assistance in manuscript preparation. Studies are supported in part by R01 NS034949 (WLY), R01 NS027713 (WLY), and K23 NS058357 (HK).

Conflict of interest statement We declare that we have no conflict of interest.

References

- Arteriovenous Malformation Study Group (1999) Arteriovenous malformations of the brain in adults. *N Engl J Med* 340: 1812–1818
- Al-Shahi R, Fang JS, Lewis SC, Warlow CP (2002) Prevalence of adults with brain arteriovenous malformations: a community based study in Scotland using capture-recapture analysis. *J Neurol Neurosurg Psychiatry* 73:547–551
- Berman MF, Sciacca RR, Pile-Spellman J, Stapf C, Connolly ES Jr, Mohr JP, Young WL (2000) The epidemiology of brain arteriovenous malformations. *Neurosurgery* 47:389–396
- Gabriel RA, Kim H, Sidney S, McCulloch CE, Singh V, Johnston SC, Ko NU, Achrol AS, Zaroff JG, Young WL (2010) Ten-year detection rate of brain arteriovenous malformations in a large, multiethnic, defined population. *Stroke* 41:21–26
- Stapf C, Mast H, Sciacca RR, Berenstein A, Nelson PK, Gobin YP, Pile-Spellman J, Mohr JP (2003) The New York Islands AVM Study: design, study progress, and initial results. *Stroke* 34: e29–e33
- Kim H, Sidney S, McCulloch CE, Poon KY, Singh V, Johnston SC, Ko NU, Achrol AS, Lawton MT, Higashida RT, Young WL (2007) Racial/ethnic differences in longitudinal risk of intracranial hemorrhage in brain arteriovenous malformation patients. *Stroke* 38: 2430–2437
- Hashimoto T, Lawton MT, Wen G, Yang GY, Chaly T Jr, Stewart CL, Dressman HK, Barbaro NM, Marchuk DA, Young WL (2004) Gene microarray analysis of human brain arteriovenous malformations. *Neurosurgery* 54:410–423
- Rothbart D, Awad IA, Lee J, Kim J, Harbaugh R, Criscuolo GR (1996) Expression of angiogenic factors and structural proteins in central nervous system vascular malformations. *Neurosurgery* 38: 915–924
- Lee CZ, Xue Z, Zhu Y, Yang GY, Young WL (2007) Matrix metalloproteinase-9 inhibition attenuates vascular endothelial growth factor-induced intracranial hemorrhage. *Stroke* 38:2563–2568
- Hashimoto T, Lam T, Boudreau NJ, Bollen AW, Lawton MT, Young WL (2001) Abnormal balance in the angiotensin-converting enzyme system in human brain arteriovenous malformations. *Circ Res* 89:111–113
- Chen Y, Fan Y, Poon KY, Achrol AS, Lawton MT, Zhu Y, McCulloch CE, Hashimoto T, Lee C, Barbaro NM, Bollen AW, Yang GY, Young WL (2006) MMP-9 expression is associated with leukocytic but not endothelial markers in brain arteriovenous malformations. *Front Biosci* 11:3121–3128
- Hashimoto T, Wen G, Lawton MT, Boudreau NJ, Bollen AW, Yang GY, Barbaro NM, Higashida RT, Dowd CF, Halbach VV, Young WL (2003) Abnormal expression of matrix metalloproteinases and tissue inhibitors of metalloproteinases in brain arteriovenous malformations. *Stroke* 34:925–931
- Chen Y, Pawlikowska L, Yao JS, Shen F, Zhai W, Achrol AS, Lawton MT, Kwok PY, Yang GY, Young WL (2006) Interleukin-6 involvement in brain arteriovenous malformations. *Ann Neurol* 59:72–80
- Chen Y, Zhu W, Bollen AW, Lawton MT, Barbaro NM, Dowd CF, Hashimoto T, Yang GY, Young WL (2008) Evidence of inflammatory cell involvement in brain arteriovenous malformations. *Neurosurgery* 62:1340–1349
- Shenkar R, Shi C, Check JJ, Lipton HL, Awad IA (2007) Concepts and hypotheses: inflammatory hypothesis in the pathogenesis of cerebral cavernous malformations. *Neurosurgery* 61:693–702
- Gao P, Chen Y, Lawton MT, Barbaro NM, Yang GY, Su H, Ling F, Young WL (2010) Evidence of endothelial progenitor cells in the human brain and spinal cord arteriovenous malformations. *Neurosurgery* 67:1029–1035
- Hao Q, Chen Y, Zhu Y, Fan Y, Palmer D, Su H, Young WL, Yang GY (2007) Neutrophil depletion decreases VEGF-induced focal angiogenesis in the mature mouse brain. *J Cereb Blood Flow Metab* 27:1853–1860
- Hao Q, Liu J, Pappu R, Su H, Rola R, Gabriel RA, Lee CZ, Young WL, Yang GY (2008) Contribution of bone marrow-derived cells associated with brain angiogenesis is primarily through leucocytes and macrophages. *Arterioscler Thromb Vasc Biol* 28:2151–2157
- Nuki Y, Matsumoto MM, Tsang E, Young WL, van Rooijen N, Kurihara C, Hashimoto T (2009) Roles of macrophages in flow-induced outward vascular remodeling. *J Cereb Blood Flow Metab* 29:495–503
- Ota R, Kurihara C, Tsou TL, Young WL, Yeghiazarians Y, Chang M, Mobashery S, Sakamoto A, Hashimoto T (2009) Roles of matrix metalloproteinases in flow-induced outward vascular remodeling. *J Cereb Blood Flow Metab* 29:1547–1558
- Marchuk DA, Srinivasan S, Squire TL, Zawistowski JS (2003) Vascular morphogenesis: tales of two syndromes. *Hum Mol Genet* 12:R97–R112
- Abdalla SA, Letarte M (2006) Hereditary haemorrhagic telangiectasia: current views on genetics and mechanisms of disease. *J Med Genet* 43:97–110
- Gallione CJ, Richards JA, Letteboer TG, Rushlow D, Prigoda NL, Leedom TP, Ganguly A, Castells A, Ploos van Amstel JK, Westermann CJ, Pyeritz RE, Marchuk DA (2006) SMAD4 mutations found in unselected HHT patients. *J Med Genet* 43:793–797
- Kim H, Marchuk DA, Pawlikowska L, Chen Y, Su H, Yang GY, Young WL (2008) Genetic considerations relevant to intracranial hemorrhage and brain arteriovenous malformations. *Acta Neurochir Suppl* 105:199–206
- Urness LD, Sorensen LK, Li DY (2000) Arteriovenous malformations in mice lacking activin receptor-like kinase-1. *Nat Genet* 26: 328–331
- Park SO, Lee YJ, Seki T, Hong KH, Fliess N, Jiang Z, Park A, Wu X, Kaartinen V, Roman BL, Oh SP (2008) ALK5- and TGFB2-independent role of ALK1 in the pathogenesis of hereditary hemorrhagic telangiectasia type 2 (HHT2). *Blood* 111:633–642
- ten Dijke P, Goumans MJ, Pardali E (2008) Endoglin in angiogenesis and vascular diseases. *Angiogenesis* 11:79–89
- Lux A, Attisano L, Marchuk DA (1999) Assignment of transforming growth factor beta1 and beta3 and a third new ligand to the type I receptor ALK-1. *J Biol Chem* 274:9984–9992
- Barbara NP, Wrana JL, Letarte M (1999) Endoglin is an accessory protein that interacts with the signaling receptor complex of multiple members of the transforming growth factor-beta superfamily. *J Biol Chem* 274:584–594
- Scharpfenecker M, van Dinther M, Liu Z, van Bezooijen RL, Zhao Q, Pukac L, Lowik CW, Ten Dijke P (2007) BMP-9 signals via ALK1 and inhibits bFGF-induced endothelial cell proliferation and VEGF-stimulated angiogenesis. *J Cell Sci* 120:964–972
- Rogers MS, D’Amato RJ (2006) The effect of genetic diversity on angiogenesis. *Exp Cell Res* 312:561–574

32. Shaked Y, Bertolini F, Man S, Rogers MS, Cervi D, Foutz T, Rawn K, Voskas D, Dumont DJ, Ben-David Y, Lawler J, Henkin J, Huber J, Hicklin DJ, D'Amato RJ, Kerbel RS (2005) Genetic heterogeneity of the vasculogenic phenotype parallels angiogenesis; implications for cellular surrogate marker analysis of antiangiogenesis. *Cancer Cell* 7:101–111
33. Pawlikowska L, Tran MN, Achrol AS, Ha C, Burchard EG, Choudhry S, Zaroff J, Lawton MT, Castro RA, McCulloch CE, Marchuk DA, Kwok PY, Young WL (2005) Polymorphisms in transforming growth factor-B-related genes ALK1 and ENG are associated with sporadic brain arteriovenous malformations. *Stroke* 36:2278–2280
34. Simon M, Franke D, Ludwig M, Aliashkevich AF, Koster G, Oldenburg J, Bostrom A, Ziegler A, Schramm J (2006) Association of a polymorphism of the ACVRL1 gene with sporadic arteriovenous malformations of the central nervous system. *J Neurosurg* 104:945–949
35. Simon M, Schramm J, Ludwig M, Ziegler A (2007) Arteriovenous malformation. *J Neurosurg* 106:732–733, Author reply to letter by Young WL et al
36. Kim H, Hysi PG, Pawlikowska L, Poon A, Burchard EG, Zaroff JG, Sidney S, Ko NU, Achrol AS, Lawton MT, McCulloch CE, Kwok PY, Young WL (2009) Common variants in interleukin-1-beta gene are associated with intracranial hemorrhage and susceptibility to brain arteriovenous malformation. *Cerebrovasc Dis* 27:176–182
37. Pawlikowska L, Tran MN, Achrol AS, McCulloch CE, Ha C, Lind DL, Hashimoto T, Zaroff J, Lawton MT, Marchuk DA, Kwok PY, Young WL (2004) Polymorphisms in genes involved in inflammatory and angiogenic pathways and the risk of hemorrhagic presentation of brain arteriovenous malformations. *Stroke* 35:2294–2300
38. Weinsheimer S, Kim H, Pawlikowska L, Chen Y, Lawton MT, Sidney S, Kwok PY, McCulloch CE, Young WL (2009) EPHB4 gene polymorphisms and risk of intracranial hemorrhage in patients with brain arteriovenous malformations. *Circ Cardiovasc Genet* 2:476–482
39. Achrol AS, Pawlikowska L, McCulloch CE, Poon KY, Ha C, Zaroff JG, Johnston SC, Lee C, Lawton MT, Sidney S, Marchuk DA, Kwok PY, Young WL (2006) Tumor necrosis factor-alpha-238G>A promoter polymorphism is associated with increased risk of new hemorrhage in the natural course of patients with brain arteriovenous malformations. *Stroke* 37:231–234
40. Pawlikowska L, Poon KY, Achrol AS, McCulloch CE, Ha C, Lum K, Zaroff J, Ko NU, Johnston SC, Sidney S, Marchuk DA, Lawton MT, Kwok PY, Young WL (2006) Apolipoprotein E epsilon2 is associated with new hemorrhage risk in brain arteriovenous malformation. *Neurosurgery* 58:838–843
41. Achrol AS, Kim H, Pawlikowska L, Poon KY, Ko NU, McCulloch CE, Zaroff JG, Johnston SC, McDermott MW, Lawton MT, Kwok PY, Young WL (2007) Association of tumor necrosis factor-alpha-238G>A and apolipoprotein E2 polymorphisms with intracranial hemorrhage after brain arteriovenous malformation treatment. *Neurosurgery* 61:731–739
42. Krebs LT, Starling C, Chervonsky AV, Gridley T (2010) Notch1 activation in mice causes arteriovenous malformations phenocopied by EphrinB2 and EphB4 mutants. *Genesis* 48:146–150
43. Klein RJ, Zeiss C, Chew EY, Tsai JY, Sackler RS, Haynes C, Henning AK, SanGiovanni JP, Mane SM, Mayne ST, Bracken MB, Ferris FL, Ott J, Barnstable C, Hoh J (2005) Complement factor H polymorphism in age-related macular degeneration. *Science* 308:385–389
44. Donoso LA, Vrabc T, Kuivaniemi H (2010) The role of complement Factor H in age-related macular degeneration: a review. *Surv Ophthalmol* 55:227–246
45. Kim H, Pawlikowska L, Weinsheimer S, Kwok PY, Zaroff JG, McCulloch CE, Young WL (2010) Genome-wide association study of intracranial hemorrhage in brain arteriovenous malformation (BAVM) patients [Abstract]. *Stroke* 41:e11 (P37)
46. Shenkar R, Elliott JP, Diener K, Gault J, Hu LJ, Cohrs RJ, Phang T, Hunter L, Breeze RE, Awad IA (2003) Differential gene expression in human cerebrovascular malformations. *Neurosurgery* 52:465–478
47. Giusti B, Rossi L, Lapini I, Magi A, Pratesi G, Lavitrano M, Biasi GM, Pulli R, Pratesi C, Abbate R (2009) Gene expression profiling of peripheral blood in patients with abdominal aortic aneurysm. *Eur J Vasc Endovasc Surg* 38:104–112
48. Sinnaeve PR, Donahue MP, Grass P, Seo D, Vonderscher J, Chibout SD, Kraus WE, Sketch M Jr, Nelson C, Ginsburg GS, Goldschmidt-Clermont PJ, Granger CB (2009) Gene expression patterns in peripheral blood correlate with the extent of coronary artery disease. *PLoS ONE* 4:e7037
49. Wang Y, Barbacioru CC, Shiffman D, Balasubramanian S, Iakubova O, Tranquilli M, Albornoz G, Blake J, Mehmet NN, Ngadimo D, Poulter K, Chan F, Samaha RR, Elefteriades JA (2007) Gene expression signature in peripheral blood detects thoracic aortic aneurysm. *PLoS ONE* 2:e1050
50. Xu H, Tang Y, Liu DZ, Ander BP, Liu X, Apperson M, Ran R, Gregg JP, Pancioli A, Jauch EC, Wagner KR, Verro P, Broderick JP, Sharp FR (2008) Gene expression in peripheral blood differs following cardioembolic compared to large vessel atherosclerotic stroke: biomarkers for the etiology of ischemic stroke. *J Cereb Blood Flow Metab* 28:1320–1328
51. Weinsheimer S, Kim H, Pawlikowska L, McCulloch CE, Xu H, Stamova B, Tian Y, Sharp FR, Young WL (2009) Genome-wide expression profiling of human blood reveals biomarkers for hemorrhage in brain arteriovenous malformation patients [Abstract]. American Society of Human Genetics 59th Annual Meeting, Honolulu, HI
52. Su H, Hao Q, Shen F, Zhu Y, Lee CZ, Young WL, Yang GY (2008) Development of cerebral microvascular dysplasia model in rodents. *Acta Neurochir Suppl* 105:185–189
53. Torsney E, Charlton R, Diamond AG, Burn J, Soames JV, Arthur HM (2003) Mouse model for hereditary hemorrhagic telangiectasia has a generalized vascular abnormality. *Circulation* 107:1653–1657
54. Srinivasan S, Hanes MA, Dickens T, Porteous ME, Oh SP, Hale LP, Marchuk DA (2003) A mouse model for hereditary hemorrhagic telangiectasia (HHT) type 2. *Hum Mol Genet* 12:473–482
55. Satomi J, Mount RJ, Toporsian M, Paterson AD, Wallace MC, Harrison RV, Letarte M (2003) Cerebral vascular abnormalities in a murine model of hereditary hemorrhagic telangiectasia. *Stroke* 34:783–789
56. Hao Q, Su H, Marchuk DA, Rola R, Wang Y, Liu W, Young WL, Yang GY (2008) Increased tissue perfusion promotes capillary dysplasia in the ALK1-deficient mouse brain following VEGF stimulation. *Am J Physiol Heart Circ Physiol* 295:H2250–H2256
57. Hao Q, Zhu Y, Su H, Shen F, Yang GY, Kim H, Young WL (2010) VEGF induces more severe cerebrovascular dysplasia in Endoglin^{+/−} than in Alk1^{+/−} mice. *Transl Stroke Res* 1:197–201
58. Xu B, Wu YQ, Huey M, Arthur HM, Marchuk DA, Hashimoto T, Young WL, Yang GY (2004) Vascular endothelial growth factor induces abnormal microvasculature in the endoglin heterozygous mouse brain. *J Cereb Blood Flow Metab* 24:237–244
59. Park SO, Wankhede M, Lee YJ, Choi EJ, Fliess N, Choe SW, Oh SH, Walter G, Raizada MK, Sorg BS, Oh SP (2009) Real-time imaging of de novo arteriovenous malformation in a mouse model of hereditary hemorrhagic telangiectasia. *J Clin Invest* 119:3487–3496
60. Mahmoud M, Allinson KR, Zhai Z, Oakenfull R, Ghandi P, Adams RH, Fruttiger M, Arthur HM (2010) Pathogenesis of arteriovenous malformations in the absence of endoglin. *Circ Res* 106:1425–1433
61. Walker E, Shen F, Halprin R, Connolly S, Nishimura SL, Young WL, Su H (2010) Regional deletion of Smad4 plus VEGF stimulation leads to vascular dysplasia in the adult mouse brain [Abstract]. *Stroke* 41:e20 (#68)

62. Lebrin F, Srun S, Raymond K, Martin S, van den Brink S, Freitas C, Breant C, Mathivet T, Larrivee B, Thomas JL, Arthur HM, Westermann CJ, Disch F, Mager JJ, Snijder RJ, Eichmann A, Mummery CL (2010) Thalidomide stimulates vessel maturation and reduces epistaxis in individuals with hereditary hemorrhagic telangiectasia. *Nat Med* 16:420–428
63. Zhang G, Zhou J, Fan Q, Zheng Z, Zhang F, Liu X, Hu S (2008) Arterial-venous endothelial cell fate is related to vascular endothelial growth factor and Notch status during human bone mesenchymal stem cell differentiation. *FEBS Lett* 582:2957–2964
64. Murphy PA, Lu G, Shiah S, Bollen AW, Wang RA (2009) Endothelial Notch signaling is upregulated in human brain arteriovenous malformations and a mouse model of the disease. *Lab Invest* 89: 971–982
65. ZhuGe Q, Zhong M, Zheng W, Yang GY, Mao X, Xie L, Chen G, Chen Y, Lawton MT, Young WL, Greenberg DA, Jin K (2009) Notch1 signaling is activated in brain arteriovenous malformation in humans. *Brain* 132:3231–3241
66. Walker EJ, Su H, Shen F, Choi EJ, Oh SP, Chen G, Lawton MT, Kim H, Chen Y, Chen W, Young WL (2011) Arteriovenous malformation in the adult mouse brain resembling the human disease. *Ann Neurol* doi: 10.1002/ana.22348

The Evolving Landscape of Neuroinflammation After Neonatal Hypoxia-Ischemia

Nancy Fathali, Nikan H. Khatibi, Robert P. Ostrowski, and John H. Zhang

Abstract Hypoxic-ischemic brain injury remains a leading cause of mortality and morbidity in neonates. The inflammatory response, which is characterized in part by activation of local immune cells, has been implicated as a core component for the progression of damage to the immature brain following hypoxia-ischemia (HI). However, mounting evidence implicates circulating immune cells recruited to the site of damage as orchestrators of neuron-glia interactions and perpetrators of secondary brain injury. This suggests that redirecting our attention from the local inflammatory response toward the molecular mediators believed to link brain-immune cell interactions may be a more effective approach to mitigating the inflammatory sequelae of perinatal HI. In this review, we focus our attention on cyclooxygenase-2, a mediator by which peripheral immune cells may modulate signaling pathways in the brain that lead to a worsened outcome. Additionally, we present an overview of emerging therapeutic modalities that target mechanisms of neuroinflammation in the hypoxic-ischemic neonate.

Keywords Hypoxia-ischemia · Neuroinflammation · Cyclooxygenase-2 · Immature brain · Neuron-glia · Immune cell

Introduction

Hypoxia-ischemia (HI) occurs in 1 to 6 per 1,000 live full-term births [1]. Of those affected, 15–20% will die in the postnatal period, and 25% of survivors will be left with long-term neurological disabilities [2–4]. Intrauterine asphyxia is the underlying mechanism of hypoxic injury and is a consequence of circulatory problems, including clotting of placental arteries and placental abruption [5]. HI in the neonate is a manifestation of systemic hypoxia combined with reduced cardiac output [6].

Studies have shown that the pathophysiology of brain injury secondary to HI consists of a biphasic profile (Fig. 1). The initial phase of HI is characterized by brain acidosis and the depletion of high-energy phosphorylated compounds, such as adenosine triphosphate and phosphocreatine [1, 7, 8]. This primary energy failure leads to the loss of membrane ionic homeostasis, depolarization of the cell, osmotic dysregulation, and inhibition of protein synthesis, further leading to necrosis [9, 10]. The secondary processes evolve over days after the brain insult and are also characterized by a depletion of high-energy phosphorylated compounds, however without tissue acidosis. Although the pathogenesis of secondary brain injury involves multiple pathophysiological processes, accumulating evidence implicates the inflammatory response as a core component of damage [11–13].

Neuroinflammation includes initial release of proinflammatory mediators by injured or dying cells, activation of microglia and astrocytes, and leukocyte infiltration. It is the synergistic actions of these events that potentiate brain damage and lead to neurological dysfunction [14]. However, experimental studies thus far have focused mainly on selectively targeting these mechanisms, which may explain why there are no pharmacotherapies proven clinically viable for

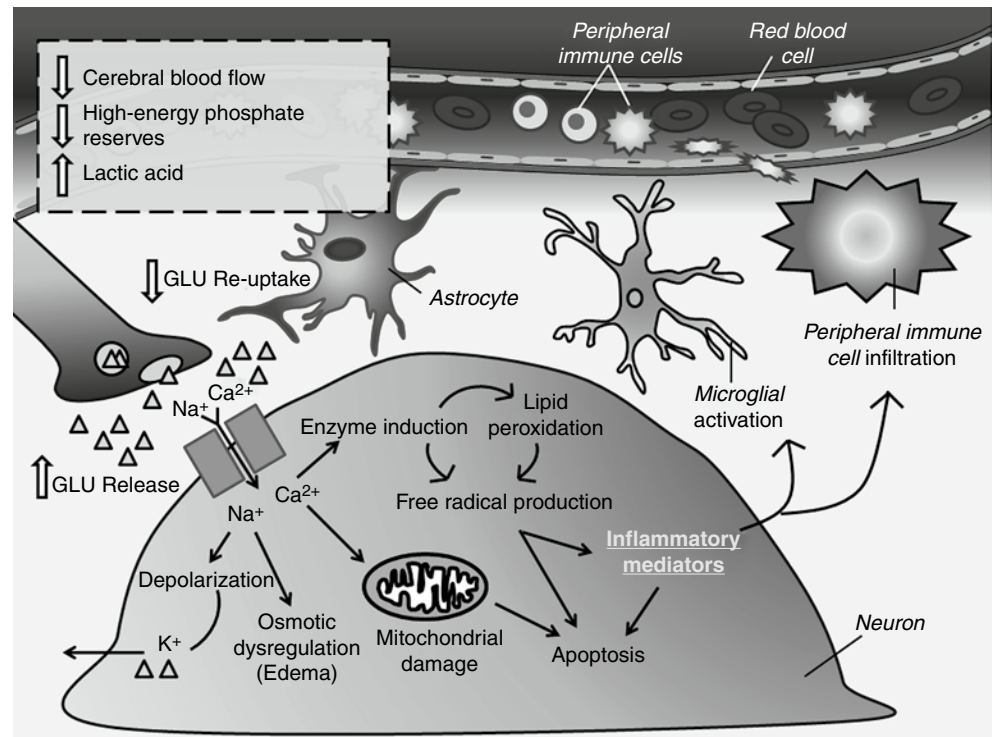
N. Fathali
Department of Human Pathology and Anatomy,
Loma Linda University, School of Medicine, Loma Linda, CA, USA

N.H. Khatibi
Department of Anesthesiology, Loma Linda University,
School of Medicine, Loma Linda, CA, USA

R.P. Ostrowski
Department of Physiology, Loma Linda University,
School of Medicine, Loma Linda, CA, USA

J.H. Zhang (✉)
Department of Anesthesiology, Loma Linda University,
School of Medicine, Loma Linda, CA, USA and
Department of Physiology, Loma Linda University,
School of Medicine, Loma Linda, CA, USA and
Department of Neurosurgery, Loma Linda University,
School of Medicine, 11234 Anderson Street, Room 2562B,
Loma Linda, CA, USA
e-mail: johnzhang3910@yahoo.com

Fig. 1 Pathophysiology of a hypoxic-ischemic event. Decrease in cerebral blood flow results in a decrease in high-energy phosphate reserves (i.e., adenosine triphosphate; phosphocreatine) and a build-up of lactic acid. Loss of membrane ionic homeostasis leads to intracellular accumulation of sodium (Na^+), calcium (Ca^{2+}), and water (edema), thereby depolarizing the cell and releasing glutamate (triangle) and potassium (K^+) into the extracellular space. Intracellular calcium ion accumulation leads to enzyme induction (i.e., lipases, proteases, endonucleases) and free fatty acid elevation, which undergo peroxidation. The result is the accumulation and/or release of inflammatory mediators (i.e., cyclooxygenase-2), which can lead to apoptosis, glial activation, and peripheral immune cell infiltration



the treatment of HI brain damage. In fact, increasing evidence suggests identifying molecular mediators responsible for orchestrating brain-immune cell interactions as a more promising approach [15–17].

This review will provide a brief overview of the current understanding of the local and peripheral inflammatory response involved in neonatal HI, and the role of cyclooxygenase-2 (COX-2) in brain-immune cell interactions and the progression of neuroinflammation.

Changing Landscape of Neuroinflammation

The immune response in the brain is highly complex and involves the participation of several different resident cells (Fig. 2). Microglia, astrocytes, and neurons directly react and contribute to neuroinflammation in the HI-injured neonate. The role of each of these cell types in propagating the local inflammatory response is important in understanding the dynamic microenvironment.

Microglia

Microglia cells serve as specialized sensors for brain tissue damage. In response to ischemia, microglia morphologically change from a resting ramified phenotype to a motile

activated amoeboid cell able to migrate to necrotic areas to remove cellular debris [10, 18]. However, in the process, these activated cells contribute to secondary brain injury by releasing a variety of pro-inflammatory mediators including cytokines, reactive oxygen species, complement factors, free radical species, and nitric oxide, which contribute to cell death, ultimately creating a vicious perpetuating cycle [2].

Mounting evidence suggests that infiltrating peripheral immune cells may be necessary for the activation of microglia, thereby exacerbating neurodegeneration after ischemia. In an *in vitro* study, microglia, when co-cultured with T-cells, become activated, thereby releasing an inflammatory cytokine [19]. In an *in vivo* study, removal of a population of infiltrating macrophages, neutrophils, B cells, and T cells by splenectomy appeared to reduce microglia activation and dramatically reduce brain damage [20]. Systemic inhibition of monocyte/macrophage or neutrophil populations has also been shown to reduce cerebral infarct volume after ischemic injury [21–23]. However, the exact mechanism by which peripheral immune cells activate and/or propagate the local inflammatory response and enhance neuronal death remains to be determined.

Astrocytes

Astrocytes, which are the predominant glial cell type in the central nervous system (CNS), have been shown to produce

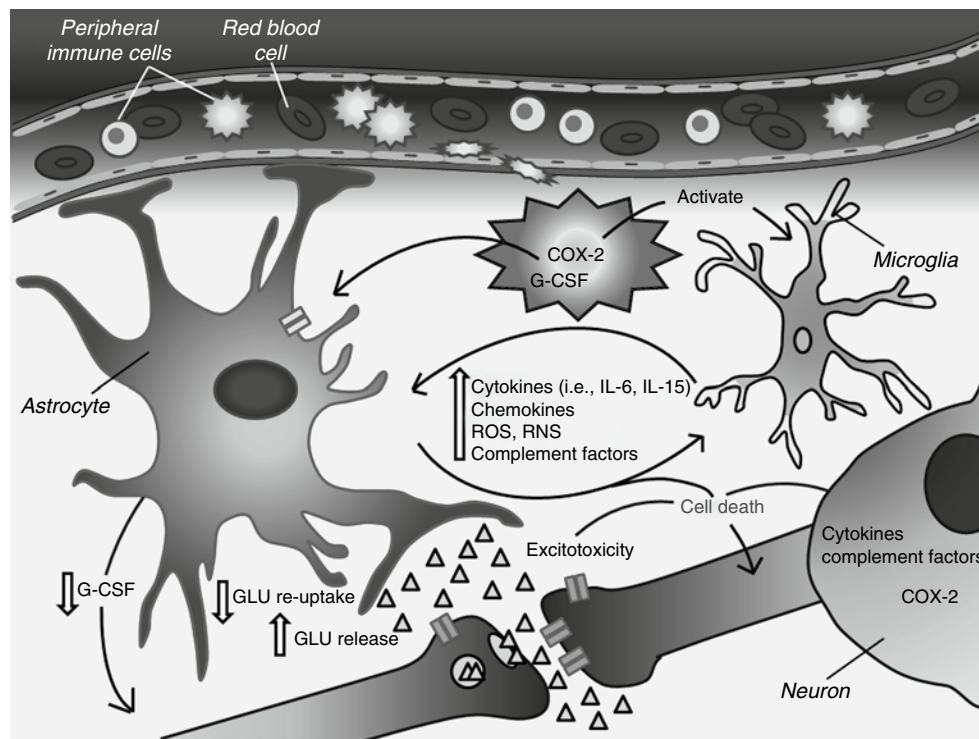


Fig. 2 Neuroinflammatory cascade after brain injury. Downstream cyclooxygenase-2 (COX-2) effectors from infiltrating peripheral immune cells activate astrocytes and microglia, which in turn release cytokines, chemokines, reactive oxygen and nitrogen species (ROS and RNS, respectively), and complement factors. These inflammatory mediators can further activate resident brain cells, thereby amplifying neuroinflammatory signals and neuronal cell death. Excessive exposure

to inflammatory mediators compromises astrocyte functions leading to downregulation of glutamate transporters, impaired glutamate re-uptake, elevated glutamate release, and decreased neurotrophic factor (i.e., granulocyte-colony stimulating factor [G-CSF]) release; all of which can lead to neuronal cell death. Neuronal release of cytokines, complement factors, and COX-2 can lead to autocrine or paracrine-mediated neuronal death

inflammatory mediators in a variety of brain injuries including HI [24, 25]. Inflammatory cytokines have been associated with neonatal HI brain damage and later development of cerebral palsy [2, 26]. Specifically, elevated levels of interleukin (IL)-6 in cerebrospinal fluid of asphyxiated newborns have been correlated with an increased degree of brain damage and poor neurological outcome [27]. Additionally, recent evidence has implicated IL-15 as playing a leading role in neuroinflammation in the injured immature rat brain [28]. Importantly, astrocytes are the main source of both IL-6 and IL-15 in CNS injury and inflammation [2, 29].

Astrocytes may also influence the local inflammatory response through their communicative partnership with neighboring cells [30]. Under pathological conditions, astrocytes play a critical role in the activation of microglia [31, 32], and by-products of reactive astrocytes such as tumor necrosis factor- α (TNF- α) and IL-6 are associated with neuronal demise after HI [33]. On the other hand, astrocytes are also a source of trophic factors, such as granulocyte-colony-stimulating factor (G-CSF) [34], and are responsible for regulating neurotransmitter and ion concentrations, removing debris, and maintaining an optimal environment for neuronal function [35]. Impairment of astrocyte function during HI is thought to influence neuron viability [33]. Therefore, it

is important to identify key molecular mediators responsible for initiating astrocyte signaling pathways involved in worsening brain injury, without eliminating the protective function of these cells.

Neurons

Once thought to be passive bystanders in neuroinflammation, neurons are now known to play a more active role. As such, neurons can be a source of inflammatory mediators, including complement, COX-2, and cytokines after HI [12, 36]. Neurons can express COX-2 at low levels under normal conditions; however, under pathological conditions, COX-2 is upregulated in response to mitogens, inflammatory mediators, and hormones [37]. Induction of COX-2 expression in neurons is also driven by physiological synaptic activity [38] and acute paradigms of excitotoxicity [39], thereby promoting local inflammatory reactions and injury to themselves [40–42]. Moreover, neurons contribute to the production of proinflammatory mediators that can alter vascular permeability and regional blood flow, and enhance chemotactic activity and thereby promote leukocyte migration [11].

Once peripheral leukocytes and monocytes enter the brain parenchyma, their actions appear to be multifaceted [43]. Certain immune cell subpopulations may directly elicit neuronal death via contact-dependent mechanisms [44] or release molecular mediators that activate resident cells, thus promoting further brain injury [45, 46]. In line with this concept, recent studies have shown that T-lymphocyte-deficient mice demonstrate attenuated brain injury and neurological deficits after experimental stroke [47, 48]. To make matters more complex, regulatory T-lymphocytes have been shown to have a protective role in the brain after stroke [49]. Immune cells have also been implicated in the generation of new neurons and improvement of spatial learning and memory performance in neurodegenerative disease [50–52].

Neuro-Glial Interactions

Astrocytes are viewed as an active participant in synaptic transmission and processing of information – a departure from the old dogma in which astrocytes were identified as merely physical supporters for neighboring neurons [35]. Moreover, opening of gap-junctional communication channels links dying astrocytes in the ischemic core with penumbral cells [53]. Therefore, astrocytes might compromise juxtaposed cells found in salvageable tissue that otherwise may have survived.

Studies have suggested that inflammatory mediators might be the driving force for altering astrocyte function and thereby impacting neuron-glia signaling. For example, astrocytes undergo IL-1 β -induced elevations in intracellular calcium, which may enhance glia-to-neuron signaling, leading to a reduction in neuron survival [54]. Proinflammatory cytokines may also be responsible for impairing astrocyte energy metabolism, thereby jeopardizing neuronal vulnerability [35]. Thus, it is reasonable to conceptualize that targeting cytokines may lead to a profound modulation of astrocyte function and improve neuronal survivability in this mechanism.

Central Role of COX-2

Cyclooxygenase is a rate-limiting enzyme responsible for catalyzing the synthesis of prostaglandins from arachidonic acid [55]. Cyclooxygenase possesses two catalytic sites: a COX active site responsible for the conversion of arachidonic acid into the endoperoxide, PGG₂, and a peroxidase active site responsible for the rapid conversion of PGG₂ into another endoperoxide, PGH₂ [56]. PGH₂ is further processed to form prostaglandins, prostacyclin, and thromboxane A₂. To date, two COX isoforms have been identified.

COX-1 is constitutively expressed in the brain, and its by-products are thought to contribute to normal physiological function [57]. COX-2 is also constitutively expressed in the brain (neurons, astrocytes, microglia, and endothelia), but can be inducible under pathological conditions [57]. In the brain, COX-2 acts as a key mediator of inflammation, orchestrating a wide spectrum of brain injuries, including excitotoxic brain injury, cerebral ischemia, traumatic brain injury, and neurodegenerative disorders [58]. COX-2 can propagate the neuroinflammatory response and contribute to tissue damage through the production of toxic prostanoids and reactive oxygen species [37]. COX-3 has also been reported in brain tissue [59], but is a splice variant of COX-1 with unknown function [60].

COX-2 Orchestrates Immunologic Responses After HI

COX-2, a well-established mediator of adult brain injury [37], is emerging as a key player in neuroinflammation after hypoxic-ischemic brain damage in the neonate [12]. Peripheral immune cells such as T-lymphocytes, B-cells, and natural killer cells have the capability to upregulate COX-2 expression when activated [61]. However, immune cell infiltration into the brain parenchyma is thought to play a beneficial role also through the production of neurotrophic factors [62]. Activated monocytes, macrophages, and neutrophils are the peripheral cell source for the neurotrophic factor, G-CSF. Peripherally produced G-CSF can also enter the brain by crossing the intact blood-brain barrier and binding to its receptor on neurons and glial cells [63, 64]. In the brain, G-CSF has been shown to protect neurons and trigger neurogenesis [65]. However, excessive and/or prolonged activation of inflammatory mediators can decrease neurotrophic support and neurogenesis in brain areas responsible for behavior and cognition [66–68]. Studies suggest COX-2 may mediate suppression of G-CSF, since inhibition of COX-2 was able to increase G-CSF production [69, 70]. This downregulation of neurotrophic factors contributes to secondary brain injury and cell death after a hypoxic-ischemic insult [71].

Emerging Therapeutic Modalities Targeting Inflammation

There are various therapeutic modalities that have attempted to modulate the neuroinflammation that results from HI brain injury in neonates. These treatment options have targeted various stages in the inflammatory cascade, including COX-2 inhibition, and also investigated the use of growth

factors such as G-CSF. In the following paragraphs, we will review these emerging therapeutic modalities and explore the various studies that have been conducted between 1970 and 2010 using relevant literature from the National Library of Medicine and National Institute of Health Database (www.pubmed.gov).

COX-2 Inhibition

To date, many studies have investigated the anti-inflammatory properties of COX-2 inhibition and the benefits with improving neurological outcomes after various adult brain injuries. Yet surprisingly, only one study to date has investigated the use of COX-2 inhibition on neonatal HI brain injury. The study led by Fathali et al. used postnatal day 10 rat pups to assess the effects of NS398, a known selective COX-2 inhibitor, on various neurologic outcomes after right common carotid artery occlusion followed by 2 h of hypoxia [12]. The authors first described that COX-2 inhibition limited morphologic damage, improved long-term functional deficits, reversed somatic growth retardation, and lowered mortality rates after a hypoxic-ischemic injury in neonatal rats. Of note, COX-2 inhibition significantly reduced the expression of IL-6, a proinflammatory cytokine, and in turn reduced the infiltration of inflammatory cells, such as macrophages and neutrophils, which suggests that the increased survivability and neuroprotection provided by COX-2 may be mediated by a reduction in neuroinflammation [12].

G-CSF Administration

G-CSF is a 20-kDa protein belonging to the cytokine family of growth factors. It is responsible for stimulating the proliferation, survival, and maturation of cells committed to the neutrophil granulocyte lineage by binding to specific G-CSF receptors [72]. In addition to its role in neutropenia, G-CSF has been shown to be neuroprotective in various brain injury models through direct apoptotic inhibition, inflammatory cell modulation, and/or trophic effects on neuronal cells.

One of the first studies to investigate the anti-inflammatory properties of G-CSF was conducted in 1992 by Gorgen et al. who looked at the role of G-CSF in gram-negative septic rodents [73]. The study showed that G-CSF could interfere with TNF- α production through a negative feedback signal. Later, in 2005, both Gibson and Komie-Kobayashi would also demonstrate the anti-inflammatory role of G-CSF by showing that treatment could modulate the inflammatory response after injury [74, 75]. Specifically,

Komie-Kobayashi demonstrated G-CSF's ability to suppress inducible nitric oxide synthase (iNOS) production and decrease activation of microglial cells expressing iNOS – according to Western blot and immunohistochemistry analysis. Gibson, on the other hand, found that G-CSF treatment only suppressed the upregulation of IL-1 β mRNA and had no effect on TNF- α and iNOS mRNA expression. Additionally, in models of peripheral infections, G-CSF-induced JAK-STAT signaling was found to reduce TNF- α , interleukin (IL)-1 β , IL-2, IL-6, and IL-8, and elevate IL-1 β receptor antagonists [76].

In terms of its neurotrophic capabilities, various studies have confirmed G-CSF as an essential neurotrophic factor, noting its ability to stimulate the release of stem cells from the bone marrow, promoting both neural repair and neural plasticity [72]. A study led by Shyu et al. in *Circulation* (2004) found that ischemic stroke rats treated with G-CSF could mobilize autologous hematopoietic stem cells into the circulation, enhance their translocation into ischemic brain, and significantly improve lesion repair [77]. Additionally, in rat ischemic models, peripherally administered G-CSF was found to enhance structural repair and function by increasing the number of newly generated neurons in both healthy and ischemic subjects [78].

In neonatal HI, only three studies can be found on PubMed using the search criteria “G-CSF and neonatal hypoxia ischemia.” Unfortunately, none of the studies looked at the role of G-CSF as an anti-inflammatory agent. Instead, the focus of attention was on the role of G-CSF in apoptosis. The first study led by Yata et al. (2007) found that five 50 $\mu\text{g}/\text{kg}$ G-CSF post-treatment injections over 4 days could reduce apoptotic neuron loss while increasing the expression of pro-survival signals [79]. Specifically, the investigators found that the anti-apoptotic protein Bcl-2 declined with injury and reversed after treatment, while the pro-apoptotic protein, Bax, increased following HI injury and again was reversed following G-CSF treatment. This is in line with another study conducted by Kim et al. (2008) that found similar neuroprotective outcomes following a single injection of 50 $\mu\text{g}/\text{kg}$ G-CSF after injury [80].

Summary

In summary, the emerging landscape of neuroinflammation reveals highly complex interactions involving neurons, glia, and peripheral immune cells in the neonatal brain injured by HI. The mechanism of these multidirectional communications and their specific involvement in brain injury began to unveil only recently. It is however important to dissect molecular orchestrators of these interactions further in order to devise novel therapeutics with increased likelihood of success in clinical trials. Recent studies demonstrated a critical

involvement of COX-2 in brain inflammation after HI and implied the use of COX inhibitors in treatment for neonatal encephalopathy in the clinical setting. While COX-2 appears to be a major neuroinflammatory mediator after HI, GCSF can negatively modulate inflammatory responses in the immature brain. Interestingly, COX-2 can also mitigate GCSF action and thereby can compromise neuronal survivability in the brain. Collectively, these findings suggest that COX-2 inhibitors and exogenous GCSF are promising treatment modalities on which to rely.

Perspective

Based on the results obtained so far, it is also reasonable to anticipate that COX-2 plays a major role in mediating neuroglial interactions as well as in orchestrating immunological cell response in HI-induced brain injury. Further studies of this matter are warranted.

In the adult stroke model, splenectomy prior to cerebral ischemia reduced brain injury by elimination of the largest pool of immunological cells in the system. Consequently, it positively verified the involvement of peripheral immune cells in the mechanism of brain injury progression after stroke. Considering that all clinical trials of anti-inflammatory agents against stroke failed, these latest findings may point towards a reassessment as to whether anti-inflammatory therapies for stroke can reduce the peripheral immune system's involvement. These new evaluation criteria would also stand true for numerous candidate treatments of neonatal HI currently being tested in neuroscience laboratories, including G-CSF. In addition, it would be worthwhile to develop immunomodulatory therapies aimed at switching the immune response after HI to Th₂ cells. Significant progress in this field should not come as a surprise quite soon considering the latest studies employing "beneficial" subtypes of T cells (Th₂/Th₃) to support neuroprotection and/or regeneration. However, the existing studies of neuro-glial-immune interactions have been conducted almost exclusively in adult stroke models. In addition, a few relevant studies of neonatal HI included unsexed animals. Thus, the peripheral immune involvement in neonatal HI awaits further investigations, considering distinct characteristics of the developing brain and immunologic immaturity of the neonate. In conclusion, the molecular circuitry of neuro-glial-immune communications in the hypoxic-ischemic neonatal brain with gender-specific investigations needs to be deciphered. It is believed that targeting master mediators of these interactions may pave the way to the first successful clinical trial with therapeutic agents that combat neuroinflammation after neonatal HI.

Acknowledgement This study was partially supported by NIH NS053407 to J.H. Zhang.

Conflict of interest statement We declare that we have no conflict of interest.

References

- Shankaran S (2009) Neonatal encephalopathy: treatment with hypothermia. *J Neurotrauma* 26(3):437–443
- Fatemi A, Wilson MA, Johnston MV (2009) Hypoxic-ischemic encephalopathy in the term infant. *Clin Perinatol* 36:835–858
- Gunn AJ (2000) Cerebral hypothermia for prevention of brain injury following perinatal asphyxia. *Curr Opin Pediatr* 12:111–115
- Vanucci RC, Perlman JM (1997) Interventions for perinatal hypoxic-ischemic encephalopathy. *Pediatrics* 100:1004–1014
- Locatelli A, Incerti M, Ghidini A, Greco M, Villa E, Paterlini G (2008) Factors associated with umbilical artery acidemia in term infants with low Apgar scores at 5 min. *Eur J Obstet Gynecol Reprod Biol* 139(2):146–150
- Liu J, Li J, Gu M (2007) The correlation between myocardial function and cerebral hemodynamics in term infants with hypoxic-ischemic encephalopathy. *J Trop Pediatr* 53(1):44–48
- Brillault J, Lam TI, Rutkowski JM, Foroutan S, O'Donnell ME (2008) Hypoxia effects on cell volume and ion uptake of cerebral microvascular endothelial cells. *Am J Physiol Cell Physiol* 294(1):C88–C96
- Hausmann R, Seidl S, Betz P (2007) Hypoxic changes in Purkinje cells of the human cerebellum. *Int J Legal Med* 121(3):175–183
- Johnston MV, Trescher WH, Ishida A, Nakajima W (2001) Neurobiology of hypoxic-ischemic injury in the developing brain. *Pediatr Res* 49:735–741
- Leonardo CC, Pennypacker KR (2009) Neuroinflammation and MMPs: potential therapeutic targets in neonatal hypoxic-ischemic injury. *J Neuroinflammation* 6:13
- Alvarez-Diaz A, Hilario E, de Cerio FG, Valls-i-Soler A, Alvarez-Diaz FJ (2007) Hypoxic-ischemic injury in the immature brain—key vascular and cellular players. *Neonatology* 92:227–235
- Fathali N, Ostrowski RP, Lekic T, Jadhav V, Tong W, Tang J, Zhang JH (2010) Cyclooxygenase-2 inhibition provides lasting protection against neonatal hypoxic-ischemic brain injury. *Crit Care Med* 38:572–578
- Ferriero DM (2004) Neonatal brain injury. *N Engl J Med* 351:1985–1995
- Pimentel VC, Belle LP, Pinheiro FV, De Bona KS, Da Luz SCA, Moretto MB (2009) Adenosine deaminase activity, lipid peroxidation and astrocyte responses in the cerebral cortex of rats after neonatal hypoxia ischemia. *Int J Dev Neurosci* 27:857–862
- Curin Y, Ritz MF, Andriantsitohaina R (2006) Cellular mechanisms of the protective effect of polyphenols on the neurovascular unit in strokes. *Cardiovasc Hematol Agents Med Chem* 4:277–288
- del Zoppo GJ (2009) Inflammation and the neurovascular unit in the setting of focal cerebral ischemia. *Neuroscience* 158:972–982
- Lo EH (2008) Experimental models, neurovascular mechanisms and translational issues in stroke research. *Br J Pharmacol* 153 (Suppl 1):S396–S405
- Kreutzberg GW (1996) Microglia: a sensor for pathological events in the CNS. *Trends Neurosci* 19:312–318
- Chabot S, Williams G, Yong VW (1997) Microglial production of TNF-alpha is induced by activated T lymphocytes. Involvement of VLA-4 and inhibition by interferon-beta-1b. *J Clin Invest* 100:604–612

20. Ajmo CT Jr, Vernon DO, Collier L, Hall AA, Garbuzova-Davis S, Willing A, Pennypacker KR (2008) The spleen contributes to stroke-induced neurodegeneration. *J Neurosci Res* 86(10):2227–2234
21. Chen H, Chopp M, Zhang RL, Bodzin G, Chen Q, Rusche JR, Todd RF 3rd (1994) Anti-CD11b monoclonal antibody reduces ischemic cell damage after transient focal cerebral ischemia in rat. *Ann Neurol* 35:458–463
22. Chopp M, Zhang RL, Chen H, Li Y, Jiang N, Rusche JR (1994) Postischemic administration of an anti-Mac-1 antibody reduces ischemic cell damage after transient middle cerebral artery occlusion in rats. *Stroke* 25:869–875
23. Zhang ZG, Chopp M, Tang WX, Jiang N, Zhang RL (1995) Postischemic treatment (2–4 h) with anti-CD11b and anti-CD18 monoclonal antibodies are neuroprotective after transient (2 h) focal cerebral ischemia in the rat. *Brain Res* 698:79–85
24. Sen E, Levison SW (2006) Astrocytes and developmental white matter disorders. *Ment Retard Dev Disabil Res Rev* 12(2):97–104
25. Svedin P, Guan J, Mathai S, Zhang R, Wang X, Gustavsson M, Hagberg H, Mallard C (2007) Delayed peripheral administration of a GPE analogue induces astrogliosis and angiogenesis and reduces inflammation and brain injury following hypoxia-ischemia in the neonatal rat. *Dev Neurosci* 29(4–5):393–402
26. Dammann O, O’Shea TM (2008) Cytokines and perinatal brain damage. *Clin Perinatol* 35(4):643–663
27. Savman K, Blennow M, Gustafson K, Tarkowski E, Hagberg H (1998) Cytokine response in cerebrospinal fluid after birth asphyxia. *Pediatr Res* 43(6):746–751
28. Maslinska D, Laure-Kamionowska M, Kaliszek A, Makarewicz D (2002) Proinflammatory cytokines in injured rat brain following perinatal asphyxia. *Folia Neuropathol* 40(4):177–182
29. Gomez-Nicola D, Valle-Argos B, Pita-Thomas DW, Nieto-Sampedro M (2008) Interleukin 15 expression in the CNS: blockade of its activity prevents glial activation after an inflammatory injury. *Glia* 56(5):494–505
30. Graeber MB, Streit WJ (2010) Microglia: biology and pathology. *Acta Neuropathol* 119:89–105
31. Ovanesov MV, Ayhan Y, Wolbert C, Moldovan K, Sauder C, Pletnikov MV (2008) Astrocytes play a key role in activation of microglia by persistent Borna disease virus infection. *J Neuroinflammation* 5:50
32. Tanuma N, Sakuma H, Sasaki A, Matsumoto Y (2006) Chemokine expression by astrocytes plays a role in microglia/macrophage activation and subsequent neurodegeneration in secondary progressive multiple sclerosis. *Acta Neuropathol* 112:195–204
33. Xiong M, Yang Y, Chen GQ, Zhou WH (2009) Post-ischemic hypothermia for 24 h in P7 rats rescues hippocampal neuron: association with decreased astrocyte activation and inflammatory cytokine expression. *Brain Res Bull* 79:351–357
34. Ding J, Li QY, Yu JZ, Wang X, Sun CH, Lu CZ, Xiao BG (2010) Fasudil, a Rho kinase inhibitor, drives mobilization of adult neural stem cells after hypoxia/reoxygenation injury in mice. *Mol Cell Neurosci* 43(2):201–208
35. Aschner M, Sonnewald U, Tan KH (2002) Astrocyte modulation of neurotoxic injury. *Brain Pathol* 12(4):475–481
36. Ten VS, Yao J, Ratner V, Sosunov S, Fraser DA, Botto M, Sivasankar B, Morgan BP, Silverstein S, Stark R, Polin R, Vannucci SJ, Pinsky D, Starkov AA (2010) Complement component C1q mediates mitochondria-driven oxidative stress in neonatal hypoxic-ischemic brain injury. *J Neurosci* 30(6):2077–2087
37. Iadecola C, Alexander M (2001) Cerebral ischemia and inflammation. *Curr Opin Neurol* 14(1):89–94
38. Yamagata K, Andreasson KI, Kaufmann WE, Barnes CA, Worley PF (1993) Expression of a mitogen-inducible cyclooxygenase in brain neurons: regulation by synaptic activity and glucocorticoids. *Neuron* 11(2):371–386
39. Adams J, Collaco-Moraes Y, de Belleruche J (1996) Cyclooxygenase-2 induction in cerebral cortex: an intracellular response to synaptic excitation. *J Neurochem* 66(1):6–13
40. Dore S, Otsuka T, Mito T, Sugou N, Hand T, Wu L, Hurn PD, Traystman RJ, Andreasson K (2003) Neuronal overexpression of cyclooxygenase-2 increases cerebral infarction. *Ann Neurol* 54(2):155–162
41. Nakayama M, Uchimura K, Zhu RL, Nagayama T, Rose ME, Stetler RA, Isakson PC, Chen J, Graham SH (1998) Cyclooxygenase-2 inhibition prevents delayed death of CA1 hippocampal neurons following global ischemia. *Proc Natl Acad Sci USA* 95(18):10954–10959
42. Nogawa S, Zhang F, Ross ME, Iadecola C (1997) Cyclo-oxygenase-2 gene expression in neurons contributes to ischemic brain damage. *J Neurosci* 17(8):2746–2755
43. Yong VW, Marks S (2010) The interplay between the immune and central nervous systems in neuronal injury. *Neurology* 74:S9–S16
44. Giuliani F, Goodyer CG, Antel JP, Yong VW (2003) Vulnerability of human neurons to T cell-mediated cytotoxicity. *J Immunol* 171:368–379
45. Arumugam TV, Granger DN, Mattson MP (2005) Stroke and T-cells. *Neuromolecular Med* 7:229–242
46. Brait VH, Jackman KA, Walduck AK, Selemidis S, Diep H, Mast AE, Guida E, Broughton BR, Drummond GR, Sobey CG (2010) Mechanisms contributing to cerebral infarct size after stroke: gender, reperfusion, T lymphocytes, and Nox2-derived superoxide. *J Cereb Blood Flow Metab* 30(7):1306–1317
47. Hurn PD, Subramanian S, Parker SM, Afentoulis ME, Kaler LJ, Vandenbark AA, Offner H (2007) T- and B-cell deficient mice with experimental stroke have reduced lesion size and inflammation. *J Cereb Blood Flow Metab* 27:1798–1805
48. Yilmaz G, Arumugam TV, Stokes KY, Granger DN (2006) Role of T lymphocytes and interferon-gamma in ischemic stroke. *Circulation* 113:2105–2112
49. Liesz A, Suri-Payer E, Veltkamp C, Doerr H, Sommer C, Rivest S, Giese T, Veltkamp R (2009) Regulatory T cells are key cerebroprotective immunomodulators in acute experimental stroke. *Nat Med* 15:192–199
50. Baron R, Nemirovsky A, Harpaz I, Cohen H, Owens T, Monsonego A (2008) IFN-gamma enhances neurogenesis in wild-type mice and in a mouse model of Alzheimer’s disease. *FASEB J* 22:2843–2852
51. Ziv Y, Ron N, Butovsky O, Landa G, Sudai E, Greenberg N, Cohen H, Kipnis J, Schwartz M (2006) Immune cells contribute to the maintenance of neurogenesis and spatial learning abilities in adulthood. *Nat Neurosci* 9:268–275
52. Ziv Y, Schwartz M (2008) Immune-based regulation of adult neurogenesis: implications for learning and memory. *Brain Behav Immun* 22:167–176
53. Lin JH, Weigel H, Cotrina ML, Liu S, Bueno E, Hansen AJ, Hansen TW, Goldman S, Nedergaard M (1998) Gap-junction-mediated propagation and amplification of cell injury. *Nat Neurosci* 1:494–500
54. Bezzi P, Volterra A (2001) A neuron-glia signaling network in the active brain. *Curr Opin Neurobiol* 11:387–394
55. Strauss KI (2008) Anti-inflammatory and neuroprotective actions of COX2 inhibitors in the injured brain. *Brain Behav Immun* 22:285–298
56. Botting RM (2006) Inhibitors of cyclooxygenases: mechanisms, selectivity and uses. *J Physiol Pharmacol* 57(5):113–124
57. Yang H, Chen C (2008) Cyclooxygenase-2 in synaptic signaling. *Curr Pharm Des* 14(14):1443–1451
58. Minghetti L (2004) Cyclooxygenase-2 (COX-2) in inflammatory and degenerative brain diseases. *J Neuropathol Exp Neurol* 63:901–910
59. Chandrasekharan NV, Dai H, Roos KLT, Evanson NK, Tomsik J, Elton TS, Simmons DL (2002) COX-3, a cyclooxygenase-1 variant inhibited by acetaminophen and other analgesic/antipyretic drugs:

- cloning, structure, and expression. *Proc Natl Acad Sci USA* 99: 13926–13931
60. Kis B, Snipes JA, Busija DW (2005) Acetaminophen and the cyclooxygenase-3 puzzle: sorting out facts, fictions, and uncertainties. *J Pharmacol Exp Ther* 315(1):1–7
 61. Chacon P, Vega A, Monteseirin J, El Bekay R, Alba G, Perez-Formoso JL, Msartinez A, Asturias JA, Perez-Cano R, Sobrino F, Conde J (2005) Induction of cyclooxygenase-2 expression by allergens in lymphocytes from allergic patients. *Eur J Immunol* 35(8):2313–2324
 62. Linker R, Gold R, Luhder R (2009) Function of neurotrophic factors beyond the nervous system: inflammation and autoimmune demyelination. *Crit Rev Immunol* 29(1):43–68
 63. Pitzer C, Krüger C, Plaas C, Kirsch F, Dittgen T, Müller R, Laage R, Kastner S, Suess S, Spoelgen R, Henriques A, Ehrenreich H, Schäbitz WR, Bach A, Schneider A (2008) Granulocyte-colony stimulating factor improves outcome in a mouse model of amyotrophic lateral sclerosis. *Brain* 131(Pt 12):335–347
 64. Schabitz WR, Kollmar R, Schwaninger M (2003) Neuroprotective effect of granulocyte colony-stimulating factor after focal cerebral ischemia. *Stroke* 34:745–751
 65. Ding J, Yu JZ, Li QY, Wang X, Lu CZ, Xiao BG (2009) Rho kinase inhibitor Fasudil induces neuroprotection and neurogenesis partially through astrocyte-derived G-CSF. *Brain Behav Immun* 23(8):1083–1088
 66. Barrientos RM, Sprunger DB, Campeau S, Higgins EA, Watkins LR, Rudy JW, Maier SF (2003) Brain-derived neurotrophic factor mRNA downregulation produced by social isolation is blocked by intrahippocampal interleukin-1 receptor antagonist. *Neuroscience* 121:847–853
 67. Ben Menachem-Zidon O, Goshen I, Kreisel T, Ben Menahem Y, Reinhartz E, Ben Hur T, Yirmiya R (2008) Intrahippocampal transplantation of transgenic neural precursor cells overexpressing interleukin-1 receptor antagonist blocks chronic isolation-induced impairment in memory and neurogenesis. *Neuropsychopharmacology* 33:2251–2262
 68. Wu CW, Chen YC, Yu L, Chen HI, Jen CJ, Huang AM, Tsai HJ, Chang YT, Kuo YM (2007) Treadmill exercise counteracts the suppressive effects of peripheral lipopolysaccharide on hippocampal neurogenesis and learning and memory. *J Neurochem* 103:2471–2481
 69. Hofer M, Pospisil M, Hola J, Vacek A, Streitova D, Znojil V (2008) Inhibition of cyclooxygenase 2 in mice increases production of G-CSF and induces radioprotection. *Radiat Res* 170:566–571
 70. Hofer M, Pospisil M, Znojil V, Hola J, Vacek A, Streitova D (2008) Meloxicam, an inhibitor of cyclooxygenase-2, increases the level of serum G-CSF and might be usable as an auxiliary means in G-CSF therapy. *Physiol Res* 57:307–310
 71. Van Bel F, Groenendaal F (2008) Long-term pharmacologic neuroprotection after birth asphyxia: where do we stand? *Neonatology* 94:203–210
 72. Solaroglu I, Jadhav V, Zhang JH (2007) Neuroprotective effect of granulocyte-colony stimulating factor. *Front Biosci* 12:712–724
 73. Gorgen I, Hartung T, Leist M, Niehörster M, Tiegs G, Uhlig S, Weitzel F, Wendel A (1992) Granulocyte colony-stimulating factor treatment protects rodents against lipopolysaccharide-induced toxicity via suppression of systemic tumor necrosis factor- α . *J Immunol* 149:918–924
 74. Gibson CL, Jones NC, Prior MJ, Bath PM, Murphy SP (2005) G-CSF suppresses edema formation and reduces interleukin-1 β expression after cerebral ischemia in mice. *J Neuropathol Exp Neurol* 64:763–769
 75. Komine-Kobayashi M, Zhang N, Liu M, Tanaka R, Hara H, Osaka A, Mochizuki H, Mizuno Y, Urabe T (2006) Neuroprotective effect of recombinant human granulocyte colony-stimulating factor in transient focal ischemia of mice. *J Cereb Blood Flow Metab* 26:402–413
 76. Heard SO, Fink MP (1999) Counterregulatory control of the acute inflammatory response: granulocyte colony-stimulating factor has anti-inflammatory properties. *Crit Care Med* 27:1019–1021
 77. Shyu WC, Lin SZ, Yang HI, Tzeng YS, Pang CY, Yen PS (2004) Functional recovery of stroke rats induced by granulocyte colony stimulation factor stimulated stem cells. *Circulation* 110:1847–1854
 78. Schneider A, Krüger C, Steigleder T, Weber D, Pitzer C, Laage R, Aronowski J, Maurer MH, Gassler N, Mier W, Hasselblatt M, Kollmar R, Schwab S, Sommer C, Bach A, Kuhn HG, Schäbitz WR (2005) The hematopoietic factor G-CSF is a neuronal ligand that counteracts programmed cell death and drives neurogenesis. *J Clin Invest* 115:2083–2098
 79. Yata K, Matchett GA, Tsubokawa T, Tang J, Kanamaru K, Zhang JH (2007) Granulocyte-colony stimulating factor inhibits apoptotic neuron loss after neonatal hypoxia-ischemia in rats. *Brain Res* 1145:227–238
 80. Kim BR, Shim JW, Sung DK, Kim SS, Jeon GW, Kim MJ, Chang YS, Park WS, Choi ES (2008) Granulocyte stimulating factor attenuates hypoxic-ischemic brain injury by inhibiting apoptosis in neonatal rats. *Yonsei Med J* 49(5):836–842

Red Blood Cell Lysis and Brain Tissue-Type Transglutaminase Upregulation in a Hippocampal Model of Intracerebral Hemorrhage

Fan Zhao, Shuijiang Song, Wenquan Liu, Richard F. Keep, Guohua Xi, and Ya Hua

Abstract Red blood cell (RBC) lysis and iron release contribute to intracerebral hemorrhage (ICH)-induced brain injury. Tissue-type transglutaminase (tTG), which has a role in neurodegeneration, is upregulated after ICH. The current study investigated the effect of RBC lysis and iron release on brain tTG levels and neuronal death in a rat model of ICH. This study had three parts: (1) Male Sprague-Dawley rats received an intrahippocampal injection of 10 μ L of either packed RBCs or lysed RBCs; (2) rats had a 10 μ L injection of either saline, hemoglobin or FeCl₂; (3) rats received a 10 μ L injection of hemoglobin and were treated with an iron chelator, deferoxamine or vehicle. All rats were killed 24 h later, and the brains were sectioned for tTG and Fluoro-Jade C staining. Lysed but not packed RBCs caused marked tTG upregulation ($p < 0.05$) and neuronal death ($p < 0.05$) in the ipsilateral hippocampus CA-1 region. Both hemoglobin and iron mimicked the effects of lysed RBCs, resulting in tTG

expression and neuronal death ($p < 0.05$). Hemoglobin-induced tTG upregulation and neuronal death were reduced by deferoxamine ($p < 0.05$). These results indicate that RBC lysis and iron toxicity contribute to neurodegeneration after ICH.

Keywords Cerebral hemorrhage · Iron · Tissue-type transglutaminase · Neurodegeneration

Introduction

Intracerebral hemorrhage (ICH) is a subtype of stroke with high morbidity and mortality [1]. Community-based studies have indicated a mortality of more than 40%, and many survivors are left with significant neurological deficits [2, 3]. Previous studies have demonstrated that lysed red blood cells (RBC) but not packed RBCs result in marked brain edema at 24 h in a rat ICH model [4]. Both in vivo and in vitro experiments have demonstrated that hemoglobin and its degradation products, especially iron, contribute to brain injury after ICH [5, 6].

Tissue-type transglutaminase (tTG) is abundantly expressed in the brain, and upregulation of tTG may contribute to the pathology of several neurodegenerative conditions, including Alzheimer's disease, Parkinson's disease, and Huntington's disease [7, 8]. Neurodegeneration also occurs after ICH, and evidence indicates that ICH induces perihematomal tTG upregulation and that cystamine, a tTG inhibitor, can reduce ICH-induced brain swelling and neurological deficits [3]. Fluoro-Jade C staining has been used to detect neuronal degeneration [9], and we have developed the intra-hippocampal injection model in rats [10]. In this study, we investigated the effect of iron on the expression of tTG and neuronal death in the hippocampus.

F. Zhao

Department of Neurosurgery, University of Michigan, Ann Arbor, MI, USA and

Department of Neurosurgery, Huashan Hospital, Fudan University, Shanghai, China

S. Song

Department of Neurosurgery, University of Michigan, Ann Arbor, MI, USA and

Department of Neurology, The Second Affiliated Hospital, Zhejiang University, Hangzhou, China

W. Liu, R.F. Keep, and G. Xi

Department of Neurosurgery, University of Michigan, Ann Arbor, MI, USA

Y. Hua (✉)

Department of Neurosurgery, University of Michigan, Room 5018 BSRB, 109 Zina Pitcher Place, 48109-2200 Ann Arbor, MI, USA
e-mail: yahua@umich.edu

Materials and Methods

Animal Preparation and Intracerebral Infusion

The University of Michigan Committee on the Use and Care of Animals approved the animal protocols. Adult male Sprague-Dawley rats (275–350 g, Charles River Laboratories, Portage, MI) were anesthetized with pentobarbital (45 mg/kg, i.p.). Physiological parameters were recorded immediately before intrahippocampal injections and were in the normal range. Core body temperature was maintained at 37.5°C. Saline, hemoglobin (Hb), FeCl₂, packed RBCs and lysed RBCs were infused into the right hippocampus stereotactically (coordinates: 3.8 mm posterior, 3.2 mm ventral, and 3.5 mm lateral to the bregma).

Experiment Groups

This study has three parts: (1) rats ($n=6$, each group) received an intrahippocampal injection of 10 μ L of either packed RBCs or lysed RBCs; (2) rats ($n=6$ each group) had a 10 μ L injection of saline, bovine Hb (150 mg/mL) or FeCl₂ (1 mM); (3) rats ($n=6$ each group) received a 10 μ L injection of bovine Hb (150 mg/mL) and were treated with either deferoxamine (100 mg/kg, i.p. given immediately after Hb injection and then every 12 h) or vehicle. All rats were killed 24 h later, and the brains were sectioned for immunohistochemistry and Fluoro-Jade C staining.

Immunohistochemistry

Rats were anesthetized with pentobarbital (60 mg/kg; i.p.) and underwent transcardiac perfusion with 4% paraformaldehyde in 0.1 mol/L (pH 7.4) phosphate-buffered saline. Brains were removed and kept in 4% paraformaldehyde for 6 h, then immersed in 30% sucrose for 3 to 4 days at 4°C. Brains were then placed in optimal cutting temperature embedding compound (Sakura Finetek, Inc., Torrance, CA) and 18- μ m sections taken on a cryostat. Sections were examined using the avidin-biotin complex technique. The primary antibody was mouse anti-transglutaminase-2 monoclonal antibody (1:200 dilution, NeoMarkers, Fremont, CA), and the secondary antibody was anti-mouse immunoglobulin G antibody (1:500 dilution, Vector Laboratories, Inc., Burlingame, CA). Normal horse immunoglobulin G (Vector Laboratories, Inc. Burlingame, CA) was used as a negative control. The number of tTG positive cells in the CA1 region was counted.

Fluoro-Jade C Staining

Brain sections were kept in 0.06% potassium permanganate (KMnO₄) for 15 min and rinsed in distilled water. Sections were stained by gently shaking for 30 min in a working solution of Fluoro-Jade C (10 mL 0.01% Fluoro-Jade C in distilled water and 90 mL 0.1% acetic acid), then rinsed in distilled water three times. After drying with a blower, slides were quickly dipped into xylol and covered after mounting with DPX. Fluoro-Jade-positive C cells were counted in the CA1 on the pictures taken by a digital camera at high power ($\times 40$ magnification) [11].

Statistical Analysis

All the data in this study are presented as mean \pm SD. Data were analyzed by Student's *t* test. A level of $P < 0.05$ was considered statistically significant.

Results

After lysed RBC injection, tTG positive cells were mostly expressed in the ipsilateral hippocampus with very few in the contralateral hippocampus. The number of tTG positive cells was significantly higher in the ipsilateral CA-1 area after injection of lysed RBCs compared to packed RBCs (91 ± 22 vs. 29 ± 13 cells/mm, $p < 0.01$, Fig. 1a). Lysed RBCs, but not packed RBCs, also induced more Fluoro-Jade C-positive cells in the ipsilateral CA-1 region (81 ± 28 vs. 15 ± 11 cells/mm, $n=6$, $p < 0.01$; Fig. 1b).

Intrahippocampal injection of Hb and iron mimicked the effects of lysed RBCs on tTG expression and neuronal degeneration. Much higher numbers of tTG positive cells were induced in the ipsilateral hippocampus CA-1 by Hb (125 ± 44 cells/mm) and FeCl₂ (127 ± 35 cells/mm) compared to saline (6 ± 6 cell/mm; $p < 0.01$, Fig. 2a). Also, there were many more Fluoro-Jade-positive cells in the ipsilateral hippocampus after Hb (92 ± 31 cells/mm) and iron injection (110 ± 35 cells/mm) than after saline injection (7 ± 6 cells/mm, $p < 0.01$, Fig. 2b).

Deferoxamine was used to examine the effect of iron in Hb-induced tTG upregulation and neuronal death. Hb-induced neuronal degeneration was abolished by deferoxamine (tTG positive cells: 29 ± 13 vs. 101 ± 45 cell/mm in vehicle-treated group, $p < 0.01$, Fig. 3a; Fluoro-Jade C-positive cells: 48 ± 30 vs. 100 ± 26 cells/mm in vehicle-treated group, $p < 0.05$, Fig. 3b).

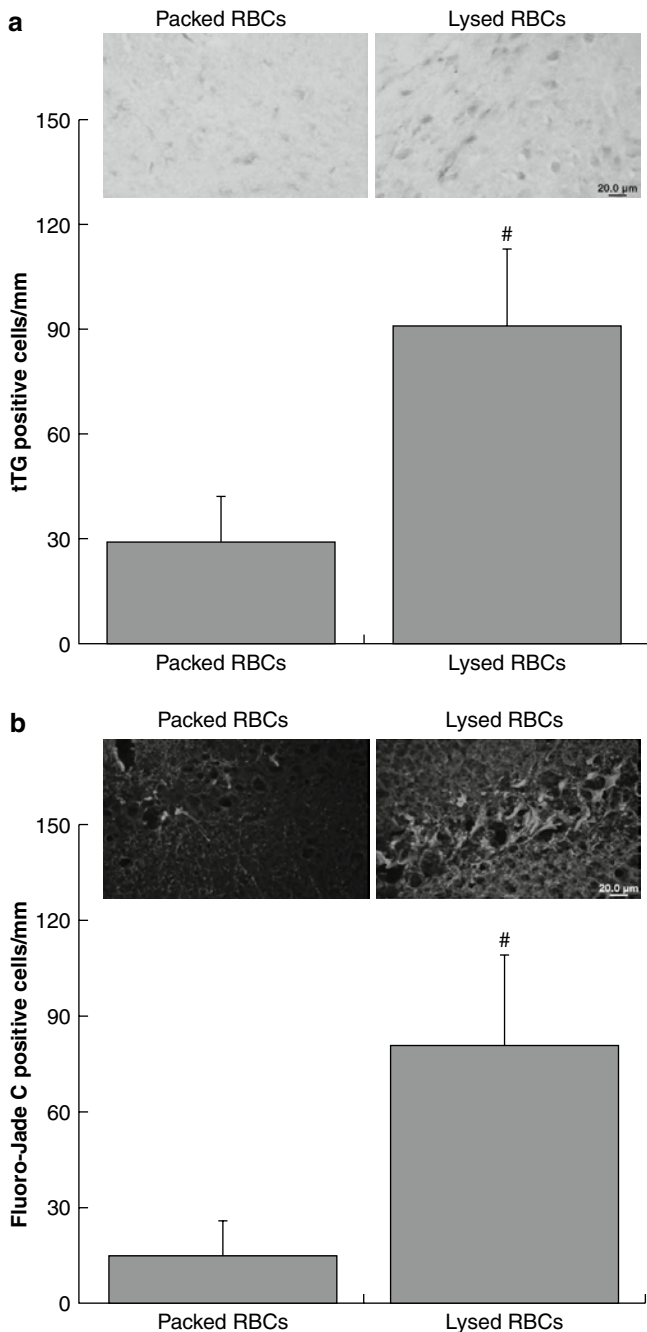


Fig. 1 tTG (a) and Fluoro-Jade C (b) positive cells in the ipsilateral hippocampus CA-1 area 24 h after an injection of 10 μ L lysed RBCs or packed RBCs. Values are expressed as mean \pm SD, $n=6$, # $p<0.01$ vs. packed RBCs

Discussion

In this study we demonstrate: (1) lysis of RBCs induces brain tTG expression and causes neuronal death in the hippocampus; (2) Hb and iron can mimic the effect of lysed RBCs, causing expression of tTG in hippocampus and resulting in

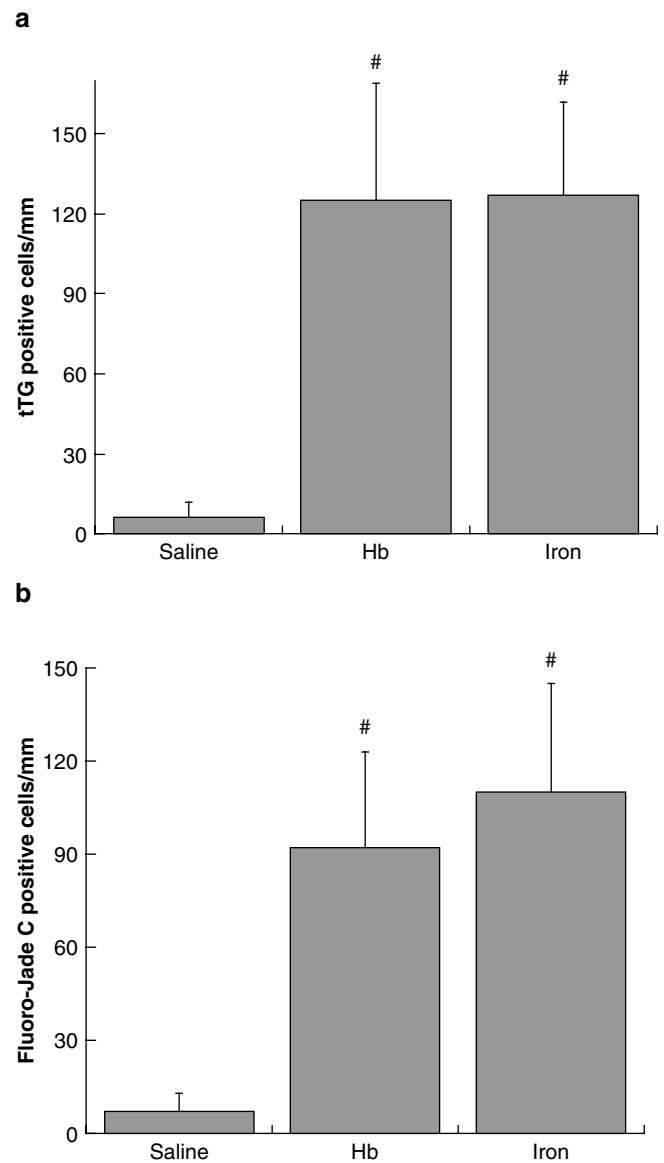


Fig. 2 tTG (a) and Fluoro-Jade C (b) positive cells in the ipsilateral hippocampus CA-1 area 24 h after injection of 10 μ L saline, Hb (150 mg/mL) or FeCl₂ (iron, 1 mM) into the right hippocampus. Values are mean \pm SD, $n=6$, # $p<0.01$ vs. saline

neuronal death; (3) deferoxamine blocks Hb-induced tTG upregulation and neuronal death.

Tissue-type transglutaminase (tTG) has been implicated in various neurodegenerative diseases. tTG has a role in neural development and function [8], but several studies have demonstrated that tTG is present in cells and tissues during apoptotic cell death and is associated with apoptosis [12]. Thus, upregulation of brain tTG has been found in different animal models of CNS diseases, including cerebral ischemia, traumatic brain injury, calcium-induced hippocampal damage and spinal cord injury [13–16]. Our recent study

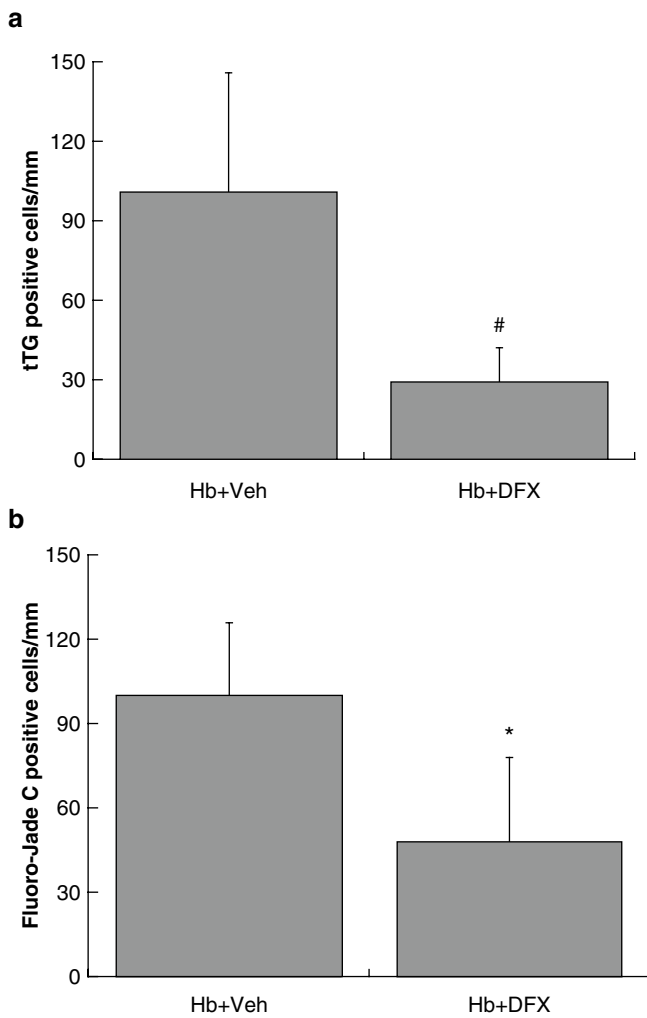


Fig. 3 tTG (a) and Fluoro-Jade C (b) positive cells in the ipsilateral hippocampus CA-1 area 24 h after an injection of 10 μ L hemoglobin (150 mg/mL) in rats treated with either deferoxamine (100 mg/kg) or vehicle. Values are mean \pm SD, n=6, # p <0.01, * p <0.05 vs. vehicle-treated group

showed that brain tTG levels are increased in the perihematomal area after ICH, and cystamine, a tTG inhibitor, reduces ICH-induced brain edema and neurological deficits [3]. Release of Hb from RBCs and Hb breakdown products cause brain damage after ICH. Iron overload occurs in the brain after ICH, and intracerebral infusion of iron causes brain damage, such as brain edema and oxidative brain injury [17]. The results from our current study suggest that iron can upregulate brain tTG and that such upregulation may contribute to iron-induced brain damage.

To clarify the role of iron in Hb-induced tTG upregulation, an iron chelator, deferoxamine, was used. We found that deferoxamine attenuates Hb-induced upregulation of brain tTG, suggesting that the effects of Hb on tTG are, at least partially, mediated by iron. The mechanisms by which Hb

and iron upregulate tTG still need to be fully elucidated. However, it is known that oxidative stress can upregulate tTG in neuronal and astrocyte cultures [18, 19]. This effect may be via both transcriptional regulation [18, 19] and inhibition of proteasomal degradation [20]. In conclusion, iron can increase brain tTG levels and cause brain injury.

Acknowledgements This study was supported by grants NS-017760, NS-039866 and NS-057539 from the National Institutes of Health (NIH) and 0755717Z and 0840016 N from the American Heart Association (AHA). The content is solely the responsibility of the authors and does not necessarily represent the official views of the NIH and AHA.

Conflict of interest statement We declare that we have no conflict of interest.

References

1. Qureshi AI, Tuhim S, Broderick JP, Batjer HH, Hondo H, Hanley DF (2001) Spontaneous intracerebral hemorrhage. *N Engl J Med* 344: 1450–1460
2. Mendelow AD, Gregson BA, Fernandes HM, Murray GD, Teasdale GM, Hope DT, Karimi A, Shaw MD, Barer DH (2005) Early surgery versus initial conservative treatment in patients with spontaneous supratentorial intracerebral haematomas in the International Surgical Trial in Intracerebral Haemorrhage (STICH): a randomised trial. *Lancet* 365:387–397
3. Okauchi M, Xi G, Keep RF, Hua Y (2009) Tissue-type transglutaminase and the effects of cystamine on intracerebral hemorrhage-induced brain edema and neurological deficits. *Brain Res* 1249: 229–236
4. Xi G, Keep RF, Hoff JT (1998) Erythrocytes and delayed brain edema formation following intracerebral hemorrhage in rats. *J Neurosurg* 89:991–996
5. Hua Y, Nakamura T, Keep RF, Wu J, Schallert T, Hoff JT, Xi G (2006) Long-term effects of experimental intracerebral hemorrhage: the role of iron. *J Neurosurg* 104:305–312
6. Wagner KR, Sharp FR, Ardizzone TD, Lu A, Clark JF (2003) Heme and iron metabolism: role in cerebral hemorrhage. *J Cereb Blood Flow Metab* 23:629–652
7. Citron BA, Suo Z, SantaCruz K, Davies PJ, Qin F, Festoff BW (2002) Protein crosslinking, tissue transglutaminase, alternative splicing and neurodegeneration. *Neurochem Int* 40:69–78
8. Lesort M, Tucholski J, Miller ML, Johnson GV (2000) Tissue transglutaminase: a possible role in neurodegenerative diseases. *Prog Neurobiol* 61:439–463
9. Gu Y, Hua Y, Keep RF, Morgenstern LB, Xi G (2009) Deferoxamine reduces intracerebral hematoma-induced iron accumulation and neuronal death in piglets. *Stroke* 40:2241–2243
10. Song S, Hua Y, Keep RF, Hoff JT, Xi G (2007) A new hippocampal model for examining intracerebral hemorrhage-related neuronal death: effects of deferoxamine on hemoglobin-induced neuronal death. *Stroke* 38:2861–2863
11. Schmued LC, Albertson C, Slikker W Jr (1997) Fluoro-Jade: a novel fluorochrome for the sensitive and reliable histochemical localization of neuronal degeneration. *Brain Res* 751:37–46
12. Fesus L (1998) Transglutaminase-catalyzed protein cross-linking in the molecular program of apoptosis and its relationship to neuronal processes. *Cell Mol Neurobiol* 18:683–694

13. Festoff BW, SantaCruz K, Arnold PM, Sebastian CT, Davies PJ, Citron BA (2002) Injury-induced "switch" from GTP-regulated to novel GTP-independent isoform of tissue transglutaminase in the rat spinal cord. *J Neurochem* 81:708–718
14. Tolentino PJ, DeFord SM, Notterpek L, Glenn CC, Pike BR, Wang KK, Hayes RL (2002) Up-regulation of tissue-type transglutaminase after traumatic brain injury. *J Neurochem* 80:579–588
15. Tolentino PJ, Waghay A, Wang KK, Hayes RL (2004) Increased expression of tissue-type transglutaminase following middle cerebral artery occlusion in rats. *J Neurochem* 89:1301–1307
16. Tucholski J, Roth KA, Johnson GV (2006) Tissue transglutaminase overexpression in the brain potentiates calcium-induced hippocampal damage. *J Neurochem* 97:582–594
17. Xi G, Keep RF, Hoff JT (2006) Mechanisms of brain injury after intracerebral haemorrhage. *Lancet Neurol* 5:53–63
18. Campisi A, Caccamo D, Li Volti G, Curro M, Parisi G, Avola R, Vanella A, Ientile R (2004) Glutamate-evoked redox state alteration are involved in tissue transglutaminase upregulation in primary astrocyte cultures. *FEBS Lett* 578:80–84
19. Curro M, Condello S, Caccamo D, Ferlazzo N, Parisi G, Ientile R (2009) Homocysteine-induced toxicity increases TG2 expression in neuron2a cells. *Amino Acids* 36:725–730
20. Luciani A, Vilella VR, Vasaturo A, Giardino I, Raia V, Pettoello-Mantovani M, D'Apolito M, Guido S, Leal T, Quarantino S, Maiuri L (2009) SUMOylation of tissue transglutaminase as link between oxidative stress and inflammation. *J Immunol* 183: 2775–2784

Cytoprotective Role of Haptoglobin in Brain After Experimental Intracerebral Hemorrhage

Xiurong Zhao, Shen Song, Guanghua Sun, Jie Zhang, Roger Strong, Lihua Zhang, James C. Grotta, and Jaroslaw Aronowski

Abstract After intracerebral hemorrhage (ICH), hemoglobin (Hb) that is released from erythrocytes within the brain hematoma is highly cytotoxic and leads to severe brain edema and direct neuronal damage. Therefore, neutralization of Hb could represent an important target for reducing the secondary injury after ICH. Haptoglobin (Hp), an endogenous Hb-binding protein in blood plasma, is found in this study to be upregulated in the hematoma-affected brain after ICH. Both in vivo and in vitro studies indicate that Hp upregulation is primarily mediated by oligodendrocytes. Hp acts as a secretory protein capable of neutralizing the cell-free Hb. We also found in an “ICH-like” injury that Hp-KO mice show the most severe brain injury and neurological deficits, whereas Hp-Tg mice are the most resistant to ICH injury, suggesting that a higher Hp level is associated with the increased resistance of animals to hemolytic product-mediated brain injury after ICH. We conclude that brain-derived Hp plays a cytoprotective role after ICH, and Hp may represent a new potential therapeutic target for management of ICH.

Keywords Haptoglobin · Hemoglobin · Oligodendrocyte · Intracerebral hemorrhage · Hematoma and neuroprotection

X. Zhao, S. Song, G. Sun, J. Zhang, R. Strong, L. Zhang, J.C. Grotta, and J. Aronowski (✉)
Stroke Program – Department of Neurology, University of Texas Health Science Center, Medical School at Houston, Houston, TX 77030, USA
e-mail: j.aronowski@uth.tmc.edu

Introduction

Haptoglobin (Hp) is an endogenous hemoglobin (Hb)-binding protein present in blood plasma. In blood, Hp binds cell-free Hb (derived from damaged or senescent erythrocytes) to form highly stable Hb-Hp complexes [1]. This process is capable of shielding and stabilizing the heme iron within the Hb hydrophobic pocket and thereby blocking the pro-oxidative property of Hb [2, 3]. Normally, Hp is produced by hepatocytes and then released to the blood [4, 5] where it binds the cell-free Hb and mediates the fast removal of Hb from circulation [6, 7]. The clearance of the Hp-Hb complexes occurs via circulating blood monocytes and tissue macrophages that express the Hb scavenger receptor CD163 [8–10]. In addition, the uptake of Hp-Hb complexes by hepatocytes plays an important role in iron recycling. Hp indirectly exerts a broad range of anti-inflammatory activities and plays an anti-oxidant role most notably by virtue of its ability to bind free Hb, accelerating the rapid clearance of Hb by monocytes and macrophages.

The Hp reservoir in blood plasma is relatively high, allowing for efficient buffering of the Hb in case of acute hemolytic events. Although the role of Hp in intravascular hemolysis is well accepted, the role of Hp in the brain is essentially unknown [11]. Limited studies suggest the presence of Hp in the neural retina [12] and subarachnoid blood clot [13]; however, its expression profile and role in the brain is not clear.

Following ICH, a large amount of Hb is released into the brain parenchyma after erythrocytes undergo hemolysis within the hematoma [14, 15]. The cell-free Hb is a potent neurotoxin capable of initiating deleterious reactions by causing oxidative damage to lipids, DNA and proteins [16, 17]; caspase activation [18, 19]; blood-brain-barrier (BBB) disruption [14, 15, 20]; and irreversible neuronal damage [21–23]. We postulate that Hp may benefit the brain

after ICH assuming Hp can either penetrate to the brain through the disrupted BBB or being locally produced by the brain cells. Here, we review our finding [24] regarding the expression, localization and biological function of Hp in the brain after ICH.

Results

Hp Is Increased in the Brain After ICH: The Role of Oligodendrocytes

To explore the role of Hp in the brain after ICH, we first tested the expression of Hp protein in the brain using Western blot analysis. In naïve Sprague-Dawley (SD) rats, Hp expression in the brain is very low. However, Hp protein in the brain increases robustly after ICH, which is seen in as soon as 3 h and subsequently increases over time in the first 3 days and remains at higher levels for at least 7 days in the hematoma-affected brain tissues [24]. To verify the origin of brain Hp protein, we measured the Hp mRNA changes in the brain tissue using RT-PCR. We found that Hp mRNA levels share a similar temporal pattern with Hp protein changes, suggesting that Hp is produced locally in the brain. However, we cannot rule out that additional Hp protein may enter the brain through a disrupted BBB.

Next, we studied the spatial distribution of Hp in the brain using immunofluorescence [24]. We found that the Hp signal is strong in the hematoma-affected cortex, corpus callosum and striatum (Fig. 1A, a–c). Using double immunolabeling to identify the specific cell types that express Hp, we found that Hp is primarily co-localized within the MBP-positive oligodendrocytes [24]. Specifically, Hp immunopositive signals localize in the oligodendrocytes' soma within the grey matter, as well in the fine processes around the myelinated nerve tract in the white matter at the corpus callosum and striatum.

To further validate the *in vivo* findings, we studied Hp expression using a primary neuron-glial co-culture system generated from E-18 rat embryos. We found that Hp protein and mRNA are uniquely expressed by MBP-positive oligodendrocytes (Fig. 1B, d–f). Interestingly, the Hp immunopositive signal is detected throughout the soma and fine processes, which is similar to the Hp localizations detected in the rat brains [24].

Using Hp ELISA, we found that Hp is a secretory protein as it can be released by oligodendrocytes into the culture media [24].

Hp Produced by Oligodendrocytes Is Protective to Neurons and Oligodendrocytes

To establish if the Hp produced and secreted by oligodendrocytes is biologically functional, we employed oligodendrocytes cultured from Hp-KO [25] and Hp-Tg [26] mice brains. As expected, at 20 days in culture, Hp-KO oligodendrocytes have practically no Hp presence in the culture media, whereas Hp-Tg oligodendrocytes release high levels of Hp into the culture media (Fig. 2a, b). We then collected the oligodendrocyte-conditioned media and transferred it to the neuron cultures. Compatibility of the media transfer was also confirmed. Next, we measured the injury to the neurons caused by hemolytic products by subjecting the neurons to an “ICH-like” injury (lysed RBC + hypoxia) and assessing the LDH released into the culture media by the injured neurons. At 24 h after adding lysed RBCs, the neurons in the medium from Hp-overexpressing oligodendrocytes demonstrated significantly less injury as compared to the neurons in the medium from Hp-deficient oligodendrocytes (Fig. 2c, d). This suggests that Hp produced by oligodendrocytes can neutralize the hemolytic product-mediated neurotoxicity. In parallel studies, we found that the Hp-Tg oligodendrocytes, similar to neurons, are much more resistant than the Hp-KO oligodendrocytes to the RBC lysate-mediated damage, suggesting that Hp is cytoprotective not only to neurons, but also to oligodendrocytes, the cells that produce Hp [24].

The Levels of Hp Expression Are Associated with Resistance to ICH-Mediated Brain Damage

To further define the relationship between Hp and ICH, we subjected the Hp-KO, Hp-Tg and WT control mice to a modified ICH injury (*M-ICH*). In this *M-ICH* injury model, we injected lysed RBCs (not whole blood) into the basal ganglia to better mimic the events associated with blood toxicity following hemolysis in the hematoma. At 7 days after *M-ICH*, we assessed brain damage by determining the neurological deficits (NDS; a composite score from a battery of behavioral tests, including foot fault, cylinder, postural reflex and corner tests) [27]. As predicted, Hp-KO mice suffer the most severe neurological deficits, whereas Hp-Tg mice are the least susceptible to *M-ICH* injury (Fig. 3), demonstrating that Hp in the brain is in fact important in protecting the animals from hemolytic product-mediated brain damage after ICH.

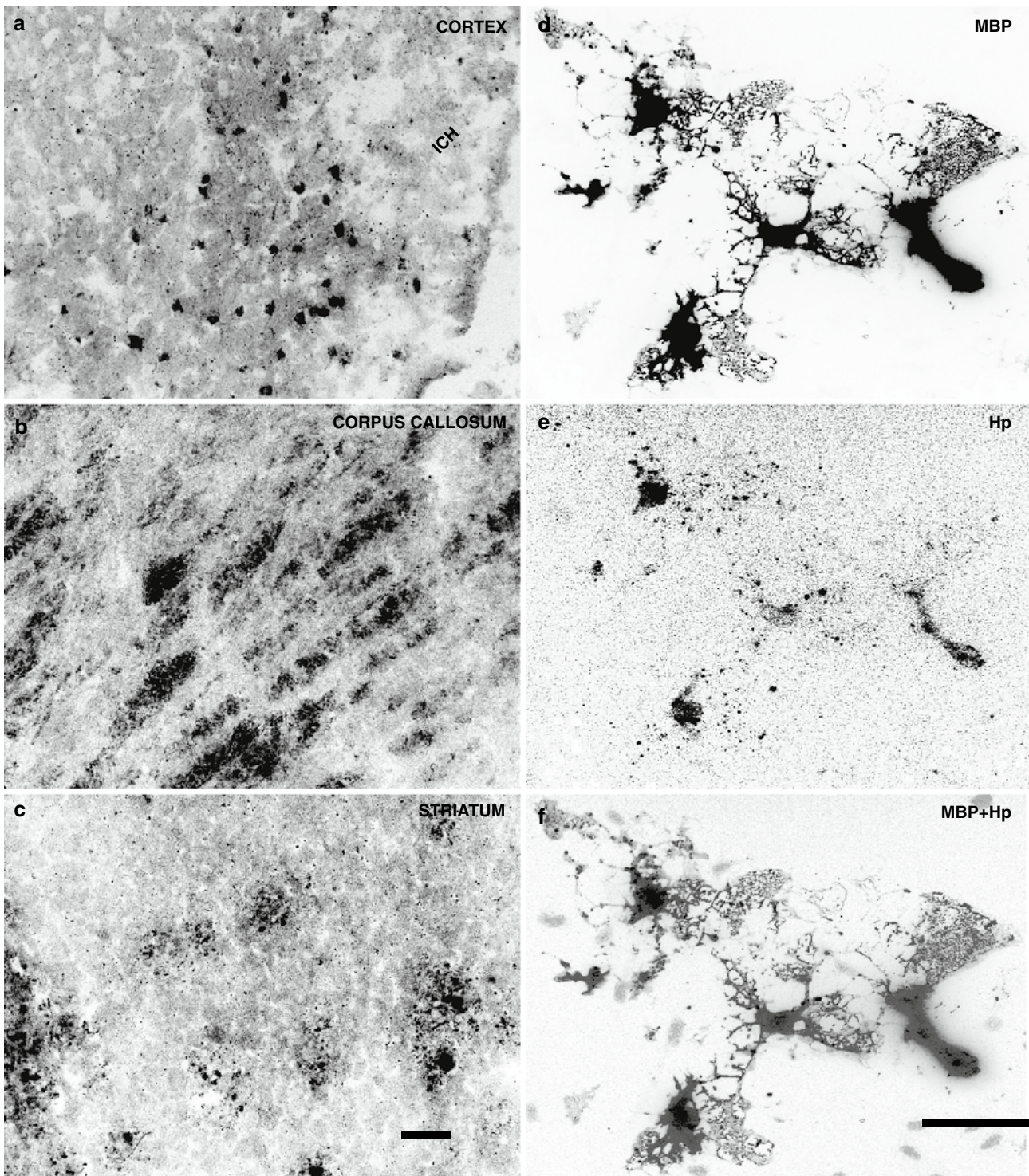


Fig. 1 (A) The representative Hp immunofluorescence to show Hp localization in the ICH-affected brain. The SD rats were subjected to M-ICH and analyzed for presence of Hp at 24 h using immunofluorescence (now converted to black and white and inverted). Hp immunopositive cells were detected in cerebral cortex (a), corpus callosum (b) and basal ganglia (c) adjacent to the hematoma. Scale bar=50 μ m. ICH: location of ICH. (B) Photograph of Hp localization in the rat primary

neuron-glia co-cultures. The oligodendrocytes are visualized with anti-myelin basic protein antibody (MBP, d). The rat Hp is visualized with sheep anti-Hp (e). A merged image of Hp and MBP is shown in (f). The scale bar=100 μ m. *Note:* Among all of the brain cell types in the field, only MBP-positive cells are immunopositive for Hp. Hp proteins localize in the soma and the fine processing of MBP-positive oligodendrocytes

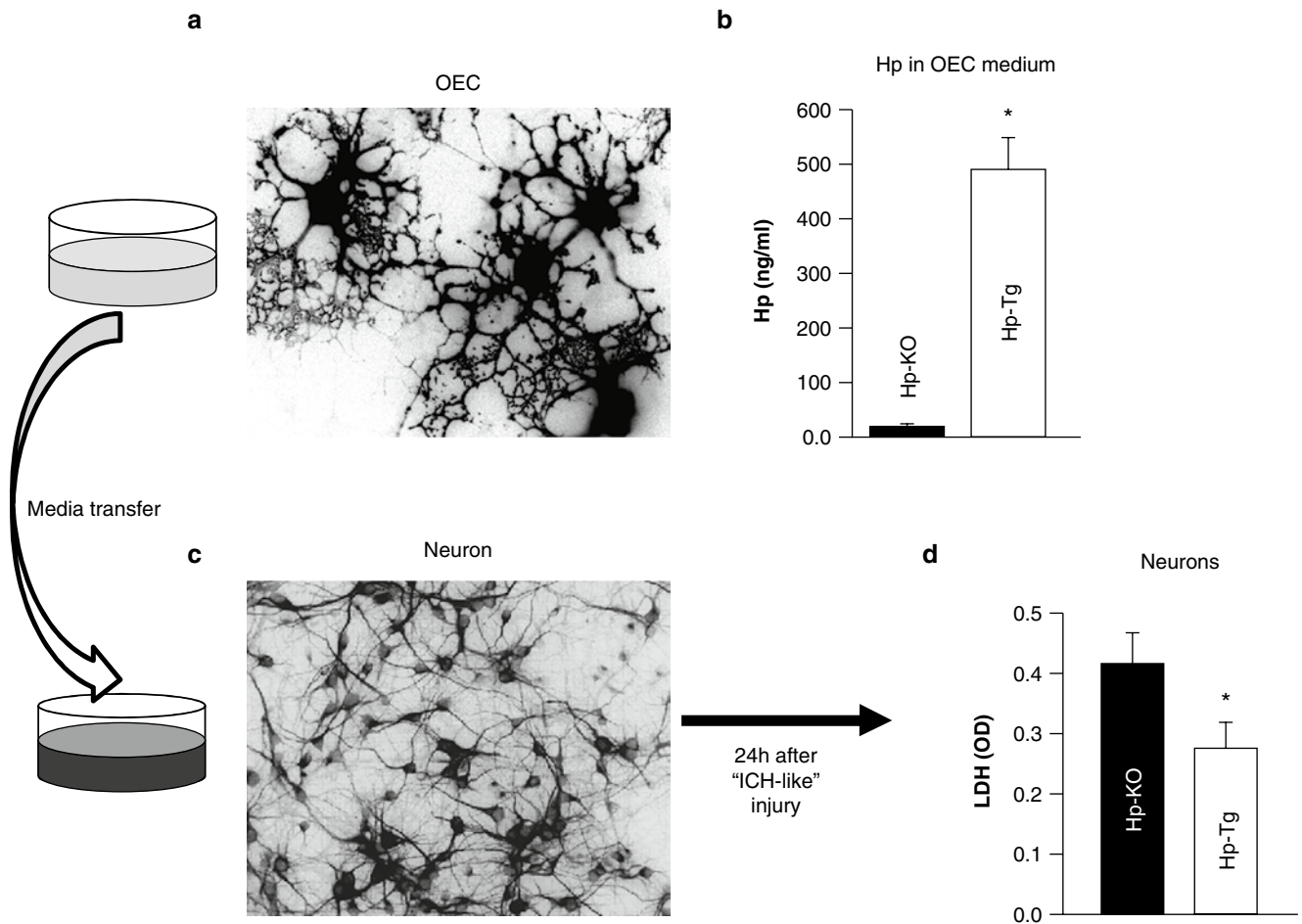


Fig. 2 Hp produced by oligodendrocytes is cytoprotective. **(a)** A representative photograph of oligodendrocytes-enriched culture (*OEC*) prepared from mouse brain at 20 days in vitro. The oligodendrocytes are visualized with MBP immunofluorescence. **(b)** Bar graph of quantifying Hp protein in the *OEC* culture media prepared from Hp-KO and Hp-Tg mice, as determined using Hp ELISA. * $p \leq 0.05$. **(c)** A representative photograph of mouse primary cortical neuron cultured for 15 days. The neurons are visualized with MAP2 immunofluorescence.

(d) Bar graph of LDH showing the injury to neurons in culture in response to “ICH-like” injury (lysed RBC+hypoxia) in presence of media conditioned by *OEC* from Hp-KO or Hp-Tg mice. The *OEC* conditioned media was directly transferred into the neuronal culture by replacing 2/3 volume of the neuronal culture medium and incubated for 15 min before “ICH-like” injury. The LDH in culture media was determined at 24 h. The data are displayed as mean \pm SEM ($n=3$). * $p \leq 0.05$

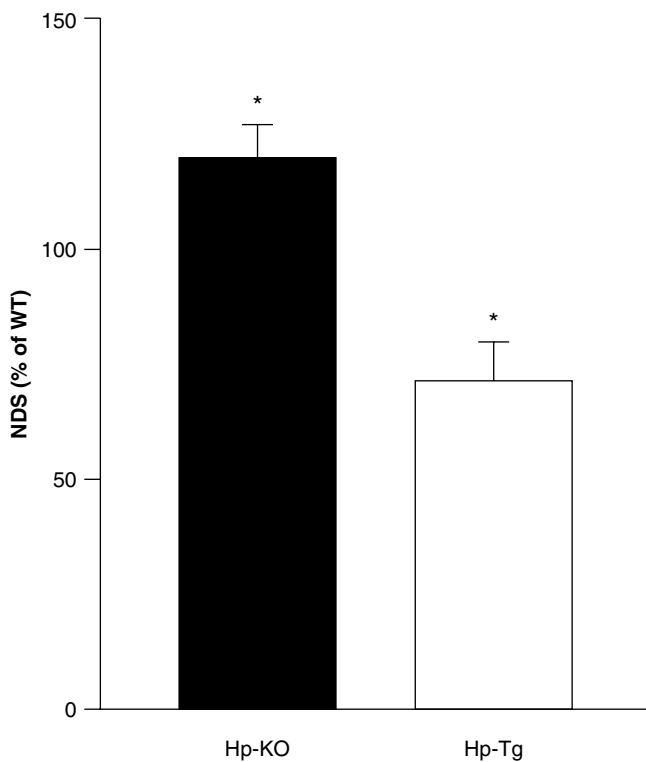


Fig. 3 Neurological deficit score (NDS) after M-ICH. The Hp-KO, Hp-Tg and WT control mice were subjected to M-ICH, and the neurological deficit was measured at day 7 by a battery of behavioral tests. The data are expressed as mean \pm SEM ($n=9$) and displayed as percent changes of the NDS in WT mice. * $p \leq 0.05$, from all other groups

Conclusion

Hp expression after ICH is increased in the brain, where it is primarily confined to oligodendrocytes, and can be secreted into the extracellular space to play a cytoprotective role against the toxicity of hemolysis products. The temporal and spatial profile of Hp synthesis in the brain appears to be highly strategic for optimal control of hemolysis-mediated cytotoxicity [28, 29]. We propose that Hp could be a potential therapeutic target for ICH.

Acknowledgements This study was supported in part by NIH/NINDS projects RO1NS060768, R21NS057284 and RO1NS064109. We thank Drs. Franklin G. Berger and Karen Barbour (University of South Carolina, Columbia, SC), who kindly provided us the Hp-Tg and Hp-KO mice.

Conflict of interest statement We declare that we have no conflict of interest.

References

- Wada T et al (1970) Autoradiographic study on the site of uptake of the haptoglobin-hemoglobin complex. *J Reticuloendothel Soc* 8(2):185–193
- Zuwala-Jagiello J (2006) Haemoglobin scavenger receptor: function in relation to disease. *Acta Biochim Pol* 53(2):257–268
- Yang F et al (2003) Haptoglobin reduces lung injury associated with exposure to blood. *Am J Physiol Lung Cell Mol Physiol* 284(2):L402–L409
- Hoj L et al (1984) Secretion rates of immunoglobulins, albumin, haptoglobin and complement factors C3 and C4 in the perfused jejunum and ileum of human Salmonella carriers. *Acta Pathol Microbiol Immunol Scand C* 92(2):129–132
- Bowman BH, Kurosky A (1982) Haptoglobin: the evolutionary product of duplication, unequal crossing over, and point mutation. *Adv Hum Genet* 12:189, 453–454
- Schaer DJ et al (2006) CD163 is the macrophage scavenger receptor for native and chemically modified hemoglobins in the absence of haptoglobin. *Blood* 107(1):373–380
- Philippidis P et al (2004) Hemoglobin scavenger receptor CD163 mediates interleukin-10 release and heme oxygenase-1 synthesis: antiinflammatory monocyte-macrophage responses in vitro, in resolving skin blisters in vivo, and after cardiopulmonary bypass surgery. *Circ Res* 94(1):119–126
- Ascenzi P et al (2005) Hemoglobin and heme scavenging. *IUBMB Life* 57(11):749–759
- Schaer DJ et al (2005) Soluble hemoglobin-haptoglobin scavenger receptor CD163 as a lineage-specific marker in the reactive hemophagocytic syndrome. *Eur J Haematol* 74(1):6–10
- Schaer DJ, Alayash AI, Buehler PW (2007) Gating the radical hemoglobin to macrophages: the anti-inflammatory role of CD163, a scavenger receptor. *Antioxid Redox Signal* 9(7):991–999
- D'Armiento J, Dalal SS, Chada K (1997) Tissue, temporal and inducible expression pattern of haptoglobin in mice. *Gene* 195(1):19–27
- Chen W et al (1998) Expression of the protective proteins hemopexin and haptoglobin by cells of the neural retina. *Exp Eye Res* 67(1): 83–93
- Borsody M et al (2006) Haptoglobin and the development of cerebral artery vasospasm after subarachnoid hemorrhage. *Neurology* 66(5):634–640
- Bhasin RR et al (2002) Experimental intracerebral hemorrhage: effect of lysed erythrocytes on brain edema and blood-brain barrier permeability. *Acta Neurochir Suppl* 81:249–251
- Xi G, Keep RF, Hoff JT (1998) Erythrocytes and delayed brain edema formation following intracerebral hemorrhage in rats. *J Neurosurg* 89(6):991–996
- Nakamura T et al (2006) Iron-induced oxidative brain injury after experimental intracerebral hemorrhage. *Acta Neurochir Suppl* 96:194–198
- Nakamura T et al (2005) Oxidative DNA injury after experimental intracerebral hemorrhage. *Brain Res* 1039(1–2):30–36
- Regan RF, Panter SS (1993) Neurotoxicity of hemoglobin in cortical cell culture. *Neurosci Lett* 153(2):219–222
- Wang X et al (2002) Hemoglobin-induced cytotoxicity in rat cerebral cortical neurons: caspase activation and oxidative stress. *Stroke* 33(7):1882–1888
- Keep RF et al (2008) Blood-brain barrier function in intracerebral hemorrhage. *Acta Neurochir Suppl* 105:73–77

21. Aronowski J, Hall CE (2005) New horizons for primary intracerebral hemorrhage treatment: experience from preclinical studies. *Neurol Res* 27(3):268–279
22. Xi G, Keep RF, Hoff JT (2006) Mechanisms of brain injury after intracerebral haemorrhage. *Lancet Neurol* 5(1):53–63
23. Koeppen AH, Dickson AC, McEvoy JA (1995) The cellular reactions to experimental intracerebral hemorrhage. *J Neurol Sci* 134(Suppl):102–112
24. Zhao X et al (2009) Neuroprotective role of haptoglobin after intracerebral hemorrhage. *J Neurosci* 29(50):15819–15827
25. Lim SK et al (1998) Increased susceptibility in Hp knockout mice during acute hemolysis. *Blood* 92(6):1870–1877
26. Yang F et al (1993) Characterization of the mouse haptoglobin gene. *Genomics* 18(2):374–380
27. Zhao X et al (2007) Transcription factor Nrf2 protects the brain from damage produced by intracerebral hemorrhage. *Stroke* 38(12):3280–3286
28. Wagner KR, Dwyer BE (2004) Hematoma removal, heme, and heme oxygenase following hemorrhagic stroke. *Ann NY Acad Sci* 1012:237–251
29. Wagner KR et al (2003) Heme and iron metabolism: role in cerebral hemorrhage. *J Cereb Blood Flow Metab* 23(6):629–652

Effects of Aging on Autophagy After Experimental Intracerebral Hemorrhage

Ye Gong, Yangdong He, Yuxiang Gu, Richard F. Keep, Guohua Xi, and Ya Hua

Abstract Intracerebral hemorrhage (ICH) causes severe brain injury in aged rats. Autophagy occurs in the brain after ICH, and the present study examined the effects of aging on autophagy after ICH. Aged (18–22-month) and young (4–6-month) male Fischer rats received an intracerebral injection of 100- μ L autologous whole blood. Rats were killed at day 7 for Western blot analysis to measure microtubule-associated protein light chain-3 (LC3), a biomarker of autophagosome, and cathepsin D, a lysosomal biomarker. Rats were killed at 11 weeks after ICH for brain histology. Age-related changes in neurological deficits were also examined. Western blotting showed that the LC3-I/LC3-II conversion ratio in the ipsilateral basal ganglia was higher in aged compared to young rats ($p < 0.05$). Perihematomal cathepsin D levels were also higher in aged rats ($p < 0.05$). Neurological deficits after ICH were more severe in aged rats, and they had a slower recovery of function ($p < 0.05$). In addition, there were more ferritin and OX-42 positive cells in the ipsilateral basal ganglia in aged than in young rats 11 weeks after ICH ($p < 0.05$). Brain atrophy was found in both young and aged rats. In conclusion, ICH causes more severe autophagy and neurological deficits in aged rats.

Keywords Aging · Autophagy · Cerebral hemorrhage · Ferritin

Y. Gong and Y. Gu
Department of Neurosurgery, University of Michigan,
Ann Arbor, MI, USA and
Department of Neurosurgery, Huashan Hospital, Fudan University,
Shanghai, China

Y. He, R.F. Keep, and G. Xi
Department of Neurosurgery, University of Michigan,
Ann Arbor, MI, USA

Y. Hua (✉)
Department of Neurosurgery, University of Michigan, Room 5018
BSRB, Ann Arbor, MI 48109-0532, USA
e-mail: yahua@umich.edu

Introduction

Age is an important factor affecting brain injury after ischemic and hemorrhagic stroke. Intracerebral hemorrhage (ICH) causes more severe brain swelling and neurological deficits in aged than in young rats [1], but the mechanisms underlying the enhanced injury have not been well studied.

Autophagy plays an important role in cellular homeostasis, and is involved in ICH and cerebral ischemia. Iron has an important role in autophagic cell death after ICH [2]. Light chain 3 (LC3) is a marker of autophagosomes. LC3 has two forms: type I is cytosolic and type II is membrane-bound. During autophagy, LC3-II is increased by conversion from LC3-I [3]. Cathepsin D is an enzyme in lysosomes that is associated with autophagy [4].

Ferritin, a naturally occurring iron chelator, is involved in maintaining brain iron homeostasis. Ferritin levels are upregulated in the brain after ICH [5, 6], and they may limit iron-induced brain injury. Microglia are cells within the brain that respond to injury such as cerebral ischemia and ICH [7, 8].

The present study examined the effect of aging on autophagic cell death after ICH. Neurological deficit and brain ferritin levels were also examined.

Materials and Methods

Animal Preparation and Intracerebral Infusion

Animal use protocols were approved by the University of Michigan Committee on the Use and Care of Animals. Male Fischer rats at different ages (4–6 and 18–22 months old, Geriatrics Center, University of Michigan or NIH) were used in this study. The animals were anesthetized with pentobarbital (45 mg/kg i.p.). The right femoral artery was catheterized for continuous blood pressure monitoring and blood

sampling. Blood was obtained from the catheter for analysis of blood pH, PaO₂, PaCO₂, hematocrit, and blood glucose. Core temperature was maintained at 37°C with use of a feedback-controlled heating pad. The rats were positioned in a stereotaxic frame (Kopf Instrument), and a cranial burr hole (1 mm) was drilled on the right coronal suture 3.5 mm lateral to the midline. Autologous whole blood (100 µL) was infused into the right caudate nucleus at a rate of 10 µL/min through a 26-gauge needle (coordinates: 0.2 mm anterior, 5.5 mm ventral and 3.5 mm lateral to the bregma) with the use of a microinfusion pump. The needle was removed, the burr hole was filled with bone wax, and the skin incision was closed with sutures after infusion. Animals were killed at 1 or 11 weeks after ICH and the brains used for immunohistochemistry or Western blot analysis.

Immunohistochemistry

Rats were anesthetized with pentobarbital (60 mg/kg, i.p.) and perfused with 4% paraformaldehyde in 0.1 M pH 7.4 phosphate-buffered saline. Brains were removed, kept in 4% paraformaldehyde for 4–6 h, then immersed in 25% sucrose for 3–4 days at 4°C. The brains were embedded in OCT compound (Sakura Finetek USA Inc.) and sectioned on a cryostat (18 µm thick). Immunohistochemistry was performed using the avidin-biotin complex technique as previously described [9]. The primary antibodies were rabbit anti-human ferritin IgG (1:400 dilution; DAKO) and mouse anti-rat CD11b (MRC OX42; 1:200 dilution; Serotec, Oxford, UK). Normal rabbit or mouse IgG was used for negative controls.

Cell Counts

Coronal sections from 1 mm anterior and 1 mm posterior to the blood injection site were used for cell counts. Three high-power images (×40 magnification) were taken in the basal ganglia using a digital camera. Ferritin and OX-42 positive cells were counted.

Western Blot Analysis

Western blot analysis was performed as previously described [9]. Briefly, brain samples were sonicated with Western blot lysis buffer. The protein concentration was determined using a Bio-Rad Laboratories (Hercules, CA) protein assay kit. Fifty micrograms of protein from each sample was separated

by sodium dodecyl sulfate-polyacrylamide gel electrophoresis and transferred to a hybond-C pure nitrocellulose membrane (Amersham, Piscataway, NJ). Membranes were blocked in Carnation nonfat milk and probed with primary and secondary antibodies. The primary antibodies were mouse anti-cathepsin D antibody (Sigma, St Louis, MO; 1:1,000 dilution) and rabbit anti-MAP-LC3 antibody (Abgent Inc., San Diego, CA; 1:400 dilution). The secondary antibodies were goat anti-mouse and goat anti-rabbit IgG (BioRad; 1:2,500 dilution). Relative densities of bands were analyzed with NIH Image program (version 1.61).

Behavioral Tests

For the behavioral tests, all animals were tested before and after surgery, and scored by experimenters who were blind to both neurological and treatment conditions. Three behavioral tests were used: forelimb placing, forelimb use asymmetry (cylinder) and corner turn tests [10]. (A) *Forelimb Placing Test*. Forelimb placing was scored using a vibrissae-elicited forelimb-placing test. Independent testing of each forelimb was induced by brushing the vibrissae ipsilateral to that forelimb on the edge of a tabletop once per trial for ten trials. Intact animals placed the forelimb quickly onto the countertop. Percent successful placing responses were determined. There is a reduction in successful responses in the forelimb contralateral to the site of the injection after ICH [10]. (B) *Forelimb Limb-Use Asymmetry Test*. Forelimb use during explorative activity was analyzed by videotaping rats in a transparent cylinder for 3–10 min depending on the degree of activity during the trial. Behavior was quantified by determining the occasions when the non-impaired (ipsilateral) forelimb was used as a percentage of total number of limb use observations on the wall (I). The occasions when the impaired forelimb (contralateral to the blood-injection site) was used as a percentage of total number of limb use observations on the wall (C), and the occasions when “both” forelimbs were used simultaneously as a percentage of total number of limb use observations on the wall (B). A single overall limb use asymmetry score was calculated as: $\text{Limb use asymmetry score} = (I/(I+C+B)) - (C/(I+C+B))$. (C) *Corner Turn Test*. The rat was allowed to proceed into a corner, the angle of which was 30°. To the exit the corner, the rat could turn either to the left or the right, and this was recorded. This was repeated 10–15 times, with at least 30 s between trials, and the percentage of right turns calculated. Only turns involving full rearing along either wall were included. The rats were not picked up immediately following each turn so that they did not develop an aversion for their prepotent turning response.

Statistical Analysis

Kruskal-Wallis test and ANOVA test were used. Values are mean \pm SD. Statistical significance was set at $p < 0.05$.

Results

Physiological data were measured prior to intracerebral blood infusion. The physiological variables, including mean arterial blood pressure, blood pH, blood gases and blood glucose, were not different between the two groups.

In young rats the ratio of LC3-II to LC3-I in the ipsilateral basal ganglia was higher than that in the contralateral basal ganglia 7 days after ICH ($p < 0.05$, Fig. 1a). The ratio of LC3-II to LC3-I in the ipsilateral basal ganglia of aging rats was much higher compared with that in young rats (1.76 ± 0.16

vs. 1.14 ± 0.03 , $p < 0.05$, Fig. 1a). Cathepsin D protein levels in the ipsilateral basal ganglia 7 days after ICH were also significantly higher in aged compared to young rats ($2,480 \pm 146$ vs. $1,476 \pm 533$ pixels, $p < 0.05$, Fig. 1b).

Immunohistochemistry showed age-related differences in ferritin immunoreactivity and microglia activation in the ipsilateral basal ganglia 11 weeks after ICH. There were more ferritin-positive cells in the ipsilateral basal ganglia in aged rats ($p < 0.05$, Fig. 2a). Most ferritin positive cells were microglia-like. OX-42 staining confirmed more microglia in the ipsilateral basal ganglia in aged than in young rats (Fig. 2b).

Aged rats had slow recovery after ICH. Marked neurological deficits were found 1 day after ICH in young and aged rats, and there were no significant differences between the groups for the initial behavioral deficits at day 1. Young rats showed better forelimb using asymmetry scores from day 3 (Fig. 3a), better forelimb placing scores from day 7 (Fig. 3b) and better corner turn scores from week 7 (Fig. 3c).

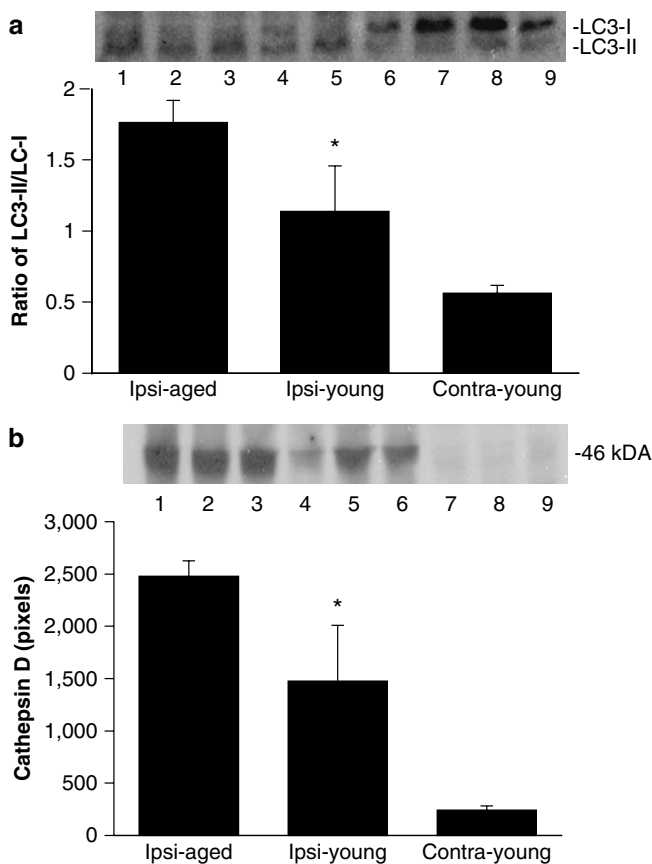


Fig. 1 Western blot analysis showing LC3-I (18 kDa), LC3-II (16 kDa) (a) and cathepsin D levels (b) in the ipsilateral (*ipsi*) basal ganglia of aging (lanes 1–3) or young (lanes 4–6) rats and in the contralateral (*contra*) basal ganglia of young (lanes 7–9) rats 7 days after ICH. Values are mean \pm SD, * $p < 0.05$ vs. the other groups

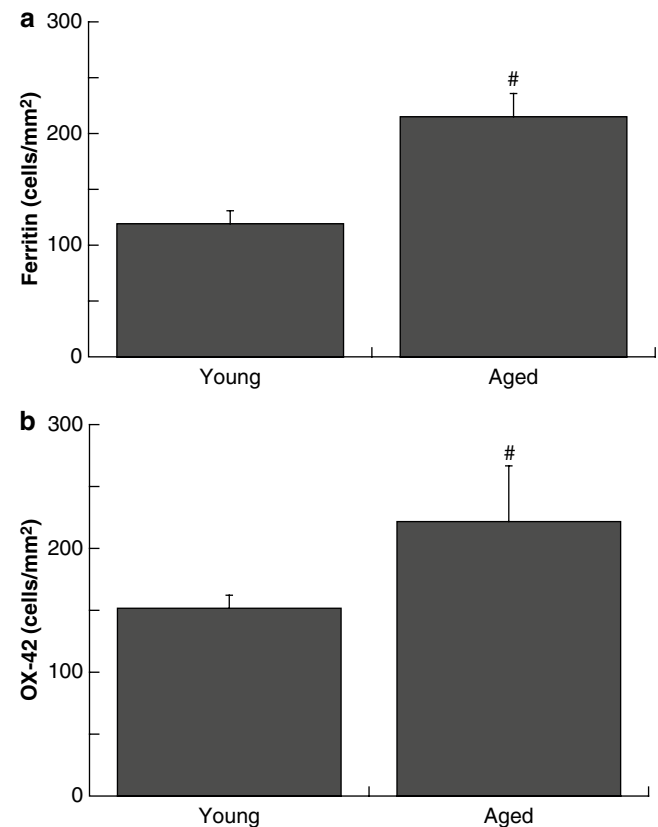
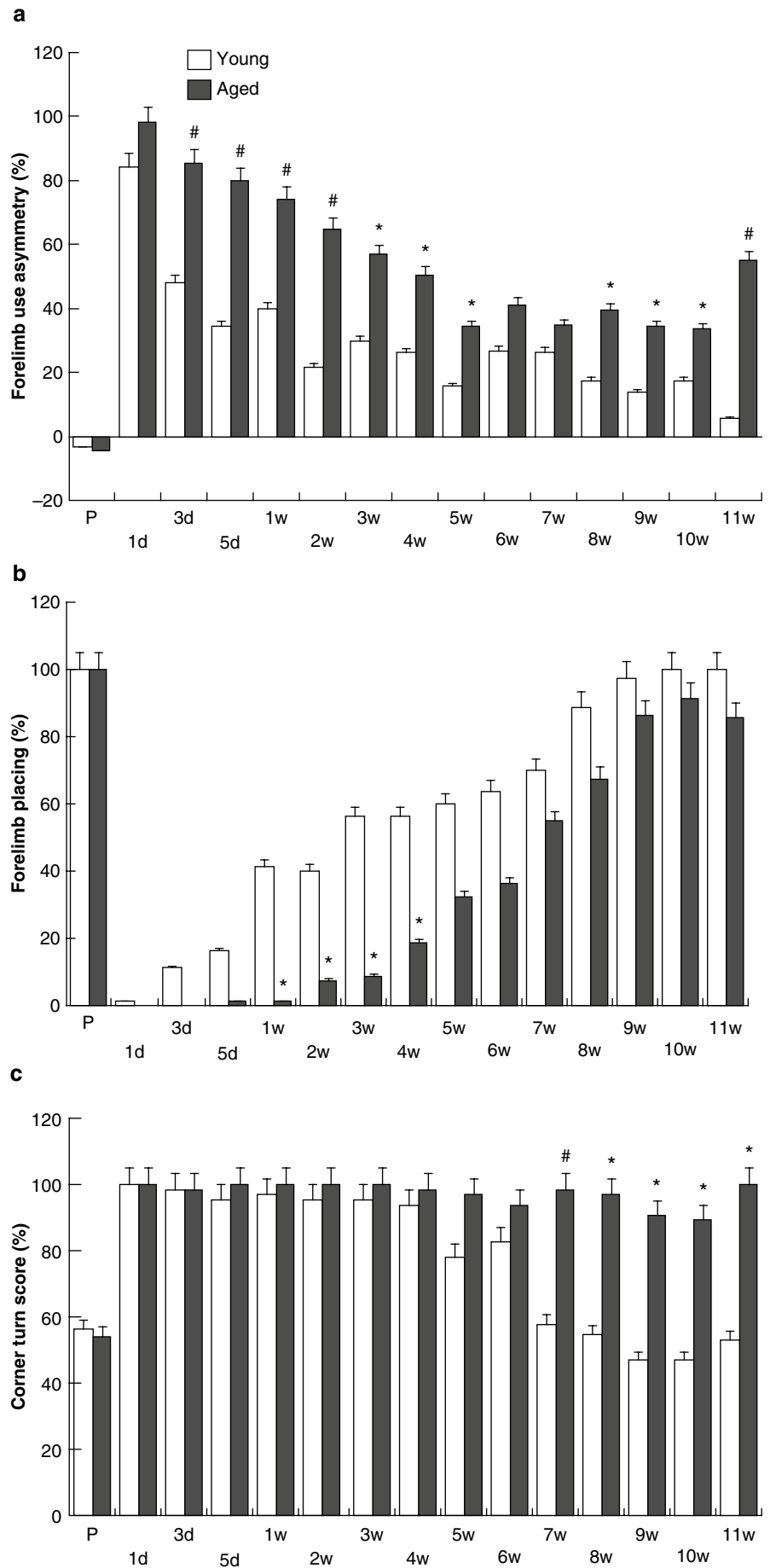


Fig. 2 Ferritin (a) and OX-42 (b) positive cells in the ipsilateral basal ganglia 11 weeks after ICH. Values are mean \pm SD, $n = 7-8$, # $p < 0.01$ vs. young rats

Fig. 3 Forelimb use asymmetry (a), forelimb placing (b) and corner turn (c) tests were performed prior to ICH (P) and then at days 1, 3, 5 and weeks 1–11 after ICH. Values are mean ± SD, $n = 7-8$. * $p < 0.05$, # $p < 0.01$ vs. young rats



Discussion

ICH results in stronger autophagic responses in aged compared to young rats. Autophagy is a cellular degradation process in which cellular proteins and organelles are sequestered in double-membrane vesicles known as autophagosomes, delivered to lysosomes, and digested by lysosomal hydrolases. We examined ICH-induced autophagy in young and aged rats at day 7 after autophagy in the perihematomal area peaks at that time [2]. The function of autophagy after ICH still remains unclear, and autophagy could be beneficial or harmful. During autophagic processes, injured cellular components are degraded in the lysosome. Enhanced autophagy in aged ICH rats may result from severe brain injury. Our previous studies have demonstrated that brain swelling is more severe in aged compared to young rats and that aged animals have stronger microglial activation [1]. However, over-activated autophagy may actually cause neuronal death. Thus, there is evidence showing that autophagy in certain pathological situations can trigger and mediate programmed cell death [11, 12].

Iron accumulates in the brain after ICH, reaching very high levels. Iron causes brain injury after ICH and is not cleared from the brain for at least several weeks [6, 13, 14]. Our previous studies found that iron can induce autophagy in the brain and deferoxamine, an iron chelator, reduces ICH-induced autophagy. This suggests an important role of iron in autophagy following ICH [2]. In this study, there were more ferritin positive cells after ICH in aged rats. Ferritin is the iron storage protein and can be upregulated in the brain after ICH [6]. Iron may participate in the induction of autophagy in aged rats, and it would be interesting to know whether iron overload after ICH is more severe in aged rats.

Microglia is activated in response to injury. In normal brain, microglia are quiescent, but after ICH they become highly phagocytic and are involved in clearing debris from areas of damage [15]. Microglia become progressively activated with age in humans [8, 16]. Inhibition of microglia activation by minocycline reduces ICH-induced brain injury [17]. Activated microglia secretes many toxic materials. In the present study we found that there were greater neurological deficits after ICH in aged rats. Future studies should determine if greater autophagy and microglia activation cause worse behavioral deficits in aged rats. Clarification of the mechanisms of brain injury after ICH in the aging brain should help develop new therapeutic strategies for hemorrhagic brain injury.

Acknowledgment This study was supported by grants NS-017760, NS-039866 and NS-057539 from the National Institutes of Health (NIH) and 0755717Z, 0840016N from the American Heart Association (AHA). The content is solely the responsibility of the authors and does not necessarily represent the official views of the

NIH and AHA. Drs. Gong and Gu were supported by NSFC30872675 and NSFC30700864 from the China National Natural Science Foundation.

Conflict of interest statement We declare that we have no conflict of interest.

References

- Gong Y, Hua Y, Keep RF, Hoff JT, Xi G (2004) Intracerebral hemorrhage: effects of aging on brain edema and neurological deficits. *Stroke* 35:2571–2575
- He Y, Wan S, Hua Y, Keep RF, Xi G (2008) Autophagy after experimental intracerebral hemorrhage. *J Cereb Blood Flow Metab* 28:897–905
- Kabeya Y, Mizushima N, Ueno T, Yamamoto A, Kirisako T, Noda T, Kominami E, Ohsumi Y, Yoshimori T (2000) LC3, a mammalian homologue of yeast Apg8p, is localized in autophagosome membranes after processing. *EMBO J* 19:5720–5728
- Yan L, Vatner DE, Kim SJ, Ge H, Masarekar M, Massover WH, Yang G, Matsui Y, Sadoshima J, Vatner SF (2005) Autophagy in chronically ischemic myocardium. *Proc Natl Acad Sci USA* 102:13807–13812
- Koeppen AH, Dickson AC, McEvoy JA (1995) The cellular reactions to experimental intracerebral hemorrhage. *J Neurol Sci* 134:102–112
- Wu J, Hua Y, Keep RF, Nakamura T, Hoff JT, Xi G (2003) Iron and iron-handling proteins in the brain after intracerebral hemorrhage. *Stroke* 34:2964–2969
- Schwartz M (2003) Macrophages and microglia in central nervous system injury: are they helpful or harmful? *J Cereb Blood Flow Metab* 23:385–394
- Wu J, Yang S, Xi G, Song S, Fu G, Keep RF, Hua Y (2008) Microglial activation and brain injury after intracerebral hemorrhage. *Acta Neurochir Suppl* 105:59–65
- Xi G, Keep RF, Hua Y, Xiang JM, Hoff JT (1999) Attenuation of thrombin-induced brain edema by cerebral thrombin preconditioning. *Stroke* 30:1247–1255
- Hua Y, Schallert T, Keep RF, Wu J, Hoff JT, Xi G (2002) Behavioral tests after intracerebral hemorrhage in the rat. *Stroke* 33:2478–2484
- Tolkovsky AM, Xue L, Fletcher GC, Borutaite V (2002) Mitochondrial disappearance from cells: a clue to the role of autophagy in programmed cell death and disease? *Biochimie* 84:233–240
- Yu L, Alva A, Su H, Dutt P, Freundt E, Welsh S, Baehrecke EH, Lenardo MJ (2004) Regulation of an ATG7-beclin 1 program of autophagic cell death by caspase-8. *Science* 304:1500–1502
- Wu G, Xi G, Hua Y, Sagher O (2010) T2* magnetic resonance imaging sequences reflect brain tissue iron deposition following intracerebral hemorrhage. *Transl Stroke Res* 1:31–34
- Xi G, Keep RF, Hoff JT (2006) Mechanisms of brain injury after intracerebral haemorrhage. *Lancet Neurol* 5:53–63
- Streit WJ, Walter SA, Pennell NA (1999) Reactive microgliosis. *Prog Neurobiol* 57:563–581
- Streit WJ, Sparks DL (1997) Activation of microglia in the brains of humans with heart disease and hypercholesterolemic rabbits. [comment]. *J Mol Med* 75:130–138
- Wu J, Yang S, Xi G, Fu G, Keep RF, Hua Y (2009) Minocycline reduces intracerebral hemorrhage-induced brain injury. *Neurol Res* 31:183–188

Effects of Gender on Heart Injury After Intracerebral Hemorrhage in Rats

Zi Ye, Qing Xie, Guohua Xi, Richard F. Keep, and Ya Hua

Abstract Intracerebral hemorrhage (ICH)-induced brain injury is less in female than in male rats, and estrogen can reduce such injury in males. Myocardial injury occurs after ischemic and hemorrhagic stroke, and the current study investigated the effects of gender on heart injury after ICH in rats. In the first part of the study, male and female rats had an intracerebral injection of 100 μ L autologous blood, and sham-operated rats had a needle insertion. In the second part of the study, male rats were treated with 17 β -estradiol or vehicle 2 h after ICH. All rats were then killed after 3 days and heart samples collected for histology and Western blot analysis. ICH caused heart injury, including petechial hemorrhage in male and female rats. To quantify heart stress following ICH, heat shock proteins (HSP) 32 and 27 were measured by Western blot analysis. We found that heart HSP-32 levels were higher in female compared to male rats after ICH ($p < 0.01$), but there was no effect of gender in sham-operated rats ($p > 0.05$), nor were there gender differences in myocardial HSP27 levels. Treatment with 17 β -estradiol increased HSP-32 levels in male ICH rats ($p < 0.05$). In conclusion, an ICH results in heart injury by an unknown mechanism. Gender and estrogen affect the heart response to ICH.

Keywords Intracerebral hemorrhage · Gender · Heat shock protein · Myocardium

Introduction

Myocardial injury, such cardiac arrhythmias, elevated troponin T and cardiac dysfunction, has been documented clinically after ischemic stroke, intracerebral hemorrhage (ICH) and subarachnoid hemorrhage [1–4]. Heart damage has also been found in experimental cerebral ischemia and ICH [5, 6].

There are gender differences in brain injury after ischemic stroke, ICH and cardiovascular diseases [7–9]. However, it is not clear if gender affects myocardial injury after ICH. Heat shock protein (HSP)-27 and -32 are two sensitive stress markers. Increases of HSP-27 or -32 levels have been found in the myocardium during hypoxia, apoptosis and other pathophysiological processes [10–13] and are associated with protective effects.

The current study investigated the effects of gender and estrogen on heart injury and expression of HSP-27 and -32 following ICH in rats.

Materials and Methods

Animal Groups

The University of Michigan Committee on the Use and Care of Animals approved the animal use protocols. There were two groups of experiments in this study. In the first, male or female Sprague-Dawley rats (250–300 g) were randomized to sham or ICH groups. In the second, male rats had an ICH

Z. Ye and Q. Xie
Department of Neurosurgery, University of Michigan,
Ann Arbor, MI, USA and
Department of Neurosurgery Huashan Hospital, Fudan University,
Shanghai, China

G. Xi and R.F. Keep
Department of Neurosurgery, University of Michigan,
Ann Arbor, MI, USA

Y. Hua (✉)
Department of Neurosurgery, University of Michigan, R5018 BSRB,
109 Zina Pitcher Place, Ann Arbor, MI, USA
e-mail: yahua@umich.edu

and were treated with 17 β -estradiol (5 mg/kg dissolved in 1% gelatin in saline) or vehicle (1% gelatin in saline) subcutaneously 2 h after ICH. All rats were sacrificed 3 days later and heart samples harvested for histology and Western blot analysis.

Intracerebral Injection

All animals were anesthetized with pentobarbital (40 mg/kg, i.p.). The right femoral artery was catheterized for continuous blood pressure monitoring and blood sampling. Blood was obtained from the catheter for analysis of blood pH, PaO₂, PaCO₂, hematocrit and blood glucose. Core temperature was maintained at 37°C with use of a feed back-controlled heating pad. Rats were positioned in a stereotactic frame, and a cranial burr hole (1 mm) was drilled in the right coronal suture 3.5 mm lateral to the midline. ICH rats received a 100 μ L injection of autologous blood into the right caudate nucleus at a rate of 10 μ L/min through a 26-gauge needle using a microinfusion pump. The needle was removed and the skin incision closed with sutures after infusion. Sham rats only had a needle insertion.

Histology and Immunohistochemistry

Rats were reanesthetized with pentobarbital and perfused with 4% paraformaldehyde in 0.1 M phosphate-buffered saline, pH 7.4. Hearts were placed in optimal cutting temperature embedding compound (Sakura Finetek, Inc., Torrance, CA) and sectioned coronally on a cryostat (8- μ m-thick slices). Hematoxylin and eosin (H&E) staining was used to study myocardial pathological changes.

For immunohistochemistry, myocardial sections were examined using the avidin-biotin complex technique. The primary antibodies were rabbit anti-rat HSP-32 or rabbit anti-mouse HSP-27 (1:400 dilutions, Stressgen). The secondary antibody was anti-rabbit immunoglobulin G (1:1,000 dilution, Vector Laboratories, Inc., Burlingame, CA).

Western Blot Analysis

After extraction of myocardial protein, samples were boiled at 95°C for 5 min; 50- μ g protein samples were then separated on 15% SDS-polyacrylamide gels and transferred to nitrocellulose membranes. The membranes were incubated with primary antibodies against HSP-32, HSP-27 (Stressgen) or

β -actin (Sigma) for 2 h at room temperature after blocking with 5% non-fat milk containing 0.1% Tween 20. The membranes were hybridized with HRP-conjugated goat anti-rabbit IgG antibody for another hour and detected with the ECL chemiluminescence system (Amersham Biosciences) and exposed to Kodak film. The relative pixels of the protein bands were analyzed with NIH Image software, version 1.61.

Statistical Analysis

Statistical analyses were performed using KaleidaGraph 4.0 software. All data are expressed as means \pm SD. Differences between the groups were determined by Student's *t*-test or ANOVA. Differences were set at $p < 0.05$.

Results

Hematoxylin-eosin staining showed there were petechial hemorrhages in the myocardium of both male and female rats after ICH (Fig. 1a, b). There were also inflammatory cells and myocardial necrosis spots around the hemorrhage area. These changes were not observed in sham-operated animals.

The stress-related proteins HSP-27 and -32 were examined in the myocardium by Western blot analysis. There was no difference in HSP-32 in sham-operated male or female rats. However, HSP-32 levels were significantly higher in females compared to male rats after ICH (11,413 \pm 1,873 pixels vs. 6,907 \pm 1,694 pixels, $p < 0.01$; Fig. 2). To examine the effects of estrogen on myocardial HSP-32 expression after ICH, male rats were treated with 17 β -estradiol 2 h after ICH. We found that HSP-32 levels in the heart were higher in rats treated with 17 β -estradiol (9,610 \pm 1,532 pixels vs. 5,754 \pm 1,606 pixels in the vehicle-treated rats, $p < 0.05$, Fig. 3).

In contrast to HSP-32, HSP-27 levels were not significantly different between male and female rats after sham operation or ICH.

Discussion

The myocardial injury after ICH suggests a brain-heart connection. Many studies have described neurogenic heart disease. Multifocal small subendocardial petechial hemorrhages and myocytolysis have been described in the myocardium of patients with severe intracranial hemorrhages, particularly subarachnoid hemorrhage [14]. This myocytolysis has been classified as one of three major patterns of myocardial

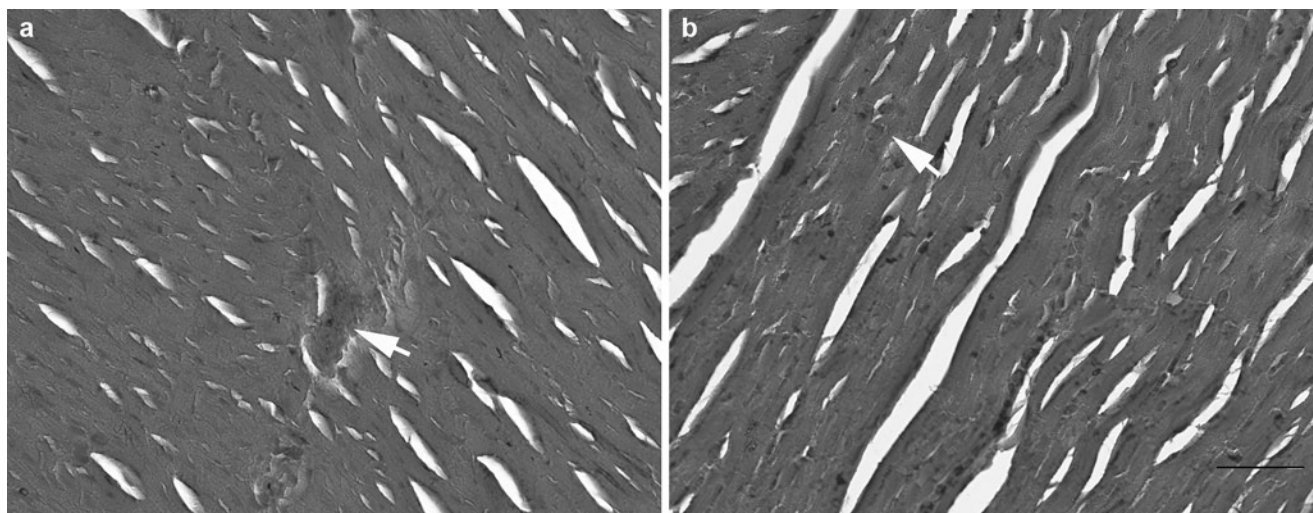


Fig. 1 H&E staining showing petechial hemorrhages (indicated by arrows) in male (a) or female myocardium (b) 3 days after ICH. Scale bar = 200 μ m

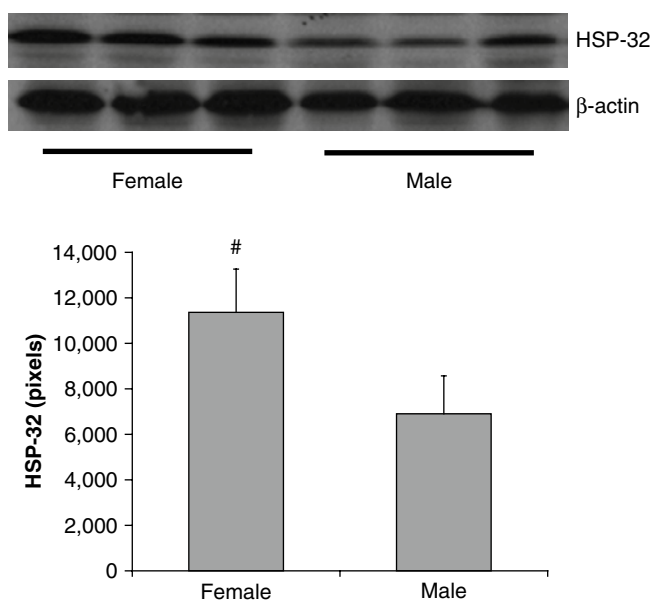


Fig. 2 Myocardial HSP-32 protein levels in male and female rats 3 days after ICH. Values are mean \pm SD, $n=3-6$, # $p < 0.01$ vs. male

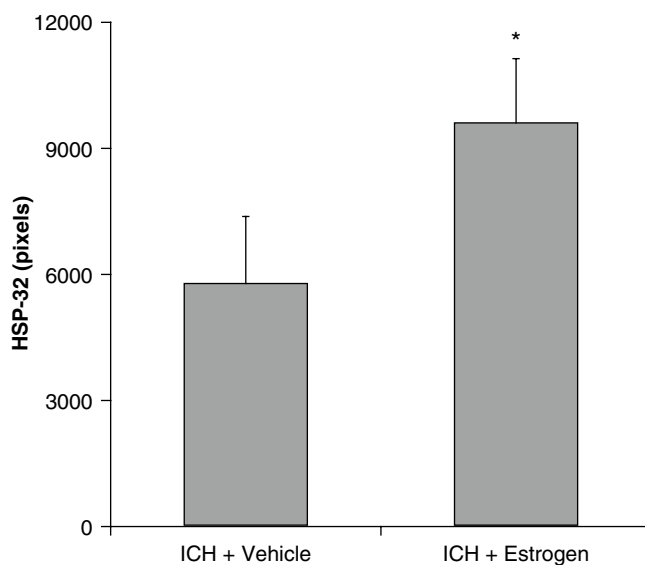


Fig. 3 Myocardial HSP-32 protein levels of HSP-32 in male rats 3 days after ICH. Rats were treated with 17 β -estradiol or vehicle 2 h after ICH. Values are mean \pm SD, $n=3-6$, * $p < 0.05$ vs. ICH + Vehicle

infarction, called coagulative myocytolysis. This was found not only in the heart after sudden death, but also in hearts exposed to high levels of catecholamine [15]. Recently, Min et al. found cardiac contractile band necrosis after permanent middle cerebral artery occlusion, and the cardiac dysfunction was associated with elevated levels of norepinephrine [6]. Also, intracerebral hemorrhage could damage cardiomyocyte contractility, damage initiated by intracellular calcium dysregulation [5]. In the current study, we found scattered

coagulative myocytolysis foci with petechial hemorrhages in myocardium of both male and female ICH rats.

Our results suggest that there may be a difference in myocardial injury between genders after ICH. Many clinical trials and animal studies have shown gender differences in tissue injury after cardiovascular disease and stroke. Our previous studies showed that gender and estrogen play important roles in ICH-induced brain injury in rats [8]. The stress-related proteins, HSP-32 and -27, are expressed in the

myocardium, but they can be further induced under stress-protecting myocytes. We found female rats had a higher HSP-32 level than males after ICH and that 17β -estradiol treatment induced higher levels of HSP-32 in male rats after ICH. This suggests that gender differences in myocardial HSP-32 may be related to estrogen. Further studies are needed to elucidate the exact role of gender in HSP-32 expression in the myocardium after ICH.

Acknowledgment This study was supported by grants NS-017760, NS-039866 and NS-057539 from the National Institutes of Health (NIH) and 0755717Z, 0840016N from the American Heart Association (AHA). The content is solely the responsibility of the authors and does not necessarily represent the official views of the NIH and AHA.

Conflict of interest statement We declare that we have no conflict of interest.

References

- Garrett MC, Komotar RJ, Starke RM, Doshi D, Otten ML, Connolly ES (2010) Elevated troponin levels are predictive of mortality in surgical intracerebral hemorrhage patients. *Neurocrit Care* 12:199–203
- Hurst JW (2003) Electrocardiographic changes in intracranial hemorrhage mimicking myocardial infarction. *N Engl J Med* 349:1874–1875, author reply 1874–1875
- Jung F, Setzer M, Hohnloser SH (2001) Severe intracranial bleeding mimicking acute inferior myocardial infarction with right ventricular involvement. *Cardiology* 95:48–50
- Laowattana S, Zeger SL, Lima JA, Goodman SN, Wittstein IS, Oppenheimer SM (2006) Left insular stroke is associated with adverse cardiac outcome. *Neurology* 66:477–483, discussion 463
- Fang CX, Wu S, Ren J (2006) Intracerebral hemorrhage elicits aberration in cardiomyocyte contractile function and intracellular Ca^{2+} transients. *Stroke* 37:1875–1882
- Min J, Farooq MU, Greenberg E, Aloka F, Bhatt A, Kassab M, Morgan JP, Majid A (2009) Cardiac dysfunction after left permanent cerebral focal ischemia: the brain and heart connection. *Stroke* 40:2560–2563
- Mackman N, Smyth S (2009) Cardiovascular disease in women. *Arterioscler Thromb Vasc Biol* 29:277–278
- Nakamura T, Hua Y, Keep R, Park J, Xi G, Hoff J (2005) Estrogen therapy for experimental intracerebral hemorrhage. *J Neurosurg* 103:97–103
- Xi G, Keep RF, Hoff JT (2006) Mechanisms of brain injury after intracerebral hemorrhage. *Lancet Neurol* 5:53–63
- Burger D, Xiang F, Hammoud L, Lu X, Feng Q (2009) Role of heme oxygenase-1 in the cardioprotective effects of erythropoietin during myocardial ischemia and reperfusion. *Am J Physiol Heart Circ Physiol* 296:H84–H93
- Efthymiou CA, Mocanu MM, de Bellerche J, Wells DJ, Latchmann DS, Yellon DM (2004) Heat shock protein 27 protects the heart against myocardial infarction. *Basic Res Cardiol* 99:392–394
- Latchman DS (2001) Heat shock proteins and cardiac protection. *Cardiovasc Res* 51:637–646
- Yeh CH, Chen TP, Wang YC, Lin YM, Lin PJ (2009) HO-1 activation can attenuate cardiomyocyte apoptosis via inhibition of NF-kappaB and AP-1 translocation following cardiac global ischemia and reperfusion. *J Surg Res* 155:147–156
- Lin NN, Kuo JS, Cheng CC, Tung KC, Cheng FC, Chiu YT (2008) Early cardiac damage after subarachnoid hemorrhage in rats. *Int J Cardiol* 129:433–437
- Samuels MA (2007) The brain-heart connection. *Circulation* 116:77–84

Iron Accumulation and DNA Damage in a Pig Model of Intracerebral Hemorrhage

Yuxiang Gu, Ya Hua, Yangdong He, Lin Wang, Hua Hu, Richard F. Keep, and Guohua Xi

Abstract Cerebral iron overload causes brain injury after intracerebral hemorrhage (ICH) in rats and pigs. The current study examined whether an iron chelator, deferoxamine, can reduce ICH-induced DNA damage in pigs. Pigs received an injection of autologous blood into the right frontal lobe. Deferoxamine (50 mg/kg, i.m.) or vehicle was given 2 h after ICH and then every 12 h up to 7 days. Animals were killed at day 3 or day 7 after ICH to examine iron accumulation and DNA damage. We found that ICH resulted in the development of a reddish perihematomal zone, with iron accumulation and DNA damage within that zone. Deferoxamine treatment reduced the perihematomal reddish zone, and the number of Perls' ($p < 0.01$) and TUNEL ($p < 0.01$) positive cells. In conclusion, iron accumulates in the perihematomal zone and causes DNA damage. Systemic deferoxamine treatment reduces ICH-induced iron overload and DNA damage in pigs.

Keywords Cerebral hemorrhage · Deferoxamine · Iron · Perls' reaction · TUNEL

Introduction

Iron accumulation occurs in the brain after intracerebral hemorrhage (ICH) and results in brain injury [1–3]. Iron-induced brain injury including DNA damage may result from oxidative stress [4, 5]. Terminal deoxynucleotidyl transferase-mediated dUTP nick end-labeling (TUNEL) is a DNA injury marker that is often used to detect double-strand DNA damage [4].

Deferoxamine (DFX), an iron chelator, is a FDA-approved drug for the treatment of acute iron intoxication and chronic iron overload due to transfusion-dependent anemia. DFX reduces brain edema, neuronal death and neurological deficits following ICH in rats [6–8]. DFX also reduces hemorrhagic transformation in a rat model of cerebral ischemia [9].

The current study examined whether systemic DFX treatment reduces brain iron accumulation and DNA damage in a pig model of ICH.

Materials and Methods

Animal Preparation, Intracerebral Infusion and DFX Treatment

Animal use protocols were approved by the University of Michigan Committee on the Use and Care of Animals. Male pigs (8–10 kg, Michigan State University) were sedated with ketamine (25 mg/kg, i.m.) and anesthetized with isoflurane. After a surgical plane of anesthesia was reached, animals were orotracheally intubated. The right femoral artery was catheterized for monitoring of blood pressure, blood gases and glucose concentrations. Body temperature was maintained at $37.5 \pm 0.5^\circ\text{C}$.

A cranial burr hole (1.5 mm) was drilled 11 mm to the right of the sagittal and 11 mm anterior to the coronal suture. A 20-gauge sterile plastic catheter was then placed stereotaxically

Y. Gu

Department of Neurosurgery, University of Michigan, Ann Arbor, MI, USA and

Department of Neurosurgery, Huashan Hospital, Fudan University, Shanghai, China

Y. Hua, Y. He, L. Wang, H. Hu, and R.F. Keep

Department of Neurosurgery, University of Michigan, Ann Arbor, MI, USA

G. Xi (✉)

Department of Neurosurgery, University of Michigan, 109 Zina Pitcher Place, Ann Arbor, MI 48109-2200, USA
e-mail: guohuaxi@umich.edu

into the center of the right frontal cerebral white matter and cemented in place. Silicone elastomer tubing connected to the arterial catheter was filled with 5 mL of autologous arterial blood. An infusion pump was connected, and 1.0 mL of whole blood was injected over 15 min. After a 5 min break, another 1.5 mL of whole blood was injected over 15 min [10].

Brain Histology

Pigs were treated with DFX (50 mg/kg; i.m., given at 2 h after ICH and then every 12 h for up to 7 days) or vehicle. Pigs were reanesthetized on day 3 or day 7, and the brains perfused with 10% formalin. Paraffin-embedded brain was cut coronally into 10- μ m-thick sections.

Enhanced Perls' Staining

Enhanced Perls' staining was performed to detect iron accumulation [11]. Paraffin sections were deparaffinized in xylol and alcohols of descending concentration, rinsed in distilled water, and incubated in Perls' Prussian blue staining solution (1:1, 5% potassium ferrocyanide/5% hydrochloric acid) for 45 min, followed by washing with distilled water. The sections were then incubated in 0.5% diamine benzidine tetrahydrochloride with nickel for 45 min.

Immunohistochemistry

Ferritin was examined by immunohistochemistry. The primary antibody was polyclonal rabbit anti-human ferritin IgG (DACO, 1:400 dilution). Normal rabbit IgG was used as a negative control.

Terminal Deoxynucleotidyl Transferase-Mediated dUTP Nick End-Labeling (TUNEL)

TUNEL staining was performed using a ApopTag Peroxidase Kit (Intergen). First, 3% hydrogen peroxide in 0.1MPBS was applied to sections for 5 min to quench endogenous peroxidases. After washing with PBS and equilibrating with the solution supplied, the specimens were incubated with TdT enzyme at 37°C for 1 h. The reaction was stopped by washing with buffer for 10 min. Anti-digoxigenin peroxidase conjugate was then applied to the slide for 30 min at room temperature. 3,3' diaminobenzidine (DAB) was used for visualization. Omission of the terminal deoxynucleotidyl transferase was used as the negative control.

Photography for Cell Counting

Light microphotographs ($\times 40$, 4 fields from each distance) were taken at 200, 500 and 1,000 μ m from the edge of the hematoma.

Statistical Analysis

Data from different animal groups and brain sites were expressed as mean \pm SD and analyzed by Student's *t*-test. Differences were considered significant at $p < 0.05$.

Results

ICH resulted in the development of a reddish zone around the clot in pigs at day 3 and 7. Systemic DFX treatment reduced this reddish zone (Fig. 1). There were many Perls'-

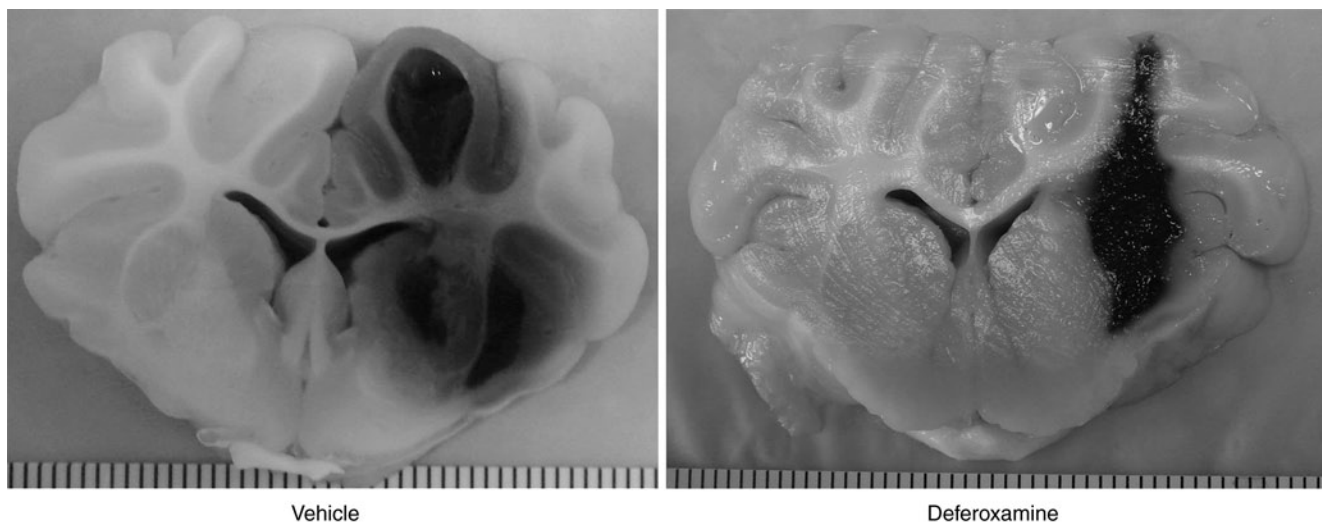


Fig. 1 Deferoxamine reduces the area of the reddish zone around the clot at 3 days after ICH

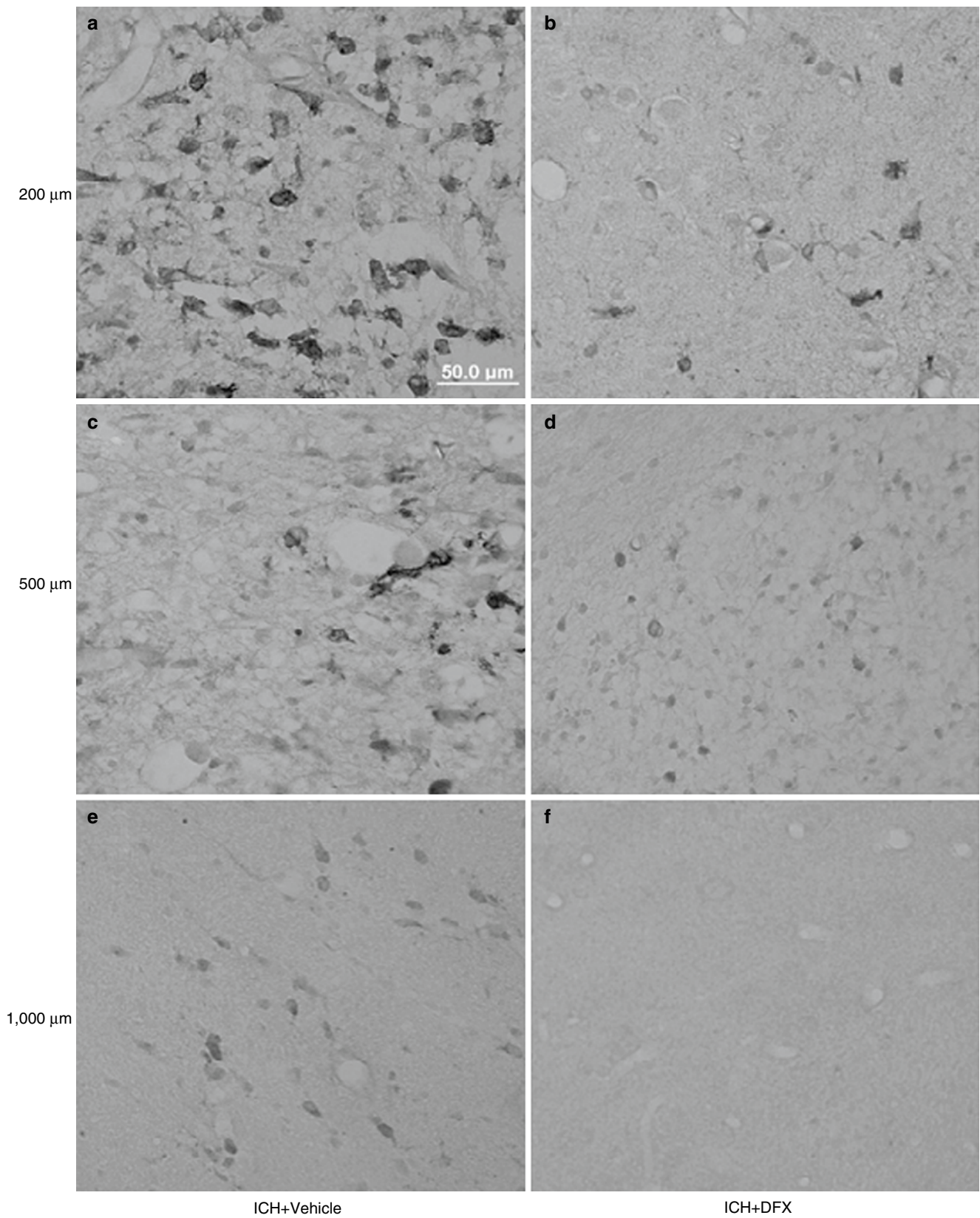


Fig. 2 Ferritin-positive cells in the perihematoma zone at different distances away from the edge of hematoma at day 7 after ICH. (a, b) 200 μm , (c, d) 500 μm and (e, f) 1,000 μm from the hematoma edge.

The rats were treated by vehicle (a, c, e) or deferoxamine (b, d, f). Scale bar=50 μm . (g) Quantification of ferritin-positive cells. Values are means \pm SD, $\#p < 0.01$ vs. ICH+Vehicle

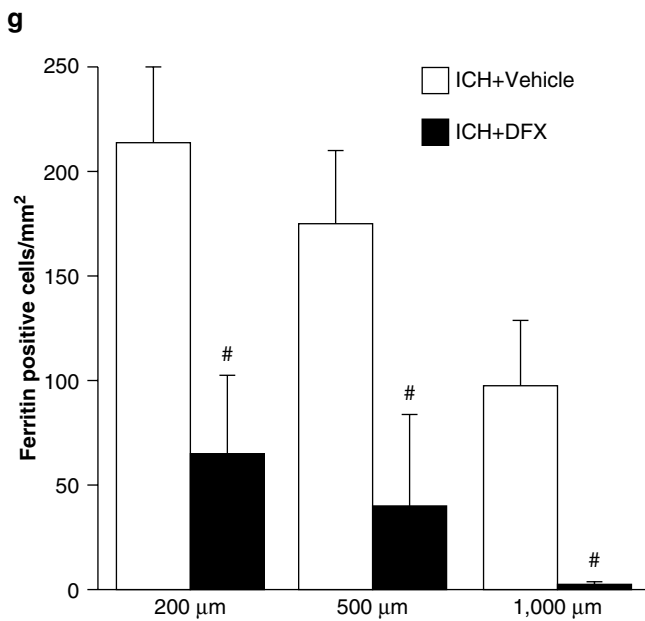


Fig. 2 (continued)

positive cells in the reddish zone, and DFX also reduced the number of these cells ($p < 0.01$).

Ferritin was upregulated in the perihematoma area. Ferritin-positive cells around the hematoma were glia-like (Fig. 2). Most ferritin-positive cells were detected immediately next to the clot. There were fewer ferritin-positive cells in DFX-treated compared to vehicle-treated pigs (Fig. 2).

TUNEL staining was used to detect DNA damage in the brain. TUNEL-positive cells were found in the vicinity of

the clot (Fig. 3). DFX treatment reduced the number of TUNEL-positive cells around the hematoma ($p < 0.01$, Fig. 3).

Discussion

This study found that systemic DFX treatment reduces perihematoma iron accumulation and DNA damage in pigs. Our previous studies found that DFX is neuroprotective and can reduce brain edema and atrophy after ICH in young and aged rats [6–8]. DFX has protective effects in ICH models in two species (rats and pigs), as well as in young and aged animals, suggesting that DFX may also work in humans.

DNA damage was found in the perihematoma zone in pigs. Two pathways that can result in DNA damage are endonuclease-mediated DNA fragmentation and oxidative injury [12]. It is well known that reactive oxygen species can attack DNA directly, forming oxidative base damage and strand breaks [13], and that DNA damage by reactive oxygen species can be greatly amplified in the presence of free iron [14]. Our previous study showed that oxidative stress is a major cause of DNA damage in a rat model of ICH [4]. The current results suggest that iron released from the clot can cause DNA damage in pigs.

Iron overload following ICH is toxic to the brain. The duration over which clot lysis and iron release occurs is likely to be dependent on hematoma size. Our former data in rats [6–8] and present results in pigs show that DFX is effective in reducing brain injury in different ICH models with different sizes of clots.

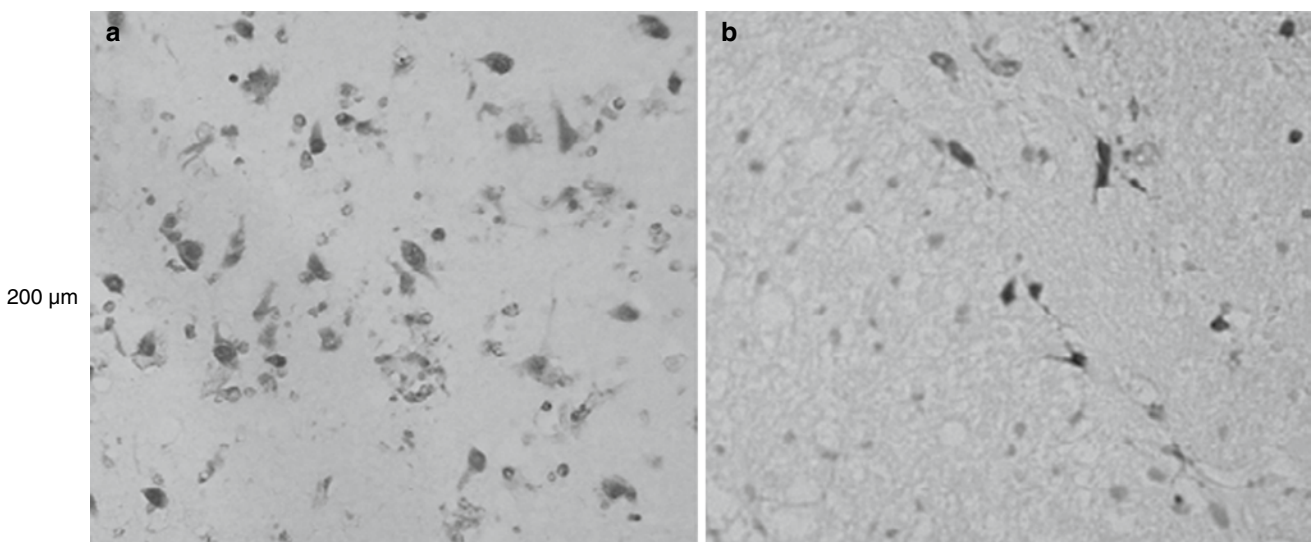


Fig. 3 TUNEL staining in the perihematoma zone at different distances away from the edge of the hematoma 3 days after ICH. (a, b) 200 μm, (c, d) 500 μm and (e, f) 1,000 μm from the edge. Rats were treated with

vehicle (a, c, e) or deferoxamine (b, d, f). Scale bar=50 μm. (g) Quantification of TUNEL-positive cells. Values are means ± SD, * $p < 0.05$, # $p < 0.01$ vs. ICH+ Vehicle

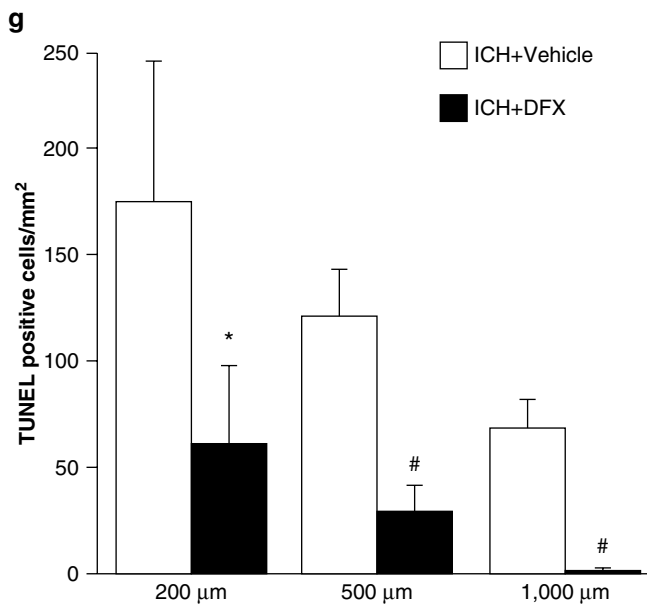
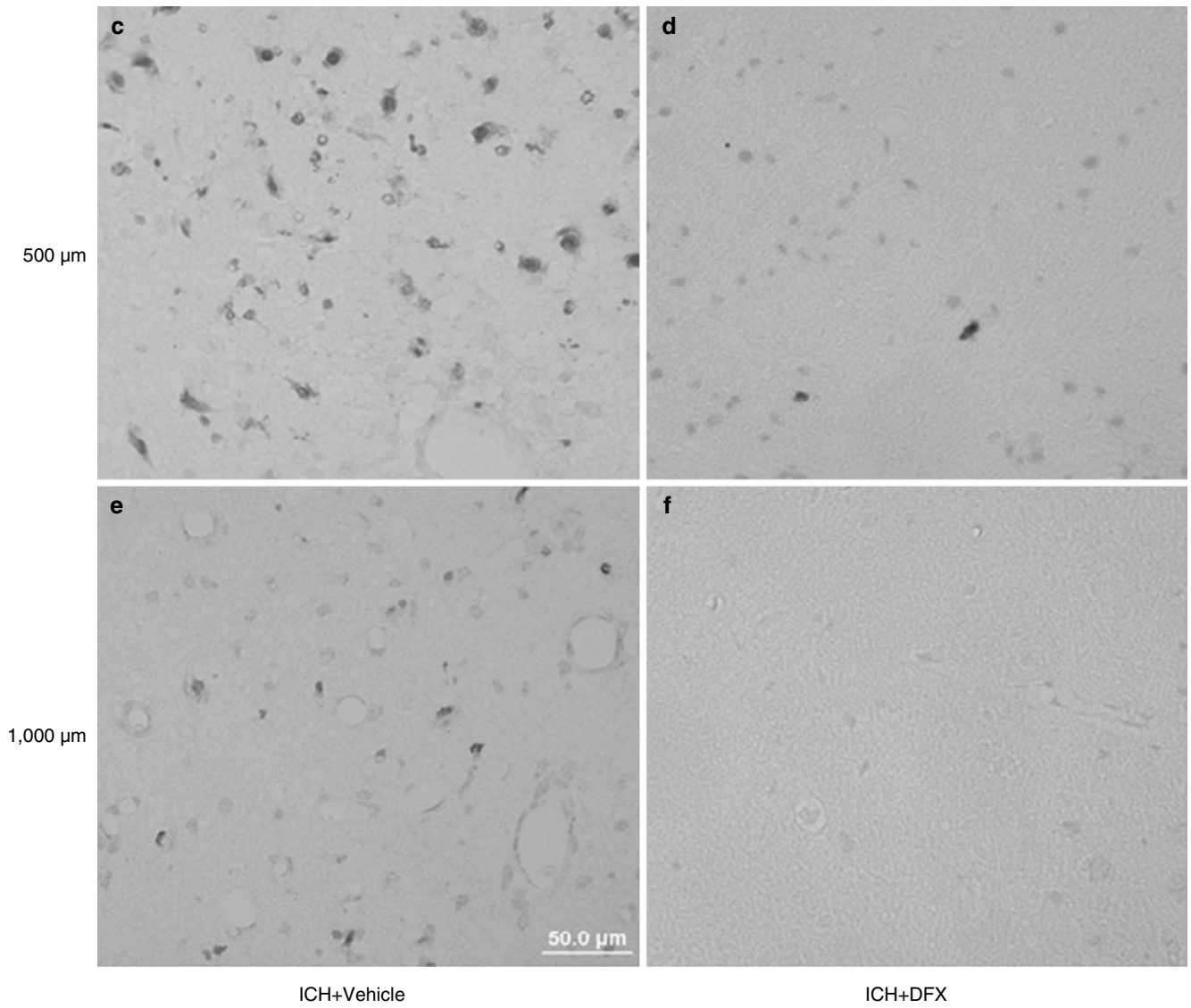


Fig. 3 (continued)

In conclusion, iron accumulation occurs in the pig brain, and systemic DFX treatment reduces ICH-induced DNA damage.

Acknowledgment This study was supported by grants NS-017760, NS-039866, NS-052510 and NS-057539 from the National Institutes of Health (NIH) and 0840016N from the American Heart Association (AHA). The content is solely the responsibility of the authors and does not necessarily represent the official views of the NIH and AHA. Dr. Gu was supported by a grant 30700864 from the China National Natural Science Foundation.

Conflict of interest statement We declare that we have no conflict of interest.

References

1. Wagner KR, Sharp FR, Ardizzone TD, Lu A, Clark JF (2003) Heme and iron metabolism: role in cerebral hemorrhage. *J Cereb Blood Flow Metab* 23:629–652
2. Wu G, Xi G, Hua Y, Sagher O (2010) T2* Magnetic resonance imaging sequences reflect brain tissue iron deposition following intracerebral hemorrhage. *Transl Stroke Res* 1:31–34
3. Xi G, Keep RF, Hoff JT (2006) Mechanisms of brain injury after intracerebral hemorrhage. *Lancet Neurol* 5:53–63
4. Nakamura T, Keep RF, Hua Y, Hoff JT, Xi G (2005) Oxidative DNA injury after experimental intracerebral hemorrhage. *Brain Res* 1039:30–36
5. Nakamura T, Kuroda Y, Yamashita S, Zhang X, Miyamoto O, Tamiya T, Nagao S, Xi G, Keep RF, Itano T (2008) Edaravone attenuates brain edema and neurologic deficits in a rat model of acute intracerebral hemorrhage. *Stroke* 39:463–469
6. Hua Y, Nakamura T, Keep RF, Wu J, Schallert T, Hoff JT, Xi G (2006) Long-term effects of experimental intracerebral hemorrhage: the role of iron. *J Neurosurg* 104:305–312
7. Nakamura T, Keep R, Hua Y, Schallert T, Hoff J, Xi G (2004) Deferoxamine-induced attenuation of brain edema and neurological deficits in a rat model of intracerebral hemorrhage. *J Neurosurg* 100:672–678
8. Okauchi M, Hua Y, Keep RF, Morgenstern LB, Schallert T, Xi G (2010) Deferoxamine treatment for intracerebral hemorrhage in aged rats: therapeutic time window and optimal duration. *Stroke* 41:375–382
9. Xing Y, Hua Y, Keep RF, Xi G (2009) Effects of deferoxamine on brain injury after transient focal cerebral ischemia in rats with hyperglycemia. *Brain Res* 1291:113–121
10. Xi G, Wagner KR, Keep RF, Hua Y, de Courten-Myers GM, Broderick JP, Brott TG, Hoff JT (1998) The role of blood clot formation on early edema development following experimental intracerebral hemorrhage. *Stroke* 29:2580–2586
11. Wu J, Hua Y, Keep RF, Nakamura T, Hoff JT, Xi G (2003) Iron and iron-handling proteins in the brain after intracerebral hemorrhage. *Stroke* 34:2964–2969
12. Graham SH, Chen J (2001) Programmed cell death in cerebral ischemia. *J Cereb Blood Flow Metab* 21:99–109
13. Nagayama T, Lan J, Henshall DC, Chen D, O'Horo C, Simon RP, Chen J (2000) Induction of oxidative DNA damage in the perinfarct region after permanent focal cerebral ischemia. *J Neurochem* 75:1716–1728
14. Aruoma OI, Halliwell B, Dizdaroglu M (1989) Iron ion-dependent modification of bases in DNA by the superoxide radical-generating system hypoxanthine/xanthine oxidase. *J Biol Chem* 264:13024–13028

Subarachnoid Hemorrhage Causes Pulmonary Endothelial Cell Apoptosis and Neurogenic Pulmonary Edema in Mice

Hidenori Suzuki, Takumi Sozen, Yu Hasegawa, Wanqiu Chen, Kenji Kanamaru, Waro Taki, and John H. Zhang

Abstract *Objects:* Neurogenic pulmonary edema (NPE) is a well-known complication of subarachnoid hemorrhage (SAH), which potentially causes a poor outcome. The aim of this study was to examine if NPE occurs in the *endovascular perforation model of SAH* in mice and if apoptosis contributes to NPE development after SAH in mice.

Methods: Sham-operated or SAH mice were treated with an intraperitoneal administration of vehicle or an antiapoptotic drug Z-Val-Ala-Asp-fluoromethylketone (Z-VAD-FMK) 1 h post-SAH. Pulmonary edema measurements and evaluation of apoptosis occurrence were performed on the lung at 24 h post-SAH.

Results: SAH caused NPE, which was associated with apoptosis of pulmonary endothelial cells. Z-VAD-FMK significantly prevented apoptosis and NPE.

Conclusions: Pulmonary endothelial cell apoptosis contributes to the pathophysiology of NPE after SAH in mice.

Keywords Apoptosis · Caspase inhibitor · Pulmonary edema · Subarachnoid hemorrhage

Introduction

Neurogenic pulmonary edema (NPE) is a potentially life-threatening complication sometimes associated with a worse clinical grade of aneurysmal subarachnoid hemorrhage (SAH) [1]. Although the true incidence of NPE remains unclear, acute pulmonary edema has been documented in approximately 90% of sudden deaths from spontaneous SAH [1]. In addition, NPE may impair brain oxygenation, aggravate neurogenic injury, and impede aggressive treatments for SAH and the subsequent ischemia, worsening neurological recovery in survivors. Only few studies, however, have focused on NPE after SAH, and therefore the mechanism for post-SAH NPE development has been poorly understood. We examined if lung cell apoptosis contributes to NPE after SAH in mice in this study.

Materials and Methods

All procedures were approved by Loma Linda University animal care committee.

Experimental Model of SAH and Study Protocol

SAH was produced by endovascular perforation of the left anterior cerebral artery, and sham-operated rats underwent identical procedures except that the suture was withdrawn

H. Suzuki

Department of Neurosurgery, Mie University Graduate School of Medicine, Tsu, Japan and
Department of Physiology, Loma Linda University of Medicine, School of Medicine, Loma Linda, CA, USA

T. Sozen, Y. Hasegawa, and W. Chen
Department of Physiology, Loma Linda University of Medicine, School of Medicine, Loma Linda, CA, USA

K. Kanamaru
Department of Neurosurgery, Suzuka Kaisei Hospital, Suzuka, Japan

W. Taki
Department of Neurosurgery, Mie University Graduate School of Medicine, Tsu, Japan

J.H. Zhang (✉)
Department of Neurosurgery, Loma Linda University of Medicine, School of Medicine, Loma Linda, CA, USA and
Department of Physiology, Loma Linda University of Medicine, School of Medicine, Risely Hall, Room 223, Loma Linda, CA 92354, USA
e-mail: johnzhang3910@yahoo.com

without puncture in CD-1 mice (35–40 g, Harlan, Indianapolis, IN) as described previously [2]. The SAH mice were treated with an intraperitoneal administration of vehicle or an antiapoptotic drug Z-Val-Ala-Asp-fluoromethylketone (Z-VAD-FMK, 6 mg/kg; Sigma-Aldrich, St. Louis, MO) 1 h post-SAH. The production of SAH or sham model was continued until the number of each group was 10. All surviving mice were sacrificed, and SAH grading scores (0–18 in one number steps) were assessed after evaluating neurological scores (3–21 in one number steps) 24 h post-surgery as previously described [2]. The lung water content was measured on the left lobes ($n=6$ per group), and Western blots were performed on the right lobes ($n=6$ per group). Also, histological assessment was performed on the lungs ($n=4$ per group).

Lung Water Content (Pulmonary Edema)

Left lungs were sharply dissected free of nonparenchymal tissue and weighed (wet weight). The lung specimens were dried in an oven at 105°C for 24 h and weighed again (dry weight). This was repeated until there was no weight change over a 24-h period at which time the samples were determined to be dry. Lung water was expressed as a wet-to-dry weight ratio (W/D) [3].

Western Blot Analyses

Western blot analysis was performed as previously described [4]. Equal amounts of protein samples (50 µg) were loaded on a Tris glycine gel, electrophoresed and transferred to a nitrocellulose membrane. Membranes were blocked with a blocking solution, followed by incubation overnight at 4°C with the rabbit polyclonal anti-cleaved caspase-3 antibody (1:1,000; Cell Signaling, Danvers, MA). Immunoblots were processed with appropriate secondary antibodies (1:2,000, Santa Cruz Biotechnology, Santa Cruz, CA) for 1 h at 21°C, and bands were detected with a chemiluminescence reagent kit (ECL Plus; Amersham Bioscience, Arlington Heights, IL). Blot bands were quantified by densitometry with Image J software (NIH, Bethesda, MD). β -Actin (1:2,000, Santa Cruz Biotechnology, Santa Cruz, CA) was blotted on the same membrane as a loading control.

Histological Assessments

Lungs were fixed by cardiovascular perfusion with phosphate-buffered saline and 10% paraformaldehyde. The lungs were postfixed in 10% paraformaldehyde followed by 30%

sucrose (weight/volume) for 3 days. Ten-micron-thick coronal sections were cut on a cryostat (Leica Microsystems LM3050S) and mounted on poly-L-lysine-coated slides. Hematoxylin-eosin, terminal deoxynucleotidyl transferase-mediated uridine 5'-triphosphate-biotin nick end-labeling (TUNEL; in situ cell death detection kit; Roche, Indianapolis, IN) and 4',6-diamidino-2-phenylindole (DAPI; VECTASHIELD; Vector, Burlingame, CA) staining were performed according to the manufacturer's protocol. The TUNEL-positive cells were counted in the three fields in each case at $\times 400$ magnification in a blinded manner, and the average number of cells was expressed.

We also immunostained the sections with the rabbit polyclonal anti-von Willebrand factor (vWF) antibody (1:50, Santa Cruz Biotechnology, Santa Cruz, CA) and then subjected the sections to TUNEL and DAPI staining as previously described [4]. The sections were visualized with a fluorescence microscope, and pictographs were recorded and analyzed with MagnaFire SP 2.1B software (Olympus, Melville, NY).

Statistics

All values were expressed as mean \pm SD. Unpaired *t* tests or one-way analysis of variance with Scheffé correction was used as appropriate with $P < 0.05$ considered statistically significant.

Results

Pulmonary Edema

SAH-induced brain injury was similar in terms of neurological impairment and the severity of SAH between the vehicle- and Z-VAD-FMK-treated SAH groups (7.3 ± 2.7 vs. 8.8 ± 0.8 and 6.3 ± 1.0 vs. 6.6 ± 1.2 , respectively) at 24 h post-SAH. Pulmonary edema in the vehicle-treated SAH group was significantly increased compared with the sham-operated group, while Z-VAD-FMK treatment significantly reduced pulmonary edema after SAH (Fig. 1). Hematoxylin-eosin stains showed that alveoli were filled with fluid, but only a few inflammatory cells were observed in the vehicle-treated SAH group having NPE, while little or no alveolar edema was observed in the Z-VAD-FMK-treated SAH group.

Apoptosis

SAH caused a significant increase in the number of TUNEL positive cells, which was significantly reduced by

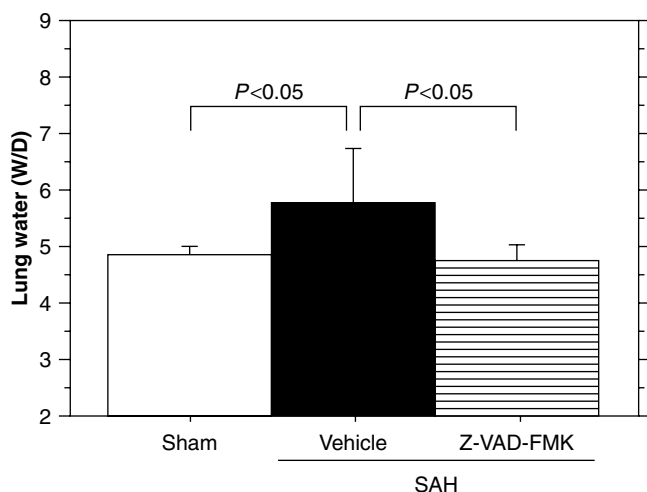


Fig. 1 Pulmonary edema at 24h post-SAH. $N=6$ mice per group

Z-VAD-FMK treatment in the lung 24h post-SAH (Fig. 2a). Western blot analysis showed that changes in cleaved caspase-3 levels in the lung 24h post-SAH were similar to those in the number of TUNEL-positive cells (Fig. 2). Immunofluorescence showed that apoptosis occurred in the pulmonary endothelial cells after SAH (Fig. 3).

Discussion

This study showed that NPE occurred in the endovascular perforation model of SAH in mice, associated with the apoptosis of pulmonary endothelial cells. Moreover, the prevention of pulmonary endothelial cell apoptosis by Z-VAD-FMK significantly reduced NPE. These results suggest that pulmonary endothelial cell apoptosis contributes to the development of NPE after SAH.

NPE typically develops within minutes or hours after SAH [1]. Although the exact mechanism remains unclear, hemodynamic changes by catecholamine are considered to be the main pathogenetic factor [1, 5, 6]. The increased intracranial pressure as well as toxic or ischemic injury of inhibitory neurons at so-called NPE trigger zones following SAH may cause severe sympathetic discharge, which results in transient left ventricular dysfunction or pulmonary vasoconstriction. As a result, elevated pulmonary capillary pressure (hydrostatic pressure) occurs, leading to the development of NPE [1, 6]. The hydrostatic pressure-independent mechanism has also been suggested, but remains unknown. For example, an excessive release of catecholamines not only leads to hydrostatic pulmonary edema, but also causes an activation of cytokines and inflammation [5] or lung cell apoptosis [7]. Inflammatory reactions can cause pulmonary edema associated with recruitment of neutrophils, which release matrix metalloproteinases that damage the alveolar-capillary barrier

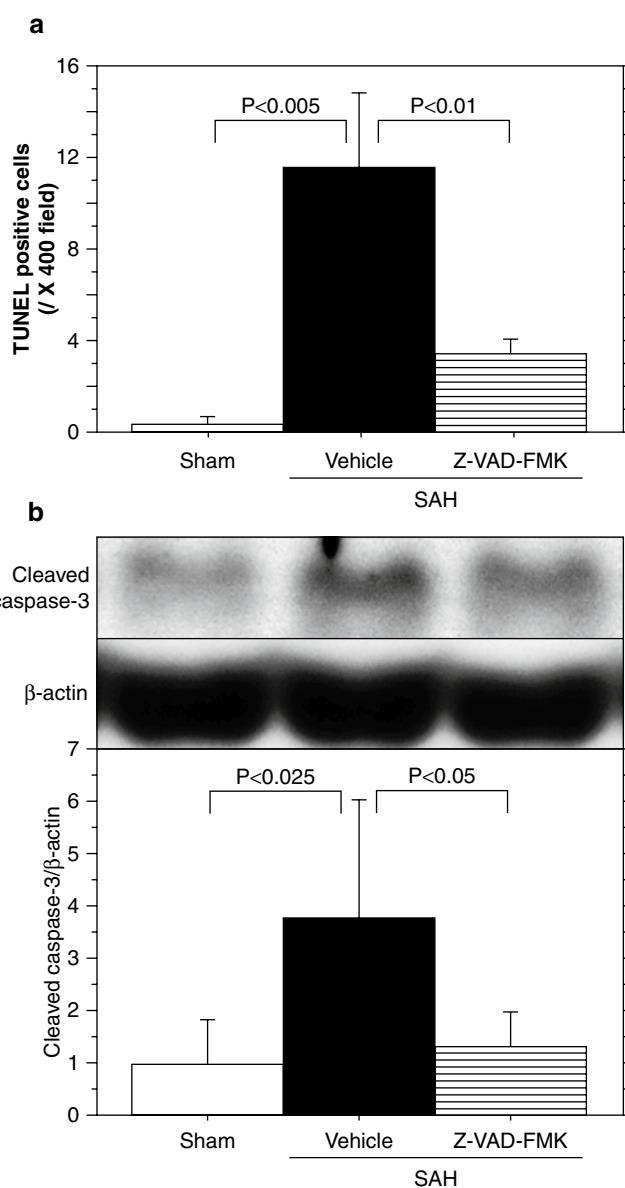


Fig. 2 Z-VAD-FMK treatment prevents lung tissue apoptosis at 24h post-SAH. (a) number of TUNEL-positive pulmonary cells per $\times 400$ field. $N=4$ mice per group. (b) Western blot of cleaved caspase-3 in the right pulmonary lobes. $N=6$ mice per group

[3]. However, inflammation is considered not to be involved in the development of NPE, but potentially to contribute to maintaining and aggravating the edema by increasing capillary permeability [5, 6]. On the other hand, the possibility that apoptosis is involved in the pathogenesis of NPE has not been sufficiently investigated. This study showed that post-SAH NPE was associated with lung cell apoptosis, but not with a significant increase in neutrophil infiltration, and that Z-VAD-FMK prevented lung cell apoptosis and NPE. As Z-VAD-FMK is not known to cause an immediate decrease in hydrostatic pressure but prevents apoptosis, our findings suggest that apoptosis is involved in the development of NPE. These findings are consistent with our previous study [8],

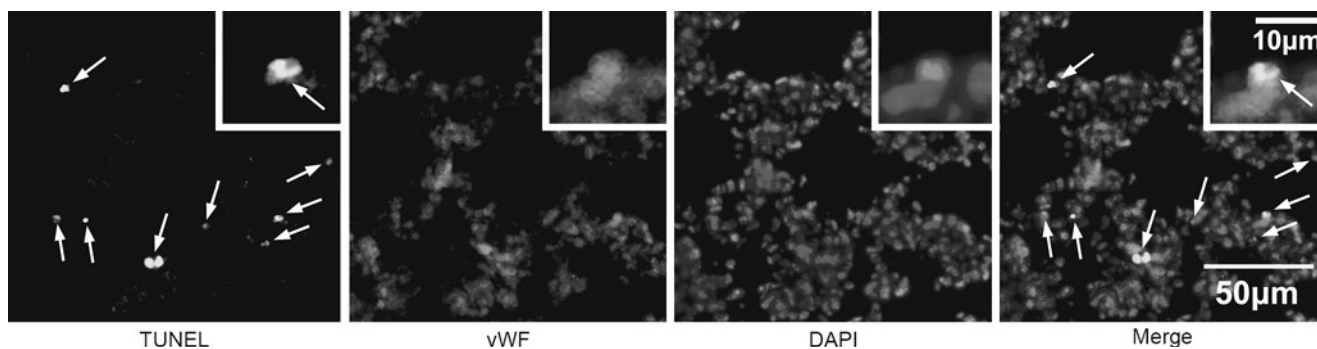


Fig. 3 Representative photographs of combined TUNEL/endothelial cell (vWF)/DAPI immunostaining in the lungs at 24h post-SAH. Arrows, TUNEL-positive nuclei

in which a caspase-1 inhibitor Ac-YVAD-CMK prevented lung cell apoptosis and NPE via the inactivation of interleukins-1 β [9] and/or other mechanisms independent of its caspase-1 inhibitor activity [10]. We speculate that pulmonary endothelial cell apoptosis weakens the alveolar-capillary barrier and diminishes the capacity to withstand increased hydrostatic pressure by a release of catecholamines, resulting in NPE.

The cornerstone of NPE management is early and appropriate treatment of the underlying neurological cause [1]: the most frequent underlying factor is SAH [11]. However, the specific treatment for NPE has not yet been developed, and therefore NPE is only supportively treated [6]. This study suggests that anti-apoptotic therapy may prove to be a novel approach for the prevention and treatment of NPE after SAH.

Acknowledgement This study is partially supported by NIH NS053407 to J.H. Zhang.

Conflict of interest statement We declare that we have no conflict of interest.

References

- Baumann A, Audibert G, McDonnell J, Mertes PM (2007) Neurogenic pulmonary edema. *Acta Anaesthesiol Scand* 51:447–455
- Sozen T, Tsuchiyama R, Hasegawa Y, Suzuki H, Jadhav V, Nishizawa S, Zhang JH (2009) Role of interleukin-1 β in early brain injury after subarachnoid hemorrhage in mice. *Stroke* 40: 2519–2525
- Steinberg J, Halter J, Schiller H, Gatto L, Carney D, Lee HM, Golub L, Nieman G (2005) Chemically modified tetracycline prevents the development of septic shock and acute respiratory distress syndrome in a clinically applicable porcine model. *Shock* 24:348–356
- Hasegawa Y, Suzuki H, Sozen T, Rolland W, Zhang JH (2010) Activation of sphingosine 1-phosphate receptor-1 by FTY720 is neuroprotective after ischemic stroke in rats. *Stroke* 41:368–374
- Raßler B, Reißig C, Briest W, Tannapfel A, Zimmer HG (2003) Pulmonary edema and pleural effusion in norepinephrine-stimulated rats: hemodynamic or inflammatory effect? *Mol Cell Biochem* 250:55–63
- Sedy J, Zicha J, Kunes J, Jendelova P, Sykova E (2008) Mechanisms of neurogenic pulmonary edema development. *Physiol Res* 57: 499–506
- Uhal BD, Rayford H, Zhuang J, Li X, Lauka J, Soledad-Conrad V (2003) Apoptosis-dependent acute lung injury and repair after intratracheal instillation of noradrenaline in rats. *Exp Physiol* 88: 269–275
- Suzuki H, Sozen T, Hasegawa Y, Chen W, Zhang JH (2009) Caspase-1 inhibitor prevents neurogenic pulmonary edema after subarachnoid hemorrhage in mice. *Stroke* 40:3872–3875
- Zhang XH, Zhu RM, Xu WA, Wan HJ, Lu H (2007) Therapeutic effects of caspase-1 inhibitors on acute lung injury in experimental severe acute pancreatitis. *World J Gastroenterol* 13:623–627
- Zhang Y, Rosenberg PA (2004) Caspase-1 and poly (ADP-ribose) polymerase inhibitors may protect against peroxynitrite-induced neurotoxicity independent of their enzyme inhibitor activity. *Eur J Neurosci* 20:1727–1736
- Fontes RBV, Aguiar PH, Zanetti MV, Andrade F, Mandel M, Teixeira MJ (2003) Acute neurogenic pulmonary edema: case reports and literature review. *J Neurosurg Anesthesiol* 15:144–150

Hemoglobin Expression in Neurons and Glia After Intracerebral Hemorrhage

Yangdong He, Ya Hua, Richard F. Keep, Wenquan Liu, Michael M. Wang, and Guohua Xi

Abstract The purpose of this study was to examine the expression of hemoglobin (Hb) in the brain after intracerebral hemorrhage (ICH) and the effects of hemin and iron on neuronal Hb.

For the *in vivo* studies, male Sprague-Dawley rats received either a sham operation or an ICH. The rats were killed 1, 4, 24 or 72 h later, and brains were used for real-time polymerase chain reaction (PCR) and immunohistochemistry. For the *in vitro* study, primary cultured neurons were exposed to either hemin or vehicle. Some neurons also received treatment with deferoxamine, an iron chelator. Neurons were collected 24 h later for real-time PCR.

We found that α -globin (HbA) and β -globin (HbB) mRNA levels in the ipsilateral basal ganglia are significantly increased after ICH, and Hb is localized in neurons and glia cells. Exposure of neurons to hemin also upregulated HbA and HbB mRNA levels. Hemin-induced HbA and HbB expression in cultured neurons was reduced by deferoxamine treatment.

These results indicate that ICH increases HbA and HbB expression in neurons and glia cells, and that heme and iron may be important factors in inducing endogenous Hb expression after ICH.

Keywords Intracerebral hemorrhage · Hemoglobin · Hemin · Iron · Deferoxamine

Introduction

Vertebrate hemoglobin (Hb) is a heterotetramer of two α -globin (HbA) and two β -globin (HbB) subunits. Each subunit contains a hydrophobic pocket in which a heme molecule binds tightly and allows for the reversible binding of oxygen [1]. Vertebrate Hb has been traditionally thought to be exclusively present in cells of erythroid lineage. However, recent studies have shown that Hb is expressed in a variety of nonhematopoietic tissues and cell lines, including macrophages, epithelial cells and mesangial cells [2–4]. The presence of Hb in neurons has also been reported, and neuronal Hb is inducible after cerebral and ischemic preconditioning [5–8].

Intracerebral hemorrhage (ICH) is a common and often fatal subtype of stroke. After ICH, erythrocyte lysis can happen in the early phase, and Hb is released from the lysed blood cells [9]. There is evidence suggesting that free Hb is deleterious to the brain after ICH. Exogenous Hb can cause brain injury when injected into the brain *in vivo* [10, 11] or added to cerebral cortical neurons *in vitro* [12, 13]. Currently, the effects of ICH on endogenous Hb expression are unknown. In this study, we examined the change of endogenous Hb expression after ICH. The effects of hemin and iron on neuronal Hb expression were also examined.

Materials and Methods

Animal Preparation and Intracerebral Infusion

The University of Michigan Committee on the Use and Care of animals approved the protocols for these studies. Adult male Sprague-Dawley rats (275–325 g; Charles River Laboratories, Portage, MI) were used. Rats were anesthetized with pentobarbital (40 mg/kg, *i.p.*). A polyethylene catheter (PE-50) was then inserted into the right femoral artery to monitor arterial blood pressure and blood gases,

Y. He, Y. Hua, R.F. Keep, and W. Liu
Department of Neurosurgery, University of Michigan,
Ann Arbor, MI, USA

M.M. Wang
Department of Neurology, University of Michigan, Ann Arbor,
MI, USA

G. Xi (✉)
Department of Neurosurgery, University of Michigan,
Ann Arbor, MI, USA and
Department of Neurosurgery, University of Michigan,
R5018 Biomedical Science Research Building, Ann Arbor,
48109-2200, MI, USA
e-mail: guohuaxi@umich.edu

and to obtain blood for intracerebral blood infusion. Body temperature was maintained at 37.5°C by using a feedback-controlled heating pad. The animals were positioned in a stereotactic frame (Kopf Instruments, Tujunga, CA), and a cranial burr hole (1 mm) was drilled. Autologous blood was infused into the right caudate nucleus through a 26-gauge needle at a rate of 10 μ L/min using a microinfusion pump (Harvard Apparatus Inc., South Natick, MA). The coordinates were 0.2 mm anterior and 3.5 mm lateral to the bregma at a depth of 5.5 mm. After intracerebral infusion, the needle was removed and the skin incision closed with sutures. The rats received either a needle insertion (sham) or an intracerebral infusion of 100 μ L autologous whole blood and were killed 1, 4, 24 or 72 h ($n=8$, each time point) later for real-time polymerase chain reaction (PCR) and immunohistochemistry staining.

Cell Culture

Primary neuronal cultures were obtained from embryonic day-17 Sprague-Dawley rats (Charles River Laboratories, Portage, MI). Cultures were prepared according to a previously described procedure with some modifications [14]. The neurons were used for experiments after 7 days.

There were two parts to the in vitro study. In the first part, neurons were treated with either vehicle or hemin (50 or 100 μ M; Sigma, St. Louis, MO). Cells were collected 24 h later for real-time PCR and Western blot analysis. In the second part, neurons were treated with hemin (50 μ M) with or without deferoximine (50 μ M). Cells were used for real-time PCR 24 h later.

Real-Time PCR

Rats were anesthetized and decapitated. The brains were quickly removed, and a 3-mm-thick coronal brain slice was cut approximately 4 mm from the frontal pole. The slice was separated into ipsi- and contralateral basal ganglia. The samples were frozen in liquid nitrogen. In vitro, cell medium was removed and the plates washed three times with chilled PBS. The cells were quickly scraped and collected by centrifugation at 4°C, then stored at -80°C.

Total RNA was extracted from the frozen brain tissue and cultured cells with Trizol reagent (Gibco BRL, Grand Island, NY), and 1 μ g RNA was digested with deoxyribonuclease I (DNaseI, Amplification-grade, Gibco BRL, Grand Island, NY). Complimentary DNA was synthesized by reverse transcription using the digested 1- μ g RNA (11 μ L) with 14 μ L reaction buffer (Perkin Elmer, Foster City, CA) containing

dNTP (dATP, dCTP, dGTP and dTTP), 25 mmol/L MgCl₂, 10 \times polymerase chain reaction (PCR) buffer II, Random Hexamer Primer, Rnase inhibitor and MuL V reverse transcriptase. The reaction was performed at 42°C for 30 min and terminated at 99°C after 5 min. Diethyl pyrocarbonate water (75 μ L) was added to dilute the complimentary DNA to 100 μ L and stored at -20°C for later use.

Real-time quantitative PCR was performed with SYBR green as a double-strand DNA-specific dye using an Eppendorf Mastercycler EP Realplex (Eppendorf North America Inc., NY). The primers for rat HbA and HbB were designed from known sequences of rat HbA-mRNA (GeneBank no. U29528) and HbB-mRNA (GeneBank no. NM_033234) identified by PrimerQuest (Integrated DNA Technologies Inc., Coralville, IA). The primers were as follows: rat HbA 5'-TGATCC-ACCTCCT-TCTCTGCCCAA-3' (forward primer) and 5'-ATCAGTTGCCCAAGTGCTTCT TGC-3' (reverse primer), HbB 5'-ATGGCCTGAAACACTT GGACAACC-3' (forward primer) and 5'-TGGTGGCCCA AC-ACAATCACAATC-3' (reverse primer). Primers for rat GAPDH, a housekeeping gene, served as a control. They were as follows: 5'-CCGTGCCAAGATGAAATTGGCTGT-3' (forward) and 5'-TGTGCATATGTGCGTGTGTGTGTG-3' (reverse). PCR reactions were run in triplicate on a 96-well plate with a total volume of 20 μ L per well using 2.5 \times SYBR[®] Green universal master mix. Cycling conditions were 2 min at 95°C, 30 s at 95°C, 30 s at 60°C, 1 min at 72°C, 40 cycles, and a melting-curve program (60°C to 95°C with warming of 1.75°C per minute). The relative quantification analysis module was used to compare expression levels of a target gene. The expression levels were calculated by using the $\Delta\Delta C_T$ method [15]. Fold changes in gene expression of the target gene were equivalent to $2^{-\Delta\Delta C_T}$. With this method, a value equal to 1 represents no change in relative expression between untreated (set to 1.0) and treated samples. We defined overexpression when $2^{-\Delta\Delta C_T} > 1$ and underexpression when $2^{-\Delta\Delta C_T} < 1$.

Immunohistochemistry

Immunocytochemistry staining was performed according to the method described previously [16]. The primary antibody was polyclonal rabbit anti-hemoglobin antibody (1:400 dilution, Cappel, MP Biomedicals Inc., OH). Rhodamine-conjugated goat anti-rabbit antibody (Chemicon International Inc., Temecula, CA; 1:600 dilution) was used as second antibody. Normal rabbit immunoglobulin G was used as a negative control.

For immunofluorescent double labeling, the primary antibodies were rabbit anti-hemoglobin (Cappel, MP Biomedicals Inc., OH; 1:100 dilution), mouse anti-gial fibrillary acid protein (GFAP) (Chemicon International Inc. Temecula, CA;

1:100 dilution), mouse anti-rat neuronal nuclei (NeuN) (Chemicon International Inc., Temecula, CA; 1:100 dilution) and mouse anti-rat CD11b (MRC OX42; Serotec, Oxford, UK; 1:100 dilution). Rhodamine-conjugated goat anti-rabbit antibody (Chemicon International Inc., Temecula, CA; 1:100 dilution) and fluorescein isothiocyanate (FITC)-labeled horse anti-mouse antibody (Vector Laboratories, Burlingame, CA; 1:100 dilution) were used as second antibodies. The double labeling was analyzed using a fluorescence microscope.

Statistical Analysis

All data in this study are presented as mean \pm SD. Data were analyzed with Student's *t*-test and analysis of variance, or Kruskal-Wallis test and Mann-Whitney *U*-rank test. Statistical significance was set at 0.05.

Results

The time-course study demonstrated that HbA mRNA expression in the ipsilateral basal ganglia was significantly increased after ICH, reaching a peak at 4 h. HbB mRNA expression in the ipsilateral basal ganglia also peaked at 4 h after ICH and remained high at 24 h. There was a 10.7 ± 6.9 -fold increase in HbA mRNA and 59.5 ± 69 -fold increase in HbB mRNA in the ipsilateral basal ganglia at 4 h after ICH compared to shams ($p < 0.05$, Mann-Whitney *U*-rank test).

By immunohistochemistry, Hb-positive cells were found in the brains of both sham-operated and ICH rats. The negative control showed no immunoreactivity. After blood injection, Hb-positive cells were significantly increased in the ipsilateral basal ganglia compared to both the contralateral hemisphere and sham operated rats, particularly 72 h after ICH (Fig. 1). Double-labeling revealed that Hb-positive cells in the perihematomal area 72 h after ICH were colocalized with NeuN-positive, GFAP-positive and OX-42-positive cells, indicating that Hb is present not only in neurons, but also in glial cells.

Primary cultured neurons were treated with either hemin (50 or 100 μ M) or vehicle for 24 h. Some neurons also received deferoxamine (50 μ M), an iron chelator. Quantitative real-time PCR showed a 44.1 ± 21.2 - and 60.8 ± 11.8 -fold increase in HbA mRNA compared to the control after treatment with 50 or 100 μ M hemin, respectively ($p < 0.05$, Mann-Whitney *U*-rank test). HbB mRNA expression also increased by 3.19 ± 0.69 - and 2.76 ± 0.32 -fold, respectively, ($p < 0.05$, Mann-Whitney *U*-rank test). Deferoxamine had no significant effect on HbA and HbB mRNA expression under the

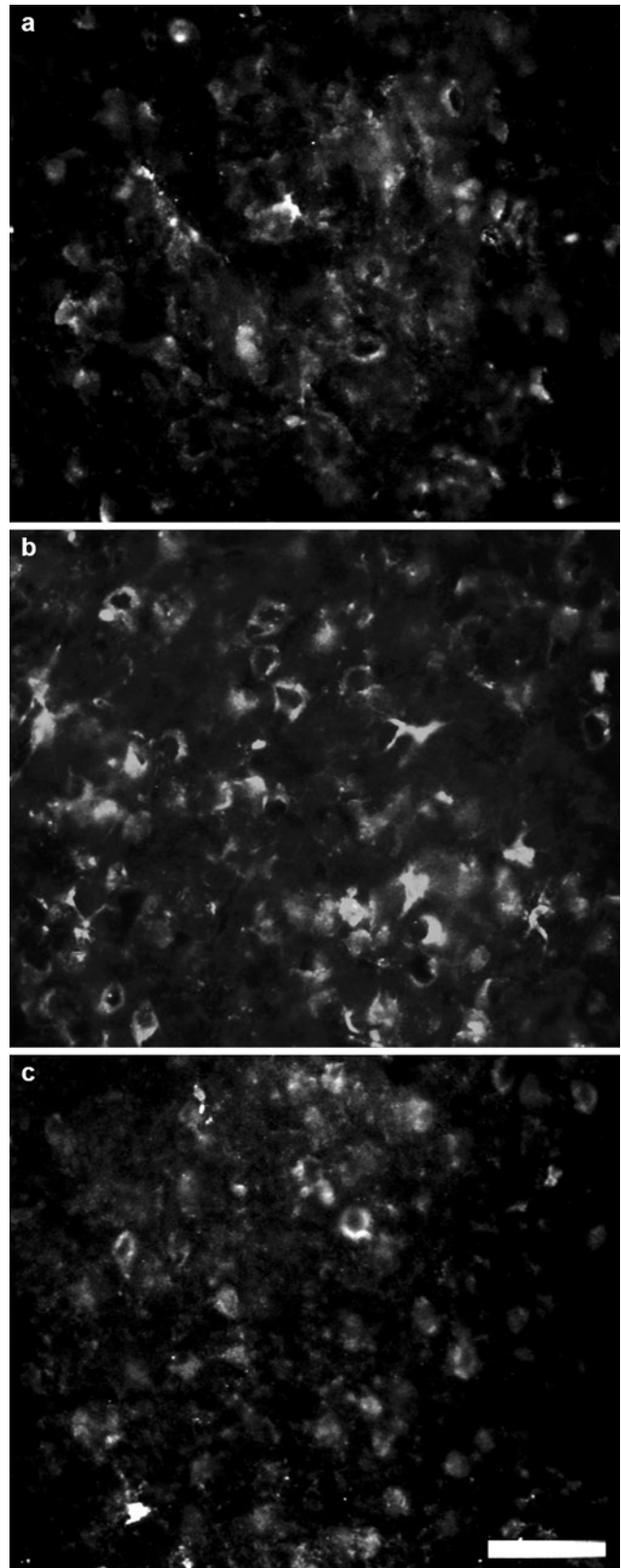


Fig. 1 Hb immunoreactivity in the ipsilateral basal ganglia 72 h after sham operation (a) and in the ipsilateral (b), and contralateral (c) basal ganglia 72 h after blood injection. Scale bar = 50 μ m

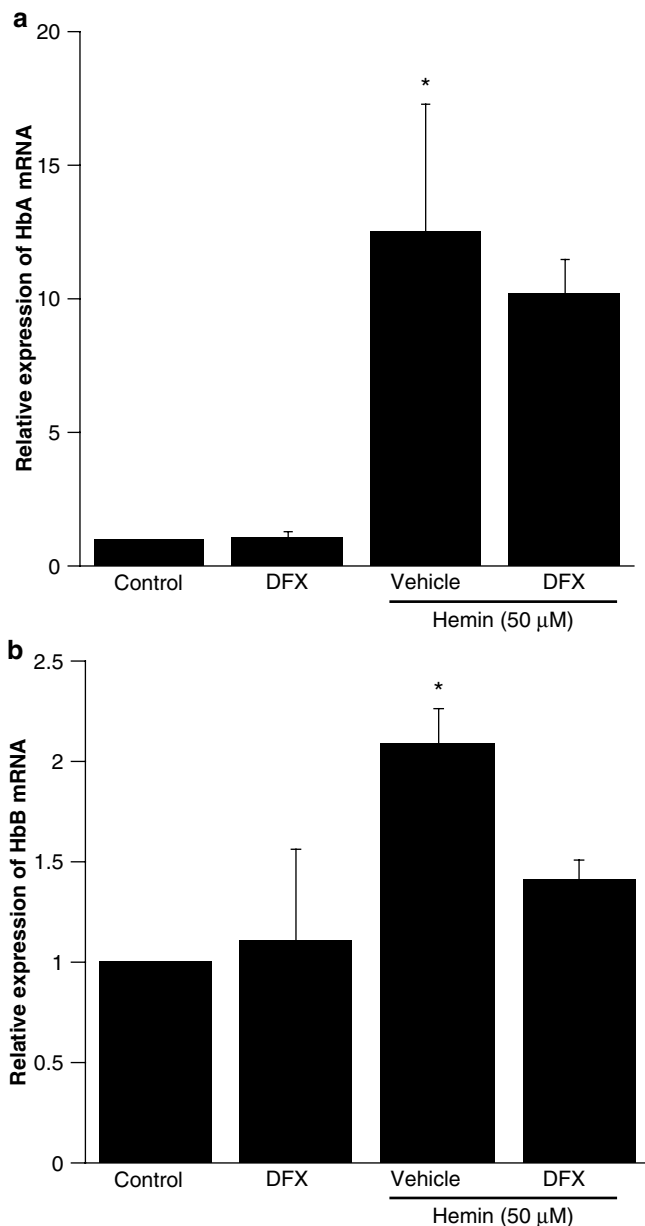


Fig. 2 Relative expression in HbA (a) and HbB (b) mRNA in primary cultured cerebral neurons after treatment with medium, deferoximine, hemin+vehicle or hemin+deferoximine for 24 h. Value are expressed as mean \pm S.D., $n=3$ per group; * $p<0.05$ versus other groups

normal conditions. However, hemin induction of HbA and HbB mRNA expression was significantly decreased by deferoxamine ($p<0.05$, Mann-Whitney U -rank test, Fig. 2).

Discussion

Our previous studies have demonstrated that Hb is induced after cerebral ischemia and ischemic preconditioning [5]. In this study, we found that Hb-positive cells were significantly

increased in the ipsilateral basal ganglia after blood injection. Double labeling demonstrated that Hb-positive cells in the perihematomal area were colocalized with NeuN-, GFAP- and OX42-positive cells, suggesting that Hb is expressed not only in neurons, but also in glial cells. Endogenous Hb in the neuron and glial cells can be derived from lysed red blood cells or local synthesis within the cells. To further confirm the expression of Hb in the brain after ICH, quantitative real-time PCR was performed. We found that both HbA and HbB mRNA levels were significantly increased after ICH, suggesting that local synthesis of Hb within the cells is involved in ICH-induced endogenous Hb upregulation.

Heme is released from hemoglobin after ICH. Extracellular heme can be transported into the cytoplasm of cells by binding to its transport protein hemopexin or heptoglobin [17]. Previous studies have shown that heme participates in the regulation of α - and β -globin gene expression in erythroid cells [18, 19]. Hemin, the ferric chloride salt of heme, has also been shown to regulate Hb gene expression [20–22]. In this study, we found that neuronal HbA and HbB mRNA levels were markedly upregulated by hemin.

Iron is another important structural component of Hb, which is released from heme by heme oxygenase (HO). Two HO isoforms have been identified in the brain. HO-1 is expressed at very low levels in normal brain, but it is rapidly induced in glia cells after ICH [23]. HO-2 is constitutively expressed in neurons in the brain [24]. Our previous studies have shown that iron concentration in the brain can reach very high levels and non-heme iron is not cleared from the brain within 4 weeks of ictus [23]. In the present study, we found that deferoxamine had no significant effects on HbA and HbB mRNA expression under normal conditions, but it did significantly reduce hemin-induced HbA and HbB mRNA expression, indicating that iron participates in the regulation of hemin-induced Hb expression. However, the effects of deferoxamine were incomplete, suggesting that factors other than iron may participate in the regulation of Hb expression by hemin.

In conclusion, our present study demonstrates that Hb expression is increased after ICH and Hb is localized in the neuron and astrocytes. ICH-induced Hb expression may be related to heme and iron released from hematoma. The function of Hb upregulation after ICH is still unknown, although it may impact iron homeostasis.

Acknowledgements This study was supported by grants NS-017760, NS-039866 and NS-057539 from the National Institutes of Health (NIH) and 0755717Z and 0840016N from the American Heart Association (AHA). The content is solely the responsibility of the authors and does not necessarily represent the official views of the NIH and AHA. MMW is supported by NS-062816 and NS-054724.

Conflict of interest statement We declare that we have no conflict of interest.

References

1. Poyart C, Wajcman H, Kister J (1992) Molecular adaptation of hemoglobin function in mammals. *Respir Physiol* 90:3–17
2. Liu L, Zeng M, Stamler JS (1999) Hemoglobin induction in mouse macrophages. *Proc Natl Acad Sci USA* 96:6643–6647
3. Newton DA, Rao KM, Dluhy RA, Baatz JE (2006) Hemoglobin is expressed by alveolar epithelial cells. *J Biol Chem* 281:5668–5676
4. Nishi H, Inagi R, Kato H, Tanemoto M, Kojima I, Son D, Fujita T, Nangaku M (2008) Hemoglobin is expressed by mesangial cells and reduces oxidant stress. *J Am Soc Nephrol* 19:1500–1508
5. He Y, Hua Y, Liu W, Hu H, Keep RF, Xi G (2009) Effects of cerebral ischemia on neuronal hemoglobin. *J Cereb Blood Flow Metab* 29:596–605
6. Ohyagi Y, Yamada T, Goto I (1994) Hemoglobin as a novel protein developmentally regulated in neurons. *Brain Res* 635:323–327
7. Richter F, Meurers BH, Zhu C, Medvedeva VP, Chesselet MF (2009) Neurons express hemoglobin alpha- and beta-chains in rat and human brains. *J Comp Neurol* 515:538–547
8. Schelshorn DW, Schneider A, Kuschinsky W, Weber D, Kruger C, Dittgen T, Burgers HF, Sabouri F, Gassler N, Bach A, Maurer MH (2009) Expression of hemoglobin in rodent neurons. *J Cereb Blood Flow Metab* 29:585–595
9. Xi G, Keep RF, Hoff JT (1998) Erythrocytes and delayed brain edema formation following intracerebral hemorrhage in rats. *J Neurosurg* 89:991–996
10. Huang FP, Xi G, Keep RF, Hua Y, Nemoianu A, Hoff JT (2002) Brain edema after experimental intracerebral hemorrhage: role of hemoglobin degradation products. *J Neurosurg* 96:287–293
11. Sadrzadeh SM, Anderson DK, Panter SS, Hallaway PE, Eaton JW (1987) Hemoglobin potentiates central nervous system damage. *J Clin Invest* 79:662–664
12. Regan RF, Panter SS (1993) Neurotoxicity of hemoglobin in cortical cell culture. *Neurosci Lett* 153:219–222
13. Wang X, Mori T, Sumii T, Lo EH (2002) Hemoglobin-induced cytotoxicity in rat cerebral cortical neurons: caspase activation and oxidative stress. *Stroke* 33:1882–1888
14. Jiang Y, Wu J, Hua Y, Keep RF, Xiang J, Hoff JT, Xi G (2002) Thrombin-receptor activation and thrombin-induced brain tolerance. *J Cereb Blood Flow Metab* 22:404–410
15. Livak KJ, Schmittgen TD (2001) Analysis of relative gene expression data using real-time quantitative PCR and the $2^{-\Delta\Delta C(T)}$ Method. *Methods* 25:402–408
16. Xi G, Keep RF, Hua Y, Xiang J, Hoff JT (1999) Attenuation of thrombin-induced brain edema by cerebral thrombin preconditioning. *Stroke* 30:1247–1255
17. Wagner KR, Sharp FR, Ardizzone TD, Lu A, Clark JF (2003) Heme and iron metabolism: role in cerebral hemorrhage. *J Cereb Blood Flow Metab* 23:629–652
18. Tahara T, Sun J, Igarashi K, Taketani S (2004) Heme-dependent up-regulation of the alpha-globin gene expression by transcriptional repressor Bach1 in erythroid cells. *Biochem Biophys Res Commun* 324:77–85
19. Tahara T, Sun J, Nakanishi K, Yamamoto M, Mori H, Saito T, Fujita H, Igarashi K, Taketani S (2004) Heme positively regulates the expression of beta-globin at the locus control region via the transcriptional factor Bach1 in erythroid cells. *J Biol Chem* 279:5480–5487
20. Fibach E, Kollia P, Schechter AN, Noguchi CT, Rodgers GP (1995) Hemin-induced acceleration of hemoglobin production in immature cultured erythroid cells: preferential enhancement of fetal hemoglobin. *Blood* 85:2967–2974
21. Rutherford TR, Clegg JB, Weatherall DJ (1979) K562 human leukaemic cells synthesise embryonic haemoglobin in response to haemin. *Nature* 280:164–165
22. Zhu Y, Sun Y, Jin K, Greenberg DA (2002) Hemin induces neuroglobin expression in neural cells. *Blood* 100:2494–2498
23. Wu J, Hua Y, Keep RF, Nakamura T, Hoff JT, Xi G (2003) Iron and iron-handling proteins in the brain after intracerebral hemorrhage. *Stroke* 34:2964–2969
24. Vincent SR, Das S, Maines MD (1994) Brain heme oxygenase isoenzymes and nitric oxide synthase are co-localized in select neurons. *Neuroscience* 63:223–231

Experimental Treatment for Cerebral Hemorrhage

Isoflurane Preconditioning Affords Functional Neuroprotection in a Murine Model of Intracerebral Hemorrhage

Paul R. Gigante, Geoffrey Appelboom, Brian Y. Hwang, Raqeeb M. Haque, Mason L. Yeh, Andrew F. Ducruet, Christopher P. Kellner, Justin Gorski, Sarah E. Keesecker, and E. Sander Connolly Jr.

Abstract Introduction: Exposure to isoflurane gas prior to neurological injury, known as anesthetic preconditioning, has been shown to provide neuroprotective benefits in animal models of ischemic stroke. Given the common mediators of cellular injury in ischemic and hemorrhagic stroke, we hypothesize that isoflurane preconditioning will provide neurological protection in intracerebral hemorrhage (ICH).

Methods: 24 h prior to intracerebral hemorrhage, C57BL/6J mice were preconditioned with a 4-h exposure to 1% isoflurane gas or room air. Intracerebral hemorrhage was performed using a double infusion of 30- μ L autologous whole blood. Neurological function was evaluated at 24, 48 and 72 h using the 28-point test. Mice were sacrificed at 72 h, and brain edema was measured.

Results: Mice preconditioned with isoflurane performed better than control mice on 28-point testing at 24 h, but not at 48 or 72 h. There was no significant difference in ipsilateral hemispheric edema between mice preconditioned with isoflurane and control mice.

Conclusion: These results demonstrate the early functional neuroprotective effects of anesthetic preconditioning in ICH and suggest that methods of preconditioning that afford protection in ischemia may also provide protection in ICH.

Keywords Intracerebral hemorrhage · Preconditioning · Isoflurane

Introduction

Intracerebral hemorrhage (ICH) is associated with the highest fatality rate of any stroke subtype, yet remains the cerebrovascular disease with perhaps the least impactful treatment options [1]. Strategies designed to prevent hematoma expansion have been minimally effective, and no therapy currently exists to mitigate injury to parenchyma surrounding the hematoma [2]. Spontaneous intracerebral hemorrhage is thought to impose mechanical stress on the surrounding parenchyma with consequent dysfunctional cellular and mitochondrial activity, as well as abnormal neurotransmission [3, 4]. Within hours of ictus, hemoglobin, cellular degradation products and coagulation factors induce vasogenic and cytotoxic edema by disruption of the blood-brain barrier and initiation of apoptosis. Peri-hematoma histology is characterized by edema, neuronal damage, macrophages and neutrophils and nests of intact neural tissue within and surrounding the hematoma [5]. Evidence also suggests that local mass effect may result in reduced cerebral blood flow to the hematoma periphery, placing intact neural tissue at particularly high risk for infarction [6]. Given evidence of multiple mechanisms involving post-hemorrhagic tissue injury, an area of at-risk tissue adjacent to the hematoma may exist at which novel therapeutic interventions can be directed.

Isoflurane, one of the most commonly utilized inhaled anesthetics, has been studied as a neuroprotective agent in ischemia [7]. Pretreatment with volatile anesthetics has been shown to induce prolonged neuroprotection in vitro and in vivo primarily by decreasing apoptosis and excitatory stress and increasing neuronal stability [8]. Studies in a rodent model of middle cerebral artery occlusion demonstrated significant reduction in infarct volume after pretreatment with isoflurane [7] and highlight the potential for preconditioning in reducing ischemic injury. Given the mechanisms of perihematoma cellular injury in ICH may reflect those found in ischemic injury and apoptosis, we hypothesized that isoflurane preconditioning would mitigate neurological injury in our murine model of intracerebral hemorrhage.

P.R. Gigante (✉), G. Appelboom, B.Y. Hwang, R.M. Haque, M.L. Yeh, A.F. Ducruet, C.P. Kellner, J. Gorski, S.E. Keesecker, and E.S. Connolly Jr.
Department of Neurological Surgery, Columbia University Medical Center, New York, 10032, NY, USA
e-mail: pg2223@columbia.edu

Materials and Methods

Isoflurane Preconditioning

Adult male C57BL/6J rats (8–10 weeks, 25–30 g body weight) (Jackson Laboratory, Bar Harbor, ME) were housed in the Barrier Facility of the Columbia University Medical Center, maintained at $22 \pm 2^\circ\text{C}$ with constant humidity under a 12:12 h light:dark cycle, and were allowed free access to water and laboratory chow. Experiments were carried out in accordance with the guidelines set forth by the IACUC Guide for the Care and Use of Laboratory Animals. Isoflurane preconditioning was carried out by placing mice in an air-tight anesthesia induction chamber while delivering 1% isoflurane in room air. Body temperature was controlled as needed using a feedback-regulated heat lamp. Mice were preconditioned with 1% isoflurane or room air alone for 4 h. Twenty-four hours after preconditioning, mice subsequently underwent experimental ICH ($n=16$) according to our established model of double-injection of autologous blood [9].

Experimental Intracerebral Hemorrhage

Preconditioned adult male C57BL/6J mice were subjected to experimental intracerebral hemorrhage (ICH) using autologous blood infusion via our model as previous described [9]. Mice were anesthetized with ketamine/xylazine (1 mg/kg) throughout the duration of surgery. Body temperature was regulated using a rectal probe connected to a feedback-controlled heat lamp. Once experimental ICH was achieved, mice were allowed to fully recover from anesthesia in an intensive care unit set at 37°C with constant humidity for 1 h. Once the mice were fully recovered from anesthesia, they were placed in a clean cage with access to food and water in our satellite facility.

Assessment of Neurological Deficit

Neurological deficit was determined using a 28-point test as outlined by Clark et al. [10]. At 24, 48 and 72 h post-ICH, all animals were assessed according to the 28-point test, evaluating body symmetry, gait, climbing, circling behavior, front-limb symmetry, compulsory circling and sensory response.

Preparation of Brain Samples

Three days after experimental ICH, mice were anesthetized with ketamine/xylazine (1 mg/kg) and were transcardially perfused with cold saline followed by removal of the brain for albumin Western blots ($n=16$).

Albumin Western Blot

Protein samples were loaded onto a NuPAGE 4–12% Bis-Tris Gel, and electrophoresis was performed in MOPS buffer at room temperature. Samples were then transferred to a 0.2- μm pore size nitrocellulose membrane, which was then blocked in 1.5% gelatin, 100 mM NaCl and 25 mM Tris pH 7.5 for 1 h at room temperature. Membranes were then washed and incubated with anti-albumin horseradish peroxidase conjugated antibody (A90-134P; Bethyl Laboratories) in 1% gelatin, 100 mM NaCl, 25 mM Tris pH 7.5 and 0.1% Tween-20 for 1 h at room temperature. Antibodies were then visualized using chemiluminescence (Supersignal West Pico Chemiluminescent Substrate; Pierce, Rockford, IL). Densitometric analysis was performed using ImageJ software (NIH, <http://rsb.info.nih.gov/ij>), and results were normalized to beta-actin expression.

Quantitative Assessment and Statistical Analysis

All data in this study are presented as mean \pm standard error. Data were analyzed with a Student's *t*-test, and significance levels were measured at $p < 0.05$.

Results

Functional Performance

Two cohorts of mice underwent functional testing following experimental ICH. Isoflurane-preconditioned mice ($n=8$) were administered 1% isoflurane in an air-tight chamber prior to ICH, and room air-preconditioned mice ($n=8$) were administered room air in the same preconditioning chamber prior to ICH. Functional 28-point testing was performed at 24, 48 and 72 h after ICH. Mice preconditioned with isoflurane performed significantly better than room air-preconditioned mice at 24 h (10.44 ± 0.87 vs. 14.1 ± 0.57 $p=0.009$). Though a continued trend was seen towards improved performance in mice preconditioned with isoflurane, the difference was not significant at 48 h (8.11 ± 1.39 vs. 11.30 ± 1.14 , $p=0.27$) and 72 h (6.22 ± 0.66 vs. 8.10 ± 0.92 , $p=0.33$) (Fig. 1). As demonstrated in previous experiments with our murine autologous double injection ICH model, the likelihood of observing significant functional deficits by 72 h diminishes considerably because all animals show a gradual recovery of function by 72 h after ICH [9].

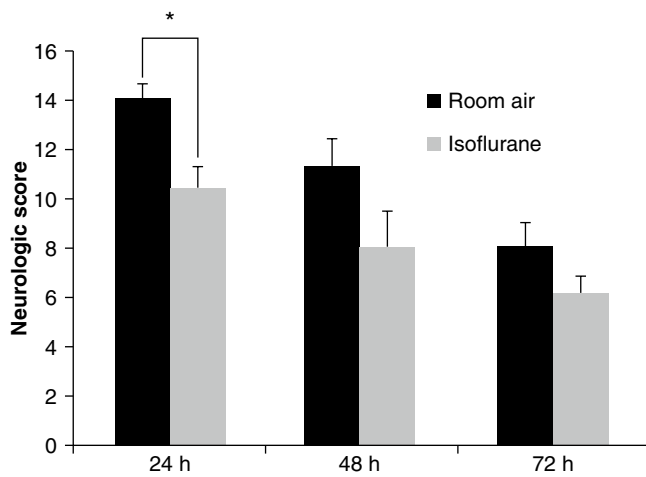


Fig. 1 Neurological score as assessed by 28-point testing in room air- and isoflurane-preconditioned mice at 24, 48 and 72 h. Values are expressed as mean \pm SEM. An *asterisk* represents significant difference by Student's T-testing ($p < 0.05$)

Brain Edema

Perihematomal brain edema was assessed by albumin content in the basal ganglia and cortex ipsilateral to the ICH ($n = 12$). Brain edema was not significantly less in mice preconditioned with isoflurane compared to control mice (5357.39 ± 341.58 vs. 7782.52 ± 1582.13 , $p = 0.165$) (Fig. 2).

Discussion

In light of recent evidence demonstrating the neuroprotective effects of preconditioning with volatile anesthetics in animal models of cerebral ischemia [11], we hypothesized that anesthetic preconditioning would also afford neurological protection in ICH, a condition that subjects neurological tissue to multiple, complex mechanisms of cellular injury [5, 12]. Cell death and ischemia may occur in salvageable perihematomal tissue following ICH, as microvasculature is subjected to mass effect, mechanical deformation, edema and inflammation. Although the relevance of “penumbral” ischemia in ICH remains controversial, and the precise mechanisms of neuroprotection in ischemic preconditioning are yet undefined, a historical overlap of neuroprotective interventions successful in both ischemic injury and ICH suggests a significant overlap in their contributory mechanisms of injury [13].

Our study is the first report of anesthetic preconditioning-induced neuroprotection in ICH and demonstrates that isoflurane pretreatment affords functional neuroprotection at 24 h after ICH, as assessed by 28-point testing. The only other report of preconditioning-induced protective effects we

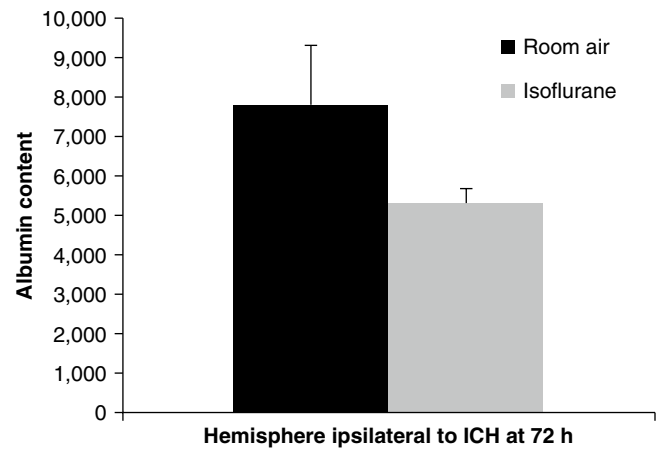


Fig. 2 Edema in the hemisphere ipsilateral to the ICH as measured by albumin content, assessed by Western blot from brains sacrificed at 72 h. Values are expressed as mean \pm SEM

identified in the ICH literature was a report of reduced perihematomal edema after hyperbaric oxygen preconditioning in rats [14]. That functional protection occurred in isoflurane-preconditioned mice at 24 h but not at 48 and 72 h may be a reflection of the tendency for functional deficits to improve by 2–3 days in our particular ICH model. Whether a reflection of the animal model alone or a true failure of anesthetic preconditioning to provide sustained neuroprotection in ICH, improved early recovery may still have important clinical implications.

This study did not demonstrate a significant reduction in ipsilateral hemispheric edema in preconditioned mice. Though in human ICH the contribution of brain edema to functional outcome remains controversial [5], we evaluated edema as an outcome measure because previous rodent ICH studies have suggested an association between reduced edema and improved functional performance, despite no direct evidence of a causal relationship [15–17]. Furthermore, the only other ICH preconditioning study, with hyperbaric oxygen pretreatment, demonstrated a significant reduction in perihematomal edema [14, 18]. However, our results support the notion that functional protection can be achieved in the absence of significant edema reduction, which both reflects human ICH studies demonstrating that absolute edema volume is not an independent predictor of outcome [19, 20] and points toward other mechanisms of neuronal injury modulation with experimental anesthetic preconditioning. At present, the downstream molecular effects of isoflurane preconditioning are incompletely understood [21]. A majority of the data showing neuroprotection with volatile anesthetics comes from animal models of ischemia, and has been hypothesized to involve the enactment of gene upregulation and long-term neuronal tolerance to ischemic insults [21–24]. Immediate early genes, ubiquitous transcription factors induced by a stress response, are thought to be the main component of tolerance when preconditioned hours to

days before an insult [7, 22]. The inducible nitric oxide synthase (iNOS) gene, whose downstream effects include modulation of glutamate signaling and the vasodilatory response, has been heavily implicated as one of these mediators in anesthetic preconditioning [7, 25, 26].

A limitation of the present study is a lack of comprehensive investigation of the potential mechanisms of protection, including assessment of the role of the iNOS and other candidate genes, and histological evaluation of peri-hematoma inflammatory cell infiltration and apoptotic cell death. Further studies are critical to determine the molecular and cellular processes of protection, which will ultimately lead us toward the optimal therapeutic targets for mitigation of injury in human ICH.

Conflict of interest statement We declare that we have no conflict of interest.

References

- Qureshi AI, Tuhim S, Broderick JP, Batjer HH, Hondo H, Hanley DF (2001) Spontaneous intracerebral hemorrhage. *N Engl J Med* 344:1450–1460
- Nyquist P (2010) Management of acute intracranial and intraventricular hemorrhage. *Crit Care Med* 38:946–953
- Lusardi TA, Wolf JA, Putt ME, Smith DH, Meaney DF (2004) Effect of acute calcium influx after mechanical stretch injury in vitro on the viability of hippocampal neurons. *J Neurotrauma* 21:61–72
- Qureshi AI, Ali Z, Suri MF, Shuaib A, Baker G, Todd K et al (2003) Extracellular glutamate and other amino acids in experimental intracerebral hemorrhage: an in vivo microdialysis study. *Crit Care Med* 31:1482–1489
- Xi G, Keep RF, Hoff JT (2006) Mechanisms of brain injury after intracerebral haemorrhage. *Lancet Neurol* 5:53–63
- Nath FP, Jenkins A, Mendelow AD, Graham DI, Teasdale GM (1986) Early hemodynamic changes in experimental intracerebral hemorrhage. *J Neurosurg* 65:697–703
- Kapinya KJ, Lowl D, Futterer C, Maurer M, Waschke KF, Isaev NK et al (2002) Tolerance against ischemic neuronal injury can be induced by volatile anesthetics and is inducible NO synthase dependent. *Stroke* 33:1889–1898
- Zheng S, Zuo Z (2003) Isoflurane preconditioning reduces purkinje cell death in an in vitro model of rat cerebellar ischemia. *Neuroscience* 118:99–106
- Rynkowski MA, Kim GH, Komotar RJ, Otten ML, Ducruet AF, Zacharia BE et al (2008) A mouse model of intracerebral hemorrhage using autologous blood infusion. *Nat Protoc* 3:122–128
- Clark WM, Lessov NS, Dixon MP, Eckenstein F (1997) Monofilament intraluminal middle cerebral artery occlusion in the mouse. *Neurol Res* 19:641–648
- Bhardwaj A, Castro IA, Alkayed NJ, Hurn PD, Kirsch JR (2001) Anesthetic choice of halothane versus propofol: impact on experimental perioperative stroke. *Stroke* 32:1920–1925
- Gong C, Boulis N, Qian J, Turner DE, Hoff JT, Keep RF (2001) Intracerebral hemorrhage-induced neuronal death. *Neurosurgery* 48:875–882, discussion 882–873
- Ducruet AF, Hassid BG, Mack WJ, Sosunov SA, Otten ML, Fusco DJ et al (2008) C3a receptor modulation of granulocyte infiltration after murine focal cerebral ischemia is reperfusion dependent. *J Cereb Blood Flow Metab* 28:1048–1058
- Qin Z, Song S, Xi G, Silbergleit R, Keep RF, Hoff JT et al (2007) Preconditioning with hyperbaric oxygen attenuates brain edema after experimental intracerebral hemorrhage. *Neurosurg Focus* 22:E13
- Gong Y, Hua Y, Keep RF, Hoff JT, Xi G (2004) Intracerebral hemorrhage: effects of aging on brain edema and neurological deficits. *Stroke* 35:2571–2575
- Nakamura T, Keep RF, Hua Y, Schallert T, Hoff JT, Xi G (2003) Deferoxamine-induced attenuation of brain edema and neurological deficits in a rat model of intracerebral hemorrhage. *Neurosurg Focus* 15:ECP4
- Thiex R, Mayfrank L, Rohde V, Gilsbach JM, Tsirka SA (2004) The role of endogenous versus exogenous tPA on edema formation in murine ICH. *Exp Neurol* 189:25–32
- Qin Z, Xi G, Keep RF, Silbergleit R, He Y, Hua Y (2008) Hyperbaric oxygen for experimental intracerebral hemorrhage. *Acta Neurochir Suppl* 105:113–117
- Gebel JM, Jauch EC, Brott TG, Khoury J, Sauerbeck L, Salisbury S et al (2002) Relative edema volume is a predictor of outcome in patients with hyperacute spontaneous intracerebral hemorrhage. *Stroke* 33:2636–2641
- Jauch E, Gebel J, Salisbury S, Broderick J, Brott T, Kothari R et al (1999) Lack of association between early edema and outcome in spontaneous intracerebral hemorrhage. *Stroke* 30:249, Abstract
- Zheng S, Zuo Z (2004) Isoflurane preconditioning induces neuroprotection against ischemia via activation of P38 mitogen-activated protein kinases. *Mol Pharmacol* 65:1172–1180
- Clarkson AN (2007) Anesthetic-mediated protection/preconditioning during cerebral ischemia. *Life Sci* 80:1157–1175
- Kawaguchi M, Kimbro JR, Drummond JC, Cole DJ, Kelly PJ, Patel PM (2000) Isoflurane delays but does not prevent cerebral infarction in rats subjected to focal ischemia. *Anesthesiology* 92:1335–1342
- Li QF, Wang XR, Yang YW, Su DS (2006) Up-regulation of hypoxia inducible factor 1alpha by isoflurane in Hep3B cells. *Anesthesiology* 105:1211–1219
- Huang PL (2004) Nitric oxide and cerebral ischemic preconditioning. *Cell Calcium* 36:323–329
- Westphalen RI, Hemmings HC (2006) Volatile anesthetic effects on glutamate versus GABA release from isolated rat cortical nerve terminals: 4-aminopyridine-evoked release. *J Pharmacol Exp Ther* 316:216–223
- Blanck TJ, Haile M, Xu F, Zhang J, Heerdt P, Veselis RA et al (2000) Isoflurane pretreatment ameliorates postischemic neurologic dysfunction and preserves hippocampal Ca²⁺/calmodulin-dependent protein kinase in a canine cardiac arrest model. *Anesthesiology* 93:1285–1293
- Matchett GA, Allard MW, Martin RD, Zhang JH (2009) Neuroprotective effect of volatile anesthetic agents: molecular mechanisms. *Neurol Res* 31:128–134
- Mocco J, Mack WJ, Ducruet AF, Sosunov SA, Sughrue ME, Hassid BG et al (2006) Complement component C3 mediates inflammatory injury following focal cerebral ischemia. *Circ Res* 99:209–217
- Rynkowski MA, Kim GH, Garrett MC, Zacharia BE, Otten ML, Sosunov SA et al (2009) C3a receptor antagonist attenuates brain injury after intracerebral hemorrhage. *J Cereb Blood Flow Metab* 29:98–107

The Neuroprotective Effects of Cyclooxygenase-2 Inhibition in a Mouse Model of Aneurysmal Subarachnoid Hemorrhage

R. Ayer, V. Jadhav, T. Sugawara, and John H. Zhang

Abstract The CNS inflammatory reaction occurring after aneurysmal subarachnoid hemorrhage (SAH) involves the upregulation of numerous cytokines and prostaglandins. Cyclooxygenase (COX) inhibition is a well-established pharmacological anti-inflammatory agent. Previous studies have shown marked increases in COX-2 expression in neurons, astrocytes, microglia, and endothelial cells following brain injury. COX-2 inhibition has been shown to be beneficial following various types of brain injury. This experiment investigates the role of COX-2 activity in early brain injury following SAH. CD-1 mice were subjected to an endovascular perforation model of SAH or SHAM surgery. Following experimental SAH animals were treated with the specific COX-2 inhibitor, NS398, in dosages of either 10 or 30 mg/kg. Neurological performance and brain edema were evaluated 24 and 72 h after SAH. NS398 at 30 mg/kg significantly reduced SAH-induced neurological deterioration. NS 398 at 30 mg/kg resulted in a trend toward the reduction of SAH-induced cerebral edema. Treatment had no effect on mortality. This experiment provides preliminary evidence that COX-2 inhibition is an effective pharmacological intervention for the prevention of brain edema and the preservation of neurological function following SAH.

Keywords Aneurysmal subarachnoid hemorrhage · Early brain injury · Cyclooxygenase inhibition · COX-2 · Cerebral edema

Introduction

Inflammation is designed as an active defense reaction against insults in multicellular organisms, but is often associated with the overexpression of various cell signals that contribute to the pathogenesis of neurodegenerative brain diseases, traumatic brain injury, and stroke [1]. Inflammation is triggered by several factors including signals derived from injured or dying cells, proinflammatory mediators from endogenous cells, as well as molecular signals from infiltrating immune cells [2]. Deleterious molecules in the form of cytokines and free radical oxygen species are produced during the early stages of brain inflammation and correlate with reduced neuronal survival and the progression of gliosis. Glial cells (e.g., astrocytes and microglia) are activated by proinflammatory mediators released from infiltrating immune cells and contribute to the propagation of the inflammatory cascade through the production of their own proinflammatory mediators [3–6]. These processes induce glial scarring, which is a significant obstacle to axonal regeneration and likely affects clinical recovery following a CNS insult [7–9].

Among the several types of proinflammatory mediators, prostanoids, a product of arachidonic acid (AA) metabolism, are generated through the COX pathway. These compounds are also largely produced by activated glial cells and act as potent local regulators of the pathogenic processes in brain inflammation [10]. Evidence has shown that the COX-2 isoform, but not COX-1, plays a crucial role in inflammation-induced pathology. Treatment with selective inhibitors of COX-2 has been found to reduce brain inflammation [11–18] and increase neuronal survival in focal ischemia models [19]. Studies of the COX-2-null mouse have indicated that COX-2 deficiency attenuates ischemia-induced brain damage and

R. Ayer

Department of Neurosurgery, Loma Linda University Medical Center, Loma Linda, CA, USA

V. Jadhav and T. Sugawara

Department of Physiology and Pharmacology, Loma Linda University Medical Center, Loma Linda, CA, USA

J.H. Zhang (✉)

Department of Neurosurgery, Loma Linda University Medical Center, Loma Linda, CA, USA and

Department of Anesthesiology, Loma Linda University Medical Center, Loma Linda, CA, USA and

Department of Physiology and Pharmacology, Loma Linda University Medical Center, Loma Linda, CA, USA and

Department of Neurosurgery, Loma Linda University Medical Center, 11234 Anderson Street, Room 2562B, Loma Linda, CA, USA

e-mail: johnzhang3910@yahoo.com

protects neurons from excitotoxic insult [20]. COX-2 is therefore thought to be a promising pharmacological target for the treatment of brain inflammation. Aneurysmal subarachnoid hemorrhage has a significant inflammatory component induced by the toxicity of the extravasated blood as well as that induced by the ischemia and recruitment of immune cells that follows aneurysm rupture [21], and several studies document an increase in COX-2 expression following experimental SAH [22–24]. This experiment tests the role of COX-2 inhibition following experimental aneurysmal subarachnoid hemorrhage as a potential treatment for the preservation of neurological function and the reduction of brain swelling following aneurysmal SAH.

Materials and Methods

Animals

This protocol was evaluated and approved by the Institutional Animal Care and Use Committee at Loma Linda University, Loma Linda, California. Forty-four male CD-1 mice weighing 20–25 g were used for all studies (Harlan Corp., Indianapolis, IN). Animals were housed in a climate-controlled environment with strict day/night light cycles prior to surgery. Animals were divided into four groups: SHAM=Vehicle, SAH+Vehicle, SAH+10 mg/kg NS398, and SAH + 30 mg/kg NS398.

Treatment

After SHAM surgery or experimental SAH, NS-398 (Cayman Chemical Co., Ann Arbor, MI) was dissolved in 50 mL dimethyl sulfoxide, and diluted 10-fold with saline prior to intraperitoneal injection in a dosages of either 10 mg/kg or 30 mg/kg. Treatments were administered at 1, 6, and 12 h in accordance with previous dosages effective in treating ischemic brain injury [12, 13, 15, 16, 18].

Brain Injury

Prior to surgery general anesthesia was induced with Ketamine (80 mg/kg intraperitoneally) and xylazine (10 mg/kg intraperitoneally). Spontaneous ventilation without airway management was permitted by this anesthetic combination. Core body temperature was kept at $37 \pm 0.5^\circ\text{C}$. Mice underwent endovascular perforation of the internal carotid artery bifurcation as previously described [25, 26].

In summary, a sharpened 5-0 nylon suture was threaded through the ICA to puncture the cerebral vasculature at the ICA bifurcation.

Neurological Testing and Measurement of Brain Edema

All neurological scoring and brain edema measurements were performed by an independent researcher blinded to the experimental conditions. A modified 21-point Garcia scoring system was used to assess neurological function in the mice 24 and 72 h after surgery [27, 28]. Additional testing included evaluation of the animals' performance on previously established beam balance [29] and wire hang tests [30]. Brain edema was evaluated at 24 and 72 h by measuring brain water content. Briefly, brains were sectioned, immediately weighed, dried for 48 h, and weighed again to calculate brain water content: $([\text{wet weight} - \text{dry weight}] / \text{wet weight}) \times 100$. One-way ANOVA testing with a p value of 0.05 was used to test for statistical significance.

Results

Mortality

Six of the 44 experimental animals died within 1 h of SAH prior to any vehicle or NS398 administration. No SHAM animals died. Ten of the remaining 38 animals were sacrificed at 24 h; their brains were preserved and will be the subject of more detailed studies. Therefore, 38 animals were assessed neurologically at 24 h, 30 of which were then killed (20 to brain edema, 10 to other studies). The remaining eight were assessed at 72 h and then killed for brain edema measurements.

Neurological Function

Experimental SAH created significant neurological deficits in all groups versus vehicle-injected animals in each of the three neurological assessments given (Figs. 1 and 2). Treatment with 30 mg/kg of NS398 mitigated neurological deficits following SAH in comparison to the SAH+Vehicle treated group (Figs. 1 and 2a; $p < 0.05$) at 24 h; this trend continued at 72 h after injury, but did not reach significance because of the small sample size (Figs. 1 and 2b). Low dose treatment (10 mg/kg) did not mitigate neurological deterioration 24 h following SAH ($p > 0.05$) and was not tested at 72 h.

Brain Edema

Experimental SAH created edema in the left frontal hemisphere of mice 24 and 72 h after SAH. Treatment with 30 mg/kg of NS 398 shows a trend toward the prevention of increases in brain water content 24 and 72 h after experimental SAH (Fig. 3). Brain edema at 72 h after SAH was not tested in the 10 mg/kg group.

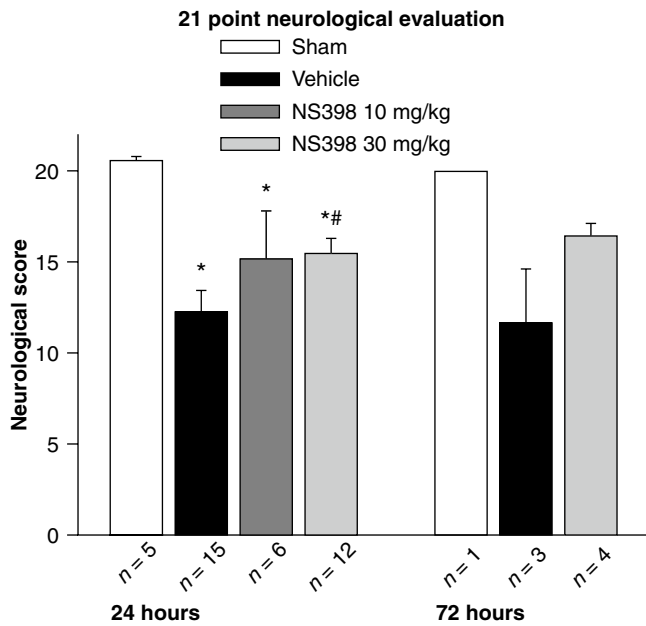


Fig. 1 SAH induced significant declines in neurological function at 24 and 72 h after injury. Treatment with high-dose NS398 leads to a significant improvement in neurological function versus SAH+ Vehicle. Treatment was administered at 1, 6 and 12 h following SAH. * $p < 0.05$ vs. SHAM, # $p < 0.05$ vs. SAH+ Vehicle; ANOVA

Discussion

Increases in COX-2 activity following brain injury have been associated with increased neurological injury, and its expression is significantly increased following SAH [22–24]. Accordingly, this experiment is the first to provide evidence that COX-2 inhibition is an effective pharmacological intervention for the prevention of brain edema and the preservation of neurological function following aneurysmal SAH. In vivo studies by Nakayama et al. [15, 19] have indicated that selective COX-2 inhibition by SC58125 prevented CA1 hippocampal neurons from global ischemia [15, 19]. Similar protection may be provided by COX-2 inhibitors in aneurysmal SAH as its victims also experience global ischemia as a result of elevated ICP and reduced perfusion pressure following aneurysm rupture. In addition to global ischemia, aneurysmal SAH elicits a characteristic inflammatory response [31] and has associated increases in COX-2 expression [22–24]. Candelario-Jali et al. demonstrated that breakdown of the BBB, increased MMP expression, and oxidative stress were attenuated by the administration of COX-2 inhibitors [32]. Spreading depression (SD) is a wave of sustained depolarization that challenges the energy metabolism of cells and can contribute to a sustained mechanism of continued cell death following subarachnoid hemorrhage [33]. Koistinaho et al. demonstrated that SD induces COX-2 mRNA expression in neurons and thus is a likely contributor to COX-2 expression following SAH [34]. Several studies not only suggest that COX-2 inhibition will reduce cerebral edema and neuronal cell death following aneurysmal SAH, but also support the possibility that COX-2 inhibition will help with function recovery and corroborate

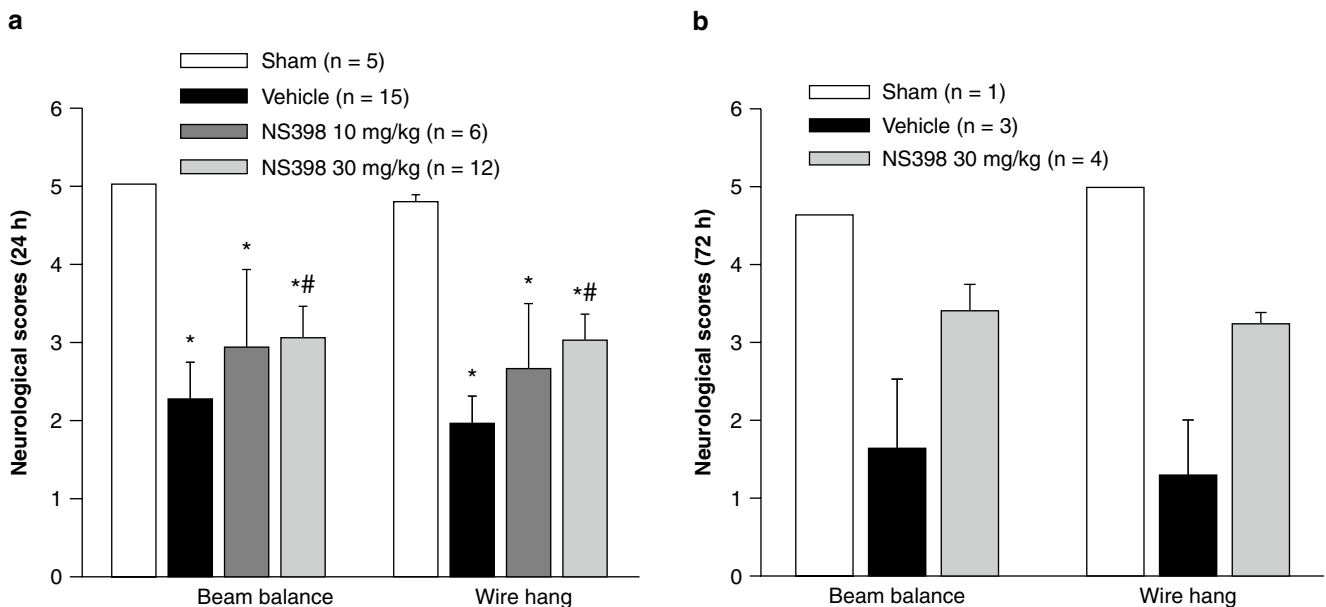


Fig. 2 Beam balance and wire hang testing at 24 h (a) and 72 h (b) demonstrate the neuroprotection provided by high dosages of the COX-2 inhibitor NS398. * $p < 0.05$ vs. SHAM, # $p < 0.05$ vs. SAH+ Vehicle; ANOVA

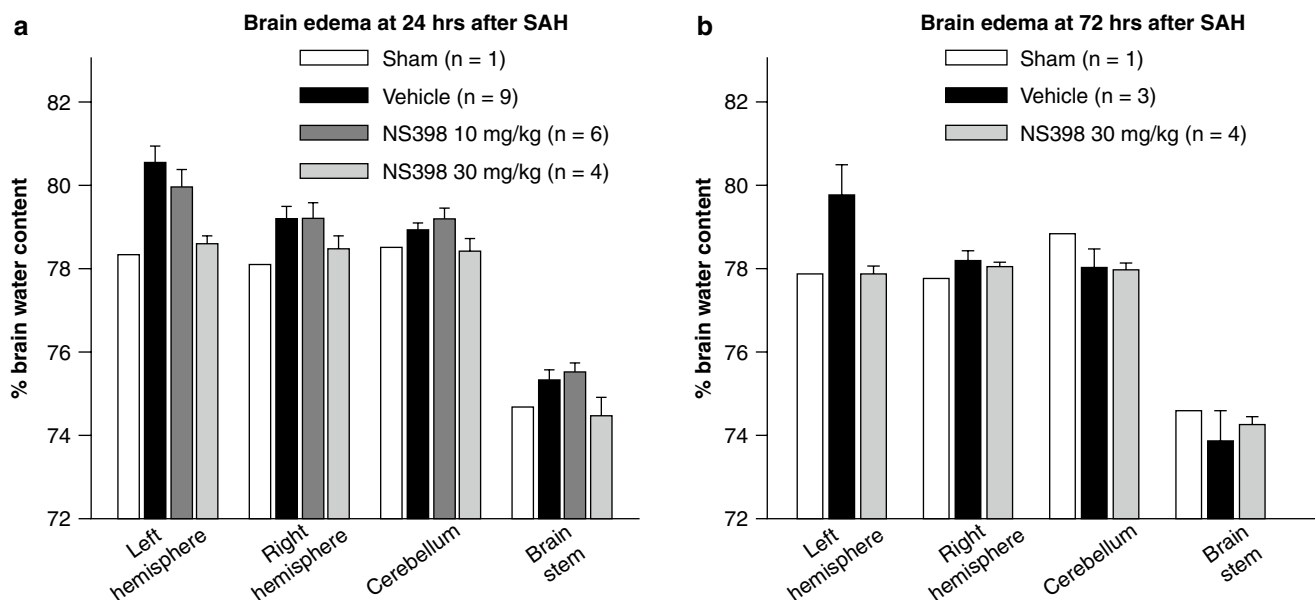


Fig. 3 Data demonstrating a trend toward reduced cerebral edema following treatment with 30 mg/kg of NS398. Treatment was administered at 1, 6, and 12 h following SAH. Brains were collected and

sectioned at 24 h (a) and 72 h (b) after injury. The *left* hemisphere typically demonstrated the greatest amount of edema as this area is next to the location of arterial rupture

a role for COX-2 inhibition following neurological injury. In experimental models of neurodegeneration high levels of COX-2 induction occurred in the brain, and treatment with the selective COX-2 inhibitor, Celecoxib, enhanced functional recovery [35]. Additional studies found functional recovery in neonatal global ischemia models following COX-2 inhibition [36].

In summary, our experiment contributes to the small but growing body of evidence showing that COX-2 inhibition provides neuroprotection in neurological injury and is the first to do so concerning aneurysmal subarachnoid hemorrhage. It is important to note that the previously wide use of COX-2 inhibitors for various inflammatory pathologies was severely restricted in the face of concerns for thrombotic cardiac events in the early part of this past decade. This concern was made most public by the worldwide withdrawal of the drug rofecoxib (Vioxx) from the market in 2004 amidst these concerns. However, it is likely that the potential benefits of selective COX-2 inhibition during the relatively brief period of early brain injury will outweigh these thrombotic risks in the treatment aneurysmal SAH and may provide a new venue for the application of this class of drug.

Acknowledgements This study was partially supported by grants from NIH to JHZ.

Conflict of interest statement We declare that we have no conflict of interest.

References

- Cederberg D, Siesjo P (2010) What has inflammation to do with traumatic brain injury? *Childs Nerv Syst* 26(2):221–226
- Dong Y, Benveniste EN (2001) Immune function of astrocytes. *Glia* 36(2):180–190
- Giulian D, Baker TJ, Shih LC, Lachman LB (1986) Interleukin 1 of the central nervous system is produced by ameboid microglia. *J Exp Med* 164(2):594–604
- Norton WT, Aquino DA, Hozumi I, Chiu FC, Brosnan CF (1992) Quantitative aspects of reactive gliosis: a review. *Neurochem Res* 17(9):877–885
- Sawada M, Kondo N, Suzumura A, Marunouchi T (1989) Production of tumor necrosis factor- α by microglia and astrocytes in culture. *Brain Res* 491(2):394–397
- Iadecola C, Sugimoto K, Niwa K, Kazama K, Ross ME (2001) Increased susceptibility to ischemic brain injury in cyclooxygenase-1-deficient mice. *J Cereb Blood Flow Metab* 21(12):1436–1441
- Liuzzi FJ, Lasek RJ (1987) Astrocytes block axonal regeneration in mammals by activating the physiological stop pathway. *Science* 237(4815):642–645
- Reier PJ, Houle JD (1988) The glial scar: its bearing on axonal elongation and transplantation approaches to CNS repair. *Adv Neurol* 47:87–138
- Eddleston M, Mucke L (1993) Molecular profile of reactive astrocytes – implications for their role in neurologic disease. *Neuroscience* 54(1):15–36
- Minghetti L, Levi G (1998) Microglia as effector cells in brain damage and repair: focus on prostanooids and nitric oxide. *Prog Neurobiol* 54(1):99–125
- Candelario-Jalil E, Gonzalez-Falcon A, Garcia-Cabrera M, Leon OS, Fiebich BL (2007) Post-ischaemic treatment with the cyclooxygenase-2 inhibitor nimesulide reduces blood-brain barrier disruption and leukocyte infiltration following transient focal cerebral ischaemia in rats. *J Neurochem* 100(4):1108–1120

12. Kawano T, Anrather J, Zhou P et al (2006) Prostaglandin E2 EP1 receptors: downstream effectors of COX-2 neurotoxicity. *Nat Med* 12(2):225–229
13. Kunz A, Anrather J, Zhou P, Orio M, Iadecola C (2007) Cyclooxygenase-2 does not contribute to postischemic production of reactive oxygen species. *J Cereb Blood Flow Metab* 27(3):545–551
14. Kunz T, Marklund N, Hillered L, Oliw EH (2002) Cyclooxygenase-2, prostaglandin synthases, and prostaglandin H2 metabolism in traumatic brain injury in the rat. *J Neurotrauma* 19(9):1051–1064
15. Nagayama M, Niwa K, Nagayama T, Ross ME, Iadecola C (1999) The cyclooxygenase-2 inhibitor NS-398 ameliorates ischemic brain injury in wild-type mice but not in mice with deletion of the inducible nitric oxide synthase gene. *J Cereb Blood Flow Metab* 19(11):1213–1219
16. Nogawa S, Zhang F, Ross ME, Iadecola C (1997) Cyclo-oxygenase-2 gene expression in neurons contributes to ischemic brain damage. *J Neurosci* 17(8):2746–2755
17. Scali C, Giovannini MG, Prosperi C, Bellucci A, Pepeu G, Casamenti F (2003) The selective cyclooxygenase-2 inhibitor rofecoxib suppresses brain inflammation and protects cholinergic neurons from excitotoxic degeneration in vivo. *Neuroscience* 17(4):909–919
18. Sugimoto K, Iadecola C (2003) Delayed effect of administration of COX-2 inhibitor in mice with acute cerebral ischemia. *Brain Res* 960(1–2):273–276
19. Nakayama M, Uchimura K, Zhu RL et al (1998) Cyclooxygenase-2 inhibition prevents delayed death of CA1 hippocampal neurons following global ischemia. *Proc Natl Acad Sci USA* 95(18):10954–10959
20. Iadecola C, Alexander M (2001) Cerebral ischemia and inflammation. *Curr Opin Neurol* 14(1):89–94
21. Ayer RE, Zhang JH (2008) The clinical significance of acute brain injury in subarachnoid hemorrhage and opportunity for intervention. *Acta Neurochir Suppl* 105:179–184
22. Osuka K, Suzuki Y, Watanabe Y, Takayasu M, Yoshida J (1998) Inducible cyclooxygenase expression in canine basilar artery after experimental subarachnoid hemorrhage. *Stroke* 29(6):1219–1222
23. Osuka K, Watanabe Y, Yamauchi K et al (2006) Activation of the JAK-STAT signaling pathway in the rat basilar artery after subarachnoid hemorrhage. *Brain Res* 1072(1):1–7
24. Tran Dinh YR, Jomaa A, Callebert J et al (2001) Overexpression of cyclooxygenase-2 in rabbit basilar artery endothelial cells after subarachnoid hemorrhage. *Neurosurgery* 48(3):626–633
25. Schwartz AY, Masago A, Sehba FA, Bederson JB (2000) Experimental models of subarachnoid hemorrhage in the rat: a refinement of the endovascular filament model. *J Neurosci Methods* 96(2):161–167
26. Sozen T, Tsuchiyama R, Hasegawa Y et al (2009) Role of interleukin-1beta in early brain injury after subarachnoid hemorrhage in mice. *Stroke* 40(7):2519–2525
27. Bravo TP, Matchett GA, Jadhav V et al (2008) Role of histamine in brain protection in surgical brain injury in mice. *Brain Res* 1205:100–107
28. Garcia JH, Wagner S, Liu KF, Hu XJ (1995) Neurological deficit and extent of neuronal necrosis attributable to middle cerebral artery occlusion in rats. Statistical validation. *Stroke* 26(4):627–634
29. Colombel C, Lalonde R, Caston J (2002) The effects of unilateral removal of the cerebellar hemispheres on motor functions and weight gain in rats. *Brain Res* 950(1–2):231–238
30. Manaenko A, Lekic T, Sozen T, Tsuchiyama R, Zhang JH, Tang J (2009) Effect of gap junction inhibition on intracerebral hemorrhage-induced brain injury in mice. *Neurol Res* 31(2):173–178
31. Kubota T, Handa Y, Tsuchida A, Kaneko M, Kobayashi H, Kubota T (1993) The kinetics of lymphocyte subsets and macrophages in subarachnoid space after subarachnoid hemorrhage in rats. *Stroke* 24(12):1993–2000
32. Candelario-Jalil E, Taheri S, Yang Y et al (2007) Cyclooxygenase inhibition limits blood-brain barrier disruption following intracerebral injection of tumor necrosis factor-alpha in the rat. *J Pharmacol Exp Ther* 323(2):488–498
33. Dreier JP, Woitzik J, Fabricius M et al (2006) Delayed ischaemic neurological deficits after subarachnoid haemorrhage are associated with clusters of spreading depolarizations. *Brain* 129(Pt 12):3224–3237
34. Koistinaho J, Chan PH (2000) Spreading depression-induced cyclooxygenase-2 expression in the cortex. *Neurochem Res* 25(5):645–651
35. Gobbo OL, O'Mara SM (2004) Post-treatment, but not pre-treatment, with the selective cyclooxygenase-2 inhibitor celecoxib markedly enhances functional recovery from kainic acid-induced neurodegeneration. *Neuroscience* 125(2):317–327
36. Fathali N, Ostrowski RP, Lekic T et al (2010) Cyclooxygenase-2 inhibition provides lasting protection against neonatal hypoxic-ischemic brain injury. *Crit Care Med* 38(2):572–578

Sonic Hedgehog Agonist Fails to Induce Neural Stem Cell Precursors in a Porcine Model of Experimental Intracranial Hemorrhage

Jing Tong, Jonathan M. Latzman, Judah Rauch, David S. Zagzag, Jason H. Huang, and Uzma Samadani

Abstract Background: The role of endogenous neural stem cell progenitors in recovery from intracranial hemorrhage remains to be elucidated. Proliferation of such stem cells in the subventricular zone has been described in rodent models of experimental intracranial hemorrhage. Administration of a sonic hedgehog agonist at the time of hemorrhage was hypothesized to increase the quantity of such precursor cells.

Methods: Two groups of pigs were subjected to injection of autologous blood into the right frontal lobe. One group was also injected at the same site with a sonic hedgehog agonist at the time of the hemorrhage to stimulate cell growth, and the other was given a vehicle control. The pigs received intravenous BrdU for 5 days postoperatively to label replicating cells, and then were sacrificed at intervals up to 21 days.

Results: Pigs in the hemorrhage only group demonstrated increased and more persistent BrdU staining in the subventricular zone relative to pigs in the group that received sonic hedgehog agonist. The latter group demonstrated increased BrdU activity in non-neural lineage cells in the area of the hemorrhage.

Conclusion: Sonic hedgehog agonist did not induce subventricular zone neural stem cell progenitor division after experimental intracranial hemorrhage in a pig model.

Keywords Intracranial hemorrhage · Neurogenesis · Sonic hedgehog · Stem cell · Stroke

Introduction

There exists a population of neuronal precursor cells within the subventricular zone (SVZ) and dentate gyrus of the adult human brain [1] that is induced to proliferate and differentiate by ischemia, trauma or neurodegenerative insult (reviewed in [2]). In animal models, migration of these precursor cells and spontaneous differentiation into functioning neurons has been seen after ischemia [3].

This population of endogenous neural precursors represents a tantalizing target for exogenous manipulation of cellular fate [4]. The signal transduction molecule and putative morphogen sonic hedgehog (SHH) secreted by the floor plate and notochord, which is itself regulated by retinoic acid [5], FOX (Forkhead box) proteins [6] and cytokines [7, 8], induces ventral cell types and suppresses dorsal cell types in the neural tube. SHH induces dopaminergic and other neuronal phenotypes in chick mesencephalic explants [9], and its retrovirally mediated expression in the chick neural tube induces ventral markers in the dorsal brain [10]. SHH functions through a concentration gradient; lower concentrations of SHH result in differentiation of precursor cells into motor neurons whereas higher concentrations result in floor plate cells [11]. SHH works both in conjunction with and independently from other molecules including the BMP (bone morphogenetic proteins) and FGF (fibroblast growth factor) proteins [12, 13] and is required both early and late for induction of motor neurons rather than interneurons [11].

Recognition of the role of SHH in neural development has led to experimentation with SHH and associated factors as potential therapeutic modalities for the treatment of conditions requiring neurogenesis [14–17]. Injection of SHH into the rat striatum shows induction of PTCH in the SVZ [18] and results in a reduction of behavioral deficits in a rat

J. Tong and J.H. Huang
Department of Neurosurgery, University of Rochester,
New York, NY, USA

J.M. Latzman, J. Rauch, and U. Samadani (✉)
Department of Neurosurgery, New York University,
423 E. 23rd St MC 112, 4168N, New York,
NY 10010, USA
e-mail: uzma.samadani@med.nyu.edu

D.S. Zagzag
Department of Pathology, New York University

Parkinsonian model [19]. Similar reductions in motor impairment have been seen in a marmoset MPTP Parkinson model [20]. SHH and FGF-8 have been used to manipulate embryonic stem cells in vitro, differentiating them into dopaminergic neurons for injection into striatum and partial reversal of Parkinsonian symptoms in rats [21]. SHH in combination with retinoic acid results in conversion of embryonic stem cells into motor neurons capable of receiving synaptic output and eliciting trains of action potentials [22].

The non-peptidyl sonic hedgehog agonist HH-Ag [23] was used in conjunction with retinoic acid to generate motor neurons from stem cells that were capable of generating long axons, and establishing motoneuron connections that result in in vitro muscle contraction [24]. Transplant of these motor neurons into injured spinal cord showed that connecting axons did form [24].

The purpose of this work is to evaluate the impact of sonic hedgehog agonist administration on neuronal stem cell precursor division in a model of porcine intracranial hemorrhage.

Materials and Methods

The double-injection of autologous venous blood porcine model for intracranial hemorrhage has been described previously [25–27]. We took 20–25 kg male pigs and administered general endotracheal anesthesia. Under sterile conditions a 3 mm twist drill hole was placed 1.7 cm in front of the coronal suture and 6 mm right of midline. A Fogarty catheter was passed through the hole to a depth of 1 cm and gently inflated with 1 cc of air to create a cavity within the right frontal cortex. A ventricular catheter attached to an Ommaya reservoir was then inserted into the brain and 7 mL of blood were injected into the brain with a 2 min pause between the first 2 and last 5 mL. The wound was sutured in anatomic layers and anesthesia was reversed.

Pigs that received SHH agonist were administered 1 mg of agonist in 1 mL of saline immediately prior to hemorrhage placement. Sham operated pigs underwent the entire procedure excepting the drilling of a twist hole for the Fogarty, ommaya and hemorrhage placement.

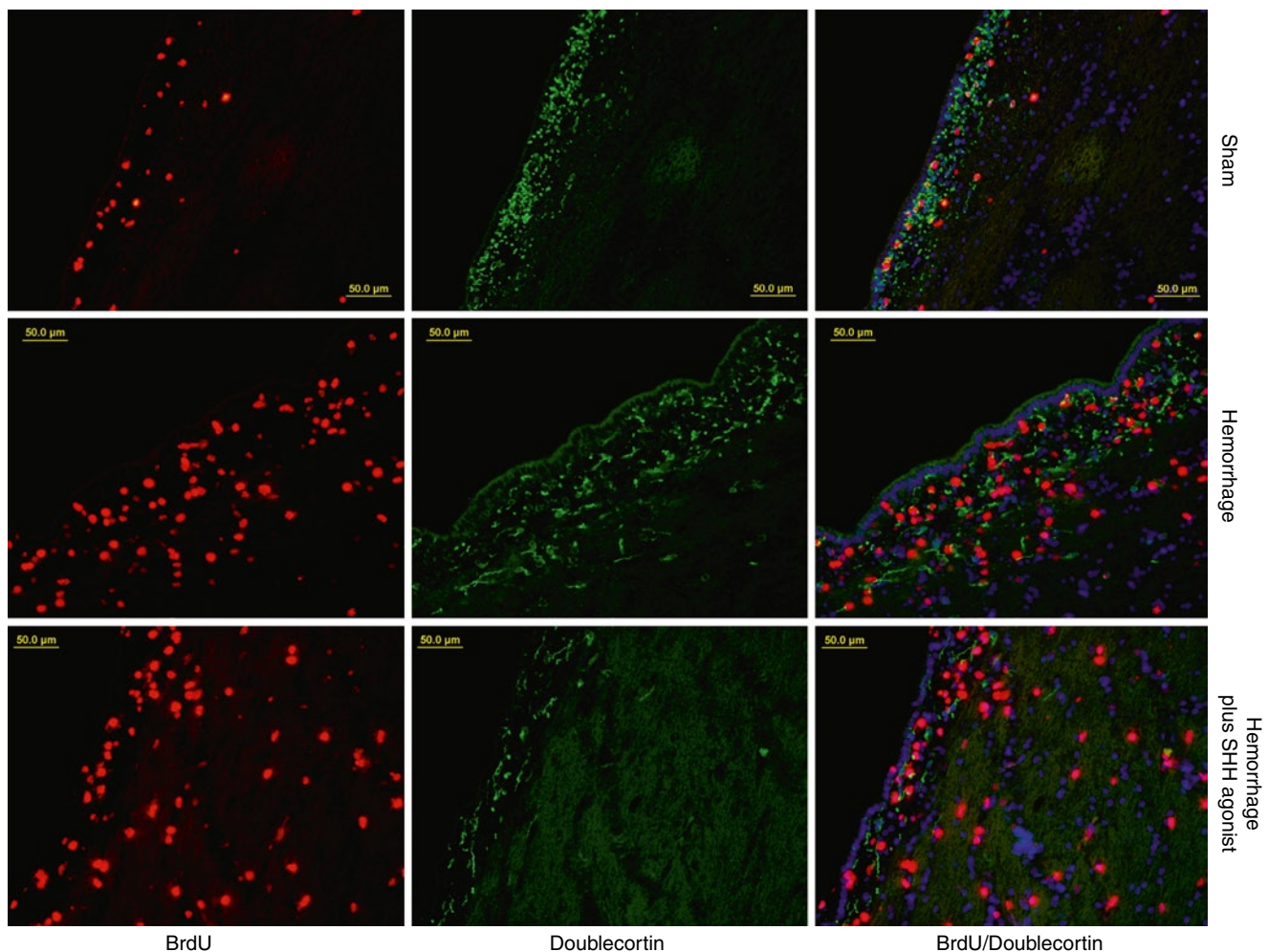


Fig. 1 Staining of 7.5 day post-experimental intracranial hemorrhage porcine subventricular zone demonstrates that relative to sham animals (*top row*), both hemorrhaged animals (*middle row*) and hemorrhaged

animals administered SHH agonist (*bottom row*) had increased BrdU and Doublecortin staining activity

Animals were perfused with 4% paraformaldehyde between posthemorrhage days 7 and 8, and brains were resected, cut, sectioned and stained as described previously [28]. Antibodies used for staining were mouse anti-NeuN 1:400 (Millipore, cat#MAB377), mouse anti-GFAP 1:400 (Sigma, cat#G3893), rat anti-BrdU 1:200 (Abcam, cat#Ab6326) and rabbit anti-DCX 1:200 (Cell signaling, cat#4604). Quantitative immunohistochemistry was performed to 100 μ m from the ventricle using the Image J counting program software. Data shown represents the average of two pigs in each of the test groups.

Results

At the 7–8 day time point, pigs in the hemorrhage only group demonstrated increased and more persistent BrdU staining in the subventricular zone relative to pigs in the group that received sonic hedgehog agonist. The latter group demonstrated increased BrdU activity in non-neural lineage cells in the area of the hemorrhage (Figs. 1 and 2).

Doublestaining with BrdU and DCX revealed that relative to sham control, hemorrhage did not significantly alter the number of stem cells present adjacent to the subventricular zone (Fig. 1). However addition of SHH agonist significantly reduced the number of doublecortin and BrdU positively stained cells (Figs. 1 and 2). Representative staining is shown in Fig. 2.

Discussion

SHH agonists have been shown to be necessary [29, 30] and sufficient [31] to induce division of neural stem cell precursors in the subventricular zone of adult animals in conditional

gene expression models. Our very limited results, consisting of just one concentration of SHH agonist, administered at a single time point right at hemorrhage placement, and with outcomes analyzed at 7.5 days using only the stem cell marker doublecortin, preliminarily appear to suggest that at least under these circumstances SHH agonist did not result in neural stem cell proliferation. While we did see an increase in the number of neural stem cells after placement of an experimental hemorrhage, which is consistent with previous ICH responses in a rodent model [32], SHH agonist administration did not further increase these stem cell numbers.

Further studies are underway with additional stem and mature cell markers, and longer time points to confirm and expand these results.

Conflict of interest statement We declare that we have no conflict of interest.

References

- Gage FH (2000) Mammalian neural stem cells. *Science* 287: 1433–1438
- Goldman SA, Sim F (2005) Neural progenitor cells of the adult brain. *Novartis Found Symp* 265:66–80; discussion 82–97
- Lichtenwalner RJ, Parent JM (2006) Adult neurogenesis and the ischemic forebrain. *J Cereb Blood Flow Metab* 26:1–20
- Cayuso J, Marti E (2005) Morphogens in motion: growth control of the neural tube. *J Neurobiol* 64:376–387
- Ribes V, Wang Z, Dolle P, Niederreither K (2006) Retinaldehyde dehydrogenase 2 (RALDH2)-mediated retinoic acid synthesis regulates early mouse embryonic forebrain development by controlling FGF and sonic hedgehog signaling. *Development* 133:351–361
- Filosa S, Rivera-Perez JA, Gomez AP, Gansmuller A, Sasaki H, Behringer RR, Ang SL (1997) Goosecoid and HNF-3beta genetically interact to regulate neural tube patterning during mouse embryogenesis. *Development* 124:2843–2854
- Lin W, Kemper A, McCarthy KD, Pytel P, Wang JP, Campbell IL, Utset MF, Popko B (2004) Interferon-gamma induced medulloblastoma in the developing cerebellum. *J Neurosci* 24: 10074–10083
- Wang J, Lin W, Popko B, Campbell IL (2004) Inducible production of interferon-gamma in the developing brain causes cerebellar dysplasia with activation of the Sonic hedgehog pathway. *Mol Cell Neurosci* 27:489–496
- Wang MZ, Jin P, Bumcrot DA, Marigo V, McMahon AP, Wang EA, Woolf T, Pang K (1995) Induction of dopaminergic neuron phenotype in the midbrain by Sonic hedgehog protein. *Nat Med* 1: 1184–1188
- Zhang XM, Lin E, Yang XJ (2000) Sonic hedgehog-mediated ventralization disrupts formation of the midbrain-hindbrain junction in the chick embryo. *Dev Neurosci* 22:207–216
- Ericson J, Morton S, Kawakami A, Roelink H, Jessell TM (1996) Two critical periods of Sonic Hedgehog signaling required for the specification of motor neuron identity. *Cell* 87:661–673
- Gutin G, Fernandes M, Palazzolo L, Paek H, Yu K, Ornitz DM, McConnell SK, Hebert JM (2006) FGF signalling generates ventral telencephalic cells independently of SHH. *Development* 133: 2937–2946
- Ye W, Shimamura K, Rubenstein JL, Hynes MA, Rosenthal A (1998) FGF and Shh signals control dopaminergic and serotonergic cell fate in the anterior neural plate. *Cell* 93:755–766

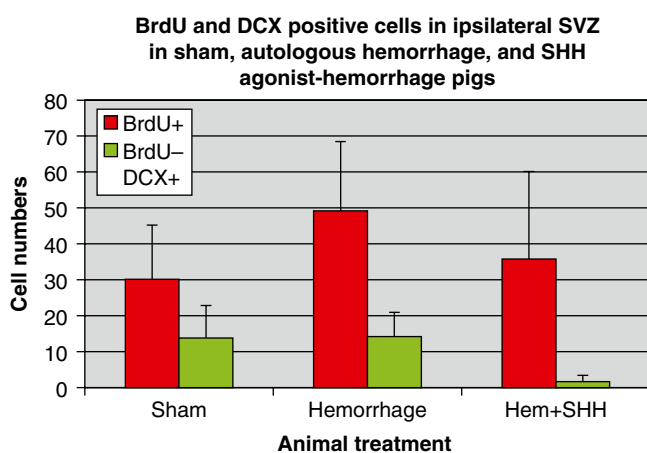


Fig. 2 Quantitative immunohistochemistry of BrdU and Doublecortin stained subventricular zone demonstrates a statistically significant decrease in double stained cells in SHH agonist treated/hemorrhaged animals relative to hemorrhage alone animals

14. Ahmad I, Das AV, James J, Bhattacharya S, Zhao X (2004) Neural stem cells in the mammalian eye: types and regulation. *Semin Cell Dev Biol* 15:53–62
15. Dellovade T, Romer JT, Curran T, Rubin LL (2006) The Hedgehog pathway and neurological disorders. *Annu Rev Neurosci* 29: 539–563
16. Longo FM, Yang T, Xie Y, Massa SM (2006) Small molecule approaches for promoting neurogenesis. *Curr Alzheimer Res* 3:5–10
17. Stecca B, Ruiz i Altaba A (2005) Brain as a paradigm of organ growth: Hedgehog-Gli signaling in neural stem cells and brain tumors. *J Neurobiol* 64:476–490
18. Charytoniuk D, Traffort E, Hantraye P, Hermel JM, Galdes A, Ruat M (2002) Intrastratial sonic hedgehog injection increases patched transcript levels in the adult rat subventricular zone. *Eur J Neurosci* 16:2351–2357
19. Tsuboi K, Shults CW (2002) Intrastratial injection of sonic hedgehog reduces behavioral impairment in a rat model of Parkinson's disease. *Exp Neurol* 173:95–104
20. Dass B, Iravani MM, Jackson MJ, Engber TM, Galdes A, Jenner P (2002) Behavioural and immunohistochemical changes following supranigral administration of sonic hedgehog in 1-methyl-4-phenyl-1, 2, 3, 6-tetrahydropyridine-treated common marmosets. *Neuroscience* 114:99–109
21. Fu YS, Cheng YC, Lin MY, Cheng H, Chu PM, Chou SC, Shih YH, Ko MH, Sung MS (2006) Conversion of human umbilical cord mesenchymal stem cells in Wharton's jelly to dopaminergic neurons in vitro: potential therapeutic application for Parkinsonism. *Stem Cells* 24:115–124
22. Soundararajan P, Miles GB, Rubin LL, Brownstone RM, Rafuse VF (2006) Motoneurons derived from embryonic stem cells express transcription factors and develop phenotypes characteristic of medial motor column neurons. *J Neurosci* 26:3256–3268
23. Frank-Kamenetsky M, Zhang XM, Bottega S, Guicherit O, Wichterle H, Dudek H, Bumcrot D, Wang FY, Jones S, Shulok J, Rubin LL, Porter JA (2002) Small-molecule modulators of Hedgehog signaling: identification and characterization of smoothed agonists and antagonists. *J Biol* 1:10
24. Harper JM, Krishnan C, Darman JS, Deshpande DM, Peck S, Shats I, Backovic S, Rothstein JD, Kerr DA (2004) Axonal growth of embryonic stem cell-derived motoneurons in vitro and in motoneuron-injured adult rats. *Proc Natl Acad Sci USA* 101:7123–7128
25. Rohde V, Rohde I, Thiex R, Ince A, Jung A, Duckers G, Groschel K, Rottger C, Kuker W, Muller HD, Gilsbach JM (2002) Fibrinolysis therapy achieved with tissue plasminogen activator and aspiration of the liquefied clot after experimental intracerebral hemorrhage: rapid reduction in hematoma volume but intensification of delayed edema formation. *J Neurosurg* 97:954–962
26. Thiex R, Kuker W, Muller HD, Rohde I, Schroder JM, Gilsbach JM, Rohde V (2003) The long-term effect of recombinant tissue-plasminogen-activator (rt-PA) on edema formation in a large-animal model of intracerebral hemorrhage. *Neurol Res* 25:254–262
27. Wagner KR, Xi G, Hua Y, Zuccarello M, de Courten-Myers GM, Broderick JP, Brott TG (1999) Ultra-early clot aspiration after lysis with tissue plasminogen activator in a porcine model of intracerebral hemorrhage: edema reduction and blood-brain barrier protection. *J Neurosurg* 90:491–498
28. Thiex R, Weis J, Krings T, Barreiro S, Yakisikli-Alemi F, Gilsbach JM, Rohde V (2007) Addition of intravenous N-methyl-D-aspartate receptor antagonists to local fibrinolytic therapy for the optimal treatment of experimental intracerebral hemorrhages. *J Neurosurg* 106:314–320
29. Balordi F, Fishell G (2007) Hedgehog signaling in the subventricular zone is required for both the maintenance of stem cells and the migration of newborn neurons. *J Neurosci* 27:5936–5947
30. Balordi F, Fishell G (2007) Mosaic removal of hedgehog signaling in the adult SVZ reveals that the residual wild-type stem cells have a limited capacity for self-renewal. *J Neurosci* 27: 14248–14259
31. Ahn S, Joyner AL (2005) In vivo analysis of quiescent adult neural stem cells responding to Sonic hedgehog. *Nature* 437: 894–897
32. Masuda T, Isobe Y, Aihara N, Furuyama F, Misumi S, Kim TS, Nishino H, Hida H (2007) Increase in neurogenesis and neuroblast migration after a small intracerebral hemorrhage in rats. *Neurosci Lett* 425:114–119

NC1900, an Arginine Vasopressin Analogue, Fails to Reduce Brain Edema and Improve Neurobehavioral Deficits in an Intracerebral Hemorrhagic Stroke Mice Model

Anatol Manaenko, Tim Lekic, John H. Zhang, and Jiping Tang

Abstract Objective: There is mounting evidence suggesting that arginine vasopressin via its V1a receptor interaction is involved in the regulation of the brain water channel, aquaporin-4 (AQP4). The role of AQP4 in brain edema resolution has been thoroughly investigated in knock-out animal studies, which showed that its depletion increases brain water content in models of vasogenic edema. As a result, we tested the hypothesis that the activation of V1a receptor by its selective agonist will decrease brain edema in a mouse intracerebral hemorrhage (ICH) model.

Materials and Methods: ICH was induced by injection of bacterial collagenase into the right basal ganglia in CD1 male mice (weight 30–35 g). The animals were divided into the following groups: sham, ICH+vehicle, and ICH+AVP V1a receptor agonist. Brain edema and neurological outcomes were evaluated at 24 and 72 h post-ICH.

Results: We found that collagenase injection increased brain edema and resulted in subsequent neurobehavioral deficits at both time points. Treatment with our agonist had no effect on the ICH outcomes at both time points.

Conclusions: Our results suggest that the activation of the V1a receptor has no beneficial effect on secondary brain injury following ICH in mice.

Keywords Arginine vasopressin · Brain edema · ICH · Neuroprotection

Introduction

Development of perihematomal brain edema is one of the most life-threatening events following an intracerebral hemorrhage (ICH). Two types of edema can present after ICH – namely vasogenic and cytotoxic edema. Vasogenic edema occurs predominantly as a result of BBB disruption, whereas cytotoxic edema refers to the intracellular accumulation of water that is released following death. Today, despite promising basic science research aimed at reducing and/or eliminating cerebral edema, bench work has not been translated into clinical improvements. This is partly due to the lack of clear understanding behind the pathophysiology of edema evolution.

Arginine vasopressin (AVP) is a cyclic non-peptide that regulates water and electrolyte homeostasis in the body [1]. Niermann et al. demonstrated that AVP via its G protein-coupled receptor V1a can modulate the most abundant bidirectional water channel in the brain, called aquaporin-4 (AQP4) [2]. Aquaporins play an important role in the maintenance of tissue water homeostasis. Specifically AQP-4, the most abundant water channel in the brain, has been implicated in a number of brain injury-induced cerebral edema cases [3–5]. AQP-4 is an integral membrane protein; it is located in the blood-brain interface and regulates the flow of water in and out of the membrane [6].

In this study, we investigated the role of AVP V_{1a} receptor activation and its effects on cerebral edema and neurobehavioral functioning after intracerebral hemorrhage (ICH). We hypothesized that treatment with a selective V_{1a} agonist will ameliorate the brain water increase and improve neurobehavioral deficits in mice after ICH injury.

Materials and Methods

This study was in accordance with the guidelines of the National Institute of Health for the treatment of animals and was approved by the Institutional Animal Care and Use

A. Manaenko, T. Lekic, and J. Tang
Department of Physiology and Pharmacology,
Loma Linda University, Loma Linda, CA, USA

J.H. Zhang (✉)
Department of Physiology and Pharmacology,
Loma Linda University, Loma Linda, CA, USA and
Department of Anesthesiology, Loma Linda Medical Center,
Loma Linda, CA, USA and
Department of Neurosurgery, Loma Linda University Medical Center,
11234 Anderson Street, Room 2562B, Loma Linda, CA, 92354, USA
e-mail: johnzhang3910@yahoo.com

Committee at Loma Linda University. Male CD1 mice (weight 35–45 g, Charles River, MA) were housed in a 12-h light/dark cycle at controlled temperature and humidity with free access to food and water. Mice were divided into the following groups: sham ($n=5$), ICH ($n=5$), and ICH treated with agonist (NC1900 10 ng/kg; $n=5$),

Operative Procedure. The collagenase-induced ICH model was adapted as previously described in mice [7]. Briefly, mice were anesthetized intraperitoneally with a ketamine (100 mg/kg)/xylazine (10 mg/kg) cocktail, and positioned prone in a stereotaxic head frame (Stoelting, Wood Dale, IL). An electronic thermostat-controlled warming blanket was used to maintain the core temperature at 37°C. The calvarium was exposed by a midline scalp incision from the nose to the superior nuchal line, and the skin was retracted laterally. With a variable speed drill (Fine Scientific Tools, Foster City, CA), a 1.0-mm burr hole was made 0.9 mm posterior to the bregma and 1.45 mm right-lateral to the midline. A 26-G needle on a Hamilton syringe was inserted with stereotaxic guidance 4.0 mm into the right deep cortex/basal ganglia at a rate of 1 mm/min. Collagenase (0.075 units in 0.5 μ L saline; Sigma, St Louis, MO) was then infused into the brain at a rate of 0.25 μ L/min over 2 min using an automatic infusion pump (Stoelting, Wood Dale, IL). The needle was left in place for an additional 10 min after injection to prevent the possible leakage of collagenase solution. After removal of the needle, the incision was sutured closed, and mice were allowed to recover. Sham operation was performed with needle insertion only.

Treatment Method. The agonist (NC1900) was kindly provided by Nippon Chemiphar Co., Ltd., Japan. NC1900 (10 ng/kg) was dissolved in saline and administered as a single dose subcutaneously 1 h after ICH.

Brain Water Content. Brain water content was measured as previously described [7]. Briefly, rats were sacrificed at 24 and 72 h post ICH, and brains were immediately removed and divided into five parts: ipsilateral frontal, contralateral frontal, ipsilateral parietal, contralateral parietal, and cerebellum. The cerebellum was used as an internal control for brain water content. Tissue samples were then weighed on an electronic analytical balance (APX-60, Denver Instrument; Arvada, CO) to the nearest 0.1 mg to obtain the wet weight (WW). The tissue was then dried at 105°C for 48 h to determine the dry weight (DW). The percent brain water content was calculated as $[(WW - DW)/WW] \times 100$.

Assessment of Neurobehavioral Deficits. Neurobehavioral deficits were assessed by a blind observer at 24 and 72 h post ICH using the Modified Garcia Score [15]. The Modified Garcia Score is a 21-point sensorimotor assessment system consisting of seven tests with scores of 0–3 for each test (maximum score=21). These seven tests included: (1) spontaneous activity, (2) side stroking, (3) vibris touch, (4) limb symmetry, (5) climbing, (6) lateral turning, and (7) forelimb walking.

Additionally, beam balance and wire hang testing were performed. Both the beam (590 cm in length by 51 cm in width) and wire (550 cm in length by 51 mm in width) were constructed and held in place by two platforms on each side. Mice were put on the center of the beam or wire and allowed to reach the platform. Mice were observed for both their time and behavior until they reached one platform and scored according to six grades. The test was repeated three times, and an average score was taken [minimum score 0; maximum score (healthy mouse)] [9].

Western Blotting of Aquaporin-4. Animals were perfused with 0.1 M PBS at 72 h post-ICH. The peri-hematoma region was then isolated and snap-frozen in liquid nitrogen for analysis. Individual protein samples (50 μ g each) were subjected to electrophoresis and then transferred to a nitrocellulose membrane for 80 min at 70 V (Bio-Rad). Blotting membranes were incubated for 2 h with 5% nonfat milk in Tris-buffered saline containing 0.1% Tween 20 and then incubated overnight at 4°C with primary antibody (anti-aquaporin 4) (1:200; Santa Cruz Biotechnology, Santa Cruz, CA). The membranes were incubated for 1 h with secondary antibodies (1:1,000; Santa Cruz Biotechnology) and processed with an enhanced chemiluminescent reagent kit (Amersham Bioscience, Arlington Heights, IL) on X-ray film (Kodak, Rochester, NY).

Statistical Analysis. Quantitative data were expressed as the mean \pm SEM. One-way ANOVA and Tukey test were used to determine significance in differences between the means. Neurological scores were evaluated using the Dunn method. A p -value < 0.05 was considered statistically significant.

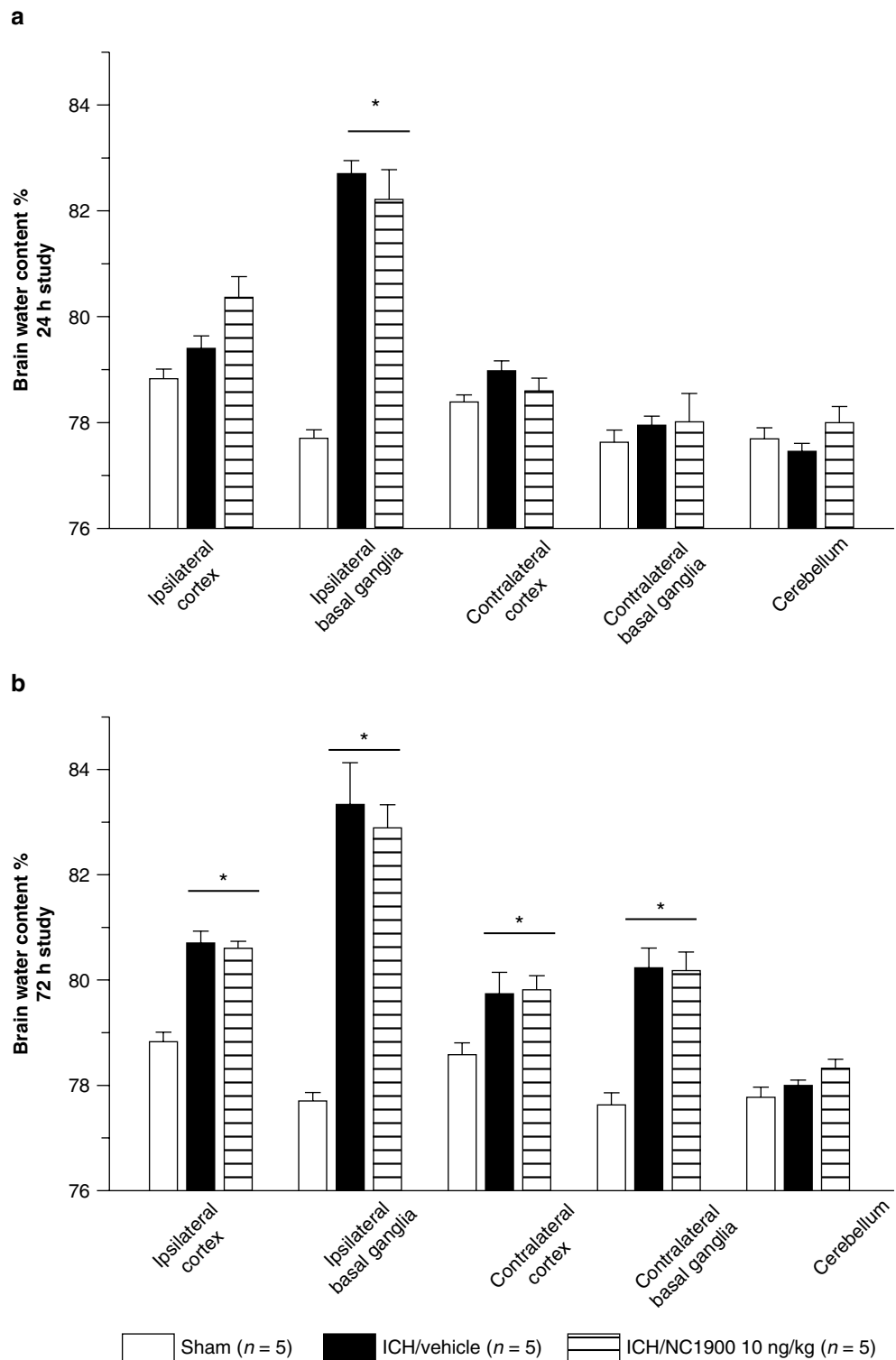
Results

AVP V_{1a} receptor activation has no effect on cerebral edema after ICH injury. Vehicle groups demonstrated a consistently elevated level of cerebral edema in the ipsilateral hemisphere compared to the sham animals ($p < 0.05$). Activation of the AVP V_{1a} receptor using NC1900 was not able to reduce the cerebral edema at 24 and 72 h post injury (Fig. 1).

AVP V_{1a} receptor activation does not improve neurobehavioral deficits. Neurobehavioral deficits were present in all animals following collagenase injection. No effects were observed with NC1900 treatment. The neurobehavioral deficits were evaluated by the Modified Garcia test (Fig. 2a(1) and (2)), and the beam balance and wire hanging test (Fig. 2b(1) and (2)).

AVP V_{1a} receptor activation and AQP4 expression. Western blot measurement of AQP4 protein expression showed no difference between the vehicle and NC1900 (Fig. 3).

Fig. 1 All animals after collagenase injection have a significant increase of brain water content. NC1940 has no effect on brain edema at 24 h (a) and 72 h (b) as well. *Significant difference vs. sham ($p < 0.05$); (a) 24 h: sham=5; (vehicle)=5; (ICH+10 ng/kg NC1900); (b) 72 h: sham=5; (vehicle)=5; (ICH+10 ng/kg NC1900)



Discussion

The aim of this study was to determine the effects of the AVP V_{1a} receptor agonist NC1900 on AQP4 production, and resulting effects on brain edema and neurobehavioral deficits. We

demonstrated that activation of the AVP V_{1a} receptor with NC1900 had no effect on AQP4 production, the ICH-induced increase in brain water content and neurobehavioral deficits.

AVP’s actions are modulated through one of its three receptors. In the brain, the predominant receptor is the V_1

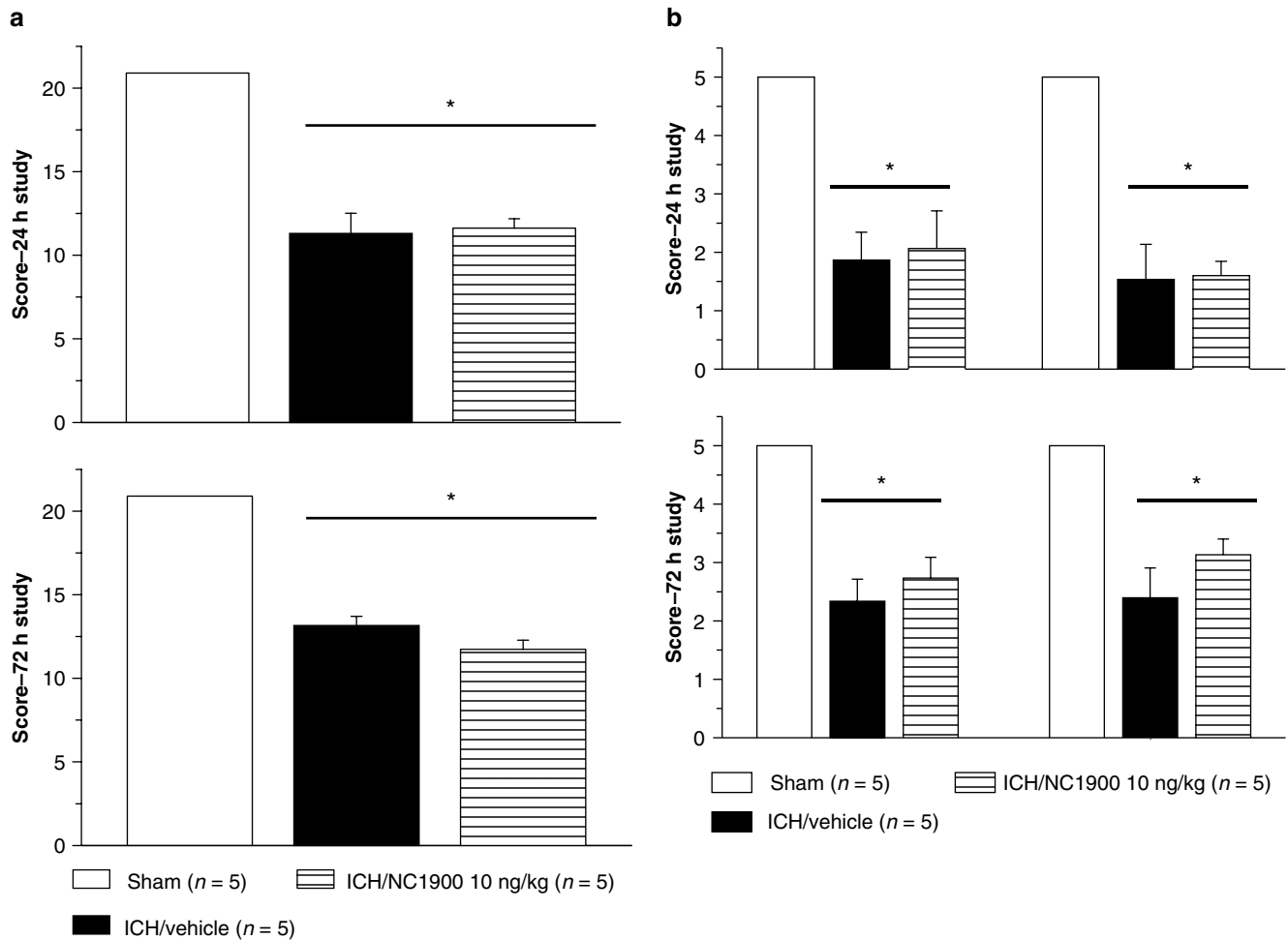


Fig. 2 Neurobehavioral deficits were present in all animals following collagenase injection. NC1900 had no effect on ICH-induced neurobehavioral deficit at 24 (a) and at 72 h (b). *Significant difference vs. sham ($p < 0.05$)

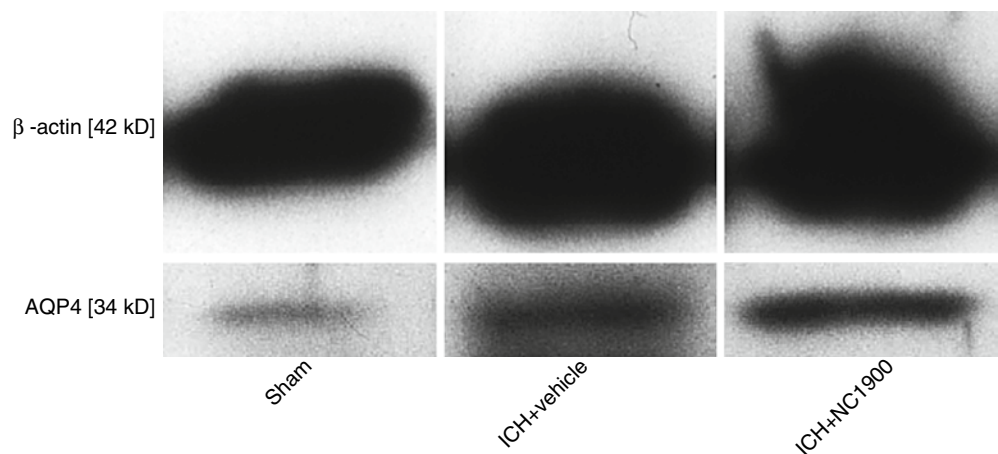


Fig. 3 NC1900 does not change the production of AQP4 at 72 h

receptor, which exists in two subtypes V_{1a} and V_{1b} . It has been demonstrated that activation of V_{1a} but not other types of receptors can activate AQP4 [2, 14]. AQP4 provides bidirectional water flow between the blood and the brain, and has

been implicated as a key component in water homeostasis in normal brain and the cause of brain edema during injury [8]. Experiments with knock-out animals demonstrated that AQP4 is essential in reducing the duration and onset of

vasogenic edema and that its depletion can cause a significant increase in brain water content in models of vasogenic edema [5]. Hirt et al. demonstrated that early aquaporin induction has a protective effect, and his team was able to reduce the edema formation after a middle cerebral artery occlusion model [10]. Similarly, Badaut et al. demonstrated that induction of AQP4 can preserve the tissue and ameliorate edema formation following injury [11]. In order to test whether the pharmacological activation of V_{1a} receptor will have an effect on brain water content after ICH, we investigated the effect of V_{1a} receptor agonist NC1900.

NC1900 is an AVP analog with a strong affinity for the V_{1a} receptor in rodents compared to other known AVP agonist types [12, 16]. In this study, we tested the effects of this drug on various delayed time points in which vasogenic edema has been suggested to be most present. Since AQP4 upregulation peaks 72 h after ICH [13], we tested the effect of NC1900 on AQP4 production at this time point.

Conclusion

We conclude that AVP V_{1a} receptor activation has no effect on AQP 4 production and ICH-induced brain damage in mice.

Acknowledgement This study is partially supported by NIH NS053407 to J.H. Zhang and NS060936 to J. Tang.

Conflict of interest statement We declare that we have no conflict of interest.

References

1. Antoni FA (1993) Vasopressinergic control of pituitary adrenocorticotropin secretion comes of age. *Front Neuroendocrinol* 14:76–122
2. Niermann H, Amiry-Moghaddam M, Holthoff K, Witte O, Ottersen O (2001) A novel role of vasopressin in the brain: modulation of activity-dependent water flux in the neocortex. *J Neurosci* 21(9): 3045–3051
3. Gu YT, Zhang H, Xue YX (2007) Dexamethasone treatment modulates aquaporin-4 expression after intracerebral hemorrhage in rats. *Neurosci Lett* 413:126–131
4. Manley GT, Fujimura M, Ma T, Noshita N, Filiz F, Bollen AW, Chan P, Verkman AS (2000) Aquaporin-4 deletion in mice reduces brain edema after acute water intoxication and ischemic stroke. *Nat Med* 6:159–163
5. Papadopoulos MC, Manley GT, Krishna S, Verkman AS (2004) Aquaporin-4 facilitates reabsorption of excess fluid in vasogenic brain edema. *FASEB J* 18:1291–1293
6. Yukutake Y, Yasui M (2010) Regulation of water permeability through aquaporin-4. *Neuroscience* 168(4):885–891
7. Tang J, Liu J, Zhou C, Alexander JS, Nanda A, Granger DN, Zhang JH (2004) Mmp-9 deficiency enhances collagenase-induced intracerebral hemorrhage and brain injury in mutant mice. *J Cereb Blood Flow Metab* 24:1133–1145
8. Benarroch E (2007) Aquaporin-4, homeostasis, and neurologic disease. *Neurology* 69:2266–2268
9. Manaenko A, Lekic T, Sozen T, Tsuchiyama R, Zhang JU, Tang J (2009) Effect of gap junction inhibition on intracerebral hemorrhage-induced brain injury in mice. *Neurol Res* 31:173–178
10. Hirt L, Ternon B, Price M, Mastour N, Brunet JF, Badaut J (2009) Protective role of early aquaporin 4 induction against postischemic edema formation. *J Cereb Blood Flow Metab* 29(2):423–433
11. Badaut J, Ashwal S, Tone B, Regli L, Tian HR, Obenaus A (2007) Temporal and regional evolution of aquaporin-4 expression and magnetic resonance imaging in a rat pup model of neonatal stroke. *Pediatr Res* 62:248–254
12. Mishima K, Tsukikawa H, Miura I, Inada K, Abe K, Matsumoto Y, Egashira H, Iwasaki K, Fujiwara M (2003) Ameliorative effect of NC1900, a new AVP4–9 analog, through vasopressin V_{1A} receptor on scopolamine-induced impairments of spatial memory in the eight-arm radial maze. *Neuropharmacology* 44:541–552
13. Qing WG, Dong YQ, Ping TQ, Lai LG, Fang LD, Min HW, Xia L, Heng PY (2009) Brain edema after intracerebral hemorrhage in rats: the role of iron overload and aquaporin 4. *J Neurosurg* 110:462–468
14. Brinton RE, Gee KW, Wamsley JK, Davis TP, Yamamura HI (1984) Regional distribution of putative vasopressin receptors in rat brain and pituitary by quantitative autoradiography. *Proc Natl Acad Sci USA* 81:7248–7252
15. Garcia JH, Wagner S, Liu KF, Hu XJ (1995) Neurological deficit and extent of neuronal necrosis attributable to middle cerebral artery occlusion in rats. Statistical validation. *Stroke* 26: 627–634
16. Matsuoka T, Sumiyoshi T, Tanaka K, Tsunoda M, Uehara T, Itoh H, Kurachi M (2005) NC-1900, an arginine-vasopressin analogue, ameliorates social behavior deficits and hyperlocomotion in MK-801-treated rats: therapeutic implications for schizophrenia. *Brain Res* 1053:131–136

Geldanamycin Reduced Brain Injury in Mouse Model of Intracerebral Hemorrhage

Anatol Manaenko, Nancy Fathali, Shammah Williams, Tim Lekic, John H. Zhang, and Jiping Tang

Abstract We investigated the effect of the heat shock protein inducer geldanamycin on the development of secondary brain injury after ICH in mice. The effect of the drug at two different concentrations was evaluated at two time points: 24 and 72 h after ICH induction. In the first part of this study, a total of 30 male CD-1 mice were randomly divided into four groups: one sham group and three ICH groups. ICH animals received either an intraperitoneal injection of vehicle or geldanamycin (1 or 10 mg/kg). Neurological deficits and brain water content were evaluated 24 h after ICH. In the second part of this study, the effect of a high concentration of geldanamycin was evaluated 72 h after ICH. Neurological deficits were evaluated by the Garcia neuroscoring, wire hanging and beam balance tests. For estimation of brain water content, the “wet/dry weight” method was used. We demonstrated that administration of geldanamycin (10 mg/kg) ameliorated ICH-induced increase of brain water content significantly in both parts of the study. Geldanamycin improved the neurological outcome according to performance on Garcia and beam balance tests in the 72 h part of this study. Geldanamycin-induced induction of heat shock protein after ICH has a neuroprotective effect and may be a therapeutic target for ICH.

Keywords Geldanamycin · HSP · ICH Neuroprotection

Introduction

Intracerebral hemorrhage (ICH) is a devastating clinical event with greater than 40% initial mortality, leaving many of the survivors permanently disabled. Currently, there is

neither an effective therapy to increase survival after intracerebral hemorrhage nor a treatment to improve the quality of life of survivors [1]. There are biphasic effects of intracerebral hemorrhage upon brain tissue. Initial injury is in response to the expanding hematoma imposing sheer forces and mass effect upon the cerebral tissues [2]. Intracerebral bleeding leads to increased intracranial pressures and could lead to transtentorial herniation secondary to the mass effect [3]. A later phase involves hematoma-induced neuronal and glial apoptotic cell death at the surrounding parenchymal rim [4], inflammation and progressive rupture of the blood-brain-barrier, and rising brain edema [5]. Geldanamycin belongs to the family of ansamycin antibiotics. Biochemical and structural studies have demonstrated that geldanamycin binds specifically to the ATP pocket of the constitutively induced heat shock protein (HSP) 90 and inhibits its chaperone activity and its ability to bind to target proteins [6]. HSP 90 affects multiple signal transduction pathways [7] and has been shown to regulate more than 100 proteins involved in cellular signaling [7]. HSP 90 is a negative regulator of heat shock factor 1 (HSF 1). The binding between HSP 90 and geldanamycin makes HSP 90 unable to associate with HSF 1 [8]. The free HSF 1 initiates production of other HSPs, specifically HSP 70 [9]. A neuroprotective effect of geldanamycin-induced HSP70 upregulation was demonstrated previously [10, 11]. To date, no study has assessed the effects of geldanamycin on the outcomes of intracerebral hemorrhage. In the present study we aimed to investigate if post-treatment with the HSP modulator geldanamycin will result in decreased brain edema and improvement in neurological outcomes

Methods

Experimental animals: All procedures and methods for these studies were approved by the Animal Care and Use Committee at Loma Linda University and complied with the Guide for the Care and Use of Laboratory Animals

A. Manaenko, N. Fathali, S. Williams, T. Lekic, J.H. Zhang, and J. Tang (✉)
Department of Physiology and Pharmacology, Loma Linda University, School of Medicine, Loma Linda, CA 92350, USA
e-mail: jtang@llu.edu

(<http://research.ltu.edu/forms/appendixb.doc>). A total of 30 male CD-1 mice were divided into four groups: sham, ICH treated with vehicle, ICH treated with low-dose geldanamycin (1 mg/kg), and ICH treated with high-dose geldanamycin (10 mg/kg). Geldanamycin was dissolved in 2.5% of DMSO and administered intraperitoneally 1 h after ICH induction. Animals were tested for neurological function and euthanized for brain edema measurements at 24 and 72 h after ICH. *Intracerebral hemorrhage induction:* We adopted the collagenase-induced intracerebral hemorrhage model as previously described in mice [12]. Briefly, mice were anesthetized with ketamine (100 mg/kg) and xylazine (10 mg/kg, intraperitoneal injection) and positioned prone in a stereotaxic head frame (Stoelting, Wood Dale, IL). An electronic thermostat-controlled warming blanket was used to maintain the core temperature at 37°C. The calvarium was exposed by a midline scalp incision from the nasion to the superior nuchal line, and the skin was retracted laterally. With a variable speed drill (Fine Scientific Tools, Foster City, CA) a 1.0-mm burr hole was made 0.9 mm posterior to bregma and 1.45 mm to the right of the midline. A 26-gauge needle on a Hamilton syringe was inserted with stereotaxic guidance 4.0 mm into the right deep cortex/basal ganglia at a rate 1 mm/min. The collagenase (0.075 units in 0.5 μ L saline, VII-S; Sigma, St Louis, MO) in the syringe was infused into the brain at a rate of 0.25 μ L/min over 2 min with an infusion pump (Stoelting, Wood Dale, IL). The needle was left in place for an additional 10 min after injection to prevent the possible leakage of collagenase solution. After removal of the needle, the incision was closed, and the mice were allowed to recover. A sham operation was performed with needle insertion only.

Brain water content: The brain water content was measured as previously described [12]. Briefly, mice were euthanized under deep anesthesia. Brains were removed immediately and divided into five parts: ipsilateral and contralateral basal ganglia, ipsilateral and contralateral cortex, and cerebellum. The cerebellum was used as an internal control for brain water content. Tissue samples were weighed on an electronic analytical balance (model AE 100; Mettler Instrument Co., Columbus, OH) to the nearest 0.1 mg to obtain the wet weight. The tissue was then dried at 100°C for 24 h to determine the dry weight. Brain water content (%) was calculated as [(wet weight – dry weight)/wet weight] \times 100.

Neurological deficits: Neurological scores were assessed by an independent researcher blinded to the procedure 24 and 72 h after ICH using a modification of scoring (21 points) (maximum 3 = healthy animal) [13]. In addition, beam balance and wire hang tests were performed.

Statistical analysis: Quantitative data are expressed as the mean \pm SEM. Statistical significance was verified by analysis of variance (ANOVA; Bonferroni test) for analysis of acute effect (24 h) and by ANOVA (Tukey test) for analysis of delayed effect (72 h). $P < 0.05$ was considered statistically significant.

Results

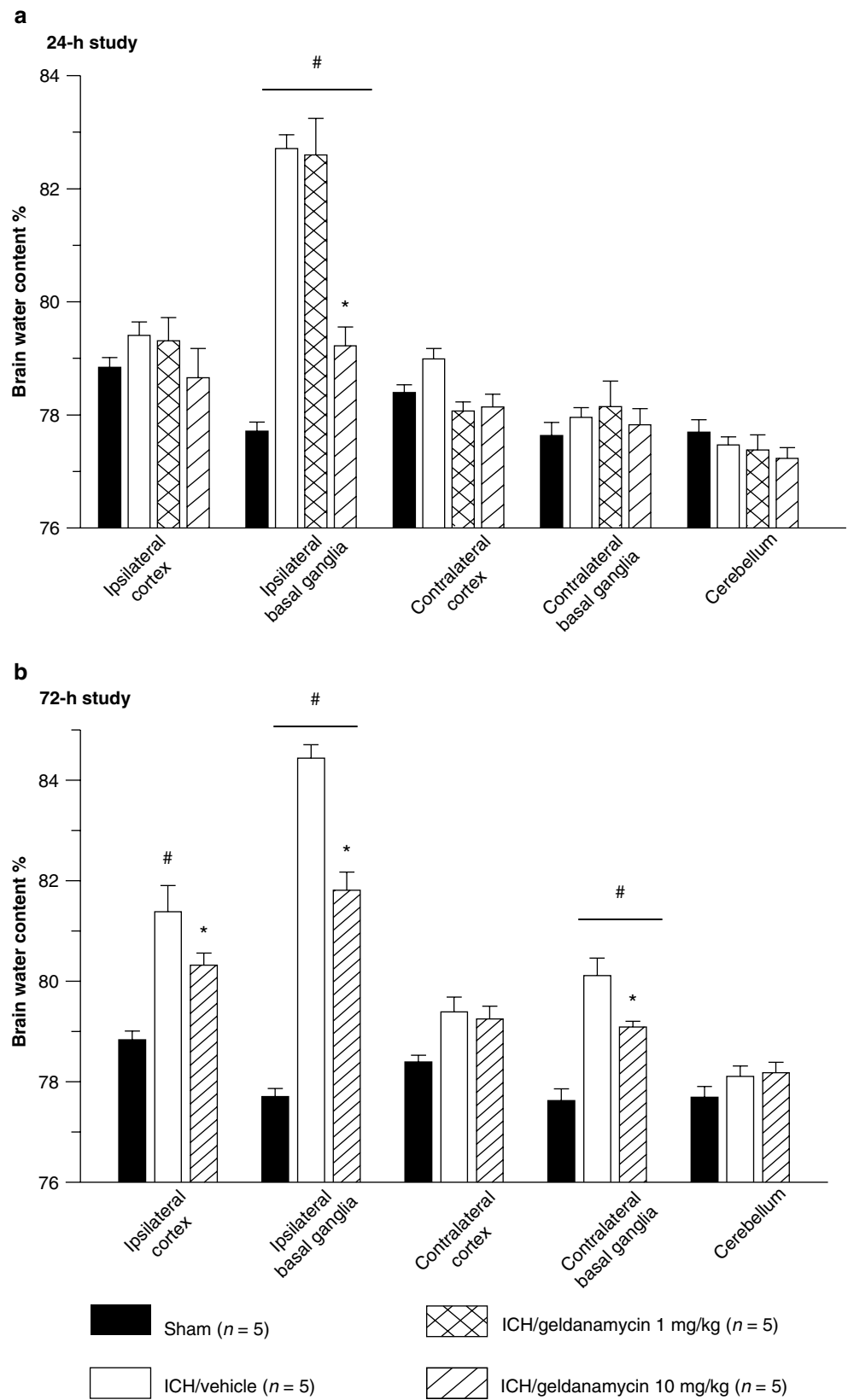
Geldanamycin reduced brain edema: In the 24-h study, collagenase injection caused a significant rise in brain water content in the ipsilateral basal ganglia of all ICH animals ($p < 0.001$, ANOVA, Bonferroni test). The high dose of geldanamycin treatment significantly reduced brain edema in the ipsilateral basal ganglia when compared with the vehicle-treated and low-dose-treated ICH groups ($p < 0.001$, ANOVA, Bonferroni test). Low-dose geldanamycin did not reduce brain water content (Fig. 1a). In the 72-h study, we observed that injection of collagenase caused an increase of brain water content in both basal ganglia and in the ipsilateral cortex. High-dose geldanamycin treatment reduced brain water content significantly ($p < 0.001$, ANOVA, Bonferroni test) (Fig. 1b). *High-dose geldanamycin reduced neurological deficits at 72 h after ICH:* Neurological deficits were present in all animals after collagenase injection. Neither the low dose nor high dose of geldanamycin led to any improvement of neurological function when compared with the vehicle-treated intracerebral hemorrhage group at 24 after ICH (Fig. 2a). In the 72-h study, high-dose geldanamycin treatment significantly reduced neurological deficits that were indicated by improvements in the Garcia test ($*p < 0.05$, ANOVA, Dunn's method) and wire hanging test ($*p < 0.05$ ANOVA, Bonferroni *t*-test) (Fig. 2b). Beam balance test results tended to improve after high-dose geldanamycin treatment; however, this change did not reach statistical significance ($p = 0.072$).

Discussion

Our study demonstrated that (1) geldanamycin at a dose of 10 mg/kg significantly reduced brain edema at 24 and 72 h after ICH; (2) geldanamycin at a dose of 10 mg/kg significantly improved neurological function at 72 h after ICH; (3) geldanamycin at a dose of 1 mg/kg did not produce a significant effect on ICH-induced brain edema and neurological deficits.

The neuroprotective effect of geldanamycin has been demonstrated in several in vitro and in vivo models of neuronal injury. It has been shown that administration of geldanamycin after middle cerebral artery occlusion in rats reduced infarct volume and brain swelling, and significantly improved the neurological function [10, 11]. In an animal model of hemorrhage, intraperitoneal administration of geldanamycin 16 h before hemorrhage preserved energy loss by amelioration of hemorrhage-induced ATP breakdown [14]. Moreover, geldanamycin pre-treatment affects caspase-3 activity in the brain in an animal model of hemorrhage [15]. The mechanism of geldanamycin-induced neuroprotection appears to be due to its ability to affect HSP

Fig. 1 (a) The 24-h study: Brain edema detected in ipsilateral basal ganglia was significantly higher among ICH groups when compared with sham-operated animals ($\#p < 0.001$ vs. sham, ANOVA). Geldanamycin (10 mg/kg) reduced the brain water content of ipsilaterally basal ganglia significantly ($*p < 0.001$ vs. vehicle, ANOVA). A low concentration of drug remains ineffective. (b) The 72-h study: Brain edema spread into other brain compartment of vehicle-treated mice compared with sham-operated animals ($\#p < 0.001$ vs. sham, ANOVA). Geldanamycin (10 mg/kg) reduced brain water content significantly ($*p < 0.001$ vs. vehicle, ANOVA)



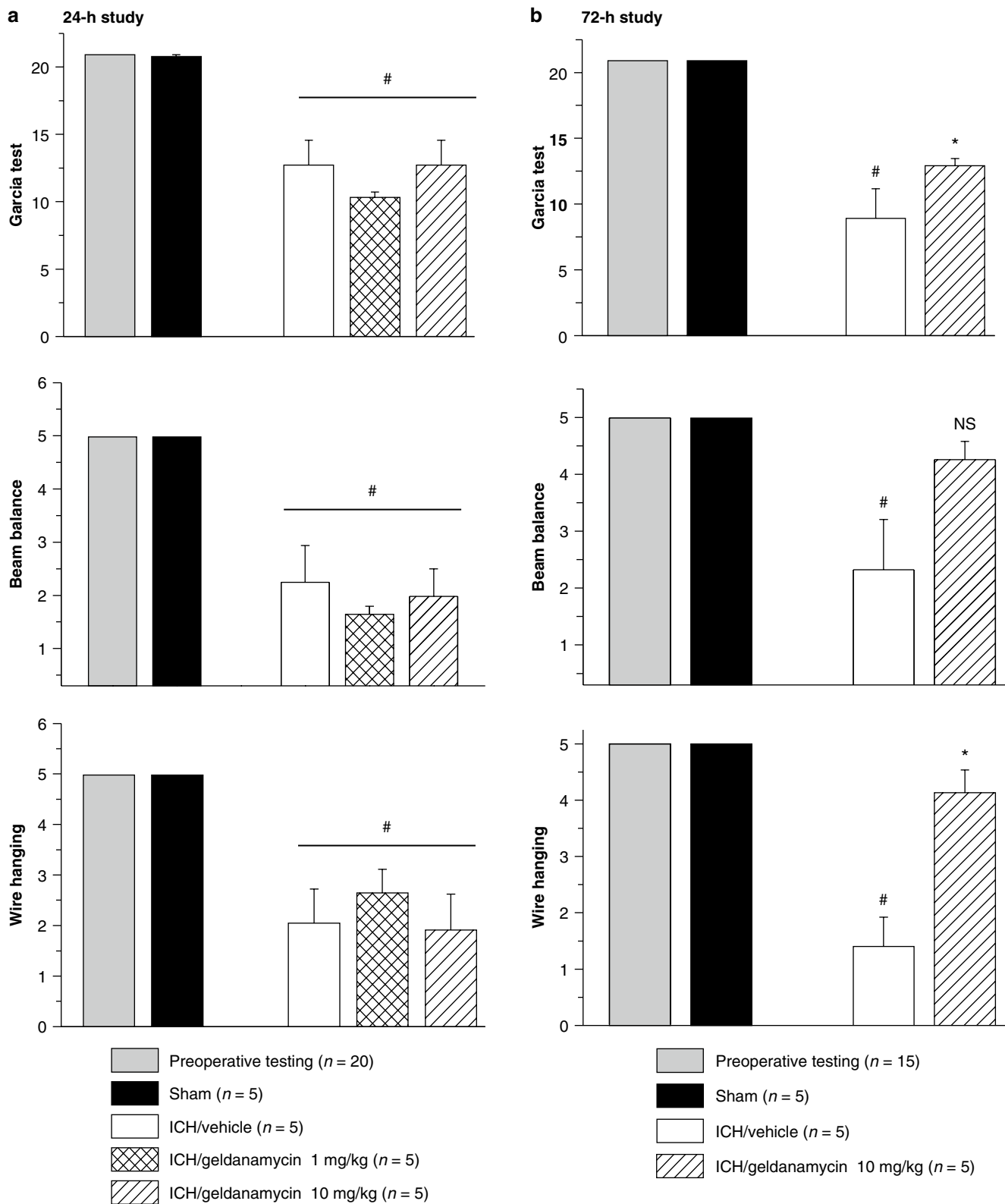


Fig 2 Neurological function tests. In the 24-h study (a), significant neurological deficits were observed in all animals receiving collagenase ($*p < 0.05$, vs. sham). However, no differences were observed between vehicle- and geldanamycin-treated groups. The data of wire hanging and beam balance tests are represented as the average of three

trials per animal. (b) In the 72-h study, a high concentration of geldanamycin leads to significant improvement of the neurological deficit according to performance on Garcia and wire hanging tests. Tendency to improvement in the beam balance test remains insignificant (NS $p = 0.072$)

70 [9]. HSP 70 is an inducible form of heat shock protein. It is the major inducible stress protein and has long been thought to contribute to cell survival following potentially lethal stresses. The neuroprotective effect of HSP 70 upregulation has been described in several models of brain injury [16]. Transgenic animals overexpressing HSP 70 have fewer apoptotic cells compared with wild-type animals after permanent focal ischemia [17]. Similar results were demonstrated by Matsumori et al. by studying the activation of mitochondrial apoptotic pathways in mice overexpressing HSP 70 in a model of neonatal hypoxia-ischemia. They showed that high constitutive expression of HSP 70 protects the brain from hypoxia-ischemia in the neonatal period and affects the apoptotic pathways [18].

This study provides the first evidence that geldanamycin treatment protects the brain against intracerebral hemorrhage. Geldanamycin decreases brain water content in acute (24 h after ICH induction) and delayed (72 h after ICH induction) phases. Moreover, the administration of geldanamycin improved the neurological deficit in the delayed phase.

Acknowledgement This study is partially supported by NIH NS053407 to J.H. Zhang and NS060936 to J. Tang.

Conflict of interest statement We declare that we have no conflict of interest.

References

1. D'Ambrosio AL, Sughrue ME, Yorgason JG, Mocco JD, Kreiter KT, Mayer SA, McKhann GM II, Connolly ES Jr (2005) Decompressive hemicraniectomy for poor-grade aneurysmal subarachnoid hemorrhage patients with associated intracerebral hemorrhage: clinical outcome and quality of life assessment. *Neurosurgery* 56:12–19
2. Aronowski J, Hall CE (2005) New horizons for primary intracerebral hemorrhage treatment: experience from preclinical studies. *Neurol Res* 27:268–279
3. Badjatia N, Rosand J (2005) Intracerebral hemorrhage. *Neurologist* 11:311–324
4. Felberg RA, Grotta JC, Shirzadi AL, Strong R, Narayana P, Hill-Felberg SJ, Aronowski J (2002) Cell death in experimental intracerebral hemorrhage: the “black hole” model of hemorrhagic damage. *Ann Neurol* 51:517–524
5. Qureshi AI, Ling GS, Khan J, Suri MF, Miskolczi L, Guterman LR, Hopkins LN (2001) Quantitative analysis of injured, necrotic, and apoptotic cells in a new experimental model of intracerebral hemorrhage. *Crit Care Med* 29:152–157
6. Prodromou C, Roe SM, O'Brien R, Ladbury JE, Piper PW, Pearl LH (1997) Identification and structural characterization of the ATP/ADP-binding site in the Hsp90 molecular chaperone. *Cell* 90:65–75
7. Pratt WB, Galigniana MD, Harrell JM, DeFranco DB (2004) Role of hsp90 and the hsp90-binding immunophilins in signalling protein movement. *Cell Signal* 16:857–872
8. Whitesell L, Mimnaugh EG, De Costa B, Myers CE, Neckers LM (1994) Inhibition of heat shock protein HSP90-pp 60v-src heteroprotein complex formation by benzoquinone ansamycins: essential role for stress proteins in oncogenic transformation. *Proc Natl Acad Sci USA* 91:8324–8328
9. Voellmy R, Boellmann F (2007) Chaperone regulation of the heat shock protein response. *Adv Exp Med Biol* 594:89–99
10. Kwon HM, Kim Y, Yang SI, Kim YJ, Lee SH, Yoon BW (2008) Geldanamycin protects rat brain through overexpression of HSP70 and reducing brain edema after cerebral focal ischemia. *Neurol Res* 30:740–745
11. Lu A, Ran R, Parmentier-Batteur S, Nee A, Sharp FR (2002) Geldanamycin induces heat shock proteins in brain and protects against focal cerebral ischemia. *J Neurochem* 81:355–364
12. Tang J, Liu J, Zhou C, Alexander JS, Nanda A, Granger DN, Zhang JH (2004) Mmp-9 deficiency enhances collagenase-induced intracerebral hemorrhage and brain injury in mutant mice. *J Cereb Blood Flow Metab* 24:1133–1145
13. Garcia JH, Wagner S, Liu KF, Hu XJ (1995) Neurological deficit and extent of neuronal necrosis attributable to middle cerebral artery occlusion in rats. Statistical validation. *Stroke* 26:627–634
14. Kiang JG, Bowman PD, Lu X, Li Y, Ding XZ, Zhao B, Juang YT, Atkins JL, Tsokos GC (2006) Geldanamycin prevents hemorrhage-induced ATP loss by overexpressing inducible HSP70 and activating pyruvate dehydrogenase. *Am J Physiol Gastrointest Liver Physiol* 291:G117–G127
15. Kiang JG, Bowman PD, Lu X, Li Y, Wu BW, Loh HH, Tsen KT, Tsokos GC (2007) Geldanamycin inhibits hemorrhage-induced increases in caspase-3 activity: role of inducible nitric oxide synthase. *J Appl Physiol* 103:1045–1055
16. Shen HY, He JC, Wang Y, Huang QY, Chen JF (2005) Geldanamycin induces heat shock protein 70 and protects against MPTP-induced dopaminergic neurotoxicity in mice. *J Biol Chem* 280:39962–39969
17. Tsuchiya D, Hong S, Matsumori Y, Shiina H, Kayama T, Swanson RA, Dillman WH, Liu J, Panter SS, Weinstein PR (2003) Overexpression of rat heat shock protein 70 is associated with reduction of early mitochondrial cytochrome C release and subsequent DNA fragmentation after permanent focal ischemia. *J Cereb Blood Flow Metab* 23:718–727
18. Matsumori Y, Hong SM, Aoyama K, Fan Y, Kayama T, Sheldon RA, Vexler ZS, Ferriero DM, Weinstein PR, Liu J (2005) HSP 70 overexpression sequesters AIF and reduces neonatal hypoxic/ischemic brain injury. *J Cereb Blood Flow Metab* 25(7):899–910

Combined Systemic Thrombolysis with Alteplase and Early Hyperbaric Oxygen Therapy in Experimental Embolic Stroke in Rats: Relationship to Functional Outcome and Reduction of Structural Damage

Lea Küppers-Tiedt*, Anatol Manaenko*, Dominik Michalski, Albrecht Guenther, Carsten Hobohm, Armin Wagner, John H. Zhang, and Dietmar Schneider

Abstract Introduction: The only causal therapy in ischemic stroke is thrombolysis with recombinant tissue plasminogen activator (rtPA), but it is feasible only for few patients, and new therapies are needed. This study investigates the effects of systemic thrombolysis with rtPA combined with hyperbaric oxygen therapy (HBOT) in embolic stroke in rats.

Methods: In 22 male Wistar rats, an embolic ischemic stroke was induced. The animals were randomized to one of four groups: control, thrombolysis alone, HBOT sequential or HBOT parallel with thrombolysis. HBOT (2.4 ATA, 1 h) started 45 min (sequential) or 120 min (parallel) after stroke. rtPA was given intravenously 120 min after stroke onset. Functional tests were performed after stroke induction and after treatment. After 6 h infarct volume and intracerebral hemorrhagic complications were assessed.

Results: Compared to the control group only the combination of HBOT and thrombolysis significantly improved the functional outcome ($p=0.03$) and reduced the infarct volume ($p=0.01$), whereas thrombolysis alone did not show a significant benefit. In all treatment groups there was a trend towards fewer hemorrhagic transformations.

Conclusion: Hyperbaric oxygen in combination with thrombolysis shows neuroprotection in acute ischemic stroke in rats by reducing infarct volume and improving functional outcome in the early poststroke period.

Keywords Embolic stroke · Rat · Hyperbaric oxygen therapy · Thrombolysis

Introduction

In ischemic stroke an arterial vessel occlusion leads to an acute regional lack of cerebral perfusion. Depending on the remaining perfusion, at first the functional metabolism of the affected cells ceases, and secondly they lose their ability to maintain structure, resulting in cell death. The so-called “penumbra” describes ischemic tissue with extinct functional but preserved structural metabolism. So the penumbra is the target of all acute therapeutic efforts and can recover completely if the perfusion is restored in time [4]. The only causal therapy for acute ischemic stroke is thrombolysis with recombinant tissue plasminogen activator (rtPA), but its use remains very low in stroke patients because of numerous contraindications and a narrow time window [18]. The most feared side effect of thrombolytic therapy is secondary hemorrhagic transformation of the ischemic brain tissue [25]. The risk of hemorrhagic transformation rises with increasing infarction size and time window [12]. The expansion of the therapeutic window for thrombolysis and reduction of its risks by an adjuvant therapy would represent great progress in stroke therapy.

The most important therapeutic goal following cerebral ischemia is to restore, or at least improve, the oxygenation of ischemic brain tissue [11]. Hyperbaric oxygen therapy (HBOT) can increase the partial oxygen pressure in blood several fold. Because of the high pressure gradient, oxygen can diffuse passively deeper into the ischemic tissue, so the cells are able to maintain their cellular integrity longer. By optimizing the oxygen supply also the ischemic damage to the endothelium of the vessels should be decreased and

L. Küppers-Tiedt (✉), D. Michalski, A. Guenther, C. Hobohm, A. Wagner, and D. Schneider
Department of Neurology, University of Leipzig, Liebigstraße 20, 04103, Leipzig, Germany
e-mail: kueppers-tiedt@gmx.de

A. Manaenko (✉)
Department of Neurology, University of Leipzig, Liebigstraße 20, 04103, Leipzig, Germany and
Department of Physiology and Pharmacology, Loma Linda University, School of Medicine, Loma Linda, CA, USA
e-mail: amanaenko@llu.edu

J.H. Zhang
Department of Physiology and Pharmacology, Loma Linda University, School of Medicine, Loma Linda, CA, USA

*Equally contributed

therefore the risk of hemorrhagic transformation [19, 24]. In several models of experimental focal cerebral ischemia, HBOT has proved to be beneficial when used early after onset of the ischemia [7, 9, 21, 23]. Clinical pilot studies [1, 16, 20], however, have failed to show a benefit from HBOT, potentially because of the long time window between symptom onset and initiation of therapy, and prohibition of thrombolytic therapy [30]. In this study we combined HBOT and thrombolytic therapy in an embolic stroke model in rats to analyze the effects of the combination therapy on infarction size, functional outcome and incidence of secondary hemorrhagic transformations in the early post-stroke period.

Materials and Methods

Experimental Protocol

In 22 male Wistar rats (Charles River, Sulzfeld, Germany) weighing 325 ± 30 g an embolic stroke was induced. Afterwards the animals were randomized to one of four groups: control (room air, placebo, $n=6$), thrombolysis (room air, rtPA, $n=5$), HBOT sequential (HBOT, rtPA, $n=5$) and HBOT parallel (HBOT, rtPA, $n=6$). In the sequential setting, HBOT started 45 min and thrombolysis (rtPA) 120 min post stroke. In the parallel treatment group, gas and rtPA were administered 120 min after stroke. The experimental protocol involving animals was approved by the local authorities (Regierungspräsidium Leipzig, TVV-no. 35/03).

Embolus Preparation and Embolic Middle Cerebral Artery Occlusion (eMCAO)

Arterial blood (200 μ l) was withdrawn from the rat 24 h prior to surgery and allowed to clot in PE-50 tubing at room temperature for 2 h. Then the clot was extruded into a Petri dish filled with calcium chloride and stored at 4°C for 22 h. As embolus a single clot of 20 mm was collected into PE-10 tubing. Anesthesia was performed with isoflurane in 70% N₂O/30% O₂. Body temperature was adjusted to 37.0 ± 0.5 °C. Embolic MCAO was induced using the protocol described by Zhang [28]. Briefly, the right common carotid (CCA), internal carotid (ICA) and external carotid (ECA) arteries were exposed and the ECA ligated. PE-10 tubing was inserted into the ECA proximal to its ligation and forwarded gently into the ICA to reach the origin of the middle cerebral artery. There the clot was injected with a volume of 40 μ l of saline. After 10 min the catheter was removed and the incision closed.

Thrombolysis and Hyperbaric Oxygenation

For thrombolysis rtPA 0.9 mg/100 g body weight was used, with saline as placebo. rtPA or placebo was given intravenously (volume 1 ml) 120 min after the embolic stroke over 30 min. HBOT was performed 45 or 120 min after MCAO depending on the experimental group. The animals were pressurized within 10 min to 2.4 ATA of 100% O₂, maintained for 60 min, and thereafter decompressed within 10 min. Controls were also transferred into the chamber, but breathed room air at 1.0 ATA.

Functional Testing

After the embolic stroke, as soon as the animals recovered from anesthesia, and after complete treatment, functional testing after Menzies [13] was performed (scoring: no apparent deficits=0; contralateral forelimb flexion=1; decreased grip of the contralateral forelimb while tail pulled=2; spontaneous movement in all directions; contralateral circling only if pulled by tail=3; spontaneous contralateral circling=4; death=5).

Analysis of Infarct Volume and Hemorrhagic Transformation

Six hours after the embolic stroke animals were sacrificed. Brains were cut into five 2-mm coronal slices, stained with triphenyltetrazolium chloride (TTC) and fixed in 4% phosphate-buffered paraformaldehyde. Infarct volumes were determined using Scion Image (Scion Corporation, Walkersville, MD). For statistics, infarct volumes were expressed as percentage of the right hemisphere. Hemorrhagic transformation was analyzed macroscopically using the TTC-stained brain slices without quantitative assessment.

Statistical Analysis

Data are expressed as mean \pm standard deviation. Differences between experimental groups were statistically evaluated with the *T*-test or by analysis of variance (ANOVA), as appropriate. The incidence of hemorrhagic transformations was analyzed using Fisher's exact test. Statistical significance was set at $\alpha=0.05$.

Results

Functional Testing

Directly after the embolic stroke and after complete treatment (i.e., after 3 h), functional testing of the animals was performed (after 13). As shown in Fig. 1 after the operation, all animals presented a severe neurological deficit (score 3.9 ± 0.4) without any differences between the groups. The control animals showed no neurological recovery during the experiment; rather there was a trend to deterioration when evaluated after 3 h. The animals treated with rtPA alone showed a trend to clinical recovery compared to the control group (T -test, $p=0.082$). Only the combination of HBOT, sequential or parallel, with the thrombolytic therapy, led to a significant improvement of the neurological deficit after 3 h (T -test, HBOT sequential $p=0.031$; HBOT parallel $p=0.030$).

Infarction Size

As shown in Fig. 2, 6 h after embolic stroke we found infarctions of about 50% of the hemisphere in control animals ($51.2 \pm 14.0\%$). With thrombolytic therapy, after 2 h we did

not observe a significant decrease in infarction size ($43.4 \pm 16.1\%$, T -test $p=0.415$). The combination therapy of thrombolysis and HBOT by contrast led to a significant decrease in infarction size. In the parallel treatment group (HBOT and thrombolysis after 120 min), we observed the largest reduction of the infarcted area ($18.9 \pm 20.0\%$ control versus HBOT, T -test $p=0.010$). Similar results were obtained with the sequential treatment concept (HBOT after 45 min, thrombolysis after 120 min). This combination therapy could significantly reduce the infarcted area to $21.8 \pm 15.6\%$ compared to the control group (T -test $p=0.011$).

Hemorrhagic Transformation

In addition to the infarction size, we analyzed the percentage of hemorrhagic transformations of the infarcted tissue. We observed a difference in the rate of hemorrhagic transformations depending on the treatment strategy (Table 1). In the control group, 50% of the animals showed a hemorrhagic transformation of ischemic tissue; all treatment groups showed a lower rate of hemorrhagic complications: 20% in the rtPA treated animals ($n=5$) and 9% in the groups with the combination of thrombolysis and HBOT ($n=11$; sequential setting 0%, $n=5$; parallel setting 17%, $n=6$). These results

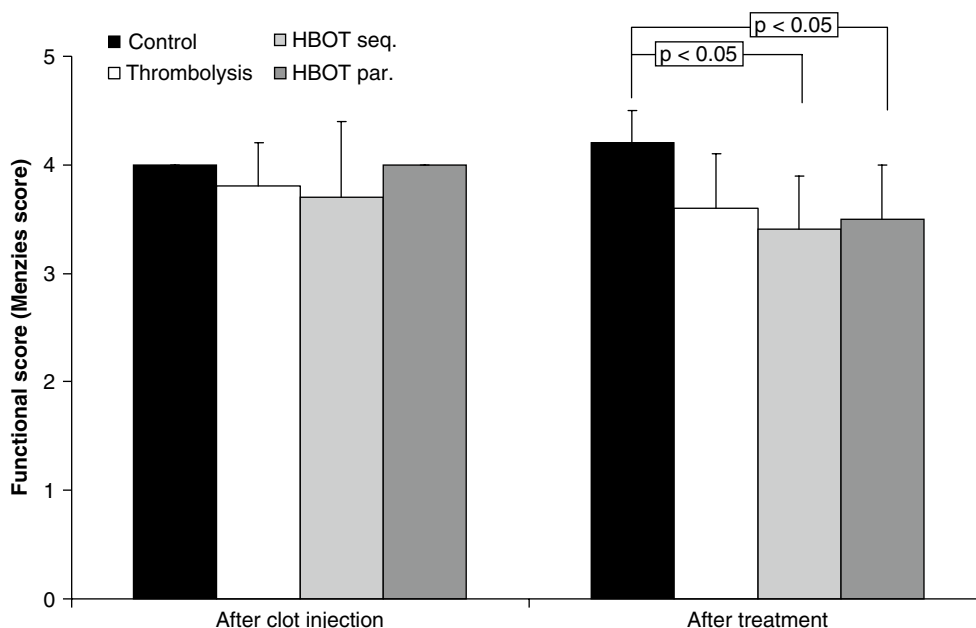


Fig. 1 Effects of HBOT/room air in combination with thrombolysis on the functional outcome using the Menzies score. *Left column:* After induction of the embolic stroke the animals showed a severe neurological deficit without any significant difference between the groups. *Right column:* After treatment the control animals experienced no clinical

recovery. By thrombolysis alone no statistically significant neurological improvement could be achieved, but both groups treated with HBOT and thrombolysis showed a significantly better functional outcome in comparison to the control group

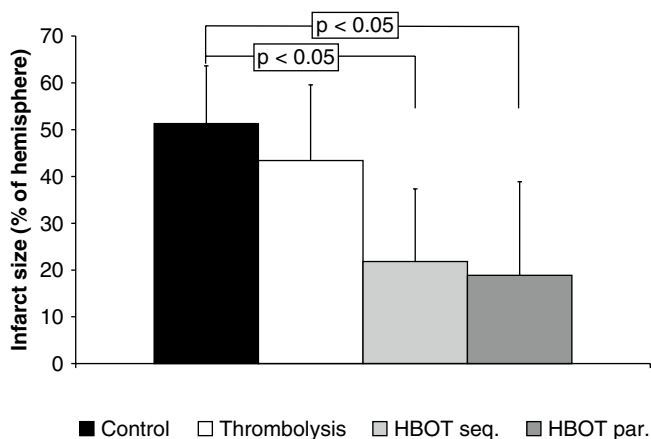


Fig. 2 Effects of HBOT/room air in combination with thrombolysis on the infarction size using TTC-stained brain slices, assessed 6 h after stroke. The control group ($n=6$) featured a mean infarction size of $51.2 \pm 14.0\%$ of the hemisphere (column 1). Treatment with rtPA alone ($n=5$, column 2) did not reduce the infarction size significantly ($43.4 \pm 16.1\%$ of the hemisphere, T -test $p=0.415$). Combination of rtPA and HBOT reduced the infarction size significantly compared with the control group, using the sequential (column 3; $n=5$; $21.8 \pm 15.6\%$ of the hemisphere; T -test $p=0.011$) or parallel treatment strategy (column 4; $n=6$; $18.9 \pm 20.0\%$ of the hemisphere; T -test $p=0.010$)

Table 1 Incidence of hemorrhagic transformation of the ischemic tissue using TTC-stained brain slices assessed 6 h after stroke. In the control group we observed in three of the six animals a hemorrhagic transformation of the brain infarct; in the group treated with thrombolysis alone in one of the five animals. Hemorrhagic transformation in the animals treated with the combination of rtPA and HBOT was 0% (sequential setting) and 17% (parallel setting), respectively

	Hemorrhagic transformation	Overall count (n)	Percentage (%)
Control	3	6	50.0
Thrombolysis	1	5	20.0
HBOT seq.	0	5	00.0
HBOT par.	1	6	17.0

did not reach statistical significance, but showed a clear trend toward the treatment groups (control versus all animals treated with rtPA and HBOT, Fisher's exact test $p=0.099$).

Discussion

The only approved clinical therapy for ischemic stroke is thrombolysis with rtPA within 4.5 h after symptom onset [8]. But this therapy has a narrow time window and holds severe risks, most notably of secondary hemorrhagic transformation of the infarcted brain tissue, and is only an option for a few stroke patients. So there is great need for new adjuvant

therapies. Up to now, no neuroprotective agent could show a benefit in clinical use.

It has already been shown in animal models that HBOT applied within the first hours is highly effective in reducing infarction size and functional deficits and optimizing metabolic parameters in ischemic stroke [19, 21, 23, 24, 26, 27]. Mostly the filament model of occlusion and reperfusion was used and reperfusion induced mechanically. But reperfusion in human stroke is much more likely a dynamic process with fibrin deposition and fibrinolysis and different degrees of reperfusion [6]. To more closely resemble the clinical situation, the present study used a rat model of embolic middle cerebral artery occlusion [28]. As has been shown before, HBOT is also effective using this stroke model [9], and it was demonstrated that after clot injection, there is no difference in infarct volume between the experimental groups. Therefore, in this study we forwent a determination of infarct volume before treatment.

In this study we could demonstrate a reduction of infarction size of more than 50% by the combination of thrombolytic and hyperbaric oxygen therapy compared to control conditions. Thrombolytic therapy alone after 2 h, relatively late in rats [22], however, reduced the ischemic damage only slightly. Thus, HBOT seems to be an effective adjuvant treatment strategy to deliver oxygen to the ischemic tissue until reperfusion is achieved. Interestingly, we could not observe any difference between the sequential and parallel use of HBOT. Theoretically, a better effect of the sequential therapy would be expected because of the earlier supply of the ischemic area with oxygen. However, we have to consider that rtPA does not lead to an immediate (complete) reperfusion [3]. Thus, in the sequential therapy there was some time window between finishing of HBOT and effective recanalization. This could explain our observation that sequential therapy is not superior to the parallel treatment strategy. Otherwise, HBOT could reduce the reperfusion damage during parallel treatment via stabilization of the blood-brain barrier [24]. This result is pleasing, as only the parallel treatment seems to make sense under clinical conditions.

Due to the short survival time of the animals, functional assessment was very limited. Parallel to the results assessing the infarction size, only the combination of HBOT and thrombolysis led to a significant neurological improvement. Further experiments with longer survival times are needed to obtain information about the final functional outcome.

An important aspect of the present study is the incidence of hemorrhagic transformations of the infarcted brain tissue. In comparison to the data available in human and experimental embolic stroke [2, 29], we observed a high incidence of hemorrhagic transformations in control animals (50%). This finding could be explained by the use of the thromboembolic model itself, because we have to face a rate of spontaneous, but late reperfusion in our model [9]. Fagan [5]

has shown that late reperfusion is a risk factor for hemorrhagic transformations in stroke. The higher rate of late reperfusion in comparison to other embolic stroke studies with a lower rate of hemorrhagic transformations [29] might be explained by different preparation of the clot material [15]. Additionally, the huge infarction volume is a risk factor of secondary hemorrhagic transformation [10]. In contrast to the human data with an increased risk of hemorrhagic complications using rtPA in acute stroke [17], in our study all treatment groups showed a lower rate of hemorrhagic complications compared to the control group. Most likely due to the small experimental groups, these results did not reach statistical significance, but showed a protective trend toward the treatment groups without any difference between the animals treated with thrombolysis alone or in combination with HBOT. Interestingly, we did not observe any secondary intracerebral hemorrhages in the sequentially treated group. Qin [19] described an attenuation of hemorrhagic complications in transient focal cerebral ischemia using HBOT. A possible explanation could be the better preserved endothelium of the vessels affected by ischemia using early HBOT. During the following reperfusion there could be less “leaking” of the vessels and therefore less hemorrhagic transformation. Veltkamp [24] also described a better preserved blood-brain barrier as well as a reduced degradation of the basal lamina under hyperbaric oxygenation. Although the methods used in our study are not adequate to reveal underlying mechanisms of HBOT, our data support the hypothesis that the neuroprotective effect of HBOT is mediated through improved oxygen supply to the ischemic periphery [23] and increased blood-brain barrier integrity [14, 24]. As we reported previously, HBOT is able to modify the inflammatory response in the ischemic penumbra in a model of permanent cerebral ischemia [7] by upregulating astrocytes and reducing activated microglia. Further experiments should investigate the effect of the combination therapy on the microglial and astrocytic reaction using the thromboembolic stroke model.

Acknowledgments This study was supported by a junior research grant of the Medical Faculty of the University of Leipzig.

Conflict of interest statement We declare that we have no conflict of interest.

References

- Anderson DC, Bottini AG, Jagiella WM, Westphal B, Ford S, Rockswold GL, Loewenson RB (1991) A pilot study of hyperbaric oxygen in the treatment of human stroke. *Stroke* 22:1137–1142
- Brinker G, Pillekamp F, Hossmann KA (1999) Brain hemorrhages after rt-PA treatment of embolic stroke in spontaneously hypertensive rats. *NeuroReport* 10(9):1943–1946
- Christou I, Alexandrov AV, Burgin WS, Wojner AW, Felberg RA, Malkoff M, Grotta JC (2000) Timing of recanalization after tissue plasminogen activator therapy determined by transcranial Doppler correlates with clinical recovery from ischemic stroke. *Stroke* 31(8):1812–1816
- Fisher M (2004) The ischemic penumbra: identification, evolution and treatment concepts. *Cerebrovasc Dis* 17(Suppl):1–6
- Fagan SC, Nagaraja TN, Fenstermacher JD, Zheng J, Johnson M, Knight RA (2003) Hemorrhagic transformation is related to the duration of occlusion and treatment with tissue plasminogen activator in a nonembolic stroke model. *Neurol Res* 25(4):377–382
- Gerriets T, Postert T, Goertler M, Stolz E, Schlachetzki F, Sliwka U, Seidel G, Weber S, Kaps M (2000) DIAS I: duplex-sonographic assessment of the cerebrovascular status in acute stroke. A useful tool for future stroke trials. *Stroke* 31:2342–2345
- Günther A, Küppers-Tiedt L, Schneider PM, Kunert I, Berrouschot J, Schneider D, Rossner S (2005) Reduced infarct volume and differential effects on glial cell activation after hyperbaric oxygen treatment in rat permanent focal cerebral ischaemia. *Eur J Neurosci* 21(11):3189–3194
- Hacke W, Kaste M, Bluhmki E, Brozman M, Dávalos A, Guidetti D, Larrue V, Lees KR, Medeghri Z, Machnig T, Schneider D, von Kummer R, Wahlgren N, Toni D, ECASS Investigators (2008) Thrombolysis with alteplase 3 to 4.5 hours after acute ischemic stroke. *N Engl J Med* 359(13):1317–1329
- Henninger N, Küppers-Tiedt L, Sicard KM, Günther A, Schneider D, Schwab S (2006) Neuroprotective effect of hyperbaric oxygen therapy monitored by MR-imaging after embolic stroke in rats. *Exp Neurol* 201(2):316–323
- Kerenyi L, Kardos L, Szász J, Szatmári S, Bereczki D, Hegedüs K, Csiba L (2006) Factors influencing hemorrhagic transformation in ischemic stroke: a clinicopathological comparison. *Eur J Neurol* 13:1251–1255
- Khaja AM, Grotta JC (2007) Established treatments for acute ischaemic stroke. *Lancet* 369:319–330
- Larrue V, von Kummer R, del Zoppo G, Bluhmki E (1997) Hemorrhagic transformation in acute ischemic stroke: potential contributing factors in the European Cooperative Acute Stroke Study. *Stroke* 28:957–960
- Menzies SA, Hoff JT, Betz AL (1992) Middle cerebral artery occlusion in rats: a neurological and pathological evaluation of a reproducible model. *Neurosurgery* 31(1):100–106; discussion 106–107
- Mink RB, Dutka AJ (1995) Hyperbaric oxygen after global cerebral ischemia in rabbits reduces brain vascular permeability and blood flow. *Stroke* 26(12):2307–2312
- Niessen F, Hilger T, Hoehn M, Hossmann KA (2003) Differences in clot preparation determine outcome of recombinant tissue plasminogen activator treatment in experimental thromboembolic stroke. *Stroke* 34:2019–2024
- Nighoghossian N, Trouillas P, Adeleine P, Salord F (1995) Hyperbaric oxygen in the treatment of acute ischemic stroke. A double-blind pilot study. *Stroke* 26:1369–1372
- NINDS rt-PA Stroke Study Group (1997) Intracerebral hemorrhage after intravenous tPA therapy for ischemic stroke. *Stroke* 28:2109–2118
- Quinn TJ, Dawson J, Lees KR (2008) Past, present and future of alteplase for acute ischemic stroke. *Expert Rev Neurother* 8(2):181–192
- Qin Z, Karabiyikoglu M, Hua Y, Silbergleit R, He Y, Keep RF, Xi G (2007) Hyperbaric oxygen-induced attenuation of hemorrhagic transformation after experimental focal transient cerebral ischemia. *Stroke* 38(4):1362–1367
- Rusyniak DE, Kirk MA, May JD, Kao LW, Brizendine EJ, Welch JL, Cordell WH, Alonso RJ (2003) Hyperbaric oxygen therapy in acute ischemic stroke: results of the hyperbaric oxygen in acute ischemic stroke trial pilot study. *Stroke* 34:571–574

21. Schabitz WR, Schade H, Heiland S, Kollmar R, Bardutzky J, Henninger N, Muller H, Carl U, Toyokuni S, Sommer C, Schwab S (2004) Neuroprotection by hyperbaric oxygenation after experimental focal cerebral ischemia monitored by MRI. *Stroke* 35: 1175–1179
22. Schatlo B, Henning EC, Pluta RM, Latour LL, Golpayegani N, Merrill MJ, Lewin N, Chen Y, Oldfield EH (2008) Nitrite does not provide additional protection to thrombolysis in a rat model of stroke with delayed reperfusion. *J Cereb Blood Flow Metab* 28(3): 482–489
23. Veltkamp R, Warner DS, Domoki F, Brinkhous AD, Toole JF, Busija DW (2000) Hyperbaric oxygen decreases infarct size and behavioural deficit after transient focal cerebral ischemia in rats. *Brain Res* 853:68–73
24. Veltkamp R, Siebing DA, Sun L, Heiland S, Bieber K, Marti HH, Nagel S, Schwab S, Schwaninger M (2005) Hyperbaric oxygen reduces blood-brain barrier damage and edema after transient focal cerebral ischemia. *Stroke* 36:1679–1683
25. Walters MR, Muir KW, Harbison J, Lees KR, Ford GA (2005) Intravenous thrombolysis for acute ischaemic stroke: preliminary experience with recombinant tissue plasminogen activator in the UK. *Cerebrovasc Dis* 20(6):438–442
26. Yin D, Zhou C, Kusaka I, Calvert JW, Parent AD, Nanda A, Zhang JH (2003) Inhibition of apoptosis by hyperbaric oxygen in a rat focal cerebral ischemic model. *J Cereb Blood Flow Metab* 23: 855–864
27. Yin D, Zhang JH (2005) Delayed and multiple hyperbaric oxygen treatments expand therapeutic window in rat focal cerebral ischemic model. *Neurocrit Care* 2(2):206–211
28. Zhang RL, Chopp M, Zhang ZG, Jiang Q, Ewing JR (1997) A rat model of focal embolic cerebral ischemia. *Brain Res* 766(1–2):83–92
29. Zhang RL, Chopp M, Zhang ZG, Divine G (1998) Early (1 h) administration of tissue plasminogen activator reduces infarct volume without increasing hemorrhagic transformation after focal cerebral embolization in rats. *J Neurol Sci* 160(1):1–8
30. Zhang JH, Singhal AB, Toole JF (2003) Oxygen therapy in ischemic stroke. *Stroke* 34:152–153

Neutrophil Depletion Diminishes Monocyte Infiltration and Improves Functional Outcome After Experimental Intracerebral Hemorrhage

Lauren H. Sansing, Tajie H. Harris, Scott E. Kasner, Christopher A. Hunter, and Katalin Kariko

Abstract Inflammation contributes to secondary injury and neuronal loss after intracerebral hemorrhage, but the role of individual immune populations in these processes is unclear. In a mouse model, the injection of autologous blood into the striatum was associated with an intense inflammatory cell infiltrate composed of neutrophils, monocytes, and dendritic cells. Selective depletion of neutrophils resulted in decreased infiltration of monocytes and improved functional outcomes at day 3 post-hemorrhage. These findings indicate that neutrophil infiltration into the site of hemorrhage contributes to brain injury either by direct cellular damage or the recruitment of monocytes.

Keywords Intracerebral hemorrhage · Inflammation · Neutrophils · Monocytes

Introduction

Intracerebral hemorrhage (ICH) is a devastating stroke subtype without specific treatment. Activation of the innate immune system after ICH leads to perihematomal inflammation and neuronal loss over the first 3 days [1]. As neurons have limited regeneration, neuronal loss likely contributes to poor functional outcome. More detailed understanding of the triggers of the inflammatory response and the particular effector immune cells involved may lead to development of therapies that can mitigate the secondary injury response after ICH and improve outcome.

At the site of the hemorrhage, there is an intense inflammatory response evident by activation of resident microglia and an acute influx of neutrophils that accumulate at the edge of the hematoma [1–5]. Similarly, neutrophils are also observed in models of acute cerebral ischemia and have been associated with poor outcome. For example, inhibition of neutrophil elastase reduced infarct volume and blood-brain barrier permeability in transient middle cerebral artery occlusion [6]. The protective role of cannabinoid 2 receptors after ischemia has been shown to be mediated solely through inhibited neutrophil recruitment [7]. In addition, depletion of neutrophils with vinblastine reduced hemorrhagic transformation of ischemic brain after tPA administration [8]. Thus, there is accumulating evidence of deleterious effects of infiltrating neutrophils in the sterile brain injury models of cerebral ischemia and hemorrhage.

Although previous studies have documented the presence of perihematomal neutrophils after ICH, the specific role of neutrophils in the pathogenesis of secondary injury has not been investigated. This study used immunohistochemistry and flow cytometry to quantify the degree of neutrophil, monocyte, and dendritic cell infiltration after experimental hemorrhage. Moreover, as neutrophils may serve a pathogenic role in this sterile injury model, the effects of neutrophil depletion on the composition of the inflammatory infiltrate and on functional outcome in the first 3 days after ICH were determined.

L.H. Sansing (✉)

Department of Neurology, University of Pennsylvania Medical Center,
3 W Gates, 3400 Spruce Street, Philadelphia, PA, USA
e-mail: lauren.sansing@uphs.upenn.edu

T.H. Harris and C.A. Hunter

Department of Pathobiology, School of Veterinary Medicine,
University of Pennsylvania, Philadelphia, PA, USA

S.E. Kasner

Department of Neurology, University of Pennsylvania Medical Center,
Philadelphia, PA, USA

K. Kariko

Department of Neurosurgery, University of Pennsylvania Medical
Center, Philadelphia, PA, USA

Methods and Materials

Mice: C3H/HeO_uJ mice were obtained from Jackson Laboratories (Bar Harbor, ME). Male mice aged 14–18 weeks and weighing 28–35 g were used for all experiments. All procedures were carried out with the approval of the Institutional Animal Use and Care Committee of the University of Pennsylvania.

Intracerebral hemorrhage surgery: Mice were anesthetized with inhaled 70% N₂O, 30% O₂, and 1–5% Isoflurane, and given buprenorphine 0.1 mg/kg subcutaneously for analgesia. Autologous blood from the ventral tail artery was injected at 0.5 μ l/min for a total of 15 μ l by microinfusion pump (World Precision Instruments, Sarasota, FL) with a 5-min pause midway through the infusion, at coordinates 2.5 mm right of the bregma, angled 5° medial and 3 mm deep. The needle was left in place for 30 additional minutes to allow blood clotting and then withdrawn at 1 mm/min. Incisions were closed using Vetbond (3 M, St. Paul, MN). Body core temperature was maintained at 37 \pm 0.5°C by rectal thermometer using a thermistor-controlled heating pad throughout the procedure. Sham surgeries were also performed that included all procedures (including needle insertion) except blood injection.

Immediately after sacrifice, the brain was inspected for ICH success based on gross inspection of a coronal section at the needle insertion site, blinded to mouse treatment. Hemorrhages that tracked down to the base of the brain, up the needle track past the corpus callosum, or into the ventricles were deemed unsuccessful and that mouse was eliminated from all analyses. Three mice were eliminated after ICH resulting in a success rate 81%.

Neutrophil depletion: Mice were injected intraperitoneally with rat anti-mouse Ly6G monoclonal antibody (clone 1A8, BD Biosciences, San Jose, CA), 5 mg/kg, $n=6$, to deplete circulating neutrophils or control rat IgG (5 mg/kg, $n=6$) 12 h prior to ICH surgery and then every 36–48 h until sacrifice on post-ICH day 3.

Quantification of neurobehavioral deficit: Cylinder testing was performed postoperatively each morning, blinding to treatment, and videotaped for review of the scoring. Each mouse was placed in a 12-cm-diameter clear glass cylinder and observed for 20 rears. The initial placement of the forelimbs on the wall of the cylinder was scored per rear. Subsequent movements (such as lateral exploration) were not scored until the mouse returned to the ground; the next rear was then scored. The laterality index was calculated as (number of right forelimb placements on the side of the cylinder – number of left forelimb placements)/(number of right + number of left + number of both), where 0 indicates no forelimb preference, and 1 indicates only the right forelimb was used.

Immunohistochemistry: Mice were euthanized at 72 \pm 2 h after ICH; their brains were removed and immediately frozen

in Tissue-tek O.C.T. (Andwin Scientific, Addison, IL), and stored at –80°C until analysis. Then 6- μ m sections were fixed with 75% acetone/25% ethanol and blocked with 2% normal goat serum. Slides were incubated with rat anti-mouse Ly6G (5 μ g/ml) or rat anti-mouse CD11b (2.5 μ g/ml) (eBioscience, San Diego, CA) followed by secondary antibody [Cy3 Affinipure goat anti-rat IgG (Jackson ImmunoResearch, West Grove, PA)] at 1:500. DAPI was used at 0.5 μ g/ml (Roche Diagnostics, Mannheim, Germany).

Images were acquired using a Nikon E600 fluorescence microscope equipped with a CoolSNAP CCD camera (Photometrics, Tucson, AZ) and processed with NIS Elements software (Nikon, Melville, NY). Neutrophil infiltration was quantified by summing the number of perihematomal neutrophils in five perihematomal 40 \times fields per mouse to yield the neutrophil count for each mouse. CD11b-positive cells were quantified by summing the number of positive cells in five 20 \times fields.

Tissue preparation for flow cytometry: Immediately following sacrifice, 1 ml of venous blood was withdrawn and mixed with heparin 200 U/ml. Mice were then perfused with 50 mL of ice cold PBS, and the brains and spleens removed. The two cerebral hemispheres were divided along the inter-hemispheric fissure so that the ipsilateral and contralateral hemispheres could be analyzed separately. Each hemisphere was placed in 4 ml of complete RPMI 1640 (Life Technologies, Gaithersburg, MD) medium supplemented with 10% fetal calf serum, 1% sodium pyruvate, 1% non-essential amino acids, 0.1% β -mercaptoethanol, 100 U penicillin/mL, and 100 μ g/ml streptomycin (all Gibco, Invitrogen Incorporation, Grand Island, NY). Tissues were mechanically dissociated and incubated with 100 μ l of collagenase/dispase (10 mg/ml, Roche Diagnostics, Indianapolis, IN) and 300 μ l DNase (10 mg/ml, Sigma) for 45 min at 37°C. The suspension was then passed through a 70- μ m cell strainer, pelleted at 2,000 \times g for 10 min, and resuspended in 60% isotonic Percoll (GE Healthcare, Pittsburgh, PA) solution, overlaid with 30%, and centrifuged at 1,000 \times g for 25 min. Brain mononuclear cells were harvested at the 60% and 30% inter-phase layer.

Peripheral blood leukocytes were overlaid on 4 ml Lympholyte-M and centrifuged at 800 \times g for 20 min. Leukocytes at the interface were harvested and washed with complete RPMI.

Flow cytometry: Cells were washed in PBS and then blocked with 50 μ l Fc block [10% CD16/CD32 10 μ g/ml, BD Biosciences, 0.5% normal rat IgG in FACS buffer (1 \times PBS, 0.2% BSA, and 2 mM EDTA)] for 15 min prior to staining with CD45-APC, CD11b-PerCp Cy5.5, Ly6G-Pacific Blue, CD11c-PECy7, CD3-FITC, CD19-FITC, NK1.1-FITC, and Gr-1-PE (eBioscience) for 15 min. Data were acquired on a BD Canto II using FACsDIVA 6.0 software (BD Biosciences). Analysis was performed using

FlowJo software (Treestar Inc., Ashland, OR). Microglia were identified as CD45^{int}CD11b⁺Gr-1⁻ cells. Neutrophils were identified as CD45^{hi}CD3⁻CD19⁻NK1.1⁻CD11b⁺Ly6G⁺F4/80⁻ cells. Monocytes were identified as CD45^{hi}CD3⁻CD19⁻NK1.1⁻CD11b⁺Ly6G⁻CD11c⁺F4/80^{int} cells. Dendritic cells were identified as CD45^{hi}CD3⁻CD19⁻NK1.1⁻CD11b⁺Ly6G⁻CD11c⁺ cells.

Statistical analysis: Cell counts by immunohistochemistry and flow cytometry were tested for normality, and differences between treatment groups were compared by two-sided *t*-test or Wilcoxon rank sum, as appropriate. Cells counts in peripheral blood were compared by *t*-test. The ratios of ipsilateral/contralateral neutrophils, monocytes, and dendritic cells in the brain were calculated to account for differences in the success of perfusion in each mouse and compared by *t*-test. Cylinder test results on each day were compared by ANOVA followed by *t*-tests for each pair of cohorts since the comparisons were pre-specified and distribution was normal. Analysis was performed with Stata IC/10 (College Station, TX).

Results

Localized Inflammatory Response After Experimental ICH

In order to better understand how inflammation contributes to the pathogenesis of ICH, a murine model of autologous blood injection was used. In these studies, mice were infused with 15 μ l of blood into the right striatum or a sham injection, and at 3 days post injection brain tissue was removed and used for immunohistochemistry and flow cytometry. Neutrophils were identified immunohistochemically by characteristic bright Ly6G staining and multi-lobed nuclei. Rare neutrophils were found in the needle track after sham surgery (Fig. 1a). In contrast, after ICH, neutrophils were readily identified at the rim of the lesion but did not extend more than 50 μ m from the edge of the hematoma (Fig. 1b). The median number of neutrophils in five 40 \times perihematomal fields was 21.5 neutrophils (IQR 16–22) after ICH and two [2, 9, 10] after sham surgery, $p=0.006$.

Also present in both cohorts were CD11b⁺ cells of different morphologies. After sham surgery most CD11b⁺ cells had small cell bodies with multiple processes, resembling resting microglia (Fig. 1c). At the hematoma there were also large CD11b⁺ cells, with at least 1 diameter greater than 10 μ m, and vacuolated cytoplasm, which were present within the hemorrhage and extended 50–100 μ m from the edge of the hematoma, and smaller cells with processes and without vacuolated cytoplasm (Fig. 1d). Quantification of the populations of CD11b⁺ cells revealed that the ICH resulted in

approximately a 60% increase in the numbers, with a mean of 255.6 ± 77.3 cells in five 20 \times fields after ICH and 161.7 ± 22.5 cells after sham, $p>0.05$.

Consistent with the immunohistochemistry, flow cytometric analysis of the mononuclear cell preparations revealed that the inflammatory infiltrate consisted of neutrophils, monocytes, dendritic cells, and microglia (gating shown in Fig. 1e). The ratios of cells in the ipsilateral/contralateral hemispheres are shown in Fig. 1f. In the ipsilateral hemisphere, there was a 9-fold increase in neutrophils, a 29-fold increase in monocytes, a 24-fold increase in dendritic cells, and a 3-fold increase in microglia after ICH. These results confirm an intense, localized inflammation associated with experimental ICH.

Neutrophil Depletion Reduced Monocyte Infiltration into Perihematomal Brain

The presence of perihematomal neutrophils after ICH and their association with poor outcome in other models of sterile brain injury led to experiments to assess the contribution of these cells to the development of inflammation. Therefore, prior to ICH surgery, mice were treated with a neutrophil-specific (anti-Ly6G) antibody that spared other myeloid cell lines [10], but led to the depletion of 96.5% of blood neutrophils (data not shown). In these experiments, neutrophil depletion did not alter the twofold increase in ipsilateral microglia observed after ICH. However, this treatment did result in a significant reduction in the number of monocytes that infiltrated into perihematomal brain (neutrophil-depleted mean ratio 2.8 ± 1.7 vs. control 10.2 ± 6.6 , $p<0.05$). There was also a trend toward fewer dendritic cells in the neutrophil-depleted mice, although this did not reach significance. The ratios of cell counts by treatment are shown in Fig. 2a. These results indicate an important role for neutrophils in recruiting monocytes to the injured brain.

Neutrophil Depletion Improved Functional Outcome

To assess the importance of the modified inflammatory response on injury and recovery, the laterality index on the cylinder test was compared among neutrophil-depleted, control IgG-treated, and untreated mice. There was no difference in the laterality indices among untreated ($n=5$), control IgG-treated ($n=5$), and neutrophil-depleted mice ($n=6$) on post-ICH day 1 (Fig. 2b). However, the neutrophil-depleted mice significantly improved each day (post-ICH day 2: $p=0.03$, post-ICH day 3: $p=0.002$, laterality indices

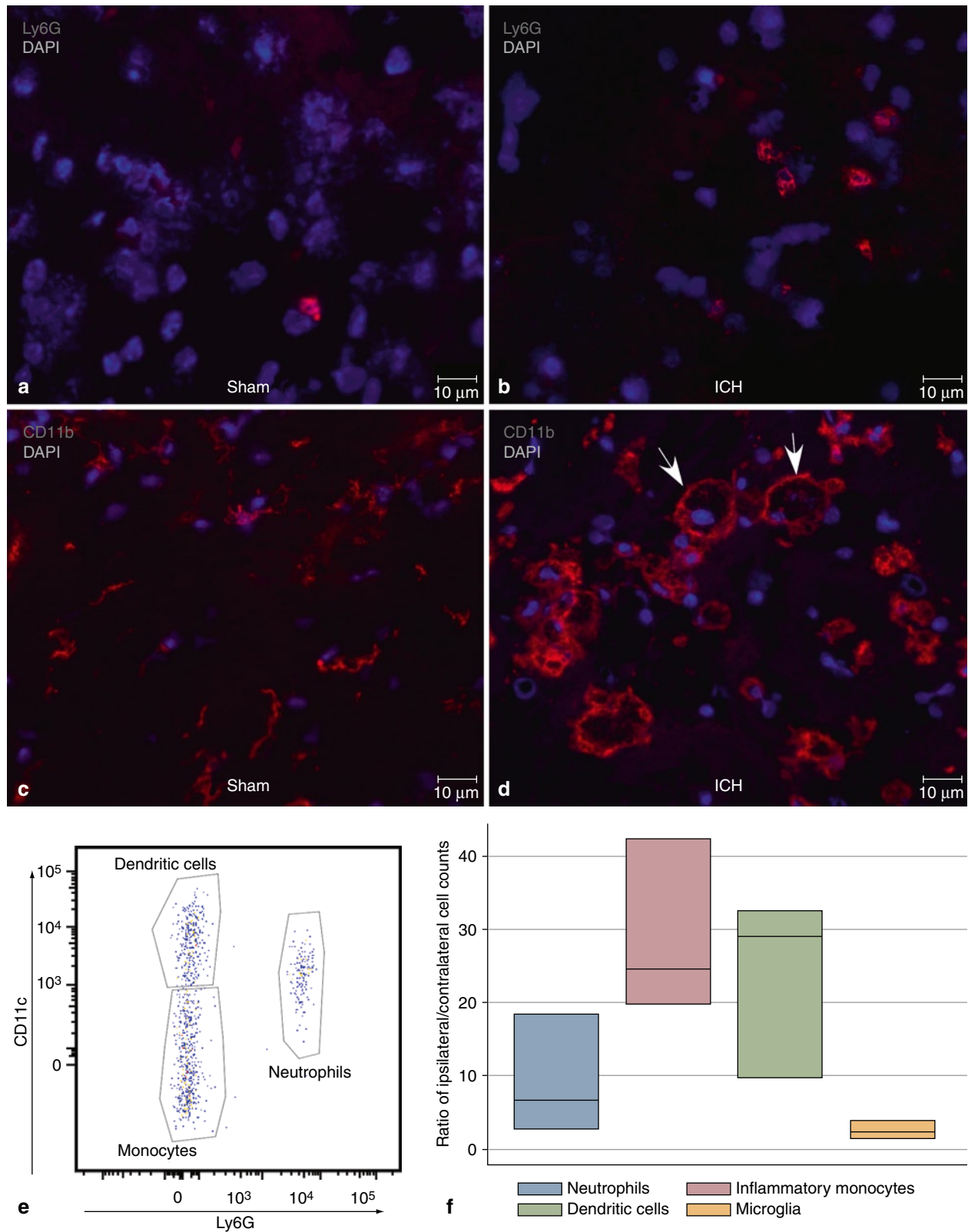


Fig. 1 Immunohistochemistry of perihematomal brain post-ICH day 3 in an untreated mouse. **(a)** Ly6G staining (*red*) identifies rare neutrophils after sham surgery. **(b)** Increased numbers of infiltrating neutrophils are seen at the periphery of the hematoma. **(c)** After sham surgery, most CD11b⁺ (myeloid-derived) cells are small and resemble resting microglia. **(d)** After ICH, CD11b⁺ cells have differing morphologies

both within and at the periphery of the hematoma. Larger, vacuolated cells are indicated by the arrows. **(e)** Flow cytometry plot of CD45^{hi}CD3-CD19-NK1.1-CD11b⁺ cells plotted Ly6G against CD11c to show three separate populations of dendritic cells (CD11c⁺Ly6G⁻), inflammatory monocytes (CD11c⁺Ly6G⁺), and neutrophils (Ly6G⁺). **(f)** Ratios of ipsilateral/contralateral cell counts in brain, $n=3$

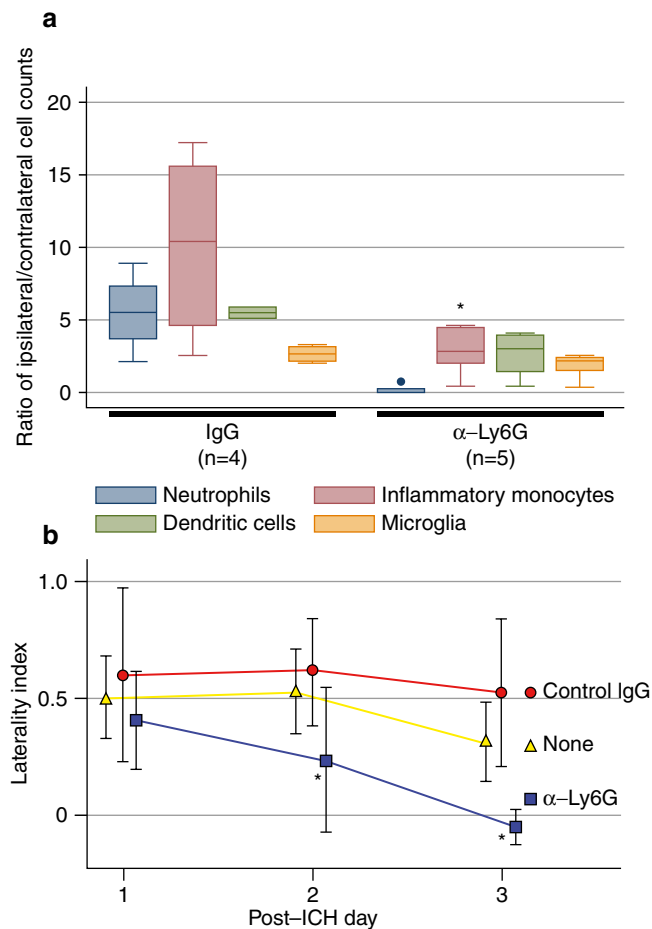


Fig. 2 Neutrophil depletion reduced inflammatory response and improved functional outcome. (a) Ratios of ipsilateral/contralateral cell counts in brain after neutrophil depletion or control IgG treatment. (b) Cylinder score results on post-ICH days 1-3 by treatment

compared by ANOVA). On post-ICH day 3 they had no measurable forelimb preference (laterality index mean -0.14 ± 0.23), whereas the other two groups remained with significant left-sided weakness (untreated laterality index 0.32 ± 0.17 ; control IgG-treated 0.52 ± 0.31). There was no difference in the laterality indices between untreated and IgG-treated mice at any time point. Thus, neutrophil depletion resulted in improved functional recovery after ICH, indicating that neutrophils are a mediator of secondary injury and a potential target for therapeutic intervention.

Discussion

A substantial neutrophil infiltration was identified in the perihematomal brain on day 3 after ICH by immunohistochemistry and flow cytometry. Thus, we hypothesized that neutrophil infiltration into brain after sterile injury

contributes to secondary brain injury. Neutrophil depletion prior to ICH with a selective (anti-Ly6G) antibody led to significantly fewer neutrophils and monocytes infiltrating into the perihematomal region and improved functional outcome. The basis for this protection is unclear, but possible mechanisms include decreased direct brain injury by neutrophil degranulation and decreased monocyte recruitment. The timing of granule release from neutrophils is coordinated with the stage of migration into tissues, with primary and secondary granules being released after successful extravasation into tissue [11]. Contents of these granules include collagenase, elastase, and myeloperoxidase, among others, which may cause direct injury to neurons and astrocytes and contribute to the poor outcomes seen after ICH. Neutrophil-derived serine proteases also regulate the immune response via cytokine activation and release, including IL-8 [12], IL-6 [13], TNF- α , and IL-1 β [9, 14], which may contribute to additional injury [15–18]

Neutrophils have a key role in the recruitment of monocytes to infected or injured tissue. When neutrophils adhere to the endothelial surface, the contents of secretory granules are released, including cationic antimicrobial protein of 37 kD (CAP37)/azurocidin and proteinase 3, leading to endothelial cell activation, increased cellular adhesion molecule expression, and increased monocyte adhesion [19–21]. Neutrophils also contribute to monocyte chemotaxis by releasing LL-37 [22] and cathepsin G [23], and enhancing endothelial cell release of monocyte chemoattractant protein-1 [24]. Thus, our observation that neutrophil depletion led to decreased monocyte infiltration after ICH is consistent with a model in which the early recruitment of neutrophils establishes a local environment that allows monocytes to enter the injured brain. Nevertheless, it is unclear based on this study whether the diminished monocyte response contributed to the benefit on functional outcome. Monocytes may contribute to acute injury by releasing inflammatory cytokines and chemokines. Alternatively, monocytes may contribute to recovery by aiding in phagocytosis of red blood cells and cellular debris or by shifting response to a less inflammatory one. Additional studies will be required to elucidate the role of monocytes in the perihematomal region.

An early study on the detrimental effect of circulating leukocytes after ICH demonstrated decreased cerebral edema after whole body irradiation and increased edema after brain irradiation [25]. The irradiation depleted all leukocyte cell lines and platelets and used a microballoon (inert) model of ICH, indicating that blood-derived cells contribute to local inflammation after tissue disruption in the brain. More recently, CD18 deficiency has been shown to reduce brain edema after ICH, confirming the role of leukocyte migration in the pathogenesis of inflammation after ICH [26]. Identification of which immune cells are pathogenic in the acute phase after ICH may lead to new potential therapies in

blocking specific cell trafficking and signaling while leaving beneficial responses intact. Thus, the finding of an injurious role of neutrophils after ICH invites further investigation of potential therapies to mitigate their effect. While antagonizing neutrophil migration or function may leave critically ill patients at high risk of infection, selective inhibition of neutrophil trafficking across the blood-brain barrier or antagonism of specific neutrophil-mediated detrimental processes may offer more specific/tangible benefits.

Acknowledgments Funded by a fellowship from the Institute for Translational Medicine and Therapeutics, University of Pennsylvania (LHS), T32-AI055400 and AI081478 (TH), and AI41158 (CAH).

Disclosure/conflict of interest statement We declare that we have no conflict of interest.

References

- Wasserman JK, Schlichter LC (2007) Neuron death and inflammation in a rat model of intracerebral hemorrhage: effects of delayed minocycline treatment. *Brain Res* 1136:208–218
- Bigio MRD, Yan HJ, Buist R, Peeling J, del Zoppo GJ (1996) Experimental intracerebral hemorrhage in rats: magnetic resonance imaging and histopathological correlates. *Stroke* 27:2312–2320
- Gong C, Hoff JT, Keep RF (2000) Acute inflammatory reaction following experimental intracerebral hemorrhage in rat. *Brain Res* 871:57–65
- Guo FQ, Li XJ, Chen LY, Yang H, Dai HY, Wei YS, Huang YL, Yang YS, Sun HB, Xu YC, Yang ZL (2006) Study of relationship between inflammatory response and apoptosis in perihematoma region in patients with intracerebral hemorrhage. *Zhongguo Wei Zhong Bing Ji Jiu Yi Xue* 18:290–293
- Xue M, Del Bigio MR (2000) Intracerebral injection of autologous whole blood in rats: time course of inflammation and cell death. *Neurosci Lett* 283:230–232
- Stowe AM, Adair-Kirk TL, Gonzales ER, Perez RS, Shah AR, Park TS, Gidday JM (2009) Neutrophil elastase and neurovascular injury following focal stroke and reperfusion. *Neurobiol Dis* 35:82–90
- Murikinati S, Juttler E, Keinert T, Ridder DA, Muhammad S, Waibler Z, Ledent C, Zimmer A, Kalinke U, Schwaninger M (2010) Activation of cannabinoid 2 receptors protects against cerebral ischemia by inhibiting neutrophil recruitment. *FASEB J* 24:788–798
- Gautier S, Ouk T, Petrault O, Caron J, Bordet R (2009) Neutrophils contribute to intracerebral haemorrhages after treatment with recombinant tissue plasminogen activator following cerebral ischaemia. *Br J Pharmacol* 156:673–679
- Coeshott C, Ohnemus C, Pilyavskaya A, Ross S, Wieczorek M, Kroona H, Leimer AH, Cheronis J (1999) Converting enzyme-independent release of tumor necrosis factor α and IL-1 β from a stimulated human monocytic cell line in the presence of activated neutrophils or purified proteinase 3. *Proc Natl Acad Sci USA* 96:6261–6266
- Daley JM, Thomay AA, Connolly MD, Reichner JS, Albina JE (2008) Use of Ly6G-specific monoclonal antibody to deplete neutrophils in mice. *J Leukoc Biol* 83:64–70
- Soehnlein O, Weber C, Lindbom L (2009) Neutrophil granule proteins tune monocytic cell function. *Trends Immunol* 30:538–546
- Padrines M, Wolf M, Walz A, Baggiolini M (1994) Interleukin-8 processing by neutrophil elastase, cathepsin G and proteinase-3. *FEBS Lett* 352:231–235
- Li T, Wang H, He S (2006) Induction of interleukin-6 release from monocytes by serine proteinases and its potential mechanisms. *Scand J Immunol* 64:10–16
- Elssner A, Duncan M, Gavrilin M, Wewers MD (2004) A novel P2X7 receptor activator, the human cathelicidin-derived peptide LL37, induces IL-1 β processing and release. *J Immunol* 172:4987–4994
- Fang HY, Ko WJ, Lin CY (2007) Inducible heat shock protein 70, interleukin-18, and tumor necrosis factor alpha correlate with outcomes in spontaneous intracerebral hemorrhage. *J Clin Neurosci* 14:435–441
- Holmin S, Mathiesen T (2000) Intracerebral administration of interleukin-1 β and induction of inflammation, apoptosis, and vasogenic edema. *J Neurosurg* 92:108–120
- Hua Y, Wu J, Keep RF, Nakamura T, Hoff JT, Xi G (2006) Tumor necrosis factor- α increases in the brain after intracerebral hemorrhage and thrombin stimulation. *Neurosurgery* 58:542–550; discussion 542–550
- Mayne M, Ni W, Yan HJ, Xue M, Johnston JB, Del Bigio MR, Peeling J, Power C (2001) Antisense oligodeoxynucleotide inhibition of tumor necrosis factor- α expression is neuroprotective after intracerebral hemorrhage. *Stroke* 32:240–248
- Lee TD, Gonzalez ML, Kumar P, Grammas P, Pereira HA (2003) CAP37, a neutrophil-derived inflammatory mediator, augments leukocyte adhesion to endothelial monolayers. *Microvasc Res* 66:38–48
- Soehnlein O, Xie X, Ulbrich H, Kenne E, Rotzius P, Flodgaard H, Eriksson EE, Lindbom L (2005) Neutrophil-derived heparin-binding protein (HBP/CAP37) deposited on endothelium enhances monocyte arrest under flow conditions. *J Immunol* 174:6399–6405
- Taekema-Roelvink MEJ, Van Kooten C, Heemskerk E, Schroeijers W, Daha MR (2000) Proteinase 3 interacts with a 111-kD membrane molecule of human umbilical vein endothelial cells. *J Am Soc Nephrol* 11:640–648
- Yang D, Chen Q, Schmidt AP, Anderson GM, Wang JM, Wooters J, Oppenheim JJ, Chertov O (2000) IL-37, the neutrophil granule- and epithelial cell-derived cathelicidin, utilizes formyl peptide receptor-like 1 (FPRL1) as a receptor to chemoattract human peripheral blood neutrophils, monocytes, and T cells. *J Exp Med* 192:1069–1074
- Sun R, Iribarren P, Zhang N, Zhou Y, Gong W, Cho EH, Lockett S, Chertov O, Bednar F, Rogers TJ, Oppenheim JJ, Wang JM (2004) Identification of neutrophil granule protein cathepsin G as a novel chemotactic agonist for the G protein-coupled formyl peptide receptor. *J Immunol* 173:428–436
- Taekema-Roelvink MEJ, Kooten CV, Kooij SVD, Heemskerk E, Daha MR (2001) Proteinase 3 enhances endothelial monocyte chemoattractant protein-1 production and induces increased adhesion of neutrophils to endothelial cells by upregulating intercellular cell adhesion molecule-1. *J Am Soc Nephrol* 12:932–940
- Kane PJ, Modha P, Strachan RD, Cook S, Chambers IR, Clayton CB, Mendelow AD (1992) The effect of immunosuppression on the development of cerebral oedema in an experimental model of intracerebral haemorrhage: whole body and regional irradiation. *J Neurol Neurosurg Psychiatry* 55:781–786
- Titova E, Kevil CG, Ostrowski RP, Rojas H, Liu S, Zhang JH, Tang J (2008) Deficiency of CD18 gene reduces brain edema in experimental intracerebral hemorrhage in mice. *Acta Neurochir Suppl* 105:85–87

Hydrogen Inhalation is Neuroprotective and Improves Functional Outcomes in Mice After Intracerebral Hemorrhage

Anatol Manaenko, Tim Lekic, Qingyi Ma, Robert P. Ostrowski, John H. Zhang, and Jiping Tang

Abstract Objective: Oxidative stress contributes significantly to the development of secondary brain injury after intracerebral hemorrhage (ICH). It has been previously demonstrated that hydrogen gas can decrease oxidative stress by scavenging reactive oxygen species. We hypothesized that hydrogen therapy will reduce brain oxidative stress in mice after ICH and thereby will lead to reduced brain edema and improved neurological outcomes.

Materials and Methods: CD1 male mice (weight 30–35 g) were divided into the following groups: sham, ICH+vehicle (room air), ICH+1-h hydrogen treatment, and ICH+2-h hydrogen treatment. ICH was induced by injection of bacterial collagenase into the right basal ganglia. The evaluation of outcomes was done at two time points: 24 and 72 h post-ICH. Brain water content was measured for assessment of brain edema (wet/dry weight method), and three neurological tests were performed pre- and postoperatively.

Results: Collagenase injection was found to induce brain edema and impair functional performance of rats. The hydrogen inhalation reduced these effects acutely (24 h); however it exhibited only a tendency to improvement in the delayed study (72 h).

Conclusions: Our results suggest that hydrogen inhalation exerts an acute brain-protective effect in the mouse ICH model. However, the acute hydrogen therapy alone is not sufficient to improve delayed ICH outcomes in this model.

Keywords ROS · Antioxidant · Brain edema · ICH · Neuroprotection

A. Manaenko, T. Lekic, Q. Ma, R.P. Ostrowski, and J.H. Zhang
Department of Physiology and Pharmacology, Loma Linda University,
School of Medicine, Loma Linda, CA, USA

J. Tang (✉)
Department of Physiology and Pharmacology, Loma Linda University,
School of Medicine, Loma Linda, CA, USA and
Department of Physiology and Pharmacology, Loma Linda University,
School of Medicine, Risley Hall, Room 219, 92350, Loma Linda,
CA, USA
e-mail: jtang@llu.edu

Introduction

The role of reactive oxygen species (ROS) as mediators of oxidative brain damage after ICH is well accepted. Overproduction of ROS, which cannot be balanced by endogenous antioxidant defenses of brain tissues, results in lipid peroxidation, disruption of the blood-brain barrier (BBB), an increase in brain edema, and neurological deficits. Beneficial effects of antioxidant agents in the ICH model have been recently demonstrated in our laboratory [1]. The inhalation with hydrogen selectively reduced hydroxyl radical and peroxynitrite levels in vitro and exerted an antioxidant effect, reflected by a decreased brain concentration of 4-hydroxynonenal (4-HNE) (the specific marker for lipid peroxidation) and 8OHG (nucleic acid oxidation marker) in a rat MCAO model [2]. To date, no study has assessed the effects of hydrogen gas therapy in the animal model of ICH. In this study, we examined whether hydrogen inhalation provides neuroprotective effects by decreasing brain water content and ameliorating neurological deficits.

Methods

Experimental animals: All procedures and methods for these studies were approved by the Animal Care and Use Committee at Loma Linda University and complied with the Guide for the Care and Use of Laboratory Animals (<http://research.llu.edu/forms/appendixb.doc>). A total of 30 male CD-1 mice were assigned into the acute (24 h) or delayed (72 h) study. The animals in the acute experiment were divided into sham, ICH treated with vehicle (room air), ICH treated with hydrogen for 1 h, and ICH treated with hydrogen for 2 h. At 24 h after ICH, the animals were tested for neurological deficits and euthanized for brain edema measurements. The animals assigned to the delayed group were partitioned into ICH treated with vehicle and ICH treated with hydrogen for 1 h (since 1-h treatment was effective in the 24-h study).

Animals were checked for neurological deficits and euthanized for brain water content measurements at 72 h post-ICH. Since no increase in brain water content was observed after sham surgery, the same group of sham-operated animals was used for the 72-h time point.

Intracerebral hemorrhage induction: We adopted the collagenase-induced intracerebral hemorrhage model in mice, as we described before [3]. Briefly, mice were anesthetized intraperitoneally with a ketamine (100 mg/kg)/xylazine (10 mg/kg) cocktail and positioned prone in a stereotaxic head frame (Stoelting, Wood Dale, IL). An electronic thermostat-controlled warming blanket was used to maintain the core temperature at 37°C. The calvarium was exposed by a midline scalp incision from the nose to the superior nuchal line, and the skin was retracted laterally. With a variable speed drill (Fine Scientific Tools, Foster City, CA), a 1.0-mm burr hole was made 0.9 mm posterior to the bregma and 1.45 mm right-lateral to the midline. A 26-G needle on a Hamilton syringe was inserted with stereotaxic guidance 4.0 mm into the right deep cortex/basal ganglia at a rate 1 mm/min. Collagenase (0.075 units in 0.5 μ L saline; Sigma, St Louis, MO) was then infused into the brain at a rate of 0.25 μ L/min over 2 min using an automatic infusion pump (Stoelting, Wood Dale, IL). The needle was left in place for an additional 10 min after injection to prevent the possible leakage of collagenase solution. After removal of the needle, the incision was sutured closed, and mice were allowed to recover. Sham operation was performed with needle insertion only.

Brain water content: Mice were euthanized under deep anesthesia. Brains were removed immediately and divided into five parts: ipsilateral and contralateral basal ganglia, ipsilateral and contralateral cortex, and cerebellum. Tissue samples were weighed on an electronic analytical balance. The tissue was then dried at 100°C for 24 h to determine the dry weight. Brain water content (%) was calculated as [(wet weight – dry weight)/wet weight] \times 100.

Neurological deficits: Neurological scores were assessed by an independent researcher blinded to the procedure 24 and 72 h after ICH. Three tests were implemented for evaluation of neurological deficits: (1) Modified Garcia test [4]. The Modified Garcia Score is a 21-point sensorimotor assessment system consisting of seven tests with scores of 0–3 for each test (maximum score=21). These seven tests included: (1) spontaneous activity, (2) side stroking, (3) vibris touch, (4) limb symmetry, (5) climbing, (6) lateral turning, and (7) forelimb walking. Additionally, beam balance and wire hang testing were performed as described before [3]. Both the beam (590 cm in length by 51 cm in width) and wire (550 cm in length by 51 mm in width) were constructed and held in place by two platforms on each side.

Mice were put on the center of the beam or wire and allowed to reach the platform. Mice were observed for both their time and behavior until they reached one platform, and scored according to six grades. The test was repeated three times, and an average score was taken [minimum score 0; maximum score (healthy mouse)].

Statistical analysis: Quantitative data are expressed as the mean \pm SEM. Statistical significance was verified by analysis of variance (ANOVA) (Dunn's method) for analysis of acute effect (24-h) and by ANOVA (Tukey test) for analysis of delayed effect (72-h). $P < 0.05$ was considered statistically significant.

Results

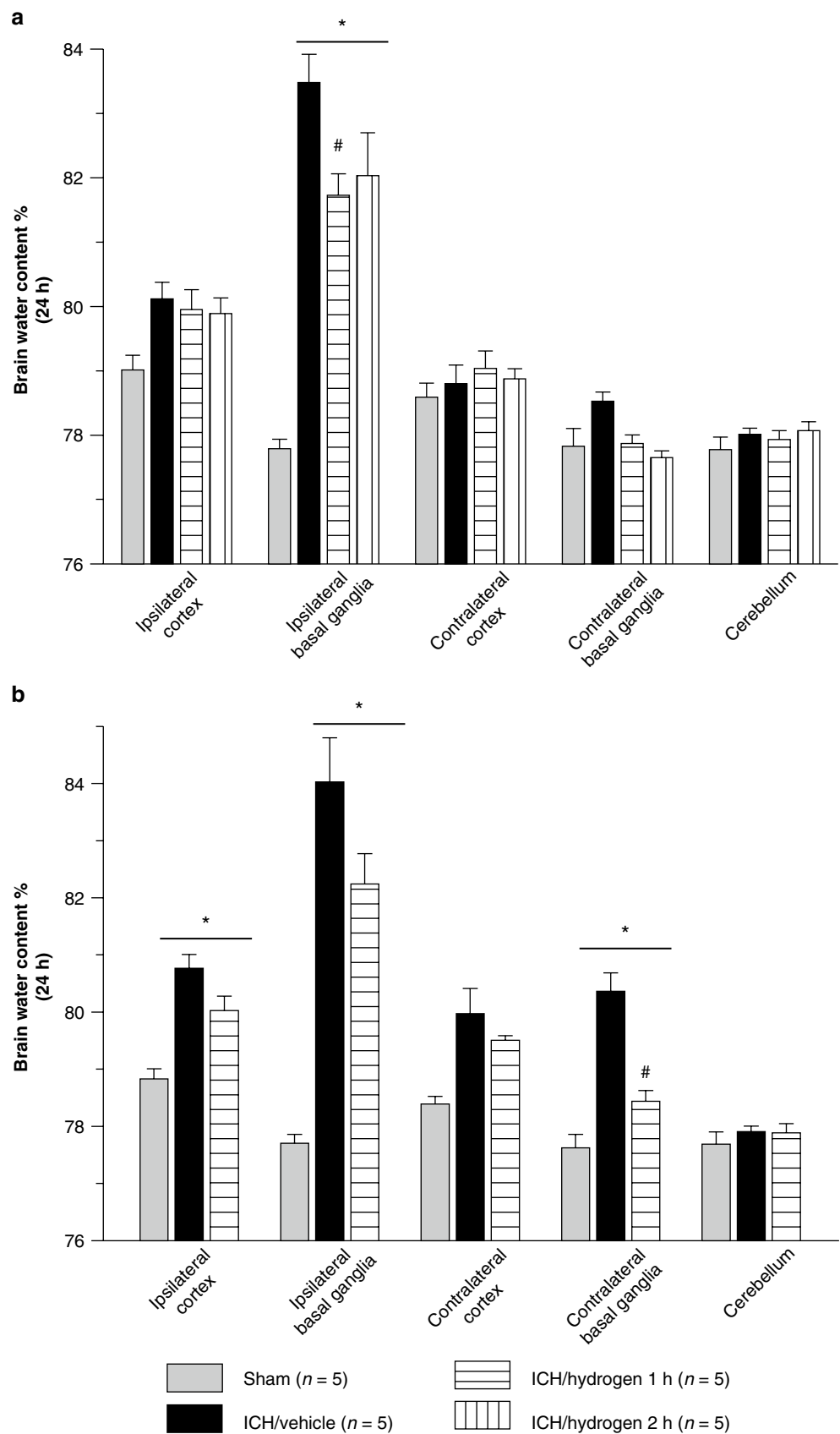
Effect of Inhalation Hydrogen Therapy on Brain Edema

At 24 h after ICH, the water content significantly increased in the ipsilateral basal ganglia of all collagenase-injected animals (Fig. 1a). Hydrogen treatment resulted in a dose-dependent effect where 1-h of inhalation significantly decreased brain water content in hydrogen vs. room-air treated animals, while 2-h of hydrogen inhalation showed no effect. Brain edema progressed to involve bilateral basal ganglia as well as the ipsilateral cortex at 72 h post-ICH (Fig. 1b). At this time point, 1-h of hydrogen inhalation showed only the tendency towards reducing water content in these brain regions (Fig. 1b). Since there was no statistical difference between the brain water content of naïve (non-operated animals) and sham-operated animals at the 24-h time point, we did not expect the formation of brain edema at a later time-point and used the same group of sham-operated animals in both studies.

Effect of Inhalation Hydrogen Therapy on Neurological Outcomes

Neurological deficits were evident in all ICH-animals 24 and 72-h after ICH as tested by the modified Garcia test, wire hanging and beam balance tests. One hour but not 2-h of hydrogen inhalation was able to attenuate these ICH-induced effects in 24-h study (Fig. 2). However, 72-h post-ICH, hydrogen therapy showed only a tendency towards an improvement of neurological deficit. This tendency did not reach statistical significance (Fig. 3).

Fig. 1 All animals after collagenase injection had a significant increase of brain water content. One but not 2 h of hydrogen therapy reduced brain edema in the 24-h study group. (a) One hour of hydrogen therapy tended to decrease brain water content in (b) the 72-h group. * Significant difference vs. sham ($p < 0.05$). #Significant difference vs. sham ($p < 0.05$). (a) 24 h: sham=5; (vehicle)=5; (ICH+Hydrogen 1 h)=5; (ICH+hydrogen 2 h)=5. (b) 72 h: sham=5; (vehicle)=5; (ICH+hydrogen 1 h)



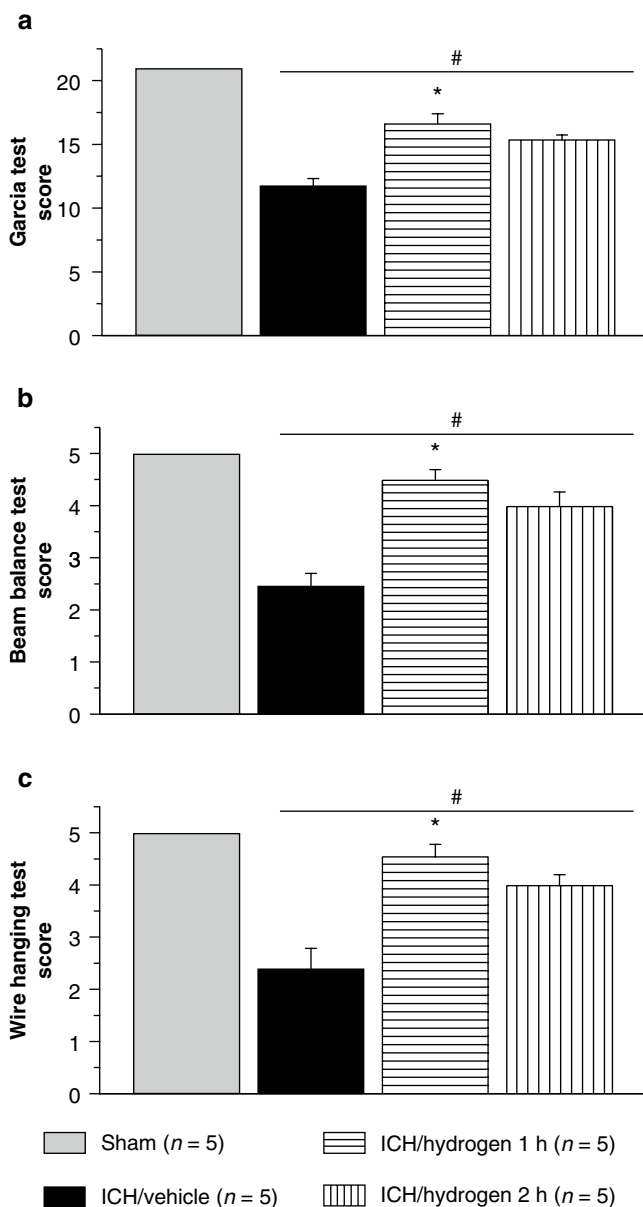


Fig. 2 One hour hydrogen inhalation improved neurological deficit in the 24-h study according to performance on Garcia (a), beam balance (b) and wire hanging (c) tests. Significant difference vs. sham ($p < 0.05$); #significant difference vs. vehicle ($p < 0.05$)

Discussion

Several studies have shown that antioxidants confer a neuroprotective effect in ICH [5]. Since previous work had demonstrated the antioxidative effects of hydrogen inhalation therapy [2], we postulated that the hydrogen gas treatment will reduce oxidative stress and will protect against brain injury following ICH. In our study we tested the effects of inhalation with hydrogen in the mouse intracerebral hemorrhage model. We used 2.0% of hydrogen since it is known

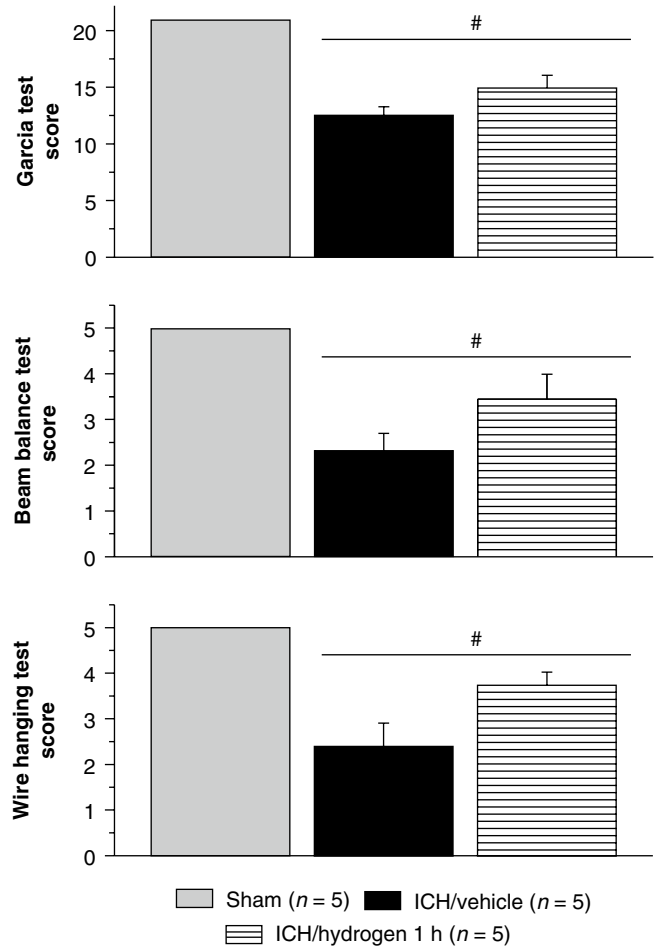


Fig. 3 One hour hydrogen inhalation tended to improve neurological deficit in 72 h. *Significant difference vs. sham ($p < 0.05$)

that (1) at such a concentration (less 4% in air), H_2 is neither explosive nor harmful; (2) this concentration of hydrogen was most effective in the previous studies [2, 6]. We tested the acute effect (24-h after ICH induction) of hydrogen therapy and compared it to the delayed effect (72-h after ICH). In the acute study, hydrogen inhalation significantly reduced the ICH-induced increase in brain water content and improved the neurological deficit in ICH animals. In the 72-h study, the hydrogen inhalation tended to decrease brain edema; however, the difference between groups did not reach statistical significance. There are several possible explanations for this result. The limited efficacy of hydrogen therapy at 72-h after ICH may relate to the increased severity of inflammatory cell infiltration in the delayed phase after ICH [7]. One of the ROS sources after ICH are peripheral immune cells, which start invading the brain shortly after the hemorrhage and participate in microglial activation. The activated microglia further increase the ROS formation. It has been reported that leukocyte infiltration and microglial activation reached a maximum at 3 days after ICH [8]. Concordantly, Liao et al.

observed maximal superoxide production in the perihematomal region on day 3 after ICH induction [9]. Another possibility is that hydroxyl radicals, which are the most aggressive reactive oxygen species, overwhelmed the beneficial effect of hydrogen in the delayed phase of hemorrhagic brain injury. Hydroxyl radicals can cause lipid peroxidation, protein oxidation, as well as DNA damage in the cell [10, 12]. These radicals are produced by Fenton chemistry, which requires free iron for the formation of transition metal complexes. Wu et al. demonstrated that ICH upregulated heme oxygenase-1 levels and resulted in iron overload in the brain [11]. The release of iron from the breakdown of hemoglobin occurred during intracerebral hematoma formation. The authors observed a time-dependent increase in iron level in the ipsilateral versus contralateral basal ganglia. The difference was insignificant on the first day after ICH induction, however became significant 72 h later [11]. In conclusion, hydrogen therapy can protect the brain against acute injury following ICH. However, further studies are needed to establish the regimen of treatment that would provide lasting protection.

Acknowledgement This study is partially supported by NIH NS053407 to J.H. Zhang and NS060936 to J. Tang.

Conflict of interest statement We declare that we have no conflict of interest.

References

1. Rojas H, Lekic T, Chen W, Jadhav V, Titova E, Martin RD, Tang H, Zhang J (2008) The antioxidant effects of melatonin after intracerebral hemorrhage in rats. *Acta Neurochir Suppl* 105:19–21
2. Ohsawa I, Ishikawa M, Takahashi K, Watanabe M, Nishimaki K, Yamagata K, Katsura K, Katayama Y, Asoh S, Ohta S (2007) Hydrogen acts as therapeutic antioxidant by selectively reducing cytotoxic oxygen radicals. *Nat Med* 13:688–694
3. Manaenko A, Lekic T, Sozen T, Tsuchiyama R, Zhang JH, Tang J (2009) Effect of gap junction inhibition on intracerebral hemorrhage-induced brain injury in mice. *Neurol Res* 31:173–178
4. Garcia JH, Wagner S, Liu KF, Hu XJ (1998) Neurological deficit and extent of neuronal necrosis attributable to middle cerebral artery occlusion in rats. Statistical validation. *Stroke* 29:871–872
5. Lekic T, Hartman R, Rojas H, Manaenko A, Chen W, Ayer R, Tang J, Zhang JH (2010) Protective effect of melatonin upon neuropathology, striatal function, and memory ability after intracerebral hemorrhage in rats. *J Neurotrauma* 27(3):627–637
6. Hayashida K, Sano M, Ohsawa I, Shinmura K, Tamaki K, Kimura K, Endo J, Katayama T, Kawamira A, Kohsaka S, Makino S, Ohta S, Ogawa S, Fakuda K (2008) Inhalation of hydrogen gas reduces infarct size in the rat model of myocardial ischemia-reperfusion injury. *Biochem Biophys Res Commun* 373(1):30–35
7. Wang J, Rogove AD, Tsirka AE, Tsirka SE (2003) Protective role of tuftsin fragment 1–3 in an animal model of intracerebral hemorrhage. *Ann Neurol* 54:655–664
8. Gong C, Hoff JT, Keep RF (2000) Acute inflammatory reaction following experimental intracerebral hemorrhage in rat. *Brain Res* 871:57–65
9. Liao W, Zhong J, Yu J, Xie J, Liu Y, Du L, Yang S, Liu P, Xu J, Wang J, Han Z, Han ZC (2009) Therapeutic benefit of human umbilical cord derived mesenchymal stromal cells in intracerebral hemorrhage rat: implications of anti-inflammation and angiogenesis. *Cell Physiol Biochem* 24:307–316
10. Valko M, Leibfritz D, Moncol J, Cronin MT, Mazur M, Telser J (2007) Free radicals and antioxidants in normal physiological functions and human disease. *Int J Biochem Cell Biol.* 39: 44–84
11. Wu J, Hua Y, Keep RF, Nakamura T, Hoff JT, Xi G (2003) Iron and iron-handling proteins in the brain after intracerebral hemorrhage. *Stroke* 34:2964–2969
12. Chan PH (1996) Role of oxidants in ischemic brain damage. *Stroke* 27:1124–1129

Deferoxamine Reduces Cavity Size in the Brain After Intracerebral Hemorrhage in Aged Rats

Tetsuhiro Hatakeyama, Masanobu Okauchi, Ya Hua, Richard F. Keep, and Guohua Xi

Abstract This study investigated whether deferoxamine (DFX), an iron chelator, reduces cavity size after ICH in aged rats. Aged male Fischer rats (18 months old) had an intracaudate injection of 100 μ L autologous blood and were treated with DFX or vehicle. Rats were euthanized at day 56 and brains were perfused for histology and immunohistochemistry. Hematoxylin and eosin staining was used to examine hematoma cavity presence and size. Immunohistochemistry was performed to measure the number of cells positive for ferritin, heme oxygenase-1 (HO-1), glial fibrillary acidic protein (GFAP) and OX-6. Neurological deficits were also examined. In aged rats with ICH, a cavity formed in the caudate in 7 out of 12 vehicle-treated rats and 1 out of 9 DFX-treated rats. DFX treatment significantly reduced the size of the ICH-induced cavity ($p < 0.05$) as well as neurological deficits ($p < 0.05$). DFX also reduced the number of ferritin ($p < 0.05$) and HO-1 ($p < 0.01$) positive cells in the ipsilateral basal ganglia. However, DFX had no effect on brain GFAP and OX-6 immunoreactivity 2 months after ICH.

In conclusion, DFX reduces cavity size, neurological deficits, and immunoreactivity for ferritin and HO-1 after ICH in aged rats, supporting the suggestion that DFX may reduce brain injury in ICH patients.

Keywords Deferoxamine · Iron · Cerebral hemorrhage · Cavity size · Oxidative stress

Introduction

Intracerebral hemorrhage (ICH) is a common and often fatal subtype of stroke. If the patient survives the ictus, the hematoma gradually resolves within several months, but restoration of function is usually incomplete [1].

Iron is a hemoglobin degradation product, and iron overload in the brain can cause free radical formation and oxidative damage, such as lipid peroxidation, after ICH [2]. After erythrocyte lysis, brain iron concentrations can reach very high levels. Our previous study showed that non-heme iron increases about three-fold after ICH in a rat model, and brain iron levels remain high for at least several weeks [3]. Deferoxamine (DFX), an iron chelator, can rapidly penetrate the blood-brain barrier and accumulate in the brain tissue at a significant concentration after systemic administration [4, 5]. Our previous study showed that DFX reduces ICH or hemoglobin-induced brain injury in rats and pigs [6–9].

In ICH patients, a cavity is formed after the hematoma is absorbed. Age is an important factor affecting brain injury after ICH. This study investigated whether DFX reduces cavity size after ICH in aged rats.

Materials and Methods

Animal Preparation and Intracerebral Infusion

Animal use protocols were approved by the University of Michigan Committee on the Use and Care of Animals. Aged male Fischer 344 rats (18 months old; weight, 380–450 g; NIH) were used in this study. Rats were anesthetized with

T. Hatakeyama and M. Okauchi
Department of Neurosurgery, University of Michigan, Ann Arbor, MI, USA and
Department of Neurosurgery, Kagawa University, Takamatsu, Kagawa, Japan

Y. Hua and R.F. Keep
Department of Neurosurgery, University of Michigan, Ann Arbor, MI, USA

G. Xi (✉)
Department of Neurosurgery, University of Michigan,
109 Zina Pitcher Place, 48109-2200, Ann Arbor, MI, USA
e-mail: guohuaxi@umich.edu

pentobarbital (45 mg/kg, i.p.). The right femoral artery was catheterized for continuous blood pressure monitoring and blood sampling. Blood was obtained from the catheter for analysis of blood pH, PaO₂, PaCO₂, hematocrit and blood glucose levels. Core temperature was maintained at 37°C with use of a feedback-controlled heating pad. Rats were positioned in a stereotactic frame (Kopf Instruments), and a cranial burr hole (1 mm) was drilled on the right coronal suture 3.5 mm lateral to the midline. A 26-gauge needle was inserted stereotactically into the right basal ganglia (coordinates: 0.2 mm anterior, 5.5 mm ventral, 3.5 mm lateral to the bregma). Autologous whole blood (100 µL) was injected at a rate of 10 µL/min using a microinfusion pump. After injection, the needle was removed, the burr hole was filled with bone wax, and the skin incision was closed with sutures.

Experimental Groups

All rats had an ICH and were either treated with DFX (100 mg/kg; *n*=9) or vehicle (*n*=12) 2 and 6 h post ICH and then every 12 h for 7 days. Behavioral tests were undertaken on the day before surgery, and then 1, 28 and 56 days after surgery. All rats were killed at day 56, and brains were perfused for histology and immunohistochemistry.

Hematoma Cavity Measurement

Rats were reanesthetized (pentobarbital 60 mg/kg; i.p.) and underwent transcardiac perfusion with 4% paraformaldehyde in 0.1 mol/L phosphate-buffered saline (pH 7.4). The brains were removed and kept in 4% paraformaldehyde for 6 h, then immersed in 30% sucrose for 3–4 days at 4°C. Brains were then placed in optimal cutting temperature embedding compound (Sakura Finetek, Inc.) and 18-µm sections taken on a cryostat. Coronal sections from 1 mm posterior to the blood injection site were stained with hematoxylin and eosin (H&E) and scanned. Hematoma cavities were outlined on a computer and the areas measured using ImageJ (version 1.37v; National Institutes of Health). All measurements were repeated three times, and the mean value was used.

Immunohistochemistry

The immunohistochemistry method using the avidin-biotin complex technique has been described previously [4]. Sections were incubated overnight with a primary antibody: rabbit anti-HO-1 (HSP32; 1:200 dilution, Assay Designs,

Ann Arbor, MI), rabbit anti-human ferritin (1:400 dilution; DAKO, Glostrup, Denmark), mouse anti-rat MHC CLASSII(OX-6; 1:200 dilution; Serotec, Oxford, UK) and mouse anti-rat GFAP (1:200 dilution; Chemicon, Temecula, CA). Normal rabbit or mouse serum and the absence of primary antibody were used as negative controls.

Cell Counts

To assess the effects of deferoxamine on astrocyte, ferritin and microglia reaction, we used 18-µm-thick coronal sections from 1-mm posterior to the blood injection site. High-power images (×40 magnification) were taken from the caudate with the cavity using a digital camera. GFAP, ferritin, HO-1 and OX6- positive cells were counted. Counts were performed on four areas in each of 9 deferoxamine-treated or 12 vehicle-treated rat brain sections.

Behavioral Tests

For behavioral tests, all animals were tested before and after surgery, and scored by experimenters who were blind to treatment group. The following two types of tests were used.

Forelimb-Placing Test

Forelimb placing was scored using a vibrissae-elicited forelimb placing test. Independent testing of each forelimb was induced by brushing the vibrissae ipsilateral to that forelimb on the edge of a tabletop once per trial for ten trials. Intact animals placed the forelimb quickly onto the countertop. Percentage of successful placing responses was determined. There is a reduction in successful responses in the forelimb contralateral to the site of injection after ICH.

Corner Turn Test

The rat was allowed to proceed into a corner, the angle of which was 30°. To the exit the corner, the rat could turn either to the left or the right, and this was recorded. This was repeated 10–15 times, with at least 30 s between trials and the percentage of right turns calculated. Only turns involving full rearing along either wall were included. Rats were not picked up immediately after each turn so that they did not develop an aversion for their prepotent turning response.

Statistical Analysis

All data in this study are presented as means \pm SD. Data were analyzed with Student's *t*-test or Wilcoxon-Mann-Whitney rank sum test. Differences were considered significant at $P < 0.05$.

Results

All physiological variables were measured immediately before an intracerebral infusion. Mean arterial blood

pressure, blood pH, PaO₂, PaCO₂, hematocrit and blood glucose level were within normal ranges.

In aged rats with ICH, a cavity formed in the caudate in 7 out of 12 vehicle-treated rats and 1 out of 9 DFX-treated rats. DFX treatment significantly reduced the size of the ICH-induced cavity (0.03 ± 0.08 vs. 0.17 ± 0.25 mm² in the vehicle-treated group, $p < 0.05$; Fig. 1).

Ferritin is an iron storage protein. DFX treatment significantly reduced the ferritin positive cells around the cavity in the ipsilateral basal ganglia (287 ± 46 versus 358 ± 70 /mm² in the vehicle-treated group, $p < 0.05$). DFX treatment also reduced HO-1 positive cells around the hemorrhage cavity

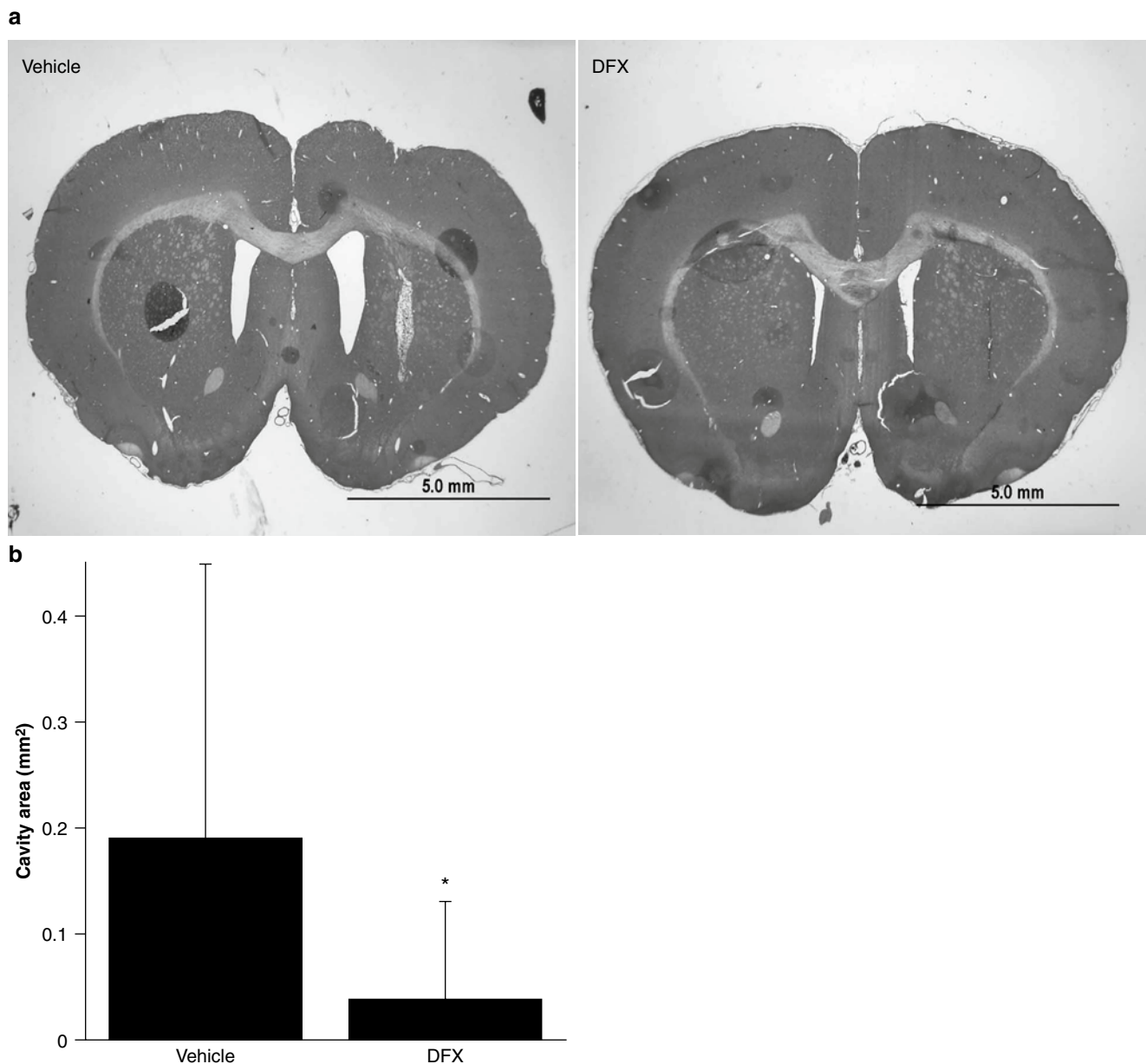


Fig. 1 (a) Coronal gross hematoxylin and eosin sections 8 weeks after ICH in rats treated with vehicle or DFX. Scale bar=5.0 mm. (b) Bar graph showing cavity area. Values are expressed as means \pm SD. * $p < 0.05$ vs. the vehicle group

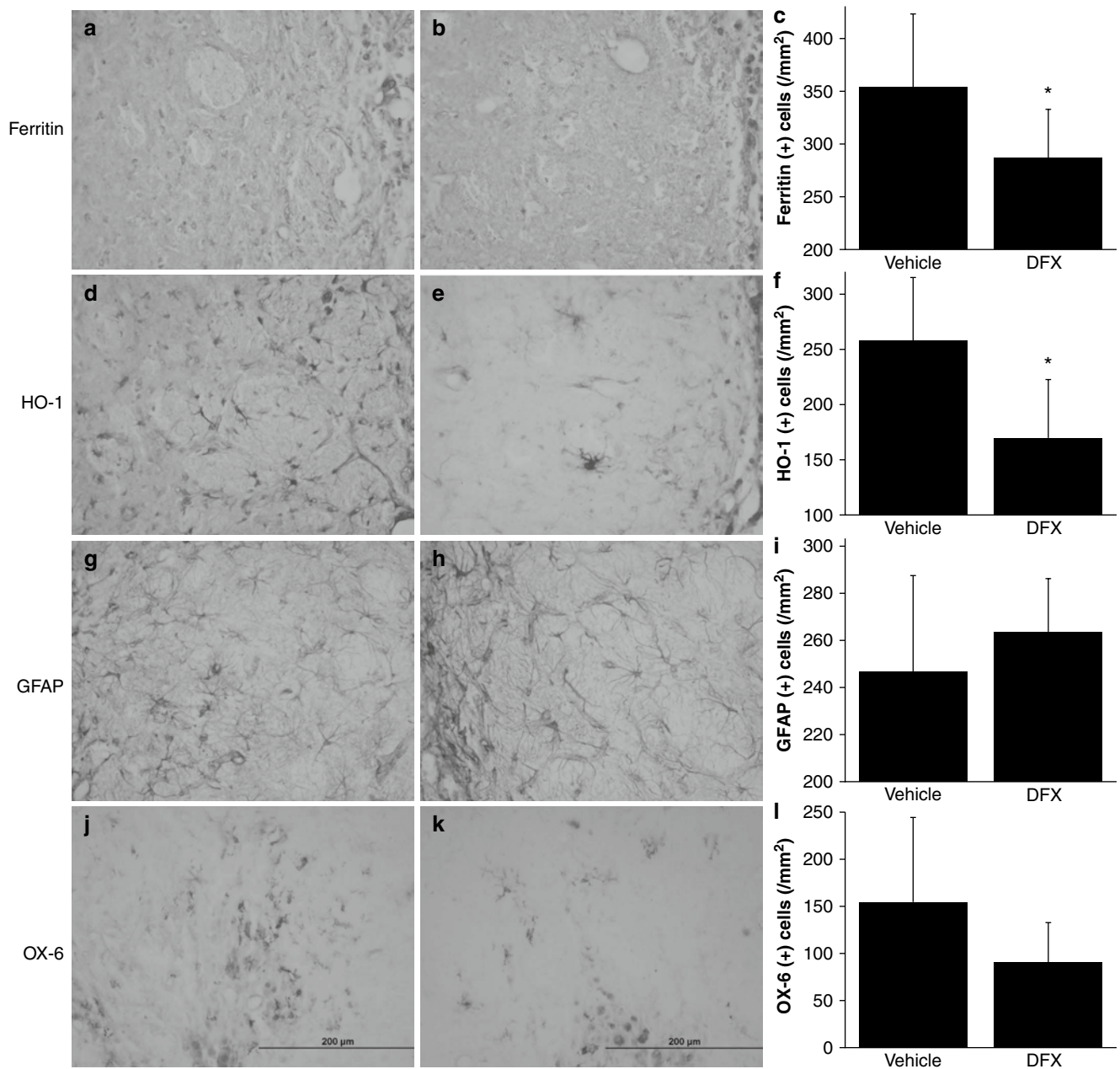


Fig. 2 Immunohistochemistry for ferritin, HO-1, GFAP and OX-6 in the ipsilateral basal ganglia 2 months after ICH. (a), (d), (g) and (j) are vehicle. (b), (e), (h) and (k) are DFX. (c), (f), (i) and (l) are

immune-positive cell count. Scale bar = 200 μ m. Values are expressed as means \pm SD. * p < 0.05 vs. the vehicle group

(170 ± 53 versus $253 \pm 66/\text{mm}^2$ in the vehicle-treated group, $p < 0.01$). However, DFX had no effect on brain GFAP (263 ± 22 versus $247 \pm 40/\text{mm}^2$ in the vehicle-treated group, $p > 0.05$) and OX-6, a marker of activated microglia, (89 ± 42 versus $157 \pm 90/\text{mm}^2$ in the vehicle-treated group, $p > 0.05$) 2 months after ICH (Fig. 2a–l).

Behavioral tests including the forelimb placing and the corner turn tests were performed before ICH, and 1, 28 and 56 days after ICH. In vehicle-treated ICH rats, a partial recovery of forelimb placing occurred with time, but residual neurological deficits were still present at 56 days

($64 \pm 35\%$, the normal level is 100%). When rats were treated with DFX, ICH-induced forelimb placing deficits showed a greater recovery (>95% at 28 and 56 days). In the corner turn test, the percentage of turns to the right was significantly decreased at 28 days in DFX treatment groups compared to the vehicle group ($60 \pm 7\%$ versus $79 \pm 10\%$ in the vehicle-treatment group, $p < 0.01$; the normal level is $\sim 50\%$). ICH-induced corner turn deficits were almost normalized at 56 days in the DFX treatment group ($58 \pm 8\%$ versus $70 \pm 10\%$ in the vehicle-treatment group, $p < 0.05$).

Discussion

In this study, we found that DFX treatment reduces cavity size, ferritin and HO-1 immunoreactivity around the cavity, and improves functional outcomes after ICH in aged rats. These results suggest that iron chelation may reduce brain injury for patients with ICH.

Oxidative brain injury and neuronal death occur after intracerebral infusion of autologous blood [10–12]. Iron-induced brain damage may result from oxidative stress [2], and free iron can stimulate the formation of free radicals, leading to neuronal damage. Deferoxamine, an iron chelator, is approved by the FDA for treatment of acute iron intoxication and chronic iron overload in transfusion-dependent anemia. Its molecular weight is 657, and DFX can rapidly penetrate the blood-brain barrier and accumulate in brain tissue at a significant concentration after systemic administration [4, 5]. We have previously reported that systemic DFX attenuates brain edema in rats after intracerebral infusion of autologous whole blood or hemoglobin [8, 13].

In the present study, we found that DFX reduces ferritin and HO-1 immunoreactivity around the cavity. Ferritin, a naturally occurring iron chelator, is involved in maintaining brain iron homeostasis. Ferritin protein synthesis is regulated mostly post-transcriptionally by iron-mediated or non-iron-mediated induction [3]. Heme oxygenase-1 is a key enzyme in hemoglobin degradation, converting heme to iron, carbon monoxide and biliverdin. HO-1 is markedly upregulated in the brain after ICH [3], and heme oxygenase inhibition reduces brain injury after ICH [14]. Our present data found downregulation of ferritin and HO-1 in the DFX treatment group, suggesting that DFX may reduce iron overload in the aged rat ICH model.

In ICH patients, a cavity forms after the hematoma is absorbed. In the current study, we showed that a cavity is also formed in aged rats after ICH and that DFX reduces the occurrence and the size of cavity. In a clinical ICH study, serum glutamate concentrations are correlated with the size of the residual cavity, and its size is independent of initial ICH volume [15]. Also DFX decreased brain tissue levels of the glutamate in an experimental ischemic model [16]. In addition, there are some studies showing the correlation among matrix metalloproteinase-9 (MMP-9), MMP-3, growth factors and cavity volume [17, 18]. Further studies are required to identify the mechanisms of cavity formation after ICH.

We found that DFX reduced ICH-induced neurological deficits in aged rats at 4 and 8 weeks. Both sensorimotor behavioral tests appear to be well suited to models of unilateral brain injury because they measure asymmetry. These sensorimotor tests are also not altered by repeated testing and do not require special training or food deprivation [7, 19]. The degree of improvement in neurological deficits with DFX was almost a complete normalization of

forelimb-placing and corner test scores in DFX-treated animals by 28 days.

In summary, DFX reduces cavity size, neurological deficits, and ferritin and HO-1 levels after ICH in aged rats. These results suggest that DFX may reduce brain injury in ICH patients

Acknowledgements This study was supported by grants NS-017760, NS-039866 and NS-057539 from the National Institutes of Health (NIH) and 0755717Z and 0840016N from the American Heart Association (AHA). The content is solely the responsibility of the authors and does not necessarily represent the official views of the NIH and AHA.

Conflict of interest statement We declare that we have no conflict of interest.

References

1. Kase CS, Caplan LR (1994) Intracerebral hemorrhage. Kase CS, Caplan LR eds. Butterworth-Heinemann, Boston
2. Wu J, Hua Y, Keep RF, Schallert T, Hoff JT, Xi G (2002) Oxidative brain injury from extravasated erythrocytes after intracerebral hemorrhage. *Brain Res* 953:45–52
3. Wu J, Hua Y, Keep RF, Nakamura T, Hoff JT, Xi G (2003) Iron and iron-handling proteins in the brain after intracerebral hemorrhage. *Stroke* 34:2964–2969
4. Keberle H (1964) The biochemistry of desferrioxamine and its relation to iron metabolism. *Ann NY Acad Sci* 119:758–768
5. Palmer C, Roberts RL, Bero C (1994) Deferoxamine posttreatment reduces ischemic brain injury in neonatal rats. *Stroke* 25:1039–1045
6. Gu Y, Hua Y, Keep RF, Morgenstern LB, Xi G (2009) Deferoxamine reduces intracerebral hematoma-induced iron accumulation and neuronal death in piglets. *Stroke* 40:2241–2243
7. Hua Y, Nakamura T, Keep RF, Wu J, Schallert T, Hoff JT, Xi G (2006) Long-term effects of experimental intracerebral hemorrhage: the role of iron. *J Neurosurg* 104:305–312
8. Nakamura T, Keep RF, Hua Y, Schallert T, Hoff JT, Xi G (2004) Deferoxamine-induced attenuation of brain edema and neurological deficits in a rat model of intracerebral hemorrhage. *J Neurosurg* 100:672–678
9. Song S, Hua Y, Keep RF, Hoff JT, Xi G (2007) A new hippocampal model for examining intracerebral hemorrhage-related neuronal death: effects of deferoxamine on hemoglobin-induced neuronal death. *Stroke* 38:2861–2863
10. Nakamura T, Keep RF, Hua Y, Hoff JT, Xi G (2005) Oxidative DNA injury after experimental intracerebral hemorrhage. *Brain Res* 1039:30–36
11. Nakamura T, Xi G, Park JW, Hua Y, Hoff JT, Keep RF (2005) Holo-transferrin and thrombin can interact to cause brain damage. *Stroke* 36:348–352
12. Xi G, Keep RF, Hoff JT (2006) Mechanisms of brain injury after intracerebral haemorrhage. *Lancet Neurol* 5:53–63
13. Huang FP, Xi G, Keep RF, Hua Y, Nemoianu A, Hoff JT (2002) Brain edema after experimental intracerebral hemorrhage: role of hemoglobin degradation products. *J Neurosurg* 96:287–293
14. Wagner KR, Hua Y, de Courten-Myers GM, Broderick JP, Nishimura RN, Lu SY, Dwyer BE (2000) Tin-mesoporphyrin, a potent heme oxygenase inhibitor, for treatment of intracerebral hemorrhage:

- in vivo and in vitro studies. *Cell Mol Biol (Noisy-le-grand)* 46:597–608
15. Castillo J, Davalos A, Alvarez-Sabin J, Pumar JM, Leira R, Silva Y, Montaner J, Kase CS (2002) Molecular signatures of brain injury after intracerebral hemorrhage. *Neurology* 58:624–629
 16. Papazisis G, Pourzitaki C, Sardeli C, Lallas A, Amaniti E, Kouvelas D (2008) Deferoxamine decreases the excitatory amino acid levels and improves the histological outcome in the hippocampus of neonatal rats after hypoxia-ischemia. *Pharmacol Res* 57:73–78
 17. Alvarez-Sabin J, Delgado P, Abilleira S, Molina CA, Arenillas J, Ribo M, Santamarina E, Quintana M, Monasterio J, Montaner J (2004) Temporal profile of matrix metalloproteinases and their inhibitors after spontaneous intracerebral hemorrhage: relationship to clinical and radiological outcome. *Stroke* 35:1316–1322
 18. Sobrino T, Arias S, Rodriguez-Gonzalez R, Brea D, Silva Y, de la Ossa NP, Agulla J, Blanco M, Pumar JM, Serena J, Davalos A, Castillo J (2009) High serum levels of growth factors are associated with good outcome in intracerebral hemorrhage. *J Cereb Blood Flow Metab* 29:1968–1974
 19. Schallert T, Fleming SM, Leasure JL, Tillerson JL, Bland ST (2000) CNS plasticity and assessment of forelimb sensorimotor outcome in unilateral rat models of stroke, cortical ablation, parkinsonism and spinal cord injury. *Neuropharmacology* 39:777–787

Post-treatment with SR49059 Improves Outcomes Following an Intracerebral Hemorrhagic Stroke in Mice

Anatol Manaenko, Nancy Fathali, Nikan H. Khatibi, Tim Lekic, Kenneth J. Shum, Robert Martin, John H. Zhang, and Jiping Tang

Abstract Intracerebral hemorrhage (ICH) is a devastating stroke subtype characterized by severe brain edema formation leading to cerebral blood flow compromise and parenchymal damage. Arginine vasopressin (AVP), a non-peptide antidiuretic hormone, has recently been implicated as a modulator of brain edema following injury. In this study, we investigated the effects of SR49059, a highly specific AVP V1a receptor antagonist, on brain injury outcomes following ICH, specifically assessing the ability of SR49059 in reducing brain edema and improving neurobehavioral deficits. Male CD1 mice ($n=35$) were randomly assigned to the following groups: sham, ICH, ICH with SR49059 at 0.5 mg/kg, and ICH with SR49059 at 2 mg/kg. ICH was induced by using the collagenase injection model, and treatment was given 1 h after surgery. Post-assessment was conducted at 24 and 72 h after surgery, and included brain water content and neurobehavioral testing. The study found that SR49059

significantly reduced cerebral edema at 24 and 72 h post-ICH injury and improved neurobehavioral deficits at 72 h. Our study suggests that blockage of the AVP V1a receptor is a promising treatment target for improving ICH-induced brain injury. Further studies will be needed to confirm this relationship and determine future clinical direction.

Keywords Intracerebral hemorrhage (ICH) · Arginine vasopressin (AVP) · SR49059

Introduction

Intracerebral hemorrhage (ICH) is a devastating stroke subtype victimizing over 120,000 Americans each year. One of the major reasons for its severity is the development of perihematomal edema – on average, close to 40% of victims have a 1–2% increase, resulting in an increased intracranial pressure and heightened risk for brain herniation. Today, despite extensive research focusing on ameliorating or reducing the development of edema, research has not been effective in developing a treatment option for this ICH-induced outcome.

Arginine vasopressin (AVP) is a non-peptide antidiuretic hormone responsible for regulating water and electrolyte homeostasis in the body. Normally, AVP is produced in the hypothalamus and then released into the circulation by the posterior pituitary. However, recent studies have suggested an alternate pathway for AVP, specifically suggesting that AVP can be released directly into the brain where it acts as a neurotransmitter, regulating water permeability, ion homeostasis, and cerebrospinal fluid production [1]. In an acute ischemic stroke model, AVP injection directly into the brain exacerbated already accumulating brain edema, while injection of an AVP anti-serum reduced edema formation [2].

Accordingly, in the present study we investigated the role of AVP inhibition and its effects on cerebral edema formation and neurobehavioral functioning. We hypothesize that

A. Manaenko, N. Fathali, T. Lekic, and K.J. Shum
Department of Physiology and Pharmacology,
Loma Linda University, School of Medicine,
Loma Linda, CA, USA

N.H. Khatibi and R. Martin
Department of Anesthesiology, Loma Linda Medical Center,
Loma Linda, CA, USA

J.H. Zhang
Department of Physiology and Pharmacology,
Loma Linda University, School of Medicine,
Loma Linda, CA, USA and
Department of Anesthesiology, Loma Linda Medical Center,
Loma Linda, CA, USA and
Department of Neurosurgery, Loma Linda University Medical Center,
Loma Linda, CA, USA

J. Tang (✉)
Department of Physiology and Pharmacology,
Loma Linda University, School of Medicine,
Loma Linda, CA, USA and
Department of Neurosurgery, Loma Linda University Medical Center,
11234 Anderson Street, Room 2562B, 92354, Loma Linda, CA, USA
e-mail: jtang@llu.edu

SR49059, a highly specific AVP V1a receptor competitive antagonist, could reduce brain edema accumulation and improve neurobehavioral functioning following an ICH brain injury in mice.

Materials and Methods

This study was in accordance with the guidelines of the National Institute of Health for the treatment of animals and was approved by the Institutional Animal Care and Use Committee at Loma Linda University. Male CD1 mice (weight 35–45 g, Charles River, MA) were housed in a 12-h light/dark cycle at a controlled temperature and humidity with free access to food and water. Mice were divided into the following groups: sham ($n=5$), ICH ($n=5$), ICH treated with low-dose antagonist (SR49059 at 0.5 mg/kg; $n=5$), and ICH treated with high-dose antagonist (SR49059 at 2 mg/kg; $n=5$).

Operative Procedure. The collagenase-induced intracerebral hemorrhage model [3] was adapted as previously described in mice [4]. Briefly, mice were anesthetized intraperitoneally with a ketamine (100 mg/kg)/xylazine (10 mg/kg) cocktail and positioned prone in a stereotaxic head frame (Stoelting, Wood Dale, IL). An electronic thermostat-controlled warming blanket was used to maintain the core temperature at 37°C. The calvarium was exposed by a midline scalp incision from the nose to the superior nuchal line, and the skin was retracted laterally. With a variable speed drill (Fine Scientific Tools, Foster City, CA), a 1.0-mm burr hole was made 0.9 mm posterior to the bregma and 1.45 mm right-lateral to the midline. A 26-G needle on a Hamilton syringe was inserted with stereotaxic guidance 4.0 mm into the right deep cortex/basal ganglia at a rate 1 mm/min. Collagenase (0.075 units in 0.5 μ L saline; Sigma, St Louis, MO) was then infused into the brain at a rate of 0.25 μ L/min over 2 min using an automatic infusion pump (Stoelting, Wood Dale, IL). The needle was left in place for an additional 10 min after injection to prevent the possible leakage of collagenase solution. After removal of the needle, the incision was sutured closed, and mice were allowed to recover. Sham operation was performed with needle insertion only.

Treatment Method. SR49059 (Tocris Bioscience, Ellisville, MO) was dissolved in 0.5% DMSO and administered one time intraperitoneally approximately 1 h after ICH induction.

Brain Water Content. Brain water content was measured as previously described [5]. Briefly, rats were sacrificed at 24 h and 72 h post ICH, and brains were immediately removed and divided into five parts: ipsilateral frontal, contralateral frontal, ipsilateral parietal, contralateral parietal, and cerebellum. The cerebellum was used as an internal

control for brain water content. Tissue samples were then weighed on an electronic analytical balance (APX-60, Denver Instrument; Arvada, CO) to the nearest 0.1 mg to obtain the wet weight (WW). The tissue was then dried at 105°C for 48 h to determine the dry weight (DW). The percent brain water content was calculated as $[(WW - DW)/WW] \times 100$.

Assessment of Neurobehavioral Deficits. Neurological outcomes were assessed by a blind observer at 24 h and 72 h post ICH using the Modified Garcia Score [6]. The Modified Garcia Score is a 21-point sensorimotor assessment system consisting of seven tests with scores of 0–3 for each test (maximum score=21). These seven tests included: (1) spontaneous activity, (2) side stroking, (3) vibris touch, (4) limb symmetry, (5) climbing, (6) lateral turning, and (7) forelimb walking.

Additionally, beam balance and wire hang testing was performed. Both the beam (590 cm in length by 51 cm in width) and wire (550 cm in length by 51 mm in width) were constructed and held in place by two platforms on each side. Mice were put on the center of the beam or wire and allowed to reach the platform. Mice were observed for both their time and behavior until they reached one platform and scored according to six grades. The test was repeated three times, and an average score was taken [minimum score 0; maximum score (healthy mouse)] [2].

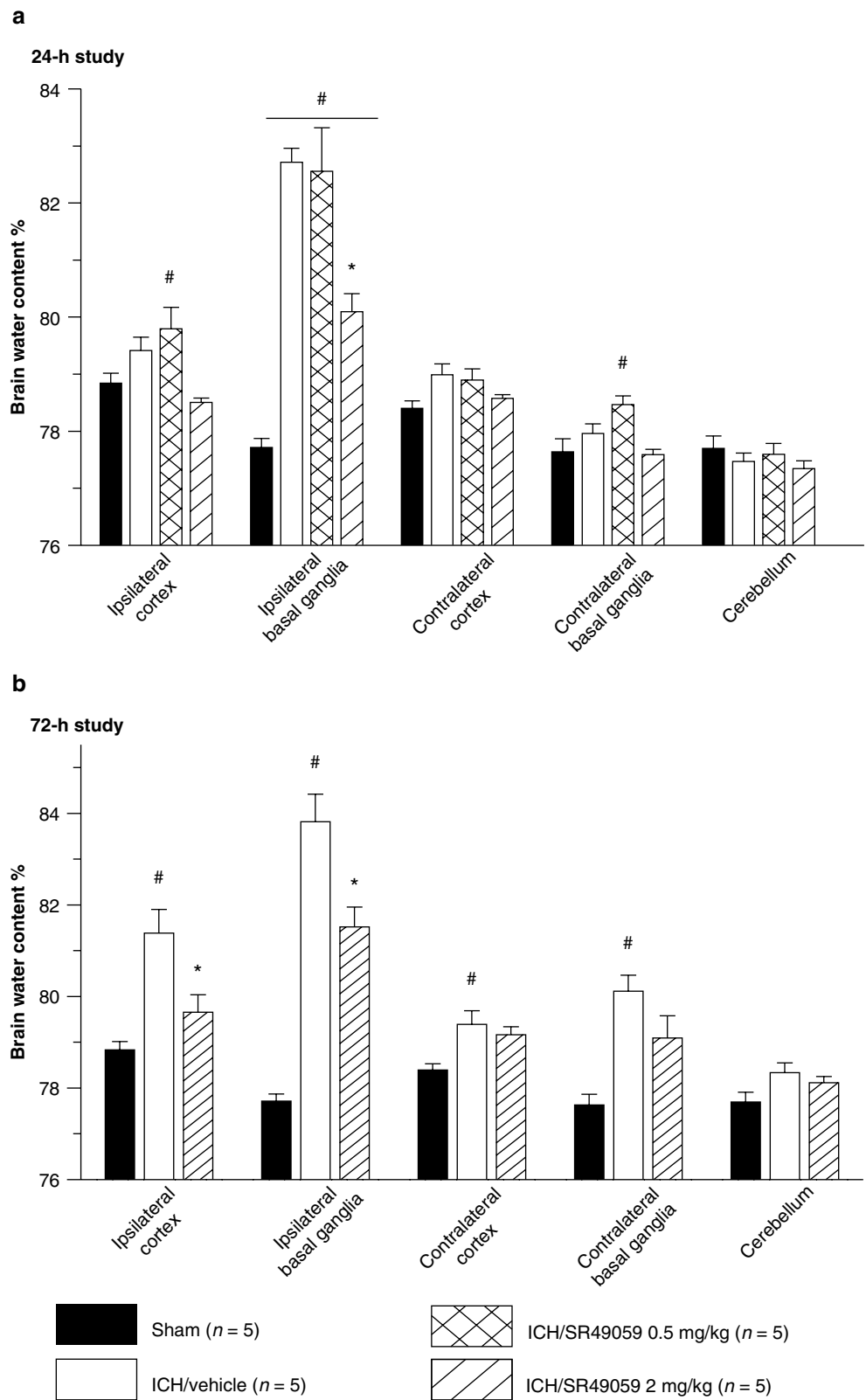
Statistical Analysis. Quantitative data were expressed as the mean \pm SEM. One-way ANOVA and Tukey test were used to determine significance in differences between the means. Neurological scores were evaluated using the Dunn method. A p -value < 0.05 was considered statistically significant.

Results

SR49059 decreases cerebral edema formation after ICH injury in mice. Vehicle groups demonstrated a consistently elevated level of cerebral edema in the ipsilateral basal ganglia. Inhibition of the AVP V1a receptor using high-dose SR49059 was able to significantly reduce the cerebral edema at 24 and 72 h post injury ($p < 0.05$) (Fig. 1). Low dose SR49059 failed to reduce cerebral edema at both time points.

SR49059 improves neurobehavioral deficits. Neurobehavioral deficits were present in all animals after collagenase injection. At 24 h, treatment with SR49059 failed to improve deficits. However, at 72 h post-injury, high-dose SR49059 significantly improved neurobehavioral deficits according to the Modified Garcia test, beam balance, and wire hang tests (Figs. 2 and 3). Additionally, improvements were not seen with low-dose SR49059.

Fig. 1 High-dose SR49059 significantly reduced ICH-induced brain edema at 24 (a) and 72 h (b) *Significant difference vs. sham ($p < 0.05$); #significant difference vs. vehicle ($p < 0.05$); (a) 24 h: sham=5; (vehicle)=5; (ICH+0.5 mg/kg SR49059)=5; (ICH+2 mg/kg SR49059)=5. (b) 72 h: sham=5; (vehicle)=5; (ICH+0.5 mg/kg SR49059)=5; (ICH+2 mg/kg SR49059)=5



Discussion

The aim of this study was to determine the effects of AVP V1a receptor inhibition on ICH-induced brain injury in mice. Using high-dose SR49059, a highly specific AVP V1a receptor competitive antagonist, we found there was a strong reduction in brain edema accumulation and improvement in neurobehavioral deficits in our treated versus untreated mice groups. This suggests a key role for AVP in ICH-induced

brain injury outcomes. To the best of our knowledge, this is the first study to elucidate the benefits of AVP inhibition in ICH injured mice.

Brain injury following an ICH involves a wide array of consequences, including cerebral edema formation, blood-brain barrier (BBB) disruption, apoptotic cell death, direct injury from the expanding hematoma, and secondary changes from hemoglobin breakdown products and inflammation.

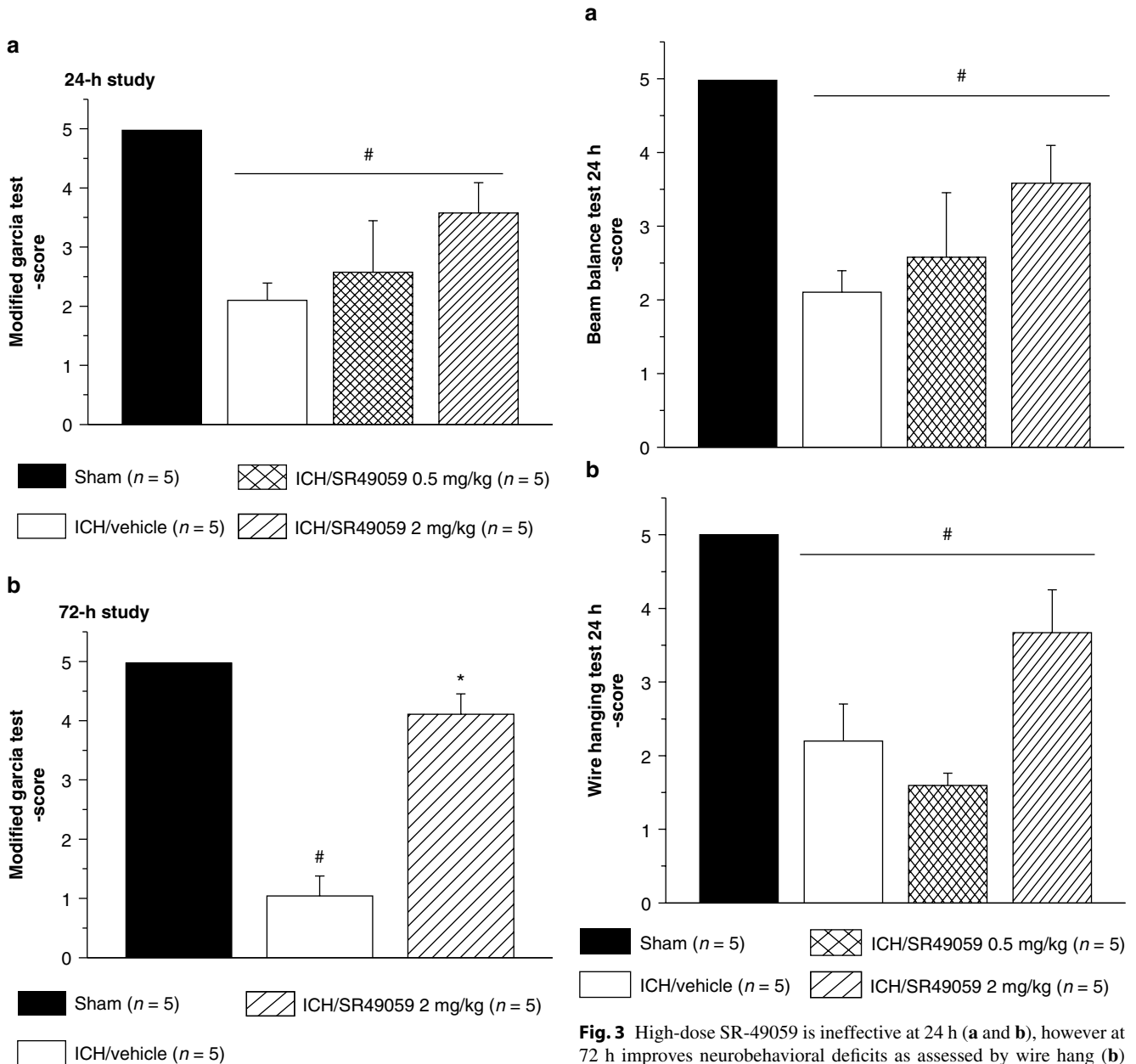


Fig. 2 High-dose SR49059 has no effect on ICH-induced neurological deficit at 24 h (a), however improved it at 72 h (b). *Significant difference vs. sham ($p < 0.05$); #significant difference vs. vehicle ($p < 0.05$); (a) 24 h: sham=5; (vehicle)=5; (ICH+0.5 mg/kg SR49059)=5; (ICH+2 mg/kg SR49059)=5; (b) 72 h: sham=5; (vehicle)=5; (ICH+2 mg/kg SR49059)=5

Fig. 3 High-dose SR-49059 is ineffective at 24 h (a and b), however at 72 h improves neurobehavioral deficits as assessed by wire hang (b) and beam balance (d) tests. *Significant difference vs. sham ($p < 0.05$); #significant difference vs. vehicle ($p < 0.05$); (a) beam balance, 24 h: sham=5; (vehicle)=5; (ICH+0.5 mg/kg SR49059)=5; (ICH+2 mg/kg SR49059)=5; (b) wire hang, 24 h: sham=5; (vehicle)=5; (ICH+0.5 mg/kg SR49059)=5; (ICH+2 mg/kg SR49059)=5; (c) beam balance, 72 h: sham=5; (vehicle)=5; (ICH+2 mg/kg SR49059)=5; (d) wire hang, 72 h: sham=5; (vehicle)=5; (ICH+2 mg/kg SR49059)=5

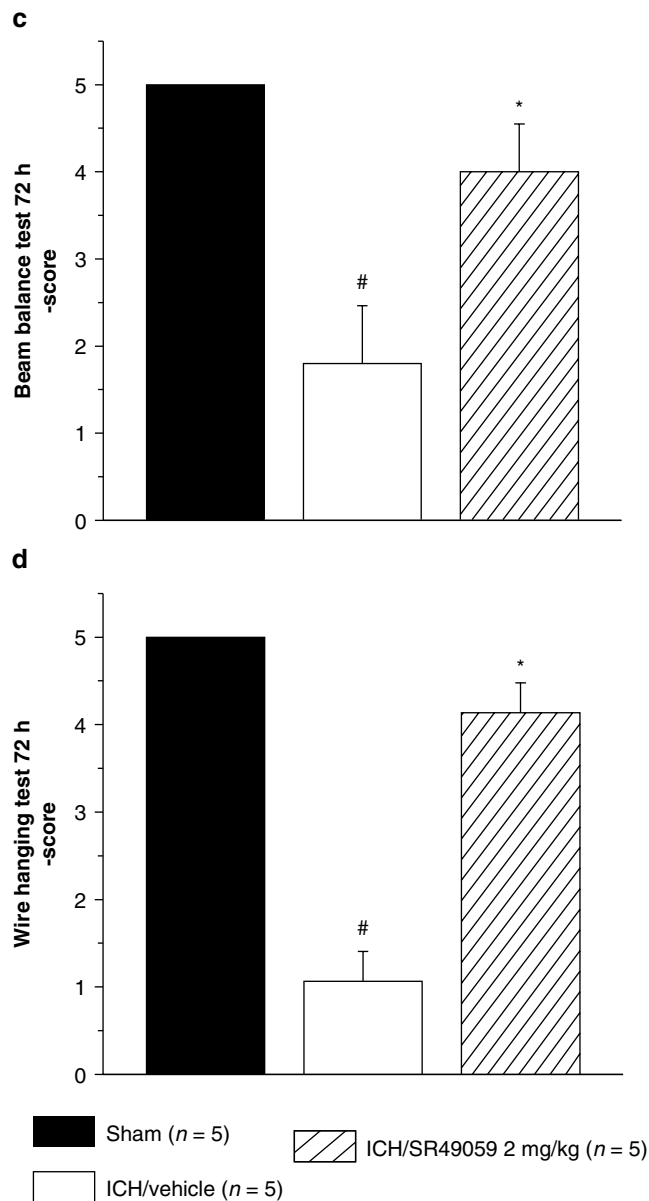


Fig.3 (continued)

Of these, cerebral edema formation seems to be the most devastating – responsible for increasing intracranial pressure that can lead to brain herniation and death [7]. In our bodies, the BBB prevents the movement of large molecules from the blood to the brain, allowing for proper water and ion homeostasis. During an ICH injury, the BBB gets disrupted by various mediators – including inflammatory cells, thrombin, hemoglobin breakdown products, and enzyme activation – which no longer permit the BBB from carrying out its functions [8]. In our study, we found a significant increase in brain edema with ICH injury and subsequent reduction with high-dose SR49059 treatment. This was similar to previous studies in other brain injury models that have looked at the effects of SR49059 on brain edema.

To date, many brain injury studies, including traumatic brain injury (TBI) and middle cerebral artery occlusion (MCAO), have demonstrated AVP's role in mediating brain edema formation [9, 10]. Although no formal mechanism has been determined, we speculate that AVP may in fact play a role in activating aquaporin channels in the brain, specifically, AQP4. In previous studies, upregulation of AQP4 has been observed in surrounding tissue injury sites in MCAO injury models and focal cerebral ischemic rat models [11]. This relationship could possibly explain the increase in brain edema formation following ICH injury. We acknowledge the fact that more studies will be needed, specifically to look at the relationship between these two proteins.

Conclusion

We conclude that AVP V1a receptor inhibition using SR49059, a specific receptor competitive antagonist, can in fact reduce brain edema and improve neurobehavioral deficits following an ICH injury in mice.

Acknowledgement This study is partially supported by NIH NS053407 to J.H. Zhang and NS060936 to J. Tang.

Conflict of interest statement We declare that we have no conflict of interest.

References

- Vakili A, Hiroharu K, Plesnila N (2005) Role of arginine vasopressin V1 and V2 receptors for brain damage after transient focal cerebral ischemia. *J Cereb Blood Flow Metab* 25: 1012–1019
- Liu X, Jin Y, Zheng H, Chen G (1996) Arginine vasopressin gene expression in supraoptic nucleus and paraventricular nucleus of hypothalamus following cerebral ischemia and reperfusion. *Chin Med Sci J* 15:157–161
- Rosenberg GA, Mun-Bryce S, Wesley M, Kornfeld M (1990) Collagenase-induced intracerebral hemorrhage in rats. *Stroke* 21: 801–807
- Choudhri TF, Hoh BL, Solomon RA, Connolly ES, Pinsky D (1997) Use of a spectrophotometric hemoglobin assay to objectively quantify intracerebral hemorrhage in mice. *Stroke* 28: 296–2302
- Yang GY, Betz AL, Chenevert TL, Brunberg JA, Hoff JT (1994) Experimental intracerebral hemorrhage: relationship between brain edema, blood flow, and blood-brain barrier permeability in rats. *J Neurosurg* 81:93–102
- Garcia JH, Wagner S, Liu KF, Hu XJ (1995) Neurological deficit and extent of neuronal necrosis attributable to middle cerebral artery occlusion in rats. Statistical validation. *Stroke* 26:627–634
- Diringer MN (1993) Intracerebral hemorrhage: pathophysiology and management. *Crit Care Med* 2:159–1603

8. Keep RF, Xi G, Hua Y, Hoff JT (2005) The deleterious or beneficial effects of different agents in intracerebral hemorrhage: think big, think small, or is hematoma size important? *Stroke* 6: 1594–1596
9. Liu X, Nakayama S, Ottersen OP, Bhardwaj A (2000) Arginine vasopressin V1 but not V2 receptor antagonism modulates infarct volume, brain water content, and aquaporin-4 expression following experimental stroke. *Neurocrit Care* 12 (1):124–131
10. Trabold R, Krieg S, Scholler K (2008) Role of vasopressin v1a and v2 receptors for the development of secondary brain damage after traumatic brain injury in mice. *J Neurotrauma* 25: 1459–1465
11. Yang M, Gao F, Liu H, Yu WH, Sun SQ (2009) Temporal changes in expression of aquaporin-3, -4, -5 and -8 in rat brains after permanent focal cerebral ischemia. *Brain Res* 1290:121–132

Deferoxamine Affects Heat Shock Protein Expression in Heart after Intracerebral Hemorrhage in Aged Rats

Hua Hu, Lin Wang, Masanobu Okauchi, Richard F. Keep, Guohua Xi, and Ya Hua

Abstract Cardiac dysfunction can occur after intracerebral hemorrhage (ICH). This study examined the expression of heat shock proteins (HSPs) in the heart after ICH in aged rats and whether deferoxamine (DFX), an iron chelator, affects HSP expression. Male Fischer 344 rats (18 months old) received an injection of 100 μ l autologous blood into the right caudate, whereas sham-operated rats had a needle insertion. The rats were treated with DFX or vehicle at 2 and 6 h after ICH and then every 12 h for 3 days. Rats were killed 3 days after ICH, and the hearts were sampled for Western blot analysis of HSP-27 and HSP-32. Western blotting showed that levels of HSP-32 were reduced in the heart after ICH ($p < 0.05$), and this reduction was normalized by DFX ($p < 0.05$). DFX had no effects on heart HSP-32 levels in sham-operated rats. ICH also resulted in a reduction in HSP-27 ($p < 0.05$), but DFX treatment reduced HSP-27 further ($p < 0.05$). In addition, DFX reduced HSP-27 levels in sham rats. In conclusion, ICH causes HSP-27 and -32 reductions in the heart of aged rats. Deferoxamine treatment has different effects on the expression of HSP-27 and HSP-32.

Keywords Cerebral hemorrhage · Deferoxamine · Heart · Heat shock proteins

H. Hu and L. Wang
Department of Neurosurgery, University of Michigan,
Ann Arbor, MI, USA and
Department of Neurosurgery, 2nd Affiliated Hospital,
Zhejiang University, Zhejiang, China

M. Okauchi, R.F. Keep, and G. Xi
Department of Neurosurgery, University of Michigan,
Ann Arbor, MI, USA

Y. Hua (✉)
Department of Neurosurgery, University of Michigan,
109 Zina Pitcher Place, 48109–2200 Ann Arbor, MI, USA
e-mail: yahua@umich.edu

Introduction

Brain damage may result in heart injury, and this phenomenon has been called “the brain-heart connection” [1]. Clinically, neurogenic heart injury has been found in ischemic and hemorrhagic stroke patients [2–5]. Cerebral ischemia and intracerebral hemorrhage (ICH) can also cause heart damage in animals [6, 7].

ICH is mostly a disease of the elderly, but current experimental ICH models have primarily used young animals. Age is an important factor affecting brain injury in ischemic stroke in animals and humans. Recently, we found that ICH caused greater neurological deficits, more severe brain swelling, greater induction of heat shock proteins (HSPs), and enhanced microglial activation in aged rats compared to young rats [8]. These results suggest that age is a significant factor in determining brain injury after ICH [9].

Deferoxamine (DFX), an iron chelator, can reduce ICH – and hemoglobin-induced brain injury. Our recent data showed that DFX reduces ICH-induced brain edema, brain atrophy, and neurological deficits in aged rats and in pigs [10, 11].

This study examined whether ICH causes heart stress in aged rats and the effects of DFX on such stress. HSP-27 and HSP-32 were used as stress markers.

Materials and Methods

Animal Preparation and Intracerebral Infusion

Animal use protocols were approved by the University of Michigan Committee on the Use and Care of Animals. Male Fisher 344 rats (18 months old, from the National Institutes of Health) were used in this study. Animals were anesthetized with pentobarbital (40 mg/kg i.p.). The right femoral artery was catheterized for continuous blood pressure monitoring

and blood sampling for injection and monitoring of pH, PaO₂, PaCO₂, hematocrit, and glucose levels. Core temperature was maintained at 37°C with use of a feedback-controlled heating pad. Rats were positioned in a stereotactic frame (Kopf Instruments) and a cranial burr hole (1 mm) drilled on the right coronal suture 3.5 mm lateral to the midline. All rats received an injection of 100 µl autologous whole blood into the right caudate nucleus at a rate of 10 µl/min through a 26-gauge needle (coordinates 0.2 mm anterior, 5.5 mm ventral, and 3.5 mm lateral to bregma) with the use of a microinfusion pump. The needle was removed and the skin incision closed with suture after infusion [12].

Animal Groups

Rats received an intracaudate injection of 100 µl autologous blood or a needle insertion (sham). They were then treated with DFX (100 mg/kg, i.m.) or vehicle 2 h after ICH and then every 12 h for 3 days. Thus, the four groups in this study were: Sham+Vehicle, Sham+DFX, ICH+Vehicle, and ICH+DFX. Rats were killed 3 days after ICH and the left heart ventricles sampled for Western blot analysis. Levels of heat shock proteins (HSP-27 or -32) were determined.

Western Blot Analysis

Heart tissues were immersed in 0.5 ml Western sample buffer (62.5 mM Tris-HCl, pH 6.8, 2.3% sodium dodecyl sulfate, 10% glycerol, and 5% β-mercaptoethanol) and sonicated for 10 s. Ten-microliters of the sample solution was taken for protein assay (Bio-Rad), while the rest was frozen at -20°C for Western blot. Western blot analysis was performed as described previously [8]. Briefly, 50 µg of protein was run on polyacrylamide gels with a 4% stacking gel (SDS-PAGE) after 5 min boiling at 95°C. The protein was transferred to a hybond-C pure nitrocellulose membrane (Amersham). The membranes were blocked in 5% Carnation non-fat dry milk in TBST (150 mM NaCl, 100 mM Tris-base, 0.1% Tween 20, pH 7.6) buffer for 1 h at 37°C. After washing in TBST buffer three times, membranes were probed with primary antibodies against HSP-32, HSP27 (Stressgen) for 90 min at room temperature. After washing with TBST buffer three times, membranes were immunoprobed again with the second antibody for 1 h at room temperature. Finally, membranes were washed three times in TBST buffer and the antigen-antibody complexes visualized with the ECL chemiluminescence system (Amersham) and exposed to Kodak X-OMAT film. The relative densities of the protein bands were analyzed with a public domain NIH Image program (NIH Image Version 1.61).

Statistical Analysis

Student's *t* test and analysis of variance (ANOVA) were used. Values are mean ± SD. Statistical significance was set at $p < 0.05$.

Results

Western blotting showed that levels of HSP-32 were reduced in the heart 3 days after ICH (1,158 ± 221 vs. 1,685 ± 115 pixels in the sham rats, $p < 0.05$, Fig. 1a). The reduction of heart HSP-32 following ICH was normalized by DFX treatment ($p < 0.05$, Fig. 1a). DFX had no effect on heart HSP-32 levels in sham rats (3,030 ± 637 pixels vs. 3,631 ± 589 pixels in sham + vehicle group, $p > 0.05$, Fig. 1b).

ICH also decreased HSP-27 expression in heart. Western blot analysis showed the levels of HSP-27 in heart 3 days after ICH were lower than in sham-operated rats (1,347 ± 165 vs. 1,874 ± 151 pixels, respectively, $p < 0.05$, Fig. 2a). In addition, DFX treatment significantly reduced heart HSP-27 levels in aged rats with sham operation (1,870 ± 628 vs. 3,454 ± 613 pixels in sham + vehicle group, $p < 0.01$, Fig. 2b).

Discussion

In this study, we demonstrated that ICH causes a reduction of heart HSP-32 in aged rats, and systemic DFX treatment normalizes cardiac HSP-32 levels. HSP-32 is a protective protein in the heart [13, 14]. Upregulation of heart HSP-32 contributes to erythropoietin-mediated cardioprotection during myocardial ischemia-reperfusion [13]. A recent report has shown that ICH causes heart damage in young rats [6], and the lower HSP-32 levels in heart after ICH found in our study may reflect ICH-induced heart injury.

It is not clear how DFX can normalize heart HSP-32 levels after ICH. However, there are at least two possibilities. First, DFX reduces brain injury caused by ICH and then reduces heart stress. Our recent studies have shown that iron overload has a key role in brain damage after ICH, and DFX can reduce ICH-induced brain edema, neuronal death, and brain atrophy in young and aged rats, as well as in pigs [10, 11]. Second, DFX can cause hypoxia-inducible factor-1α (HIF-1α) accumulation, and HSP-32 is a HIF-1α target gene [15].

ICH also reduced heart HSP-27 protein levels, another protective protein. Overexpressing HSP-27 in heart protects from lethal ischemia/reperfusion injury in mice [16]. Interestingly, DFX reduces heart HSP-27 in sham-operated aged rats via an unknown mechanism.

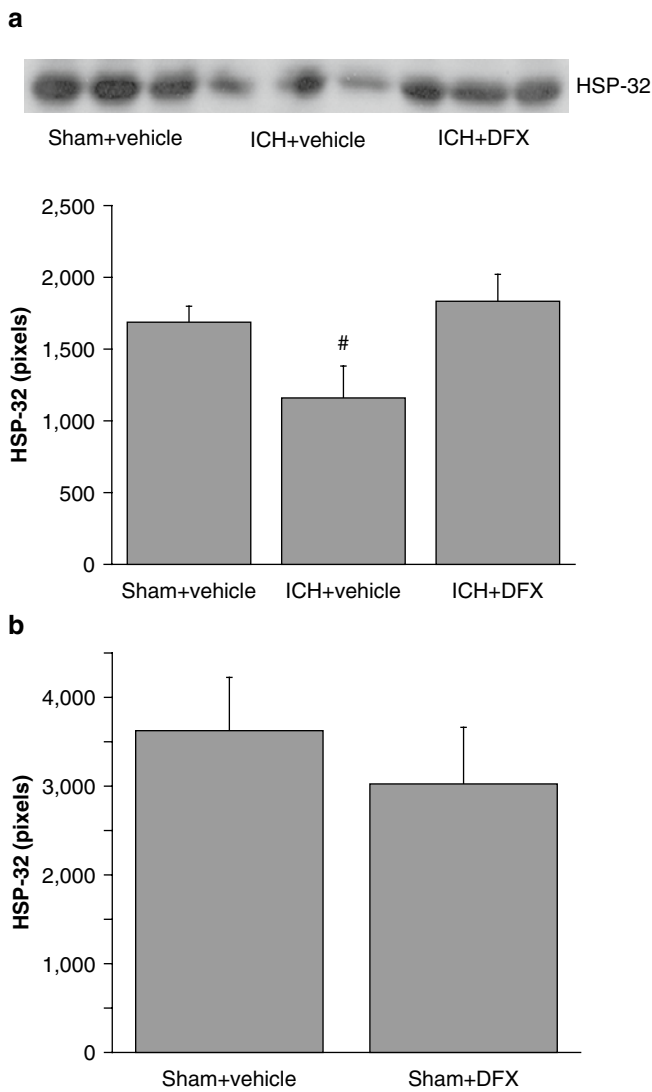


Fig. 1 (a) Protein levels of heat shock protein 32 (HSP-32) in the heart of 18-month-old rats 3 days after ICH or a sham operation. Rats were treated with vehicle or deferoxamine. Values are mean \pm SD, [#] $p < 0.01$ vs. the other groups. (b) Heart HSP-32 levels 3 days after sham operation. Rats were treated with vehicle or deferoxamine. Values are mean \pm SD

In conclusion, our results showed that ICH causes HSP-27 and -32 reductions in the heart of the aged rats, which may be associated with heart injury caused by ICH. Deferoxamine has differential roles in the expression of heart HSP-27 and HSP-32.

Acknowledgment This study was supported by grants NS-017760, NS-039866, NS-052510, and NS-057539 from the National Institutes of Health (NIH) and 0840016N from the American Heart Association (AHA). The content is solely the responsibility of the authors and does not necessarily represent the official views of the NIH and AHA.

Conflict of interest statement We declare that we have no conflict of interest.

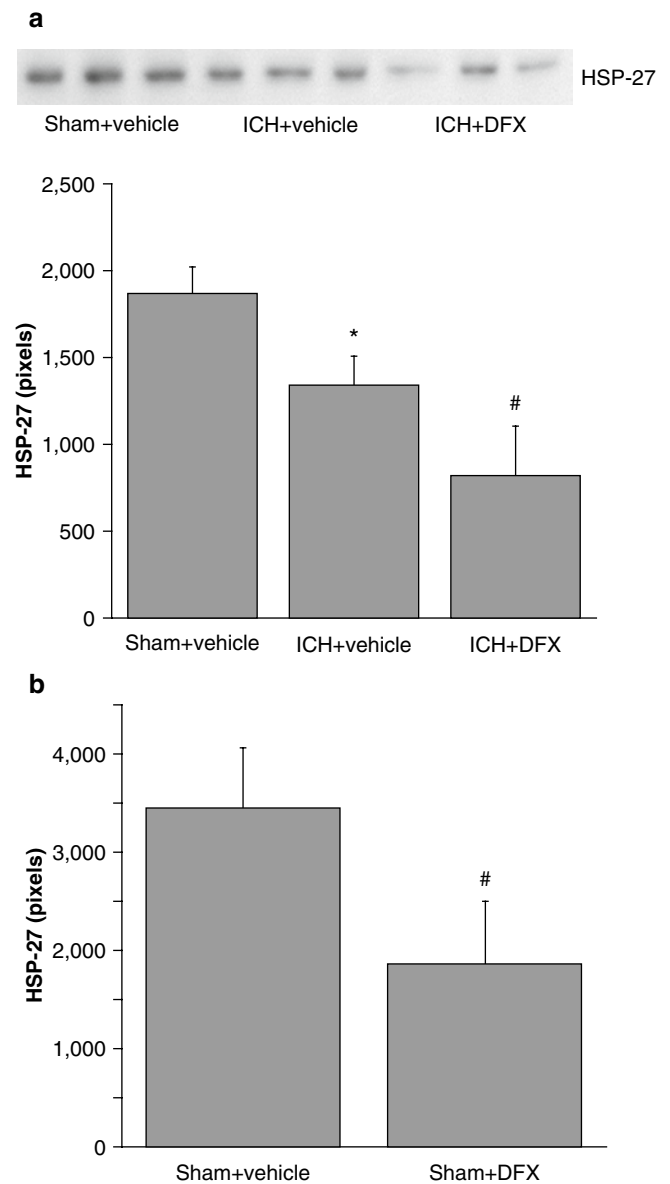


Fig. 2 (a) Protein levels of heat shock protein 27 (HSP-27) in the heart of 18-month-old rats 3 days after ICH or a sham operation. Rats were treated with vehicle or deferoxamine. Values are mean \pm SD, ^{*} $p < 0.05$, [#] $p < 0.01$ vs. the other groups. (b) Heart HSP-27 levels 3 days after sham operation. Rats were treated with vehicle or deferoxamine. Values are mean \pm SD. [#] $p < 0.01$ vs. sham + vehicle

References

- Samuels MA (2007) The brain-heart connection. *Circulation* 116:77–84
- Garrett MC, Komotar RJ, Starke RM, Doshi D, Otten ML, Connolly ES (2009) Elevated troponin levels are predictive of mortality in surgical intracerebral hemorrhage patients. *Neurocrit Care* 12(2): 199–203
- Hurst JW (2003) Electrocardiographic changes in intracranial hemorrhage mimicking myocardial infarction. *N Engl J Med* 349: 1874–1875, author reply 1874–1875

4. Jung F, Setzer M, Hohnloser SH (2001) Severe intracranial bleeding mimicking acute inferior myocardial infarction with right ventricular involvement. *Cardiology* 95:48–50
5. Laowattana S, Zeger SL, Lima JA, Goodman SN, Wittstein IS, Oppenheimer SM (2006) Left insular stroke is associated with adverse cardiac outcome. *Neurology* 66:477–483
6. Fang CX, Wu S, Ren J (2006) Intracerebral hemorrhage elicits aberration in cardiomyocyte contractile function and intracellular Ca_2+ transients. *Stroke* 37:1875–1882
7. Min J, Farooq MU, Greenberg E, Aloka F, Bhatt A, Kassab M, Morgan JP, Majid A (2009) Cardiac dysfunction after left permanent cerebral focal ischemia: the brain and heart connection. *Stroke* 40:2560–2563
8. Gong Y, Hua Y, Keep RF, Hoff JT, Xi G (2004) Intracerebral hemorrhage: effects of aging on brain edema and neurological deficits. *Stroke* 35:2571–2575
9. Xi G, Keep RF, Hoff JT (2006) Mechanisms of brain injury after intracerebral hemorrhage. *Lancet Neurol* 5:53–63
10. Gu Y, Hua Y, Keep RF, Morgenstern LB, Xi G (2009) Deferoxamine reduces intracerebral hematoma-induced iron accumulation and neuronal death in piglets. *Stroke* 40:2241–2243
11. Okauchi M, Hua Y, Keep RF, Morgenstern LB, Schallert T, Xi G (2010) Deferoxamine treatment for intracerebral hemorrhage in aged rats: therapeutic time window and optimal duration. *Stroke* 41:375–382
12. He Y, Hua Y, Lee J, Liu W, Keep RF, Wang MM, Xi G (2010) Brain alpha – and beta-globin expression after intracerebral hemorrhage. *Transl Stroke Res* 1:48–56
13. Burger D, Xiang F, Hammoud L, Lu X, Feng Q (2009) Role of heme oxygenase-1 in the cardioprotective effects of erythropoietin during myocardial ischemia and reperfusion. *Am J Physiol Heart Circ Physiol* 296:H84–H93
14. Latchman DS (2001) Heat shock proteins and cardiac protection. *Cardiovasc Res* 51:637–646
15. Bergeron M, Gidday JM, Yu AY, Semenza GL, Ferriero DM, Sharp FR (2000) Role of hypoxia-inducible factor-1 in hypoxia-induced ischemic tolerance in neonatal rat brain. *Ann Neurol* 48: 285–296
16. Efthymiou CA, Mocanu MM, de Bellerche J, Wells DJ, Latchmann DS, Yellon DM (2004) Heat shock protein 27 protects the heart against myocardial infarction. *Basic Res Cardiol* 99:392–394

Neuroprotection by Melatonin after Germinal Matrix Hemorrhage in Neonatal Rats

Tim Lekic, Anatol Manaenko, William Rolland, Kelly Virbel, Richard Hartman, Jiping Tang, and John H. Zhang

Abstract *Background:* Germinal matrix hemorrhage (GMH) is a devastating neurological disorder of very low birth weight premature infants that leads to post-hemorrhagic hydrocephalus, cerebral palsy, and mental retardation. Melatonin is a potent antioxidant known to reverse free-radical mediated injury in the brain. This study investigated the effect of melatonin treatment after GMH injury.

Methods: Clostridial collagenase was infused into the right germinal matrix region of neonatal rats with stereotaxic technique. Cognitive function, sensorimotor ability, cerebral, cardiac and splenic growths were measured in juvenile animals.

Results: Systemic melatonin treatment ameliorated cognitive and sensorimotor dysfunction at the juvenile developmental stage. This hormone also normalized brain atrophy, splenomegaly, and cardiac hypertrophy consequences at 1 month after injury.

Conclusion: This study supports the role of free radicals in acute neonatal hemorrhagic brain injury. Melatonin is an effective antioxidant that can protect the infant's brain from the post-hemorrhagic consequences of mental retardation and cerebral palsy. Further mechanistic studies are

warranted to determine the mechanisms behind these neuroprotective effects.

Keywords Melatonin · Neurological deficits · Stroke · Experimental

Introduction

Germinal matrix hemorrhage (GMH) is a clinical condition of very low birth weight (VLBW $\leq 1,500$ g) premature neonates in which immature blood vessels rupture within the anterior caudate (sub-ventricular) brain region during the first 7 days of life [1, 2]. This affects approximately 3.5/1,000 births in the United States each year [3]. The consequences of this brain injury are hydrocephalus (post-hemorrhagic ventricular dilation), developmental delay, and a lifetime of cerebral palsy and mental retardation [4, 5]. Although this is an important disease, experimental studies investigating therapeutic modalities are lacking [6].

Interventions targeting free-radical mechanisms have been shown to be neuroprotective after brain hemorrhage in adult rats [7–11]. Thrombin is released from the clot, and erythrocytes undergo lysis to release the neurotoxins hemoglobin, heme, and iron [12–14]. These will, in turn, diffusely oxidatively damage proteins, lipid, and DNA within the first day after brain hemorrhage [15–21]. Melatonin is a potent antioxidant and free-radical scavenger [22–24] shown to inhibit free-radical-associated red blood cell lysis [25], hemoglobin degradation [26], neuronal cell death [27], and hippocampal and nigrostriatal degeneration [28].

In light of this evidence, we hypothesized that melatonin can be a reasonable therapeutic modality for the amelioration of hemorrhage-mediated free-radical brain injury mechanisms in neonatal rats. This intervention could improve juvenile cognitive and sensorimotor outcomes after neonatal germinal matrix hemorrhage.

T. Lekic, A. Manaenko, W. Rolland, K. Virbel, and J. Tang
Department of Physiology, Loma Linda University,
School of Medicine, Loma Linda, CA, USA

R. Hartman
Department of Psychology, Loma Linda University,
School of Medicine, Loma Linda, CA, USA

J.H. Zhang (✉)
Department of Anesthesiology, Loma Linda University,
School of Medicine, Loma Linda, CA, USA and
Department of Neurosurgery, Loma Linda University,
School of Medicine, Loma Linda, CA, USA and
Department of Physiology, Loma Linda University,
School of Medicine, Risley Hall, Room 223,
92354 Loma Linda, CA, USA
e-mail: johnzhang3910@yahoo.com

Methods and Materials

Animal Groups and General Procedures

This study was in accordance with the National Institutes of Health guidelines for the treatment of animals and was approved by the Institutional Animal Care and Use Committee at Loma Linda University. Timed pregnant Sprague-Dawley rats were housed with food and water available *ad libitum*. Treatment consisted of melatonin (Sigma Aldrich) dissolved in 10% ethanol and diluted with 0.9% normal saline. This was administered (I.P.) at 60 min after collagenase infusion using treatment dosages of 5 mg/kg and 10 mg/kg. Postnatal day 7 (P7) pups were blindly assigned to the following ($n=8$ /group): sham (naive), needle (control), GMH (collagenase-infusion), GMH+5 mg/kg melatonin, and GMH+10 mg/kg melatonin. All groups were evenly divided within each litter.

Experimental Model of GMH

Using an aseptic technique, rat pups were gently anaesthetized with 3% isoflurane (in mixed air and oxygen) while placed prone on a stereotaxic frame. Betadine sterilized the surgical scalp area, which was incised in the longitudinal plane to expose the skull and reveal the bregma. The following stereotaxic coordinates were determined: 1 mm (anterior), 1.5 mm (lateral), and 3.5 mm (ventral) from the bregma. A bore hole (1 mm) was drilled, into which a 27-gauge needle was inserted at a rate of 1 mm/min. A microinfusion pump (Harvard Apparatus, Holliston, MA) infused 0.3 units of clostridial collagenase VII-S (Sigma, St Louis, MO) through a Hamilton syringe. The needle remained in place for an additional 10 min after injection to prevent “back-leakage.” After needle removal, the burr hole was sealed with bone wax, the incision sutured closed, and the animals allowed to recover. The entire surgery took on average 20 min. Upon recovering from anesthesia, the animals were returned to their dams. Needle controls consisted of needle insertion alone without collagenase infusion, while naive animals did not receive any surgery.

Cognitive Measures

Higher order brain function was assessed during the third week after collagenase infusion. The T-Maze assessed short-term (working) memory [29]. Rats were placed into the stem (40 cm × 10 cm) of a maze and allowed to explore until one arm (46 cm × 10 cm) was chosen. From the sequence of ten

trials, of left and right arm choices, the rate of spontaneous alternation (0% = none and 100% = complete, alternations/trial) was calculated, as routinely performed [30, 31]. The Morris water maze assessed spatial learning and memory on four daily blocks, as described previously in detail [11, 32]. The apparatus consisted of a metal pool (110 cm diameter), filled to within 15 cm of the upper edge, with a platform (11 cm diameter) for the animal to escape onto, which changed location for each block (maximum = 60 s/trial), and data were digitally analyzed by Noldus Ethovision tracking software. Cued trials measured place learning with the escape platform visible above water. Spatial trials measured spatial learning with the platform submerged, and probe trials measured spatial memory once the platform was removed. For the locomotor activity, in an open field, the path length in open-topped plastic boxes (49 cm long, 35.5 cm wide, 44.5 cm tall) was digitally recorded for 30 min and analyzed by Noldus Ethovision tracking software [32].

Sensorimotor Function

At 4 weeks after collagenase infusion, the animals were tested for functional ability. Neurodeficit was quantified using a summation of scores (maximum = 12) given for (1) postural reflex, (2) proprioceptive limb placing, (3) back pressure towards the edge, (4) lateral pressure towards the edge, (5) forelimb placement, and (6) lateral limb placement (2 = severe, 1 = moderate, 0 = none), as routinely performed [30]. For the rotarod, striatal ability was assessed using an apparatus consisting of a horizontal, accelerated (2 rpm/5 s), rotating cylinder (7 cm-diameter × 9.5 cm-wide) requiring continuous walking to avoid falling recorded by the photo-beam circuit (Columbus Instruments) [11, 32]. For foot fault, the number of complete limb missteps through the openings was counted over 2 min while exploring over an elevated wire (3 mm) grid (20 cm × 40 cm) floor [31].

Assessment of Treatment upon Cerebral and Somatic Growth

At the completion of experiments, the brains were removed and hemispheres separated by midline incision (loss of brain weight has been used as the primary variable to estimate brain damage in juvenile animals after neonatal brain injury [33]). For organ weights, the spleen and heart were separated from surrounding tissue and vessels. The quantification was performed using an analytical microbalance (model AE 100; Mettler Instrument Co., Columbus, OH) capable of 1.0 μg precision.

Statistical Analysis

Significance was considered at $P < 0.05$. Data were analyzed using analysis of variance (ANOVA) with repeated measures (RM-ANOVA) for long-term neurobehavior. Significant interactions were explored with conservative Scheffé *post hoc* and Mann-Whitney rank sum test when appropriate.

Results

Collagenase infusion led to significant cognitive dysfunction in the T-maze (working) memory and water maze (spatial) learning and memory (Figs. 1a–c, $P < 0.05$). Melatonin treatment normalized T-maze deficits (Fig. 1a, $P > 0.05$ compared to controls) and water maze (spatial) learning deficits (Fig. 1b, $P < 0.05$ compared to GMH), without improving spatial memory (Fig. 1c, $P > 0.05$). Both doses of melatonin also normalized ($P < 0.05$) the significant sensorimotor dysfunction (compared to juvenile GMH animals), demonstrated by the neurodeficit score, number of foot faults, and accelerating rotarod falling latency (Figs. 2a–c, $P < 0.05$). Broad cytoprotection by melatonin was confirmed by the improvement upon brain atrophy (Fig. 3a, $P < 0.05$ compared to GMH), and normalization of peripheral splenomegaly and cardiomegaly (Fig. 3b and c, $P > 0.05$ compared to controls) at 4 weeks after injury.

Discussion

These results indicate that systemic melatonin treatment after neonatal injury can reduce long-term brain atrophy, and return sensorimotor and cognitive function to near-normal levels in juvenile animals. In support of the findings from others, these outcomes provide preliminary evidence about the importance of oxidative stress mechanisms on outcomes after neonatal GMH [7, 8, 10].

Beyond the improvements in sensorimotor function and brain atrophy, the cognitive normalization by melatonin could have mechanistic benefits beyond reductions of periventricular free radical injury. Hippocampal neurons have receptors for melatonin [34, 35], upon which can be modulated excitability, synaptic transmission, and plasticity [35–38]. These targets could augment melatonin's neuroprotective effects beyond a reduction of oxidative stress alone [38–44]. Mechanistic studies can investigate these processes further, as a window of opportunity for lasting neuroprotection after neonatal GMH.

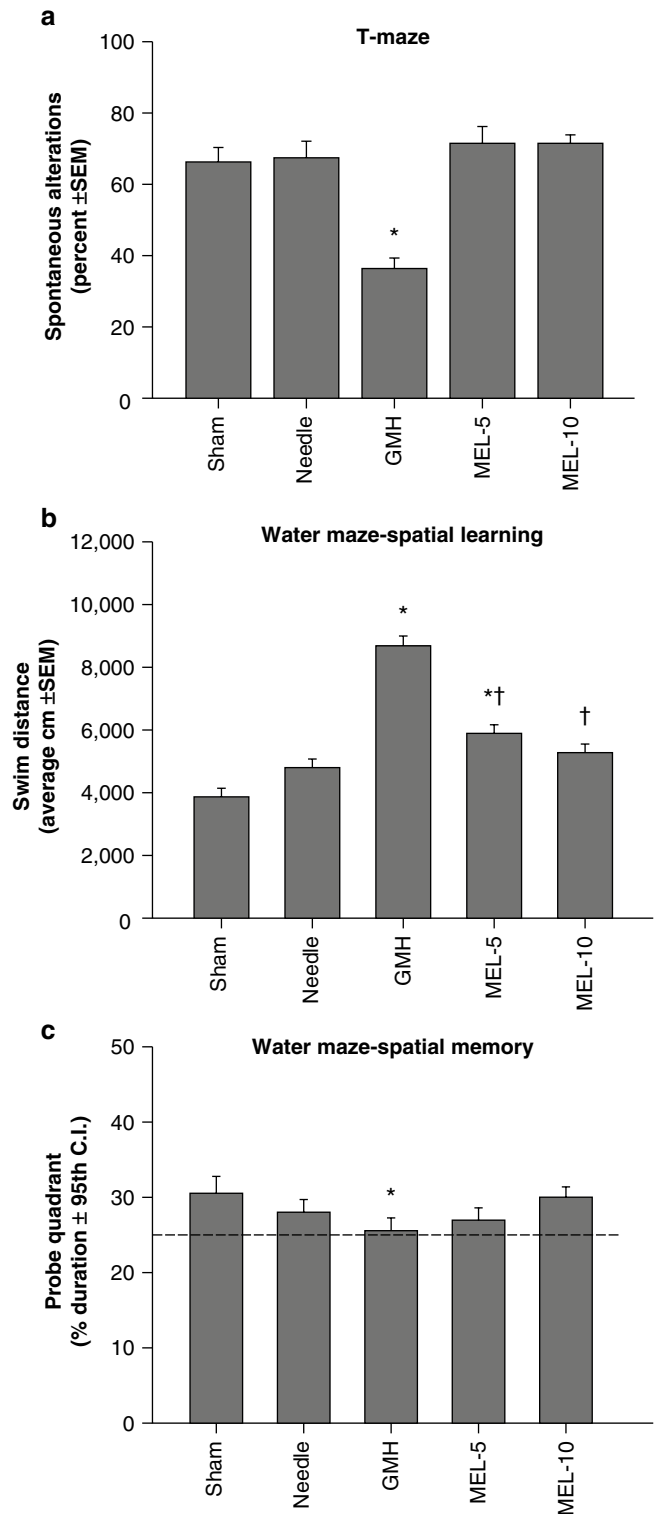


Fig. 1 Cognitive function normalization in juvenile rats by melatonin (MEL) after neonatal GMH. Higher order function was measured at the third week after collagenase infusion: (a) T-maze, (b) spatial learning water maze, (c) spatial memory (Probe) water maze. Values expressed as mean \pm 95th CI (probe quadrant) or mean \pm SEM (all others), $n = 8$ (per group), * $P < 0.05$ compared with controls (sham and needle trauma), and † $P < 0.05$ compared with GMH

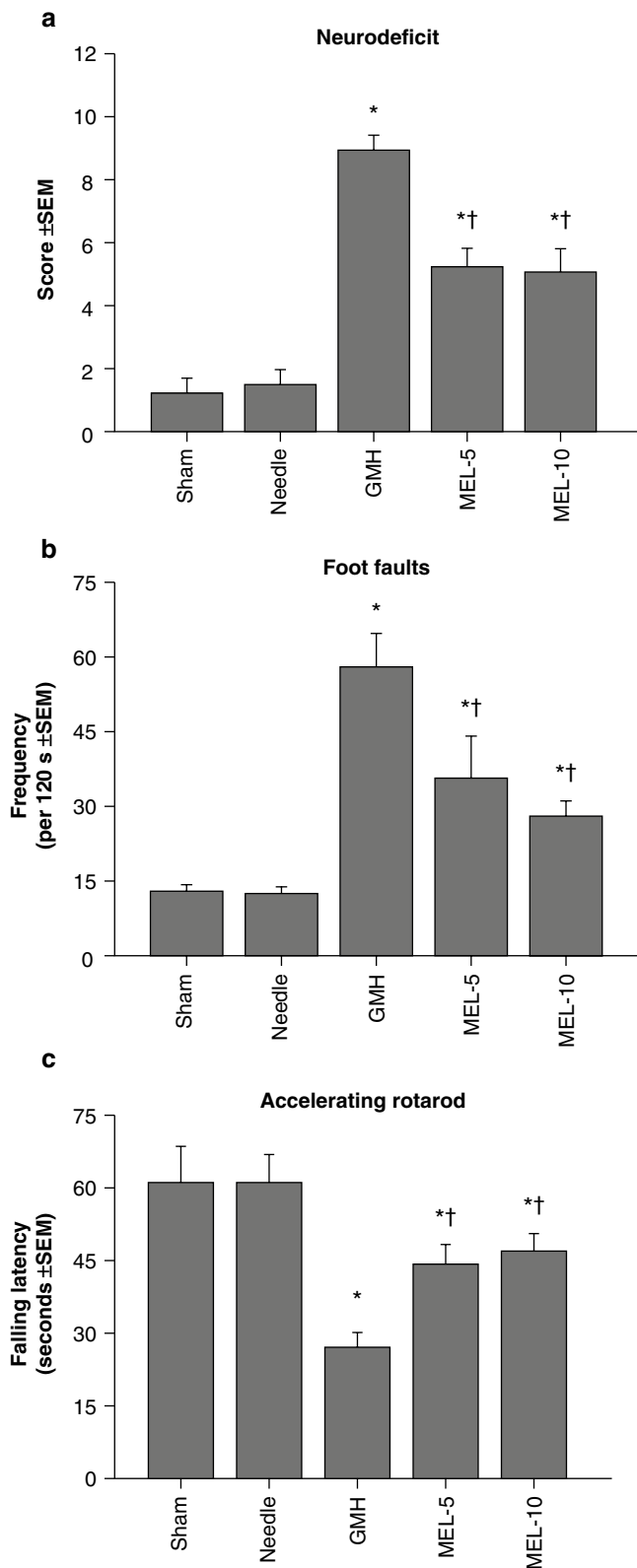


Fig. 2 Sensorimotor function normalization in juvenile rats by melatonin (MEL) after neonatal GMH. Cerebral palsy measurements were performed in the juveniles at 1 month after collagenase infusion: (a) neurodeficit score, (b) foot faults and (c) rotarod. Values expressed as mean \pm SEM, $n=8$ (per group), * $P<0.05$ compared with controls (sham and needle trauma), and † $P<0.05$ compared with GMH

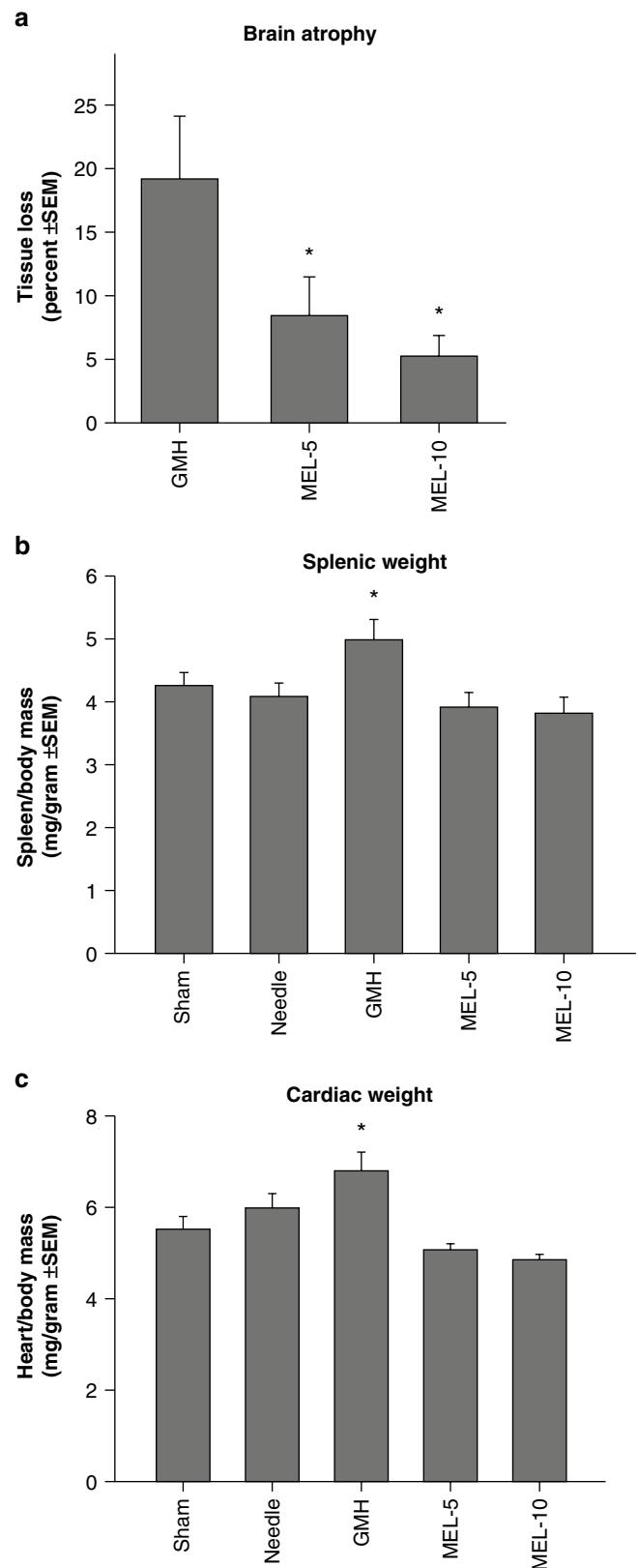


Fig. 3 Cerebral and somatic growth normalization in juvenile rats by melatonin (MEL) after GMH. (a) Brain atrophy (percent tissue loss), (b) splenic weight, and (c) cardiac weight were measured at 4 weeks after injury. Values expressed as mean \pm SEM, $n=8$ (per group), * $P<0.05$ compared with controls (sham and needle trauma)

Melatonin is a widely tested neuroprotectant shown to ameliorate brain injury in adult animal models of cerebral ischemia [45] and hemorrhage [11]. This study supports the notion that the application of melatonin has no adverse effects in neonatal rats and can lead to improvements in functional outcomes after brain injury from hemorrhagic stroke in premature infants as well.

Acknowledgements and Funding This study was partially supported by a grant (NS053407) from the National Institutes of Health to J.H. Zhang.

Conflict of interest statement We declare that we have no conflict of interest.

References

- Ballabh P (2010) Intraventricular hemorrhage in premature infants: mechanism of disease. *Pediatr Res* 67:1–8. doi:10.1203/PDR.0b013e3181c1b176
- Kadri H, Mawla AA, Kazah J (2006) The incidence, timing, and predisposing factors of germinal matrix and intraventricular hemorrhage (GMH/IVH) in preterm neonates. *Childs Nerv Syst* 22:1086–1090. doi:10.1007/s00381-006-0050-6
- Heron M, Sutton PD, Xu J, Ventura SJ, Strobino DM, Guyer B (2010) Annual summary of vital statistics: 2007. *Pediatrics* 125:4–15. doi:peds.2009-2416 [pii] 10.1542/peds.2009-2416
- Ballabh P, Braun A, Nedergaard M (2004) The blood-brain barrier: an overview: structure, regulation, and clinical implications. *Neurobiol Dis* 16:1–13. doi:10.1016/j.nbd.2003.12.016 S0969996103002833 [pii]
- Murphy BP, Inder TE, Rooks V, Taylor GA, Anderson NJ, Mogrige N, Horwood LJ, Volpe JJ (2002) Posthaemorrhagic ventricular dilatation in the premature infant: natural history and predictors of outcome. *Arch Dis Child Fetal Neonatal Ed* 87:F37–41
- Balasubramaniam J, Del Bigio MR (2006) Animal models of germinal matrix hemorrhage. *J Child Neurol* 21:365–371
- Peeling J, Del Bigio MR, Corbett D, Green AR, Jackson DM (2001) Efficacy of disodium 4-[(tert-butylimino)methyl]benzene-1, 3-disulfonate N-oxide (NXY-059), a free radical trapping agent, in a rat model of hemorrhagic stroke. *Neuropharmacology* 40:433–439. doi:S002839080001702 [pii]
- Peeling J, Yan HJ, Chen SG, Campbell M, Del Bigio MR (1998) Protective effects of free radical inhibitors in intracerebral hemorrhage in rat. *Brain Res* 795:63–70. doi:S0006-8993(98)00253-4 [pii]
- Peeling J, Yan HJ, Corbett D, Xue M, Del Bigio MR (2001) Effect of FK-506 on inflammation and behavioral outcome following intracerebral hemorrhage in rat. *Exp Neurol* 167:341–347. doi:10.1006/exnr.2000.7564 S0014-4886(00)97564-2 [pii]
- Nakamura T, Kuroda Y, Yamashita S, Zhang X, Miyamoto O, Tamiya T, Nagao S, Xi G, Keep RF, Itano T (2008) Edaravone attenuates brain edema and neurologic deficits in a rat model of acute intracerebral hemorrhage. *Stroke* 39:463–469. doi:STROKEAHA.107.486654 [pii] 10.1161/STROKEAHA.107.486654
- Lekic T, Hartman R, Rojas H, Manaenko A, Chen W, Ayer R, Tang J, Zhang JH (2010) Protective effect of melatonin upon neuropathology, striatal function, and memory ability after intracerebral hemorrhage in rats. *J Neurotrauma* 27:627–637. doi:10.1089/neu.2009.1163
- Wagner KR, Sharp FR, Ardizzone TD, Lu A, Clark JF (2003) Heme and iron metabolism: role in cerebral hemorrhage. *J Cereb Blood Flow Metab* 23:629–652. doi:10.1097/01.WCB.0000073905.87928.6D
- Wu J, Hua Y, Keep RF, Nakamura T, Hoff JT, Xi G (2003) Iron and iron-handling proteins in the brain after intracerebral hemorrhage. *Stroke* 34:2964–2969. doi:10.1161/01.STR.0000103140.52838.45 01.STR.0000103140.52838.45 [pii]
- Xi G, Keep RF, Hoff JT (2006) Mechanisms of brain injury after intracerebral haemorrhage. *Lancet Neurol* 5:53–63. doi:S1474-4422(05)70283-0 [pii] 10.1016/S1474-4422(05)70283-0
- Xi G, Wagner KR, Keep RF, Hua Y, de Courten-Myers GM, Broderick JP, Brott TG, Hoff JT (1998) Role of blood clot formation on early edema development after experimental intracerebral hemorrhage. *Stroke* 29:2580–2586
- Nakamura T, Keep RF, Hua Y, Hoff JT, Xi G (2005) Oxidative DNA injury after experimental intracerebral hemorrhage. *Brain Res* 1039:30–36. doi:S0006-8993(05)00104-6 [pii] 10.1016/j.brainres.2005.01.036
- Lee KR, Colon GP, Betz AL, Keep RF, Kim S, Hoff JT (1996) Edema from intracerebral hemorrhage: the role of thrombin. *J Neurosurg* 84:91–96
- Xi G, Keep RF, Hoff JT (1998) Erythrocytes and delayed brain edema formation following intracerebral hemorrhage in rats. *J Neurosurg* 89:991–996
- Huang FP, Xi G, Keep RF, Hua Y, Nemoianu A, Hoff JT (2002) Brain edema after experimental intracerebral hemorrhage: role of hemoglobin degradation products. *J Neurosurg* 96:287–293
- Nakamura T, Keep RF, Hua Y, Nagao S, Hoff JT, Xi G (2006) Iron-induced oxidative brain injury after experimental intracerebral hemorrhage. *Acta Neurochir Suppl* 96:194–198
- Zhao X, Sun G, Zhang J, Strong R, Song W, Gonzales N, Grotta JC, Aronowski J (2007) Hematoma resolution as a target for intracerebral hemorrhage treatment: role for peroxisome proliferator-activated receptor gamma in microglia/macrophages. *Ann Neurol* 61:352–362. doi:10.1002/ana.21097
- Tan DX, Manchester LC, Terron MP, Flores LJ, Reiter RJ (2007) One molecule, many derivatives: a never-ending interaction of melatonin with reactive oxygen and nitrogen species? *J Pineal Res* 42:28–42. doi:JPI407 [pii] 10.1111/j.1600-079X.2006.00407.x
- Cervantes M, Morali G, Letechipia-Vallejo G (2008) Melatonin and ischemia-reperfusion injury of the brain. *J Pineal Res* 45:1–7. doi:JPI551 [pii] 10.1111/j.1600-079X.2007.00551.x
- Peyrot F, Ducrocq C (2008) Potential role of tryptophan derivatives in stress responses characterized by the generation of reactive oxygen and nitrogen species. *J Pineal Res* 45:235–246. doi:JPI580 [pii] 10.1111/j.1600-079X.2008.00580.x
- Tesoriere L, D'Arpa D, Conti S, Giaccone V, Pintaudi AM, Livrea MA (1999) Melatonin protects human red blood cells from oxidative hemolysis: new insights into the radical-scavenging activity. *J Pineal Res* 27:95–105
- Tesoriere L, Allegra M, D'Arpa D, Butera D, Livrea MA (2001) Reaction of melatonin with hemoglobin-derived oxoferryl radicals and inhibition of the hydroperoxide-induced hemoglobin denaturation in red blood cells. *J Pineal Res* 31:114–119. doi:jpi310204 [pii]
- Hayter CL, Bishop GM, Robinson SR (2004) Pharmacological but not physiological concentrations of melatonin reduce iron-induced neuronal death in rat cerebral cortex. *Neurosci Lett* 362:182–184. doi:10.1016/j.neulet.2004.02.024 S0304394004002083 [pii]
- Lin AM, Ho LT (2000) Melatonin suppresses iron-induced neurodegeneration in rat brain. *Free Radic Biol Med* 28:904–911. doi:S0891-5849(00)00169-6 [pii]
- Hughes RN (2004) The value of spontaneous alternation behavior (SAB) as a test of retention in pharmacological investigations of memory. *Neurosci Biobehav Rev* 28:497–505. doi:S0149-7634(04)00073-9 [pii] 10.1016/j.neubiorev.2004.06.006
- Fathali N, Ostrowski RP, Lekic T, Jadhav V, Tong W, Tang J, Zhang JH (2010) Cyclooxygenase-2 inhibition provides lasting protection against neonatal hypoxic-ischemic brain injury. *Crit Care Med* 38:572–578. doi:10.1097/CCM.0b013e318cb1158

31. Zhou Y, Fathali N, Lekic T, Tang J, Zhang JH (2009) Glibenclamide improves neurological function in neonatal hypoxia-ischemia in rats. *Brain Res* 1270:131–139. doi:S0006-8993(09)00520-4 [pii] 10.1016/j.brainres.2009.03.010
32. Hartman R, Lekic T, Rojas H, Tang J, Zhang JH (2009) Assessing functional outcomes following intracerebral hemorrhage in rats. *Brain Res* 1280:148–157. doi:S0006-8993(09)00957-3 [pii] 10.1016/j.brainres.2009.05.038
33. Andine P, Thordstein M, Kjellmer I, Nordborg C, Thiringer K, Wennberg E, Hagberg H (1990) Evaluation of brain damage in a rat model of neonatal hypoxic-ischemia. *J Neurosci Methods* 35:253–260
34. Morgan PJ, Barrett P, Howell HE, Helliwell R (1994) Melatonin receptors: localization, molecular pharmacology and physiological significance. *Neurochem Int* 24:101–146
35. Musshoff U, Riewenherm D, Berger E, Fauteck JD, Speckmann EJ (2002) Melatonin receptors in rat hippocampus: molecular and functional investigations. *Hippocampus* 12:165–173. doi:10.1002/hipo.1105
36. Wan Q, Man HY, Liu F, Braunton J, Niznik HB, Pang SF, Brown GM, Wang YT (1999) Differential modulation of GABAA receptor function by Mel1a and Mel1b receptors. *Nat Neurosci* 2:401–403. doi:10.1038/8062
37. Hogan MV, El-Sherif Y, Wieraszko A (2001) The modulation of neuronal activity by melatonin: in vitro studies on mouse hippocampal slices. *J Pineal Res* 30:87–96
38. Wang LM, Suthana NA, Chaudhury D, Weaver DR, Colwell CS (2005) Melatonin inhibits hippocampal long-term potentiation. *Eur J Neurosci* 22:2231–2237. doi:EJN4408 [pii] 10.1111/j.1460-9568.2005.04408.x
39. Gorfine T, Zisapel N (2007) Melatonin and the human hippocampus, a time dependent interplay. *J Pineal Res* 43:80–86. doi:JPI446 [pii] 10.1111/j.1600-079X.2007.00446.x
40. Bob P, Fedor-Freybergh P (2008) Melatonin, consciousness, and traumatic stress. *J Pineal Res* 44:341–347. doi:JPI540 [pii] 10.1111/j.1600-079X.2007.00540.x
41. Talaei SA, Sheibani V, Salami M (2009) Light deprivation improves melatonin related suppression of hippocampal plasticity. *Hippocampus*. doi:10.1002/hipo.20650
42. Fukunaga K, Horikawa K, Shibata S, Takeuchi Y, Miyamoto E (2002) Ca₂⁺/calmodulin-dependent protein kinase II-dependent long-term potentiation in the rat suprachiasmatic nucleus and its inhibition by melatonin. *J Neurosci Res* 70:799–807. doi:10.1002/jnr.10400
43. Baydas G, Ozer M, Yasar A, Tuzcu M, Koz ST (2005) Melatonin improves learning and memory performances impaired by hyperhomocysteinemia in rats. *Brain Res* 1046:187–194. doi:S0006-8993(05)00549-4 [pii] 10.1016/j.brainres.2005.04.011
44. Larson J, Jessen RE, Uz T, Arslan AD, Kurtuncu M, Imbesi M, Manev H (2006) Impaired hippocampal long-term potentiation in melatonin MT2 receptor-deficient mice. *Neurosci Lett* 393:23–26. doi:S0304-3940(05)01098-0 [pii] 10.1016/j.neulet.2005.09.040
45. Macleod MR, O'Collins T, Horky LL, Howells DW, Donnan GA (2005) Systematic review and meta-analysis of the efficacy of melatonin in experimental stroke. *J Pineal Res* 38:35–41. doi:JPI172 [pii] 10.1111/j.1600-079X.2004.00172.x

Endothelin Receptor-A (ET_A) Inhibition Fails to Improve Neonatal Hypoxic-Ischemic Brain Injury in Rats

Nikan H. Khatibi, Lillian K. Lee, Yilin Zhou, Wanqiu Chen, William Rolland, Nancy Fathali, Robert Martin, Richard Applegate, Gary Stier, and John H. Zhang

Abstract Cerebral hypoxia-ischemia (HI) is an important cause of mortality and disability in newborns. It is a result of insufficient oxygen and glucose circulation to the brain, initiating long-term cerebral damage and cell death. Emerging evidence suggests that endothelin receptor-A (ET_A) activation can play an important role in mediating brain damage. In this study, we investigated the role of ET_A receptor inhibition using ABT-627 in neonatal HI injured rats. Postnatal day 10 Sprague-Dawley rat pups ($n=91$) were assigned to the following groups: sham ($n=28$), HI (vehicle, $n=32$), and HI with ABT-627 at 3 mg/kg ($n=31$). The Rice-Vannucci model was used to induce ischemia by ligating the right common carotid artery, followed by a 2 h hypoxic episode using 8% oxygen in a 37°C chamber. Postoperative assessment was conducted at 48 h after injury and again at 4 weeks. At the acute time point, investigative markers included cerebral edema, infarction volume, and body weight change. Neurobehavioral testing was measured at 4 weeks post-injury. Our findings indicated that ABT-627 had no effect on the measured parameters. This study suggests that ET_A receptor blockade using ABT-627 post-treatment fails to improve neurological outcomes in neonatal HI injured rats.

Keywords ABT-627 · Endothelin receptor-A (ET_A) · Hypoxic-ischemic (HI) · Endothelins · Brain injury

Introduction

Cerebral hypoxia-ischemia (HI) is a fatal, life-threatening event during the perinatal period responsible for a large number of mortalities and disabilities in newborns [1, 2]. With a reported incidence of 2–9 per 1,000 births, HI can be caused by a number of events, including a reduction in uterine circulation from uterine contractions, umbilical cord compression, and placental abruption to name a few [3]. The concern with HI is the mounting inflammatory response produced by a reduction in cerebral blood flow. To date, adequate therapeutic interventions aimed at treating the short- and long-term consequences of HI are limited. Although multiple studies have shown mild improvements with various treatment modalities, including erythropoietin and hypothermia, there continue to be significant limitations in their ability to improve neurobehavioral deficits or reduce mortality [4]. Therefore, development of a new treatment intervention that can reduce a wide spectrum of HI-induced consequences is highly desirable.

Endothelins (ET) are vasomotor peptides produced primarily in the endothelium that are responsible for maintaining vascular homeostasis [5, 6]. In order to carry out downstream effects, ETs must bind to one of two distinct receptor subtypes, either ET_A or ET_B. Within the brain, ETs and their receptors are localized to neurons, glial cells, and smooth muscle cells where they modulate neuronal function and regulate cerebral blood flow [7]. Specifically, activation of ET_A receptors, which are found predominantly in vascular smooth muscle cells, may lead to blood vessel vasoconstriction and propagation of ischemic damage. In an adult model of focal ischemia, ET_A receptor inhibition improved brain edema formation, decreased infarction volume, attenuated BBB disruption, and improved overall mortality [7].

N.H. Khatibi, L.K. Lee, Y. Zhou, R. Martin, R. Applegate, and G. Stier
Department of Anesthesiology, Loma Linda Medical Center, Loma Linda, CA, USA

W. Chen, W. Rolland, and N. Fathali
Department of Physiology and Pharmacology, Loma Linda University, School of Medicine, Loma Linda, CA, USA

J.H. Zhang (✉)
Department of Anesthesiology, Loma Linda Medical Center, Loma Linda, CA, USA and
Department of Physiology and Pharmacology, Loma Linda University, School of Medicine, Loma Linda, CA, USA and
Department of Neurosurgery, Loma Linda Medical Center, Loma Linda, CA, USA and
Department of Neurosurgery, Loma Linda Medical Center, 11234 Anderson Street, Room 2562B, Loma Linda, CA 9235, USA
e-mail: johnzhang3910@yahoo.com

Therefore, in this study, we investigated the role of ET_A receptor inhibition on both short- and long-term outcomes in the HI-injured neonatal rat, specifically, determining the role of ABT627, a selective ET_A receptor competitive antagonist, on edema formation, infarction volume, body weight change, and neurobehavioral deficits.

Materials and Methods

Animal Groups. All procedures for this study were approved by the Animal Care and Use Committee at Loma Linda University and complied with the NIH Guide for the Care and Use of Laboratory Animals. Ninety-one postnatal day 10 pups were randomly divided into the following three groups: sham surgery ($n=28$), vehicle ($n=32$), and HI + 3 mg/kg ABT627 post-treatment ($n=31$).

Operative Procedure. The surgery was conducted as previously described using the Rice-Vannucci model [8]. Briefly, pups were placed on a surgical table maintained at 37°C and anesthetized by inhalation with isoflurane (3% in mixed air and oxygen). HI groups had the right common carotid artery permanently ligated. After 1 h of recovery, pups were placed in a glass jar submerged in a water bath maintained at 37°C and perfused with 8% oxygen for 2 h. At 48 h, pups were euthanized and decapitated.

Treatment Method. Treated pups were given a single IP injection of 3 mg/kg ABT627 immediately after HI. Vehicle pups followed the same injection regimen, but were given saline solution.

Brain Water Content. Brain water content was measured as previously described [9]. Briefly, pups were sacrificed at 48 h post-HI, and brains were immediately removed and divided into three parts: ipsilateral frontal, contralateral frontal, and cerebellum. The cerebellum was used as an internal control for brain water content. Tissue samples were then weighed on an electronic analytical balance (APX-60, Denver Instrument; Arvada, CO) to the nearest 0.1 mg to obtain the wet weight (WW). The tissue was then dried at 105°C for 48 h to determine the dry weight (DW). The percent brain water content was calculated as $[(WW - DW)/WW] \times 100$.

Infarct Volume. 2, 3, 5-Triphenyltetrazolium chloride monohydrate (TTC) staining was used to measure infarct volume as previously described [10]. At 48 h post-HI, brains were removed and sectioned into 2-mm slices, then immersed into 2% TTC solution at 37°C for 5 min, followed by 10% formaldehyde. The infarct volume was traced and analyzed by Image-J software.

Assessment of Neurobehavioral Deficits. Four weeks after HI and prior to sacrifice, rats were tested for spontaneous alternation on a T-shaped maze as previously described [11].

Rats were placed at the stem of the T-maze [measured 40 (stem) \times 46 (arm) \times 10 (width) cm] and allowed to freely explore the two arms of the maze throughout a ten-trial continuous alternation session. Once an arm was chosen, the rat was placed in the stem of the maze again, and the trial was repeated. Absolute numbers of left and right choices were recorded, and the spontaneous alternation rate was calculated as the ratio of the alternating choices to the total number of the choices.

In the foot-fault test, rats were placed on a horizontal grid floor (wire diameter 0.4 cm) for 2 min. Foot fault was defined as when the animal inaccurately placed a fore- or hindlimb, and it fell through one of the openings in the grid. The numbers of foot faults for each animal were recorded. Previous study has shown that intact animals place their paws on the grid frame or foot holds while moving around on the grid [12]. Limb misplacements in intact animals were infrequent.

Finally, for the wire grip tests [13], rats were placed on a metal wire (45 cm long) suspended 45 cm above a foam pad and were allowed to traverse the wire for 40 s. The latency that a rat remained on the wire within a 40 s interval was measured. The test was repeated two times and the average of the two values was recorded.

Statistics. Quantitative data were expressed as the mean \pm SEM. One-way ANOVA and Tukey test were used to determine significance in differences between the means. Neurological scores were evaluated using the Dunn method. A p -value < 0.05 was considered statistically significant.

Results

ET_A receptor inhibition has no effect on brain edema formation. Brain water content was measured 48 h post-HI (Fig. 1a, b). The results showed that vehicle mice presented with significantly worse brain edema compared to sham mice. After post-treatment with ABT627, brain edema failed to reduce significantly in both cerebral hemispheres compared to the vehicle group.

ET_A receptor inhibition did not improve body weight after HI. Prior to decapitation at 48 h post-HI, body weight was measured and compared to initial body weight prior to surgery (Fig. 1c). Compared to sham groups, vehicle groups showed a marked reduction in body weight gain after 48 h. Unfortunately, the decrease in body weight did not improve with ABT627 treatment.

Infarction volume failed to improve with ET_A receptor inhibition. Infarction volume was measured by TTC staining at 4 weeks post-HI (Fig. 2). The results indicate there was a significant increase in infarct volume between sham and vehicle rat pups. Treatment with ABT627, however, failed to reverse or attenuate the volume of infarction.

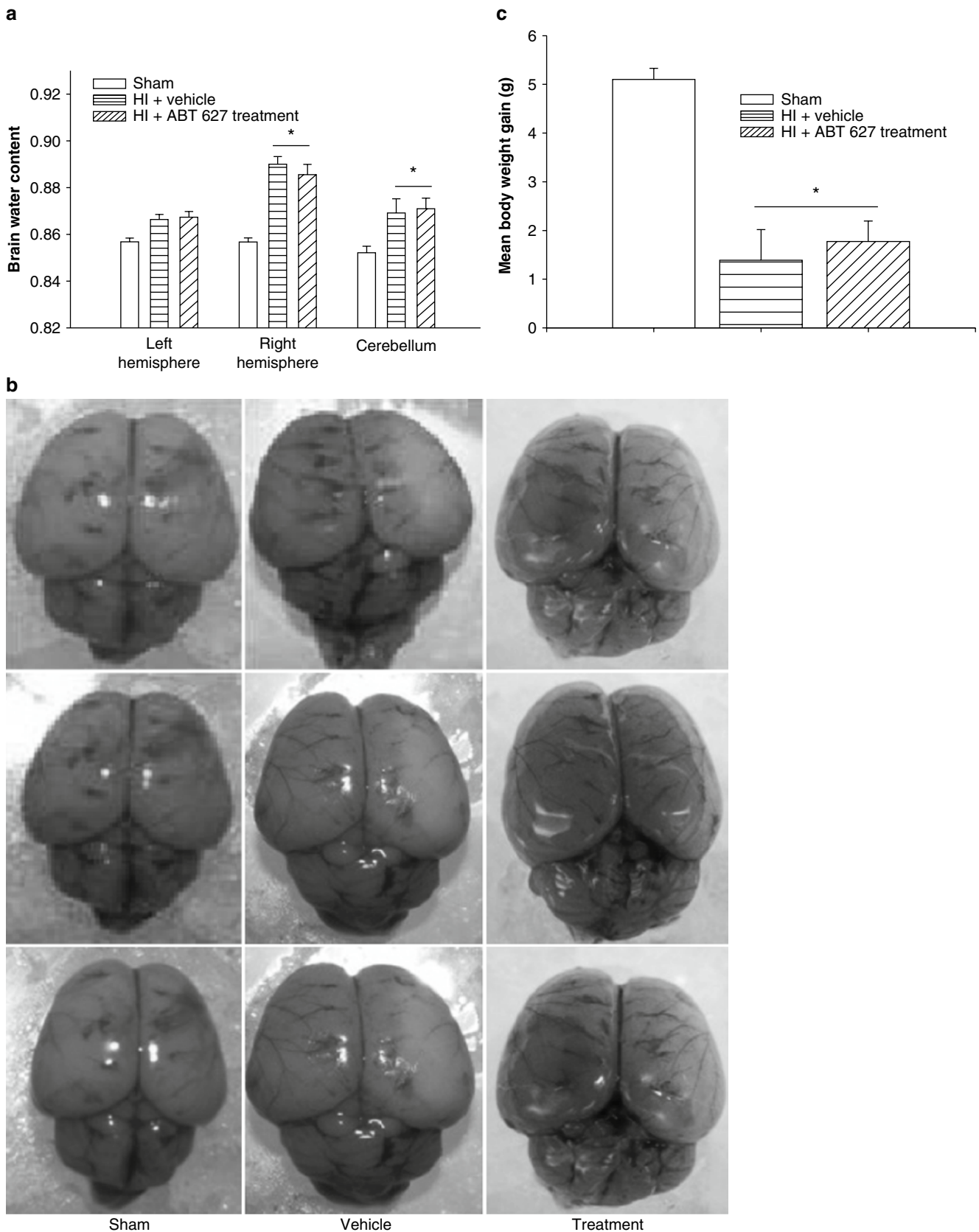
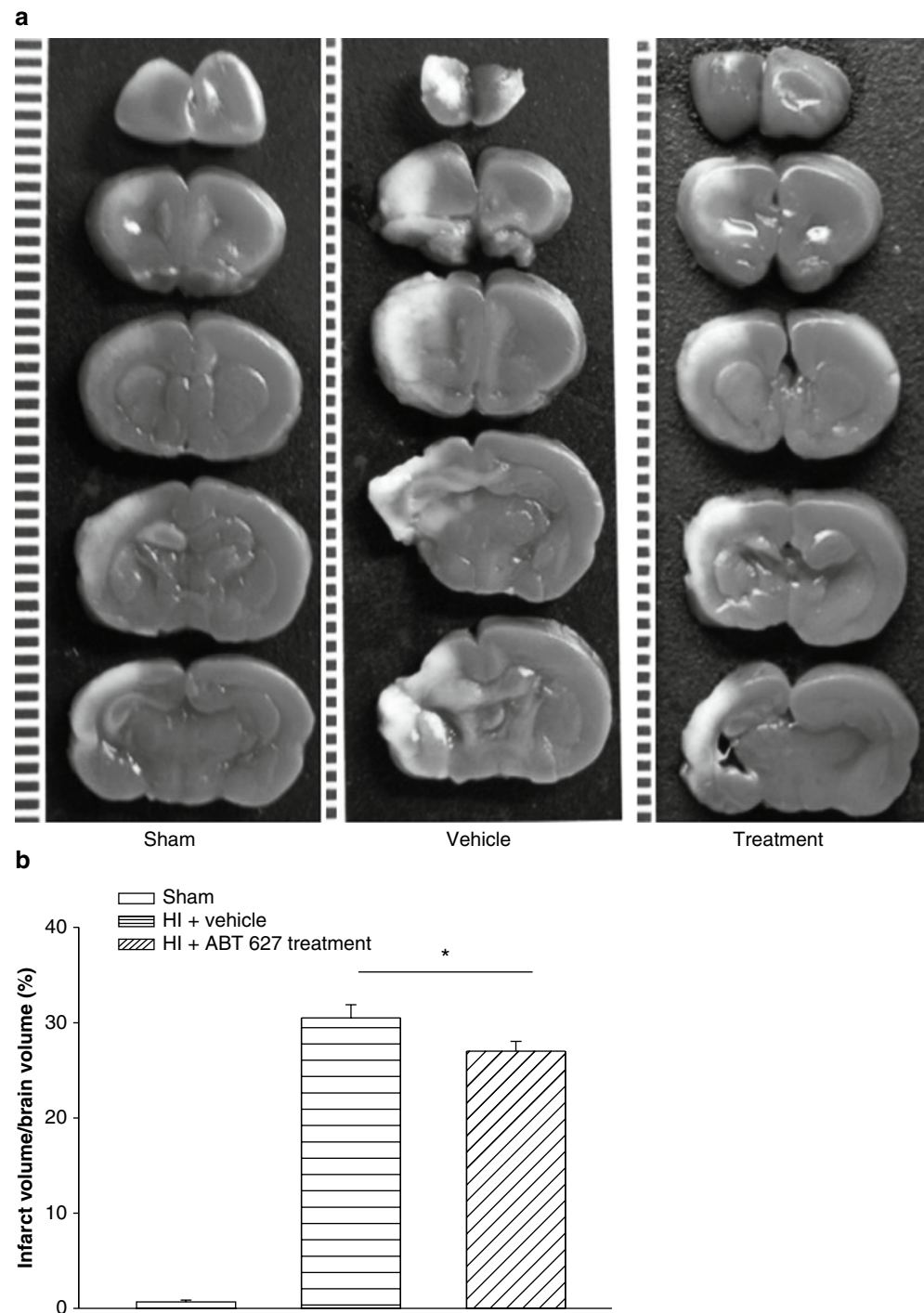


Fig. 1 Forty-eight hour edema and somatic growth outcome. **(a)** Treatment failed to reduce brain edema at 48 h post-injury. **(b)** Gross brains collected at 48 h post-injury. **(c)** Mean body weight failed to improve with treatment at 48 h post-injury; *significant difference vs. sham ($p < 0.05$)

Fig. 2 Infarction volume. (a) TTC staining showing a significant difference in infarction volume between vehicle and sham animals. Treatment with ABT627 did not show any improvement. (b) Percent infarction increased substantially in vehicle rats, but failed to improve with treatment. *Significant difference vs. sham ($p < 0.05$)



Neurobehavioral deficits did not improve with ET_A receptor inhibition. Neurobehavioral functioning was conducted at 4 weeks post-HI (Fig. 3). Three different means of testing for neurobehavioral deficits were performed, including the foot fault test, T-maze test, and wire grip test. The results showed no significant improvement in behavior with treatment.

Discussion

Neonatal cerebral HI is a fatal perinatal event that currently has no effective treatment option. Even if infants survive the initial attack, the inflammatory response that occurs as a result of cerebral hypoperfusion triggers a series of events leading to cerebral edema formation, neuronal cell death,

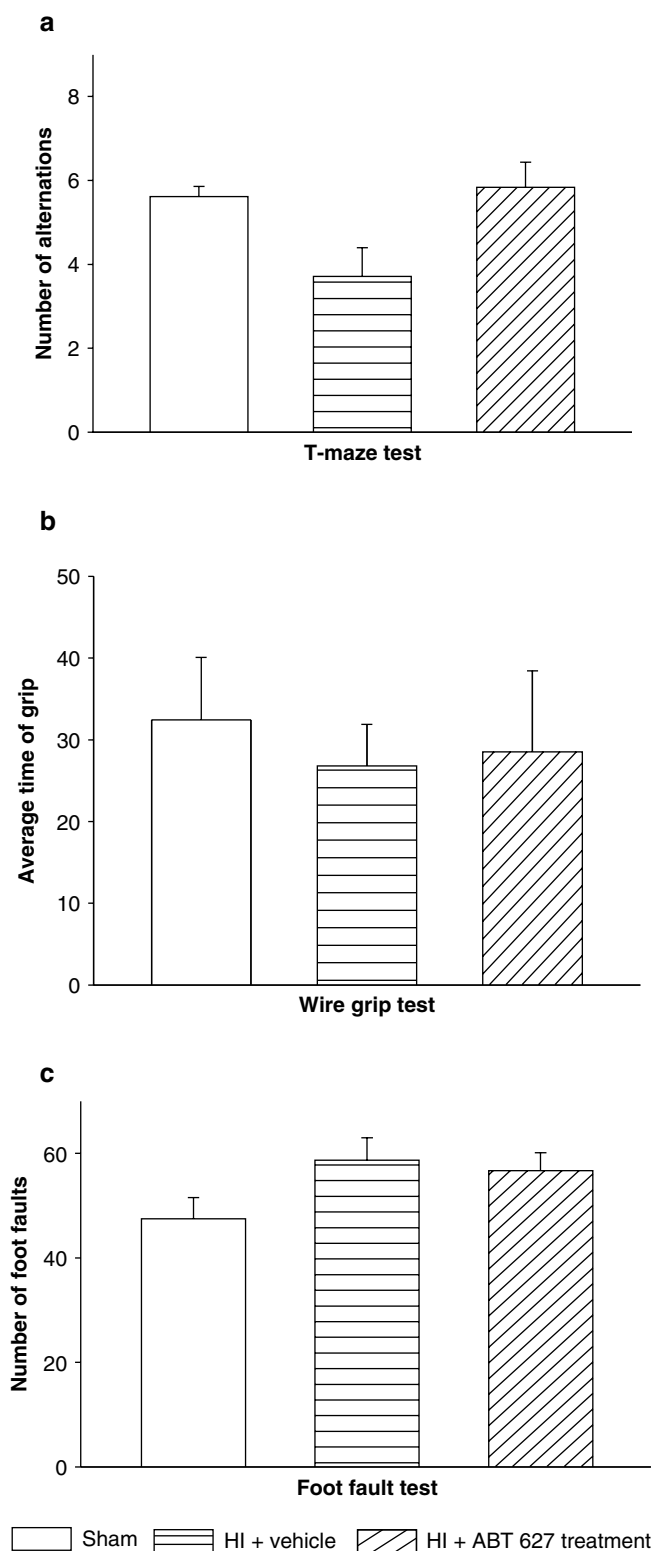


Fig. 3 Neurobehavioral testing. There was no significant difference among the three groups after neurobehavioral testing

somatic growth retardation, and motor behavioral problems [8]. In the present study, we investigated whether ET_A receptor inhibition with ABT627, a selective ET_A receptor competitive

antagonist, would reduce brain edema formation and infarction volume while improving weight gain at 48 h post-injury. Additionally, we wanted to determine whether post-treatment could attenuate the long-term neurobehavioral deficits measured at 4 weeks post-injury. In this study, we found that post-treatment with ABT627 had no effect on brain injury outcomes in our neonatal HI rat population at both short- and long-term time intervals.

It was originally hypothesized that rats subjected to HI brain injury would develop significant brain edema and infarction, and that ABT627 post-treatment would reduce these consequences by blocking the harmful effects of endothelins. The data collected, however, do not support this hypothesis. The increased brain water content levels found 48 h after HI failed to decrease with drug administration. Furthermore, there was no difference in infarction volume between the treatment and vehicle groups. Normally, the devastating consequences following an HI are a result of hypoperfusion and subsequent physiological changes [14]. One of the mechanisms responsible for edema formation and cell death includes activation of a number of vasoactive factors during hypoperfusion, including endothelins [15]. A potent vasoconstrictor with mitogenic properties, endothelins have been found to be increased in patients with ischemic stroke. Stanimirovic et al. [16] showed that endothelins enhance the permeability of the BBB via ET_A receptor activation by increasing the expression of intercellular adhesion molecule-1 and interleukin-8 on brain capillary endothelial cells. Additionally, by reducing the blood supply to the brain through vasoconstriction, endothelins are propagating the ischemic damage and increasing the volume of infarction. Thus, we had hoped that inhibition of the endothelin receptor could reduce the damages following injury – however, this was not the case.

Assessment of neurobehavior was conducted by three tests: T-maze, wire grip, and the foot fault test. The T-maze spontaneous alternation task has been shown to test exploratory behavior and working memory by hippocampal dysfunction [17, 18], while the foot-fault and wire grip tests look more at motor and strength capabilities [8]. In our study, we failed to show an improvement in neurobehavioral deficits with post-treatment. This is contrary to previous studies in various models that have shown an improvement in neurobehavior after ET_A receptor inhibition [7]. The lack of significant improvement in our study was likely attributed to the failure in improvement of brain edema and infarction volume after injury.

The reason why ABT627 post-treatment failed to work is unclear. The limited dosing amount, however, may be an explanation. A one-time drug injection after injury may not be sufficient to elicit a protective response. It is possible that multiple treatments are needed in order to combat the early and delayed phases of brain injury. Additionally, previous

authors have found that excitotoxicity plays a key role in brain edema production and neuronal cell death, which was not addressed with our choice of therapy. Studies have shown that with a decrease in oxidative phosphorylation and subsequent reduction in available energy production, membrane depolarization results in the release of excitatory amino acids, enhancing the neuronal destructive process [19].

Conclusion

These results suggest that inhibition with ABT627, a selective ET_A receptor inhibitor, does not provide major benefits for brain integrity, neurobehavioral deficits, and body weight after neonatal HI. Collectively, these results establish the need for further studies investigating possible alternative methods of targeting endothelins.

Acknowledgement This study is partially supported by NIH NS053407 to J.H. Zhang.

Conflict of interest statement We declare that we have no conflict of interest.

References

- Gomella TL (1999) Neonatology: management, procedures, on-call problems, diseases, and drugs, 4th edn. Appleton & Lange, Stamford
- Vannucci RC (1990) Experimental biology of cerebral hypoxia-ischemia: relation to perinatal brain damage. *Pediatr Res* 27:317–326
- O'Brien JR, Usher RH, Maughan GB (1966) Causes of birth asphyxia and trauma. *Can Med Assoc J* 94(21):1077–1085
- Zhu C, Kang W, Xu F, Cheng X, Zhang Z (2009) Erythropoietin improved neurologic outcomes in newborns with hypoxic-ischemic encephalopathy. *Pediatrics* 124:218–226
- Takahashi K, Ghatei M, Jones PM, Murphy JK, Lam HC (1990) Endothelin in human brain and pituitary gland; presence of immunoreactive endothelin, endothelin mRNA and endothelin receptors. *J Clin Endocrinol Metab* 72:693–699
- Yoshimoto S, Ishizaki Y, Kurihara H, Sasaki T, Yoshizumi M (1990) Cerebral microvessel endothelium is producing endothelin. *Brain Res* 508:283–285
- Matsuo Y, Mihara S, Ninomiya M (2001) Protective effect of endothelin type A receptor antagonist on brain edema and injury after transient middle cerebral artery occlusion in rats. *Stroke* 32:2143–2148
- Fathali N, Ostrowski RP, Lekic T, Jadhav V, Tong W (2010) Cyclooxygenase-2 inhibition provides lasting protection against neonatal hypoxic-ischemic brain injury. *Crit Care Med* 38:572–578
- Chen W, Jadhav V, Tang J, Zhang JH (2008) HIF-1 alpha inhibition ameliorates neonatal brain injury in a rat pup hypoxic-ischemic model. *Neurobiol Dis* 31:433–441
- Yin D, Zhou C, Kusaka I, Calvert JW, Parent AD, Nanda A, Zhang JH (2003) Inhibition of apoptosis by hyperbaric oxygen in a rat focal cerebral ischemic model. *J Cereb Blood Flow Metab* 23:855–864
- Matchett GA, Calinisan JB, Matchett GC, Martin RD, Zhang JH (2007) The effect of granulocyte-colony stimulating factor in global cerebral ischemia in rats. *Brain Res* 1136:200–207
- Barth TM, Stanfield BB (1990) The recovery of forelimb-placing behavior in rats with neonatal unilateral cortical damage involves the remaining hemisphere. *J Neurosci* 10:3449–3459
- Berpohl D, You Z, Korsmeyer SJ, Moskowitz MA, Whalen MJ (2006) Traumatic brain injury in mice deficient in Bid: effects on histopathology and functional outcome. *J Cereb Blood Flow Metab* 26:625–633
- Leonardo CC, Pennypacker KR (2009) Neuroinflammation and MMPs: potential therapeutic targets in neonatal hypoxic-ischemic injury. *J Neuroinflammation* 6:13
- Lo AC, Chen AY, Hung VK, Yaw LP, Fung M (2005) Endothelin-1 overexpression leads to further water accumulation and brain edema after middle cerebral artery occlusion via aquaporin 4 expression in astrocytic end-feet. *J Cereb Blood Flow Metab* 25:998–1011
- Stainirovic DB, Bertrand N, McCarron R, Uematsu S (1994) Arachidonic acid release and permeability changes induced by endothelins in human cerebrovascular endothelium. *Acta Neurochir Suppl* 60:71–75
- Gerlai R (2001) Behavioral tests of hippocampal function: simple paradigms complex problems. *Behav Brain Res* 125:269–277
- Ishibashi S, Kuroiwa T, Endo S, Okeda R, Mizusawa H (2003) Neurological dysfunctions versus regional infarction volume after focal ischemia in Mongolian gerbils. *Stroke* 34:1501–1506
- Calvert JW, Zhang JH (2007) Oxygen treatment restores energy status following experimental neonatal hypoxia-ischemia. *Pediatr Crit Care* 8:165–173

FTY720 is Neuroprotective and Improves Functional Outcomes After Intracerebral Hemorrhage in Mice

William B. Rolland II, Anatol Manaenko, Tim Lekic, Yu Hasegawa, Robert Ostrowski, Jiping Tang, and John H. Zhang

Abstract Intracerebral hemorrhage (ICH) accounts for 20% of all strokes and is the most devastating form across all stroke types. Lymphocytes have been shown to potentiate cerebral inflammation and brain injury after stroke. FTY720 (Fingolimod) is an immune-modulating drug that prevents the egress of peripheral lymphocytes from peripheral stores. We hypothesized that FTY720 would reduce peripheral circulating lymphocytes, resulting in reduced brain injury and improved functional outcomes. CD-1 mice were anesthetized and then injected with collagenase into the right basal ganglia. Animals were divided into three groups: sham, ICH+ Vehicle, and ICH+FTY720, by the intra-peritoneal route at 1 h after ICH induction. Brain water content was measured at 24 and 72 h. Neurobehavioral tests included corner test, forelimb use asymmetry, paw placement, wire-hang test, beam balance test, and a Neuroscore. FTY720 significantly reduced brain edema and improved neurological function at all time points tested. Lymphocyte modulation with FTY720 is an effective neuroprotective strategy to reduce brain injury and promote functional recovery after ICH.

Keywords Intracerebral hemorrhage · FTY720 · Fingolimod · Lymphocytes · Neuroprotection · Brain edema · Neurological function

W.B. Rolland II, A. Manaenko, T. Lekic, Y. Hasegawa, R. Ostrowski, and J. Tang

Department of Physiology, Loma Linda University,
School of Medicine, Loma Linda, CA, USA

J.H. Zhang (✉)

Department of Physiology, Loma Linda University,
School of Medicine, Loma Linda, CA, USA and
Department of Neurosurgery, Loma Linda University,
School of Medicine, Loma Linda, CA, USA and
Department of Physiology and Pharmacology,
Loma Linda University, School of Medicine,
Risley Hall, Room 219, Loma Linda, CA 92350, USA and
Department of Anesthesiology, Loma Linda University,
School of Medicine, Loma Linda, CA, USA
e-mail: jhzhang@llu.edu

Introduction

Intracerebral hemorrhage (ICH) is a spontaneous bleeding event in the brain for which there are no effective therapies. ICH accounts for about 20% of all strokes and affects 1 in 6,000 people each year [1]. ICH results in a higher mortality rate than ischemic stroke, and 40–50% of patients in the United States die within the first 30 days [2].

The inflammatory response after ICH is a highly complex process that includes acute and delayed events requiring local and peripheral cellular cross-talk. Significant orchestrators of this inflammatory process are blood-derived immune cells, trafficking from the periphery into the brain parenchyma [3]. Monocyte and neutrophil infiltration, along with microglia and macrophage activation, occur in and around the hematoma within hours after ictus and peak within a few days [3, 4], leading to the production of proinflammatory mediators, such as TNF- α , IL-1 β , and proteolytic enzymes, such as MMP-9. While the myeloid branch of the immune system includes the above cell types involved in inflammation, lymphoid cells also interact with resident and infiltrated cells in the CNS, potentiating the inflammatory response. T-cells have been shown to play a major role in the numerous neurological diseases, such as Parkinson's disease, Alzheimer's disease, and multiple sclerosis [5–7], as well as the deleterious events following stroke [8]. It has been demonstrated that T-cells are significantly increased in the brain as early as 24 h after stroke [9]. These lymphocytes are responsible for further driving the local inflammatory reaction, leading to increased blood-brain barrier (BBB) permeability, edema formation, cell death, and neurological deficits following stroke.

FTY720 (Fingolimod), a sphingosine-1-phosphate(S1P) analog that is an agonist for S1P receptors (S1P1, 3, 4, and 5), has a half life of 20 h [10, 11]. FTY720's immunosuppressive activity results from inhibition of S1P1 receptor-dependent lymphocyte egress mediated by downregulating S1P1 receptor on T-cells [12]. Therefore, a single administration of FTY720 causes peripheral lymphopenia. It has

been shown to be effective in several phase II clinical trials at reducing the incidence of relapsing/remitting MS [13, 14] and for renal transplantation [15]. In a recent study in our laboratory, FTY720 administration was shown to be neuroprotective following 2 h middle cerebral artery occlusion in rats [16].

In the present study, we hypothesized that FTY720 administration following ICH would reduce brain edema and improve neurological function in mice. To test this hypothesis, we administered FTY720 to reduce circulating peripheral lymphocytes, and then evaluated brain edema and neurological deficits 24 and 72 h following collagenase-induced intracerebral hemorrhage.

Materials and Methods

Experimental Animal Preparation

All procedures for this study were approved by the Animal Care and Use Committee at Loma Linda University, and were in compliance with the NIH *Guide for the Care and Use of Laboratory Animals*.

Eight-week-old CD-1 mice were used in our study and were housed on a 12:12 light/dark cycle in a pathogen-free facility with controlled temperature and humidity, and were given food and water ad libitum.

Experimental Protocol

In total, 30 mice were used in this study. Mice were divided into three groups: sham (needle insertion), ICH+vehicle (ICH), and ICH+FTY720 treatment (1 mg/kg, i.p.). FTY720 was dissolved in 2% DMSO and given 1 h after ICH induction. Both sham and vehicle animals received the same volume of i.p. 2% DMSO in saline. All animals were neurologically tested, and brains were harvested 24 and 72 h after ICH induction. Evaluation of neurological deficits was carried out by a blinded investigator. Brain samples were collected for measurement of brain edema.

Intracerebral Hemorrhage Model in Mice

ICH was induced by intrastriatal collagenase injection as described by Rosenberg et al. [17, 18]. Briefly, mice were anesthetized with ketamine (100 mg/kg, i.p.) and xylazine (10 mg/kg, i.p.) (2:1 v/v), and positioned prone in a stereotactic head frame (Kopf Instruments, Tujunga, CA). A bore-

hole (1 mm) was drilled near the right coronal suture 1.7 mm lateral to the midline. A 27-gauge needle was inserted stereotactically into the right basal ganglia according to the coordinates: 0.9 mm posterior to the bregma, 1.7 mm lateral to the midline, and 3.7 mm below the surface of the calvaria. Clostridal collagenase (VII-S, Sigma; 0.1 U in 0.5 μ L of saline) was infused into the brain over 2 min at a rate of 0.25 μ L/min with a microinfusion pump (Harvard Apparatus, Holliston, MA). Sham-operated mice were subjected to needle insertion only. The needle was left in place for an additional 10 min after injection to prevent possible leakage or backflow of the collagenase solution. After removing the needle, the bore hole was closed with bone wax, the incision closed with sutures, and mice were allowed to recover. To avoid postsurgical dehydration, 0.5 ml of normal saline was given subcutaneously to each mouse after surgery.

Testing Neurological Function

All neurological tests were performed during the light cycle. Neurological deficits were evaluated by using a modified Garcia test [19], beam balance and wire-hanging tests [20]. In the modified Garcia test, seven items, including spontaneous activity, side stroke, vibrissae touch, limb symmetry, lateral turning, forelimb walking, and climbing were tested (the total possible neurological score was 21 for a healthy mouse). For both the modified beam balance and wire-hanging test, the total possible score for healthy mice was five. The behavior testing was conducted at 24 and 72 h after ICH induction by a blinded investigator.

Measurement of Brain Edema

Brain water content was measured as previously described [18]. Briefly, mice were decapitated under deep anesthesia. Brains were immediately removed and cut into 4-mm sections. Each section was divided into four parts: ipsilateral and contralateral basal ganglia, ipsilateral and contralateral cortex. The cerebellum was used as an internal control. Tissue samples were weighed to obtain the wet weight (WW) and then dried at 100°C for 24 h to determine the dry weight (DW). Brain water content (%) was calculated as $[(WW - DW)/WW] \times 100$.

Statistical Analysis

All the data were expressed as Mean \pm SEM. Statistical differences were analyzed by one way-ANOVA Tukey test or

Dunn's test on rank. A P value of <0.05 was considered statistically significant.

Results

Brain Water Content

Brain water content was tested at 24 and 72 h after ICH (Fig. 1). There was a very significant increase in brain water content for the ICH+Vehicle group at both 24 and 72 h, respectively, in the ipsilateral basal ganglia (ICH+Vehicle[24h], 83.62 ± 0.48 & ICH+Vehicle[72 h], 82.79 ± 0.41 vs. sham, 78.27 ± 0.24 , $P < 0.05$) and cortex (ICH+Vehicle[24 h], 80.46 ± 0.36 & ICH+Vehicle[72 h], 80.48 ± 0.34 vs. sham, 78.96 ± 0.22 , $P < 0.05$) compared to the sham group. Brain edema was also significantly increased in the contralateral basal ganglia for ICH+Vehicle at 24 and 72 h (ICH+Vehicle[24 h], 81.12 ± 0.20 and ICH+Vehicle[72 h], 80.34 ± 0.13 vs. Sham, 78.25 ± 0.11 , $P < 0.05$) compared to the sham group. FTY720 treatment (1 mg/kg) significantly reduced brain edema in the ipsilateral basal ganglia at 24 and 72 h (ICH+FTY720[24 h], 82.16 ± 0.28 vs. ICH+Vehicle [24 h], 83.62 ± 0.48 and ICH+FTY720[72 h], 81.28 ± 0.33 vs. ICH+Vehicle[72 h], 82.79 ± 0.41 , $P < 0.05$) and in the contralateral basal ganglia at 72 h after ICH (ICH+FTY720 [72 h], 79.70 ± 0.15 vs. ICH+Vehicle[72 h], 80.34 ± 0.13). FTY720 treatment also significantly reduced brain edema in the ipsilateral cortex (ICH+FTY720[72 h], 79.59 ± 0.17 vs.

ICH+Vehicle[72 h], 80.48 ± 0.34 , $P < 0.05$) and contralateral cortex at 72 h after ICH (ICH+FTY720[72 h], 78.89 ± 0.09 vs. ICH+Vehicle[72 h], $79. \pm 0.11$).

Neurobehavioral Testing and Neurological Function

Neurobehavioral evaluations were completed at 24 and 72 h after ICH induction by using the modified Garcia test, wire-hanging test, and beam balance test (Fig. 2a–c). At 24 and 72 h after ICH, the ICH+Vehicle group demonstrated significant deficits compared to the sham group for the modified Garcia test, wire-hanging test, and beam walking test ($P < 0.05$). After FTY720 treatment, the Garcia neurological score was significantly improved at both time points ($P < 0.05$). FTY720 treatment significantly improved performance on the beam balance and wire-hanging tests at 24 h after ICH ($P < 0.05$) and showed a trend to improve performance at 72 h after ICH; however, we did not find significant results.

Discussion

Hemorrhagic stroke is the most fatal stroke type, and currently there is no effective treatment. The extravasated blood and blood components trigger a complex series of events leading to the production of inflammatory mediators and the infiltration

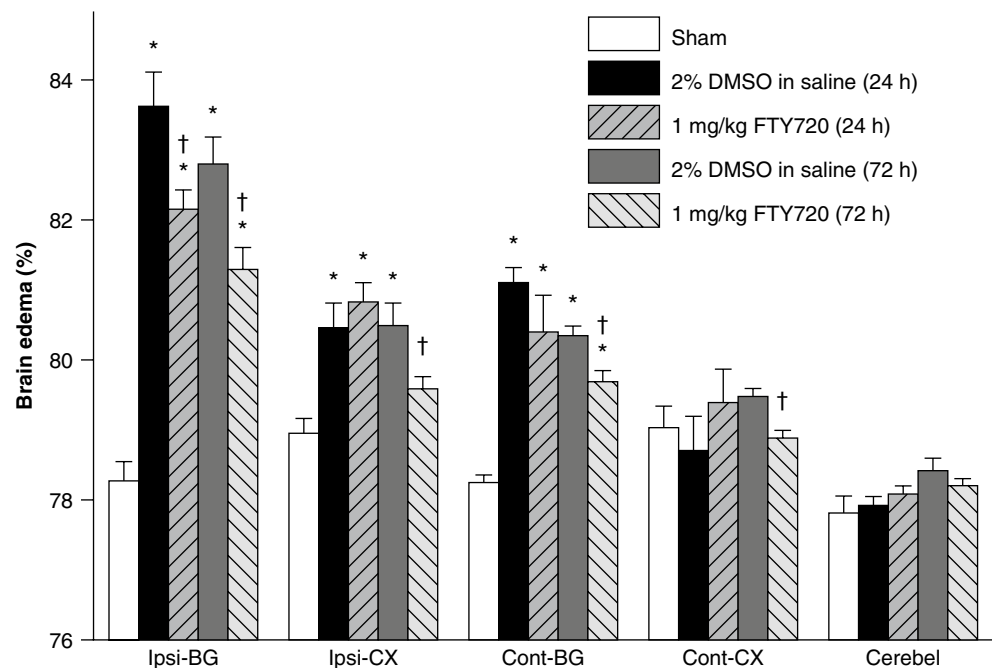


Fig. 1 FTY720 treatment improved brain edema at 24 and 72 h after ICH. Cont-CX, contralateral cortex; Ipsi-CX, ipsilateral cortex; Cont-BG, contralateral basal ganglia; Ipsi-BG, ipsilateral basal ganglia; Cerebel, cerebellum. Values are expressed as mean \pm SEM. * $P < 0.01$ vs. Sham; † $P < 0.05$ vs. Vehicle

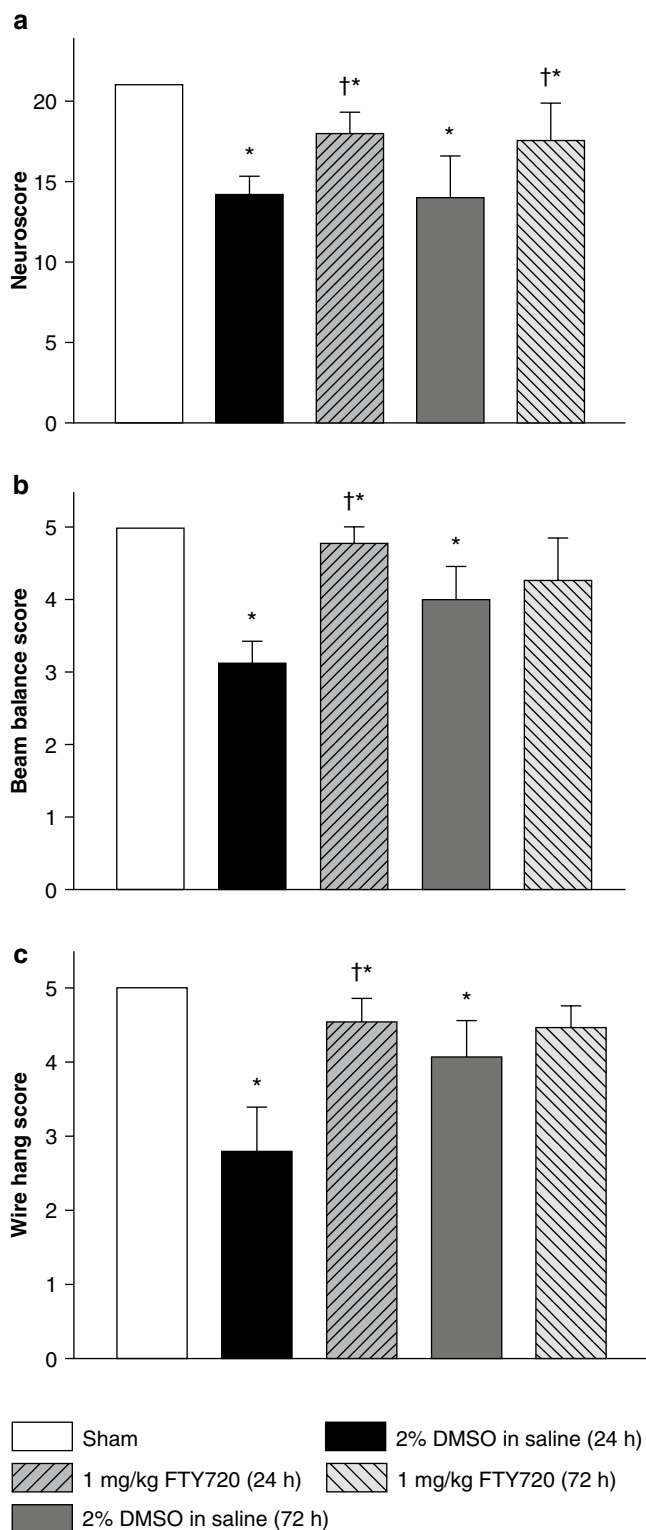


Fig. 2 FTY720 treatment improved neurological function at 24 and 72 h after ICH. (a) Modified Garcia test; (b) wire-hanging test; (c) beam balance test. Values are expressed as mean \pm SEM. * $P < 0.01$ vs. Sham; † $P < 0.05$ vs. Vehicle

of a wide variety of immune cells, resulting in edema formation, cell death, and permanent neurological deficits. The present study used a clinically relevant immunosuppressant that is

already in clinical trials and has been submitted for regulatory approval in the US and EU for oral administration to treat MS patients. We found that administration of FTY720 reduced brain edema, improved neurological function, and offered neuroprotection after ICH. This is the first study to demonstrate the neuroprotective effect of FTY720 in a mouse intracerebral hemorrhage model.

Although T-cells are not the largest population of immune cells in the brain after stroke, their presence is certainly important. Inhibition of T-cell activation in rats with FK-506 and knockout mice for CD18 (a lymphocyte-associated adhesion molecule) leads to decreased cell death and improved functional outcome in the days and weeks following ICH [21, 22]. FTY720 binds to four of the five known S1P receptors and has been repeatedly shown to induce peripheral lymphopenia when administered at doses around 0.1 mg/kg [10, 23]. Our dosage of 1 mg/kg can be safely assumed to be causing the same effect in mice, which will reduce the amount of T-cells available for trafficking into the brain after ICH. This reduction in T-cells available for trafficking in effect reduces the driving force behind inflammation, leading to reduced brain edema and neurological deficits.

FTY720 has been shown to have an endothelial barrier enhancement capacity by inhibiting VEGF induced vascular permeability in vitro and in vivo [24]. Moreover, FTY720 has been shown to induce the translocation of vascular endothelial cadherin and β -catenin, via S1P1 or S1P3 activation, to the focal contacts between endothelial cells, promoting adherens junction assembly [25]. Lastly, it has been demonstrated that activation of S1P1 with FTY720 induces anti-apoptotic signaling, rescuing cells from the brink of death. In a recent study in our laboratory, FTY720 treatment was shown to increase the levels of phospho-Akt, phospho-Erk, and Bcl-2 as well as reduced cleaved caspase-3 after middle cerebral artery occlusion in rats.

In summary, FTY720 post-treatment reduced the brain edema and improved neurological function after intracerebral hemorrhage in mice. This result may be explained by its anti-inflammatory effect.

Acknowledgement This study is partially supported by NIH NS053407 to J.H. Zhang and NS060936 to J. Tang.

Conflict of interest statement We declare that we have no conflict of interest.

References

- Dennis MS, Burn JP, Sandercock PA, Bamford JM, Wade DT, Warlow CP (1993) Long-term survival after first-ever stroke: the Oxfordshire Community Stroke Project. *Stroke* 24:796–800
- James ML, Warner DS, Laskowitz DT (2008) Preclinical models of intracerebral hemorrhage: a translational perspective. *Neurocrit Care* 9:139–152

3. Wang J, Dore S (2007) Inflammation after intracerebral hemorrhage. *J Cereb Blood Flow Metab* 27:894–908
4. Hickenbottom SL, Grotta JC, Strong R, Denner LA, Aronowski J (1999) Nuclear factor-kappaB and cell death after experimental intracerebral hemorrhage in rats. *Stroke* 30:2472–2477, discussion 2477–2478
5. Brochard V, Combadiere B, Prigent A, Laouar Y, Perrin A, Beray-Berthet V, Bonduelle O, Alvarez-Fischer D, Callebert J, Launay JM, Duyckaerts C, Flavell RA, Hirsch EC, Hunot S (2009) Infiltration of CD4+ lymphocytes into the brain contributes to neurodegeneration in a mouse model of Parkinson disease. *J Clin Invest* 119:182–192
6. Smith D (2009) Interferon-beta therapy for multiple sclerosis—is the injection site the relevant action site? *J Neuroimmunol* 215:117–121
7. Togo T, Akiyama H, Iseki E, Kondo H, Ikeda K, Kato M, Oda T, Tsuchiya K, Kosaka K (2002) Occurrence of T cells in the brain of Alzheimer's disease and other neurological diseases. *J Neuroimmunol* 124:83–92
8. Shichita T, Sugiyama Y, Ooboshi H, Sugimori H, Nakagawa R, Takada I, Iwaki T, Okada Y, Iida M, Cua DJ, Iwakura Y, Yoshimura A (2009) Pivotal role of cerebral interleukin-17-producing gammadeltaT cells in the delayed phase of ischemic brain injury. *Nat Med* 15:946–950
9. Campanella M, Sciorati C, Tarozzo G, Beltramo M (2002) Flow cytometric analysis of inflammatory cells in ischemic rat brain. *Stroke* 33:586–592
10. Brinkmann V, Davis MD, Heise CE, Albert R, Cottens S, Hof R, Bruns C, Prieschl E, Baumruker T, Hiestand P, Foster CA, Zollinger M, Lynch KR (2002) The immune modulator FTY720 targets sphingosine 1-phosphate receptors. *J Biol Chem* 277:21453–21457
11. Meno-Tetang GM, Li H, Mis S, Pyszczyński N, Heining P, Lowe P, Jusko WJ (2006) Physiologically based pharmacokinetic modeling of FTY720 (2-amino-2[2-(–4-octylphenyl)ethyl]propane-1, 3-diol hydrochloride) in rats after oral and intravenous doses. *Drug Metab Dispos* 34:1480–1487
12. Chiba K (2005) FTY720, a new class of immunomodulator, inhibits lymphocyte egress from secondary lymphoid tissues and thymus by agonistic activity at sphingosine 1-phosphate receptors. *Pharmacol Ther* 108:308–319
13. Kappos L, Radue EW, O'Connor P, Polman C, Hohlfeld R, Calabresi P, Selmaj K, Agoropoulou C, Leyk M, Zhang-Auberson L, Burtin P (2010) A placebo-controlled trial of oral fingolimod in relapsing multiple sclerosis. *N Engl J Med* 362:387–401
14. O'Connor P, Comi G, Montalban X, Antel J, Radue EW, de Vera A, Pohlmann H, Kappos L (2009) Oral fingolimod (FTY720) in multiple sclerosis: two-year results of a phase II extension study. *Neurology* 72:73–79
15. Tedesco-Silva H, Mourad G, Kahan BD, Boira JG, Weimar W, Mulgaonkar S, Nashan B, Madsen S, Charpentier B, Pellet P, Vanrenterghem Y (2004) FTY720, a novel immunomodulator: efficacy and safety results from the first phase 2A study in de novo renal transplantation. *Transplantation* 77:1826–1833
16. Hasegawa Y, Suzuki H, Sozen T, Rolland W, Zhang JH (2010) Activation of sphingosine 1-phosphate receptor-1 by FTY720 is neuroprotective after ischemic stroke in rats. *Stroke* 41:368–374
17. Rosenberg GA, Mun-Bryce S, Wesley M, Kornfeld M (1990) Collagenase-induced intracerebral hemorrhage in rats. *Stroke* 21:801–807
18. Tang J, Liu J, Zhou C, Alexander JS, Nanda A, Granger DN, Zhang JH (2004) Mmp-9 deficiency enhances collagenase-induced intracerebral hemorrhage and brain injury in mutant mice. *J Cereb Blood Flow Metab* 24:1133–1145
19. Garcia JH, Wagner S, Liu KF, Hu XJ (1995) Neurological deficit and extent of neuronal necrosis attributable to middle cerebral artery occlusion in rats. Statistical validation. *Stroke* 26:627–634, discussion 635
20. Hartman R, Lekic T, Rojas H, Tang J, Zhang JH (2009) Assessing functional outcomes following intracerebral hemorrhage in rats. *Brain Res* 1280:148–157
21. Peeling J, Yan HJ, Corbett D, Xue M, Del Bigio MR (2001) Effect of FK-506 on inflammation and behavioral outcome following intracerebral hemorrhage in rat. *Exp Neurol* 167:341–347
22. Titova E, Ostrowski RP, Kevil CG, Tong W, Rojas H, Sowers LC, Zhang JH, Tang J (2008) Reduced brain injury in CD18-deficient mice after experimental intracerebral hemorrhage. *J Neurosci Res* 86:3240–3245
23. Chiba K, Yanagawa Y, Masubuchi Y, Kataoka H, Kawaguchi T, Ohtsuki M, Hoshino Y (1998) FTY720, a novel immunosuppressant, induces sequestration of circulating mature lymphocytes by acceleration of lymphocyte homing in rats. I. FTY720 selectively decreases the number of circulating mature lymphocytes by acceleration of lymphocyte homing. *J Immunol* 160:5037–5044
24. Sanchez T, Estrada-Hernandez T, Paik JH, Wu MT, Venkataraman K, Brinkmann V, Claffey K, Hla T (2003) Phosphorylation and action of the immunomodulator FTY720 inhibits vascular endothelial cell growth factor-induced vascular permeability. *J Biol Chem* 278:47281–47290
25. Brinkmann V, Cyster JG, Hla T (2004) FTY720: sphingosine 1-phosphate receptor-1 in the control of lymphocyte egress and endothelial barrier function. *Am J Transplant* 4:1019–1025

Thrombin Preconditioning Reduces Iron-Induced Brain Swelling and Brain Atrophy

Shuijiang Song, Haitao Hu, Ya Hua, Jianan Wang, and Guohua Xi

Abstract Cerebral preconditioning with a low dose of thrombin attenuates brain edema induced by intracerebral hemorrhage (ICH), a large dose of thrombin or iron. This study examined whether or not thrombin preconditioning (TPC) reduces neuronal death and brain atrophy caused by iron. The right hippocampus of rats was pretreated with or without thrombin, and iron was then injected into the same location 3 days later. Rats were killed at 1 day or 7 days after iron injection, and the brains were used for histology. We found that TPC reduced neuronal death and brain swelling in the hippocampus 1 day after iron injection, and hippocampal atrophy 7 days later. Western blots showed that thrombin activates p44/42 mitogen-activated protein kinase (p44/42 MAPK) and 70-kDa ribosomal protein S6 kinase (p70 S6K). Our results indicate that TPC reduction of iron-induced neuronal death may be through the p44/42 MAPK /p70 S6K signal transduction pathway.

Keywords Hippocampus · Iron · p44/42 MAPK · Preconditioning · Thrombin

Introduction

Preconditioning has been used for heart and brain surgery [1, 2]. Our previous studies have demonstrated that prior treatment with a low dose of thrombin attenuates the brain edema induced by thrombin, iron or hemorrhage [3–5]. We call this phenomena thrombin preconditioning (TPC).

Iron overload occurs in the brain after intracerebral hemorrhage (ICH) and has a key role in ICH-induced brain damage. It is known that increased brain iron levels contribute to brain edema, oxidative injury and brain atrophy following ICH [6–8]. Deferoxamine, an iron chelator, reduces ICH-induced brain injury in rats and piglets [9–12].

Preconditioning-induced protection is associated with new protein synthesis [13, 14]. Activation of 70-kDa ribosomal protein S6 kinase (p70 S6K) is essential for preconditioning in the heart [15, 16]. The p44/42 mitogen-activated protein kinase (p44/42 MAPK) can activate p70 S6K [15]. The target of the activated kinase is the 40S ribosomal protein S6, a major regulator of protein synthesis [17].

In this study, we examined whether TPC reduces iron-induced neuronal death and brain atrophy. Whether or not thrombin activates the p44/42 MAPK-P70S6K pathway in the hippocampus was also examined.

Materials and Methods

Animal Preparation and Intrahippocampal Injection

The University of Michigan Committee on the Use and Care of Animals approved the protocols for these studies. Male Sprague-Dawley rats (275–325 g, Charles River Laboratories, Portage, MI) were anesthetized with pentobarbital (40 mg/kg, i.p.). A polyethylene catheter (PE-50) was then inserted into the right femoral artery to monitor arterial

S. Song and H. Hu
The Second Affiliated Hospital, Zhejiang University, Hangzhou, China and
Department of Neurosurgery, University of Michigan, Ann Arbor, MI, USA

Y. Hua
Department of Neurosurgery, University of Michigan, Ann Arbor, MI, USA

J. Wang (✉)
The Second Affiliated Hospital, Zhejiang University, #88 Jiefang Road, Hangzhou, China
e-mail: wang_jian_an@tom.com

G. Xi (✉)
Department of Neurosurgery, University of Michigan, 109 Zina Pitcher Place, Ann Arbor, MI 48109–2200, USA
e-mail: guohuaxi@umich.edu

blood pressure and to obtain blood samples for analysis of blood gases, blood pH, hematocrit, and blood glucose concentration. Body temperature was maintained at 37.5°C by using a feedback-controlled heating pad. The animals were positioned in a stereotactic frame, and a cranial burr hole (1 mm) was drilled. Thrombin and ferrous iron were infused into the right hippocampus through a 26-gauge needle at a rate of 2 μ L/min using a microinfusion pump. The coordinates were 3.8 mm posterior and 3.5 mm lateral to the bregma at a depth of 3.2 mm. After intrahippocampal infusion, the needle was removed and the skin incision closed with suture.

Experimental Groups

This study was divided into two parts. In the first part, rats were pretreated intrahippocampally with 10 μ L thrombin (Sigma, St Louis, MO, 1U/mL in saline) or a needle insertion (control). After 3 days, rats had another intrahippocampal infusion of 10 μ L ferrous chloride (1 mM in saline). Rats were killed at 1 day or 7 days later for brain histology. In the second part, rats received either a needle insertion (control) or an intrahippocampal infusion of 10 μ L thrombin (1U/mL) and were killed at 3 or 7 days later for Western blot analysis.

Histological Assessments

Rats were reanesthetized at 1 or 7 days after iron injection and were perfused with 4% paraformaldehyde in 0.1 M phosphate-buffered saline (pH 7.4). The brains were removed and kept in 4% paraformaldehyde overnight, then immersed in 30% sucrose for 3–4 days at 4°C. After embedding in the mixture of 30% sucrose and OCT (SAKURA Finetek, Torrance, CA), 18- μ m sections were taken on a cryostat.

The brain sections from 1 mm posterior to the blood injection site were stained with hematoxylin and eosin and scanned. The hippocampus was outlined and measured with NIH Image. All measurements were repeated three times, and the mean value was used.

Fluoro-Jade C Staining

Brain sections were processed for Fluoro-Jade C staining as described previously [18]. Fluoro-Jade C-positive cells were counted on the hippocampus from TPC or control rat brain sections.

Western Blot Analysis

Western blot analysis was performed as previously described [5]. The primary antibodies were polyclonal rabbit phospho-p44/42 MAPK antibody (1:2,000; Cell Signaling, MA) and polyclonal rabbit phospho-p70S6K (Thr421/Ser424) antibody (1:1,000; Cell Signaling, MA). The relative densities of phospho-p44/42 MAPK and phospho-p70 S6K protein bands were analyzed using NIH image software (version 1.63).

Statistical Analysis

All results are expressed as mean \pm SD. Data were statistically analyzed by Student's *t*-test. Differences were considered significant at the $p < 0.05$ level.

Results

Physiological parameters were recorded immediately before intrahippocampal injections. The mean arterial blood pressure (MABP), blood pH, blood gases, hematocrit and blood glucose were controlled within normal ranges (MABP, 80–120 mmHg; pO_2 , 80–120 mmHg; pCO_2 , 35–45 mmHg; hematocrit, 38–42%; blood glucose, 80–120 mg/dL).

Fluoro-Jade C staining was used to examine neuronal death at day 1 after iron injection. Iron caused neuronal death in the hippocampus, and TPC reduced iron-induced neuronal death in the hippocampal CA-1 region (Fluoro-Jade C positive cells: 27.8 ± 7.8 cells/mm vs. 38.8 ± 6.3 cells/mm in the control group, $p < 0.01$, Fig. 1). Iron also caused swelling in the ipsilateral hippocampus. TPC reduced hippocampal swelling induced by iron (5.9 ± 0.2 vs. 6.6 ± 0.6 mm² in the control group, $p < 0.05$; Fig. 2).

Iron-induced hippocampal tissue loss was examined at day 7. We found that hippocampal sizes in the contralateral side were same in the TPC and control group. Iron injection resulted in significant tissue loss in the ipsilateral hippocampus (Fig. 2). TPC reduced iron-induced hippocampal atrophy (5.4 ± 0.4 vs. 4.5 ± 0.2 mm², $p < 0.01$, Fig. 2).

To determine whether the p44/42 MAPK/p70 S6K pathway involves in TPC-induced neuron protection, we measured levels of activated p44/42 MAPK and p70 S6K by Western blots and found that thrombin can activate p44/42 MAPK and p70 S6K in the hippocampus (Fig. 3).

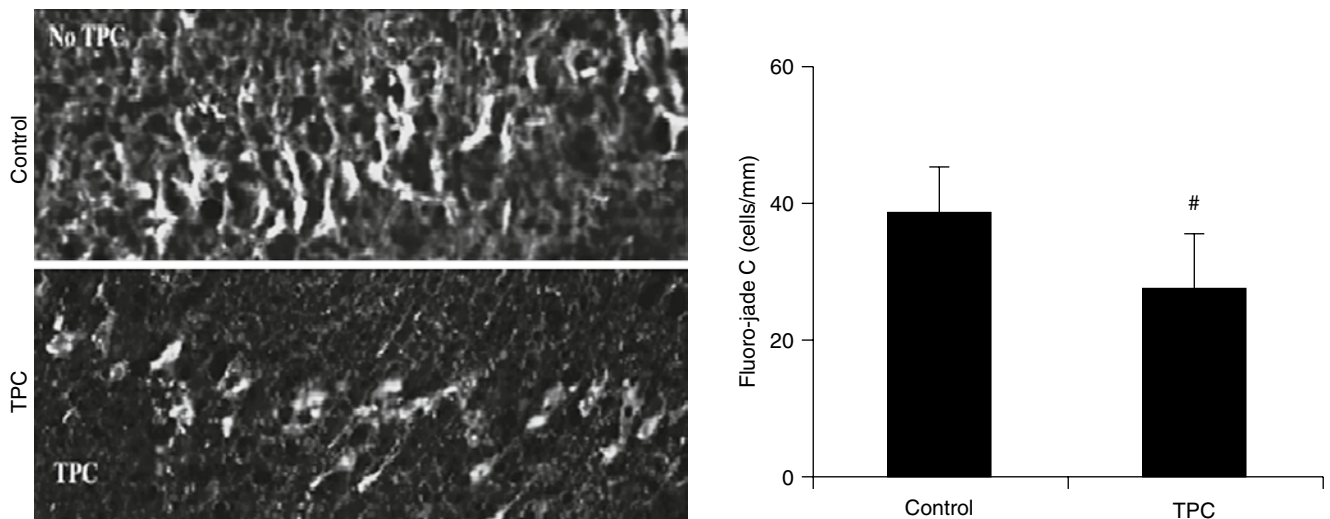


Fig. 1 Fluoro-Jade C staining in the ipsilateral hippocampus 1 day after iron injection. Values are expressed as mean \pm SD, $n=5$, $\#p<0.01$ vs. control

Discussion

Although high concentrations of thrombin are deleterious to the brain, low concentrations of thrombin are neuroprotective in vitro and in vivo [3, 19]. In vitro studies have shown that thrombin protects rat primary astrocytes from hypoglycemia- or oxidative stress-induced cell death. Thrombin also protects rat primary hippocampal neurons from cell death

produced by hypoglycemia, hypoxia or growth supplement deprivation [20, 21]. In vivo studies have shown that prior intracerebral injection of a low dose of thrombin reduces the brain injury that follows a subsequent intracerebral injection of a high dose of thrombin, an effect abolished by co-injection of a thrombin inhibitor [5]. TPC reduces brain ICH-induced edema [4] and brain injury following focal cerebral ischemia [22]. We have also shown that TPC can protect against brain

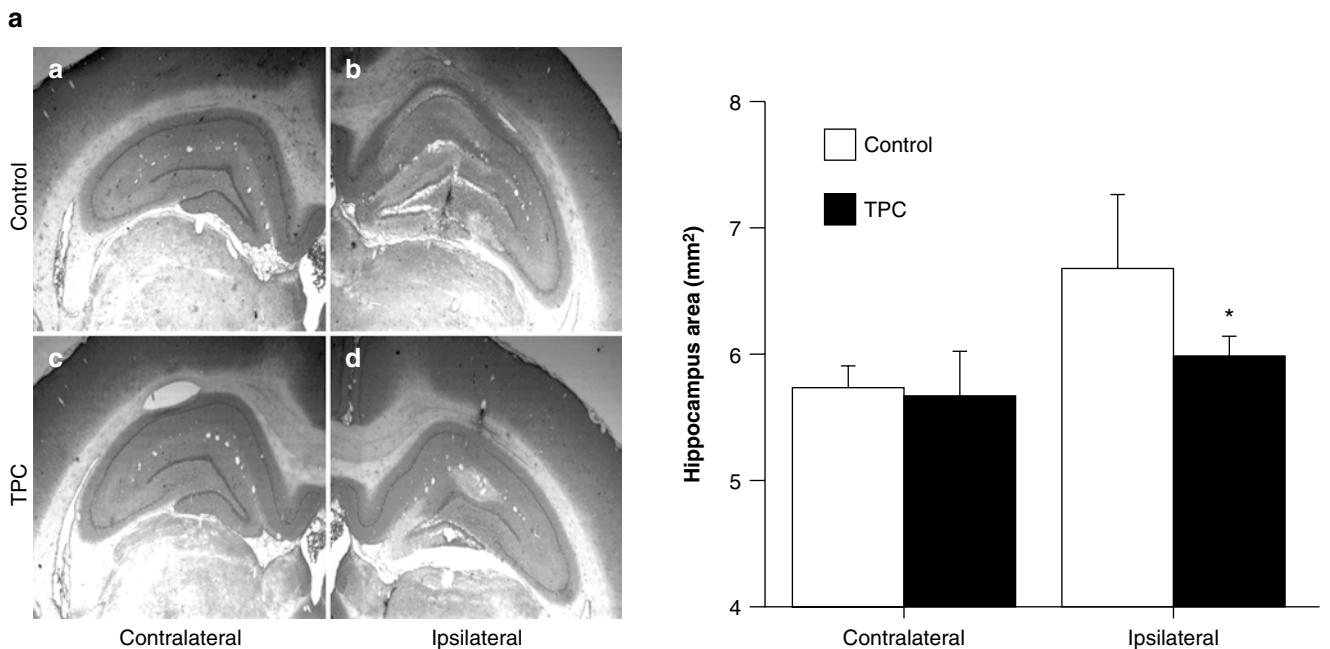


Fig. 2 H&E staining showing hippocampal swelling (a) and hippocampal atrophy (b) after iron injection. Values are expressed as mean \pm SD, $n=4-6$, $*p<0.05$, $\#p<0.01$ vs. control

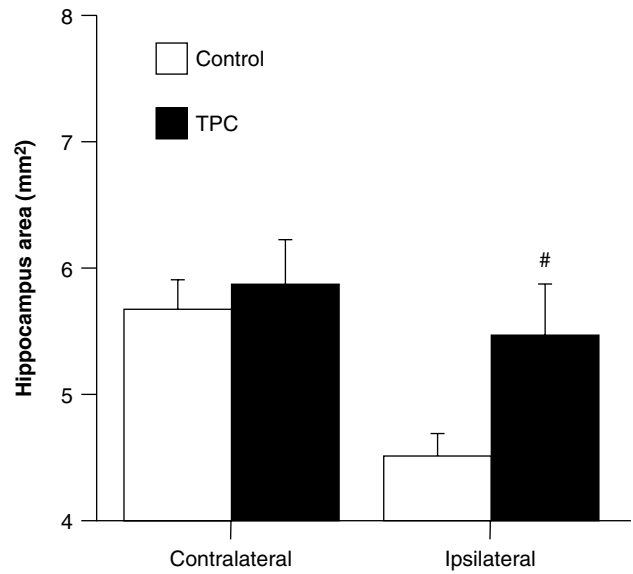
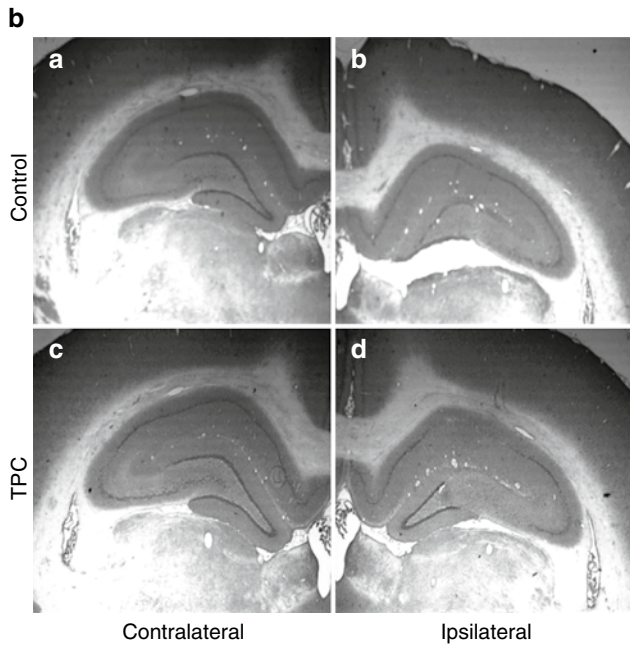


Fig. 2 (continued)

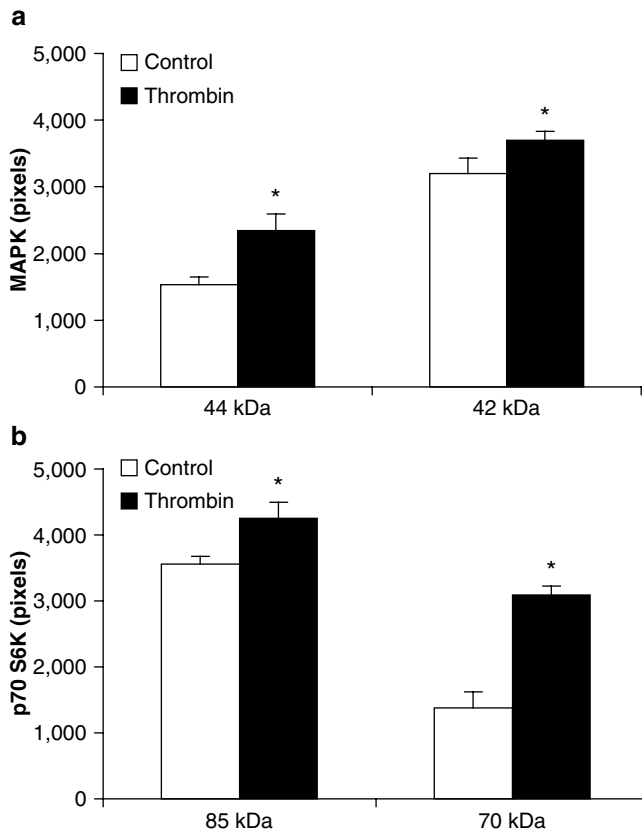


Fig. 3 Western blot analysis showing levels of activated p44/42 MAPK (a) and p70S6K (b) in the hippocampus after thrombin injection or a needle insertion (control). Values are mean ± S.D., **p* < 0.05 vs. control

edema induced by intracerebral injection of iron [3, 23]. In addition, TPC reduces brain injury in a rat Parkinson’s model [24, 25]. In this study, we demonstrate that TPC reduces neuronal death and brain atrophy induced by iron.

Our current results also show that thrombin can also activate p44/42 MAPK and p70 S6K, which may be related to protein synthesis. We have demonstrated that protein synthesis (e.g., heat shock proteins) may contribute to neuroprotection induced by TPC. Reports have shown that protein synthesis is associated to cerebral ischemic preconditioning [13], and it may also have a role in cerebral TPC.

TPC reduces iron-mediated brain injury, suggesting a potential role of iron-handling proteins in TPC. Evidence indicates that brain injury after ICH is, in part, due to the release of iron from hemoglobin [26]. We have examined the effects of a low dose of thrombin on brain transferrin and transferrin receptor, proteins involved in iron transport, which might modulate iron-induced toxicity. We found that thrombin upregulates brain transferrin and transferrin receptor [3]. Thrombin also increases ceruloplasmin levels in vivo [27]. The role of the p44/42 MAPK/p70 S6K pathway and iron-handling proteins in TPC should be examined in the future.

Acknowledgment This study was supported by grants NS-017760, NS-039866 and NS-057539 from the National Institutes of Health (NIH) and 0755717Z, 0840016N from the American Heart Association (AHA). The content is solely the responsibility of the authors and does not necessarily represent the official views of the the NIH and AHA.

Conflict of interest statement We declare that we have no conflict of interest.

References

1. Gidday JM (2010) Pharmacologic preconditioning: translating the promise. *Transl Stroke Res* 1:19–30
2. Keep RF, Wang MM, Xiang J, Hua Y, Xi G (2010) Is there a place for cerebral preconditioning in the clinic? *Transl Stroke Res* 1:4–18
3. Hua Y, Keep RF, Hoff JT, Xi G (2003) Thrombin preconditioning attenuates brain edema induced by erythrocytes and iron. *J Cereb Blood Flow Metab* 23:1448–1454
4. Xi G, Hua Y, Keep RF, Hoff JT (2000) Induction of colligin may attenuate brain edema following intracerebral hemorrhage. *Acta Neurochir Suppl* 76:501–505
5. Xi G, Keep RF, Hua Y, Xiang JM, Hoff JT (1999) Attenuation of thrombin-induced brain edema by cerebral thrombin preconditioning. *Stroke* 30:1247–1255
6. Hua Y, Nakamura T, Keep RF, Wu J, Schallert T, Hoff JT, Xi G (2006) Long-term effects of experimental intracerebral hemorrhage: the role of iron. *J Neurosurg* 104:305–312
7. Nakamura T, Keep R, Hua Y, Schallert T, Hoff J, Xi G (2004) Deferoxamine-induced attenuation of brain edema and neurological deficits in a rat model of intracerebral hemorrhage. *J Neurosurg* 100:672–678
8. Xi G, Keep RF, Hoff JT (2006) Mechanisms of brain injury after intracerebral hemorrhage. *Lancet Neurol* 5:53–63
9. Gu Y, Hua Y, Keep RF, Morgenstern LB, Xi G (2009) Deferoxamine reduces intracerebral hematoma-induced iron accumulation and neuronal death in piglets. *Stroke* 40:2241–2243
10. Okauchi M, Hua Y, Keep RF, Morgenstern LB, Schallert T, Xi G (2010) Deferoxamine treatment for intracerebral hemorrhage in aged rats: therapeutic time window and optimal duration. *Stroke* 41:375–382
11. Okauchi M, Hua Y, Keep RF, Morgenstern LB, Xi G (2009) Effects of deferoxamine on intracerebral hemorrhage-induced brain injury in aged rats. *Stroke* 40:1858–1863
12. Song S, Hua Y, Keep RF, Hoff JT, Xi G (2007) A new hippocampal model for examining intracerebral hemorrhage-related neuronal death: effects of deferoxamine on hemoglobin-induced neuronal death. *Stroke* 38:2861–2863
13. Dirnagl U, Simon RP, Hallenbeck JM (2003) Ischemic tolerance and endogenous neuroprotection. *Trends Neurosci* 26:248–254
14. Gidday JM (2006) Cerebral preconditioning and ischaemic tolerance. *Nat Rev Neurosci* 7:437–448
15. Hausenloy DJ, Mocanu MM, Yellon DM (2004) Cross-talk between the survival kinases during early reperfusion: its contribution to ischemic preconditioning. *Cardiovasc Res* 63:305–312
16. Hausenloy DJ, Tsang A, Mocanu MM, Yellon DM (2005) Ischemic preconditioning protects by activating prosurvival kinases at reperfusion. *Am J Physiol Heart Circ Physiol* 288:H971–H976
17. Berven LA, Crouch MF (2000) Cellular function of p70S6K: a role in regulating cell motility. *Immunol Cell Biol* 78:447–451
18. Schmued LC, Stowers CC, Scallet AC, Xu L (2005) Fluoro-Jade C results in ultra high resolution and contrast labeling of degenerating neurons. *Brain Res* 1035:24–31
19. Xi G, Reiser G, Keep RF (2003) The role of thrombin and thrombin receptors in ischemic, hemorrhagic and traumatic brain injury: deleterious or protective? *J Neurochem* 84:3–9
20. Striggow F, Riek M, Breder J, Henrich-Noack P, Reymann KG, Reiser G (2000) The protease thrombin is an endogenous mediator of hippocampal neuroprotection against ischemia at low concentrations but causes degeneration at high concentrations. *Proc Natl Acad Sci USA* 97:2264–2269
21. Vaughan PJ, Pike CJ, Cotman CW, Cunningham DD (1995) Thrombin receptor activation protects neurons and astrocytes from cell death produced by environmental insults. *J Neurosci* 15:5389–5401
22. Masada T, Xi G, Hua Y, Keep RF (2000) The effects of thrombin preconditioning on focal cerebral ischemia in rats. *Brain Res* 867:173–179
23. Xi G, Wu J, Jiang Y, Hua Y, Keep RF, Hoff JT (2003) Thrombin preconditioning upregulates transferrin and transferrin receptor and reduces brain edema induced by lysed red blood cells. *Acta Neurochir Suppl* 86:449–452
24. Cannon JR, Keep RF, Hua Y, Richardson RJ, Schallert T, Xi G (2005) Thrombin preconditioning provides protection in a 6-hydroxydopamine Parkinson's disease model. *Neurosci Lett* 373:189–194
25. Cannon JR, Keep RF, Schallert T, Hua Y, Richardson RJ, Xi G (2006) Protease-activated receptor-1 mediates protection elicited by thrombin preconditioning in a rat 6-hydroxydopamine model of Parkinson's disease. *Brain Res* 1116:177–186
26. Huang F, Xi G, Keep RF, Hua Y, Nemoianu A, Hoff JT (2002) Brain edema after experimental intracerebral hemorrhage: role of hemoglobin degradation products. *J Neurosurg* 96:287–293
27. Yang S, Hua Y, Nakamura T, Keep RF, Xi G (2006) Up-regulation of brain ceruloplasmin in thrombin preconditioning. *Acta Neurochir Suppl* 96:203–206

Capsaicin Pre-treatment Provides Neurovascular Protection Against Neonatal Hypoxic-Ischemic Brain Injury in Rats

Nikan H. Khatibi, Vikram Jadhav, Shelton Charles, Jeffrey Chiu, John Buchholz, Jiping Tang, and John H. Zhang

Abstract Capsaicin, a transient receptor potential vanilloid 1 (TRPV1) agonist, has recently been shown to provide neuroprotection against brain injury in experimental adult models of cerebral ischemia. Accordingly, in this study, we investigated the way in which capsaicin-mediated TRPV1 modulation could attenuate damage in an experimental hypoxic-ischemic (HI) neonatal brain injury model. The Rice-Vannucci method was used in 10-day-old rat pups by performing unilateral carotid artery ligation followed by 2 h of hypoxia (8% O₂ at 37°C). Capsaicin was administered intraperitoneally (0.2 mg/kg or 2.0 mg/kg) at 3 h pre-HI or 1 h post-HI. Post assessment included measurement of infarction volume at 24 and 72 h in addition to an assessment of the vascular dynamics of the middle cerebral artery (MCA) at 6 h post-HI. The results indicated that pre-treatment with capsaicin reduced infarction volume significantly with either low-dose or high-dose treatment. Pre-treatment also improved myogenic tone and decreased apoptotic changes in the distal MCA. We concluded that capsaicin pre-treatment may provide neurovascular protection against neonatal HI.

Keywords Transient receptor potential vanilloid 1 (TRPV1) · Capsaicin · Neonatal hypoxia ischemia

Introduction

Perinatal brain injury can occur because of a wide variety of events, including hypoxia-ischemia (HI), intrauterine infections, and cerebral hemorrhage. Of these three, HI is the most common cause of perinatal brain injury, and is responsible for a large number of morbidities and mortalities [1]. In the past, many studies have been aimed at determining the cause of brain damage in an effort to reduce the major consequences of injury, including cerebral palsy, seizure disorders and motor/cognitive disabilities [2]. To date, various mechanisms including excitotoxicity have been implicated as a key component of brain damage in HI. Unfortunately, the lack of effective therapeutic options to combat excitotoxic cell death and prevent further damage has driven the need for additional research in this field.

Transient receptor potential vanilloid 1 (TRPV1, or capsaicin receptor) is a nonspecific cation channel belonging to the TRP superfamily [3]. It is highly expressed in spinal and peripheral nerve terminals and has an important role in nociception as well as analgesia [3, 4]. In order for TRPV1 to be activated, it must be exposed to various noxious and painful stimuli, such as low pH (<5.9), heat (>43°C), capsaicin and endocannabinoids. In doing so, activated TRPV1 causes an increase in calcium influx, thereby promoting excitotoxic cell death mechanisms in neurons [3]. Recently, experimental adult models have shown that capsaicin administration may provide neuroprotection against excitotoxic and ischemic brain injury by desensitizing the TRPV1 receptor [5].

Accordingly, in the present study we investigated whether modulation of TRPV1 with capsaicin provides neuroprotection after HI brain injury using the established Rice-Vannucci neonatal rat model. Specifically, we investigated the effects of capsaicin treatment on infarction volume and vascular dynamics in our brain-injured neonatal rat pups.

N.H. Khatibi
Department of Anesthesiology, Loma Linda Medical Center,
Loma Linda, CA, USA

V. Jadhav, S. Charles, J. Chiu, and J. Buchholz
Department of Physiology, Loma Linda University,
School of Medicine, Loma Linda, CA, USA

J. Tang (✉)
Department of Physiology, Loma Linda University,
School of Medicine, Loma Linda, CA, USA and
Department of Physiology and Pharmacology, Loma Linda University,
School of Medicine, Loma Linda, CA, 92354, USA
e-mail: jtang@llu.edu

J.H. Zhang
Department of Anesthesiology, Loma Linda Medical Center,
Loma Linda, CA, USA and
Department of Physiology, Loma Linda University,
School of Medicine, Loma Linda, CA, USA and
Department of Neurosurgery, Loma Linda Medical Center,
Loma Linda, CA, USA

Materials and Methods

Animal Groups. All procedures for this study were approved by the Animal Care and Use Committee at Loma Linda University and complied with the NIH Guide for the Care and Use of Laboratory Animals. Ninety-five 10-day-old rat pups were randomly divided into the following groups: sham, HI ($n=39$), HI+0.2 mg/kg capsaicin pre-treatment ($n=14$), HI+2 mg/kg capsaicin pre-treatment ($n=14$), HI+0.2 mg/kg capsaicin post-treatment ($n=14$) and HI+0.2 mg/kg capsaicin post-treatment ($n=14$).

Operative Procedure. Timed pregnant female Sprague-Dawley rats were obtained from Harlan Laboratories (Indianapolis, IN) and housed in individual cages. The day of birth was considered day 0. After birth, pups were housed with their dam under a 12:12-h light-dark cycle, with food and water available ad libitum throughout the study. A modified Rice-Vannucci model was adopted as follows [6]: 10-day-old postnatal pups were anesthetized with isoflurane. The right common carotid artery of each pup was permanently ligated with 5-0 surgical silk through a near-midline incision. After recovering with their dams for 2 h, the pups were then placed in a jar perfused with a humidified and pre-warmed gas mixture (8% oxygen balanced with nitrogen) for 2 h. A constant temperature of 37°C was maintained throughout all the procedures. After hypoxia, the animals were returned to their dams, and the ambient temperature was maintained at 37°C for 24 h. Sham animals underwent anesthesia, and the common carotid artery was exposed without ligation and hypoxia.

Treatment Method. Capsaicin (Tocris Bioscience, MO), a TRPV1 agonist, was administered intraperitoneally as a single treatment in two doses of 0.2 mg/kg and 2.0 mg/kg based on previous studies [7] either as pretreatment (3 h prior to HI) or post-treatment (1 h after HI). The drugs were constituted in 1% dimethyl sulfoxide (DMSO).

Immunohistochemistry. Naïve pups (10 days old) were transcardially perfused under deep anesthesia with PBS followed by 4% paraformaldehyde. The brains were then removed and post-fixed in formalin. Paraffin-embedded brains were sectioned into 10- μ m-thick slices by cryostat (CM3050S; Leica Microsystems). Double immunofluorescent staining was performed using the following primary antibodies: rabbit polyclonal anti-TRPV1 antibody (Tocris Biosciences, 1:200), goat polyclonal anti-vWF (Santa Cruz Biotechnology, 1:200) and mouse anti-NeuN antibody (Chemicon, MAB377, 1:200) as described before [8].

Infarct Volume Measurement. 2, 3, 5-Triphenyltetrazolium chloride monohydrate (TTC) staining was used to measure infarct volume as previously described [9]. Briefly, at 24 h and 72 h after HI, animals were perfused transcardially with PBS under deep anesthesia. The brains were removed and

sectioned into 2-mm slices, then immersed into 2% TTC solution at 37°C for 5 min, followed by 10% formaldehyde. The infarction volume was traced and analyzed by Adobe Photoshop 6.0 by an investigator blinded to the treatment groups.

Vascular Dynamics. These experiments were carried out on distal MCA segments. All methods used for tissue dissection and mounting in the organ were performed as described previously [10]. Briefly, rat brains were rapidly removed from the cranial cavity after decapitation and placed in ice cold PBS at a pH level of 7.4 via stepwise addition of 1 M NaOH. Distal MCA was dissected from the brain surface, cut into lengths of 5 mm and mounted on cannulas in an organ chamber (Living Systems, Burlington, VT). In the organ chamber, the proximal cannula was connected in parallel to a pressure transducer, a reservoir of PSS, and a servo-controlled pump system used to set transmural pressure. The distal cannula was connected to a luer-lock valve that was open to gently flush the lumen during the initial cannulation. After cannulation, the distal valve was closed, and all measurements were conducted under no-flow conditions. Arterial diameter was recorded with the SoftEdge Acquisition Subsystem (Ion-Optix, Milton, MA). The percent myogenic tone at each pressure (20, 40, 60 and 80 mmHg) was calculated as passive diameter (diameter in zero Ca^{2+} PSS) minus active diameter (diameter in PSS) divided by passive diameter times 100 [10].

Statistics. All the data were expressed as mean \pm SEM. Statistical differences between groups were analyzed by using one-way ANOVA followed by Holm-Sidak post-hoc analysis.

Results

Ubiquitous expression of TRPV1 in the neonatal brain. The distribution of TRPV1 in the neonatal brain using double-labeling fluorescent immunostaining was examined. We found that the receptor was widely distributed in the neonatal brain, including the cortex, hippocampus, striatum and sub-ventricular zone, as shown in Fig. 1, similar to the distribution in the adult brain, as reported by others [7, 11]. TRPV1 immunoreactivities (blue color) were expressed in both neuronal as well as non-neuronal cell types as indicated by the partial co-localization with a neuronal marker (NeuN, red immunoreactivities) in the merged images shown in Fig. 1b. TRPV1 immunoreactivities were also expressed in the cerebral vasculature (distal MCA). There was partial co-localization with vWF, an endothelial marker indicating presence of TRPV1 on the endothelial as well as non-endothelial cells in the vasculature (Fig. 1c).

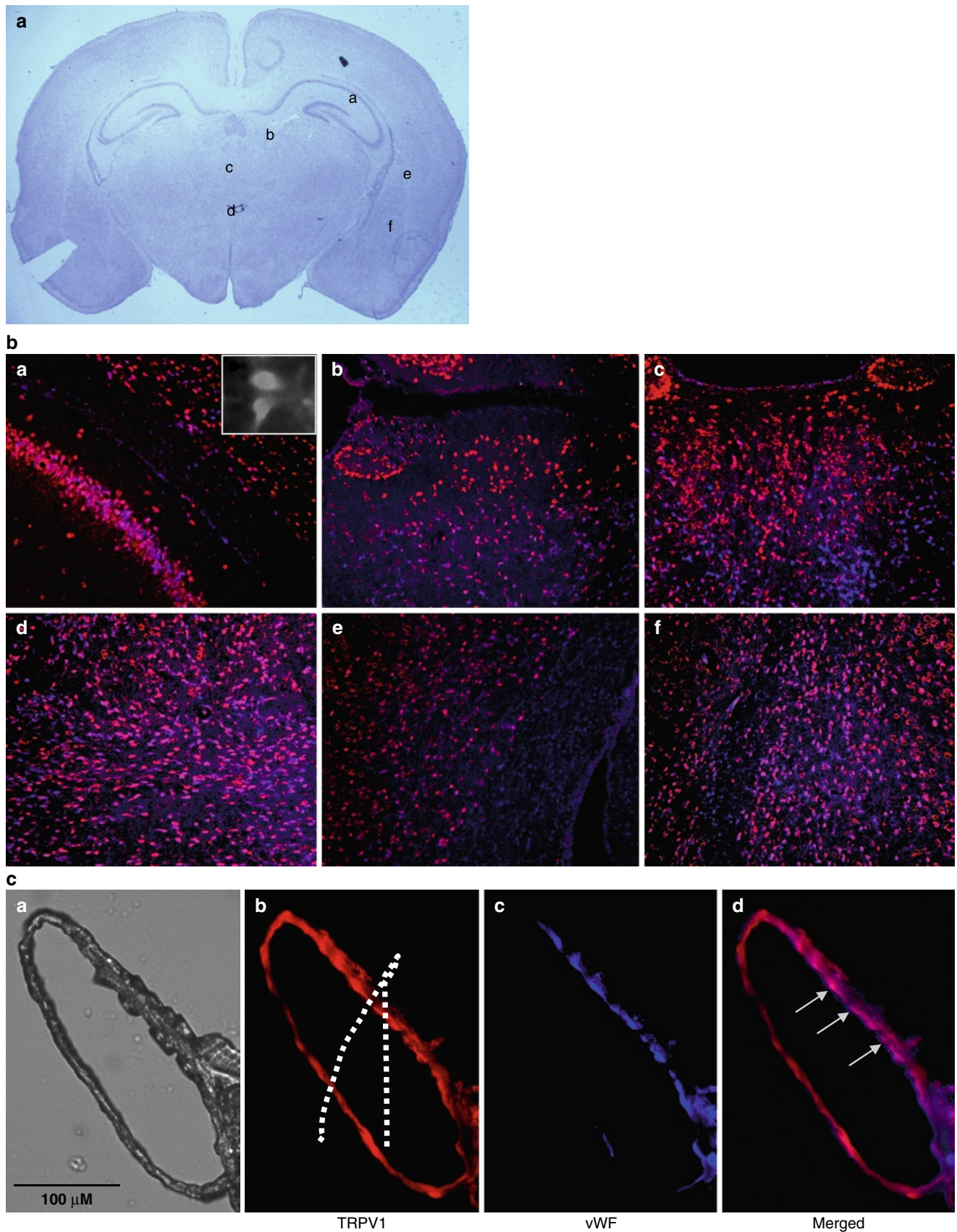


Fig. 1 Cell-specific distribution of TRPV1. (b) The double immunofluorescent images in panels a–f show the TRPV1 immunoreactivities (blue color) and neuronal marker, NeuN (red color), in different areas of the neonatal brain as indicated in Fig. 1a. (c) Panels a–d show the

presence of TRPV1 immunoreactivities (panel b, red color) and endothelial marker, vWF (panel c, blue color), merged at some areas (panel d, indicated by arrows) in the middle cerebral artery (panel a) from neonatal rat brain

Infarction volume after neonatal hypoxia ischemia. Based on existing reports in adult models [5], TRPV1 modulation was done using an agonist (capsaicin, 0.2 and 2 mg/kg, i.p) at 3 h before HI and at 1 h after HI. Both doses of capsaicin pre-treatment significantly reduced the infarction volume at

24 h and 72 h after neonatal HI (Fig. 2a, b). However, when capsaicin was administered as a post-treatment, there were no effects on infarction size at either 24 h or 72 h (Fig. 2c).

Vascular dynamics after neonatal HI. Distal MCA segments were obtained from sham ($n=3$), vehicle ($n=6$) and

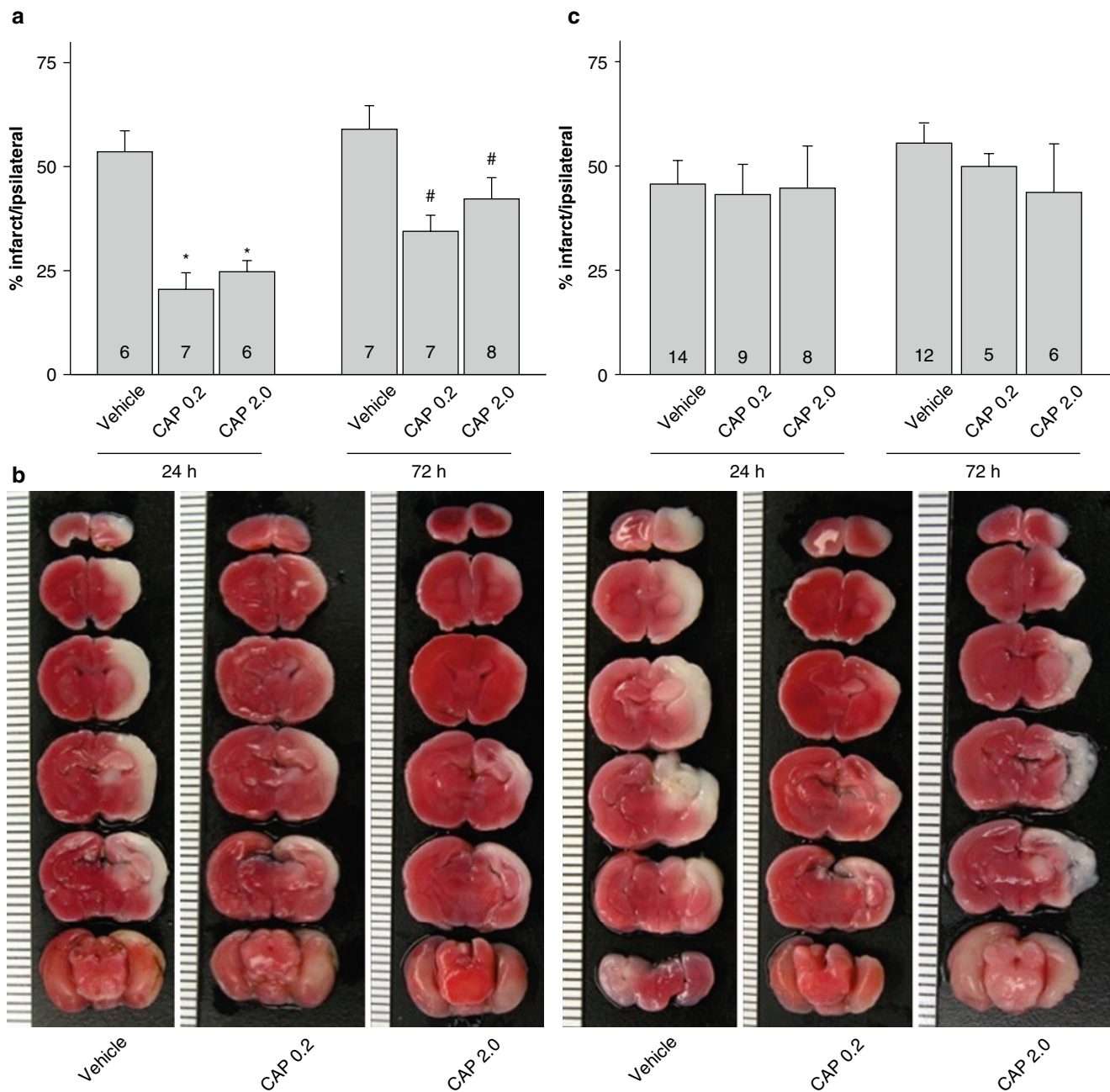


Fig. 2 Infarction volume with capsaicin pre/post treatment. (a) Bar graph showing the quantified results of infarction volume calculated from TTC-stained brain coronal slices from pre-treatment groups (3 h pre-HI): vehicle, capsaicin 0.2 mg/kg, capsaicin 2 mg/kg at 24 h and 72 h post-HI. The data indicated that both capsaicin pretreated groups significantly decreased infarction volume as compared to respective vehicle-treated groups at 24 h ($*p < 0.05$) and 72 h ($\#p < 0.05$)

post-HI. (b) Represented brain slices stained with TTC. The vertical scale on the left side of the brain slices in the lower panel has a count of 1 mm. (c) Bar graph showing similar tests as in 2a, however with 1 h post-treatment. The data indicated that capsaicin post-treated groups did not have any effects on the infarction volume as compared to respective vehicle-treated groups at 24 h and 72 h ($p < 0.05$)

capsaicin pre-treated (0.2 mg/kg, $n=6$) pups at 6 h post-HI, i.e., during the development of infarction. This time point was chosen specifically to allow for studying the vascular dynamics of the MCA during the progression of infarction. There was significant loss of myogenic tone (Fig. 3a) and increased diameter (Fig. 3b) (loss of the ability to contract and maintain tone) in the arterial segments obtained from vehicle-treated animals. The capsaicin pretreatment group significantly improved the myogenic tone in the MCA segments at 60 and 80 mmHg pressure as compared to

the vehicle-treated group. Capsaicin pretreatment showed slightly improved vascular diameter dynamics; however, the values were not significant as compared to the vehicle-treated group.

Discussion

Neonatal HI brain injury is a major cause of morbidity and mortality in infants and children. Even if newborns are able to survive the initial attack, the damage to the brain is so severe that most individuals are left with chronic neurobehavioral disabilities and limited growth capabilities. In this study, we investigated the effects of capsaicin treatment on HI brain injury, specifically investigating its potential to reduce the acute changes that occur after injury. Our study suggests that for the first time, pre-treatment with capsaicin may provide neurovascular protection in neonatal HI by reducing the volume of infarction and improving overall vascular dynamics of major arteries in the brain.

TRPV1 receptors are calcium cation channels responsible for transducing the nociceptive effects of sensory neurons in the body as well as in the brain. In various adult species, immunohistochemistry markers have demonstrated TRPV1's expression in various regions of the brain including the cortex, hippocampus, dentate gyrus, central amygdala, striatum, hypothalamus, thalamus and cerebellum [7]. Where it has not been confirmed is in the immature, neonatal brain. Nevertheless, in our study, we found a similar degree of distribution of TRPV1 receptors in the neonatal rat brain through the use of double immunofluorescence. Specifically, we found the ubiquitous presence of TRPV1 in neuronal and endothelial cells within the cerebral vasculature. As a result of their widespread distribution in the brain, we felt that by inhibiting TRPV1, we could potentially reduce the damages induced by HI injury.

Many of the damaging initial occurrences after an HI event are a result of the body's attempt to cope with the surrounding environment. With an inadequate amount of oxygen reaching the brain, anaerobic glycolysis is quickly initiated, leading to an insufficient supply of energy. As a result, key processes in the brain responsible for maintaining cellular survival shut down, such as energy-dependent ion pumps [12]. This effect can occur from activation of TRPV1 receptors by pathophysiologic mediators, such as cell membrane breakdown products, endocannabinoids and pH changes, which occur after HI [3]. This leads to an overstimulation of glutamate-dependent NMDA receptors and an abnormal rise in intracellular calcium levels. Consequently, a high production of reactive oxygenated species (ROS) and activation of nitric oxide synthase occurs, ultimately resulting in neuronal excitotoxicity. In previous works, capsaicin

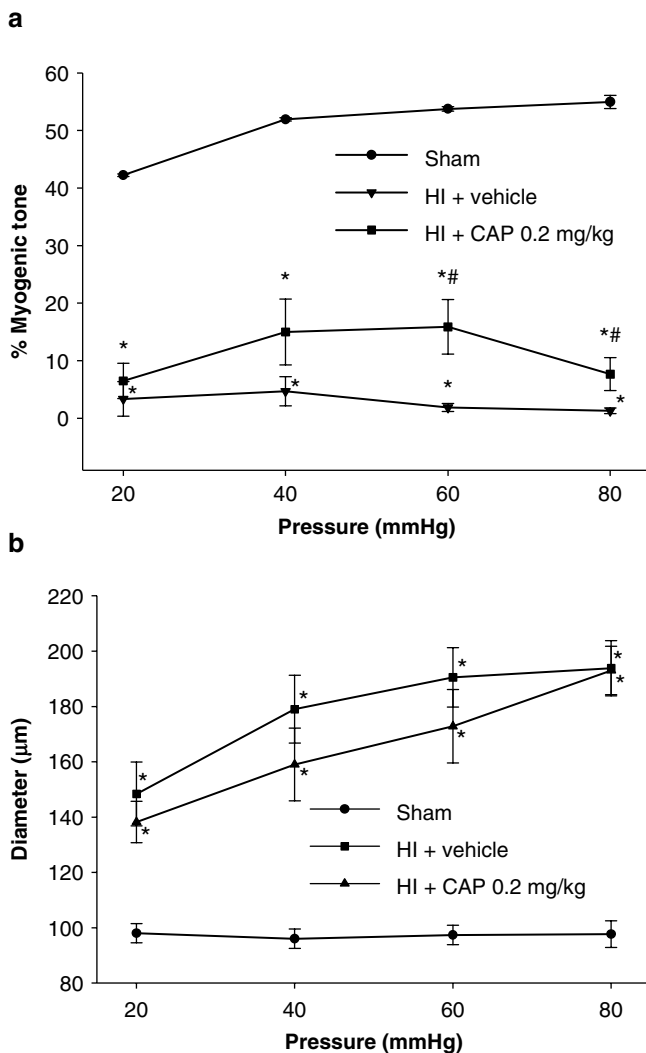


Fig. 3 Vascular dynamics after neonatal HI. Effects of changes in myogenic tone (a) and diameter (b) of distal MCA post-HI. Sequential pressure steps from 20 to 80 mmHg were applied after exposing the arteries to normal PSS or zero calcium PSS (3 mM EDTA), respectively. The arterial segments showed significant loss of myogenic tone and increased diameter in both capsaicin pretreated ($n=6$) and vehicle-treated ($n=6$) groups compared to sham ($n=3$). The capsaicin-pretreated group showed significant improvement in myogenic tone at 60 and 80 mmHg as compared to the vehicle-treated group (Fig. 3a). ($p < 0.05$, denoted by *v/s sham and #v/s vehicle)

treatment has been suggested to desensitize the TRPV1 receptor [5], and thus lead to a decrease in Ca^{++} influx post-ischemia and a significant reduction in excitotoxic damage. In our study we found similar results. Both the low- and high-dose capsaicin pre-treatment groups were found to decrease the volume of infarction in our neonatal rat population. This may be due to the reduction in excitotoxic damage caused by TRPV1 inhibition by capsaicin.

The brain area supplied by the MCA is known to include the penumbra after the hypoxic ischemic insult. Without intervention, the infarction after neonatal HI has been shown to progress and increase in size over 72 h, but the earliest irreversible changes, such as activation of caspase-3 in the penumbra, were seen as early as 3 h after neonatal HI [13]. The myogenic response is critical in autoregulation, which is a hallmark of cerebral circulation. In recent studies, it was suggested that the activation of TRPV1 can regulate the myogenic tone via release of vasoactive neuropeptides [14]. To examine the effects of capsaicin on the cerebral vasculature and the vascular dynamics during this acute and critical phase, we harvested the distal MCA from the ipsilateral brain at 6 h after neonatal HI to study the vascular dynamics in the vessel. We found that there was a loss in myogenic tone in the distal MCA after injury, which was attenuated with capsaicin pre-treatment. The results of this study suggest that TRPV1 modulation by capsaicin provides vascular protection.

Conclusion

In summary, this study provides evidence that capsaicin, a TRPV1 agonist, provides neurovascular protection against neonatal HI brain damage. This effect may be partly exerted by improvement of vascular dynamics and inhibition of TRPV1-mediated excitotoxic cell damage. Further studies will need to be conducted to determine its potential in the clinical setting.

Acknowledgement This study is partially supported by NIH NS043338 to J.H. Zhang, and NS060936 to J. Tang.

Conflict of interest statement We declare that we have no conflict of interest.

References

1. Bracci R, Perrone S, Buonocore G (2006) The timing of neonatal brain damage. *Biol Neonate* 90:145–155
2. Northington FJ, Ferriero DM, Martin LJ (2001) Neurodegeneration in the thalamus following neonatal hypoxia–ischemia is programmed cell death. *Dev Neurosci* 23:186–191
3. Pedersen SF, Owsianik G, Nilius B (2005) TRP channels: an overview. *Cell Calcium* 38(3–4):233–252, Review
4. Caterina MJ (2007) Transient receptor potential ion channels as participants in thermosensation and thermoregulation. *Am J Physiol Regul Integr Comp Physiol* 292(1):R64–R76, Epub 2006 Sep 14. Review
5. Pegorini S, Braidà D, Verzoni C, Guerini-Rocco C, Consalez GG, Croci L, Sala M (2005) Capsaicin exhibits neuroprotective effects in a model of transient global cerebral ischemia in Mongolian gerbils. *Br J Pharmacol* 144(5):727–735
6. Chen W, Jadhav V, Tang J, Zhang JH (2008) HIF-1 α inhibition ameliorates neonatal brain injury in a rat pup hypoxic-ischemic model. *Neurobiol Dis* 31(3):433–441
7. Mezey E, Tóth ZE, Cortright DN, Arzubi MK, Krause JE, Elde R, Guo A, Blumberg PM, Szallasi A (2000) Distribution of mRNA for vanilloid receptor subtype 1 (VR1), and VR1-like immunoreactivity, in the central nervous system of the rat and human. *Proc Natl Acad Sci USA* 97(7):3655–3660
8. Hayes P, Meadows HJ, Gunthorpe MJ, Harries MH, Duckworth DM, Cairns W, Harrison DC, Clarke CE, Ellington K, Prinjha RK, Barton AJ, Medhurst AD, Smith GD, Topp S, Murdock P, Sanger GJ, Terrett J, Jenkins O, Benham CD, Randall AD, Gloger IS, Davis JB (2000) Cloning and functional expression of a human orthologue of rat vanilloid receptor-1. *Pain* 88(2):205–215
9. Zhong B, Wang DH (2008) N-oleoyldopamine, a novel endogenous capsaicin-like lipid, protects the heart against ischemia-reperfusion injury via activation of TRPV1. *Am J Physiol Heart Circ Physiol* 295(2):H728–H735
10. Charles SM, Zhang L, Longo LD, Buchholz JN, Pearce WJ (2007) Postnatal maturation attenuates pressure-evoked myogenic tone and stretch-induced increases in Ca^{2+} in rat cerebral. *Am J Physiol Regul Integr Comp Physiol* 293(2):R737–R744
11. Cristino L, de Petrocellis L, Pryce G, Baker D, Guglielmotti V, Di Marzo V (2006) Immunohistochemical localization of cannabinoid type 1 and vanilloid transient receptor potential vanilloid type 1 receptors in the mouse brain. *Neuroscience* 139(4):1405–1415, Epub 2006 Apr 17
12. Kaur C, Ling EA (2009) Periventricular white matter damage in the hypoxic neonatal brain: role of microglial cells. *Prog Neurobiol* 87(4):264–280
13. Manabat C, Han BH, Wendland M, Derugin N, Fox CK, Choi J, Holtzman DM, Ferriero DM, Vexler ZS (2003) Reperfusion differentially induces caspase-3 activation in ischemic core and penumbra after stroke in immature brain. *Stroke* 34(1):207–213
14. Scotland RS, Chauhan S, Davis C, De Felipe C, Hunt S, Kabir J, Kotsonis P, Oh U, Ahluwalia A (2004) Vanilloid receptor TRPV1, sensory C-fibers, and vascular autoregulation: a novel mechanism involved in myogenic constriction. *Circ Res* 95(10):1027–1034

Effects of Recombinant Osteopontin on Blood-Brain Barrier Disruption After Subarachnoid Hemorrhage in Rats

Hidenori Suzuki, Yu Hasegawa, Robert Ayer, Takashi Sugawara, Wanqiu Chen, Takumi Sozen, Kenji Kanamaru, Waro Taki, and John H. Zhang

Abstract *Objects:* We determined effects of recombinant OPN (r-OPN), a pleiotropic extracellular matrix protein, on blood-brain barrier (BBB) disruption and matrix metalloproteinase (MMP)-9 activation after subarachnoid hemorrhage (SAH) in rats.

Methods: The endovascular perforation model of SAH was used. SAH or sham-operated rats were treated with pre-SAHA intracerebroventricular administration of two dosages of r-OPN, r-OPN+GRGDSP (an L-arginyl-glycyl-L-aspartate-dependent integrin receptor antagonist), albumin or vehicle. Neurological impairments, brain edema and BBB disruption were evaluated, and Western blot analyses were performed in the brain at 24 h after SAH.

Results: r-OPN significantly prevented brain edema and BBB disruption compared with the control rats, associated

with the suppression of nuclear factor- κ B and mitogen-activated protein kinase pathways, leading to MMP-9 inactivation. These effects were blocked by GRGDSP.

Conclusions: L-arginyl-glycyl-L-aspartate-dependent integrin receptor-mediated multiple signaling pathways may be involved in the protective effects of r-OPN against BBB disruption after SAH.

Keywords Osteopontin · Blood-brain barrier · Brain injury · Subarachnoid hemorrhage

Introduction

The primary cause of poor outcome after aneurysmal subarachnoid hemorrhage (SAH) is not only cerebral vasospasm, but also early brain injury, whose key pathologic manifestation is the blood-brain barrier (BBB) disruption [1]. Osteopontin (OPN) is a multifunctional extracellular matrix glycoprotein, and recombinant OPN (r-OPN) was reported to be protective against BBB disruption after SAH [1]. However, there are many mediators of BBB disruption [2], and the effects of r-OPN on them have not been determined. The aim of this study was to determine the effects of r-OPN on some upstream mediators of matrix metalloproteinase (MMP)-9 in the endovascular perforation model of SAH in rats.

Materials and Methods

All procedures were approved by Loma Linda University animal care committee.

H. Suzuki, Y. Hasegawa, T. Sugawara, W. Chen, and T. Sozen
Departments of Physiology, Loma Linda University,
School of Medicine, Loma Linda, CA, USA

R. Ayer
Departments of Neurosurgery, Loma Linda University,
School of Medicine, Loma Linda, CA, USA

K. Kanamaru
Department of Neurosurgery, Suzuka Kaisei Hospital, Suzuka, Japan

W. Taki
Department of Neurosurgery, Mie University Graduate
School of Medicine, Tsu, Japan

J.H. Zhang (✉)
Departments of Physiology, Loma Linda University,
School of Medicine, Loma Linda, CA, USA
Departments of Neurosurgery, Loma Linda University,
School of Medicine, Loma Linda, CA, USA
Department of Physiology, Loma Linda University,
School of Medicine, Risley Hall, Room 223, Loma Linda,
CA 92354, USA
e-mail: johnzhang3910@yahoo.com

Experimental Model of SAH and Study Protocol

The endovascular perforation model of SAH was produced in male adult Sprague-Dawley rats (300–370 g, Harlan, Indianapolis, IN) as previously described [1]. A sharpened 4-0 monofilament nylon suture was advanced rostrally into the left internal carotid artery from the left external carotid artery stump until resistance was felt, and then pushed 3 mm further to perforate the bifurcation of the anterior and middle cerebral arteries. Sham-operated rats underwent the identical procedures except that the suture was withdrawn once resistance was felt, without puncture.

One hundred forty-eight rats were divided into sham + vehicle ($n=17$), sham + r-OPN ($n=17$), SAH + vehicle ($n=33$), SAH + 0.1 μg of bovine serum albumin (BSA; $n=11$), SAH + 0.02 μg of r-OPN ($n=28$), SAH + 0.1 μg of r-OPN ($n=31$) and SAH + 0.1 μg of r-OPN + GRGDSP (L-arginyl-glycyl-L-aspartate [RGD] motif-containing hexapeptide; $n=11$) groups. Neurological scores, the severity of SAH, brain edema ($n=5$ per group) and BBB disruption ($n=6$ per group) were assessed, and Western blot analyses ($n=6$ per group) were performed at 24 h post-SAH.

Neurological Scoring

Neurological scores (3–18) were blindly evaluated prior to SAH and at 24 h after SAH as previously described [3]. The scores were calculated by summing up scores of six tests (spontaneous activity, symmetry in the movement of all four limbs, forepaw outstretching, climbing, body proprioception and response to whisker stimulation) that were scored 0–3 or 1–3.

Severity of SAH

The severity of SAH was blindly assessed in all animals at the sacrifice as previously described [3]. The subarachnoid cistern was divided into six segments, and each segment was allotted a grade from 0 to 3 depending on the amount of SAH. The animals received a total score ranging from 0 to 18 after adding the scores.

Intracerebroventricular Infusion

The needle of a 10- μL Hamilton syringe (Hamilton Company, Reno, NV) was inserted through a burr hole into the left

lateral ventricle using the following coordinates relative to the bregma: 1.5 mm posterior; 1.0 mm lateral; 3.2 mm below the horizontal plane of bregma [1]. Sterile phosphate-buffered saline (PBS) vehicle (1 μL) or mouse r-OPN (0.02 or 0.1 μg in 1 μL ; EMD Chemicals, La Jolla, CA) was infused at a rate of 0.5 $\mu\text{L}/\text{min}$ irrespective of the animal's body weight at 1 h before the SAH production or sham operation. GRGDSP (Sigma-Aldrich, St. Louis, MO) was dissolved in 0.1°N acetic acid and was further diluted in PBS (final concentration of acetic acid <1.74%). GRGDSP (100 pmol in 1 μL) was infused together with r-OPN.

Brain Water Content

After sacrificing rats, brains were immediately divided into the right and left cerebral hemispheres, brain stem and cerebellum. Brain specimens were dried in an oven at 105°C for 72 h. The following formula was used to calculate the percentage of water content: $([\text{wet weight} - \text{dry weight}]/\text{wet weight}) \times 100\%$ [1].

BBB Permeability

Evans blue dye (2%; 5 mL/kg) was injected over 2 min into the left femoral vein and allowed to circulate for 60 min. Rats were sacrificed by intracardiac perfusion with PBS, and brains were removed and divided into the same regions as in the water content study. Spectrophotometric quantification of extravasated Evans blue dye was performed as previously described [1].

Western Blot Analyses

Western blot analysis was performed as previously described [1]. Brains were divided into the same regions as in the water content study, and the left (perforation side) cerebral hemisphere was used. Equal amounts of protein samples (50 μg) were loaded on Tris glycine gel, electrophoresed and transferred to a nitrocellulose membrane. Membranes were blocked with a blocking solution, followed by incubation overnight at 4°C with the primary antibodies: rabbit polyclonal anti-phospho-inhibitor of nuclear factor (NF)- κB (I κB)- α (1:200), goat polyclonal anti-phospho-I κB kinase (IKK) α/β (1:200), mouse monoclonal anti-phospho-c-Jun N-terminal kinase (JNK; 1:200), mouse monoclonal anti-phospho-p38 (1:200), rabbit polyclonal anti-phospho-extracellular signal-regulated kinase (ERK)1/2 (1:200) antibodies

(Santa Cruz Biotechnology, Santa Cruz, CA), rabbit polyclonal anti-MMP-9 (1:1,500), and mouse monoclonal anti-vascular endothelial growth factor (VEGF) antibodies (1:1,000, Millipore, Temecula, CA). Immunoblots were processed with appropriate secondary antibodies (1:2,000, Santa Cruz Biotechnology, Santa Cruz, CA) for 1 h at 21°C, and bands were detected with a chemiluminescence reagent kit (ECL Plus; Amersham Bioscience, Arlington Heights, IL). Blot bands were quantified by densitometry with Image J software (NIH, Bethesda, MD). β -Actin (1:2,000, Santa Cruz Biotechnology, Santa Cruz, CA) was blotted on the same membrane as a loading control.

Statistical Analysis

Data were expressed as mean \pm SD, and unpaired *t* tests, chi-square tests or one-way analysis of variance with Tukey-Kramer *post hoc* tests was used as appropriate. $p < 0.05$ was considered significant.

Results

Comparisons of physiological parameters revealed no significant differences among the groups (data not shown). None of the sham-operated rats died. In SAH rats, the

mortality rate in the r-OPN+GRGDSP treatment group (45.5%, 5 of 11 rats) was significantly higher than the 0.1 μ g of r-OPN treatment group (16.1%, 5 of 31 rats), but not the vehicle (24.2%, 8 of 33 rats), 0.1 μ g of BSA (18.2%, 2 of 11 rats) and 0.02 μ g of r-OPN (17.8%, 5 of 28 rats) treatment groups. Among surviving animals, 8 vehicle-, 3 BSA-, 9 0.1 μ g and 6 0.02 μ g of r-OPN-treated SAH rats were not used for further analysis, because their SAH grading scores were nine or less, suggesting that the BBB disruption was mild [1].

The average SAH grading score was similar among the groups in each analysis (12.4 ± 1.9 , 12.8 ± 1.2 , 13.6 ± 2.5 , 12.3 ± 2.2 and 11.7 ± 0.5 in the vehicle [$n = 17$], BSA [$n = 6$], 0.02 μ g of r-OPN [$n = 17$], 0.1 μ g of r-OPN [$n = 17$] and r-OPN+GRGDSP [$n = 6$] treatment groups). The vehicle-, BSA and r-OPN+GRGDSP-treated, but not r-OPN-treated SAH rats showed significant neurological impairment compared with the vehicle- ($n = 17$) or r-OPN-treated sham-operated rats ($n = 17$; Fig. 1). SAH caused a significant increase in brain water content ($n = 5$ per group) and Evans blue dye extravasation ($n = 6$ per group) in all brain regions, which were significantly attenuated by r-OPN treatment in the bilateral cerebral hemispheres (Fig. 2a, b). BSA, a protein with an equivalent weight to r-OPN, had no protective effect on post-SAH Evans blue dye extravasation.

Western blot analysis of the left cerebral hemisphere showed that r-OPN significantly inhibited post-SAH upregulation of VEGF-A and phospho-JNK that was prevented by GRGDSP, as well as increased phosphorylation of IKK α/β

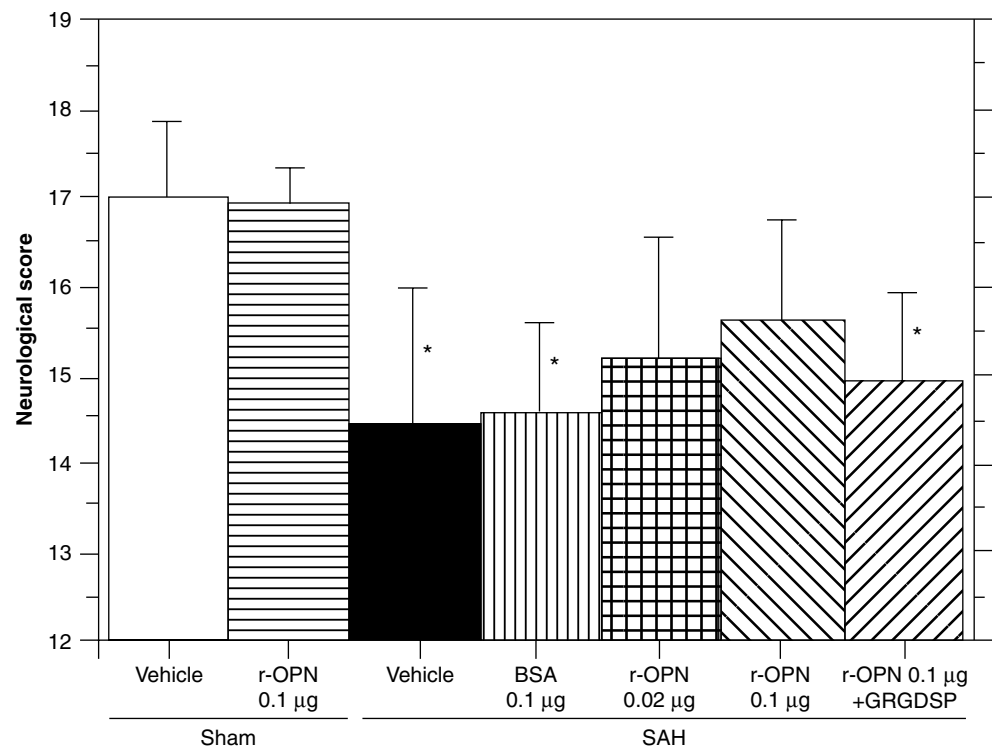


Fig. 1 Effects of r-OPN on neurological scores ($n = 17$): sham operated rats treated with vehicle or r-OPN and SAH rats treated with vehicle, 0.02 μ g or 0.1 μ g of r-OPN; $n = 6$, SAH rats treated with BSA or r-OPN+GRGDSP. * $p < 0.05$ vs. sham-operated rats

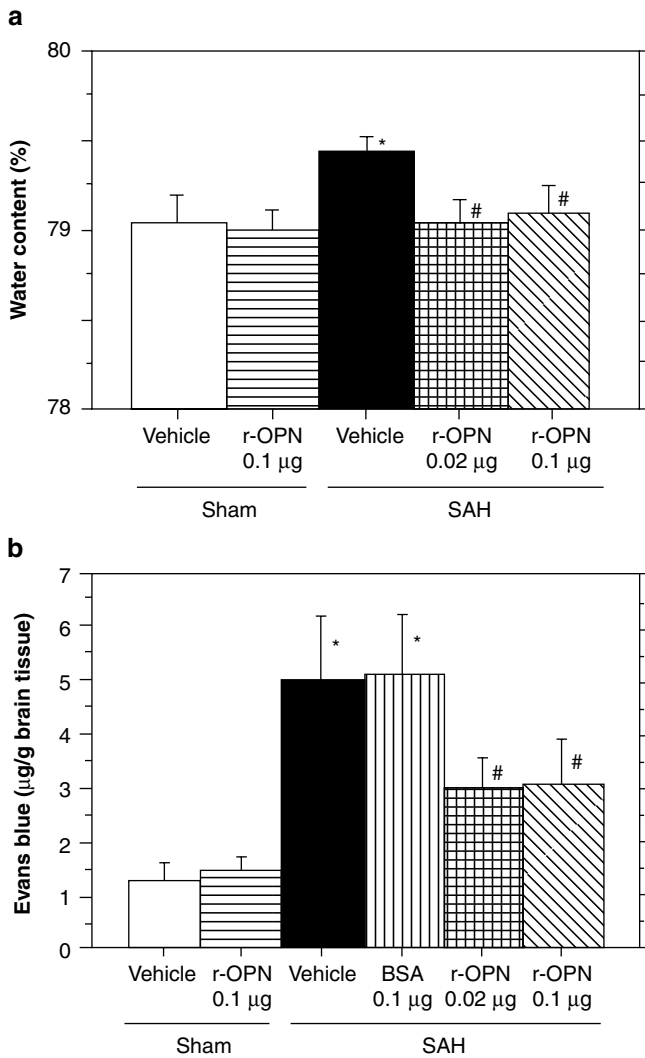


Fig. 2 Effects of r-OPN on brain edema (a) and BBB disruption (b) in the left cerebral hemisphere at 24 h post-SAH. (a) $n=5$ per group; (b) $n=6$ per group; * $p<0.01$ vs. sham-operated rats treated with vehicle or r-OPN; # $p<0.05$ vs. SAH rats treated with vehicle or BSA

and I κ B- α demonstrating the NF- κ B activation ($n=6$, respectively; Fig. 3). Phospho-p38 and phospho-ERK1/2 levels were not significantly changed. SAH significantly increased active MMP-9 expression, which was significantly inhibited by r-OPN treatment at 24 h post-SAH (Fig. 3b).

Discussion

This study confirmed our previous findings that r-OPN treatment improved neurological impairment, brain edema and BBB disruption associated with the inactivation of NF- κ B and MMP-9 after SAH [1]. r-OPN also prevented VEGF-A upregulation and JNK phosphorylation, which were blocked by GRGDSP at 24 h post-SAH.

Accumulated evidence supports a role for MMP-9 in the BBB disruption after SAH [1, 4]. Interleukin-1 β has been repeatedly reported to be induced in the brain after SAH [1, 5, 6], and interleukin-1 β -induced MMP-9 secretion from astrocytes is critically dependent on NF- κ B and mitogen-activated protein kinase (MAPK) signaling pathways [7]. The activation of NF- κ B has been also detected in the cerebral cortices adjacent to SAH [1, 8], suggesting its importance in post-SAH BBB disruption. However, the expression levels of MAPK after SAH were diverse according to reports, possibly because of a limited injury of irregular pattern in cerebral cortex [5, 9, 10].

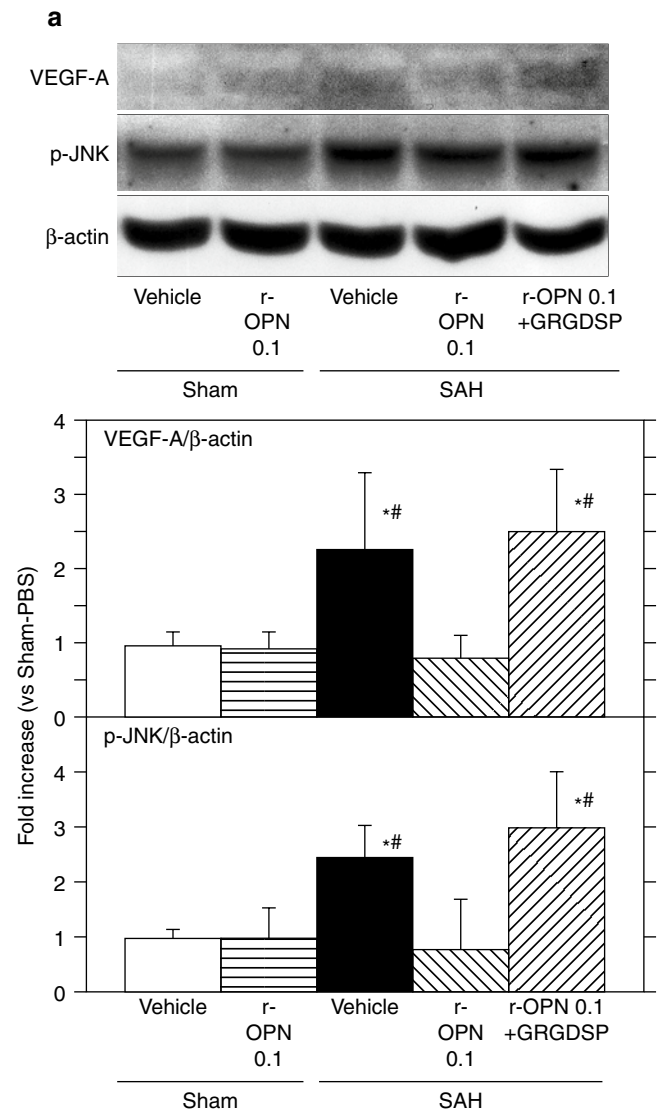


Fig. 3 Effects of r-OPN on VEGF-A, phospho-JNK, (a) phospho-IKK α/β , phospho-I κ B- α and MMP-9 (b) levels in the left cerebral hemisphere at 24 h post-SAH. Expression levels of each protein are expressed as a ratio of β -actin levels for normalization; $n=6$ per group. * $p<0.05$ vs. sham-operated rats; # $p<0.05$, $^{\dagger}p<0.05$ vs. SAH rats treated with 0.1 and 0.02 μ g of r-OPN, respectively

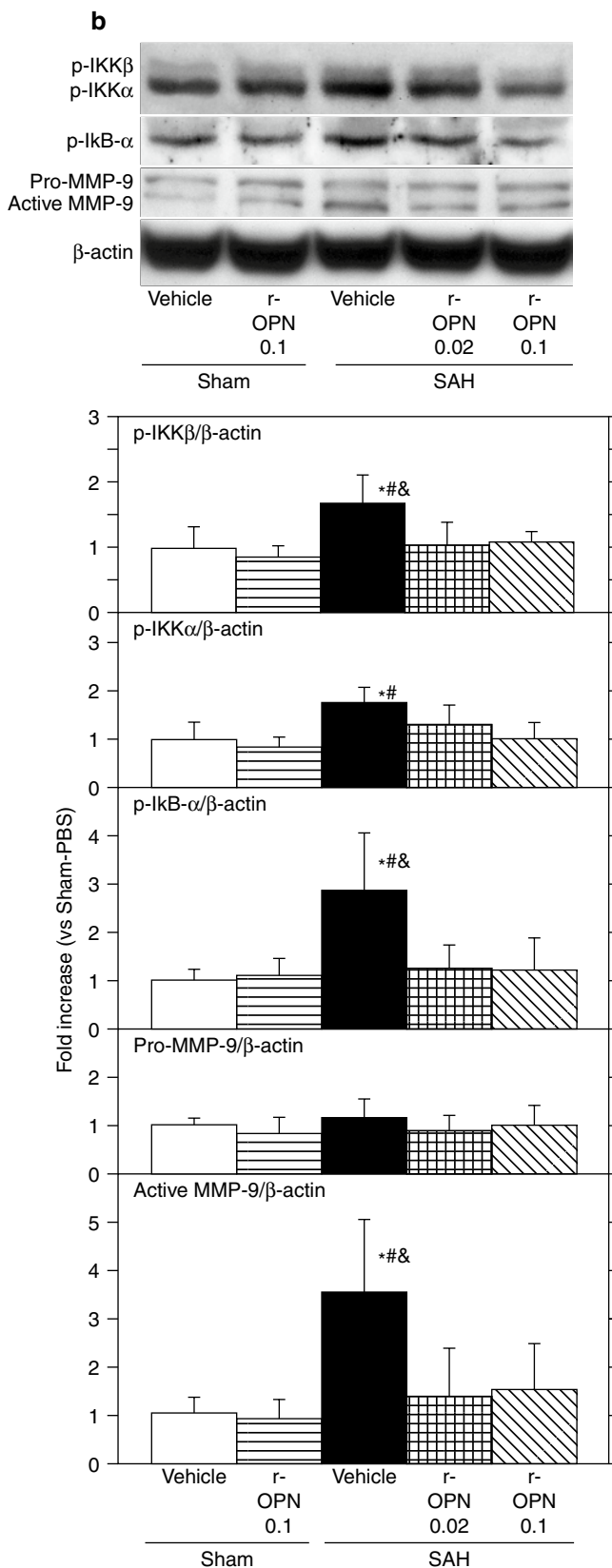


Fig.3 (continued)

VEGF-A, another potent inducer of BBB disruption [2], was also reported to be increased in the cerebral cortex with BBB disruption after SAH [9–11]. MAPK not only mediates the effect of VEGF-A on the BBB permeability, but also induces VEGF-A expression [9, 12]. Interestingly, inhibition of MAPK by an Src-family kinase inhibitor or a JNK inhibitor consistently suppressed VEGF-A expression and prevented BBB disruption after SAH [9, 10]. Taken together, our findings in this study suggest the following three possibilities as the mechanisms of r-OPN-induced MMP-9 suppression and BBB protection: (1) r-OPN may inactivate the NF- κ B pathway; (2) r-OPN may inactivate the JNK pathway, which may be upstream and downstream of VEGF-A, and (3) r-OPN may inactivate VEGF-A and then JNK. r-OPN may suppress these independent or interconnected signaling pathways via binding to RGD-dependent integrin receptors and may prevent post-SAH BBB disruption.

Acknowledgement This study was partially supported by NIH NS053407 to J.H. Zhang.

Conflict of interest statement We declare that we have no conflict of interest.

References

- Suzuki H, Ayer R, Sugawara T, Chen W, Sozen T, Hasegawa Y, Kanamaru K, Zhang JH (2010) Protective effects of recombinant osteopontin on early brain injury after subarachnoid hemorrhage in rats. *Crit Care Med* 38:612–618
- Nag S, Manias JL, Stewart DJ (2009) Pathology and new players in the pathogenesis of brain edema. *Acta Neuropathol* 118: 197–217
- Sugawara T, Ayer R, Jadhav V, Zhang JH (2008) A new grading system evaluating bleeding scale in filament perforation subarachnoid hemorrhage rat model. *J Neurosci Methods* 167: 327–334
- Sehba FA, Mostafa G, Knopman J, Friedrich V Jr, Bederson JB (2004) Acute alterations in microvascular basal lamina after subarachnoid hemorrhage. *J Neurosurg* 101:633–640
- Sozen T, Tsuchiyama R, Hasegawa Y, Suzuki H, Jadhav V, Nishizawa S, Zhang JH (2009) Role of interleukin-1 β in early brain injury after subarachnoid hemorrhage in mice. *Stroke* 40:2519–2525
- Sugawara T, Jadhav V, Ayer R, Chen W, Suzuki H, Zhang JH (2009) Thrombin inhibition by argatroban ameliorates early brain injury and improves neurological outcomes after experimental subarachnoid hemorrhage in rat. *Stroke* 40:1530–1532
- Wu CY, Hsieh HL, Jou MJ, Yang CM (2004) Involvement of p42/p44 MAPK, p38 MAPK, JNK and nuclear factor-kappa B in interleukin-1beta-induced matrix metalloproteinase-9 expression in rat brain astrocytes. *J Neurochem* 90:1477–1488
- Simard JM, Geng Z, Woo SK, Ivanova S, Tosun C, Melnichenko L, Gerzanich V (2009) Glibenclamide reduces inflammation,

- vasogenic edema, and caspase-3 activation after subarachnoid hemorrhage. *J Cereb Blood Flow Metab* 29:317–330
9. Kusaka G, Ishikawa M, Nanda A, Granger DN, Zhang JH (2004) Signaling pathways for early brain injury after subarachnoid hemorrhage. *J Cereb Blood Flow Metab* 24:916–925
 10. Yatsushige H, Ostrowski RP, Tsubokawa T, Colohan A, Zhang JH (2007) Role of c-Jun N-terminal kinase in early brain injury after subarachnoid hemorrhage. *J Neurosci Res* 85:1436–1448
 11. Ostrowski RP, Colohan ART, Zhang JH (2005) Mechanisms of hyperbaric oxygen-induced neuroprotection in a rat model of subarachnoid hemorrhage. *J Cereb Blood Flow Metab* 25: 554–571
 12. Paul R, Zhang ZG, Eliceiri BP, Jiang Q, Boccia AD, Zhang RL, Chopp M, Cheres DA (2001) Src deficiency or blockade of Src activity in mice provides cerebral protection following stroke. *Nat Med* 7:222–227

Protective Effect of Hydrogen Gas Therapy After Germinal Matrix Hemorrhage in Neonatal Rats

Tim Lekic, Anatol Manaenko, William Rolland, Nancy Fathali, Mathew Peterson, Jiping Tang, and John H. Zhang

Abstract *Background:* Germinal matrix hemorrhage (GMH) is a neurological disease of very low birth weight premature infants leading to post-hemorrhagic hydrocephalus, cerebral palsy, and mental retardation. Hydrogen (H₂) is a potent antioxidant shown to selectively reverse cytotoxic oxygen-radical injury in the brain. This study investigated the therapeutic effect of hydrogen gas after neonatal GMH injury.

Methods: Neonatal rats underwent stereotaxic infusion of clostridial collagenase into the right germinal matrix brain region. Cognitive function was assessed at 3 weeks, and then sensorimotor function, cerebral, cardiac and splenic growths were measured 1 week thereafter.

Results: Hydrogen gas inhalation markedly suppressed mental retardation and cerebral palsy outcomes in rats at the juvenile developmental stage. The administration of H₂ gas, early after neonatal GMH, also normalized the brain atrophy, splenomegaly and cardiac hypertrophy 1 month after injury.

Conclusion: This study supports the role of cytotoxic oxygen-radical injury in early neonatal GMH. Hydrogen gas inhalation is an effective strategy to help protect the infant

brain from the post-hemorrhagic consequences of brain atrophy, mental retardation and cerebral palsy. Further studies are necessary to determine the mechanistic basis of these protective effects.

Keywords Hydrogen gas · Neurological deficits · Stroke, experimental

Introduction

Germinal matrix hemorrhage (GMH) is a clinical condition where immature blood vessels rupture within the sub-ventricular (anterior caudate) region during the first week of life [1, 2]. This affects approximately 3.5 per 1,000 births in the United States each year [3]. The clinical consequences are hydrocephalus (post-hemorrhagic ventricular dilation), developmental delay, cerebral palsy and mental retardation [4, 5]. Although this is an important clinical problem, experimental studies investigating therapeutic modalities are lacking [6].

Interventions that target free-radical mechanisms are neuroprotective after brain hemorrhage in adult rats [7–10]. The lysis of red-blood cells after bleeding leads to the release of hemoglobin and other neurotoxins like heme and iron [11–13]. Thrombin will also contribute to this free radical-mediated injury [14–16]. This leads to oxidative damage to proteins, lipids and DNA within the first day [15, 17–20]. As a therapeutic intervention, hydrogen gas is a potent antioxidant that can selectively attenuate neurotoxic oxygen radicals and is known to protect the brain after injury in adult rats after ischemic stroke [21].

In light of this evidence, we hypothesized that hydrogen gas can be a therapeutic strategy for the amelioration of free-radical-mediated brain injury mechanisms. This can improve juvenile cognitive and sensorimotor outcomes after germinal matrix hemorrhage in neonatal rats.

T. Lekic, A. Manaenko, W. Rolland, M. Peterson, and J. Tang
Departments of Physiology, Loma Linda University,
School of Medicine, Loma Linda, CA 92354, USA

N. Fathali
Department of Human Pathology and Anatomy, Loma Linda
University, School of Medicine, Loma Linda, CA 92354, USA

J.H. Zhang (✉)
Departments of Physiology, Loma Linda University,
School of Medicine, Loma Linda, CA 92354, USA and
Department of Human Pathology and Anatomy, Loma Linda
University, School of Medicine, Loma Linda, CA 92354, USA and
Department of Neurosurgery, Loma Linda University,
School of Medicine, Loma Linda, CA 92354, USA and
Department of Physiology, Loma Linda University, School of
Medicine, Risley Hall, Room 223, Loma Linda, CA 92354, USA
e-mail: johnzhang3910@yahoo.com

Methods and Materials

Animal Groups and General Procedures

This study was in accordance with the National Institutes of Health guidelines for the treatment of animals and was approved by the Institutional Animal Care and Use Committee at Loma Linda University. Timed pregnant Sprague-Dawley rats were housed with food and water available *ad libitum*. Treatment consisted of 1 h of hydrogen gas (2.9%, mixed with air and oxygen) administered at 1 h after collagenase infusion. Postnatal day 7 (P7) pups were blindly assigned to the following (n=8/group): sham (naïve), needle (control), needle+hydrogen gas (treatment control), GMH (collagenase-infusion) and GMH+hydrogen gas (treatment). All groups were evenly divided within each litter.

Experimental Model of GMH

Using aseptic technique, rat pups were gently anaesthetized with 3% isoflurane (in mixed air and oxygen) while placed prone onto a stereotaxic frame. Betadine sterilized the surgical scalp area, which was incised in the longitudinal plane to expose the skull and reveal the bregma. The following stereotactic coordinates were determined: 1 mm (anterior), 1.5 mm (lateral) and 3.5 mm (ventral) from bregma. A bore hole (1 mm) was drilled, into which a 27-gauge needle was inserted at a rate of 1 mm/min. A microinfusion pump (Harvard Apparatus, Holliston, MA) infused 0.3 units of clostridial collagenase VII-S (Sigma, St Louis, MO) through a Hamilton syringe. The needle remained in place for an additional 10 min after injection to prevent back-leakage. After needle removal, the burr hole was sealed with bone wax, the incision sutured closed and the animals allowed to recover. The entire surgery took on average 20 min. Upon recovering from anesthesia, the animals were returned to their dams. Needle controls consisted of needle insertion alone without collagenase infusion, while naïve animals did not receive any surgery.

Cognitive Measures

Higher order brain function was assessed during the third week after collagenase infusion. The T-maze assessed short-term (working) memory [22]. Rats were placed into the stem (40 cm × 10 cm) of a maze and allowed to explore until one arm (46 cm × 10 cm) was chosen. From the sequence of

ten trials, of left and right arm choices, the rate of spontaneous alternation (0% = none and 100% = complete, alternations/trial) was calculated, as routinely performed [23, 24]. The Morris water maze assessed spatial learning and memory on four daily blocks, as described previously in detail [25, 26]. The apparatus consisted of a metal pool (110 cm diameter), filled to within 15 cm of the upper edge, with a platform (11 cm diameter) for the animal to escape onto, that changed location for each block (maximum=60 s/trial), and the data were digitally analyzed by Noldus Ethovision tracking software. Cued trials measured place learning with the escape platform visible above water. Spatial trials measured spatial learning with the platform submerged, and probe trials measured spatial memory once the platform was removed. For the locomotor activity, in an open field, the path length in open-topped plastic boxes (49 cm-long, 35.5 cm-wide, 44.5 cm-tall) was digitally recorded for 30 min and analyzed by Noldus Ethovision tracking software [26].

Sensorimotor Function

At 4 weeks after collagenase infusion, the animals were tested for functional ability. Neurodeficit was quantified using a summation of scores (maximum = 12) given for (1) postural reflex, (2) proprioceptive limb placing, (3) back pressure towards the edge, (4) lateral pressure towards the edge, (5) forelimb placement, and (6) lateral limb placement (2 = severe, 1 = moderate, 0 = none), as routinely performed [23]. For the rotarod, striatal ability was assessed using an apparatus consisting of a horizontal, accelerated (2 rpm/5 s), rotating cylinder (7 cm-diameter × 9.5 cm-wide), requiring continuous walking to avoid falling recorded by photobeam circuit (Columbus Instruments) [25, 26]. For foot fault, the number of complete limb missteps through the openings was counted over 2 min while exploring over an elevated wire (3 mm) grid (20 cm × 40 cm) floor [24].

Assessment of Treatment upon Cerebral and Somatic Growth

At the completion of the experiments, the brains were removed and hemispheres separated by midline incision (loss of brain weight has been used as the primary variable to estimate brain damage in juvenile animals after neonatal brain injury [27]). For organ weights, the spleen and heart were separated from surrounding tissue and vessels. The

quantification was performed using an analytical microbalance (model AE 100; Mettler Instrument Co., Columbus, OH) capable of 1.0 µg precision.

Statistical Analysis

Significance was considered at $p < 0.05$. Data were analyzed using analysis of variance (ANOVA), with repeated measures (RM-ANOVA) for long-term neurobehavior. Significant interactions were explored with conservative Scheffé *post hoc* and Mann-Whitney rank sum when appropriate.

Results

Collagenase infusion led to significant cognitive dysfunction in the T maze (working) memory and water maze (spatial) learning and memory (Fig. 1a–c, $p < 0.05$), while hydrogen inhalation significantly ameliorated T maze and water maze (spatial) learning deficits (Fig. 1a, b, $p < 0.05$), without improving spatial memory (Fig. 1c, $p > 0.05$). H₂ also normalized ($p < 0.05$) sensorimotor dysfunction in juvenile GMH animals as shown by the neurodeficit score, number of foot faults and accelerating rotarod falling latency (Fig. 2a–c, $p < 0.05$). Neurological amelioration by hydrogen was confirmed with improvement upon brain atrophy, splenomegaly and cardiomegaly, compared to the juvenile vehicle-treated animals (Fig. 3a–c, $p < 0.05$).

Discussion

The findings of this study indicate that the inhalation of hydrogen gas, early after neonatal GMH, can improve brain atrophy, mental retardation, cerebral palsy, splenomegaly and cardiac hypertrophy in juvenile animals 1 month later. The therapeutic implications of H₂ inhalation point to the pathophysiological role of cytotoxic oxygen-radical injury [21]. These outcomes support the findings from other brain injury studies to provide preliminary evidence about the importance of oxidative stress mechanisms on outcomes after neonatal GMH [7, 8, 10].

H₂ inhalation is a neuroprotectant shown to ameliorate brain injury in an adult animal model of cerebral ischemia [21]. This study supports the notion that the hydrogen gas has no adverse affects in neonatal rats, and can be applied as a strategy to improve functional outcomes after brain injury from hemorrhagic stroke in premature infants. Further investigation is needed to determine the mechanistic basis of these neuroprotective effects.

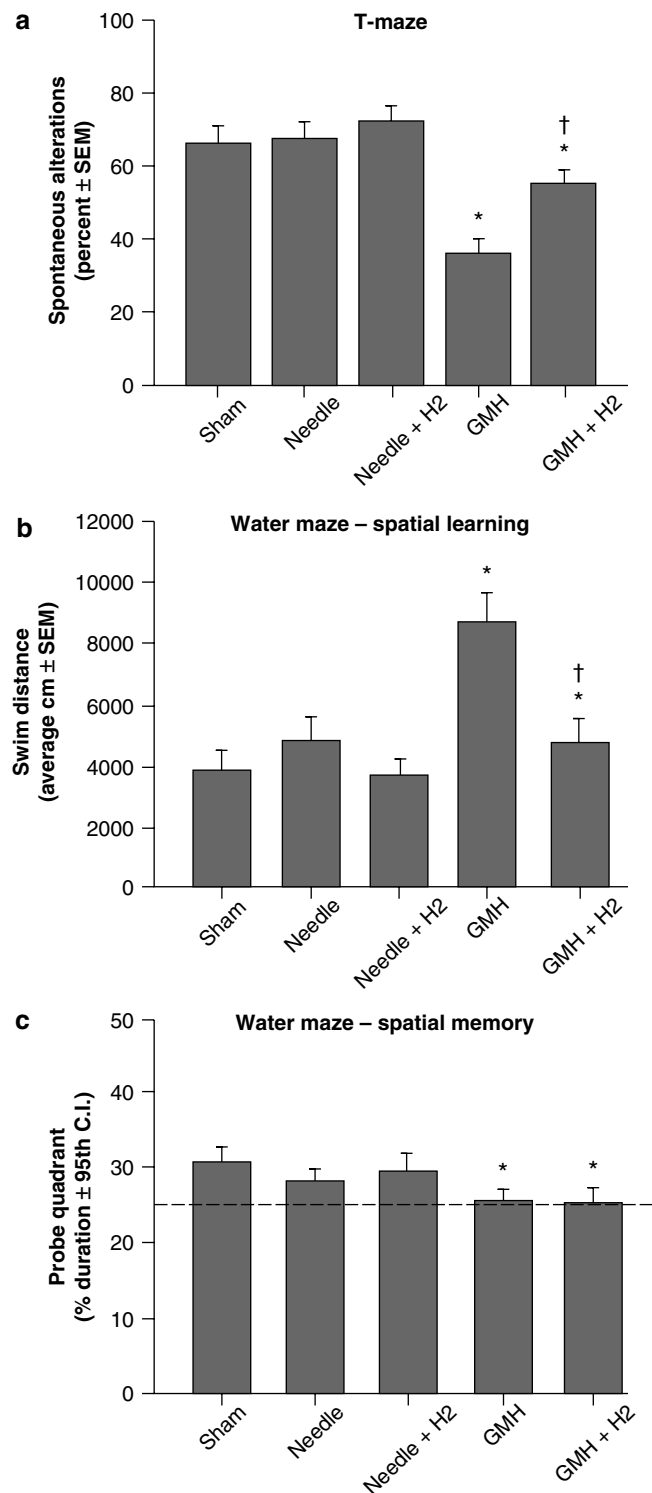


Fig. 1 Cognitive function normalization in juvenile rats by hydrogen gas (H₂) after neonatal GMH. Higher order function was measured at the third week after collagenase infusion: (a) T maze, (b) spatial learning water maze, (c) spatial memory (probe) water maze. Values expressed as mean ± 95th CI (probe quadrant) or mean ± SEM (all others), $n = 8$ (per group), * $p < 0.05$ compared with controls (sham and needle trauma) and † $p < 0.05$ compared with GMH

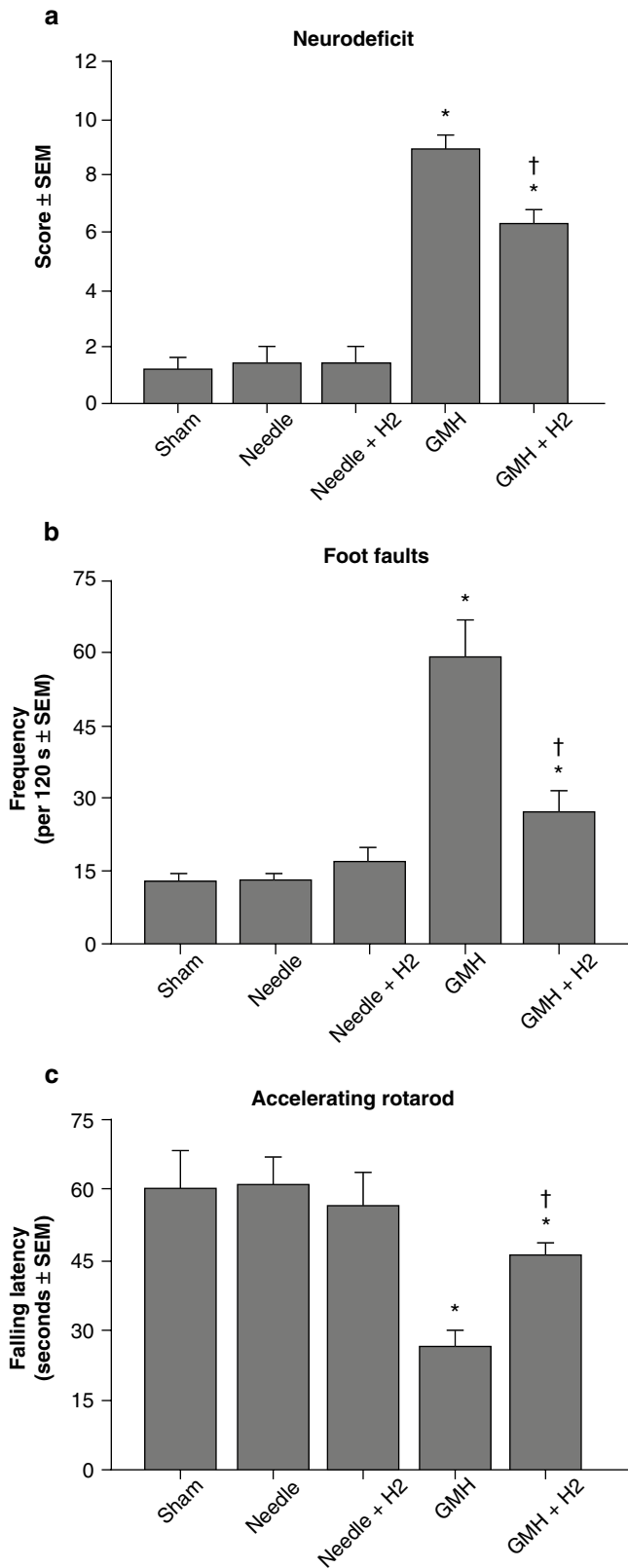


Fig. 2 Sensorimotor function normalization in juvenile rats by hydrogen gas (H₂) after neonatal GMH. Cerebral palsy measurements were performed in the juveniles at 1 month after collagenase infusion: (a) neurodeficit score, (b) foot faults and (c) rotarod. Values expressed as mean ± SEM, *n* = 8 (per group), **p* < 0.05 compared with controls (sham and needle trauma), and †*p* < 0.05 compared with GMH

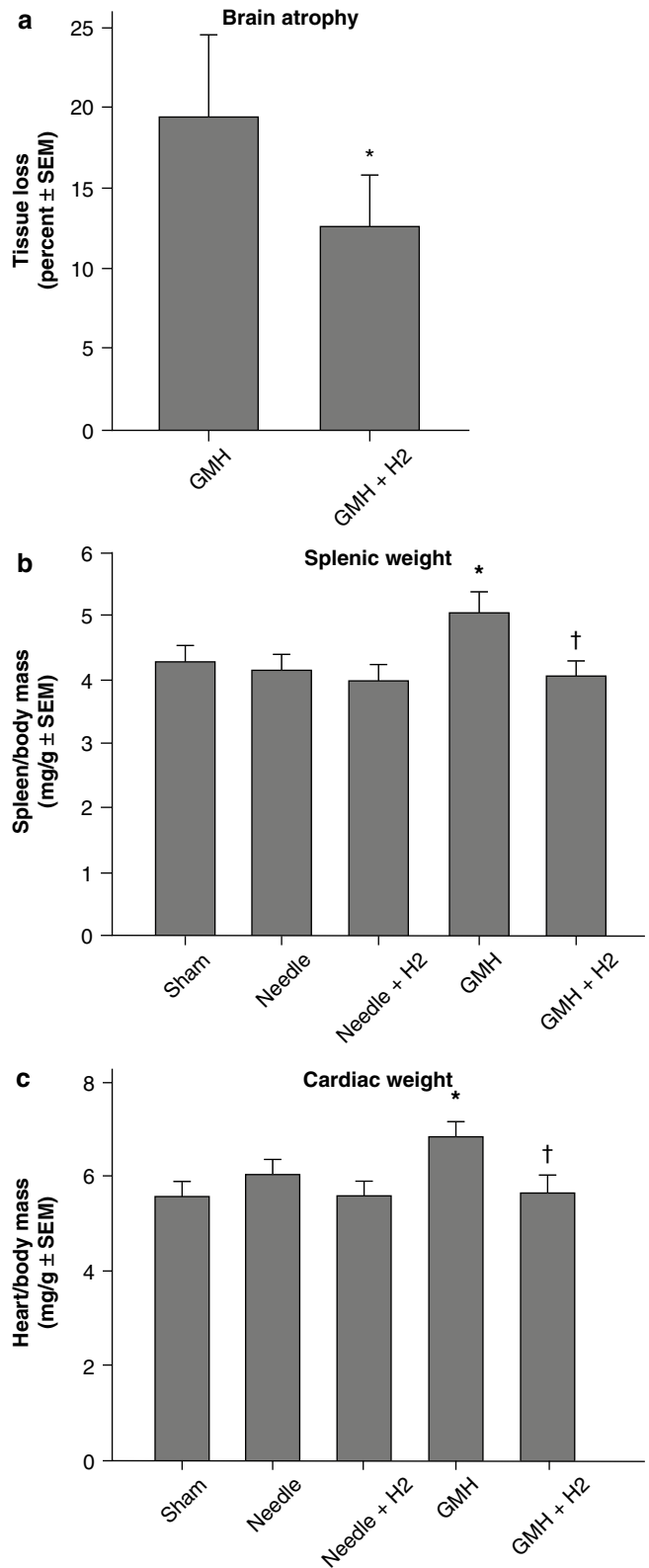


Fig. 3 Cerebral and somatic growth normalization in juvenile rats by hydrogen gas (H₂) after GMH. (a) Brain atrophy (percent tissue loss), (b) splenic weight and (c) cardiac weight were measured at 4 weeks after injury. Values expressed as mean ± SEM, *n* = 8 (per group), **p* < 0.05 compared with controls (sham and needle trauma), and †*p* < 0.05 compared with GMH

Acknowledgements This study was partially supported by a grant (NS053407) from the National Institutes of Health to J.H.Z.

Conflict of interest statement We declare that we have no conflict of interest.

References

- Ballabh P (2010) Intraventricular hemorrhage in premature infants: mechanism of disease. *Pediatr Res* 67:1–8. doi:10.1203/PDR.0b013e3181c1b176
- Kadri H, Mawla AA, Kazah J (2006) The incidence, timing, and predisposing factors of germinal matrix and intraventricular hemorrhage (GMH/IVH) in preterm neonates. *Childs Nerv Syst* 22:1086–1090. doi:10.1007/s00381-006-0050-6
- Heron M, Sutton PD, Xu J, Ventura SJ, Strobino DM, Guyer B (2010) Annual summary of vital statistics: 2007. *Pediatrics* 125:4–15. doi:peds.2009-2416 [pii], 10.1542/peds.2009-2416
- Ballabh P, Braun A, Nedergaard M (2004) The blood-brain barrier: an overview: structure, regulation, and clinical implications. *Neurobiol Dis* 16:1–13. doi:10.1016/j.nbd.2003.12.016, S0969996103002833 [pii]
- Murphy BP, Inder TE, Rooks V, Taylor GA, Anderson NJ, Mogridge N, Horwood LJ, Volpe JJ (2002) Posthaemorrhagic ventricular dilatation in the premature infant: natural history and predictors of outcome. *Arch Dis Child Fetal Neonatal Ed* 87:F37–F41
- Balasubramaniam J, Del Bigio MR (2006) Animal models of germinal matrix hemorrhage. *J Child Neurol* 21:365–371
- Peeling J, Del Bigio MR, Corbett D, Green AR, Jackson DM (2001) Efficacy of disodium 4-[(tert-butylimino)methyl]benzene-1, 3-disulfonate N-oxide (NXY-059), a free radical trapping agent, in a rat model of hemorrhagic stroke. *Neuropharmacology* 40:433–439. doi:S0028390800001702 [pii]
- Peeling J, Yan HJ, Chen SG, Campbell M, Del Bigio MR (1998) Protective effects of free radical inhibitors in intracerebral hemorrhage in rat. *Brain Res* 795:63–70. doi:S0006-8993(98)00253-4 [pii]
- Peeling J, Yan HJ, Corbett D, Xue M, Del Bigio MR (2001) Effect of FK-506 on inflammation and behavioral outcome following intracerebral hemorrhage in rat. *Exp Neurol* 167:341–347. doi:10.1006/exnr.2000.7564, S0014-4886(00)97564-2 [pii]
- Nakamura T, Kuroda Y, Yamashita S, Zhang X, Miyamoto O, Tamiya T, Nagao S, Xi G, Keep RF, Itano T (2008) Edaravone attenuates brain edema and neurologic deficits in a rat model of acute intracerebral hemorrhage. *Stroke* 39:463–469. doi:STROKEAHA.107.486654 [pii], 10.1161/STROKEAHA.107.486654
- Wagner KR, Sharp FR, Ardizzone TD, Lu A, Clark JF (2003) Heme and iron metabolism: role in cerebral hemorrhage. *J Cereb Blood Flow Metab* 23:629–652. doi:10.1097/01.WCB.0000073905.87928.6D
- Wu J, Hua Y, Keep RF, Nakamura T, Hoff JT, Xi G (2003) Iron and iron-handling proteins in the brain after intracerebral hemorrhage. *Stroke* 34:2964–2969. doi:10.1161/01.STR.0000103140.52838.45, 01.STR.0000103140.52838.45 [pii]
- Xi G, Keep RF, Hoff JT (2006) Mechanisms of brain injury after intracerebral haemorrhage. *Lancet Neurol* 5:53–63. doi: S1474-4422(05)70283-0 [pii], 10.1016/S1474-4422(05)70283-0
- Xi G, Wagner KR, Keep RF, Hua Y, de Courten-Myers GM, Broderick JP, Brott TG, Hoff JT (1998) Role of blood clot formation on early edema development after experimental intracerebral hemorrhage. *Stroke* 29:2580–2586
- Nakamura T, Keep RF, Hua Y, Hoff JT, Xi G (2005) Oxidative DNA injury after experimental intracerebral hemorrhage. *Brain Res* 1039:30–36. doi:S0006-8993(05)00104-6 [pii], 10.1016/j.brainres.2005.01.036
- Lee KR, Colon GP, Betz AL, Keep RF, Kim S, Hoff JT (1996) Edema from intracerebral hemorrhage: the role of thrombin. *J Neurosurg* 84:91–96
- Xi G, Keep RF, Hoff JT (1998) Erythrocytes and delayed brain edema formation following intracerebral hemorrhage in rats. *J Neurosurg* 89:991–996
- Huang FP, Xi G, Keep RF, Hua Y, Nemoianu A, Hoff JT (2002) Brain edema after experimental intracerebral hemorrhage: role of hemoglobin degradation products. *J Neurosurg* 96:287–293
- Nakamura T, Keep RF, Hua Y, Nagao S, Hoff JT, Xi G (2006) Iron-induced oxidative brain injury after experimental intracerebral hemorrhage. *Acta Neurochir Suppl* 96:194–198
- Zhao X, Sun G, Zhang J, Strong R, Song W, Gonzales N, Grotta JC, Aronowski J (2007) Hematoma resolution as a target for intracerebral hemorrhage treatment: role for peroxisome proliferator-activated receptor gamma in microglia/macrophages. *Ann Neurol* 61:352–362. doi:10.1002/ana.21097
- Ohsawa I, Ishikawa M, Takahashi K, Watanabe M, Nishimaki K, Yamagata K, Katsura K, Katayama Y, Asoh S, Ohta S (2007) Hydrogen acts as a therapeutic antioxidant by selectively reducing cytotoxic oxygen radicals. *Nat Med* 13:688–694. doi:nm1577 [pii], 10.1038/nm1577
- Hughes RN (2004) The value of spontaneous alternation behavior (SAB) as a test of retention in pharmacological investigations of memory. *Neurosci Biobehav Rev* 28:497–505. doi:S0149-7634(04)00073-9 [pii], 10.1016/j.neubiorev.2004.06.006
- Fathali N, Ostrowski RP, Lekic T, Jadhav V, Tong W, Tang J, Zhang JH (2010) Cyclooxygenase-2 inhibition provides lasting protection against neonatal hypoxic-ischemic brain injury. *Crit Care Med* 38:572–578. doi:10.1097/CCM.0b013e3181cb1158
- Zhou Y, Fathali N, Lekic T, Tang J, Zhang JH (2009) Glibenclamide improves neurological function in neonatal hypoxia-ischemia in rats. *Brain Res* 1270:131–139. doi:S0006-8993(09)00520-4 [pii], 10.1016/j.brainres.2009.03.010
- Lekic T, Hartman R, Rojas H, Manaenko A, Chen W, Ayer R, Tang J, Zhang JH (2010) Protective effect of melatonin upon neuropathology, striatal function, and memory ability after intracerebral hemorrhage in rats. *J Neurotrauma* 27:627–637. doi:10.1089/neu.2009.1163
- Hartman R, Lekic T, Rojas H, Tang J, Zhang JH (2009) Assessing functional outcomes following intracerebral hemorrhage in rats. *Brain Res* 1280:148–157. doi:S0006-8993(09)00957-3 [pii], 10.1016/j.brainres.2009.05.038
- Andine P, Thordstein M, Kjellmer I, Nordborg C, Thiringer K, Wennberg E, Hagberg H (1990) Evaluation of brain damage in a rat model of neonatal hypoxic-ischemia. *J Neurosci Methods* 35:253–260

Pretreatment with Normobaric and Hyperbaric Oxygenation Worsens Cerebral Edema and Neurologic Outcomes in a Murine Model of Surgically Induced Brain Injury

David Westra, Wanqiu Chen, Reiko Tsuchiyama, Austin Colohan, and John H. Zhang

Abstract *Background:* Hyperbaric oxygenation is a readily available treatment modality, and its ability to improve neurological outcomes in a variety of animal models has been demonstrated. This study was designed to investigate the use of a single pretreatment regimen of either hyperbaric oxygenation or normobaric oxygenation to determine its effects in a murine model of surgically induced brain injury (SBI). *Materials and Methods:* Hyperbaric oxygen (2.5ATM, 1 h), normobaric oxygen (100% FIO₂, 1 h) or room air (21% FIO₂, 1 h) was applied on CD-1 mice immediately, or at 1, 2 or 3 h followed by SBI or sham surgical operation. Neurological assessment of the animals was done by a blinded observer at 24 and 72 h using a 21-point modified Garcia scale, wire hanging test, and beam balance test. The brain edema was evaluated using brain water content at 24 and 72 h after SBI. *Results:* There was no statistically significant difference in the mortality rate after treatment compared with the SBI group. The brain water content after SBI was significantly increased in the right (ipsilateral) frontal lobe surrounding the site of surgical resection compared with the sham group. Both hyperbaric and normobaric oxygen treatment significantly increased the brain edema and worsened the neurological outcomes using a 21-point Garcia score compared

with the SBI group. The brain edema at 24 h after injury was most pronounced in the group treated with normobaric oxygenation 2 h prior to surgery. These differences disappeared at 72 h after SBI. *Conclusion:* Immediate pretreatment with either hyperbaric (2.5ATM, 1 h) or normobaric oxygen (100% FIO₂, 1 h) increased brain edema and worsened neurological function at 24 h following SBI.

Keywords Hyperbaric oxygenation · Lipid peroxidation · Surgically induced brain injury

Introduction

Hyperbaric oxygenation (HBO) is a treatment modality that is currently available in many hospitals throughout the world. Its use in experimental animal models of brain injury secondary to ischemia, neonatal hypoxia, and traumatic brain injury, among others, is widespread and has given us insight into the underlying pharmacology of hyperbaric oxygenation. In addition, it has been shown to reduce the mortality rate in prospective randomized trials of severely brain injured patients by up to 50% [1, 2]. The main mechanism appears to be a significant increase in brain PO₂ after injury [3]. Other mechanisms include preserving the integrity of the blood-brain-barrier [4–6], reduction of cerebral blood flow and cerebral edema [5, 7], reduction of acute stage endothelin [8], reduction of neutrophil adhesion and infiltration [9, 10], caspase 9 activity [11], and inhibition of HIF-1 α and its target genes [12, 13]. However, it has also been reported that HBO treatment increased expression of cytochrome C [14], Bcl-2 [15], Bax [14], metalloproteinase-2, metalloproteinase-9 [10], and L-arginine (Demchenko et al. 2002). In addition, it has been shown in animals and in humans to enhance aerobic metabolism at the cellular level through improvements in mitochondrial recovery [2, 5]. As levels of oxygen increase, the levels of oxygen-free radicals also increase, which causes an increase in lipid peroxidation

D. Westra and A. Colohan
Department of Neurosurgery, Loma Linda University Medical Center,
Loma Linda, CA, USA

W. Chen and R. Tsuchiyama
Department of Physiology and Pharmacology, Loma Linda University,
School of Medicine, Loma Linda, CA, USA

J.H. Zhang (✉)
Department of Neurosurgery, Loma Linda University Medical Center,
Loma Linda, CA, USA and
Department of Physiology and Pharmacology, Loma Linda University,
School of Medicine, Loma Linda, CA, USA and
Department of Physiology and Pharmacology, Loma Linda University,
School of Medicine, Risley Hall, Room 214, Loma Linda, CA
92350, USA
e-mail: johnzhang3910@yahoo.com

[3, 16]. However, this increase in brain lipid peroxidation has not been demonstrated in all animal models [4]. Lipid peroxidation can cause damage to cellular organelles and can lead to cell lysis through oxidative DNA damage [17]. Despite the possible side effects caused by lipid peroxidation, hyperbaric oxygenation would be a desirable therapy since hyperbaric chambers are already present in hospitals around the world for wound care and could be readily adapted for use in the neurosurgical patient population.

Surgically induced brain injury (SBI) takes place during every intramedullary cranial surgery, and it can adversely affect patient outcomes and increase mortality. The brain reacts to insult through breakdown of the blood-brain-barrier and secondary activation of the immune system leading to neutrophil infiltration, release of inflammatory mediators, and cerebral edema. Cerebral edema adversely affects neuronal function in the area affected and can lead to worse patient outcomes. Marked cerebral edema can lead to increased intracranial pressure, herniation syndromes, and death. In animal models of surgically induced brain injury and traumatic brain injury, multiple exposures to hyperbaric oxygenation preoperatively have resulted in attenuation of cerebral edema through vasoconstriction and improvement in neurological outcomes [5]. In addition, in animals undergoing middle cerebral artery occlusion, hyperbaric oxygenation appeared to attenuate tissue hypoxia in the penumbra and improve neurological outcomes [17, 18].

Given the widespread presence of hyperbaric oxygen chambers throughout the world and various beneficial reports, it would be helpful to be able to utilize this already present resource to decrease postoperative complications and improve outcomes in the neurosurgical patient population. If this model were successfully applied to the neurosurgical

patient population, every patient undergoing elective cranial surgery would have to be admitted 5 days preoperatively in order to receive hyperbaric oxygenation. Given the limited resources and increasing costs of health care, it would be beneficial if these same effects could be obtained through a single hyperbaric oxygenation pretreatment on the morning of surgery.

Materials and Methods

Surgical Procedure

All procedures were approved by Loma Linda University Animal Care Committee. Following anesthesia with ketamine (100 mg/kg) and xylazine (10 mg/kg) intraperitoneally, the CD-1 mice were placed in a stereotaxic frame. A 1-cm midline incision was made on the back of the head, and a right frontal craniotomy using the high speed drill was made from the bregma anteriorly, midline medially, 2–3 mm medial to the orbit laterally, and 5 mm posterior to the bregma. The underlying brain was cauterized using monopolar cautery until the visible brain was removed to the base of the anterior cranial fossa (Fig. 1). Once hemostasis was obtained using cautery, irrigation, and packing sponges, the overlying skin was closed with interrupted 3-0 silk suture. Sham-operated animals underwent the same surgical procedure; however, only craniotomy was included without any dural incisions. Vital signs were monitored throughout the procedure. All mice were kept under a heating lamp to maintain the core body temperature at 35°C until recovery.

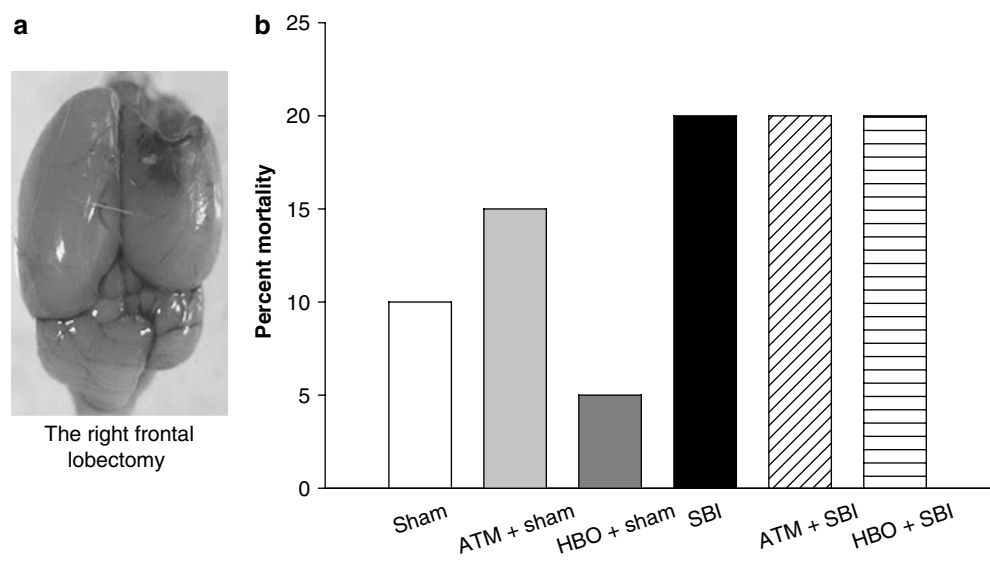


Fig. 1 Surgical brain injury and mortality rate. (a) Top view of the right frontal lobectomy in the surgically induced brain injury model. (b) Mortality rate of six experimental groups, including sham, ATM+sham, HBO+sham, SBI, ATM+SBI, HBO+SBI

Experiment Groups

There were a total of six groups in the experiment, including sham, ATM+sham, HBO+sham, SBI, ATM+SBI, and HBO+SBI. The HBO pretreatment groups were placed into the hyperbaric oxygen chamber with 100% O₂, and the pressure was increased to 2.5 ATM where it was held for 1 h. The ATM pretreatment groups were placed into the hyperbaric oxygenation chamber where they inhaled 100% oxygen at 1.0 ATM for 1 h and then removed. The sham group had no pretreatment and underwent sham surgery.

The experiment was subdivided into two parts. (1) To examine the effectiveness of the normobaric and hyperbaric preoperative oxygenation in reducing cerebral edema 24 h postoperatively, 20 CD-1 mice were placed in each of six groups, and preoperative 2.5 ATM HBO or 1.0 ATM 100% O₂ was given followed by sham operation or SBI. (2) To determine the optimum timeframe to administer the preoperative oxygenation, five mice were assigned to each of six groups, and 1 h pretreatment was received. Afterwards, SBI or sham surgery was performed immediately (0 h) or at 1, 2, or 3 h elapsed time between the time when the pretreatment finished and the operative intervention began.

Brain Water Content

The brain water content was calculated similarly as in previous studies [19]. The animals were killed under deep anesthesia 24 h after surgery, and the brains were immediately removed and divided into six parts: right frontal lobe, left frontal lobe, right parietal lobe, left parietal lobe, cerebellum, and brain stem. These parts were weighed immediately (wet weight) and weighed again after drying in an oven at 105°C for 72 h (dry weight). The percentage of water content was calculated as [(wet weight – dry weight)/wet weight] × 100%.

Neurological Behavioral Tests

All mice underwent neurological scoring 24 and 72 h after surgery. Three neurological tests were used, including a modified 21-point Garcia score, wire hanging, and beam balance test as previously described [19]. All the tests were recorded by an observer blinded to the experimental groups. The 21-point Garcia score consists of seven areas of evaluation: spontaneous activity, response to side stroking, response to vibration touch, evaluation of limb usage symmetry, lateral turning, climbing, and forelimb walking. Each area was

graded from 0 to 3, with 3 being a perfect score. The numbers were then added to obtain the total 21-point Garcia neurological score. The wire hanging and beam balance tests were scored from 0 to 5, considering the time spent and distance traveled.

Statistics

All the data are expressed as mean ± SEM. The statistical significance was verified by one-way ANOVA statistical analysis. The mortality rate was analyzed by chi-square test. A probability value of $p < 0.05$ was considered statistically significant.

Results

There were no statistically significant differences in the mortality rate between either the ATM+sham with SBI group (20% vs. 20%) or HBO+sham with SBI group (20% vs. 20%) (Fig. 1b). Brain edema was assessed by measuring the brain water content in different areas of the brain 24 h after surgery (Fig. 2). There was significantly increased brain water content in the right frontal brain subjected to SBI when compared with the sham group (83.3% ± 0.37 vs. 80.6% ± 0.16, * $p < 0.05$, ANOVA). There was no significant difference in the brain water content between the SBI and sham groups in other brain areas. One hour 1.0 ATM pretreatment significantly increased right frontal brain water content compared with the SBI group (86.6% ± 0.79 vs. 83.3% ± 0.37, $p < 0.05$, ANOVA). In the ATM+SBI group, the brain water content in the right frontal (86.6% ± 0.79), right parietal (82.2% ± 0.59), and left parietal (80.9% ± 0.33) area was significantly higher compared with the comparable brain areas in the ATM+sham group (* $p < 0.05$, ANOVA). In the HBO+SBI group, there was significantly increased brain water content in the right parietal (81.2% ± 0.42) and left parietal (80.3% ± 0.34) brain when compared with the HBO+sham group ($p < 0.05$, ANOVA). Moreover, both ATM and HBO pretreatment significantly increased the brain water content in the right frontal area when compared with the SBI group (* $p < 0.05$). There was no significant difference in the brain water content among all the three sham groups in all the brain areas.

Neurological function evaluation was performed 24 and 72 h after surgery (Fig. 3). For the 21-point Garcia neurological scoring, the mice subjected to SBI had worsened scores when compared with the sham group (* $p < 0.05$) 24 h, but not 72 h after SBI. Moreover, there was a statistically significant worsening of neurological scores between the HBO+SBI and SBI group (11.6 ± 1.24 vs. 16.2 ± 1.23,

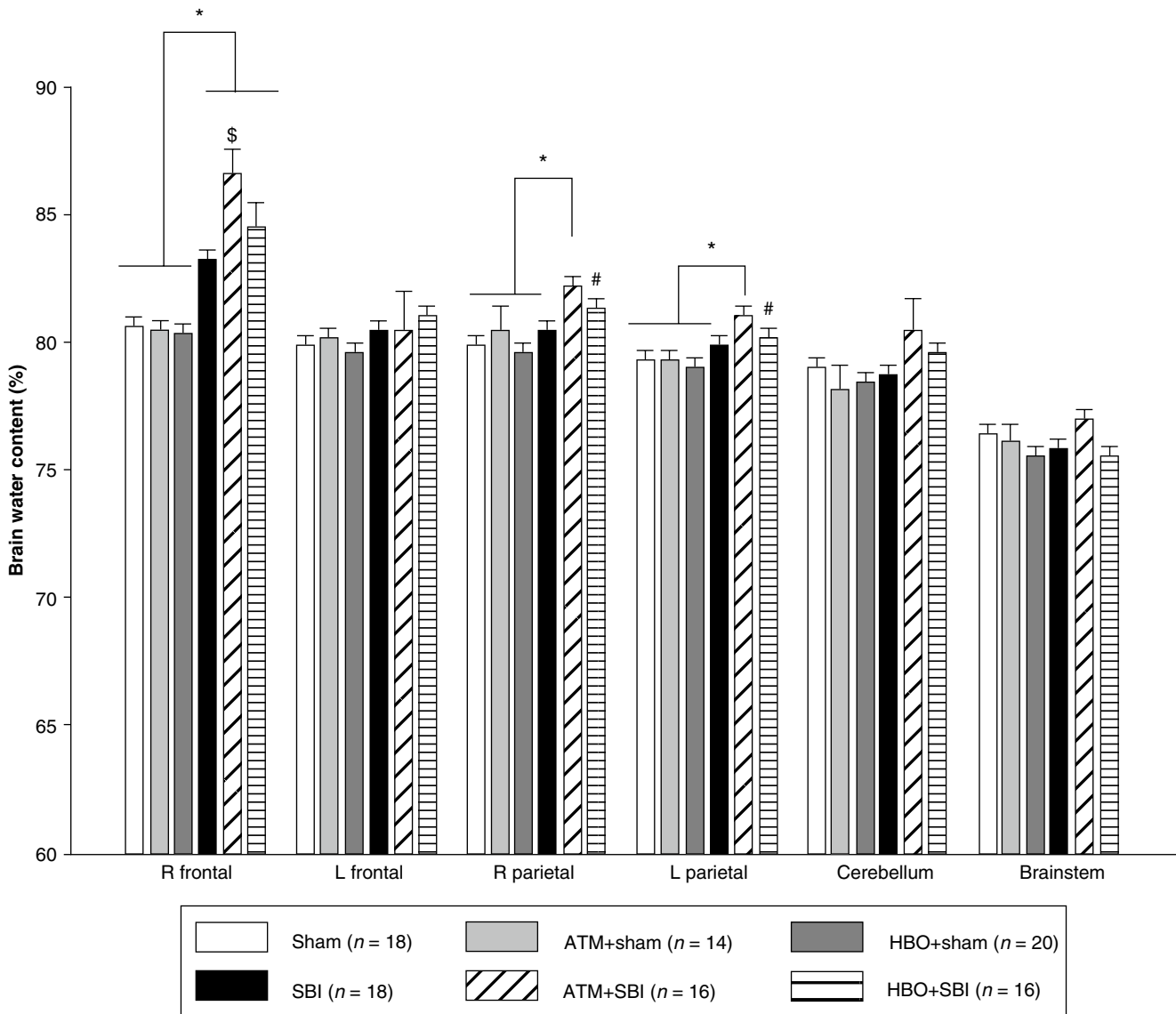


Fig. 2 Brain edema at 24 h following SBI. Quantification of brain water content in the right frontal lobe, left frontal lobe, right parietal lobe, left parietal lobe, cerebellum, and brain stem at 24 h after SBI or sham operation. After SBI, there was significantly increased brain water content in the right frontal area compared with the sham group ($*p < 0.05$, ANOVA). One hour 1.0 ATM pretreatment significantly increased right frontal brain water content compared with the SBI group

($*p < 0.05$, ANOVA). Both ATM and HBO pretreatment significantly increased right frontal brain water content compared with the comparable sham group ($*p < 0.05$, ANOVA). In the HBO+SBI group, the brain water content in the right and left parietal area was significantly increased compared with the HBO+sham group ($*p < 0.05$, ANOVA). There was no statistical difference among the groups in the left frontal area, cerebellum, and brain stem. All vertical bars indicate SEM

$\#p < 0.05$, ANOVA) and ATM+SBI and SBI group (10.2 ± 1.43 vs. 16.2 ± 1.23 , $p < 0.05$, $\#p < 0.05$, ANOVA) 24 h after SBI. For the 72 h 21-point Garcia neurological scoring, there was a significant difference between the ATM+SBI and ATM+sham group (16.3 ± 1.65 vs. 20.4 ± 0.50 , $*p < 0.05$). However, there was no difference in Garcia score between the HBO+SBI and SBI group 72 h following surgery. For the 24 h wire hanging test (Fig. 3b), the mice subjected to SBI had worsened scores when compared with the sham group (2.4 ± 0.36 vs. 4.6 ± 0.19 , $*p < 0.001$, ANOVA). Both

ATM+SBI and HBO+SBI groups did not improve their neurological performance. There was no statistically significant difference after either ATM or HBO pretreatment compared with SBI groups ($p > 0.05$). At 72-h wire hanging test, there was no difference among all the groups. For the 24-h beam balance test, the mice subjected to SBI had worsened scores when compared with the sham group (2.2 ± 0.41 vs. 4.9 ± 0.13 , $*p < 0.001$, ANOVA). Both ATM and HBO pretreatment did not improve the score. At 72-h beam balance test, there was no difference among all the groups.

Fig. 3 Neurological score 24 and 72 h following SBI. **(a)** The 21-point Garcia score test. At 24 h following SBI, the mice had worsened scores when compared with the sham group at 24 h ($*p < 0.05$, ANOVA), but not 72 h after SBI. Both ATM and HBO pretreatment significantly worsen the score compared with the SBI group ($*p < 0.05$, ANOVA). At 72 h following SBI, the score for the ATM+SBI group is significantly worse than for the ATM+sham group ($*p < 0.05$, ANOVA). **(b)** Wire hanging test. The mice subjected to SBI had worsened scores when compared with the sham group ($*p < 0.05$, ANOVA) 24 h after SBI. Both ATM and HBO pretreatment did not improve the score. There was no difference among all the groups at 72 h following SBI. **(c)** Beam score test. For the 24 h beam balance test, the mice scored significantly worse after SBI ($*p < 0.001$, ANOVA). Both ATM and HBO pretreatment did not improve the score. For the 72 h beam balance test, there was no difference among all the groups

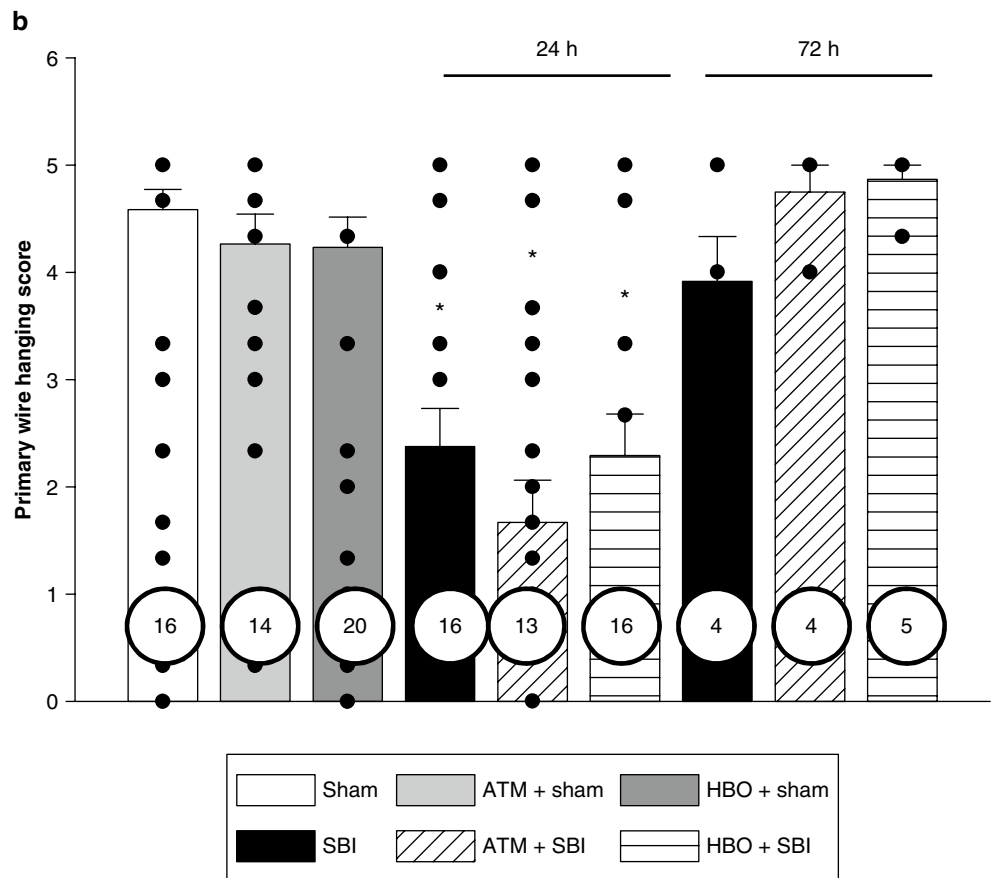
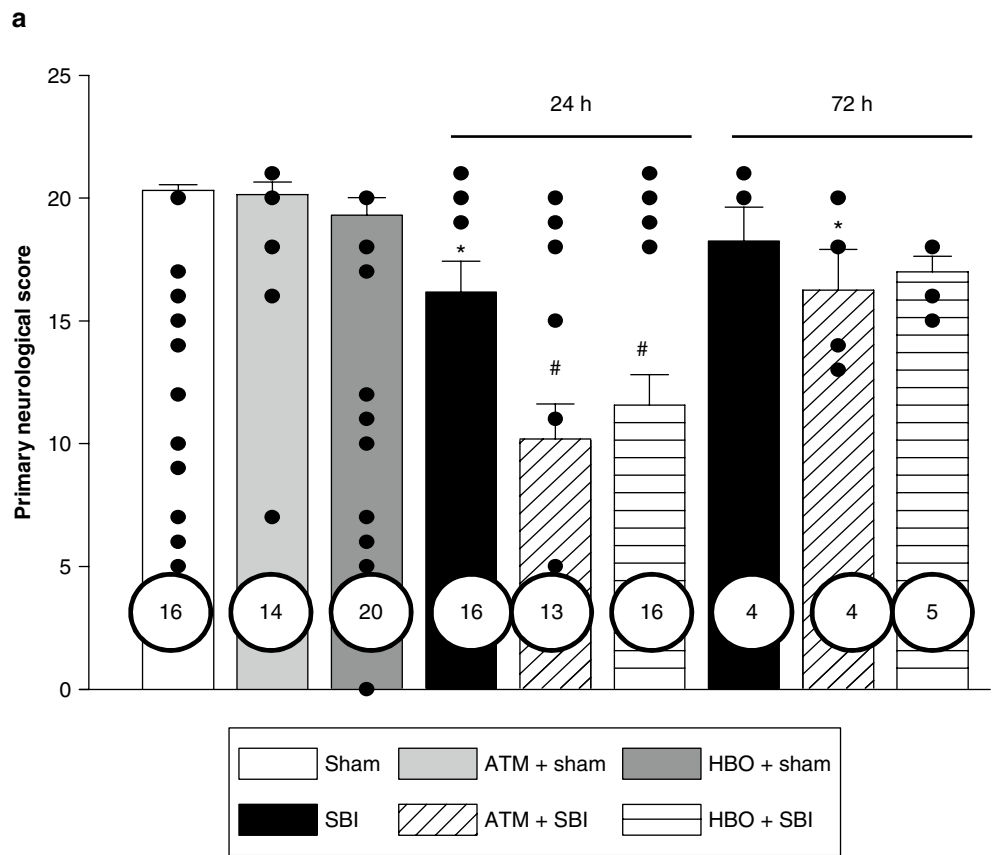
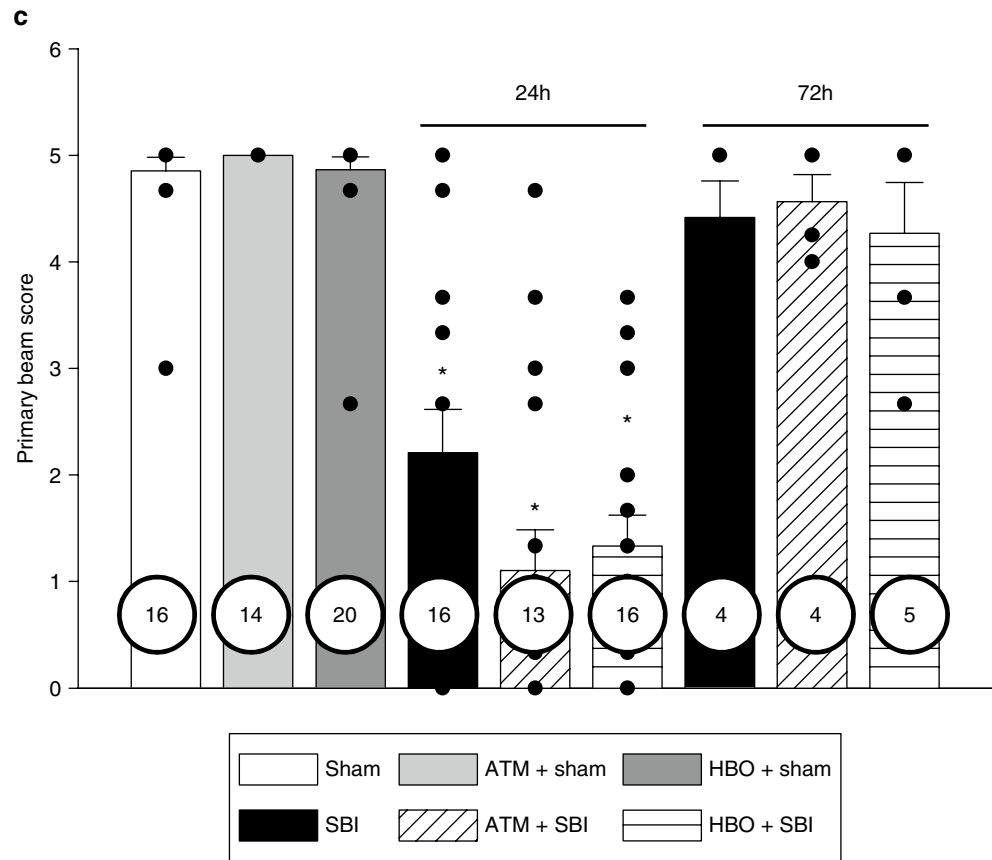


Fig. 3 (continued)



The optimum time to administer the preoperative oxygenation was determined using neurological evaluation (Fig. 4). For the 21-point Garcia neurological scoring, the score for the ATM+SBI group was significantly worse than for the ATM+sham group when 1-h 1.0 ATM was applied 0, 2, and 3 h before SBI. More importantly, the score for the ATM+SBI group was significantly worse than for the SBI group when 1 h 1.0 ATM was applied 3 h before SBI (5.5 ± 0.50 vs. 16.2 ± 1.24 , $*p < 0.05$, ANOVA). In the wire hanging test, when HBO treatment was applied 2 h before SBI, the score for the HBO+SBI group was significantly worse than for the SBI group (1.2 ± 0.29 vs. 2.4 ± 0.36 , $#p < 0.05$, ANOVA). Meanwhile, when ATM treatment was applied 3 h before SBI, the score for the ATM+SBI group was significantly worse than for the SBI group (0.7 ± 0.67 vs. 2.4 ± 0.36 , $*p < 0.05$, ANOVA). In the beam balance test, when the HBO treatment was applied 2 h before SBI, the score for the HBO+SBI group was significantly worse than for the SBI group (0.6 ± 0.29 vs. 2.2 ± 0.41 , $#p < 0.05$). Meanwhile, when ATM treatment was applied 3 h before SBI, the score for the ATM+SBI group was significantly worse than for the SBI group ($*p < 0.05$).

Discussion

This study evaluates the effects of pretreatment with normobaric or hyperbaric oxygenation SBI after neurosurgical operation. Our results suggest that both 1.0 ATM (100% FIO_2 , 1 h) and HBO (2.5 ATM, 1 h) treatment given in a single dose immediately preoperatively appear to have a deleterious effect on brain edema and neurological scoring. The brain edema results showed that 100% O_2 1.0 ATM treatment increased edema formation in the ipsilateral frontal brain compared with the SBI group. Moreover, 100% O_2 2.5 ATM treatment increased edema formation in the ipsilateral parietal brain compared with the SBI group. However, the mortality rate showed no difference between the treated and non-treated groups. Correlated with the brain edema data, the neurological function at 24 h after SBI was worse after either 1.0 ATM or 2.5 ATM O_2 treatment.

The increased brain edema formation appears to be partly due to lipid peroxidation (data not shown). Most lipid peroxidation was seen in the hyperbaric oxygenation group, and this correlated with the worsened outcomes and higher mortality rates that were encountered in this group compared to

Fig. 4 At 24 h, the neurological score following different treatment time points. **(a)** The 21-point Garcia score test. ATM pretreatment significantly worsens the score when applied 0, 2, and 3 h before SBI ($*p < 0.05$, ANOVA). HBO pretreatment significantly worsens the score when applied 3 h before SBI ($*p < 0.05$, ANOVA). **(b)** Wire hanging test. HBO pretreatment significantly worsens the score when applied 2 h before SBI ($*p < 0.05$, ANOVA). ATM pretreatment significantly worsens the score when applied 3 h before SBI ($*p < 0.05$, ANOVA). **(c)** Beam score test. HBO pretreatment significantly worsens the score when applied 2 h before SBI ($*p < 0.05$, ANOVA). ATM pretreatment significantly worsens the score when applied 3 h before SBI ($*p < 0.05$, ANOVA)

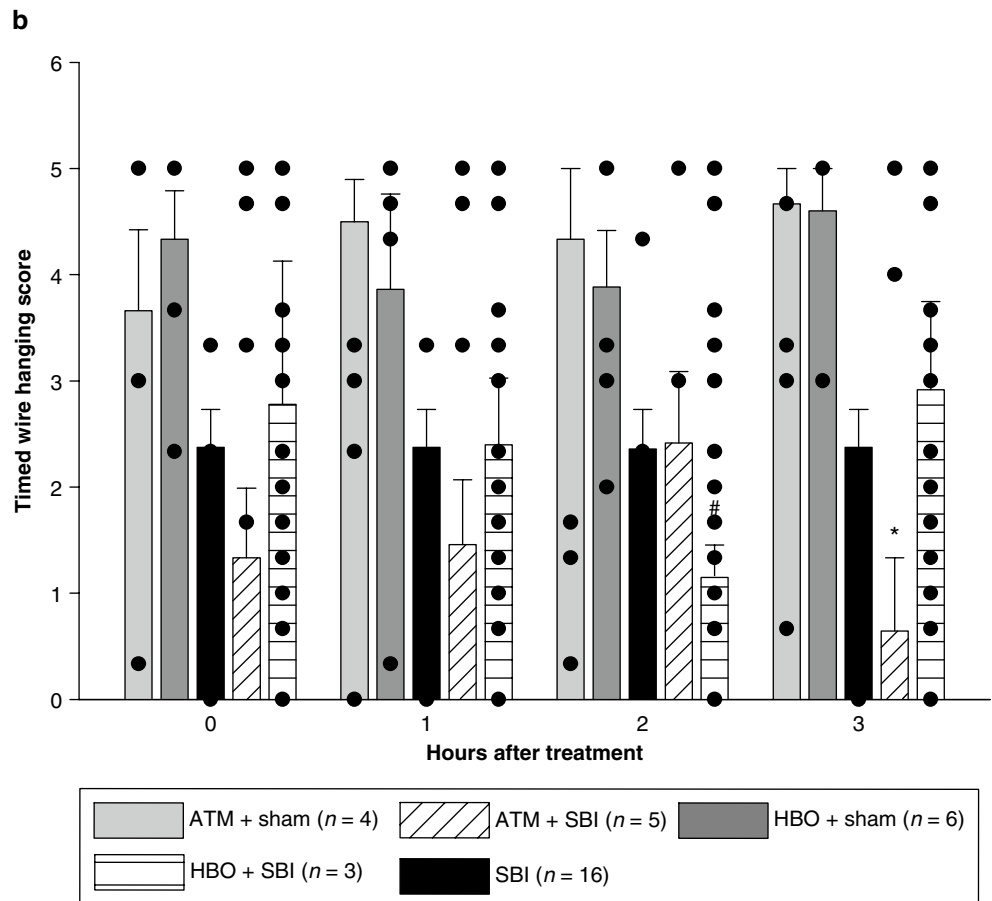
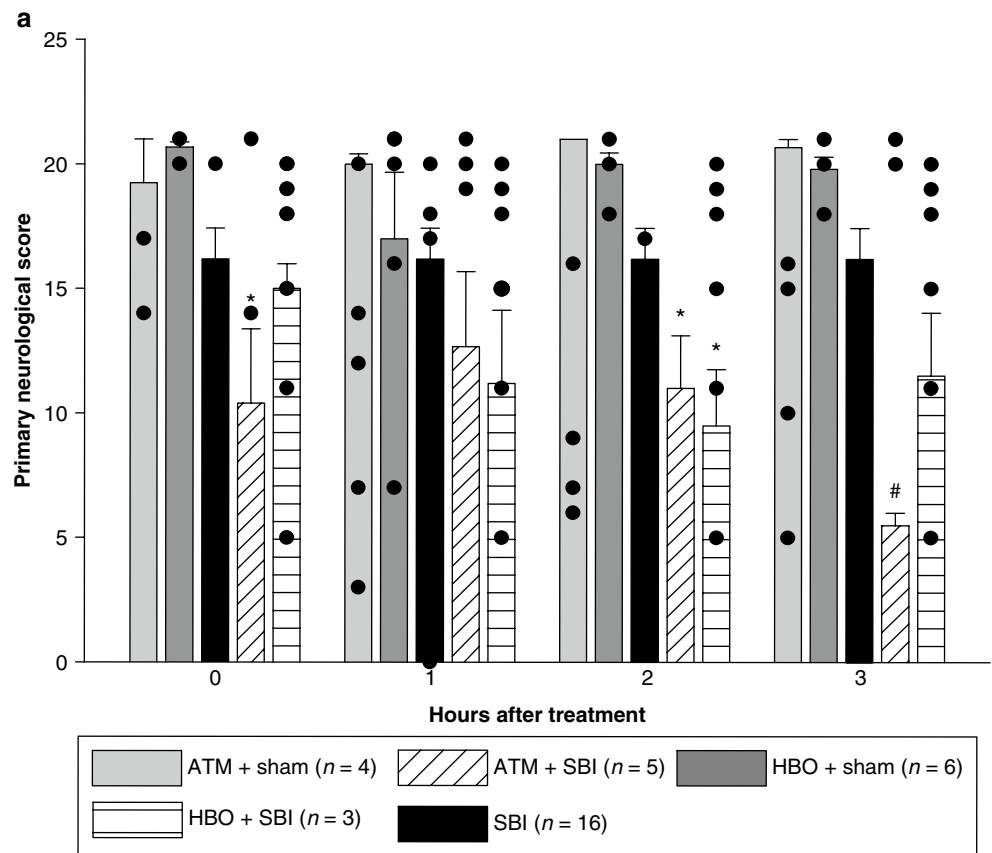
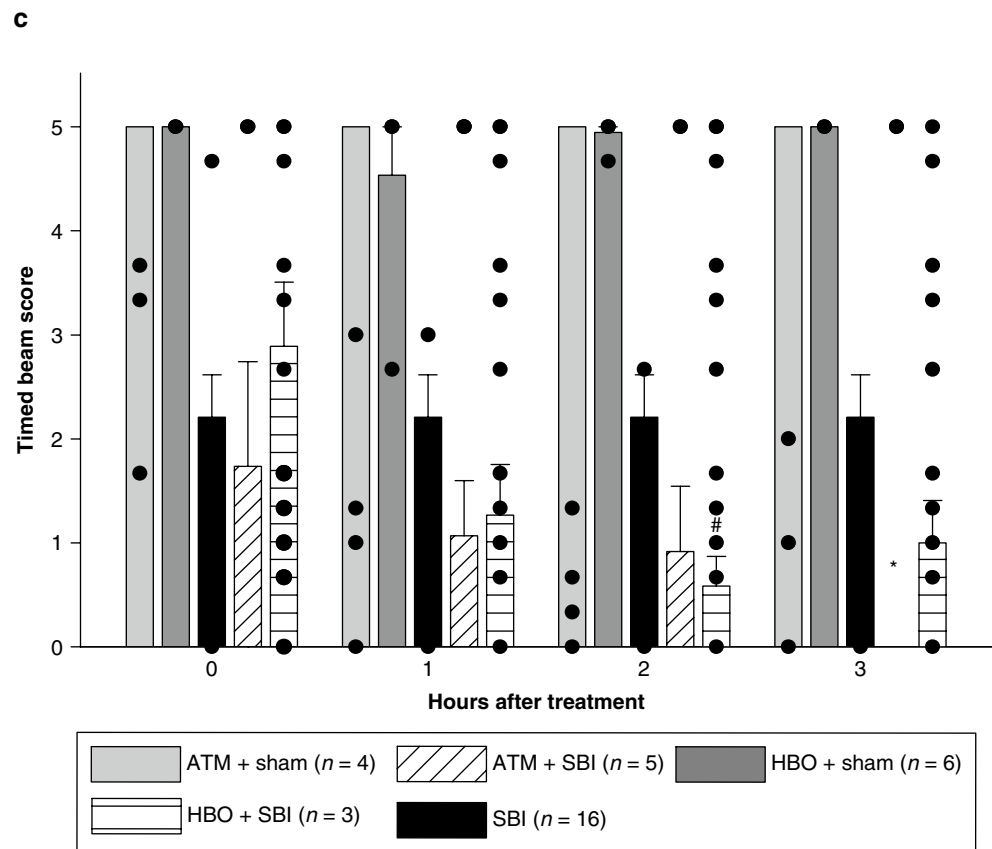


Fig. 4 (continued)



the untreated group. In this study, this effect was most pronounced in lung parenchyma, but the underlying mechanisms are probably at work in cerebral tissue as well. It is possible that this effect might also be due to differences in regulation of nitric oxide in normobaric and hyperbaric conditions [20]. In addition, reactive oxygen species were demonstrated to be present in normobaric conditions and accounted for increased neuronal damage in a middle cerebral artery occlusion mouse model treated with normobaric oxygen [21]. However, the underlying mechanisms need to be clarified in the future.

Niklas et al. postulated that the protective mechanism in hyperbaric oxygenation was the upregulation of DNA repair mechanisms that counteract the effects of lipid peroxidation. They noted that HBO induces oxidative DNA damage in blood cells of healthy subjects, but that this damage was only found after the first hyperbaric oxygen treatment but not after the second or further treatments. Therefore, they concluded that more than one hyperbaric session may be necessary to achieve good clinical results, and our results are in agreement with this conclusion. Qin et al. utilized pretreatment with hyperbaric oxygenation in a rat model of intracerebral hemorrhage and concluded that fewer than five sessions of hyperbaric oxygen preconditioning did not significantly

attenuate cerebral edema after the insult. They noted that the key pathway was the activation of p44/42 mitogen-activated protein kinase [22]. However, this mechanism was not found to be a key mechanism in all strains of mice examined. Overall, the literature supports multiple pretreatments with hyperbaric oxygenation prior to cerebral surgery in order to optimally activate the noted mechanisms instead of a single pretreatment. Our study demonstrates worsened outcomes at 24 h postoperatively when a single pretreatment was given. These effects were most pronounced when the pretreatment was completed 2 or 3 h prior to surgery. This worsening was attenuated at 72 h, suggesting that these results could be due to the immediate deleterious effects of lipid peroxidation since this improvement in scores was most pronounced in the pretreatment groups. More research is needed to elucidate the precise molecular steps in the known mechanisms and how to manipulate them optimally to improve neurological outcomes. In addition, there are probably molecular mechanisms yet to be discovered that could hold the key to improving neurological outcomes through oxygen pretreatment.

Acknowledgement This study is partially supported by NIH NS053407 to J.H. Zhang.

Conflict of interest statement We declare that we have no conflict of interest.

References

1. Rockswold GL, Ford SE (1985) Preliminary results of a prospective randomized trial for treatment of severely brain-injured patients with hyperbaric oxygen. *Minn Med* 68:533–535
2. Rockswold SB, Rockswold GL, Vargo JM, Erickson CA, Sutton RL, Bergman TA, Biros MH (2001) Effects of hyperbaric oxygenation therapy on cerebral metabolism and intracranial pressure in severely brain injured patients. *J Neurosurg* 94:403–411
3. Daugherty WP, Levasseur JE, Sun D, Rockswold GL, Bullock MR (2004) Effects of hyperbaric oxygen therapy on cerebral oxygenation and mitochondrial function following moderate lateral fluid-percussion injury in rats. *J Neurosurg* 101:499–504
4. Mink RB, Dutka AJ (1995) Hyperbaric oxygen after global cerebral ischemia in rabbits does not promote brain lipid peroxidation. *Crit Care Med* 23:1398–1404
5. Rockswold SB, Rockswold GL, Defillo A (2007) Hyperbaric oxygen in traumatic brain injury. *Neurol Res* 29:162–172
6. Veltkamp R, Siebing DA, Sun L, Heiland S, Bieber K, Marti HH, Nagel S, Schwab S, Schwaninger M (2005) Hyperbaric oxygen reduces blood-brain barrier damage and edema after transient focal cerebral ischemia. *Stroke* 36:1679–1683
7. Calvert JW, Cahill J, Zhang JH (2007) Hyperbaric oxygen and cerebral physiology. *Neurol Res* 29:132–141
8. Ren H, Wang W, Ge Z, Zhang J (2001) Clinical, brain electric earth map, endothelin and transcranial ultrasonic Doppler findings after hyperbaric oxygen treatment for severe brain injury. *Chin Med J (Engl)* 114:387–390
9. Buras JA, Reenstra WR (2007) Endothelial-neutrophil interactions during ischemia and reperfusion injury: basic mechanisms of hyperbaric oxygen. *Neurol Res* 29:127–131
10. Vlodayvsky E, Palzur E, Soustiel JF (2006) Hyperbaric oxygen therapy reduces neuroinflammation and expression of matrix metalloproteinase-9 in the rat model of traumatic brain injury. *Neuropathol Appl Neurobiol* 32:40–50
11. Palzur E, Zaaroor M, Vlodayvsky E, Milman F, Soustiel JF (2008) Neuroprotective effect of hyperbaric oxygen therapy in brain injury is mediated by preservation of mitochondrial membrane properties. *Brain Res* 1221:126–133
12. Ostrowski RP, Colohan AR, Zhang JH (2005) Mechanisms of hyperbaric oxygen-induced neuroprotection in a rat model of subarachnoid hemorrhage. *J Cereb Blood Flow Metab* 25:554–571
13. Peng Z, Ren P, Kang Z, Du J, Lian Q, Liu Y, Zhang JH, Sun X (2008) Up-regulated HIF-1 α is involved in the hypoxic tolerance induced by hyperbaric oxygen preconditioning. *Brain Res* 1212:71–78
14. Liu Z, Jiao QF, You C, Che YJ, Su FZ (2006) Effect of hyperbaric oxygen on cytochrome C, Bcl-2 and Bax expression after experimental traumatic brain injury in rats. *Chin J Traumatol* 9:168–174
15. Vlodayvsky E, Palzur E, Feinsod M, Soustiel JF (2005) Evaluation of the apoptosis-related proteins of the BCL-2 family in the traumatic penumbra area of the rat model of cerebral contusion, treated by hyperbaric oxygen therapy: a quantitative immunohistochemical study. *Acta Neuropathol* 110:120–126
16. Nemoto EM, Betterman K (2007) Basic physiology of hyperbaric oxygen in brain. *Neurol Res* 29:116–126
17. Niklas A, Brock D, Schober R, Schulz A, Schneider D (2004) Continuous measurements of cerebral tissue oxygen pressure during hyperbaric oxygenation—HBO effects on brain edema and necrosis after severe brain trauma in rabbits. *J Neurol Sci* 219:77–82
18. Veltkamp R, Sun L, Herrmann O, Wolferts G, Hagmann S, Siebing DA, Marti HH, Veltkamp C, Schwaninger M (2006) Oxygen therapy in permanent brain ischemia: potential and limitations. *Brain Res* 1107:185–191
19. Lee S, Jadhav V, Ayer RE, Rojas H, Hyong A, Lekic T, Tang J, Zhang JH (2009) Dual effects of melatonin on oxidative stress after surgical brain injury in rats. *J Pineal Res* 46(1):43–48
20. Demchenko IT, Welty-Wolf KE, Allen BW, Piantadosi CA (2007) Similar but not the same: normobaric and hyperbaric pulmonary oxygen toxicity, the role of nitric oxide. *Am J Physiol Lung Cell Mol Physiol* 293:L229–L238
21. Nonaka Y, Shimazawa M, Yoshimura S, Iwama T, Hara H (2008) Combination effects of normobaric hyperoxia and edaravone on focal cerebral ischemia-induced neuronal damage in mice. *Neurosci Lett* 441:224–228
22. Qin Z, Song S, Xi G, Silbergleit R, Keep RF, Hoff JT, Hua Y (2007) Preconditioning with hyperbaric oxygen attenuates brain edema after experimental intracerebral hemorrhage. *Neurosurg Focus* 22:E13
23. Demchenko IT, Boso AE, O'Neill TJ, Bennett PB, Piantadosi CA (2000) Nitric oxide and cerebral blood flow responses to hyperbaric oxygen. *J Appl Physiol* 88(4):1381–1389

Beneficial Effect of Hyperbaric Oxygenation After Neonatal Germinal Matrix Hemorrhage

Tim Lekic, Anatol Manaenko, William Rolland, Robert P. Ostrowski, Kelly Virbel, Jiping Tang, and John H. Zhang

Abstract *Background:* Germinal matrix hemorrhage (GMH) is a potentially devastating neurological disease of very low birth weight premature infants. This leads to post-hemorrhagic hydrocephalus, cerebral palsy, and mental retardation. Hyperbaric oxygen (HBO) treatment is a broad neuroprotectant after brain injury. This study investigated the therapeutic effect of HBO after neonatal GMH.

Methods: Neonatal rats underwent stereotaxic infusion of clostridial collagenase into the right germinal matrix (anterior caudate) brain region. Cognitive function was assessed at 3 weeks, and then sensorimotor, cerebral, cardiac, and splenic growths were measured 1 week thereafter.

Results: Hyperbaric oxygen (HBO) treatment markedly improved upon the mental retardation and cerebral palsy outcome measurements in rats at the juvenile developmental stage. The administration of HBO early after neonatal GMH also normalized brain atrophy, splenomegaly, and cardiac hypertrophy 1 month after injury.

Conclusion: This study supports the role of hyperbaric oxygen (HBO) treatment in the early period after neonatal GMH. HBO is an effective strategy to help protect the infant's brain from the post-hemorrhagic consequences of

brain atrophy, mental retardation, and cerebral palsy. Further studies are necessary to determine the mechanistic basis of these neuroprotective effects.

Keywords Hyperbaric oxygenation · Neurological deficits · Stroke, experimental

Introduction

Germinal matrix hemorrhage (GMH) is a potentially devastating clinical condition with life-long consequences. This occurs when immature blood vessels rupture within the subventricular (anterior caudate) region during the first 7 days of life [1, 2]. Approximately 20–25% of very low birth weight (VLBW $\leq 1,500$ g) premature infants will be affected, accounting for around 3.5 per 1,000 births in the United States every year [3–6]. The long-term consequences of GMH are hydrocephalus (post-hemorrhagic ventricular dilation), developmental delay, cerebral palsy, and mental retardation [4, 7]. This is an important clinical problem for which experimental studies investigating therapeutic modalities are generally lacking [8].

Hyperbaric oxygen (HBO) treatment will induce multiple neuroprotective pathways across a wide domain of brain injury [9]. HBO has been shown in randomized controlled trials to improve cognition and overall functioning in autistic children [10], and may ameliorate outcomes after cerebral palsy as well [11]. Emerging evidence shows that both HBO and normobaric oxygen (NBO) treatments exert similar neuroprotective mechanisms to improve outcomes after adult ischemic stroke [12], and perhaps after neonatal hypoxia-ischemia as well [13].

In light of this evidence, we hypothesized that HBO therapy can be a therapeutic strategy to ameliorate brain injury mechanisms, to thereby improve cognitive and sensorimotor outcomes after germinal matrix hemorrhage in neonatal rats.

T. Lekic, A. Manaenko, W. Rolland, R.P. Ostrowski, K. Virbel, and J. Tang

Departments of Physiology, Loma Linda University, School of Medicine, Loma Linda, CA, USA

J.H. Zhang (✉)

Departments of Physiology, Loma Linda University, School of Medicine, Loma Linda, CA, USA and Departments of Anesthesiology, Loma Linda University, School of Medicine, Loma Linda, CA, USA and Departments of Neurosurgery, Loma Linda University, School of Medicine, Loma Linda, CA, USA and Department of Physiology, Loma Linda University, School of Medicine, Risley Hall, Room 223, Loma Linda, CA 92354, USA
e-mail: johnzhang3910@yahoo.com

Methods and Materials

Animal Groups and General Procedures

This study was in accordance with the National Institutes of Health guidelines for the treatment of animals and was approved by the Institutional Animal Care and Use Committee at Loma Linda University. Timed pregnant Sprague-Dawley rats were housed with food and water available *ad libitum*. Treatment consisted of 1 h normobaric oxygen (NBO, 0 atm) or hyperbaric oxygen (HBO, 2.5 atm) administration beginning 1 h after collagenase infusion. Postnatal day 7 (P7) pups were blindly assigned to the following ($n=8$ /group): sham (naive), needle (control), GMH (collagenase-infusion), GMH+NBO, and GMH+HBO. All groups were evenly divided within each litter.

Experimental Model of GMH

Using aseptic technique, rat pups were gently anesthetized with 3% isoflurane (in mixed air and oxygen) while placed prone onto a stereotaxic frame. Betadine sterilized the surgical scalp area, which was incised in the longitudinal plane to expose the skull and reveal the bregma. The following stereotactic coordinates were determined: 1 mm (anterior), 1.5 mm (lateral), and 3.5 mm (ventral) from the bregma. A bore hole (1 mm) was drilled, into which a 27-gauge needle was inserted at a rate of 1 mm/min. A microinfusion pump (Harvard Apparatus, Holliston, MA) infused 0.3 units of clostridial collagenase VII-S (Sigma, St Louis, MO) through a Hamilton syringe. The needle remained in place for an additional 10 min after injection to prevent back-leakage. After needle removal, the burr hole was sealed with bone wax, the incision sutured closed, and the animals allowed to recover. The entire surgery took on average 20 min. Upon recovering from anesthesia, the animals were returned to their dams. Needle controls consisted of needle insertion alone without collagenase infusion, while naïve animals did not receive any surgery.

Cognitive Measures

Higher order brain function was assessed during the third week after collagenase infusion. The T-maze assessed short-term (working) memory [14]. Rats were placed into the stem (40 cm × 10 cm) of a maze and allowed to explore until one arm (46 cm × 10 cm) was chosen. From the sequence of ten

trials, of left and right arm choices, the rate of spontaneous alternation (0% = none and 100% = complete, alternations/trial) was calculated, as routinely performed [15, 16]. The Morris water maze assessed spatial learning and memory on four daily blocks, as described previously in detail [17, 18]. The apparatus consisted of a metal pool (110 cm diameter) filled to within 15 cm of the upper edge, with a platform (11 cm diameter) for the animal to escape onto, which changed location for each block (maximum = 60 s/trial), and data were digitally analyzed by Noldus Ethovision tracking software. Cued trials measured place learning with the escape platform visible above water. Spatial trials measured spatial learning with the platform submerged, and probe trials measured spatial memory once the platform was removed. For the locomotor activity, in an open field, the path length in open-topped plastic boxes (49 cm long, 35.5 cm wide, 44.5 cm tall) was digitally recorded for 30 min and analyzed by Noldus Ethovision tracking software [18].

Sensorimotor Function

At 4 weeks after collagenase infusion, the animals were tested for functional ability. The neurodeficit was quantified using a summation of scores (maximum = 12) given for (1) postural reflex, (2) proprioceptive limb placing, (3) back pressure towards the edge, (4) lateral pressure towards the edge, (5) forelimb placement, and (6) lateral limb placement (2 = severe, 1 = moderate, 0 = none), as routinely performed [15]. For the rotarod, striatal ability was assessed using an apparatus consisting of a horizontal, accelerated (2 rpm/5 s), rotating cylinder (7 cm-diameter × 9.5 cm-wide), requiring continuous walking to avoid falling, recorded by photo-beam circuit (Columbus Instruments) [17, 18]. For foot fault, the number of complete limb missteps through the openings while exploring over an elevated wire (3 mm) grid (20 cm × 40 cm) floor was counted over 2 min [16].

Assessment of Treatment upon Cerebral and Somatic Growth

At the completion of experiments, the brains were removed and hemispheres separated by midline incision (loss of brain weight has been used as the primary variable to estimate brain damage in juvenile animals after neonatal brain injury [19]). For organ weights, the spleen and heart were separated from surrounding tissue and vessels. The quantification was performed using an analytical microbalance (model AE 100; Mettler Instrument Co., Columbus, OH) capable of 1.0 µg precision.

Statistical Analysis

Significance was considered at $p < 0.05$. Data were analyzed using analysis of variance (ANOVA) with repeated measures (RM-ANOVA) for long-term neurobehavior. Significant interactions were explored with conservative Scheffé post hoc and Mann-Whitney rank sum when appropriate.

Results

HBO and NBO treatment normalized T-maze deficits (Fig. 1a, $p > 0.05$ compared to controls) and water maze (spatial) learning deficits (Fig. 1b, $p < 0.05$ compared to GMH), without improving spatial memory (Fig. 1c, $p > 0.05$). Oxygenation treatment also normalized ($p < 0.05$) sensorimotor dysfunction (compared to juvenile GMH animals) in the neurodeficit score, the number of foot faults, and accelerating rotarod falling latency (Fig. 2a–c, $p < 0.05$). This was confirmed with normalization of brain atrophy (Fig. 3a, $p < 0.05$ compared to GMH), splenomegaly, and cardiomegaly (Fig. 3b, c, $p > 0.05$ compared to controls).

Discussion

These results indicate that hyperbaric oxygen (HBO) treatment after neonatal GMH can reduce long-term brain atrophy and return sensorimotor and cognitive functional deficits back to near-normal levels in juvenile animals. In support of the findings from others, this provides preliminary evidence about the importance of HBO-mediated mechanisms upon improvement of outcomes after neonatal injury [10–13].

Hyperbaric oxygen (HBO) treatment can induce multiple neuroprotective pathways across a wide domain of cerebral pathophysiology [9]. Our results support descriptive clinical studies using HBO to improve cognition and overall functioning in autistic and cerebral palsy children [10, 11]. In agreement with our findings, recent evidence shows that both HBO and normobaric oxygen (NBO) therapy can upregulate neuroprotective mechanisms and improve outcomes in adult ischemic stroke models [12]. Although hyper-oxygenation treatment has been shown to be protective after neonatal hypoxia-ischemia [13], our study demonstrates the first preliminary evidence, in this patient sub-population, advocating the use of oxygenation after hemorrhagic brain injury as well.

This study supports the notion that HBO treatment has no adverse affects in neonatal rats and can be applied as a strategy to improve functional outcomes after brain injury from hemorrhagic stroke in premature infants. Further investigation

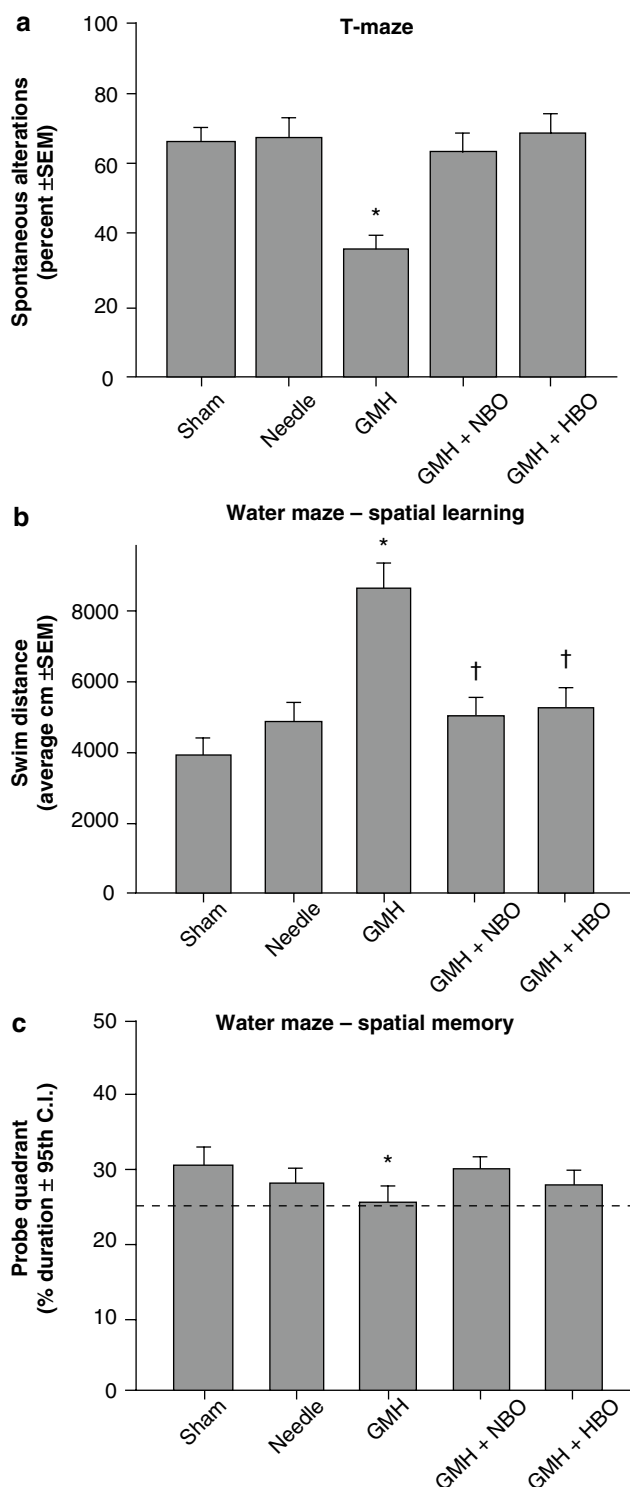


Fig. 1 Cognitive function normalization in juvenile rats by HBO/NBO after neonatal GMH. Higher order function was measured at the 3rd week after collagenase infusion: (a) T-maze, (b) spatial learning water maze, (c) spatial memory (probe) water maze. Values expressed as mean \pm 95th CI (probe quadrant) or mean \pm SEM (all others), $n = 8$ (per group), * $p < 0.05$ compared with controls (sham and needle trauma), and † $p < 0.05$ compared with GMH

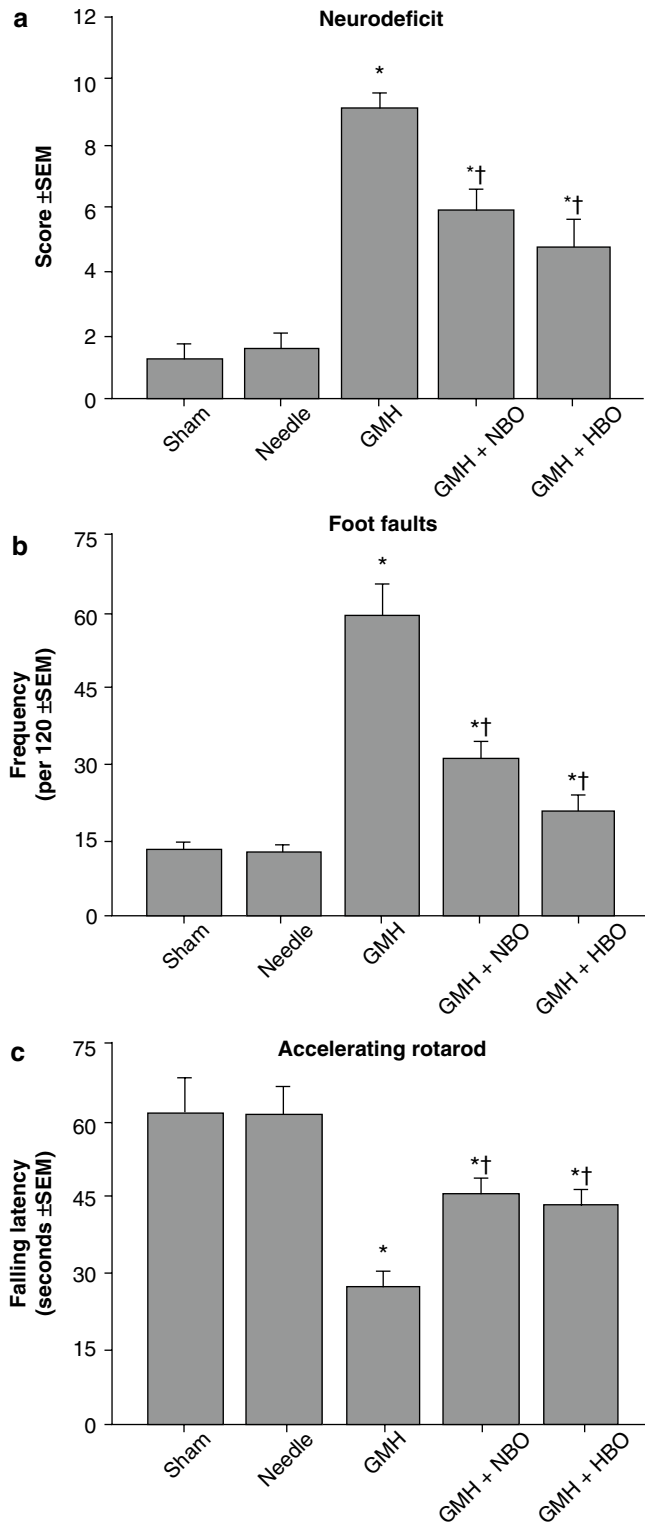


Fig. 2 Sensorimotor function normalization in juvenile rats by HBO/NBO after neonatal GMH. Cerebral palsy measurements were performed in the juveniles at 1 month after collagenase infusion: (a) neurodeficit score, (b) foot faults and (c) rotarod. Values expressed as mean ± SEM, $n=8$ (per group), * $p<0.05$ compared with controls (sham and needle trauma), and † $p<0.05$ compared with GMH

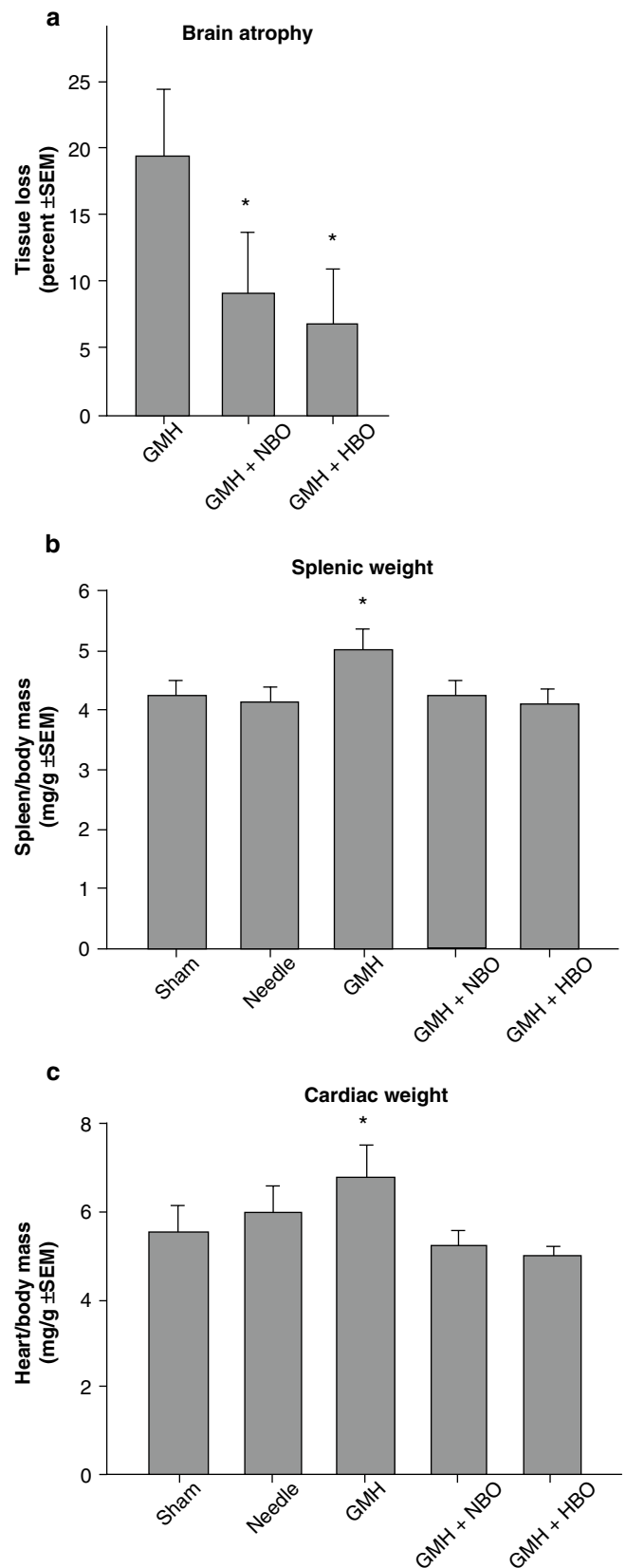


Fig. 3 Cerebral and somatic growth normalization in juvenile rats by HBO/NBO after GMH. (a) Brain atrophy (percent tissue loss), (b) splenic weight, and (c) cardiac weight. Values expressed as mean ± SEM, $n=8$ (per group), * $p<0.05$ compared with controls (sham and needle trauma)

is needed to determine the mechanistic basis of these neuro-protective effects.

Acknowledgements This study was partially supported by a grant (NS053407) from the National Institutes of Health to J.H.Z.

Conflict of interest statement We declare that we have no conflict of interest.

References

- Ballabh P (2010) Intraventricular hemorrhage in premature infants: mechanism of disease. *Pediatr Res* 67:1–8. doi:10.1203/PDR.0b013e3181c1b176
- Kadri H, Mawla AA, Kazah J (2006) The incidence, timing, and predisposing factors of germinal matrix and intraventricular hemorrhage (GMH/IVH) in preterm neonates. *Childs Nerv Syst* 22:1086–1090. doi:10.1007/s00381-006-0050-6
- Vohr BR, Wright LL, Dusick AM, Mele L, Verter J, Steichen JJ, Simon NP, Wilson DC, Broyles S, Bauer CR, Delaney-Black V, Yolton KA, Fleisher BE, Papile LA, Kaplan MD (2000) Neurodevelopmental and functional outcomes of extremely low birth weight infants in the National Institute of Child Health and Human Development Neonatal Research Network, 1993–1994. *Pediatrics* 105:1216–1226
- Murphy BP, Inder TE, Rooks V, Taylor GA, Anderson NJ, Mogridge N, Horwood LJ, Volpe JJ (2002) Posthaemorrhagic ventricular dilatation in the premature infant: natural history and predictors of outcome. *Arch Dis Child Fetal Neonatal Ed* 87:F37–41
- Vermont-Oxford (1993) The Vermont-Oxford Trials Network: very low birth weight outcomes for 1990. Investigators of the Vermont-Oxford Trials Network Database Project. *Pediatrics* 91:540–545
- Heron M, Sutton PD, Xu J, Ventura SJ, Strobino DM, Guyer B (2010) Annual summary of vital statistics: 2007. *Pediatrics* 125:4–15. doi:peds.2009-2416 [pii], 10.1542/peds.2009-2416
- Ballabh P, Braun A, Nedergaard M (2004) The blood-brain barrier: an overview: structure, regulation, and clinical implications. *Neurobiol Dis* 16:1–13. doi:10.1016/j.nbd.2003.12.016, S0969996103002833 [pii]
- Balasubramaniam J, Del Bigio MR (2006) Animal models of germinal matrix hemorrhage. *J Child Neurol* 21:365–371
- Zhang JH, Lo T, Mychaskiw G, Colohan A (2005) Mechanisms of hyperbaric oxygen and neuroprotection in stroke. *Pathophysiology* 12:63–77. doi:S0928-4680(05)00013-1 [pii], 10.1016/j.pathophys.2005.01.003
- Rossignol DA, Rossignol LW, Smith S, Schneider C, Logerquist S, Usman A, Neubrandner J, Madren EM, Hintz G, Grushkin B, Mumper EA (2009) Hyperbaric treatment for children with autism: a multicenter, randomized, double-blind, controlled trial. *BMC Pediatr* 9:21. doi:1471-2431-9-21 [pii], 10.1186/1471-2431-9-21
- Hardy P, Collet JP, Goldberg J, Ducruet T, Vanasse M, Lambert J, Marois P, Amar M, Montgomery DL, Lecomte JM, Johnston KM, Lassonde M (2002) Neuropsychological effects of hyperbaric oxygen therapy in cerebral palsy. *Dev Med Child Neurol* 44:436–446
- Poli S, Veltkamp R (2009) Oxygen therapy in acute ischemic stroke – experimental efficacy and molecular mechanisms. *Curr Mol Med* 9:227–241
- Calvert JW, Zhang JH (2007) Oxygen treatment restores energy status following experimental neonatal hypoxia-ischemia. *Pediatr Crit Care Med* 8:165–173. doi:10.1097/01.PCC.0000257113.75488.84
- Hughes RN (2004) The value of spontaneous alternation behavior (SAB) as a test of retention in pharmacological investigations of memory. *Neurosci Biobehav Rev* 28:497–505. doi:S0149-7634(04)00073-9 [pii], 10.1016/j.neubiorev.2004.06.006
- Fathali N, Ostrowski RP, Lekic T, Jadhav V, Tong W, Tang J, Zhang JH (2010) Cyclooxygenase-2 inhibition provides lasting protection against neonatal hypoxic-ischemic brain injury. *Crit Care Med* 38:572–578. doi:10.1097/CCM.0b013e3181cb1158
- Zhou Y, Fathali N, Lekic T, Tang J, Zhang JH (2009) Glibenclamide improves neurological function in neonatal hypoxia-ischemia in rats. *Brain Res* 1270:131–139. doi:S0006-8993(09)00520-4 [pii], 10.1016/j.brainres.2009.03.010
- Lekic T, Hartman R, Rojas H, Manaenko A, Chen W, Ayer R, Tang J, Zhang JH (2010) Protective effect of melatonin upon neuropathology, striatal function, and memory ability after intracerebral hemorrhage in rats. *J Neurotrauma* 27:627–637. doi:10.1089/neu.2009.1163
- Hartman R, Lekic T, Rojas H, Tang J, Zhang JH (2009) Assessing functional outcomes following intracerebral hemorrhage in rats. *Brain Res* 1280:148–157. doi:S0006-8993(09)00957-3 [pii], 10.1016/j.brainres.2009.05.038
- Andine P, Thordstein M, Kjellmer I, Nordborg C, Thiringer K, Wennberg E, Hagberg H (1990) Evaluation of brain damage in a rat model of neonatal hypoxic-ischemia. *J Neurosci Methods* 35:253–260

Thrombin Preconditioning Attenuates Iron-Induced Neuronal Death

Haitao Hu, Shiro Yamashita, Shuijiang Song, Ya Hua, Richard F. Keep, and Guohua Xi

Abstract Pretreatment with a low dose of thrombin attenuated brain injury after intracerebral hemorrhage (ICH) or cerebral ischemia. This phenomenon has been called thrombin preconditioning (TPC). The current study investigated whether or not TPC reduces neuronal death induced by iron in cultured neurons. The roles of protease-activated receptors (PARs) and the p44/42 mitogen-activated protein kinase (p44/42MAPK)/70-kDa ribosomal protein S6 kinase (p70S6K) signal transduction pathway in TPC were also examined. This study had three parts: (1) primary cultured neurons were pretreated with vehicle, thrombin or PAR agonists. Cell death was induced by ferrous iron (500 μ M) 24 h later. After 48 h, culture medium was collected for lactate dehydrogenase measurement; (2) neurons were treated with vehicle, thrombin or thrombin plus PPACK (D-Phe-Pro-Arg chloromethylketone) thrombin and were collected for Western blotting; (3) the effect PD098059 on TPC was examined. Cells were treated with 20 μ M PD098059 or vehicle 1 h before TPC. Neuron viability was measured 24 h following exposure to ferrous iron. Preconditioning with thrombin or PAR agonists reduced iron-induced neuronal death ($p < 0.05$). Thrombin, but not PPACK thrombin, upregulated the protein levels of activated p44/42 MAPK and p70 S6K ($p < 0.05$) in neurons. PD098059 also abolished the TPC-induced

neuronal protection against iron ($p < 0.05$). In conclusion, the protective effect of thrombin preconditioning is partially achieved through activating PARs and the p44/42 MAPK/p70S6K signal transduction pathway.

Keywords Thrombin · Preconditioning · Cerebral hemorrhage · Protease-activated receptors · p44/42 mitogen activated protein kinase · p70 S6K

Introduction

High concentrations of intracerebral thrombin cause brain edema and neuronal death, but low concentrations are neuroprotective [1–13]. Thus, we have found that prior treatment with a low dose of thrombin attenuates the brain edema induced by thrombin, iron or hemorrhage [6, 11, 12], significantly reduces infarct size in a rat middle cerebral artery occlusion model [8] and reduces brain damage in a rat model of Parkinson's disease [1, 14]. We have termed this phenomena thrombin preconditioning (TPC) or thrombin-induced brain tolerance.

Preconditioning has been used for heart and brain surgery, and is now a clinical reality [15, 16]. Many of the protective effects of preconditioning are delayed and involve new protein synthesis prior to the injury-inducing insult [17, 18]. In heart, there is evidence that activation of 70-kDa ribosomal protein S6 kinase (p70 S6K) is essential for preconditioning [19, 20]. p70 S6K is activated by phosphorylation on multiple sites. Thus, as well as the PI3K-Akt pathway that phosphorylates thr389, the p44/42 mitogen-activated protein kinase (MAPK) pathway phosphorylates p70 S6K on thr421/ser424 [19]. The major target of the activated kinase is the 40S ribosomal protein S6, a major regulator of protein synthesis [21].

In this study, we examined whether thrombin preconditioning reduces neuronal death induced by ferrous iron, and whether activation of protease-activated receptors and the p44/42 MAPK-p70S6K pathway contributes to TPC-induced neuroprotection.

H. Hu and S. Song
Department of Neurosurgery, University of Michigan,
Ann Arbor, MI, USA and
Department of Neurology, 2nd Affiliated Hospital, Zhejiang
University, Zhejiang, China

S. Yamashita, Y. Hua, and R.F. Keep
Department of Neurosurgery, University of Michigan,
Ann Arbor, MI, USA

G. Xi (✉)
Department of Neurosurgery, University of Michigan,
Room 5018 Biomedical Science Research Building,
109 Zina Pitcher Place, Ann Arbor, MI, USA
e-mail: guohuaxi@umich.edu

Materials and Methods

Experiment Groups

To examine the effect of TPC-induced neuronal protection, primary neuronal cultures were used. This study was divided into three parts. In the first part, cells were pretreated with vehicle, low-dose thrombin (1 U/ml) or thrombin receptor (also called protease activated receptor, PAR) agonists (PAR-1 agonist, NeomPS, San Diego, CA; PAR-3 and PAR-4 agonists, Bachem, Torrance, CA) for 24 h. Neuronal death was induced by 500 μ M ferrous iron. Lactate dehydrogenase (LDH) in the culture medium was measured after 48 h. In the second part, neurons were pretreated with a thrombin inhibitor, PPACK (D-Phe-Pro-Arg chloromethylketone, 1 μ M; Bachem, Torrance, CA) or vehicle 30 min before thrombin (1 U/ml) treatment. After 24 h, neurons were collected for Western blot analysis detecting levels of activated p44/42 MAPK and p70 S6K. In the third part, neurons were treated with either 20 μ M PD98059 (Calbiochem, La Jolla, CA), a p44/42 MAPK kinase inhibitor, or vehicle 1 h before thrombin (1 U/ml) pretreatment. Cell viability was assayed 48 h after exposure to 500 μ M ferrous iron.

Cell Preparation

Primary neuron cultures were prepared from E17 fetal rats (Sprague-Dawley, Charles River). Brains were removed and cortices dissected out, and freed of meninges and blood vessels. Tissues were triturated in modified Hanks' Balanced Solution (25 mM HEPES, 1% Antibiotic-Antimycotic, Invitrogen, Carlsbad, CA). After centrifuging at 800 g \times 5 min, the supernatant was removed and the tissue digested for 20 min in 0.5% trypsin at 37°C, then DNase I and 3.8% MgSO₄ were applied for 5 min at room temperature. After centrifuging, the tissue was resuspended in neurobasal medium (supplemented 2% B27 and 1 mM glutamine; Invitrogen, Carlsbad, CA). The cells were plated at a density of 3.0 \times 10⁵/cm² on poly-L-lysine coated 6- or 24-well plates and then incubated at 37°C in an atmosphere of 5% CO₂/95% air. The medium was replaced every 3 days with fresh neurobasal medium. Cultures were used after 7–10 days.

Lactate Dehydrogenase (LDH) Measurement

At the end of the experiment, neuronal toxicity was assessed by measurement of LDH release using a CytoTox-96 Non-Radioactive Cytotoxicity Assay kit (Promega, Madison, WI)

according to the manufacturer's instruction. Absorbance of the resulting solution was measured in a microplate reader (EL 800, Bio-Tek Instruments, Winooski, VT) at 490 nm with a reference wavelength of 630 nm. Results were analyzed with microplate data analysis software, KC junior (Bio-Tek Instruments, Inc.).

Western Blot Analysis

Neurons were collected, immersed in 0.1 mL of Western blot sample buffer and then sonicated for Western blot analysis. The sample solution (10 μ L) was taken for protein assay (Bio-Rad protein assay kit). Protein (20 μ g) was separated by SDS-PAGE gel and transferred to a hybond-C pure nitrocellulose membrane. Membranes were probed with the following primary antibodies: polyclonal rabbit phospho-p44/42 MAPK antibody (1:2,000; Cell Signaling, MA) and polyclonal rabbit phospho-p70s6k (Thr421/Ser424) antibody (1:1,000; Cell Signaling, MA). The relative densities of phospho-p44/42 MAPK and phospho-p70 S6K protein bands were analyzed using NIH image software (version 1.63).

Statistical Analysis

All results are expressed as mean \pm SD. Data were statistically analyzed by analysis of variance with Scheffé multiple comparisons or Student's *t*-test. Differences are considered significant at the $p < 0.05$ level.

Results

Thrombin Preconditioning and Thrombin Receptor Agonists Preconditioning Reduce Ferrous Iron-Induced Neuronal Death

To investigate whether pretreatment with a low dose of thrombin can induce neuronal tolerance to the toxic effects of iron and to determine whether activation of the thrombin-receptor mediates the neuroprotective effect of TPC, we pretreated the cells with 1 U/mL thrombin, thrombin receptor (PAR-1, PAR-3 and PAR-4) agonists (50 nM) or vehicle for 24 h before exposure to 500 μ M ferrous iron. Ferrous iron (500 μ M) resulted in marked neuronal death. Thrombin and PAR preconditioning reduced neuronal death caused by iron (e.g., TPC: 62.2 \pm 15.2% vs. 100 \pm 11.9% in the control group, $p < 0.05$, Fig. 1).

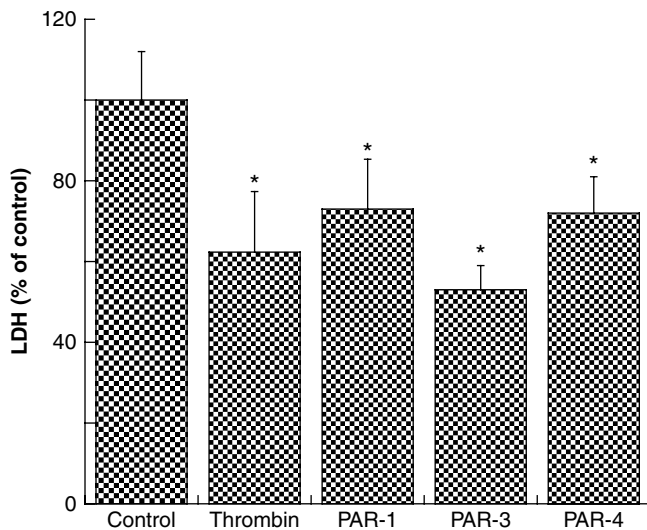


Fig. 1 Lactate dehydrogenase (LDH) release expressed as percent of control in neuronal culture medium after incubation with 500 μ M FeCl₂ for 48 h. Neurons were pretreated with thrombin (1U/mL), or PAR-1, PAR-3 and PAR-4 agonists (50 nM), or vehicle (control) for 24 h. Values are mean \pm SD, $n=12$, * $p<0.05$ vs. the control group

Thrombin Activates the p44/42 MAPK-p70 S6K Pathway in Cultured Neurons

To determine whether TPC can activate the p44/42 MAPK-p70 S6K pathway, we examined activated p44/42 MAPK and p70 S6K levels by Western blot analysis. We found that activated p44/42 MAPK and p70 S6K levels were significantly higher after thrombin (1 U/mL) treatment ($p<0.01$, Fig. 2). To confirm the specificity of thrombin, PPACK was used. PPACK thrombin could not activate p44/42 MAPK and p70 S6K (Fig. 2).

PD98059 Blocks the Neuroprotective Effect of TPC

To examine the effect of p44/42 MAPK activation on TPC-induced neuroprotection, neurons were treated with 20 μ M PD98059, a p44/42 MAPK kinase inhibitor or vehicle 1 h before TPC. Cell viability was measured 48 h after exposure to 500 μ M ferrous iron. We found that TPC reduced iron-induced neuronal death and PD98059 blocked TPC-induced neuroprotection (Fig. 3).

Discussion

The precise mechanisms of thrombin-induced brain tolerance to hemorrhagic and ischemic stroke are not known.

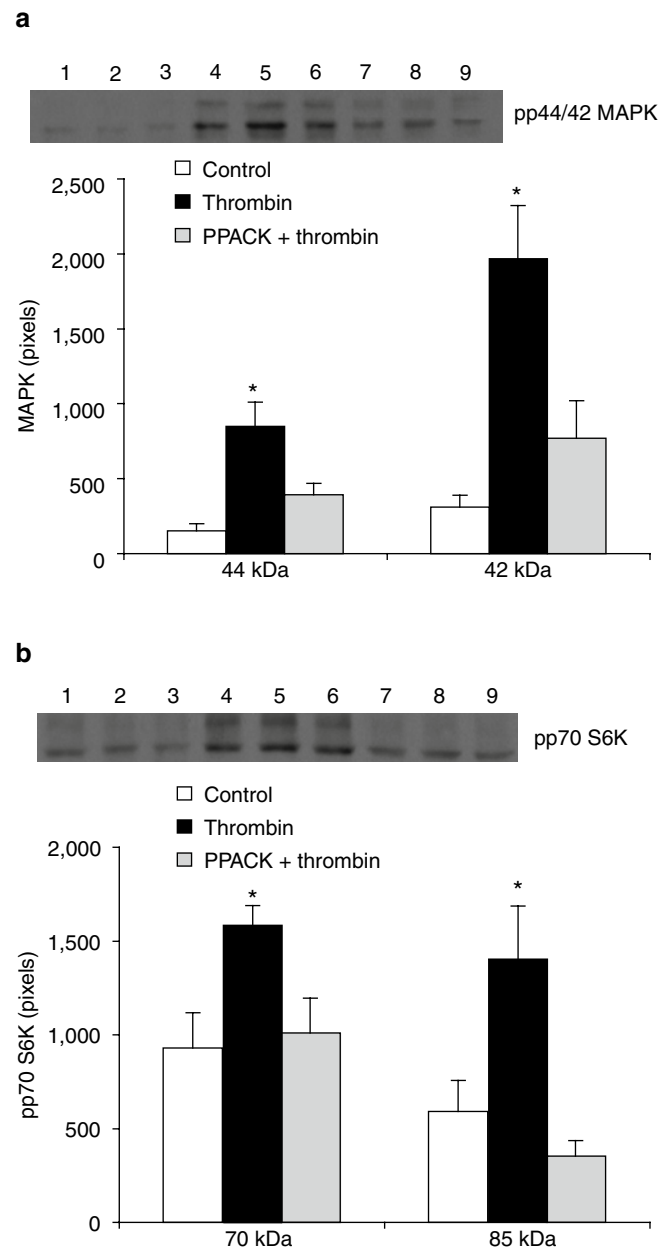


Fig. 2 Western blot analysis showing phosphorylated p44/42 MAPK (a) and p70 S6K(Thr421/Ser424) (b) levels in primary cultured neurons 24 h after treatment with vehicle (lanes 1–3), thrombin (lanes 4–6) or PPACK + thrombin (lanes 7–9). Values are mean \pm SD, * $p<0.05$ vs. the other groups

However, activation of thrombin receptors, upregulation of thrombin inhibitors, iron handling proteins and heat shock proteins in the brain may be associated with the induced tolerance [6, 7, 11–14, 22, 23]. Thrombin has a vital role in hemostasis through cleavage of fibrinogen to fibrin. Other important cellular activities of thrombin, such as p44/42 mitogen-activated protein kinase activation, appear to be receptor mediated. Thrombin receptors are seven transmembrane G protein-coupled receptors that are activated by

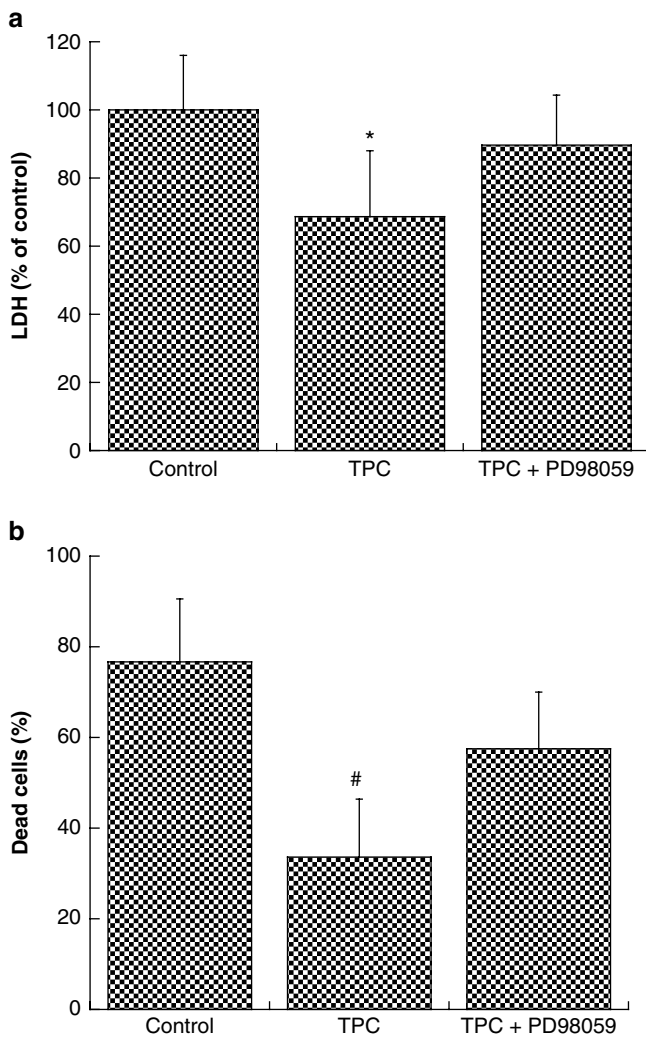


Fig. 3 The effects of PD98059 on TPC-induced neuroprotection against iron. (a) LDH levels and (b) dead neurons (%). Values are mean \pm SD, * p <0.01, # p <0.05, vs. the other groups

proteolytic cleavage rather than by ligand binding. Three protease-activated receptors, PAR-1, -3 and -4, can be activated by thrombin [24]. The present results suggest that activation of PARs can induce neuroprotection.

The data show that a low dose of thrombin activates p44/42 MAPK in neurons and PD98059, a specific inhibitor of p44/42 MAPK kinase, blocks tolerance induced by thrombin, indicating an important role of p44/42 MAPK in TPC. p44/42 MAPKs are well-known cytoplasmic signal transducers, and Gonzalez-Zulueta et al. report that activation of the p44/42 MAPK pathway is required for preconditioning induced by oxygen glucose deprivation in primary cortical cell cultures [25].

Our results also show that thrombin can also activate p70 S6K, which may be related to protein synthesis, in cultured neurons. Our previous studies have shown protein synthesis occurs following TPC and may contribute to TPC-induced

neuroprotection. New protein synthesis is key to cerebral ischemic preconditioning [17], and it may also play an important role in TPC. Recent studies indicate that the PI3K/p70S6K and ERK/p70 S6K pathways contribute to cell protection induced by ischemic preconditioning [19, 20, 26–28]. The role of ERK/p70 S6K pathway activation and new protein synthesis (e.g., iron-handling protein synthesis) in TPC need to be studied further.

In summary, thrombin and PAR agonists can induce neuronal tolerance against iron toxicity. Thrombin activates p44/42 MAPK and p70 S6K, and inhibition of p44/42 MAPK kinase abolishes thrombin-induced tolerance, suggesting a potential role of the p44/42 MAPK/p70 S6K pathway in TPC.

Acknowledgment This study was supported by grants NS-017760, NS-039866 and NS-057539 from the National Institutes of Health (NIH) and 0840016N from the American Heart Association (AHA). The content is solely the responsibility of the authors and does not necessarily represent the official views of the NIH and AHA.

Conflict of interest statement We declare that we have no conflict of interest.

References

1. Cannon JR, Keep RF, Hua Y, Richardson RJ, Schallert T, Xi G (2005) Thrombin preconditioning provides protection in a 6-hydroxydopamine Parkinson's disease model. *Neurosci Lett* 373:189–194
2. Choi SH, da Lee Y, Kim SU, Jin BK (2005) Thrombin-induced oxidative stress contributes to the death of hippocampal neurons in vivo: role of microglial NADPH oxidase. *J Neurosci* 25:4082–4090
3. Choi SH, da Lee Y, Ryu JK, Kim J, Joe EH, Jin BK (2003) Thrombin induces nigral dopaminergic neurodegeneration in vivo by altering expression of death-related proteins. *Neurobiol Dis* 14:181–193
4. Henrich-Noack P, Striggow F, Reiser G, Reymann KG (2006) Preconditioning with thrombin can be protective or worsen damage after endothelin-1-induced focal ischemia in rats. *J Neurosci Res* 83:469–475
5. Hua Y, Keep R, Hoff J, Xi G (2007) Brain injury after intracerebral hemorrhage: the role of thrombin and iron. *Stroke* 38:759–762
6. Hua Y, Keep RF, Hoff JT, Xi G (2003) Thrombin preconditioning attenuates brain edema induced by erythrocytes and iron. *J Cereb Blood Flow Metab* 23:1448–1454
7. Jiang Y, Wu J, Hua Y, Keep RF, Xiang J, Hoff JT, Xi G (2002) Thrombin-receptor activation and thrombin-induced brain tolerance. *J Cereb Blood Flow Metab* 22:404–410
8. Masada T, Xi G, Hua Y, Keep RF (2000) The effects of thrombin preconditioning on focal cerebral ischemia in rats. *Brain Res* 867:173–179
9. Striggow F, Riek M, Breder J, Henrich-Noack P, Reymann KG, Reiser G (2000) The protease thrombin is an endogenous mediator of hippocampal neuroprotection against ischemia at low concentrations but causes degeneration at high concentrations. *Proc Natl Acad Sci USA* 97:2264–2269
10. Vaughan PJ, Pike CJ, Cotman CW, Cunningham DD (1995) Thrombin receptor activation protects neurons and astrocytes from

- cell death produced by environmental insults. *J Neurosci* 15: 5389–5401
11. Xi G, Hua Y, Keep RF, Hoff JT (2000) Induction of colligin may attenuate brain edema following intracerebral hemorrhage. *Acta Neurochir Suppl* 76:501–505
 12. Xi G, Keep RF, Hua Y, Xiang JM, Hoff JT (1999) Attenuation of thrombin-induced brain edema by cerebral thrombin preconditioning. *Stroke* 30:1247–1255
 13. Yang S, Hua Y, Nakamura T, Keep RF, Xi G (2006) Up-regulation of brain ceruloplasmin in thrombin preconditioning. *Acta Neurochir Suppl* 96:203–206
 14. Cannon JR, Keep RF, Schallert T, Hua Y, Richardson RJ, Xi G (2006) Protease-activated receptor-1 mediates protection elicited by thrombin preconditioning in a rat 6-hydroxydopamine model of Parkinson's disease. *Brain Res* 1116:177–186
 15. Gidday JM (2010) Pharmacologic preconditioning: translating the promise. *Transl Stroke Res* 1:19–30
 16. Keep RF, Wang MM, Xiang J, Hua Y, Xi G (2010) Is there a place for cerebral preconditioning in the clinic? *Transl Stroke Res* 1:4–18
 17. Dirnagl U, Simon RP, Hallenbeck JM (2003) Ischemic tolerance and endogenous neuroprotection. *Trends Neurosci* 26:248–254
 18. Gidday JM (2006) Cerebral preconditioning and ischaemic tolerance. *Nat Rev Neurosci* 7:437–448
 19. Hausenloy DJ, Mocanu MM, Yellon DM (2004) Cross-talk between the survival kinases during early reperfusion: its contribution to ischemic preconditioning. *Cardiovasc Res* 63:305–312
 20. Hausenloy DJ, Tsang A, Mocanu MM, Yellon DM (2005) Ischemic preconditioning protects by activating prosurvival kinases at reperfusion. *Am J Physiol Heart Circ Physiol* 288:H971–H976
 21. Berven LA, Crouch MF (2000) Cellular function of p70S6K: a role in regulating cell motility. *Immunol Cell Biol* 78:447–451
 22. Hua Y, Xi G, Keep RF, Wu J, Jiang Y, Hoff JT (2002) Plasminogen activator inhibitor-1 induction after experimental intracerebral hemorrhage. *J Cereb Blood Flow Metab* 22:55–61
 23. Xi G, Reiser G, Keep RF (2003) The role of thrombin and thrombin receptors in ischemic, hemorrhagic and traumatic brain injury: deleterious or protective? *J Neurochem* 84:3–9
 24. Coughlin SR (2000) Thrombin signalling and protease-activated receptors. *Nature* 407:258–264
 25. Gonzalez-Zulueta M, Feldman AB, Klesse LJ, Kalb RG, Dillman JF, Parada LF, Dawson TM, Dawson VL (2000) Requirement for nitric oxide activation of p21(ras)/extracellular regulated kinase in neuronal ischemic preconditioning. *Proc Natl Acad Sci USA* 97:436–441
 26. Kis A, Yellon DM, Baxter GF (2003) Second window of protection following myocardial preconditioning: an essential role for PI3 kinase and p70S6 kinase. *J Mol Cell Cardiol* 35:1063–1071
 27. Malhotra S, Savitz SI, Ocava L, Rosenbaum DM (2006) Ischemic preconditioning is mediated by erythropoietin through PI-3 kinase signaling in an animal model of transient ischemic attack. *J Neurosci Res* 83:19–27
 28. Wynne AM, Mocanu MM, Yellon DM (2005) Pioglitazone mimics preconditioning in the isolated perfused rat heart: a role for the pro-survival kinases PI3K and P42/44MAPK. *J Cardiovasc Pharmacol* 46:817–822

Granulocyte Colony-Stimulating Factor Treatment Provides Neuroprotection in Surgically Induced Brain Injured Mice

Nikan H. Khatibi, Vikram Jadhav, Mehdi Saidi, Wanqiu Chen, Robert Martin, Gary Stier, Jiping Tang, and John H. Zhang

Abstract Surgically induced brain injury (SBI) is a common concern after a neurosurgical procedure. Current treatments aimed at reducing the postoperative sequela are limited. Granulocyte-colony stimulating factor (G-CSF), a hematopoietic growth factor involved in the inflammatory process, has been shown in various animal models to be neuroprotective. Consequently, in this study, we investigated the use of G-CSF as a treatment modality to reduce cell death and brain edema, while improving neurobehavioral deficits following an SBI in mice. Eleven-week-old C57 black mice ($n=76$) were randomly placed into four groups: sham ($n=19$), SBI ($n=21$), SBI with G-CSF pre-treatment ($n=15$) and SBI with G-CSF pre/post-treatment ($n=21$). Treated groups received a single dose of G-CSF intraperitoneally at 24, 12 and 1 h pre-surgery and/or 6 and 12 h post-surgery. Postoperative assessment occurred at 24 h and included neurobehavioral testing and measurement for both cell death and brain edema. Results indicated that pre-treatment with G-CSF reduced both cell death and brain edema, while post-treatment reduced neurobehavioral deficits. This study

implies that the morphological changes in the brain are effected by pre-treatment; however, in order to activate and/or amplify targets involved in the recovery process, more dosing regimens may be needed.

Keywords Granulocyte colony-stimulating factor (G-CSF) · Surgically induced brain injury (SBI) · Neurosurgery

Introduction

Surgically induced brain injury (SBI) refers to the wide range of unintentional injuries that take place during routine neurosurgical procedures. These injuries occur more commonly along the edge of tissue resection because of direct surgical trauma, electrocautery burn, stretch damage from tissue retraction and intraoperative bleeding [1, 2]. The concern with SBI is the heightened inflammatory response that mounts in an attempt to orchestrate the effects of tissue damage. Side effects of this response include disruption of blood-brain-barrier (BBB) integrity, apoptotic cell death and subsequent neurobehavioral deterioration. Unfortunately, current therapies aimed at battling the effects of SBI are limited. Consequently, discovering direct anti-inflammatory therapies that could potentially decrease brain edema and cell death while improving neurobehavioral function would be of great benefit.

Granulocyte colony-stimulating factor (G-CSF) is a hematopoietic growth factor, cytokine, and glycoprotein responsible for the proliferation, survival, and maturation of neutrophil precursors [3]. It stimulates the bone marrow to produce and release neutrophilic precursors as well as hematopoietic stem cells (HSC) into the circulation. It has been discovered that G-CSF plays a key role in the central nervous system (CNS), where it provides a level of neuroprotection [3]. The underlying mechanism involved in the G-CSF induced protection is unknown; however, in various stroke models G-CSF has been shown to exert neuroprotective

N.H. Khatibi, R. Martin, and G. Stier
Department of Anesthesiology, Loma Linda Medical Center,
Loma Linda, CA, USA

V. Jadhav, M. Saidi, and W. Chen
Department of Physiology, Loma Linda University,
School of Medicine, Loma Linda, CA, USA

J. Tang (✉)
Department of Physiology, Loma Linda University,
School of Medicine, Loma Linda, CA, USA and
Department of Physiology and Pharmacology, Loma Linda University,
School of Medicine, Loma Linda, CA 92354, USA
e-mail: jtang@llu.edu

J.H. Zhang
Department of Anesthesiology, Loma Linda Medical Center,
Loma Linda, CA, USA and
Department of Physiology, Loma Linda University,
School of Medicine, Loma Linda, CA, USA and
Department of Neurosurgery, Loma Linda Medical Center,
Loma Linda, CA, USA

actions through the inhibition of apoptosis, inflammation and the stimulation of both neurogenesis and angiogenesis [4].

Accordingly, in this study, we investigated the effects of G-CSF pre- and post-treatment on cerebral edema, neuronal cell death and neurobehavioral functioning in SBI mice. Two dosing regimens were used to evaluate these outcomes.

Materials and Methods

Animal Groups

All procedures for this study were approved by the Animal Care and Use Committee at Loma Linda University and complied with the NIH Guide for the Care and Use of Laboratory Animals. Seventy-six Sprague-Dawley mice weighing between 35 and 45 g were randomly divided into the following four groups: sham surgery ($n=19$), SBI ($n=21$), SBI with G-CSF pre-treatment ($n=15$) and SBI with G-CSF pre-/post-treatment ($n=21$).

Operative Procedure

The SBI model was adapted as previously described in mice [5]. Briefly, mice were anesthetized with a ketamine (100 mg/kg)/xylazine (10 mg/kg) combination intraperitoneal injection and positioned prone in a stereotaxic head frame (Stoelting, Wood Dale, IL). A 3 mm by 3 mm cranial window was created 1 mm anterior and 2 mm lateral to the coronal and sagittal sutures, respectively. Using a flat blade (6 mm \times 1.5 mm), two incisions were made along the sagittal and coronal planes leading away from the bregma and extending to the edge of the craniotomy window. The sectioned brains were weighed and were not significantly different between animals. Electrocautery was utilized for 2 s along the medial coronal and posterior sagittal borders at a power level consistent with the coagulation setting used in the operating room. Sham surgery included only a craniotomy window and replacement of the bone flap without any dural incisions.

Treatment Method

A 100 μ g/kg G-CSF (Neupogen, Amgen, Thousand Oaks, CA) intraperitoneal injection was given at 24, 12 and 1 h pre-surgery in the pre-treatment group, while the post-treatment group received an additional treatment at 6 and 12 h post-surgery. Normal saline injections in similar volumes were

given to the sham and vehicle groups on the same dosing schedule as G-CSF.

Assessment of Neurobehavioral Deficits

Prior to sacrificing at 24 h, neurological outcomes were assessed by a blind observer using the Modified Garcia Score [6], beam balance test and modified wire hanging test [7].

The Modified Garcia Score is a 21-point sensorimotor assessment system consisting of seven tests with scores of 0–3 for each test (maximum score=21). These seven tests included: (1) spontaneous activity, (2) side stroking, (3) vibrios touch, (4) limb symmetry, (5) climbing, (6) lateral turning and (7) forelimb walking.

Additionally, beam balance and wire hanging testing were performed. Both the beam (590 cm in length by 51 cm in width) and wire (550 cm in length by 51 mm in width) were constructed and held in place by two platforms on each side. Mice were observed for both their time and behavior until they reached one platform and scored according to six grades. The test was repeated three times, and an average score was taken [minimum score 0; maximum score (healthy rat) 5].

Brain Water Content

Brain water content was measured as previously described [8]. Briefly, mice were killed 24 h post-SBI, and the brains were immediately removed and divided into three parts: ipsilateral frontal, contralateral frontal and cerebellum. The cerebellum was used as an internal control for brain water content. Tissue samples were then weighed on an electronic analytical balance (APX-60, Denver Instrument; Arvada, CO) to the nearest 0.1 mg to obtain the wet weight (WW). The tissue was then dried at 105°C for 48 h to determine the dry weight (DW). The percent brain water content was calculated as $[(WW - DW)/WW] \times 100$.

Assessing Cell Death

Cell Death Detection ELISA kit (Roche Applied Science) was used to quantify cell death in the ipsilateral frontal cortex 24 h after SBI. For quantification of DNA fragmentation, which indicates apoptotic cell death, we used a commercial enzyme immunoassay to determine cytoplasmic histone-associated DNA fragments (Roche Molecular Biochemicals).

Statistical Analysis

Quantitative data were expressed as the mean \pm SEM. One-way ANOVA and Tukey test were used to determine significance in differences between the means. Neurological scores were evaluated using the Dunn method. A p -value <0.05 was considered statistically significant.

Results

G-CSF Pre-Treatment Reduces Brain Edema

Brain water content was measured 24 h post-SBI (Fig. 1). The results showed that vehicle mice presented with significantly worse brain edema compared to sham mice. After pre-treatment with G-CSF, brain edema reduced significantly in the contralateral frontal cortex compared to vehicle group. The ipsilateral cortex increased in brain edema, which is attributed to the direct BBB disruption from frontal lobe removal.

G-CSF Pre-Treatment Reduces Cell Death

Cell death was also measured via an absorbance assay at 24 h post-SBI (Fig. 2). The results showed that vehicle mice presented with a significant increase in the number of cell

deaths compared to sham mice. After pre-treatment with G-CSF, the number of cell deaths reduced significantly.

Post-Treatment with G-CSF Improves Neurobehavioral Deficits

To evaluate the sensorimotor deficits after SBI, the modified Garcia test, wire hanging test and beam balance test were conducted 24 h post-SBI. The results showed that vehicle mice presented with severe neurobehavioral deficits compared to sham mice. After both pre- and post-treatment with G-CSF, a significant improvement in neurobehavioral function was seen with the beam balance and wire hanging neurological tests (Fig. 3a); there was no improvement with the modified Garcia test (Fig. 3b).

Discussion

The aim of this study was to determine the effects of G-CSF treatment after SBI. We showed for the first time that pre-treatment with G-CSF could reduce cell death and attenuate brain edema following a SBI in mice. Additionally, at 24 h post-injury, we observed a marked improvement in neurobehavioral deficits after pre- and post-treatment with G-CSF. Consequently, this study suggests that the morphologic changes in the brain are effected by G-CSF pre-treatment;

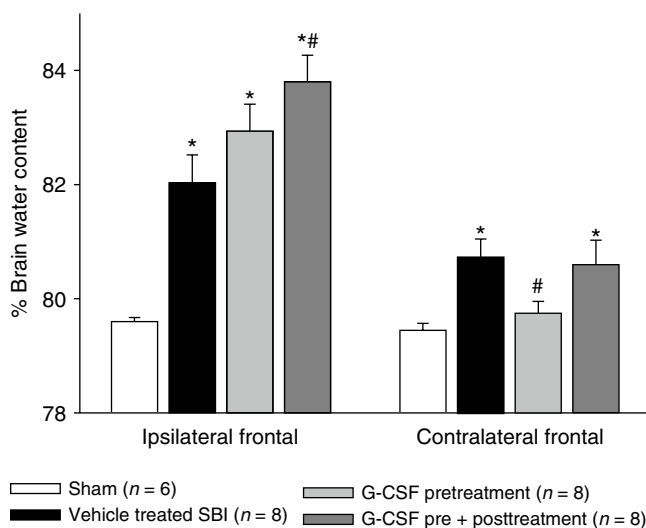


Fig. 1 Brain water content. The results showed that vehicle mice presented with significantly worse brain edema compared to sham mice. After pre-treatment with G-CSF, brain edema reduced significantly in the contralateral frontal cortex compared to vehicle group. The ipsilateral cortex increased in brain edema, which is attributed to the direct BBB disruption from frontal lobe removal. *Significant difference vs. sham ($p < 0.05$)

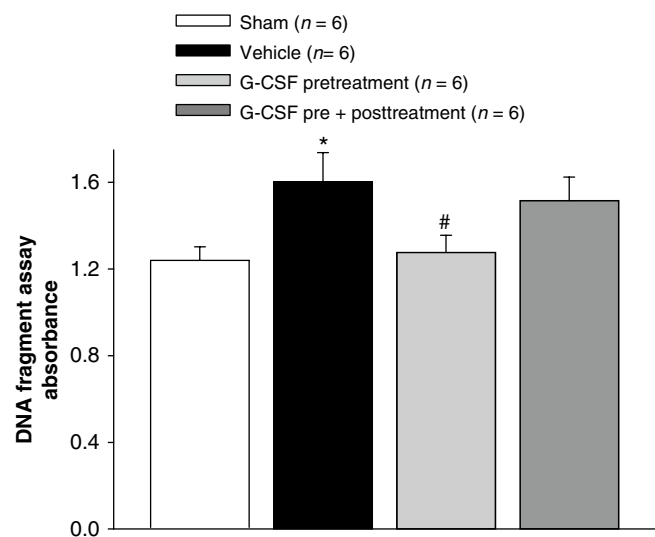


Fig. 2 Cell death measurement 24 h post SBI. The results showed that vehicle mice presented with a significant increase in the number of cell deaths compared to sham mice. After pre-treatment with G-CSF, the number of cell deaths reduced significantly. *Significant difference vs. sham ($p < 0.05$); #significant difference vs. vehicle ($p < 0.05$)

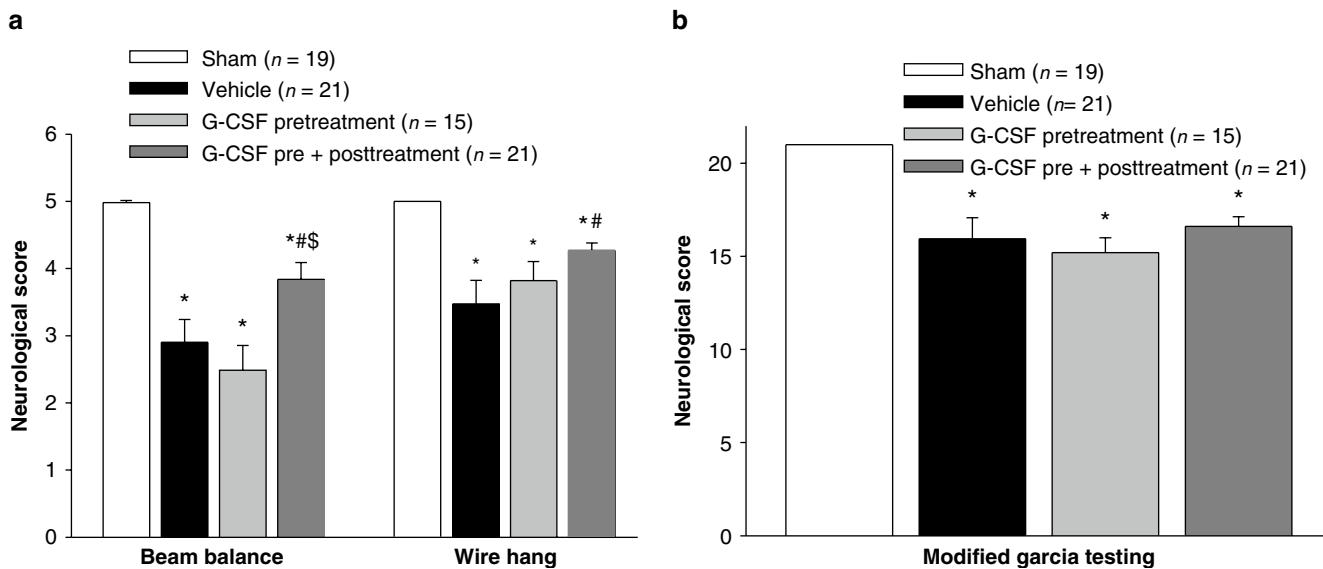


Fig. 3 Neurobehavioral deficits. The results showed that vehicle mice presented with severe neurobehavioral deficits compared to sham mice. After both pre- and post-treatment with G-CSF, a significant improvement in neurobehavioral function was seen with the beam balance and

wire hanging neurological tests (a); there was no improvement with the modified Garcia test (b). *Significant difference vs. sham ($p < 0.05$); #significant difference vs. vehicle ($p < 0.05$)

however, in order to activate and/or amplify targets involved in the plasticity process and improve neurobehavioral functioning, more dosing regimens may be needed after injury.

Cell death following a SBI is not an uncommon phenomenon. Previous works in SBI have shown massive neuronal degeneration and death in the area of injury [9], specifically, finding increased expression of pro-apoptotic BAX and active caspase-3 in cortical neurons. In particular, studies in transient focal ischemic models in mice found that G-CSF exerted a protective effect by upregulating anti-apoptotic proteins, such as STAT3 and Bcl-2. This was confirmed by Schabitz [10], who also found an elevation of STAT3 expression in the infarction penumbra in ischemic injured rats treated with G-CSF. In our study, we found that the vehicle group had a significant increase in neuronal cell deaths – an effect partially reduced by pre-treatment with G-CSF – thus suggesting that G-CSF may play a role in decreasing neuronal cell death after SBI.

In addition to its effects on neuronal cell death, SBI has been implicated in increasing the formation of brain edema by disrupting the BBB. According to Jadhav [11], infiltration of inflammatory markers, such as matrix metalloproteinases, to the site of injury is responsible for disrupting the BBB and subsequently causing an influx of edema. In a focal ischemic mouse model, G-CSF treatment was shown to decrease the amount of edema accumulated in the penumbral brain tissue [12]. G-CSF has also been found to reduce brain edema and inflammatory cell infiltration in a rat intracerebral hemorrhage model [13]. These studies are in line with our results, which showed a significant reduction in brain edema in the contralateral brain hemisphere, corresponding to the penumbral region. This implies that G-CSF pre-treatment

may reduce damage associated with inflammatory infiltration caused by SBI. Although our results did show an increase in brain edema in the ipsilateral frontal cortex, this increase is most likely due to the direct BBB disruption from performing the model. Consequently, the contralateral side was evaluated, investigating the potential of G-CSF to reduce penumbral edema following a SBI.

Although there were morphological improvements with G-CSF pre-treatment, it took additional treatments after the injury to reduce neurobehavioral deficits. In our mouse population, we found a significant improvement with motor and strength testing after both pre- and post-G-CSF treatments compared to vehicle. This was confirmed using the beam balance and wire hanging tests. Previous works have found similar results. In a focal ischemic rat model, G-CSF was found to improve lesion repair and improve neuronal plasticity and vascularization [14], while in a MCAO model, a post-treatment dose of G-CSF improved long-term functional and cognitive outcomes [15].

Conclusion

This study implies that the morphologic changes in the brain are effected by G-CSF pre-treatment; however, in order to activate and/or amplify targets involved in the plasticity process and improve neurobehavioral deficits, more dosing regimens may be needed after the initial injury. Consequently, further studies will be needed to explore the use of G-CSF in the clinical setting of SBI.

Acknowledgement This study is partially supported by NIH NS053407 to J.H. Zhang and NS060936 to J. Tang.

Conflict of interest statement We declare that we have no conflict of interest.

References

1. Andrews RJ, Muto RP (1992) Retraction brain ischaemia: cerebral blood flow, evoked potentials, hypotension and hyperventilation in a new animal model. *Neurol Res* 14(1):12–18
2. Hernesniemi J, Leivo S (1996) Management outcome in third ventricular colloid cysts in a defined population: a series of 40 patients treated mainly by transcallosal microsurgery. *Surg Neurol* 45(1):2–14
3. Schneider A, Hans-George K (2005) A role for G-CSF in the central nervous system. *Cell Cycle* 4(12):1753–1757
4. Lu CZ, Xiao G (2006) G-CSF and neuroprotection: a therapeutic perspective in cerebral ischaemia. *Biochem Soc Trans* 34:6
5. Jadhav V et al (2007) Neuroprotection against surgically induced brain injury. *Surg Neurol* 67(1):15–20, discussion 20
6. Garcia JH et al (1995) Neurological deficit and extent of neuronal necrosis attributable to middle cerebral artery occlusion in rats. Statistical validation. *Stroke* 26(4):627–634, discussion 635
7. Yamaguchi M et al (2007) Matrix metalloproteinase inhibition attenuates brain edema in an in vivo model of surgically-induced brain injury. *Neurosurgery* 61(5):1067–1075, discussion 1075–1076
8. Tang J, Liu J, Zhou C, Alexander JS, Nanda A, Granger DN, Zhang JH (2004) Mmp-9 deficiency enhances collagenase-induced intracerebral hemorrhage and brain injury in mutant mice. *J Cereb Blood Flow Metab* 24:1133–1145
9. Sulejczak D, Grieb P, Walski M (2008) Apoptotic death of cortical neurons following surgical brain injury. *Folia Neuropathol* 46(3): 213–219
10. Schabitz WR, Kollmar R, Schwaninger M (2003) Neuroprotective effect of G-CSF after focal cerebral ischemia. *Stroke* 34:745–751
11. Jadhav V, Yamaguchi M, Obenaus A, Zhang JH (2008) Matrix metalloproteinase inhibition attenuates brain edema after surgical brain injury. *Acta Neurochir Suppl* 102:357–361
12. Gibson CL, Jones NC, Prior MJ (2005) G-CSF suppresses edema formation and reduces interleukin-1b expression after cerebral ischemia in mice. *J Neuropathol Exp Neurol* 64:763–769
13. Park HK, Chu K, Lee ST (2005) Granulocyte colony-stimulating factor induces sensorimotor recovery in intracerebral hemorrhage. *Brain Res* 1041:125–131
14. Shyu WC, Lin SZ, Yang HI (2004) Functional recovery of stroke rats induced by granulocyte colony-stimulating factor-stimulated stem cells. *Circulation* 110:1847–1854
15. Gibson CL, Bath PM, Murphy SP (2005) G-CSF reduces infarct volume and improves functional outcome after transient focal cerebral ischemia in mice. *J Cereb Blood Flow Metab* 25(4):431–439

Tamoxifen Treatment for Intracerebral Hemorrhage

Qing Xie, Jian Guan, Gang Wu, Guohua Xi, Richard F. Keep, and Ya Hua

Abstract Tamoxifen is a selective estrogen receptor modulator. In this study we investigated whether or not tamoxifen reduces intracerebral hemorrhage (ICH)-induced brain injury in rats. In all experiments, adult male Sprague-Dawley rats received an injection of 100 μ L autologous whole blood into the right basal ganglia. In the first set of experiments, rats were treated with tamoxifen (2.5 mg/kg or 5 mg/kg, i.p.) or vehicle 2 and 24 h after ICH and were killed at day 3 for brain edema measurement. In the second set of experiments, rats were treated with tamoxifen (5 mg/kg) or vehicle and magnetic resonance imaging (MRI), and behavior tests were performed at days 1, 7, 14 and 28. Rats were killed at day 28 for brain histology. We found that tamoxifen at 5 but not at 2.5 mg/kg reduced perihematomal brain edema at day 3 ($p < 0.05$). Brain histology showed that tamoxifen reduced caudate atrophy at day 28 ($p < 0.01$). Tamoxifen also improved functional outcome ($p < 0.05$). MRI demonstrated a tendency to smaller T2* lesions in tamoxifen-treated rats. However, two out of five rats treated with tamoxifen developed hydrocephalus. These results suggest that tamoxifen has neuroprotective effects in ICH, but the cause of hydrocephalus development following tamoxifen treatment needs to be examined further.

Keywords Cerebral hemorrhage · Brain edema · Brain atrophy · Hydrocephalus · Tamoxifen

Introduction

Gender has an important role in brain injury after ischemic and hemorrhagic stroke. Our previous studies demonstrated that brain edema after intracerebral hemorrhage (ICH) is less in female compared to male rats [1–3], a gender difference that appears to involve activation of estrogen receptors (ER) in the female rats. Several estrogen receptors have been discovered, including estrogen receptor (ER)- α , - β , -X and a membrane estrogen receptor [4]. Estrogen-induced neuroprotection can be ER mediated or ER independent [4].

Tamoxifen is a selective estrogen receptor modulator, which was discovered and named ICI 46,474 in 1967 [5]. Tamoxifen has also been reported to have a neuroprotective in ischemic stroke [6, 7] and Parkinson's disease [8]. However, it is still not clear whether or not tamoxifen is protective for the brain after ICH. This study examined whether tamoxifen reduces ICH-induced brain edema, brain atrophy and neurological deficits in male rats.

Materials and Methods

Animal Preparation and Intracerebral Infusion

Animal use protocols were approved by the University of Michigan Committee on the Use and Care of Animals. Male Sprague-Dawley rats (Charles River Laboratories, Portage, MI), 275–300 g each, were used in this study. Rats were anesthetized by pentobarbital (50 mg/kg, i.p.). Rectal body temperature was maintained at 37.5°C by using a feedback-controlled heating pad. The right femoral artery was catheterized to obtain blood for injection, to monitor blood

Q. Xie and G. Wu
Department of Neurosurgery, University of Michigan,
Ann Arbor, MI, USA and
Department of Neurosurgery, Huashan Hospital,
Fudan University, Shanghai, China

J. Guan, R.F. Keep, and G. Xi
Department of Neurosurgery, University of Michigan,
Ann Arbor, MI, USA

Y. Hua (✉)
Department of Neurosurgery, University of Michigan, R5018 BSRB,
109 Zina Pitcher Place, Ann Arbor, MI 48109–2200, USA
e-mail: yahua@umich.edu

pressure and to analyze blood pH, PaO₂, PaCO₂, hematocrit and glucose concentrations. Rats were placed in a stereotactic frame (Kopf Instruments) and a 1-mm cranial burr hole drilled on the right coronal suture 3.5 mm lateral to the midline. A 26-gauge needle was inserted stereotactically into the right basal ganglia (coordinates: 0.2 mm anterior, 5.5 mm ventral, 3.5 mm lateral to the bregma). Autologous whole blood (100 µL) was infused at a rate of 10 µL/min using a microinfusion pump. The needle was then removed, the burr hole sealed with bone wax, the skin incision closed with sutures and the animal allowed to recover.

Experimental Groups

There were two sets of experiments in this study. In the first set, ICH rats were treated with tamoxifen (2.5 or 5 mg/kg in 4% DMSO, i.p., 2 and 24 h after ICH, Tocris Bioscience, Ellisville, MO, $n=6$) or vehicle ($n=6$). Rats were euthanized at day 3 to determine brain water content. In the second set, rats were treated with tamoxifen (5 mg/kg, $n=5$) or vehicle ($n=8$) at 2 and 24 h after ICH. Rats had both T2-weighted and T2*-weighted gradient-echo MR scans at days 1, 7, 14 and 28 after ICH, and then were euthanized for brain histology. Body weight and neurological deficits were measured on days 1, 3, 7, 14, 21 and 28 after operation.

Brain Water Content

Animals were euthanized by decapitation under deep pentobarbital anesthesia (100 mg/kg, i.p.) to measure brain water content. The rat brains were removed immediately, and a 3-mm-thick coronal brain slice 4 mm from the frontal pole was cut with a sharp blade. The slice was divided into four samples, ipsi- and contralateral basal ganglion and ipsi- and contralateral cortex. The cerebellum was also obtained as a control. Each of these five brain tissue samples was weighed on an electronic analytical balance to the nearest 0.1 mg to obtain the wet weight (WW). Samples were then dried in a gravity oven at 100°C for 24 h to obtain the dry weight (DW). Brain water content (%) was calculated as $((WW - DW)/WW) \times 100\%$.

Behavioral Tests

To assess neurological deficits, forelimb placing, forelimb use asymmetry and corner turn tests were used. These have been described in detail previously [9]. All animal behavioral

tests were evaluated at 1, 3, 7, 14, 21 and 28 days by an investigator who was blinded to the treatment.

Magnetic Resonance Imaging

Head MRI scans were performed to get T2 and T2* images at 1, 7, 14 and 28 days after ICH as described in our previous studies [10, 11]. All measurements were repeated three times and mean values used.

Brain Atrophy Measurement

Brain atrophy was measured as previously described [10]. Coronal sections from 1 mm posterior to the blood injection site were stained with hematoxylin and eosin (H&E) and scanned. The caudate in each hemisphere was outlined on a computer and caudate size measured using Image. Brain tissue loss was calculated by the formula as: $(\text{contralateral basal ganglia} - \text{ipsilateral basal ganglia}) / \text{contralateral basal ganglia} \times 100\%$.

Statistical Analysis

All data in this study are presented as mean \pm SD. Data were analyzed with Student's *t* test or one-way analysis of variance (ANOVA). Differences were set significant at $p < 0.05$.

Results

During the long-term experiments, body weight was monitored. It decreased on the first and third day after ICH, but then gradually increased. There was no significant difference in body weight between tamoxifen-treated and vehicle-treated groups ($p > 0.05$).

ICH causes brain edema in rats. Tamoxifen treatment at the dose 5 mg/kg significantly reduced brain water content (82.2 ± 0.7 vs. $83.4 \pm 1.1\%$ in vehicle treated group, $p < 0.05$) in the ipsilateral basal ganglia 3 days after ICH. However, tamoxifen at a dose of 2.5 mg failed to reduce ICH-induced brain edema at day 3 ($p > 0.05$).

Behavioral tests, including forelimb placing, corner turn and forelimb use asymmetry tests, were performed at days 1, 3, 7, 14, 21 and 28 after ICH. Tamoxifen treatment improved the forelimb placing score (e.g., day 14: 40 ± 10 vs. $24 \pm 15\%$ in the vehicle-treated group, $p < 0.05$), forelimb using asymmetry

score (e.g. day 28: 3 ± 6 vs. $22 \pm 8\%$ in the vehicle-treated group, $p < 0.05$) and corner turn score ($p < 0.05$). Brain tissue loss in the ipsilateral caudate at day 28 was significantly less in tamoxifen-treated rats (21.9 ± 4.3 vs. $30.3 \pm 1.8\%$ in vehicle-treated group, $p < 0.05$, Fig. 1).

On T2* images, there was no significant difference between the two groups ($p > 0.05$) in T2* lesion size from day 1 to 28 (data not shown), although at day 28 there was a tendency for smaller T2* lesions in tamoxifen-treated rats (28.5 ± 4.7 vs. 34.3 ± 6.1 mm³ in vehicle-treated group, $p = 0.14$, Fig. 2). On T2 images, we found that two of five tamoxifen-treated rats developed obvious dilation of ventricles starting 7 days after treatment (Fig. 3), but no vehicle-treated rats showed such dilation.

Discussion

In this study, we found that tamoxifen treatment (5 mg/kg) reduced brain edema, brain atrophy and neurological deficits after ICH. However, surprisingly, we found that with this dosage, hydrocephalus developed in two out of five rats.

The half-life of tamoxifen is 9–12 h after an initial dose, and tamoxifen is still detectable after 28 days after 7 days of chronic use [12]. We therefore chose 2 and 24 h for injection time points. We tried two different doses and found that only the higher dose (5 mg/kg) reduced acute brain edema after ICH, and this higher dose was chosen for our long-term study.

In animal experiments, high-dose tamoxifen has also been used in studies of cerebral ischemia [6, 7] and Parkinson's

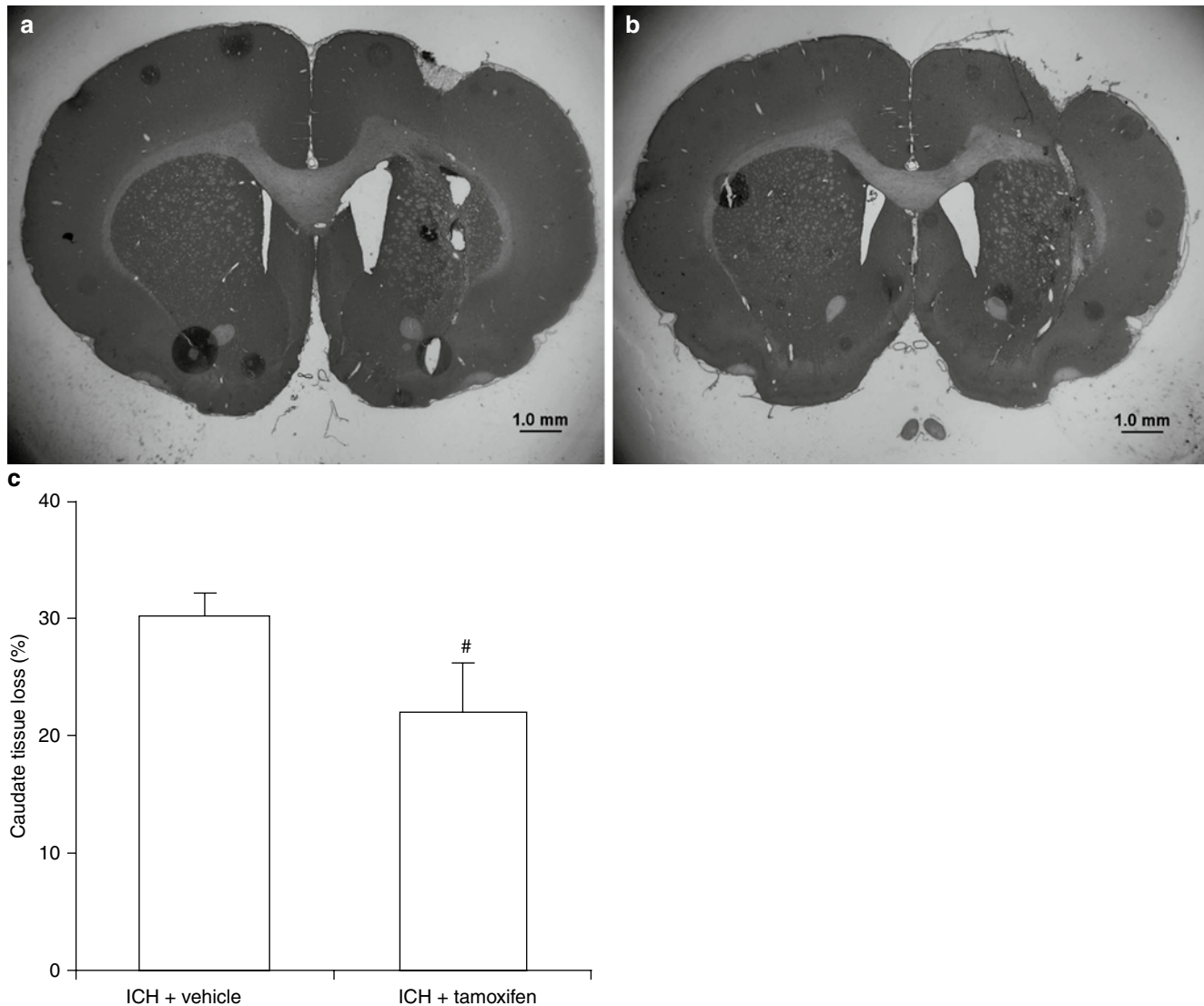


Fig. 1 Coronal brain sections at day 28 after ICH in rats treated with (a) vehicle or (b) tamoxifen. (c) The ipsilateral caudate tissue loss in rats treated with vehicle or tamoxifen at day 28. Values are mean \pm SD, $n = 5$, $\#p < 0.01$ vs. ICH + Vehicle

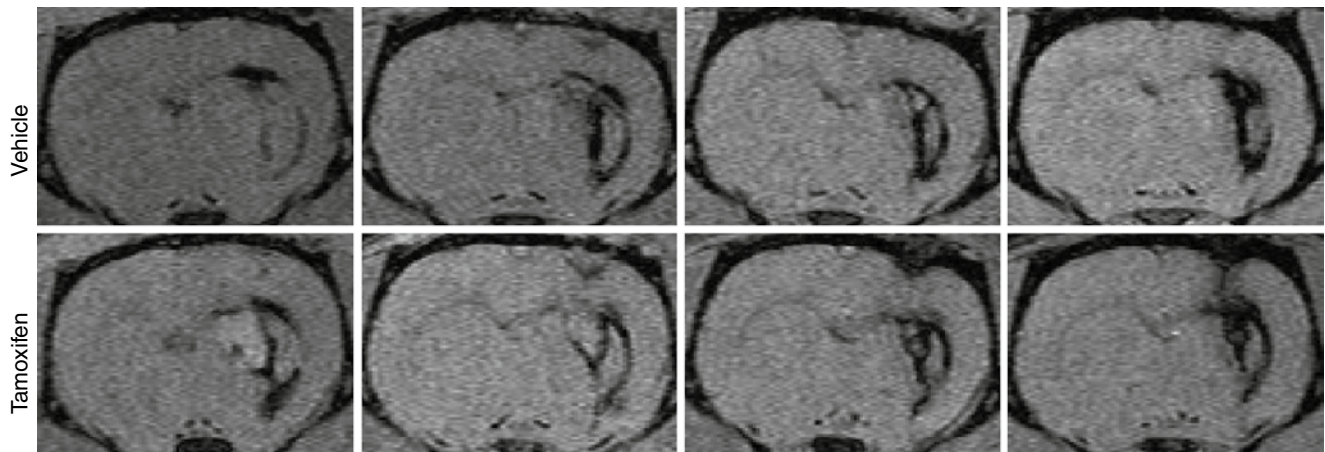


Fig. 2 MR T2*-weighted MRI showing T2* lesions in rats treated with vehicle or tamoxifen (5 mg/kg at 2 and 24 h after ICH) 28 days after ICH

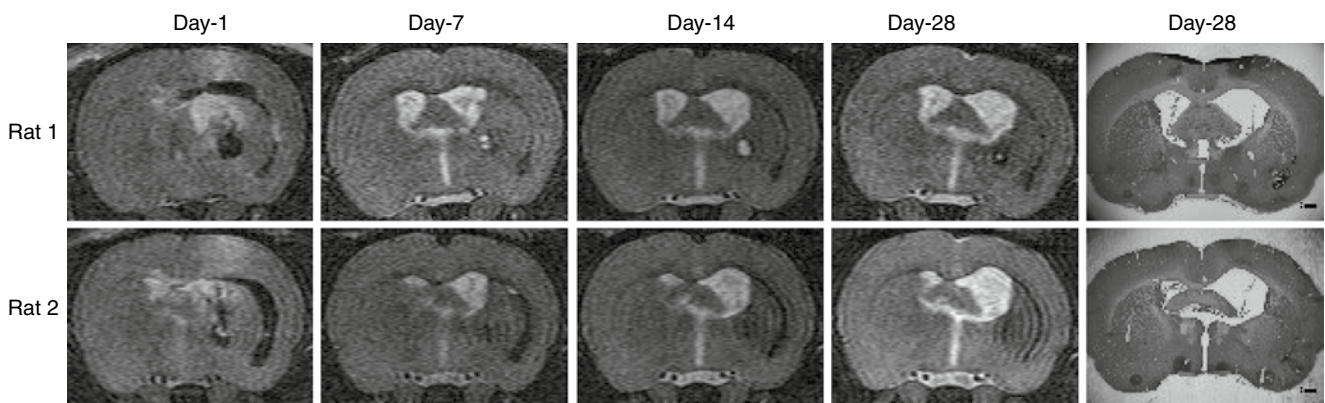


Fig. 3 T2-weighted MR images and coronal section of H&E staining showing hydrocephalus in two out of five rats treated with tamoxifen after ICH

disease [8, 13]. Most of the experiments conclude that doses higher, but not lower, than 5 mg/kg/day, have beneficial effects and that the high doses are generally well tolerated. Tamoxifen-induced neuroprotection may be estrogen receptor mediated, although some reports indicate that protection with high dose tamoxifen is not through estrogen receptors but through anti-oxidative actions [14]. It is well known that oxidative stress has a major role in brain injury following ICH [3].

Hydrocephalus developed in two of five tamoxifen-treated rats in our study, suggesting that tamoxifen may affect the process of production, circulation or absorption of cerebrospinal fluid. There are only a few experiments focusing on long-term changes and side effects in animals after tamoxifen treatment [15]. So far, in clinical trials with MRI follow-up, no tamoxifen-induced hydrocephalus cases have been reported [16, 17]. Whether or not tamoxifen only induces hydrocephalus after intracerebral hemorrhage should be studied further.

Acknowledgment This study was supported by grants NS-017760, NS-039866 and NS-057539 from the National Institutes of Health (NIH) and 0755717Z, 0840016N from the American Heart Association (AHA). The content is solely the responsibility of the authors and does not necessarily represent the official views of the NIH and AHA. Dr. Xie was supported by NSFC-30901549 from the China National Natural Science Foundation.

Conflict of interest statement We declare that we have no conflict of interest.

References

1. Hurn PD, Macrae IM (2000) Estrogen as a neuroprotectant in stroke. *J Cereb Blood Flow Metab* 20:631–652
2. Nakamura T, Hua Y, Keep RF, Park JW, Xi G, Hoff JT (2005) Estrogen therapy for experimental intracerebral hemorrhage in rats. *J Neurosurg* 103:97–103
3. Xi G, Keep RF, Hoff JT (2006) Mechanisms of brain injury after intracerebral haemorrhage. *Lancet Neurol* 5:53–63

4. Rau SW, Dubal DB, Bottner M, Gerhold LM, Wise PM (2003) Estradiol attenuates programmed cell death after stroke-like injury. *J Neurosci* 23:11420–11426
5. Harper MJ, Walpole AL (1967) A new derivative of triphenylethylene: effect on implantation and mode of action in rats. *J Reprod Fertil* 13:101–119
6. Kimelberg HK, Feustel PJ, Jin Y, Paquette J, Boulos A, Keller RW Jr, Tranmer BI (2000) Acute treatment with tamoxifen reduces ischemic damage following middle cerebral artery occlusion. *NeuroReport* 11:2675–2679
7. Zhang Y, Jin Y, Behr MJ, Feustel PJ, Morrison JP, Kimelberg HK (2005) Behavioral and histological neuroprotection by tamoxifen after reversible focal cerebral ischemia. *Exp Neurol* 196:41–46
8. Obata T, Kubota S (2001) Protective effect of tamoxifen on 1-methyl-4-phenylpyridine-induced hydroxyl radical generation in the rat striatum. *Neurosci Lett* 308:87–90
9. Hua Y, Schallert T, Keep RF, Wu J, Hoff JT, Xi G (2002) Behavioral tests after intracerebral hemorrhage in the rat. *Stroke* 33:2478–2484
10. Okauchi M, Hua Y, Keep RF, Morgenstern LB, Schallert T, Xi G (2010) Deferoxamine treatment for intracerebral hemorrhage in aged rats: therapeutic time window and optimal duration. *Stroke* 41:375–382
11. Wu G, Xi G, Hua Y, Sagher O (2010) T2* magnetic resonance imaging sequences reflect brain tissue iron deposition following intracerebral hemorrhage. *Transl Stroke Res* 1:31–34
12. Fabian C, Sternson L, El-Serafi M, Cain L, Hearne E (1981) Clinical pharmacology of tamoxifen in patients with breast cancer: correlation with clinical data. *Cancer* 48:876–882
13. Smith CP, Oh JD, Bibbiani F, Collins MA, Avila I, Chase TN (2007) Tamoxifen effect on L-DOPA induced response complications in parkinsonian rats and primates. *Neuropharmacology* 52:515–526
14. Zhang Y, Milatovic D, Aschner M, Feustel PJ, Kimelberg HK (2007) Neuroprotection by tamoxifen in focal cerebral ischemia is not mediated by an agonist action at estrogen receptors but is associated with antioxidant activity. *Exp Neurol* 204:819–827
15. Atakisi E, Kart A, Atakisi O, Topcu B (2009) Acute tamoxifen treatment increases nitric oxide level but not total antioxidant capacity and adenosine deaminase activity in the plasma of rabbits. *Eur Rev Med Pharmacol Sci* 13:239–243
16. Puchner MJ, Giese A, Lohmann F, Cristante L (2004) High-dose tamoxifen treatment increases the incidence of multifocal tumor recurrences in glioblastoma patients. *Anticancer Res* 24:4195–4203
17. Sankar T, Caramanos Z, Assina R, Villemure JG, Leblanc R, Langleben A, Arnold DL, Preul MC (2008) Prospective serial proton MR spectroscopic assessment of response to tamoxifen for recurrent malignant glioma. *J Neurooncol* 90:63–76

Prostaglandin E₂ EP₁ Receptor Inhibition Fails to Provide Neuroprotection in Surgically Induced Brain-Injured Mice

Nikan H. Khatibi, Vikram Jadhav, Brenden Matus, Nancy Fathali, Robert Martin, Richard Applegate, Jiping Tang, and John H. Zhang

Abstract Recent trials have shown that the prostaglandin E₂ EP₁ receptor is responsible for NMDA excitotoxicity in the brain after injury. Consequently, in this study, we investigated the use of SC-51089, a selective prostaglandin E₂ EP₁ receptor antagonist, as a pre-treatment modality to decrease cell death, reduce brain edema, and improve neurobehavioral function after surgically induced brain injury (SBI) in mice. Eleven-week-old C57 black mice ($n=82$) were randomly assigned to four groups: sham ($n=31$), SBI ($n=27$), SBI treated with SC51089 at 10 $\mu\text{g}/\text{kg}$ ($n=7$), and SBI treated with SC51089 at 100 $\mu\text{g}/\text{kg}$ ($n=17$). Treated groups received a single dose of SC51089 intraperitoneally at 12 and 1 h pre-surgery. SBI was performed by resecting the right frontal lobe using a frontal craniotomy. Postoperative assessment occurred at 24 and 72 h, and included neurobehavioral testing and measurement of brain water content and cell death. Results indicated that neither low- nor high-dose EP₁ receptor inhibition protected against the SBI-related effects on brain edema formation or cell death. There was however a significant improvement in neurobehavioral

function 24 h post-SBI with both dosing regimens. Further studies will be needed to assess the potential therapeutic role of EP₁ receptor targeting in SBI.

Keywords SC-51089 · Prostaglandin E₂ · EP₁ Receptor · Surgically induced brain injury (SBI) · Neurosurgery

Introduction

Neurosurgical procedures can damage viable brain tissue unintentionally by a wide range of methods. These surgically induced brain injuries (SBI) can be a result of direct surgical trauma, intraoperative bleeding, thermal injury from electrocautery, or stretch damage from tissue retraction [1, 2]. The concern with these injuries is the heightened inflammatory response that is mounted in an attempt to combat the effects of brain tissue damage. Propagation of this local response may result in direct cell death, enhanced disruption of the blood-brain-barrier (BBB) causing an increase in brain edema formation, and subsequent deterioration in neurobehavioral function [3]. Unfortunately, current therapies, such as steroids and diuretics, are relatively non-specific and focus mostly on reducing the postoperative edema that has already transpired [4]. Therefore, recent studies have looked into targeting specific anti-inflammatory mediators, which may be more effective at reducing cell death and brain edema while improving neurobehavior.

Cyclooxygenase-2 (COX-2) is a rate-limiting enzyme responsible for catalyzing the synthesis of prostaglandins at sites of injury. In the brain, COX-2 acts as a key mediator of inflammation, orchestrating a wide spectrum of brain injuries, including excitotoxic brain injury, cerebral ischemia, traumatic brain injury, and neurodegenerative disorders [5]. A key downstream effector of COX-2 neurotoxicity is prostaglandin E₂ (PGE₂), an endogenous signaling molecule produced by the enzymatic transformation of arachidonic acid by COX-2 [6, 7]. PGE₂ has been linked to BBB disruption during CNS inflammation [8–10], and through its

N.H. Khatibi, R. Martin, and R. Applegate
Department of Anesthesiology, Loma Linda Medical Center,
Loma Linda, CA, USA

V. Jadhav, B. Matus, and N. Fathali
Department of Physiology, Loma Linda University,
School of Medicine, Loma Linda, CA, USA

J. Tang (✉)
Department of Physiology, Loma Linda University,
School of Medicine, Loma Linda, CA, USA
Department of Physiology and Pharmacology, Loma Linda University,
School of Medicine, Loma Linda, CA 92354, USA
e-mail: jtang@llu.edu

J.H. Zhang
Department of Anesthesiology, Loma Linda Medical Center,
Loma Linda, CA, USA
Department of Physiology, Loma Linda University,
School of Medicine, Loma Linda, CA, USA
Department of Neurosurgery, Loma Linda Medical Center,
Loma Linda, CA, USA

interaction with the G-protein coupled receptor, EP1, it can enhance peripheral microvessel endothelial cell permeability and thereby cause a substantial amount of brain edema accumulation. Aside from its role in BBB disruption and edema formation, the EP1 receptor may also be involved in excitotoxic cell death [7].

Recently, selective COX-2 enzyme inhibitors have come under scrutiny because of an increased occurrence of cardiovascular events [11, 12], suggesting that downstream signaling pathways in the inflammatory cascade may be a safer target. Consequently, in this study, we investigated the role of the PGE₂ EP1 receptor on brain edema formation, neuronal cell death, and neurobehavioral function after SBI. We hypothesized that EP1 receptor inhibition will result in marked improvement in these three parameters in our mouse population.

Materials and Methods

Animal Groups

All procedures for this study were approved by the Animal Care and Use Committee at Loma Linda University and complied with the NIH Guide for the Care and Use of Laboratory Animals. Eighty-two male Sprague-Dawley mice weighing between 35 and 45 g were randomly divided into the following four groups: sham ($n=31$), SBI ($n=27$), SBI treated with SC51089 at 10 $\mu\text{g}/\text{kg}$ ($n=7$), and SBI treated with SC51089 at 100 $\mu\text{g}/\text{kg}$ ($n=17$).

Operative Procedure

The SBI model was adapted as previously described in mice [4]. Briefly, mice were anesthetized with a ketamine (100 mg/kg)/xylazine (10 mg/kg) combination intraperitoneal injection and positioned prone in a stereotaxic head frame (Stoelting, Wood Dale, IL). A 3 mm by 3 mm cranial window was created 1 mm anterior and 2 mm lateral to the coronal and sagittal sutures, respectively. Using a flat blade (6 mm \times 1.5 mm), two incisions were made along the sagittal and coronal planes, leading away from the bregma and extending to the edge of the craniotomy window. The brain sections were weighed and were not significantly different between animals. Electrocautery was utilized for 2 s along the medial coronal and posterior sagittal borders at a power level consistent with the coagulation setting used in the operating room. Sham surgery included only a craniotomy

window and replacement of the bone flap without any dural incisions.

Treatment Method

SC51089 (Enzo Life Sciences, Plymouth Meeting, PA) was dissolved in 0.5% DMSO and administered intraperitoneally approximately 12 h and 1 h before SBI induction. Treated mice were divided into two groups, depending on the concentration of drug received – either a low-dose concentration (10 $\mu\text{g}/\text{kg}$) or a high-dose concentration (100 $\mu\text{g}/\text{kg}$).

Assessment of Neurobehavioral Deficits

Neurological outcomes were assessed by a blind observer at 24 h post-SBI using the Modified Garcia Score [13], beam balance test, and modified wire hanging test [3].

The Modified Garcia Score is a 21-point sensorimotor assessment system consisting of seven tests with scores of 0–3 for each test (maximum score=21). These seven tests included: (1) spontaneous activity, (2) side stroking, (3) vibris touch, (4) limb symmetry, (5) climbing, (6) lateral turning, and (7) forelimb walking.

Additionally, beam balance and wire hanging tests were performed. Both the beam (590 cm in length by 51 cm in width) and wire (550 cm in length by 51 mm in width) were constructed and held in place by two platforms on each side. Mice were observed for both their time and behavior until they reached one platform, and were scored according to six grades. The test was repeated three times, and an average score was taken [minimum score 0; maximum score (healthy rat) 5].

Brain Water Content

Brain water content was measured as previously described [14]. Briefly, mice were killed at 24 and 72 h post SBI, and brains were immediately removed and divided into three parts: ipsilateral frontal, contralateral frontal, and cerebellum. The cerebellum was used as an internal control for brain water content. Tissue samples were then weighed on an electronic analytical balance (APX-60, Denver Instrument; Arvada, CO) to the nearest 0.1 mg to obtain the wet weight (WW). The tissue was then dried at 105°C for 48 h to determine the dry weight (DW). The percent brain water content was calculated as $[(\text{WW} - \text{DW})/\text{WW}] \times 100$.

Assessing Cell Death

The Cell Death Detection ELISA kit (Roche Applied Science) was used to quantify cell death in the ipsilateral frontal cortex 24 h after SBI. For quantification of DNA fragmentation, which indicates apoptotic cell death, we used a commercial enzyme immunoassay to determine cytoplasmic histone-associated DNA fragments (Roche Molecular Biochemicals).

Statistical Analysis

Quantitative data were expressed as the mean \pm SEM. One-way ANOVA and Tukey tests were used to determine significance in differences between the means. Neurological scores were evaluated using the Dunn method. A p -value < 0.05 was considered statistically significant.

Results

PGE₂ EP₁ Receptor Inhibition Failed to Reduce Brain Edema After SBI

Brain water content was measured at 24 and 72 h post-SBI (Fig. 1). The results showed that vehicle mice presented with significantly worse brain edema compared to sham mice. After treatment with low-dose (10 μ g/kg) or high-dose (100 μ g/kg) SC51089, brain edema failed to reduce

significantly in the ipsilateral and contralateral frontal cortex compared to vehicle groups.

PGE₂ EP₁ Receptor Inhibition Transiently Improves Neurobehavioral Scores at 24 h

To evaluate the sensorimotor deficits after SBI, the modified Garcia test, wire hanging test, and beam balance test were conducted at 24 and 72 h post-SBI. The results showed that vehicle mice presented with severe neurobehavioral deficits compared to sham mice. After treatment with low-dose or high-dose SC51089, a significant improvement in neurobehavioral function was seen with the modified Garcia test at 24 h (Fig. 2a); however, with the wire hanging and beam balance tests, there was no improvement in neurobehavioral function noted compared to the vehicle group (Fig. 2b, c). At 72 h, there was no improvement seen with either treatment dose compared to vehicle.

Cell Death Fails to Reduce with EP₁ Receptor Inhibition

Cell death was also measured via an absorbance assay at 24 h post-SBI (Fig. 3). The results showed that vehicle mice presented with a significant increase in the number of cell deaths compared to sham mice. After treatment with high-dose (100 μ g/kg) SC51089, the number of cell deaths failed to reduce significantly.

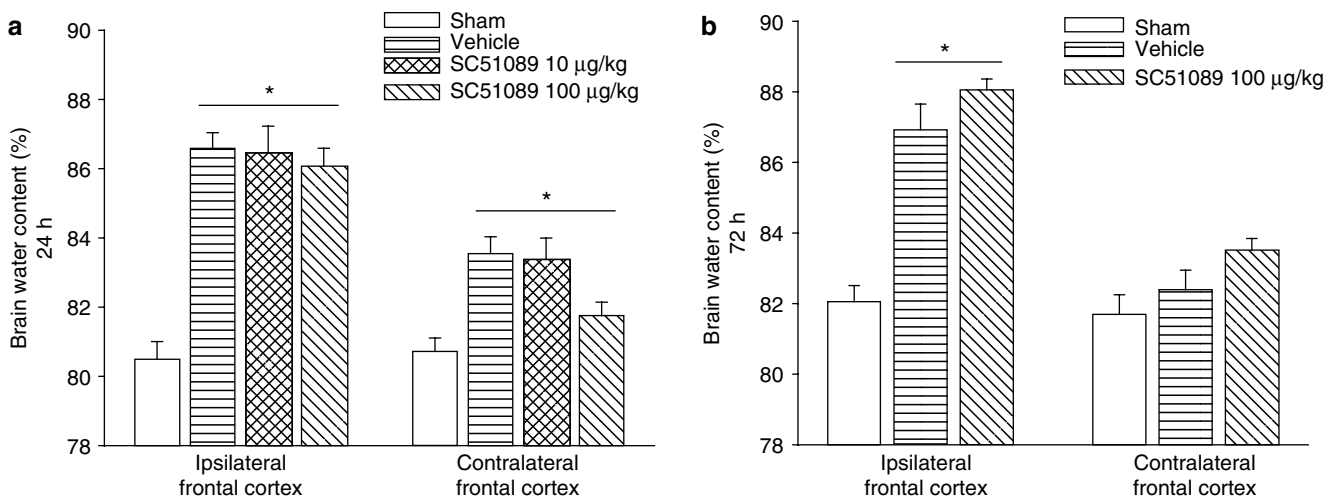


Fig. 1 Brain water content. Brain water content increased significantly in the ipsilateral basal ganglia at 24 and 72 h post-SBI injury. This increase was not affected by SC51089 treatment. *Significant difference

vs. sham ($p < 0.05$); (a) 24 h: sham = 14; (vehicle) = 14; (ICH + SC51089 10 μ g/kg) = 7; (ICH + SC51089 100 μ g/kg) = 6. (b) 72 h: sham = 11; (vehicle) = 7; (ICH + SC51089 100 μ g/kg) = 5

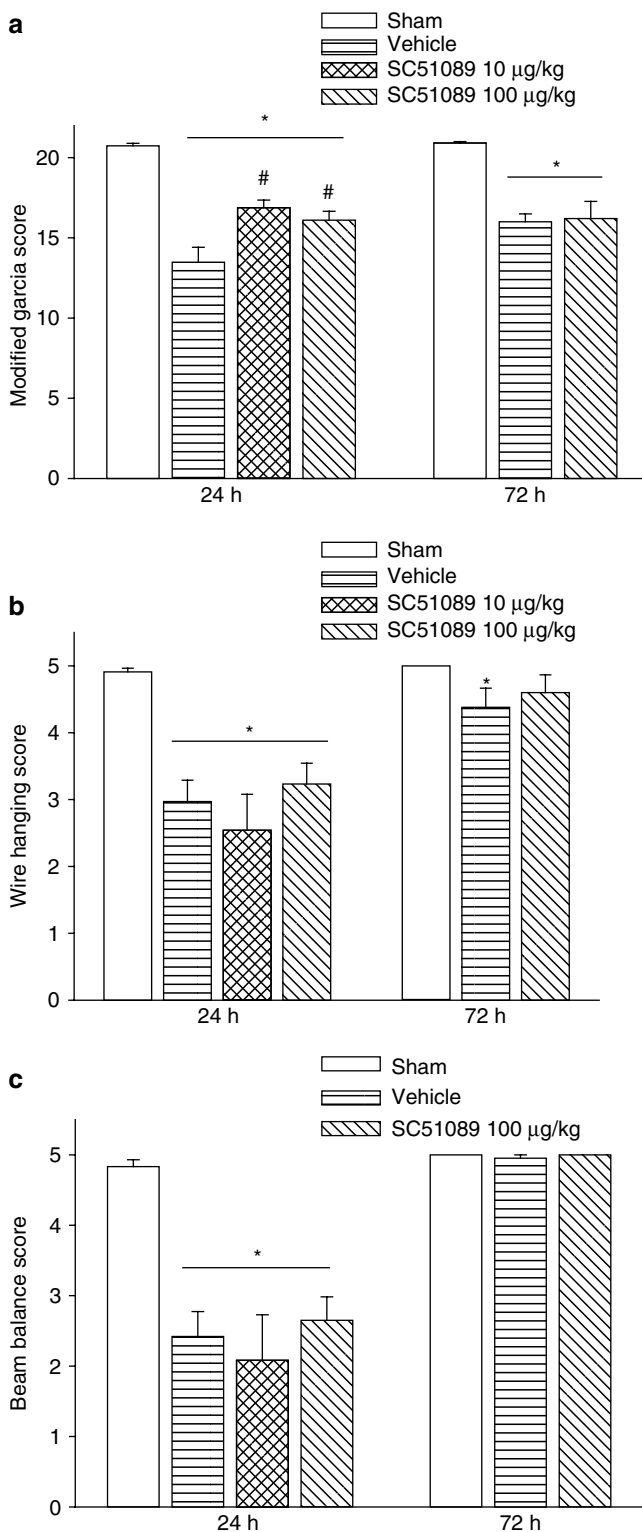


Fig. 2 Neurobehavioral function. Neurobehavioral deficits were present in all vehicle compared to sham animals. With SC51089 treatment, there was a significant improvement in Garcia behavioral testing scores at 24 h post SBI. *Significant difference vs. sham ($p < 0.05$); #significant difference vs. vehicle ($p < 0.05$); (a) modified Garcia scoring; (b) wire hanging score; (c) beam balance score

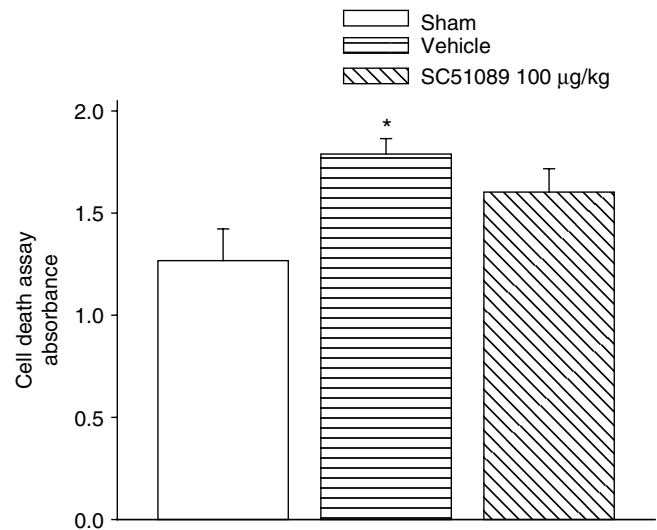


Fig. 3 Cell death measurement 24 h post SBI. There were significant differences between the sham and vehicles groups. However, no improvement was seen with SC51089 treatment *Significant difference vs. sham ($p < 0.05$); #significant difference vs. vehicle ($p < 0.05$); (A) 24 h: sham=6; (vehicle)=6; (ICH+SC51089 100 µg/kg)=6

Discussion

In this study, we used a mouse SBI model to investigate the role by which the COX-2 downstream receptor, EP1, contributed to brain injury outcomes. Using SC51089, a selective EP1 receptor inhibitor, we showed for the first time that receptor inhibition failed to attenuate cell death and reduce brain edema after SBI. Additionally, at 24 h post injury, we observed a marked improvement in neurobehavioral deficits; however, those improvements reversed by 72 h. Consequently, this study suggests that EP1 receptor inhibition has limited neuroprotective effects in SBI mice.

The downstream COX-2 effector, PGE₂, has been implicated in causing neuronal cell death in the brain [15]. By binding to the G-protein coupled receptor, EP1, PGE₂ can activate the IP3 signaling pathway causing an influx of calcium into the cell and in doing so disrupt normal calcium homeostasis. As a result of this calcium influx, NMDA receptor activation also occurs, causing significant excitotoxic damage and neuronal cell death [16]. This being true, blocking of the EP1 receptor should prevent damage and reduce neuronal cell death; however, this was not the case in our study. Instead, we found that neuronal cell death did not improve with EP1 receptor inhibition at 24 h post-injury. There was neither a reduction nor an increase in the number of cell deaths, implying that SC51089 had no effect on our outcome. This begs the question of whether COX-2-mediated inflammation is involved with delayed cell death rather than the acute phase of injury after SBI. Therefore, further studies

will need to investigate the effects of COX-2 inhibition on neuronal cell death at later time points.

Aside from neuronal cell death, brain edema can be an additionally encountered postoperative complication following neurosurgical procedures. Its accumulation leads to significant brain swelling [11, 12], resulting in a dramatic rise in intracranial pressure. In SBI, disruption of the BBB is responsible for brain edema formation. In our study we found that brain edema formation was not affected by SC51089 treatment.

Although neuronal cell death and brain edema did not improve, we did find a reduction in neurobehavioral deficits in our mouse population. At 24 h post-injury, there was an improvement in neurobehavioral deficits with EP1 receptor inhibition. Testing was conducted using the modified Garcia test and both the wire hanging and beam balance tests. Improvements with treatment were only seen with the modified Garcia test, which is more sensitive to acute neurological deficits than the other tests [13]. However, the improvement in neurobehavioral function was transient, quickly deteriorating by 72 h after injury. This is most likely a result of delayed cell death in brain regions associated with neurobehavioral function [17, 18]. In the central region of injury, blood flow is compromised, which leads to energy failure and subsequent cell death; however, in the surrounding peri-injury sites, neurons remain viable for prolonged periods [19, 20]. Hence, the area of the brain responsible for neurobehavioral function may not have been affected until later in the course of the injury.

There is one main limitation that needs to be acknowledged and addressed regarding the present study. The limitation concerns the timing of treatment. In this study, we chose to give SC51089 treatment at 12 and 1 h pre-surgery as a means of preventing and/or decreasing potential damage from neurological surgery. However, we failed to take into account the half-life of the drug. We recognize the need for studies to investigate the pharmacodynamics of SC51089 in order to best determine when to give treatment.

Conclusion

We conclude that EP1 receptor inhibition fails to improve the injuries of an SBI in adult male mice. Further studies will be needed to confirm this relationship and determine the future clinical direction.

Acknowledgement This study is partially supported by NIH NS053407 to J.H. Zhang and NS060936 to J. Tang.

Conflict of interest statement We declare that we have no conflict of interest.

References

- Andrews RJ, Muto RP (1992) Retraction brain ischaemia: cerebral blood flow, evoked potentials, hypotension and hyperventilation in a new animal model. *Neurol Res* 14(1):12–18
- Hernesniemi J, Leivo S (1996) Management outcome in third ventricular colloid cysts in a defined population: a series of 40 patients treated mainly by transcallosal microsurgery. *Surg Neurol* 45(1):2–14
- Yamaguchi M et al (2007) Matrix metalloproteinase inhibition attenuates brain edema in an in vivo model of surgically-induced brain injury. *Neurosurgery* 61(5):1067–1075, discussion 1075–1076
- Jadhav V et al (2007) Neuroprotection against surgically induced brain injury. *Surg Neurol* 67(1):15–20, discussion 20
- Minghetti L (2004) Cyclooxygenase-2 (COX-2) in inflammatory and degenerative brain diseases. *J Neuropathol Exp Neurol* 63(9):901–910
- Carlson NG (2003) Neuroprotection of cultured cortical neurons mediated by the cyclooxygenase-2 inhibitor APHS can be reversed by a prostanoid. *J Neurosci Res* 71(1):79–88
- Kawano T et al (2006) Prostaglandin E2 EP1 receptors: downstream effectors of COX-2 neurotoxicity. *Nat Med* 12(2):225–229
- Jaworowicz DJ Jr et al (1998) Nitric oxide and prostaglandin E2 formation parallels blood-brain barrier disruption in an experimental rat model of bacterial meningitis. *Brain Res Bull* 46(6):541–546
- Mark KS, Trickler WJ, Miller DW (2001) Tumor necrosis factor- α induces cyclooxygenase-2 expression and prostaglandin release in brain microvessel endothelial cells. *J Pharmacol Exp Ther* 297(3):1051–1058
- Payne DK, Fuseler JW, Owens MW (1994) Modulation of endothelial cell permeability by lung carcinoma cells: a potential mechanism of malignant pleural effusion formation. *Inflammation* 18(4):407–417
- Marmarou A et al (2000) Contribution of edema and cerebral blood volume to traumatic brain swelling in head-injured patients. *J Neurosurg* 93(2):183–193
- Marmarou A et al (2006) Predominance of cellular edema in traumatic brain swelling in patients with severe head injuries. *J Neurosurg* 104(5):720–730
- Garcia JH et al (1995) Neurological deficit and extent of neuronal necrosis attributable to middle cerebral artery occlusion in rats. Statistical validation. *Stroke* 26(4):627–634, discussion 635
- Tang J, Liu J, Zhou C, Alexander JS, Nanda A, Granger DN, Zhang JH (2004) Mmp-9 deficiency enhances collagenase-induced intracerebral hemorrhage and brain injury in mutant mice. *J Cereb Blood Flow Metab* 24:1133–1145
- Andreasson K (2010) Emerging roles of PGE(2) receptors in models of neurological disease. *Prostaglandins Other Lipid Mediat* 91(3–4):104–112. Epub 2009 Apr 11
- Zhou P et al (2008) Neuroprotection by PGE2 receptor EP1 inhibition involves the PTEN/AKT pathway. *Neurobiol Dis* 29(3):543–551
- Caggiano AO, Breder CD, Kraig RP (1996) Long-term elevation of cyclooxygenase-2, but not lipoxygenase, in regions synaptically distant from spreading depression. *J Comp Neurol* 376(3):447–462
- Hewett SJ et al (2000) Cyclooxygenase-2 contributes to N-methyl-D-aspartate-mediated neuronal cell death in primary cortical cell culture. *J Pharmacol Exp Ther* 293(2):417–425
- Dereski MO et al (1993) The heterogeneous temporal evolution of focal ischemic neuronal damage in the rat. *Acta Neuropathol* 85(3):327–333
- Garcia JH et al (1993) Progression from ischemic injury to infarct following middle cerebral artery occlusion in the rat. *Am J Pathol* 142(2):623–635

Mucosal Tolerance to Brain Antigens Preserves Endogenous TGF β -1 and Improves Neurological Outcomes Following Experimental Craniotomy

N. Jafarian, R. Ayer, J. Eckermann, W. Tong, N. Jafarian, R.L. Applegate II, G. Stier, R. Martin, J. Tang, and John H. Zhang

Abstract Intracranial surgery causes brain damage from cortical incisions, intraoperative hemorrhage, retraction, and electrocautery; collectively these injuries have recently been coined surgical brain injury (SBI). Inflammation following SBI contributes to neuronal damage. This study develops T-cells that are immunologically tolerant to brain antigen via the exposure of myelin basic protein (MBP) to airway mucosa. We hypothesize that these T-cells will migrate to the site of corticotomy, secrete immunosuppressive cytokines, such as TGF β 1, reduce inflammation, and improve neurological outcomes following SBI. A standard model for SBI was used for this experiment. C57 mice were divided into six groups: SHAM+ Vehicle, SHAM+ Ovalbumin, SHAM+ MBP, SBI+ Vehicle, SBI+ OVA, and SBI+ MBP. Induction of mucosal tolerance to vehicle, ovalbumin, or MBP was performed prior to SBI. Neurological scores and TGF β 1 cytokine levels were measured 48 h postoperatively. Mice receiving craniotomy demonstrated a reduction in neurological score. Animals tolerized to MBP (SBI+ MBP) had better postopera-

tive neurological scores than SBI+ Vehicle and SBI+ OVA. SBI inhibited the cerebral expression TGF β 1 in PBS and OVA treated groups, whereas MBP treated-animals preserved preoperative levels. Mucosal tolerance to MBP leads to significant improvement in neurological outcome that is associated with the preservation of endogenous levels of brain TGF β 1.

Keywords Brain injury · Neuroprotection · Mucosal tolerance · Inflammation · TGF β 1

Introduction

There are over 200,000 cranial neurosurgical operations performed each year (www.neurosurgerytoday.org). During each of these operations, unavoidable brain damage is incurred as a result of cortical incisions, brain retraction, and thermal electrocautery, in addition to the inherent surgical risks of intra-operative hypotension, blood loss, transient cerebral ischemia, and the possible need for temporary vascular occlusion. This unavoidable inherent risk for surgically induced insult to the brain is acknowledged by the neurosurgical community through the development of minimally invasive surgical techniques [1–3]. In addition, the use of osmotic agents to maximize brain relaxation and burst suppression to reduce the CNS metabolic demands is a means of medical neuroprotection to address these issues [4, 5]. The concept of pre-treating patients in order to protect them against the subsequent damage incurred by craniotomy procedures has recently come into focus, and the term surgical brain injury (SBI) has been adopted to incorporate damage to the nervous system inherent to the craniotomy procedure itself [6, 7]. The study of the clinical impact of SBI is difficult because it cannot be easily demarcated from the underlying brain pathology; however, the adaptation of the aforementioned perioperative treatments acknowledges its significance.

N. Jafarian, R.L. Applegate II, G. Stier, and R. Martin
Department of Anesthesiology, Loma Linda University Medical Center, Loma Linda, CA, USA

R. Ayer and J. Eckermann
Department of Neurosurgery, Loma Linda University Medical Center, Loma Linda, CA, USA

W. Tong, N. Jafarian, and J. Tang
Department of Physiology and Pharmacology, Loma Linda University Medical Center, Loma Linda, CA, USA

J.H. Zhang (✉)
Department of Physiology and Pharmacology, Loma Linda University Medical Center, Loma Linda, CA, USA
Department of Neurosurgery, Loma Linda University Medical Center, Loma Linda, CA, USA
Department of Anesthesiology, Loma Linda University Medical Center, Loma Linda, CA, USA
Department of Neurosurgery, Loma Linda University Medical Centre, 11234 Anderson Street, Room 2562B, Loma Linda, CA, USA
e-mail: johnzhang3910@yahoo.com

Inflammation is a key component leading to the exacerbation of brain injuries resulting from different etiologies such as neurodegeneration, trauma, ischemia, and SBI [8–11]. In the brain, inflammation can be particularly detrimental because it can increase intracranial pressure because of increased blood flow and edema. Immunosuppressive agents have been shown to improve outcome in experimental models of brain injury [12–14]. Unfortunately, immunosuppressives have systemic side effects that often limit their use and may account for their limited efficacy in human trials for CNS injury [15]. In our experiment we attempt to control brain inflammation following SBI by inducing mucosal tolerance to the central nervous system (CNS) antigen, myelin basic protein (MBP). Mucosal tolerance is a long-recognized method of inducing peripheral immune tolerance to a specific antigen by exposing that antigen to the mucosal surfaces [16, 17]. Tolerance develops after repetitive low-dose feeding of the antigen [18–20], and upon restimulation with the appropriate antigen, T cells in tolerized animals secrete cytokines such as transforming growth factor b1 (TGF β 1), which suppress cell-mediated immune responses [18–22]. Since experimental craniotomy causes BBB breakdown and exposes antigens that are typically hidden from immune surveillance to the systemic immune system [9, 23], we hypothesize that tolerization to MBP prior to experimental craniotomy will result in neuroprotection against inherent brain injury through the induction of TGF β 1-secreting T cells that subsequently inhibit inflammation at the craniotomy site.

Materials and Methods

Animals

This protocol was evaluated and approved by the Institutional Animal Care and Use Committee at Loma Linda University, Loma Linda, CA. Male CD57 mice weighting 20–25 g were used for all studies (Harlan Corporation, Indianapolis, IN). Animals were housed in a climate-controlled environment with strict day/night light cycles prior to surgery. Seventy-five animals were subjected to a tolerizing regimen of vehicle (PBS), OVA, or MBP prior to craniotomy, and were divided as follows: SHAM+PBS=12, SHAM+OVA=12, SHAM+MBP=12, SBI+PBS=11, SBI+OVA=14, and SBI+MBP=14. Six animals randomly selected from each group were then sacrificed at 48 h, and their brains were used for brain molecular analysis.

Treatment

Before sham surgery or SBI craniotomy, 50 μ g of bovine MBP (50 μ g/10 μ L of vehicle), 50 μ g of ovalbumin (OVA;

50 μ g/10 μ L of vehicle), or 10 μ L of vehicle (phosphate buffer solution; PBS) was instilled into the nasal pharynx, 5 μ L each nostril, every other day for a total of five doses. Surgery was performed 1 day after the last instillation. MBP was chosen for the induction of tolerance because it can prevent experimental allergic encephalomyelitis [18, 21] and previously has been shown to improve outcome in experimental models of stroke [24–26]. Animals were briefly sedated for the nasal application of with MBP, OVA, or PBS with the use of isoflurane anesthetic 0.5–5% in 70% medical air with 30% oxygen.

Brain Injury

In this study we used a variation of the surgical brain injury (SBI) model described in previous reports [23, 27]. Prior to surgery, general anesthesia was induced with ketamine (80 mg/kg intraperitoneally) and xylazine (10 mg/kg intraperitoneally). Spontaneous ventilation without airway management was permitted by this anesthetic combination. After induction of general anesthesia, mice were placed in the prone position in a Benchmark Stereotaxic frame under a surgical operating microscope. Scalp fur and skin were cleaned and prepared in a sterile manner. A no. 11 blade was used to incise the skin down to the skull through a single sagittal incision. The periosteum was reflected to expose the right frontal skull. Using the bregma as a landmark, a small square of skull (approximately 4 mm \times 4 mm) was thinned and removed with a bone drill. The dura was excised with a no. 22-gauge needle. The entire right frontal lobe anterior to the bregma was excised by sharp dissection and electrocautery. The resection was carried down to the skull base. Preliminary studies were conducted to demonstrate the consistency of the size of resection based on the weight of the removed specimen. Once the brain tissue had been excised, intraoperative packing and saline irrigation along with brief (~1 s) bipolar electrocautery application to the cut surfaces was used to control bleeding. Hemostasis was confirmed by close observation after removal of packing. After hemostasis was assured, the skin was closed with 3-0 silk suture (Ethicon Inc., Cornelia, GA). Sham surgery included general anesthesia, skin incision, and craniotomy, but no dural incisions. A heating pad was used to maintain the body temperature at 36.0 \pm 0.5 $^{\circ}$ C during surgery and while the animal recovered from anesthesia postoperatively.

Modified Garcia Testing

All scoring was performed by an independent researcher blinded to the experimental conditions. A modified 21-point Garcia scoring system was used to assess neurological function

in the mice 24 and 48 h after surgery [23, 28]. The scoring system was applied to mice by a blinded observer.

Brain Cytokine Levels

Western blot analysis was performed as described previously with some modification [29]. Briefly, animals were euthanized under anesthesia (isoflurane anesthetic 5% in 70% medical air with 30% oxygen) 48 h after SBI, and brains were immediately removed and stored at -80°C until analysis ($n=6$ for each group). Protein extraction from right hemisphere (ipsilateral to the craniotomy) was obtained by gently homogenizing in RIPA lysis buffer (Santa Cruz Biotechnology, Inc., sc-24948) and further centrifuged at 14,000 g at 4°C for 30 min. The supernatant was used as whole cell protein extract, and the protein concentration was determined by using a detergent compatible assay (Bio-Rad, Dc protein assay). Equal amounts of protein (50 μg) were loaded on an SDS-PAGE gel. After being electrophoresed and transferred to a nitrocellulose membrane, the membrane was then blocked and incubated with the primary antibody, anti-TGFβ1 (Cell Signaling, catalog no. 3711), overnight at 4°C . Nitrocellulose membranes were then incubated with secondary antibodies (Santa Cruz Biotechnology) for 1 h at room temperature. Immunoblots were then probed with an ECL Plus chemiluminescence reagent kit (Amersham Biosciences, Arlington Heights, IL) and exposed to films. The data were analyzed by the software ImageJ 1.41 (NIH).

Statistics

Data are expressed as mean \pm standard error of the mean (SEM). All data were analyzed using ANOVA to account for differences between groups and expressed as mean \pm standard error using Sigma Stat for Windows, version 3.5. Data were found to be significant at $p < 0.05$. Analysis of variance (ANOVA) was used to compare all groups at 24 and 48 h for neurological outcome and at 48 h for cytokine expression.

Results

Neurological Score

There were no significant reductions in neurological score in sham mice receiving a tolerizing regimen with either OVA or MBS ($p > 0.05$ SHAM+PBS vs. SHAM+OVA/MBP; one-way ANOVA). All mice receiving SBI craniotomy demonstrated a significant reduction in neurological score versus their corresponding SHAM groups at 24 and 48 h ($p < 0.05$ SHAM+PBS

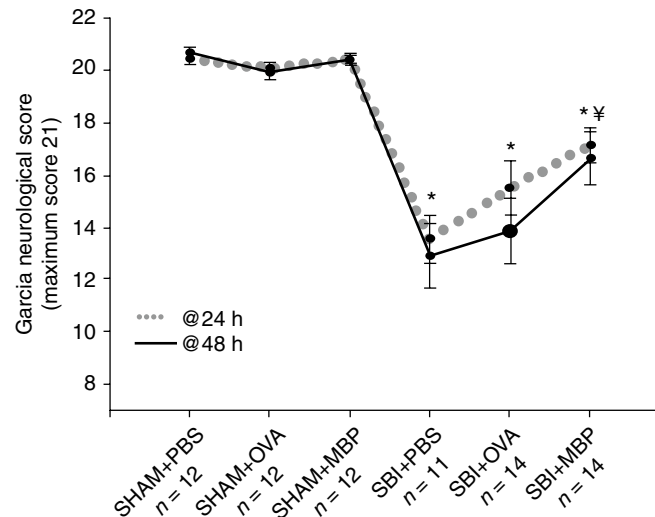


Fig. 1 Neurological scores of mice 24 and 48 h following SBI. SBI resulted in significant neurological injury in all groups ($*p < 0.05$ vs. sham groups). Mucosal tolerance treatment with MBP improved post-surgical neurological scores versus vehicle and PBS-treated groups. $\ddagger p < 0.05$ vs. SBI+PBS/OVA at 48 h

vs. SBI+PBS; SHAM+OVA vs. SBI+OVA; SHAM+MBP vs. SBI+MBP; one-way ANOVA). Animals tolerized to MBP prior to craniotomy had a trend to increased neurological scores at 24 h versus PBS- and OVA-treated groups. This trend reached statistical significance at 48 h ($p < 0.05$ SBI+MBP vs. SBI+PBS/OVA; one-way ANOVA) (Fig. 1).

Brain Cytokine Level

Western blot analysis of the right frontal lobe showed that TGFβ1 levels in sham animals were not affected by tolerization with either OVA or MBP ($p > 0.05$ SHAM+PBS vs. SHAM+OVA/MBP; one-way ANOVA). Craniotomy decreased the expression of TGFβ1 in PBS- and OVA-treated groups ($p < 0.05$ SHAM+PBS/OVA/MBP vs. SBI+PBS/OVA; one-way ANOVA). However, animals tolerized to MBP preserved their preoperative levels of TGFβ1 (Table 1).

Table 1 Relative TGFβ1 levels collected from the cerebral hemisphere 48 h after SBI

Group	N	TGFβ1
SHAM+PBS	6	1.000 \pm 0.000
SHAM+OVA	6	1.029 \pm 0.111
SHAM+MBP	6	1.093 \pm 0.0761
SBI+PBS	6	0.478 \pm 0.0348*
SBI+OVA	6	0.604 \pm 0.0452*
SBI+PBS	6	0.976 \pm 0.0602

Optical density is normalized to SHAM+PBS for comparison
* $p < 0.05$ vs. SHAM groups

Discussion

Inflammation is a significant contributor to the secondary injury associated with cerebral insults such as trauma and ischemic injury [9–11]. Significant increases in inflammatory mediators have also been documented following experimental craniotomy [9, 23]. Anti-inflammatory treatment strategies have been employed following a variety of CNS insults and have met with variable success. While steroids in the setting of traumatic brain injury have proven to be detrimental to outcome [15], their use in spinal cord injury is still highly debated [30]. Additionally, anti-inflammatory treatments in ischemic stroke models have been shown to improve outcome [31], while human trials have been less successful [32]. To date, the contribution of inflammation to the brain injury associated with experimental craniotomy in the SBI model has not been clearly defined, and previous attempts at inhibiting inflammation have not shown improved outcome [9, 23]. Systemic anti-inflammatory agents are frequently limited in their clinical utility by systemic effects [15, 33]. This is why this experiment chose to limit CNS inflammation in a site-specific manner through the induction of low-dose oral tolerance to MBP, a CNS-specific antigen. Our data demonstrated that such induction leads to significant improvement in neurological score following craniotomy versus untreated controls. The efficacy of mucosal tolerance in our experiment is supported by the preservation of endogenous levels of TGF β 1 in the brain when pre-treated with MBP. This provides evidence that inflammatory cytokines have an important role in modulating the clinical effects of the CNS inflammatory response following SBI. These findings are supported by similar work done in ischemic stroke by Becker and Gee et al. [24–26]. Becker et al. found that mucosal tolerance before MCAO occlusion reduced infarct size [24]. Gee et al. demonstrated that brain lymphocytes collected 1 month after MCAO occlusion in animals who had undergone MBP immune tolerance expressed higher levels of the regulatory cytokine TGF β 1 in comparison to the autoimmune-associated cytokine INF γ [26]. This is in contrast to control animals that were treated with proteins irrelevant to the CNS who had lymphocytes that produced elevated levels of INF γ . The elevation of relative levels of TGF β 1 was associated with improved neurological outcome and reduced brain atrophy. Our findings parallel those by Gee et al. in that the perseveration of TGF β 1 in the CNS following craniotomy improved outcomes.

In summary, our study suggests that the induction of immune tolerance prior to elective or semi-elective craniotomy will provide neuroprotection against surgically induced injury through the modulation of post-surgical inflammation and the preservation of endogenous levels of TGF β 1.

Acknowledgment This study was partially supported by NIH NS053407 to J.H. Zhang and NS060936 to J. Tang.

Conflict of interest statement We declare that we have no conflict of interest.

References

- Li KW, Nelson C, Suk I, Jallo GI (2005) Neuroendoscopy: past, present, and future. *Neurosurg Focus* 19(6):E1
- Maciunas RJ (2006) Computer-assisted neurosurgery. *Clin Neurosurg* 53:267–271
- Tharin S, Golby A (2007) Functional brain mapping and its applications to neurosurgery. *Neurosurgery* 60(4 suppl 2):185–201
- Raivich G, Bohatschek M, Kloss CU, Werner A, Jones LL, Kreutzberg GW (1999) Neuroglial activation repertoire in the injured brain: graded response, molecular mechanisms and cues to physiological function. *Brain Res Brain Res Rev* 30(1):77–105
- Rozet I, Tontisirin N, Muangman S et al (2007) Effect of equiosmolar solutions of mannitol versus hypertonic saline on intraoperative brain relaxation and electrolyte balance. *Anesthesiology* 107(5):697–704
- Jadhav V, Solaroglu I, Obenaus A, Zhang JH (2007) Neuroprotection against surgically induced brain injury. *Surg Neurol* 67(1):15–20
- Jadhav V, Zhang JH (2008) Surgical brain injury: prevention is better than cure. *Front Biosci* 13:3793–3797
- Williams AJ, Wei HH, Dave JR, Tortella FC (2007) Acute and delayed neuroinflammatory response following experimental penetrating ballistic brain injury in the rat. *J Neuroinflammation* 4:17
- Hyong A, Jadhav V, Lee S et al (2008) Rosiglitazone, a PPAR gamma agonist, attenuates inflammation after surgical brain injury in rodents. *Brain Res* 1215:218–224
- Wang Q, Tang XN, Yenari MA (2007) The inflammatory response in stroke. *J Neuroimmunol* 184(1–2):53–68
- Esiri MM (2007) The interplay between inflammation and neurodegeneration in CNS disease. *J Neuroimmunol* 184(1–2):4–16
- Allahtavakoli M, Moloudi R, Arababadi K, Shamsizadeh A, Kazem JM (2009) Delayed post ischemic treatment with Rosiglitazone attenuates infarct volume, neurological deficits and neutrophilia after embolic stroke in rat. *Brain Res* 1271:121–127
- Solaroglu I, Cahill J, Tsubokawa T, Beskonakli E, Zhang JH (2009) Granulocyte colony-stimulating factor protects the brain against experimental stroke via inhibition of apoptosis and inflammation. *Neurol Res* 31(2):167–172
- Yi JH, Park SW, Brooks N, Lang BT, Vemuganti R (2008) PPARgamma agonist rosiglitazone is neuroprotective after traumatic brain injury via anti-inflammatory and anti-oxidative mechanisms. *Brain Res* 1244:164–172
- Roberts I, Yates D, Sandercock P et al (2004) Effect of intravenous corticosteroids on death within 14 days in 10008 adults with clinically significant head injury (MRC CRASH trial): randomised placebo-controlled trial. *Lancet* 364(9442):1321–1328
- Khoury SJ, Lider O, al-Sabbagh A, Weiner HL (1990) Suppression of experimental autoimmune encephalomyelitis by oral administration of myelin basic protein. III. Synergistic effect of lipopolysaccharide. *Cell Immunol* 131(2):302–310
- Miller A, Lider O, Weiner HL (1991) Antigen-driven bystander suppression after oral administration of antigens. *J Exp Med* 174(4):791–798
- Chen Y, Kuchroo VK, Inobe J, Hafler DA, Weiner HL (1994) Regulatory T cell clones induced by oral tolerance: suppression of autoimmune encephalomyelitis. *Science* 265(5176):1237–1240
- Khoury SJ, Hancock WW, Weiner HL (1992) Oral tolerance to myelin basic protein and natural recovery from experimental autoimmune encephalomyelitis are associated with downregulation of inflammatory cytokines and differential upregulation of transforming

- growth factor beta, interleukin 4, and prostaglandin E expression in the brain. *J Exp Med* 176(5):1355–1364
20. Miller A, Lider O, Roberts AB, Sporn MB, Weiner HL (1992) Suppressor T cells generated by oral tolerization to myelin basic protein suppress both in vitro and in vivo immune responses by the release of transforming growth factor beta after antigen-specific triggering. *Proc Natl Acad Sci USA* 89(1):421–425
 21. Chen Y, Inobe J, Kuchroo VK, Baron JL, Janeway CA Jr, Weiner HL (1996) Oral tolerance in myelin basic protein T-cell receptor transgenic mice: suppression of autoimmune encephalomyelitis and dose-dependent induction of regulatory cells. *Proc Natl Acad Sci USA* 93(1):388–391
 22. Fukaura H, Kent SC, Pietrusiewicz MJ, Khoury SJ, Weiner HL, Hafler DA (1996) Induction of circulating myelin basic protein and proteolipid protein-specific transforming growth factor-beta1-secreting Th3 T cells by oral administration of myelin in multiple sclerosis patients. *J Clin Invest* 98(1):70–77
 23. Bravo TP, Matchett GA, Jadhav V et al (2008) Role of histamine in brain protection in surgical brain injury in mice. *Brain Res* 1205:100–107
 24. Becker KJ, McCarron RM, Ruetzler C et al (1997) Immunologic tolerance to myelin basic protein decreases stroke size after transient focal cerebral ischemia. *Proc Natl Acad Sci USA* 94(20):10873–10878
 25. Becker KJ, Kindrick DL, Lester MP, Shea C, Ye ZC (2005) Sensitization to brain antigens after stroke is augmented by lipopolysaccharide. *J Cereb Blood Flow Metab* 25(12):1634–1644
 26. Gee JM, Kalil A, Thullbery M, Becker KJ (2008) Induction of immunologic tolerance to myelin basic protein prevents central nervous system autoimmunity and improves outcome after stroke. *Stroke* 39(5):1575–1582
 27. Jadhav V, Matchett G, Hsu FP, Zhang JH (2007) Inhibition of Src tyrosine kinase and effect on outcomes in a new in vivo model of surgically induced brain injury. *J Neurosurg* 106(4):680–686
 28. Garcia JH, Wagner S, Liu KF, Hu XJ (1995) Neurological deficit and extent of neuronal necrosis attributable to middle cerebral artery occlusion in rats. Statistical validation. *Stroke* 26(4):627–634
 29. Ayer R, Chen W, Sugawara T, Suzuki H, Zhang JH (2009) Role of gap junctions in early brain injury following subarachnoid hemorrhage. *Brain Res* 1315:150–158
 30. Nesathurai S (1998) Steroids and spinal cord injury: revisiting the NASCIS 2 and NASCIS 3 trials. *J Trauma* 45(6):1088–1093
 31. Becker K, Kindrick D, Relton J, Harlan J, Winn R (2001) Antibody to the alpha4 integrin decreases infarct size in transient focal cerebral ischemia in rats. *Stroke* 32(1):206–211
 32. Enlimomab Acute Stroke Trial Investigators (2001) Use of anti-ICAM-1 therapy in ischemic stroke: results of the Enlimomab Acute Stroke Trial. *Neurology* 57(8):1428–1434
 33. Edwards P, Arango M, Balica L et al (2005) Final results of MRC CRASH, a randomised placebo-controlled trial of intravenous corticosteroid in adults with head injury-outcomes at 6 months. *Lancet* 365(9475):1957–1959

Effects of Progesterone and Testosterone on ICH-Induced Brain Injury in Rats

Zheng Chen, Guohua Xi, Ying Mao, Richard F. Keep, and Ya Hua

Abstract Studies have shown that progesterone reduces brain injury, whereas testosterone increases lesion size after ischemic stroke. This study examined the effects of progesterone and testosterone on intracerebral hemorrhage (ICH)-induced brain injury.

Male Sprague-Dawley rats received an injection of 100 μ L autologous whole blood into the right basal ganglia. Progesterone (16 mg/kg), testosterone (15 mg/kg) or vehicle was given intraperitoneally 2 h after ICH. Behavioral tests were performed, and the rats were killed after 24 h for brain edema measurement.

Perihematomal brain edema was reduced in progesterone-treated rats compared to vehicle-treated rats ($p < 0.05$). Progesterone also improved functional outcome following ICH ($p < 0.05$). Testosterone treatment did not affect perihematomal edema formation, but resulted in lower forelimb placing score ($p < 0.05$).

In conclusion, progesterone can reduce brain edema and improve functional outcome, whereas testosterone may have a deleterious effect after ICH in male rats.

Introduction

Intracerebral hemorrhage (ICH), a common and devastating event, accounts for approximately 10–15% of all strokes [1, 2]. It often leads to secondary injury and severe neurological deficits. Clinically, stroke is increasingly recognized as a sexually dimorphic disease [3, 4]. Female rats or mice have better outcomes for an equivalent insult after focal or global cerebral ischemia, ICH and brain trauma [5–8]. Estrogen has been frequently reported to have neuroprotective and potential therapeutic effects [6–9]. Fewer studies have focused on the effects of progesterone. Among them, most reports have indicated a beneficial effect of progesterone and its metabolite, allopregnanolone, on experimental traumatic brain injury, and focal and global cerebral ischemia [10].

Emerging data from laboratory studies suggest that testosterone and its potent metabolite, dihydrotestosterone, are important factors in the male response to cerebral ischemia and trauma [10]. Testosterone depletion 6 h before stroke attenuates ischemia-reperfusion injury, and stress-induced testosterone reduction contributes to ischemic tolerance in cerebral ischemia-reperfusion injury in males [11, 12]. Other reports have also revealed that chronic in vivo treatment with estrogen or testosterone has opposite effects on cerebral artery reactivity: estrogen decreases vascular tone by enhancing production of endothelium-dependent vasodilators, whereas chronic testosterone treatment increases cerebrovascular tone [13, 14].

This study examined the effects of progesterone and testosterone on ICH-induced brain injury in male rats.

Materials and Methods

Animal Preparation and Intracerebral Infusion

Animal use protocols were approved by the University of Michigan Committee on the Use and Care of Animals. Three-month-old male Sprague-Dawley rats (Charles River

Z. Chen
Department of Neurosurgery, University of Michigan,
Ann Arbor, MI, USA and
Department of Neurosurgery, Huashan Hospital, Fudan University,
Shanghai, China

G. Xi and R.F. Keep
Department of Neurosurgery, University of Michigan,
Ann Arbor, MI, USA

Y. Mao
Department of Neurosurgery, Huashan Hospital, Fudan University,
Shanghai, China

Y. Hua (✉)
Department of Neurosurgery, Huashan Hospital, Fudan University,
Shanghai, China and
Department of Neurosurgery, University of Michigan, Room 5018,
BSRB, 109 Zina Pitcher Place, Ann Arbor, MI 48109–2200, USA
e-mail: yahua@umich.edu

Laboratories, Wilmington, MA) were used in this study. Animals were anesthetized with pentobarbital (40 mg/kg, i.p.). The right femoral artery was catheterized for continuous blood pressure monitoring and blood sampling. Blood was obtained from the catheter for analysis of blood pH, PaO₂, PaCO₂, hematocrit and blood glucose. Core temperature was maintained at 37°C with use of a feedback-controlled heating pad. Rats were positioned in a stereotactic frame (Kopf Instruments), and a cranial burr hole (1 mm) was drilled on the right coronal suture 3.5 mm lateral to the midline. All rats received an injection of 100 µL autologous whole blood into the right caudate nucleus at a rate of 10 µL per minute through a 26-gauge needle (coordinates 0.2 mm anterior, 5.5 mm ventral and 3.5 mm lateral to bregma) with the use of a microinfusion pump. The needle was removed, and the skin incision was closed with sutures after infusion [15].

Experimental Groups

A total of 27 male Sprague-Dawley rats were divided into three groups. The first group was treated with progesterone at doses of 16 mg/kg [16], the second group was treated with testosterone at doses of 15 mg/kg, and the third group received vehicle (2-hydroxypropyl-β-cyclodextrin solution). All three reagents were given intraperitoneally 2 h after ICH. Twenty-four hours after ICH, behavioral tests were performed, and then the rats were euthanized for brain water, sodium and potassium content measurements.

Brain Water and Ion Contents

Rats were reanesthetized (pentobarbital 60 mg/kg; i.p.) and decapitated 24 h after intracerebral blood injection. The brains were removed immediately, and a coronal brain slice (approximately 4 mm thick) 3 mm from the frontal pole was cut with a blade. The brain slice was divided into ipsi- and contralateral cortex, and ipsi- and contralateral basal ganglia. The cerebellum served as control. Brain samples were weighed on an electronic analytical balance (Modal AE100, Mettler Instrument, Hightstown, NJ) to obtain the wet weight (WW). Brain samples were dried in a gravity oven at 100°C for 24 h to obtain the dry weight (DW). Brain water content was determined as follows: (WW-DW)/WW. The dehydrated samples were digested in 1 mL of 1 mol/L nitric acid for a week, after which the Na⁺ and K⁺ contents were measured using a flame photometer (Model IL 943, Instrumentation Laboratory, Inc., Lexington, MA). Ion

contents were expressed in micro-equivalents per gram of dehydrated brain tissue (µEq/g dry weight) [17].

Behavioral Tests

To assess behavior, forelimb-placing and the forelimb-use asymmetry (cylinder) tests were used [18]. For the forelimb-placing test, independent testing of each forelimb was induced by brushing the vibrissae ipsilateral to that forelimb on the edge of a tabletop once per trial for ten trials. A score of 1 was given each time the rat placed its forelimb onto the edge of the table in response to vibrissae stimulation. The results were expressed as percent (ipsilateral or contralateral/total × 100). Forelimb use during explorative activity was analyzed by observing rats in a 20 cm × 30 cm plastic cylinder until 20 forelimb placements had occurred. Forelimb use asymmetry was calculated as (right forelimb use + 1/2 both)/total (right + left + both) × 100.

Statistical Analysis

Student's *t* test was used. Values are expressed as mean ± SD. Statistical significance was set at *p* < 0.05.

Results

Physiological variables were measured before blood injection. Mean blood pressure, blood pH, PO₂ and PCO₂ were in the normal range.

Brain edema in the ipsilateral basal ganglia was less in progesterone-treated rats than in the vehicle-treated rats (80.1 ± 0.8 vs. 81.0 ± 0.8%, *p* < 0.05, Fig. 1a) at 24 h after ICH. The reduction of water content was associated with less sodium ion accumulation (301 ± 70 vs. 368 ± 49 µEq/g dry wt in the vehicle-treated group, *p* < 0.05, Fig. 1b) and less potassium loss (379 ± 23 vs. 333 ± 28 µEq/g dry weight, *p* < 0.01, Fig. 1c). Treatment with testosterone did not affect perihematomal brain edema at 24 h (Fig. 1).

ICH induced marked neurological deficits. Progesterone treatment improved forelimb placing score (18 ± 6% vs. 3 ± 2% in the vehicle-treated group, *p* < 0.05, Fig. 2a; normal score = 100%) and forelimb-using asymmetry score (39.6 ± 1.4% vs. 44.3 ± 0.9% in the vehicle-treated group, *p* < 0.05, Fig. 2b; normal score = 0). Testosterone treatment caused worse forelimb placing (*p* < 0.05), but it did not significantly affect the forelimb-using asymmetry score.

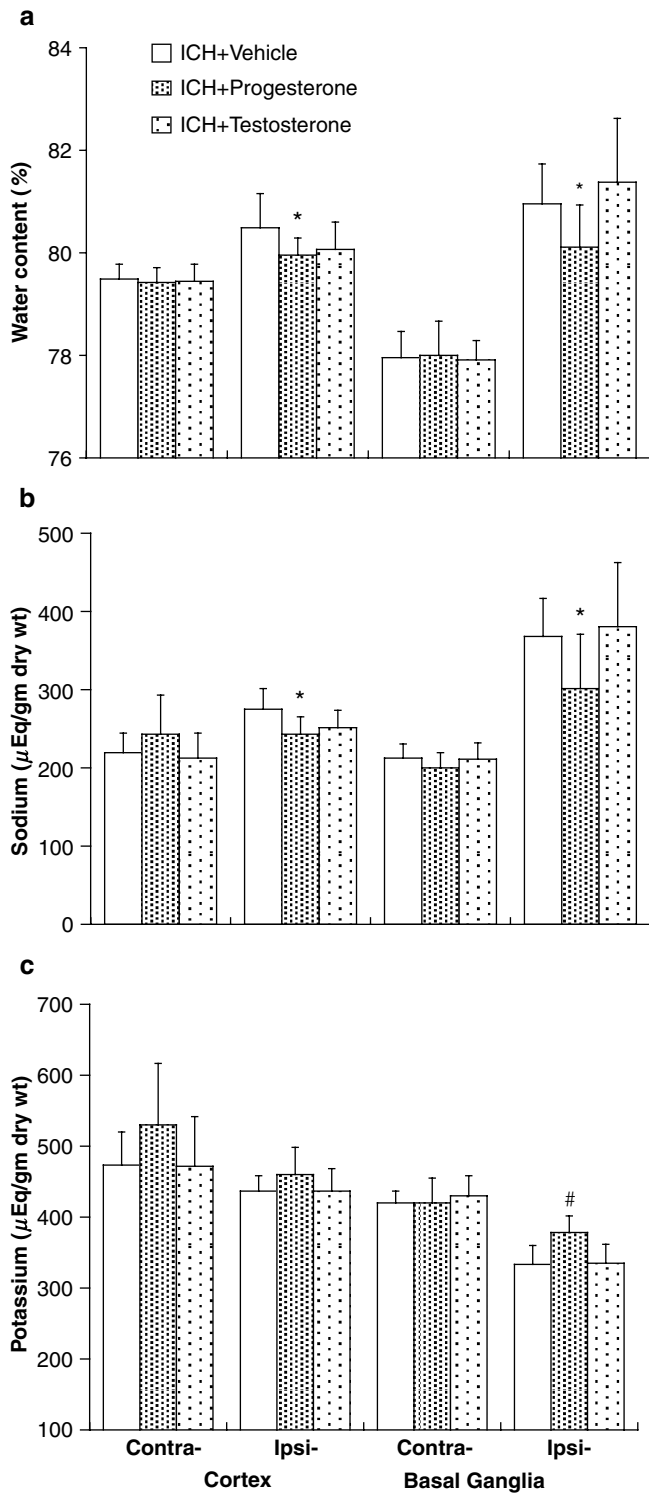


Fig. 1 Brain water (a), sodium (b) and potassium ion (c) contents 24 h after ICH in rats treated with vehicle, progesterone or testosterone. Values are mean ± SD, n=9. *p<0.05 vs. vehicle-treated group

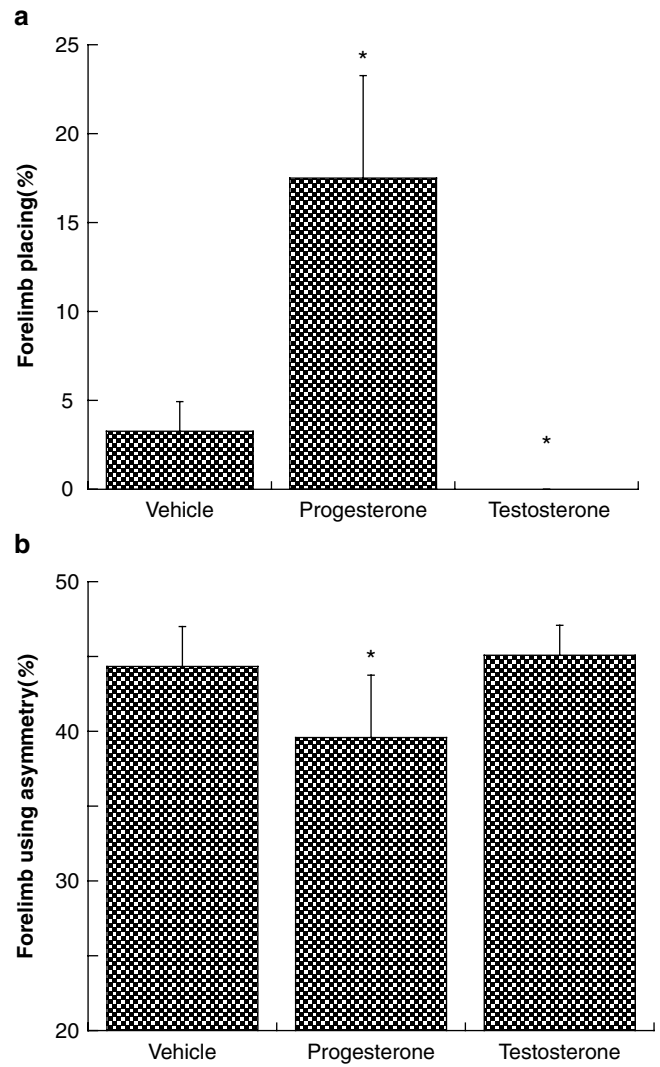


Fig. 2 Forelimb placing (a) and forelimb-use asymmetry (b) scores 24 h after ICH in rats treated with vehicle, progesterone or testosterone. Values are mean ± SD, n=9. *p<0.05 vs. vehicle-treated group

Discussion

There were two major findings in this study. First, progesterone had a protective effect against ICH-induced brain injury in male rats. Second, testosterone did not affect ICH-induced brain edema, but resulted in more severe forelimb placing deficits at 24 h.

The dose of progesterone (16 mg/kg) selected for this study has been shown to improve short-term motor recovery and attenuate edema, secondary inflammation and cell death after traumatic brain injury in aged male rats [16]. This dose

of progesterone improved ICH outcome and reduced brain swelling. It reduced brain edema not only in the striatum, but also in the nearby cortex. Vasogenic and cytotoxic edema occur following brain injury because of disruption of the blood-brain barrier, failure of the sodium pump and death of neurons [19, 20]. Ovarian hormones benefit ischemic stroke and traumatic brain injury in part by reducing the blood-brain barrier permeability and decreasing cytotoxic and vasogenic brain edema [10, 21, 22]. More work is needed to determine if progesterone has similar effects in ICH.

Progesterone receptors are broadly expressed throughout the brain and can be detected in every neural cell type. The distribution of such receptors beyond the hypothalamic borders suggests a much broader role of progesterone in regulating neural function than previously thought [23]. The interaction of estrogen and progesterone is controversial in intact or ovariectomized rats or even in vitro [24, 25]. Co-administration of estrogen and progesterone rescues neuronal loss in some rodent models of injury but not others [26]. Some recent findings indicate that in vitro progesterone can decrease expression of both estrogen receptors (ER), α and β , and as a consequence also reduces both ER-dependent transcriptional activity and neuroprotection [25]. That, in our study, progesterone could alleviate brain injury after ICH in male rats suggests that such protection is through an estrogen-independent mechanism. As yet it is uncertain whether co-administration of progesterone and estrogen would be more effective than progesterone or estrogen alone in attenuating brain injury after ICH. This will be an important clinical issue for hormone therapy, especially for female patients after ICH.

Due in part to poor agreement about “normal” levels of androgens in humans over their lifespans, less is known about the effects of male sex steroids on brain injury in patients [10], and very little is known about how testosterone might affect ICH-induced brain injury. Our study indicated that testosterone did not significantly affect brain swelling at 24 h after ICH in male rats. However, there was evidence of increased neurological deficits in those rats. Thus, we were unable to induce a forelimb placing reflex in all nine testosterone-treated rats, though forelimb-using asymmetry appeared to be equally impaired as in vehicle-treated rats. The forelimb placing test is a sensitive indicator of neurological deficits after ICH in the rat [18].

Androgens have been reported to induce a number of gene candidates in the presence or absence of ischemia, including which might cause impaired blood-brain barrier function, apoptosis and ionic imbalance [27]. In addition, testosterone can augment endotoxin-mediated cerebrovascular inflammation [28]. The dose from that study was used in the current experiments (15 mg/kg).

Stressors, such as ischemia, ischemia-reperfusion and halothane anesthesia, can cause a rapid decrease in plasma testosterone in male rats [10–12]. Whether this response also

occurs after ICH has yet to be investigated. Determining plasma androgen levels after ICH will help elucidate whether endogenous androgens may impact ICH-induced brain injury.

In summary, progesterone had a protective effect in ICH, whereas testosterone may have a deleterious effect. Sex hormones could be therapeutic targets for ICH patients.

Acknowledgment This study was supported by grants NS-017760, NS-039866 and NS-057539 from the National Institutes of Health (NIH) and 0755717Z, 0840016N from the American Heart Association (AHA). The content is solely the responsibility of the authors and does not necessarily represent the official views of the NIH and AHA.

Conflict of interest statement We declare that we have no conflict of interest.

References

1. Qureshi AI, Mendelow AD, Hanley DF (2009) Intracerebral haemorrhage. *Lancet* 373:1632–1644
2. Xi G, Keep RF, Hoff JT (2006) Mechanisms of brain injury after intracerebral hemorrhage. *Lancet Neurol* 5:53–63
3. Thorvaldsen P, Kuulasmaa K, Rajakangas AM, Rastenyte D, Sarti C, Wilhelmsen L (1997) Stroke trends in the WHO MONICA project. *Stroke* 28:500–506
4. Wyller TB (1999) Stroke and gender. *J Gend Specif Med* 2:41–45
5. Alkayed NJ, Murphy SJ, Traystman RJ, Hurn PD, Miller VM (2000) Neuroprotective effects of female gonadal steroids in reproductively senescent female rats. *Stroke* 31:161–168
6. Nakamura T, Hua Y, Keep RF, Park JW, Xi G, Hoff JT (2005) Estrogen therapy for experimental intracerebral hemorrhage in rats. *J Neurosurg* 103:97–103
7. Roof RL, Duvdevani R, Stein DG (1993) Gender influences outcome of brain injury: progesterone plays a protective role. *Brain Res* 607:333–336
8. Zhang YQ, Shi J, Rajakumar G, Day AL, Simpkins JW (1998) Effects of gender and estradiol treatment on focal brain ischemia. *Brain Res* 784:321–324
9. Nakamura T, Xi G, Keep RF, Wang M, Nagao S, Hoff JT, Hua Y (2006) Effects of endogenous and exogenous estrogen on intracerebral hemorrhage-induced brain damage in rats. *Acta Neurochir Suppl* 96:218–221
10. Vagnerova K, Koerner IP, Hurn PD (2008) Gender and the injured brain. *Anesth Analg* 107:201–214
11. Yang SH, Liu R, Wen Y, Perez E, Cutright J, Brun-Zinkernagel AM, Singh M, Day AL, Simpkins JW (2005) Neuroendocrine mechanism for tolerance to cerebral ischemia-reperfusion injury in male rats. *J Neurobiol* 62:341–351
12. Yang SH, Perez E, Cutright J, Liu R, He Z, Day AL, Simpkins JW (2002) Testosterone increases neurotoxicity of glutamate in vitro and ischemia-reperfusion injury in an animal model. *J Appl Physiol* 92:195–201
13. Gonzales RJ, Krause DN, Duckles SP (2004) Testosterone suppresses endothelium-dependent dilation of rat middle cerebral arteries. *Am J Physiol Heart Circ Physiol* 286:H552–H560
14. Ospina JA, Krause DN, Duckles SP (2002) 17 β -estradiol increases rat cerebrovascular prostacyclin synthesis by elevating cyclooxygenase-1 and prostacyclin synthase. *Stroke* 33:600–605
15. He Y, Hua Y, Lee J, Liu W, Keep RF, Wang MM, Xi G (2010) Brain alpha- and beta-globin expression after intracerebral hemorrhage. *Transl Stroke Res* 1:48–56

16. Cutler SM, Cekic M, Miller DM, Wali B, VanLandingham JW, Stein DG (2007) Progesterone improves acute recovery after traumatic brain injury in the aged rat. *J Neurotrauma* 24:1475–1486
17. Xi G, Keep RF, Hoff JT (1998) Erythrocytes and delayed brain edema formation following intracerebral hemorrhage in rats. *J Neurosurg* 89:991–996
18. Hua Y, Schallert T, Keep RF, Wu J, Hoff JT, Xi G (2002) Behavioral tests after intracerebral hemorrhage in the rat. *Stroke* 33:2478–2484
19. Wagner KR, Xi G, Hua Y, Kleinholz M, de Courten-Myers GM, Myers RE (1998) Early metabolic alterations in edematous perihematomal brain regions following experimental intracerebral hemorrhage. *J Neurosurg* 88:1058–1065
20. Xi G, Keep RF, Hoff JT (2002) Pathophysiology of brain edema formation. *Neurosurg Clin N Am* 13:371–383
21. Betz AL, Coester HC (1990) Effect of steroids on edema and sodium uptake of the brain during focal ischemia in rats. *Stroke* 21:1199–1204
22. Marques-Vidal P, Sie P, Cambou JP, Chap H, Perret B (1995) Relationships of plasminogen activator inhibitor activity and lipoprotein(a) with insulin, testosterone, 17 beta-estradiol, and testosterone binding globulin in myocardial infarction patients and healthy controls. *J Clin Endocrinol Metab* 80:1794–1798
23. Brinton RD, Thompson RF, Foy MR, Baudry M, Wang J, Finch CE, Morgan TE, Pike CJ, Mack WJ, Stanczyk FZ, Nilsen J (2008) Progesterone receptors: form and function in brain. *Front Neuroendocrinol* 29:313–339
24. Carroll JC, Rosario ER, Pike CJ (2008) Progesterone blocks estrogen neuroprotection from kainate in middle-aged female rats. *Neurosci Lett* 445:229–232
25. Jayaraman A, Pike CJ (2009) Progesterone attenuates oestrogen neuroprotection via downregulation of oestrogen receptor expression in cultured neurones. *J Neuroendocrinol* 21:77–81
26. Schumacher M, Guennoun R, Stein DG, De Nicola AF (2007) Progesterone: therapeutic opportunities for neuroprotection and myelin repair. *Pharmacol Ther* 116:77–106
27. Cheng J, Alkayed NJ, Hurn PD (2007) Deleterious effects of dihydrotestosterone on cerebral ischemic injury. *J Cereb Blood Flow Metab* 27:1553–1562
28. Razmara A, Krause DN, Duckles SP (2005) Testosterone augments endotoxin-mediated cerebrovascular inflammation in male rats. *Am J Physiol Heart Circ Physiol* 289:H1843–H1850

Drug Repurposing for Vascular Protection After Acute Ischemic Stroke

Weihua Guan, Anna Kozak, and Susan C. Fagan

Abstract The attempts to develop new treatments for acute ischemic stroke have been fraught with costly and spectacularly disappointing failures. Repurposing of safe, older drugs provides a lower risk alternative. Vascular protection is a novel strategy for improving stroke outcome. Promising targets for vascular protection after stroke have been identified, and several of these targets can be approached with “repurposed” old drugs, including statins, angiotensin receptor blockers (ARBs), and minocycline.

We tested the vascular protection (ability to reduce hemorrhagic transformation) of three marketed drugs (candesartan, minocycline, and atorvastatin) in the experimental stroke model using three different rat strains [Wistar, spontaneously hypertensive rats (SHR) and type 2 diabetic Goto-Kakizaki (GK) rats]. All agents decreased the infarct size, improved the neurological outcome and decreased bleeding. Mechanisms identified include inhibition of MMP-9, activation of Akt, and increased expression of proangiogenic growth factors. Premorbid vascular damage (presence of either diabetes or hypertension) increased the likelihood of vascular injury after ischemia and reperfusion and improved the response to vascular protection.

Keywords Stroke · Drug repurposing · Hemorrhagic transformation

W. Guan and A. Kozak
Program in Clinical and Experimental Therapeutics, University of Georgia College of Pharmacy, Charlie Norwood VA Medical Center, Augusta, GA, USA

S.C. Fagan (✉)
Program in Clinical and Experimental Therapeutics, University of Georgia College of Pharmacy, Charlie Norwood VA Medical Center, Augusta, GA, USA and
University of Georgia College of Pharmacy, Charlie Norwood VA Medical Center, HM-1220 Medical College of Georgia, 1120 15th St., Augusta, GA, USA
e-mail: sfagan@georgiahealth.edu

Introduction

Drug repurposing has emerged as an antidote to the sluggish drug development pipeline [1–3], where marketed drugs are exploited for their secondary activity. This strategy is particularly well-suited to the public sector, where off-patent agents can undergo high throughput screening for their ability to interact with identified molecular targets both in vitro and in vivo [1]. Since neuroprotection has failed for stroke therapy, we have focused on vascular protection with an eye toward better success. Promising targets for vascular protection after stroke have been identified and include the inhibition of endogenous mediators of vascular damage (superoxide, endothelin, matrix metalloproteases, cytokines and caspases) and the stimulation of endogenous protectors (nitric oxide, angiopoietin 1, vascular endothelial growth factor-VEGF and superoxide dismutases) [4]. Several of these targets can be approached with “repurposed” old drugs, including statins, angiotensin receptor blockers (ARBs) and minocycline [5].

The purpose of this investigation was to compare the vascular protective properties of these agents in experimental stroke both with and without premorbid vascular disease.

Methods

The Institutional Animal Care and Use Committee (IACUC) of the Augusta VA Medical Center approved the protocol. Male Wistar rats ($n=90$) and spontaneously hypertensive rats ($n=45$) from the Charles River Breeding Company (Wilmington, MA) and GK rats ($n=40$) from Taconic Farms, Inc. (Germantown, NY) within a narrow range of body weight (270–305 g) were used. Data from previously published reports [6–11] and unpublished data (Minocycline IP) from our group were included.

Experimental Cerebral Ischemia

Anesthesia was performed by using 2% isoflurane via inhalation. Cerebral ischemia was induced using the intraluminal suture middle cerebral artery occlusion (MCAO) model [12]. Then 19–21 mm 3-0 surgical nylon filament was introduced from the external carotid artery lumen into the internal carotid artery to block the origin of the right MCA. The animals were kept under anesthesia for only 15 min for the surgical procedure. Temperature was constantly maintained at 36.5–37.0°C using a controlled heating system. The suture was removed after 3 h of occlusion, and the animals were returned to their cages. At reperfusion, animals received one of the following drugs or vehicle: atorvastatin (5 or 15 mg/kg) (Pfizer Inc., NY, NY), candesartan (0.1, 0.3 or 1 mg/kg) (Astra Zeneca), hydralazine 1 mg/kg, enalapril (either 5 or 10 mg/kg) or minocycline (45 mg/kg IP or 3 mg/kg IV with tissue plasminogen activator-tPA, 10 mg/kg, Sigma Chemical and Genentech, Inc.). In the case of atorvastatin and minocycline, a second dose was administered 12 h later.

Assessment of Infarct Volume and Hemoglobin Content

At 24 h after the onset of MCAO, anesthesia was performed with intramuscular ketamine 75 mg/kg and xylazine 13 mg/kg (cocktail); animals were then perfused with saline and killed, and their brains were removed. The brain tissue was sliced into seven 2 mm thick slices in the coronal plane and stained with 2% solution of 2,3,5-triphenyltetrazolium chloride (TTC) (Sigma Chemical Co., St. Louis, MO) for 15–20 min. Images of the stained sections were taken. Using image analysis software (Zeiss-KS300, Oberkochen, Germany), infarction zones were measured, and infarct volume was calculated. The ischemic and non-ischemic hemispheres of the slices taken from the core of the infarct for the enzyme-linked immunosorbent assay (ELISA) were separated and processed using the non-ischemic side as a control. After homogenizing the slices in the core of the infarct and taking the supernatants, ELISA was performed to measure the hemoglobin in the brain tissue [13].

Conversion and Analysis

In order to convert percent of contralateral hemisphere to cubic millimeters for infarct size, and hemoglobin per gram of protein to hemoglobin per gram of tissue, we used data from the control group of the study of the effect of candesartan 1 mg/kg

in temporary MCAO [8], where both measures were performed. In those animals, total volume of the ipsilateral hemisphere was 1,192 mm³, and there was 0.17 g protein/g tissue.

For each of the three strains of rats, the line describing the relationship between infarct size and hemoglobin excess was determined and compared. The slopes of the lines were compared using analysis of covariance testing for slope homogeneity using SAS 9.2.

Results

Wistar: In animals treated with either saline or either of two doses of enalapril, the slope of the line describing the relationship between infarct size and degree of hemorrhagic transformation was significantly different from zero ($p < 0.05$) (Fig. 1). Hydralazine was similar to enalapril, but did not achieve statistical significance. Candesartan treatment resulted in significantly more vascular protection than neuroprotection.

In animals treated with minocycline IP, neither neuroprotection nor vascular protection was demonstrated (not shown). Animals receiving tPA alone had more vascular injury; however, when minocycline 3 mg/kg IV was administered to animals receiving tPA, both neuro and vascular protection was demonstrated.

Diabetes: Diabetic (GK) animals had much higher vascular injury than Wistars when treated with saline. Atorvastatin significantly reduced neurovascular injury, and the line describing the relationship between infarct size and bleeding was significantly steeper in the GKs than in the Wistars ($p = 0.0022$). This suggests an improved response to vascular protection in these animals (Fig. 2).

SHRs: Previously hypertensive animals experienced the largest injuries in response to the 3 h of MCAO and reperfusion, with the vascular injury being predominant compared to Wistars (values above the curve describing Wistars). Again, these animals appeared to have increased sensitivity to candesartan when compared to Wistar rats, but none of the slopes of the raw data in the SHRs were significantly different from zero (Fig. 3).

Discussion

The vascular injury that occurs during cerebral ischemia and leads to hemorrhagic transformation varies directly with infarct size. Neuroprotective agents reduce bleeding (vascular injury) as a result of decreasing infarct size. Vascular protective agents are particularly effective in reducing vascular

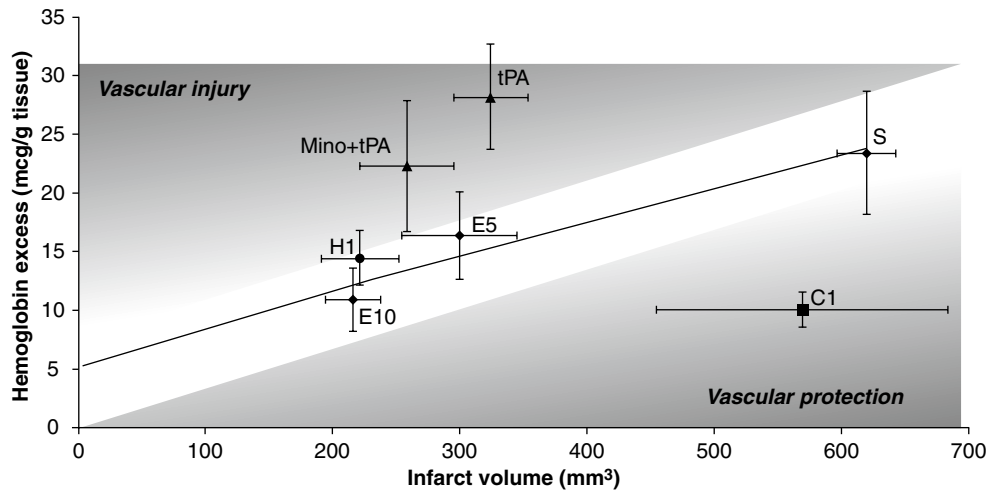


Fig. 1 Wistar rats. The trendline describes the relationship between infarct volume and hemorrhage formation in the saline- and enalapril-treated animals. Candesartan resulted in more vascular protection, and minocycline provided vascular protection when combined with tPA.

tPA = tissue plasminogen activator 10 mg/kg ($n=13$); Mino + tPA = minocycline 3 mg/kg IV + tPA 10 mg/kg IV ($n=11$); S = saline ($n=12$); C1 = candesartan 1 mg/kg IV ($n=19$); E5 = enalapril 5 mg/kg ($n=6$); E10 = enalapril 10 mg/kg ($n=9$); H1 = hydralazine 1 mg/kg ($n=8$)

injury and bleeding out of proportion to the reduction in infarct size. In the analysis presented, candesartan and atorvastatin were predominantly vascular protective, especially in animals with preexisting vascular damage (diabetes, hypertension). Minocycline demonstrated vascular protection when

administered in combination with tPA. Acute vascular protection after cerebral ischemia can reduce excess risk caused by pre-morbid vascular injury and improve outcome. Vascular protection should be pursued, particularly in stroke patients with known hypertension and diabetes.

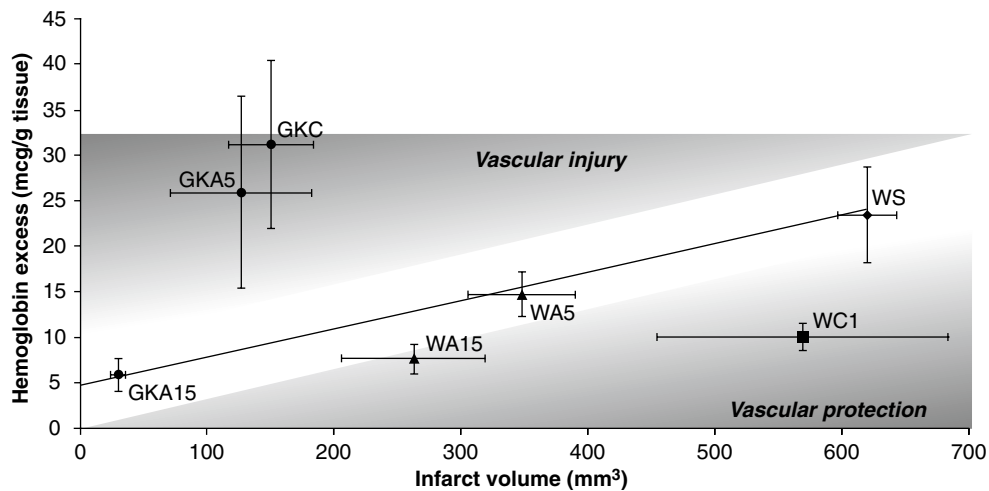


Fig. 2 Diabetic rats. The trendline describes the relationship between infarct volume and hemorrhage formation in the saline- and enalapril-treated Wistar animals (as in Fig. 1). Diabetic (GK) rats had a steeper slope than Wistar rats and treatment with atorvastatin (A) significantly reduced the injury in a dose-dependent manner. A15mg/kg IV showed the best vascular protection in both Wistars (W) and GKs. A treatment

showed more vascular protection than neuroprotection in GK rats. GK C = GK control ($n=10$); GK A5 = GK atorvastatin 5 mg/kg ($n=6$); GK A15 = GK atorvastatin 15 mg/kg ($n=5$); W S = Wistar saline ($n=12$); W A5 = Wistar atorvastatin 5 mg/kg ($n=8$); W A15 = Wistar atorvastatin 15 mg/kg ($n=8$); W C1 = Wistar candesartan 1 mg/kg IV ($n=19$)

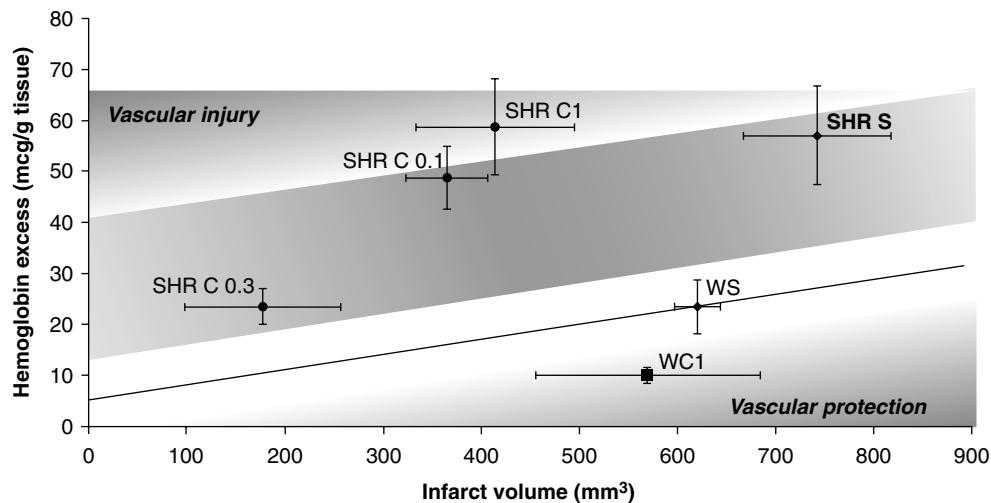


Fig. 3 Spontaneously hypertensive rats (SHRs). The trendline describes the relationship between infarct volume and hemorrhage formation in the saline- and enalapril-treated Wistar animals (as in Fig. 1). SHRs had predominant vascular injury compared to Wistars, but the relationship between infarct volume and hemorrhage was not significant in any of the four treatment groups. Candesartan 0.3 mg/kg showed the best

neurovascular protection in SHR rats. SHR S=SHR saline ($n=16$); SHR C1=SHR candesartan 1 mg/kg IV ($n=11$); SHR C 0.3=SHR candesartan 0.3 mg/kg IV ($n=11$); SHR C 0.1=SHR candesartan 0.1 mg/kg IV ($n=7$); W S=Wistar saline ($n=12$); W C1=Wistar candesartan 1 mg/kg IV ($n=19$)

Acknowledgment SCF has received grant support from Pfizer, Inc, VA Merit Review (BX000891) and NIH-NINDS (RO1 - NS063965)

Conflict of interest statement SCF is a consultant for Pfizer, Inc and Genentech, Inc. Candesartan was a gift from Astra Zeneca and tPA was a gift from Genentech, Inc.

References

1. Bisson WH, Cheltsov AV, Bruey-Sedano N, Lin B, Chen J, Goldberger N, May LT, Christopoulos A, Dalton JT, Sexton PM, Zhang XK, Abagyan R (2007) Discovery of antiandrogen activity of nonsteroidal scaffolds of marketed drugs. *Proc Natl Acad Sci USA* 104:11927–11932
2. Boguski MS, Mandl KD, Sukhatme VP (2009) Repurposing with a difference. *Science* 324:1394–1395
3. Duenas-Gonzalez A, Garcia-Lopez P, Herrera LA, Medina-Franco JL, Gonzalez-Fierro A, Candelaria M (2008) The prince and the pauper. A tale of anticancer targeted agents. *Mol Cancer* 7:82
4. Fagan SC, Hess DC, Pollock DM, Hohnadel EJ, Ergul A (2004) Targets for vascular protection after acute ischemic stroke. *Stroke* 35(9):2220–2225
5. Fagan SC, Hess DC, Machado LS, Hohnadel EJ, Pollock DM, Ergul A (2005) Tactics for vascular protection after acute ischemic stroke. *Pharmacotherapy* 25(3):387–395
6. Elewa HF, Kozak A, Johnson MH, Ergul A, Fagan SC (2007) Blood pressure lowering after experimental cerebral ischemia provides neurovascular protection. *J Hypertens* 25:855–859
7. Elewa HF, Kozak A, Frye RF, Johnson MH, Ergul A, Fagan SC (2009) Early atorvastatin reduces hemorrhage after acute cerebral ischemia in diabetic rats. *J Pharmacol Exp Ther* 330:532–540
8. Fagan SC, Kozak A, Hill WD, Pollock DM, Xu L, Johnson MH, Ergul A, Hess DC (2006) Hypertension after experimental cerebral ischemia: candesartan provides neurovascular protection. *J Hypertens* 24:535–539
9. Kozak A, El-Remessy AB, Ergul A, Machado LS, Elewa HF, Johnson MH, Abdelsaid M, Wiley DA, Fagan SC (2009) Candesartan augments ischemia-induced proangiogenic state and results in sustained functional improvement after stroke. *Stroke* 40:1870
10. Kozak W, Kozak A, Elewa HF, Johnson MH, Fagan SC (2008) Vascular protection with candesartan after experimental acute stroke in hypertensive rats: a dose-response study. *J Pharmacol Exp Ther* 326:773–782
11. Machado LS, Sazanava I, Kozak A, Wiley DC, El-Remessy AB, Ergul A, Hess DC, Fagan SC (2009) Minocycline and tissue plasminogen activator for stroke: assessment of interaction potential. *Stroke* 40:3028–3033
12. Longa EZ, Weinstein PR, Carlson S, Cummins R (1989) Reversible middle cerebral artery occlusion without craniectomy in rats. *Stroke* 20:84–91
13. Hilali HM, Simpkins AN, Hill WD, Waller JL, Knight RA, Fagan SC (2004) Single slice method for quantification of hemorrhagic transformation using direct ELISA. *Neurol Res* 26:93–98

Erythropoietin Attenuates Inflammatory Factors and Cell Death in Neonatal Rats with Intracerebral Hemorrhage

Monica Chau, Dongdong Chen, and Ling Wei

Abstract Stroke affects infants at a rate of 26/100,000 live births each year. Of these strokes, approximately 6.7 are hemorrhagic strokes. Erythropoietin (EPO) is an anti-apoptotic and neuroprotective hormone. In adult rodents, EPO attenuates inflammatory factor expression and blood–brain barrier damage after intracerebral hemorrhage (ICH). However, the effect of EPO in neonatal ICH stroke remains unexplored. This investigation aimed to elucidate the underpinnings of inflammation after ICH in postnatal day 7 (P7) rats and the effect of human recombinant EPO (hrEPO) treatment on ICH-induced inflammation. The P7 rat pups were pretreated with hrEPO (5,000 U/kg i.p.) or saline vehicle 4 h prior to the induction of ICH by blood injection into the right cerebral cortex and basal ganglia. Supplemental half doses of hrEPO treatment or saline injections were subsequently given 16 h after ICH induction. Real-time PCR done 24 h after ICH showed reductions in interleukin1- β (IL1- β), interleukin-6 (IL-6) and tumor necrosis factor- α (TNF α) mRNA expression in the basal ganglia of the hrEPO-treated rats compared to saline-treated rats. Terminal deoxynucleotidyl transferase dUTP nick end labeling (TUNEL) staining indicated fewer dying cells in the hrEPO-treated brain. Our data suggest that hrEPO has an anti-inflammatory action in neonates after ICH. The suppression of inflammatory cascades likely contributes to hrEPO's neuroprotective effect, which may be explored as a therapeutic treatment for ICH.

Keywords Intracerebral hemorrhage · Recombinant human erythropoietin · Inflammatory factors · Interleukins · Tumor necrosis factor α · Neuroprotection

M. Chau, D. Chen, and L. Wei (✉)
Department of Anesthesiology, Emory University School of Medicine,
Atlanta, GA 30322, USA
e-mail: lwei7@emory.edu

Introduction

Intracerebral hemorrhage (ICH) is a devastating disorder that can lead to serious debilitation or death. Of the neonatal strokes that affect 26 of 100,000 live births each year, different studies report a range of 0.7–6.7 incidents as ICH, or hemorrhagic stroke [1–3]. In a California-wide hospital discharge study of 2,278 first-stroke admissions between 1991 and 2000, the incident rate of stroke was 2.3 per 100,000 [3]. Of these, 49% were hemorrhagic stroke cases. Thus, ICH cases may comprise up to about half of total stroke cases. In a study on surveying stroke and stroke subtypes, the 30-day mortality rate for intracerebral hemorrhage and subarachnoid hemorrhage in children was 22%, which was higher than the 14% mortality rate for cerebral infarct [2]. The authors concluded that infants and children have at least the same rate of hemorrhagic stroke as ischemic stroke [2]. Even though pediatric stroke represents a great health problem, there is a lack of understanding of the mechanism of ICH in the developing brain, and there are few consensus guidelines established for treatment of child ICH because of the limited attention to basic and clinical studies [4, 5]. The causes and outcomes of neonatal stroke have not been well studied and, ICH has been even less studied.

Among all the risk factors of ICH, including hematological disorders, cerebrovascular disruption, sepsis, intracranial tumors, aneurysms and liver failure, trauma and vascular malformation are the most common risk factors [6–9]. Newborns and infants are particularly vulnerable to head trauma because their skulls are thin and pliable. ICH is also related to coagulation disorders, such as hemophilia, thrombocytopenia and leukemia [5]. Even with recent cerebral imaging advances, improved neonatal care and understanding of inflammation, full neurological repair of ICH damage does not exist. Finding a neuroprotective treatment for ICH lesions in neonates could ameliorate long-term developmental defects and reduce mortality.

ICH occurs when a blood vessel in the brain bursts. Misdirected blood in the tissue increases intracranial pressure. This displaced blood starves the cells of oxygen and metabolites, making the tissue ischemic and thus disrupting normal neurological function. Both necrosis and apoptosis occur after ICH [10, 11]. A secondary cell death may be induced by inflammatory factors initiated from the primary phase of cell death. The cells in the secondary phase likely undergo apoptosis rather than necrosis and are potentially rescued by neuroprotective agents, such as erythropoietin (EPO) [11].

EPO is a glycoprotein hormone that was originally known for its hematopoietic effects. It has recently been recognized as a neuroprotective hormone that attenuates brain damage and inflammation in ischemic and hemorrhagic stroke models [11, 12]. EPO modulates certain cell-death-related pathways including mitochondria-related cytochrome c release, bcl-2/bcl-x ratio and reactive oxygen species production [12, 13]. Thus, mitochondrial pathways present possible mechanisms for EPO protection. [Under anoxic in vitro insult, EPO attenuates cytochrome c release and mitochondrial depolarization possibly the modulation of protein kinase B (Akt), a protein involved in cell survival pathways [14, 15]. EPO's neuroprotection may also be mediated by regulating intracellular signals such as the Akt1 pathway, suppressing caspase activities, DNA damage and microglia activation [12, 14]. EPO has trophic factor-like actions. In the adult rodent ICH model, EPO increases angiogenesis, and decreases inflammatory factor expression, edema and matrix metalloproteases (MMP) [16–18]. EPO treatment in neonates with ischemic stroke improves cognitive function and sensorimotor function, and reduces infarction [19, 20]. EPO may increase proliferation of neural progenitors in the subventricular zone and promote cell migration to the ischemic infarct region [21]. Our previous investigations showed that in models of adult and neonatal ischemic stroke, EPO increases angiogenesis and neurogenesis [21–23]. EPO helps maintain the blood-brain barrier with the interplay of MMPs and tissue inhibitor of matrix metalloproteases (TIMP) [16, 24]. EPO treatment in adult ICH rats upregulates TIMP and reduces the breakdown activity of MMPs. Upon analysis of MMP-2, pretreatment of EPO into the adult ICH rat showed an attenuation of active MMP-2 expression with the increase of TIMP, which suggests that EPO reduces deleterious remodeling of the vessel basement membrane of the blood-brain barrier in ICH animals.

Nonetheless, the effect of EPO in neonatal ICH stroke remains unexplored. The present investigation examined inflammation after ICH in postnatal day 7 (P7) rats and the effect of EPO treatment on this inflammation.

Methods

ICH Induction Model

Animal procedures were approved by the Institutional Animal Care and Use Committee (IACUC) at Emory University. Wistar rat dams and pups were maintained in a climate-controlled room at 21°C with a 12-h light-dark cycle. Animals had free access to water and food. Pups were anesthetized by the hypothermia method as previously used [21]. Surgery was performed when the animal showed no response to pinches to test reflexes. Blood was collected from the tail vein, and coagulation of collected blood was prevented with the addition of heparin. With a Hamilton's syringe, 15 μ L of blood was injected through the soft skull into the barrel cortex and basal ganglia of the animal. The incision was closed with surgical glue (3M Corporate, St. Paul, MN). After surgery, animals were warmed up manually under a heat lamp to reverse hypothermic anesthetic effects.

Brain Tissue Dissection

Dissection of the brain caudate putamen and cortex was performed 24 h after ICH surgery. Animals were anesthetized with hypothermia before decapitation and dissection. The animals' brains were promptly dissected from the cranium after decapitation. A 5-mm coronal section was cut out to include the injury area, embedded and flash frozen in OCT mounting media on dry ice. Brains were preserved at -80°C until cryostat sectioning.

TUNEL Staining and Analysis

Dissected tissues were sectioned on a cryostat microtome at -13°C into 10- μm sections using design-based stereology. On each slide, every tenth section was collected such that there is at least 100 μm between the sections to avoid double-counting the same cells on a single slide. Tissues were fixed with 10% buffered formalin, incubated in a -20°C ethanol/acetic acid solution and permeabilized with 0.2% Triton X100. In between each step, the tissues were washed three times with phosphate-buffered saline (PBS). Tissues were blocked with a TUNEL detection kit (Promega, Madison, WI) equilibration buffer and incubated at 37°C in TdT and nucleotide solution. Hoescht solution made in PBS (1:25,000) was applied to the slides to stain the nuclei. Stained sections

were analyzed by fluorescent microscopy. The injury site was localized with TUNEL-positive cells. The number of TUNEL-positive cells immediately surrounding the injury site was counted.

Quantitative Real-Time PCR

Quantitative real-time polymerase chain reaction (qRT-PCR) was performed on the dissected ipsilateral caudate putamen of the P7 pups. Total RNA was isolated from the homogenized caudate putamen tissue dissected 24 h after ICH induction with Trizol (Invitrogen, Carlsbad, CA). Reverse transcription was performed with 1 μ g total RNA using a high-capacity cDNA kit (Applied Biosystems, Foster City, CA). Quantitative real-time PCR was used to assess mRNA levels in brain tissues using Applied Biosystems StepOnePlus with SYBR Green mastermix (Applied Biosystems). The following primers were used in this investigation: IL-1 β Forward: 5'CATCTTTGAAGAAGAGCCCG3'; IL-1 β Reverse: 5'AGCTTTCAGCTCACATGGGT3'; IL-6 Forward: 5'GCCCTTCAGGAACAGCTATG3'; IL-6 Reverse: 5'CCGGACTTGTGAAGTAGGA3'; TNF α Forward: 5'CCCATTACTCTGACCCCTT3'; TNF α Reverse: 5'TTGTGGAAATTCTGAGCCC3'. Fold changes in expression levels were calculated by the $\Delta\Delta$ cycle threshold (C_t) method, using 18S ribosomal subunit amplification as the internal control.

Statistical Analyses

All analyses were performed using Graphpad Prism 4.0 statistical software (GraphPad Software, Inc., La Jolla, CA). Single comparisons were performed using Student's *t* test. Multiple comparisons were performed by one-way analysis of variance (ANOVA) followed by Tukey's post hoc analysis. Changes were identified as significant if the *p*-value was less than 0.05. Mean values are reported with the standard error of the mean (SEM).

Results

Postnatal day 7 (P7) Wistar pups from the same litter were randomly separated into three experimental groups: (1) sham control that received an incision over the skull, but no ICH induction; (2) ICH + saline vehicle injection; (3) ICH + hrEPO

treatment. ICH insult and brain damaged were induced by autologous blood injection into the right cortex and basal ganglia. In groups 2 and 3, P7 rat pups received saline injection and rhEPO (5,000 U/kg i.p.) 4 h before ICH. This pretreatment allowed i.p.-injected rhEPO to reach peak serum concentration before ICH induction [25, 26]. A supplemental half dose of hrEPO or saline was injected 16 h after ICH.

TUNEL staining for cell death assay detected a few positive cells diffusely throughout the cerebral cortex and basal ganglia (Fig. 1a). Strong TUNEL-positive staining revealed massive cell death in the injection site 24 h after ICH (Fig. 1b). rhEPO treatment attenuated the number of TUNEL-positive cells compared to vehicle-treated animals (Fig. 1c).

Quantitative real-time PCR was used to assess relative levels of IL-6, IL-1 β and TNF α mRNA in brain tissues from sham controls, ICH plus saline and ICH plus hrEPO treatment animals. ICH insult resulted in multi-fold increases in these three factors (Fig. 2). rhEPO treatment substantially blocked the inflammatory factor increases in the brain (Fig. 2).

Discussion

This investigation examined ICH-induced cell death in the neonatal brain. TUNEL staining demonstrated massive cell death and multifold increases of three key inflammatory factors following ICH insult. We showed that hrEPO pretreatment was highly effective in preventing inflammatory factor increases and significantly reduced ICH-induced cell death in the ICH region of the neonatal brain. This is consistent with previous results using hrEPO in adult ICH animals. It is suggested that ICH-induced inflammation is likely a main mechanism contributing to cell death and neonatal brain injury. hrEPO acts as an anti-inflammatory reagent and is neuroprotective against ICH injury in the neonatal brain.

Cytokines mediate the inflammatory and immune response [27]. They are upregulated in stroke injury and exacerbate injury. Previous studies have demonstrated a reduction of proinflammatory cytokines in vitro and in vivo with EPO treatment [28, 29]. In the present study, we focused on the cytokines, IL-1 β , IL-6 and TNF α , which are believed to be primary inflammatory factors. EPO may attenuate cell death by attenuating the inflammatory response, including inflammatory cell infiltration such as activated glia and microglia to the infarct [30]. Cytokines can increase the production of other cytokines in a positive feedback way [31]. They can also induce the expression of each other, such as in the case with IL-1 β and TNF α [31]. IL-1 β has a prominent role in inflammation and activates other inflammatory factors, such

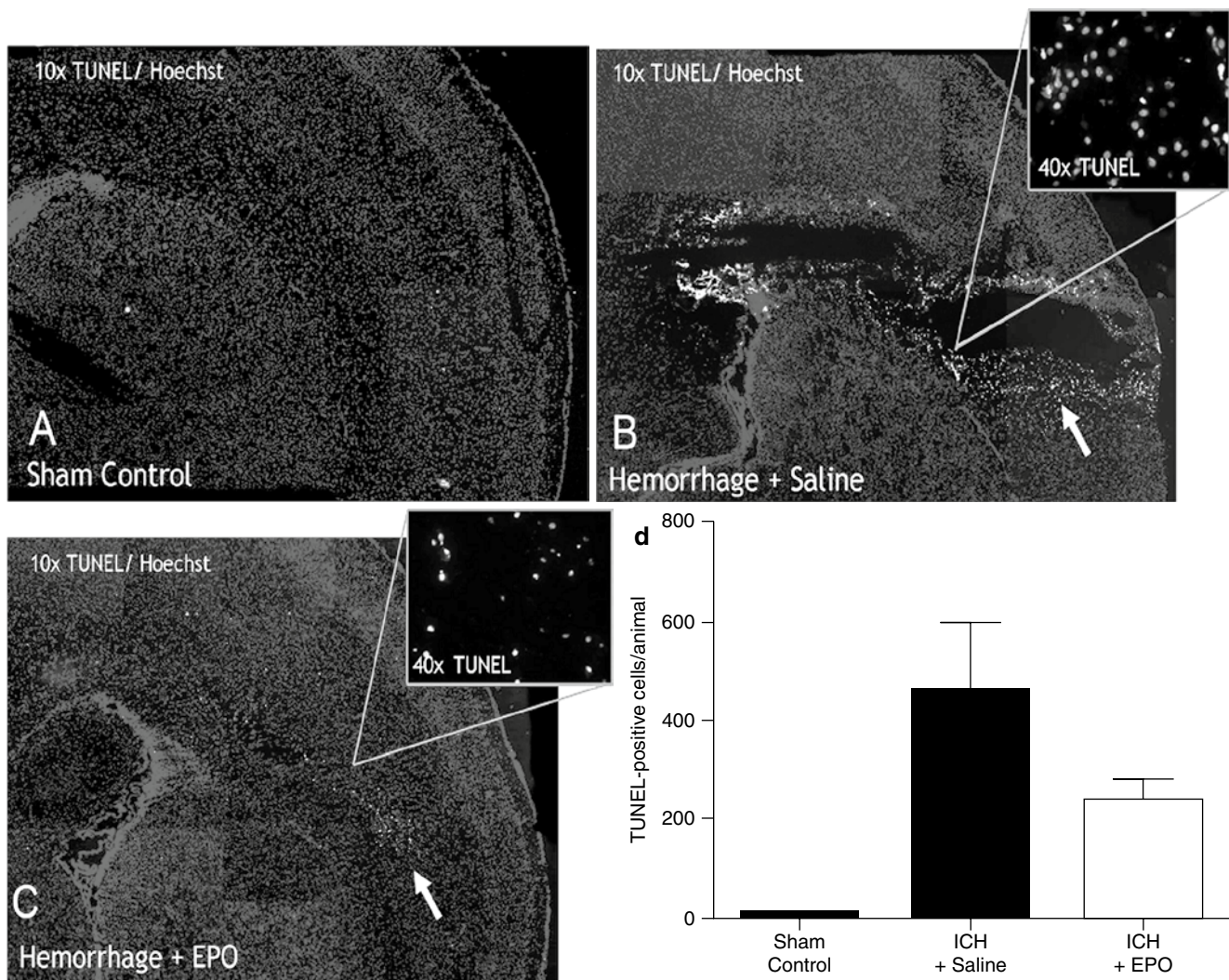


Fig. 1 ICH induced cell death and an hrEPO protective effect in the neonatal brain. TUNEL staining was performed 24 h after ICH in the brain coronal section containing the ICH induction site. (A) Sham control shows very few scattered TUNEL-positive cells (green) in the normal brain. Blue color is Hoechst 33342 staining of cell nuclei. (B) At the blood injection site (arrow), an infarct region was surrounded by

many TUNEL-positive cells (green). The insert shows an enlarged image of TUNEL-positive cells. (C) hrEPO treatment (5,000 IU/kg, i.p. 4 h before and 16 h after ICH) substantially prevented ICH-induced cell death. The insert shows an enlarged image of the ICH site. (D) Summary graph of TUNEL-positive cells in the ICH peripheral area. * $P < 0.05$ vs. ICH plus saline; $n = 7-8$ in each group

as lymphokines, IL-2, IL-3, IL-4 and IL-6 [32]. We report an upregulation of TNF α , IL-1 β and IL-6 mRNA expression after ICH induction. IL-1 β is upregulated after ischemic stroke [33], which is a potent mediator of inflammation because of its neutrophil recruitment and increase in brain water content after stroke [34]. IL-1 β is found in the traumatized brain and mediates astroglial proliferation at the site of the injury [34, 35]. Overexpression of the IL-1 receptor antagonist reduces edema and inflammation from intracerebral hemorrhage, suggesting IL-1 is a key molecule in the pathological events [36]. TNF α and IL-1 contribute to the breakdown of the BBB and cause brain edema [37–39]. It was positively correlated with perihematoma edema size in a clinical study [40]. TNF α also increases after ICH [40, 41]. Even though some argue that TNF α is protective [42, 43], TNF α has been generally recognized as an injurious factor in

stroke models [44–46]. The protective effects of EPO were abrogated when JAK2 and phosphatidylinositol 3-kinase (PI3K) inhibitors were incubated with TNF α cultures treated with EPO, which suggests that JAK2 and PI3K pathways play roles in EPO neuroprotection. In an in vivo EPO study, EPO provides neuroprotection through an attenuation of the mRNA of inflammatory factors such as IL-1 β and inflammatory cytokines in the ischemic model of the neonatal rat [29, 30]. We therefore suggest that the suppression effect of hrEPO on these factors contributes to the neuroprotection after ICH.

While pretreatment is not a common clinical practice for brain injury, we used it to test our hypothesis as a “proof of concept” investigation. It is possible that EPO is neuroprotective in a post-treatment paradigm. Previous work has translated EPO pretreatment into post-treatment in ischemic stroke models and ICH adult models [14, 16, 21–23, 47].

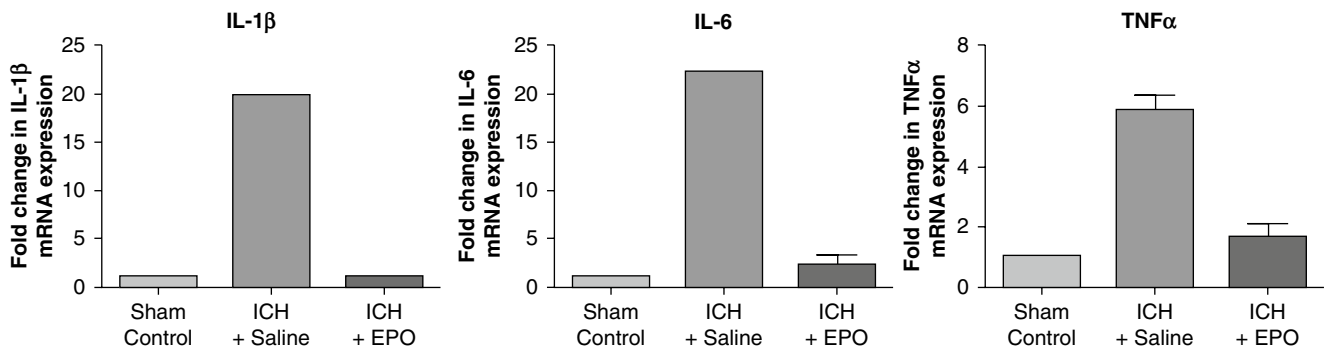


Fig. 2 ICH induced inflammatory factor expression, and the effect of hrEPO qRT-PCR was performed 24 h after ICH to detect mRNA expression of inflammatory factors, IL-6, IL-1 β and TNF α , in the ipsilateral site of the ICH brain. All three factors existed at low levels in sham control animals. ICH insult (ICH plus saline) markedly enhanced

mRNA levels of IL-6, IL-1 β and TNF α . Treatment with hrEPO showed a strong inhibitory effect on the upregulation of these inflammatory factors, enabling them to stay at the normal or near normal levels. $n=2$. Fold change was calculated by the $\Delta\Delta$ cycle threshold (C_t) method using 18S ribosomal subunit amplification as the internal control

EPO has been employed in clinical trials for subarachnoid hemorrhage, which has overlapping mechanisms of cell death with ICH. The results of these findings suggest that post-treating with EPO is a promising therapeutic tool for adults younger than 60 years of age and that EPO reduces delayed ischemic injury by reducing vasospasms [48–50]. Although there have been successes in using EPO treatment in the clinical arena, much work needs to be done, especially for the treatment of neonatal ICH injury.

In summary, the available data suggest that the EPO not only attenuates inflammation and brain damage in adult ICH animals, but also has a similar anti-inflammatory action in neonates after ICH. The suppression of inflammatory cascades may help reduce cell death and brain damage. EPO's anti-inflammatory/anti-apoptotic properties could be explored as a therapeutic treatment for ICH. Further experiments should be performed to further compare EPO's effect in adults and neonates.

Acknowledgments This work was supported by NIH grants NS058710 and NS062097, NS045155 and NS045810, and the American Heart Association Established Investigator Award.

Conflict of interest statement We declare that we have no conflict of interest.

References

- Lloyd-Jones D, Adams RJ, Brown TM, Carnethon M, Dai S, De Simone G, Ferguson TB, Ford E, Furie K, Gillespie C, Go A, Greenlund K, Haase N, Hailpern S, Ho PM, Howard V, Kissela B, Kittner S, Lackland D, Lisabeth L, Marelli A, McDermott MM, Meigs J, Mozaffarian D, Mussolino M, Nichol G, Roger VL, Rosamond W, Sacco R, Sorlie P, Stafford R, Thom T, Wasserthiel-Smoller S, Wong ND, Wylie-Rosett J (2010) Executive summary: heart disease and stroke statistics – 2010 update: a report from the American Heart Association. *Circulation* 121:948–954. doi:10.1161/CIRCULATIONAHA.109.192666 [pii]
- Broderick J, Talbot GT, Prenger E, Leach A, Brott T (1993) Stroke in children within a major metropolitan area: the surprising importance of intracerebral hemorrhage. *J Child Neurol* 8:250–255
- Fullerton HJ, Wu YW, Zhao S, Johnston SC (2003) Risk of stroke in children: ethnic and gender disparities. *Neurology* 61:189–194
- Sofronas M, Ichord RN, Fullerton HJ, Lynch JK, Massicotte MP, Willan AR, deVeber G (2006) Pediatric stroke initiatives and preliminary studies: what is known and what is needed? *Pediatr Neurol* 34:439–445. doi:S0887-8994(05)00636-3 [pii] 10.1016/j.pediatrneurol.2005.10.016
- Lynch JK, Hirtz DG, DeVeber G, Nelson KB (2002) Report of the National Institute of Neurological Disorders and Stroke workshop on perinatal and childhood stroke. *Pediatrics* 109:116–123
- Zakhary MM, Wesolowski JR, Sewick AE, Carlson M, Mehrotra N, Maly P, Sundgren PC (2009) Prevalence and etiology of intracranial hemorrhage in term children under the age of two years: a retrospective study of computerized tomographic imaging and clinical outcome in 798 children. *Acad Radiol* 16:572–577. doi:S1076-6332(09)00035-X [pii] 10.1016/j.acra.2009.01.007
- Schoenberg BS, Mellinger JF, Schoenberg DG (1978) Cerebrovascular disease in infants and children: a study of incidence, clinical features, and survival. *Neurology* 28:763–768
- Lanthier S, Carmant L, David M, Larbrisseau A, de Veber G (2000) Stroke in children: the coexistence of multiple risk factors predicts poor outcome. *Neurology* 54:371–378
- Meyer-Heim AD, Boltshauser E (2003) Spontaneous intracranial haemorrhage in children: aetiology, presentation and outcome. *Brain Dev* 25:416–421. doi:S0387760403000299 [pii]
- Lipton P (1999) Ischemic cell death in brain neurons. *Physiol Rev* 79:1431–1568
- Liu XB, Wang JA, Yu SP, Keogh CL, Wei L (2008) Therapeutic strategy of erythropoietin in neurological disorders. *CNS Neurol Disord Drug Targets* 7:227–234
- Chong ZZ, Kang JQ, Maiese K (2003) Erythropoietin fosters both intrinsic and extrinsic neuronal protection through modulation of microglia, Akt1, bad, and caspase-mediated pathways. *Br J Pharmacol* 138:1107–1118. doi:10.1038/Sj.Bjp.705161
- Youle RJ, Strasser A (2008) The BCL-2 protein family: opposing activities that mediate cell death. *Nat Rev Mol Cell Biol* 9:47–59. doi:nrm2308 [pii] 10.1038/nrm2308
- Chong ZZ, Lin SH, Kang JQ, Maiese K (2003) Erythropoietin prevents early and late neuronal demise through modulation of Akt1 and induction of caspase 1, 3, and 8. *J Neurosci Res* 71:659–669. doi:10.1002/jnr.10528
- Kennedy SG, Kandel ES, Cross TK, Hay N (1999) Akt/Protein kinase B inhibits cell death by preventing the release of cytochrome c from mitochondria. *Mol Cell Biol* 19:5800–5810

16. Li Y, Ogle ME, Wallace GC, Lu ZY, Yu SP, Wei L (2008) Erythropoietin attenuates intracerebral hemorrhage by diminishing matrix metalloproteinases and maintaining blood-brain barrier integrity in mice. *Acta Neurochir Suppl* 105:105–112
17. Lee ST, Chu K, Sinn DI, Jung KH, Kim EH, Kim SJ, Kim JM, Ko SY, Kim M, Roh JK (2006) Erythropoietin reduces perihematomal inflammation and cell death with eNOS and STAT3 activations in experimental intracerebral hemorrhage. *J Neurochem* 96:1728–1739. doi:10.1111/J.1471-4159.2006.03697.X
18. Grasso G, Graziano F, Sfacteria A, Carletti F, Meli F, Maugeri R, Passalacqua M, Certo F, Fazio M, Buemi M, Iacopino DG (2009) Neuroprotective effect of erythropoietin and darbepoetin alfa after experimental intracerebral hemorrhage. *Neurosurgery* 65:763–769. doi:10.1227/01.NEU.0000347475.73347.5F; discussion 769–770
19. Gonzalez FF, Abel R, Almlri CR, Mu D, Wendland M, Ferriero DM (2009) Erythropoietin sustains cognitive function and brain volume after neonatal stroke. *Dev Neurosci* 31:403–411. doi:000232558 [pii] 10.1159/000232558
20. Kim SS, Lee KH, Sung DK, Shim JW, Kim MJ, Jeon GW, Chang YS, Park WS (2008) Erythropoietin attenuates brain injury, subventricular zone expansion, and sensorimotor deficits in hypoxic-ischemic neonatal rats. *J Korean Med Sci* 23:484–491. doi:200806484 [pii] 10.3346/jkms.2008.23.3.484
21. Wei L, Han BH, Li Y, Keogh CL, Holtzman DM, Yu SP (2006) Cell death mechanism and protective effect of erythropoietin after focal ischemia in the whisker-barrel cortex of neonatal rats. *J Pharmacol Exp Ther* 317:109–116. doi:jpet.105.094391 [pii] 10.1124/jpet.105.094391
22. Li Y, Lu Z, Keogh CL, Yu SP, Wei L (2007) Erythropoietin-induced neurovascular protection, angiogenesis, and cerebral blood flow restoration after focal ischemia in mice. *J Cereb Blood Flow Metab* 27:1043–1054. doi:9600417 [pii] 10.1038/sj.jcbfm.9600417
23. Keogh CL, Yu SP, Wei L (2007) The effect of recombinant human erythropoietin on neurovasculature repair after focal ischemic stroke in neonatal rats. *J Pharmacol Exp Ther* 322:521–528. doi:jpet.107.121392 [pii] 10.1124/jpet.107.121392
24. Deng XL, Lau CP, Lai K, Cheung KF, Lau GK, Li GR (2007) Cell cycle-dependent expression of potassium channels and cell proliferation in rat mesenchymal stem cells from bone marrow. *Cell Prolif* 40:656–670
25. Brines ML, Ghezzi P, Keenan S, Agnello D, de Lanerolle NC, Cerami C, Itri LM, Cerami A (2000) Erythropoietin crosses the blood-brain barrier to protect against experimental brain injury. *Proc Natl Acad Sci USA* 97:10526–10531. doi:97/19/10526 [pii]
26. Brines M (2002) What evidence supports use of erythropoietin as a novel neurotherapeutic? *Oncology (Williston Park)* 16:79–89
27. Arai K, Lee F, Miyajima A, Miyatake S, Arai N, Yokota T (1990) Cytokines: coordinators of immune and inflammatory responses. *Annu Rev Biochem* 59:783–836
28. Pregi N, Wenker S, Vittori D, Leiros CP, Nesse A (2009) TNF-alpha-induced apoptosis is prevented by erythropoietin treatment on SH-SY5Y cells. *Exp Cell Res* 315:419–431. doi:10.1016/J.Yexcr.2008.11.005
29. Sun Y, Calvert JW, Zhang JH (2005) Neonatal hypoxia/ischemia is associated with decreased inflammatory mediators after erythropoietin administration. *Stroke* 36:1672–1678. doi:10.1161/01.Str.0000173406.04891.8c
30. Villa P, Bigini P, Mennini T, Agnello D, Laragione T, Cagnotto A, Viviani B, Marinovich M, Cerami A, Coleman TR, Brines M, Ghezzi P (2003) Erythropoietin selectively attenuates cytokine production and inflammation in cerebral ischemia by targeting neuronal apoptosis. *J Exp Med* 198:971–975. doi:10.1084/Jem.20021067
31. Turrin NP, Plata-Salaman CR (2000) Cytokine-cytokine interactions and the brain. *Brain Res Bull* 51:3–9. doi:S0361-9230(99)00203-8 [pii]
32. Dinarello CA (1987) The biology of interleukin-1 and comparison to tumor necrosis factor. *Immunol Lett* 16:227–331
33. Minami M, Kuraishi Y, Yabuuchi K, Yamazaki A, Satoh M (1992) Induction of interleukin-1 beta mRNA in rat-brain after transient forebrain ischemia. *J Neurochem* 58:390–392
34. Yamasaki Y, Matsuura N, Shozuhara H, Onodera H, Itoyama Y, Kogure K (1995) Interleukin-1 as a pathogenetic mediator of ischemic brain-damage in rats. *Stroke* 26:676–680
35. Giulian D, Lachman LB (1985) Interleukin-1 stimulation of astroglial proliferation after brain injury. *Science* 228:497–499
36. Masada T, Hua Y, Xi G, Yang GY, Hoff JT, Keep RF (2001) Attenuation of intracerebral hemorrhage and thrombin-induced brain edema by overexpression of interleukin-1 receptor antagonist. *J Neurosurg* 95:680–686. doi:10.3171/jns.2001.95.4.0680
37. Gordon CR, Merchant RS, Marmarou A, Rice CD, Marsh JT, Young HF (1990) Effect of murine recombinant interleukin-1 on brain oedema in the rat. *Acta Neurochir Suppl (Wien)* 51:268–270
38. Megyeri P, Abraham CS, Temesvari P, Kovacs J, Vas T, Speer CP (1992) Recombinant human tumor necrosis factor alpha constricts pial arterioles and increases blood-brain barrier permeability in newborn piglets. *Neurosci Lett* 148:137–140
39. Holmin S, Mathiesen T (2000) Intracerebral administration of interleukin-1beta and induction of inflammation, apoptosis, and vasogenic edema. *J Neurosurg* 92:108–120. doi:10.3171/jns.2000.92.1.0108
40. Castillo J, Davalos A, Alvarez-Sabin J, Pumar JM, Leira R, Silva Y, Montaner J, Kase CS (2002) Molecular signatures of brain injury after intracerebral hemorrhage. *Neurology* 58:624–629
41. Hua Y, Wu J, Keep RF, Nakamura T, Hoff JT, Xi G (2006) Tumor necrosis factor-alpha increases in the brain after intracerebral hemorrhage and thrombin stimulation. *Neurosurgery* 58:542–550. doi:10.1227/01.NEU.0000197333.55473.AD00006123-200603000-00017 [pii]; discussion 542–550
42. Nawashiro H, Tasaki K, Ruetzler CA, Hallenbeck JM (1997) TNF-alpha pretreatment induces protective effects against focal cerebral ischemia in mice. *J Cereb Blood Flow Metab* 17:483–490. doi:10.1097/00004647-199705000-00001
43. Figiel I (2008) Pro-inflammatory cytokine TNF-alpha as a neuroprotective agent in the brain. *Acta Neurobiol Exp (Wars)* 68:526–534. doi:6855 [pii]
44. Barone FC, Arvin B, White RF, Miller A, Webb CL, Willette RN, Lysko PG, Feuerstein GZ (1997) Tumor necrosis factor-alpha. A mediator of focal ischemic brain injury. *Stroke* 28:1233–1244
45. Meistrell ME, Botchkina GI, Wang HC, DiSanto E, Cockcroft KM, Bloom O, Vishnubhakat JM, Ghezzi P, Tracey KJ (1997) Tumor necrosis factor is a brain damaging cytokine in cerebral ischemia. *Shock* 8:341–348
46. Pettigrew LC, Kindy MS, Scheff S, Springer JE, Kryscio RJ, Li Y, Grass DS (2008) Focal cerebral ischemia in the TNFalpha-transgenic rat. *J Neuroinflammation* 5:47. doi:1742-2094-5-47 [pii] 10.1186/1742-2094-5-47
47. Tseng MY, Hutchinson PJ, Richards HK, Czornyka M, Pickard JD, Erber WN, Brown S, Kirkpatrick PJ (2009) Acute systemic erythropoietin therapy to reduce delayed ischemic deficits following aneurysmal subarachnoid hemorrhage: a Phase II randomized, double-blind, placebo-controlled trial. *Clinical article. J Neurosurg* 111:171–180. doi:10.3171/2009.3.JNS081332
48. Tseng MY, Hutchinson PJ, Kirkpatrick PJ (2010) Interaction of neurovascular protection of erythropoietin with age, sepsis, and statin therapy following aneurysmal subarachnoid hemorrhage. *J Neurosurg* 112:1235–1239. doi:10.3171/2009.10.Jns09954

49. Tseng MY, Richards H, Czosnyka M, Pickard JD, Kirkpatrick PJ (2007) Acute systemic erythropoietin therapy reduces cerebral vasospasm and delayed ischemic deficits after aneurysmal subarachnoid hemorrhage: a phase II randomized, double-blind, placebo-controlled trial. *J Neurosurg* 106:A768
50. Tseng MY, Hutchinson PJ, Richards HK, Czosnyka M, Pickard JD, Erber WN, Brown S, Kirkpatrick PJ (2009) Acute systemic erythropoietin therapy to reduce delayed ischemic deficits following aneurysmal subarachnoid hemorrhage: a Phase II randomized, double-blind, placebo-controlled trial. *J Neurosurg* 111:171–180. doi:10.3171/2009.3.Jns081332

Protective Effects of Hydrogen on Fetal Brain Injury During Maternal Hypoxia

Wenwu Liu, Oumei Chen, Chunhua Chen, Bihua Wu, Jiping Tang, and John H. Zhang

Abstract This study aimed to investigate the effects of hydrogen on fetal brain injury during maternal hypoxia. Pregnant rats ($n=12$, at gestational day 17) were randomly assigned into three groups; air, hypoxia, and hypoxia plus hydrogen groups were put into a chamber and flushed with room air (21% O₂ and 79% N₂), hypoxia (8% O₂ and 92% N₂), and hypoxia with hydrogen mixture (2% H₂, 8% O₂ and 90% N₂), respectively, for 4 consecutive hours. After birth, body and brain weights, body-righting reflex, and negative geotropism of neonates were measured, and then pups were killed at days 1 and 7. Oligodendrocytes were studied at post-natal day 1 by immunohistochemistry. We found significant decreases in body weight in the hypoxia group ($P<0.05$ vs. room air group), but not in the hypoxia plus hydrogen group ($P>0.05$ vs. room air group). Even though brain weight was not different among groups, the brain weight to body weight ratio in the room air group was significantly ($P<0.05$) lower than that in the hypoxia alone or hypoxia plus hydrogen groups. Body-righting reflex at day 1 and negative geotropism at days 3–4 showed deficiency in hypoxia animals when compared with the room air group ($P<0.05$). Hydrogen treatment improved the body-righting reflex and negative geotropism

($P<0.05$ vs. room air group). The above-mentioned functional changes caused by hypoxia were not associated with morphology and cell death of oligodendrocytes. Therefore, the maternal hypoxia-induced body weight loss, and functional abnormalities and hydrogen treatment during hypoxia offered a protective effect and improved functions in neonates.

Keywords Maternal hypoxia · Neonates · Hydrogen · Functional evaluation

Introduction

Pathological conditions during pregnancy, such as hypoxia, seizures, and infection, are known to cause fetal brain damage [1]. Among these factors, low brain oxygenation is associated with an increased risk of cerebral palsy and periventricular leukomalacia (PVL) in newborns [2]. Depending on the type, the severity, and the duration, hypoxia produces either temporary brain dysfunction or permanent brain injury [1]. During hypoxia, excessive production of reactive oxygen species (ROS) actively oxidizes protein, DNA, and lipid, and results in cellular injury. Among these ROSs, the hydroxyl radical ($\cdot\text{OH}$) and peroxynitrite (ONOO^-) are more noticeable because there is not a known detoxification system in human body for $\cdot\text{OH}$ and ONOO^- [3].

Recently, the protective effects of hydrogen have attracted attention in ischemic and hypoxic insults because of its electric neutrality, cellular permeability, harmless metabolite (H₂O), and non-interference with metabolic oxidation-reduction reactions [4]. Hydrogen seems to selectively scavenge $\cdot\text{OH}$ and ONOO^- during ischemia and reperfusion injury [4] in focal ischemia, neonatal hypoxia-ischemia, Parkinson's, and stress-induced impairment rat models [4–7]. Therefore, the aim of this study is to investigate the effect of hydrogen on fetal neurodevelopmental brain damage in an established maternal hypoxia rat model.

W. Liu

Department of Physiology and Pharmacology, Loma Linda University, School of Medicine, Loma Linda, CA, USA and
Department of Diving Medicine, The Second Military Medical University, Shanghai, People's Republic of China

O. Chen, C. Chen, B. Wu, and J. Tang

Department of Physiology and Pharmacology, Loma Linda University, School of Medicine, Loma Linda, CA, USA

J.H. Zhang (✉)

Department of Physiology and Pharmacology, Loma Linda University, School of Medicine, Loma Linda, CA, USA and
Department of Physiology, Loma Linda University, School of Medicine, Risley Hall, Room 223, Loma Linda, 92354, CA, USA
e-mail: johnzhang3910@yahoo.com

Materials and Methods

Experimental Regimen

Pregnant Sprague-Dawley (SD) rats at gestational day 17 were assigned randomly to the following groups: room air group ($n=4$), hypoxia group ($n=4$), and hypoxia plus hydrogen group ($n=4$). The rats in the room air, hypoxia, and hypoxia plus hydrogen group were put into a chamber and flushed with room air (21% O₂ and 79% N₂), hypoxia (8% O₂ and 92% N₂), and hypoxia with a hydrogen mixture (2% H₂, 8% O₂ and 90% N₂), respectively, for 4 consecutive hours. Then, the mother rats were taken out, and maintained in a normal atmosphere and humidity-controlled condition with a 12:12-h light-dark cycle. The Animal and Ethics Review Committee at the Loma Linda University evaluated and approved the protocol used in this study.

Negative Geotropism

Pups were placed on a sloping rough surface (at an angle of 20°, size 300 × 330 mm) head downwards. The magnitude of rotation of the animal to reach the normal head-upwards position was assessed during a 1-min period using a four-point scale: 0=no reaction; 1=weak rotation (up to 90°); 2=incomplete rotation (from 90°); 3=complete rotation (180°) [8]. Negative geotropism was tested daily from 3 days after delivery.

Body Righting

Pups were gently placed on their backs, and a score was given according to the following criteria: 0=no response; 1=weak response; 2=incomplete response (e.g., a leg remaining beneath the animal's body); 3=complete response [8]. In addition, the time taken before the animal showed the complete righting response was measured (cutoff: 60 s). Body-righting was tested daily.

Body and Brain Weight

Animals were weighed daily and killed at postnatal day 1 (P1) and day 7 (P7). The brains were removed and weighed. The ratio of brain weight to body weight was obtained.

Immunohistochemistry

Brains were obtained and fixed in formaldehyde followed by frozen sectioning. Then sections were washed with PBS three times and treated with 0.3% Triton×100 for 15 min. After washing with PBS three times, antigen retrieval was performed in sodium citrate solution. Then, sections were washed with PBS three times and treated with 3% hydrogen peroxide. After washing with PBS three times, sections were blocked with 3% donkey serum in PBS for 1 h at room temperature followed by incubation with primary antibody (Anti-CNPase, 1:200; Millipore, USA) overnight. Then, sections were washed with PBS three times and treated with secondary antibody (1:200) for 2 h. Color development was performed according to the manufacturer's instructions (Santa Cruz, USA). The number of oligodendrocytes was counted under a light microscope.

Results

Body and Brain Weights

The mean body weight of neonates in the room air group was higher at days 1, 6, and 7 than in the hypoxia group. Hydrogen treatment increased body weight even though statistical significance was not obtained ($P>0.05$ vs. hypoxia group, Fig. 1a). Daily body weight gain was calculated, and animals in the room air group had significant gains at days 5 and 7 when compared to the hypoxia groups ($P<0.05$ vs. hypoxia, hypoxia+hydrogen groups). No statistical significance was obtained between the hypoxia and hypoxia plus hydrogen groups (Fig. 1b).

Brain weights were obtained at days 1 and 7, and no differences were observed among these three groups ($P>0.05$), although there was a trend that the brain weight in room air and hypoxia plus hydrogen groups were higher than in the hypoxia group at day 7 (Fig. 1c). Brain to body weight ratio was calculated, and a significantly higher ratio was observed in the hypoxia, but not in the hypoxia plus hydrogen groups when compared with room air animals ($P<0.05$, Fig. 1d).

Functional Evaluation

A transient but marked deficiency of body-righting reflex was observed at day 1 in the hypoxia group when compared with room air animals ($P<0.05$), and hydrogen treatment abolished the deficiency of body-righting reflex

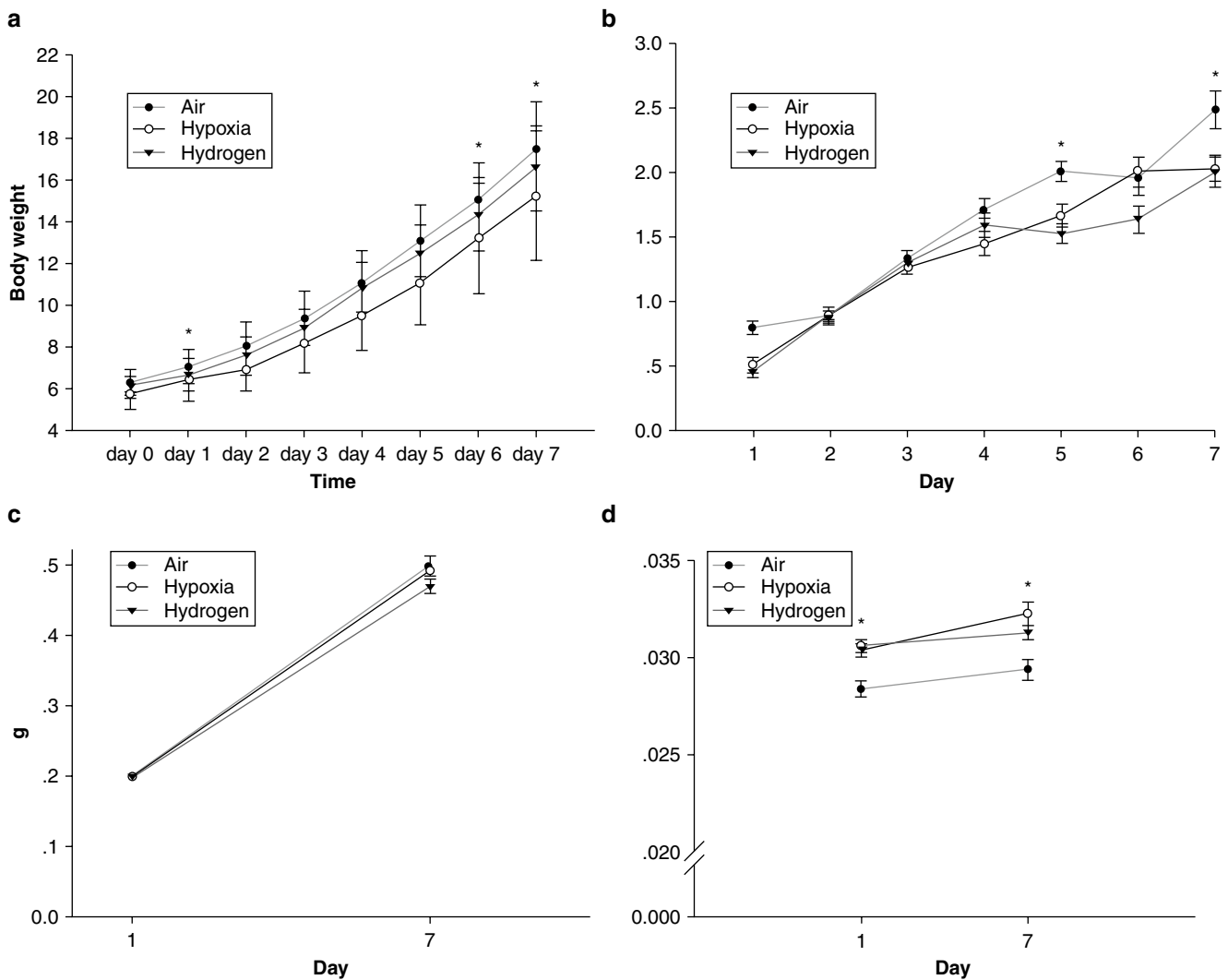


Fig. 1 (a) Body weight among groups ($*P < 0.05$, air group vs. hydrogen group or hypoxia group). (b) Body weight gain among groups ($*P < 0.05$, air group vs. hydrogen group or hypoxia group). (c) Brain

weight among groups. (d) Brain weight to body weight ratio among groups ($*P < 0.05$, air group vs. hydrogen group or hypoxia group)

($P < 0.05$ vs. hypoxia, Fig. 2a). Similarly, a marked deficiency of negative geotropism was observed at days 3–4 in the hypoxia group when compared with room air animals ($P < 0.05$). Again, hydrogen treatment improved significantly the deficiencies ($P < 0.05$ vs. hypoxia group, Fig. 2b).

Oligodendrocytes Morphology

Oligodendrocytes and their precursors begin to arise in significant numbers in the developing rodent forebrain around embryonic day 18, and they are sensitive to hypoxia [9]. Therefore, we killed pups on day 1 (E18) to observe oligodendrocytes.

The number of oligodendrocytes was counted at a magnification of 100. We did not observe morphological abnormalities in this animal model ($P > 0.05$, Fig. 3a). The cell numbers of oligodendrocytes tended to be lower in the hypoxia group without statistical significance ($P > 0.05$ vs. room air). Hydrogen treatment failed to affect the number of oligodendrocytes ($P > 0.05$ vs. hypoxia or room air groups, Fig. 3b).

Discussion

In this study, a mild and transient maternal hypoxia retarded brain and body development slightly and reversibly, similar

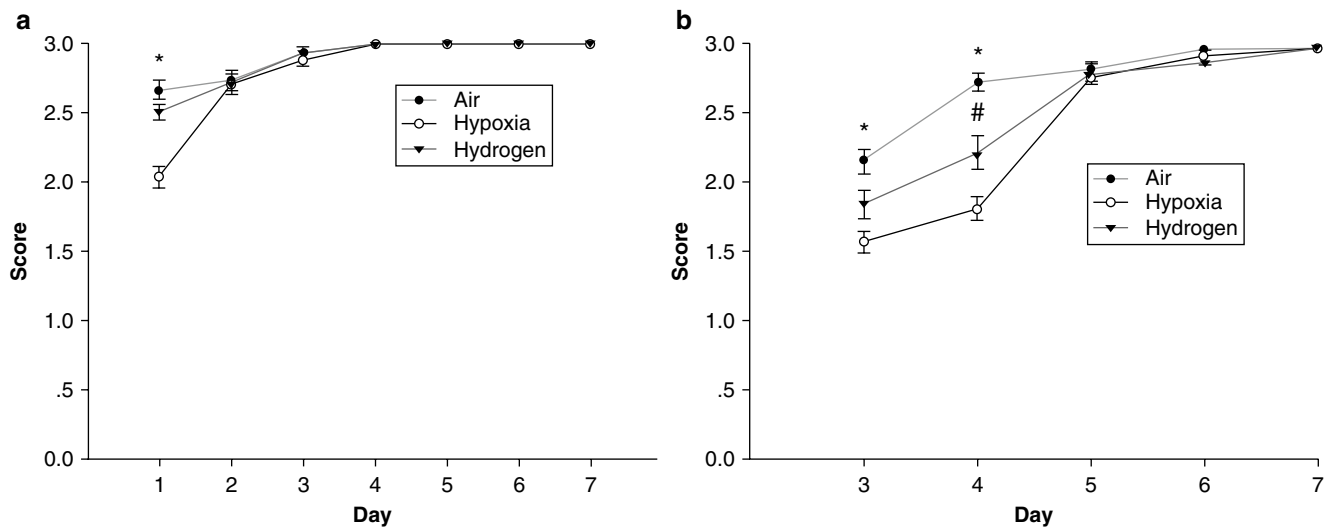


Fig. 2 (a) Body-righting reflex among groups (* $P < 0.05$, air group vs. hydrogen group or hypoxia group). (b) Negative geotropism in different groups (* $P < 0.05$, air group vs. hydrogen group or hypoxia group; # $P < 0.05$ hydrogen group vs. hypoxia group)

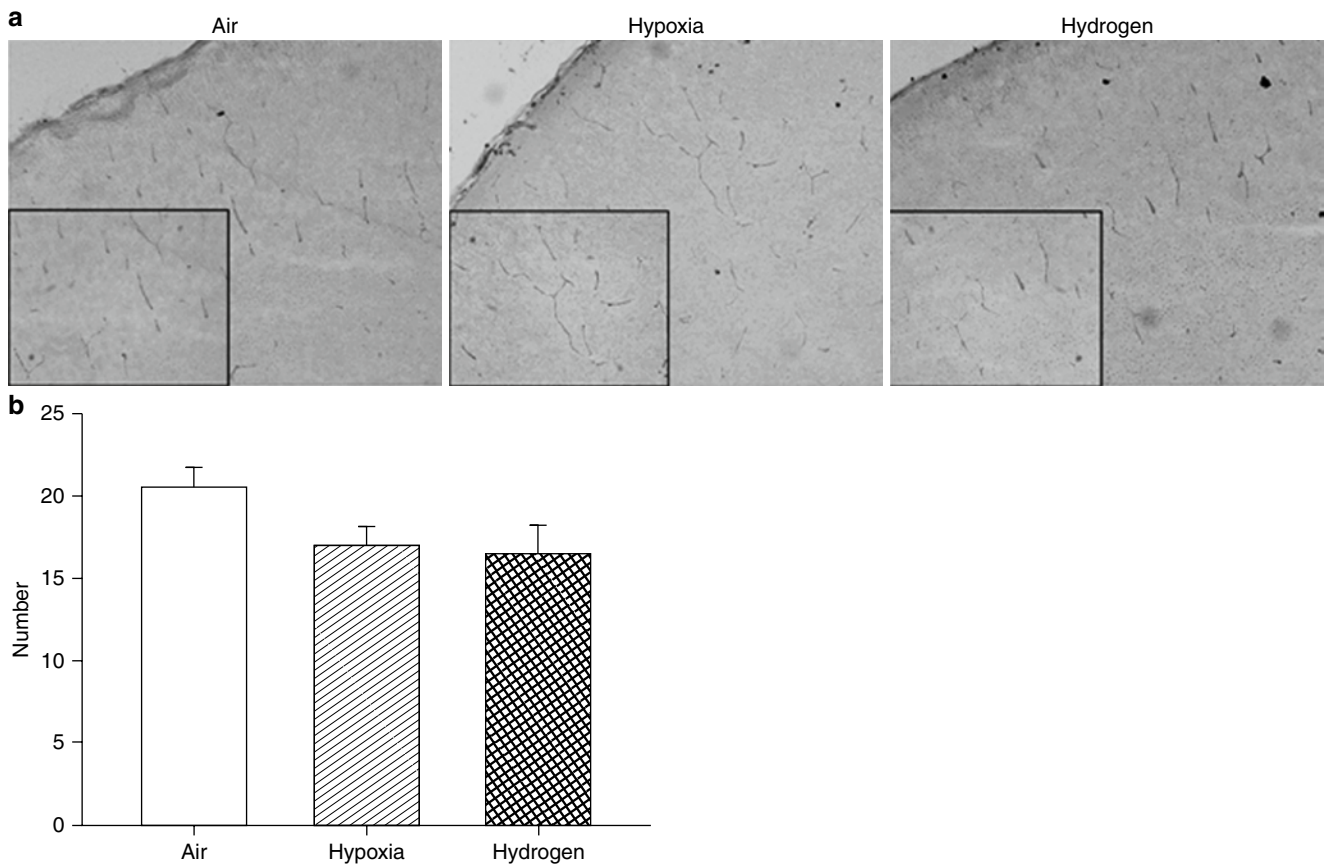


Fig. 3 (a) Representative photographs of oligodendrocytes in the cortex. No marked morphological changes were noted in oligodendrocytes in any groups. (b) The number of oligodendrocytes was counted, and no significant difference was observed among three groups

to the low brain oxygenation-caused perinatal brain injury in human [10]. This mild developmental retardation is accompanied by an abnormal body-righting reflex observed at day 1

and abnormal negative geotropism noted at days 3 and 4. Both sensory reflexes returned to normal level rapidly after birth. Oligodendrocytes and their precursors begin to arise

in significant numbers in the developing rodent forebrain around embryonic day 18 (E18) [9]. Oligodendrocytes are particularly vulnerable to neonatal hypoxia/ischemia insults and are preferentially lost following neonatal unilateral carotid ligation combined with hypoxia in rodents. This mild and transient maternal hypoxia does not produce morphological brain abnormalities or oligodendrocyte cell death.

Mouse and rat brains at the last trimester of gestation paralleled the developmental stage of a human fetal brain at the first-second trimester. Study showed delays in the development of various sensory and motor reflexes were observed during the first month of rodent life after maternal hypoxia exposure [11]. Negative geotropism is essential for adaptation to the environment and is developed during the first postnatal week in the rat and mouse. Zhuravin et al. [12] indicated acute prenatal hypoxia delayed the development of this ability. Any one of the neuromuscular responses aims to restore the body to its normal upright position when it has been displaced, which is called the righting reflex and represents a sensory reflex. A similar trend of slower development in newborns exposed to prenatal or neonatal hypoxia/ischemia, as compared to control groups, has been reported for other sensorimotor reflexes, including the righting reflex [13]. Despite the delay in reflex development, it is important to note that newborns exposed to hypoxia/ischemia pre- or neonatally do complete the development of all the sensorimotor reflexes tested [11]. Our results were consistent with previous study in which researchers showed abnormal sensory reflexes could resolve [11–13].

We tested the potential therapeutic effect of hydrogen in this mild and transient maternal hypoxic pup model, because a recent study reported that inhalation of hydrogen gas could selectively neutralize $\cdot\text{OH}$ and peroxynitrite ($\text{ONOO}\cdot$) and protect the brain against ischemia/reperfusion injury [4]. Even though the results of hydrogen on body weight, body weight gain, and brain weight to body weight ratio are inconsistent, hydrogen treatment during hypoxia improved the body-righting reflex and negative geotropism. In summary, mild and transient maternal hypoxia caused neurological functional abnormalities in this animal model, and hydrogen may be an alternative treatment to prevent subtle brain injury and especially improve functional outcomes.

Acknowledgments This study was supported by grants HD43120 and NS54695 from the National Institutes of Health to John H. Zhang and NS60936 to Jiping Tang.

Conflict of interest statement We declare that we have no conflict of interest.

References

1. Volpe JJ (1995) Hypoxic-ischemic encephalopathy. In: Volpe JJ (ed) *Neurology of the newborn*, 3rd edn. W.B. Saunders, Philadelphia, pp 211–369
2. Inder TE, Volpe JJ (2000) Mechanisms of perinatal brain injury. *Semin Neonatol* 5:3–16
3. Kiliç I, Güven C, Kiliç K (2003) Effect of maternal NG-nitro-L-arginine administration on fetal growth and hypoxia-induced changes in newborn rats. *Pediatr Int* 45:375–378
4. Ohsawa I, Ishikawa M, Takahashi K et al (2007) Hydrogen acts as a therapeutic antioxidant by selectively reducing cytotoxic oxygen radicals. *Nat Med* 13:688–694
5. Cai JM, Kang ZM, Liu WW et al (2008) Hydrogen therapy reduces apoptosis in neonatal hypoxia-ischemia rat model. *Neurosci Lett* 441:167–172
6. Fu Y, Ito M, Fujita Y et al (2009) Molecular hydrogen is protective against 6-hydroxydopamine-induced nigrostriatal degeneration in a rat model of Parkinson's disease. *Neurosci Lett* 453:81–85
7. Nagata K, Nakashima-Kamimura N, Mikami T et al (2009) Consumption of molecular hydrogen prevents the stress-induced impairments in hippocampus-dependent learning tasks during chronic physical restraint in mice. *Neuropsychopharmacology* 34:501–508
8. Thullier F, Lalonde R, Cousin X et al (1997) Neurobehavioral evaluation of lurcher mutant mice during ontogeny. *Brain Res Dev Brain Res* 100(1):22–28
9. Robinson S, Petelenz K, Li Q, Cohen ML et al (2005) Developmental changes induced by graded prenatal systemic hypoxic-ischemic insults in rats. *Neurobiol Dis* 18:568–581
10. Nyakas C, Buwalda B, Luiten PG (1996) Hypoxia and brain development. *Prog Neurobiol* 49:1–51
11. Golan H, Huleihel M (2006) The effect of prenatal hypoxia on brain development: short- and long-term consequences demonstrated in rodent models. *Dev Sci* 9:338–349
12. Zhuravin IA, Dubrovskaya NM, Tumanova NL (2004) Neuroscience and postnatal physiological development of rats after acute prenatal hypoxia. *Behav Physiol* 34:809–816
13. Golan H, Kashtutsky I, Hallak M et al (2004) Maternal hypoxia during pregnancy delays the development of motor reflexes in newborn mice. *Dev Neurosci* 26:24–29

Cerebral Hemorrhage Clinical Manifestations

Neuroglobin Expression in Human Arteriovenous Malformation and Intracerebral Hemorrhage

Kunlin Jin, XiaoOu Mao, Lin Xie, and David A. Greenberg

Abstract We reported previously that Notch signaling is activated in human arteriovenous malformations (AVMs) and that intracerebral hemorrhage (ICH) in humans is accompanied by increased neurogenesis. The former phenomenon may be involved in AVM pathogenesis and the latter in the brain's response to ICH-induced injury. Here we describe increased expression of the hypoxia-inducible neuroprotective protein, neuroglobin (Ngb), in neurons surrounding unruptured AVMs and in the perihematomal region adjacent to ICH. In these disorders, as in other clinical settings, such as ischemic stroke, AVM- and ICH-induced overexpression of Ngb may be stimulated by ischemic hypoxia and may help to constrain brain injury.

Keywords Neuroglobin · Arteriovenous malformation · Intracerebral hemorrhage · Hypoxia · Ischemia

Introduction

Intracerebral hemorrhage (ICH) accounts for approximately 10–15% of strokes and is associated with high early mortality. Causes include head trauma, chronic hypertension, vascular malformations, amyloid angiopathy, bleeding into primary or metastatic tumors, coagulopathy and therapeutic anticoagulation [1]. Despite extensive clinical experience with ICH, its pathophysiology [2, 3] and optimal treatment [4, 5] are poorly defined.

One important class of lesions associated with ICH – vascular malformations of the brain, including arteriovenous malformations (AVMs) – are thought to arise during embryonic development, but typically present in middle age and

appear to grow over time [3]. This suggests that the brain may have the opportunity to mount postnatal adaptive responses that limit tissue dysfunction, as is observed in other pathological processes, such as ischemia or tumor. By extension, it may be possible to intervene medically to check the growth of vascular malformations or mitigate their clinical sequelae by targeting these responses.

ICH has been considered to produce symptoms – typically altered consciousness and focal neurological deficits – through a combination of tissue destruction, mass effect and perhaps ischemia in the surrounding brain tissue. However, the role of perihematomal ischemia has been questioned by recent studies [2]. This may have important clinical implications, because the desire to avoid exacerbating ischemia has limited enthusiasm for reducing blood pressure early in the course of ICH, despite the fact that some studies show a beneficial effect of blood pressure reduction [4].

In previous work related to AVM and ICH, we investigated mechanisms that could be involved in the pathophysiology and in the brain's response to these disorders. In one study, we examined the role of Notch signaling in human AVMs [6]. Notch1 signaling was activated in smooth muscle and endothelial cells of AVMs compared to normal cerebral blood vessels. Activated Notch1 (Notch intracellular domain, or NICD) was detected immunohistochemically in brain AVMs but not control vessels. Notch1 ligands (Jagged1 and Delta-like 4) and a downstream target (Hes1) were also overexpressed in AVMs. A functional role for Notch1 signaling in AVMs was supported by the finding that Notch1 activation in rats promoted angiogenesis, which could contribute to the development of AVMs.

In another study, we reported that neurogenesis, which is stimulated by a variety of experimental brain lesions and by cerebral ischemia in humans [7], was increased in the brains of patients with ICH [8]. This was manifested by the expression of neural stem or progenitor cell markers together with markers of cell proliferation in regions of the basal ganglia and parietal lobe surrounding brain hematomas. Thus, the brain may respond to ICH, as it does to infarction, with an

K. Jin, X. Mao, L. Xie, and D.A. Greenberg (✉)
Buck Institute for Age Research, 8001 Redwood Boulevard,
Novato, CA 94945, USA
e-mail: dgreenberg@buckinstitute.org

increased capacity for generating new neurons. As in infarction, this may be a mechanism for moderating the extent of injury [9].

Here we report findings regarding the expression of neuroglobin (Ngb), a hypoxia-inducible neuroprotective protein, in the brains of patients with AVM or ICH. Ngb is expressed, predominantly in neurons, at low basal levels [10]. In response to hypoxia, ischemia or related insults, Ngb is transcriptionally activated [11]. Evidence for a neuroprotective role of Ngb includes the observations that infarct size and associated neurobehavioral abnormalities following occlusion of the middle cerebral artery are reduced in rodents that overexpress Ngb [12, 13], whereas knockdown of Ngb expression exacerbates these deficits [13]. Ngb expression is also increased in the vicinity of cerebral infarcts in humans [14]. However, the role of Ngb in cerebral responses to other vascular lesions has not been reported.

Materials and Methods

The provenance of brain specimens from and clinical features of patients with cerebral AVM and presumed hypertensive ICH have been described previously [6, 8]. All studies were conducted under protocols approved by local Institutional Research Review Boards. Single-label Ngb immunohistochemistry was conducted using 6- μ m paraffin-embedded sections, which were deparaffinized with xylene and rehydrated with ethanol, following antigen retrieval with antigen unmasking solution (Vector Laboratories) according to the manufacturer's instructions. Rabbit polyclonal anti-Ngb (1: 500; Sigma) was added in blocking buffer and incubated with sections at 4°C overnight. Sections were then washed with PBS and incubated with biotinylated anti-rabbit IgG for 1 h at room temperature. Avidin-biotin complex (Vector Elite; Vector Laboratories) and Ni solution (Vector Laboratories) were used to obtain a visible reaction product. A Nikon microscope and Nikon digital color camera were used to examine and photograph the slides, respectively. For double-label immunohistochemistry, the primary antibodies used were rabbit polyclonal anti-Ngb (1:200; Sigma), mouse monoclonal anti-NeuN (1:200; Chemicon) and mouse monoclonal anti-GFAP (1:150; Sigma), and the secondary antibodies were FITC-conjugated anti-rabbit and rhodamine-conjugated anti-mouse IgG (1:200; Jackson Immuno Research). DAPI (Molecular Probes) was used to counterstain nuclei. Fluorescence signals were detected using an LSM 510 NLO Confocal Scanning System mounted on an Axiovert 200 inverted microscope equipped with a

two-photon Chameleon laser. Controls included omitting primary or secondary antibody or preabsorbing primary antibody.

Results

Basal expression of Ngb immunoreactivity in normal human brain was low (Fig. 1), as noted previously [14]. In contrast, immunoreactivity was higher in brain parenchyma adjacent to AVM and ICH. Within these regions, Ngb was co-localized with the neuronal marker NeuN, but not the astroglial marker GFAP, consistent with its preferential expression in neurons [10].

Discussion

These results indicate that neuronal Ngb expression is induced in brain tissue surrounding human AVM and ICH, as reported before for ischemic stroke [14]. In the case of ischemic stroke, increased Ngb expression in penumbral brain tissue has been attributed to ischemic hypoxia, but how AVM and ICH induce Ngb is less obvious.

Brain parenchyma adjacent to AVMs may show reactive gliosis, necrosis and hemosiderin deposition, which are thought to result from some combination of increased pressure, thrombosis, venous congestion, ischemia and bleeding [15]. Astrocytic expression of vascular endothelial growth factor (VEGF), a hypoxia-inducible angiogenic factor, is increased in surgical specimens from some patients with AVM [16], suggesting that hypoxia in the surrounding tissue might be responsible for inducing Ngb expression as well.

The role of perihematomal ischemia in the pathophysiology of ICH is controversial [2]. Neuronal expression of hypoxia-inducible factor-1 α is increased in the perihematomal region after experimental ICH in rats [17], consistent with ischemic hypoxia. Magnetic resonance imaging in patients with ICH suggests the existence of an ischemic penumbra around hematomas in some [18] but not other [19] studies, perhaps reflecting clinical heterogeneity [20]. Alternative explanations for perihematomal tissue dysfunction include impaired mitochondrial respiration [21] and iron-induced oxidative injury [22], but whether these processes rather than ischemic hypoxia could account for induction of Ngb is unclear.

We conclude that both unruptured AVM and presumed hypertensive ICH induce expression of Ngb in neurons located in the surrounding tissue, but the mechanism through which this occurs is unknown. It is also uncertain whether, as appears to be the case for ischemia stroke [12, 13], AVM- or

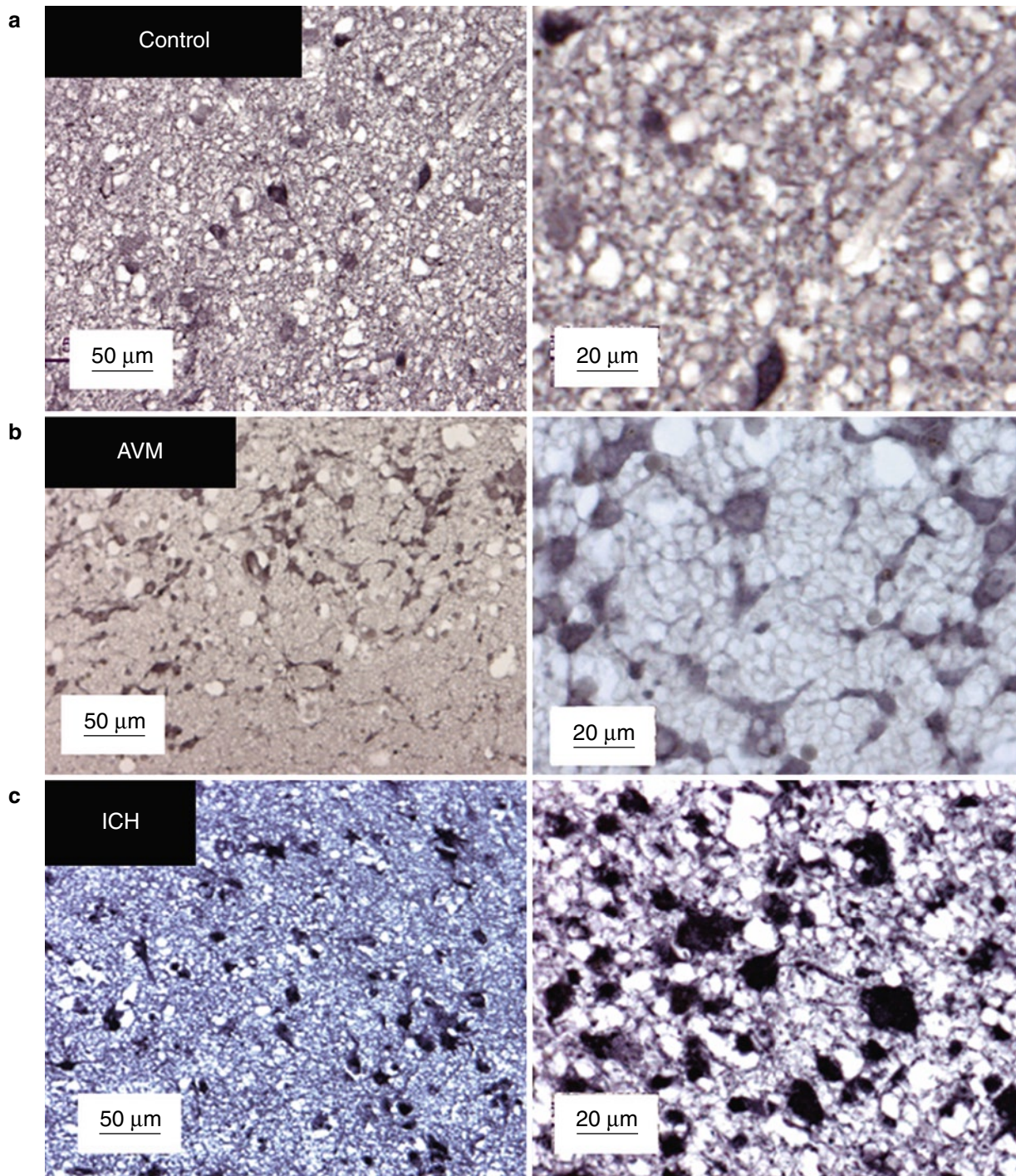


Fig. 1 Ngb expression in normal human brain, AVM and ICH. Low basal expression of Ngb immunoreactivity in normal human brain (a) is increased in brain parenchyma adjacent to AVM (b) and ICH (c), each

shown at low (*left*) and high (*right*) magnification. Double-label immunohistochemistry shows co-localization of Ngb with the neuronal marker NeuN (d), but not the astroglial marker GFAP (e)

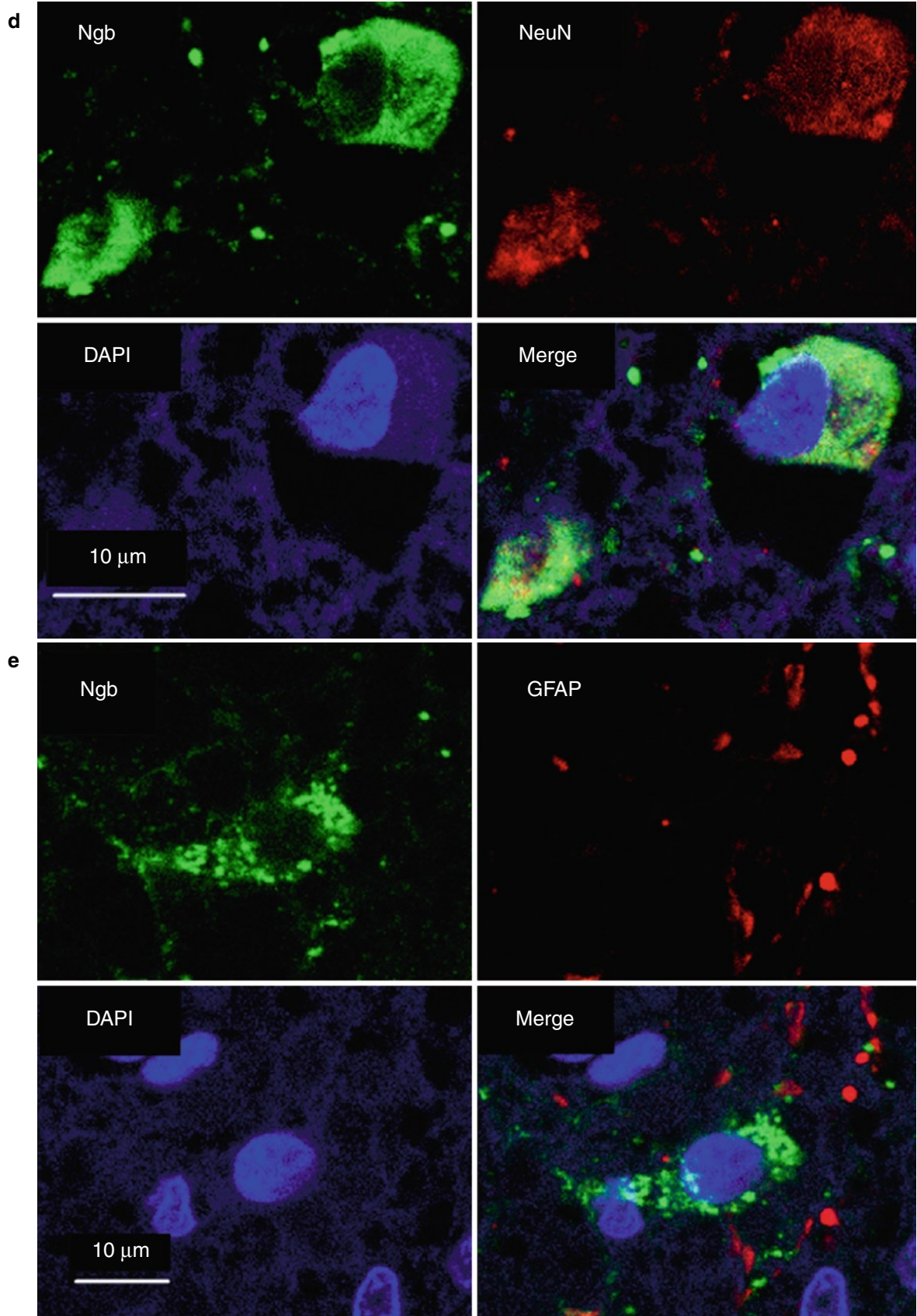


Fig. 1 (continued)

ICH-induced overexpression of Ngb helps to mitigate the resulting tissue injury and dysfunction.

Acknowledgments Supported by USPHS grant NS62040 to David A. Greenberg.

Conflict of interest statement We declare that we have no conflict of interest.

References

- Linn J, Bruckmann H (2009) Differential diagnosis of nontraumatic intracerebral hemorrhage. *Klin Neuroradiol* 19:45–61
- Elijovich L, Patel PV, Hemphill JC 3rd (2008) Intracerebral hemorrhage. *Semin Neurol* 28:657–667
- Leblanc GG, Golanov E, Awad IA, Young WL (2009) Biology of vascular malformations of the brain. *Stroke* 40:e694–e702
- Anderson CS (2009) Medical management of acute intracerebral hemorrhage. *Curr Opin Crit Care* 15:93–98
- Rincon F, Mayer SA (2010) Intracerebral hemorrhage: getting ready for effective treatments. *Curr Opin Neurol* 23:59–64
- ZhuGe Q, Zhong M, Zheng W, Yang GY, Mao X, Xie L, Chen G, Chen Y, Lawton MT, Young WL, Greenberg DA, Jin K (2009) Notch-1 signalling is activated in brain arteriovenous malformations in humans. *Brain* 132:3231–3241
- Jin K, Wang X, Xie L, Mao XO, Zhu W, Wang Y, Shen J, Mao Y, Banwait S, Greenberg DA (2006) Evidence for stroke-induced neurogenesis in the human brain. *Proc Natl Acad Sci USA* 103:13198–13202
- Shen J, Xie L, Mao X, Zhou Y, Zhan R, Greenberg DA, Jin K (2008) Neurogenesis after primary intracerebral hemorrhage in adult human brain. *J Cereb Blood Flow Metab* 28:1460–1468
- Jin K, Wang X, Xie L, Mao XO, Greenberg DA (2010) Transgenic ablation of doublecortin-expressing cells suppresses adult neurogenesis and worsens stroke outcome in mice. *Proc Natl Acad Sci USA* 107(17):7993–8
- Burmester T, Weich B, Reinhardt S, Hankeln T (2000) A vertebrate globin expressed in the brain. *Nature* 407:520–523
- Sun Y, Jin K, Mao XO, Zhu Y, Greenberg DA (2001) Neuroglobin is upregulated by and protects neurons from hypoxic-ischemic injury. *Proc Natl Acad Sci USA* 98:15306–15311
- Khan AA, Wang Y, Sun Y, Mao XO, Xie L, Miles E, Graboski J, Chen S, Ellerby LM, Jin K, Greenberg DA (2006) Neuroglobin-overexpressing transgenic mice are resistant to cerebral and myocardial ischemia. *Proc Natl Acad Sci USA* 103:17944–17948
- Sun Y, Jin K, Mao XO, Zhu Y, Greenberg DA (2003) Neuroglobin protects the brain from experimental stroke in vivo. *Proc Natl Acad Sci USA* 100:3497–3500
- Jin K, Mao Y, Mao X, Xie L, Greenberg DA (2010) Neuroglobin expression in ischemic stroke. *Stroke* 41:557–559
- Challa VR, Moody DM, Brown WR (1995) Vascular malformations of the central nervous system. *J Neuropathol Exp Neurol* 54:609–621
- Sonstein WJ, Kader A, Michelsen WJ, Llena JF, Hirano A, Casper D (1996) Expression of vascular endothelial growth factor in pediatric and adult cerebral arteriovenous malformations: an immunocytochemical study. *J Neurosurg* 85:838–845
- Jiang Y, Wu J, Keep RF, Hua Y, Hoff JT, Xi G (2002) Hypoxia-inducible factor-1 α accumulation in the brain after experimental intracerebral hemorrhage. *J Cereb Blood Flow Metab* 22:689–696
- Pascual AM, Lopez-Mut JV, Benlloch V, Chamarro R, Soler J, Lainez MJ (2007) Perfusion-weighted magnetic resonance imaging in acute intracerebral hemorrhage at baseline and during the 1st and 2nd week: a longitudinal study. *Cerebrovasc Dis* 23:6–13
- Schellinger PD, Fiebich JB, Hoffmann K, Becker K, Orakcioglu B, Kollmar R, Juttler E, Schramm P, Schwab S, Sartor K, Hacke W (2003) Stroke MRI in intracerebral hemorrhage: is there a perihemorrhagic penumbra? *Stroke* 34:1674–1679
- Warach S (2003) Editorial comment – Is there a perihematomal ischemic penumbra? More questions and an overlooked clue. *Stroke* 34:1680
- Kim-Han JS, Kopp SJ, Dugan LL, Dinger MN (2006) Perihematomal mitochondrial dysfunction after intracerebral hemorrhage. *Stroke* 37:2457–2462
- Nakamura T, Keep RF, Hua Y, Nagao S, Hoff JT, Xi G (2006) Iron-induced oxidative brain injury after experimental intracerebral hemorrhage. *Acta Neurochir Suppl* 96:194–198

Intracerebral Hemorrhage and Meteorological Factors in Chongqing, in the Southwest of China

Xin Li, John H. Zhang, and Xinyue Qin

Abstract Studies have reported the relationship between intracerebral hemorrhage (ICH) and meteorological factors. However, few of those study analyses were dependent on daily meteorological factors. The aim of this study is to evaluate the relationship between various meteorological data and ICH cases from Chongqing, in the southwest of China. One thousand nineteen intracerebral hemorrhage events registered in our hospital were recorded from 1 January 2006 to 30 August 2009. Meteorological parameters were analyzed, including season, month, air temperature, humidity, atmospheric pressure, visibility, presence of fog, and wind velocity. The chi-square test for goodness of fit was used for statistical evaluations. Significant differences in seasonal and monthly patterns of ICH onset were observed. The incidence of ICH attack was highest in winter and lowest in summer ($p < 0.0001$). The monthly variation was consistent with the above pattern ($p = 0.002$). Daily air temperature ($p < 0.0001$), humidity ($p = 0.002$), and atmospheric pressure ($p < 0.0001$) were associated with the admission rate. However, no significant relationships were found between visibility ($p = 0.62$), presence of fog ($p = 0.32$), or wind velocity ($P = 0.5$) and the

risk of ICH. Our study demonstrates that the incidence of ICH is closely related to some meteorological factors, such as season, daily air temperature, humidity, and atmospheric pressure.

Keywords ICH · Meteorological factors · Seasons · Weather

Introduction

The relationship between intracerebral hemorrhage (ICH) and the weather have been reported in recent decades. In those studies, the most recognized conclusion was that ICH has a significant association with low temperature [1–5], whereas other studies did not reach this conclusion [6–8]. Most of this research depended on monthly data. Besides temperature, some other meteorological factors, such as humidity, atmospheric pressure, visibility, wind velocity, and fog, may affect humans' physiological functions independently and be associated with onset of some diseases [9–12]. Few studies have shown that air pressure is associated with cerebrovascular disease; the relationship between those meteorological factors and ICH is still limited. Among the studies, seasonal and monthly variations have been analyzed intensively, though few reports focused on daily meteorological data [3, 4].

The published studies were mainly from America, Europe, Japan, and other countries. Our study was focused on the inland areas of China. The 1,019 patients with ICH came from Chongqing, in the southwest of China. Patients with ICH in Chongqing were analyzed based on daily meteorological parameters to evaluate the seasonal and monthly variations in the onset of ICH and the relationship between ICH and meteorological factors.

X. Li

Department of Neurology, The First Affiliated Hospital of Chongqing Medical University, Chongqing, China

J.H. Zhang

Department of Neurosurgery, Loma Linda University, School of Medicine, Loma Linda, CA, USA

X. Qin (✉)

Department of Neurology, The First Affiliated Hospital of Chongqing Medical University, Chongqing, China and
Department of Neurology, The First Affiliated Hospital of Chongqing Medical University, Chongqing 400016, China
e-mail: qinxinyue@yahoo.com

Materials and Methods

Patient Population

A total of 1,019 patients with ICH were admitted to the Departments of Neurology and Neurosurgery, and the Intensive Care Unit of the First Affiliated Hospital, Chongqing Medical University, between January 2006 and August 2009. The diagnosis of ICH was based on computed tomography (CT).

Seasons

The seasons were defined based on local climatology: winter (December to February), spring (March to May), summer (June to August), and autumn (September to November).

Meteorological Data

The meteorological data from January 2006 to August 2009 were obtained from Weather Underground (<http://www.wunderground.com/>), providing daily mean temperature (°C), daily mean humidity (%), atmospheric pressure (hPa), visibility (km), wind speed (km/h), and events (presence of fog).

Statistical Analysis

A one-way chi-square test for goodness of fit was applied to compare whether the number of events differed significantly in each time period and various weather conditions.

Distributions of ICH onset were tested for uniformity, with an assumption that season, month, and meteorological factors had no effects. The observed events of ICH (O) were compared with the expected values (E). The relative risk of ICH onset in specific times or various weather conditions was evaluated by O/E. $P < 0.05$ was considered statistically significant. Data analysis was performed with SPSS 16.0.

Results

Population characteristics of the patients are shown in Table 1.

The study comprised 1,019 patients; 669 were men and 350 women; age ranged from 3 to 108 years. In all six age groups, the numbers of ICHs in men were higher than in women. The mean age of women at onset was significantly higher than that of men with ICH. However, the numbers of ICH events significantly increased after age 50 in both men and women.

Seasons

All ICH patients were unevenly distributed throughout the four seasons ($P < 0.0001$), as shown in Table 2. The onset of ICH was significantly higher in winter (O/E = 1.23) than in spring and autumn. The lowest number of ICHs occurred in summer (O/E = 0.76). Table 3 shows the distribution of ICH across 12 months, and demonstrates that it was uneven and corresponded with the season distribution. Most onsets of ICH (O/E = 1.34) occurred in December, and the fewest (O/E = 0.67) in August. We analyzed 859 ICH patients in this part, with all cases from 2006 to 2008.

Table 1 Characteristics of the ICH patients ($n = 1,019$)

	Sample	Age						Mean age
		<30	30–40	41–50	51–60	61–70	>70	
Male	669	22	49	96	191	144	167	51.19 ± 14.81
Female	350	12	16	51	97	73	101	60.79 ± 15.28

Table 2 Evaluation of ICH by season

	Spring	Summer	Autumn	Winter	χ^2	p
ICH $n = 859$					23.93	2.59E-05
Observed	213	164	219	263		
Expected	212.40	216.32	216.32	213.97		
O/E	1.00	0.76	1.01	1.23		

A χ^2 test for goodness of fit was used for evaluations

E means expected values, in chi square test, if null hypothesis was accepted, the theoretical frequency would recorded as expected values. In this study, the null hypothesis is that the cases in difference meteorological factors is equal.

Temperature

There was a tendency for ICH to occur more frequently at a low mean temperature. When the mean temperature was lower than 8 °C, ICH occurred more frequently, and when the mean temperature was higher than 24 °C, it occurred at a lower frequency. The highest frequency occurred at very low temperatures (mean temperature <4 °C O/E=1.71), and the lowest frequency occurred at very high mean temperatures (mean temperature >32 °C, O/E=0.17), as shown in Table 4.

Relative Humidity and Air Pressure

Table 5 shows ICH in relation to daily relative humidity. There was a statistically significant uneven distribution. Although there was no clear pattern, one thing we could assume was that when humidity was more than 75%, humidity was a negative factor in relation to ICH.

The relationship between ICH and daily air pressure is shown in Table 6. There is a tendency for the onset of ICH to occur more frequently than expected at higher mean air pressures. The highest frequency occurred at 1,028–1,030 hPa (O/E=1.86).

Visibility, Wind, and Fog

There was no statistically significant difference between occurrence of ICH and visibility (Table 7), wind (Table 8), or fog, (Table 9) (p>0.05).

Discussion

Firstly, our study showed a significant seasonal variation in the incidence of ICH in that a characteristic winter peak and a lowest point in summer were observed. The monthly variation

Table 3 Evaluation of ICH by month

	Month												χ^2	p
	Jan	Feb	Mar	Apr	May	Jun	Jul	Aug	Sep	Oct	Nov	Dec		
ICH n = 859													29.45	0.002
Observed	91	74	68	73	72	57	58	49	68	83	68	98		
Expected	72.89	66.62	72.89	70.54	72.89	70.54	72.89	72.89	70.54	72.89	70.54	72.89		
O/E	1.25	1.11	0.93	1.03	0.99	0.81	0.80	0.67	0.96	1.14	0.96	1.34		

A χ^2 test for goodness of fit was used for evaluations

Table 4 Evaluation of ICH by daily mean temperature

	Temperature, °C										χ^2	p
	0–3	4–7	8–11	12–15	16–19	20–23	24–27	28–31	>32			
ICH n = 1,019											63.27	1.06E-10
Observed	39	148	147	136	117	217	120	79	4			
Expected	22.83	105.02	148.40	127.85	111.87	213.08	157.53	108.82	23.59			
O/E	1.71	1.12	0.99	1.06	1.05	1.02	0.76	0.73	0.17			

A χ^2 test for goodness of fit was used for evaluations

Table 5 Evaluation of ICH by daily mean humidity

	Humidity, %										χ^2	p
	<45	45–50	51–56	57–62	63–68	69–74	75–80	81–86	87–92	>92		
ICH n=1019											26.04	0.002
Observed	6	20	28	81	93	100	180	217	206	88		
Expected	9.89	17.50	31.96	74.58	96.65	146.11	179.57	211.56	181.88	69.251		
O/E	0.61	1.14	0.88	1.087	0.96	0.68	1.00	1.03	1.13	1.27		

A χ^2 test for goodness of fit was used for evaluations

Table 6 Evaluation of ICH by daily mean sea level pressure

	Sea level pressure (hPa)										χ^2	<i>p</i>
	<1,000	1,000–1,003	1,004–1,007	1,008–1,011	1,012–1,015	1,016–1,019	1,020–1,023	1,024–1,027	1,028–1,031	>1,031		
ICH <i>n</i> = 1019											56.64	0
Observed	12	79	132	149	135	161	142	114	82	13		
Expected	18.26	102.74	178.84	137.74	136.22	152.2	139.26	98.17	44.14	11.42		
O/E	0.66	0.77	0.74	1.08	0.99	1.06	1.02	1.16	1.86	1.14		

A χ^2 test for goodness of fit was used for evaluations

Table 7 Evaluation of ICH by daily visibility

	Visibility (km)													χ^2	<i>p</i>
	0	1	2	3	4	5	6	7	8	9	10	11	–		
ICH <i>n</i> =1019														9.92	0.62
Observed	8	99	183	176	136	146	63	70	30	30	37	23	18		
Expected	7.61	90.56	163.62	177.31	144.59	133.18	74.58	68.49	31.96	35	46.42	25.87	19.79		
O/E	1.05	1.09	1.12	0.99	0.94	1.09	0.84	1.02	0.94	0.86	0.79	0.89	0.91		

A χ^2 test for goodness of fit was used for evaluations

Table 8 Evaluation of ICH by wind

	Wind (km/h)							χ^2	<i>p</i>
	0–2	3–5	6–8	9–11	12–14	15–17	>17		
ICH <i>n</i> =1019								5.37	0.497
Observed	105	451	273	125	46	12	7		
Expected	98.17	459.64	273.96	124.04	46.42	6.85	9.89		
O/E	1.07	0.98	1.00	1.00	0.99	1.75	0.71		

A χ^2 test for goodness of fit was used for evaluations

Table 9 Evaluation of ICH by fog

	Fog	Non-fog	χ^2	<i>p</i>
ICH <i>n</i> = 1,019			0.99	0.32
Observed	295	724		
Expected	280.81	738.17		
O/E	1.05	0.98		

A χ^2 test for goodness of fit was used for evaluations

was consistent with the pattern of seasonal variation, and additionally the onset of ICH was more frequent in colder months, but less in warmer months. These results agreed with most previous studies [8, 13–16], though some other studies have shown no significant seasonal variation [2, 8, 17–19], which may be related to the environments or small sample size of patients.

The explanation of the pattern was usually dependent on air temperature [1, 3, 5, 20]; a significant inverse relationship between temperature and the occurrence of ICH has been reported in many studies based on monthly mean temperature, but few studies were based on daily temperature or pointed out how temperature affected the onset of ICH. Our

study demonstrated that low temperatures, particularly lower than 8°C, were strongly associated with the occurrence of ICH. The interval of daily mean temperature between 8°C and 23°C had no significant effect on the onset of ICH, and extremely high or low temperatures did not enhance the risk of ICH, though they were often reported to result in the death of old people.

An interesting discovery is the relationship between air pressure and the onset of ICH. Based on more intervals of daily mean air pressure and many more ICH cases, we found that high air pressure is a risk factor for ICH. The risk at the high level between 1,028 hPa to 1,031 hPa was three times as great as that at the lowest level of air pressure. The findings on the relation between ICH and air pressure are inconsistent. Capon et al. [17] found no correlation between the onset of ICH and changes in air pressure. Similarly, Ohwaki et al. [21] found that the correlation of ICH with atmospheric pressure was not statistically significant. However, Chen et al. [3] believed that the onset of ICH was approximately twice as great on high-pressure days as that on low-pressure days. Our study corresponds with this pattern.

Although there were some inconsistent conclusions dependent on different statistical methods and local climatic characteristics [4, 6, 7, 22], in the relationship between important meteorological factors and onset of ICH, we found that humidity had an effect on the occurrence of ICH. In the present study, the onset of ICH was significantly different at different intervals ($P=0.002$), and the risk strongly increased when the humidity was high. The effect of humidity on the onset of ICH is not as intense as the effect of temperature and air pressure; it seems to be a mild factor among meteorological influence, but it does have an effect on occurrence of ICH.

The biological reasons for how weather affects the higher occurrence of ICH are not clear, but elevated blood pressure may be the trigger for ICH. Blood pressure has a seasonal variation that is well known [23–25], and air pressure is associated with blood pressure. Some studies suggested another mechanism to explain this phenomenon, such as platelets, red cell count, blood viscosity, and so on [26–28], but they may be not the key reasons in terms of stroke risk.

In conclusion, marked differences in seasonal and monthly patterns of ICH onset were found, and our study strongly suggests that temperature, air pressure, and humidity variation were significantly associated with the onset of ICH in Chongqing, China.

Conflict of interest statement We declare that we have no conflict of interest.

References

- Anlar O, Tombul T, Unal O, Kayan M (2002) Seasonal and environmental temperature variation in the occurrence of ischemic strokes and intracerebral hemorrhages in a Turkish adult population. *Int J Neurosci* 112:959–963
- Biller J, Jones MP, Bruno A, Adams HP Jr, Banwart K (1988) Seasonal variation of stroke—does it exist? *Neuroepidemiology* 7:89–98
- Chen ZY, Chang SF, Su CL (1995) Weather and stroke in a subtropical area: Ilan, Taiwan. *Stroke* 26:569–572
- Nakaguchi H, Matsuno A, Teraoka A (2008) Prediction of the incidence of spontaneous intracerebral hemorrhage from meteorological data. *Int J Biometeorol* 52:323–329
- Passero S, Reale F, Ciacci G, Zei E (2000) Differing temporal patterns of onset in subgroups of patients with intracerebral hemorrhage. *Stroke* 31:1538–1544
- Feigin VL, Nikitin YP, Bots ML, Vinogradova TE, Grobbee DE (2000) A population-based study of the associations of stroke occurrence with weather parameters in Siberia, Russia (1982–92). *Eur J Neurol* 7:171–178
- Field TS, Hill MD (2002) Weather, Chinook, and stroke occurrence. *Stroke* 33:1751–1757
- Rothwell PM, Wroe SJ, Slattery J, Warlow CP (1996) Is stroke incidence related to season or temperature? The Oxfordshire Community Stroke Project. *Lancet* 347:934–936
- Gloster J, Champion HJ, Mansley LM, Romero P, Brough T, Ramirez A (2005) The 2001 epidemic of foot-and-mouth disease in the United Kingdom: epidemiological and meteorological case studies. *Vet Rec* 156:793–803
- Nacher M, Couppie P, Carne B, Clyti E, Sainte Marie D, Guibert P, Pradinaud R (2002) Influence of meteorological parameters on the clinical presentation of cutaneous leishmaniasis in French Guiana and on the efficacy of pentamidine treatment of the disease. *Ann Trop Med Parasitol* 96:773–780
- O'Toole TE, Conklin DJ, Bhatnagar A (2008) Environmental risk factors for heart disease. *Rev Environ Health* 23:167–202
- Ricketts KD, Charlett A, Gelb D, Lane C, Lee JV, Joseph CA (2009) Weather patterns and Legionnaires' disease: a meteorological study. *Epidemiol Infect* 137:1003–1012
- Caicoya M, Rodriguez T, Lasheras C, Cuello R, Corrales C, Blazquez B (1996) Stroke incidence in Asturias, 1990–1991. *Rev Neurol* 24:806–811
- Inagawa T (2003) Diurnal and seasonal variations in the onset of primary intracerebral hemorrhage in individuals living in Izumo City, Japan. *J Neurosurg* 98:326–336
- Jakovljevic D, Salomaa V, Sivenius J, Tamminen M, Sarti C, Salmi K, Kaarsalo E, Narva V, Immonen-Raiha P, Torppa J, Tuomilehto J (1996) Seasonal variation in the occurrence of stroke in a Finnish adult population. The FINMONICA Stroke Register. Finnish Monitoring Trends and Determinants in Cardiovascular Disease. *Stroke* 27:1774–1779
- Wang H, Sekine M, Chen X, Kagamimori S (2002) A study of weekly and seasonal variation of stroke onset. *Int J Biometeorol* 47:13–20
- Capon A, Demeurisse G, Zheng L (1992) Seasonal variation of cerebral hemorrhage in 236 consecutive cases in Brussels. *Stroke* 23:24–27
- Khan FA, Engstrom G, Jerntorp I, Pessah-Rasmussen H, Janzon L (2005) Seasonal patterns of incidence and case fatality of stroke in Malmo, Sweden: the stroma study. *Neuroepidemiology* 24:26–31
- Sobel E, Zhang ZX, Alter M, Lai SM, Davanipour Z, Friday G, McCoy R, Isack T, Levitt L (1987) Stroke in the Lehigh Valley: seasonal variation in incidence rates. *Stroke* 18:38–42
- Shinkawa A, Ueda K, Hasuo Y, Kiyohara Y, Fujishima M (1990) Seasonal variation in stroke incidence in Hisayama, Japan. *Stroke* 21:1262–1267
- Ohwaki K, Yano E, Murakami H, Nagashima H, Nakagomi T (2004) Meteorological factors and the onset of hypertensive intracerebral hemorrhage. *Int J Biometeorol* 49:86–90
- Wang XY, Barnett AG, Hu W, Tong S (2009) Temperature variation and emergency hospital admissions for stroke in Brisbane, Australia. *Int J Biometeorol* 53(6):535–41
- Charach G, Rabinovich PD, Weintraub M (2004) Seasonal changes in blood pressure and frequency of related complications in elderly Israeli patients with essential hypertension. *Gerontology* 50:315–321
- Choi JH, Xu QS, Park SY, Kim JH, Hwang SS, Lee KH, Lee HJ, Hong YC (2007) Seasonal variation of effect of air pollution on blood pressure. *J Epidemiol Community Health* 61:314–318
- Frohlich ED (2004) Seasonal variations in blood pressure. *Am J Geriatr Cardiol* 13:274–275
- Crawford VL, McNerlan SE, Stout RW (2003) Seasonal changes in platelets, fibrinogen and factor VII in elderly people. *Age Ageing* 32:661–665
- Gill J (1989) Seasonal changes in the red blood cell system in the European bison, *Bison bonasus* L. *Comp Biochem Physiol A Comp Physiol* 92:291–298
- Stout RW, Crawford V (1991) Seasonal variations in fibrinogen concentrations among elderly people. *Lancet* 338:9–13

Timing Pattern of Onset in Hypertensive Intracerebral Hemorrhage Patients

Jinzhou Feng, John H. Zhang, and Xinyue Qin

Abstract The temporal pattern of onset of hypertensive intracerebral hemorrhage (ICH) has been evaluated in previous reports, but there are few published data on this pattern in Chongqing, China. The purpose of this study is to explore the temporal pattern of diurnal, weekly and monthly variations in the onset of hypertensive ICH from a hospital-based population. The study retrospectively reviewed 230 residents who suffered from hypertensive ICH between January 2008 and August 2009 in our hospital. The temporal pattern was investigated by hours, days and months. Chi-square test for goodness of fit was used for statistical analysis. Significant differences of the onset time of hypertensive ICH patients could be seen in diurnal variation ($p=0.000$) and in monthly variation ($p=0.000$), but could not be found in weekly variation ($p=0.466$). There was a bimodal distribution in diurnal variation, and monthly variation showed that the occurrence of hypertensive ICH mainly focuses on the period from December to May. Our study demonstrated the existence of diurnal and monthly variations and no significant weekly variation can be found in the time of onset of hypertensive ICH.

Keywords Hypertensive ICH · Temporal pattern · Diurnal · Weekly · Monthly · Onset

Introduction

The onset of ICH shows chronobiological variations, including diurnal variation, weekly variation and seasonal variation. In the past decades, time variation in the onset of ICH has been extensively evaluated in many community- and hospital-based studies [1–9]. But the conclusions derived from those studies are not all the same.

Hypertension is a recognized factor in the etiology of ICH [9], and blood pressure is the most significant risk factor for ICH [7]. Hypertensive ICH is the most common type of spontaneous intracerebral hemorrhage. Proof of a temporal pattern in the occurrence of hypertensive ICH may provide helpful clues to its pathogenesis, rational treatment or swift prevention. As far as we know, little research has been performed in order to evaluate the temporal pattern in the onset of hypertensive ICH patients in Chongqing, China. This study aimed to conduct diurnal, weekly and monthly variations in the onset of hypertensive ICH by using hospital-based data. It may reveal some regulation of the onset of ICH and help physicians and patients to know the clinical characteristics of this disease.

Materials and Methods

A total of 230 available cases were registered during the study period from January 2008 to August 2009 in our hospital. The time of the first known sign or symptom, such as vertigo, vomiting, headache or coma and so on, was defined as the onset time, and it was reported by the patients themselves or the person discovering the events. The average age of all patients was 62.4 ± 13.2 years (range 31–98 years). Among them, 149 patients were men (61.1 ± 12.9 years, range 36–95 years), and 81 were women (64.8 ± 13.5 years, range 40–98 years). Fifteen patients could not report the precise time of onset because they were found unconscious or because they could not remember the symptom of onset.

J. Feng and X. Qin (✉)
Department of Neurology, The First Affiliated Hospital of Chongqing Medical University, Chongqing, 400016, China
e-mail: qinxinyue@yahoo.com

J.H. Zhang
Department of Physiology and Pharmacology,
Department of Neurosurgery, Department of Anesthesiology,
Loma Linda University, School of Medicine, Loma Linda, CA, USA

Diagnosis of hypertensive ICH was based on hypertension history, clinical symptoms and neurological imaging examination. All of the patients were given a routine neurological imaging examination by CT or MRI. ICH caused by head trauma, brain tumor, aneurysms, arteriovenous malformations, moyamoya disease, cavernous hemangioma, hemorrhagic transformation of a previous cerebral infraction, severe bleeding tendency or coagulation disorder was not covered in this study.

The date of the time of onset was classified according to hours and day of the week and month, and 24 h in a day was divided into 12 2-h intervals for analysis (0:00~1:59, 2:00~3:59,...22:00~23:59).

The chi-square test for goodness of fit was used to evaluate the patterns of variation by examining the null hypothesis that the frequency of the time of onset was evenly distributed across the 12 2-h intervals, or 7 days in a week or 12 months in a year. Furthermore, data were analyzed with the chi-square test in order to determine whether there was a significant gender difference in the frequency distribution. Statistical analysis was processed by SPSS 13.0 for Windows. A statistically significant probability value was defined as $P < 0.05$.

Results

Diurnal Variation

The distribution of hypertensive ICH patients according to 12 2-h intervals in a day is shown in Table 1. The null hypothesis of assumed uniform frequency distribution of the time of onset was rejected ($X^2 = 68.86, p = 0.000$). No significant difference was found in the frequency distribution between men and women ($X^2 = 7.450, p = 0.762$). The frequency distribution of the onset of hypertensive ICH presented a bimodal distribution with two peak times: a slightly higher peak between 10 a.m. and 12 a.m., and a relatively lower peak between 6 p.m. and 8 p.m. From midnight to 6 a.m. is the lowest time of hypertensive ICH onset (Fig. 1).

Weekly Variation

The distribution of hypertensive ICH patients according to 7 days in a week is shown in Table 2. The null hypothesis of

Table 1 Distribution of hypertensive ICH by 2-h time intervals

	12 2-h Time intervals												χ^2	p	
	1	2	3	4	5	6	7	8	9	10	11	12			T
M	3	3	9	11	14	24	12	8	23	11	9	9	136	7.450	0.762
W	1	0	2	9	10	14	5	8	12	6	6	6	79		
T	4	3	11	20	24	38	17	16	35	17	15	15	215		

Numbers 1–12 under the words 2-h time intervals stand for the time periods 0:00–1:59; 2:00–3:59;...22:00–23:59 accordingly

Chi-square test was used to determine whether there was a significant difference between male and female groups

Chi-square test for goodness of fit was used to evaluate the pattern of diurnal variation in total patients

M men, W women, T total patients

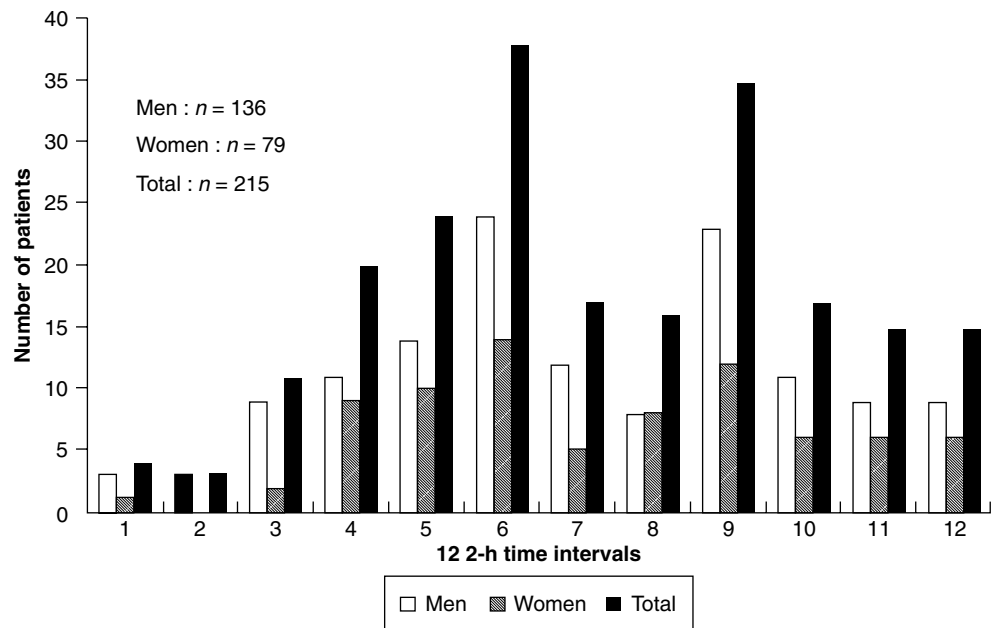


Fig. 1 Frequency distribution of hypertensive ICH by 12 2-h time intervals. Bar graph presenting a bimodal pattern in diurnal variation, with peak times between 10 a.m. and 12 a.m. and a second one between 6 p.m. and 8 p.m. The lowest time of onset was midnight to 6 a.m.

assumed uniform frequency of onset time was accepted ($X^2=5.625, p=0.466$). No significant difference in frequency distribution was found between men and women ($X^2=8.074, p=0.233$).

Monthly Variation

The frequency distribution of hypertensive ICH patients according to 12 months in a year is shown in Table 3. The frequency distribution for the time of onset over 12 months showed a significant difference ($X^2=40.574, p=0.000$). The occurrence of hypertensive ICH was mainly focused on the period from December to May (Fig. 2). The chi-square test had a result of $P=0.483$, suggesting no significant difference between men and women.

Discussion

The temporal pattern of the onset of ICH has been extensively investigated in many previous studies, however, sometimes differences existed in the results they demonstrated. This phenomenon may result from clinical, methodological, environmental and statistical factors [7], and very few studies can obtain all data at the same time [5]. In this study, we evaluated the diurnal, weekly and monthly variations in the time of onset of hypertensive ICH by evaluating 230 resident cases in our hospital. In order to reduce the influencing

factors and obtain accurate conclusions, hypertensive ICH was exclusively chosen from all kinds of ICH.

Among previous studies on diurnal variation, some have reported a bimodal pattern in the occurrence of ICH [6, 8, 10, 11], with one peak time in the morning and a smaller one in the afternoon or evening. Others demonstrated that there was only one peak time during the morning [3, 7]. We also found a bimodal pattern in diurnal variation, with a peak time between 10 a.m. and 12 a.m. and a second one between 6 p.m. and 8 p.m. The lowest time of onset lay in the interval from midnight to 6 a.m. This diurnal variation may mainly relate to the circadian pattern of blood pressure, which was demonstrated by Degaute et al. [12]. According to them, the typical blood pressure and heart rate patterns were bimodal, with a morning peak (around 10 a.m.), a small afternoon nadir (around 3 p.m.) and an evening peak (around 8 p.m.), and a profound nocturnal nadir (around 3 a.m.). In addition, the two peak times are during very busy times of the day, when people may encounter more stressful events and physical activities. As is well known, stressful events and physical activities can lead to a prompt and substantial increase in BP, and these factors may act on the occurrence of hypertensive ICH through the effect on BP. Fasting plasma glucose levels and glycemc abnormalities were also significant factors in the morning and waking blood pressure summit [13]. Some researchers found that hypertensive status, smoking, drinking and diabetes had no effect on the time variation of stroke onset [8], whereas others hold the opposite opinion [7].

Only a few studies have evaluated the weekly variation of ICH onset. Kelly-Hayes et al. [14] reported that more ICH

Table 2 Distribution of hypertensive ICH by week

	Week								χ^2	P
	Mon	Tue	Wen	Thu	Fri	Sat	Sun	T		
M	17	28	27	24	18	21	14	149	8.074	0.233
W	9	12	9	15	14	7	15	81		
T	26	40	36	39	32	28	29	230	5.625	0.466

Chi-square test was used to determine whether there was a significant difference between male and female groups

Chi-square test for goodness of fit was used to evaluate the pattern of weekly variation in total patients

M men, W women, T total patients

Table 3 Distribution of hypertensive ICH by month

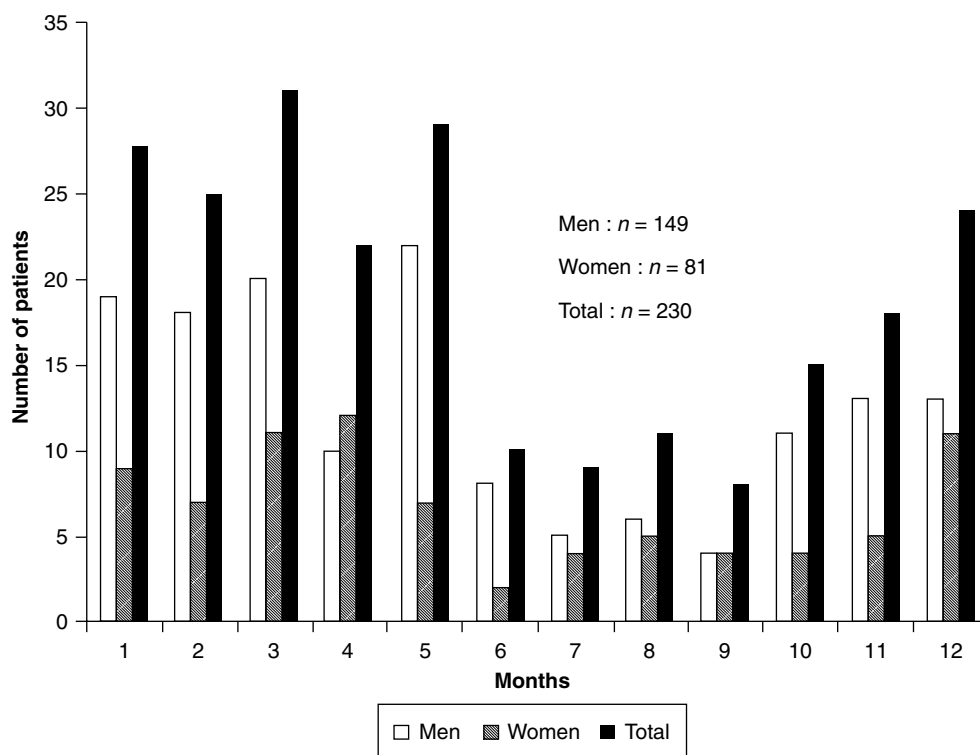
	Month												χ^2	P	
	1	2	3	4	5	6	7	8	9	10	11	12			T
M	19	18	20	10	22	8	5	6	4	11	13	13	149	10.538	0.483
W	9	7	11	12	7	2	4	5	4	4	5	11	81		
T	28	25	31	22	29	10	9	11	8	15	18	24	230	40.574	0.000

Chi-square test was used to determine whether there was a significant difference between male and female groups

Chi-square test for goodness of fit was used to evaluate the pattern of monthly variation in total patients

M men, W women, T total patients

Fig. 2 Frequency distribution of hypertensive ICH by month. *Bar graph* presenting a monthly variation with a peak in December to May, which is the period of winter and spring



events occurred on Mondays than on any other days, whereas Wang et al. [9] demonstrated a more frequent incidence on weekdays than weekends. In this study, we could not find any weekly variations in the total population, and this result conforms to the conclusion reported by Passero et al. [7]. Reasons for weekly variation in ICH onset are not well understood. Willich et al. [15] hypothesized that external factors, such as sudden changes in physical and mental activity in the transition from the weekend to workdays, may trigger vascular events. Stress concerning returning to work after the weekend might cause changes in physiological parameters such as blood pressure and give rise to the incidence of ICH [7]. No significant variation could be found in our study, perhaps because Chongqing is a leisure city with a slow life tempo, and inconspicuous stress changes could be found from weekend to weekdays. On other hand, the number of study patients may not be large enough.

Considering monthly variation, most studies prefer to investigate seasonal variation instead. In the great majority of studies, the occurrences of ICH mainly focused on the winter months [4, 7, 9], but some others reported that the peak incidence occurred in the autumn [16] or April [17], or that no significant seasonal variation was found [14, 18]. In our study, we demonstrated a monthly variation with a peak in December to May. In other words, it is the period of winter and spring. This result is basically consistent with those from previous reports. It has been documented that exposure to cold causes peripheral constriction and an increase in blood

pressure [19], and temperature variation in a year may cause a seasonal variation of BP, with the highest levels in winter and the lowest in summer [20, 21]. As a consequence, elevated blood pressure during cold days maybe an important trigger of ICH. According to Passero et al. [7], an acute cold-induced rise in BP is probably a much more significant precipitating factor of bleeding than seasonal variations in BP. People who are more often exposed to cold environments in winter are more likely to have ICH. The inverse relationship between ambient temperature and the occurrence of ICH turned out to be the most constant finding, but other factors, such as hours of sunshine, humidity, atmospheric pressure, rainfall and windchill, were also involved [1]. The climate during winter and spring in Chongqing is cold, rainy and humid, while summer days are very hot. This could be the main reason why the occurrence of hypertensive ICH largely took place in winter and spring.

In summary, we observed temporal patterns of diurnal and monthly variations in the occurrence of hypertensive ICH in a hospital-based population. No significant weekly variation was found. These findings suggest that there are periods of increased risk of hypertensive ICH that may be useful for therapeutic and preventive strategies. BP change may be one of the most substantial factors in the temporal pattern, but temporal variability may be affected by a complex combination of pathophysiological changes, environmental factors, gender, aging and so on. Other risk factors should be considered in further study.

Conflict of interest statement We declare that we have no conflict of interest.

References

1. Capon A, Demeurisse G, Zheng L (1992) Seasonal variation of cerebral hemorrhage in 236 consecutive cases in Brussels. *Stroke* 23:24–27
2. Foerch C, Korf HW, Steinmetz H, Sitzer M (2008) Arbeitsgruppe Schlaganfall Hessen: Abrupt shift of the pattern of diurnal variation in stroke onset with daylight saving time transitions. *Circulation* 118:284–290
3. Gallerani M, Manfredini R, Ricci L et al (1993) Chronobiological aspects of acute cerebrovascular diseases. *Acta Neurol Scand* 87: 482–487
4. Gallerani M, Trappella G, Manfredini R et al (1994) Acute intracerebral hemorrhage: circadian and circannual patterns of onset. *Acta Neurol Scand* 89:280–286
5. Inagawa T, Takechi A, Yahara K et al (2000) Primary intracerebral and aneurysmal subarachnoid hemorrhage in Izumo City, Japan. Part I: Incidence and seasonal and diurnal variations. *J Neurosurg* 93:958–966
6. Omama S, Yoshida Y, Ogawa A, Onoda T, Okayama A (2006) Differences in circadian variation of cerebral infarction, intracerebral haemorrhage and subarachnoid hemorrhage by situation at onset. *J Neurol Neurosurg Psychiatry* 77:1345–1349
7. Passero S, Reale F, Ciacci G et al (2000) Differing temporal patterns of onset in subgroups of patients with intracerebral hemorrhage. *Stroke* 31:1538–1544
8. Turin TC, Kita Y, Rumana N et al (2009) Diurnal variation in onset of hemorrhagic stroke is independent of risk factor status: Takashima Stroke Registry. *Neuroepidemiology* 34(1):25–33
9. Wang H, Sekine M, Chen X, Kagamimori S (2002) A study of weekly and seasonal variation of stroke onset. *Int J Biometeorol* 47(1):13–20
10. Spengos K, Vemmos KN, Tsvigoulis G, Synetos A et al (2003) Two-peak temporal distribution of stroke onset in Greek patients: a hospital-based study. *Cerebrovasc Dis* 15:70–77
11. Stergiou GS, Vemmos KN, Pliarchopoulou KM et al (2002) Parallel morning and evening surge in stroke onset, blood pressure, and physical activity. *Stroke* 33:1480–1486
12. Degaute JP, van de Borne P, Linkowski P et al (1991) Quantitative analysis of the 24-hour blood pressure and heart rate patterns in youngmen. *Hypertension* 18:199–210
13. Shimizu M, Ishikawa J, Eguchi K et al (2009) Association of an abnormal blood glucose level and morning blood pressure surge in elderly subjects with hypertension. *Am J Hypertens* 22:611–616
14. Kelly-Hayes M, Wolf PA, Kase CS et al (1995) Temporal patterns of stroke onset: the Framingham study. *Stroke* 26:1343–1347
15. Willich SM, LoÈwel H, Lewis M, HoÈrmann A, Arntz H-R, Keil U (1994) Weekly variation of acute myocardial infarction: increased Monday risk in the working population. *Circulation* 90:87–93
16. Ricci S, Celani MG, Vitali R et al (1992) Diurnal and seasonal variations in the occurrence of stroke: a community-based study. *Neuroepidemiology* 11:59–64
17. Rosenow F, Hojer C, Meyer-Lohmann C et al (1997) Spontaneous intracerebral hemorrhage. Prognostic factors in 896 cases. *Acta Neurol Scand* 96:174–182
18. Rothwell PM, Wroe SJ, Slattery J, Warlow CP (1996) on behalf of the Oxfordshire Community Stroke Project. Is stroke related to season or temperature? *Lancet* 347:934–936
19. Minami J, Kawano Y, Ishimitsu T, Yoshimi H, Takishita S (1996) Seasonal variations in office, home and 24 h ambulatory blood pressure in patients with essential hypertension. *J Hypertens* 14: 1421–1425
20. Inagawa T (2003) Diurnal and seasonal variations in the onset of primary intracerebral hemorrhage in individuals living in Izumo City, Japan. *J Neurosurg* 98:326–336
21. Wang Y, Levi CR, Attia JR et al (2003) Seasonal variation in stroke in the Hunter Region, Australia: a 5-Year hospital-based study, 1995–2000. *Stroke* 34:1144–1150

“Weekend Effects” in Patients with Intracerebral Hemorrhage

Fan Jiang, John H. Zhang, and Xinyue Qin

Abstract Studies have shown that weekend admissions are associated with outcomes of patients with different diseases. Our aim is to evaluate the weekend effects in patients with intracerebral hemorrhage (ICH) in our hospital. A retrospective analysis of patients with ICH was performed. Weekend admission was defined as the period from Friday, 6:01 p.m., to Monday, 7:59 a.m. The ICH score was used to evaluate severity on admission. The chi-square goodness-of-fit test was applied to analyze weekly distribution. The rank sum test was conducted to calculate the functional outcomes (modified Rankin scale, MRS), and the mortality was compared by binary logistic regression. Between 2008 and 2009, 313 patients with ICH were included, of which 30% (95/313) were admitted on the weekend. Patients with ICH were equally distributed on weekdays and weekends ($P=0.7123$). Weekend admission was not a statistically significant predictive factor for in-hospital mortality ($P=0.315$) and functional outcomes ($P=0.128$) in patients with ICH. However, a significant correlation was found between the ICH score and the mortality (OR=6.819, 95%CI: 4.323–10.757; $P=0.009$). Our results suggest that compared with weekday admission, weekend admission is not significantly associated with increased short-term mortality and poorer functional outcome among patients hospitalized with ICH.

F. Jiang

Department of Neurology, The First Affiliated Hospital of Chongqing Medical University, Chongqing, China

J.H. Zhang

Department of Physiology and Pharmacology,
Department of Neurosurgery, Department of Anesthesiology,
Loma Linda University, School of Medicine, Loma Linda, CA, USA

X. Qin (✉)

Department of Neurology, The First Affiliated Hospital of Chongqing Medical University, Chongqing, China and
Department of Neurology, The First Affiliated Hospital of Chongqing Medical University, Chongqing 400016, China
e-mail: qinxinyue@yahoo.com

Keywords Intracerebral hemorrhage · Weekend · Mortality · Outcome

Introduction

Prior studies have demonstrated that in-hospital mortality for patients presenting on weekends is higher than for those presenting on weekdays, including cases of heart failure, myocardial infarction, upper gastrointestinal hemorrhage, pulmonary embolism and so on [1–4]. This is known as the “weekend effect” [5, 6]. However, some other literature has shown that there is no statistical difference among the outcomes of patients with some of these diseases [7, 8]. To investigate the theory, we examined the circaseptan variation in fatality and function outcome of patients with intracerebral hemorrhage by day of admission.

Patients and Methods

A retrospective study of all patients with ICH admitted in our hospital (a major teaching hospital) from January 2007 to August 2009 was performed. They were identified by data using the International Classification of Disease, ninth revision, Clinical modification diagnosis code for intracerebral hemorrhage, 431. Patients who were transferred from other hospitals were excluded. The characteristics, including age, sex, comorbid disease, symptoms and complications, were collected.

Criteria for Grouping and Evaluation

Patients were categorized into two groups: weekend admission and weekday admission. Weekend admission was defined as the period from Friday, 6:01 p.m., to Monday, 7:59 a.m.

Weekday admission was defined as the rest of the time. ICH score was performed to evaluate the severity on admission [9]. Functional outcome was measured by the modified Rankin Scale (MRS). Poor functional outcome was defined as MRS 3–6. In-hospital mortality was also calculated.

Statistical Analysis

T test was used to calculate the ICH score variation between two groups. The chi-square goodness-of-fit test was applied to analyze weekly distribution. The functional outcomes (modified Rankin scale, MRS) were tested by the rank sum test method. In-hospital mortality was compared by binary logistic regression and adjusted for ICH score.

Results

This study involved 313 patients with ICH, 30.35% (95/313) of whom were admitted on the weekend. Table 1 shows the baseline characteristics of all the ICH patients on admission. The ICH score indicated no statistically significant difference

between weekday admission and weekend admission groups ($P > 0.05$, Table 2), nor for the incidence of the two groups ($P > 0.05$, Table 3). The rank sum test demonstrated that the function outcome of weekend admission had no significant difference with weekday admission (Table 4). A positive correlation was found between ICH score and in-hospital mortality (OR = 6.819, 95%CI: 4.323–10.757; $P = 0.009$). However, weekend admission was not associated with increased mortality ($P = 0.315$, Table 4).

Discussion

Recently, an analysis was performed including 13,821 patients with ICH using the Agency for Healthcare Research and Quality Health Care Utilization Project Nationwide Inpatient Sample (NIS) data from 1,004 US hospitals across 37 states adjusting for admission severity of illness. They found weekend admission was associated with increased mortality [10]. There have been conflicting reports on the “weekend effect” among patients with ICH in Australia. There were 30,522 chronic obstructive pulmonary disease (COPD), 17,910 acute myocardial infarction, 4,183 acute hip fracture and 1,781 intracerebral hemorrhage patient admissions involved in the

Table 1 Baseline characteristics of ICH patients

ICH (n=313)	–	Weekday admission (n=218)	Weekend admission (n=95)
Age group	<30 years	7 (3.21%)	3 (3.15%)
	30–39 years	8 (3.67%)	5 (5.26%)
	40–49 years	28 (12.84%)	18 (18.94%)
	50–59 years	58 (26.61%)	23 (24.21%)
	60–69 years	52 (23.85%)	20 (21.05%)
	70–79 years	42 (19.27%)	19 (20.00%)
	>80 years	23 (10.55%)	7 (7.37%)
Sex	Female	71 (32.57%)	35 (36.84%)
	Male	147 (67.43%)	60 (63.16%)
Comorbid disease	Hypertension	91 (41.74%)	33 (34.74%)
	Hyperlipidemia	26 (11.93%)	16 (16.84%)
	Diabetes	16 (7.34%)	11 (11.58%)
	Gout	2 (0.92%)	2 (2.11%)
	Fibrillation atrial	4 (1.83%)	0 (0)
	Pulmonary emphysema	2 (0.92%)	1 (1.05%)
	Pulmonary tuberculosis	1 (0.46%)	1 (1.05%)
Coronary heart disease	3 (1.38%)	3 (3.16%)	
ICH score	–	1.18 ± 1.405	1.05 ± 1.266*

* $P > 0.05$ compared with weekday admission

Table 2 Distribution variation between weekend admission and weekday admission

ICH (n=313)	Weekday admission	Weekend admission	X ²	P
–	–	–	0.136	0.712
Observed	218	95	–	–
Expected	221	92*	–	–
O/E	0.99	1.03	–	–

*P>0.05 compared with weekday admission

Table 3 Modified Rankin Scale

Weekday admission (n=218)		Weekend admission (n=95)		P=0.218
MRS	n	MRS	MRS	–
0	51	0	0	–
1	53	1	1	–
2	20	2	2	–
3	25	3	3	–
4	13	4	4	–
5	7	5	5	–
6	49	6	6	–

Table 4 Adjusted risk of in-hospital death associated with weekend admission and ICH score

ICH (n=313)	Weekday admission	Weekend admission	OR	95% CI	P
Percent in-hospital mortality	21.56	17.89	–	–	0.315
ICH score	–	–	6.819	4.323 – 10.757	0.009

retrospective analysis of state-wide administrative data from public hospitals, but a significant weekend effect was only found for acute myocardial infarction [2].

A positive correlation was found between increased mortality and weekend admissions among patients with heart failure, myocardial infarction, upper gastrointestinal hemorrhage and pulmonary embolism [1–4]. However, different results were reported among patients suffering from trauma, tumor, upper gastrointestinal bleeding caused by peptic ulcers, subarachnoid hemorrhage, COPD and so on [2, 7, 8, 11, 12]. Based on these data, we can propose that the “weekend effect” is associated with service provision factors (e.g., access to invasive procedures).

Global mortality was similar in both the weekend and weekday group among patients admitted to the emergency

department from 1999 to 2003 in Spain [13]. The inverse correlations were also found in the pediatric intensive care unit (PICU) and intensive care unit (ICU) [14–17]. These studies were generally consistent in postoperative and non-operative patients. A subgroup analysis indicated a positive correlation between weekend admission and higher adjusted hospital mortality rates in the surgical ICU, but not in the medical or multispecialty ICUs [18]. For patients with myocardial infarction, the difference in mortality at 30 days between the weekend and weekday admission group became insignificant after additional adjustment for invasive cardiac procedures. The result is that higher mortality is associated with lower use of invasive cardiac procedures [19]. The authors [20] suggested that preoperative delay will influence the quality of outcome.

In addition, Albright et al. [21] observed that no significant differences were found in comprehensive stroke centers (CSC) when comparing stroke patients with weekend admission and weekday admission groups. Their results suggested that CSC may ameliorate the “weekend effect” in stroke patients. On the other hand, nosocomial external factors may also influence the “weekend effect.” A study of weekly variation of stroke showed that the onset of stroke was more frequent on weekdays than on weekends [22]. This phenomenon may be associated with changes in lifestyle between working days and the weekend, such as alcohol consumption, smoke, reveling until dawn, etc. Chinese people, especially middle-aged women, enjoy sitting down at the table and playing mah-jong for the whole night without moving much. Onset of stroke during the weekend is associated with longer median delay (11–16 h) rather than onset on a weekday (4–8.5 h) [23]. All these above-mentioned factors may contribute to the “weekend effect.” The difference between these studies could be due to all the data collected from hospitals with stratification of service levels.

Conclusion

Our study found that patients with ICH who were admitted on weekends had the same risk of mortality and disability in our hospital, which is equipped with patient management guidelines and staffed by intensivists on call 24 h. The “weekend effect” was found in many diseases, especially diseases with short time to peak and for which invasive procedures are needed. This phenomenon alerts people to the need to improve medical service quality on the weekends.

Conflict of interest statement We declare that we have no conflict of interest.

References

- Aujesky D, Jiménez D, Mor MK, Geng M, Fine MJ, Ibrahim SA (2009) Weekend versus weekday admission and mortality after acute pulmonary embolism. *Circulation* 119(7):962–968
- Clarke MS, Wills RA, Bowman RV, Zimmerman PV, Fong KM, Coory MD, Yang IA (2010) Exploratory study of the ‘weekend effect’ for acute medical admissions to public hospitals in Queensland, Australia. *Intern Med J* 40(11):777–783, 2009 Oct 7
- Dorn SD, Shah ND, Berg BP, Naessens JM (2010) Effect of weekend hospital admission on gastrointestinal hemorrhage outcomes. *Dig Dis Sci* 55(6):1658–1666, Epub 2009 Aug 12
- Horwich TB, Hernandez AF, Liang L, Albert NM, Labresh KA, Yancy CW, Fonarow GC, Get With Guidelines Steering Committee and Hospitals (2009) Weekend hospital admission and discharge for heart failure: association with quality of care and clinical outcomes. *Am Heart J* 158(3):451–458, Epub 2009 Aug 4
- Barnett MJ, Kaboli PJ, Sirio CA, Rosenthal GE (2002) Day of the week of intensive care admission and patient outcomes: a multisite regional evaluation. *Med Care* 40(6):530–539
- Cram P, Hillis SL, Barnett M, Rosenthal GE (2004) Effects of weekend admission and hospital teaching status on in-hospital mortality. *Am J Med* 117(3):151–157
- Crowley RW, Yeoh HK, Stukenborg GJ, Medel R, Kassell NF, Dumont AS (2009) Influence of weekend hospital admission on short-term mortality after intracerebral hemorrhage. *Stroke* 40(7):2387–2392, Epub 2009 May 21
- Nahon S, Pariente A, Latrive JP, Group of Investigators of the Association Nationale des Gastroentérologues des Hôpitaux Généraux (ANGH) (2009) Weekend admission does not influence the mortality of upper gastrointestinal bleeding caused by peptic ulcers: results of a French prospective study of the association nationale des gastroentérologues des hôpitaux généraux group. *Clin Gastroenterol Hepatol* 7(8):911; author reply 912. Epub 2009 Mar
- Hemphill JC 3rd, Bonovich DC, Besmertis L, Manley GT, Johnston SC (2001) The ICH score: a simple, reliable grading scale for intracerebral hemorrhage. *Stroke* 32(4):891–897
- Crowley RW, Yeoh HK, Stukenborg GJ, Ionescu AA, Kassell NF, Dumont AS (2009) Influence of weekend versus weekday hospital admission on mortality following subarachnoid hemorrhage. Clinical article. *J Neurosurg* 111(1):57–58; discussion 58–59
- Arbabi S, Jurkovich GJ, Wahl WL, Kim HM, Maier RV (2005) Effect of patient load on trauma outcomes in a level I trauma center. *J Trauma* 59(4):815–818; discussion 819–820
- Busse JW, Bhandari M, Devereaux PJ (2004) The impact of time of admission on major complications and mortality in patients undergoing emergency trauma surgery. *Acta Orthop Scand* 75(3):333–338
- Barba R, Losa JE, Velasco M, Guijarro C, García de Casasola G, Zapatero A (2006) Mortality among adult patients admitted to the hospital on weekends. *Eur J Intern Med* 17(5):322–324
- Arabi Y, Alshimemeri A, Taher S (2006) Weekend and weeknight admissions have the same outcome of weekday admissions to an intensive care unit with onsite intensivist coverage. *Crit Care Med* 34(3):605–611
- Arias Y, Taylor DS, Marcin JP (2004) Association between evening admissions and higher mortality rates in the pediatric intensive care unit. *Pediatrics* 113(6):e530–e534
- Hixson ED, Davis S, Morris S, Harrison AM (2005) Do weekends or evenings matter in a pediatric intensive care unit? *Pediatr Crit Care Med* 6(5):523–530
- Sheu CC, Tsai JR, Hung JY, Yang CJ, Hung HC, Chong IW, Huang MS, Hwang JJ (2007) Admission time and outcomes of patients in a medical intensive care unit. *Kaohsiung J Med Sci* 23(8):395–404, 43
- Ensminger SA, Morales IJ, Peters SG, Keegan MT, Finkielman JD, Lymp JF, Afessa B (2004) The hospital mortality of patients admitted to the ICU on weekends. *Chest* 126(4):1292–1298, 81
- Kostis WJ, Demissie K, Marcella SW, Shao YH, Wilson AC, Moreyra AE, Myocardial Infarction Data Acquisition System (MIDAS 10) Study Group (2007) Weekend versus weekday admission and mortality from myocardial infarction. *N Engl J Med* 356(11):1099–1109
- Smektala R, Hahn S, Schröder P, Bonnaire F, Schulze Raestrup U, Siebert H, Fischer B, Boy O (2010) Medial hip neck fracture: influence of pre-operative delay on the quality of outcome: results of data from the external in-hospital quality assurance within the framework of secondary. *Unfallchirurg* 113(4):287–292, 2009 Sep 12
- Albright KC, Raman R, Ernstrom K, Hallevi H, Martin-Schild S, Meyer BC, Meyer DM, Morales MM, Grotta JC, Lyden PD, Savitz SI (2009) Can comprehensive stroke centers erase the ‘weekend effect’? *Cerebrovasc Dis* 27(2):107–113
- Wang H, Sekine M, Chen X, Kagamimori S (2002) A study of weekly and seasonal variation of stroke onset. *Int J Biometeorol* 47:13–20
- Rainer Fogelholm, Kari Murros, Aimo Rissanen, Matti Ilmavirta (1996) Factors Delaying Hospital Admission After Acute Stroke. *Stroke* 27(3):398–400

Disparities in Medical Expenditure and Outcomes Among Patients with Intracranial Hemorrhage Associated with Different Insurance Statuses in Southwestern China

Yuhan Kong, Yonghong Wang, John H. Zhang, Xiaolin Wang, and Xinyue Qin

Abstract As the economic impact of intracranial hemorrhage (ICH) has not been well characterized before, the purpose of this study is to investigate the prognosis of ICH patients with different insurances in southwestern China. This study used hospital data from December 2005 to September 2009. All patients with a final discharge diagnosis of acute ICH were enrolled. Patients were divided by payer sources. Hospital expenditure, length of hospital stay (LOS) and outcome during hospitalization were analyzed. SAS 9.1 software was utilized for the Kruskal-Wallis test and multivariate logistic regression analysis.

There were 1,091 adult subjects who met the inclusion criteria of ICH. Hospital costs were remarkably higher for local medical insurance beneficiaries than for the nonlocally insured group and the uninsured group. The locally insured group had the longest LOS compared to the uninsured and nonlocally insured groups. There were significant outcome differences between the locally insured and uninsured groups. However, we noted that locally insured patients seemed to have higher in-hospital mortality from ICH. In spite of acquiring insurance, these ICH subjects did not

appear to have better outcomes. The results emphasize the need for improvement in health care policy.

Keywords Intracranial hemorrhage · Medical insurance · Hospital expenditure · Outcome

Introduction

Stroke is one of the most common chronic diseases in China. Cerebral vascular diseases are now the second leading cause of death in China's population [1]. For years, health care has been the most concerning issue for China's population [2]. The prices of medical service provided by medical resources (especially high quality medical care in cities) are higher than the economic paying capacity and psychological endurance of common patients. Despite well-documented discrepancies associated with health care across insured and uninsured groups, few studies have explored the insurance-related disparities in outcomes of patients with intracranial hemorrhage (ICH). The purpose of this paper is to provide an overview of the outcomes of patients with different insurance statuses in Chongqing, one of the municipalities directly under the Central Government in southwestern China.

Materials and Methods

This is a retrospective study using hospital data from December 2005 to September 2009. All patients with a final discharge diagnosis of acute ICH during that time were enrolled. The principal diagnosis was based on the *International Classification of Diseases*, 10th Revision codes. We used code I61.902, representing non-traumatic intracranial hemorrhage as the principle diagnosis code. Then, we excluded discharged patients who had been transferred to other hospitals to avoid double counts.

Y. Kong and Y. Wang
Department of Neurology, The First Affiliated Hospital of Chongqing Medical University, Chongqing, China

J.H. Zhang
Department of Physiology and Pharmacology,
Department of Neurosurgery, Department of Anesthesiology,
Loma Linda University, School of Medicine,
Loma Linda, CA, USA

X. Wang
Medical Examination Center, The First Affiliated
Hospital of Chongqing Medical University,
Chongqing, China

X. Qin (✉)
Department of Neurology, The First Affiliated Hospital of Chongqing Medical University, Chongqing, China
e-mail: qinxinyue@yahoo.com

Firstly, the patients were categorized into three groups: locally insured, nonlocally insured and uninsured (who had no insurance and had to pay out-of-pocket). Secondly, after 2008, because of the nation's new insurance policy, the insured patients were divided into three patterns of insurances: metropolitan medical insurance, rural cooperative medical insurance and non-metropolitan medical insurance. So the patients enrolled after 2008 were divided into four groups, which were the three insured groups and the uninsured group. Thirdly, the insured groups were compared to the uninsured (out-of-pocket) group.

The primary results included the disparities in hospital costs (the costs have been changed to USD; \$1 USD is equivalent to 6.9 RMB) and length of hospital stay between the groups. Secondary results were differences in the patients' outcomes between insured and uninsured groups during the initial hospitalization. We also compared the outcomes across the subjects of the three groups of medical insurances to subjects without insurance.

Statistical analysis was performed using SAS 9.1 software, which was utilized for the Kruskal-Wallis test (analysis of costs and LOS) and multivariate logistic regression analysis (analysis of outcome). Results of the multivariate logistic regression are presented as odds ratios (OR) and their 95% confidence intervals (95% CIs). The statistical test was significant if the *P* value was <0.05.

Results

There were 1,091 adult subjects who met the inclusion criteria of ICH (717 males and 374 females, mean age 60 years \pm 15 and 61 years \pm 15). Of the subjects, 41.3% had local medical insurance, 35.3% had nonlocal insurance, and 23.4% were uninsured. Outcomes were recovery, improvement, death and other conditions (such as no improvement or abandoning treatment because of financial problems). There was no significant difference among ages in the four types of outcomes (*P*=0.29) (Table 1).

Table 2 compares hospital costs and LOS of locally insured, nonlocally insured and uninsured patients. For the three groups, hospital costs were remarkably higher for local medical insurance beneficiaries than for the nonlocally insured group and uninsured group, with an average of USD

Table 2 Hospital costs and LOS of three patterns of payer sources

	Locally insured	Nonlocally insured	Uninsured	<i>P</i> value
Total hospital costs	4,766.33	2,905.19	2,989.50	0.0001
Length of stay	28.94	17.62	18.29	0.0001
Average costs/day	255.54	227.55	218.62	0.1204

Costs and days were expressed by mean values (\bar{x}); standard deviations were omitted because of space limitations

\$4,766 in total (*P*=0.0001). Locally insured patients also had the longest LOSs. During hospitalization, locally insured patients had an average LOS of 28.9 days compared to nonlocally insured and uninsured subjects with an average LOS of 17.6 days and 18.3 days (*P*=0.0001). However, the average cost per day was not significantly different among the three groups (*P*=0.1204). Nonlocally insured patients had almost equivalent hospital costs and LOS as the uninsured group.

In Table 3, outcomes between locally insured and uninsured patients are shown to be significantly different (OR=10.48, 95% CI: 7.53–14.58). Outcomes were also significantly different between nonlocally insured and uninsured groups (OR=7.55, 95% CI: 5.42–10.52). Locally insured patients had the highest constituent ratio of death (21.51%), whereas nonlocally insured and uninsured groups had 7.52% and 13.7%. However, the cure constituent ratios of locally insured, nonlocally insured and uninsured groups were 11.20%, 12.47% and 6.27%, respectively.

In Table 4, analyses comparing hospital costs and LOS among the metropolitan insurance, rural cooperative medical insurance, non-metropolitan medical insurance and uninsured are shown. There was a significant difference in hospital costs (*P*=0.0027) and a tendency with LOS (*P*=0.0663), but no significant difference in daily fees. Metropolitan medical insured patients had the highest total hospital costs, and their LOS was also the longest.

Table 5 compares outcomes of the insured groups with the uninsured group. There was no significant difference among the groups (*P*>0.05). However, the constituent ratio of death in the metropolitan insurance group was highest again (23.97%), and in the rural cooperative medical insurance group, non-metropolitan medical insurance group and uninsured groups were 12.28%, 10.17% and 7.41%, respectively.

Table 1 Age of males and females with different outcomes

	Males	Females	Age ($\bar{X} \pm s$)
Recovery	448	247	61.91 \pm 14.64
Improvement	80	37	59.79 \pm 14.87
Death	97	64	60.71 \pm 14.97
Other	91	26	58.44 \pm 14.58
Total	717	374	

Discussion

According to our research, there is some discrepancy among medical expenditures, outcomes and insurance status. The explanation for these findings remains to be fully determined. Indeed, the disparate results may be due to a series of factors.

Table 3 Disparities in outcomes of patients with three different payer sources

	Cure	Improvement	Death	Others	Total	<i>P</i> value
Locally insured	54 (11.97)	266 (58.98)	97 (21.51)	34 (7.54)	451	0.0001
Nonlocally insured	48 (12.47)	257 (66.75)	29 (7.53)	51 (13.25)	385	0.0001
Uninsured	16 (6.27)	172 (67.45)	35 (13.73)	32 (12.55)	255	

Table 4 Hospital costs and LOS of patients covered by four patterns of insurance

	M-insured	Co-insured	NM-insured	Uninsured	<i>P</i> value
Total hospital costs	6,105.78	3,755.64	5,339.56	3,441.12	0.0027
Length of stay	28.34	16.63	24.93	17.11	0.0663
Average costs/day	352.45	345.66	292.11	279.59	0.2258

M-insured metropolitan medical insurance coverage, *Co-insured* rural cooperative medical insurance coverage, *NM-insured* non-metropolitan medical insurance coverage

Costs and days were expressed by mean values (\bar{x}); standard deviations were omitted because of space limitations

Table 5 Disparities in outcomes of patients covered by four patterns of insurance

	Recovery	Improvement	Death	Others	Total	<i>P</i> value
M-insured	21 (17.35)	62 (51.24)	29 (23.97)	9 (7.44)	121	0.3663
Co-insured	7 (12.28)	31 (54.39)	7 (12.28)	12 (21.05)	57	0.3641
NM-insured	9 (15.25)	36 (61.02)	6 (10.17)	8 (13.56)	59	0.9917
Uninsured	6 (11.11)	37 (68.52)	4 (7.41)	7 (12.96)	54	

M-insured metropolitan medical insurance coverage, *Co-insured* rural cooperative medical insurance coverage, *NM-insured* non-metropolitan medical insurance coverage

Table 6 Hospital costs and LOS of four types of outcomes

	Recovery	Improvement	Death	Other conditions	<i>P</i> value
Total hospital costs	7,727.97	3,382.61	2,900.15	2,570.87	0.0001
Length of stay	35.18	25.54	10.92	7.17	0.0001
Average costs/day	218.12	152.75	490	408.99	0.0001

Costs and days were expressed by mean values (\bar{x}), standard deviations were omitted owing to space limitations

In our study, the insured patients mainly came from urban areas. They worked in state-owned enterprises or public institutions. The nonlocal patients might have come from other areas where the policy might be different from local ones. The uninsured patients included the majority of workers, unemployed population and farmers in the rural areas. As for the insurance, insured patients could have longer hospital stays and afford higher expenditures than the others on average. Even with the data after the new division was carried out, the metropolitan and non-metropolitan insured patients also had longer hospital stays and better medical conditions. That is, they had more chances to improve their health. Moreover, we found the patients with rural cooperative insurance had nearly the same expenditures and LOSs as the uninsured, and their outcomes were not significantly different from uninsured patients. Two years ago, they were just

uninsured. So we concluded that rural cooperative medical insurance is insufficient at present.

With more than 1.3 billion people, China is becoming the world's largest and most populous country in the world, and the economy is increasingly improving. The nation's health care policy should be appropriate to the times. However, the policy of health care is still in practising stage. The challenge has been undertaken for years, but it will take a long time to achieve success [3–7]. A better outcome requires better medical conditions and long hospital stays. In China, however, more than 35% of urban households and 43% of rural households have difficulty affording health care [8]. The rural cooperative medical scheme, for instance, reimburses only approximately 30% of inpatient expenditures [9].

The social health insurance program (SHI) has been established in China to ensure that the citizens can obtain

health care economically and equitably. However, access to primary care for poor people has not really improved, and financial protection against high health care expenses remains very limited [10]. In 2005–2006, 66.5% of Chinese inpatients were not SHI beneficiaries. Drug expenditures for SHI inpatients were significantly higher than for non-SHI inpatients [11]. In our study, we also found that the insurance coverage was associated with higher hospital costs.

Discrepancies in hospital care across insurance subgroups have been widely documented, indicating that uninsured or unfavorable health insurance status could contribute to reduced access to high-quality care and to an increased likelihood of experiencing poorer outcomes than other patients [12–15]. According to previous studies, insured patients tended to be aware of chronic risk factors [16, 17]. For example, hypertension and hypercholesterolemia, which lead to stroke, can be more easily detected and controlled if patients are aware of them [18, 19]. Furthermore, being uninsured can create stress or other hazards that make patients less likely to adhere to medication and lifestyle modifications (e.g., smoking cessation, low-sodium diet and physical activities) to control chronic risk factors for stroke [20, 21].

Interestingly, in spite of acquiring insurance, according to the results of this study, locally insured patients, especially metropolitan insurance coverage patients, have higher in-hospital mortality in case of ICH. In Table 3, we show the calculations of the constituent ratio of death of locally insured, nonlocally insured and uninsured groups. The ratios were 21.51%, 7.53% and 13.73%, respectively ($P=0.0001$, by chi-square test). The recovery rates of the three groups were 11.97%, 12.47% and 6.27%, respectively. The improvement rates were 58.98%, 66.75% and 67.45%, respectively. The rates of other conditions (abandoned treatment or left hospital without improvement) were 7.54%, 13.25 and 12.55%, respectively. We found that although locally insured patients had the longest hospital stays, expended the most and had good compliance, they did not seem to have better outcomes. Conversely, the rate of death was the highest, and the rate of improvement was the lowest. However, this was not a coincidence. In Table 5, the latest 2 years' data show that the metropolitan insurance coverage patients also had the highest death rate of the four groups. These phenomena should not be totally attributed to insurance discrepancies.

Some research concerning a carotid disease reported the phenomenon that uninsured patients have fewer cardiovascular risk factors [22]. The possible causes are as follows: on one hand, Chongqing is a heavily industrial city, and urban citizens suffer with environmental pollution, which can lead to health problems. On the other, as social competition gets fierce, increasing stress and intense lifestyles over the coming years might aggravate the problem. And thirdly, the workers and farmers in the uninsured group engage mostly in manual labor. In other words, they engage in intense physical activity, so they are in better physical condition when overcoming diseases.

In conclusion, our findings indicate that future efforts need to be made to improve health care delivery to uninsured populations. Recently, the government has approved guidelines and an action plan to reform the health care system. The government has made a schedule to provide insurance coverage for all citizens. The aims are to provide safe, effective, convenient and affordable basic care for all citizens by 2020 [23]. The work is arduous. In addition, the results concerning health problems in urban residents emphasize the need for effective prevention, and citizens should pay more attention to health care. Efforts should be made to enhance public education and improve awareness of warning signs related to cerebral vascular diseases.

Conflict of interest statement We declare that we have no conflict of interest.

References

1. World Bank (2005) Public expenditure and the role of government in Chinese health sector, briefing note series newsletter 33234, October 2005. World Bank, Washington, DC
2. Shi L (2001) The convergence of vulnerable characteristics and health insurance in the US. *Soc Sci Med* 53:519–529
3. Ayanian JZ, Zaslavsky AM, Weissman JS, Schneider EC, Ginsburg JA (2003) Undiagnosed hypertension and hypercholesterolemia among uninsured and insured adults in the Third National Health and Nutrition Examination Survey. *Am J Public Health* 93:2051–2054
4. Barr J, McKinley S, O'Brien E, Herkes G (2006) Patient recognition of and response to symptoms of TIA or stroke. *Neuroepidemiology* 26:168–175
5. Rice T, Lavarreda SA, Ponce NA, Brown ER (2005) The impact of private and public health insurance on medication use for adults with chronic diseases. *Med Care Res Rev* 62:231–249
6. Wagstaff A, Lindelow M, Gao J, Xu L, Qian J (2007) Extending health insurance to the rural population: an impact evaluation of China new cooperative scheme, policy research working paper 4150, March 2007. World Bank, Washington, DC
7. Wang M, Liu K, Wang D, Zhao J, Wang S, Zhao Y, Kang S (2005) The current situation and issues on direct disease burden of intracerebral hemorrhage in China. *Chin Health Econ* 24:43–46
8. Zhao Y (2005) Assessing government health expenditure in China, working paper 34529, October 2005. World Bank, Washington, DC
9. Moy E, Bartman BA, Weir MR (1995) Access to hypertensive care. Effects of income, insurance, and source of care. *Arch Intern Med* 155:1497–1502
10. Giacobelli JK, Egorova N, Nowygrod R, Gelijns A, Kent KC, Morrissey NJ (2008) Insurance status predicts access to care and outcomes of vascular disease. *J Vasc Surg* 48(4):905–911
11. Fan M (2008) Health care tops list of concerns in China. *Washington Post*, Washington, DC. <http://www.washingtonpost.com/wp-dyn/content/article/2008/01/09/AR2008010903222.html>. Accessed 10 Jan 2008
12. Shen JJ, Wan TTH, Perlin JB (2001) An exploration of the complex relationship of socioecological factors in the treatment and outcomes of acute myocardial infarction in disadvantaged populations. *Health Serv Res* 36:711–732
13. World Bank (2004) Taking stock of China's rural health challenges, briefing note series newsletter 33231, October 2004. World Bank, Washington, DC

14. Yip W, Hsiao WC (2008) MarketWatch: the Chinese health system at a crossroads. *Health Aff* 27:460–468
15. Zhou B, Yang L, Sun Q, Gu H, Wang B (2008) Social health insurance and drug spending among cancer inpatients in China. *Health Aff (Millwood)* 27:1020–1027
16. Liu Y, Rao K, Hu SL (2002) People's Republic of China: toward establishing a rural health protection system. Asian Development Bank, Manila
17. Opinions of the CPC Central Committee and the State Council on deepening the health care system reform (2009) Communist Party of China Central Committee, State Council, National Development and Reform Commission Web site. http://shs.ndrc.gov.cn/ygjd/ygwj/t20090408_271138.htm. Accessed 17 Mar 2009
18. Ayanian JZ, Weissman JS, Schneider EC, Ginsburg JA, Zaslavsky AM (2000) Unmet health needs of uninsured adults in the United States. *JAMA* 284:2061–2069
19. Dollar D (2007) Poverty, inequality, and social disparities during China's economic reform, policy research working paper 2453. World Bank, Washington, DC
20. Gandelman G, Aronow WS, Varma R (2004) Prevalence of adequate blood pressure control in self-pay or Medicare patients versus Medicaid or private insurance patients with systemic hypertension followed in a university cardiology or general medicine clinic. *Am J Cardiol* 94:815–816
21. Institute of Medicine (2002) Coverage matters: insurance and health care. National Academies, Washington, DC
22. Bradbury RC, Golec JH, Steen PM (2001) Comparing uninsured and privately insured hospital patients: admission severity, health outcomes and resource use. *Health Serv Manage Res* 14:203–210
23. Meng Q, Li L, Eggleston K (2005) Health service delivery in China, a review, working paper 33233, February 2005. World Bank, Washington, DC

Clinical Analysis of Electrolyte Imbalance in Thalamic Hemorrhage Patients Within 24 H After Admission

Zhenwei Guo, Tianzhu Wang, John H. Zhang, and Xinyue Qin

Abstract We have observed that patients with thalamic hemorrhage are more likely to have electrolyte disturbances than those with non-thalamic hemorrhage. Here, we are attempting to provide some comprehensive information on electrolyte disturbances in patients with thalamic hemorrhage. Retrospectively, 67 patients with thalamic hemorrhage (TH group) and 256 with non-thalamic hemorrhage (N-TH group) were found from computer tomography images. Electrolytes of these patients were tested within 24 h after hospitalization. Chi-square test was used to compare the incidence of electrolyte imbalance. Serum K^+ levels were found to be abnormal in 37.31% of the patients in the TH group and 24.21% in the N-TH group, and the difference was significant ($p < 0.05$). Such a difference was also observed for the levels of serum Na^+ and Cl^- . Incidences of abnormal serum K^+ ($p < 0.05$), Na^+ ($p < 0.01$) and Cl^- ($p < 0.01$) levels were different among thalamic hemorrhage, basal ganglia area hemorrhage and lobar hemorrhage patients. In the TH group, the mortality of patients with electrolyte disturbances (42.50%) was higher than that of patients with normal electrolyte levels (14.81%, $p < 0.05$). The incidence of electrolyte imbalance is higher in patients with thalamic hemorrhage than in those with non-thalamic hemorrhage. The reason may be partly related to the location of the hemorrhage. Electrolyte disturbance may contribute to the higher mortality of patients with thalamic hemorrhage.

Keywords Thalamic hemorrhage · Electrolyte imbalance · Hypokalemia · Hyponatremia

Z. Guo, T. Wang, and X. Qin (✉)
Department of Neurology, The First Affiliated Hospital of Chongqing Medical University, Chongqing, 400016, China
e-mail: qinxinyue@yahoo.com

J.H. Zhang
Department of Physiology and Pharmacology,
Department of Neurosurgery, Department of Anesthesiology,
Loma Linda University, School of Medicine, Loma Linda, CA, USA

Introduction

Cerebral hemorrhage is also described as spontaneous intracerebral hemorrhage, and its incidence is 20–30% [1]. The mortality is 30–40% in the acute phase. It is a type of acute cerebrovascular disease, causing the highest number of deaths in China [1]. In addition, the number of patients who have to go to the hospital for cerebral hemorrhage has not fallen worldwide in the past 10 years [2]. These hemorrhages consist of putaminal (35%), thalamic (10–15%) [3], cerebellar (5–10%) and pontine (5%) [4]. At the beginning of the last century, Dejerine and Roussy [5] provided detailed records on thalamic syndrome. Then, in 1930, after an interval of about 10 years, Lhermitte [6] and Baudouin et al. [7] made important contributions toward defining the characteristics of thalamic hemorrhage (TH). Fisher [8] came up with concept of three characteristics of thalamic hemorrhage in 1959, which included Parinaud syndrome, consciousness disturbance and sensory disorder. In the past decades, the clinical features and prognosis of thalamic hemorrhage have been reported [9–13]; however, little is known about electrolyte levels after thalamic hemorrhage [10, 14–16]. Furthermore, special information on electrolyte imbalance in thalamic hemorrhage is practically absent in the literature. Thus, we attempt to provide some new information about electrolyte imbalances in patients with thalamic hemorrhage.

Patients and Methods

Subjects and Inclusion/Exclusion Criteria

The clinical characteristics of patients with intracranial hemorrhage were retrospectively reviewed according to their medical files. Three hundred thirty patients diagnosed with cerebral hemorrhage by cranial computer tomography (CT) were admitted to our hospital from February 2008 to April 2009.

Their electrolyte levels, including serum sodium, potassium and chlorine, were tested within 24 h after admission by an automatic biochemical analyzer (model: M305593, USA). Patients with traumatic hemorrhage or without electrolyte records were excluded.

Groups

First, patients were divided into the TH group and NTH group. Our criteria for electrolyte imbalance were rooted in classical Chinese medical textbooks [17, 18]. The criteria were as follows: hypokalemia <3.5 mmol/L, hyperkalemia >5.5 mmol/L, hyponatremia <135 mmol/L, hypernatremia >145 mmol/L, hypochloremia <95 mmol/L and hyperchloremia >105 mmol/L. Meanwhile, the N-TH group was further assigned into the basal ganglia area hemorrhage group and lobar hemorrhage group to investigate the relationship between them concerning the incidence of electrolyte imbalance and the locations of hemorrhage.

Variables and Statistical Analysis

Variables consisted of serum potassium, sodium and chloride levels. Chi-square test was used to compare the incidence of electrolyte imbalance in TH and NTH. SPSS version 16.0 for Windows (SPSS Inc., Chicago, IL), $\alpha=0.05$ or 0.025, was used for calculations.

Results

Baseline Characteristics of Hemorrhage

Seventy-four patients were confirmed to have TH, but only 67 medical files conformed to the inclusion criteria standards, accounting for 22.42%. Of these, 40 TH patients had electrolyte disturbances according to the criteria [17, 18]. Another 256 patients with non-thalamic hemorrhage were collected, including 116 persons with electrolyte imbalances within 24 h of admission. Their clinical characteristics of hemorrhage are provided in Table 1.

Incidence of Electrolyte Disturbance

The general incidence of electrolyte imbalance of thalamic hemorrhage (59.70%) and non-thalamic hemorrhage (45.31%)

Table 1 Baseline characteristics of hemorrhage

Characteristics	TH (n=67)%	NTH (n=256)%
Means age (years)	66.77 ± 11.03	59.17 ± 15.70
Age stratification		
≤45 years	5 (7.47)	43 (16.80)
>45 years	62 (92.53)	213 (83.20)
Gender		
Male	40 (59.70)	174 (67.97)
Female	27 (40.30)	82 (32.03)
Hypertension		
	59 (88.60)	209 (81.64)
Blood pressure		
Mean SBP (mmHg)	180.00 ± 37.36	162.97 ± 55.51
Mean DBP (mmHg)	106.46 ± 21.91	100.52 ± 45.33
Smoking	13 (19.40)	49 (19.14)
Alcohol consumption	12 (17.91)	52 (20.31)
GCS at hospital admission*		
<6	19 (28.36)	69 (26.95)
6–12	27 (40.30)	144 (56.25)
>12	21 (31.34)	75 (29.30)
Hypercholesterolemia	12 (17.91)	48 (18.75)

*Three levels of the Glasgow Coma Scale were grouped according to one previous article [19]

patients was different ($p<0.05$) (Table 2). In detail, hypopotassemia was found in 25 patients, but none of the patients in the TH group suffered from hyperkalemia. Compared to the TH group, 57 persons had hypopotassemia and 5 had hyperpotassemia in the NTH group, and the difference was significant for hypopotassemia ($p<0.05$). Thirty-six patients suffered from hyponatremia and 12 patients experienced hypernatremia in the NTH group. Compared to the TH group, their difference was significant for hypernatremia ($p<0.01$). A similar phenomenon also could be found for serum chloride (Table 3).

Electrolyte Disturbance in Different Locations

Serum Potassium

Twenty-seven patients experienced hypopotassemia (19.15%), but none with basal ganglia area hemorrhage suffered from hyperpotassemia. Another 83 patients experienced lobar hemorrhage, 18 of whom had hypopotassemia (21.68%); 3 had hyperpotassemia (3.61%). The incidence of abnormal serum potassium in thalamic hemorrhage patients (37.31%) was higher than in those with basal ganglia area hemorrhage (20.75%, $p<0.025$) (Table 4).

Table 2 General incidence of electrolyte disturbance in TH and NTH

Group	N of normal level	N of abnormal level	Total	Incidence (%)
TH	27 (40.30%)	40 (59.70%)	67	59.70
NTH	140 (54.69%)	116 (45.31%)	256	45.31
Total	167	156	323	48.30

TH thalamic hemorrhage, NTH non-thalamic hemorrhage, N numbers

* $P < 0.05$

Table 3 Electrolyte imbalance between TH and NTH

Group		Hypo-	Normal	Hyper-	Total
K ⁺	TH	25 (37.31%) ^a	42	0 (0%) ^b	67
	NTH	57 (22.27%) ^a	194	5 (1.95%) ^b	256
	Total	82 (25.39%)	236	5 (1.55%)	323
Na ⁺	TH	14 (20.90%) ^b	41	12 (17.91%) ^c	67
	NTH	36 (14.06%) ^b	208	12 (4.69%) ^c	256
	Total	50 (15.78%)	249	24 (7.43%)	323
Cl ⁻	TH	12 (17.91%) ^b	44	11 (16.42%) ^c	67
	NTH	29 (11.33%) ^b	214	13 (5.08%) ^c	256
	Total	41 (12.69%)	258	24 (7.43%)	323

TH thalamic hemorrhage, N-TH non-thalamic hemorrhage

^aFisher's exact test, $p < 0.05$

^bChi-square test, $p > 0.05$

^cContinuity correction of chi-square test, $p < 0.01$

Table 4 Electrolyte imbalance among three locations of hemorrhage (K⁺)

Group	Abnormal level	Normal	Total
K ⁺ TH ^a	25 (37.31%)	42 (62.69%)	67
BGAH ^b	27 (19.15%)	114 (80.85%)	141
LH ^c	21 (25.30%)	62 (74.70%)	83
Total	73 (25.08%)	218 (74.92%)	291

TH thalamic hemorrhage, BGAH basal ganglia area hemorrhage, LH lobar hemorrhage

^aChi-square test, $p < 0.05$. A general comparison among TH, BGAH and LH

^b $p < 0.025$, compared to TH group

^c $p > 0.025$, compared to TH

Serum Sodium

The incidence of abnormal serum sodium levels in patients with thalamic hemorrhage (hyponatremia, 20.90%; hypernatremia, 17.91%) was higher than in basal ganglia hemorrhage patients (hyponatremia, 9.22%; hypernatremia, 2.13%; $p < 0.025$), but there was no difference when compared to those with lobar hemorrhage (hyponatremia, 24.09%; hypernatremia, 4.81%, $p > 0.025$) (Table 5).

Table 5 Electrolyte imbalance among three locations of hemorrhage (Na⁺, Cl⁻)

Group	Hypo-	Hyper-	Normal	Total
Na ⁺ TH ^a	14 (20.90%)	12 (17.91%)	41 (61.19%)	67
BGAH ^{ab}	13 (9.22%)	3 (2.13%)	125 (88.65%)	141
LH ^{ac}	20 (24.09%)	4 (4.81%)	59 (71.10%)	83
Total	47 (16.15%)	19 (6.52%)	225 (77.33%)	291
Cl ⁻ TH ^d	12 (17.91%)	11 (16.42%)	44 (65.67%)	67
BGAH ^{de}	13 (9.22%)	6 (4.26%)	122 (86.52%)	141
LH ^{df}	15 (18.72%)	7 (8.43%)	61 (72.85%)	83
Total	40 (13.74%)	24 (8.24%)	227 (79.02%)	291

TH thalamic hemorrhage, BGAH basal ganglia area hemorrhage, LH lobar hemorrhage

^aChi-square test, $p < 0.05$; a general comparison among TH, BGAH and LH

^b $p < 0.025$, compared to TH group

^c $p > 0.025$, compared to TH

^dChi-square test, $p < 0.05$. A general comparison among TH, BGAH and LH

^e $p < 0.025$, compared to TH group

^f $p > 0.025$, compared to TH

Serum Chloride

The incidence of abnormal serum chloride levels among patients with thalamic, basal ganglia area and lobar hemorrhage was different ($p < 0.05$). Moreover, the incidence of electrolyte imbalance in thalamic hemorrhage patients was higher than in those with basal ganglia area hemorrhage (Table 5).

Mortality of Thalamic Hemorrhage

We found that 17 persons (42.50%) with electrolyte disturbances died during hospitalization, more than in the normal electrolyte level group (14.81%). The difference was significant ($p < 0.05$) (Table 6).

Discussion

The first 24 h after admission is the easiest time for electrolytes to deteriorate after hemorrhage [20]. Some drugs, such as

Table 6 Mortality of TH in normal or abnormal level of electrolytes

Group	Survival group	Death group	Total	Mortality (%)
Abnormal level	23 (57.50%) ^a	17 (42.50%)	40	42.50
Normal level	23 (85.19%)	4 (14.81%)	27	14.81
Total	46 (68.66%)	21 (31.34%)	67	31.34

^aChi-Square test, $P < 0.05$

hypertonic mannitol, may lead to an electrolyte imbalance. To avoid this influence, we focused on the blood electrolyte changes within 24 h. These data indicated that a large proportion of thalamic hemorrhage patients had electrolyte problems within 24 h after admission; a previous study [21] collected data on electrolytes within 2 weeks after admission.

Our study showed that the incidence of hypopotassemia was higher in thalamic hemorrhage than in non-thalamic hemorrhage patients, but not of hyperpotassemia (Table 3). Recently, Gao [22] reported that some patients developed hypopotassemia after thalamic hemorrhage, but no cases of hyperpotassemia were reported in his study. The study showed that the incidence of hypernatremia was higher in thalamic hemorrhage (17.91%) than in NTH patients (4.69%), but this was not the case for hyponatremia. The incidence of hypernatremia or hyponatremia was not reported, but Kusuda et al. [21] have done research on hemorrhages. They found that about 44% of patients with hemorrhage suffered from hypernatremia. This is higher than our results (7.43%). The reason may be that their data were recorded 2 weeks after admission, whereas our data were recorded only in the first 24 h. Twelve patients with TH had hypernatremia, and half of them died during hospitalization. About half of the patients with hypernatremia (41.67%) had a history of diabetes mellitus (DM). Therefore, diabetes may be a risk factor for hypernatremia. The occurrence of acute hypernatremia can lead neurons to dehydrate. Na^+ and K^+ enter the intracellular state in the acute phase of neuron dehydration. Thus, the concentration of Na^+ , K^+ increases in neurons. It can have adverse effects on the neurons' metabolism and physiological functioning. The mortality of thalamic hemorrhage patients with hypernatremia was greatly augmented [23–25]. Intracranial pressure rises quickly after hemorrhage, so the body also comes into a high-stress state. Adrenocorticotrophic hormone (ACTH) increases 10- to 20-fold, and the kidney's function of reabsorbing Na^+ is augmented. This causes patients to develop hypernatremia [19, 26, 27]. Therefore, DM and high intracranial pressure may be two of the causes of hypernatremia in patients with thalamic hemorrhage. Some patients developed only one type of electrolyte imbalance, but the others could suffer from two or three types of electrolyte disturbance. We defined

the former as single electrolyte imbalance and the latter as multi-electrolyte disturbance. Finally, we found that 15 patients had single electrolyte imbalance (22.39%) and 25 multi-electrolyte disturbance (37.31%).

The reasons for electrolyte imbalance 24 h after admission for thalamic hemorrhage are not well known. The hypothalamus is the center of the neuroendocrine system and regulates endocrine activity [28]. Once thalamic hemorrhage occurs, it may disturb the regulating function of the hypothalamus. The body is in a stress state when cerebral hemorrhage takes place. The sympathetic nerve is excited, and epinephrine and adrenal cortical hormone secretion is greatly increased to activate the beta-2 receptor in the cytoplasmic membrane, which has a correlation with the activity of the Na^+/K^+ ATP enzyme. The receptor precipitates potassium ions into the cells [29]. This may be one of the causes of hypopotassemia. Some patients with cerebral hemorrhage suffer from arrhythmia. This augments catecholamine and also decreases serum potassium levels. We had 13 patients (52%) who suffered from vomiting. Vomiting is probably another cause of hypopotassemia.

This study indicated that the incidence of hyperchloremia was higher in thalamic hemorrhage (16.42%) than in non-thalamic hemorrhage (5.08%) patients. Abnormal levels of chlorine in TH patients were also not well described in the previous literature. When thalamic hemorrhage occurs, the hypothalamus is impaired directly or indirectly. Thus, the renin-angiotensin-aldosterone system and antidiuretic hormone (ADH) system cannot work well. It is likely the syndrome of inappropriate antidiuretic hormone secretion (SIADH) is generated [29–31]. Previously, Oppenheimer and Hachinski [32] reported that 14% of patients of cerebral hemorrhage had SIADH, which may be a cause of hyponatremia. The clinical characteristics of cerebral salt-wasting syndrome (CSWS) are hyponatremia, and an increase in urinary sodium and hypovolemia. CSWS may be another cause of hyponatremia [31, 33]. The causes of hypochloremia in thalamic hemorrhage patients have not been stated clearly. Vomiting may be an indicator of hypochloremia because half of the patients (50%) with hemorrhage suffered from it. But we found only a small proportion of patients (9.09%) with vomiting in the hyperchloremia group.

The incidence of abnormal levels of serum potassium in patients with thalamic hemorrhage (37.31%) was higher than in those with basal ganglia area hemorrhage (19.15%, $p < 0.025$; TH was excluded), but not in those with lobar hemorrhage ($p > 0.025$). A similar phenomenon also appeared in serum sodium and chloride levels. Thus, we came to the conclusion that the reason for electrolyte imbalance may be partly related to the hemorrhage location. The reason may be that thalamic hemorrhage impairs the center of the neuroendocrine system and hypothalamus, and causes hypothalamic

dysfunction, while other locations are not as easily injured as the hypothalamus during thalamic hemorrhage. Kusuda et al. [21] reported that the incidence of hypernatremia was the highest in brain stem hemorrhage patients, but our study indicated that the incidence of hypernatremia was highest in thalamic hemorrhage patients. The highest incidence of hyponatremia and hypochloremia was in lobar hemorrhage patients in this study.

The results showed that the mortality of thalamic hemorrhage patients with electrolyte disturbance (42.50%) was higher than in those with normal levels (14.81%) of electrolytes (Table 6). Therefore, electrolyte imbalance may have a relationship with the prognosis for thalamic hemorrhage patients. Other factors, such as initial consciousness, pyramid sign [34, 35], size of the hematoma [34, 36], hydrocephalus [9, 37] and ventricular extension, could forecast the prognosis of thalamic hemorrhage patients. In these articles, none of the authors reported that electrolyte disturbance was related to the prognosis for thalamic hemorrhage. We found that an electrolyte imbalance 24 h after admission was possibly related to mortality during hospitalization. Hypernatremia [38] and hyponatremia [39] have a close relationship with mortality. Hypernatremia leads to higher mortality, perhaps because of the higher rate of complications [38], such as pneumonia, upper gastrointestinal bleeding, secondary epilepsy and renal dysfunction. Our study showed that five patients (41.67%) experienced pneumonia, four suffered from upper gastrointestinal bleeding (33.33%), and eight developed renal dysfunction (66.67%) in case of hypernatremia.

Conclusion

In summary, the incidence of electrolyte imbalance was higher in thalamic hemorrhage than in non-thalamic hemorrhage patients within 24 h after hospitalization, perhaps because of the location of the hemorrhage and SIADH or CSWS. Electrolyte disturbance could lead to a poor prognosis for thalamic hemorrhage patients during hospitalization. We need to pay attention to electrolyte imbalances in patients with TH in our clinical practice.

Conflict of interest statement We declare that we have no conflict of interest.

References

1. Wu J, Jia JP, Cui LY (2007) *Neurology*, 1st edn. People's Medical Publishing House, Beijing, p 170
2. Qureshi AI, Mendelow AD, Hanley DF (2009) Intracerebral haemorrhage. *Lancet* 373:1632–1644
3. Walshe TM, Davis KD, Fisher CM (1977) Thalamic hemorrhage: a computed tomographic-clinical correlation. *Neurology (Minneapolis)* 27:217–222
4. Kase CS, Mohr JP, Caplan LR (1998) Intracerebral hemorrhage. In: Barnett HJM, Mohr JP, Stein MB (eds) *Stroke: pathology, diagnosis and management*. Saunders, Philadelphia, pp 649–700
5. Dejerine J, Roussy G (1906) Le syndrome thalamique. *Rev Neurol* 14:521–532
6. Lhermitte J (1925) Les syndromes thalamiques dissociés: les formes analgésique et hémialgésique. *Ann Med* 17:488–501
7. Baudouin A, Lhermitte J, Lereboullet J (1930) Une observation anatomo-clinique d'hémorragie du thalamus. *Rev Neurol* 2:102–109
8. Fisher CM (1959) The pathologic and clinical aspects of thalamic hemorrhage. *Trans Am Neurol Assoc* 84:56–59
9. Kumral E, Kocaer T, Ertübey NO et al (1995) Thalamic hemorrhage: a prospective study of 100 patients. *Stroke* 26:964–970
10. Kwak R, Kadoya S, Suzuki T (1983) Factors affecting the prognosis in thalamic hemorrhage. *Stroke* 14:493–500
11. Shah SD, Kalita J, Misra UK (2005) Prognostic predictors of thalamic hemorrhage. *J Clin Neurosci* 12:559–561
12. Wakasugi H (1987) A comparative study on the prognosis and factors affecting putaminal hemorrhage and thalamic hemorrhage. *Nippon Ika Daigaku Zasshi* 54:63–77
13. Whael K, Stefanache F, Hodorog DN (2008) Clinical and prognostic considerations in thalamic hemorrhage. *Clinical study on 117 cases*. *Rev Med Chir Soc Med Nat Iasi* 112:366–370
14. Hirota K, Hara T, Hosoi S (2005) Two cases of hyperkalemia after administration of hypertonic mannitol during craniotomy. *J Anesth* 19:75–77
15. Rohana AG, Ming W, Norlela S, Norazmi MK (2007) Functioning adrenal adenoma in association with congenital adrenal hyperplasia. *Med J Malaysia* 62:158–159
16. Yamamoto N, Miyamoto N, Seo H, Matsui N, Kuwayama A, Terashima K (1987) Hyponatremia with high plasma ANP level—report of two cases with emphasis on the pathophysiology of cerebral salt wasting. *No Shinkei Geka* 15:1019–1023
17. Chen WB, Pan XL (2008) *Diagnostics*, 7th edn. People's Medical Publishing House, Beijing, p 388
18. Ye RG, Lu ZY (2005) *Internal medicine*, 6th edn. People's Medical Publishing House, Beijing, pp 847–851
19. Imura H, Nakao K, Itoh H (1992) The natriuretic peptide system in the brain: implications in the central control of cardiovascular and neuroendocrine functions. *Front Neuroendocrinol* 13:217–249
20. Mayer SA, Sacco RL, Shi T, Mohr JP (1994) Neurologic deterioration in noncomatose patients with supratentorial intracerebral hemorrhage. *Neurology* 44:1379–1384
21. Kusuda K, Saku Y, Sadoshima S, Kozo I, Fujishima M (1989) Disturbances of fluid and electrolyte balance in patients with acute stroke. *Nippon Ronen Igakkai Zasshi* 26:223–227
22. Gao SR (2008) Clinical analysis of thalamic in 30 patients. *J Brain Nerv Dis* 16:640–641
23. Liu XY, Xu Y, Wu SN (2005) Common causes of hypernatremia and its treatment strategies in SICU. *Chin Med Works* 13:78–79
24. Zhang JJ, Cheng WX, Zhang CM (2002) The causes of hypernatremia and clinical analysis of its treatments. *Chin Crit Care Med* 14:750–752
25. Zhang XJ, Chen ZQ, Li H (2007) Clinical study of hypernatremia after intracerebral hemorrhage. *Brain Neurol Disord* 15:437–439
26. Han ZY, Tang SM, Shi BX (1996) *Practical cerebrovascularology*. Shanghai Science and Technology Press, Shanghai, pp 389–390
27. Song YJ, Chen SD (1997) Nervous system diseases and water-electrolyte metabolism disorder. *J Chin Pract Intern Med* 11:217
28. Bai SL (2003) *Systematic anatomy*, 5th edn. People's Medical Publishing House, Beijing, p 361
29. Trauer JM, Wrobel JP, Young AC (2008) The syndrome of inappropriate anti-diuretic hormone secretion concurrent with an acute exacerbation of cystic fibrosis. *J Cyst Fibros* 7:573–575

30. Hew-Butler T, Noakes TD, Siegel AJ (2008) Practical management of exercise-associated hyponatremic encephalopathy: the sodium paradox of non-osmotic vasopressin secretion. *Clin J Sport Med* 18: 350–354
31. Vingerhoets F, de Tribolet N (1988) Hyponatremia hypo-osmolarity in neurosurgical patients. “Appropriate secretion of ADH” and “cerebral salt wasting syndrome”. *Acta Neurochir (Wien)* 91:50–54
32. Oppenheimer S, Hachinski V (1992) Complications of acute stroke. *Lancet* 339:721–724
33. Cerdà-Esteve M, Cuadrado-Godia E, Chillaron JJ (2008) Cerebral salt wasting syndrome: review. *Eur J Intern Med* 19:249–254
34. Barraquer-Bordas L, Illa I, Escartin A, Rusalleda J, Marti-Vilalta JL (1981) Thalamic hemorrhage. A study of 23 patients with diagnosis by computed tomography. *Stroke* 12:524–527
35. Wen LY, Jiang AY, Kang JM, Liu CH (1996) The clinical characters and CT of severe cerebral hemorrhage. *J Stroke Neurol Dis* 13: 158–159
36. Chung CS, Caplan LR, Han W, Pessin MS, Lee KH, Kim JM (1996) Thalamic haemorrhage. *Brain* 119:1873–1886
37. Mori S, Sadoshima S, Ibayashi S, Fujishima M, Iino K (1995) Impact of thalamic hematoma on six-month mortality and motor and cognitive functional outcome. *Stroke* 26:620–626
38. Zhang XJ, Chen ZQ (2007) Clinical research of hypernatremia after hemorrhage. *J Brain Nerv Dis* 15:437–439
39. Liu B, Liu H (2009) Serum electrolytes changes and its clinical significance in patients with hemorrhagic stroke. *China Mod Doct* 47:154–155

Characteristics of Pulse Pressure Parameters in Acute Intracerebral Hemorrhage Patients

Tao Tao, Tianzhu Wang, John H. Zhang, and Xinyue Qin

Abstract We explored the features of changes in pulse pressure (PP) in patients with intracerebral hemorrhage (ICH). Two hundred one patients with ICH were admitted to our hospital from January 2008 to August 2009. Meanwhile, another 201 people matching in age and gender with these patients were assigned as controls. Blood Pressures (BP) were collected within the first 24 h after admission. PP was calculated from the BP readings. The mean of PPs was compared via *T*-test. The distributed frequency of the PP level was analyzed using the chi-square test. PPs in the ICH group were higher than those of the controls ($P < 0.001$). Chi-square test showed a significant difference in distribution ratios of PP ($P < 0.01$) between the ICH and control group. The largest PP range in the ICH group was from 80 to 99 mmHg, which accounted for 33.3%; PP of the control group was from 40 to 49 mmHg (30.3%). The PP level in the 40–89-year-old case group was higher than that in the 40–89-year-old control group. PP increased with age. Our investigation indicates that higher PP is correlated with acute ICH and that PP is important in predicting the risk of ICH.

Keywords Acute intracerebral hemorrhage · Pulse pressure · Mean artery pressure · Blood pressure

Introduction

Intracerebral hemorrhage (ICH) is a disease with high rates of incidence, death and mutilation, accounting for 10–15% of all cerebrovascular accidents [1]. Hypertension, resulting in damage to blood vessel walls [2], is the most common cause of primary ICH. It is widely believed that different components of BP are important not only for the effect on the progress of cerebrovascular diseases, but also for the appropriate application of antihypertensive treatment. More recently, PP, an indicator of arterial stiffness (pulsatile load), has been shown to be useful in predicting cardiovascular disease (CVD) events in the elderly [3–5]; MAP serves as an indicator of peripheral resistance and cardiac output (steady flow load) [6]. However, there is still some uncertainty regarding the utility of PP for predicting ICH. Therefore, we sought to determine whether PP might be helpful for predicting ICH risk in order to provide a reference for further developing the prevention and treatment of ICH.

Materials and Methods

Case Data

This was a retrospective study of 201 consecutive patients with acute ICH who were admitted to the Department of Neurology and Neurosurgery of the First Affiliated Hospital of Chongqing Medical University from January 2008 to August 2009. All of the patients had been diagnosed in the clinic, with CT confirmation, within 24 h after onset. Of these 201 patients (mean age, 61.6 ± 14.6 years), 135 were male and 66 were female. Hemorrhagic stroke patients were not included in our study if they had one of the following secondary causes: neoplasm, coagulation disorders, trauma and hemorrhagic transformation of an ischemic stroke. Another 201 people, 141 males and 60 females

T. Tao, T. Wang, and X. Qin (✉)
Department of Neurology, The First Affiliated Hospital of Chongqing Medical University, Chongqing 400016, China
e-mail: qinxinyue@yahoo.com

J.H. Zhang
Department of Physiology and Pharmacology,
Department of Neurosurgery, Department of Anesthesiology,
Loma Linda University, School of Medicine, Loma Linda, CA, USA

(mean age, 57.2 ± 10.7 years), coming to our hospital for physical examination in the same period were selected as the normal control group. Their neurological examination results were normal, and CT examination showed no history of cerebrovascular diseases. No history of severe complications of the heart, lung, liver and kidney were found in their medical records. Between the two groups, no statistically significant difference was found in age and gender.

Measurement of BP

The first BPs were measured by a trained nurse using a calibrated sphygmomanometer immediately after the patients' arrival in the emergency room, under the condition that each patient had not taken anti-hypertensive drugs or other treatments. The control group rested peacefully for at least 15 min before having BP measured. MAP and PP could be calculated with the following formulas: MAP (mmHg) = (systolic pressure + 2 diastolic pressure) / 3; PP (mmHg) = systolic pressure - diastolic pressure.

Statistical Analysis

All data were analyzed with SPSS 16.0 software. Univariate analysis was performed using the X^2 test in nominal and ordinal data and the t test in continuous data; data were expressed as mean \pm SD. Values of $P=0.05$ were considered significant.

Results

General Data

Of 201 cases in the ICH group, 98 patients had hypertension (48.8%). In the control group, only 75 had hypertension (37.3%).

Comparison of Blood Pressure Parameters Between Subjects in the Two Groups

In the ICH group, mean SBP was 168.4 ± 36.7 mmHg, and in the control group it was 133.3 ± 19.6 mmHg ($t=49.89$, $p<0.001$). Mean DBP was 98.2 ± 20.8 mmHg in the ICH group and 79.6 ± 12.2 mmHg in the control group ($t=32.94$, $p<0.001$). Mean PP was 70.2 ± 25.6 mmHg in the ICH group and 54.2 ± 13.6 mmHg in the control group ($t=64.66$, $p<0.001$). Mean MAP was 121.3 ± 24.9 mmHg in the ICH group and 97.6 ± 13.7 mmHg in the control group ($t=44.87$, $p<0.001$). All parameters of BP had extremely significant differences between the ICH group and control group (Table 1).

Analysis of PP and MAP in Non-Hypertensive Subjects in the Two Groups

The mean MAP and PP of 103 non-hypertensive patients in the ICH group were 115.7 ± 22.6 mmHg and 64.9 ± 24.4 mmHg, respectively, and of 126 non-hypertensive patients in the control group were 89.7 ± 7.9 mmHg and 48.6 ± 8.9 mmHg, respectively. PP and MAP pressures were higher in the ICH group than in the control group, with a significant difference ($t=68.96$, $P<0.001$).

Distribution Variation of Different PP Levels in the Two Groups

Chi-square test demonstrated that there was a statistically significant difference in the proportion of PP distributed frequency between the two groups ($X^2=63.28$, $p<0.001$) (Table 2). In the ICH group, PP was mostly distributed between 80 and 99 mmHg (33.3%), and for most subjects in the control group, PP was from 40 to 49 mmHg (30.3%). The analysis suggested that the incidence rate of intracranial hemorrhages in the ICH group was higher when the PP was above 80 mmHg.

Table 1 Variation of blood pressure parameters in the two groups

Variables (mmHg)	ICH group	Control group	t	P
SBP, mean \pm SD	168.4 ± 36.7	133.3 ± 19.6	49.89	<0.001
DBP, mean \pm SD	98.2 ± 20.8	79.6 ± 12.2	32.94	<0.001
MAP, mean \pm SD	121.3 ± 24.9	97.6 ± 13.7	44.87	<0.001
PP, mean \pm SD	70.2 ± 25.6	54.2 ± 13.6	64.66	<0.001

SBP indicates systolic blood pressure, DBP diastolic blood pressure, MAP mean arterial pressure, PP pulse pressure

Table 2 The proportion of PP frequency distribution in the two groups (n/%)

PP (mmHg)	ICH group	Control group
<39	18/9.0	26/12.9
40~49	22/10.9	61/30.3
50~59	40/19.9	58/28.9
60~69	28/13.9	27/13.4
70~79	26/13.0	17/8.5
>80	67/33.3	12/6.0

ICH group compared with control group $p < 0.001$

Analysis of the Relationship Between Age Distribution and PP

Mean PP was significantly higher in the ICH group than in the healthy group in the age range from 40 to 89 years ($P < 0.001$), and our investigation showed an increasing tendency of PP with the development of age in both groups (Table 3). This suggested PP was increasing with age.

Discussion

Intracerebral hemorrhage is an important public health problem with an annual incidence of 10–30/100,000 population [7, 8], accounting for 2 million (10–15%) of about 15 million strokes worldwide each year [9]. The number of incidences of ICH has increased in the past 10 years [10], mostly because of the increase in the number of elderly people [7], most of whom lack monitoring of blood pressure. Systolic pressure, diastolic pressure, mean arterial pressure and pulse pressure are common parameters for arterial pressure. The positive association between either systolic blood pressure (SBP) or diastolic blood pressure (DBP) and the risk of cardiovascular disease (CVD) is well established [11]. We have traditionally considered DBP the most important component of blood pressure and the primary target of antihypertensive therapy. However, numerous epidemiological studies found the

importance of SBP over 30 years ago, and elevated SBP is the most common form of hypertension in old people because SBP increases progressively with age. Recent research has suggested that the predictive value of SBP is superior to that of DBP. Therefore, active efforts to reduce SBP are of great importance in reducing the mortality rate and decreasing the incidence rate of cerebrovascular diseases. Morfis et al. [12] investigated the blood pressure of newly hospitalized patients with acute stroke and found significantly higher SBP and DBP, which were higher than those in the normal control group. Our analysis supports this view. As we know, the principal components of blood pressure consist of both a steady component (MAP) and a pulsatile component (PP). MAP is the result of the ventricle injection and peripheral vessel resistance, and PP reflects interaction between ventricle injection and the viscoelastic properties of the large arteries (direct) and wave reflection (indirect) [13, 14]. PP has been observed to be a significant and independent indicator of myocardial infarction, even among normotensive individuals [15], whereas stroke is best predicted by MAP [16]. However, there has been increasing evidence that PP is an independent risk factor for the occurrence of death from cardiovascular diseases and cerebrovascular diseases [17, 18]. Its predictive value is superior to that of SBP and DBP. Both SBP and DBP in young individuals increase proportionally as vascular resistance rises; however, SBP rises more than DBP after reaching middle age, resulting in elevation of PP [8, 19]. DBP rises with increased peripheral arterial resistance and falls with increased central artery stiffness; the relative contributions of these two opposing forces determine DBP and ultimately PP [17]. An increased stiffness of large elastic arteries in middle-aged and elderly subjects is a well-recognized mechanism of the increase in PP [8, 20]. There is abundant evidence that the increase in pulse pressure (PP) after the sixth decade of life is a surrogate risk marker for central artery stiffness [16]. Similarly, our data show that the PPs of patients with ICH are all higher than those of the healthy group, whether the patients had hypertension or not.

The pathophysiology and pathogenesis of high blood pressure in ICH patients are not absolutely clear, and it is not fully understood whether hypertension is caused by ICH or vice versa. Most researchers have considered that transient

Table 3 Relationship between age distribution and PP

Age (year)	ICH group (n=201)		Control group (n=201)		t	p
	n	PP (mmHg)	n	PP (mmHg)		
<40	12	58.7±25.2	12	46.2±15.2	2.407	0.135
40~49	32	66.0±28.2	39	45.5±7.5	26.638	<0.001
50~59	50	65.0±23.0	60	50.1±11.7	13.981	<0.001
60~69	40	70.9±28.9	57	58.7±14.6	20.726	<0.001
>70	67	77.8±22.7	33	63.8±13.3	9.360	0.003

post-ICH hypertension is caused by several different factors. The fact that the majority of patients with ICH have chronic hypertension and elevation at the time of admission is merely a reflection of the untreated hypertension [21]. It could also be a reaction to compression of the brain stem, also known as the Cushing-Kocher response, in order to maintain cerebral perfusion [22, 23]. The stress response leading to abnormal sympathetic activity, altered parasympathetic activity, raised levels of circulating catecholamines [24] and brain natriuretic peptide may also contribute to acute hypertension [25]. In our research, there was a significant difference of PP in the two groups. Moreover, PP increased with the development of age both in the ICH group and control group, and PP was especially higher in patients aged 40–89 years, which was strikingly higher in the ICH group than in the control group. All of these above factors indicate that the increase in PP can be a stable and reliable evaluation standard.

In summary, the mechanism of hypertension in acute ICH and its treatment are highly controversial. Decompression should be adopted carefully and adaptively. Our findings suggest that high PP is independently associated with an increased risk of ICH. PP provides an important predictive value for ICH events in normotensive and untreated hypertensive middle-aged and elderly adults. There is a tendency for PP to be higher with increasing age. In the future, public health recommendations should focus on PP as the prime target for defining risk and goal therapy in middle-aged and elderly individuals.

Conflict of interest statement We declare that we have no conflict of interest.

References

- Brown DL, Morgenstern LB (2005) Stopping the bleeding in intracerebral hemorrhage. *N Engl J Med* 352(8):828–830
- Fazekas F, Kleinert R, Roob G, Kleinert G, Kapeller P, Schmidt R (1999) Histopathologic analysis of foci of signal loss on gradient-echo T2*-weighted MR images in patients with spontaneous intracerebral hemorrhage: evidence of microangiopathy-related microbleeds. *Am J Neuroradiol* 20(4):637–642
- Blacher J, Staessen JA, Girerd X, Gasowski J (2000) Pulse pressure not mean pressure determines cardiovascular risk in older hypertensive patients. *Arch Intern Med* 160:1085–1089
- Darne B, Girerd X, Safar M, Cambien F, Guize L (1989) Pulsatile versus steady component of blood pressure: a cross-sectional analysis and a prospective analysis on cardiovascular mortality. *Hypertension* 13:392–400
- Gasowski J, Fagard RH, Staessen JA, Grodzicki T, Pocock S, Boutitie F, Gueyffier F, Boissel JP (2002) Pulsatile blood pressure component as predictor of mortality in hypertension: a meta-analysis of clinical trial control groups. *J Hypertens* 20:141–151
- Franklin SS, Lopez VA, Wong ND, Mitchell GF, Larson MG, Vasan RS, Levy D (2009) Single versus combined blood pressure components and risk for cardiovascular disease: the Framingham Heart Study. *Circulation* 119(2):243–250
- Feigin VL, Lawes CMM, Bennett DA, Anderson CS (2003) Stroke epidemiology: a review of population-based studies of incidence, prevalence, and case-fatality in the late 20th century. *Lancet Neurol* 2:43–53
- Franklin SS, Gustin WG, Wong ND (1997) Hemodynamic patterns of age-related changes in blood pressure: the Framingham Study. *Circulation* 96:308–315
- Sudlow CL, Warlow CP (1997) Comparable studies of the incidence of stroke and its pathological types: results from an international collaboration. *Stroke* 28:491–499
- Qureshi AI, Suri MFK, Nasar A (2007) Changes in cost and outcome among US patients with stroke hospitalized in 1990 to 1991 and those hospitalized in 2000 to 2001. *Stroke* 38:2180–2184
- Joint National Committee on Prevention, Detection, Evaluation, and Treatment of High Blood Pressure (1997) The sixth report of the Joint National Committee on Prevention, Detection, Evaluation, and Treatment of High Blood Pressure. *Arch Intern Med* 157:2413–2446
- Morfis L, Schwartz RS, Poulos R (1997) Blood pressure changes in acute cerebral infarction and hemorrhage. *Stroke* 28:1401–1405
- Nichols WW, Nicolini FA, Pepine CJ (1992) Determinants of isolated systolic hypertension in the elderly. *J Hypertens* 10(suppl 6):S73–S77
- Nichols WW, O'Rourke MF (1998) McDonald's blood flow in arteries. Lea & Febiger, Philadelphia
- Franklin SS (2004) Pulse pressure as a risk factor. *Clin Exp Hypertens* 26(7–8):645–652, Review
- Millar JA, Lever AF, Burke V (1999) Pulse pressure as a risk factor for cardiovascular events in the MRC Mild Hypertension Trial. *J Hypertens* 17:1065–1072
- Franklin SS, Khan SA, Wong ND, Larson MG, Levy D (1999) Is pulse pressure useful in predicting risk for coronary heart disease? The Framingham Heart Study. *Circulation* 100(4):354–360
- Verdecchia P, Schillaci G, Reboldi G, Franklin SS, Porcellati C (2001) Different prognostic impact of 24-hour mean blood pressure and pulse pressure on stroke and coronary artery disease in essential hypertension. *Circulation* 103(21):2579–2584
- Berne RM, Levy MN (1992) Cardiovascular physiology. Mosby, St Louis, pp 113–144
- Witterman JCM, Grobbee DE, Valkenburg HA (1994) J-shaped relation between change in diastolic blood pressure and progression of aortic atherosclerosis. *Lancet* 343:504–507
- Arboix A, Roig H, Rossich R, Martinez EM, Garcia-Eroles L (2004) Differences between hypertensive and non-hypertensive ischemic stroke. *Eur J Neurol* 11(10):687–692
- Qureshi AI, Geocadin RG, Suarez JI, Ulatowski JA (2000) Long-term outcome after medical reversal of transtentorial herniation in patients with supratentorial mass lesions. *Crit Care Med* 28(5):1556–1564
- Qureshi AI, Tuhim S, Broderick JP, Batjer HH, Hondo H, Hanley DF (2001) Spontaneous intracerebral hemorrhage. *N Engl J Med* 344:1450–1460
- Cheung RT, Hachinski V (2004) Cardiac effects of stroke. *Curr Treat Options Cardiovasc Med* 6(3):199–207
- Nakagawa K, Yamaguchia T, Seida M, Yamadab S, Imaea S, Tanakac Y (2005) Plasma concentrations of brain natriuretic peptide in patients with acute ischemic stroke. *Cerebrovasc Dis* 19(3):157–164
- Giroud M, Gras P, Chadan N, Beuriat P, Milan C, Arveux P (1991) Cerebral haemorrhage in a French prospective population study. *J Neurol Neurosurg Psychiatry* 54(7):595–598
- Labovitz DL, Halim A, Boden-Albala B, Hauser WA, Sacco RL (2005) The incidence of deep and lobar intracerebral hemorrhage in whites, blacks, and Hispanics. *Neurology* 65:518–522

Electrocardiographic Abnormalities in Patients with Intracerebral Hemorrhage

Qing Liu, Yanhui Ding, Pengcheng Yan, John H. Zhang, and Han Lei

Abstract *Background:* Stroke is frequently followed by electrocardiographic changes. Although electrocardiographic abnormalities are well known in ischemic stroke and subarachnoid hemorrhage, these changes have only rarely been investigated systematically in patients with intracerebral hemorrhage. The purpose of this study is to investigate the prevalence and characterization of ECG abnormalities in a consecutive series of ICH patients who had no history of heart disease. *Methods:* The study was retrospective, and 304 intracerebral hemorrhage patients who met the study criteria were entered in the study. The ECG changes of the 304 acute hemorrhagic stroke patients without primary heart disease were analyzed. The relationship among the electrocardiographic abnormalities, the location of hematoma, and the clinical outcome were investigated to determine cardiac involvement in the cerebral hemorrhage in these patients.

Results: A total of 304 patients were included. Two hundred and four patients (67.1%) had one or more ECG abnormalities. These changes included morphological waveform changes and arrhythmias, such as QTc prolongation, ST-T morphological changes, sinus bradycardia, inverted T wave, and conduction block. These ECG changes were not related to the level of the cerebral lesion, but were related to its location and the outcome.

Conclusions: Electrocardiographic abnormalities frequently occur after intracerebral hemorrhage, and these changes were not related to the level of the cerebral lesion, but were related to the location of the cerebral lesion and the outcome.

Keywords Intracerebral hemorrhage (ICH) · Electrocardiographic (ECG) abnormalities · Cerebrocardiac syndrome (CCS)

Introduction

For many years, clinicians have known that ECG abnormalities are seen frequently in patients with ICH [1]. The electrocardiographic abnormalities and cardiac dysfunction as a result of cerebrovascular diseases are collectively called cerebral-cardiac syndrome (CCS) [2]. Since these ECG changes are suggestive of myocardial ischemia, they can mislead physicians in the initial diagnosis of the patient. This misdiagnosis may result in adverse consequences, especially in patients with hemorrhagic stroke, because of the treatment of myocardial ischemia [3]. The incidence of CCS in China has been increasing in recent years, and it may lead to diagnostic and therapeutic difficulties for cardiologists and neurologists.

ICH is a serious neurological disorder that is often complicated by the occurrence of electrocardiographic abnormalities unexplained by preexisting cardiac conditions [4]. For further study of the cardiac dysfunction arising from the acute cerebral hemorrhage in these patients, we retrospectively reviewed the medical records of patients diagnosed with intracerebral hemorrhage who visited the First Affiliated Hospital of Chongqing Medical University from 1 January 1998 to 31 March 2009. Relevant variable information about these populations was analyzed and discussed.

Materials and Methods

Case Selection

The study population consisted of all consecutive patients with non-traumatic, intraparenchymal ICH admitted to the First Affiliated Hospital of Chongqing Medical University

Q. Liu (✉), Y. Ding, P. Yan, and H. Lei
Department of Clinical Research Center, The First Affiliated Hospital of Chongqing Medical University, Chongqing, 400016, China
e-mail: qingliu5566@yahoo.cn

J.H. Zhang
Department of Neurosurgery, Loma Linda University,
School of Medicine, Loma Linda, CA, USA

between 1 January 1998 and 31 March 2009. Three hundred four patients were entered into the study: 203 male patients, accounting for 66.8%, and 101 female patients, accounting for 33.2%. The age range was 14 to 108 years, and the average age was 58.36 ± 16.39 years old.

All patients met the following inclusion criteria:

1. "Completed" hemorrhagic stroke: in all cases, the diagnosis of intracerebral hemorrhage was made by relevant findings on cranial computed tomography and magnetic resonance imaging.
2. At least one ECG within 3 days after admission.
3. No conclusive history of heart disease prior to the initial intracerebral hemorrhage, including coronary disease, valve sickness, arrhythmia, etc., according to the previous medical history record, and the patient or a family member.
4. Ruling out of the possibility or presence of brain trauma and subarachnoid hemorrhage.

Statistical Methods

Adapted SPSS software was used to analyze the data. The *t*-test was applied to compare the mean difference between two calculated data points, and a χ^2 examination was used to compare the differences between multiple groups of calculated data. SARS software was used to make the logistic regression analysis in view of the multi-factors. Statistical significance was set at $p < 0.05$.

Results

All 304 patients had ECG recordings available for review. Two hundred four patients (67.1%) had one or more ECG abnormalities, while normal ECG results were seen in 100

patients (32.9%). These abnormalities included both morphological waveform changes in the 12-lead ECG and arrhythmias, such as QTc prolongation, ST-T morphological changes, sinus bradycardia, inverted T wave, conduction block, and atrial fibrillation.

A wide variety of morphological waveform changes and arrhythmias have been observed following all types of intracerebral hemorrhage. Hematoma location of patients accompanied with electrocardiographic abnormalities was distributed as follows: basal ganglia 77.3%; thalamus, 19 patients (14.84%); lobar, 15 patients (11.72%); pons, 5 patients (3.91%); cerebellum, 4 patients (3.13%); other, 7 patients (5.47%). This set of data showed that ECG changes correlated with the location of ICH. The closer the hematoma location was to the center brain, such as the thalamus, basal ganglia, and brain stem, the higher the incidence of ECG abnormalities. In contrast, the closer the hematoma location was to the edge, such as the lobe, the lower the incidence of ECG abnormalities, according to the statistical analysis ($P = 0.0022$, $\chi^2 = 14.6194$). The detailed relationship between ECG abnormalities and hematoma location is presented in Table 1.

We divided the patients into the coma group and conscious group; the incidences of ECG abnormalities between the two groups were compared, but we did not find a statistically significant difference ($p = 0.1948$, $\chi^2 = 1.6812$). The details are presented in Table 2.

The possible relationship between ECG and prognosis was analyzed as shown in Table 3. ECG abnormalities are related to the prognosis of the patients.

Table 1 Electrocardiographic abnormalities and hematoma location

Hematoma location	Cases (<i>n</i>)	Rate of normal ECG (<i>n</i> %)	Rate of abnormal ECG(<i>n</i> %)				
			A	B	C	D	E
Thalamus and basal nucleus	174	27.6	20.1	4.6	12.6	7.5	27.6
Brainstem	22	22.7	40.9	0	4.5	4.5	27.3
Cerebral cortex	90	46.7	20.0	5.6	15.6	2.2	10.0
Cerebellum	18	27.8	16.7	16.7	16.7	11.1	11.1
Total	304	32.9	21.4	5.3	13.2	5.9	21.4

Allorhythmia (A) including sinus bradycardia, sinus tachycardia, atrial premature, ventricular premature beat, ventricular tachycardia, supraventricular tachycardia, junctional rhythm; conduction defects (B) including ST-segment depression or elevation, QTc prolongation and abnormal T and U waves; repolarization abnormalities (C) including bundle branch block, I or II atrioventricular block; others (D) including left ventricular hypertrophy with strain, ventriculus sinister high tension, hyperpotassemia; combined abnormality (E) means those people with two or more abnormalities at the same time

Table 2 Level of consciousness and ECG abnormalities

Level of consciousness	Cases (<i>n</i>)	Rate of abnormal ECG (<i>n</i> %)
Coma	25	80.0
Conscious	279	65.9
Total	304	67.1

Table 3 Multifactor logistic regression analysis of the prognosis

Factors	β	SE	Wald χ^2	<i>P</i>	OR	OR (95%CI)
Level of consciousness	1.7643	0.4519	15.2398	<0.0001	5.837	2.407~14.155
ECG abnormalities	0.9266	0.4429	4.3772	0.0364	2.526	1.060~6.017

Discussion

The concept that the cerebral vascular system and cardiovascular systems are closely linked was recognized as early as 1900 by Cushing [1]. To date, the interrelationship between cerebrovascular disease and cardiovascular disease has been repeatedly emphasized. They have common risk factors, such as hypertension, diabetes, hyperlipidemia, and cigarette smoking, and frequently coexist [2]. Decompensation in one system may adversely affect the other, whether or not the patient has recognized disease of both systems. Cardiac disease may cause acute cerebral manifestations. On the other hand, it is well known that patients with acute cerebrovascular accidents have a high incidence of electrocardiographic changes and of arrhythmias [3, 4]. Through the neurotransmitters released by the sympathetic nerve and parasympathetic nerve, the cardiac function can be regulated by the cerebrum [2, 15]. Therefore, cerebral vascular accidents can cause previously normal functions of the heart to enter a series of physiological pathological changes.

A total of 304 ICH patients who had no history of heart disease were analyzed. Two hundred four patients had one or more ECG abnormalities. However, we found that there was no direct relationship between ECG abnormalities and entry consciousness, indicating entry ECG abnormalities may not correlate with the intensity of initial brain injury. This result conflicts with He [2], who suggested that there is a relationship between ECG changes and the lesion intensity of the brain. In addition, the relationship between the hemorrhage location and the incidence of the ECG abnormality in our study is in agreement with the results of published papers [5–7]. The pathogenesis behind this relation is unclear. It was presumed that the deep brain lesion location may influence the autonomic nervous system located in the bottom of the thalamus, inducing the dysfunction of the cardiovascular autonomic system [8]. Besides the effects of catecholamine, the effect of NPY in the progress of CCS is an alternative explanation. The action of NPY in the cardiovascular system has been established [9]. NPY levels were increased in CCS patients [3].

There are several studies using hemorrhagic and ischemic CCS models [10–13]. Xu et al. [10] found that there was a different level of necrosis of the cardiac muscle cell according to the timing of bleeding in a hemorrhagic CCS model. The characteristic pattern of myocardial lesions suggested that the damaging catecholamines are released from intramyocardial

nerve endings rather than from the general circulation [4]. Elrifai et al. [11] found that the bleeding lesion increased intracranial pressure and enhanced catecholamine release, inducing the injuries in cardiac muscle in dogs. Xu et al. [14] found that once the cerebral hemorrhage has occurred, NPY levels in the brain stem of rats increased, so NPY may interact with catecholamine, acetylcholine, histamine, glucocorticoids, and vasopressin to regulate the cardiovascular system by affecting sympathetic and parasympathetic systems.

Of the 304 patients, the fatality rate of the normal ECG group was 7.5%, and of the abnormal ECG group 20.7%. This marked difference in mortality suggests that neurologists need to keep in mind the potential cardiac dysfunction of ICH patients, especially in unconscious patients or in patients with aphasia in whom the cardiovascular signs may be masked, and that the diagnosis of CCS depends almost entirely on ECG recordings.

Conflict of interest statement We declare that we have no conflict of interest.

References

- Cushing H (1903) The blood pressure reaction of acute cerebral compression illustrated by cases of intracranial hemorrhage. *Am J Med Sci* 125:1017–1044
- He DB, Guo ZQ et al (2009) The prognosis of aged patients of acute cerebrovascular disease with brain-heart syndrome. *J Brain Nerve Dis* 17(1)
- Xu ZQ, Zhou HD et al (2005) Cardiac response in patients with acute cerebral vascular disease and its mechanism. *Chin J Geriatric Heart Brain Vessel Dis* 7(6)
- Chen LJ et al (2002) Heart and lung complication of cerebrovascular disease. *Foreign Med Sci Cerebrovasc* 10(2):110–112
- Liu JL et al (1994) The relationship between apoplexy site and ECG alteration. *Chin J Pract Intern Med* 14(1):35
- Gawaz M (2004) Role of platelets in coronary thrombosis and reperfusion of ischemic myocardium. *Cardiovasc Res* 61(3):498–511
- Eckardt M, Gerlach L, Weelter FL (1999) Prolongation of the frequency-corrected QT dispersion following cerebral strokes with involvement of the insula of Reil. *Eur Neurol* 42(4):190–197
- Shi YQ, Zhou XD et al (2004) *Neurology in practice*, 3rd edn. Shanghai Technological Publishing Company, Shanghai, pp 794–796
- Zeng CY (1997) The effect of neuropeptide Y on cerebro-cardiac axis response in experiment intracerebral hemorrhage. *Adv Cardiovasc Dis* 18(3):164–167
- Xu ZQ, Chen ME, Jiang XJ et al (2001) Establishment of the animal model of CCS. *Chin J Geriatric Heart Brain Vessel Dis* 3(2)

11. Elrifai AM, Bailes JE, Shih SR et al (1996) Characterization of the cardiac effects of acute subarachnoid hemorrhage in dogs. *Stroke* 27(4):737-741
12. Wang L, Sun LH, Chen ZY et al (2007) Establishment of the rat model of CCS. *Chin Pharma Bull* 23(5)
13. Zhou MQ (2004) A research into mechanism of acupuncture protection on animal model of cerebral-cardiac syndrome. *Chin J Basic Med Traditional Chin Med* 10(6)
14. Xu ZQ, Jiang XJ, Chen ME et al (2002) Experimental study of mechanism of cerebral-cardiac syndrome. *J Brain Nerve Dis* 10(6)
15. Catanzaro JN, Meraj PM, Zheng S (2008) Electrocardiographic T-wave changes underlying acute cardiac and cerebral events. *Am J Emerg Med* 26(6):716-720

ECG Change of Acute Subarachnoid Hemorrhagic Patients

Qing Liu, Yan-Hui Ding, John H. Zhang, and Han Lei

Abstract Objective: This study intends to investigate whether the entry electrocardiographic (ECG) abnormalities of patients with acute subarachnoid hemorrhage (SAH) are related to the prognosis. **Methods:** From 1998 to the present, 106 SAH patients who had no history of heart disease and were diagnosed with head CT were recruited. **Results:** Abnormal ECG changes of acute subarachnoid hemorrhage patients were observed, with a total incidence rate of 63.2% (67/106). The incidence rate of allorhythmia was 22.6% (24/106), the repolarization abnormality was 14.2% (15/106), the conduction abnormality was 1.9% (2/106), and the combined abnormality was 21.7% (23/106). However, dividing the patients into two groups according to their entry consciousness state, no difference was observed between coma and alert groups ($P=1.0000$). In addition, the ECG changes had no relationship with the lesion degree and the outcome prognosis according to logistic regression analysis ($P=0.0844$). **Conclusions:** In 106 SAH patients, we could not identify any relationship between the ECG and lesion degree and outcome prognosis.

Keywords Cerebrocardiac syndrome (CCS) · Electrocardiographic (ECG) · Subarachnoid hemorrhage (SAH)

Introduction

Since Levin's first report regarding ECG change in acute subarachnoid hemorrhagic patients, more reports have appeared in the literature. This syndrome was named cerebrocardiac syndrome (CCS) [1]. Several reports indicated that there are relationships between CCS and the outcome

prognosis, but others failed to establish this relationship [1]. We made a retrospective analysis of 106 SAH patients from our hospital from 1998 to 2009 to examine a possible link between the ECG and prognosis; we excluded patients with traumatic SAH and those with combined heart disease.

Materials and Methods

A total of 106 subjects with acute SAH were prospectively evaluated. There were 53 men and 53 women, with an age range of 21 to 80, the average being 54.87 ± 14.99 .

All the subjects were selected according to these standardizations:

1. Diagnosed with a head CT.
2. Had the ECG within 2 days of admission to the hospital.
3. According to the medical history, no definite heart disease before admission to the hospital, excluding coronary artery disease, valvular heart disease, and arrhythmia.
4. Excluded traumatic SAH.

We divided the subjects into two groups according to whether or not CCS was present: the negative group (group I), with 39 subjects (36.8%) – 15 men and 24 women, average age 54.15 ± 14.52 ; positive group (group II), with a total of 67 subjects (63.2%) – 38 men and 29 women, average age 55.28 ± 12.11 . There was no difference in the number of patients and the gender of patients between these two groups ($t=-0.43$, $P=0.6680$).

Hypertension history: There were 13 subjects in group I and 21 in group II, and there was no patent difference between the two groups ($\chi^2=0.0448$, $P=0.8324$).

Statistical Analysis

Statistical analysis was carried out with SAS software, using a t -test between two group measurement data and χ^2 test for

Q. Liu (✉), Y.-H. Ding, J.H. Zhang, and H. Lei
The Clinical Research Center, The First Affiliated Hospital,
Chongqing Medical University, Chongqing 400016, China
e-mail: qingliu5566@yahoo.cn

numeration data. Logistic analysis was aimed at the factors affecting the prognosis, with significance at $P < 0.05$.

Results

ECG changes are shown in Table 1. Using the consciousness of the subjects upon admission to the hospital, we divided patients into the coma group and alertness group. Comparing the incidence of ECG abnormality between the two groups, we found no statistical difference ($\chi^2 = 0.0000$, $P = 1.0000$). Therefore, we could not identify any relationship between ECG abnormality and the severity of the SAH. See Table 2.

ECG and prognosis: In group I, 38 subjects fully recovered from SAH, and there was 1 death. In group II, there were 58 recoveries and 9 deaths. The prognosis of the two groups showed no significant difference ($\chi^2 = 2.2549$, $P = 0.1332$), as shown in Table 3.

Table 1 Classification of ECG

ECG	Number	%
Allorhythmia	24	22.6
Repolarization abnormality	15	14.2
Conduction abnormality	2	1.9
Combined abnormality	23	21.7
Others	3	2.8
Normal ECG	39	36.8

Allorhythmia includes sinus bradycardia, sinus tachycardia, atrial premature, ventricular premature beat, ventricular tachycardia, supraventricular tachycardia, junctional rhythm; repolarization abnormality includes bundle branch block, atrioventricular block I or II; conduction abnormality includes ST-T alteration, QTc prolongation, and constitutional T wave change; others include left ventricular hypertrophy with strain, ventriculus sinister high tension, hyperpotassemia; combined abnormality means those people with two or more abnormalities at the same time

Table 2 ECG and consciousness

Consciousness	Cases (n)	Abnormal ECG rate (%)
Coma group	8	62.5
Alertness group	98	63.3
All	106	63.2

Discussion

There are many causes of SAH, such as cerebral aneurysm, cerebral arteriovenous malformations (AVM), hypertension, cerebral arteriosclerosis, and moyamoya disease. Though we had discharged the subjects with basic cardiac disease before admission to the hospital, most of the senile patients may have had risks such as hypertension, diabetes mellitus, hyperlipidemia, hyperviscosamia, smoking, and chronic alcoholic intoxication. During bleeding effluence, cerebral edema, electrolyte disturbances, and acid-base imbalance aggravate the anoxia of the cardiac and cerebral vascular system, thus strengthening the stress reaction and evoking cardiac disease [1].

Hematoceles in the skull base directly activate the autonomic nerves, inducing the gangliated nerve to stress and hyperadrenocorticism. Catecholamine increases in blood upon SAH, and coronarospasm can eventually lead to myocardial ischemia [2]. Pathology research confirms that the abnormality of the ECG is very closely related to the hypothalamus lesion [3]. During SAH, the hypothalamus and cerebral secondary edema, nucleus denaturation, infundibulum, and mamillary body are covered by blood, inducing third ventricle extension, mamillary body displacement downward, bleeding, and infarction around the vessel. These may cause the intracranial pressure to rise, brain tissue ischemia and anoxia, autonomic nerve center dysfunction, gangliated nerve and parasympathetic nerve loss of equilibrium, affecting the conducting system of the heart, and repolarization of the cardiac muscle. Elrifai [4] did experiments in dogs and found that the bleeding lesion made the intracranial pressure increase and activated the center of autonomic nerve accommodation to deliver catecholamine, inducing injuries and increasing the oxygen consumption of the cardiac muscle, increasing the burden of the heart and lungs. There are reports showing that the neurogenic ECG alteration may be caused by catecholamine, which is released by the nerve ending to the cardiac muscle, since there is no increase of catecholamine in blood [5].

In this study, the incidence of CCS in these 106 subjects was 63.2%. The potential relationship between CCS and consciousness has not been established. In addition, no direct correlation exists between the ECG with the incidence of CCS or prognosis. Catanzaro [6] found that there was a different electrocardiographic T-wave change between heart disease patients and SAH patients with CCS. Some of the SAH patients may have CCS, but the alteration of ECG has no effect on the prognosis of the patients, with allorhythmia having the most effect, so we can consider the ECG

Table 3 Logistic analysis of the SAH patients' prognosis

Factor	β	SE	Wald χ^2	P	OR	OR (95% CI)
Intercept	-6.0907	2.6176	5.4143	0.0200		
Age	0.0206	0.0361	0.3256	0.5682	1.021	0.951–1.096
Gender	0.7257	0.8179	0.7873	0.3749	2.066	0.416–10.265
BP	-0.0725	0.8874	0.0067	0.9348	0.930	0.163–5.295
Consciousness	3.2677	1.0077	10.5149	0.0012	26.250	3.642–189.188
ECG	2.2252	1.2894	2.9781	0.0844	9.255	0.739–115.861

alteration of most parts to be convertible. Nonetheless, the clinician must consider the alteration of heart function of SAH patients in the routine examination. There are different degrees of consciousness and aphasia in these patients, and the signs of cardiovascular problems may be masked; therefore, the diagnosis of CCS depends on the ECG.

Conflict of interest statement We declare that we have no conflict of interest.

References

1. Shi YQ, Zhou XD et al (2004) Practical neurology, 3rd edn. Shanghai Scientific Technical Publishing Company, Shanghai, pp 794–796
2. Pilati CF, Clark RS, Gilloteaux J, Bosso FJ, Holcomb P, Maron MB (1990) Excessive sympathetic nervous system activity decreases myocardial contractility. *Proc Soc Exp Biol Med* 193:225–231
3. Harries AD (1981) Subarachnoid hemorrhage and the electrocardiogram — a review. *Postgrad Med J* 57(667):294–296
4. Elrifai AM, Bailes JE, Shih SR et al (1996) Characterization of the cardiac effects of acute subarachnoid hemorrhage in dogs. *Stroke* 27(4):737–741
5. Chen LJ et al (2002) Heart and lung complication of cerebrovascular disease. *Foreign Med Sci Cerebrovasc* 10(2):110–112
6. Catanzaro JN, Meraj PM, Zheng S et al (2008) Electrocardiographic T-wave changes underlying acute cardiac and cerebral events. *Am J Emerg Med* 26(6):716–720

Diagnosis and Treatment of Hemorrhagic Pituitary Adenomas

Gang Huo, Qing-Lin Feng, Mao-Yuan Tang, and Dong Li

Abstract We retrospectively analyzed the clinical manifestations, imaging results, and surgical treatment conditions of 72 patients who were diagnosed with hemorrhagic pituitary adenoma between January 2006 and May 2009 at our Department of Neurosurgery. We reached the conclusion that the CT-positive rate was 55.17% and the MRI-positive rate was 94.44%. Sixty-six patients underwent transsphenoidal operations; 6 patients, transfrontal operations; 52, total resections; 10, subtotal resections; and 10, partial resections. All procedures alleviated patients' headaches and stopped vomiting; patients with impaired consciousness gradually became clear-headed after the operations; patients whose preoperative eyesight had been impaired improved to different degrees, and ophthalmoplegia improved. Fifty-six patients were followed, 14 were cured, 32 had alleviated symptoms but 4 did not, and 6 relapsed. Our finding suggests that MRI scanning is superior to CT scanning in the diagnosis of hemorrhagic pituitary adenomas. Surgical decompression should be performed as soon as possible, and transsphenoidal microsurgery is the optimal treatment.

Keywords Pituitary adenoma · Hemorrhage · Pituitary apoplexy · Transsphenoidal microsurgery

Introduction

Pituitary adenoma is a common intracranial tumor, and the disease conditions develop slowly. However, the diseases of hemorrhagic pituitary adenomas start quickly, can cause severe visual impairment and consciousness disturbance, can lead to disability, and can even threaten the patients'

lives. Of 400 patients who were diagnosed with pituitary adenoma between January 2006 and May 2009 at our department, 72 consecutive patients were diagnosed with hemorrhagic pituitary adenomas. This paper analyzes the 72 patients retrospectively, and the literature is reviewed for discussion.

Materials and Methods

General Information

The patients comprised 42 males and 30 female, with a male:female ratio of 1.4:1. The age range was 18–69 years, with an average age of 43.5 years. Sixteen patients (22.22%) had prolactin adenomas (PRL adenoma), 6 (8.33%) had adrenocorticotrophic hormone adenomas (ACTH adenoma), 4 (5.56%) had growth hormone adenomas (GH adenoma), 4 (5.56%) had mixed-secreting adenomas, and 42 (58.33%) had non-secreting adenomas (Table 1). Non-secreting adenomas accounted for 58.33%, while non-secreting pituitary adenomas in non-pituitary adenoma apoplexy in the same period accounted for 14.28%; both had a statistically significant difference ($P < 0.05$, X^2 test). Fifty patients had invasive pituitary adenomas, and 22 had non-invasive pituitary adenomas. The tumor diameter of 64 patients was larger than 1 cm. Four patients with PRL adenomas had a history of taking bromocriptine; 2 with recurrent adenomas had histories of surgery and radiation therapy; 3 had a history of hypertension; 1 had accepted a CRH test; 1 had a history of liver cirrhosis; the others had unclear predisposing factors.

Clinical Manifestations

In addition to the original clinical symptoms of pituitary adenoma, 58 patients had symptoms of hemorrhagic pituitary adenomas, which were mainly manifested as sudden

G. Huo (✉), Q.-L. Feng, M.-Y. Tang, and D. Li
Department of Neurosurgery, The First Affiliated Hospital of
Chongqing Medical University, Chongqing 400016,
People's Republic of China
e-mail: xiaomin198171@tom.com

Table 1 Clinical features of 72 patients

Clinical features	Cases (%)	Clinical features	Cases (%)
<i>Pathological type</i>		<i>Clinical manifestation</i>	
Prolactin adenoma	16 (22.22)	Headache	54 (75.00)
Adrenocorticotrophic hormone adenomas	6 (8.33)	Vomiting	48 (66.67)
Growth hormone adenoma	4 (5.56)	Visual deterioration	44 (61.11)
Mixed-secreting adenoma	4 (5.56)	Ophthalmoplegia	38 (52.78)
Non-secreting adenoma	42 (58.33)	Consciousness disturbance	16 (22.22)
<i>Operation time after admission</i>			
<24 h	18 (25.00)		
1–3 days	44 (61.11)		
4–7 days	10 (13.89)		

headache (54 patients, 75%), vomiting (48 patients, 66.67%), sudden deterioration in visual acuity (44 patients, 61.11%), ophthalmoplegia (38 patients, 52.78%), and consciousness disturbance (16 patients, 22.22%) (Table 1). Another 14 patients did not have sudden deterioration of disease conditions, and only pituitary adenoma hemorrhage was discovered by CT imaging, MRI examination, or in operations. Of 72 patients, 4 had outbreaks of pituitary adenoma apoplexy (type I), 24 had acute pituitary adenoma apoplexy (type II), 30 had subacute pituitary adenoma apoplexy (type III), and 14 had chronic pituitary adenoma apoplexy (type IV).

Imaging Examination

All 72 patients agreed to undergo MRI examinations, of whom 58 also agreed to CT examination at the same time. Tumor hemorrhage or infarction in saddle areas was discovered in 68 patients by MRI examination (Fig. 1), and high density blood clots in the saddle areas were discovered in 32 patients by CT examination.

Treatment

Seventy-two patients with hemorrhagic pituitary adenomas underwent surgical treatment, except for six who underwent transfrontal resection because of giant tumors or problematic sphenoid sinus. The other 66 patients underwent transsphenoidal microsurgery for cutting the tumors. Operation time after admission was 24 h for 18 patients (25%), 1–3 days for 44 patients (61.11%), and in 4–7 days for 10 patients (13.89%) (Table 1).

Postoperative Follow-up Visit

Fifty-six patients had been followed up. Follow-up time was 3 months to 6 years, with an average of 2.8 years. Efficacy evaluation criteria were as follows: cure: no abnormalities were seen on MRI review and/or no internal secretion symptoms and signs were found, and biochemical detection indexes were normal; alleviation: no abnormalities were seen on MRI review, endocrine hyperactivity performance was



Fig. 1 MRI scan: sagittal zones are flat and show hemorrhage with high signals within the pituitary adenoma

partially alleviated or biochemical detection indexes were not completely normal; no alleviation: no abnormalities were seen on MRI review, and visual damages and endocrine function abnormalities were not improved; however, there were no signs of clinical relapse; recurrence: MRI examination confirmed that tumors had recurred or that endocrine disorders had recurred after having once been normal.

Result

Surgical Results

Fifty-two patients underwent surgical removal of the whole tumor (Fig. 2), 10 had subtotal resection, and 10 underwent partial removal of the tumor. Headaches were alleviated by the operation, vomiting was stopped, patients with impaired consciousness gradually became clear-headed, patients whose preoperative eyesight had been impaired improved to different degrees, and patients with ophthalmoplegia before admission improved. Thirty-two patients had concurrent postoperative diabetes insipidus after operations. The symptoms of one patient disappeared after 36 months by taking

Minirin, and the symptoms of another 31 patients disappeared automatically within 2 weeks after the operations or after treatment. Four patients had cerebrospinal fluid rhinorrhea. This condition resolved on its own in two patients and in two others was cured by nasal endoscopic operations to promote healing. There were no operative deaths.

Prognosis

In the follow-up of 56 patients, 14 were cured (the cure rate was 25%), 32 had symptom alleviation (the alleviation rate was 44.44%), 4 had no alleviation (the no alleviation rate was 5.56%), and 6 had recurrences (8.33%) (Table 2). Two patients with recurrence underwent transfrontal tumor resection again, two had r-knife treatment, and two refused further treatment. Thirty-eight of 56 patients had visual impairment before surgery: 10 of 76 eyes were fully blind before surgery, 4 eyes returned to eye front finger counting, another 6 eyes did not show improvement, and the visual ability of another 66 eyes was improved or returned to normal levels. Thirty patients needed to use prednisone for replacement therapy after surgery.

Discussion

Pituitary adenoma apoplexy is a group of syndromes caused by the infarction or bleeding of a pituitary adenoma and mainly manifests as a series of clinical symptoms [1], such as unexpected headache, vomiting, acute visual impairment, cranial nerve palsy, hypothalamic dysfunction, and even coma and the like. Although simple infarction can cause pituitary adenoma apoplexy, pituitary adenoma apoplexy caused by bleeding is the most common clinically. Some studies report that the possibility of pituitary tumor bleeding is about 5.4 times more than in other intracranial tumors [2]. Therefore, this chapter discusses the clinical features and the methods of diagnosis and treatment of 72 patients with hemorrhagic pituitary adenomas that were found during operations.



Fig. 2 MRI scans: sagittal zone is flat and shows that pituitary adenoma was totally removed in the second year after operation

Table 2 Prognosis conditions of 56 follow-up patients

Prognosis	Cases (%)
Healing	14 (25.00)
Alleviation	32 (44.44)
Non-alleviation	4 (5.56)
Recurrence	6 (8.33)

Pathogenesis and Predisposing Factors

At present, the reasons for hemorrhage are unknown. Some scholars believe that it is related to the pituitary-specific blood supply. Increased tumor size compresses the vessels that supply blood, thereby causing ischemia and necrosis of the tumor and anterior pituitary [3]. The hemorrhagic pituitary adenomas in this group were mainly observed in large adenomas and were also observed in invasive pituitary adenomas simultaneously. There is support for this view. Whether the diseases are caused by tumor cells involving vessels needs to be clarified by pathological evidence. The majority of cases of pituitary adenoma apoplexy do not have known causes; known predisposing factors only account for 25–30% of the patients. The main factors associated with the condition reported in the literature are the following: abnormal blood coagulation status caused by anticoagulant therapy or blood system diseases; low blood pressure and hypertension of any cause; radiation exposure; the use of dopamine receptor excitants such as bromocriptine or cabergoline, etc.; and other predisposing factors such as pituitary function tests, heart surgery, closed craniocerebral injury, or inflammation and other factors that also may cause pituitary adenoma apoplexy [4]. A hypercoagulable state is a factor inducing ischemic apoplexy. In the group, 11 patients had predisposing factors: 6 took bromocriptine and underwent radiotherapy, 3 had a history of hypertension, 1 had undergone a CRH test, and 1 had a history of liver cirrhosis. The other predisposing factors were unclear.

Clinical Features

Pituitary adenoma apoplexy is mainly observed in middle-aged men, and the tumors are mainly non-secreting adenomas and invasive pituitary adenomas. Studies show that more than 70% of patients with pituitary apoplexy have non-functional pituitary adenomas [5]. The patients in this group lack typical clinical manifestations in the early stage, and symptoms cannot be observed until the tumors grow to be large enough and cause hypopituitarism. Patients always have pituitary adenoma apoplexy as the first clinical manifestation. In this group, 64 patients had large adenomas, accounting for 88.89%, and 42 had non-secreting adenomas, accounting for 58.33%. Not all pituitary adenoma bleedings have clinical symptoms. This only occurs when a certain amount of blood has collected and compresses the surrounding structures or when bleeding enters the subarachnoid space to generate meningeal irritation symptoms and the symptoms of pituitary adenoma hemorrhage are generated. Common symptoms include: headache, vomiting, visual deterioration and visual field loss, ophthalmoplegia, and consciousness disturbance [6].

Typical manifestations are unexpected pains in the forehead, eye socket, and suboccipital areas. This can be accompanied by nausea and vomiting simultaneously, and headache is the most common clinical symptom. After pituitary apoplexy, the increased intrasellar pressure leads to compression of the cavernous sinus on both sides and leads to symptoms caused by the compression of cranial nerves (III, IV, V, and VI). Approximately 70% of patients have diplopia and other cranial nerve palsy symptoms in the clinic. Approximately 75% of patients have visual deterioration, blindness, and visual field loss. In patients with cranial nerve palsy, about 50% have oculomotor nerve palsy [7]. In this group, 54 patients (75%) had sudden headaches, 48 (66.67%) had vomiting, 44 (61.11%) had sudden visual deterioration, 38 cases (52.78%) had ophthalmoplegia, and 16 cases (22.22%) had consciousness disturbance (Table 1). This is basically consistent with the results reported in the literature. Relatively rare clinical symptoms comprise hemiplegia and anepia, mainly caused by necrotic tissue or bleeding into the cerebrospinal fluid, promoting intracranial arterial spasm, secondary ischemia [8], and Horner's syndrome [3] because of sympathetic nerve fiber damage.

Diagnosis

Early diagnosis, timely hormone therapy, and surgical decompression have great significance for improving prognosis. Patients with typical hemorrhagic symptoms of pituitary adenoma can be diagnosed easily. If patients are not aware of pituitary adenomas with the outbreak of diseases, the patients can be easily misdiagnosed, and the diseases should be strictly distinguished from aneurysmal subarachnoid hemorrhage, cavernous sinus thrombosis, Sheehan syndrome, and Rathke cyst hemorrhage [9]. Laboratory examinations should include electrolyte, glucose, and pituitary hormone measurements. CT examination is of certain help for confirming the diagnosis. CT scanning can show high-density or mixed-density lesions in saddle areas with unobvious enhancement. The density can be reduced after a few days, and the periphery is intensified after enhancement. However, about half of the patients have positive findings. MRI examination in the saddle areas is the best auxiliary examination method at present and can be used to detect bleeding that cannot be observed by CT. The positive rate is more than 90%. Hemorrhage or necrosis in tumors, the growth direction of tumors, and the relation between the tumors and surrounding structures can be clearly displayed [2].

In the study group, 72 patients underwent MRI examination, wherein tumor hemorrhage or infarction was discovered in saddle zones of 68 patients, and the positive rate was 94.44%. Conventional MRI cannot identify necrotic pituitary

large adenomas and craniopharyngioma (since they have peripheral enhancement). The adoption of restricted water diffusion-weighted MRI is conducive to achieving an early diagnosis of pituitary apoplexy. For patients with bleeding in saddle regions suspected to be caused by an aneurysm, cerebral angiography should be carried out for clarification. Cerebrospinal fluid examination has little significance for establishing the diagnosis. Analysis results of cerebrospinal fluid are often normal, unless the necrotic materials or bleeding have reached the subarachnoid space.

Treatment

Once the diagnosis is made, hormone replacement therapy should be given at once. The necessity to relieve compression of the hypothalamus and visual pathway in time through surgical decompression, thereby saving eyesight and life, is indisputable for type I and II patients with rapid onset and rapid disease progression. Although some authors adopt conservative treatment for type III and IV patients with slow disease progression and relatively stable disease conditions, also with good efficacy, the recovery of the optic nerve and the dominant eye muscle's cranial nerve function is worse compared with surgical decompression patients. The occurrence rate of hypopituitarism is higher, not to mention tumor tissues can be cut simultaneously. According to the improved vision of patients, we conclude that the operation effect within a week is better than the effect after a week, so patients should accept surgical decompression as soon as possible [10]. We agree with this view. A majority of patients in the group agreed to operations within 3 days after admission to the hospital. Patients with the sudden visual loss and consciousness disturbance should accept emergency operations. The transsphenoidal microsurgical operation approach is the best. The texture is thin and soft after tumor hemorrhage and necrosis, and can be scratched and absorbed easily in operations. Simultaneously, the influence on the optic nerve and optic chiasm blood supply due to transfrontal approach tumor cutting is also avoided, which is conducive to visual recovery after operations. Only when the tumors are huge and growth to the area is beyond the saddle area, or there is bad sphenoidal sinus gasification, should transfrontal or under wing point

tumor resection be used. Patients with tumor hemorrhage cystic changes can easily develop cerebrospinal fluid rhinorrhea after transsphenoidal operation, as occurred in four patients in the study group. Muscles should be filled in the saddle zones for patients with cerebrospinal fluid leakage during operations. The bottom of the saddles should be repaired using artificial meninges, and postoperative cerebrospinal fluid rhinorrhea can be reduced. The incidence rate of hypopituitarism for pituitary adenoma apoplexy after operations is high. Endocrinological examinations should be carried out after operations, and the patients should be followed up. Long-term steroid hormone and hormone replacement therapy is necessary [3].

Conflict of interest statement We declare that we have no conflict of interest.

References

1. Yang S, Lee K, Lee K et al (2008) Pituitary apoplexy producing internal carotid artery compression: a case report. *J Korean Med Sci* 23:1113–1117
2. Semple P, Jane J, Lopes B et al (2008) Pituitary apoplexy: correlation between magnetic resonance imaging and histopathological results. *J Neurosurg* 108:909–915
3. Murad-Kejbou S, Eggenberger E (2009) Pituitary apoplexy: evaluation, management, and prognosis. *Curr Opin Ophthalmol* 20:456–461
4. Telesca M, Santini F, Mazzucco A (2009) Adenoma related pituitary apoplexy disclosed by ptosis after routine cardiac surgery: occasional reappearance of a dismal complication. *Intensive Care Med* 35:185–186
5. Nawar R, AbdelMannan D, Selman W et al (2008) Pituitary tumor apoplexy: a review. *J Intensive Care Med* 23:75–90
6. Dubuisson AS, Beckers A, Stevenaert A (2007) Classical pituitary tumour apoplexy: clinical features, management and outcomes in a series of 24 patients. *Clin Neurol Neurosurg* 109:63–70
7. Kim S, Lee K, Kim S (2007) Cranial nerve palsies accompanying pituitary tumour. *J Clin Neurosci* 14:1158–1162
8. Ahmed FS, Semple FP (2008) Cerebral ischaemia in pituitary apoplexy. *Acta Neurochir* 150:1193–1196
9. Binning M, Liu J, Gannon J et al (2008) Hemorrhagic and nonhemorrhagic Rathke cleft cysts mimicking pituitary apoplexy. *J Neurosurg* 108:3–8
10. Muthukumar N, Rossette D, Soundaram M et al (2008) Blindness following pituitary apoplexy: timing of surgery and neuro-ophthalmic outcome. *J Clin Neurosci* 15:873–879

Characteristics of Acute Cerebral Hemorrhage with Regard to Lipid Metabolism and Glycometabolism Among Different Age Groups

Xiaolin Wang, Yuhan Kong, Hui Chen, John H. Zhang, and Yonghong Wang

Abstract Objective: This study investigated the lipid metabolism and glycometabolism of patients with acute cerebral hemorrhage from 2006–2008 in order to find a possible association among lipid metabolism, glycometabolism and different age groups of adults in the Chinese Chongqing population. **Methods:** Data on levels of total cholesterol (TC), triglyceride (TG), high density lipoprotein (HDL-C), low density lipoprotein (LDL-C) and fasting serum glucose (GLU) were obtained from records of patients (548) from the Department of Neurology of the First Affiliated Hospital of Chongqing Medical University. Participants ranging in age from 21–94 years were divided into three groups; the first group was the young group in which all participants were 21–44 years old; the second group was the middle-age group in which all participants were 45–59 years old, and the last group was the elderly group in which all participants were 60–94 years old. **Results:** Levels of TC, TG, HDL-C, LDL-C and GLU were not significantly different among the three groups ($P > 0.05$). Proportions of hypercholesterolemia high LDL-C, low HDL-C, impaired fasting glucose and diabetes mellitus were not different among the three groups ($P > 0.05$).

Only the proportion of hypertriglyceridemia patients was significantly different. The risk of being diagnosed with hypertriglyceridemia in the middle-age group was increased 2.371 times (95% CI: 1.542–3.645) and in the young group increased 2.281 times (95% CI: 1.211–4.296). **Conclusion:** Age and hypertriglyceridemia are risk factors associated with an increased incidence rate of acute cerebral hemorrhage in the Chongqing population in China.

Keywords Cerebral hemorrhage · Lipid Metabolism · Glycometabolism

Introduction

In the United States, stroke is the third most common cause of death. Stroke also causes substantial health-care expenditures [1]. In 2005, stroke resulted in an estimated 5.7 million deaths, and 87% of these deaths were in low-income and middle-income countries. Without intervention, the number of global stroke deaths is projected to rise to 6.5 million in 2015 and to 7.8 million in 2030, and the majority of these deaths will be in low-income and middle-income countries, especially in China [2].

The best way to prevent a first-time stroke is to identify at-risk patients and control as many risk factors as possible. Some risk factors, such as smoking, can be eliminated; others, such as hypertension and carotid artery stenosis, can be controlled or treated to reduce the risk of stroke [3]. Therefore, in this study, in order to study lipid metabolism and glycometabolism of acute cerebral hemorrhage and do our best to prevent stroke, we analyzed a possible association among lipid metabolism, glycometabolism and different age groups of adults with acute cerebral hemorrhage in the Chinese Chongqing population.

X. Wang and Y. Wang (✉)

The Medical Examination Center, The First Affiliated Hospital of Chongqing Medical University, Chongqing, China
e-mail: wyh0231029@yahoo.com.cn

Y. Kong

Department of Neurology, The First Affiliated Hospital of Chongqing Medical University, Chongqing, China

H. Chen

Clinical Laboratories, The First Affiliated Hospital of Chongqing Medical University, Chongqing, China

J.H. Zhang

Department of Neurosurgery, Loma Linda University, School of Medicine, Loma Linda, CA, USA

Data and Methods

Data Source

The data were obtained from records of patients who suffered from cerebral hemorrhage within 24 h (acute cerebral hemorrhage) in the Department of Neurology of the First Affiliated Hospital of Chongqing Medical University. The variables of participants selected for this study included age, gender, levels of total cholesterol (TC), triglycerides (TG), high density lipoprotein (HDL-C), low density lipoprotein (LDL-C) and fasting serum glucose (GLU).

All participants were Chongqing Chinese residents ($n=548$). The age of participants ranged between 21–94 years. The participants were divided into three groups by age: (1) the young-age group in which all participants were 21–44 years old; (2) the middle-age group in which all participants were 45–59 years old; (3) the elderly group in which all participants were 60–94 years old.

Measurements of Lipids and Serum Glucose

Blood samples were obtained from the antecubital vein in all participants after an overnight fasting period. The blood was transferred into glass tubes and allowed to clot at room temperature. Immediately following clotting, serum was separated by centrifugation for 15 min at 3,000 rpm. The levels of TC, TG, HDL-C and LDL-C in the different samples were determined enzymatically using commercially available kits. All determinations were performed with an auto analyzer in our Clinical Science Experiment Center of the First Affiliated Hospital of Chongqing Medical University. The clinical laboratory (no. ML000036) passed the accreditation criteria for the quality and competence of medical laboratories (ISO15189, no. ML000036).

Diagnostic Criteria

The normal values of serum TC, TG, HDL-C and LDL-C in our Clinical Science Experiment Center were 3.10–5.72, 0.56–1.70, 0.91–1.81 and 1.70–3.61 mmol/L, respectively. Individuals with TC > 5.72 mmol/L and/or TG > 1.70 mmol/L were defined as hyperlipidemic patients [4]. Individuals with GLU > 7.0 mmol/L were defined as hyperglycemic patients [5].

Statistical Analysis

The analysis of variance was used to determine the difference in TC, TG, HDL-C, LDL-C and GLU values among the

different groups. The prevalence of TC, TG, HDL-C, LDL-C and GLU in the three groups was calculated. The chi-square test method was used to calculate differences in TC, TG, HDL-C, LDL-C and GLU prevalence among the three groups. A logistic model was developed to determine the odds ratio of the impact of age on adult hyperlipidemia and hyperglycemia. The SAS 9.1 statistical program was used to analyze the data.

Results

Population Characteristics

For the whole group of 548 participants with acute cerebral hemorrhage for whom we had complete data for all components of TC, TG, HDL-C, LDL-C and GLU, 356 participants (65%) were men and 162 (35%) were women. A total of 57 participants (10.40%) were in the young-age group, 182 participants (33.21%) were in the middle-age group, and 309 participants (56.39%) were in the elderly group. The comparison of sex distribution among the three groups showed no significant difference ($P>0.05$), as shown in Table 1. The characteristics of age in each group are shown in Fig. 1. We analyzed the four lipid metabolism indexes and fasting glucose levels. The proportion of high TG (36.88%), high TC (23.49%), low HDL-C (10.58%) and hyperglycemia (31.02%) were higher. But high LDL-C (14.96%) was lower as compared to the rate of high TG (26.3%), high TC (20.0%), high LDL-C (16.5%), low HDL-C (4.0%) and DM (2.7%) [20], respectively, in China, which is evident in the literature [4].

Acute Cerebral Hemorrhage Led to a High Proportion of High TG in the Young-Age Group

In Table 2 below, the various components included in this study are shown in the three groups. Participants exposed to acute cerebral hemorrhage in the young-age group had a high proportion of high TG (TG > 1.70 mmol/L) and had an OR of

Table 1 Gender distribution among the three groups

Group	Male <i>n</i> (%)	Female <i>n</i> (%)	Total <i>n</i> (%)
Young-age group	38 (66.67)	19 (33.33)	57 (10.40)
Middle-age group	114 (62.64)	68 (37.36)	182 (33.21)
Elderly group	204 (66.02)	105 (33.98)	309 (56.39)
χ^2		0.6567	
F		0.7201	

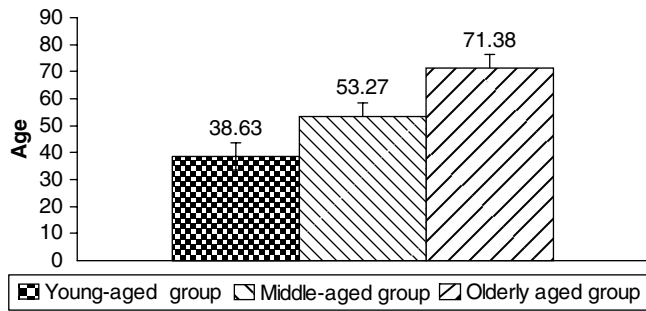


Fig. 1 Age distribution of the three groups

2.28 (1.21, 4.30) as compared to those in the elderly group. The levels of TC, TG, LDL-C, HDL-C and GLU and the proportion of high TC, high LDL-C, low HDL-C and hyperglycemia were not significantly higher in the young-age group as compared to the elderly group, as shown in Table 2.

Acute Cerebral Hemorrhage Led to a High Proportion of High TG in Middle-Age Group

In the middle-age group, there was a trend towards significantly higher levels of TG, and the proportion of high TG

(TG > 1.70 mmol/L) was more than in those who were in the elderly group. Participants who were affected by acute cerebral hemorrhage in the elderly age period had an OR of 2.37 (1.54, 3.65, vs. elderly group) for high TG and had an OR of 1.58 (1.06, 2.34, vs. elderly group). However, compared to the elderly group no trends towards significantly different levels of LDL-C, HDL-C, GLU and the proportion of high LDL-C, low HDL-C and hyperglycemia in the middle-age group were noted.

Discussion

Recurrent stroke is common, but whether young or middle-age patients have a discrepancy of serum lipid and glucose compared to old-age patients is not fully understood. The results in this study demonstrate that participants who were acute cerebral hemorrhage patients had high proportions of high TG, high TC, low HDL-C and hyperglycemia. With increasing patient age, the level of TC, TG, LDL-C, HDL-C and GLU and the proportion of high TC, high LDL-C, low HDL-C and hyperglycemia did not become high, except for TG. This means that hypertriglyceridemia of patients in the young- or middle-age period is

Table 2 Characteristics of TC, TG, LDL-C, HDL-C, and GLU according to different age groups of acute cerebral hemorrhage in adulthood

	Young-age group	Middle-age group	Elderly group
TC (M±SD) mmol/L	4.82±1.05	4.92±1.04	4.62±1.10
Number of TCs>5.72 mmol/L	19	66	82
Proportion of high TC (%)	33.33	36.26	26.54
Odds ratio of high TC (95%CI)	1.384 (0.76–2.54)	1.58 (1.06–2.34) ^a	–
TG(M(Q))mmol/L	1.16 (1.16)	1.33 (0.91) ^b	1.12 (0.69)
Number of TGs>1.70 mmol/L	18	59	52
Proportion of high TG (%)	31.58 ^c	32.42 ^c	16.83
Odds ratio of high TG (95%CI)	2.28 (1.21–4.30) ^d	2.37 (1.54–3.65) ^d	–
HDL(M±SD)mmol/L	1.42±0.52	1.38±0.47	1.35±0.41
Number of HDL-C<0.90 mmol/L	5	22	31
Proportion of low HDL (%)	8.77	12.09	10.03
Odds ratio of low HDL (95% CI)	0.86 (0.32–2.32)	1.23 (0.69–2.20)	–
LDL (mean±SD) mmol/L	2.85±0.85	2.73±0.78	2.64±0.87
Number of LDL-Cs>3.60 mmol/L	8	31	43
Proportion of high LDL (%)	14.04	17.03	13.92
Odds ratio of high LDL (95% CI)	1.10 (0.45–2.28)	1.27 (0.77–2.10)	–
GLU (mean±SD) mmol/L	6.56±2.97	6.77±2.21	6.79±2.52
Number of DMs	13	63	94
Proportion of DMs (%)	22.81	34.62	30.42
Odds ratio of DMs (95% CI)	0.68 (0.35–1.31)	1.21 (0.82–1.79)	–

^{a,d}Significantly different from participants in elderly group, P<0.05 (linear regression analysis)

^{b,c}Indicates P<0.05 vs. elderly group

a risk factor that shows an increase in the incidence rate of acute cerebral hemorrhage among the Chongqing population in China.

Stroke is a largely preventable disease, but it also remains the second or third leading cause of death among the Chinese, even with dramatic economic development in recent years [6]. As the most populated country, China has the largest number of stroke victims in the world [7]. With the aging population and the change of Chinese traditional lifestyles in recent years, the prevalence and incidence of stroke have been increasing. The rank of stroke as a cause of death in the disease spectrum is shifting forward [8]; socioeconomic costs of stroke are climbing very rapidly [9–11], and there is no definite evidence that these trends will change in the near future.

There are two main subtypes of stroke; one is hemorrhagic stroke, and the other is ischemic. As shown in epidemiological studies, cerebral hemorrhage occurs at younger ages than ischemic stroke. The incidence of cerebral hemorrhage reaches a peak at about 55–65 years of age [7]. In our study, we found that the proportion of cerebral hemorrhage was highest among Chongqing participants who were more than 60 years old. This discrepancy is largely due to the increasing age of people; the prevalence of hypertension and arteriosclerosis is also increasing. Thus, an increased proportion of elderly people in a given population will increase the age at which hemorrhagic stroke occurs.

Epidemiological evidence suggests that there are many risk factors for hemorrhagic stroke, such as hypertension [12], arteriosclerosis, a high serum lipoprotein (a) concentration and low apolipoprotein A-I [13]. Another study showed that the most frequent vascular risk factors were hypertension, hyperlipidemia, and diabetes [14]. In this study, we found that participants who were acute cerebral hemorrhage patients had a higher proportion of high TG, high TC, low HDL-C, and hyperglycemia than normal people. Although dyslipidemia and hyperglycemia are not directly involved in the incidence of cerebral hemorrhage, they can lead to atherosclerosis and indirectly lead to the occurrence of cerebral hemorrhage. Serum cholesterol and triglyceride levels are strong independent predictors of in-hospital mortality of patients with spontaneous supratentorial cerebral hemorrhage [15]. However, some studies suggest that there are no significant differences in blood lipid levels between the patients with cerebral hemorrhage and normal people [16].

Lipids metabolism has been extensively studied between the large number of patients with cerebral hemorrhage and normal people. However, the different ages of patients with cerebral hemorrhage were customarily excluded from most studies. Results of this study indicated that in subtypes of dyslipidemia, only hypertriglyceridemia is a risk factor for acute cerebral hemorrhage for patients in the young or middle-age periods. These results support the existence of a

vicious cycle between ethanol and fat. Within this vicious cycle, ethanol and fat act synergistically to increase TG levels, and these phenomena are reversed by gemfibrozil, which lowers TG levels [17]. We suggest that the high levels of TG were caused by ethanol consumption in the young and middle-age population.

There are some matters that need to be considered in interpreting our findings, such as BMI, socioeconomic status, and health care. In addition, this study is a retrospective study, so we need an epidemiological investigation in order to further clarify the relationships among different ages of patients with acute cerebral hemorrhage and the lipid metabolism and glycometabolism.

Acknowledgments In this study, we thank all participants: the data collection team of the First Affiliated Hospital of Chongqing Medical University, Chongqing, China. Gopall Roshnee has provided great help in modifying the language of this article. The work was supported by the Foundation of the First Affiliated Hospital of Chongqing Medical University (YXJJ2009-14).

Conflict of interest statement The study is supported by a foundation issued by the First Affiliated Hospital of Chongqing Medical University.

References

- Centers for Disease Control and Prevention (CDC) (2007) Prevalence of stroke—United States, 2005. *MMWR Morb Mortal Wkly Rep* 56:469–474
- Strong K, Mathers C, Bonita R (2007) Preventing stroke: saving lives around the world. *Lancet Neurol* 6:182–187
- Sauerbeck LR (2006) Primary stroke prevention. *Am J Nurs* 106:40–41, 43–45, 48–49; quiz 49–50
- Juan Z, Yonghong W, Jihong W (2007) Clinical research of lipid metabolism feature and lipid metabolism disorders of 9528 health examination people in Chongqing. *Chin J Health Lab Technol* 17:299–301
- Allende-Vigo M (2001) Diabetes mellitus: current concepts in diagnosis, classification and coding. *P R Health Sci J* 20:119–122
- He J, Gu D, Wu X, Reynolds K, Duan X, Yao C, Wang J, Chen CS, Chen J, Wildman RP, Klag MJ, Whelton PK (2005) Major causes of death among men and women in China. *N Engl J Med* 353:1124–1134
- Xu G, Liu X (2008) Impacts of population aging on the subtypes of stroke. *Stroke* 39:e102–e103; author reply e104–105
- Kincannon CL, He W, West LA (2005) Demography of aging in China and the United States and the economic well-being of their older populations. *J Cross Cult Gerontol* 20:243–255
- Heeley E, Anderson CS, Huang Y, Jan S, Li Y, Liu M, Sun J, Xu E, Wu Y, Yang Q, Zhang J, Zhang S, Wang J (2009) Role of health insurance in averting economic hardship in families after acute stroke in China. *Stroke* 40:2149–2156
- Lim SJ, Kim HJ, Nam CM, Chang HS, Jang YH, Kim S, Kang HY (2009) Socioeconomic costs of stroke in Korea: estimated from the Korea national health insurance claims database. *J Prev Med Public Health* 42:251–260
- Wang YL, Wu D, Liao X, Zhang W, Zhao X, Wang YJ (2007) Burden of stroke in China. *Int J Stroke* 2:211–213

12. Zhang XF, Attia J, D'Este C, Yu XH (2004) Prevalence and magnitude of classical risk factors for stroke in a cohort of 5,092 Chinese steelworkers over 13.5 years of follow-up. *Stroke* 35:1052–1056
13. Woo J, Lau E, Lam CW, Kay R, Teoh R, Wong HY, Prall WY, Kreel L, Nicholls MG (1991) Hypertension, lipoprotein (a), and apolipoprotein A-I as risk factors for stroke in the Chinese. *Stroke* 22: 203–208
14. Leoo T, Lindgren A, Petersson J, Von Arbin M (2008) Risk factors and treatment at recurrent stroke onset: results from the Recurrent Stroke Quality and Epidemiology (RESQUE) Study. *Cerebrovasc Dis* 25:254–260
15. Roquer J, Rodriguez Campello A, Gomis M, Ois A, Munteis E, Bohm P (2005) Serum lipid levels and in-hospital mortality in patients with intracerebral hemorrhage. *Neurology* 65: 1198–1202
16. Xu H, Yang Q, Tang B (1998) Studies on stroke and blood lipid level. *Zhonghua Yu Fang Yi Xue Za Zhi* 32:366–368
17. Barson JR, Karatayev O, Chang GQ, Johnson DF, Bocarsly ME, Hoebel BG, Leibowitz SF (2009) Positive relationship between dietary fat, ethanol intake, triglycerides, and hypothalamic peptides: counteraction by lipid-lowering drugs. *Alcohol* 43:433–441

Prognosis of Cerebral Hemorrhage

The Role of a High Augmentation Index in Spontaneous Intracerebral Hemorrhage to Prognosticate Mortality

Lee Hock Keong, Ab Rahman Izaini Ghani, Mohamed Saufi Awang, Sani Sayuthi, Badrisyah Idris, and Jafri Malin Abdullah

Abstract The aim of the study was to determine the prognostic value of a high augmentation index, which was a surrogate marker of arterial stiffness in patients with spontaneous intracerebral hemorrhage. The outcome was divided into two groups in which the following data were collected in a computer running SphygmoCor CvMS software version 8.2. Logistic regression analysis was carried out among significant variables to identify an independent predictor of 6-month outcome and mortality. Sixty patients were recruited into the study. Admission Glasgow Coma Scale score (OR, 0.7; 95% CI, 0.450–0.971; $P=0.035$), total white cell count (OR, 1.2; 95% CI, 1.028–1.453; $P=0.023$) and hematoma volume (OR, 1.1; 95% CI, 1.024–1.204; $P=0.011$) were found to be statistically significant for identifying poor 6-month outcome in multivariate analysis.

Factors independently associated with mortality were a high augmentation index (OR, 8.6; 95% CI, 1.794–40.940; $P=0.007$) and midline shift (OR, 7.5; 95% CI, 1.809–31.004; $P=0.005$). Admission Glasgow Coma Scale score, total white cell count and hematoma volume were significant predictors for poor 6-month outcome, and a high augmentation index and midline shift were predictors for 6-month mortality in this study.

Keywords Augmentation index · Intracerebral hemorrhage · Glasgow Coma Scale

L.H. Keong, Ab R.I. Ghani, M.S. Awang, S. Sayuthi, B. Idris, and J.M. Abdullah (✉)
Department of Neurosciences, School of Medical Sciences, Universiti Sains Malaysia, Health Campus, Jalan Sultanah Zainab 2, Kubang Kerian, Kota Bharu, 16150, Kelantan, Malaysia
e-mail: brainsciences@gmail.com

Introduction

Intracerebral hemorrhage (ICH) accounts for 15–30% of all strokes and had an estimated incidence of 37,000 cases per year [1]. The 6-month morbidity and mortality of ICH reported in one recent study were 30–50%, and only 20% of patients regain functional independence at 6 months [2]. The aim of the study was to analyze whether a high augmentation index was associated with poor 6-month outcome (Modified Rankin Scale 5 and 6) or 6-month mortality in ICH patients.

Materials and Methods

This prospective study was conducted at Hospital University Sciences in Malaysia from May 2006 to May 2008. Patients were eligible for inclusion if they gave consent or if assent was obtained from the relatives, if aged between 18 and 85 years, and if evidence of spontaneous supratentorial intracerebral hemorrhage was present on the initial CT brain scan. Other exclusion criteria were history of severe heart disease, previous history of stroke, end-stage renal failure and severe systemic diseases (like malignant disease and chronic lung diseases) that could interfere with the assessment of the outcome, and severe preexisting physical or mental disability.

The diagnosis of spontaneous supratentorial intracerebral hemorrhage was based on a history of typical acute clinical onset and confirmed with the finding of a CT scan of the brain. Spontaneous intracerebral hematomas were those that occurred without an associated history of trauma, coagulopathy or surgery. Demographic data such as age and sex were recorded initially. The risk factors for ICH, including hypertension (HPT), diabetes mellitus (DM), smoking status and hypercholesterolemia, were recorded. Glasgow Coma Scale score (GCS) at the emergency department was recorded. The height (Ht), weight (Wt), body mass index (BMI), systolic blood pressure (SBP), diastolic blood pressure (DBP),

mean arterial pressure (MAP), heart rate (HR), right carotid blood flow (right CBF), left carotid blood flow (left CBF) and augmentation index (AIx) were measured and recorded on admission. The bilateral internal carotid blood flow was measured using a DWL Embo-Dop Doppler machine with a 2-MHz probe. The augmentation index was defined as the proportion of central pulse pressure due to late systolic peak, which was in turn attributed to the reflected pulse wave. The SphygmoCor System (AtCor Medical, Sydney, Australia) was used to record radial artery pressure waveform data by a small handheld tonometer. The acquired data were used to calculate central pressure through a generalized mathematical transfer function. Those with values of higher than normal range were labeled high augmentation index (high AIx), which was suggestive of arterial stiffness. The cardiothoracic ratio was measured from the chest X-ray to rule out cardiomegaly (cardiothoracic ratio >0.5). The CT scan findings, such as the side of hematoma, site of hematoma, volume of hematoma, any evidence of midline shift (MLS), ventricular extension (IVH) and hydrocephalus, were recorded. Supratentorial intracranial hematoma can be classified into lobar (frontal, parietal, temporal or occipital) or ganglionic (basal ganglia, thalamic).

Intracranial hematoma volume was measured with the ABC/2 method, in which A was the greatest diameter on the largest hemorrhage slice, B was the diameter perpendicular to A, and C was the appropriate number of axial slices with the hematoma multiplied by the slice thickness. Patients were followed up for a maximum period of 6 months from the onset of stroke. The outcome measure was the score on the modified Rankin scale at 6 months. The 6-month outcomes were divided into two groups; good outcome was defined as a score of 0–4, and poor outcome was defined as a score of 5 and 6. Data entry and analysis were done using Statistical Package for Social Sciences (SPSS) version 12.0 for Windows (SPSS Inc., Chicago, IL). A *P* value of less than 0.05 was considered statistically significant for univariate analysis. The final model of factors was examined for fitness by using the Hosmer-Lemeshow goodness-of-fit test.

Result

The univariate analysis as shown in Table 1 revealed GCS ($p=0.003$), TWC ($p=0.048$), site of hematoma ($p=0.009$), volume of hematoma ($p=0.21$), MLS ($p<0.0001$) and hydrocephalus ($p=0.007$) were associated with poor 6-month outcome. Parameters associated with 6-month mortality in univariate analysis were DM ($p=0.030$), HR ($p=0.050$), right CBF ($p=0.023$), high AIx ($p=0.005$), RBS ($p=0.029$), urea ($p=0.004$), creatinine ($p=0.001$), midline shift ($p=0.003$) and hydrocephalus ($p=0.006$). The final variables

predicting 6-month outcome and mortality in this study are shown in Table 2 and 3.

Discussion

This prospective study showed that a high augmentation index (OR, 8.6; 95% CI, 1.748–40.940; $P=0.007$) was a significant predictor for 6-month mortality in patients with ICH. Patients with a high augmentation index had 8.6 times the risk of mortality. The augmentation index as one of the surrogate markers for arterial stiffness was proven to be useful in predicting cardiovascular event in end-stage renal failure [3], coronary artery disease [4] and patients undergoing percutaneous coronary interventions [5]. Old age was an important factor linked to poorer prognosis in ICH [6–8]. A recent study done by Smajlovic et al. to explore 30-day prognosis in 352 patients with intracerebral hemorrhage concluded that age was an independent predictor for 30-day mortality [9]. Our study showed no significant association between age and outcome, which was probably due to the small sample size. On analyzing the risk factors (hypertension, diabetes mellitus, current smoker and hypercholesterolemia) for ICH in this study, none of these factors had an association with ICH outcome and mortality. Smajlovic et al. reported that hypertension, diabetes mellitus and smoking were not associated with ICH outcome and mortality [9].

Togha et al. and Passero et al. had shown diabetes mellitus was associated with poor outcome and mortality in ICH [10, 11]. With regard to various clinical parameters in this study, Glasgow Coma Scale score was the significant predictor of ICH 6-month outcome. Patients with high GCS scores had 0.7 times the chance of being associated with poor outcome. These findings were in accordance with many other studies that found GCS to be the most important and consistent predictor of ICH outcome and mortality [11–16]. In our study, the hemoglobin and platelet levels were not associated with ICH outcome and mortality. Hematoma volume (OR, 1.1; 95% CI, 1.024–1.204; $P=0.011$) was the significant predictor of a poor 6-month outcome, whereas MLS (OR, 7.5; 95% CI, 1.809–31.004; $P=0.005$) was a significant predictor of ICH 6-month mortality.

Larger hematoma volume carried 1.1 times the risk of poor outcome. A study done by Delgado et al. involving 98 ICH patients showed an ICH volume >30 mL was an independent predictor for ICH mortality [17]. Associated intraventricular hemorrhage and hydrocephalus were important predictors of poor outcome in ICH [18]. In this study, radiological factors such as hydrocephalus and intraventricular hemorrhage did not significantly affect the ICH outcome and mortality. This could be because the type of in-patient treatment (conservative or surgical) and surgical treatments

Table 1 Univariate analysis of various demographic, clinical, laboratory, radiographic and treatment parameters in relation to 6-month mortality

Continuous variables	Survived (<i>n</i> =38) mean±SD	Fatal (<i>n</i> =22) mean±SD	<i>p</i> -value	
Age	55.4±10.8	59.0±9.6	0.830	
Height (m)	1.60±0.07	1.60±0.09	0.081	
Weight (kg)	70.1±9.9	68.2±12.4	0.124	
BMI (kg/m ²)	27.7±3.9	26.4±3.2	0.369	
SBP (mmHg)	193.2±25.9	202.3±28.0	0.427	
DBP (mmHg)	112.0±15.5	109.1±14.5	0.749	
MAP (mmHg)	139.1±17.4	140.3±17.7	0.549	
HR (/min)	81.6±18.4	80.4±14.2	0.050	
AIx	25.0±10.1	29.6±12.3	0.438	
Right CBF (cm/s)	17.3±4.5	18.9±7.0	0.023	
Left CBF (cm/s)	17.0±5.2	18.2±7.9	0.943	
GCS	13.0±2.4	8.7±3.1	0.260	
TWC (×10 ³ /μL)	11.1±3.6	14.5±7.1	0.162	
HB (g/dL)	13.8±2.0	13.5±2.1	0.507	
PLT (×10 ³ /μL)	245.8±60.3	268.7±75.9	0.103	
RBS (mmol/L)	7.08±2.46	8.66±3.99	0.029	
Na (mmol/L)	136.9±4.8	136.6±3.9	0.455	
K (mmol/L)	3.32±0.48	3.52±0.54	0.362	
Urea (mmol/L)	6.17±1.99	6.93±4.79	0.004	
Creatinine (mmol/L)	116.5±38.9	164.2±151.2	0.001	
INR	1.06±0.10	1.05±0.11	0.644	
APTT (s)	31.2±6.2	29.6±7.0	0.402	
LDL (mmol/L)	3.70±1.31	3.92±1.55	0.692	
TG (mmol/L)	1.17±0.51	1.60±0.90	0.053	
Total cholesterol (mmol/L)	5.48±1.49	6.03±1.78	0.858	
HDL (mmol/L)	1.25±0.31	1.35±0.40	0.377	
Volume of hematoma (mL)	14.6±17.5	31.2±16.7	0.924	
Categorical variables	Good outcome <i>n</i> (%)	Poor outcome <i>n</i> (%)	<i>p</i> value	OR (95% CI)
Gender			0.662 ^a	0.786 (0.266–2.317)
Male	22 (61.1)	14 (38.9)		
Female	16 (66.7)	8 (33.3)		
HPT			1.000 ^b	1.167 (0.100–13.656)
Yes	36 (63.2)	21 (36.8)		
No	2 (66.7)	1 (33.3)		
DM			0.030 ^a	3.692 (1.093–12.477)
Yes	6 (40)	9 (60)		
No	32 (71.1)	13 (28.9)		
smoking			0.705 ^a	1.238 (0.410–3.740)
Yes	12 (60)	8 (40)		
No	26 (65)	14 (35)		
hypercholesterolemia			0.388 ^a	1.603 (0.548–4.691)
Yes	13 (56.5)	10 (43.5)		
No	25 (67.6)	12 (32.4)		
high AIx			0.005 ^a	5.500 (1.559–19.400)
Yes	5 (33.3)	10 (66.7)		
No	33 (73.3)	12 (26.7)		

(continued)

Table 1 (continued)

Categorical variables	Good outcome <i>n</i> (%)	Poor outcome <i>n</i> (%)	<i>p</i> value	OR (95% CI)
cardiomegaly			0.047 ^a	0.320 (0.102–1.006)
Yes	30 (71.4)	12 (28.6)		
No	8 (44.4)	10 (55.6)		
site of hematoma			0.191 ^a	0.254 (0.028–2.263)
Lobar	6 (85.7)	1 (14.3)		
Ganglionic	32 (60.4)	21 (39.6)		
side of hematoma			0.694 ^a	1.235 (0.431–3.538)
Right	21 (63.6)	11 (36.4)		
Left	17 (60.7)	11 (39.3)		
MLS			0.003 ^a	5.417 (1.709–17.167)
Yes	8 (38.1)	13 (61.9)		
No	30 (76.9)	9 (23.1)		
IVH			0.095 ^a	2.476 (0.845–7.259)
Yes	14 (51.9)	13 (48.1)		
No	24 (72.7)	9 (27.3)		
hydrocephalus			0.006 ^a	5.885 (1.541–22.474)
Yes	4 (30.8)	9 (69.2)		
No	34 (72.3)	13 (27.7)		
Treatment			0.958 ^a	1.042 (0.224–4.854)
Conservative	33 (63.5)	19 (36.5)		
Surgery	5 (62.5)	3 (37.5)		
EVD			0.659 ^b	1.842 (0.338–10.033)
Yes	3 (50)	3 (50)		
No	35 (64.8)	19 (35.2)		
craniotomy			0.528 ^b	0
Yes	2 (100)	0 (0)		
No	36 (62.1)	22 (37.9)		

^aChi-square test^bFisher's exact test**Table 2** Final model with significant variables predicting poor 6-month outcome

Variable	B	SE	Wald	OR (95% CI)	<i>P</i> value
GCS	-0.414	0.196	4.458	0.7 (0.450–0.971)	0.035
TWC	0.200	0.088	5.149	1.2 (1.028–1.453)	0.023
Volume of hematoma	0.105	0.041	6.395	1.1 (1.024–1.204)	0.011

Adjusted for GCS, TWC, site of hematoma, volume of hematoma, MLS and hydrocephalus

Constant = 1.881

Hosmer and Lemeshow test *p*-value = 0.188

Overall percentage correct = 85%

Table 3 Final model with significant variables predicting 6-month mortality

Variable	B	SE	Wald	OR (95% CI)	<i>P</i> value
High AIX	2.148	0.798	7.250	8.6 (1.748–40.940)	0.007
MLS	2.014	0.725	7.718	7.5 (1.809–31.004)	0.005

Adjusted for DM, HR, right CBF, high AIX, cardiomegaly, RBS, urea, creatinine, MLS and hydrocephalus

Constant = -2.280

Hosmer and Lemeshow test *p*-value = 0.141

Overall percentage correct = 78.3%

(EVD or craniotomy) were not associated with outcome and mortality in this study because of the small sample size.

Conclusions

This prospective study involving 60 ICH patients, the 6-month mortality of 36.7% and 60% of them had poor 6-month outcome (Modified Rankin Scale score 5 and 6). Glasgow Coma Scale score (OR, 0.7; 95% CI, 0.450–0.971; $P=0.035$), total white cell count (OR, 1.2; 95% CI, 1.028–1.453; $P=0.023$) and volume of hematoma (OR, 1.1; 95% CI, 1.024–1.204; $P=0.011$) were the independent predictors of 6-month outcome in multivariate analysis. The significant predictors for 6-month mortality in ICH patients were high augmentation index (OR, 8.6; 95% CI, 1.794–40.940; $P=0.007$) and midline shift (OR, 7.5; 95% CI, 1.809–31.004; $P=0.005$). There was no difference between these results compared to a 3-month follow-up study published recently [19]

Acknowledgments Prof Jafri Malin Abdullah FASc, MD, PhD, FRCS (Ed), FACS, FICS (USA), FWFNS, DSCN (Belgium) Chairperson of Task Force of the Academy of Science Malaysia in improving Research and Development in Health and Medical Sciences

Conflict of interest statement We declare that we have no conflict of interest.

References

- Thompson KM, Gerlach SY, Jorn HK, Larson JM, Brott TG, Files JA (2007) Advances in the care of patients with intracerebral hemorrhage. *Mayo Clin Proc* 82:987–990
- Sacco RL, Mayer SA (1994) Epidemiology of intracerebral hemorrhage. In: Feldmann E (ed) *Intracerebral hemorrhage*. Futura Publishing, New York, pp 3–23
- London GM, Blacher J, Pannier B, Guerin AP, Marchais SJ, Safar ME (2001) Arterial wave reflections and survival in end-stage renal failure. *Hypertension* 38:434–438
- Chirinos JA, Zambrano JP, Chakko S, Veerani A, Schob A, Willens HJ, Perez G, Mendez AJ (2005) Aortic pressure augmentation predicts adverse cardiovascular events in patients with established coronary artery disease. *Hypertension* 45:980–985
- Weber T, Auer J, O'Rourke MF, Kvas E, Lassnig E, Lamm G, Stark N, Rammer M, Eber B (2005) Increased arterial wave reflections predict severe cardiovascular events in patients undergoing percutaneous coronary interventions. *Eur Heart J* 26:2657–2663
- Fieschi C, Carolei A, Fiorelli M, Argentino C, Bozzao L, Fazio C, Salvetti M, Bastianello S (1988) Changing prognosis of primary intracerebral hemorrhage: results of a clinical and computed tomographic follow-up study of 104 patients. *Stroke* 19:192–195
- Franke CL, van Swieten JC, Algra A, van Gijn J (1992) Prognostic factors in patients with intracerebral haematoma. *J Neurol Neurosurg Psychiatry* 55:653–657
- Hardemark HG, Wesslen N, Persson L (1999) Influence of clinical factors, CT findings and early management on outcome in supratentorial intracerebral hemorrhage. *Cerebrovasc Dis* 9:10–21
- Smajlovic D, Salihovic D, Ibrahimagic OC, Sinanovic O, Vidovic M (2008) Analysis of risk factors, localization and 30-day prognosis of intracerebral hemorrhage. *Bosn J Basic Med Sci* 8:121–125
- Passero S, Ciacci G, Olivelli M (2003) The influence of diabetes and hyperglycemia on clinical course after intracerebral hemorrhage. *Neurology* 61:1351–1356
- Togha M, Bakhtavar K (2004) Factors associated with in-hospital mortality following intracerebral hemorrhage: a three-year study in Tehran, Iran. *BMC Neurol* 4:9
- Karnik R, Valentin A, Ammerer HP, Hochfelner A, Donath P, Slany J (2000) Outcome in patients with intracerebral hemorrhage: predictors of survival. *Wien Klin Wochenschr* 112:169–173
- Marti-Fabregas J, Belvis R, Guardia E, Cocho D, Munoz J, Marruecos L, Vilalta JLM (2003) Prognostic value of pulsatility Index in acute intracerebral hemorrhage. *Neurology* 61:1051–1056
- Muiz AJ, Abdullah J, Naing NN, Ghazaim G, Ariff AR (2003) Spontaneous intracerebral hemorrhage in northeast Malaysian patients: a four-year study. *Neuroepidemiology* 22:184–195
- Roquer J, Rodríguez Campello A, Gomis M, Ois A, Puente V, Munteis E (2005) Previous antiplatelet therapy is an independent predictor of 30-day mortality after spontaneous supratentorial intracerebral hemorrhage. *J Neurol* 252:412–416
- Schwarz S, Hafner K, Aschoff A, Schwab S (2000) Incidence and prognostic significance of fever following intracerebral hemorrhage. *Neurology* 54:354–361
- Delgado P, Alvarez-Sabin J, Abilleira S, Santamarina E, Purroy F, Arenillas JF, Molina A, Cadenas IF, Rosell A, Montaner J (2006) Plasma D-dimer predicts poor outcome after acute intracerebral hemorrhage. *Neurology* 67:94–98
- Razzaq AA, Hussain R (1998) Determinants of 30-day mortality of spontaneous intracerebral hemorrhage in Pakistan. *Surg Neurol* 50:336–342; discussion 342–343
- Lee HK, Ghani AR, Awang MS, Sayuthi S, Idris B, Abdullah JM (2010) Role of high Augmentation Index in Spontaneous Intracerebral Haemorrhage. *Asian J. Surg* 33:42–50.

Effect of Minimally Invasive Aspiration in Treatment of Massive Intracerebral Hemorrhage

Guangqin Li, Xinyue Qin, Guoguang Pen, Wanfu Wu, Jun Yang, and Qin Yang

Abstract Objective: To observe the effect of minimally invasive aspiration combined with medication in patients with massive spontaneous intracerebral hemorrhage.

Methods: Twenty-three patients with massive primary intracerebral hematoma (>50 mL), presenting with depressed consciousness, were recruited. Minimally invasive aspiration was applied within 72 h after onset, along with mannitol or furosemide to lower the intracranial pressure and symptomatic treatment.

Results: Within 1 month after hemorrhage, three patients recovered to normal activity; the consciousness level of eight had improved; three patients remained stable; three patients had aggravated conditions and were discharged automatically (two with rehemorrhage and one with complications). Six patients died (hematoma volume of all patients was above 80 mL).

Conclusions: Minimally invasive aspiration may be effective in patients with massive intracerebral hemorrhage, but it had a poor prognosis for those patients whose hematoma volume was above 80 mL.

Keywords Intracerebral hemorrhage · Aspiration · Prognosis

Introduction

The role of minimally invasive surgery in the treatment of intracerebral hemorrhage (ICH) has gained attention over the past decade. This can be attributed to the lack of validated therapeutic options for this form of stroke as well as to the high morbidity and mortality associated with it. Massive

spontaneous ICH is associated with poor response either to medications or to craniotomy operations [1]. Traditional medical and surgical approaches, proposed mainly based on clinical experience, have been unable to favorably modify the neurological outcome of these patients. This study aims to examine whether minimally invasive aspiration in patients with massive intracerebral hemorrhage associated with depressed consciousness improves the ultimate outcome.

Materials and Methods

Patient Selection

Twenty-three patients admitted for massive primary intracerebral hematoma (hematoma > 50 mL), confirmed by CT, were recruited from 2007 to 2009. The exclusion criteria were: a hemorrhage due to tumor, trauma, aneurysm, arteriovenous malformation, or coagulopathy. Eighteen patients were male and five female, and the age range was 31–84. Eighteen patients had hypertension, two had hypertension and diabetes, and three had had ICH in the past.

Aspiration Time

Minimally invasive aspiration was applied between 6 and 72 h after onset (17 patients) or within 6 h after the hematoma enlarged (6 patients).

Procedure of Aspiration

CT scans were performed on the patients to locate the hematoma before aspiration. Under local anesthesia, a burr hole was drilled ipsilaterally by a YL-1 type metal needle, and a

G. Li (✉), X. Qin, G. Pen, W. Wu, J. Yang, and Q. Yang
Department of Neurology, The First Affiliated Hospital of Chongqing Medical University, Chongqing, China
e-mail: liguangqin@tom.com

tube was used for drainage. The volume of the first aspiration was less than half of the total volume of the hematoma. Urokinase (40,000 IU/day) was administered through a needle. The needle was removed when repeat CT scanning revealed the volume of the residual hematoma was below one third of the hematoma before aspiration. The patients were also given mannitol or furosemide to decrease the intracranial pressure and symptomatic treatment.

Results

Six patients (26%) were 31–50 years old, nine (39%) were 51–70, and eight (35%) were over 70. Twelve patients (52%) were in a coma, eight (35%) in a stupor, and three (13%) in somnolent state before aspiration. The hematoma of 18 patients (78%) was in the basal ganglia, for only 5 patients (22%) in the cerebral lobe. The hematoma volume of 14 patients (61%) was 50–80 mL and of 9 patients (39%) was above 80 mL.

Within 1 month after hemorrhage, three (13%) patients recovered to normal activity levels; eight (35%) patients had improved conscious levels; three (13%) remained stable; three (13%) had aggravated conditions and were discharged automatically (two because of rehemorrhage and one because of complications). Six (26%) patients died (hematoma volume of all cases was above 80 mL): two died within 24 h after aspiration because of cerebral herniation, the other four had pulmonary infections (two had multiple organ failure).

Discussion

Intracerebral hemorrhage (ICH) has high mortality and morbidity, especially massive ICH. Thirty-day mortality after ICH approaches 50%. Evacuation of the hematoma via craniotomy is controversial. Minimally invasive aspiration is as effective as conventional craniotomy for reducing the volume of brain edema caused by hematomas, and has the shortest operative time and the least amount of blood loss, especially endoscopic surgery [2]. However, the effect of minimally invasive aspiration on massive ICH has not been extensively reported.

In this study, 23 patients with massive ICH whose hematoma volume was above 50 mL and associated with depressed consciousness were given minimally invasive aspiration. Eleven patients (48%) had ameliorated conditions, and six patients (26%) died. Most of the patients had a good outcome. Chen et al. [3] reported a newly developed endoscopic sheath for the removal of large putaminal hematomas (the volume >40 mL) within 5 h after onset; the

mean Glasgow Outcome Scale (GCS) score increased from 8 preoperatively to 12 postoperatively; the 1-month mortality rate was 16%; 1 year postoperatively, the mean GCS score was 2.7. Thus, endoscopic removal of large putaminal hematomas is safe and effective.

According to the literature, most hematoma enlargement occurs within 6 h after ictus. If performed during an unstable period, acute decompression (<2 h from onset) can provoke rebleeding. Thus, many authors agreed that the waiting time for the removal of a hematoma should be more than 6 h after onset. In this study, the waiting time for aspiration was therefore set for at least 6 h after onset or within 6 h after the hematoma enlarged. The hematomas of six patients enlarged in our study. However, recently some authors reported that the removal of hematomas within 6 h after onset is safe and effective [3].

If the amount of hematoma first removed is too much, it will provoke rebleeding because of the decreased pressure. Therefore, the amount of first removal was less than 1/2 of the hematoma, and urokinase was injected into the hematoma daily to facilitate drainage [4]. In this study, the hematoma volume of all the patients was more than 50 mL. The patients whose hematoma volume was more than 80 mL had a poor prognosis and very high mortality.

Conclusion

This study suggested that minimally invasive aspiration may be effective for patients with massive intracerebral hemorrhage, and therefore, it may be a promising method. However, it had a poor prognosis for those patients whose hematoma volume was above 80 mL.

Conflict of interest statement We declare that we have no conflict of interest.

References

1. Broderick J, Connolly S, Feldmann E et al (2007) Guidelines for the management of spontaneous intracerebral hemorrhage in adults: 2007 update. *Stroke* 38:2001–2023
2. Cho DY, Chen CC, Chang CS et al (2006) Endoscopic surgery for spontaneous basal ganglia hemorrhage: comparing endoscopic surgery, stereotactic aspiration, and craniotomy in noncomatose patients. *Surg Neurol* 65:547–556
3. Chen CC, Chung HC, Liu CL et al (2009) A newly developed endoscopic sheath for the removal of large putaminal hematomas. *J Clin Neurosci* 16:1338–1341
4. Xu DF (2009) Clinical research of minimally invasive needle combined urokinase in treatment of cerebral hematoma. *Chin J Mod Drug Appl* 3:16–18

Retrospective Analysis of the Predictive Effect of Coagulogram on the Prognosis of Intracerebral Hemorrhage

Yonghong Wang, Xiaolin Wang, Yuhan Kong, Fengzeng Li, and Hui Chen

Abstract Objective: To determine the effective index of coagulogram after acute intracerebral hemorrhage (ICH) for predicting the outcome of ICH.

Methods: A total of 641 patients with ICH were divided into two groups: the effective treatment group (healing well and improving) and ineffective treatment group (non-improving and dying). The coagulogram results of the two groups were analyzed with SPSS software 13.0, including PT, APTT, TT, and Fbg. The differences in these parameters were found by independent samples *T* test and Kruskal-Wallis test between the two groups. Then, the different parameters were obtained by logistic regression, which were significantly associated with the prognosis of acute cerebral hemorrhage patients. In addition, the odds ratio for the special indicators was calculated by chi-square test.

Results: Only PT had a significant difference between the groups ($p < 0.05$) among the four parameters. The binary logistic regression analysis indicated that PT ($p = 0.003$) and APTT ($p = 0.043$) were related to the outcome of ICH patients. According to the chi-square test, the OR (odds ratio) of prolonged PT is 2.40 (1.34–4.29 with 95% CI) and that of prolonged APTT is 1.57 (1.01–2.42 with 95% CI).

Conclusion: Prolonged PT and APTT are risk factors affecting the prognosis of ICH patients. Monitoring and controlling PT and APTT are advisable for improving the prognosis of ICH patients.

Keywords Intracerebral hemorrhage · Coagulogram · Prognosis

Y. Wang, X. Wang, and Y. Kong
The Medical Examination Center, The First Affiliated Hospital of Chongqing Medical University, People's Republic of China 400016, Chongqing

F. Li and H. Chen (✉)
Clinical laboratories, The First Affiliated Hospital of Chongqing Medical University, People's Republic of China 400016, Chongqing
e-mail: chen1970chen@yahoo.com

Introduction

With the increasing of aging population and the changing of dietary habit, the incidence of cerebrovascular diseases has been increasing yearly. Among these, acute intracerebral hemorrhage (ICH) is one of the important leading causes of death. Many debates are ongoing about how to treat ICH patients, including the use of coagulants to enhance the function of clotting or the use of anticoagulants to minimize thrombin damage of the nerve cells. In order to provide more evidence for the treatment of ICH in practice, the relationship between changes of coagulation function and prognosis of ICH deserves to be investigated further. In this study, we analyzed the association between coagulogram and the prognosis of 641 ICH patients retrospectively in order to find an effective index for predicting the turnover of ICH, and to provide reference for clinical treatment.

Materials and Methods

From May 2005 to September 2009, 641 ICH patients were included in our research group. These patients were primarily admitted to the Department of Neurology of The First Affiliated Hospital of Chongqing Medical University. All patients underwent either a CT scan or MRI of the brain, and met the diagnostic criteria of cerebrovascular disease established in the All-China Conference of Cerebrovascular Disease in 1995.

These patients were divided into three groups: (1) effective treatment group (healing well and improving, $n = 473$); (2) ineffective treatment group (non-improving and dying, $n = 131$); (3) follow-up failure group ($n = 37$, did not participate in follow-up research).

All venous blood samples were collected after admission before drug administration; 0.9% sodium citrate was used as an anticoagulant for the sample (0.2 ml 0.9% sodium citrate vs. 1.8 ml venous blood). The coagulogram

was tested by a Sysmex CA1500 coagulation analyzer with Dade Behring's reagent. The following parameters were analyzed: prothrombin time (PT), activated partial thromboplastin time (APTT), thrombin time (TT), and fibrinogen (Fbg).

SPSS13.0 statistical package was used to synthesize the relevant data. The *T* test and Kruskal-Wallis test were used to compare the four parameters between two groups, depending on whether or not there were homogeneous variances. The logistic regression model was used to identify the parameters directly associated with the outcome of acute ICH. Chi-square test was used to calculate the odds ratio for the predictors.

Results

The Basic Situation of Patients with Acute Cerebral Hemorrhage

There were a total of 604 patients, including the effective treatment group ($n=473$) and ineffective treatment group ($n=131$). Of the 604 enrolled patients, 412 (68%) were male and 192 (32%) female. The results of the statistical analysis are shown in Table 1.

The chi-square test showed that there was no significant difference regarding genders between the two groups ($p=0.85$). As for age, significant differences existed between groups ($p<0.001$), as shown by *T* test. It seems that the older the patient is, the poorer the outcome is.

Table 1 The basic situation of the two groups

Mean \pm s	Gender		Age (years old)
	Male (<i>n</i>)	Female (<i>n</i>)	
Effective treatment group	325	158	57.0 \pm 15.7
Ineffective treatment group	87	44	63.4 \pm 15.2*

* $p<0.001$

Table 2 The difference of coagulogram between the two groups

Group	<i>N</i>	Mean \pm s			
		PT*	APTT (s)	TT (s)	Fbg (g/L)
Effective treatment group	473	286.6**	25.7 \pm 10.8	18.9 \pm 8.1	3.0 \pm 1.0
Ineffective treatment group	131	360.0**	26.15 \pm 7.4	19.0 \pm 4.1	3.1 \pm 1.1

*Mean rank ** $p<0.001$

The Difference of Coagulogram Between the Two Groups

In our hospital, the coagulogram profile included PT, APTT, TT, and Fbg. The differences in APTT, TT, and Fbg were compared with the *T* test, and PT with the Kruskal-Wallis test because of their unequal variances (Levene's test, $p<0.05$). The results of statistical analysis are shown in Table 2.

The PT of the ineffective group was significantly higher than that of the effective group ($p<0.001$), and there were no significant differences in APTT, TT, and Fbg between the two groups ($p>0.05$).

Estimation of the Prognosis of ICH with Coagulogram

The binary logistic regression analysis was done with the forward LR procedure. The elimination criterion is $p>0.05$, while for $p<0.05$, the parameter was identified as significantly related to the outcome of acute ICH. Chi-square test was used to calculate the odds ratio. The results of statistical analysis are shown in Table 3.

The binary logistic regression analysis indicates that PT and APTT are associated with the turnover of ICH ($p<0.05$). According to the chi-square test, the OR (odds ratio) of elongated PT is 2.40 (1.34–4.29 with a 95% confidence interval (CI) and that of elongated APTT is 1.57 (1.01–2.42 with 95% CI).

Table 3 The odds ratio of PT and APTT

Parameters	B estimate	Standard error	P	OR(95%CI)
Age	0.400	0.128	0.002	
PT	0.876	0.297	0.003	2.40 (1.34~4.29)
APTT	0.449	0.222	0.043	1.57 (1.01~2.42)

Discussion

In recent years, the incidence of acute ICH has shown a rising trend, especially in the elderly, with a high disability rate and mortality. The balance among coagulation, anticoagulation and fibrinolysis profile is disrupted after ICH. The body responds to the imbalance, which eventually has an impact on the prognosis of ICH. Therefore, we retrospectively analyzed the relationship between the change of the coagulogram and the prognosis of ICH in order to find some useful data from the coagulogram (including PT, APTT, TT, and Fbg) and to provide help in the treatment and prognosis of ICH.

After acute ICH, the body's coagulation system is activated. A large number of thrombin is converted from thrombogen [1], which is a key enzyme in the process of coagulation. The body is in a hypercoagulable status with decreasing fibrinolytic activity [2], and a large number of clotting factors are consumed, resulting in prolonged PT, APTT, and TT, and reduced Fbg. PT and APTT are the main indicators of exogenous and endogenous coagulation systems, respectively. In this study, the results of 604 patients with ICH showed that PT had a significant difference between the two groups. In the ineffective treatment group, PT was higher than that in the effective treatment group ($P < 0.001$). This hinted that prolonged PT may be a risk factor for ICH. Furthermore, the binary logistic regression analysis indicated that PT was a significant risk factor for the prognosis of ICH ($p = 0.003$). The OR was 2.40 (1.34–4.29 with 95% CI) with statistical significance. The logistic regression analysis indicated that APTT was also a significant factor for the prognosis of ICH ($p = 0.043$), although there was no significant difference between the two groups ($p = 0.71$). The OR was 1.57 (1.01–2.42 with 95% CI), which was smaller than that of PT. We supposed that the possible mechanism in the acute phase of ICH (within 24 h) is that a large number of clotting factors are consumed, such as prothrombin and other coagulation factors. This results in the decrease of the coagulation function and leads to an increased risk of secondary brain hemorrhage. Hence, the prolonged PT may indicate a bad prognosis to a certain extent. However, Zhang and Antovic reported that after acute ICH, the values of PT and APTT were significantly lower than those of control group ($P < 0.01$). This hinted that the patients of ICH were in a hypercoagulable status, and coagulation was hyperfunctioning [3, 4]. It seems that there was a difference in our results compared to theirs. However, this was not the case as we compared the parameters between the effective treatment group and ineffective treatment group, while Zhang and Antovic investigated between patients with ICH and had healthy patients as control.

As for TT and Fbg, our data showed that there was no significant difference between the two groups ($p > 0.05$). Furthermore, logistic regression analysis indicated TT and

Fbg were not significantly associated with the prognosis of ICH ($p > 0.05$). Liang [5] reported that Fbg of patients with ICH was lower than that of the control group. The possible reason is that a large amount of Fbg is consumed after acute ICH, but Zhang [1] reached the opposite conclusion that Fbg of the ICH patients was markedly increased, while TT showed no significant change. Chen [6] reported that there was no significant difference in TT and Fbg between the ICH group and control groups. In general, there has not been any conclusive relationship determined between the patients with ICH and control group. Our goal is to place emphasis on the coagulogram difference between the effective treatment and ineffective treatment groups. This mandates further research in the future.

Conclusion

In summary, via retrospective analysis of the relationship between the coagulogram and the prognosis of 604 patients with ICH, we found that prolonged PT and APTT may be risk factors for the prognosis of ICH. Monitoring and controlling the coagulation function may be advisable for improving the prognosis of ICH.

Acknowledgments In this study, we thank all participants and the data collection team of the First Affiliated Hospital of Chongqing Medical University. The contract grant sponsor was The First Affiliated Hospital of Chongqing Medical University, contract grant no. YXJJ2009-14.

Conflict of interest statement We declare that we have no conflict of interest.

References

1. Gong Y, Xi G, Hu H, Gu Y, Huang F, Keep RF, Hua Y (2008) Increase in brain thrombin activity after experimental intracerebral hemorrhage. *Acta Neurochir Suppl* 105:47–50
2. Xue H (2007) The function of coagulation and fibrinolysis in acute cerebral hemorrhage. *Shanxi Med J* 36:1644–1647
3. Antovic J, Bakic M, Zivkovic M, Ilic A, Blomback M (2002) Blood coagulation and fibrinolysis in acute ischaemic and haemorrhagic (intracerebral and subarachnoid haemorrhage) stroke: does decreased plasmin inhibitor indicate increased fibrinolysis in subarachnoid haemorrhage compared to other types of stroke? *Scand J Clin Lab Invest* 62(3):195–199
4. Zhang XJ (2004) The changes of coagulogram in patients with acute cerebrovascular disease. *Chin J Thromb Hemost* 10:78–80
5. Liang YT (2009) The differences of coagulation between cerebral hemorrhage and cerebral thrombosis. *Chin J Gerontol* 29:1308–1309
6. Chen YN, Sun L (2004) Correlation of prognosis with the changes of blood glucose and blood lipid and blood coagulation in patients with cerebral hemorrhage. *Chin J Clin Rehabil* 8:4512–4513

Risk Factors of Early Death in Patients with Hypertensive Intracerebral Hemorrhage During Hospitalization

Xiao Hu, John H. Zhang, and Xinyue Qin

Abstract Hypertensive intracerebral hemorrhage (ICH) is the deadliest, most disabling and least treatable form of acute cerebral accident. A large number of patients die in a short time after the hemorrhage. However, the risk factors of early death in this pattern are still in debate. A case control study of 273 patients with hypertensive ICH admitted to our hospital was carried out. The patients were divided into the death group and survival group according to clinical outcome during hospitalization. Any possible risk factors were assessed using univariate and multivariate analysis. The logistic regression analysis revealed that the following four factors were independently associated with early death: age [odds ratio (OR), 0.966; 95% confidence interval (CI), 0.936–0.997; $P=0.0327$], GCS score (OR, 1.192; 95% CI, 1.090–1.303; $P<0.001$) and systolic pressure (OR, 0.939; 95% CI, 0.772–1.142; $P<0.001$) at admission, and hematoma volume (OR, 0.8000; 95% CI, 0.807–0.959; $P=0.0037$). Cranial computed tomography imaging is an important examination method to evaluate the clinical outcome. Effective prevention of hypertension and adequate reduction of blood pressure at admission are recommended as the major measures to improve the prognosis of hypertensive ICH.

Keywords Early death · Factors · Hypertensive intracerebral hemorrhage (ICH) · Logistic regression analysis

X. Hu and X. Qin (✉)

Department of Neurology, The First Affiliated Hospital of Chongqing Medical University, Chongqing 400016, China
e-mail: qinxinyue@yahoo.com

J.H. Zhang

Department of Physiology and Pharmacology,
Department of Neurosurgery, Department of Anesthesiology,
Loma Linda University, School of Medicine, Loma Linda, CA, USA

Introduction

Hypertensive intracerebral hemorrhage (ICH) is a serious acute cerebral accident. Despite the improvement of medical treatment and surgical therapy, the mortality and the incidence of hypertensive ICH are still high. The average mortality rate for the patients with hypertensive ICH ranges from 25% to 58% [1], and about half of them will die within 30 days from onset. Most survivors will have sequelae with different degrees. Hence, the assessment of risk factors of early death is of important clinical significance and of necessity so as to predict the prognosis of hypertensive ICH. Although some predictors of poor prognosis of hypertensive ICH have been verified clinically in many countries [2–5] in recent years, there may also be possible bias concerning the predictors among different countries because of the differences in race, individual financial conditions, personal educational level and medical care in different regions. Here, we reviewed 273 cases with hypertensive ICH admitted at our hospital and tried our best to assess the risk factors of early death in order to provide neurologists with evidence for proper medical management of patients with hypertensive ICH.

Materials and Methods

Patient Population

We reviewed 273 patients with hypertensive ICH retrospectively (182 males and 91 females), with an average age of 65.82 ± 12.39 years, diagnosed at the Department of Neurology and Neurosurgery of the People's Hospital of Guizhou province from January 2005 to June 2009. All patients were admitted to our hospital within 72 h of onset or at the time of the manifestation of symptoms. Clinicians made a definite diagnosis of each patient according to the diagnostic criteria from the Fourth National Cerebrovascular Disease Congress

of China in 1995. Unenhanced computed tomographic (CT) scan or magnetic resonance imaging (MRI) was routinely performed for each patient within 24 h of admission. Angiography was performed if aneurysmal bleeding was suspected. Patients with ICH were excluded from this study for definite intracranial disease such as cerebral aneurysm, vascular malformation, amyloid angiopathy, moyamoya disease, and trauma-induced ICH. In addition, patients in need of immediate surgery and lacking in complete information were also excluded. All patients underwent standardized medical treatment at the unit according to the institutional protocol for acute cerebrovascular diseases.

The Definition of Early Death After Hypertensive ICH

The patients with hypertensive ICH died within 30 days from onset [6].

Groups

All patients with hypertensive ICH were divided into two groups: Patients who died within 30 days from onset at the hospital were designated as the death group ($n=59$), and the others who did not die served as the survival group ($n=214$).

Data Collection

The patients' neurological findings were assessed, and blood pressure was measured immediately at admission. The previous diseases and ICH onset time (defined by acute onset of headache or neurological deficit) were obtained by interviewing the patients and/or their relatives. The medications, laboratory parameters, and death time were also recorded. CT brain scans were performed with 5-mm-thick slices in all patients to define the volume, shape and locations of the hematoma. Hematoma volume (in cubic centimeters) was calculated according to Tian's formula: $V/\text{mL} = \pi/6 \times A \times B \times C$, also $(A \times B \times C)/2$; A was the maximum hematoma diameter within the maximum hemorrhage area according to CT; B was the vertical diameter to A; C was the multiplication of the involved slice number and slice thickness. Variables related to the hematoma locations included the subcortex, basal ganglia, thalamus, and cerebellum and pons. The shape of the hematoma was recorded as regular or irregular.

Intraventricular hemorrhage was recorded if present, but was not included in the hematoma volume. The second CT scan was usually obtained when the patient demonstrated neurological deterioration. Hematoma volume in the initial and the second CT scans was measured to confirm the presence or absence of hematoma growth. Hematoma enlargement was evaluated based on the study by Kazui et al. [7]. All records of the 273 patients were completed, with no missing data.

Variables

Discrete variables were gender, diabetes history, intraventricular hemorrhage, the volume, location, and shape of the hematoma, cerebral herniation, and hematoma enlargement during hospitalization. Continuous variables were age, Glasgow Coma Scale* (GCS) score, and systolic and diastolic blood pressure at admission, and white blood cell and platelet count.

Statistical Analysis

Univariate analysis of discrete variables was carried out by using the chi-square test and continuous variables by using the *T* test to detect the risk factors significantly related to early death after hypertensive ICH onset. $P < 0.05$ was of statistical significance. Then, among all the risk factors, the variables independently associated with early death were determined by using logistic regression analysis. Dependent variables were coded as zero for survival and one for early deceased patients. All statistical analyses were processed by SPSS 13.0 for Windows software.

Results

Univariate Analysis of Predictors of Early Death

Fifty-nine patients (21.6% of all 273 patients) died within 30 days, and the average time of death was 8.7118 ± 9.2644 days from onset; 49.15% of the deaths occurred in the first 3 days. The univariate analysis results of discrete data and

*The GCS [8] is a scoring system that aims to provide reliable and objective way of recording the state of the state of consciousness following hypertensive ICH.

continuous data are shown in Table 1 and in Table 2 respectively. The incidence of early death increased significantly with increasing age, systolic blood pressure at admission, white blood cell and hematoma volume, and decreased with the increase of GCS score at admission. Patients with intraventricular hemorrhage, cerebral herniation, or hematoma enlargement had a higher incidence of early death. Patients with irregularly shaped hematomas had a higher incidence of early death than patients with regularly shaped hematomas.

Multivariate Analysis of Risk Factors of Early Death

The multivariate analysis (Table 3) revealed that hematoma volume (OR, 0.8000; 95% CI, 0.807–0.959; $P=0.0037$) was negatively associated with early death. Poor GCS score (OR, 1.192; 95% CI, 1.090–1.303; $P<0.001$) and high systolic blood pressure (OR, 0.939; 95% CI, 0.772–1.142; $P<0.001$) at admission were factors independently associated with early deaths. In addition, a significant increase in

the incidence of early death was observed in older patients (OR, 0.966; 95% CI, 0.936–0.997; $P=0.0327$).

Discussion

Hypertensive ICH is a major clinical problem worldwide, and its mortality rate is comparatively high. The exploration of the risk factors of early death after hypertensive ICH onset might improve the prognosis and enhance life quality in patients. In this study, the deceased and the survivors were reported as outcome predictors of hypertensive ICH. We retrospectively reviewed 273 hospital patients with hypertensive ICH. Fifty-nine of the subjects died within 30 days from onset; 49.15% of the deaths occurred in the first 3 days. Previous studies also reported a higher mortality rate in the first 2–4 days after onset. Our study demonstrated early mortality with a higher rate of death in men (62.71%) than in women (37.29%), which is consistent with previously reported studies [9].

Univariate analysis showed that the factors associated with early death included large hemorrhagic volume, irregularly shaped hematomas, the presence of intraventricular

Table 1 Univariate analysis of discrete data

Factors		Death group <i>n</i> (%)	Survival group <i>n</i> (%)	χ^2	P value
Gender	Female	22 (37.29)	69 (32.24)	0.530	0.467
	Male	37 (62.71)	145 (67.76)		
Diabetes history	Yes	9 (15.25)	21 (9.81)	1.400	0.237
	No	50 (84.75)	193 (90.19)		
Hematoma shape ^a	Regular	46 (77.97)	202 (94.39)	15.001	0.001
	Irregular	13 (12.03)	12 (5.61)		
Hematoma location	Subcortex	8 (13.56)	50 (23.36)	3.852	0.278
	Basal ganglia	30 (50.85)	102 (47.66)		
	Thalamus	8 (13.56)	31 (14.49)		
	Cerebellum and pons	13 (22.03)	31 (14.49)		
Intraventricular hematoma ^a	Yes	30 (50.85)	40 (18.69)	25.082	0.001
	No	29 (49.15)	174 (81.31)		
Cerebral herniation ^a	Yes	8 (11.86)	1 (0.47)	24.865	0.001
	No	51 (88.14)	213 (99.53)		
Hematoma enlargement ^a	Yes	10 (16.95)	8 (3.77)	15.466	0.001
	No	49 (83.05)	206 (96.23)		
Hematoma volume ^a	<20 mL	9 (15.25)	141 (65.88)	66.052	0.001
	20~50 mL	21 (5.59)	54 (25.23)		
	>50 mL	29 (49.15)	19 (8.88)		

n indicates number of cases.

^aThere was a significant ($P<0.05$) difference between patients with and those without early death after hypertensive ICH

Table 2 Univariate analysis of continuous data

Factors	Death group ($\bar{x} \pm s$)	Survival group ($\bar{x} \pm s$)	<i>t</i>	<i>P</i> value
Age (years) ^a	68.05 ± 13.21	63.59 ± 11.57	2.5403	0.0116
Glasgow Coma Scale score ^a	6.34 ± 4.55	11.05 ± 3.94	7.2333	<0.001
Systolic blood pressure (mmHg) ^a	174.32 ± 33.18	162.56 ± 25.09	2.9593	0.0034
Diastolic blood pressure (mmHg)	99.19 ± 18.40	95.91 ± 14.51	1.4461	0.1493
White blood cell count (×10 ⁹ /L) ^a	11.75 ± 5.18	8.87 ± 3.47	5.0286	<0.001
Platelet count (×10 ⁹ /L)	153.66 ± 73.71	169.57 ± 58.11	1.7514	0.0810

^aThere was a significant ($P < 0.05$) difference between patients with and those without early death after hypertensive ICH

Table 3 Evaluation of independent factors associated with early death in 273 patients with hypertensive ICH by multiple logistic regression analysis

Factors	B coefficient	Odds ratio	95% Confidence interval	<i>P</i> value
Age	-0.035	0.966	0.936–0.997	0.0327
Glasgow Coma score	0.175	1.192	1.090–1.303	<0.001
Hematoma volume	-0.128	0.800	0.807–0.959	0.0037
Systolic blood pressure	-0.063	0.939	0.772–1.142	<0.001

hemorrhage, cerebral herniation, and hematoma enlargement, poor GCS score and high systolic blood pressure at admission, old age, and increased white blood cell count. However, univariate statistical analysis was deficient in evaluating the interrelations among variables. Therefore, a logistic regression analysis for predicting early death was constructed by using the factors with statistical significance ($p < 0.05$) in univariate analysis in order to preclude the interaction between the independent variables and the dependent variable in our study.

The multivariate analysis revealed that only old age, poor GCS score, and high systolic pressure at admission, and large hemorrhagic volume were independent predictors of early death after hypertensive ICH onset. To begin with, a poor GCS score was significantly associated with an increased incidence of early death [10, 11] and a GCS score between 3 and 15 (13 or higher correlates with a mild cerebral injury, 9–12 with a moderate injury, and 8 or less with severe cerebral injury). In this study, the GCS score of 67.80% death cases was eight or less, but the GCS score of only 28.04% of the survival cases was eight or less. Accordingly, consciousness disturbance after hypertensive ICH is the predictor of worsening ICH, and it directly shows the degree of intracerebral injury, and serious consciousness disturbances, such as coma, are a prelude to death and also the inevitable result of serious hypertensive ICH. Then, exorbitant blood pressure in the acute period of hypertensive ICH often indicates a bad prognosis [5, 12]. Except original hypertension, elevated blood pressure means autoregulation induced by acute cerebral edema and intracranial hypertension after intracerebral impairment. After onset, the increase of blood

pressure may induce cerebral herniation and hematoma enlargement, and further result in serious intracranial hypertension. In this study, we found that systolic blood pressure at admission is mainly attributable to early death of hypertensive ICH, and the increase of systolic blood pressure might be associated with hematoma enlargement in the early period. Furthermore, the mortality rate enhances with age [13, 14]. The high mortality rate among older patients with hypertensive ICH may be related to their weak immunotolerance and multiple complications. Finally, the hematoma volume is independently related to the prognosis of hypertensive ICH [15]. Franke et al. [16] found that the mortality rate increased significantly with hematomas >40 mL. In this study, 57.63% death cases showed hematomas >40 mL, but only 9.81% of survival cases showed hematomas >40 mL. For patients with hypertensive ICH, less hemorrhagic volume means a small degree of pressure on cerebral tissue and relatively minor secondary brain injury, which could be compensated for by autoregulation. However, large hemorrhagic volume may induce evident cerebral edema and damage brain tissue seriously so that death occurs easily by cerebral herniation.

Preventing these risk factors is an important issue in patients with hypertensive ICH. Hence, careful observation and treatment of patients with a high likelihood of early death are advisable. Clinicians should pay attention to patients' states of consciousness and be adept at GCS application. For old patients with hypertensive ICH, clinicians should take a positive and prudent attitude, and select the optimum therapy program based on comprehensive assessment of each patient's health status. Meanwhile, education about risk factors of

hypertensive ICH and incentives among high-risk populations should be strengthened and the strategy of early diagnosis and early treatment advocated. Adequate reduction of blood pressure at admission is of important significance. In the acute period of hypertensive ICH, lowering blood pressure quickly is not recommended clinically; the decreased range of blood pressure within 2 h should be less than 25%, and blood pressure should be dropped gradually within 2–10 h, usually down to 150–160/90–100 mmHg. Clinicians should also pay more attention to the problems demonstrated by CT. Compared with the clinical features, CT is an important examination measure to predict the prognosis of hypertensive ICH because CT features of hypertensive ICH could objectively reflect the pathological changes of acute ICH and the severity of ICH. Clinically, clinicians should select proper therapy and evaluate the prognosis through comprehensive analysis of patients' status and patients' CT outcome. For patients with hypertensive ICH, surgical removal of hematoma at the proper time on the basis of conventional medical treatment could recover compressed nerve cells, save patients' lives, and reduce disability in survivors. Moreover, it could keep cerebral dysfunction to a minimum.

Conflict of interest statement We declare that we have no conflict of interest.

References

- Ovary C, Suzuki K, Nagy Z (2004) Regional differences in incidence rates, outcome predictors and survival of stroke. *Neuroepidemiology* 23:240–246
- Ariesen MJ, Claus SP, Rinkel GJ, Algra A (2003) Risk factors for intracerebral hemorrhage in the general population: a systematic review. *Stroke* 34:2060–2065
- Crowley RW, Yeoh HK, Stukenborg GJ, Medel R, Kassell NF, Dumont AS (2009) Influence of weekend hospital admission on short-term mortality after intracerebral hemorrhage. *Stroke* 40:2387–2392
- Kimura K, Iguchi Y, Inoue T, Shibasaki K, Matsumoto N, Kobayashi K, Yamashita S (2007) Hyperglycemia independently increases the risk of early death in acute spontaneous intracerebral hemorrhage. *Neurol Sci* 263:228–229
- Tetri S, Juvela S, Saloheimo P, Pyhtinen J, Hillbom M (2009) Hypertension and diabetes as predictors of early death after spontaneous intracerebral hemorrhage. *Neurosurgery* 110:411–417
- Hemphill JC, Bonovich DC, Besmertis L, Manley GT, Johnston SC (2001) The ICH score: a simple, reliable grading scale for intracerebral hemorrhage. *Stroke* 32:891–897
- Kazui S, Naritomi H, Yamamoto H, Sawada T, Yamaguchi T (1996) Enlargement of spontaneous intracerebral hemorrhage: incidence and time course. *Stroke* 27:1783–1787
- Teasdale G, Knill-Jones R, Van der Sande J (1978) Observer variability in assessing impaired consciousness and coma. *J Neurol Neurosurg Psychiatry* 41:603–610
- Lisk DR, Pasteur W, Rhoades H, Putnam RD, Grotta JC (1994) Early presentation of hemispheric intracerebral hemorrhage prediction of outcome and guidelines for treatment allocation. *Neurology* 44:133–139
- Heppner P, Ellegala DB, Durieux M, Jane JA Sr, Lindner JR (2006) Contrast ultrasonographic assessment of cerebral perfusion in patients undergoing decompressive craniectomy for traumatic brain injury. *Neurosurgery* 104:738–745
- Nilsson OG, Lindgren AR, Brandt L, Saveland H (2002) Prediction of death in patients with primary intracerebral hemorrhage: a prospective study of a defined population. *Neurosurgery* 97:531–536
- Willmot M, Leonardi-Bee J, Bath PM (2004) High blood pressure in acute stroke and subsequent outcome: a systematic review. *Hypertension* 43:18–24
- Arboix A, Vall-Llosera A, Garcia-Eroles L, Massons J, Oliveres M, Targa C (2002) Clinical features and functional outcome of intracerebral hemorrhage in patients aged 85 and older. *Am Geriatr Soc* 50:449–454
- Togha M, Bakhtavar K (2004) Factors associated with in-hospital mortality following intracerebral hemorrhage: a three-year study in Tehran Iran. *BMC Neurol* 4:9
- Davis SM, Broderick J, Hennerici M, Brun NC, Diringer MN, Mayer SA, Begtrup K, Steiner T (2006) Hematoma growth is a determinant of mortality and poor outcome after intracerebral hemorrhage. *Neurology* 66:1175–1181
- Franke CL, van Swieten JC, Algra A, van Gijn J (1992) Prognostic factors in patients with intracerebral haematoma. *J Neurol Neurosurg Psychiatry* 55:653–657

Effects of Early Serum Glucose Levels on Prognosis of Patients with Acute Intracerebral Hemorrhage

Yanyue Wang, Tianzhu Wang, John H. Zhang, and Xinyue Qin

Abstract Studies have indicated that hyperglycemia might cause cerebral damage to patients after acute intracerebral hemorrhage (ICH). But systematic studies on the effects of diabetes, stress hyperglycemia and normal serum glucose level on the prognosis of ICH patients are insufficient. It is essential to explore the prognosis among them. According to their serum glucose level within 24 h, 189 patients with ICH were divided into three groups: diabetes (group A), stress hyperglycemia (group B) and normal serum glucose (group C). The activity of daily living ability of patients was evaluated by Barthel index at 30 days after admission. The data analysis was done using cumulative logit model and rank sum test. Significant differences were observed in prognosis between group A and group C (OR: 0.056; CI: 0.022–0.143; $p < 0.0001$), B and C (OR: 0.081; CI: 0.039–0.167; $p < 0.0001$), respectively; there was no significant difference between A and B ($p > 0.05$). No difference was found between A and B in the early serum glucose level, but significant differences were observed between A and C, and between B and C. Early hyperglycemia may worsen the prognosis of ICH patients, though patients with diabetes or stress hyperglycemia after ICH may have similar outcomes when early serum glucose levels fluctuate within the same range.

Keywords Acute intracerebral hemorrhage · Clinical analysis · Prognosis · Serum glucose

Introduction

ICH accounts for 10–15% of all strokes and is associated with a higher mortality rate [1–3]; some scholars believe that hyperglycemia could have damaging effects on brain tissue, worsen the condition of patients and hinder the recovery of neurological functional defects [4]. A high proportion of patients suffering an acute stress such as stroke may develop hyperglycemia, even in the absence of a preexisting diagnosis of diabetes [5]. More than 3 decades ago, many studies demonstrated the risk for ICH was dramatically higher among patients with diabetes and among those without diabetes [6–8]. The following factors have been identified as predictors of ICH: male sex, age, hypertension, alcohol intake, smoking and diabetes mellitus [9, 10]. But systematic studies on the effects of diabetes, stress hyperglycemia and normal serum glucose level on the prognosis of ICH patients are lacking. The authors studied and compared 189 patients with ICH treated in the Department of Neurology, the First Affiliated Hospital of Chongqing Medical University, from January 2008 to August 2009, and probed the influence of early serum glucose on the prognosis of these patients. The results were reported as follows.

Materials and Methods

Clinical Materials

All 189 patients were proven to have cerebral hemorrhage with CT or MRI scanning. The patients were divided into three groups: the diabetes with ICH group (group A) had 31 patients. Among them, 15 were males, and 16 were females, with ages ranging from 45 to 88 years old (63.71 ± 9.99 years old). The diagnostic criterion of diabetes was from the World Health Organization (WHO) in 1999. The stress hyperglycemia group (group B) had 70 patients; 45 were males,

Y. Wang, T. Wang, and X. Qin (✉)

Department of Neurology, The First Affiliated Hospital of Chongqing Medical University, Chongqing, 400016, China
e-mail: qinxinyue@yahoo.com

J.H. Zhang

Department of Physiology and Pharmacology, Department of Neurosurgery, Department of Anesthesiology, Loma Linda University, School of Medicine, Loma Linda, CA, USA

and 25 were females, with ages ranging from 17 to 87 years old (58.51 ± 16.42 years old). The normal serum glucose level group (group C) had 88 patients; 56 were males, and 32 were females, with ages ranging from 14 to 95 years old (58.75 ± 16.53 years old). The patients with serum glucose levels from 6.1 mmol/l to 6.8 mmol/l were excluded.

The fasting serum glucose values of all patients were tested in the first 24 h after hospitalization, and the various interference factors that increased serum glucose were eliminated before drawing blood. Except for cases of diabetes, early serum glucose levels higher than 6.8 mmol/l were considered to be stress hyperglycemia. All patients received conservative internal medicine treatment by reducing intracranial hypertension, cerebral nerve nutrition agents and antibiotics, and were supported by symptomatic treatment and rehabilitation training. The patients with hyperglycemia were simultaneously treated with anti-diabetic drugs.

The ABC/2 [11] formula was used for measuring the volume of hemorrhage, where A and B are the greatest hemorrhage diameter by MRI or CT scanning. C represents the thickness of the ICH. The daily living ability of surviving patients was measured by the Barthel index at 30 days after admission. The evaluation contents included that independently taking a bath scored 5 points, beautifying their outward appearance 5, dining 10, dressing 10, going to the lavatory 10, controlling their bowel movement and urination 10, respectively, walking up and down the stairs 10, moving the bed and chairs 15, and walking on flat land 45 m 15. The score of 100 was independence, 75–95 slight dependence, 50–70 moderate dependence, 25–45 severe dependence, and 0–25 complete dependence. The death cases were classified into complete dependence during the treatment and prognosis judged as ineffective treatment cases.

Statistical Methods

Statistics analysis was done using the SAS8.2 analysis system. Table 1 shows the frequency distribution of prognosis among the three groups. Considering the impact of confounding factors on prognosis, such as age, gender, hemorrhage volume, hemorrhage sites and complications (Table 2),

Table 1 Frequency distribution of prognosis among the three groups

Prognosis groups	Mild dependence	Moderate dependence	Severe dependence	Complete dependence (death)
Group A	2	6	14	4 (5)
Group B	12	13	21	9 (15)
Group C	55	14	13	3 (3)

a cumulative logit model was made to determine those factors that could be considered as independent predictors of prognosis and remove the confounding factors to compare the prognosis among the three groups. Five confounding factors and inter-group factors (early serum glucose level) were all involved in the cumulative logit model (hemorrhage sites with six dummies, complications with five dummies and inter-group factors with two dummies). Significance for inter-group differences in early serum level was assessed by the rank sum test.

Results

It was revealed by cumulative logit model that the following three factors were associated with the prognosis ICH: hemorrhage volume (OR: 0.012; 95% CI: 0.004–0.032; $p < 0.0001$), hemorrhage sites (OR: 0.463; CI: 0.243–0.882; $p = 0.0192$), complications (OR: 0.058; CI: 0.004–0.775; $p = 0.0313$). After removing these confounding factors, significant differences were observed in prognosis between group A and group C (OR: 0.056; CI: 0.022–0.143; $p < 0.0001$), and between groups B and C (OR: 0.081; CI: 0.039–0.167; $p < 0.0001$), respectively. However, the difference between A and B in prognosis, owing to the variable, did not enter the logistic regression equation; there was no significant difference between A and B ($p > 0.05$). Table 3 demonstrates that significant differences were found among the three groups in the early serum glucose levels ($X^2 = 141.2$, $p < 0.001$); early serum glucose levels in group A and group B were significantly higher than those in group C. However, there was no difference between A and B.

Discussion

The scholars have paid close attention to the relationship between early serum glucose level and ICH. As early as 1973, the Framingham Study demonstrated an increased morbidity and mortality from cerebrovascular disease in patients with diabetes [12]. Similar conclusions have been drawn from subsequent studies of patients with diabetes [13, 14]. Diabetes increases the risk for disorders that predispose individuals to hospitalization, including coronary artery, cerebrovascular and peripheral vascular disease, nephropathy, infection and lower extremity amputations [15]. The level of Advanced Glycation End Products (AGEs) in diabetes patients was significantly elevated [16]. The increased AGEs caused dysfunctional endothelial cells [17], stimulated smooth muscle cell proliferation, and accelerated atherosclerosis and thrombosis [18].

Table 2 Frequency distribution of confounding factors among the three groups

	Group A	Group B	Group C
Gender			
Male	15	45	56
Female	16	25	32
Age (years)	63.71 ± 9.99	58.51 ± 16.42	58.75 ± 16.53
Hemorrhage sites <i>n</i> (%)			
Basal ganglia	13 (41.94)	33 (47.14)	46 (52.27)
Lobe brain	6 (19.35)	12 (17.14)	19 (21.59)
Thalamencephalon	4 (12.90)	9 (12.86)	7 (7.95)
Cerebellum	3 (9.68)	6 (8.57)	4 (4.55)
Brain stem	2 (6.45)	4 (5.71)	7 (7.95)
Subarachnoidcavity	1 (3.23)	3 (4.29)	2 (2.27)
Others	2 (6.45)	3 (4.29)	3 (3.41)
Hemorrhage volume <i>n</i> (%)			
≤30 mL	20 (64.52)	46 (65.71)	72 (81.82)
>30 mL	11 (35.48)	24 (34.29)	16 (18.18)
Complications <i>n</i> (%)			
Pulmonary infection	4 (12.90)	20 (28.57)	13 (14.77)
Electrolyte disturbance	4 (12.90)	8 (11.43)	6 (6.82)
Cerebral hernia	1 (3.23)	5 (7.14)	2 (2.27)
Arrhythmia	1 (3.23)	4 (5.71)	2 (2.27)
Hemorrhage of			
Digestive tract	1 (3.23)	4 (5.71)	2 (2.27)
No complications	20 (64.52)	29 (41.43)	63 (71.59)

Table 3 Comparisons of the early serum level among the three groups

Groups	Cases (n)	$\bar{x} \pm s$
Group A	31	9.47 ± 1.86 ^a
Group B	70	9.19 ± 2.54 ^b
Group C	88	5.29 ± 0.47

^aMeans there were significant differences between group A and group C

^bMeans there were significant differences between group B and group C

There were no significant differences between group A and group B

Hyperglycemia can damage cerebral tissue. The pathological basis was that hyperglycemia increased anaerobic glycolysis and caused a further increase of lactic acid in cerebral tissue under the circumstances of cerebral ischemia and anoxia. These cause intracellular acidosis [19], causing the thalamic barrier to open by interfering with the process of mitochondrial oxidative phosphorylation and aggravating cerebral edema [4] to worsen the prognosis. In one study brain edema after ICH with hyperglycemia increased in both lesioned and nonlesioned hemispheres, and this may be more attributable to vasogenic edema [20]. Relative insulin deficiency liberates circulating free fatty acids,

which, together with hyperglycemia, reportedly diminish vascular reactivity [21]. Hyperglycemia may disrupt the blood-brain barrier [22] and promote hemorrhagic infarct conversion [23].

The mechanism of hyperglycemia after ICH was that elevated intracranial pressure could directly or indirectly influence the structure and function of the hypothalamus-pituitary-thyroid axis; the midline shifting, which was caused by the hemorrhage, excited the hypothalamus-pituitary system after ICH, which led to the increase of hydrocortisone, growth hormone and glucagon, and the reduction of triiodothyronine (T_3). The combined effect of these hormones increased serum glucose [24]. Second, catecholamine excess occurs as a component of the stress response, resulting in glycogenolysis and increased hepatic glucose production. Catecholamines are the initial mediators of hyperglycemia via this mechanism. [25] Third, insulin resistance occurs in the setting of stress, which evaluates the serum glucose level [26]. Last, patients without diabetes who develop stress hyperglycemia are likely to have dysglycemia or undiagnosed diabetes when not stressed. Patients with dysglycemia or undiagnosed diabetes have a higher risk of vascular disease than patients with normal blood glucose levels [27].

The principles should be grasped to treat hyperglycemia with ICH patients as follows: (1) actively treat the primary disease and eliminate stressors as soon as possible, control complications in time, and correct water electrolyte and acid-base equilibrium disorders; (2) iatrogenic hyperglycemia will also aggravate the damage of brain tissue [28], so reasonable intravenous infusions should be adopted to control exogenous glucose, and a high-fat low-sugar diet should be given to reduce glucose intake, with dietary fiber to delay gastric emptying, thereby inhibiting the production of glucose. (3) Using insulin should follow the principles of efficiency, safety, stability and adjustability to control the serum glucose level. The dose of insulin is difficult to control by intravenous transfusion because of the large fluctuations often observed in serum glucose. An insulin pump is recommended to control serum glucose more accurately. The dose of insulin must be individualized. The multivariate logistic regression analysis revealed that daily insulin dosage and serum glucose level both were the independent positive predictors of patients' mortality rates; namely, the higher the daily dose of insulin was, the higher the serum glucose level was, and the higher mortality was [29]. (4) Regularly monitoring their serum glucose levels is important, as is regularly adjusting the dose of anti-diabetic drugs and avoiding hypoglycemic reactions.

To sum up, the authors consider that admission hyperglycemia may lead to a poor prognosis of ICH patients, although patients with diabetes or stress hyperglycemia after ICH may have similar outcomes under the circumstance that early serum glucose levels fluctuate within the same range. The authors remind clinicians that they must monitor serum glucose levels of patients in a timely manner and effectively control hyperglycemia to improve the prognosis of ICH patients and raise survival rates.

Conflict of interest statement We declare that we have no conflict of interest.

References

- Dennis MS, Burn JP, Sandercock PA, Bamford JM, Wade DT, Warlow CP (1993) Long-term survival after first-ever stroke: the Oxfordshire Community Stroke Project. *Stroke* 24(6):796–800
- Fewel ME, Thompson G Jr, Hoff JT (2003) Spontaneous intracerebral hemorrhage: a review. *Neurosurg Focus* 15(4):E1
- Qureshi AI, Tuhim S, Broderick JP, Batjer HH, Hondo H, Hanley DF (2001) Spontaneous intracerebral hemorrhage. *N Engl J Med* 344(19):1450–1460
- Levetan CS (2004) Effect of hyperglycemia on stroke outcomes. *Endocr Pract* 10(supply 2):34–39
- Capes SE, Hunt D, Malmberg K, Pathak P, Gerstein HC (2001) Stress hyperglycemia and prognosis of stroke in nondiabetic and diabetic patients. *Stroke* 32(10):2426–2432
- Fuller JH, Shipley MJ, Rose G, Jarrett RJ, Keen H (1983) Mortality from coronary heart disease and stroke in relation to degree of glycaemia: the Whitehall study. *Br Med J* 287:867–870, Clin Res Ed. J (6393)
- Stamler J, Vaccaro O, Neaton JD, Wentworth D (1993) Diabetes, other risk factors, and 12-yr cardiovascular mortality for men screened in the multiple risk factor intervention trial. *Diab Care* 16(2):434–444
- Wolf PA, D'Agostino RB, Belanger AJ, Kannel WB (1991) Probability of stroke: a risk profile from the Framingham study. *Stroke* 22(3):312–318
- Ariesen MJ, Claus SP, Rinkel GJ, Algra A (2003) Risk factors for intracerebral hemorrhage in general population: a systematic review. *Stroke* 34(8):2060–2065
- Kazui S, Minematsu K, Yamamoto H, Sawada T, Yamaguchi T (1997) Predisposing factors to enlargement of spontaneous intracerebral hematoma. *Stroke* 28(12):2370–2375
- Kothari RU, Brott T, Broderick JP, Barsan WG, Sauerbeck LR, Zuccarello M, Khoury J (1996) The ABCs of measuring intracerebral hemorrhage volumes. *Stroke* 27(8):1304–1305
- Garcia MJ, McNamara PM, Gordon T, Kannel WB (1974) Morbidity and mortality in diabetics in the Framingham population. *Diabetes* 23(2):1105–1112
- Kessler II (1971) Mortality experience of diabetic patients. A twenty-six-year follow-up study. *Am J Med* 51(6):715–724
- Lehto S, Ronnema T, Pyorala K, Laakso M (1996) Predictors of stroke in middle-aged patients with non-insulin-dependent diabetes. *Stroke* 27(1):63–68
- Clement S, Braithwaite SS, Magee MF, Ahmann A, Smith EP, Schafer RG, Hirsch IB (2004) American Diabetes Association Diabetes in Hospitals Writing Committee (2004) Management of diabetes and hyperglycemia in hospitals. *Diab Care* 27(2):553–591
- Okada S, Shikata MM, Ogawa D, Usui H, Kido Y, Nagase R, Wada J, Shikata Y, Makino H (2003) Intercellular adhesion molecule deficient mice are resistant against renal injury after induction of diabetes. *Diabetes* 52(10):2586–2588
- Chavakis T, Bierhaus A, Nawroth PP (2004) PRAGE(receptor for advanced glycation end products): a central player in the inflammatory response. *Microbes Infect* 6(13):1219–1225
- Basta G, Schmidt AM, De Caterina R (2004) Advanced glycation end products and vascular inflammation; implications for accelerated atherosclerosis in diabetes. *Cardiovasc Res* 63(4):582–592
- Levine SR, Welch KM, Helpert JA, Chopp M, Bruce R, Selwa J, Smith MB (1988) Prolonged deterioration of ischemic brain energy metabolism and acidosis associated with hyperglycemia: human cerebral infarction studied by serial 31P NMR spectroscopy. *Ann Neurol* 23(4):416–418
- Song EC, Chu K, Jeong SW, Jung KH, Kim SH, Kim M, Yoon BW (2003) Hyperglycemia exacerbates brain edema and perihematomal cell death after intracerebral hemorrhage. *Stroke* 34(9):2215–2220
- Lindsberg PJ, Roine RO (2004) Hyperglycemia in acute stroke. *Stroke* 35(2):363–364
- Dietrich WD, Alonso O, Busto R (1993) Moderate hyperglycemia worsens acute blood-brain barrier injury after forebrain ischemia in rats. *Stroke* 24(1):111–116
- De Courten-Myers GM, Kleinholz M, Holm P, DeVoe G, Schmitt G, Wagner KR, Myers RE (1992) Hemorrhagic infarct conversion in experimental stroke. *Ann Emerg Med* 21(2):120–126
- Laird AM, Miller PR, Kilgo PD, Meredith JW, Chang MC (2004) Relationship of early hyperglycemia to mortality in trauma patients. *J Trauma* 56(5):1058–1062
- Young B, Ott L, Dempsey R, Haack D, Tibbs P (1989) Relationship between admission hyperglycemia and neurologic outcome of severely brain-injured patients. *Ann Surg* 210(4):466–473
- Lange MP, Dahn MS, Jacobs LA (1985) The significance of hyperglycemia after injury. *Heart Lung* 14(5):470–472

27. Coutinho M, Gerstein HC, Wang Y, Yusuf S (1999) The relationship between glucose and incident cardiovascular events: a meta regression analysis of published data from 20 studies of 95,783 individuals followed for 12.4 years. *Diab Care* 22(2):233–240
28. Efron D, South M, Volpe JJ, Inder T (2003) Cerebral injury in association with profound iatrogenic hyperglycemia in a neonate. *Eur J Paediatr Neurol* 7(4):167–171
29. Van den Berghe G, Wouters PJ, Bouillon R, Weekers F, Verwaest C, Schetz M, Vlasselaers D, Ferdinande P, Lauwers P (2003) Outcome benefit of intensive insulin therapy in the critically ill: insulin dose versus glycolic control. *Crit Care Med* 31(2):359–366

Prognosis Study of 324 Cases with Spontaneous Intracerebral Hemorrhage in Chongqing, China

Qian Li, Xin-Yue Qin, John H. Zhang, and Jun Yang

Abstract We aimed to investigate the clinical characteristics of intracerebral hemorrhage (ICH) in Chongqing City, China, and evaluate some factors predicting the prognosis of ICH. We collected 324 cases with spontaneous intracerebral hemorrhage in our hospital from January 2008 to November 2009. Univariate variance analyses were used for comparison of characteristics. Odds ratios (ORs) were calculated by logistic regression. Potential confounders were adjusted, including gender, age, smoking, and drinking status. Hypertension was the major cause of the spontaneous intracerebral hemorrhage, accounting for 75% of all patients in this study. Hemorrhages were located in lobes (22.5%), basal ganglia (65.3%), cerebral ventricles (2.6%), cerebellum (4.2%), and brain stem (7.4%). Serum glucose and consciousness status were independently associated with in-hospital mortality after ICH. Comparing subjects who died in the hospital to those who survived, the adjusted ORs of serum glucose were 1.248 (95% CI 1.013–1.537, $p=0.037$), and the adjusted ORs of consciousness status were 1.995 (95% CI 1.519–2.621, $p<0.001$). In China, spontaneous intracerebral hemorrhage is mostly caused by hypertension and is usually located in the basal ganglia. Serum glucose and consciousness status independently predict the prognosis of ICH.

Keywords ICH · Serum glucose · In-hospital mortality · Prognosis

Q. Li, X.-Y. Qin, and J. Yang (✉)

Department of Neurology, The First Affiliated Hospital of Chongqing Medical University, Chongqing 400016, China
e-mail: yangweixiao222@yahoo.com.cn

J.H. Zhang

Department of Neurology, Loma Linda University,
School of Medicine, Loma Linda, CA, USA

Introduction

Spontaneous (non-traumatic) intracerebral hemorrhage (ICH) can be defined as an acute and spontaneous bleeding into the brain parenchyma [1], which is distinct from subarachnoid hemorrhage (SAH) and isolated intraventricular hemorrhage (IVH). It is an important public health problem leading to high morbidity and mortality. ICH accounts for 2 million (10–15%) [2] of about 15 million strokes worldwide each year [3]. The annual incidence of ICH is 10–30 cases per 100,000 people [1, 4]. In more than two-thirds of cases, ICH is classified as primary ICH, as it occurs from spontaneous rupture of small vessels damaged by hypertension (60%–70% of cases) [5] or cerebral amyloid angiopathy (CAA) (15% of cases) [6]. Secondary ICH, in a minority of patients, results from vascular abnormalities (arteriovenous malformations and aneurysm) or other causes (e.g., ischemic stroke or tumor). Other important etiologies of both primary and secondary ICH include coagulopathy, sympathomimetic drugs of abuse, vasculitides, and moyamoya disease [7].

In previous studies, ethnicity has been reported to contribute to ICH risk. Non-white races have been consistently associated with higher rates of ICH [8, 9]. Hispanic and Asian patients have higher rates of ICH, which may be partially explained by higher rates of cerebral vascular anomalies such as cavernous malformations and moyamoya disease [10, 11]. Because of ethnicity and socioeconomic factors, ICHs in Chinese patients may have different characteristics. This study was designed to investigate the clinical characteristics of ICH in Chongqing City, China, and evaluate the factors that can predict the prognosis of ICH.

Materials and Methods

A medical records review of patients with ICH treated in the First Affiliated Hospital of Chongqing Medical University from January 2008 to November 2009 was undertaken

for elementary data collection. In total, 324 subjects (34% women) aged from 14 to 105 years were recruited in this study.

All variables used for the model were extracted from data available at the time of initial ICH evaluation. The Glasgow Coma Scale (GCS) score at admission was used. The systolic blood pressure (SBP), diastolic blood pressure (DBP), and heart rate (HR), measured after hospital admission, were recorded. Other information including sex, age, smoking habit, alcohol intake, and medical history were obtained from medical files. Only the first laboratory tests by our hospital staff were recorded. Outcome was assessed by mortality in the hospital after ICH.

Comparison for baseline characteristics between two sets of patients (dead and alive) was performed with ANOVA for continuous parameters and χ^2 test for categorical parameters. Continuous data were expressed as mean \pm standard deviation (SD). Multivariate logistic regression analyses were used to assess the contribution of baseline characteristics to mortality in hospital after ICH. Adjusted variables were gender, age, smoking, and drinking status. Statistical analyses were performed using SPSS software version 15.0 (SPSS Inc., Chicago, IL).

Results

Location of ICH

Hypertension is the major cause of spontaneous intracerebral hemorrhage, accounting for 75% of all ICHs in this study. Hemorrhages were located in lobes (22.5%), basal ganglia (65.3%), cerebral ventricles (2.6%), cerebellum (4.2%), and brain stem (7.4%) (Fig. 1).

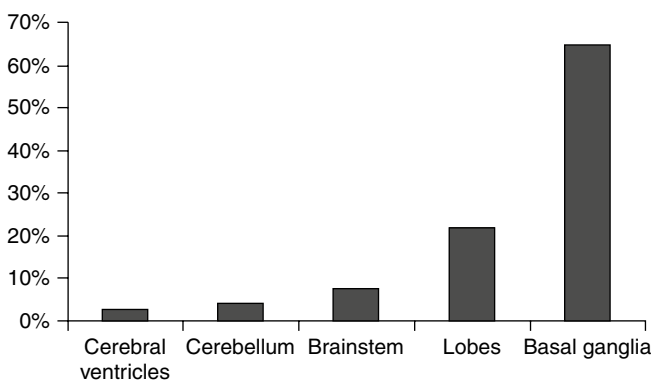


Fig. 1 Locations of intracerebral hemorrhages

Independent Predictor for Prognosis of ICH

Overall hospital mortality was 26.5% ($n=86$), with no sex difference (24.8% in males and 30.0% in females, $p=0.190$). Significant differences were found between the dead and surviving patients in the hospital for the following variables: age (62.71 ± 16.43 years, 58.30 ± 15.60 years, $p=0.046$), GCS score (7.83 ± 4.14 , 13.36 ± 2.41 , $p<0.001$), SBP (176.77 ± 41.57 mmHg, 158.53 ± 29.44 mmHg, $p<0.001$), DBP (100.28 ± 23.73 mmHg, 94.81 ± 16.62 mmHg, $p=0.018$), HR (87.25 ± 21.18 beats/min, 79.56 ± 15.42 beats/min, $p=0.001$), and levels of serum glucose (8.59 ± 3.15 mmol/L, 6.34 ± 1.49 mmol/L, $p<0.001$), urea nitrogen (urea) (7.37 ± 5.36 mmol/L, 5.90 ± 2.70 mmol/L, $p=0.004$), and serum creatinine (Scr) (128.23 ± 141.67 mmol/L, 84.17 ± 85.59 mmol/L, $p=0.003$). The comparison of baseline characteristics between two sets of patients is shown in Table 1.

Eight factors may contribute to the prognosis of ICH and were selected for further investigation. Multivariate logistic regression analyses showed that only serum glucose levels

Table 1 Characteristics of study subjects dead or alive in hospital

Characteristics	Dead in hospital ($n=86$)	Alive in hospital ($n=238$)	p
% (n)			
Male	61.6 (53)	67.6 (161)	0.190
Current smoking	29.1 (25)	28.6 (68)	0.530
Current drinking	27.9 (24)	29.0 (69)	0.470
Mean \pm SD			
Age (years)	62.71 ± 16.43	58.30 ± 15.60	0.046
GCS score	7.83 ± 4.14	13.36 ± 2.41	<0.001
SBP (mmHg)	176.77 ± 41.57	158.53 ± 29.44	<0.001
DBP (mmHg)	100.28 ± 23.73	94.81 ± 16.62	0.018
HR (beats/min)	87.25 ± 21.18	79.56 ± 15.42	0.001
Glu (mmol/L)	8.59 ± 3.15	6.34 ± 1.49	<0.001
Na (mmol/L)	140.13 ± 6.53	139.48 ± 4.57	0.364
K (mmol/L)	3.93 ± 0.81	3.87 ± 0.53	0.475
Urea (mmol/L)	7.37 ± 5.36	5.90 ± 2.70	0.004
Scr (mmol/L)	128.23 ± 141.67	84.17 ± 85.59	0.003
LDL-C (mmol/L)	2.70 ± 0.81	2.75 ± 0.88	0.774
HDL-C (mmol/L)	1.50 ± 0.47	1.32 ± 0.63	0.149
TC (mmol/L)	5.05 ± 1.19	4.77 ± 1.01	0.184
TG (mmol/L)	1.28 ± 0.85	1.45 ± 0.84	0.319

GCS Glasgow Coma Scale, SBP systolic blood pressure, DBP diastolic blood pressure, HR heart rate, Glu serum glucose, TP total protein, ALB albumin, Na serum sodium, K potassium, Urea urea nitrogen, Scr serum creatinine, LDL-C low-density lipoprotein cholesterol, HDL-C high-density lipoprotein cholesterol, TC total cholesterol, TG triglycerides

Table 2 Multivariable logistic regression analysis predicting the likelihood of in-hospital mortality after ICH

Variables	Exp (B)	95% CI Exp (B)	<i>p</i>
Age	1.032	1.001–1.065	0.045
Glu	1.248	1.013–1.537	0.037
Conscious status	1.995	1.519–2.621	<0.001
SBP	1.000	0.979–1.021	0.970
DBP	1.014	0.976–1.054	0.465
HR	1.015	0.995–1.035	0.140
Urea	0.998	0.835–1.192	0.981
Cre	1.008	0.999–1.017	0.082

SBP systolic blood pressure, *DBP* diastolic blood pressure, *HR* heart rate, *Glu* serum glucose, *Urea* urea nitrogen, *Scr* serum creatinine

and consciousness status were significantly associated with prognosis of ICH (dead in hospital versus alive in hospital: OR for serum glucose, 1.248; 95% CI, 1.013–1.537; $p=0.037$; OR for consciousness status, 1.995; 95% CI, 1.519–2.621; $p<0.001$) (Table 2).

Discussion

Intracerebral hemorrhage commonly affects cerebral lobes, the basal ganglia, the thalamus, the brain stem (predominantly the pons), and the cerebellum as a result of ruptured vessels affected by hypertension-related degenerative changes or cerebral amyloid angiopathy [1]. In our study, spontaneous intracerebral hemorrhage was mostly caused by hypertension (75%). The proportion was slightly higher than that reported before (60–70%). This could be due to the poorly controlled hypertension in our country. Intracerebral hemorrhage commonly affects cerebral lobes, the basal ganglia, the thalamus, the brain stem (predominantly the pons), and the cerebellum as a result of ruptured vessels affected by hypertension-related degenerative changes or cerebral amyloid angiopathy [1]. In the present study, ICH was mostly located in the basal ganglia (65.3%).

The GCS score, which is a reproducible and reliable neurological assessment tool [12], has been used in many predictive models [13–16]. Recently, it has been proven that hyperglycemia may worsen the prognosis of ICH [17, 18]. In our study, consciousness status and serum glucose independently predicted the in-hospital mortality of ICH.

This study is subject to certain limitations. Firstly, hospital mortality may not be as effective in assessing the outcome of ICH as 30-day mortality. Some patients who were alive in the hospital could have died soon after being discharged. The hospital mortality (26.5%) of ICH patients in our study was smaller

than 30-day mortality in other studies (45%) [19]. Secondly, the sample size of this study limited the conclusion.

Conflict of interest statement We declare that we have no conflict of interest.

References

1. Qureshi AI, Tuhim S, Broderick JP et al (2001) Spontaneous intracerebral hemorrhage. *N Engl J Med* 344:1450–1460
2. Sudlow CL, Warlow CP (1997) Comparable studies of the incidence of stroke and its pathological types: results from an international collaboration. *Stroke* 28:491–499
3. American Heart Organization (2007) International cardiovascular disease statistics: cardiovascular disease (CVD). <http://www.americanheart.org/downloadable/heart/1140811583642InternationalCVD.pdf>
4. Labovitz DL, Halim A, Boden-Albala B, Hauser WA, Sacco RL (2005) The incidence of deep and lobar intracerebral hemorrhage in whites, blacks, and Hispanics. *Neurology* 65:518–522
5. McCormick WF, Rosenfield DB (1973) Massive brain hemorrhage: a review of 144 cases and an examination of their causes. *Stroke* 4: 946–954
6. Marietta M, Pedrazzi P, Girardis M, Torelli G (2007) Intracerebral haemorrhage: an often neglected medical emergency. *Intern Emerg Med* 2:38–45
7. Eljovich L, Patel PV, Hemphill JC 3rd (2008) Intracerebral hemorrhage. *Semin Neurol* 28:657–667
8. Qureshi AI, Suri MA, Safdar K, Ottenlips JR, Janssen RS, Frankel MR (1997) Intracerebral hemorrhage in blacks. Risk factors, subtypes, and outcome. *Stroke* 28:961–964
9. Sturgeon JD, Folsom AR, Longstreth WT Jr, Shahar E, Rosamond WD, Cushman M (2007) Risk factors for intracerebral hemorrhage in a pooled prospective study. *Stroke* 38:2718–2725
10. Gunel M, Awad IA, Finberg K, Anson JA, Steinberg GK, Batjer HH, Kopitnik TA, Morrison L, Giannotta SL, Nelson-Williams C, Lifton RP (1996) A founder mutation as a cause of cerebral cavernous malformation in Hispanic Americans. *N Engl J Med* 334: 946–951
11. Kuriyama S, Kusaka Y, Fujimura M, Wakai K, Tamakoshi A, Hashimoto S, Tsuji I, Inaba Y, Yoshimoto T (2008) Prevalence and clinicoepidemiological features of moyamoya disease in Japan: findings from a nationwide epidemiological survey. *Stroke* 39:42–47
12. Hemphill JC 3rd, Bonovich DC, Besmertis L, Manley GT, Johnston SC (2001) The ICH score: a simple, reliable grading scale for intracerebral hemorrhage. *Stroke* 32:891–897
13. Dennis MS (2003) Outcome after brain haemorrhage. *Cerebrovasc Dis* 16:9–13
14. Grau AJ, Boddy AW, Dukovic DA, Buggle F, Lichy C, Brandt T, Hacke W (2004) CAPRIE investigators: leukocyte count as an independent predictor of recurrent ischemic events. *Stroke* 35: 1147–1152
15. Lisk DR, Pasteur W, Rhoades H, Putnam RD, Grotta JC (1994) Early presentation of hemispheric intracerebral hemorrhage: prediction of outcome and guidelines for treatment allocation. *Neurology* 44:133–139
16. Tuhim S, Horowitz DR, Sacher M, Godbold JH (1999) Volume of ventricular blood is an important determinant of outcome in supratentorial intracerebral hemorrhage. *Crit Care Med* 27: 617–621

17. Pongvarin N, Bhoopat W, Viriyavejakul A, Rodprasert P, Buranasiri P, Sukondhabant S, Hensley MJ, Strom BL (1987) Effects of dexamethasone in primary supratentorial intracerebral hemorrhage. *N Engl J Med* 316:1229–1233
18. Tuhrim S, Dambrosia JM, Price TR, Mohr JP, Wolf PA, Hier DB, Kase CS (1991) Intracerebral hemorrhage: external validation and extension of a model for prediction of 30-day survival. *Ann Neurol* 29:658–663
19. Yu YL, Kumana CR, Lauder IJ, Cheung YK, Chan FL, Kou M, Chang CM, Cheung RT, Fong KY (1992) Treatment of acute cerebral hemorrhage with intravenous glycerol. A double-blind, placebo-controlled, randomized trial. *Stroke* 23:967–971

Retrospective Analysis of the Predictive Effect of Routine Biochemical Results on the Prognosis of Intracerebral Hemorrhage

Hui Chen, Fengzeng Li, Xiaolin Wang, Yuhan Kong, and Yonghong Wang

Abstract Objective: To find the effective biochemical factors for predicting the outcome of acute intracerebral hemorrhage (ICH). **Methods:** According to the outcome, 497 ICH patients were divided into two groups (effective treatment group, ineffective treatment group). The routine biochemical results were analyzed between groups with SPSS software 13.0, including TC, TG, HDL-c, LDL-c, UA, and Glu. The differences of these items were found by independent sample *T* test and Kruskal-Wallis test between groups. Then the items, which were significantly associated with the prognosis of ICH patients, were obtained by the logistic regression. In addition, we calculated the odds ratio (OR) for the special indicators by chi-square test. **Results:** Only UA, Glu, and HDL-c had significant differences between groups ($P < 0.05$) among the six biochemical items. The binary logistic regression analysis indicated that high Glu and UA were related to the outcome of ICH ($P < 0.01$). By chi-square test, the OR of high Glu was 3.95 (2.27–6.87 with 95% CI) and that of high UA was 2.19 (1.16–4.11 with 95% CI), but HDL-c's OR was only 0.90 (0.41–1.98 with 95% CI) without statistical significance. **Conclusion:** High Glu and UA were risk factors for the prognosis of ICH; monitoring and controlling the Glu and UA may be advisable improving the prognosis of ICH.

Keywords Intracerebral hemorrhage · Glucose · Uric acid · Prognosis

H. Chen and F. Li
Clinical Laboratories, The First Affiliated of Hospital Chongqing Medical University, Chongqing 400016, People's Republic of China

X. Wang, Y. Kong, and Y. Wang (✉)
The Medical Examination Center, The First Affiliated Hospital of Chongqing Medical University, Chongqing 400016, People's Republic of China
e-mail: wyh0231029@yahoo.com.cn

Introduction

With the sociodemographic changes in aging and changes in diet structure, the incidence of cerebrovascular disease has been increasing yearly. Acute intracerebral hemorrhage (ICH) is one of the important leading causes of death. In China, there are great disparities in technical facilities and medical techniques among hospitals of different grades. For the primary and community hospitals, it is important to judge the prognosis of ICH using simple and effective laboratory equipment and to take pertinent measures for the risk factors, which may be a better way to reduce medical disputes and the incidence and mortality of ICH. In this study, for finding the effective index to predict the outcome of ICH, we analyzed the association between routine biochemical results and the prognosis of ICH retrospectively.

Material and Methods

From May 2005 to September 2009, 507 ICH patients were admitted to the Department of Neurology of the First Affiliated Hospital, Chongqing Medical University, Chongqing, China. All those examined had brain CT- or MRI-based diagnoses, and met with the diagnostic criteria of cerebrovascular disease established at the 1995 All-China Conference on Cerebrovascular Disease. These patients were divided into three groups: effective treatment group (healing well and improving, $n = 420$), ineffective treatment group (non-improving and dying, $n = 77$), and follow-up failure group ($n = 10$, did not participate in follow-up research). The venous blood samples were collected on the status of empty stomachs the next morning after admission. All the routine biochemical items were tested by an automatic biochemical analyzer, Olympus Au640, including serum total cholesterol (TC), triglycerides (TG), high density lipoprotein cholesterol (HDL-c), low density lipoprotein cholesterol (LDL-c), uric acid (UA), and

glucose (Glu). Our laboratory passed the accreditation criteria for the quality and competence of medical laboratories (ISO15189).

SPSS13.0 statistical package was used to deal with the data. The *T* test or Kruskal-Wallis test was used to compare the two groups, depending on whether or not they were variance homogenous. The logistic regression model was used to identify the items associated with the outcome of acute ICH. Chi-square test was used to calculate the odds ratio for the prediction.

Results

The Basic Situation of Patients with Acute Intracerebral Hemorrhage

Among the total 497 patients, including 179 (36%) males and 318 (64%) females, the chi-square test showed that there were no significant gender differences between the two groups ($P=0.56$). The ages of the effective treatment group ($n=420$) and ineffective treatment group ($n=77$) were 61.2 ± 13.0 years and 67.6 ± 13.2 years (mean \pm SD), respectively; significant differences existed between them ($P<0.001$) with the *T*-test. It seems the older the patient is, the poorer the outcome is.

Differences Between the Lipid Levels of the Two Groups

The four lipid items included TC, TG, HDL-c, and LDL-c. The difference in TC and HDL-c levels was compared with the *T* test, and in TG and LDL-c with the Kruskal-Wallis test because of its unequal variances (Levene's test, $P<0.05$). The statistical results are shown in Table 1.

The HDL-c levels of the ineffective treatment group was significantly higher than that of effective treatment group ($P<0.05$). There were no significant differences in TC, TG, and LDL-c levels between the two groups ($P>0.05$).

Differences in Plasma Glucose and Serum Uric Acid Between the Two Groups

The difference in plasma glucose (Glu) levels was compared with the Kruskal-Wallis test because of its unequal variances (Levene's test, $P<0.05$). The difference in serum uric acid (UA) was compared with *T* test. The results are shown in Table 2.

Table 1 The differences of lipids between the two groups

Group	<i>n</i>	TC (Mean \pm SD, mmol/L)	TG ^a (Mean rank)	HDL-c (Mean \pm SD, mmol/L)	LDL-c ^a (Mean rank)
Effective group	420	4.74 \pm 1.02	250.46	1.34 \pm 0.41	249.85
Ineffective group	77	4.82 \pm 1.22	241.05	1.48 \pm 0.50	244.36*
<i>P</i>		0.523	0.597	0.020*	0.758

Note: * $P<0.05$

^aMean Rank

Table 2 The differences in Glu and UA between the two groups

Group	<i>n</i>	Glu (mean rank)	UA (mean \pm SD, μ mmol/L)
Effective treatment group	420	231.18 ^a	305.47 \pm 110.84**
Ineffective treatment group	77	346.23 ^a	348.35 \pm 139.23**

** $P<0.01$

^aMean rank, $P<0.01$

Table 3 The odds ratio of HDL-c, Glu, and UA

Parameter	B estimate	Standard error	<i>P</i>	OR (95% CI)
Age	-0.041	0.011	<0.001	
HDL-c	-0.724	0.298	0.015	0.90 (0.41-1.98)
Glu	-0.271	0.049	<0.001	3.95 (2.27-6.87)
UA	1.24	0.44	0.008	2.19 (1.16-4.11)

Both Glu and (UA) exhibited significant differences between the two groups ($P<0.001$). Both Glu and UA levels of the ineffective treatment group were significantly higher than those of the effective treatment group.

Estimates of the Prognosis of ICH Patients by Biochemical Items

The binary logistic regression analysis was done by the forward LR procedure; the eliminated criterion was $P>0.05$, while if $P<0.05$, the item was identified as significant related to the outcome of acute ICH. Chi-square test was used to calculate the OR, the statistical analysis results of which are shown in Table 3.

The binary logistic regression analysis indicated the Glu, UA, and HDL-c levels were associated with the outcome of ICH ($P<0.05$). By chi-square test, the OR of high Glu was 3.2 (1.5-6.7 with 95% CI), and that of high UA was 3.8 (1.7-8.7 with 95% CI). However, the OR of low HDL-c was 0.90 (0.41-1.98 with 95% CI) without statistical difference.

Discussion

In recent years, the incidence of acute intracerebral hemorrhage (ICH) has been increasing, with high disability and mortality rates, especially in elderly people. Among the causes of ICH, hypertension and atherosclerosis are considered the main ones. However, there is no general consensus on the prognosis of ICH. In order to offer guidance to basic hospitals and community hospitals, we analyzed the relationship between routine biochemical factors and the prognosis of ICH retrospectively; this might help them judge the prognosis correctly and decrease the mortality and disability rates of ICH.

Effects of Abnormal Lipid Metabolism on Prognosis of ICH

Lipid metabolic disorders, including increased TC, TG, LDL-c and/or decreased HDL-c levels, play an important role in pathophysiological processes of atherosclerosis. Among many risk factors of intracerebral hemorrhage, hypertension and atherosclerosis, especially the joint action, are considered the main causes [1]. In our study, among 497 patients with ICH, serum lipid results had no significant differences between the effective treatment group and ineffective treatment group, except for HDL-c levels ($P < 0.05$). However, the OR of HDL-c was only 0.90 (0.41–1.98, 95% CI) without statistical significance. Recently, related studies have reported that low levels of serum TC, TG, HDL-c [2], and LDL-c [3] were considered strong predictors for poor outcome in patients with ICH, which is different from our data. The possible reason for the difference may be that we compared the lipids only and did not take hypertension into consideration. So, it is necessary for us to study the joint action of lipids and hypertension on ICH further.

Effects of Hyperglycemia on the Prognosis of ICH

Hyperglycemia is a common condition after ICH as a stress response to the severity of the bleeding [4]. But does hyperglycemia affect the prognosis of ICH? Our data showed that hyperglycemia may be a risk factor for poor outcome after ICH. The possible pathogenesis may be as follows: hyperglycemia aggravates the intracellular acidosis after ICH, damages nerve cells, and dilates blood vessels; all this will aggravate brain edema, increase intracranial pressure, and intensify brain damage. Schlenk reported that blood glucose

levels >7.8 mmol/L (140 mg/dl), but not levels >6.1 mmol/L (110 mg/dl), independently predicted unfavorable outcomes, and cerebral glucose increased only at blood levels >7.8 mmol/L (140 mg/dl). He suggested that the acceptable blood glucose level was up to 7.8 mmol/L (140 mg/dl) after SAH [5]. Godoy's results supported ours; he states that a 1.0 mmol/L (18 mg/dl) increase in the Glu concentration at admission was associated with a 33% mortality increase (OR: 1.33; 95%CI: 1.22–1.46; $P < 0.0001$) [6]. Ho reported maintenance of lower normoglycemia (4–8 mmol/L) with continuous titrated insulin therapy is associated with improved cerebral hemodynamics ($P < 0.001$), especially in the first 12 h [7].

Effects of Hyperuricemia on Prognosis of ICH

Hyperuricemia is a part of metabolic disease and occurs commonly in patients with type 2 diabetes; it has interactions with hypertension, so in our study, we analyzed the relationship between uric acid level and prognosis of ICH. We showed that UA of the ineffective treatment group was significantly higher than that of the effective treatment group, and hyperuricemia was a predictor of poor prognosis with OR 2.19 (1.16–4.11, 95% CI). Our results were consistent with Karagiannis's conclusions ($P = 0.001$; OR = 1.37; 95% CI = 1.13–1.67) [8]. Newman reported that urate levels of greater than 0.42 mmol/L predicted increased likelihood of suffering an independent event, including myocardial infarction, recurrent stroke, or vascular death [9]. The possible reason is as follows: Because of cerebral vasospasm and hematoma after ICH, focal cerebral ischemia causes the body to release more adenosine for regulating vascular relaxation; however, the adenosine is metabolized into uric acid in the vascular endothelial cell, which results in elevated blood UA. Thus, the UA level may reflect the severity of ICH to a certain extent, and hyperuricemia was considered a poor predictor of ICH.

In summary, by retrospectively analyzing relationships between the routine biochemical items and the prognosis of 497 patients with ICH, we found that both high Glu and high UA levels were risk factors for the prognosis of ICH; monitoring and controlling the Glu and UA may be advisable for improving the prognosis of ICH.

Acknowledgments In this study, we thank all participants and the data collection team of the First Affiliated Hospital of Chongqing Medical University. The contract grant sponsor was The First Affiliated Hospital of Chongqing Medical University, contract grant no. YXJJ2009-14.

Conflict of interest statement We declare that we have no conflict of interest.

References

1. Inagawa T (2007) Risk factors for primary intracerebral hemorrhage in patients in Izumo City, Japan. *Neurosurg Rev* 30:225–234 (discussion 234)
2. Li W, Liu M, Wu B, Liu H, Wang LC, Tan S (2008) Serum lipid levels and 3-month prognosis in Chinese patients with acute stroke. *Adv Ther* 25:329–341
3. Ramirez-Moreno JM, Casado-Naranjo I, Portilla JC, Calle ML, Tena D, Falcon A, Serrano A (2009) Serum cholesterol LDL and 90-day mortality in patients with intracerebral hemorrhage. *Stroke* 40:1917–1920
4. Tetri S, Juvela S, Saloheimo P, Pyhtinen J, Hillbom M (2009) Hypertension and diabetes as predictors of early death after spontaneous intracerebral hemorrhage. *J Neurosurg* 110:411–417
5. Schlenk F, Vajkoczy P, Sarrafzadeh A (2009) Inpatient hyperglycemia following aneurysmal subarachnoid hemorrhage: relation to cerebral metabolism and outcome. *Neurocrit Care* 11:56–63
6. Godoy DA, Pinero GR, Svampa S, Papa F, Di Napoli M (2008) Hyperglycemia and short-term outcome in patients with spontaneous intracerebral hemorrhage. *Neurocrit Care* 9:217–229
7. Ho CL, Ang CB, Lee KK, Ng IH (2008) Effects of glycaemic control on cerebral neurochemistry in primary intracerebral haemorrhage. *J Clin Neurosci* 15:428–433
8. Karagiannis A, Mikhailidis DP, Tziomalos K, Sileli M, Savvatanos S, Kakafika A, Gossios T, Krikis N, Moschou I, Xochellis M, Athyros VG (2007) Serum uric acid as an independent predictor of early death after acute stroke. *Circ J* 71:1120–1127
9. Newman EJ, Rahman FS, Lees KR, Weir CJ, Walters MR (2006) Elevated serum urate concentration independently predicts poor outcome following stroke in patients with diabetes. *Diabetes Metab Res Rev* 22:79–82

Clinical Management

Alteplase (rtPA) Treatment of Intraventricular Hematoma (IVH): Safety of an Efficient Methodological Approach for Rapid Clot Removal

J. Bartek Jr., J. Hansen-Schwartz, O. Bergdal, J. Degn, B. Romner, K.L. Welling, and W. Fischer

Abstract Intraventricular hemorrhage (IVH) subsequent to intracerebral hemorrhage (ICH) or subarachnoid hemorrhage (SAH) is associated with high mortality and morbidity. The use of fibrinolytic agents to treat this condition has previously been reported in small clinical trials with limited numbers of patients. Variability regarding inclusion criteria, method of administration and outcome have made it difficult to draw firm conclusions regarding the efficacy of antifibrinolytic therapy. Nine patients with CT-diagnosed IVH were treated with Alteplase intrathecally for 3 to 5 days according to the CT-verified clearance of IVH. After the treatment period, a repeat CT scan was performed to evaluate treatment effect.

In this safety study, we achieved rapid removal of IVH compared to retrospective controls, without incidents of re-bleeding, with only 33% permanent shunt placements and a neurological outcome of GOS of 4–5 in 44% of the patients. Based on the above results, the treatment protocol was considered safe and highly effective. A prospective randomized national multicenter trial has been initiated in order to evaluate the efficacy of this novel method also in terms of outcome and shunt dependency.

Keywords Intraventricular hemorrhage (IVH) · Intracerebral hemorrhage (ICH) · Subarachnoid hemorrhage (SAH) ·

Extraventricular drainage (EVD) · Intraventricular thrombolysis · Recombinant tissue plasminogen activator (rt-PA) · Hydrocephalus

Introduction

Intraventricular hemorrhage (IVH) is observed in approximately 40% of all patients with spontaneous hypertensive intracerebral hemorrhage (ICH) and in 30% of all patients with SAH [1, 2]. A significant IVH component is associated with both poorer outcome and a mortality rate of up to 90% [2–8]. The reason why IVH in itself carries a poor prognosis is not understood. It has been suggested that poorer ICP control [9], ischemic encephalopathy due to direct compression of central structures adjacent to the ventricles [2, 10], and brain edema [5] may be contributing factors.

In the case of ICH, surgical removal is an option in the current management of these patients, with the added risk of surgery usually not being significant. However, in the case of IVH, surgical removal is a challenge and has been shown to pose significant surgical risk to the patient and is generally not thought of as a therapeutic option [3]. With the advent of fibrinolytic agents, the goal of blood removal may be pursued with minimal surgical risk as it is administered via an external ventricular drain (EVD). The use of fibrinolytic agents to treat IVH has previously been reported in smaller clinical trials [9–17]. Due to differences in protocol and inclusion criteria, the results reported are by far equivocal.

The primary purpose of the present study was to devise a clinically feasible protocol for intrathecal administration of Alteplase and to demonstrate the safety of this treatment. Secondary endpoints were the assessment of incidence of ventriculitis, frequency of drain clotting, the need for VP shunt placement and preliminary clinical outcome as measured by the Glasgow Outcome Scale (GOS) score 6 months after admission at the hospital.

J. Bartek Jr. (✉), J. Degn, B. Romner, and W. Fischer
Department of Neurosurgery, the Neuroscience Centre, Copenhagen University Hospital Rigshospitalet, Landemerket 47, 3.sal, 1119, Copenhagen, Denmark
e-mail: jiri_bartek@hotmail.com

J. Hansen-Schwartz and O. Bergdal
Department of Neurosurgery, Copenhagen University Hospital of Glostrup, Copenhagen, Denmark

K.L. Welling
Neuro Intensive Care Unit (NICU), the Neuroscience Centre, Copenhagen University Hospital Rigshospitalet, Copenhagen, Denmark

Materials and Methods

The regional science ethics committee in Copenhagen approved the study.

Over a period of 2 years (January 2008 to January 2010) nine patients were included in the study. The mean age of the included patients was 58 (range 39–78), and the median GCS score upon admission was eight (range 6–15). Treatment with EVD was according to routine clinical practice and criteria. A CT scan was performed to verify catheter position. In cases where the IVH had occurred secondary to aneurysmal hemorrhage, the offending aneurysm had been secured. Routine blood workup was performed with emphasis on the clotting parameters.

Pregnancy, lactation, being less than 18 or greater than 85 years of age, and presence of coagulopathy (either spontaneous or iatrogenic through treatment with acetylsalicylic acid or vitamin K antagonist) led to exclusion from the study. Alteplase was used as fibrinolytic agent. The dose regimen was based on the experience of previously reported clinical trials [9–17] (Table 1). The following protocol was employed:

1. After aspiration of 4 mL of CSF from the EVD, 4 mg (1 mg/mL) of Alteplase was administered through the EVD every 24 h. Two milliliters of NaCl was used to flush the EVD after the Alteplase administration.
2. Following administration of Alteplase, the EVD was closed for up to 6 h, during which the intracerebral pressure (ICP) was monitored. However, if ICP rose above 25 mmHg for a period of more than 20 min prior to the 6 h limit, the EVD was re-opened against a 20-cm water pressure gradient.
3. The EVD was re-opened after 6 h to a pressure gradient of 20 cm water.
4. Prior to the administration of Alteplase the next day, the EVD was lowered to 0 cm water resistance for 1 h in order to evacuate blood components.
5. After the third dose was administered, a CT scan was performed the following day to visualize the treatment effect. If the CT scan revealed significant amounts of residual IVH, a further 1–2 days of treatment was initialized. Another control CT was performed 2 days after termination of the Alteplase treatment to evaluate the full effect of the treatment.

The observed IVH was graded according to the system devised by LeRoux et al. ([6]; see Table 2). In brief, each of the four ventricles are scored on a scale ranging from 1 to 4, 1 representing traces of blood, and 4 representing a ventricle filled entirely with blood. Thus, the total score of an IVH ranges between 1 and 16. CT scans were scored at the time before and after the Alteplase treatment. To compare the effect of Alteplase treatment in terms of blood clearance five random historical controls with IVH and treated with EVD were identified. The CT scans obtained were analyzed at time of presentation and at day 7. Treating the LeRoux scale as semiquantitative, differences were analyzed using Student's *t*-test. *P* values lower than 0.05 were considered significant.

The patients were followed-up 6 months after discharge, at which time they were clinically scored according to the Glasgow Outcome Scale (GOS) score. The possible insertion of a shunt system was registered, and the case notes were reviewed to ascertain any sign of a rebleed, incidents of catheter clotting and incidence of possible ventriculitis.

Table 1 Demographic data and treatment outcome

Patient	Age	Sex	Diagnosis	Comorbidity	GCS admitting score	LeRoux before treatment	LeRoux after treatment	Alteplase (rt-PA) total dose (mg)	VP shunt insertion	GOS after 6 months
1.	50	M	ICH	None	6	11	3	20	Y	GOS 4
2.	39	M	SAH	None	15	15	3	20	N	GOS 5
3.	78	W	ICH	Hypertension	7	12	4	20	N	GOS 1 ^a
4.	62	M	ICH	Hypertension	7	14	4	12	N	GOS 5
5.	49	M	ICH	None	8	14	4	12	Y	GOS 3
6.	58	W	ICH	Hypertension	6	15	2	20	N	GOS 1 ^b
7.	70	W	ICH	Hypertension	10	15	8	12	N	GOS 1 ^c
8.	50	W	SAH	None	8	10	0	20	N	GOS 4
9.	65	M	SAH	None	9	15	2	20	Y	N/A ^d

^aDied during admission due to pneumonia

^bDied because of poor cerebral status

^cDied during admission because of pneumonia

^dN/A since the patient was first included in the study in January 2010

Table 2 Grading system for severity of IVH (LeRoux scale). Each ventricle ($n=4$) is graded separately. The scores are added to a total range of 1–16

Grade	
1	Trace of blood
2	Less than half of the ventricle is filled with blood
3	More than half of the ventricle is filled with blood
4	The ventricle is filled with blood and expanded

According to LeRoux et al. [6]

Results

Nine patients were included in the study, five males and four females. Mean age was 58 years (range: 39–78), and mean GCS upon admission was eight (range: 6–15). Patients were admitted to the neurointensive care unit (NICU) for 19 days on average (range 7–30 days). Three patients were treated with Alteplase for 3 days, the remainder 5 days. The average treatment dose of Alteplase was 17.3 mg, either as a 3-day treatment of 12 mg or a 5-day treatment of 20 mg totally. Substantial removal of intraventricular hematoma size was achieved in 3–5 days (Fig. 1). Upon admission the average LeRoux grade of IVH was 13.4. After treatment, the mean LeRoux grade was 3.3. The average fall in LeRoux grading was 10.1 ($P<0.0001$; see Fig. 1).

In the control group patients were admitted with an average IVH grade of 11.6 and had an IVH grade of 7.8 at 7 days after admission. All patients in the control group were treated with EVD solely, and the average hematoma reduction according to LeRoux grade was 3.8.

No new hemorrhagic events in the nine patients receiving Alteplase were recorded. None of the treated patients

experienced clotting of the ventricular drain or the need for drain replacement, and there was no occurrence of ventriculitis observed during the Alteplase treatment period. Three out of the nine treated patients (33%) had a ventriculoperitoneal shunt placed. Three out of eight patients (38%) died before reaching the 6-month follow-up, with one patient not being eligible for 6-month follow-up because of recent treatment.

Three patients died before reaching follow-up. A cerebral cause of death could be identified in one case, whereas the other two patients died of septicemia.

Six months after IVH, four patients (44%) had a good clinical outcome (GOS 4–5).

Discussion

Spontaneous or secondary IVH carries a poor prognosis as an isolated primary event in itself, but also conditions secondary to the IVH, such as hydrocephalus, often require long-term treatment with EVD and subsequent VP shunts. In many cases, treatment with EVD is accompanied by complications, most notably reduced patency of CSF drainage due to blood clots obstructing the intraventricular catheter. Long-term EVD treatment often involves an increased risk of ventriculitis/CSF infection.

In addition, the blood clot in itself can exert a mass effect on the ventricular walls compromising local cerebral blood circulation [2, 8, 18]. It has also been described that blood clots can produce secondary neuronal degeneration because of an inflammatory reaction in the subependymal tissue [5], which is especially important if such a blood clot is located in relation to the third (hypothalamus) and fourth (brainstem) ventricles, which is often seen in patients with IVH.

Therefore, fibrinolytic agents injected into the ventricular system should rapidly dissolve blood clots and thereby reduce any mass effect on the ventricular walls as well as removing any substrates for deleterious breakdown products that could challenge the integrity of adjacent neural tissue and, potentially, patient recovery.

This study demonstrates that intrathecal Alteplase treatment over a 3–5-day period was efficient and safe in removing either totally or considerably the intraventricular blood present at the time of presentation. Among other interesting observations worth mentioning, we found a low VP shunt placement percentage of 33%, compared to 40–60% in the literature [1, 3, 6, 19], a good (GOS 4–5) neurological outcome 6 months post bleeding in 44% of our patients, and finally a low mortality rate of 22% compared to historic data in the range of 40–90% [1, 3, 6, 19] (Fig. 2).

There is a paucity of randomized clinical trials aimed at determining the risk/benefit ratio of intrathecal fibrinolytic therapy for IVH. To evaluate whether fibrinolytic treatment

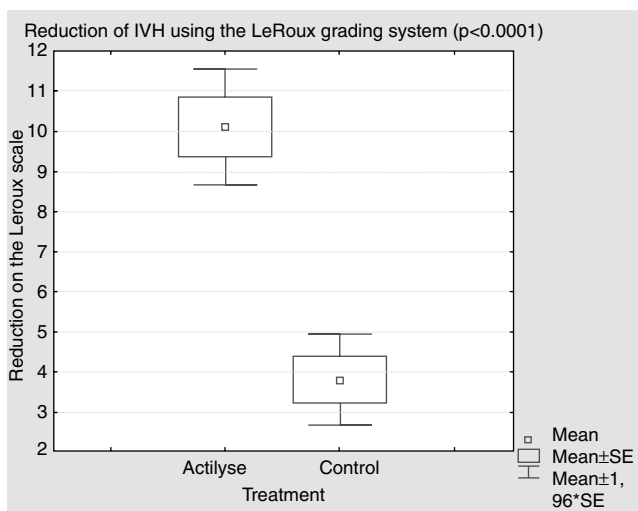
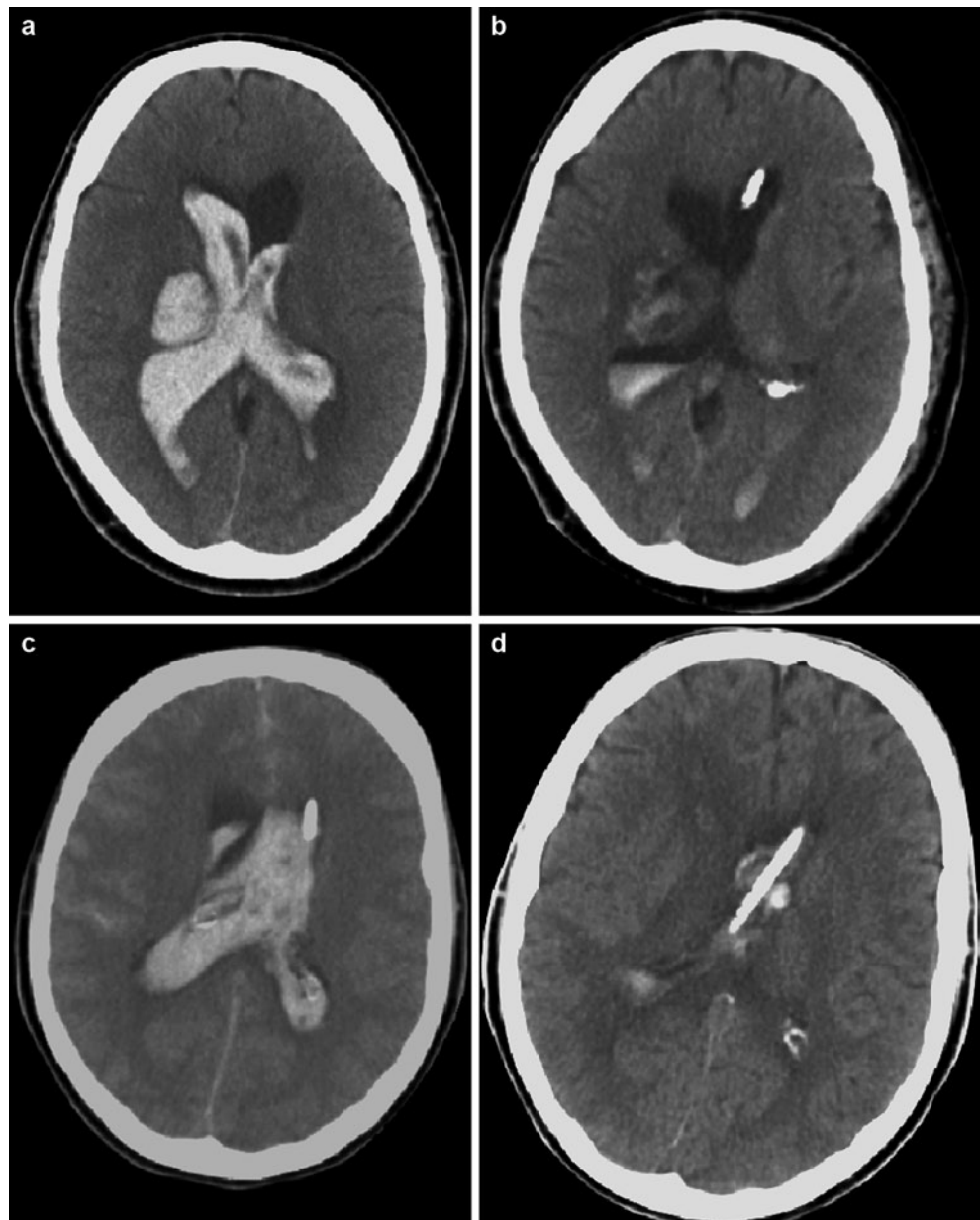


Fig. 1 Reduction of IVH, actilyse vs. control, using the LeRoux grading system ($P<0.0001$)

Fig. 2 (a and b) A 50-year-old man, initially GCS 6 with ICH+IVH (a), Alteplase treatment for 5 days with almost complete removal of IVH (b). No permanent shunt was placed. GOS 4 after 6 months. (c and d) A 40-year-old man, initially GCS 15 with SAH+IVH (c). Alteplase treatment for 5 days with almost complete removal of IVH (d). No permanent shunt was placed. GOS 5 after 6 months



carries a benefit to the patient, a Danish prospective randomized placebo-controlled multicenter study is currently being conducted to assess the effect on clinical outcome and shunt dependency. Also, this multicenter study will evaluate whether fibrinolytic therapy leads to shortened intensive care stay.

Conflicts of interest statement We declare that we have no conflict of interest.

References

1. Daverat P, Castel JP, Dartigues JF, Orgogozo JM (1991) Death and functional outcome after spontaneous intracerebral hemorrhage. A prospective study of 166 cases using multivariate analysis. *Stroke* 22(1):1–6
2. Shapiro SA, Campbell RL, Scully T (1994) Hemorrhagic dilation of the fourth ventricle: an ominous predictor. *J Neurosurg* 80(5):805–809
3. Broderick JP, Brott TG, Duldner JE, Tomsick T, Huster G (1994) Management of intracerebral hemorrhage in a large metropolitan population. *Neurosurgery* 34(5):882–887, discussion 887
4. Claassen J, Bernardini GL, Kreiter K, Bates J, Du YE, Copeland D et al (2001) Effect of cisternal and ventricular blood on risk of delayed cerebral ischemia after subarachnoid hemorrhage: the Fisher scale revisited. *Stroke* 32(9):2012–2020
5. Lee KR, Betz AL, Kim S, Keep RF, Hoff JT (1996) The role of the coagulation cascade in brain edema formation after intracerebral hemorrhage. *Acta Neurochir (Wien)* 138(4):396–400
6. LeRoux PD, Haglund MM, Newell DW, Grady MS, Winn HR (1992) Intraventricular hemorrhage in blunt head trauma: an analysis of 43 cases. *Neurosurgery* 31(4):678–684

7. Little JR, Blomquist GA Jr, Ethier R (1977) Intraventricular hemorrhage in adults. *Surg Neurol* 8(3):143–149
8. Young WB, Lee KP, Pessin MS, Kwan ES, Rand WM, Caplan LR (1990) Prognostic significance of ventricular blood in supratentorial hemorrhage: a volumetric study. *Neurology* 40(4):616–619
9. Fountas KN, Kapsalaki EZ, Parish DC, Smith B, Smisson HF, Johnston KW et al (2005) Intraventricular administration of rt-PA in patients with intraventricular hemorrhage. *South Med J* 98(8):767–773
10. Andrews CO, Engelhard HH (2001) Fibrinolytic therapy in intraventricular hemorrhage. *Ann Pharmacother* 35(11):1435–1448
11. Findlay JM, Grace MG, Weir BK (1993) Treatment of intraventricular hemorrhage with tissue plasminogen activator. *Neurosurgery* 32(6):941–947
12. Findlay JM, Jacka MJ (2004) Cohort study of intraventricular thrombolysis with recombinant tissue plasminogen activator for aneurysmal intraventricular hemorrhage. *Neurosurgery* 55(3):532–537
13. Goh KY, Poon WS (1998) Recombinant tissue plasminogen activator for the treatment of spontaneous adult intraventricular hemorrhage. *Surg Neurol* 50(6):526–531
14. LaPointe M, Haines S (2009) Fibrinolytic therapy for intraventricular hemorrhage in adults. *Cochrane Database Syst Rev* (3):CD0003692
15. Naff NJ, Hanley DF, Keyl PM, Tuhim S, Kraut M, Bederson J et al (2004) Intraventricular thrombolysis speeds blood clot resolution: results of a pilot, prospective, randomized, double-blind, controlled trial. *Neurosurgery* 54(3):577–583
16. Varelas PN, Rickert KL, Cusick J, Hacein-Bey L, Sinson G, Torbey M et al (2005) Intraventricular hemorrhage after aneurysmal subarachnoid hemorrhage: pilot study of treatment with intraventricular tissue plasminogen activator. *Neurosurgery* 56(2):205–213
17. Vereecken KK, Van HT, De BW, Parizel PM, Jorens PG (2006) Treatment of intraventricular hemorrhage with intraventricular administration of recombinant tissue plasminogen activator A clinical study of 18 cases. *Clin Neurol Neurosurg* 108(5):451–455
18. Steinke W, Sacco RL, Mohr JP, Foulkes MA, Tatemichi TK, Wolf PA et al (1992) Thalamic stroke. Presentation prognosis infarcts hemorrhages. *Arch Neurol* 49(7):703–710
19. Engelhard HH, Andrews CO, Slavin KV, Charbel FT (2003) Current management of intraventricular hemorrhage. *Surg Neurol* 60(1):15–21

Decompressive Hemi-craniectomy Is Not Necessary to Rescue Supratentorial Hypertensive Intracerebral Hemorrhage Patients: Consecutive Single-Center Experience

Norihito Shimamura, Akira Munakata, Masato Naraoka, Takahiro Nakano, and Hiroki Ohkuma

Abstract Objective: A consensus on decompressive surgery for hypertensive intracranial hemorrhage (ICH) has not been reached. We retrospectively analyzed our single-center experience with ICH. **Material and Methods:** From January 2004 to August 2009, 65 consecutive supratentorial ICH patients underwent surgery in our institute. Supratentorial ICHs that exhibited a hematoma volume of over 50 mL according to the xyz/2 method were included in this study. We compared a hematoma removal plus decompressive craniectomy group (DC) and a hematoma removal group (HR) with regard to GCS, preoperative hematoma volume, shift from the midline, time from the ictus to surgery, post-surgical hematoma volume, brain swelling, hospitalization periods, and m-RS after 3 months. Statistical analysis was done using the *t*-test or χ^2 test, and the odds ratio was calculated. **Results:** Twenty-five patients participated in this study. The DC group included 5 male patients, and the HR group 20 patients (F/M=8/12). Mean DC group age was 44.2 years, and 56.8 years for the HR group ($p<0.05$). GCS, preoperative hematoma volume, shift from the midline, time from the ictus to surgery, and postoperative hematoma volume were similar between both groups. Brain swelling on post-operative CT was demonstrated to be mild and delimited within the cranium in the DC group, similar to the HR group. Hospitalization periods increased in the DC group ($p<0.05$). The m-RS after 3 months was similar for both groups. The factors relevant for m-RS were age, postoperative hematoma volume, and GCS at 24 h after surgery. **Conclusion:** Decompressive craniectomy is not necessary for rescue in ICH if the hematoma can be removed completely.

Keywords Decompressive craniectomy · Hypertension · Intracerebral hemorrhage · Supratentorial

Introduction

In light of the randomized, prospective trial pertaining to hypertensive intracranial hemorrhage (ICH), the role of decompressive craniectomy has become controversial [1–4]. A consensus on decompressive surgery for ICH has also not been reached. We retrospectively analyzed our single-center consecutive experience with large ICHs and investigated the effect of decompressive hemi-craniectomy.

Material and Methods

From January 2004 to August 2009, 65 consecutive ICH patients underwent surgery in our institute. Supratentorial ICHs that exhibited a hematoma volume of over 50 mL according to the xyz/2 method were included in this study [5, 6]. We divided patients into two groups according to treatment methods: a hematoma removal plus decompressive hemi-craniectomy group (DC) and a simple hematoma removal by osteoplastic craniotomy group (HR). We compared the two groups with regard to GCS score, preoperative hematoma volume, shift from the midline, time from the ictus to surgery, post-surgical hematoma volume, brain swelling away from the normal inner layer of cranium (Fig. 1b), hospitalization periods, and modified Rankin Scale (m-RS) after 3 months. Statistical analysis was done using the *t*-test or χ^2 test, and the odds ratio was calculated (JMP 8.01, SAS institute Inc., Cary, NC). A *p*-value below 0.05 was accepted as statistically significant.

Perioperative treatment of patients was the same in both groups according to the AHA guideline [1]. Decompressive hemi-craniectomies were done in patients with a prospect of

N. Shimamura (✉), A. Munakata, M. Naraoka, T. Nakano, and H. Ohkuma

Department of Neurosurgery, Hirosaki University School of Medicine, 5-Zaihuchou, Hirosaki, Aomori, 036–8562, Japan
e-mail: shimab@cc.hirosaki-u.ac.jp

brain swelling or inadequate brain decompression after hematoma removal.

Illustrative Cases

Case 1. A 60-year-old male suffering with right putaminal hemorrhage was transferred to our department. He was administered warfarin because of an aortic mechanical valve. GCS score was 4, hematoma volume was 151 mL, and midline shift was 16 mm (Fig. 1a1). Removal of the hematoma and decompressive hemi-craniectomy were done on the same

day. A 5 mm brain swelling was recognized on the day after surgery (Fig. 1a2). Postoperative rebleeding did not occur (Fig. 1a3). His m-RS was five at 3 months after the ictus.

Case 2. A 69-year-old female suffering with right putaminal hemorrhage was transferred to our department (Fig. 1b1). She was administered warfarin because of arterial fibrillation. The GCS score was 10, hematoma volume was 118 mL, and midline shift was 12 mm. Simple removal of the hematoma by osteoplastic craniotomy was done on the same day. On the day after surgery, no remarkable brain swelling was recognized (Fig. 1b2). The postoperative course was uneventful (Fig. 1b2). Her m-RS was four at 3 months after the ictus.

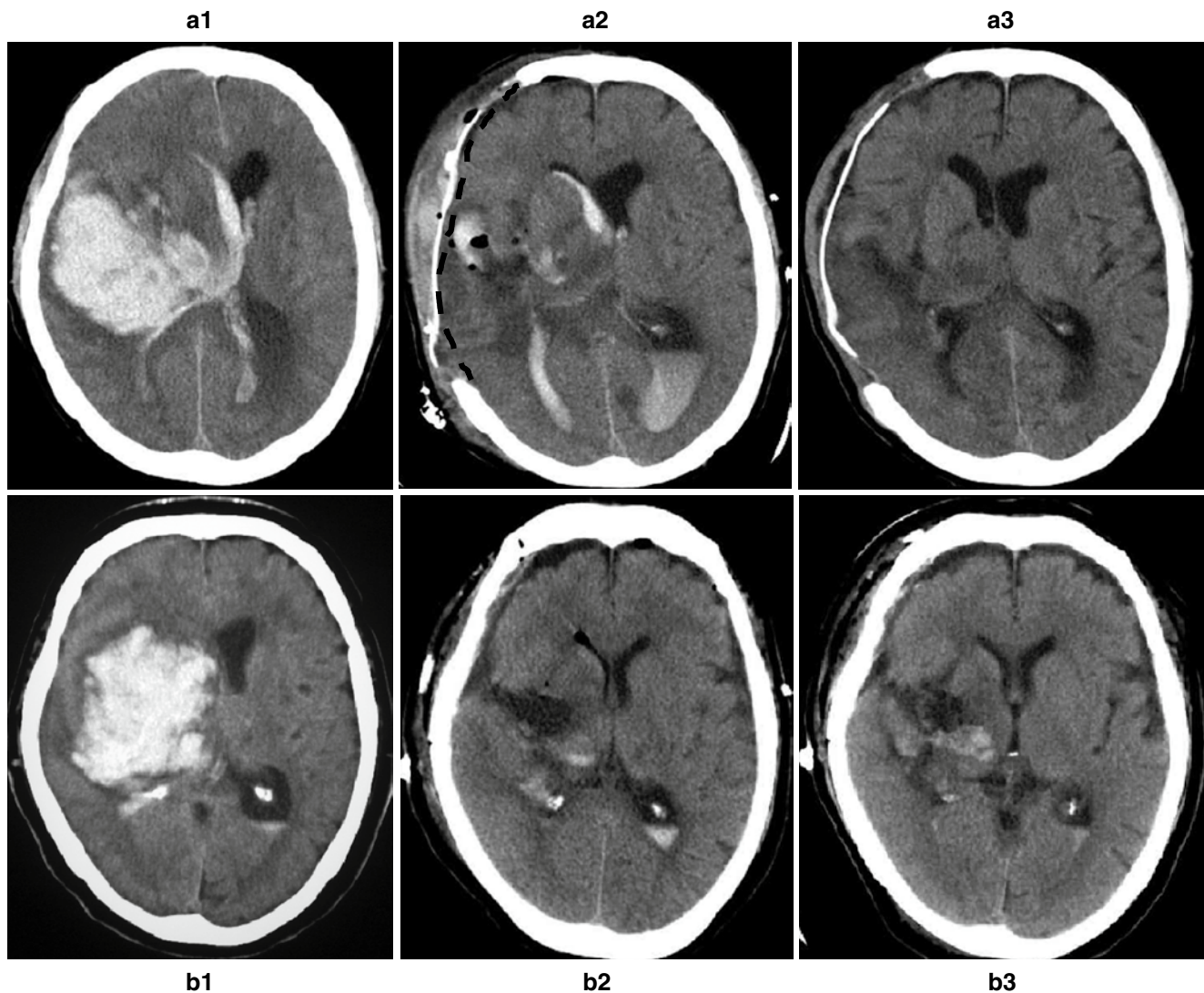


Fig. 1 Computed tomography of illustrative cases. (a) A 60-year-old male with right putaminal hemorrhage. (a1) Preoperative CT. Hematoma volume 151 mL and midline shift 16 mm. (a2) Postoperative CT at day 1. Brain swelling is at 5 mm beyond the normal inner bone (*dashed line*). (a3) Postoperative CT at day 8. No rebleeding experienced. (b) A

69-year-old female with putaminal hemorrhage. (b1) Preoperative CT. Hematoma volume 118 mL and midline shift 12 mm. (b2) Postoperative CT at day 1. No remarkable brain swelling was apparent. (b3) Postoperative CT at day 8. Her m-RS was four at 3 months after the ictus

Results

Twenty-five patients participated in this study (Table 1). The DC group included 5 male patients and the HR group 20 patients (F/M=8/12). Mean DC group age was 44.2 years and in the HR group 56.8 years ($p < 0.05$). GCS, preoperative hematoma volume, shift from the midline, time from the ictus to surgery, and postoperative hematoma volume were similar between both groups. Brain swelling on postoperative day 1 CT was demonstrated to be mild and delimited within the cranium in the DC group (Fig. 1a2), similar to the HR group. Hospitalization periods increased in the DC group ($p < 0.05$). The m-RS after 3 months was similar for both groups. The m-RS significantly correlated with patient age, preoperative hematoma volume, postoperative hematoma volume, and postoperative GCS at 24 h (Fig. 2). The relevant factors for m-RS were age (≤ 60), postoperative hematoma volume (≤ 2 mL), and GCS (≥ 10) at 24 h after surgery (Fig. 3).

Discussion

According to our results, decompressive hemi-craniectomy does not influence m-RS at 3 months after the ictus. The effectiveness of decompressive hemi-craniectomy has been demonstrated in malignant middle cerebral artery infarction and traumatic brain injury [7–11]. But there is no established evidence of the effectiveness of decompressive hemi-craniectomy for ICH. Efficient hematoma removal can reduce the need for decompressive hemi-craniectomy, while a reduction in

decompressive hemi-craniectomies reduces medical costs and hospitalization periods. We need to select candidates for decompressive hemi-craniectomy appropriately.

Pantazis et al. prospectively showed that surgical removal of large subcortical or putaminal hematomas greater than 30 mL yields better functional results than conservative therapy [12]. But they also pointed out that patients' GCS scores of under 8 or ICH volumes over 80 mL did not achieve a favorable outcome [12]. We report here for the first time that GCS scores at 24 h and hematoma volumes after surgery are predictive of patient outcome.

Our study group included five cases (20%) at GCS 3 or 4, and we treated more severe cases than previous reports [2, 12]. Cho et al. reported that surgical treatment is recommended at a GCS score of less than 12 with an ICH volume of at least 30 mL in order to save lives, and hematoma volume is more important than GCS to determine the treatment strategy [13]. Our results partially confirm their report; both preoperative hematoma volume and poor GCS are predictive of patient outcome.

Our median time from the ictus to surgery was 10 h and IQR was 6.25–20 h. In the STICH report, early surgery group median time between ictus and surgery was 30 h, and IQR was 16–46 h [2]. In the rat experimental model, inflammation and cell death start 4 h after the ICH [14]. At the same time, perihematomal increases in glucose metabolism occur after several days in human cases [15]. Early hematoma removal and reduction of intracranial pressure are beneficial for ICH.

The limitations of our study are that we did not make a comparison to conservative therapy, and this study is not randomized, nor is it a multicenter trial.

Table 1 Parameters for the two treatment groups

	Hematoma removal plus decompressive craniectomy	Simple hematoma removal
No. of patients	5	20
Gender (m/f)	5/0	12/8
Age (median, IQR)*	43 (36–53)	59 (50.3–66.5)
Side (right/left)	3/2	13/7
GCS (median, IQR)	7 (3.5–11)	8.5 (5.25–10.75)
Preop hematoma volume (mean, 95% CI)	97.8 mL (55.3–140)	80.4 mL (70.5–90.2)
Shift from the midline (mean, 95% CI)	10 mm (5.7–14.3)	8.2 mm (6.5–9.9)
Time from the ictus to surgery (mean, 95% CI)	15.7 h (8.2–18.4)	14.2 h (9.0–19.4)
Postoperative hematoma volume (mean, 95% CI)	7.55 mL (–12.2 to 27.3)	6.5 mL (1.0–12.1)
GCS at 24 h later (median, IQR)	9 (6.5–12)	10 (6–13)
Hospitalization periods (median, IQR)*	54 days (47–154)	20.5 days (15–30.5)
m-RS (median, IQR)	5 (3.5–5)	4 (4–4.75)

* $p < 0.05$

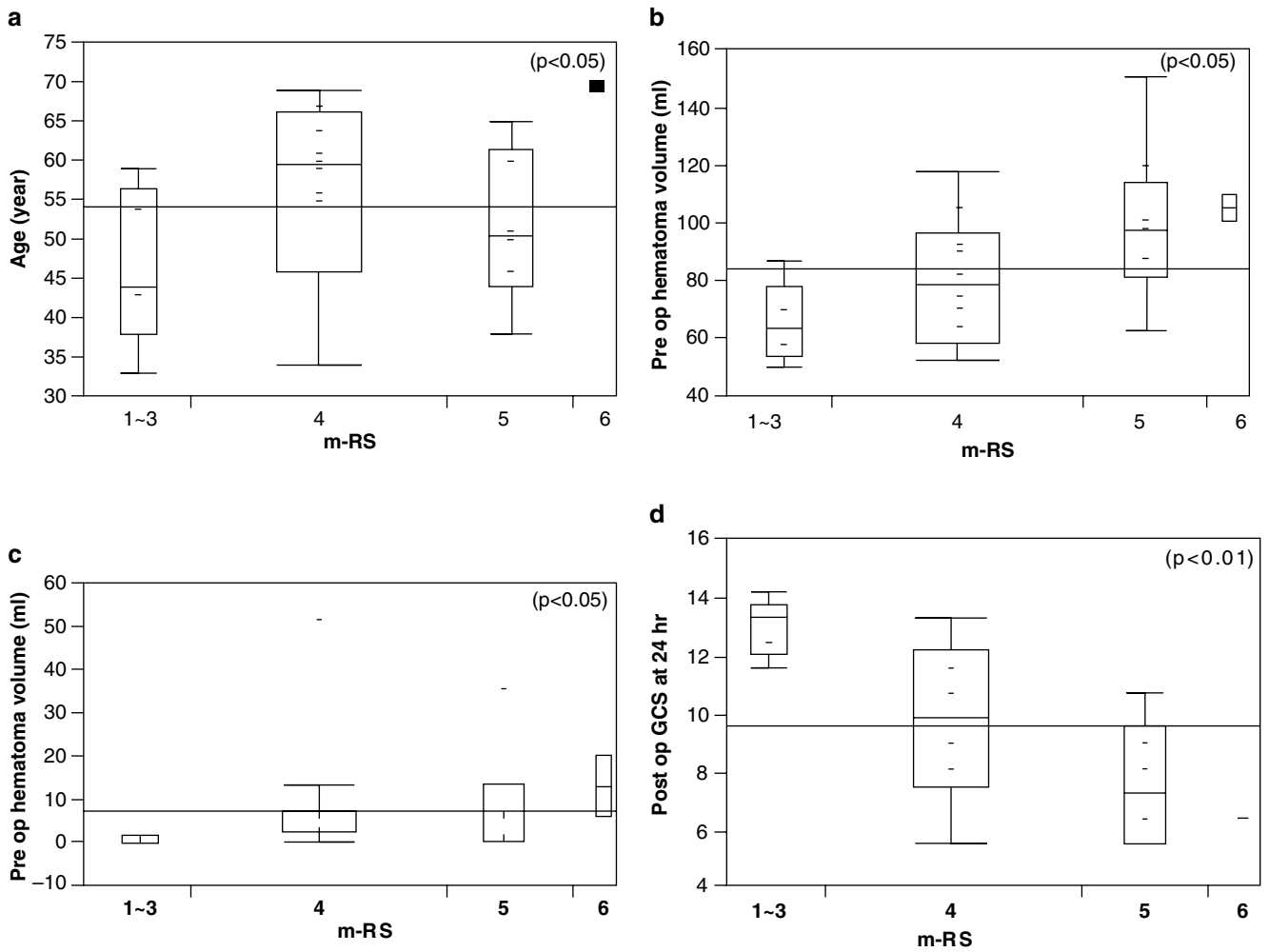


Fig. 2 Relationship to m-RS and parameters. (a) Patient age. (b) Preoperative hematoma volume. (c) Postoperative hematoma volume. (d) Postoperative GCS at 24 h

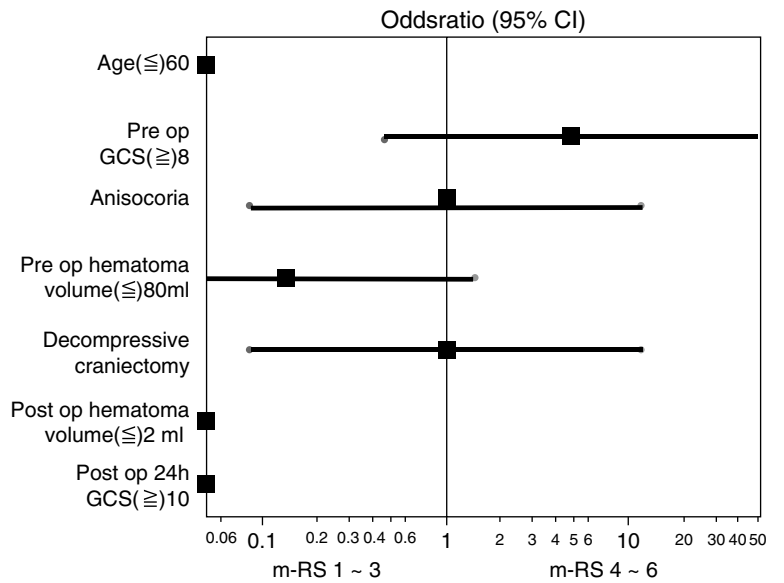


Fig. 3 Odds ratio for parameters

Conclusions

Decompressive craniectomy is not necessary for rescue in hypertensive ICH if the hematoma can be removed completely. Age, postoperative hematoma volume, and GCS at 24 h after surgery determine patient prognosis.

Conflict of interest statement We declare that we have no conflict of interest.

References

1. Broderick J, Connolly S, Feldmann E, Hanley D, Kase C, Krieger D, Mayberg M, Morgenstern L, Ogilvy CS, Vespa P, Zuccarello M (2007) Guidelines for the management of spontaneous intracerebral hemorrhage in adults: 2007 update: a guideline from the American Heart Association/American Stroke Association Stroke Council, High Blood Pressure Research Council, and the Quality of Care and Outcomes in Research Interdisciplinary Working Group. *Stroke* 38:2001–2023
2. Mendelow AD, Gregson BA, Fernandes HM, Murray GD, Teasdale GM, Hope DT, Karimi A, Shaw MD, Barer DH (2005) Early surgery versus initial conservative treatment in patients with spontaneous supratentorial intracerebral haematomas in the International Surgical Trial in Intracerebral Haemorrhage (STICH): a randomised trial. *Lancet* 365:387–397
3. Mitchell P, Gregson BA, Vindlacheruvu RR, Mendelow AD (2007) Surgical options in ICH including decompressive craniectomy. *J Neurol Sci* 261:89–98
4. Qureshi AI, Mendelow AD, Hanley DF (2009) Intracerebral haemorrhage. *Lancet* 373:1632–1644
5. Gebel JM, Sila CA, Sloan MA, Granger CB, Weisenberger JP, Green CL, Topol EJ, Mahaffey KW (1998) Comparison of the ABC/2 estimation technique to computer-assisted volumetric analysis of intraparenchymal and subdural hematomas complicating the GUSTO-1 trial. *Stroke* 29:1799–1801
6. Kothari RU, Brott T, Broderick JP, Barsan WG, Sauerbeck LR, Zuccarello M, Khoury J (1996) The ABCs of measuring intracerebral hemorrhage volumes. *Stroke* 27:1304–1305
7. Adams HP Jr, del Zoppo G, Alberts MJ, Bhatt DL, Brass L, Furlan A, Grubb RL, Higashida RT, Jauch EC, Kidwell C, Lyden PD, Morgenstern LB, Qureshi AI, Rosenwasser RH, Scott PA, Wijdicks EF (2007) Guidelines for the early management of adults with ischemic stroke: a guideline from the American Heart Association/American Stroke Association Stroke Council, Clinical Cardiology Council, Cardiovascular Radiology and Intervention Council, and the Atherosclerotic Peripheral Vascular Disease and Quality of Care Outcomes in Research Interdisciplinary Working Groups: the American Academy of Neurology affirms the value of this guideline as an educational tool for neurologists. *Stroke* 38:1655–1711
8. Albanese J, Leone M, Alliez JR, Kaya JM, Antonini F, Alliez B, Martin C (2003) Decompressive craniectomy for severe traumatic brain injury: evaluation of the effects at one year. *Crit Care Med* 31:2535–2538
9. Vahedi K, Hofmeijer J, Juettler E, Vicaut E, George B, Algra A, Amelink GJ, Schmiedeck P, Schwab S, Rothwell PM, Bousser MG, van der Worp HB, Hacke W (2007) Early decompressive surgery in malignant infarction of the middle cerebral artery: a pooled analysis of three randomised controlled trials. *Lancet Neurol* 6:215–222
10. Vahedi K, Vicaut E, Mateo J, Kurtz A, Orabi M, Guichard JP, Boutron C, Couvreur G, Rouanet F, Touze E, Guillon B, Carpentier A, Yelnik A, George B, Payen D, Bousser MG (2007) Sequential-design, multicenter, randomized, controlled trial of early decompressive craniectomy in malignant middle cerebral artery infarction (DECIMAL Trial). *Stroke* 38:2506–2517
11. Venes JL, Collins WF (1975) Bifrontal decompressive craniectomy in the management of head trauma. *J Neurosurg* 42:429–433
12. Pantazis G, Tsitsopoulos P, Mihas C, Katsiva V, Stavrianos V, Zymaris S (2006) Early surgical treatment vs conservative management for spontaneous supratentorial intracerebral hematomas: a prospective randomized study. *Surg Neurol* 66:492–501
13. Cho DY, Chen CC, Lee HC, Lee WY, Lin HL (2008) Glasgow Coma Scale and hematoma volume as criteria for treatment of putaminal and thalamic intracerebral hemorrhage. *Surg Neurol* 70:628–633
14. Xue M, Del Bigio MR (2000) Intracerebral injection of autologous whole blood in rats: time course of inflammation and cell death. *Neurosci Lett* 283:230–232
15. Zazulia AR, Videen TO, Powers WJ (2009) Transient focal increase in perihematomal glucose metabolism after acute human intracerebral hemorrhage. *Stroke* 40:1638–1643

Intravascular Hypothermia for Acute Hemorrhagic Stroke: A Pilot Study

Jafri Malin Abdullah and Andrian Husin

Abstract The use of intravascular hypothermia in the treatment of hemorrhagic stroke is currently still being researched. The exact therapeutic properties and effect of hypothermia on the natural progression of the disease are not known, and a only small number of papers has been published with results from these studies.

Mild hypothermia at 34°C was induced in six patients with hemorrhagic stroke in the first 48 h after presentation, using an intravascular catheter placed in the inferior vena cava. The hypothermia was induced and maintained for 24 h followed by gradual rewarming. Another 18 patients with hemorrhagic stroke but not receiving hypothermia were then taken as the control group, and all patients were treated with standard stroke management. The patients were then followed up using the modified Rankin Scale (mRS) for 6 months and 1 year.

There was a statistically significant improvement at 6 months and 1 year follow-up using the mRS score in the hypothermia group, indicating a possible beneficial effect of early therapeutic hypothermia in the management of acute hemorrhagic stroke. However, a larger study is needed in order to confirm our finding.

Keywords Adjunct treatment · Hypothermia · Intracerebral hemorrhage · mRS score

Introduction

The use of hypothermia in acute stroke has been gaining renewed interest in the last few years. However, a very limited number of papers have been published regarding the use

of hypothermia in the treatment of hemorrhagic stroke [1–4]. These papers are mostly pilot or feasibility studies, or studies on animal models.

Materials and Methods

Subjects

Twenty-four patients with confirmed hemorrhagic stroke on CT scan were recruited after fulfilling our inclusion and exclusion criteria. Only six patients consented to having intravascular hypothermia. Eighteen others who agreed were recruited as controls. All patients received standard management for stroke, including antihypertensive medication, physiotherapy and supportive care.

Our inclusion criteria were patients whose ages were between 18 and 80 years, intracerebral hemorrhage on confirmed radiological imaging and those who presented within 48 h of onset of the first symptoms. Exclusion criteria for our study included pregnancy or having uncontrolled severe and chronic medical problems including cardiac, renal or liver failure, AIDS, previously diagnosed vascular malformations, cancer, hemorrhage secondary to other causes such as warfarin, congenital abnormalities, presence of intraventricular hemorrhage, posterior fossa hemorrhage, hematological conditions such as Sickle cell disease, cryoglobulinemia and vasospastic disorder as well as any surgical intervention that was planned for the patient.

Study Protocol and Design

The study was a nonrandomized, prospective, controlled clinical trial. The study protocol and design were reviewed and accepted by the Ethics Committee of the School of

J.M. Abdullah (✉) and A. Husin
Department of Neurosciences, School of Medical Sciences,
Universiti Sains Malaysia, Health Campus, Jalan Sultanah Zainab 2,
Kubang Kerian, Kota Bharu 16150, Kelantan, Malaysia
e-mail: brainsciences@gmail.com

Medical Sciences, Universiti Sains Malaysia, in 2005. The study duration was January 2005 and June 2008, and the study population was made up of patients presenting to Universiti Sains Malaysia Hospital, Kubang Kerian, Kelantan, Malaysia (HUSM), with confirmed hemorrhagic stroke. We recruited patients with confirmed intracerebral hemorrhage on CT scan that presented to our hospital within 24 h of stroke symptom onset. After fulfilling our inclusion and exclusion criteria as outlined above, the patients were either selected for induction of hypothermia or observation depending on the consent given. The reason for nonrandomization of the study was that consent for the procedure was integral to our study. This was not achieved in many instances since in this 2-year period, refusal to be in the study was high because of the numerous possible complications of hypothermia, including death, were high.

The patients that were selected for hypothermia were then transferred to our High Dependency Unit and an intravascular catheter (ICY Catheter by Alsius, Irvine, CA) was inserted in the right femoral vein. The catheter was then connected to the mobile temperature management system, the CoolGard 3000 (Alsius, Irvine, CA). This system is basically a heat exchange system whereby a heat exchange balloon is built into the catheter that is placed in the inferior vena cava. Cold sterile saline then is circulated by a pump through the balloon, thus cooling the blood in the inferior vena cava. The target temperature and the rate of cooling could be adjusted between 0.5°C and 42°C. In all patients that underwent hypothermia, the highest rate of cooling was used and the target temperature set at 34°C. The temperature probe was placed in the rectum as per the instructions of the CoolGard 3000 system. This intravascular system has the advantage of better temperature control and a faster cooling rate compared to the surface cooling method, at least according to Steinberg et al. in 2004. Once the target temperature of 34°C was achieved, this was maintained for at least 24 h, after which gradual rewarming of about 1°C/h was initiated. It was imperative that the rewarming phase was gradual as it has been shown that fast rewarming can cause a rebound increase in intracranial pressure and influence outcome as described by Bloch in 1964 [5]. Once normothermia had been achieved, the catheter was removed, and the patient was then transferred to a normal ward. The control group, which did not receive hypothermia, was managed in a standard manner for hemorrhagic stroke, which included antihypertensive medications as needed.

Follow-Up Assessment

Modified Rankin Scale [6] was used in the follow-up phase to assess the outcome in these patients. The patients were

reviewed in our neurosurgery out-patient clinic and assessed by a single non-blinded observer.

Adverse Event

The first two patients in the hypothermia group met with early death within the first week of admission. The first patient died after 5 days of completing the hypothermia therapy, while the second patient died 24 h after completing the therapy. In both in patients the causes of death were not determined as autopsy was refused, but both deaths occurred suddenly in otherwise stable patients, leading to possible cardiorespiratory events causing the death. By day 90 of follow-up, two patients in the control group had died of unknown causes, both of whom had died at home and had no autopsy done. No neurological deterioration was recorded during admission for the rest of the hypothermia and control group.

Results

The baseline characteristics for both groups are shown in Table 1. The most obvious difference between the interventional group and control group were the mean age of patients and GCS score on admission.

We recorded the modified Rankin Scale score in all patients at 7 days, 3 months, 6 months and 1 year of follow-up (Table 2, Fig. 1). Those patients who were unable to attend the out-patient clinic were given a phone call, and the best description of the patient or carrier was taken as the current condition.

Discussion

The underlying neuroprotective mechanism of hypothermia involves several pathophysiological steps. The cerebral protection accorded by hypothermia may be in part due to decreased metabolic requirements according to the Q10 principle, representing the factor by which the rate of biochemical reaction increases for a 10°C rise in temperature [7]. Our inclusion criteria for the study were based on a previous review of therapeutic hypothermia [8]. We however focused on subjects with basically stable, supratentorial, spontaneous intracerebral hemorrhage that did not undergo any surgical intervention. In such a high morbidity and mortality condition, we felt that our early study needed to focus on a more stable subgroup of the hemorrhagic stroke.

Table 1 Baseline clinical characteristics of patients recruited in the study on admission. *P*-value less than or equal to 0.05 taken as significant

Characteristic	Intervention group (<i>n</i> =6)	Control group (<i>n</i> =18)	<i>P</i> -value (independent t test)
Age (years)			
Mean	49.8	60.7	0.03
Range	(42–59)	(45–70)	
Male (%) percentage GCS score	33.3	33.3	0.04
Mean	14.7	11.8	0.01
Range	(14–15)	(9–15)	
SBP (mmHg)			
Mean	162	154.3	0.13
Range	(150–178)	(138–170)	
DBP (mmHg)			
Mean	98.3	98.3	1
Range	(89–118)	(989–110)	
Temperature (°C)			
Mean	37.3	37.3	0.95
Range	(37–37.5)	(37–37.8)	

Table 2 mRS score at follow-up day 0, 7, 30 and 90. *P* values were obtained using Mann-Whitney test. The difference is significant at 6 months and 1 year of follow-up

	Intervention group (<i>n</i> =6)			Control group (<i>n</i> =18)			<i>P</i> -value
mRS day 0 Median; Mean; Range	4	3.75	(3–4)	4	4.13	(4–5)	0.090
mRS day 7 Median; Mean; Range	4	3.75	(3–4)	4	4.2	(4–5)	0.080
mRS 6 months Median; Mean; Range	3	3.0	(2–4)	4	3.87	(3–4)	0.009*
mRS 12 months Median; Mean; Range	2	2.25	(2–3)	4	3.4	(2–4)	0.016*

**P* value <0.05 taken as significant

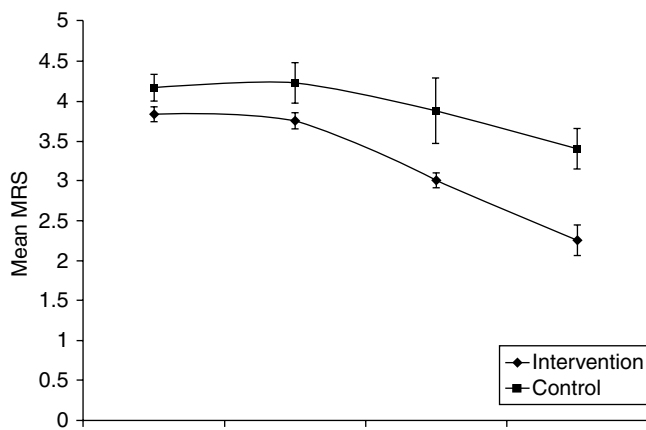


Fig. 1 Graphical representation of the mRS score between the two groups. The data obtained from the follow-up were analyzed using SPSS 12, and the Mann-Whitney test was used because of the non-normal distribution of the samples

The use of an intravascular cooling method was chosen because of the superiority of this method in comparison to other methods available with regard to rate of cooling and

maintenance of target temperature [2–4, 9]. The target temperature of 34°C (mild hypothermia) was chosen as temperatures lower than this have been shown to be associated with more complications. The duration of therapeutic hypothermia at target temperature was chosen to be 24 h and then followed by gradual rewarming to prevent a rebound increase in intracranial pressure. The use of the CoolGard 3000 system made the control of temperature precise with the placement of the exchange catheter in the inferior vena cava. We however felt that the effect of cooling the blood via the inferior vena cava resulted in cooling of the heart and lungs, causing some of the side effects of hypothermia, such as cardiac arrhythmias and increased risk of lung infection.

The baseline characteristics of both groups showed a statistically significant difference of mean age 49.8 years in the hypothermia group compared to 60.7 years for control group. This might be a reflection of the small number of patients in the intervention group. The presenting GCS was 14.7 in the hypothermia group and 11.8 in the control group, a difference of about three points in the GCS score. Thus, the hypothermia group was younger and three points better on the GCS on admission.

The results of the mRS score showed a difference of one point at 6-month follow-up and two points at 1-year follow-up ($P < 0.05$).

Conclusion

There was a statistically significant difference between the mRS score of the hypothermia group and the control group. This shows that mild hypothermia may have a beneficial effect in the treatment of acute hemorrhagic stroke. We suggest starting a larger multicenter study to analyze the effects of hypothermia on hemorrhagic stroke in the near future.

Conflict of interest statement We declare that we have no conflict of interest.

References

1. Kawanishi M, Kawai N, Nakamura T, Luo C, Tamiya T, Nagao S (2008) Effect of delayed mild brain hypothermia on edema formation after intracerebral hemorrhage in rats. *J Stroke Cerebrovasc Dis* 17(4):187–195
2. Linares G, Mayer SA (2009) Hypothermia for the treatment of ischemic and hemorrhagic stroke. *Crit Care Med* 37(7 Suppl): S243–S249
3. MacLellan CL, Davies LM, Fingas MS, Colbourne F (2006) The influence of hypothermia on outcome after intracerebral hemorrhage in rats. *Stroke* 37(5):1266–1270
4. Otani N, Takasato Y, Masaoka H, Hayakawa T, Yoshino Y, Yatsushige H, Miyawaki H, Sumiyoshi K, Chikashi A, Takeuchi S, Suzuki G (2008) Surgical outcome following decompressive craniectomy for poor-grade aneurysmal subarachnoid hemorrhage in patients with associated massive intracerebral or Sylvian hematomas. *Cerebrovasc Dis* 26(6):612–617
5. Bloch JH, Manax WG, Eyal Z, Lillehei RC, (1964) Heart Preservation in vitro with Hyperbaric Oxygenation and Hypothermia. *J Thorac Cardiovas Surg.* 48:969–83
6. Huybrechts KF, Caro JJ, Xenakis JJ, Vemmos KN (2008) The prognostic value of the modified Rankin Scale score for long-term survival after first-ever stroke. Results from the Athens Stroke Registry. *Cerebrovasc Dis* 26(4):381–387
7. Goto Y, Kassell NF, Hiramatsu K, Soleau SW, Lee KS (1993) Effects of intraischemic hypothermia on cerebral damage in a model of reversible focal ischemia. *Neurosurgery* 32(6):980–984 (discussion 984–985)
8. Jaramillo A, Illanes S, Díaz V (2008) Is hypothermia useful in malignant ischemic stroke? Current status and future perspectives. *J Neurol Sci* 266(1–2):1–8 (Epub 2007 Nov 26. Review)
9. Steinberg GK, Ogilvy CS, Shuer LM, Connolly ES Jr, Solomon RA, Lam A, Kassell NF, Baker CJ, Giannotta SL, Cockroft KM, Bell-Stephens TE, Allgren RL (2004) Comparison of endovascular and surface cooling during unruptured cerebral aneurysm repair. *Neurosurgery* 55(2):307–14 (discussion 314–5)

Use of Intralesional tPA in Spontaneous Intracerebral Hemorrhage: Retrospective Analysis

Walter D. Johnson and Peter A. Bouz

Abstract *Introduction:* Neurosurgical treatment of spontaneous intracerebral hemorrhage (ICH) is controversial, with a lack of evidence-based guidelines contributing to the high variety of treatments. In our study we examine the outcome and complication from use of intralesional tissue plasminogen activator (IL tPA).

Method: Patients who have been treated with IL tPA for spontaneous ICH were reviewed retrospectively. We compared clot sizes before and after tPA infusion, and outcome based on the modified Rankin score.

Results: Nine patients received IL tPA during the period 1999–2009. No immediate complications with use of IL tPA were found. There was a statistically significant volume reduction in clot sizes on computed tomography. Four patients recovered to independent functional status. Three patients were discharged to SNF, and two patients died as a result of ICH. Our results appear to demonstrate superior outcome to supportive management and no worse result than surgical management.

Conclusion: It appears a subset of ICH patients benefits from use of IL tPA. This study demonstrates that IL tPA use is safe and has the potential to improve outcome compared to conservative management without the risk of surgical complications. Our patient size is small, and larger prospective studies are needed to provide solid guidelines for management of ICH.

Keywords Tissue plasminogen activator · tPA · Intracerebral hemorrhage · Intralesional · ICH

Introduction

According to available statistics each year, approximately 37,000–52,400 people in the United States have an intracerebral hemorrhage [1]. Of these patients less than one-third will make a functional recovery, and 35–52% are likely to die [2–4]. Even worse prognosis has been reported with a component of intraventricular hemorrhage (IVH) [1, 2, 5].

Treatment of spontaneous ICH continues to be controversial. Multiple studies have been conducted in the past with goals of establishing guidelines for treatment of spontaneous ICH. Despite the prevalence of the condition, to date, no class I ICH-specific treatment recommendation exists [1]. Currently there are several ongoing studies looking into the benefit of intralesional tPA use with promising preliminary results.

Patients and Methods

An institutional review board-approved retrospective review of the patients who received IL tPA from the period 1999–2009. We included all patients who received bedside placement of an intralesional catheter within 24–48 h from presentation and subsequently received the IL tPA. The etiology of ICH was presumed to be hypertensive in all of the cases; aneurysmal and vascular malformation hemorrhages were excluded in all patients prior to beginning tPA treatment. After diagnosis of ICH with or without ICH component, based on non-contrast head computed tomography, the intralesional drain was placed. A Codman external ventricular drain (EVD) catheter was used in all these cases. Following the placement of the catheter, the appropriate position was confirmed using CT scan. Adjustments were made if necessary to insure a good position of the catheter prior to the administration of tPA. Using an established protocol, 2 mg/2 mL of tPA was administered once daily with

W.D. Johnson (✉) and P.A. Bouz
Department of Neurosurgery, Loma Linda University,
School of Medicine, Loma Linda, 92350, CA, USA
e-mail: wjohnson@llu.edu

periodic evaluation utilizing computed tomography. The drain was clamped for 30 min following the administration of tPA, then opened to drain. In all cases administration of IL tPA was done in the ICU setting. Blood pressure was strictly controlled as per standard post-ICH stroke protocol. We reviewed and compared the exam and functional status of all patients at the presentation as well as at the time of discharge (Fig. 1).

Results

In our study we included nine patients that received bedside intralesional catheter placement and administration of IL tPA. Average age of patients was 60 years old, ranging from 49 to 80 years old. Average clot size on presentation was 97 cc, ranging from 38 cc to 190 cc. Duration of tPA infusion varied depending on the size of the ICH and clinical

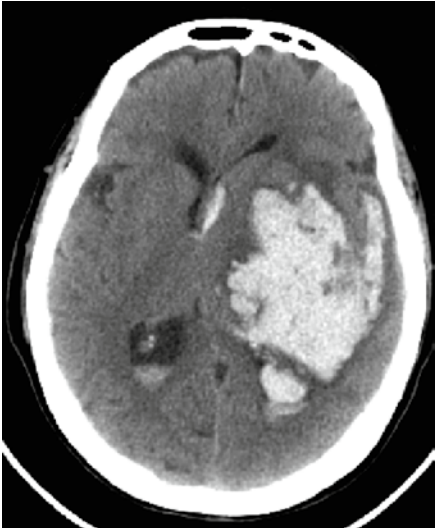
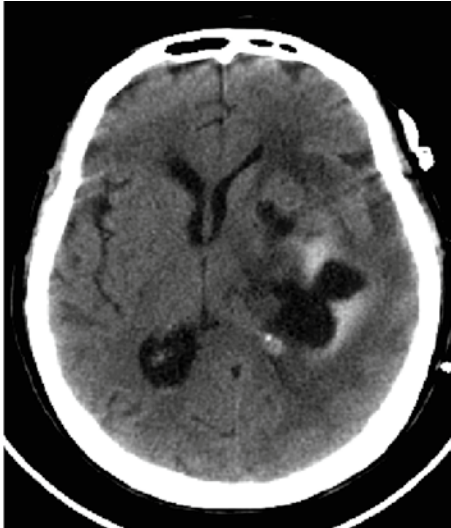


Ref to the Table 1	CT image on presentation	CT image after the completion of tPA therapy
Patient #6	Day 0 	Day 8 
Patient #5	Day 0 	Day 3 

Fig. 1 Examples of single-slice CT cuts of selected patients included in the study

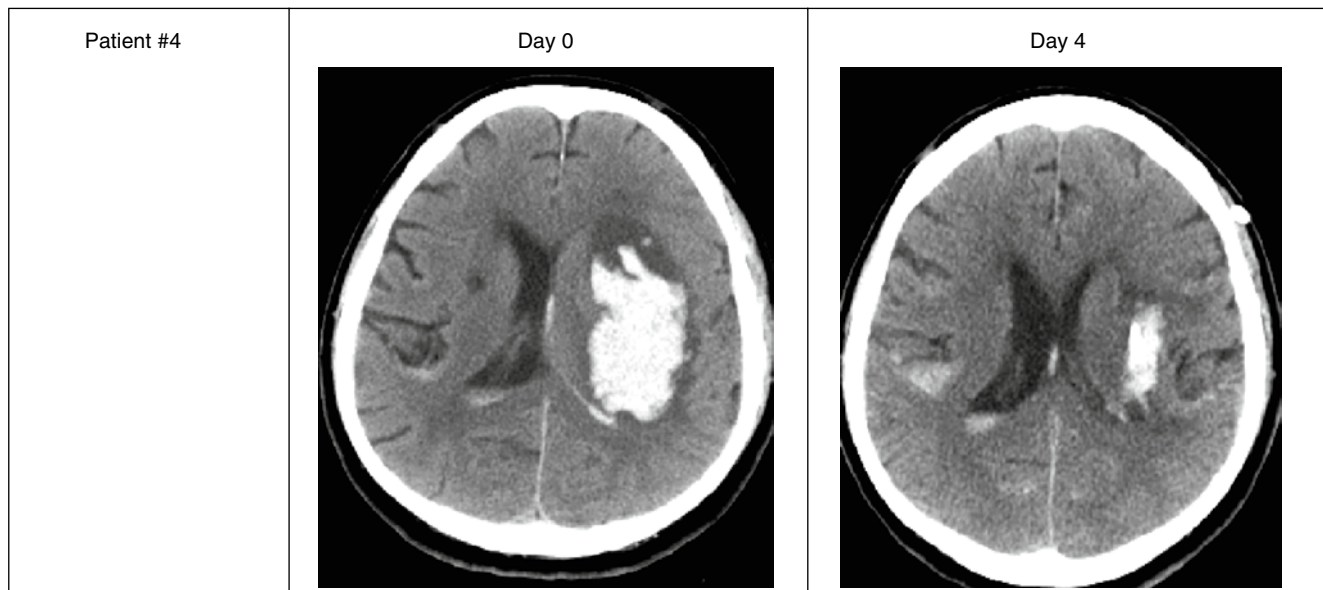


Fig. 1 (continued)

symptoms. The end point of IL tPA therapy termination was chosen based on clinical status or when acceptable clot reduction had been achieved. To analyze and compare the outcome, we used the Modified Rankin Scale. The majority of patients had a Modified Rankin Score of 5 on presentation. Table 1 summarizes the profile and the outcome of the patients.

The hematoma volume was determined using the ABC/2 equation (height, depth, and width over 2). A p value ≤ 0.05 was considered statistically significant. Using t-score analysis, we report statistically significant clot resolution with a p value < 0.05 .

We did not observe hematoma expansion in any of the patients who received IL tPA. The majority of patients showed improvement based on the Modified Rankin Scale. Mortality within 30 days associated with ICH was 28%.

Functional recovery (Modified Rankin score 2 or better) was 45%. Both parameters appeared to be better than previously reported. IVH was the most significant factor associated with poor outcome. Both mortalities in our study had a significant IVH component upon presentation. Other factors influencing the outcome were co-morbidities prior to injury, location of clot, size of the clot and catheter position.

Discussion

It has been reported that extent of ICH-mediated brain injury relates directly to clot volume and duration of blood exposure to brain [6, 7]. To date, there is no evidence suggesting that surgical intervention is superior to medical management,

Table 1 Clinical, radiological and outcome data

Patient	Age	Modified Rankin score on presentation	Modified Rankin score on discharge	Days of tPA infusion	Clot size on presentation	Clot size on termination of tPA	IVH +/-
1	67	5	5	6	38	18	+
2	53	5	6	7	146	0	+
3	60	5	3	7	38	0	-
4	54	4	1	4	68	15	-
5	49	4	2	3	60	10	-
6	80	4	2	8	152	0	-
7	52	5	6	4	190	50	+
8	51	5	2	5	86	20	-
9	79	5	3	4	100	39	-

especially given patients' frequently severe comorbidities. The medical management of acute ICH revolves around the concept of hematoma stabilization and supportive measures, generally including strict BP control and normalizing of coagulation profiles. Several surgical strategies are currently being tested against medical management: craniotomy and evacuation of the hematoma, endoscopic aspiration of the hematoma, stereotactic placement of the catheter and infusion of tPA, and bedside drain placement with subsequent infusion of tPA. A large, multicenter prospective randomized surgical trial in intracerebral hemorrhage (STICH) evaluated patients with intracerebral hemorrhage. The study compared early surgery versus conservative treatment for patients with ICH. It was concluded that patients with spontaneous supratentorial intracerebral hemorrhage in neurosurgical units showed no overall benefit from early surgery [8]. SICHPA (Stereotactic treatment of Intracerebral Hemorrhage by means of a Plasminogen Activator) was another multicenter randomized controlled trial that attempted to prove clinical benefit of using IL tPA. Even though the study was stopped prematurely because of slow patient accrual, they were able to demonstrate that stereotactic aspiration can be performed safely, leading to a reduction of 18 mL of hematoma over 7 days; comparatively the control group had a 7-mL reduction over the same period. Thus, the assumption was made that use of IL tPA may improve prognosis [9]. MISTIE (Minimally Invasive Surgery plus tPA for Intracerebral hemorrhage Evacuation) is an ongoing clinical trial. Subjects were randomized to surgery undergoing stereotactic catheter placement and clot aspiration. Following the surgical procedure, tPA is being administered as per the instituted protocol. Preliminary findings demonstrate greater clot resolution than traditional medical management [7]. With all available studies, the Cochrane Database of Systematic Review 2009 concluded that there is a need for further trials of surgery versus no surgery to identify those patients most likely to benefit, and to find effective but less invasive methods of removing the hematoma [10].

In summary, the results of our study lend support to the usefulness of IL tPA in the patient population with spontaneous ICH. There are several limitations in this study that must be mentioned. Being a retrospective study with a small number of patients, no definitive statement can be made on the long-term outcome. Our outcome measurements were made based on the single point of hospital discharge.

Conclusion

Thrombolytic therapy is a reasonable option that has the potential to modify the natural outcome of ICH. Nevertheless, questions with regard to the initiation of the therapy, duration of the therapy and drug dosing still need to be answered. Forms of treatment, cost-benefit ratio, and relative efficacies of various mechanisms of clot aspiration and drainage also need to be established.

Conflict of interest statement We declare that we have no conflict of interest.

References

1. Broderick JP, Connolly S, Feldmann E et al (2007) Guidelines for the management of spontaneous intracerebral hemorrhage in adults. 2007 Update. *Stroke* 38:2001–2023
2. Broderick JP, Adams HP, Barsan W et al (1999) Guidelines for the management of spontaneous intracerebral hemorrhage: a statement for healthcare professionals from a special writing group of the Stroke Council, American Heart Association. *Stroke* 30:905–915
3. Broderick JP, Brott T, Tomsick T et al (1993) Intracerebral hemorrhage more than twice as common as subarachnoid hemorrhage. *J Neurosurg* 78:188–191
4. Mayer SA, Brun NC, Begtrup K, Broderick J, Davis S, Diringer MN et al (2005) Recombinant activated factor VII for acute intracerebral hemorrhage. *N Engl J Med* 352:777–785
5. Tuhim S, Horowitz DR, Sacher M, Godbold JH (1999) Volume of ventricular blood is an important determinant of outcome in supratentorial intracerebral hemorrhage. *Crit Care Med* 27:617–621
6. Lapointe M, Haines S (2002) Fibrinolytic therapy for intraventricular hemorrhage in adults. *Cochrane Database Syst Rev* (3):CD003692
7. Morgan T, Zuccarello M, Naravan R, Kevl P, Lane K, Hanley D (2008) Preliminary findings of the minimally-invasive surgery plus rtPA for intracerebral hemorrhage evacuation (MISTIE) clinical trial. *Acta Neurochir Suppl* 105:147–151
8. Mendelow AD, Gregson BA, Fernandes HM et al (2005) Early surgery versus initial conservative treatment in patients with spontaneous supratentorial intracerebral haematomas in the International Surgical Trial in Intracerebral Haemorrhage (STICH): a randomised trial. *Lancet* 365(9457):387–397
9. Teernstra OP, Evers SM, Lodder J et al (2003) Stereotactic treatment of intracerebral hematoma by means of a plasminogen activator: a multicenter randomized controlled trial (SICHPA). *Stroke* 34:968–974
10. Prasad K, Mendelow AD, Gregson B (2008) Surgery for primary supratentorial intracerebral hemorrhage. *Cochrane Database Syst Rev* (4):CD000200

Endoscopic Surgical Treatment for Pituitary Apoplexy in Three Elderly Patients over the Age of 80

Yu Hasegawa, Shigetoshi Yano, Tomotaka Sakurama, Yuki Ohmori, Takayuki Kawano, Motohiro Morioka, Hank Chen, John H. Zhang, and Jun-Ichi Kuratsu

Abstract Objectives: As the population continues to live longer, the diagnosis of pituitary adenoma-induced apoplexy becomes more common in the elderly. The standard treatment options for pituitary apoplexy are debatable. Although there is little information regarding the treatment of pituitary apoplexy in elderly patients, the optimal treatment needs to be determined for this age group. The current study examined the surgical treatment of pituitary apoplexy in three patients over the age of 80.

Case Description: Three patients over the age of 80 with pituitary apoplexy were admitted to our hospital. Some symptoms caused by pituitary apoplexy, including decreased visual acuity, double vision and oculomotor paresis, had persisted for more than 14 days. Magnetic resonance imaging revealed suprasellar mass lesions extending into the cavernous sinus. The general condition of the patients was good, and we performed endoscopic transsphenoidal surgery

in each of these cases. The masses were removed, and the histological findings were diagnosed as non-functioning pituitary adenoma with presence of hemorrhagic or ischemic necrosis. Perioperative courses and general conditions were good, and the neurological deficits of each patient improved immediately.

Conclusions: Endoscopic transsphenoidal surgery has the advantage of visualization of the structures surrounding the pituitary gland. Moreover, the complication rate is relatively low because stress on the pituitary gland can be reduced by using this procedure. Even in patients over 80 years of age during the subacute phase, endoscopic surgical management is a good treatment candidate for pituitary apoplexy with mass lesion extension into the cavernous sinus.

Keywords Pituitary apoplexy · Elderly · Cavernous sinus · Endoscopic surgery

Y. Hasegawa

Department of Neurosurgery, Kumamoto University School of Medicine, 1-1-1 Honjo, 860–8556, Kumamoto, Japan and Department of Physiology, Loma Linda University, School of Medicine, Loma Linda, CA, USA

S. Yano (✉), T. Sakurama, Y. Ohmori, T. Kawano, M. Morioka, and J.-I. Kuratsu

Department of Neurosurgery, Kumamoto University School of Medicine, 1-1-1 Honjo, 860–8556, Kumamoto, Japan
e-mail: yanos@kumamoto-u.ac.jp

H. Chen

Department of Physiology, Loma Linda University, School of Medicine, Loma Linda, CA, USA

J.H. Zhang

Department of Physiology, Loma Linda University, School of Medicine, Loma Linda, CA, USA and Department of Neurosurgery, Loma Linda University, School of Medicine, Loma Linda, CA, USA

Introduction

Pituitary apoplexy is one of the most serious, life-threatening complications of pituitary adenoma. The clinical features of pituitary apoplexy usually involve the abrupt onset of typical symptoms including headache, vomiting, visual disturbances, oculomotor paresis, hemianopsia and loss of consciousness [1]. Although this disease often requires emergency treatment, the standard treatment for pituitary apoplexy remains controversial. Some have advocated routine early neurological decompression, while others have recommended a more conservative approach, especially in the absence of significant progression of neuro-ophthalmological compromise. This study demonstrates the surgical treatment of pituitary apoplexy in three patients over the age of 80 with good perioperative courses.

Case Reports

Case 1

This 82-year-old man noticed headache and appetite loss on May 16, 2002 (1st day). He had a past medical history significant for diabetes mellitus, hypertension and cardiac arrhythmia. He experienced double vision on the 5th day after onset, and general fatigue and headache on the 7th day. He was diagnosed with pituitary apoplexy and was admitted to our hospital service. According to his neurological examination at the time of admission, loss of consciousness and left abducens nerve palsy were noted. Endocrine examination revealed decreased serum levels of adrenocorticotropic hormone (ACTH) and cortisol, requiring hormonal replacement with hydrocortisone, after which his consciousness was recovered. Computed tomography (CT) revealed a suprasellar mass lesion with isodensity. Magnetic resonance imaging (MRI) demonstrated a suprasellar mass lesion with extension into the cavernous sinus (Knosp grade 2, Fig. 1a). No compression of the optic chiasm was noted. After improvement in the patient's general condition, he underwent endoscopic transsphenoidal surgery on the 14th day after onset. Following incision of the dura, no hemorrhage was noted, and we could observe necrotic solid tumor. We attempted removal of as much of the mass as possible, but to minimize complications we did not complete total removal of the tumor. The patient did well immediately postoperatively, with recovery from his abducens nerve palsy, and there was no abnormality in hormone levels or complications of diabetes insipidus. Postoperative MRI did reveal residual tumor, but successful decompression of the cavernous sinus was achieved (Fig. 1b). According to histological findings, there was an area of necrosis with a few pituitary adenoma-like cells (Fig. 1c). Three years later the patient passed away from pneumonia.

Case 2

This 85-year-old woman reported headache, deterioration of left visual acuity, right side ptosis and double vision on February 11, 2006 (1st day). Her past medical history was significant for diabetes mellitus, hypertension and thyroid tumor. She was diagnosed with pituitary apoplexy and admitted to our hospital service. On neurological examination, there were deterioration of left visual acuity, double vision and right oculomotor nerve palsy. Endocrine evaluation was normal. CT revealed a suprasellar mass lesion with homogenous hyperdensity. MRI demonstrated a suprasellar mass lesion with extension into the cavernous sinus (Knosp grade 3) with compression of the optic chiasm (Fig. 2a). She underwent endoscopic transsphenoidal surgery on the 16th day after onset. There was bleeding noted after incision of the dura (Fig. 2c). The mass was soft, and total resection was achieved (Fig. 2d and e). After the operation, the patient experienced transient diabetes insipidus for 1 week, but her overall condition was good, and immediate improvement in her neurological deficits was observed. No replacement of pituitary hormones was necessary. There was no residual tumor on postoperative MRI (Fig. 2b). Histological findings revealed a typical pituitary adenoma with red blood cells and necrosis (Fig. 2f). She had healthy evaluations for 6 months following surgery, after which time she did not maintain her follow-up appointments.

Case 3

This 80-year-old man suddenly experienced nausea on February 23, 2006 (1st day). He showed right ptosis and felt double vision on the 3rd day. His past medical history was significant for hypertension and cerebral infarction. He was

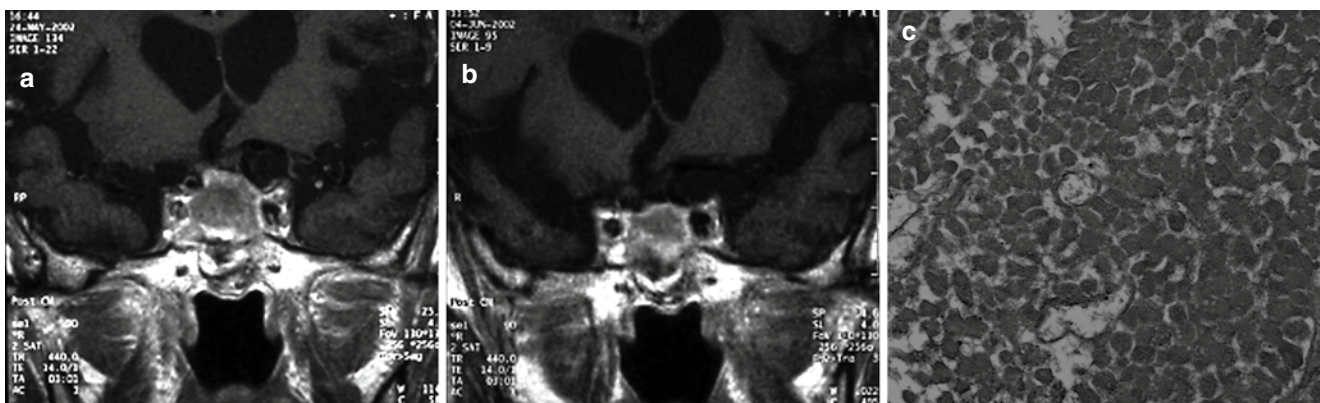


Fig. 1 Representative MRI findings preoperation (a) and postoperation (b), and hematoxylin and eosin staining (c)

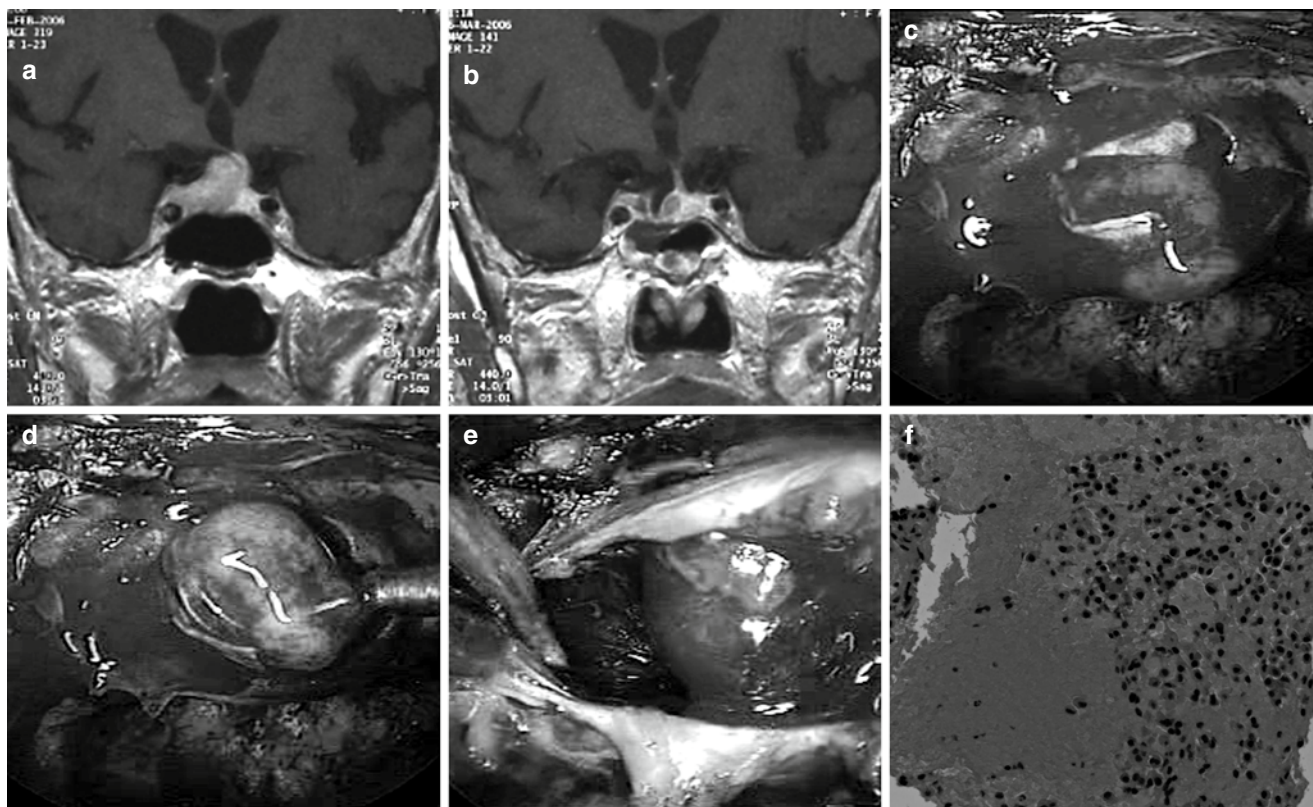


Fig. 2 Representative MRI findings preoperation (a) and postoperation (b), photographs during operation (c–d), and hematoxylin and eosin staining (f)

diagnosed with pituitary apoplexy and admitted to our hospital service. On neurological examination, double vision and right oculomotor nerve palsy were noted. Hormonal evaluation was normal. CT revealed a suprasellar mass lesion with homogenous slight hyperdensity. MRI demonstrated a suprasellar mass lesion with extension into the cavernous sinus (Knosp grade 3), but there was no compression noted of the optic chiasm (Fig. 3a). He underwent endoscopic transsphenoidal surgery on the 18th day after onset. There was bleeding noted after incision of the dura (Fig. 3d). The tumor was fairly soft with peripheral tissue adhesion to the medial wall of the cavernous sinus (Fig. 3e and f). To minimize complications, subtotal excision of the tumor was performed. His postoperative condition was good with immediate improvement in oculomotor function. Histological findings showed typical pituitary adenoma with red blood cells and necrosis (Fig. 3g). No replacement of pituitary hormones was necessary. Postoperative MRI showed residual tumor at the right side of the cavernous sinus, with decreases in size observed on subsequent imaging over the next 3 years (Fig. 3b and c). He is at present very healthy and visits our hospital on a regular basis.

Discussion

In this study, we achieved excellent results using endoscopic surgical treatment more than 14 days after the onset of pituitary apoplexy in patients over the age of 80. Pituitary apoplexy is mainly induced by hemorrhage, infarction or hemorrhagic infarction of a pituitary tumor, resulting in the aforementioned symptoms. While the frequency of pituitary apoplexy in elderly patients is observed to be 12%, similar to the rate in other age groups (6–16.6%) [2], it is observed more often in the elderly.

The most important aspects and basic concept in the treatment of pituitary apoplexy are management of the hypopituitarism and the deterioration of visual acuity. Before surgery, patients suffering from hypopituitarism require hormone replacement, as the replacement has been demonstrated to be critical in reducing morbidity and mortality in cases with pituitary apoplexy [3]. When the patients note emergent visual loss, they usually need to undergo surgery within 7 days of onset, or in some cases, emergency surgery [4, 5]. With respect to oculomotor paresis, the outcomes of surgical treatment and conservative management are similar [6].

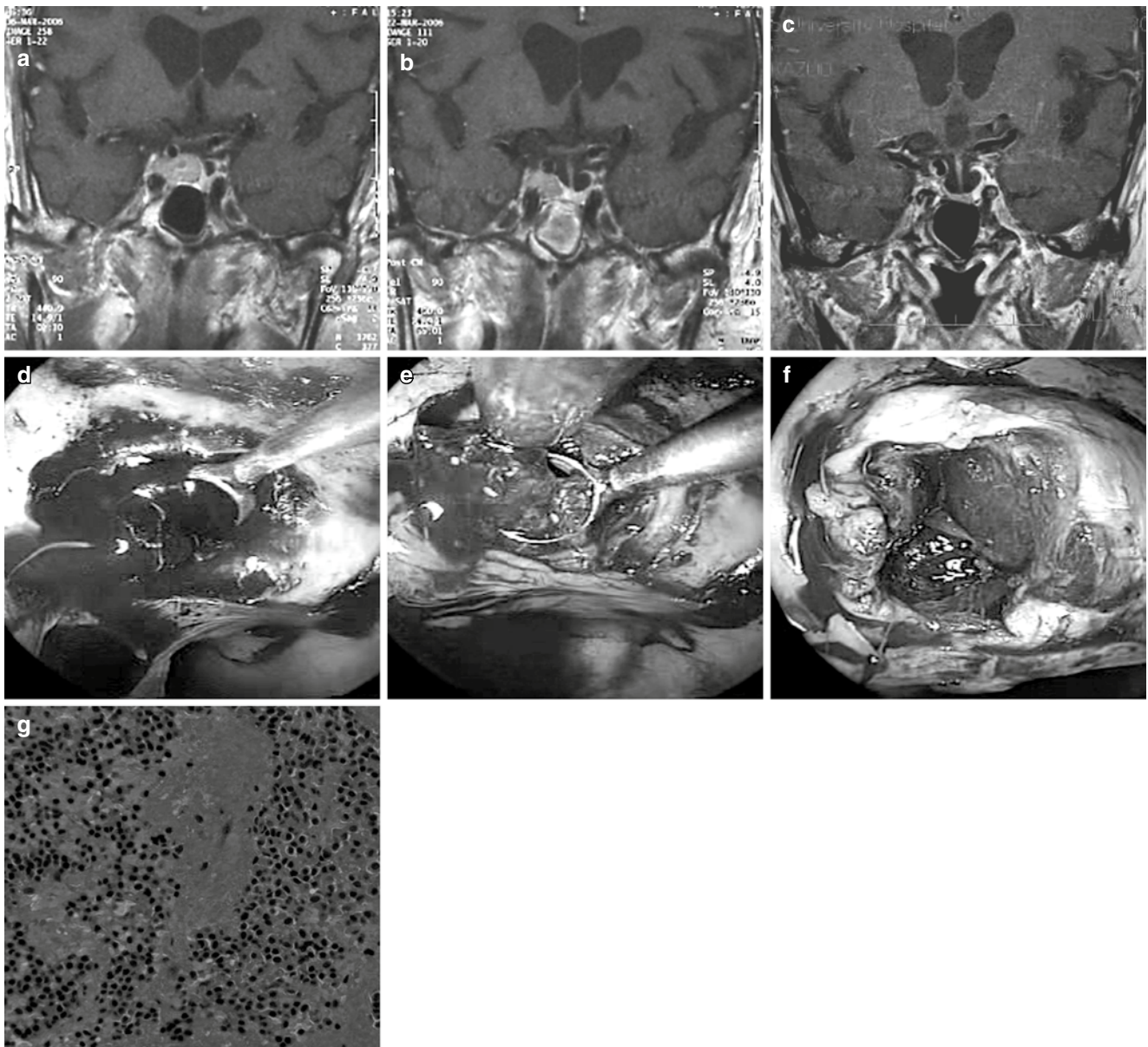


Fig. 3 Representative MRI findings preoperation (a), postoperation (b), the next 3-year follow-up postoperative MRI (c), photographs during operation (d–f) and hematoxylin and eosin staining (g)

Taking into consideration that an extended period of hospitalization may induce dementia and depression in elderly patients, we should carefully determine the best treatment on an individual basis in elderly patients, even if the symptoms are significant only for oculomotor paresis and/or subacute phase presentation. In the current cases, the symptoms of all patients improved immediately following surgery even if the treatment was performed more than 14 days after the initial presentation of pituitary apoplexy. Moreover, the regrowth of tumor and rebleeding in those patients may not have occurred. Because the frequency of recurrence and presentation of hormonally active tumors are both lower in elderly patients and transsphenoidal surgery can be performed in elderly patients

without significant risk [2], less aggressive resection may be acceptable in elderly patients.

The rate of pituitary adenoma with cavernous sinus invasion was 6–10% [7–9]. Although various surgical approaches to the sellar and parasellar region have been demonstrated to treat pituitary adenoma involving the cavernous sinus [10–12], these approaches may be limited by the deep and narrow surgical spaces involved and limited visualization under the microscope. The operation under the microscope has long been performed for pituitary apoplexy, whereas pure endoscopic endonasal transsphenoidal surgery was first described in 1996 [13]. The advantages of endoscopic surgery are excellent visualization of the pituitary gland and

surrounding structures, fewer complications compared with sublabial transsphenoidal surgery and wide exposure of the medial cavernous sinus wall [14, 15]. Therefore, stress upon the pituitary gland, regarded as the main complication after surgery, can be reduced with this versus other procedures. Postoperatively, the patients were able to assume a sitting position and begin oral intake as early as the first day following surgery, and only 3–4 days were required to recover the preoperative level of activities of daily living. Moreover, they did not reveal new hormonal deficiencies after surgery. In the current study, MRI findings showed Knosp grade 2 or 3, and the tumor could be seen using an endoscope, especially lateral extension into the cavernous sinus. Therefore, surgery with an endoscope may be more suitable for suprasellar mass lesions with extension into the cavernous sinus than surgery under the microscope in cases of elderly patients. On the other hand, there are some limitations, including difficult management of bleeding, loss of three-dimensional vision, the need for special instrumentation and appropriate operator experience with endoscopy [16].

In conclusion, even in cases of patients over 80 years of age presenting more than 14 days after onset of pituitary apoplexy, endoscopic surgical management is a good candidate treatment of the disease with mass lesion extension into the cavernous sinus, while maintaining attention to risks of anesthesia, surgical planning, extended hospitalization and fluid balance.

Conflict of interest statement We declare that we have no conflict of interest.

References

1. Semple PL, Webb MK, de Villiers JC, Laws ER Jr (2005) Pituitary apoplexy. *Neurosurgery* 56:65–72
2. Sheehan JM, Douds GL, Hill K, Farace E (2008) Transsphenoidal surgery for pituitary adenoma in elderly patients. *Acta Neurochir (Wien)* 150:571–574
3. Turgut M, Ozsunar Y, Başak S, Güney E, Kır E, Meteoglu I (2010) Pituitary apoplexy: an overview of 186 cases published during the last century. *Acta Neurochir (Wien)* 152(5):749–761 [Epub ahead of print]
4. Bills DC, Meyer FB, Laws ER Jr, Davis DH, Ebersold MJ, Scheithauer BW, Ilstrup DM, Abboud CF (1993) A retrospective analysis of pituitary apoplexy. *Neurosurgery* 33:602–608
5. Agrawal D, Mahapatra AK (2005) Visual outcome of blind eyes in pituitary apoplexy after transsphenoidal surgery: a series of 14 eyes. *Surg Neurol* 63:42–46
6. Nawar RN, AbdelMannan D, Selman WR, Arafah BM (2008) Pituitary tumor apoplexy: a review. *J Intensive Care Med* 23:75–90
7. Fahlbusch R, Buchfelder M (1988) Transsphenoidal surgery of parasellar pituitary adenomas. *Acta Neurochir (Wien)* 92:93–99
8. Knosp E, Steiner E, Kitz K, Matula C (1993) Pituitary adenomas with invasion of the cavernous sinus space: a magnetic resonance imaging classification compared with surgical findings. *Neurosurgery* 33:610–617
9. Vieira JO Jr, Cukiert A, Liberman B (2006) Evaluation of magnetic resonance imaging criteria for cavernous sinus invasion in patients with pituitary adenomas: logistic regression analysis and correlation with surgical findings. *Surg Neurol* 65:130–135
10. Fraioli B, Esposito V, Santoro A, Iannetti G, Giuffrè R, Cantore G (1995) Transmaxillophenoidal approach to tumors invading the medial compartment of the cavernous sinus. *J Neurosurg* 82:63–69
11. Kitano M, Taneda M (2001) Extended transsphenoidal approach with submucosal posterior ethmoidectomy for parasellar tumors. *J Neurosurg* 94:999–1004
12. Das K, Spencer W, Nwagwu CI, Schaeffer S, Wenk E, Weiss MH, Couldwell WT (2001) Approaches to the sellar and parasellar region: anatomic comparison of endonasal-transsphenoidal, sublabial-transsphenoidal, and transethmoidal approaches. *Neurol Res* 23:51–54
13. Jho HD, Carrau RL (1996) Endoscopy assisted transsphenoidal surgery for pituitary adenoma. technical note. *Acta Neurochir (Wien)* 138:1416–1425
14. White DR, Sonnenburg RE, Ewend MG, Senior BA (2004) Safety of minimally invasive pituitary surgery (MIPS) compared with a traditional approach. *Laryngoscope* 114:1945–1948
15. Ceylan S, Koc K, Anik I (2010) Endoscopic endonasal transsphenoidal approach for pituitary adenomas invading the cavernous sinus. *J Neurosurg* 112:99–107
16. Gondim JA, Schops M, de Almeida JP, de Albuquerque LA, Gomes E, Ferraz T, Barroso FA (2010) Endoscopic endonasal transsphenoidal surgery: surgical results of 228 pituitary adenomas treated in a pituitary center. *Pituitary* 13:68–77

Proton Pump Inhibitor Prophylaxis Increases the Risk of Nosocomial Pneumonia in Patients with an Intracerebral Hemorrhagic Stroke

Li Ran, Nikan H. Khatibi, Xinyue Qin, and John H. Zhang

Abstract *Background.* Stress-related mucosal damage is an erosive process of the gastric lining resulting from abnormally high physiologic demands. To avoid the morbidity and mortality associated with significant bleeding from the damage, prophylaxis with an acid suppression medication is given. This is especially common in stroke victims. Recent studies have suggested a link between acid suppression therapy and nosocomial pneumonia, specifically implicating proton pump inhibitors (PPI), a potent acid suppression medication, as the culprit. In this retrospective study, we reviewed the medical records of admitted intracerebral hemorrhage (ICH) patients and determined if there is a link between PPI prophylaxis and nosocomial pneumonia in our ICH population. *Materials and Methods.* Medical records of 200 ICH patients admitted to the First Affiliated Hospital of Chongqing Medical University were reviewed from January 1, 2008 to October 31, 2009. PPIs were the only accepted form of acid suppression therapy. In all, 95 patients were given PPI prophylaxis, whereas 105 patients did not receive any form of acid suppression. *Results.* The unadjusted incidence rate of pneumonia in the PPI prophylactic group was 23.2%, and 10.5% in patients not having received prophylaxis. Additionally, patients treated with PPI prophylaxis were more likely to be critically ill, defined by an increase in

conscious disturbance and dependency on mechanical ventilation and/or a nasogastric tube.

Conclusion. The use of a PPI as a prophylactic treatment against stress-related mucosal damage was associated with a higher occurrence of nosocomial pneumonia in our ICH population. This study suggests the need for further research investigating the use of PPI prophylaxis in ICH patients and the possibility of using alternate acid suppression therapeutic modalities.

Keywords Proton pump inhibitors (PPIs) · Intracerebral hemorrhage (ICH) · Nosocomial pneumonia · Stress-related mucosal damage (SRMD)

Introduction

Stress-related mucosal damage (SRMD) is an erosive process of the gastric lining resulting from abnormally high physiologic demands, such as trauma, surgery, organ failure, sepsis, and burns [1, 2]. Within hours of the injury, mucosal damage may be apparent as multiple superficial erosions. These erosions are associated with asymptomatic submucosal hemorrhages that become clinically relevant once the erosion has reached the vasculature, opening the door for internal hemorrhage [3]. To avoid the morbidity and mortality associated with perfuse bleeding from SRMD, prophylaxis with an acid suppression medication is given. This is especially common in acute brain injuries, specifically intracerebral hemorrhage (ICH). In an ICH, the growing hematoma causes a rise in intracranial pressure, signaling the parasympathetic pathway to secrete unnecessary gastric acid [4].

Current recommendations for SRMD prophylaxis include histamine-2 receptor antagonists, sucralfate, and proton pump inhibitors (PPIs). Compared with placebo, all three drug classes have been shown to reduce the occurrence and/or bleeding associated with SRMD [5–7]. Although equally effective in theory, PPIs have become common in clinical practice because of their relatively inexpensive costs, limited

L. Ran and X. Qin
First Affiliated Hospital, Chongqing Medical University,
Chongqing, China

N.H. Khatibi
Department of Anesthesiology, Loma Linda Medical Center,
Loma Linda, CA, USA

J.H. Zhang (✉)
First Affiliated Hospital, Chongqing Medical University,
Chongqing, China and
Department of Anesthesiology, Loma Linda Medical Center,
Loma Linda, CA, USA and
Division of Neurosurgery, Loma Linda University Medical Center,
11234 Anderson Street, Room 2562B, 92354 Loma Linda, CA, USA
e-mail: johnzhang3910@yahoo.com

adverse effects, and ability to maintain relatively high pH levels for longer time periods. Additionally, PPIs have the ability to block both pathways involved in acid production, i.e., histamine-induced and vagally mediated gastric acid secretion, thus making them a desirable candidate for prophylaxis.

Recently, however, concerns have been raised regarding the relationship between acid suppression therapy and nosocomial pneumonia. Specifically, prophylaxis with PPIs is associated with a 30% increase in nosocomial pneumonia [8]. To our knowledge no study has investigated the relationship between PPI prophylaxis and nosocomial pneumonia in ICH patients. Therefore, this study was undertaken to investigate whether a relationship exists between PPI prophylaxis and nosocomial pneumonia in ICH patients admitted to the hospital in Chongqing, China.

Materials and Methods

Study design and patients. This is a retrospective cohort analysis of acute stroke patients who were admitted to the First Affiliated Hospital of Chongqing Medical University from January 1, 2008 to October 31, 2009. Stroke was defined in patients with neuroimaging evidence of ICH and with a time interval from onset to treatment of less than 24 h. Patients were eligible for participation if they were 18 years of age or older, and had neuroimaging evidence of an ICH. The exclusion criteria included patients with a history of immune dysfunction and patients who were discharged home and/or had died less than 3 days from admission.

Prophylactic Treatment and Outcomes. Acid-suppressive therapy was defined as an order for a PPI by the admitting physician. The primary outcome measured in this review was the presence of nosocomial pneumonia, as defined by the Centers for Disease Control and Prevention (CDC) [9].

Variables. The following variables were collected: sex, age, tobacco use, history of heart failure, chronic obstructive pulmonary disease (COPD), diabetes mellitus, prior history of stroke, level of consciousness, location of hematoma, size of hematoma, intraventricular extension, use of mechanical ventilation, use of nasogastric tube, hospitalization time, and early antibiotic therapy. Because patient dysphagia was not

examined nor the history of gastroesophageal reflux disease determined, these particular variables were excluded.

Statistical analysis. The odds ratio was used to approximate the relative risk (RR) in order to determine the relationship between PPI prophylaxis and nosocomial pneumonia. The continuous variables were analyzed using the unpaired Student's *t*-test and described as mean \pm SD. The categorical variables were analyzed by the chi-square test and/or Fisher's exact test. Binary logistic regression analysis was then performed to control the effect of confounding variables that were found to be significant ($p < 0.05$) in the univariate analysis. All analyses were performed using the SPSS 16.0 statistical software package (Chicago, IL).

Results

Table 1 lists the number of patients who suffered from nosocomial pneumonia infection during the course of their hospital stay. A total of 200 ICH patients were eligible for inclusion in this study – 95 treated with a PPI, and 105 not treated. Of the 200, 33 were found to have suffered from nosocomial pneumonia, of whom 22 were treated with a PPI prophylaxis and 11 were not.

The demographic and clinical characteristics of ICH patients between both groups are listed in Table 2. Although the mean age of patients treated with a PPI was older than untreated patients, the difference was not statistically significant. However, patients treated with a PPI prophylaxis had a greater significant incidence of conscious disturbances (63.2% vs. 21.0%) and were more likely to be on mechanical ventilation or a nasogastric tube (17.9% vs. 4.8%, 34.7% vs. 7.6%) compared to untreated patients. Additionally, treated patients experienced significantly larger bleeding, especially within the ventricles. There was no statistical difference with hematoma location between the two groups (Table 3).

Only age and level of consciousness showed a significant difference between those individuals who experienced nosocomial pneumonia and those who did not (Table 4). No statistical differences were found between groups for all other variables. In the logistic regression analysis, the use of PPI was found to be an independent risk factor of nosocomial pneumonia.

Table 1 Cases of nosocomial pneumonia with or without PPI prophylaxis

	Total number of patients	Pneumonia cases (%)	Unadjusted odds ratio (95% CI)	Adjusted odds ratio (95% CI)
No prophylaxis	105	11 (10.5)	–	–
PPI prophylaxis	95	22 (23.2)	2.6 (1.2–5.7)	2.7 (1.2–6.7)

Table 2 Demographics of ICH patients used in this study

Variables	No prophylaxis (n = 105)	PPI prophylaxis (n = 95)	p-value
Age (years)	62.2 ± 13.6	63.7 ± 13.7	No significance
Male sex	68	66	No significance
Smoking	21	19	No significance
Diabetes mellitus	20	20	No significance
Heart failure	3	2	No significance
COPD	5	7	No significance
History of tobacco use	13	11	No significance
Consciousness disturbance	22	60	0.000*
Hospitalization time (days)	19.8 ± 12.7	17.8 ± 18.4	No significance
Nasogastric tube use	8	33	0.000*
Mechanical ventilation	5	17	0.003*
Antibiotic therapy	48	51	No significance

Patients treated with a PPI prophylaxis had a more significant incidence of conscious disturbances (63.2% vs. 21.0%) and were more likely to be on mechanical ventilation or a nasogastric tube (17.9% vs. 4.8%, 34.7% vs. 7.6%) compared to untreated patients. *p-value < 0.05

Table 3 Imaging manifestation distribution

Imaging manifestation	No prophylaxis (n = 105)	PPI prophylaxis (n = 95)	p-value
Hematoma location			No significance
Lobe of brain			
Basal ganglia	15	21	–
Thalamus	64	48	–
Brain stem	17	10	–
Cerebellum	5	11	–
Cerebellum	4	5	–
Hematoma size	–	–	0.001*
Small	58	29	–
Medium	23	27	–
Large	24	39	–
Intraventricular extension	17	38	0.000*

Patients with a significantly larger hematoma size were more likely to have PPI prophylaxis than those with a smaller hematoma. *p-value < 0.05

Discussion

In this retrospective study, we investigated the role of PPI prophylaxis on nosocomial pneumonia development in our ICH population of 200 patients admitted to the First Affiliated Hospital of Chongqing Medical University. Two key conclusions were made regarding PPI prophylaxis: (1) critically ill patients were more likely to receive treatment on admission to the hospital than their more stable counterparts; (2) therapy increased the likelihood of contracting a nosocomial pneumonia infection. To the best of our knowledge, this is the first study to elucidate the relationship between PPI prophylaxis and nosocomial pneumonia in ICH-induced brain injury.

Gastrointestinal (GI) bleeding caused by SRMD is an important complication in critically ill patients [10]. The

incidence of a GI bleed in these patients is estimated at approximately 5% and carries a 50% higher mortality compared with matched placebo [11]. As a result, it is quite common for critically ill patients to begin acid suppression prophylaxis on admissions [12]. Normally, the GI tract performs a variety of critical physiologic functions, including maintenance of mucosal integrity, secretion, and motility. These physiologic functions can be adversely affected by physiological stress at other sites of the body and indirectly lead to the development of SRMD. Additionally, many critically ill patients are placed under enormous stress from outside sources such as mechanical ventilation, extended ICU stays, thermal injuries, head injuries, and even an elevated gastric acid pH [1]. In this study, we found patients who were specifically placed on mechanical ventilation, had a nasogastric tube placement, or presented with an increased level of

Table 4 Variables included in univariate analysis

Variables	Non-nosocomial pneumonia (n=33)	Nosocomial pneumonia (n=167)	p-value
Age (years)	–	–	0.001*
<60	75	6	–
60–79	79	18	–
≥80	13	9	–
Male sex	113	21	No significance
Female sex	54	12	No significance
Smoking	33	7	No significance
Diabetes mellitus	35	4	No significance
Heart failure	4	1	No significance
COPD	10	2	No significance
History of tobacco use	18	6	No significance
Level of consciousness	–	–	0.018*
Conscious	105	13	–
Drowsy	21	6	–
Lethargic	13	8	–
Light coma	7	3	–
Deep coma	21	3	–
Hematoma location	–	–	No significance
Lobe of brain	31	5	–
Basal ganglia	93	19	–
Thalamus	25	2	–
Brain stem	12	4	–
Cerebellum	6	3	–
Hematoma size	–	–	No significance
Small	75	12	–
Medium	39	11	–
Large	53	10	–
Intraventricular extension	49	6	No significance
Hospitalization time	–	–	No significance
≤20 days	109	20	–
>20 days	58	13	–
Nasogastric tube use	30	11	No significance
Mechanical ventilation	17	5	No significance
Antibiotic therapy	78	11	No significance

Only age and level of consciousness showed a significant difference between those individuals who experienced nosocomial pneumonia and those who did not. No statistical differences were found between groups for all other variables. * p -value < 0.05

conscious disturbance were more likely to be on acid suppression therapy.

We also found it necessary to examine the relationship of PPI prophylaxis leading to the development of a nosocomial pneumonia infection. Previous works in ICH found that almost one-third of patients developed some sort of pulmonary complication, most frequently pneumonia, within the first week [13]. However, the source of the infection was

unknown. Recent studies have come out implicating PPI prophylactic therapy as the main culprit behind the increased risk of nosocomial pneumonia infection [8, 14]. Other works have supported these findings – investigating the role of acid suppression therapy with a histamine-2 receptor blocker, sucralfate, and PPI, and finding that PPI therapy specifically can increase the risk of acquiring a nosocomial pneumonia infection [8, 14]. In this study, we found that prophylaxis

with a PPI in our ICH population resulted in a significantly increased number of patients infected with nosocomial pneumonia. This can likely be attributed to the ability of PPI medications to maintain a high pH level in the stomach for prolonged periods of time, allowing for bacterial overgrowth and eventual aspiration into the lungs [15, 16].

Conclusion

The use of a PPI as a prophylactic treatment against stress-related mucosal damage is associated with a higher occurrence of nosocomial pneumonia in our ICH population and is more likely to be given to critically ill patients. As a result, this study suggests that the use of alternate acid suppression therapy in ICH patients may be warranted to prevent unnecessary infections.

Acknowledgement This study was partially supported by NIH NS053407 to J.H. Zhang.

Conflict of interest statement We declare that we have no conflict of interest.

References

- Jung R, MacLaren R (2002) Proton-pump inhibitors for stress ulcer prophylaxis in critically ill patients. *Ann Pharmacother* 36(12): 1929–37
- Smythe MA, Zarowitz BJ (1994) Changing perspectives of stress gastritis prophylaxis. *Ann Pharmacother* 28(9):1073–85
- Lucas CE et al (1971) Natural history and surgical dilemma of “stress” gastric bleeding. *Arch Surg* 102(4):266–73
- Misra UK, Kalita J, Pandey S, Mandal SK, Srivastava M (2004) A randomized placebo controlled trial of ranitidine versus sucralfate in patients with spontaneous intracerebral hemorrhage for prevention of gastric hemorrhage. *J Neurol Sci* 239:5–10
- Cook DJ et al (1991) Stress ulcer prophylaxis in the critically ill: a meta-analysis. *Am J Med* 91(5):519–27
- Lacroix J et al (1989) Prophylaxis of upper gastrointestinal bleeding in intensive care units: a meta-analysis. *Crit Care Med* 17(9):862–9
- Tryba M (1991) Prophylaxis of stress ulcer bleeding. A meta-analysis. *J Clin Gastroenterol* 13(13 Suppl 2):S44–55
- Herzig SJ et al (2009) Acid-suppressive medication use and the risk for hospital-acquired pneumonia. *JAMA* 301(20):2120–8
- Centers for Disease Control and Prevention. Guidelines for prevention of nosocomial pneumonia <http://www.cdc.gov/mmwr/preview/mmwrhtml/00045365.htm>
- Cook DJ et al (1996) Stress ulcer prophylaxis in critically ill patients resolving discordant metaanalyses. *JAMA* 275(4):308–14
- Reilly J, Fennerty MB (1998) Stress Ulcer prophylaxis: the prevention of gastrointestinal bleeding and the development of nosocomial infections in critically ill patients. *J Pharm Prac* 11:p. 418–432
- Spirit MJ (2003) Acid suppression in critically ill patients: what does the evidence support? *Pharmacotherapy* 23(10 Pt 2):87S–93S
- Maramattom BV et al (2006) Pulmonary complications after intracerebral hemorrhage. *Neurocrit Care* 5(2):115–9
- Miano TA et al (2009) Nosocomial pneumonia risk and stress ulcer prophylaxis: a comparison of pantoprazole vs ranitidine in cardiothoracic surgery patients. *Chest* 136(2):440–7
- Atherton ST, White DJ (1978) Stomach as source of bacteria colonising respiratory tract during artificial ventilation. *Lancet* 2(8097): 968–9
- du Moulin GC et al (1982) Aspiration of gastric bacteria in antacid-treated patients: a frequent cause of postoperative colonisation of the airway. *Lancet* 1(8266):242–5

Author Index

A

Abdullah, J.M., 375, 421
Ai, J., 25
Appelboom, G., 141
Applegate, R., 207, 277
Applegate II, R.L., 283
Aronowski, J., 107
Awang, M.S., 375
Ayer, R., 145, 231, 283

B

Bartek Jr, J., 409
Bergdal, O., 409
Bouz, P.A., 425
Buchholz, J., 225
Butler, W., 63

C

Charles, S., 225
Chau, M., 299
Chen, C., 307
Chen, D., 299
Chen, H., 3, 9, 15, 367, 383, 403, 429
Chen, O., 307
Chen, W., 129, 207, 231, 243, 265
Chen, Z., 289
Chiu, J., 225
Colohan, A., 243
Connolly, E.S. Jr., 141

D

Degn, J., 409
Ding, Y.-H., 353, 357
Ducruet, A.F., 141

E

Eckermann, J., 283

F

Fagan, S.C., 295
Fathali, N., 37, 93, 161, 191, 207, 237, 277
Feng, J., 327
Feng, Q.-l., 361
Fischer, W., 409

G

Ghani, Ab.R.I., 375
Gigante, P.R., 141

Gong, Y., 113
Gorski, J., 141
Greenberg, D.A., 315
Grotta, J.C., 107
Gu, Y., 113, 123
Guan, J., 271
Guan, W., 295
Guenther, A., 167
Guo, Z., 343

H

Hansen-Schwartz, J., 409
Haque, R.M., 141
Harris, T.H., 173
Hartman, R., 201
Hasegawa, Y., 129, 213, 231, 429
Hashimoto, T., 31
Hatakeyama, T., 185
He, Y., 113, 123, 133
Hobohm, C., 167
Hu, H., 123, 197, 219, 259
Hu, X., 387
Hua, Y., 71, 101, 113, 119, 123, 133, 185, 197, 219, 259, 271, 289
Huang, J.H., 151
Hunter, C.A., 173
Huo, G., 361
Husin, A., 421
Hwang, B.Y., 141

I

Idris, B., 375

J

Jadhav, V., 145, 225, 265, 277
Jafarian, N., 283
Jiang, F., 333
Jiang, X., 49
Jin, K., 315
Johnson, W.D., 425
Joshita, H., 43

K

Kanamaru, K., 129, 231
Kanematsu, M., 31
Kanematsu, Y., 31
Kariko, K., 173
Kasner, S.E., 173
Kawano, T., 429

Keep, R.F., 71, 101, 113, 119, 123, 133, 185, 197, 259, 271, 289
 Keesecker, S.E., 141
 Kellner, C.P., 141
 Kentar, M., 19
 Keong, L.H., 375
 Khatibi, N.H., 3, 93, 191, 207, 225, 265, 277, 435
 Kim, H., 83
 Kong, Y., 337, 367, 383, 403
 Kozak, A., 295
 Küppers-Tiedt, L., 167
 Kuratsu, J.-i., 429

L

Latzman, J.M., 151
 Lee, L.K., 207
 Lei, H., 353, 357
 Lekic, T., 37, 55, 155, 161, 179, 191, 201, 213, 237, 253
 Leung, W., 63
 Li, D., 361
 Li, F., 383, 403
 Li, G., 381
 Li, Q., 399
 Li, X., 321
 Liang, E.I., 31
 Liu, D.-Z., 77
 Liu, Q., 353, 357
 Liu, W., 101, 133, 307
 Lo, E.H., 63
 Lok, J., 63

M

Ma, Q., 3, 179
 Macdonald, R.L., 25
 Makino, H., 31
 Manaenko, A., 9, 37, 55, 155, 161, 167, 179, 191, 201, 213, 237, 253
 Mao, X., 315
 Mao, Y., 289
 Martin, R., 191, 207, 265, 277, 283
 Matus, B., 277
 Michalski, D., 167
 Miyazaki, H., 43
 Morioka, M., 429
 Munakata, A., 415
 Murphy, S., 63

N

Nakano, T., 415
 Naraoka, M., 415
 Noviski, N., 63
 Nuki, Y., 31

O

Ohkuma, H., 415
 Ohmori, Y., 429
 Okauchi, M., 185, 197
 Orakcioglu, B., 19
 Ostrowski, R.P., 37, 93, 179, 213, 253

P

Pawlikowska, L., 83
 Pen, G., 381
 Peterson, M., 237

Q

Qin, X., 321, 327, 333, 337, 343, 349, 381, 387, 393, 399, 435

R

Ran, L., 435
 Rauch, J., 151
 Rolland, W., 37, 55, 201, 207, 213, 237, 253
 Romner, B., 409

S

Saidi, M., 265
 Sakowitz, O.W., 19
 Sakurama, T., 429
 Samadani, U., 151
 Sansing, L.H., 173
 Santos, E., 19
 Sayuthi, S., 375
 Schiebel, P., 19
 Schneider, D., 167
 Sharp, F.R., 77
 Shimamura, N., 415
 Shiokawa, Y., 43
 Shum, K.J., 191
 Song, S., 101, 107, 219, 259
 Sozen, T., 129, 231
 Stier, G., 207, 265, 283
 Strong, R., 107
 Su, H., 83
 Sugawara, T., 145, 231
 Sun, G., 107
 Suzuki, H., 37, 129, 231

T

Tada, Y., 31
 Taki, W., 129, 231
 Tang, J., 3, 9, 25, 37, 55, 155, 161, 179, 191, 201, 213, 225, 237, 253, 265, 277, 283, 307
 Tang, M.-y., 361
 Tao, T., 349
 Tong, J., 151
 Tong, W., 283
 Tsubokawa, T., 43
 Tsuchiyama, R., 243

U

Unterberg, A., 19
 Uozumi, Y., 19

V

Virbel, K., 201, 253

W

Wada, K., 31
 Wagner, A., 167
 Wang, J., 219
 Wang, L., 123, 197
 Wang, M.M., 133
 Wang, T., 343, 349, 393
 Wang, X., 337, 367, 383, 403
 Wang, Y., 337, 367, 383, 393, 403
 Wei, L., 299
 Weinsheimer, S., 83
 Welling, K.L., 409
 Westra, D., 243
 Williams, S., 161
 Wu, B., 307
 Wu, G., 271
 Wu, W., 381

X

Xi, G., 49, 71, 101, 113, 119, 123, 133, 185,
197, 219, 259, 271, 289

Xiang, J., 71

Xie, L., 315

Xie, Q., 119, 271

Xing, Y., 49

Y

Yamashita, S., 259

Yan, P., 353

Yang, J., 381, 399

Yang, Q., 381

Yang, Y., 49

Yano, S., 429

Ye, Z., 119

Yeh, M.L., 141

Young, W.L., 83

Z

Zagzag, D.S., 151

Zhang, J., 107

Zhang, J.H., 3, 9, 15, 37, 55, 93, 129, 145, 155, 161, 167,

179, 191, 201, 207, 225, 231, 237, 243, 253, 265,

277, 283, 307, 321, 327, 333, 337, 343, 349, 353,

357, 367, 387, 393, 399, 429, 435

Zhang, L., 107

Zhao, F., 101

Zhao, X., 107

Zhou, Y., 207

Subject Index

A

- Abnormal angiogenesis, AVM, 84–85
- Activated partial thromboplastin time (APTT) analysis, 384
- Acute subdural hematoma (ASDH), 26
- Advanced glycation end products (AGEs), 394
- Aging
 - autophagy, 113, 117
 - ferritin immunoreactivity and microglia activation, 115
 - forelimb using asymmetry scores, 115–116
 - LC3-II to LC3-I ratio, ipsilateral basal ganglia, 115
 - materials and methods
 - animal preparation and intracerebral infusion, 113–114
 - behavioral tests, 114
 - cell counts, 114
 - immunohistochemistry, 114
 - statistical analysis, 115
 - western blot analysis, 114
- Albumin western blot, 142
- Alteplase treatment. *See* Intraventricular hematoma (IVH)
- Alzheimer's disease, CAA
 - canine model, 16
 - diagnostic tools, 16
 - microhemorrhages, 15
 - murine model, 16
 - non-human primate model, 15
- Angiotensin II-induced hypertension, 32–33
- Apoptosis
 - lung cell, Z-VAD-FMK treatment, 131–132
 - neuron, cell cycle re-entry induced, 79
 - SAH induced, 130–131
- Arginine vasopressin (AVP)
 - NC1900
 - AQP4, 155
 - and AQP4 expression, 156, 158
 - brain water content, 156
 - definition, 155
 - effect on cerebral edema, 156
 - intracerebral hemorrhagic stroke mice model, 156
 - neurobehavioral deficit assessment, 156
 - on neurobehavioral deficits, 156
 - role and function, 191–192
 - statistical analysis, 156
 - treatment method, 156
 - western blotting, 156
 - SR49059
 - in activating aquaporin channels, 195
 - animal study, 192
 - blood-brain barrier (BBB) disruption, 194–195
 - brain water content, 192

- decreases cerebral edema, 192, 193
- high-dose, 194–195
- improves neurobehavioral deficits, 192–193
- neurological outcomes, 192
- statistical analysis, 192
- treatment method, 192

ASDH. *See* Acute subdural hematoma (ASDH)

Astrocytes, 65–66, 94–95

Autophagy, 113, 117

B

- Binary logistic regression analysis, 384, 404, 436
- Biochemical factors, retrospective analysis of
 - abnormal lipid metabolism, effects of, 405
 - automatic biochemical analyzer, 403–404
 - binary logistic regression analysis, 404
 - hyperglycemia, effects of, 405
 - hyperuricemia, effects of, 405
 - lipid levels, 404
 - patient basic situation, 404
 - plasma glucose *vs.* serum uric acid, 404
- Blood-brain barrier (BBB) disruption
 - collagenase *vs.* blood models, 12–13
 - mitogenic signal pathways, 78
 - osteopontin (OPN), recombinant
 - BBB permeability, 232
 - brain edema, effects on, 233, 234
 - brain water content, 232
 - definition, 231
 - experimental model and study protocol, of SAH, 232
 - intracerebroventricular infusion, 232
 - MMP-9, 234
 - mortality rate, 233
 - neurological scoring, 232
 - SAH grading score, 233
 - SAH severity, 232
 - statistical analysis, 233
 - VEGF-A and phospho-JNK, effects on, 234–235
 - western blot analyses, 232–233
- Blood injection model, 4
- Blood pressure measurement, 33
- Brain
 - arteriovenous malformation (AVMs)
 - abnormal angiogenesis and inflammation, 84–85
 - in Alk1 or Eng deficient mice, 89
 - brain specimens, 316
 - double-label immunohistochemistry, 316
 - etiology and pathogenesis, 87–89
 - experimental models, 86–87

- gene studies in non-HHT patients, 85–86
 - genetic influences, 85
 - genome-wide SNP and expression studies, 86
 - magnetic resonance imaging, 316
 - morphology, 83
 - neuroglobin immunoreactivity expression, 316–318
 - Notch signaling, 315
 - perihematomal tissue dysfunction, 316
 - response-to-injury paradigm, 83–84
 - treatment, 83
 - VEGF astrocytic expression, 316
 - edema
 - FTY720 treatment, 214, 215
 - G-CSF pre-treatment, 267
 - geldanamycin, 162, 163
 - inhalation hydrogen therapy, effect of, 180, 181
 - measurement, 214
 - NC1940 effect on, 157
 - neurological testing and measurement, COX-2, 146–148
 - NS398 treatment, 147, 148
 - perihematomal, isoflurane preconditioning, 143
 - PGE₂ EP1 receptor inhibition, effect of, 279
 - SR49059 effect on, 193
 - inflammation, COX-2 inhibitors for, 145–146
 - injury, 146
 - capsaicin pre-treatment, neonatal hypoxic-ischemic, 225–230
 - fetal, protective effects of hydrogen, 307–311
 - geldanamycin, 161–165
 - neonatal hypoxic-ischemic, 207–212
 - normobaric and hyperbaric oxygenation, 243–250
 - postpartum pregnancy and, 37–40
 - progesterone and testosterone, effects of, 289–292
 - secondary, mechanisms of, 63–67
 - swelling, 52
 - tissue-type transglutaminase
 - animal preparation and intracerebral infusion, 102
 - effects of lysed RBCs, 102–103
 - fluoro-jade C staining, 102
 - Hb-induced neuronal degeneration, 102, 104
 - Hb-induced upregulation of, 104
 - immunohistochemistry, 102
 - in neural development, 103–104
 - statistical analysis, 102
 - upregulation of, 101
- C**
- CAA. *See* Cerebral amyloid angiopathy (CAA)
 - Capsaicin. *See* Transient receptor potential vanilloid 1 (TRPV1)
 - CCS. *See* Cerebrocardiac syndrome (CCS)
 - Cell culture, 134
 - Cell cycle re-entry, 79
 - Cerebral amyloid angiopathy (CAA)
 - canine model, 16
 - microhemorrhages, 15
 - murine model, 16
 - non-human primate model, 15
 - Cerebral edema risk. *See* Hyperbaric oxygenation (HBO)
 - Cerebral hypoxia-ischemia (HI), 207
 - Cerebral salt-wasting syndrome (CSWS), 346
 - Cerebrocardiac syndrome (CCS), 357, 358
 - Chronic subdural hematoma (CSDH)
 - animal models, 26–28
 - characterization and origin, 25–26
 - definition, 25
 - pathogenesis, 26
 - treatment and complications, 26
 - Clot formation, 72
 - Coagulative myocytolysis, 121
 - Coagulogram
 - chi-square test, 384
 - difference of, effective vs. ineffective group, 384
 - patient study, 383–384
 - prognosis of ICH, 384
 - PT and APTT, 384, 385
 - TT and Fbg, 385
 - Collagenase injection model, 4, 11
 - Collagenase vs. blood models
 - blood-brain barrier, 12–13
 - cell death, 13
 - functional outcome, 12
 - hematoma size, 11–12
 - Combined systemic thrombolysis
 - eMCAO, 168
 - experimental protocol, 168
 - functional testing, 168, 169
 - HBOT, 167–168
 - hemorrhagic transformation, 169–170
 - and hyperbaric oxygenation, 168
 - infarction size, 169, 170
 - infarct volume and hemorrhagic transformation, 168
 - side effect of, 167
 - statistical analysis, 168
 - Corner turn test, 186
 - CSDH. *See* Chronic subdural hematoma (CSDH)
 - CSWS. *See* Cerebral salt-wasting syndrome (CSWS)
 - Cyclooxygenase-2 (COX-2)
 - aneurysmal subarachnoid hemorrhage, inhibition in
 - animal study, 146
 - brain edema, 147, 148
 - for brain inflammation, 145–146
 - brain injury, 146
 - mortality, 146
 - neurological function, 146–147
 - neurological testing and brain edema measurements, 146
 - spreading depression (SD), 147
 - treatment, 146
 - catalytic sites, 96
 - GCSF action, 98
 - inhibition, 97
 - orchestrates immunologic responses, 96
- D**
- DBP. *See* Diastolic blood pressure (DBP)
 - Decompressive hemi-craniectomy. *See* Supratentorial hypertensive intracerebral hemorrhage
 - Deferoxamine (DFX)
 - animal preparation and intracerebral infusion, 123–124, 185–186
 - brain histology, 124
 - cell counts, 186
 - corner turn test, 186
 - coronal gross hematoxylin and eosin, 187, 188
 - for DNA damage, 126
 - enhanced Perls' staining, 124
 - experimental groups, 186
 - FDA approval, 123
 - ferritin and HO-1 immunoreactivity, 187–189
 - ferritin-positive cells, 125
 - forelimb-placing test, 186
 - hematoma cavity measurement, 186
 - HO-1 positive cells, effect on, 187–188
 - HSP-27 and HSP-32, effects on

- animal groups, 198
- animal preparation and intracerebral infusion, 197–198
- protein levels, in heart, 198, 199
- statistical analysis, 198
- western blot analysis, 198
- for ICH-induced neurological deficits, 189
- immunohistochemistry, 124, 186
- normalize heart HSP-32, 198
- statistical analysis, 124, 187
- TUNEL staining, 124, 126–127
- Deoxycorticosterone acetate (DOCA)-salt treatment, 33
- Diastolic blood pressure (DBP), 351
- Drug repurposing, vascular protection
 - conversion and analysis, 296
 - description, 295
 - experimental cerebral ischemia, 296
 - infarct volume and hemoglobin content, 296
 - neuroprotective agents, 296–297
 - results, 296–298
- E**
- Early hyperbaric oxygen therapy
 - eMCAO, 168
 - experimental protocol, 168
 - functional testing, 168, 169
 - infarction size, 169, 170
 - infarct volume and hemorrhagic transformation, 168
 - statistical analysis, 168
 - therapeutic goal, 167–168
 - thrombolysis and, 168
- Early serum glucose levels
 - advanced glycation end products, 394
 - clinical materials, 393–394
 - cumulative logit model, 394, 395
 - diabetes, 394
 - hyperglycemia, 395–396
 - statistical methods, 394, 395
- Elastase-induced intracranial aneurysm, 31–32
- Electrocardiographic (ECG) abnormalities
 - case selection, 353–354
 - CCS, 353
 - cerebral vascular vs. cardiovascular systems, 355
 - consciousness level, 354
 - vs. hematoma location, 354
 - myocardial ischemia, 353
 - NPY levels, 355
 - prognosis, multifactor logistic regression analysis, 354, 355
 - statistical methods, 354
- Electrolyte imbalance, TH
 - abnormal serum chloride levels, 345
 - abnormal serum potassium levels, 344, 345
 - abnormal serum sodium levels, 345
 - and non-thalamic hemorrhage, general incidence, 344, 345
- Embolic middle cerebral artery occlusion (eMCAO), 168
- Endogenous defense mechanisms, 72–74
- Endoscopic surgical treatment. *See* Pituitary apoplexy, elderly patients
- Endothelin receptor-A (ET_A) inhibition
 - animal groups, 208
 - brain water content, 208
 - effect on body weight gain, 208, 209
 - effect on brain edema formation, 208, 209
 - infarction volume, 208, 210
 - neonatal cerebral HI, 210–211
 - neurobehavioral deficits, 208
 - neurobehavioral testing, 210, 211
 - operative procedure, 208
 - role, 207–208
 - statistics, 208
- Erythropoietin (EPO)
 - anti-inflammatory/anti-apoptotic properties, 303
 - clinical trials, subarachnoid hemorrhage, 303
 - glycoprotein hormone, 300
 - neuroprotective agent, 300
 - protection mechanisms, 300
 - treatment, 300
- F**
- Fetal brain injury, maternal hypoxia rat model
 - body and brain weight, 308
 - body righting reflex, 308, 309
 - experimental regimen, 308
 - functional evaluation, 308–309
 - hydrogen inhalation, 311
 - immunohistochemistry, 308
 - negative geotropism, 308, 309
 - neonates, body and brain weights, 308
 - oligodendrocytes morphology, 309, 310
 - pathological conditions, 307
 - reactive oxygen species (ROS), 307
- Fibrinogen (Fbg) analysis, 384
- Fingolimod. *See* FTY720 (Fingolimod)
- Flow cytometry, 174–175
- Fluoro-Jade C staining
 - brain tissue-type transglutaminase, 102
 - iron-induced brain swelling and brain atrophy, 220, 221
- Forelimb-placing test, 186
- Free heme, 64
- FTY720 (Fingolimod)
 - brain edema measurement, 214
 - brain water content, 215
 - description, 213–214
 - endothelial barrier enhancement capacity, 216
 - experimental animal preparation, 214
 - experimental protocol, 214
 - intracerebral hemorrhage mice model, 214
 - neurobehavioral testing and neurological function, 215, 216
 - neurological function test, 214
 - statistical analysis, 214–215
- G**
- G-CSF. *See* Granulocyte colony-stimulating factor (G-CSF)
- Geldanamycin
 - brain water content, 162
 - experimental animals, 161–162
 - HSP 90, 161
 - neurological deficits, 162
 - neurological function tests, 164
 - neuroprotective effect of, 162, 165
 - in reducing brain edema, 162, 163
 - statistical analysis, 162
- Genome-wide association (GWAS), 86
- Germinal matrix hemorrhage (GMH). *See also* Hyperbaric oxygenation (HBO), neonatal GMH
 - animal groups and general procedures, 55–56
 - clinical consequences of, 57
 - cognitive dysfunction, 57, 58
 - cognitive measures, 56
 - cranial and somatic pediatric growth, 57, 59
 - definition, 55
 - developmental delays, 57
 - developmental milestones, 56

- experimental model, 56, 254
 - growth assessment, 56–57
 - hydrogen gas therapy
 - animal groups and general procedures, 238
 - cerebral and somatic growth assessment, 238–239
 - cerebral and somatic growth normalization, 239, 240
 - cognitive function normalization, 239
 - cognitive measures, 238
 - experimental model, 238
 - neuroprotective effects, 239
 - sensorimotor function, 238
 - sensorimotor function normalization, 239, 240
 - statistical analysis, 239
 - long-term consequences, 253
 - melatonin, neuroprotection by
 - animal groups and general procedures, 202
 - cerebral and somatic growth assessment, 202
 - cerebral and somatic growth normalization, 203, 204
 - cognitive function normalization, 203
 - cognitive measures, 202
 - experimental model, 202
 - role, 201
 - sensorimotor function, 202
 - sensorimotor function normalization, 203, 204
 - statistical analysis, 202
 - memory deficit, 57
 - sensorimotor dysfunction, 57, 58
 - sensorimotor outcome, 56
 - statistical analysis, 57
 - Glasgow Outcome Scale (GOS) score, 410
 - GMH. *See* Germinal matrix hemorrhage (GMH)
 - GOS score. *See* Glasgow Outcome Scale (GOS) score
 - Granulocyte colony-stimulating factor (G-CSF)
 - anti-inflammatory properties, 97
 - for neuroprotection in SBI
 - animal groups, 266
 - brain edema reduction, 267
 - brain water content, 266
 - cell death assessment, 266
 - cell death measurement, 267
 - hematopoietic growth factor, 265
 - neurobehavioral deficit assessments, 266
 - operative procedure, 266
 - post-treatment, neurobehavioral deficit, 267, 268
 - statistical analysis, 267
 - treatment method, 266
- H**
- Haptoglobin (Hp)
 - cytoprotective role of
 - in blood plasma, 107
 - definition, 107
 - ICH-mediated brain damage, resistance to, 108
 - immunofluorescence, 109
 - neuron, protection of, 108
 - oligodendrocytes, role of, 108
 - free heme, binding with, 64
 - HBO. *See* Hyperbaric oxygenation (HBO)
 - Heat shock protein (HSP) 90, 161
 - Hematoma cavity measurement, 186
 - Hematoxylin-eosin staining, 120, 121
 - Hemoglobin
 - expression
 - animal preparation and intracerebral infusion, 133–134
 - cell culture, 134
 - extracellular heme, 136
 - HbA and HbB mRNA expression, 135–136
 - immunohistochemistry, 134–135
 - immunoreactivity, ipsilateral basal ganglia, 135
 - intracerebral hemorrhage, 133
 - iron, 136
 - real-time PCR, 134
 - statistical analysis, 135
 - vertebrate hemoglobin, 133
 - measurement, 50
 - Hemorrhagic pituitary adenomas
 - clinical features, 364
 - diagnosis, 364–365
 - materials and methods
 - MRI examinations, 362
 - patients clinical features and manifestation, 361–362
 - postoperative follow-up visit, 362–363
 - treatment, 362
 - pathogenesis and predisposing factors, 364
 - prognosis conditions, 363
 - surgical results, 363
 - treatment, 365
 - Hemorrhagic transformation
 - by acute hyperglycemia, transient
 - focal ischemia model
 - animal preparation and MCAO, 49–50
 - BBB integrity, 50
 - brain swelling, 52
 - brain water content measurement, 50
 - Evans blue leakage, 51–52
 - experimental groups, 50
 - hemoglobin measurement, 50
 - histology, 50–51
 - post-ischemic HT, impact on, 53
 - statistical analysis, 51
 - cerebral infarction of, hyperglycemia and brain infarction, 44–47
 - experimental protocol, 43–44
 - ischemic-reperfusion model, 45
 - macroscopic observation and TTC staining, 44
 - MCAO and reperfusion model, 44
 - model of, 44
 - morphological assessment, 44
 - physiological data, 44
 - statistics, 44
 - Hydrogen gas therapy
 - antioxidant agents, 179
 - brain edema, effects on, 180, 181
 - brain water content, 180
 - efficacy of, 182
 - experimental animals, 179–180
 - fetal brain injury (*see* Fetal brain injury, maternal hypoxia rat model)
 - GMH
 - animal groups and general procedures, 238
 - cerebral and somatic growth assessment, 238–239
 - cerebral and somatic growth normalization, 239, 240
 - cognitive function normalization, 239
 - cognitive measures, 238
 - experimental model, 238
 - neuroprotective effects, 239
 - sensorimotor function, 238
 - sensorimotor function normalization, 239, 240
 - statistical analysis, 239
 - hydroxyl radicals, 183
 - intracerebral hemorrhage induction, 180
 - neurological deficits, 180
 - neurological outcomes, 180, 182

- neuroprotective effects after ICH, 180–182
 - statistical analysis, 180
 - Hyperbaric oxygenation (HBO)
 - neonatal GMH
 - animal groups and general procedures, 254
 - cerebral and somatic growth normalization, 255, 256
 - cognitive function normalization, 255
 - cognitive measures, 254
 - experimental model, 254
 - long-term consequences, 253
 - sensorimotor function, 254
 - sensorimotor function normalization, 255, 256
 - statistical analysis, 255
 - treatment, cerebral and somatic growth, 254
 - surgically induced brain injury
 - aerobic metabolism, 243
 - beneficial effects, 244
 - brain edema assessment, 245, 246
 - brain water content, 245
 - chi-square test, 245
 - experiment groups, 245
 - lipid peroxidation effects, 248, 250
 - mechanism, 243
 - neurological behavioral tests, 245
 - neurological function evaluation, 245–248
 - statistical analysis, 245
 - surgical procedure, 244
 - treatment time points, neurological score, 248–250
 - Hyperglycemia
 - acute ICH prognosis, 405
 - aggravating factors, 45
 - brain infarction and hemorrhagic transformation, 44–47
 - catecholamines, 395
 - hyperglycemia model, 44
 - induced hemorrhagic transformation, transient focal
 - ischemia model, 49–53
 - MCAO and reperfusion model, 44
 - mechanism, 395
 - morphological assessment, 44
 - pathological basis, 395
 - pathology, 395
 - physiological data, 44
 - risk factor of, 43
 - statistics, 44
 - treatment principles, 396
 - Hypertensive intracerebral hemorrhage (ICH)
 - average mortality rate, 387
 - blood pressure reduction, 391
 - computed tomographic features, 391
 - data collection, 388
 - discrete variables, 388
 - early death
 - definition, 388
 - risk factors, multivariate analysis, 389, 390
 - univariate predictor analysis, 388–390
 - groups, 388
 - patients
 - bimodal pattern, 329
 - chi-square test, 328
 - climatic conditions, 330
 - diagnosis, 328
 - diurnal variation distribution, 328, 329
 - monthly variation distribution, 329
 - population, 387–388
 - seasonal variation, 330
 - sign/symptom, 327
 - statistical analysis, 328
 - temporal pattern evaluation, 327
 - weekly variation distribution, 328–329
 - risk factor prevention, 390–391
 - statistical analysis, 388
 - Hyperuricemia, 405
- I**
- Inflammatory factors and cell death
 - cytokines, 301–302
 - erythropoietin (EPO)
 - anti-inflammatory/anti-apoptotic properties, 303
 - clinical trials, subarachnoid hemorrhage, 303
 - glycoprotein hormone, 300
 - neuroprotective agent, 300
 - protection mechanisms, 300
 - treatment, 300
 - human recombinant EPO effect, 301, 302
 - ICH induced
 - cell death, 301, 302
 - inflammatory factor expression, 301, 303
 - methods
 - brain tissue dissection, 300
 - ICH induction model, 300
 - qRT-PCR, 301
 - statistical analyses, 301
 - TUNEL staining and analysis, 300–301
 - stroke and stroke subtypes, 299
 - Intracerebral injection, 120
 - Intracranial aneurysm
 - angiotensin II-induced hypertension, 32–33
 - blood pressure measurement, 33
 - elastase-induced, in hypertensive mice, 31–32
 - elastase, stereotaxic injection of, 33–35
 - Intralesional tissue plasminogen activator (IL tPA), spontaneous ICH
 - average clot size, 426
 - hematoma volume, 427
 - IVH factor, 427
 - Modified Rankin score, 427
 - patients and methods
 - Codman external ventricular drain (EVD) catheter, 425
 - single-slice CT cuts, 426, 427
 - SICHPA, 428
 - tPA infusion duration, 426–427
 - t-score analysis, 427
 - Intravascular hypothermia, acute hemorrhagic stroke
 - baseline characteristics, interventional and control group, 422, 423
 - GCS score, 423
 - intravascular cooling method, 423
 - materials and methods
 - death causing events, 422
 - follow-up assessment, 422
 - inclusion and exclusion criteria, 421
 - study protocol and design, 421–422
 - modified Rankin Scale (mRS) score, 422, 423
 - neuroprotective mechanism, 422
 - Intraventricular hematoma (IVH)
 - actilyse vs. control, reduction of, 411
 - blood clots, 411
 - demographic data and treatment outcome, 410
 - dose regime, 410
 - fibrinolytic agents, 409
 - GOS score, 410
 - protocols employed, 410
 - risk/benefit ratio, intrathecal fibrinolytic therapy, 411–412
 - routine blood workup, 410
 - severity, grading systems, 410, 411
 - spontaneous/secondary, 411

- Iron accumulation and DNA damage
 animal preparation, 123–124
 brain histology, 124
 cell counting, 124
 deferoxamine, 123
 enhanced Perls' staining, 124
 ferritin-positive cells, 125–126
 immunohistochemistry, 124
 intracerebral infusion and DFX treatment, 123–124
 perihematoma zone, TUNEL staining, 126–127
 statistical analysis, 124
 TUNEL, 124
- Isoflurane
 albumin western blot, 142
 brain edema, 143
 brain sample preparation, 142
 experimental intracerebral hemorrhage, 142
 functional performance, 142–143
 ipsilateral hemispheric edema, reduction of, 143
 limitation, 144
 neurological deficit assessment, 142
 as neuroprotective agent, 141
 preconditioning, 142
 quantitative assessment and statistical analysis, 142
- IVH. *See* Intraventricular hematoma (IVH)
- K**
 Kaplan-Meier survival analysis, 39
- L**
 Lactate dehydrogenase (LDH) measurement, 260
 Leukocyte-endothelial cell interactions, 65
 Lipid metabolism and glycometabolism
 data source, 368
 diagnostic criteria, 368
 high triglycerides (TG) proportion
 middle-age group, 369
 young-age group, 368–369
 hypertriglyceridemia, 370
 lipids and serum glucose measurements, 368
 population characteristics, 368
 statistical analysis, 368
 stroke, 367, 370
- M**
 Matrix metalloproteinase (MMP), 55, 66, 84
 Medical expenditure and outcomes, Southwestern China
 age, male and female, 338
 death constituent ratio, 338, 339
 hospital care discrepancies, 340
 hospital costs and LOS, 338
 locally insured vs. uninsured patients outcome, 338, 339
 patient categorization, 338
 principle diagnosis code, 337
 social health insurance program (SHI), 339–340
 statistical analysis, 338
 Meteorological factors, Southwest China
 blood pressure, 325
 climatology, 322
 daily visibility evaluation, 323, 324
 fog evaluation, 323, 324
 humidity effects, 325
 mean temperature evaluation, 323
 meteorological data, 322
 patient population characteristics, 322
 relative humidity and air pressure, 323, 324
 statistical analysis, 322
 wind evaluation, 323, 324
- Microballoon insertion, 11
 Microballoon model, 3–4
 Microglia, 65–66, 94
 Microhemorrhages, CAA, 15
 Middle cerebral artery occlusion (MCAO), 44
 Minimally invasive aspiration, massive ICH treatment
 hematoma effect, 382
 materials and methods
 aspiration time and procedure, 381–382
 patient selection, 381
- Mitogenic signal pathways, 77, 78
 Modified Rankin score, 427
 Monocyte infiltration, perihematomal brain,
 175, 177
- Mucosal tolerance, SBI
 animal groups, 284
 anti-inflammatory treatments, 284
 brain cytokine levels, 285
 modified Garcia testing, 284–285
 neurological score, 285
 osmotic agents, 283
 peripheral immune tolerance, 284
 Sham surgery, 284
 statistical analysis, 285
 surgical risks, 283
 TGF β 1 preoperative levels, 285
 treatment, 284
- Myocardial injury, gender effects
 animal experiments, 119–120
 17 β -estradiol, 122
 hematoxylin-eosin staining, 120, 121
 histology and immunohistochemistry, 120
 intracerebral injection, 120
 myocardial HSP-32 protein levels, 121
 statistical analysis, 120
 stress-related proteins, 120, 121
 western blot analysis, 120
- N**
 NC1900. *See* Arginine vasopressin (AVP)
 Neonatal hypoxia-ischemia
 COX-2, role of, 96
 neuro-glial interactions, 96
 neuroinflammation, 93–94
 after brain injury, 95
 astrocytes, 94–95
 microglia, 94
 neurons, 95–96
 pathophysiology, 93, 94
 therapeutic modalities, 96–97
 transient receptor potential vanilloid 1 (TRPV1)
 cell-specific distribution of, 227
 description, 225
 immunohistochemistry, 226
 infarction volume after neonatal hypoxia ischemia, 228
 infarct volume measurement, 226
 statistical analysis, 226
 treatment method, 226
 ubiquitous expression of, 226–227
 vascular dynamics, 226, 228–229
- Neural progenitor cell proliferation, 79
 Neural stem cell precursors
 BrdU and DCX doublestaining, 153
 non-peptidyl sonic hedgehog agonist, 152

- porcine intracranial hemorrhage model, 152–153
 - sonic hedgehog (SHH), 151–152
 - Neurogenic pulmonary edema (NPE)
 - definition, 129
 - pathogenetic factor, 131
 - Neuro-glial interactions, 96
 - Neuroglobin immunoreactivity expression, 316–318
 - Neuron apoptosis, 79
 - Neurons, 95–96
 - Neuroprotection, SBI. *See* Granulocyte
 - colony-stimulating factor (G-CSF);
 - Prostaglandin E₂EP₁ receptor inhibition
 - Neutrophil depletion
 - animal studies, 174
 - deleterious effects of, 173
 - flow cytometry, 174–175
 - functional outcome, 175, 177
 - immunohistochemistry, 174
 - intracerebral hemorrhage surgery, 174
 - localized inflammatory response, 175, 176
 - in monocyte infiltration, perihematomal brain, 175, 177
 - neurobehavioral deficit, 174
 - recruitment of monocytes, 177
 - role of, 173
 - statistical analysis, 175
 - Non-peptidyl sonic hedgehog agonist, 152
 - Normobaric oxygenation (NBO), 243–250
 - Nosocomial pneumonia, 435–439
 - Notch signaling, 315
- O**
- Oligodendrocytes, 65–66, 108
 - Osteopontin (OPN), recombinant
 - BBB permeability, 232
 - brain edema, effects on, 233, 234
 - brain water content, 232
 - definition, 231
 - experimental model and study protocol, of SAH, 232
 - intracerebroventricular infusion, 232
 - MMP-9, 234
 - mortality rate, 233
 - neurological scoring, 232
 - SAH grading score, 233
 - SAH severity, 232
 - statistical analysis, 233
 - VEGF-A, phospho-JNK, effects on, 234–235
 - western blot analyses, 232–233
- P**
- Perihemorrhagic zone, multiparametric characterisation
 - cerebral ischemia, 21
 - cerebral perfusion, 21–22
 - ICP, CBF and P_{br}O₂, 21
 - lactate/pyruvate ratio, 22
 - porcine model
 - animal preparation, 19–20
 - monitoring, 20–21
 - operative procedure, 20
 - statistical analysis, 21
 - superficial lobar hematoma, 21
 - in swine, 22
 - Pituitary apoplexy, elderly patients
 - case reports, MRI findings, 430–432
 - clinical features, 429
 - hypopituitarism management, 431
 - pituitary gland stress, 433
 - sellar and parasellar region, surgical approach, 432
 - visual acuity deterioration, 431
 - Plasminogen activator inhibitor (PAI)-1, 73
 - Preclinical models
 - collagenase injection, 11
 - collagenase vs. blood models
 - blood-brain barrier, 12–13
 - cell death, 13
 - functional outcome, 12
 - hematoma size, 11–12
 - GMH (*see* Germinal matrix hemorrhage (GMH))
 - ICH models
 - blood injection model, 4
 - collagenase injection model, 4
 - microballoon model, 3–4
 - large animal models
 - canines, 5
 - monkeys, 4–5
 - pigs, 5
 - microballoon insertion, 11
 - single blood injection, 10–11
 - small animal models
 - mice, 6–7
 - rabbits, 5–6
 - rats, 6
 - Pregnancy, brain injury
 - animal perfusion and tissue extraction, 38
 - animals and general procedures, 38
 - cerebellar hemorrhage model, 38
 - cerebellar water, 38
 - clostridial collagenase infusion, 37, 39–40
 - hematoma volume, 38
 - immunoblots, 39, 40
 - Kaplan-Meier survival analysis, 39
 - neurological score, 38
 - postpartum ICH, 37
 - statistical analysis, 39
 - vascular permeability, 38
 - western blotting, 38–39
 - Progesterone and testosterone effects, brain injury
 - androgens, 292
 - animal preparation and intracerebral infusion, 289–290
 - behavioral tests, 290
 - brain water content, 290
 - estrogen, 289
 - experimental groups, 290
 - forelimb-placing test, 290, 291
 - forelimb-use asymmetry tests, 290, 291
 - ion contents, 290
 - perihematomal brain edema, 290, 291
 - physiological variables, 290
 - progesterone dose, 291–292
 - statistical analysis, 290
 - stressors, 292
 - Prostaglandin E₂EP₁ receptor inhibition
 - absorbance assay, cell death measurement, 279, 280
 - animal groups, 278
 - ANOVA, statistical analysis, 279
 - BBB disruption, 277, 278
 - brain edema reduction, 279
 - brain water content, 278
 - cell death detection, 279
 - downstream cyclooxygenase (COX-2) effector, 280, 281
 - neurobehavioral
 - deficits assessment, 278
 - score improvement, 279, 280

- operative procedure, 278
 - SC51089 treatment, 280, 281
 - treatment method, 278
 - Protease nexin-1 (PN-1), 73
 - Prothrombin time (PT) analysis, 384
 - Proton pump inhibitor (PPI) prophylaxis
 - acid suppression therapy, 438
 - advantages, 435–436
 - demographic and clinical characteristics, ICH, 436, 437
 - imaging manifestation distribution, 437
 - logistic regression analysis, 436
 - materials and methods
 - prophylactic treatment and outcomes, 436
 - statistical analysis, 436
 - study design and patients, 436
 - variables, 436
 - nosocomial pneumonia cases, 436
 - SRMD, 435
 - univariate analysis, variables inclusion, 436, 438
 - Pulmonary edema, 130, 131
 - Pulse pressure (PP) characteristics
 - age distribution and, 351
 - blood pressure parameter variation, 350
 - BP measurement, 350
 - case study, 349–350
 - frequency distribution, 350, 351
 - hypertension, 351–352
 - in non-hypertensive patients, 350
 - statistical analysis, 350
 - systolic and diastolic blood pressure, 351
- Q**
- Quantitative real-time polymerase chain reaction (qRT-PCR), 301
- R**
- Real-time PCR, 134
 - Red blood cell lysis
 - animal preparation and intracerebral infusion, 102
 - and brain tissue-type transglutaminase, 101
 - deferoxamine, 102
 - experiment groups, 102
 - fluoro-jade C staining, 102
 - immunohistochemistry, 102
 - intrahippocampal injection, 102–103
 - statistical analysis, 102
- S**
- SBI. *See* Surgically induced brain injury (SBI)
 - SBP. *See* Systolic blood pressure (SBP)
 - Secondary brain injury
 - astrocytes, 65–66
 - coagulation disorders, 64–65
 - free heme, 64
 - leukocytes, activation of, 65
 - microglia, 65–66
 - oligodendrocytes, 65–66
 - platelet activation, 65
 - representative pathways of, 67
 - spontaneous ICH, 63
 - traumatic ICH, 63–64
 - vascular response, 66
 - Single blood injection, 10–11
 - Sonic hedgehog (SHH), 151–152
 - Spontaneous intracerebral hemorrhage (ICH)
 - Chongqing City
 - definition, 399
 - ethnicity and socioeconomic factors, 399
 - hypertension, 400
 - independent predictor, prognosis, 400
 - in-hospital mortality, multivariable logistic regression analysis, 400, 401
 - limitations, 401
 - locations of, 400
 - materials and methods, 399–400
 - primary and secondary ICH, 399
 - high augmentation index (AIx) role
 - final variable models, 6-month outcome and mortality, 376, 378
 - materials and methods, 375–376
 - radiological factors, 376, 379
 - univariate analysis, 376–378
 - Spreading depression (SD), 147
 - SR49059. *See* Arginine vasopressin (AVP)
 - Src kinases
 - in acute brain injuries, 77, 79
 - cell cycle re-entry, 79
 - mitogenic signal pathways, 77, 78
 - neural progenitor cell proliferation, 79
 - neuron apoptosis, 79
 - SRMD. *See* Stress-related mucosal damage (SRMD)
 - Stereotactic treatment of intracerebral hemorrhage by means of a plasminogen activator (SICHPA), 428
 - Stereotaxic injection, of elastase, 33–35
 - Stress-related mucosal damage (SRMD)
 - erosive process, 435
 - gastrointestinal (GI) bleeding, 437
 - mechanical ventilation, 437–438
 - Stress-related proteins, 120, 121
 - Subarachnoid hemorrhage (SAH)
 - acute, ECG change of
 - abnormality and severity, 358
 - alteration, 358–359
 - causes, 358
 - CCS, 358
 - changes, 358
 - hematoceles, 358
 - hypertension history, 357
 - negative and positive group, 357
 - patient evaluation, 357
 - and prognosis, 358, 359
 - selection criteria, 357
 - statistical analysis, 357–358
 - apoptosis, 130–131
 - COX-2 inhibition, neuroprotective effects
 - animal study, 146
 - brain edema, 147, 148
 - brain inflammation, 145–146
 - brain injury, 146
 - mortality, 146
 - neurological function, 146, 147
 - neurological testing and brain edema measurement, 146
 - experimental model and study protocol, 129–130
 - histological assessments, 130
 - lung water content, 130
 - neurogenic pulmonary edema, 129–131
 - pulmonary endothelial cell apoptosis, 131
 - statistics, 130
 - TUNEL/endothelial cell immunostaining, 132
 - western blot analyses, 130
 - Z-VAD-FMK treatment, lung cell apoptosis, 131
 - Subdural hygroma. *See* Acute subdural hematoma (ASDH)
 - Supratentorial hypertensive intracerebral hemorrhage
 - hematoma volume, 415
 - illustrative cases, computed tomography, 416

- limitations, 417
 - m-RS vs. parameters, 417, 418
 - patient groups, 415
 - perioperative treatment, 415
 - rat experimental model, 417
 - Surgically induced brain injury (SBI)
 - brain edema, 245, 246
 - brain water content, 245
 - experiment groups, 245
 - Garcia neurological scoring, 248–250
 - hyperbaric oxygenation (HBO), 243–244
 - intramedullary cranial surgery, 244
 - and mortality rate, 244
 - neurological behavioral tests, 245
 - neurological function evaluation, 245–248
 - statistics, 245
 - surgical procedure, 244
 - Sysmex CA1500 coagulation analyzer, 384
 - Systolic blood pressure (SBP), 351
- T**
- Tamoxifen treatment
 - animal preparation and intracerebral infusion, 271–272
 - behavioral tests, 272
 - brain atrophy measurement, 272
 - brain tissue loss, 273
 - brain water content, 272
 - coronal brain sections, 273
 - dose rates, 272
 - experimental groups, 272
 - hydrocephalus development, 273, 274
 - MRI, 272–274
 - selective estrogen receptor modulator, 271
 - statistical analysis, 272
 - TGFβ-1 preservation, brain antigens. *See* Mucosal tolerance, SBI
 - TH. *See* Thalamic hemorrhage (TH)
 - Thalamic hemorrhage (TH)
 - baseline characteristics, 344
 - CSWS, 346
 - electrolyte imbalance
 - abnormal serum chloride levels, 345
 - abnormal serum potassium levels, 344, 345
 - abnormal serum sodium levels, 345
 - and non-thalamic hemorrhage, general incidence, 344, 345
 - hypernatremia, 346, 347
 - hypopotassemia, 346
 - mortality, electrolytes normal/abnormal level, 345, 346
 - patients and methods
 - groups, 344
 - inclusion/exclusion criteria, 343–344
 - statistical analysis, 344
 - variables, 344
 - prognosis factors, 347
 - Thrombin
 - clot formation and resolution after ICH, 72
 - and clot resolution, 72
 - coagulation activation of, 65
 - and endogenous defense mechanisms, 72–73
 - endogenous responses and therapeutic consequences, 73–74
 - generation and coagulation after ICH, 72
 - inhibition after ICH, 73
 - sequential endogenous response to ICH, 71–72
 - and vascular repair, 72
 - Thrombin preconditioning (TPC)
 - induced neuronal protection
 - cell preparation, 260
 - experiment groups, 260
 - LDH measurement, 260
 - neuronal tolerance, iron toxic effects, 260
 - PD98059 effects, 261, 262
 - p44/42 MAPK-p70 S6K pathway activation, 261
 - protease-activated receptors (PAR), 260
 - 40S ribosomal protein S6, 259
 - statistical analysis, 260
 - thrombin receptor activation, 260
 - western blot analysis, 260
 - iron-induced brain swelling and brain atrophy
 - animal preparation and intrahippocampal injection, 219–220
 - experimental groups, 220
 - Fluoro-Jade C staining, 220, 221
 - H&E staining, hippocampal swelling, 221, 222
 - histological assessments, 220
 - p70 S6K, 219
 - statistical analysis, 220
 - in vitro and in vivo studies, 221–222
 - western blot analysis, 220, 222
 - Thrombin time (TT) analysis, 384
 - Tissue factor (TF), 64
 - Transient receptor potential vanilloid 1 (TRPV1)
 - neonatal HI brain injury
 - cell-specific distribution of, 227
 - description, 225
 - immunohistochemistry, 226
 - infarction volume after neonatal hypoxia ischemia, 228
 - infarct volume measurement, 226
 - statistical analysis, 226
 - treatment method, 226
 - ubiquitous expression of, 226–227
 - vascular dynamics, 226, 228–229
 - TUNEL staining, 124, 126–127
- V**
- Vascular dynamics, TRPV1, 226, 228–229
 - Vascular endothelial growth factor (VEGF), 84
 - Vascular protection, acute ischemic stroke
 - conversion and analysis, 296
 - diabetic Goto-Kakizaki (GK) rats, 296, 297
 - endogenous mediators, 295
 - experimental cerebral ischemia, 296
 - hemoglobin content, 296
 - infarct volume assessment, 296
 - minocycline, 296, 297
 - spontaneously hypertensive rats (SHR), 296, 298
 - Wistar rats, 296, 297
 - Vascular repair, 72
- W**
- Weekend effect, ICH
 - baseline characteristics, 334
 - clinical modification diagnosis code, 333
 - comprehensive stroke centers (CSC), 335
 - distribution variation, weekend vs. weekday admission, 334, 335
 - modified Rankin scale, 334, 335
 - mortality rates, 335
 - patient grouping and evaluation, 333–334
 - rank sum test, 334, 335
 - statistical analysis, 334
 - Western blot analysis
 - aging, 114
 - of aquaporin-4, 156
 - Heart injury, effects of gender on, 120
 - HSP-27 and HSP-32, effects on, 198
 - iron-induced brain swelling and brain atrophy, 220, 222
 - subarachnoid hemorrhage, 130